Spatial and Temporal Models of Jōmon Settlement

Enrico R. Crema

A Thesis submitted for the degree of Doctor of Philosophy

Institute of Archaeology

University College London

January 2013

Declaration

I, Enrico Ryunosuke Crema, confirm that the work presented in this thesis is my own. Where information has been derived from other sources, I confirm that this has been indicated in the thesis.

"Ce qui est simple est toujours faux. Ce qui ne l'est pas est inutilisable" (P. Valery)

"All models are wrong, but some are useful" (George E.P. Box)

Abstract

The Jōmon culture is a tradition of complex hunter-gatherers which rose in the Japanese archipelago at the end of the Pleistocene (ca. 13,000 cal BP) and lasted until the 3rd millennium cal BP. Recent studies increasingly suggest how this long cultural persistence was characterised by repeated episodes of change in settlement pattern, primarily manifested as cyclical transitions between nucleated and dispersed distributions. Although it has been suggested that these events correlate with population dynamics, shifts in subsistence strategies, and environmental change, to date there have been very few attempts to provide a quantitative analysis of spatio-temporal change in Jomon settlement and its possible causes.

This thesis is an attempt to fill that lacuna by adopting a twin-track approach to the problem. First, two case studies from central Japan have been examined using a novel set of methods, which have been specifically designed to handle the intrinsic chronological uncertainty which characterises most prehistoric data. This facilitated the application of a probabilistic framework for quantitatively assessing the available information, making it possible to identify alternating phases of nucleated and dispersed pattern during a chronological interval between 7000 and 3300 cal BP.

Second, computer simulation (by means of an agent-based model) has been used to carry out a formal inquiry into the possible underlying processes that might have triggered the observed changes in the settlement pattern. The aim of this simulation exercise was two-fold. First, it has been used as a theory-building tool, combining several models from behavioural ecology and cultural transmission theory in order to provide explicit expectations in relation to the presence and

absence of environmental disturbances. Second, the outcome of the simulation has been used as a template for linking the observed patterns to possible underlying socio-ecological processes suggested by the agent-based model. This endeavour has shown how some of the largest changes in the empirically observed settlement patterns can be simulated as emerging from the internal dynamics of the system rather than necessarily being induced by external changes in the environment.

Contents

VOLUME 1

VOLUME 2

List of Figures

List of Tables

Acknowledgements

The completion of this thesis allowed me to look back at every single individual who dedicated a moment of her or his life, and remember all friends and relatives who helped and supported me along this long journey.

I would like to express my heartfelt gratitude to Dr Andrew Bevan and Dr Mark Lake who were and always be the best mentor a student can have. Without their patience and support this work would have been impossible. Their encouragement helped me through the hardest times, while their enthusiasm made the toughest obstacle enjoyable. I hope one day I can be as inspirational as they were to me.

Dr Rick Schulting and Dr James Steele examined this thesis and offered invaluable comments and feedbacks to which I am extremely grateful. Discussing details of this work with them was both an honour and source of great enjoyment.

The thesis have been funded by the UCL Graduate School Research Scholarship and the UCL Cross-Disciplinary Training Scholarship. Both funding gave me the opportunity to fully dedicate these years to pursue my research, and I would like to thank the graduate school for this generous support. The graduate school also allowed me to spend one year at the Centre for Advanced Spatial Analysis under the supervision of Prof Mike Batty. I am grateful for all his advices and support.

I would like to express my gratitude to the AHRC Centre for the Evolution of Cultural Diversity and its members who provided support in many ways and although many are spread across the world, they still provide continuous inspiration to my research through their work. The centre also allowed me to get access to UCL Legion High Performance Computing Facility, without which I would be

still running my simulations. I would like to thank Legion's associated support services and in particular Dr Bruno Silva for his help.

I am extremely grateful to several members of the Cultural Properties Centre at the Chiba Prefecture Education Foundation and the Gunma Archaeological Research Foundation for providing support and data which were fundamental to this project. I would particularly like to thank Masahito Nishino, Shigeru Ishizaka, Chitoshi Ouchi, and Yoshio Iijima for their advice, and all the librarians of the two foundations.

Several scholars offered their advice, supporting my existing ideas with constructive critiques or giving me the grounds for developing new ones. I am particularly grateful to (with no particular order) Prof Caitlin Buck, Prof Hiro'omi Tsumura, Dr Simon Kaner, Prof Yasuhiro Taniguchi, Prof Richard Pearson, Prof Gina Barnes, Dr Anne Kandler, Dr Junzō Uchiyama, Prof Robert Drennan, Prof Fujio Kumon, and Dr Hal Whitehead.

The Institute of Archaeology offered an exceptional environment for pursuing my research, and I would like to thank all its members of staff. I am particularly grateful to Prof Cyprian Broodbank, Prof Ken Thomas, Prof Arlene Rosen, Prof Andrew Garrard, Dr Sean Downey, Dr Louise Martin, Prof Stephen Shennan, Prof Clive Orton, Ms Lisa Daniel and Ms Manu Davies.

Dr Marcello Mannino deserves a special mention. He pointed pointed to me the right direction at the right time, and gave me a crucial life-changing advice to which I will be grateful forever.

Many friends both inside and outside the institute shared their moments of there life with me. Without their constant support, friendship, and enthusiasm this PhD would not have been the wonderful experience it was. I would like to thank past and present members of room 322b (Adi, Alice, Brenna, Anke, Isabel, Tessa, Liz, Stuart, Anna Maria, Frederik, Emmy, Valentina, Victoria, and Ying), the AGIS Lab (Michele, Denitsa, Janice, Dario, Christina, Eva, Steve, Chiara, Gary, Fernando and Yu), and other offices of the institute (Andrea, Micol, Anna, Max, and Francesco). I would like to thank my housemates for making me feel home

every evening (Clara, Caterina, Claudia), Cristian for believing in me, Laura for her continuos support, Simone for listening to my complains, the SPQR (Anna Lisa, Peppe, Fracce, Stefania, and Elisa) for growing up with me, and Simona for being always there in the best and toughest moments.

Some friends and colleagues deserve a special mention for their active engagement on my PhD. Akira Matsuda has been and will always be a great *senpai* with fruitful suggestions on many aspects of the doctoral life, Carolyn Rando read drafts of my chapters and offered me insightful advice on many themes for present and future studies, Bernardo Rondelli for endless discussions on Complex Adaptive Systems, Xavier Rubio for looking at game-theoric models, Alessio Palmisano for countless talks on settlement pattern, and Eugenio Bortolini for being a great friend and colleague and for insightful comments and discussion on literally everything in the world. I thank you all so much.

Finally, I would like to apologise to my brother, my sister, and my father and all my relatives for not being around. I would like to thank my mother for all the support and for teaching me painting when I was a boy. After many years, I fully understand the meaning of her words. And at last, but not least, I would like to thank Eleonora, who has been my shelter, my love, and source of happiness all these years.

Part I

Introduction

Chapter 1

Introduction

1.1 Problem Statement

This thesis aims to investigate the generative process behind hunter-gatherer settlement change. It seeks to understand the relationship between forces external to the system of interest (such as the onset of climatic events) and forces rooted in the evolutionary history of the system itself that might —jointly or in isolation— play a fundamental role in the transformation of settlement patterns.

A unidirectional vision of human history led people to believe for many decades that pre-agricultural societies slowly developed increasing complexity, progressing from mobile to sedentary lifestyles, with a linear change in settlement pattern. Recent studies have been increasingly providing evidence that such a vision can no longer be supported and that the evolutionary trajectories of hunter-gatherers is multilinear, with episodes of rapid changes alternating with stasis, and multiple instances of reversions rather than unidirectional stepwise developments (Rowley-Conwy 2001). The presence of reversions is particularly noteworthy; hunter-gatherers can adopt agriculture or herding and then revert to their original subsistence strategies (Schrire 1980, Oota *et al.* 2005), become sedentary and then exhibit a return to a mobile settlement pattern (Habu 2002, Chatters and Prentiss 2005, Rosen and Rivera-Collazo 2012), and more in general show transitions in all directions, more generally from simple to complex and from complex

to simple (see examples in Rowley-Conwy 2001). These transformations are triggered by different underlying processes, but share the same structure of a return to patterns and configurations that have been already exhibited in the past. Furthermore, these reversions are never instances of a complete reoccurrence of previously adopted traits, and subtle differences, innovations, and social memory of past cycles lead to divergences in the evolutionary trajectory (Holling 2001, Rosen and Rivera-Collazo 2012).

How do we explain these cyclical patterns? Are they result of adaptive responses to reoccurring selective forces? And if so, what are these forces? Are they originating from convergence in the internal dynamics of the system, by the onset of similar external forces (such as the presence of similar climatic conditions), or by complex interactions between the two?

1.1.1 Jōmon Settlement Pattern

The prehistoric Jōmon hunter-gatherers of Japan were characterised by distinct features, including the adoption of pottery (Kuzmin 2006), presence of year-round, permanent villages (Pearson 2006), and the development of resource management strategies which shared many similarities to those adopted by early agricultural communities (Crawford 2011). The most striking feature is perhaps the maintenance of the same set of cultural traits for over 10,000 years (Pearson 2007), an absolute time-span starting during the last few millennia of the Pleistocene and ending about 2,500 years ago. While in other parts the world we see transitions to agriculture, the adoption of metallurgy, and the rise and fall of early states and empires, the Japanese archipelago was characterised by the persistence of the same economic system based on hunting, fishing, and gathering.

The homogeneity of Jōmon culture hides, however, a remarkable series of almost cyclical changes; population level rose and fell (Imamura 2010), subsistence strategy exhibited shifts in primary resources (Imamura 1999a), and settlement pattern showed the disappearance and the reappearance of specific features (Taniguchi 2005) along with repeated changes in its distributional properties (Kani 1993, Uchiyama

2006).

The evolutionary changes observed in the settlement pattern are perhaps one of the most prominent aspects of the Jōmon culture that testifies to its heterogeneity and cyclical nature. The exact combination of traits and their association with other features, such as subsistence and demography, varied in space and time, and this led many scholars to develop specific regional theories, often focusing on single transitional episodes (see Habu 2001, Nishimoto *et al.* 2001, Tsumura *et al.* 2002a;b; 2003). Despite this fragmentation, an overarching sense of repeated similarities over time is shared by many authors (see examples in Suzuki and Suzuki 2010), and has been synthesised fews years ago by Uchiyama's distinction between *clumped* and *dispersed* settlement patterns (2006, 2008). The former refers to instances where there are few large sites and many smaller settlements, while the latter refers to the opposite pattern, characterised by a much more uniform distribution of sizes. Uchiyama hypothesised that these two types of settlement pattern occurred multiple times in a cyclical fashion and that their occurrence were related to different types of land-use, possibly in relation to modified environmental conditions.

To date, no attempt to formally and quantitatively test this hypothesis has been proposed. The distinction between different settlement forms has been often based on qualitative descriptions, and the chronological definition confined to a relative framework defined by pottery phases. Moreover, formal models, aiming to describe how these forms emerged and how they transformed, have not been proposed. The most commonly adopted explanations (see for example Matsugi 2007, Suzuki 2010b) are based on the notion that there was one ideal shape to Jōmon settlement pattern (usually what Uchiyama would refer to as clumped pattern) becoming suddenly unsustainable due to changes in the environmental conditions, ultimately leading to the formation of alternative settlement strategies. Details on how and why these changes occurred are rarely discussed, and in most cases reduced to few lines of suppositions.

The long time-span of the Jōmon culture was undoubtedly characterised by

climatic changes with a global scale impact (Kudo 2007), but as Anderson and colleagues have recently pointed out, ”correlation between climate and culture change, of course, does not prove they are related” (Anderson *et al.* 2007: 12). Settlement pattern could thus change *without* the onset of a climatic event, and modified environmental conditions do not necessarily determine transformations in the spatial configuration of residential units.

1.2 Research Questions

The archaeological record of the Jōmon culture offers an ideal laboratory for exploring the long-term evolution of human settlement patterns. The maintenance of the same economic system for an extremely long time-span, characterised by both intervals of stability and changes in the climatic conditions, can in fact provide insights on how changes in the interaction between individuals and their surrounding physical environment become manifest in a cyclical alternation of settlement forms. In the chapters that follow, this over-arching research agenda is addressed via the following three research questions

1. Can the claim of repeated cycles between clumped and dispersed settlement patterns be supported by a formal and quantitative assessment of the Jōmon archaeological record?

2. In principle, can shifts between these two patterns be explained without reference to environmental change or is the latter always the main cause ?

3. In practice in the Jōmon case, what are the expected effects of environmental change on settlement patterns? Does the observed change in the empirical record conform to these expectations?

1.3 Aims and Objectives

The first of the above research questions will be approached through the spatial analysis of Jōmon residential units. This will be based on a series of statistics that will seek to formalise the description of the settlement size distribution, hence offering a direct and quantitative measure for distinguishing clumped and dispersed patterns. A crucial role will be played by the treatment of temporal data and its intrinsic uncertainty. This will be tackled by the adoption of a novel method specifically designed to use the fine-grained pottery-based chronology available in the Jōmon datasets, and will result in probabilistic outputs based on Monte-Carlo methods.

The second research question is theory-building in nature, and will be addressed by means of a computer simulation. This will seek to merge two sets of ecological theories. The first focuses on the relationship between metapopulation structure and resource distribution (e.g. Fretwell and Lucas 1970), and the second on group formation dynamics and frequency dependent fitness (Sibly 1983, Clark and Mangel 1986). These will be unified and integrated into an agent-based model (ABM), which will help to determine whether transition between clumped and dispersed patterns could occur without external forces acting on the system and under what circumstances.

The third research question will be first approached by extending the agent-based model developed for the previous question. This will be conducted by integrating two possible scenarios of environmental change. The first will address the consequences of overexploitation, while the second will explore the effects derived by a general decline of resource availability. The simulation output will then be used as a template for reassessing the analysis of the empirical data (conducted for research question 1) in relation to the results of existing palaeoenvironmental studies.

1.4 Scope and Limits

The study of Jōmon settlement conducted here will be confined to the interval between the Early and Late Jōmon periods (7000-3220 cal BP; Kobayashi 2008). This will ensure the exclusion of chronological intervals where the socioeconomic features were transitional and too closely resembling the adjacent Palaeolithic and Yayoi periods. The spatial extent of the analysis will be limited to two case studies in central Japan (Chiba and Gunma), and primary confined to the spatial and temporal distribution of 2,850 residential units (1,418 units for Chiba and 1,432 for Gunma). The choice has been driven by the substantial diversity in the environmental settings of the two areas (coastal tableland vs. inland river valley) and the presence of a high number of emergency excavations, which have yielded a rich archaeological record and a large corpus of existing regional studies on Jōmon settlement pattern (Kano 2002, Ishizaka 2002, Nishino 2005).

1.5 Thesis Outline

Chapter 2 will provide an outline of the main features of Jōmon hunter-gatherers and their archaeology, with a particular emphasis placed on existing studies and models concerning settlement history, population dynamics, and subsistence. This will provide the necessary background information for the two case studies, and the basis for developing the core assumptions for the computational model building. The chapter will also briefly discuss the relative chronology adopted in this thesis and the palaeoenvironmental studies relevant to the two case studies.

Chapters 3-4 work together on the analysis of the empirical data required for answering the first research question. The former will present the theoretical background of the spatial and temporal analysis, the quantitative formalisation of the distinction between clumped and dispersed patterns, and details of a novel methodology developed specifically to overcome the problem of spatial and temporal uncertainty. Chapter 4 will illustrate the results of the analysis applied to the two case

studies along with a discussion pertaining to the first research question.

Chapters 5-7 will be dedicated to building and exploring of the computer simulation model. Chapter 5 will first provide a review of existing ecological theories on group formation dynamics, followed by an extensive description of the agent-based model. Chapter 6 will present the results of the computer simulations, and discuss these in relation to the second research question. Chapter 7 will briefly introduce two models of environmental change, and then explore their implications by means of additional modules in the agent-based simulation.

Chapter 8 will review the results of the spatial analysis presented in chapter 4, this time in relation to the palaeoenvironmental data discussed in chapter 2 and within the comparative template offered from the results of the agent-based simulation (chapters 6-7). This will answer the last research question, offering at the same time grounds for a discussion of the wider implications of this thesis. Chapter 9 will then summarise the main outputs of the work, and highlight its limitations and future perspectives.

Figures and tables, along with four appendices, will be provided on a separate volume. Appendix A will provide the spatial data-set used for the analysis of the two case study areas; appendix B will offer a technical summary of the agent-based model; appendix C will present the computer code of the simulation; appendix D will provide the entire set of graphics from the simulation outputs.

Chapter 2

Jōmon Culture of Japan

Jōmon culture has been regarded as " [...] the best researched complex hunter-gatherer tradition known to archaeology [...] " (Rowley-Conwy 2001 : 59). There are at least two different sets of evidence that support this statement: 1) the amount of data collected by an astonishingly large number of emergency excavations; and 2) the availability of an unparalleled, fine-grained, pottery-based chronological sequence. While both provide an extraordinary quantitative and qualitative framework for the Jōmon archaeological record, the bias they introduce to the data should also be taken into account. The quantity of the available cultural resource management data presents unquestionably large figures (an average of over 8,500 excavations per year between 1990 and 2003; Okamura 2005a), but is also heavily correlated with modern urbanisation, and as such different parts of the archipelago are unevenly investigated, which results in a patchy quality of evidence. Similar problems can be observed for the pottery-based chronology. In some specific spatio-temporal contexts, recent increase in scientific dating techniques has allowed cross-dating to absolute chronological sequences, offering temporal resolutions at the sub-century level (e.g. Kobayashi 2004; see also table 3). However, in other regions, pottery studies have been less intense and only relative sequences with a coarse, millennium-scale matching to absolute dates are currently available. Despite such a fragmentary vision of the past, the amount of available data provides a sufficiently detailed description of many aspects of the Jōmon culture with

an overwhelming number of papers and books published since the end of the 19th century.

In a recent review paper, Richard Pearson (2007) stated that three aspects of the Jōmon culture are particularly relevant from a world-wide comparative perspective: 1) the early beginning and the long persistence of its main traits; 2) the early onset of sedentism; and 3) the development of an intensive management of plant resources with socio-economic traits similar to those expected for agricultural communities.

Perhaps one of the most intriguing aspects among those listed by Pearson is the extremely long duration of Jōmon patterns over time. In fact, if we accept the traditional chronology and mark its beginning with the adoption of pottery (ca 17th millennium cal BP; Kuzmin 2006), and its ending with the spread of farming and metallurgy from mainland Asia (early 3rd millennium cal BP; Harunari *et al.* 2003), the entire temporal length of the Jōmon period will be over 10,000 years.

Labelling such an extremely long length of time with a single name should not lead to an unquestioned assumption of a homogenous culture. As a matter of fact, although most defining traits (e.g. use of pottery, subsistence orientation, level of sedentism, etc.) can be regarded as constant, several authors acknowledge a substantial diversity over space and time. From a purely temporal perspective, alternatives to the traditional periodisation in six stages (Incipient, Initial, Early, Middle, Late, and Final Jōmon, see section 2.2.1) have been proposed by scholars who acknowledged such an internal diversity within the 10,000 years timespan. Sasaki (2010) has recently reviewed and compared 17 of these and noticed that most authors seem to agree in drawing a threshold between Initial and Early Jōmon period and a few others between the Middle and Late Jōmon periods. The former is due to the lack of some typical Jōmon features during the Incipient and Initial stages, such as the high degree of sedentism and large population sizes (but see Pearson 2006). Imamura (2002), for example, defines the Incipient Jōmon as "Palaeolithic with a pottery tradition", and the Initial Jōmon as "Mesolithic", before binding the remnant stages under the label of "Arboreal Neolithic". The latter

threshold (between Middle and Late Jōmon periods) is mainly linked to the possibly largest population decline observed during the Jōmon period, which occurred towards the end of the Middle Jōmon stage in many parts of Japan (see section 2.2.3). Several authors suggest that the cultural response that occurred in the aftermath of such a large-scale phenomenon generated a radically different society. Sasaki (2000, 2010) labels the interval between the second half of Early Jōmon and the second half of Middle Jōmon as the "development stage" (*hatten-ki*), the end of the Middle Jōmon to the beginning of the Late Jōmon as the "transformation stage" (*henshitsu-ki*), and the second half of the Late Jōmon to the end of Final Jōmon as the "apex stage" (*ranjuku-ki*).

Imamura's use of the term "Arboreal *Neolithic*" should lead us to question how to contextualise the Jōmon culture within a worldwide comparative perspective. Many of its features (e.g. use of pottery, high degree of sedentism, large population density etc.) are generally considered as typical traits of Neolithic communities, but the substantial lack of agriculture (but see Crawford 2011, and section 2.2.2) and husbandry (but see section 2.2.2) has pushed several authors to dismiss such a label for the Jōmon. Others have instead proposed that the concept of "Neolithic" should be revised, pointing out that what happened in Japan was the development of "*another* Neolithic" (Nishida 2002).

The most common label associated with the Jōmon culture either gives emphasis to its socio-political and organisational traits (i.e. "complex hunter-gatherers" as in Price 1981, Rowley-Conwy 2001) or to the environmental richness of the Japanese archipelago (i.e. "affluent foragers" as in Koyama and Thomas 1981). Such nomenclature has been often applied in comparative studies with cultures such as the Baltic Mesolithic and Neolithic (see Price 1981, Aikens *et al.* 1986), the woodland culture in Northeast America (Aikens *et al.* 1986), and most notably the Pacific Northwest Coast and the Californian Indians (Aikens 1981, Cohen 1981, Aikens and Dumond 1986, Aikens *et al.* 1986, Watanabe 1992). The historic communities of the Northwest coast and California have also been used, along with the modern Ainu population of Hokkaidō (see Watanabe 1990), as the most common

ethnographic analogy for the Jōmon culture, due to comparable environmental settings (see Olson *et al.* 2001), the availability of similar resources (e.g. acorns and salmon, see Yamanouchi 1964), and the existence of several shared traits, including high population density, sedentism, and the presence of a prestige economy (Watanabe 1992). Perhaps the most common outcome of these comparative studies has been the (too often uncritical) claim (e.g. Watanabe 1990, Kobayashi 1992) that Jōmon culture exhibited high levels of "social complexity" (see section 2.2.5 for details) similar to those observed in these ethnographic groups.

This chapter will illustrate some of the main features of the Jōmon culture, relevant for the aims and the objectives of the thesis. I will sporadically refer to the Jōmon using the term "complex hunter-gatherer", despite the recent controversy on its definition (see section 2.2.5). While doing this, I acknowledge that using such a categorical definition is a dangerous exercise, especially when the term leads to the assumption of the existence (or not) of specific sets of traits. For example, the presence of agriculture is by definition quarantined from hunter-gatherer societies, but an increasing number of studies and discussions have questioned whether Jōmon communities practiced it or not (see section 2.2.2), with some undeniable evidence in support of the former argument. In this case the categorisation of Jōmon as "hunter-gatherers" might have played a role in limiting the acceptance of such a evidence. Nonetheless, the label "complex hunter-gatherers" helps by pointing to a broad combination of features; in this thesis the term will imply the predominance of a specific subsistence mode (without denying the existence of possible alternative strategies) in association with some traits (e.g. use of pottery, sedentism) usually linked to Neolithic and other later societies.

Section 2.1 will introduce the geographical and the environmental settings, with a brief review of the most recent and updated palaeoenvironmental reconstruction of the interval between ca 7000 and 3220 cal BP, which covers the temporal scope of this thesis. Section 2.2 will provide a detailed account of the main features of the Jōmon culture, by firstly introducing its chronological framework and then by focusing on certain aspects (e.g. subsistence, demography, and settle-

ment pattern) which are relevant to the research questions. The subsequent section (2.3) will offer an overview of the prehistory of the two case study areas (Chiba and Gunma), again looking at the interval between 7000 and 3220 cal BP. The last section (2.4) will then offer a retrospective on what explanations have been proposed so far about the major changes in demography, subsistence, and settlement patterning in the case study area. This will also provide a summary of the topics that have been introduced in the preceding sections and will help defining the methodological and the theoretical directions to be undertaken in the subsequent chapters.

2.1 Geographical Settings and Environment History

Geographical Settings

Japan is an archipelago composed of over 6,000 islands, with the four main islands (Hokkaidō, Honshū, Kyushū and Shikoku) representing ca 97% of its territory (fig. 1). The geographical setting of these islands can be summarised in three main features: 1) long latitudinal extent; 2) high diversity in elevation; and 3) narrow shape and distribution of the main islands. These three features result in a relatively high degree of environmental diversity, which suggests that the geographical and environmental setting of the Jōmon culture should not be viewed as homogenous despite its relatively small spatial extent.

The long latitudinal length of the Japanese islands (between the $20°25'$ and $45°31'$, over a distance of 2,400 km) is one of the main causes of its high diversity in temperature, with a maximum difference of ca 10 °C (the present-day annual mean temperature of Sapporo city in Hokkaido is 8.9 °C, in contrast to the 23.1 °C of Naha in Okinawa[1]; figure 2-b). The presence of high mountain ranges and volcanoes across the entire length of Honshū island (figure 2-c), combined to such a latitudinal extent promote a wide variety of climatic settings. Olson and colleagues

[1]Data retrieved from Japan Meteorological Agency (`http://www.data.jma.go.jp/obd/stats/data/en/normal/normal.html`).

(2001) place the Japanese archipelago in the *Palearctic zone* (with the exception of the Okinawa islands, identified as part of the *Indo-Malay ecoregion*), but identifies 7 ecoregions: 5 different types of *temperate broadleaf and mixed forests* and 2 different regions of *temperate conifer forests* (see figure 2-a). Figure 2 shows how diversity in the environmental settings are present in both north-south and east-west axes. While the former is mainly due to the difference in latitude, the latter is a combination of different factors, namely the high mountain range separating the effects derived by the oceanic currents from the Pacific (the *Oyashio* and the *Kuroshio* currents) and the climatic influence from mainland Asia. These two forces essentially split Honshū island between its western shores (*Nihonkai evergreen forest ecoregion*) and its eastern shores (*Taiheiyō evergreen forest ecoregion*) with a deciduous forest ecoregion in the middle.

The orographic nature of the Japanese archipelago, coupled with its distinctive shape, influence its hydrographical properties, characterised by a large number of small rivers with steep gradients and short length. The absence of large rivers (Shinano river is the longest with a length of 367 km, while Tone river has the highest drainage area of 16,840 km^2) has created very few plains, with the largest — the Kantō plain — occupying ca 17,000 km^2. The direct consequence of this combination of settings is that habitable zones in present-day Japan are relatively small and fragmented.

Environment History between 7000 and 3220 cal BP

Two key climatic shifts characterised the environmental history of the Japanese archipelago between 7000 and 3220 cal BP. The first one occurred at ca 5900 cal BP, at the end of the Early Jōmon period, and the second at ca 4500 cal BP, towards the end of the Middle Jōmon period (Kudo 2007). The relationship between these events and changes in archaeological patterns has been pointed out by several authors (e.g. Imamura 2002, Kudo 2007, Habu 2008, Crema 2012) and suggests how detailed analyses of the precise nature of these episodes are of primary interest for understanding the dynamics of the Jōmon period. The number of studies are

relatively rich in this regard, but most still rely on uncalibrated data, which heavily reduces the possibility to correlate these events with archaeologically observed patterns. The following paragraphs will summarise the few studies providing calibrated dates (see also figure 3), with a particular focus on the 4,000 year time-span between the Early and the Late Jōmon period.

Prior to the Early Jōmon (7000-5470 cal BP, see section 2.2.1), during the first few millennia after the onset of the Holocene, the entire archipelago was characterised by a relatively cool climate. Adhikari and colleagues' (2002) analysis of the diatoms at Lake Aoki (Chūbu area) points to a cooling stage between 8,800 and 8,350 cal BP, while Wang and colleagues (2005) have indicated, based on oxygen isotope records at Dongge Cave in southern China, the presence of weak Asian monsoon events between 8400 and 8000 cal BP. Both studies are correlated with the so-called 8.2 kyr event (Kobashi *et al.* 2007), or the Bond Event 5 (ca 8100 cal BP; Bond *et al.* 1997), when a sudden decrease of temperature has been recorded on a global scale. From a palynological perspective, this phase roughly corresponds to the second half of Tsukada's (1986) zone RI (10000 - 7000 ^{14}C BP; ca. 11500 - 7800 cal BP), characterised by a dominance of broadleaf deciduous forests.

Notable environmental events associated with the Early Jōmon period are the Holocene Climatic Optimum (HCO), the so-called Jōmon or Yūrakuchō Transgression, and the Akahoya eruption of the Kikai caldera (K-Ah). The first, also known as "hypsithermal" or "altithermal", refers to warming conditions which affected several regions in mid- and high-latitudes (Wanner *et al.* 2008); the second is a correlated event where the sea level rose and reached its Holocene maximum in the Japanese archipelago (Stewart 1982); while the effects derived from the third seems to be restricted to Kyūshū and southwest Japan (the volcano is located at about 200 km south of Kyūshū).

The impact of the HCO varied considerably, with different timings of its onset, duration, and magnitude (Renssen *et al.* 2009). The timing of its onset in Japan is still discussed with several conflicting pieces of evidence. Schone and colleagues' (2004) study on the intra-annual growth patterns and the oxygen isotope ratios of

Phacosoma japonicum clams suggests the presence of a warm climate at 6120-5590 cal BP, with evidence of cooler and dryer climate before (7390-6770 cal BP) and after (3869-3420 cal BP), while the diatoms of lake Aoki suggest a slightly earlier occurrence of the HCO, between 7250 and 6150 cal BP (phase HW4, Adhikari et al Adhikari *et al.* 2002).

The HCO determined major changes in flora, and marks the beginning of a new pollen zone in several studies. Tsukada (1986) describes the pollen zone RII (7,000-4,000 ^{14}C BP; ca. 7800 - 4500 cal BP) as being characterised by the expansion of *Cyclobalanopsis* and then of *Castanopsis* forests from southern to northern Japan, a trend that supports the claim of a general increase in temperature. Inoue and colleagues' (2012) pollen analysis at Soni Plateau in Kansai seems to support a more recent onset of the HCO (supporting the chronology suggested by Schone *et al.* 2004), with the pollen zone OKM-2 (6500-5500 cal BP) marked by species adapted to warmer climate (such as *Cyclobalanopsis* and *Castanea/Castanopsis*) than the previous OKM-1 (7500-6500 cal BP), characterised by deciduous broadleaf forests of *Lepidobalanus*, an indicator of cooler conditions.

The second major environmental change associated with this period is the increase of sea level, which reached its maximum of +2 to +6 meters above the current level in some parts of Japan (Habu 2004: 45). The exact timing of this marine transgression is controversial, although there seems to be an agreement that its onset was between the second half of the 8th and the end of the 7th millennium cal BP (7400-5900 cal BP, according to Habu 2004; 7300-6500 cal BP according to Ishikawa *et al.* 2009).

The third major event, the Akahoya eruption, occurred at ca 7300 cal BP (Kitagawa *et al.* 1995). Both archaeological evidence (Kuwahata 2002) and phytolith analysis (Sugiyama 2002) indicates a major impact on the flora of southern Japan, notably the temporary disappearance of lucidophyllous forests (e.g. *Castanopsis* and Lauraceae) for ca 600-900 years.

By the end of the Early Jōmon period, after the Jōmon Transgression and the HCO, several lines of evidence suggest a series of climatic changes and cooling

events. This period corresponds to the beginning of Kudo's (2007) stage VI (5900-4500 cal BP), and to the Bond Event 4 (ca 5900 cal BP; Bond *et al.* 1997), and evidence of a slight decrease in temperature has been recorded in several locations around the globe. At Lake Aoki, this period presents evidence of cooling (HC4; 6150-5250 cal BP), although several shorter intervals of warming have also been identified (Adhikari *et al.* 2002). Other proxies include a peak in the weak Asian monsoon events at ca 5500 cal BP (Wang *et al.* 2005), and a more general phase of rapid climatic change between 6000 and 5000 cal BP (Mayewski *et al.* 2004). While the temperature reduction of this phase did not cause major modification of the flora, the coastal areas saw a relatively rapid phase of marine regression between 5800 and 5200 *varve* years BP (Fukusawa *et al.* 1999).

The interval between the latter half of the 6th millennium cal BP and the first half of the subsequent millennium was characterised by relatively stable conditions. Sediments of Lake Aoki indicate a stable warmer stage between 5250 and 4000 cal BP (Adhikari *et al.* 2002), while marine biogenic production between 5900 and 4000 reached its peak near Sannai-Maruyama in northern Tōhoku (Kawahata *et al.* 2009).

This stable phase saw an abrupt end towards the second half of the 5th millennium cal BP. Several studies suggest that a rapid environmental change occurred during this period in correspondence to the Bond Event 3 (ca 4300 cal BP; Bond *et al.* 1997) and to the rapid climatic changes recorded at a global scale between 4200 and 3800 cal BP (Mayewski *et al.* 2004). Marine regression increased in intensity between 4500 and 3600 varve BP (Fukusawa *et al.* 1999) and weak Asian monsoon events have been recorded for the interval between 4500 and 4000 cal BP (Wang *et al.* 2005). Cooling has been suggested by shell samples from Tokyo Bay (dated between 4600 and 4400 cal BP; Miyaji *et al.* 2010) and the diatoms record at Lake Aoki (between 4000 and 3050 cal BP; Adhikari *et al.* 2002), while at Sannai-Maruyama a decreased biogenic productivity has been identified at ca 4100 cal BP (Kawahata *et al.* 2009).

While the previous Bond event did not lead to significant changes in the flora,

the mid-5th millennium cal BP event did cause some major transformations. Tsukada (1986) marks the beginning of the pollen zone RIII at 4000 ^{14}C BP (ca. 4500 cal BP), and describes this as characterised by a decline of laurilignosa forests and a rise and expansion of *Fagus*, both providing additional evidence of cooling. Kudo (2007) indicates how in Kantō a substitution of *Castanea crenata* with *Aesculus turbinata* took place along with an expansion of *Cryptomeria*. Similarly, at Sannai-maruyama this stage correspond to a return of broad-leaved deciduous forests after an interval characterised by groves of *Castanea* and *Juglans* which started at 5900 cal BP (Miyaji *et al.* 2010).

Finally, the 4th millennium cal BP was characterised by a period of relative stability (Kudo 2007), associated with a moderately cool climate (Adhikari *et al.* 2002, between 4000 and 3050 cal BP). However, some studies suggest the presence of rapid climatic changes during the second half of the millennium (3500-2500 cal BP, Mayewski *et al.* 2004), but these are in most cases outside the temporal scope of this thesis.

A graphical summary of the environmental history described in this section is shown on figure 3. While the presence of two major clusters of environmental change can be roughly identified in the interval between 7000 and 3220 cal BP, precise chronological definition of their occurrence is still difficult to determine. Nonetheless, figure 3 shows an alternation between intervals of relatively stable climatic conditions (7000-6100 cal BP; 5000-4600 cal BP) and episodes where concurrent changes in environment are recognised (6100-5000 cal BP, 4600-3220 cal BP).

2.2 Main Features of Jōmon Culture

2.2.1 Chronology and Chronometry

Pottery based relative chronology has been adopted as the main chronological framework of the Jōmon period (Imamura 2005), and despite the increasing avail-

ability of absolute dates it is still widely, and often exclusively, used by most Japanese scholars.

As mentioned earlier, the use of pottery itself marks the beginning of the Jōmon period, with the most recent studies suggesting its adoption towards the early 17th millennium cal BP (16800-15600 cal BP, Kuzmin 2006). Such an early beginning for the Jōmon period sparked an initial controversy amongst the Jōmon scholars, leading to a disbelief in scientific dating techniques during the 60s and the 70s (Keally 2004). The most notable example of this attitude is the "Natsushima shell-mound controversy", in which leading scholars such as Yamanouchi dismissed radiocarbon dating as "too old" (Yamanouchi and Sato 1962) on the basis of cross-comparisons with the archaeology of the mainland China. The attitude towards radiocarbon dating became even more conservative after this episode, leading to a shared belief that pottery-based chronometry was more efficient and precise, and with a complete dismissal of absolute dating for over 30 years (Keally 2004). The increasing recovery of Pleistocene pottery in Japan has slowly changed this picture, with a wider acceptance of the earlier beginning of the Jōmon period. Furthermore, comparisons with other calibrated dates of the earliest pottery in Far East Asia (Kuzmin 2006), has recently showed how the early emergence of pottery is far from unique to the Japanese archipelago, dismissing definitively Yamanouchi's thesis.

As mentioned in the beginning of this chapter, the internal subdivision of the Jōmon period is based on six distinct stages (Incipient, Initial, Early, Middle, Late and Final Jōmon periods). The start of the first stage and the end of the last one are defined by key cultural events (introduction of pottery on the hand and the adoption of rice and metallurgy on the other) while other internal subdivisions are exclusively based on the pottery-based chronological sequences.

The creation, development, and continuous update of such a chronological framework have been traditionally the primary concern of Jōmon archaeology. The number of different pottery phases are extremely large (the total number is approaching, and likely going to exceed, two hundred units; Imamura 2005) and continuously refined by new subdivisions in subphases. When cross-dating to ab-

solute sequences is possible, the chronological resolution of these sub-phases can sometimes be below the threshold of 50 years (e.g. as in Kobayashi 2004); a temporal framework unavailable for other prehistoric hunter-gatherer cultures.

Imamura (2005) identifies three core reasons why this development was possible: 1) the extremely large number of emergency excavations providing a rich archaeological record; 2) the high variety of decorative traits in Jōmon pottery; and 3) the long-lasting and abundant use of pottery for over 10,000 years. Traditional methods for the creation of pottery sequences rely primarily on the study of stratigraphic relationships of the contexts where diagnostic potsherds have been recovered. In most cases, these studies have been focused on shell-midden layers, with occasional but increasing reliance on the filling deposit of abandoned pithouses. Other methods, including seriation, have been rarely applied and the already-mentioned reluctance in adopting scientific methods (e.g. radiocarbon dating, thermoluminescence, etc.) has restricted the range of options and the development of absolute chronological sequences. The rare presence of radiocarbon dates from excavation reports (with the few exceptions often confined to uncalibrated dates) and the fact that chronological references in the literature are in most cases restricted to pottery phases, provide evidence of the most common attitude towards time and chronometry.

The floating relative chronology of the Jōmon pottery sequence has clear limits, with the most notable ones being:

- Reduced capabilities for comparative analysis with datasets based on different systems of dating. This includes climatic and environmental data, but also large-scale comparison of archaeological records based on different dating materials and different relative chronological sequences.

- Reduced spatial extent where the same pottery sequence can be applied. Large-scale analysis have to rely on cross-dating between relative chronological sequences, and its precision will most likely be negatively correlated with the spatial scale of observation.

- The unknown absolute duration of the actual phases, leading cross-temporal comparative analysis to be potentially biased.

The awareness of such limits has recently pushed a number of authors to "calibrate" the relative pottery-based chronological sequence with absolute dating derived from scientific methods. Early attempts were proposed by Tsuji (1999), who successfully matched the pottery sequence of the Sannai-Maruyama site in northern Japan to an absolute chronological framework.

More recently, Kobayashi (2008) proposed a detailed pottery sequence of the entire Jōmon period for central Japan, using a dataset based on a calibrated series of 680 AMS radiocarbon dates. These had been obtained from carbonised organic materials found in many Jōmon pottery and has been cross-matched to the existing relative sequences [2]. The result has highlighted a mismatch with the absolute chronology adopted in earlier studies, suggesting a substantial difference in the timing of key archaeological events (e.g. fig.1 and fig.7 in Crema 2012).

The chronological sequence used in the current study will be based on this work (see table 1 for the major pottery phases between Early and Late Jōmon period), with some updates and revisions for the relative sequences of the Early (table 2) and the Middle Jōmon (table 3) periods. These updates are mainly due to the presence of two slightly different sequences between the two case study regions (Chiba and Gunma) and by the fact that Kobayashi's sequence is primarily focused on the pottery assemblages from southwestern Kantō.

For the Early Jōmon period (table 2), the Gunma sequence conforms with the one used in southwest Kantō, while Chiba has its own sequence, with *Futatsuki* phase parallel to *Sekiyama I* (Ogawa 1996a), *Ario* to *Kurohama* (Mikami 1996), and *Morosio* to *Ukishima* (Ogawa 1996c) and *Okitsu* phases (Ogawa 1996b). Kobayashi does not provide an absolute chronological relationship between *Hanazumi Kasō*

[2]Notice that Kobayashi defined the absolute start and end date of each pottery phase by examining the overlap of calibrated probability distributions of radiocarbon dates from organic remains associated with diagnostic potsherds. A more robust approach (capable of computing the uncertainty associated with the start and the end date of each phase) would have been the use of Bayesian inference (see for instance Buck *et al.* 1992, Ziedler *et al.* 1998)

and *Sekiyama*, thus for the present work the two phases has been combined together, with a start date at 7000 cal BP and an end date at 6450 cal BP.

The revision of the Middle Jōmon sequence is slightly more complex, with at least four parallel sequences identifiable from the pottery assemblage recovered in the two case studies. Kobayashi offers a detailed account of the matching between the so-called *Shinchihei* sequence (Kobayashi 2004) and other major pottery sequences in the Kantō region (see table 3). This can be further updated by the works of Ouchi (2008) for the *Kasori E* phases, and of Tozawa (1996) for the *Yakemachi* phases, while the local *Miharada* pottery of Gunma appears to have been used from the *Yakemachi* phase to the end of *Kasori EI* phase (Ishizaka S., *personal communication*). The Late Jōmon cross-dating proposed by Kobayashi has instead been left unchanged, and is applicable for both case studies.

2.2.2 Subsistence Pattern

Subsistence studies have been traditionally the second most common topic within Jōmon archaeology. Despite such a strong interest, most works have been strongly affected by the poor preservation of human and animal remains, due to the highly acid soil of volcanic origins (Imamura 1996), and by the infrequent use of flotation and wet-sieving (Crawford 1983, Matsui 1996). These limits restricted archaeological interpretations to particular types of sites where the level of preservation is generally higher (e.g. water-logged sites and shell-middens) and produced sampling biases towards remains with higher archaeological visibility (e.g. larger mast seeds rather than smaller plant seeds). However, the increasing awareness of such biases, the availability of new methods (e.g. isotope analysis), the wider adoption of existing ones (e.g. flotation), and the generally higher number of emergency excavations, have enhanced the understanding of Jōmon subsistence during the last few decades.

Land mammals

The two most common faunal remains in Jōmon sites are the *Sika* deer (*Cervus nippon*) and the wild boar (*Sus scrofa*). A study conducted by Nishimoto (1991) on 60 Incipient to Final Jōmon sites has shown that these two species represent about the 68% of the total sample (37% for the wild boar, and 31% for the sika deer). The remnant 30% are generally composed by smaller animals, usually racoons (*Nyctereutes procyonoides*), monkeys (*Macaca fuscata*) and hares (*Lepus brachyurus*). Occasionally, the proportion of these smaller mammals can be slightly higher (Nishimoto 1995, Ito 1999) but the general dominance of deer and boar is the most commonly observed pattern. Dogs (*Canis lupus*) are also extensively recovered from Jōmon sites, often from burial contexts, and were likely domesticated and used to support hunting activities rather than being consumed (Nishimoto 1983).

Indirect evidence of hunting is supported by the presence of arrowheads and scrapers (Suzuki 1982; 1991) and by numerous remains of pit traps (Imamura 1983; 1996, Sato 2005). The latter suggests different types of strategies, ranging from communal "drive-hunting" where prey are chased and driven towards locations where the pits are located, to "trap-hunting", where hunters wait for prey to fall inside hidden pits. The two types of hunting systems (potentially identifiable by the location, distribution, and the structural properties of the pits; Sato 2005) suggest the existence of different types of subsistence organisation, and possibly indicate some form of territoriality linked to the allocation and maintenance of the traps.

Remains of wild boar have often been associated with some form of intensive management resembling husbandry. The claim has been proposed by Nishimoto (2003), and has only been supported by indirect evidence such as burials with dogs, the presence of boar figurines, and the recovery of remains in geographic locations (such as Hokkaidō) where wild boar did not naturally exist (indicating possible transportation by humans). Recent works by Hongo and colleagues (2007) on the metrical analysis of bone remains and evaluation of kill-off patterns do not support such a hypothesis, although local diversity should also be taken into account (Dobney *et al.* 2007) before any conclusive statement is made.

Aquatic resources

Soil acidity also affects aquatic resources from riverine and maritime environments. The presence of fish bones is in fact almost exclusively confined to shell middens, providing a biased vision of aquatic subsistence activities towards coastal environments, and heavily reducing our ability to evaluate the impact of inland riverine fisheries.

Traditionally, Japanese archaeologists considered salmon (anadromous salmonids of the genus *Oncorynchus*) as a staple resource of the Jōmon culture. This notion forms the basis of the "salmon/acorn hypothesis", suggested by Kazuo Yamanouchi (Yamanouchi 1964; see Matsui 1996 for a detailed review). The central idea of the hypothesis is that several hard mast species (including different types of acorns, horse chestnuts, chestnuts, and walnuts) and salmons were the two main staple resources during the Jōmon period, and that the higher natural abundance of the latter in cooler environments explains the higher number of sites recovered in northeast Japan. However, despite the availability of an increasingly large archaeological record in northern Japan, the presence of salmonids remains are still relatively poor. This could be the result of the way these fish were dried and stored, the weak preservation level of their bones, or the way they were consumed. Matsui's (1996) extensive study proved that with careful attention to the recovery methods (e.g. by adopting wet-sieving), a much larger quantity of salmon remains could be recovered. Nevertheless, the adoption of these methods along with the excavation of waterlogged sites have not, so far, provided sufficient evidence to support Yamanouchi's hypothesis (Habu 2004).

Other species of fish have been recovered in coastal areas, although specific details are locally variable. Broadly speaking in northern Japan the dominant species are herrings (*Clupea pallasii*), rockfishes (*Sebastiscus marmoratus*), greenlings (*Pleurogrammus azonus*) and flatfishes (*Pleuronectidae*), while in central-southern Japan sea bream (*Sparidae*), sea bass (*Lateolabrax*), blowfish (*Tetraodontidae*), sardines (*Clupeoidei*), mackerels (*Scombridae*) and *Caranginae* are most commonly found (Toizumi 2005).

Evidence of fishing is also supported by the presence of a rich variety of tools. Unfortunately, many of these instruments were made of bones and hence are subject to the same preservation issues affecting animal remains. Despite this, Watanabe (1973) provided an extensive review and showed that Jōmon people used different types of fish-hooks and harpoons, and practiced some form of net-fishing, as suggested by the recovery of net-sinkers made from pebbles and reused potsherds.

Archaeologically, the most prominent aquatic resources are undoubtedly fresh and seawater shellfish, which are often recovered in large shell-mounds (Habu *et al.* 2011). Over 3,000 shell-middens have been identified throughout the Japanese archipelago, with the highest concentration in the Kantō region, where about half of them are located on the shores of Tokyo bay and at the mouth of the Tone River (Suzuki 1989, Horikoshi 1992). The majority of these shell-middens are composed of seawater species from different coastal environments, ranging from sandy inter-tidal zones to rocky beaches (Matsushima 1982). In Kantō, the dominant species of molluscs are *Umbonium moniliferum*, *Meterix lusoria* and *Corbicula* sp., although their relative proportion varies considerably depending on their local habitats along the Tokyo bay and the Tone River estuary (see fig. 9 in Toizumi 1999b).

From a nutritional point of view, much debate has focused on whether shellfish were a dominant staple or a secondary additional resource. Suzuki (1986) provided a volumetric analysis of the shell deposits approximating the daily caloric and protein consumption of three different shell-middens in Kantō, taking in account different hypothesis of occupation length and population sizes. The outcome showed how large shell-mounds are likely the product of continuous occupation (rather than a single extensive exploitation of shellfish) and that shellfish provided a small caloric impact opposed to a fairly good protein contribution. Suzuki's analysis should be considered with care if we take into account the updated information on pottery phase duration, but nonetheless provides a rough impression of the possible dietary impact of shellfish. Habu (2004) also indicates how non-residential shell mounds have been increasingly recovered, indicating how the analysis of the

nutritional contribution should not be restricted only to these residential sites.

The consumption rate of shellfish varied considerably over time, most likely in correlation with marine regression events (Toizumi 1999b). In general terms, episodes of strong regression are in fact associated with an abrupt reduction in shell-middens, while their increase seems to be associated with stages of relative stasis in the sea-level fluctuations. Regression events usually tend to reduce or shift the extent of inter-tidal zones, where optimal habitats for shell beds are present. Toizumi (1999b) acknowledges that the fluctuation of shell midden size and number are not just a function of these regression events, noticing how these correlate with broad population dynamics occurring at inland locations as well. Collecting pressure of seashell seems to have varied through time as well, occasionally indicating episodes of overexploitation (Koike 1992b).

Plant resources

According to several scholars, the exploitation of plant resources was a key element in the Jōmon subsistence system. Imamura (2002) defines most of the Jōmon period as "Arboreal Neolithic", while Nishida (2002) points out how plant exploitation and silviculture facilitated the emergence of socio-economic properties similar to those observed in early farming groups. The possible domestication, or at least some form of controlled management of masts and other plants, has also induced several scholars to suggest that the dualism "hunter-gatherers vs. agriculturalists" (see also Smith 2001, Terrell *et al.* 2003) should be discarded for a better understanding of the Jōmon culture (Crawford 2008).

The high impact of plant resources has been widely acknowledged since Yamanouchi's "salmon-acorn hypothesis", and is further supported by different types of evidence. Koyama (1996) analysed the late 19th century historical census from northern Gifu (Chūbu region) and noticed how in some villages the caloric contribution of mast trees were over 75%, and a single week of work by the members of the whole village was sufficient to obtain the necessary yield of nuts. Such ethnographic comparison led Koyama to conclude that a plant-based subsistence could

easily sustain Jōmon economy, even when the population density was comparatively high.

Chestnut (*Castanea crenata*) and Japanese horse chestnut (*Aesculus Turbinata*) were the dominant mast species (Kitagawa and Yasuda 2008), followed by minor quantities of walnuts (*Juglans*), and different types of acorns, including *Quercus Lepidobalanus*, *Quercus Cyclobalanopsis* and Castanopsis (Kokawa 1983). Some of these required different forms of processing in order to make the mast edible, from simple soaking in water to multiple soakings, boiling, and mixing with ash (see Watanabe 1975, Takahashi and Hosoya 2002).

One of the most intriguing and debated hypotheses of Jōmon subsistence is whether plant species were actively managed and whether this caused social, cultural, and economic implications similar to those observed in agricultural communities. Nishida (1983) was one of the first scholars to engage with this topic by analysing modern rural villages and their local environments. He noticed that these villages were surrounded by thin buffers of "secondary" forests composed by deciduous trees, a considerably different flora from the one observed in the background environment, characterised instead by primary evergreen forests. These secondary forests can be regarded as anthropogenic environments capable of modifying the selective pressure of certain species, ultimately leading to a higher concentration of edible plants[3]. Nishida suggested that similar processes might have occurred during Jōmon period, since only a minor effort in plant management and a relatively high level of sedentism are required to create these artificial environments.

Some palynological studies have focused on assessing whether these symbiotic relationships between humans and local plant species existed during the Jōmon period. Minaki (1994) examined chestnut remains recovered at Sannai-mauryama site in the Tōhoku region, and concluded that observed growth in the mast size over time is evidence of domestication. About a decade later, Sato and colleagues

[3]These active management of plant resources have been recently reviewed from the perspective of niche construction theory (Odling-Smee *et al.* 2003) by Bleed and Matsui (2010, see also Smith 2011)

(Sato *et al.* 2003) supported Minaki's conclusion through the DNA analysis of chestnut samples recovered from the same site. On the other hand, Chino (1991) examined the palynological data from eight different sites concluding that while the existence of a modified plant composition can be supported, this was much smaller than the extensive secondary forests of later historical periods.

Plant remains recovered at Sannai-maruyama have been further analysed by different scholars. Kitagawa and Yasuda (2004, 2008) have pointed out how chestnuts were predominant in warm phases while Japanese horse chestnuts were dominant in colder climatic stages. This is explained by the higher susceptibility to disease of the former during episodes of colder climate, which could also explain the switch to *Aesculus* despite the higher costs required for their processing. The alternation between the adoption of *Castanea* and *Aesculus* in relation to climatic changes is not necessarily visible in other sites, and recent data seems to provide evidence that local contingencies played a crucial role in generating different histories of nut exploitation (Kudo *et al.* 2007, Kitagawa and Yasuda 2008).

Other species of plants have also been recovered, including barnyard grass (*Echinochloa crus-galli*), yams (*Dioscorea japonica*), bottle gourds (*Lagenaria siceraria*), and different species of beans such as adzuki (*Vigna*) and soy (*Glycine*). Detailed analysis at different sites from northern Japan is increasingly suggestive of the idea that Jōmon food production should be regarded as an early form of agriculture (Crawford 2008). Nevertheless, despite an increasing awareness of a more active role of Jōmon communities as niche constructors (Bleed and Matsui 2010, Crawford 2011), implications of these plant species are generally not considered as dominant as those of mast-bearing species.

The widespread presence of storage pits in the archaeological record is undoubtedly the archaeologically most visible (although indirect) evidence of plant exploitation in Jōmon economy. In some cases the contents of these pits have also been recovered, showing how different species of masts (acorns, walnuts, buckeyes) were stored with layers of leaves, wood fragments, and clay (Habu 2004: 64-67). The consequence of this storage economy has been widely discussed in the

hunter-gatherer literature (Testart 1982, Rowley-Conwy and Zvelebil 1989) and is one of the key arguments presented in support of the high levels of sedentism in Jōmon communities. Sakaguchi (2009) recently reviewed the spatial and temporal variability of the Jōmon storage economy, showing that, in northern and eastern Japan, the average volume of storage pits increased from the latter half of Early Jōmon period till the Late Jōmon period, when a decline started to become evident.

Subsistence Diversity over Time and Space

Akazawa (1986) was one of the first scholars to address the spatial diversity of Jōmon subsistence by examining different assemblages of procurement tools from 200 different Late Jōmon sites. The results of his quantitative analysis showed a substantial diversity between four different macro-regions (western Japan, inland and coastal areas of Sea of Japan, coastal areas of Tōkai and Kantō, and the coastal areas of Tōhoku and Hokkaidō). More recently, stable nitrogen and carbon isotope analysis of human remains (Minagawa and Akazawa 1992, Yoneda 2010) has showed further evidence of diversity across space, with higher protein dependency from large marine animals in northern Japan, a C3 plants/land mammals orientation in southern Japan, and a mixed subsistence (meat, shellfish and fish) in central Japan. Kaneko and colleagues (1982) approached the same problem by examining the regional distribution of faunal remains. They identified four macro-regions (northern Hokkaidō; Tōhoku and southern Hokkaidō; Kantō and Chūbu; Kansai, Chūgoku, Kyūshū and Shikoku) and subdivided each into a hierarchy of zones, with a total of over 50 different subsistence areas.

Differences in subsistence at smaller spatial scales have been approached by analysing other indirect evidence. For example, Imamura (1999a) identified a clear east-west boundary in Kantō, separating the distribution of sites associated with high number of storage pits from those where large quantities of chipped ground axes (a possible indicator for the exploitation of wild yams) were recovered. Similar studies have been conducted for lithic assemblages, which showed how differ-

ent prefectures in the same Kantō region showed different proportions of arrowheads, chipped ground axes, and grinding stones (Nishino 1999).

Fewer studies of temporal change in subsistence strategy are present in the literature. Notable exceptions include the already mentioned alternation between chestnuts and horse chestnuts, the fluctuation in shell exploitation, and several studies confined to relatively short intervals or focused on the occupational history of individual sites. One of the few authors who recognised the existence of a global trend was Imamura (1992), who claimed that towards the end of the Early Jōmon period (*Moroiso c - Jūsanbodai* phase, see table 1), the Kantō region showed a marked increase in arrowheads suggesting a transition from a plant-based subsistence to a game-based one. More recently, Imamura (1999a) noted how the Jōmon period was possibly characterised by major subsistence shifts between hunting oriented phases (e.g. end of Early Jōmon and Final Jōmon periods) and plant-gathering oriented phases (e.g. Middle Jōmon period) which were in turn correlated with major changes in population density (see also section 2.4).

2.2.3 Population Size

Estimates of Jōmon population size sparked interest from the 60s with the works of Serizawa (1960) and Yamanouchi (1964). Both scholars derived their calculations from ethnographic comparisons, the former with the Ainu of Hokkaidō and the latter with the Californian Indians, and produced different estimates ranging from 120,000 to 300,000 individuals. Their conclusion ignored spatial variation in population density, did not contemplate possible fluctuations during the Jōmon period, and their justifications for the choice of the ethnographic analogy were heavily affected by a strong degree of environmental determinism (Imamura 2010).

Shūzō Koyama (1978, Koyama and Sugito 1984) undertook a more exhaustive work that solved many of these issues and resulting in a detailed estimate of the population density of nine regions of the Japanese archipelago (Tōhoku, Kantō, Hokuriku, Tōkai, Kansai, Chūgoku, Shikoku, Kyūshū, see fig.1 during all the major Jōmon periods excluding the Incipient stage. The method used by Koyama

[4] has been criticised by several authors (e.g. Imamura 1997, 2010, Habu 2004), due to some of its underlying assumptions, including a constant and high degree of sedentism, an uniform settlement size distribution, and a fixed size ratio of 1/7 to Haji period (250 to 1,250 AD) settlements. All assumptions are weakly supported and sometimes have been contradicted by archaeological evidence (see section 2.2.4). Nonetheless, Koyama's analysis offers a general overview of Jōmon population dynamics that is still used by some scholars (e.g. Okamura 2005b), and, despite the above-mentioned problems, three points are particularly relevant and worth mentioning here:

- Population size was variable over time.
- Population size was variable over space, with northern regions being characterised by a generally higher density.
- Population dynamics were spatially diverse, with eastern Japan (Tōhoku, Kantō, Hokuriku and Tōkai) characterised by a population peak at the Middle Jōmon, followed by a decline during the Late Jōmon, and western Japan (Kinki, Chūgoku, Shikoku and Kyūshū) by a population increase during the same Late Jōmon period.

Koyama's analysis thus appears to show how population dynamics were profoundly variable, with different absolute values and even opposing dynamics over time. Typically these diversities are explained by differences in subsistence strategies and local environments (e.g. the spatial distribution of deciduous broadleaf

[4] Koyama's method was based on the following equation:

$$P_t = \frac{J_t P_h}{kH}$$

where P is the population estimate, t is an index value referring to the specific Jōmon period (e.g. Initial Jōmon = 1, Early Jōmon =2 etc), and J_t is the total number of Jōmon sites dated to t. Koyama then derived the population estimate of eighth century AD (P_h) from historically recorded data on rice production, and two constants: k, which is the reciprocal of the ratio between a Jōmon settlement and a Haji settlement (20 for Initial Jōmon, 7 for the other periods); and H, the total number of Haji sites. Notice that the parameters varies between different regions, and that the equation integrates the effects derived by the different intensity in the archaeological research by assuming that the discovery rate of Jōmon and Haji sites were roughly equal.

forest zone, see Imamura 1996 for discussions), although many of these claims remains untested (but see Koyama and Sugito 1984 for a tentative approach based on numerical simulation).

More recently, some authors have offered finer grained studies on Jōmon population dynamics. These usually have smaller study regions, and sometimes shorter temporal spans, but nonetheless follow the general trend proposed by Koyama, depicting at the same time previously unseen patterns. Imamura's (1997) work on parts of Chūbu and Kantō region was undoubtedly one of the most exhaustive examples in this regard. The dataset (originally collected by Suzuki in the mid-eighties and recently republished in Suzuki 2006) consisted of over 12,000 pithouses dated between Incipient and Final Jōmon periods, with varying degrees of chronological resolution expressed in relative pottery-phase terms. The method used by Imamura for handling temporal uncertainty was questionable (see Crema 2012) and the absolute chronological sequence proposed by Kobayashi (2008) was unavailable at the time. Nevertheless Imamura identified several episodes of fluctuations in the number of pithouses, confirming also the peak and decline between Middle and Late Jōmon periods observed previously by Koyama.

A recent re-examination of the same dataset (Crema 2012), where the problem of temporal uncertainty has been approached quantitatively, and Kobayashi's (2008) absolute chronological sequence has been adopted, offered a quantitative assessment of these patterns. The results, based on the analyses of the rate of change in pithouse counts have highlighted the following points:

1. a substantial decrease in pithouse count towards the end of the Early Jōmon (from 6,000 to 5,600 cal BP);

2. a significant increase observed at the beginning of the Middle Jōmon period (ca 5,400 cal BP);

3. a fluctuation of pithouse count during the first part of the 5^{th} millennium cal BP

4. a sudden decrease in pithouse count at ca 4,500 cal BP;

5. a much less significant decrease in pithouse count towards the end of the 5^{th} millennium cal BP.

At a smaller spatio-temporal scale, but with a refined chronological resolution, Kobayashi (2004) assessed the population dynamics of the Musashino tableland in Tokyo using the *Shinchihei* chronological sequence and deriving population size from estimates of settlement sizes [5]. The results confirmed again the peak observed during the Middle Jōmon period, and showed that high population density was maintained for a couple of centuries (instead of a single spark as described by Imamura) before a sudden drop occurring sometime between 4,590 and 4,520 cal BP.

While these data support Koyama's results for the Middle to Late Jōmon transition, there is less information available for the possible smaller peaks of the Early and Late Jōmon periods, with the exception of some hints provided by Imamura (1997) and the re-analysis of his data (Crema 2012). Habu's (1988) study on the settlement pattern of western Kantō provides a quantitative account of the possible population dynamics during the Early Jōmon period. Habu examined the number of pithouses of the *Moroiso* phases (6050-5600 cal BP, Kobayashi 2008), which were subdivided in 6 subphases (two phases for *Moroiso a*, three for *Moroiso b*, and *Moroiso c* left unchanged). This showed that the peak was reached at the first subphase of *Moroiso b* (78 pithouses), followed by a constant decline (46 and 15 for the latter *Moroiso b* phases and 4 for *Moroiso c*). In later works Habu (2001, 2002) extended the sample size (including also parts of Chūbu region), but provided only the total number of sites, rather than pithouses, using a coarser resolution based on the traditional three sub-phase subdivision of the *Moroiso* phase. The Early Jōmon decline was nonetheless confirmed with a peak during *Moroiso b* (631 sites in southwest Kantō), followed by a decrease in the number of sites during *Moroiso c* (278 sites).

[5] Kobayashi (Tsumura *et al.* 2002a, Kobayashi 2004) obtained his population estimates assuming that a single pithouse was inhabited on average by five individuals. Then he classified Jōmon settlements in three classes (large, medium, and small), and associated each with a rough estimate of the number of concurrent pithouses (20,10, and 3). Finally, for each pottery phases he computed the number of settlements of each class, and then calculated his population estimate from this.

Other regions of the archipelago have been investigated to a much lesser degree. Northern Tōhoku appears to show population dynamics similar to those observed in Central Japan (Suzuki 2010a), although quantitative evidence of this is restricted to the analyses of individual sites (e.g. Habu 2008) or shorter time-spans (e.g. Tsumura 2002). Seguchi (2009, 2010) has recently assessed the population dynamics of Kansai, using both settlement counts and the total sum of pithouse areas. The chronological subdivision of Seguchi's analysis is, however, based entirely on the relative pottery chronology (with each of the five major periods divided in three sub-periods, e.g. early Early Jōmon, middle Early Jōmon and late Early Jōmon) with no reference to absolute dates. Nevertheless, the updated dataset confirms the pattern depicted earlier by Koyama (1978), showing a rapid increase in both settlement numbers and total residential area between middle Middle Jōmon and late Middle Jōmon, with a marked decrease between middle Late Jōmon and late Late Jōmon. If the broad correlation of the pottery sequences between Kantō and Kansai were correct, the decreasing population dynamics observed in Kantō would be matched by an opposite trend in Kansai.

2.2.4 Settlement Patterns

One of the primary characteristics of Jōmon archaeology is the large record retrieved from rescue projects and the extensive nature of these excavations. A look at most publications and reports show how entire plans of settlements are uncovered (see for instance Suzuki and Suzuki 2010), often with an extent of several hectares. Both these properties, along with the fine-grained pottery-based chronology, offer an unmatched data-set for the study of complex hunter-gatherer settlement patterns.

At the smallest spatial scales, CRM excavations have highlighted the spatial disposition of residential units along with other features, including burials, storage pits, and large postholes of raised-floor structures. Early studies by Wajima (1948, 1958, see Habu 2004) have already focused on the presence of the so-called *kanjōshūraku* ("annular-layout settlements"), settlements characterised by the pres-

ence of a central plaza surrounded by a large number of residential units (sometimes reaching several hundred units) and other features including storage pits and graves. The central space is either left empty as in the case of Nanbori Shell Midden in Kanagawa Prefecture (Wajima and Okamoto 1958) and the Kusagari-shell midden in Chiba Prefecture (Suzuki 2010b), or occupied by burial pits such as in the Nishida site in Iwate prefecture (Habu 2004). Wajima suggested that such a spatial organisation was shaped by the presence of a "social rule", implying the contemporary occupation of the residential units. While some form of planning must have occurred, Wajima's hypothesis of a single occupation has been rejected, as pithouses were dated to different pottery phases.

Current debates in the literature seem to be separated into two opposing views. On one hand, several authors have argued that these sites were indeed large in their size and presented, at least at some moment in time, an annular layout (Taniguchi 2005). On the other, these spatial configurations are regarded as the result of repeated multiple occupations (Nishida 1989, Kuroo 2009, Seguchi 2009). These two divergent hypotheses form the core of further questions related to the size of Jōmon settlements, the type of spatial interaction determining the annular layout (between co-residents or between residents and remains of previously occupied pithouses), and ultimately the relationship between different sites.

Taniguchi (2005) conducted the most extensive work on *kanjōshūraku* and identified two spatial properties, which he labelled "ring structure" (*jūtaikouzō*) and "sector structure" (*bunsetsukouzō*). The former refers to the spatial allocation of different "types" of features (e.g. burial pits, storage pits, etc.) along a series of rings with the same centre (located in the middle of the central plaza) but with different radii. For example, at the Nishida site in the Tōhoku region, the central plaza is surrounded by an annulus of burial pits, then by an annulus of raised-floor structures with a larger radius, and finally by pithouses and storage pits. Taniguchi suggested four typologies of concentric structures (*Katsuzaka*-type, *Nishida*-type, *Shimousa*-type and *Uetsu*-type), defined by the presence/absence of long-houses, features in the central plaza, and the location of residential units in relation to

storage and burial pits. While the "ring structure" is a common characteristic of almost all *kanjōshūraku*, the "sector structure" is less evident and its evaluation is often based on subjective impressions, in most cases without the support of any quantitative analysis. This property can be identified by the presence of two or more spatial clusters of features, sometimes with similarities in the shape of the pithouse plan, the type of hearth, or even the decorative styles of recovered potsherds (Taniguchi 2002).

Taniguchi (2002, 2005) compared these settlements with some ethnographic cases and deduced that these two properties might be the physical manifestation of the underlying social structure. As a typical example, he mentioned the case of the Bororo hunter-gatherers of western Brazil, who constructed annular layout settlements with two main sectors and further sub-sectors based on the kin relationship between different households.

The analysis of the spatial structure of *kanjōshūraku* presented so far clearly assumes that a relatively large number of residential units were occupied at the same time. However, scholars who support the alternative viewpoint provide evidence which shows how these large settlements might have been purely a product of continuous re-occupations of a very few number of residential units (Doi 1991). If so, the annular pattern might perhaps be the continuous application of simple rules in the choice of residential location (e.g. the avoidance of the central plaza), which would also indicate that some form of cultural continuity might have existed between multiple episodes of occupation (see also Nishida 1989).

Habu (1988) was one of the first scholars who quantitatively tried to assess this alternative scenario by examining the pithouses of 51 sites in western Kantō. Habu's approach consisted of subdividing the time-span of analysis (the *Moroiso a* and *b* phases) in multiple sub-stages and for each counting the number of features minus the number of instances where pithouses were overlapping. The results of Habu's analysis showed that: 1) even the largest sites were considerably smaller than previously thought, with a maximum of 8-10 units; and that 2) these large settlements represent an extremely small proportion of the sites. Habu's analysis

thus supported the view that, in many cases, large-scale settlements were likely the product of repeated occupation, but at the same time showed how these settlements are nonetheless dominant if compared to other contemporary residential sites.

The biggest problem with Habu's analysis was the exclusive adoption of pottery-based chronology, which did not allow to take into account possible differences in the duration of the phases. This led Habu and other scholars to question whether the largest settlements were actually representing a contemporary occupation or not. For example, Suzuki (1996) analysed the pithouses recovered at Kidosaku site, a large *kanjōshūraku* in Chiba, using both the pottery-based chronology and the stratigraphic relationships among overlapping features. The result suggested that the number of contemporary pithouses were extremely small and rejected the idea that site had an annular configuration at any given point in time.

More recently, Kobayashi (2004) attempted to overcome such a limited chronometric capacity by using the *Shinchihei* sequence (see table 3), and by integrating additional sources of knowledge based on the directional analysis of the pithouse entrance, the stratigraphic relationships among overlapping features, and the distributional analysis of artefacts. The outcome of his work provides one of the best insights on the nature of Jōmon settlements and a snapshot of what these sites may have looked like at a given moment in time. The most notable example is the study of the Oohashi site in Tokyo, a large settlement of over 100 residential units dated between phase 11c and 13a of the *Shinchihei* sequence (4750-4470 cal BP, see table 3). Kobayashi identified nine phases of occupation, based on the combination of the analysis listed above and a few additional radiocarbon dates. The results showed that for some phases (Kobayashi 2004: 195), the number of pithouses were over 10, supporting the view that settlements with ca 100 individuals might have existed, but at the same time fully rejecting the idea of extremely large settlements, providing an example of how repeated episodes of occupation can easily generate such an impression.

Habu's (1988) analysis of the Jōmon site size distribution shed also light on the

existence of smaller settlements and provides the empirical evidence that *kanjōshūraku* were not the "typical" residential sites. In fact, these large settlements were not only representing a small proportion of sites at a given point in time, but their existence was also intermittent and restricted only to central and northern Japan (Taniguchi 2005). *Kanjōshūraku* first appeared between the end of the Initial Jōmon and the early stages of Early Jōmon period. Subsequently their number increased, reaching a peak towards *Kurohama* and *Moroiso a-b* phases, followed by a complete disappearance in the *Moroiso c* phase. After an interval of several centuries, during which most settlements were small sized, *kanjōshūraku* reappeared briefly between the *Katsuzaka 2* and the *Kasori E4* phases of the Middle Jōmon. The last appearance of these sites is dated to the early phases of Late Jōmon period, before a definitive disappearance after the *Horinouchi* phase (Taniguchi 2005).

Habu's study is not the first case where the co-existence of larger and smaller settlements is acknowledged. Tatsuo Kobayashi has in fact identified such a pattern in his classification of Jōmon settlements, based on the distinction of six different types of sites: (Kobayashi 1973, 1992:91, Kani 1993):

Type A Large settlements (more than 100 pithouses) located on tablelands and characterised by some form of planning in the distribution of residential units, storage pits, and graves. They provide evidence of occupation for 2-3 or more consecutive pottery phases and are associated with the presence of a large quantity of different artefacts (e.g. pottery, stone tools, etc.).

Type B Settlements composed by few residential units with a maximum of ca 10-20 pithouses. Non-residential features are present but are very few. In most cases they are characterised by an occupational length of a single pottery phase.

Type C One or two residential units located in a relatively small space, with no or very few other features and artefacts.

Type D Sites without residential features and characterised mainly by a cluster of different types of pits and hearths associated with few artefacts.

Type E Special purpose sites spatially separated from settlements (e.g. cluster of burial pits, quarries, etc).

Type F Sites recognised as traces of occasional events, such as task-group camps or butchering sites.

Kani (1993) hypothesised that the three types of residential sites (A, B, and C) were all characterised by different functional tasks, and that types B and C were dependent on A, acting as local satellite sites for subsistence tasks. Furthermore, he suggested that B and C types are distinguished as the result of differences in the seasonality of specific subsistence activities (requiring different group sizes) and the spatial variation of available resources.

Both Kani and Kobayashi supported their studies with the archaeological data from the Tama New Town Residential Area, a 30 km^2 development area in Tokyo which has been extensively excavated during the 70s. Kani's conclusion for the local settlement history suggested a broad correlation with the population dynamics observed by Imamura (1997) and with the cycles of appearance and disappearance of *kanjōshūraku* (Taniguchi 2005).

The co-existence of smaller and larger sites, which has also been confirmed by Kani's analysis, led several authors to question the process behind the emergence of this size distribution. Akayama (1990) pointed out that, broadly speaking, two competing hypotheses have been offered in the literature.

The first suggests that this pattern is the consequence of intra-annual group fission and fusion dynamics. In other words, the same individuals occupied Type A sites and type-C sites during different moments of the year. According to Watanabe's (1968) classification of hunter-gatherer residential mobility pattern, several communities are characterised by similar behaviors. For example, the Nuu-chah-nulth (formally known also as Nootka) of the Pacific Northwest coast aggregate to large settlements during summer and fission into smaller settlements during winter (Drucker 1951). Other examples include the Inuit (Mauss and Beuchat 1904) and the !Kung (Lee 1979), and show how fission-fusion is present in a variety of

environmental settings (Martin 1974), implying also that this could possibly be a convergent adaptive response to different types of selective forces.

Three commonly observed pieces of archaeological evidence seem to support this hypothesis (Akayama 1990). Firstly, Kobayashi (2002 for a recent review) noted that the first depositional layer inside abandoned pithouses was often characterised by a complete absence of artefacts, and was covered by a layer where a large number of artefacts were recovered instead. This stratigraphic pattern, known as *Fukiage* (from the name of the first site where this was identifed) is commonly found in many Jōmon sites, and led some scholars to suggest that this was evidence of a temporary abandonment of the site. Secondly, residential features of large settlements often overlap each other or show evidence of rebuilding. This has often been regarded as evidence of continuous occupation, however in several cases the post-holes of older residential units were filled with natural deposit, indicating the possibility of a period of abandonment prior to the reconstruction. The third piece of evidence is directly derived from an interpretation of Kobayashi's site classification, which suggests that the occupational length of type-A sites consist of several pottery phases, in contrast to the single- phase occupation of type-C sites. This would indicate, according to the proponents of this view, that large-scale settlements are simply the result of a continuous aggregation (fusion) to the same location, while smaller sites are the results of single episodes of fission.

The alternative to the seasonal fission/fusion hypothesis is based on the critical review of some of the supporting evidence presented above. Firstly, the absence of artefacts in the first depositional layer does not imply that this was a natural process, and could well be explained as an anthropic process. This implies that the first and second depositional layers could be close in time, and would thus reject the idea of a temporary abandonment of the site. Nishida (1989) strongly criticises the idea that the *Fukiage* pattern was the result of natural deposition, pointing out how such a claim was supported exclusively by the absence of artefacts. Recent analysis by Kenichi Kobayashi (2004) at the SFC site in Kanagawa showed that the difference in the radiocarbon date between a pot recovered from the habitation

floor of the pithouse and a potsherd recovered from the second depositional layer were extremely close in time, with the latter actually showing an older median calibrated date. Kobayashi's analysis does not reach a chronological resolution sufficient to disprove the fission/fusion hypothesis, but nonetheless supports the view that if there was an abandonment, this was extremely short in time. Secondly, the fact that small settlements are occupied by a single pottery phase does not itself supports the hypothesis that the length of occupation was seasonal, and even if we assume that they were the outcome of a fission process, the duration of such an event could have lasted several decades rather than a single season. In addition to the critiques proposed by Akayama, one should question what are the selective advantages of a fission/fusion strategy given the specific environmental settings and the spatio-temporal distribution of the resources. For example, aggregation can be induced by the availability of certain resources in key locations during specific seasons (e.g. eulachon spawning sites in the Pacific coast of North America; Mitchell and Donald 2001). If this is the case, we should expect some differences in the geographic settings between aggregation sites and dispersion sites. However, recent analysis of the settlement pattern at Chiba New Town area (Crema *et al.* 2010) has shown how type-A and type-C settlements could be located at extremely short inter-distances (less than 500 meters). A fission-fusion process at such a spatial scale, where the catchment area overlap and the environmental settings are the same, is unlikely to provide any adaptive advantage.

In order to examine the nature of these clusters of larger and small settlements, Nakamura (1996) assessed the lithic assemblages of two groups of settlements in Ibaragi prefecture (northern Kantō), dated respectively to the *Kurohama-Ukishima* and to the *Kasori EII - Horinouchi 1* phases. In both cases, he noticed that some trends were constant throughout all sites (e.g. predominance of plant processing tools), while others, such as the presence/absence of arrowheads or net-sinkers, were highly diversified and correlated with the size of the settlements. Based on this evidence, he postulated that during the Early Jōmon period smaller groups were likely aggregating to a large centre for communal hunting activities, while

during the Late Jōmon period these aggregation sites might have been related to planned activities of intense plant gathering.

Although biased by the coarse chronological resolution of the analyses, Nakamura's argument shows how seasonal aggregation could be an outcome caused by the necessity of collective tasks requiring larger group sizes, or perhaps to extremely localised concentration (in space and time) of certain resources. Communal hunting might require a relatively larger number of individuals, but this would not necessarily lead to the re-occupation of the same location every year. Resource concentration might lead to such a pattern (e.g. Mitchell and Donald 2001), but few resources (apart from the notable exception of salmon, but see section 2.2.2) amongst the Jōmon diet seem to meet these spatio-temporal characteristics. Furthermore, it is important to note that the existence of sites with different subsistence orientation does not itself indicate that this was a consequence of an intra-annual fission/fusion process. Diversification of subsistence strategy, perhaps in relation to the group size, can be equally conceived as an explanation.

A strong argument against the seasonal fission/fusion hypothesis can be derived from seasonality analyses. Koike (1980) conducted this by examining the growth-line of *Meretrix lusoria* clams on 12 different sites, and showed that in the majority of the cases a year-round collection of shellfish can by hypothesised and that these settlements were permanent and not abandoned during specific seasons. While Koike's evidence is undeniable, it is difficult to generalise her claim to inland sites where such an analysis cannot be conducted. Nonetheless her study provides a strong support that the group size distribution is more likely to be determined by different durations in the site occupation and a real unevenness in settlement sizes, rather than a reflection of seasonal aggregation and dispersion.

The spatial distribution of type-A sites could provide additional clues on the nature of Jōmon settlement system. Taniguchi's (1993, 2005) spatial analysis of the so-called *kyotenshūraku* ("Hub" settlements; corresponding to *kanjōshūraku* and type-A sites) during the Middle Jōmon western Kantō, showed how these sites were evenly distributed in the landscape, with an average inter-distance of 8.4 km

and a typical territory with a radius of 4.2 km. This study represents one of the few attempts to apply quantitative methods in Jōmon settlement archaeology, with the adoption of analyses and models widely used in Anglo-American archaeology (such as Clark and Evans' Nearest Neighbour Index and Thiessen Polygons). It should be noted, however, that Taniguchi used a coarse chronological resolution of over 500 years (between *Katsuzaka 2* and Early *Kasori E3*; 5280 - ca 4600 cal BP), and considered pairs of *Kyotenshūraku* with an inter-distance of less than 3 km as a single "twin" settlement. While examples of extremely short distances between two *kanjōshūraku* are indeed discussed in the literature, a threshold distance of 3 km might have biased the result of Taniguchi's analysis.

The advent and spread of Geographic Information Systems (GIS) in Japanese archaeology, following the seminal manual by Kaneda and colleagues (2001), has increased the number of studies where quantitative methods are integrated into the study of Jōmon settlement pattern. For example, Tsumura (2002) has analysed the spatial relationship between different types of Jōmon sites between 5,850 and 4,250 cal BP (Imamura 1999b) in the Aomori prefecture (Tōhoku region), using a combination of cost-weighted distance[6] and Hodder and Okell's A-Index (1978). The classification adopted by Tsumura is slightly different from the one used by Kobayashi (1973)[7], but nonetheless offers quantitative assessment of how the relationship between different types of sites changed over time.

The problem of coarse chronological resolutions in settlement studies has been overcome by a series of publications (Nishimoto *et al.* 2001, Tsumura *et al.* 2002a;b; 2003) where several scholars have jointly assessed the Middle Jōmon settlement pattern of the Musashino tableland in Tokyo, using the absolute chronology provided by the *Shinchihei* pottery sequence (Kobayashi 2004, see also table 3). The project involved the adoption of several analytical methods, including the creation

[6]Cost-weighted distance analysis is GIS based method which allows the quantification of some cost-based (e.g. energy, time) assessment of physical distance. In the most common case, this allows the integration of morphometric properties of landscape distinguishing for instance flat terrain (low cost) from highly rugged landscapes (higher costs) (Conolly and Lake 2006).

[7]Tsumura (2002:49) distinguishes four site "ranks": A-Rank) settlement with at least 20 residentil units; B-Rank) settlements with less than 20 pithouses; C-Rank) Non-residential sites with features such as burials, storage pits etc; and D-Rank) sites with no features and few artefacts

of Thiessen polygons, inter-visibility networks derived from viewshed analysis and trend surface analyses of different types of lithic assemblage, pottery stylistic features, hearth type and source location of obsidian. While their work uncovered different aspects of the Middle Jōmon settlements of the area, the spatial pattern was assessed in a much less formal way, with the suggested five main types of spatial relationship between residential sites distinguished purely by visual observation. The results (Tsumura *et al.* 2002a) nonetheless showed how a highly inter-connected system of large and small settlements emerged towards phase 10 and 11c (4900-4710 cal BP), followed by a fragmentation into local clusters at phase 12 (4710-4520 cal BP) and a complete dispersion to smaller settlements by the end of Middle Jōmon (phase 13, 4520-4420 cal BP).

The study of the settlement pattern of the Musashino tableland can be regarded as a milestone of recent settlement studies in Jōmon archaeology, although its impact appeared to have been much more oriented to the future role of GIS-led spatial analysis rather than a rethinking of Jōmon settlement pattern. Perhaps the analysis was narrowly centred on the case study area and the authors' aim were more focused on providing a formal method of pattern recognition, rather than proposing explicit models of the processes behind the observed pattern.

2.2.5 Social Complexity

The presence of certain features of subsistence strategy (e.g. active management of resources, delayed consumption via storage, etc.), demography (i.e. high population density), and settlement pattern (large organised settlements, high degree of residential stability) has often been viewed as evidence suggesting potentially high levels of social complexity among Jōmon hunter-gatherers. While these features have been considered as remarkable and unique in the past, the increased availability of archaeological data, coupled with the awareness of a biased representation of modern ethnographic groups (Wobst 1978), has led some authors to conclude that complex-hunter gatherers are indeed much more "common" (Shnirelman 1992), and consequently are much more representative of hu-

man prehistory than previously thought.

The critical issue that must be approached before asking whether Jōmon communities were "complex" or not, is to define the meaning of such a label and question whether its application is useful for understanding past societies. The classification of hunter-gatherers across a binary spectrum has been in vogue since the early 80s, and pushed several authors to propose their own models. This includes Binford's *Forager/Collector* (Binford 1980), Bettinger and Baumhoff's *Traveller/Processor* (Bettinger and Baumhoff 1982) and Woodburn's *Immediate-consumption/Delayed-consumption* models (Woodburn 1982). Although they are based on slightly different key features, they more or less share a similar set of properties for each category and at the same time acknowledge how such a distinction should be viewed as a continuum rather than a dichotomy. These studies led Robert Kelly (1995, after Keeley 1988) to define a set of features for distinguishing "complex" hunter-gatherers from more "simple" ones, including heavy reliance on plant and marine foods, large settlement size, low residential mobility, medium to high dependency on stored food, warfare, and slavery.

This is a commonly shared set of traits which essentially unites the dualism proposed by the scholars mentioned above and sits in a broader set of definitions shared by several authors (e.g. Price and Brown 1985) where complexity can be broadly defined "as a condition in which a system is composed of greater internal differentiation (of component parts) than *another* system to which it is being *compared* "(Fitzhugh 2003: 2; emphasis added). The key element in this definition resides in its explicitly comparative framework: a society is *more* or *less* complex than another.

A more restrictive definition of "complexity" advocated by scholars such as Arnold (1996), focuses on aspects related to the social structure of these groups. In other words, a community is socially complex if there is some form of horizontal or vertical social differentiation. Fitzhugh's definition states that "complex hunter-gatherer societies are social groups primarily engaged in a foraging mode of production with institutionalised inequality (rank or stratification) and an or-

ganisational structure integrating multiple family units into larger political formations" (Fitzhugh 2003: 3; emphasis added). In a similar way, Kelly (1995) also distinguishes between egalitarian and non-egalitarian hunter-gatherers, placing the focus on the presence/absence of social inequality.

Two major pitfalls could emerge from the adoption of either view of complexity. The first one resides in ignoring the fact that the distinction "simple-complex" is purely theoretical, and that the set of features defining one or the other is rarely present altogether. In one sense this runs parallel to Smith's (2001) discussion of the problems associated with the forager-farmer distinction. The second fundamental pitfall is to adopt a progressivist vision where simple society will naturally "develop" into complex societies over time. In a review paper on complex hunter-gatherers, Peter Rowley-Conwy (2001) illustrates evidence that challenges the assumptions derived by this progressivist vision, pointing out that change towards complexity is not necessarily gradual, nor it is unidirectional and does not necessarily lead to agriculture. More recently, the problem has been quantitatively approached by Currie and Mace (2011) who tested the progressivist "Spencerian" vision of social evolution by using phylogenetic comparative techniques on data from Austronesian-speaking societies of southern Pacific. The analysis focused on the transition between "Acephalous society", "Simple Chiefdom", "Complex Chiefdom" and "State" and showed that the most probable mode of social evolution is step-wise and bi-directional. The results from Currie and Mace are not necessarily applicable to the evolution of hunter-gatherer societies, but nonetheless support Rowley-Conwy's critique.

Given this framework, discussions on whether Jōmon hunter-gatherers were complex or not requires a precise establishment of when, where, and which definition we would like to adopt. Japanese archaeological literature seems to rely on the second, narrow definition of social complexity, with most debates surrounding the question of whether Jōmon society was *stratified* or not, (Watanabe 1990, Kosugi 1991, Hayashi 2001, Nakamura 2002, Takahashi 2004).

Perhaps one of the most influential works in this regard has been offered by Hi-

toshi Watanabe, whose strong knowledge of the Ainu (Watanabe 1973) and other ethnographic hunter-gatherer communities of the north Pacific rim led him to question the presence of social inequality among Jōmon society (Watanabe 1990). The starting point of Watanabe's work was the development of a triadic model (Watanabe 1990:63) where social stratification is deeply connected to specialisation, prestige economy, and high-level manufacturing, within the overall assumption of a sedentary lifestyle. The author then tried to apply his model in the Jōmon context, presenting evidence to support the claim that social stratification was indeed present.

A series of authors questioned Watanabe's interpretation of the archaeological evidence, showing how social stratification is not treated as an hypothesis to be tested but more as a starting assumption (Kosugi 1991), or that the premise of a sedentary life-stye is not fully supported by the archaeological data (Hayashi 2001). Hayashi (2001) also pointed out how Watanabe's vision of the typical Jomon settlement was heavily biased and ignored studies that indicated how the number of contemporary residential units were much smaller than previously assumed.

In addition to these critiques, one should note how much of the discourse on Jōmon social complexity has been confined to narrow spatio-temporal windows. Watanabe's triadic model is based on the direct analogy to the Hokkaidō Ainu communities, and a substantial part of his assumptions cannot be applied to central and southern Japan. This critique is also applicable to the evidence presented by Tatsuo Kobayashi (1992, 2004) who, in a rather simplistic fashion concluded that due to a distinct similarity of the subsistence system and the technological level of the Jōmon and the Pacific Northwest Coastal Indians, we should expect a comparable level of social stratification.

Perhaps as a consequence of the weaknesses of such broad-scale perspectives, recent efforts investigating Jōmon social structure has been restricted to smaller spatio-temporal contexts, but with finer and more sophisticated sets of evidence to support stripped-down claims about Jōmon society. Examples of this trend can be found in two edited volumes by Masahito Anzai (e.g. 2002a, 2002b) where

the link to Watanabe's original work is made explicit in the preface. Papers in these books focused on detailed aspects of the Jōmon culture, such as long distance trade (Daikuhara 2002), ritual activities (Kosugi 2002), and monumental architecture (Sasaki 2002).

Among the different approaches for examining Jōmon social complexity, it is worth mentioning the evidence provided by the analyses of ritual tooth extraction (Harunari 1986). These showed how individuals with different patterns of extraction were associated with different grave goods and burial locations, possibly suggesting a social stratification based on rules of postmarital residence. A recent study conducted by Kusaka and colleagues (2011) on the carbon and nitrogen isotope of human remains showed a clear correlation between diet and type of tooth extraction, providing further support for these initial claims.

Hayashi (2001) undertook an extensive review of Jōmon archaeological data, examining different forms of communal graveyards, such as the *kanjōdōri* of Late Jōmon Hokkaidō (Ikawa-Smith 1992), stone circles, and burial areas of *kanjōshūraku*. His conclusion supports the possible presence of leaders in certain contexts, but denies the possibility that permanent elites, similar to some stratified society of the Pacific Northwest Coast, existed.

The most recent work on Jōmon social complexity offered by Richard Pearson (2007) leads to a similar conclusion. The detailed analysis of lacquer goods and decorated pottery production in association with Jōmon burial seems to suggest how part-time specialists were likely necessary, but at the same time pointed out how the existence of hereditary elites cannot be supported.

Hayashi and Pearsons' analyses thus seem to reject the claim that Jōmon hunter-gatherer had a level of social stratification comparable to the ones observed in other cultures of the northern Pacific Rim. The analysis of tooth extraction points out that there was a social differentiation between immigrants and natives but does not provide evidence of hereditary inequality between individuals. Nonetheless, if we adopt the broad definition of complexity mentioned at the beginning of this section, Jōmon communities did indeed possess several key features uncommon to

most "simple" hunter-gatherers. The key point however does not seem to be the definitive labelling of the Jōmon to the one side or the other of the simple-complex continuum. Instead, the most interesting aspect of Jōmon prehistory is how the defining features of "complexity" were characterised by an intermittent pattern, which might suggest, instead, a continuous oscillation between the two extremes of the spectrum.

2.3 Jōmon Settlement Pattern in Kantō Region between 7000 and 3220 cal BP

Kantō provides one of the best contexts for examining diachronic changes in Jōmon settlement pattern. A long tradition of studies which started at the end of the 19th century, the exceptionally rich dataset coming from rescue excavations fostered by the expansion of new urban areas, and the preservation of a rich zooarchaeological data in numerous shell middens around the Tokyo Bay, have all contributed to the emerging picture of local settlement prehistory.

Investigations within this region started with Morse's excavation of the Ōmori shell mound in Kanagawa prefecture (Morse 1879), which coincides with the dawn of modern Japanese archaeology and marks at the same time the discovery of the Jōmon culture (Imamura 1997). Early research excavations have thus been focused primarily on the shell-middens surrounding the Tokyo bay area, while a parallel interest in settlement archaeology increased after the works of Wajima and Okamoto at the Nanbori shell midden in Kanagawa (Wajima and Okamoto 1958, Habu 2004).

The number of emergency excavations increased dramatically after the second World War, particularly in the southern Kantō area where the expansion of the residential areas of Tokyo, Yokohama, and Chiba have fostered a large number of CRM projects. Two properties of these excavations are particularly noteworthy from the standpoint of settlement archaeology: 1) their extensive nature; and 2)

the high clustering of identified sites linked to the development of new residential areas. The first point has been already mentioned, and offers an incomparable record for intra-site analysis of hunter-gatherer settlements. The second point is exemplified by the study of the Tama New Town area in Tokyo (Kobayashi 1973), which sparked an interest in the micro-regional analysis of Jōmon settlements and set the basis for Kobayashi's site classification. Similar dense clusters of excavated archaeological sites are also present in Kanagawa (Kōhoku New Town Area; Yamamoto *et al.* 2001) and Chiba (Tōnanbu New Town Area; Nishino 2005, Crema and Nishino 2012) and provide additional insights into the nature of Jōmon settlement pattern. The intensity of archaeological research has been less pronounced in other regions of Kantō, where most rescue excavation are confined to smaller expansions of local residential area and to the development of large inter-regional infrastructure networks. This high quality spatial data is coupled with a rich tradition of studies on pottery typology, which encouraged the creation of a fine-grained relative chronological framework, recently calibrated to an absolute sequence (see section 2.2.1).

2.3.1 Case Study Location and Environmental Settings

For the purpose of this project two different areas in the Kantō region (figure 9) have been chosen. The first is located in Chiba prefecture, where the rich coastal environment has supported the development of large shell middens throughout the Jōmon period. The presence of these particular sites allowed a longstanding tradition of subsistence studies (e.g. Koike 1986, Suzuki 1986), which provided crucial complemental data for the investigation of the local settlement pattern (e.g. Aonuma 1990, Toizumi and Nishino 1999, Aonuma *et al.* 2001, Nishino 2005, Tsumura 2006, Crema *et al.* 2010). The second case study is located in Gunma prefecture, at about 120 km northwest of Chiba, along the valley of the river Tone within the mountainous regions of northern Kantō. Studies on this area have been less intense than in Chiba and is limited by an almost complete absence of zooarchaeological and osteoarchaeological data. Most studies are narrowed to the anal-

ysis of single large sites, such as Miharada and Doukunmae, which have provided a rich vision of the settlement history, although focused to a very small spatial scale. Spatial analysis at larger scales has also been proposed, but in most cases only as part of a broader regional analysis (e.g. Habu 1988; 2001).

The choice of the two areas has been stimulated by an interest in how different environmental settings (a coastal tableland with a rich intertidal zone against a mountainous inland area with a large river-valley) close in latitude and grouped in the same ecoregion, contributed to the evolution of local settlement history. The selection has also been influenced by the spatial range into which Kobayashi's absolute sequence can be applied (which does not allow the choice of a case study outside the Kantō region), and by the limited number of regions where a sufficiently high intensity of excavations has been conducted. The two areas, however, should not be viewed as fully isolated from each other as testified by the analysis of the obsidian trade network (Tateishi *et al.* 2004).

Chiba

The case study for Chiba is a 15 $\times$15 km square-shaped area located inside the modern city of Chiba (see figure 5), at the western side of the Tokyo bay (UTM Zone 54N, lower left corner coordinates: Northing 3,934,225 m, Easting 419,987 m, datum: WGS84).

The area is bounded by the eastern shores of the Tokyo Bay to the west and covers a large portion of the Shimousa Tableland, an alluvial terrace fragmented by a system of drowned valleys (*ria*). These create a series of plateaus with an elevation of ca 40 meters, separated by channels with an elevation of 5 to 15 meters. Most of these channels were tributary rivers of the Miyako River, flowing from east to west to the Tokyo Bay and the Kashima River flowing from south to north to the Inba Lake.

Kikuchi (1997, 2001) has investigated the relationship between the morphology of the tableland and the location of Jōmon sites, noting how these were located on the edge of the alluvial terraces, often in proximity to the head of side-valleys. This

spatial correlation is possibly explained by the presence of water springs, which tend to concentrate at the cross section of the valleys, where the sand stratum between Kantō loam stratum and Narita stratum is exposed.

A relatively large number of studies on the past vegetation and the geomorphology of the area has allowed a good reconstruction of the palaeoenvironment, although many of them have been based on uncalibrated radiocarbon dates, making the correlation with archaeological events difficult.

The largest change in flora is associated with the cooling event of the late 5 th millennium cal BP, and sees a transition from deciduous broadleaved forests, dominated by oaks (*Quercus Lepidobalanus*) to temperate coniferous forests (*Cryptomeria*, *Abies* and *Alnus*) from ca 4000 cal BP (Inada *et al.* 2008). Kudo (2007) states that the peak of this cooling event is likely to be concurrent to the interval between *Shōmyoji 1* and *Horinouchi 1* phases, which, according to Kobayashi's sequence corresponds to the second half of the 5 th millennium cal BP (4420-3980 cal BP). Sekiguchi (1989) analysed several cores from the *Murata* river valley and noted the same major shift in plant composition occurring between the Early and Late Jōmon.

The rapid regression events, which occurred during the Early and Late Jōmon period (at ca 5800-5200 cal BP and at 4500-3600 cal BP; Fukusawa *et al.* 1999) had the largest impact on Jōmon communities as manifest in the decreased number of shell middens during these episodes (Toizumi 1999b, Habu *et al.* 2011). At the peak of the Jōmon transgression (which occurred sometime during the first few centuries of the Early Jōmon period), most of the drowned valleys of the Shimousa Tableland were under water, with a fragmented coastline surrounding the case study area. Tokyo Bay was larger and extending much deeper towards the north, while the Palaeo-Kinu Bay (about 50 km north from the case study) was largely extended to the north of the Shimousa Tableland (Komiya 1989). The subsequent episodes of regression have deeply modified this setting, with the drowned valley being filled with sandy silt and the inter-tidal zone shifting towards the Tokyo Bay and the Pacific Ocean.

Gunma

The Gunma case study is also a 15 $\times$15 km square-shaped area, and is located at the confluence of the Agatsuma River and the Tone River, close to the modern town of Shibukawa (UTM Zone 54N, lower left corner coordinates: Northing 4,032,314 m, Easting 316,604 m, datum: WGS84; figure 6). The area is located between three volcanoes, Mount Haruna on the west, Mount Komochi on the north, and Mount Akagi on the east. The presence of these volcanoes creates a wide river valley (with an elevation between 150 to 230 meters, increasing gradually towards north), surrounded by a gentle slope reaching a maximum elevation of over 800 meters.

Three volcanic eruptions appear to have occurred during the interval between the Early and Late Jōmon. The earliest event within the scope of this thesis has been registered in the deposition of the Asama-Kuni pumice (As-Kn), dated to 5410 $\pm$ 75 ^{14}C BP (6391- 5993 cal BP 1σ range; Soda *et al.* 1988). The latest event is associated with the Asama-D pumice (As-D) and has been connected with the *Kasori E* pottery phase (Aizawa 1990), and hence can be dated to 4900-4420 cal BP on the basis of Kobayashi's absolute chronological sequence (Kobayashi 2008). A tephra study at Mount Tayrappyo has shown similar pumice deposition (labelled As-T1) dated to ca 4900 cal BP, which could be the same of As-D (Kariya *et al.* 1998), confirming the cross-dating with the archaeological material. Between these two layers, a third deposition related to the eruption of Mount Kusazushirane (Kusazushirane-Kumakura pumice, Ks-Ku) has been recorded, and based on the dating of As-Kn and As-D, can be roughly dated to between 5,500 and 5,000 years ago. All three events do not seem to have had major impacts in the local environment, and the associated tephra layers are often not found in many archaeological sites in Gunma. The most prominent changes are thus the same broad climatic shifts observed in other parts of Kantō, with notable episodes of cooling towards the end of Early and Middle Jōmon periods (Kudo 2007).

2.3.2 Settlement Patterns between 7000 and 3220 cal BP in Chiba and Gunma

Chiba

The Early Jōmon period in Chiba was generally characterised by relatively few sites and residential features. The major characteristic of this phase seems to be a consistent lack of a typical structural layout in the settlement forms. Despite an overall trend that sees the spatial aggregation of residential units, storage pits, and burials, their spatial association seems to vary consistently throughout different sites. Kano (2001) notes that such an unstructured distribution of features makes the definition of settlement boundary difficult, and suggests shifting to a larger scale of observation by grouping these clusters of sites (*iseki-gun* in Japanese) as the main unit of analysis. The substantial lack of archaeological data makes also the assessment of spatial and temporal patterns quite difficult, although a small increase in the total number of residential units and the appearance of a few *kanjō-shūraku* during the second half of the Early Jōmon period is evident in other parts of the prefecture. A typical example of this can be found at Kidosaki site, a middle scale *kanjōshūraku* where the central plaza is occupied by four clusters of burial pits. It is worth mentioning that not all large-scale settlement can be categorised as *kanjōshūraku*, for instance Suzuki(2010b) indicates how Hazamahigashi site has a scattered distribution of a relatively high number of residential units. Notable examples of Early Jōmon sites in the study area include Kowashimizu (7 pithouses dated to the second half of Early Jōmon), Kidosaki (about 8 pithouses dated to the middle-late Early Jōmon and 595 pits), and Honyama (10 pithouses dated to *Ukishima II-III / Moroiso b*).

Between the end of the Early Jōmon and the early stages of the Middle Jōmon period, the number of settlements showed a considerable decrease similar to those observed in other parts of Kantō. Large *kanjōshūraku* are no longer built, and the total count of residential units becomes smaller. This trend was reversed beginning with the *Otamadai III* phase (end of 6th millennium cal BP), when sedentary

nucleated settlements with long term repeated occupation started to form (Kano 2001, Nishino 2008). These are often characterised by a high concentration of shell layers, often displaced into an annular or horse-shoe distribution, and by an annular allocation of the residential features, providing the most typical examples of *kanjōshūraku*. In some cases, these settlements can be found as pairs, as in the case of the Ariyoshi-kita and Ariyoshi-minami, or Kasori-kita and Kasori-minami shell-mounds. Other notable sites of the same period include Warabitachi (over 20 pithouses attributed between *Otamadai* and *Kasori EI* phases), Minamisaku (13 pithouses of *Otamadai III-IV*) Hagawa (mainly attributed to Kasori EII and Kasori EIII), Nakayama (12 pithouses attributed to Kasori EII), and Unarasuzu (12 pithouses attributed to Kasori EIII).

During the *Kasori EIII* phase, and more remarkably during the *Kasori EIV* and the *Shōmyōji 1* phases, these annular layout settlements were abandoned, and a relatively high number of smaller settlements emerged, often without shell layers or with smaller shell deposits. In some locations new large-scale settlements formed (e.g. Mochigasaki, Unarasuzu, and Kairō sites) but the residential units of this period exhibit a scattered spatial pattern, rather than a circular layout.

Several studies have focused on the disappearance of these *kanjōshūraku*. Kano (2002) suggested that these large nucleated settlements fissioned into a series of new sites, and noticed how several cultural trends occurred in parallel. These include the appearance of *ekagami-jukyo* ("hand-mirror shaped dwelling")[8], a new type of composite hearth, raised-floor buildings, and a new decorative style in the pottery. Tateishi and colleagues (2004) also observed that obsidian tools dating to this stage appear to be sourced from the Shinshū area (north-west Kantō), instead of the Kozu island in the Pacific, while Shibutani (1998) pointed out that the average pithouse size grew during the same stage, with an increase in the number of postholes and a change of their spatial patterning.

Recent analysis of the spatial distribution of the residential units at a micro-

[8]The absence of raw stone material in Chiba determined the diffusion of these residential units without the stone-pavement typical in other regions such as Gunma

regional scale (<1 km) has indicated a shift from a highly clustered pattern to a more random one (Crema *et al.* 2010). This might be a consequence of multiple short-span occupations, an argument supported also by the recent analysis of *Meretrix lusoria* clams by Toizumi (2007), who observed how features of Rokutsuu shell midden dating to the same pottery phase (*Shōmyōji*) were occupied during different seasons.

After a brief interval of a few centuries (*Shōmyōji 2* phase), where almost no residential units were constructed, a second increase in the number of sites occurred during the *Horinouchi phase* (Toizumi and Nishino 1999, Nishino 2005). Large *kanjōshūraku* reappeared in the landscape, along with large deposits of shell layers characterised by annular or horseshoe distribution. During the subsequent *Kasori B* and *Angyō* phases, these trends were still present. Some of the large-scale settlements ceased to exist, and the overall number of pithouses became smaller, although this might be a consequence of recovery bias and changes in site location (Nishino 2005). Examples of large-scale *Horinouchi* phase settlements include Miyauchiidosaki (1717 pits, 227 pithouses between *Kasori EIII* and *Kasori B*, of which over 80 pithouses are attributed to *Horinouchi* phase), Hanawa shell mound (28 pithouses attributed to *Horinouchi* phase), Kasori minami (18 pithouses), and Kokanzawa shell mound (17 pithouses). At *Kasori B* phase, the average settlement size seems to smaller, with usually less than 10 units for the largest ones. These include both new locations such as Idosakuminami site (8 pithouses attributed to *Kasori B1*), and sites already occupied during the *Horinouchi* phase such as Kasori minami and Miyauchiidosaki. At the *Angyō* phase, the decline observed during *Kasori B* became more tangible, with only 40 pithouses attributed to this period, 10 of which are located at the Tsujkijidai shell mound.

The high number of shell-middens during Middle and Late Jōmon periods provide some clues for identifying similarities and differences in the subsistence orientation for the two stages. For instance, Toizumi and Nishino (1999) noted that during the former period settlements were more generalised in their subsistence strategies, with an equilibrium between maritime and land resources (Nishino

(1999; 2008)) while Late Jōmon sites specialised in specific types of local resources. As mentioned eariler, the acidic soil of Japan is unsuitable for the preservation of animal remains, and as such the reconstruction of the subsistence strategy or the seasonality of occupation are mainly restricted to periods where the deposition of shell layers were intense.

Gunma

Ishizaka and Daikuhara (2001) provide an extensive review of the settlement history of Gunma. The following is a summary of their paper, updated with the absolute chronological sequence of Kobayashi (2008) and with the addition, where specified, of results obtained from other archaeological analysis.

During the *Hanazumi Kasō* phase (early 7th millennium cal BP), only few pithouses were dispersed in the landscape with a relatively high proportion of open-air hearth features. The situation remained almost unchanged in the *Sekiyama I* phase, although a slight increase in the number of residential features can be observed. Pithouses were also dug deeper in the ground, and their average size was slightly larger than the previous phase. Few sites already showed one of the most typical settlement layouts of the region, characterised by a linear alignment of the residential features in one or two parallel rows. Towards the middle of the 7th millennium cal BP, larger settlements started to emerge, and by the second half of the millennium (*Ario/Kurohama* phase) the total number of sites reached the highest of the Jōmon period in Gunma. Examples of settlements dated to this phase include Mitachimine (11 pithouses of *Sekiyama* phase) and Kawashirota (15 pithouses and 169 storage pits of *Kurohama* phase) sites.

This stage is also characterised by substantial spatial diversity in the settlement pattern and in the distribution of pottery types. *Ario*-type pottery is in fact predominant in sites located at the southwest of the prefecture, where the largest settlements are also found, while *Kurohama* pottery is commonly found in the eastern part of Gunma in association with smaller residential sites. The Tone river valley in the middle (where the case study area is located) shows a mixture of these two

patterns, with the presence of both pottery types and a mixed settlement size distribution. Linear settlements of this period are characterised by a typical pithouse inter-distance of ca 20 meters, numerous burials and storage pits, and evidence of extension and reconstruction of the residential units.

By the beginning of the 6th millennium cal BP, during the *Moroiso b* pottery phase, a radical transformation in the settlement pattern can be observed. A number of large-scale nucleated settlements, with the typical annular disposition of the residential units, become evident. These examples of *kanjōshūraku* are relatively few in number and the majority of sites are instead composed of 2 to 3 pithouses, corresponding to Kobayashi's C-type sites. Ishizaka and Daikuhara (2001) suggest that the coexistence of these two types of sites might be related to seasonal fission-fusion processes. Although ethnographic analogies provide potential evidence for this hypothesis, direct assessment of the locational properties of different types of settlement and formal methods for distinguishing aggregation and dispersion sites have not been offered yet. Examples of *Moroiso* phase settlements in the study area include, Shiraijūni (12 pithouses of *Moroiso a* and *b* phases), Anagoyama (12 pithouses mainly attributed to *Moroiso b*) and Hiromen (8 pithouses between *Moroiso b* and *c* phases).

Parallel study of the lithic assemblage of these sites has provided evidence of possible local diversity in subsistence strategy. Southeast Gunma was characterised by settlements with the predominance of grinding stones (suggesting a higher reliance on plant resources) while areas in proximity to the case study were characterised by a higher concentration of arrowheads (Habu 2001).

Both Ishizaka and Daikuhara's review and Habu's study have shown that the pattern observed from the end of the 7th and the beginning of the 6th millennium cal BP saw an abrupt change during the *Moroiso c* and *Jūsanbodai* phases (ca 5750-5470 cal BP), when the total number of sites and pithouses showed a decline, and *kanjōshūraku* were substituted by linear layout settlements of considerably smaller sizes.

These features can be observed at least until the *Otamadai Ia* and *Ib* phases ($\sim$

5320 cal BP) of the Middle Jōmon period. At this point, an increase in the number of storage pits can be observed, and some key locations, which will later become large-scale *kanjōshūraku*, began to be occupied. This pattern became more visible in the subsequent *Otamadai II* phase, where the lithic assemblage started to show a marked predominance of tools related to plant gathering and processing (e.g. ground axes, grinders, etc.). Notable *Otamadai* sites of the period include Numaminami (28 pithouses attributed between *Otamadai II* and the initial part of *Kasori EI*) and Bougaito (16 pithouses attributed to *Otamadai/Katsuzaka* phases).

The peak phase of the Middle Jōmon period can be observed between *Katsuzaka 3* and the early part of *Kasori E3* phase (ca 5000-4600 cal BP). This stage was characterised by extremely large *kanjōshūraku*, often with over 100 recovered pithouses, surrounded by smaller settlements, a pattern similar to the one observed during *Moroiso a* and *b* phases. The most notable sites are Miharada (342 pithouses mainly attributed to *Kasori E2-3* phase), followed by Dokunmae (39 pithouses from *Katsuzaka* to *Kasori E3* phase), Karasawa (34 pithouses of *Kasori E* phase), and Jinba (12 pithouses of *Kasori E*).

A sudden change in the settlement pattern can be observed from the second half of the *Kasori E3* phase. Large settlements disappear again, with a complete loss of the annular arrangement of the residential units. The total number of sites and pithouses show a drastic decrease, while a new type of pithouse, known as *ekagamishikiishi-jukyo* ("hand-mirror shape, stone paved dwelling") start to appear, along with the construction of large stone circles in previously unoccupied locations. Exceptions to this radical decrease in settlement size can be found in some late Middle Jōmon sites such as Mizoroghioomidou (20 *Shōmyōji* pithouses) and Mitahachiman (7 pithouses of the *Shōmyōji* phase).

The trends observed at the end of the Middle Jōmon persisted until the first few centuries of the 4^{th} millennium cal BP (*Horinouchi* phase), when a further reduction of sites and residential units became evident. The lack of available data does not allow for a detailed description of the settlement pattern of this stage, although at Oomichi site the spatial layout of the residential units, storage pits, and burials

forms a series of parallel belts, resembling the pattern observed in previous forms of linear layout settlements.

2.4 Models of Change

The overview of the settlement history in Chiba and Gunma provides further evidence of some of the trends introduced in section 2.2.4, which can be roughly summarised through the identification of seven distinct stages of settlement history during the Early and Late Jōmon periods:

Stage 1 (ca 7000-6500 cal BP) Small number of sites and pithouses in both regions.

Stage 2 (ca 6000-5700 cal BP) Increase in the number of sites and residential units, coupled with the appearance of *kanjōshūraku* during the second half of the Early Jōmon period (*Moroiso a* and *b* phases). The pattern is more evident in Gunma, where the total number of settlements reaches the highest peak during the Jōmon period.

Stage 3 (ca 5700-5300 cal BP) Sudden decrease in the number of sites and disappearance of *kanjōshūraku* between the end of Early Jōmon (*Moroiso c* and *Jūsanbodai* phases) and the beginning of Middle Jōmon (*Goryōgadai* phase).

Stage 4 (ca 5300-4500 cal BP) Renewed increase in the number of sites and residential units coupled with the re-appearance of *kanjōshūraku* between *Otamadai II* and *Kasori E3/EIII* phases. In Chiba, this stage is also characterised by the formation of large-scale shell-middens.

Stage 5 (ca 4500-4200 cal BP) Decrease in the total number of residential units, sites, and settlement size in association with the disappearance of *kanjōshūraku* between the end of the Middle Jōmon and first few pottery phases of the Late Jōmon period (*Shōmyōji 1* and *2*). In Chiba, large-scale shell middens disappear, and only small shell deposits are formed.

Stage 6 (ca 4200-3800 cal BP) In the eastern Tokyo Bay area, this stage shows a renewed intensification in shellfish exploitation which leads to the formation of large scale shell middens often coupled with annular layout settlements. This is paralleled by an increase in the number of sites and settlements, a trend not observed in Gunma where the settlement pattern maintains the features observed at stage 5.

Stage 7 (ca 3800-3300 cal BP) Both Chiba and Gunma show a decrease in the number of sites and residential features.

There are four notable points that can be highlighted from this summary. First, large-scale settlements and *kanjōshūraku* appear intermittently in both areas, at stage 2 (for Gunma and possibly for Chiba), stage 4 (in both areas), and stage 6 (in Chiba but not for Gunma). This confirms Taniguchi's (2005) analysis introduced in section 2.2.4. Second, some authors suggest that these large-scale settlements were surrounded by smaller ones (Aonuma *et al.* 2001, Ishizaka and Daikuhara 2001), a pattern quantitatively assessed by Habu (1988) for stage 2 in Gunma. Third, the observed patterns seem to be synchronic and parallel in the two regions, although this can be claimed only in terms of relative pottery chronology. Fourth, although no quantitative data are present, most scholars indicate episodes of fluctuation in the number of pithouses, which is roughly correlated with the appearance/disappearance of *kanjōshūraku* and to the broad dynamics of pithouse count observed at regional scales (Imamura 1997, Crema 2012).

Despite the existence of descriptive and informal accounts of these dynamics, neither a quantitative assessment of the observed settlement pattern, nor an explicit endeavour on the identification of a precise cross-dating to absolute chronological sequences has been proposed so far. As a consequence, despite the availability of such a rich dataset, almost no direct attempts have been focused on explaining *why* these patterns can be been observed. In order to seek to possible explanations for these dynamics we need to look at broader regional contexts, or to focus on studies based on other parts of Japan where similar trends has been

observed.

Uchiyama (2006, 2008) provides an elegant summary of the settlement pattern change during the Jōmon period on the basis of an extensive review of previous studies. The starting point of his model is the identification of two distinct settlement patterns: *clumped* and *dispersed* (see figure 7). The former is characterised by a "combination of a few sedentary sites and many small sites"; the latter by a "site size difference [that] became almost non-existent", often correlated with the construction of large non-residential monumental sites (Uchiyama 2006: 139). According to Uchiyama, the two patterns alternate over time in a cyclical fashion with examples of clumped systems found in southern Honshū during Early Jōmon and in northern Honshū during Middle Jōmon, and dispersed patterns observed during the Middle Jōmon in southern Honshū and the Late Jōmon in northern Honshū. Uchiyama explicitly recognises that the two patterns should be regarded as alternative strategies and state that the "sequence from a clumped to dispersed settlement pattern may not necessarily imply a decrease in population, but rather that the land use and resource development system changed from a centralised and intensive one to a more dispersed and extensive system" (Uchiyama 2006: 139).

Assessing the archaeological data from the two case studies can help testing Uchiyama's model. The descriptive accounts summarised in the previous sections seems to suggest that stages when *kanjōshūraku* were present (stages 2,4, and 6) might have been characterised by a clumped settlement pattern. Data on the remnant four stages have been explored to lesser degree, and hence determining whether these conform to a dispersed pattern or not needs to be addressed. Nonetheless, suggestions offered by some authors (Ishizaka and Daikuhara 2001, Kano 2002) seem to support the view that stage 5 might have been characterised by a dispersed pattern. If we assume for a moment that stages 2,4, and 6 were characterised by a clumped settlement pattern, then we need to ask how these settlement systems emerged, what are their structural similarities (or dissimilarities), how they (possibly) transformed into a dispersed system, and whether such an

apparent cycle is an outcome of similar processes (e.g. the onset of similar environment and/or social conditions) or the convergent product of different causes.

Imamura (1999a, 2002) provides an appealing hypothesis for explaining the fluctuations in site counts observed during the Jōmon period. He observed that plant-gathering was most likely the main mode of subsistence during phases with high density, while a hunting-centred economy was probably present during periods of low density. Based on these observations, he concluded that plant-based economy was the key element sustaining large population sizes and that the decline of these resources, and the consequent shift towards a hunting-based subsistence, led to a decrease in population size. Thus, according to Imamura, the ultimate cause of the observed demographic cycles is the fluctuation in the availability of plant resources, a process that can be easily affected by episodes of climate change. Imamura does not explicitly integrate the change of settlement forms in his model, but correlation between these and the demographic trends has been suggested by others (e.g. Taniguchi 2005), while the linkage between the spatial distribution of residential units and resource type is a well researched topic in behavioural ecology (Horn 1968, Dwyler and Minnegal 1985, Cashdan 1992) and can partly support the association between clumped pattern and plant based economy, as well as dispersed pattern and game-based economy.

The association between population decrease and shift towards a game-based subsistence economy (along with the potential transition from a clumped to a dispersed settlement pattern) is undiscussed by Imamura. Expected variations in the two type of settlement forms in relation to the availability of the spatio-temporal resources have been discussed in ecology, although models on the transformation process is comparatively under-developed (see chapter 5, section 5.2). Instances of "reversions" between economic systems can be observed in several ethnographic and archaeological cases (Layton *et al.* 1991), and has often been explained by the diet breadth model (Winterhalder *et al.* 1988). More recently, Lake and Crema (2012) have determined, through a computer simulation, how the reversion to strategies that are normally regarded as sub-optimal can easily occur in case of

overexploitation. Such a study suggests how episodes of reversion can potentially occur without the onset of external climatic change.

Other studies on the changes in the Jōmon population size and settlement pattern have focused on the narrow perspective of single transitions, usually centred on the Early Jōmon (transition from stage 2 to 3) or the Middle Jōmon "collapse" (transition from stage 4 to 5).

Habu's (2008) model for the latter transition provides several insights applicable in a broader perspective. On the basis of an extensive study of the data recovered from Sannai-Maruyama site in Tōhoku, she suggested that increased subsistence specialisation (oriented to a strong reliance on plant resources) caused a substantial change in the socio-economic organisation and a considerable increase in settlement size. This however led the inhabitants of Sannai-Maruyama to become highly "susceptible to such incidences as overexploitation or minor climate fluctuations" (Habu 2008: 581). This explanation is not dissimilar to the concept of an *evolutionary trap* (Schlaepfer *et al.* 2002). The term is used in ecology to describe instances where an organism first adapts to specific environmental conditions, and then is "trapped" when the adopted set of traits is no longer adaptive to a suddenly changed environment. The concept is usually applied to anthropogenic modifications of the environment but can be easily extended to any changes in the environment, as long as the process is fast enough to impede any process of re-adaptation to the renewed conditions. Boyd and Richerson (1992) provide an evocative metaphor (following an earlier work of Wright 1932) where the set of phenotypic traits of an organism is represented as the spatial location of an *adaptive landscape*, whereby the height of a location represents the evolutionary fitness. Any movement in such a landscape will determine a change in the phenotype, and adaptive response will essentially lead an individual to climb a peak to maximise its fitness. Environmental changes (by human impact, by exogenic environmental changes or a combination of the two) can be portrayed as a modification of such a landscape, where the unchanged absolute location of the individual (the phenotype) might potentially lead to maladaptive outcomes (see figure 8).

The crucial questions arising from Habu's model are how groups developed a specific adaptive response, and more importantly why their response to the changed condition was delayed, ultimately causing a population decline. Whitehead and Richerson (2009) have recently proposed an interesting model that could provide some clues for answering these questions. They showed, through an abstract simulation model, how slow rates of environmental changes could determine a higher reliance on social learning, with a decreased dependence on individual learning. This equilibrium makes the system brittle and can in turn determine societal collapses when sudden environmental change occurs, since the lack of individual learners will weaken the group-level responsiveness.

It is important to note that a decreased number of pithouses is not necessarily evidence of population decrease. Radical changes in the settlement system, as portrayed by Uchiyama's model, could lead to a different visibility of archaeological data and hence cause a biased impression of population decline. A highly nucleated settlement pattern (such as Uchiyama's clumped pattern) could lead to an increased archaeological visibility of larger sites, which would lead to the discovery of a high number of residential features in a relatively small spatial extent. On the contrary, a dispersed pattern will lead to decreased visibility, and each excavation will yield a smaller number of features. For example, consider that a large settlement of 50 residential units fissioned into 10 smaller settlements with 5 units each. The archaeological data will show the actual population dynamic (i.e. stability in this case), only if all the offspring settlements are discovered and investigated. In reality these smaller sites might be missed or not excavated, and both instances could determine an apparent decline in the total sum of pithouses. Other authors have pointed out the effect derived by taphonomic biases in the reconstruction of prehistoric population dynamics, showing that occasionally this might lead to the an archaeological pattern that resembles the opposite of what actually happened (Surovell and Brantingham 2007, Surovell *et al.* 2009). Changes in the degree of residential stability could also produce similar misleading trends. Since temporal analysis in archaeology is based on aggregated data in time, we

are unable to distinguish instances of high mobility (higher rate of pithouse construction) from cases of population growth (higher number of individuals building pithouses) in a given time span. The relationship between changes in spatial patterning, choice of sampling strategy, and perceived population dynamics can be partly explored through a simulation based approach. Given one or more hypothetical generative processes (suggested perhaps from ethnographic studies) and specific sampling strategies, one could investigate the bias introduced by the latter for seeking to reconstruct details of the former. By quantitatively assessing the difference between the "real" pattern (i.e. the direct output of a spatial process) and the archaeologically detected one, it is possible to determine the expected bias for different combinations of generative process and sampling strategy. Clearly such an approach should explore a variety of combinations inferred from regional studies and ethnographic analogies, but can also guide the choice of an optimal strategy for archaeological recovery suited for tackling specific research questions.

If we take in consideration these issues, a correlation between population fluctuations and changes in the settlement pattern should be taken cautiously, as the supposed linkage between the two patterns could be largely affected by taphonomic biases. This also points out how, before seeking evidence of population change during the Jōmon period, a quantitative analysis of the changes in settlement pattern is necessary.

Habu's analysis of the subsistence-settlement pattern of late Early Jōmon Kantō (Habu 2001; 2002) provides one of the best regional perspectives on the possible dynamics during the transition between stage 2 and 3. The detailed assessment of the lithic assemblage, coupled with an analysis of the settlement size and distribution, led her to conclude that at some point between the *Moroiso b* and *Moroiso c* there was: (1) a shift from a collector-like system to a forager like system in southwestern Kantō; and (2) a substantial migration towards inland regions. Habu supports her claim by providing evidence of reduced inter-site variability in lithic assemblage and settlement size, scattered distribution of the site locations, and increase in the number of sites in the mountain regions of Chūbu parallel to

a decrease in western Kantō. According to Habu, the ultimate cause for the emergence of these patterns is the reduced amount of maritime resources (caused by marine regression) that led to a higher reliance on land resources. This in turn led to a shift in settlement location and a change in the residential mobility pattern.

Imamura (1992) also tried to determine the underlying causes of the possible population decline observed during the late Early Jōmon. He first assumed that population decrease can be caused by either: 1) reduced availability of resources; 2) increase mortality by disease and/or warfare; 3) migration; 4) any combination of these. He then pointed out that that 2) and 3) would not explain the observed change in subsistence pattern, and hence indicated that the decreased availability of plant resources, possibly caused by climatic change, is the best candidate in explaining the decline of sites. The re-analysis (Crema 2012) of Imamura's (1997) study on Jōmon pithouse counts shows that some degree of correlation between environmental change and pithouse counts can be established, but determining the temporal relationship between the Early Jōmon collapse, the Middle Jōmon increase, and the climatic changes of the early 6^{th} millennium cal BP is still difficult. Moreover, the assumption that these environmental changes were rapid and had a strong impact on resource availability should not be taken for granted.

Cooling and marine regression are undoubtedly the two major environmental changes that can be correlated with each episode of transformation in settlement pattern and population size. The key assumption shared by Habu and Imamura is that mast productivity decreased significantly during these stages, and that Jōmon communities were no longer capable of sustaining higher population densities. As mentioned in section 2.2.2, Kitagawa and Yasuda (2004) suggest that during colder stages, chestnut trees fail to reproduce and become highly susceptible to disease. The same decrease of the temperature would of course have different impacts at different latitudes and thus the key point is to establish whether mast-productivity in central Japan was indeed affected by such a temperature change. The fact that in Kansai, the transition between Middle and Late Jōmon period is associated with an increase in the number of pithouses (section 2.2.3), is an additional clue that

could suggest that the same exogenic forces might have been beneficial in southern Japan. In central Japan, pollen records do show a change in the plant composition (see section 2.1), suggesting that a cooling event did take place, and did modify the plant composition sometime during the transition from stage 4 to 5. However, these data should also be taken cautiously, since Davis and Botkin (1985) showed through a computer simulation that the forest response to temperature decrease is not immediate, and could show a delay of 100 to 200 years, obscuring the difference between a rapid and a gradual change in climate. This is an important point that needs to be investigated, as the *tempo* of the climatic changes and more importantly its relation to the speed of human adaptive response might overcome the role played by the magnitude of change itself. The same issue applies to the effects of marine regression. Uchiyama (2008) dismisses its importance in relation to the decrease of shell middens in the Kantō area, pointing out how the rate of shell midden decrease was faster than the gradual change of the coastal environment.

Another set of hypotheses focuses on the active role played by human activity that might determine a change to its local environment. Uchiyama (2006), stresses this point in his analysis of Torihama site in the Chūbu region, where he compares three conflicting scenarios —exogenic environmental change, increased inter-group conflict, and human induced environmental degradation— providing palynological and geomorphological evidence to support the third hypothesis. Uchiyama is extremely careful in his conclusions and does not dismiss entirely the role played by exogenous forces, but suggests that human-induced change should be viewed as a core component. Explicit acknowledgement of similar explanations does not appear to be widely present in the literature of Jōmon studies, although Ishizaka and Daikuhara (2001) consider overexploitation as one possible hypothesis for explaining the settlement change in Gunma.

Archaeological evidence supporting the existence of trends towards overexploitation is not rare. Hiroko Koike's analysis of both seashells and bone assemblages has shown that episodes of high collecting and hunting pressure did exist and suggests that this might have caused a significant decrease to the prey biomass

(1992a). Archaeological records providing evidence for this are restricted to areas where faunal remains are preserved, but larger settlements in Chiba seem to show similar trends quite often. At Kidosaku shell mound in Chiba, the analysis of *sika* deer remains has indicated a high hunting pressure at the limit of the carrying capacity during the Late Jōmon period (Koike 1986), while the size distribution of *Meretrix lusoria* clams at Kasori shell mound in Chiba indicates a possible increase in the collecting pressure between the second half of Middle Jōmon period and the beginning of Late Jōmon period (Toizumi 1999a). Ito's (1999) analysis of the faunal remains at Ariyoshi-kita shell midden in Kantō show an increase reliance on smaller animals, which might have been caused by the expansion of the diet-breadth and the inclusion of lower-ranked species, a trend which has been observed also at Sannai-Maruyama in Tōhoku (Nishimoto 1995).

Similar evidence from the Early Jōmon period is not common, but a study conducted by Koike (1992b) on shell mounds of the middle Early Jōmon in Saitama prefecture, showed again strong evidence of shellfish overexploitation, which led her to conclude that the disappearance of shell middens were likely to have been induced by human activity.

Thus, overexploitation is not a negligible hypothesis and the available archaeological lines of evidence seem to show that towards the end of stage 4, and possibly stage 2, human exploitation had a high impact on the surrounding environment. However, several problems arise if we suggest overexploitation as a unique cause for the observed dynamics. Firstly, this hypothesis holds at a local scale, but does not explain how the population dynamics were synchronised at an inter-regional level. Secondly, the available archaeological evidence is still not sufficient, and parallel analysis, such as the comparative study of dental pathology, does not seem to support the presence of systemic stress of dietary patterns at an individual scale, indicating how "the foragers from the Middle to Late Jomon period did not undergo a nutritional crisis" (Temple 2007:1041).

The absence of osteoarchaeological evidence suggesting a nutritional "collapse" during the transition between stage 4 and 5 requires further study in this direction

and potentially suggests that a transition to a dispersed pattern might have been a successful adaptive response.

An alternative to the model presented so far, which more explicitly integrates the observed spatial pattern, looks at the effects derived by increased inter-group competition during episodes of population increase. This is closely related to the "packing" model suggested by Binford (2001), or to Carneiro's circumscription theory (Carneiro 1970). In essence this view, shared by scholars such as Taniguchi (2005), sees the emergence of large settlements as a consequence of increasing population pressure, which triggered a reduction of the catchment area and hence required an increased collaboration between households. Perhaps the problem of this model is the lack of explanation on why smaller settlements existed in the landscape. If large-scale nucleated settlements are fostered by increased cooperation between households, how do we explain the presence of smaller sites? Are they instances of "extinct" groups that did not develop into *kanjōshūraku*? Or did they play an alternative function as suggested by Kani (1993)?

2.5 Summary

The summary of explanatory models presented here often appears to agree that climate change played a fundamental role in shaping the evolution of Jōmon settlement history. The level of sophistication and detail in their explanation differ considerably, but the observed correlations of the archaeological data to the climatic events of the mid 6th millennium and mid 5th millennium cal BP (Kudo 2007, Crema 2012) are undoubtedly appealing and can easily push scholars to look exclusively for confirming evidence, dismissing entirely the possibility that their starting assumption might be wrong.

Two neglected directions of enquiry seem to be mandatory *before* any attempts at determining the (possible) role played by environmental forces is taken in consideration. First, the available archaeological data must be reviewed in light of the most recent cross-dating of the pottery phases to the absolute chronological se-

quence. This should be carried out with specific analyses designed to investigate the two patterns described by the Jōmon literature: the fluctuation in the number of residential units and the alternation between clumped and dispersed patterns. The next chapter will be dedicated to this endeavour.

Second, discussion of how hunter-gatherer decision-making ultimately affects population size and settlement pattern needs to be addressed in order to determine how much of the observed pattern can actually be a result of purely internal processes independent of external climatic forces. Several models of sedentary agricultural communities (Renfrew and Poston 1979) and early complex polities (Griffin 2011) have shown how radical shifts between settlement systems could occur *without* the active role of exogenic forces. Although these models incorporate different factors, such as inter-group competition and intensive land-use, the distinct features of Jōmon groups indicates how similar dynamics might have occurred. Chapter 5 and 6 will explore these issues, before a tentative exploration of the role played by environmental change in chapter 7.

Part II

Pattern Recognition

Chapter 3

Theory and Method: Spatial and Temporal Analysis

3.1 Spatial Dependencies

All human settlements emerge from the aggregate outcome of individual decision-making. To understand how hunter-gatherer settlements change over time, we, therefore, need to identify how the choices made by each individual were shaped by specific environmental and cultural contexts, and how these choices in turn affected the behaviour of others. Although a variety of generative processes can be conceived, two properties appear to be common to many hunter-gatherer settlement systems.

First, spatial configurations of hunter-gatherer settlements emerge primarily as a bottom-up, rather than top-down, process. While some sedentary groups are often limited by technological, economic, and social constraints in their spatial decision-making, most hunter-gatherers have a comparatively low number of constraints that limit their expressions. The absence of strong centralised authorities or institutions will produce spatial configurations where the local interactions between individuals (e.g. household inter-distance as a function of kin relationship; Whitelaw 1991) and the adaptive response to environmental properties (e.g. distancing from water sources) are primary drivers. This should not be interpreted

as lack of organisation or planning, instead, patterns emerging from these processes are maintained or rejected by further decision-making, shaped by a partial awareness of the existing spatial structure. Such a continuous interaction among individuals, and between individuals and the outcome of their own actions, ultimately results in a variety of spatio-temporal expressions.

Second, hunter-gatherer spatial configurations are characterised by a comparatively rapid rate of reorganisation. This is caused by the impermanence of their building materials and by their residential mobility strategies. The former impose hunter-gatherers to rebuild their dwellings multiple times within a lifetime. In each episode (ethnographic studies have shown that pithouses of temperate sedentary hunter-gatherers have life-spans between 3 to 15 years; Watanabe 1986, Muto 1995), an individual (or a household) has the opportunity to relocate their residential unit in response to modified social or environmental conditions. This clearly does not imply that the spatial relocation occurs exclusively between these episodes or that those groups with more permanent building materials do not relocate. Nonetheless, frequent episodes of rebuilding will offer more opportunities for relocation, which aggregate outcome is a potentially continuous change in settlement pattern. Seasonal mobility will also provide frequent circumstances for each individual to decide the spatial location of residential units. Evidence of such intra-annual movements can be found in many ethnographic examples (Woodburn 1968, Watanabe 1986, Nishida 1989), where hunter-gatherer groups relocate as a whole, fission into subgroups, or form temporary large settlements through nucleation (Watanabe 1968, Butzer 1982).

The combined effect of a stronger role played by bottom-up processes, flexibility in the decision-making, and high frequency of spatial reorganisation, provide grounds for expressing a large variety of spatio-temporal patterns, often reshaped by transformations in the underlying social, economic, and cultural frameworks. Although the reasons of these settlement changes vary cross-culturally and historically, we can still identify two underlying forces that explain why settlement patterns are not formed by random scatters of dwellings in the landscape.

Firstly, the background environment will always exhibit some patterning, and this inevitably affects human spatial processes. In other words, we should expect an uneven landscape, where physical properties vary over space, and at the same time are susceptible to variation induced by human activities and external forces. Climatic variation and the distribution of resources are typical examples of variables possessing such a spatial structure. More importantly, many of these variables are able to *induce* the spatial patterning of human settlements. Individuals might in fact choose to stay closer to key resources or avoid unsuitable locations. We can further argue that these types of external influence are generally independent of the human spatial process itself. Clearly the latter statement need not always be true as when the temporal dimension is integrated, as human activities could in many cases modify the properties of the background environment through, for example, episodes of resource depletion (Broughton *et al.* 2010), or niche construction (Smith 2007).

Secondly, humans typically organise their activities in clear spatial relation to the presence (or absence) of other individuals, households, or settlements. These behaviours can be regarded as *inherent* to the spatial process itself; suitability of specific locations are in this case not absolute, but *relative* and purely dependent on the same process of human settlement.

It is perhaps a truism to state that the location of each individual entity, whether this being a single residential unit or a large settlement, is always conditioned by a mixture of these two elements. Fortin and Dale (2005) distinguish these two forms of *spatial dependency*, as 1) *induced* or exogenous; and 2) *inherent* or endogenous (see fig. 9). Bailey and Gatrell (1995) propose instead a statistical analogy, distinguishing between *first* and *second order* properties. The former refers to global trends, generally conditioned by external covariates; the latter to local variations derived from internal properties of the system. Bailey and Gatrell's definition however implies also an assumption about the different spatial scales where the two properties act. Induced (or first order) spatial dependence affects the average density of events, and hence are acting at macro-scales, while inherent (or second order) spa-

tial dependence is restricted to smaller scales. While the latter point is acceptable as a starting assumption (although it is undeniable that long distance relationship might affect the location of human settlements; e.g. over-specialised sites economically maintained by long distance trading), the former does not necessarily operate exclusively at larger scales. Complex topographic properties of the landscape can induce the spatial location of settlements at relatively small scales where spatial interactions are also present.

The distinction between the two types of spatial dependencies is a useful starting point, but its strict and uncritical usage should be avoided. Although being external to the system, induced spatial dependency is also a function of how the environment is perceived by single individuals. The very same landscape will create different spatial dependencies to a hunter-gatherer and to a post-industrial entrepreneur. Some landscape ecologists have explored how space is perceived differently depending on which functional trait is active (a concept known as *eco-field*; Farina and Belgrano 2004), an idea discussed also by some psychologists (e.g. Gibson 1977). In other words, the inherent and induced spatial dependencies behind a settlement pattern are filtered by individual intentions and purposes, and hence it is context-variant.

Inherent spatial dependence is usually expressed in the form of *attraction* or *repulsion* between individuals. The former could be encouraged by some adaptive advantages including higher efficiency for cooperative tasks or a potential increase in the frequency of information exchange, the latter by different forms of protection of personal spaces, resources, and information. As with the induced spatial dependence, both forces could vary as a function of the properties associated with the active agent. Fletcher (1981, 1995) provided strong empirical evidence of this by showing the numerical relationship between the spatial extent of settlements and their residential density for a large body of ethnographic data, ranging from mobile hunter-gatherers to urban settlements. The results of his analysis indicated how technologically advanced societies can cope with higher interaction ranges, resulting into settlements with much larger extents. However, these societies are

characterised by lower settlement density, which implies a higher inter-distance between residential units. This is explained by Fletcher as the result of the psychological stress emerging from the repeated interactions with neighbours. Mobile hunter-gatherer groups, which are characterised by smaller residential inter-distance, can solve this problem by repeated relocations of their residential units. Diversity in the settlement density is an example of inherent spatial dependency in the form of a *repulsive* force at the smallest scale. This will determine the inter-distance of residential units, which macro-scale consequences can be observed in the overall density of the settlements. The possibility to sustain larger scales of interaction by means of a more efficient communication system is instead evidence of how the fall-off of inherent *attractive* forces are function of the social, economic, and cultural properties of the specific human group. At an even higher scale, spatial dependency can be again characterised as *repulsive* force, this time as a byproduct of competition between groups of individuals, often revealed as some form of territoriality.

This reassessment of Fletcher's study results into two conclusions. First, the empirical evidence suggests that inherent spatial dependency varies between cultures, as a function of the economic, societal and economic system. As a result, investigating its change over time can offer insights for understanding transformations in human societies. Second, inherent spatial dependence can be both *repulsive* and *attractive*, with different types of forces acting at different spatial scales, although the precise scalar boundary of one and the other is often hard to delineate. Despite these complexities, this epistemic framework is extremely useful for assessing spatial patterns, and provides an inferential tool for determining the nature of the generative processes behind them.

Inherent spatial dependencies are not always expressed as a direct interaction between two entities, but often as a result of an indirect relationship. For instance, two hunter-gatherer groups exploiting the same local resource might lead to over-exploitation, which can then drive both groups to relocate elsewhere. These dynamics could be generalised once we explicitly integrate the temporal dimension

and the framework offered by niche construction models (see Laland *et al.* 1999). The effects of the latter on metapopulation dynamics has been approached through numeric simulations (see Hui *et al.* 2004, Han *et al.* 2009), but here it is sufficient to point out that the ecological imprint generated from pre-existing populations has evolutionary consequences which are reflected in the spatial distribution of current and incumbent individuals. Figure 10 illustrates this notion with an abstract example. In case of *positive niche construction* (fig. 10:**a**), a cluster of individuals will determine a change in the environment, which over time leads to an enhancement of local suitability. This will then generate an induced form of spatial dependency, where both individuals already located within the patch and those located outside are attracted to the newly created environment (coloured in grey). The anthropogenic creation of *secondary forests* (see section 2.2.2) is an example of such a positive niche construction which might lead to higher clustering of individuals, by means of an indirect and delayed spatial interaction. Niche construction could also lead to negative effects (fig. 10:**b**), where the presence of individuals could lead to the creation of an induced form of repulsive force. The most obvious example is when a patch is overexploited by a group of individuals. The successive repulsion is generally regarded as an induced form of spatial dependency, although the historical contingency (the presence of other individuals in the past) is the deep cause of such a spatial patterning.

The effects derived from niche construction processes further blur the distinction between the two forms of spatial dependency. Nonetheless acknowledging this difference is still an useful inferential framework for tracking the evolution of the human use of space through time. Given this, it is surprising that the explicit and formal application of such conceptual models is absent in most archaeological studies pertaining to settlement systems. The introduction and the explicit discussion on the two forms of spatial dependencies have been relatively late (Orton 2004, Bevan and Connolly 2006), and only recently addressed in an extensive manner by Bevan and colleagues (under review). However several studies in the past have approached one or the other implicitly, especially since the adoption of

Geographic Information Systems (GIS) in the early 90s.

In general, much of the emphasis has been placed on induced spatial dependency, as testified by the large number of studies trying to quantitatively assess the relationship between settlement locations and background environment. Early works are prior to the advent of GIS (see Jochim 1976, Foley 1981), but the vast majority of studies have appeared since then (e.g. Kohler and Parker 1986, Maschner and Stein 1995, Wescott and Brandon 2000; Verhagen and Whitley 2011 for a recent review), by fully exploiting pre-existing statistical tools (e.g. logistic regression analysis) in conjunction with the spatial representations offered by GIS. This research framework often placed the emphasis on the predictive power of models, and consequently led to the development and adoption of tools which improved the fit between the empirical data and the statistical model at the expense of a robust explanatory perspective. This is exemplified by the adoption of methods such as artificial neural networks (Deravignone and Janica 2006) or genetic algorithms (Banks *et al.* 2008), where the efficiency in the predictive power is prioritised over a clear understanding of the generative process [1]. Although the acknowledgement of important aspects such as data uncertainty (Millard 2005), or spatial non-stationarity[2] (Bevan and Conolly 2009) has shown some fruitful adoption of sophisticated techniques, the overall trend of locational models in archaeology can be still summarised as inductive and correlative (Wheatley 2004). The main concern here is not so much with environmental determinism, which is often caused by an easier accessibility of certain types of data, but more with an inductive reasoning limited to the identification of correlations between key variables without an explicit exploration of their causal linkage in relation to specific theories of human settlement processes.

Inherent or second order spatial dependency occupied much smaller space in the archaeological literature, with most studies looking at the effects of trade and

[1] It must be noted however that often the aim of these model is pure prediction for CRM purposes, although their actual efficiency is still debatable (Wheatley 2004).

[2] Spatial non-stationarity refers to situations where the spatial relationship is not constant over space.

economic interdependence. These often relied on the adoption of network analysis and statistical physics (Rihill and Wilson 1987, Evans *et al.* 2009) applied on a narrow range of cases where archaeological data related to these interactions were rich. A parallel series of works focused on the locational analysis of settlement from a distributional perspective. Most of them involved the adoption of point pattern analysis (Orton 1982, Bevan and Connolly 2006, Mayer 2006, Crema *et al.* 2010), with the primary aim often being the detection of repulsive and attractive forces at different spatial scales. As for the locational analysis, the emphasis was placed on the assessment of broad patterns (i.e. clustering and dispersion) and relied almost exclusively on hypothesis testing procedures adopting completely random spatial distributions as the null hypothesis. Geographers have already pointed out how the rejection of this hypothesis can be regarded as a truism which does not offer much knowledge about the underlying generative process other than a more quantitative description of the observed pattern (see Gould 1970, O'Sullivan and Unwin 2003). Nonetheless, detecting significant deviations from the random distribution hypothesis can still offer solid basis for creating models of generative processes.

A transition to a model-based approach should ideally integrate both forms of spatial dependency, and seek to explicitly formulate testable hypothesis. The range of existing tools and statistical models can provide only a partial answer in this regard. On the one hand point-process modelling (Möller and Waagepetersen 2004, Illian *et al.* 2008) has achieved a high level of sophistication enabling the possibility to model induced and inherent spatial dependency at the same time. On the other hand its mathematical complexity does not allow the straightforward development of variants designed to model human settlement processes, and the existing ones are often unsuitable for such purposes. Some attempts have shown, however, promising results. For example, Bevan and colleagues (under review) have assessed the spatial distribution of Iron Age settlements in the West Bank, testing the empirical data against a model that integrated both induced (using covariates such as ridge landform, topographic wetness, and elevation) and inherent

spatial dependency (using the "area-interaction model" developed by Baddeley and Lieshout 1995). Point process model-building requires, however, high levels of abstraction which might be problematic for many human processes.

This thesis will not try to overcome these limits by exploring the recent literature on point-process modelling, but will instead try to exploit the available tools to enhance the inductive pattern-recognition exercise. The primary role of spatio-temporal analysis in this context is to establish whether an alternation between clumped and dispersed patterns did occur during the target time-span between 7000 and 3220 cal BP. For such purposes, statistical analysis will be used as an exploratory tool, with the model building exercise left to the more flexible environment of agent-based simulations (chapter 5-7).

3.2 Uncertainty in Archaeological Analysis

Before proceeding to illustrate the most suitable tools for detecting clumped and dispersed patterns, it is important to tackle one of the greatest limitation in the applicability of most spatial analysis in archaeological context: the problem of spatial and temporal uncertainty. Undoubtedly such issues are not restricted to spatial analysis and can be regarded as one of the biggest burdens in the inferential exercise. This is not limited to archaeology, as uncertainty affects other disciplines as well, including criminology (Ratcliffe and McCullagh 1998), ecology (Rochette *et al.* 2009), and climatology (De Wit *et al.* 2008) amongst others. Although the acknowledgement of such limits exists in archaeology, and has been approached from a wide range of perspectives including debates from theoretical standpoints (Wylie 2008, Lake 2010), chronometric analysis (Buck *et al.* 1992; 1996), cultural resource management (Millard 2005), classification (Nicolucci and Hermon 2002) and dissemination (Zuck *et al.* 2005), the great majority of studies neglects its implication or reduces it to a practical problem.

While such problems deserve their own deep treatise, the interest within the context of this thesis emerges from practical restrictions in adopting certain ana-

lytical tools. The proposed solutions (see section 3.2.3) suggest however a careful rethinking of the nature of uncertainty in archaeological analysis. A useful starting point is to separate in three broad domains the possible sources of uncertainty. This could originate from: 1) limitations of our tools and methods to access and measure reality; 2) the way we categorise and define our unit of analysis; and 3) the intrinsic randomness embedded in the physical world. [3]

The first type of uncertainty is perhaps the most prominent one in archaeology and can be found in David Clark's (1973) seminal definition of archaeology: " [...] the discipline with the theory and practice for the recovery of unobservable hominid behaviour patterns from *indirect traces* in *bad samples*" (*ibid.*:17; emphasis added). Errors in measurements, limited accuracy in the quantification of specific phenomena, ambiguous linkage between observed pattern and its generative process, and small sample sizes will all determine restrictions and biases in the output of our analysis. This form of uncertainty can however be improved. Radiocarbon dates can be more precise using more efficient machines (e.g. the use of accelerator mass spectrometry), or field collection in surveys can be enhanced if the surveyors have a better knowledge of the material culture.

There are however forms of uncertainty that go beyond such potential improvements, and are derived from the way we represent reality and define our analytical units (Dunnell 1971). One example of this second type of uncertainty is the controversial definition of archaeological "site", which in certain contexts (e.g. surface remains) is extremely problematic and leads to question whether its use is meaningful in our discipline (Dunnell 1992). The adoption of two or more different definitions of "site", might lead to different distributional maps (observed patterns), which will consequently lead to different outputs in the analysis and to a different interpretation of the empirical reality. This is undoubtedly derived from limits in our methods and knowledge, but its deeper root resides in the way we conceive and represent reality.

[3] This triadic structure is an extension and adaptation of the epistemic/aleatoric dichotomy suggested in other disciplines (see for instance Agarwal *et al.* 2004).

The third type of uncertainty is instead derived from stochasticities embedded in the physical phenomena under investigation. This could affect for instance the reservoir effect in radiocarbon dating, or random fluctuations of the total organic contents of lake sediments where the intrinsic uncertainty is simply unavoidable, and must be handled accordingly.

To analyse past settlement patterns, we need to tackle all three types of uncertainty in both spatial and temporal domains. While the third type of uncertainty is still relevant, its intractability allows only a formal acknowledgement of its existence. Uncertainties of the first two types are, on the other hand, domains where rooms for improvements are still existent from both methodological and theoretical standpoints. Possible endeavours in this direction should ideally start from the data collection stage, where specific choices (e.g. how to define a site, what materials to collect, etc.) could drive the future direction of inquiry. In practice this is not always possible, as archaeologists do not always have the possibility to collect new data in the way they want. This unavoidably forces many scholars to cope with the uncertainties in data collected by others, perhaps because the intended aim of the data retrieval was originally different (e.g. conservation vs. research), or simply because of a lack of rigour in the original method of data collection. Jōmon archaeological data is undoubtedly an example of the former case. The great majority of Japanese archaeological data has been collected from rescue excavations (Tsude 1995), with the intent to retrieve the broadest range of information without any explicit research question.

3.2.1 Spatial Uncertainty

Spatial uncertainty will be affected primarily by three types of problems: taphonomic processes, sampling strategy, and unit definition.

Taphonomic processes will filter the relationship between the observed pattern and the process we seek to understand, and if ignored, could determine strong biases in our inferential exercise. A typical example is the movement of small artefacts both in inter-site and intra-site contexts (Rick 1976, Gregg *et al.* 1991,

Brantingham *et al.* 2007), although this plays a marginal role for settlement pattern analysis. A much more relevant process is the chance that objects of analysis are physically destroyed (see Dewar and McBride 1992, Surovell and Brantingham 2007, Surovell *et al.* 2009). This could either occur as a consequence of natural events (e.g. earthquakes, floods etc.), or by means of anthropic destruction. The main issue of such a family of processes — referred to as *thinning* in the jargon of spatial statistics— is that it often has a non-random spatial structure and can potentially be indistinguishable from some form of induced spatial dependence. For example, certain regions might be prone to flood events, and hence thinning process might be stronger, leading ultimately to a lower concentration of recovered sites. If such a geomorphological process is ignored, the observed pattern can be mis-interpreted as a consequence of past decision-making, and described as a negative (repulsive) form of induced spatial dependency. It is vital to point out that these post-depositional events are not forms of uncertainty, but rather aspects of the archaeological patterning that can be accidentally neglected despite their critical consequences. The whole issue has deep theoretical implications (see discussion in middle range theory and behavioural archaeology; Binford 1977, Schiffer 1987) and will not be further tackled here. Nonetheless it is important to point out that such additional layers of post-depositional events will most likely filter the relationship between pattern and process, an aspect which is ignored in the spatial modelling tools developed in other disciplines.

The second form of spatial uncertainty is derived from the sampling strategy adopted by archaeologists. Several authors have discussed its implication from a strategic point of view (see Orton 2000, and references within), but less attention has been dedicated to data retrieved from rescue excavations within the context of urban expansion. In such a case, the discovery of the actual archaeological sites will be partly function of the modern population density and urban planning, which might lead to some form of patchiness in the intensity of investigations. The presence of "new town" developments in southern Kantō region in Japan, where the concentration of archaeological investigation is extremely high (see section 2.3),

is a good example of how this could lead to an illusory form of induced spatial dependency, which is ironically still dependent on the decision-making of settlement processes, although not of the period we are interested in.

The last form of uncertainty is derived from ambiguities and fuzziness in the definition of the spatial unit of analysis (Wandsnider 1998). This could refer to the living contexts that we are interested in (e.g. how to define the extent of a settlement) and the distorted remains we find in the archaeological fieldwork (e.g. how to define the extent of a site). In both domains, the problem is centred on the fact that we often rely on units that are aggregation of multiple *atomic* components (e.g. single residential units for settlements or artefacts for sites). These are generally grouped according to some "meaningful" criteria, usually expressed in some form of spatial proximity rule. For example, settlements can be defined as the spatial manifestations of living communities, with the latter defined as "group of persons who normally reside in face-to-face association" (Murdock 1949, cited in Trigger 1968), and similarly a site can be defined as "a *spatial cluster* of cultural features or items, or both [...] defined by its formal content and the *spatial and associational structure* of the population's cultural items" (Binford 1964, cited in Dunnell 1992, emphasis added).

The fuzzy nature of these definitions becomes all too obvious when the unit of analysis needs to be formally defined in practice. From an archaeological viewpoint this is a two-stage process, where we first need to define the unit on the basis of the observed empirical data (e.g. the distribution of artefacts) in relation to the chosen sampling strategy, and subsequently establish its relation to the behavioural context which produced the observed pattern (compare with Schiffer's distinction of *systemic* and *archaeological* contexts; Schiffer 1972). The ambiguous and often uncritically adopted equation "site=settlement" offers an example of how this can become problematic, with consequences that extend to the analytical and interpretative phases of the research.

Figure 11 shows an example of this. The left panel shows the location of Jinmeijinja site in Chiba, with its excavation area shown in shaded grey and the recov-

ered Jōmon pithouses depicted as black dots. As many other rescue excavations in Japan, the definition of ”site” is an idiosyncratic artefact of the recovery process. Emergency excavations fostered by the construction of a new golf club might aggregate to an individual ”site” an extremely wide variety of cultural artefacts; similarly the excavation of a large medieval castle will often lead earlier findings to be recorded as if they matched the spatial extent of the later castle. Jinmeijinja shows the consequences of such a practice, the most prominent cultural phase of the site is not dated to Jōmon period, and as such two pithouse with an inter-distance of over 200 meters are recorded as part of the same site. The right panel of figure 11 shows instead the location of Mukoaraku and Rokutsuu sites, also from Chiba. In this case two Jōmon pithouses attributed to two different ”sites” have an inter-distance of only 35 meters. The example of these three sites clearly shows how adopting the equation ”site=settlement” is misleading, and could result in major divergence in the spatial pattern as a pure function of how we define the unit of analysis. If we adopt this equation, the presence of large sites will increase the average settlement size (i.e. the number of recorded residential units per site will increase), while the fragmented allocation of a new residential area in smaller sites will result into the artificial creation of multiple settlements.

The problem of spatial uncertainty and unit definition can be approached in two distinct ways. The simplest solution involves the adoption of inseparable atomic units (e.g. single residential units, or single artefacts) and entirely avoid the process of aggregation. The theoretical advantage of this approach has, however, several limitations in practice. Firstly most archaeological data-sets cannot sustain such a qualitative detail. Exact locations of single surface artefacts in archaeological surveys are in most cases unavailable and spatial coordinates are usually associated with arbitrarily imposed units (e.g. a grid). Similarly the precise location of Jōmon pithouses within the excavation area is sometimes unknown, especially when only preliminary reports are published. The practical solution in this case is to adopt an alternative aggregation criterion that purposely sidesteps any explicit linkage to the underlying spatial process (e.g. a grid overlaid on the landscape has

no relation to the human settlement process). This will provide several benefits, most notably the faculty to replicate the process of aggregation, but nonetheless complications such as the modifiable areal unit problem[4] (MAUP, Openshaw 1984) might still arise, possibly biasing the results of the spatial analysis. The second drawback of this approach is when we acknowledge that the agency of the process generating the observed pattern is not located within atomic units, but on higher-level aggregates. For example, some decision-making might occur at the group or settlement level, and hence ignoring the presence of these aggregate entities might obscure our vision of the past.

The second solution is to adopt aggregate units. As discussed above, the main problem here resides on how we define these units. The first step involves the selection of a model and the explicit definition of the aggregation criterion. For example, one could use a threshold distance of ca 150 m, on the basis of the so called "hailing distance", which suggests a spatial limit of interaction based on acoustic properties (Roberts 1996), or alternatively choose some form of density-based threshold derived from the empirical data. For the purpose of this thesis, the advantage of using aggregate units is the possibility to have a direct relation to the clumped/dispersed model, as each group can be associated with specific size expressed in terms of number of pithouses. On the other hand, this approach filters the data by imposing a unique defining criterion for groups or settlements, and differences in the details could lead to divergent analytical outcomes. Clearly no solution can be provided for such a form of uncertainty, unless a unified, formal, and quantifiable definition of settlement is available. If this is not the case, one should opt by choosing different criteria, and explore their effects in the ultimate analytical output. Such a *sensitivity analysis* does not solve the problem of this form of spatial uncertainty, but can determine whether this can affect the output of spatial analysis.

[4]The modifiable areal unit problem refers to statistical biases derived from the process of aggregating point data into discrete spatial units such as polygons and grids.

3.2.2 Temporal Uncertainty

The role of time has long been discussed in archaeology (Plog 1973, Bailey 1983, Ramenofsky 1998, Murray 1999, Karlsson 2001, Holdaway and Wandsnider 2008), and a portion of such a literature has been dedicated to the uncertainties of chronometry, both within the domain of absolute scientific dating methods (Buck *et al.* 1996, Buck and Millard 2003), and the long lasting tradition of relative chronologies based on artefact studies (see Lyman and O'Brein 2006 for a review). Despite a shared awareness of the limitations of archaeological chronometry, it is surprising how often the implication of temporal uncertainty in the spatial domain has been largely ignored, with few exceptions limited to theoretical considerations (Rouse 1972, Dewar 1991, Dewar and McBride 1992, Lock and Harris 2002), and even fewer cases of actual implementation where temporal uncertainties are formally tackled in spatial analysis (but see Johnson 2004, Crema *et al.* 2010, Green 2011, Grove 2011).

The fundamental cause of chronometric uncertainty resides in the fact that "time is a physical process that has no physical existence" (Ramenofsky 1998:78). Thus, time cannot be directly measured but needs to be inferred from observed changes in the physical properties of objects. Whether this process is accurate and quantifiable (e.g. the radioactive decay of carbon isotopes) or constrained by the limits of qualitative descriptions (e.g. the presence/absence of decorative traits on potsherd), physical properties will act as key variables and parameters of a *model* of time. Hence, errors in their quantification (spawned by errors in measurements), or biases in the model itself, will inevitably lead to some form of uncertainty (Crema 2012). An additional source of problems resides in the distinction between *dated event* and *target event*(Dean 1978). The former refers to the actual object being dated, while the latter is what we seek to date. Congruence between the two occurs in cases we are interested in dating specific artefacts, but very often this is not what we pursue and the dating process becomes indirect. For instance, a projectile point might be indirectly dated through the radiocarbon analysis of a charcoal fragment recovered in the same context unit, and similarly Jōmon resi-

dential units are usually dated through objects recovered from its floor deposit. Needless to say, indirect dating adds an additional layer of uncertainty in archaeological chronometry.

The increasing availability of scientific dating techniques (see Buck and Millard 2003), has undoubtedly overcome many of these problems by providing a direct quantification of the uncertainty embedded into *dated events*. Calibrated radiocarbon dates offer measures of time expressed in probabilistic terms, and the adoption of Bayesian inference (Buck *et al.* 1996) extends this by means of a formal and quantitative description of *target events* (see for instance the dating of archaeological phases in Buck *et al.* 1992). However in the great majority of cases, the temporal dimension of archaeological record is expressed through the adoption of some categorical definition of time. We see more often sites dated to relative temporal units (e.g. Late Bronze Age, *Kasori E* pottery phase, etc), rather than precise absolute chronologies (e.g. between 3330 and 2870 BC). As mentioned in section 2.2.1, this is common in Jōmon archaeology, where the extraordinary amount of recovered potsherds led most scholars to exclusively rely on a relative chronological framework.

While the adoption of such temporal units provides undeniable merits (e.g. low costs, immediate dating on the field, etc.), especially compared to costly scientific dating techniques, the uncertainty embedded in these chronological frameworks can be extremely problematic. Firstly, temporal units can be regarded as conceptual blocks "imposed on the continuum of time" (Ramenofsky 1998:75), often based on separations that are simpler in diagnostic terms (e.g. the presence of a specific trait in the pottery design), but not necessarily correlated with the breaks desired for a certain research objective. Furthermore, the absolute duration of these temporal units is often unknown, and in the best cases their boundaries are imprecise and fuzzy. While methods for describing such a fuzziness in terms of probability distributions are available (see Naylor and Smith 1988, Buck *et al.* 1992, Ziedler *et al.* 1998), in the great majority of cases the boundaries of these units are defined without the explicit acknowledgement of the underlying uncer-

tainty. From the perspective of spatial analysis two major problems arise from the adoption of such a chronological framework.

First, differently sized temporal units will lead to a different diachronic patterns. The phenomena is similar to the modifiable areal unit problem mentioned above; different chronological framework will determine different sequences of temporal snapshots, and hence lead to uncertainties in the analytical outcome (Dewar and McBride 1992, Crema *et al.* 2010). Figure 12 shows an abstract example of how slicing the time-continuum with different units might determine different spatial patterning. The sequences A-B-C-D and A'-B'-C'-D' are spatial patterns (here reduced into a single dimension) derived from the subdivision of the same spatio-temporal process, portrayed here as a series of archaeological events with different durations in time (vertical bars). Although the phenomena being investigated is the same, the two sets of temporal slices (shown here as horizontal lines, with events depicted as squares) will most probably lead to different interpretations and analytical outcomes.

Second, insufficient quality and quantity of the *dated event* might lead to a chronological attribution spanning multiple phases. For instance, the lack of diagnostic traits might lead a scholar to adopt a wider chronological definition, encompassing multiple temporal units where the observed traits are shared. Such forms of uncertainty are extremely common when indirect dating is sought, since the quality and the quantity of diagnostic artefacts, along with the level of coherence of their chronological attributes, will lead scholars to adopt wider chronological definitions. For example, ca 85% of a sample of over 6,500 Jōmon pithouses from south-west Kantō region have been attributed to two or more phases due to a sufficient quality/quantity of diagnostic pottery sherds (Suzuki 2006, Crema 2012). Similarly, Bevan and colleagues (in press), have shown that pottery recovered from archaeological survey on the Greek island of Antikythera exhibits high levels of uncertainty, with chronological attribution often characterised by multiple phases that are not necessarily chronologically adjacent to one another.

An example of the consequence of this form of temporal uncertainty can be

observed in figure 13, where a subset of pithouse locations at the Middle Jōmon site of *Ariyoshi-minami* in Chiba is shown. If a researcher wishes to determine the spatial distribution of residential units during the *Kasori EIII* phase (shown as red dots in the map), she or he must take into consideration units having finer (dots in darker grey tones) and coarser resolutions (dots in lighter grey tones). The variation in the temporal uncertainty is remarkable in the specific case, as some residential units have a defined interval of possible existence which is less than a century, while others are attributed to broader ranges of one or more millennia[5]. The most common approach to solve this type of problem is to use the coarsest chronology available or to exclude records with insufficient degree of knowledge. Both approaches are unsatisfactory, as the former will limit the range of possible research questions, while the latter might exclude a considerable amount of information (in this case more than half of the dataset) and is not always applicable (see the black dots labelled *Transition to Kasori EIII* which are only partially within the duration of *Kasori EIII*). The example of *Ariyoshi-minami* clearly suggests the necessity to adopt a different solution.

3.2.3 Aoristic Analysis and Monte Carlo Simulation

While methods for dealing with the problem of spatial uncertainty are widely available, partly due to the shared problem of unit definition found in other disciplines, the problem of temporal uncertainty is more complex and deserves a slightly longer discussion than its spatial equivalent. Solutions developed in other disciplines cannot be directly used or imported to cope with the unusual problems found in archaeology, and hence addressing these issues requires the development of new methodological and theoretical frameworks.

Approaching the problem of temporal uncertainty requires a two-stage process. First, uncertainty must be formally quantified. While this is not an issue for most scientific dating methods (which already provide detailed probabilistic models of the temporal attribution) relative chronology, indirect dating, and multi-

[5]Recall that most hunter-gatherer pithouses have a life span of few decades at most

phase temporal definitions (as in fig. 13) all require formal quantifications of uncertainty. Second, quantified chronological uncertainties must be fully integrated and formally acknowledged in the archaeological analysis and its output, and not lost somewhere in the course of the research process.

The first problem —uncertainty quantification— requires some method for transforming categorical and relative definitions of time into probabilistic descriptions similar to those offered by scientific chronometry. The key concept, which supports this translation from qualitative to quantitative description, is embedded in a widely adopted and almost commonsensical notion about uncertainty: in complete absence of knowledge, any possible event can be regarded as having an equal chance of occurrence. This concept is known as the *principle of insufficient reason* (also known as *principle of indifference*, or *equal priors*; Sinn 1980, Mcgrayne 2011) and was first generalised by Pierre-Simon Laplace more than 200 years ago. The formal implementation of such a principle is the adoption of a uniform probability distribution, where two parameters —a and b— express our thresholds of knowledge, and are derived from the expected maximum and minimum values. Within the context of relative chronology, this means that given an event e attributed to a temporal unit T bounded by a_T and b_T, the probability of its occurrence will be the same for any equally long portion of T, as long as: (1) no additional information is available; and (2) the event has a negligible duration in time.

The first assumption is a crucial justification for adopting a uniform probability distribution. Any additional information should in fact be incorporated, effectively modifying the shape of the probability distribution. This process constitutes the core of Bayesian inference (Buck *et al.* 1996), where uniform probability distribution can act as a *prior* that will be combined with any additional knowledge to produce what is called a *posterior* distribution, the updated version of the original probability distribution. In practice, this is not always simple, as the dating process is in most cases based on expert knowledge that is difficult to conceptualise, never mind to quantify precisely. Bevan and colleagues (in press) for instance use the expert definition of pottery phases in terms of degree of belief, quantitatively

expressed in probabilities (e.g. 0.4 Early Bronze Age, 0.6 Middle Bronze Age). The second assumption —a negligible duration of the target event— is a slightly more complex issue from a mathematical standpoint, especially if the actual duration of the event is unknown. Strictly speaking no events have a complete absence of duration, and hence any use of a uniform probability distribution can be regarded as an approximation, where the temporal length of the event is treated as negligible. From a practical point of view this depends on the scale of observation. If we are looking at multi-millennial dynamics, an event of five years could be considered as almost instantaneous, while if the processes we are interested in have a decadal scale this approximation can no longer be supported. In the latter case one could still use the principle of insufficient reason, assuming that any possible allocation of the event e within the temporal unit T has the same probability of occurrence. This approach can be still applied even when the duration of the event is unknown. In such a case any possible duration of the event (with a maximum value corresponding to the length of the temporal unit itself) along with all possible ways to allocate the event within T will have an equality probability (see online supplementary material in Crema 2012).

The adoption of equal priors for tackling the problem of temporal uncertainty has been first introduced in the field of criminology, where unknown crime events are often bounded by a *terminus ante quem* and a *terminus post quem*, in a way strikingly similar to the vast majority of archaeological record. The implementation of such a solution has been suggested by Jerry Ratcliffe —under the name of *aoristic analysis* (Ratcliffe and McCullagh 1998, Ratcliffe 2000)— who needed to construct time-series of crime events and was limited by the presence of data-sets showing different levels of temporal uncertainty. His solution involved the following three steps (fig. 14):

1. Divide the time-continuum into equally sized discrete segments (*time-blocks*) choosing a specific size (temporal resolution).

2. For each event e define its *time-span*, defined as the interval of time within

which the event might have occurred, and round its length to the chosen temporal resolution (event **a** in fig. 14).

3. For each event, define the *aoristic weight* for each time block within its *time-span*, as the reciprocal of the number of time blocks within the *time-span* itself (i.e. 1 divided by the number of time-blocks within the *time-span* of e). As a result, events with longer time-span (e.g. **c** in fig. 14) will have smaller aoristic weights compared to those with shorter time-spans (e.g. **b** in fig. 14).

Such a three-step algorithm is clearly an implementation of a uniform probability distribution, where the boundaries of each *time-span* are the parameters a and b introduced above. In fact, if we assume a simple continuous uniform distribution, the rounding in step 2 becomes unnecessary, although the aoristic weight (which is essentially the probability of existence) will not be equal for all time-blocks related to a specific event (Crema 2012, see also event **d** in figure 14).

As mentioned above the duration of the event should be short compared to the scale of observation. An useful heuristic for evaluating this is to compute the ratio between the average duration of the event and the length of the temporal block. If this is sufficiently small (i.e. $< 0.05 \sim 0.1$) one could safely ignore the effect derived by the duration of the events [6]. If this is too large one should opt for larger temporal blocks.

Adopting an aoristic approach thus requires the knowledge of the time-span of each archaeological event. For relative chronological frameworks this means that we could simply translate the relation between the sequence of temporal units (e.g. the sequence of archaeological phases) and the time-span of each event into a sequence of probability values (aoristic weights) based on *a priori* defined subdivision of the time continuum in equally long time-blocks (see fig 15).

[6]The problem of events with long durations is the possibility that these can potentially exists in more than one time-blocks. The probability of such an event can be computed with the following equation:

$$P = \frac{(d-1) \times (N-1)}{N \times r}$$

where d is the duration of a event, N is the number of time-blocks within the time-span of existence, and r is the resolution of the time-block.

Once the temporal uncertainty of each event is measured in probabilistic terms (either through aoristic analysis or other means such as scientific dating or Bayesian inference), the new information should be integrated into the actual spatial analysis, which can be computed for each of the artificially created temporal blocks. Two different approaches can be adopted to do this. The first one involves the use of weighted analyses, where the contribution of each observation to the assessment of the general pattern will be proportional to its aoristic weight. The second will instead use simulation-based techniques to create a series of artificial data-sets, which will be separately examined and combined in probabilistic terms.

Early applications of aoristic analysis offered the simplest form of weighted analysis, which involves the sum of all aoristic weights for each temporal block (see for instance Ratcliffe 2000:fig.2) . This creates a time-series that illustrates the variation in the intensity of the process over time (e.g. crime events or deposition of potsherds), weighted by our degree of knowledge. Archaeological applications of aoristic sum has been offered by Ian Johnson (2004), who also proposed a standardised version of the analysis to better compensate for the correlation between the length of the time-span and the date of the artefact (more recent artefacts generally exhibit shorter time-spans). The same concept of weighted analysis can be also extended to spatial pattern assessment. For instance Crema, Bevan, and Lake (2010) have assessed the spatial locations of Jōmon pithouses by calculating the shift of the weighted mean centre of distribution, while more recently Grove (2011) has examined the spatial pattern of mesolithic sites from Atlantic Iberia, using probability values obtained from radiocarbon dating and a weighted version of density estimates.

The main limit of weighted analysis is its incapacity to handle problems of diachronic nature, and by the fact that uncertainty is embedded but not represented in the outcome: a low cumulative sum of aoristic weights could equally indicate the presence of few well-known events or many unknown events. Such limit can be shown with the practical example illustrated in figure 16 (see also Crema 2012). The aoristic sum shown on the left is derived from three events, showing an in-

crease from time-block t_1 to t_2, followed by a decrease from t_2 to t_3. Since the number of possible permutations is only four (scenario A, B, C, and D on the right of 16) we can actually calculate the probability of all possible dynamics that might have occurred using the *multiplication rule*[7]. The results shows how the time-series suggested by the aoristic sum (increase followed by decrease) occurs only for scenario A (with probability 0.4), that the pattern which has the highest probability is an uniform number of events over time (scenarios B and C, with a total probability of 0.5), and that there is a 10% chance that a decrease was followed by and increase (scenario D).

The example shown in figure 16 suggests how the adoption of weighted and cumulative measures have strong limitations for assessing dynamics of change. Furthermore, weighted data requires additional layers of complexity for their computation that limits the straightforward application of available tools. The most direct solution to such a problem is offered by the example on figure 16 and consists of calculating the probability of each possible permutation and combine the results in order to express, in probabilistic terms, the likelihood that a specific pattern occurred. Thus, for example, one could evaluate the spatial pattern of each time-block by independently analysing every possible permutation and sum the probabilities of the instances where a specific condition (e.g. a certain degree of clustering) is met. Such an approach will fully exploit the available information on temporal uncertainty, and provide statistical answers with the most precise statement of the current state of knowledge. However this becomes unfeasible when the number of events to be considered becomes high. If we wish to assess the spatio-temporal pattern of 50 pithouses, each with time-spans of four temporal blocks, we would need to compute the probability of ca 1.27×10^{30} different possible permutations (Crema 2012).

Clearly computing the probability of each permutation is unfeasible in most cases. A solution, which would avoid such a heavy computation and at the same

[7]The *multiplication rule* states that the probability of co-occurrence of two events can be computed as the product of their own probabilities. Thus for instance if the probability of event a is 0.2 and the probability of event b is 0.5, the probability of both events occurring will be $0.2 \times 0.5 = 0.1$.

time produce outputs that will maintain a probabilistic nature, is the application of Monte-Carlo methods. The name of said technique refers to a wide range of different simulation-based approaches for solving complex computational problems by means of repeated sampling from defined probability distributions (Robert and Casella 2004). The method is increasingly used in archaeology: Buck, Litton, and Smith (1992) have used it for Bayesian calibrations of radiocarbon dates; Lake and Woodman (2000) have assessed the site location of hunter-gatherers in relation to the visibility of the surrounding landscape in the Scottish Island of Islay; and Whitehead and colleagues (2008) have analysed the ancient water supply system of the Early Bronze Age site of Jawa in Jordan.

The extreme flexibility of Monte-Carlo methods offers a simple solution for integrating temporal uncertainty in the spatio-temporal analysis, providing at the same time a probabilistic assessment of the observed patterns. This can be achieved with the following workflow:

1. Measure the temporal uncertainty of each event as a discrete probability distribution defined by the temporal blocks $t_1, t_2, ...t_n$.

2. Randomly sample from these distributions, so that each event will be associated with one, and one only, temporal-block (e.g. t_4).

3. For each temporal block obtain some statistical measure X of the events (e.g. total counts, average spatial inter-distance, etc.)

4. Repeat step 2 and 3 s times

5. Obtain the distribution of X (with length s) for each time-block.

This sequence of steps allows the creation of s spatio-temporal patterns that might have occurred given the knowledge derived from our probabilistic definition of temporal uncertainty. Each simulated data-set will not have uncertainty associated with its events, and as such, standard statistical methods for spatial

analysis can be easily applied. The repetition of such a procedure, and the consequent production of s analytical outputs (rather than a single result per time-block) will offer the basis for a probabilistic assessment of the observed pattern. If the number of simulation runs (s) is sufficiently high, the probabilistic estimate should approximate the one which can be obtained by assessing the probability of all permutations (as done in fig. 16). The workflow presented above is not dissimilar to the so-called multiple-imputation method (Schafer 1999), a widely known technique for survey statistics where missing values are simulated, in order to allow the use of standard statistical analysis on the one hand, and incorporate the uncertainty derived by such missing values on the other (see Rhode and Arriaza 2006 for an osteoarchaeological application of this).

There are other benefits derived from this method. One could in fact simulate possible durations of each event (Crema 2012), or assume that some have conditional probability distributions, and hence add an additional knowledge in our pattern recognition exercise. The latter is particularly relevant when some topological relation between events is known. For instance if event b is known to have occurred right after event a, then we could simulate first the latter, and then sample a possible time-block for b, given the newly obtained temporal definition of a, ensuring consequently the maintenance of the topological relation (see fig. 17).

3.3 Detecting instances of Dispersed and Clumped Patterns

The combination of aoristic analysis and Monte-Carlo simulation offers a straightforward solution for measuring and integrating temporal uncertainty in the analysis of settlement patterns. Having established such a framework, we then need to choose a method which can provide a direct answer to the first research question of this thesis — whether Jōmon settlement pattern exhibited repeated changes between clumped and dispersed patterns over time. In section 3.2.1, I have pointed

how the problem of spatial uncertainty could be potentially solved in two distinct ways: (1) find a suitable parameter-based criterion for aggregating pithouses into clusters comparable to settlements, and conduct a *sensitivity analysis* to explore the effects derived by parameter variation; and (2) shift the unit of analysis from aggregate units (settlements) to atomic units (individual pithouses). The former has the advantage of being directly compatible to the nature of the research question, which requires a pattern recognition exercise of the evolution of group (settlement) size distribution. The latter lacks such a straightforward link to Uchiyama's distinction between clumped and dispersed patterns, but is more robust, as it is independent from how we define our unit of analysis.

3.3.1 Group Size Distribution Analysis

The first necessary step for investigating the size distribution of Jōmon settlements is to establish a criterion for aggregating its atomic components (residential units). In the absence of additional information, the simplest solution is to adopt a parameter-based cluster algorithm that ensures the possibility to determine the effects of different assumptions in the analytical output. In the specific case, the basic assumption is that spatial proximity is a proxy of higher likelihood of interaction, and hence a defining criterion of a settlement.

Giving these assumptions, the necessary criterion for defining the analytical unit should ideally be a clustering algorithm with some parameter defining the spatial range (limit) of aggregation. Most common hierarchical cluster analyses will do this, as the output tree can be ideally cut into segments based on defined thresholds. However these methods have not been explicitly designed to deal with spatial data, where arbitrary shape of the clusters and differences in density might play an active role in defining groups. One possible algorithm, which solves many of these problems, has been proposed by Ester and colleagues (2009). Their DBSCAN (Density Based Spatial Clustering of Applications with Noise) [8] is based on two parameters: *eps* (the spatial threshold distance); and *mnpts* (the minimum

[8]The clustering algorithm is implemented in the *fpc* package in R (Hennig 2010)

number of points necessary to form a cluster). We can safely set to a single unit the latter parameter (allowing the possibility to have groups with one residential unit), while *eps* should be swept across a range of values in order to evaluate the sensitivity of its variation in the final output.

Once we have established how to create our basic unit of analysis we need to determine what we need to measure. Since the definition of clumped and dispersed patterns are entirely based on the difference in sizes between settlements (see section 2.4), we can treat our observed data as a set $D = \{x_1, x_2...x_n\}$, where x denotes the number of residential units associated with each of the n observed settlements. We thus need to describe D with some quantitative measure that will indicate its relationship to the theoretical description of clumped and dispersed pattern. The former will be characterised by a few large groups and many smaller ones (eg. $D_{clumped} = \{100, 4, 3, 5, 60, 2, 1, 1\}$), while the latter will be characterised by a more uniform size distribution (e.g. $D_{dispersed} = \{20, 18, 22, 17, 12, 24, 21\}$).

Most standard summary statistics (such as mean, or median) are not suited for distinguishing these two forms of distributions. A simple and widely adopted alternative consists of ranking the sizes of the settlements and plotting the logarithm of these against the ordered logarithm of the ranks. Such a *log-log* plot provides the basis of a family of *rank-size* analysis, and offers a method for describing a wide range of different scaling systems, from plant communities (Collins *et al.* 2008), to the severity of terrorists attacks and surname frequencies (Bentley *et al.* 2009). One commonly found property of these scaling systems has been summarised by the following equation (Zipf 1949):

$$S_r = S_1 \cdot r^{-q} \tag{3.1}$$

where the size of a given observation (S_r) can be predicted if its rank r, the size of the largest observation (S_1), and the constant q are known. Equation 3.1 essentially establishes a power-law relation between size and rank, a relationship visible from how the observations are along a straight line on the *log-log* plot. The

exponent q is crucial in this model, as it will determine how this relationship is substantiated. When $q > 1$, highly ranked observations dominate with their sizes, while when $q < 1$ a more uniform distribution of sizes can be observed. Zipf (1949) defines q as the balance between *forces of unification*, which push single subunits defining the sizes (e.g. single residential units in the case of settlement sizes) towards few aggregations (e.g. settlements), and *forces of diversification*, which foster the maximum dispersion of the subunits. When the two forces are in equilibrium, q will be equal to one and the observed distribution will be known as *Zipfian* (or *Zipf's law* distribution).

This equilibrium point can be used as a theoretical boundary for distinguishing settlement systems characterised by the dominance of few large groups (i.e. clumped pattern), from those where the system is less integrated and with a more uniform distribution of sizes (i.e. dispersed pattern). The former will have $q > 1$, and is often referred to as a *primate* distribution; the latter will have $q < 1$, and is labelled as *convex* distribution. In an extensive review and comparative study of historical data, Johnson (1980) provides a wide range of settlement size distributions, showing how higher or lower level of system integration could easily determine deviations from the theoretical *Zipf's law* distribution. However, these deviations do not always follow a straight-line. Falconer and Savage (1995) have shown how in some cases the forces of unification and the forces of diversification act at different ranks, effectively leading to a mixed non-linear relationship between rank and size. This often has a *primo-convex* shape, where at higher ranks a primate pattern is evident and at lower ranks a convex pattern can be observed, or a *double-convex* shape, where a much more complex relationship between the two forces becomes apparent (see figure 18).

Savage (1997) offers a literature review with a wide range of explanations and expectations for each type of settlement size distribution depicted in figure 18. These include colonial processes, relation to theoretical models, sampling issues, and co-existence of multiple settlement systems. Details of Savage's review will not be illustrated here, as most of these models refer to urbanised societies and

hence not applicable in this context. Furthermore, it should be noted that rank-size analyses will be used exclusively as a pattern-recognition tool, and the ultimate interpretation of the output will be independent from these models, and will instead be made in conjunction with the output of agent-based simulations.

Estimating q on the basis of the sample distribution is a relatively simple exercise of linear model fitting, and several authors (e.g. Falconer and Savage 1995, Savage 1997) have used basic statistical analysis to test against the null hypothesis of a Zipfian distribution. In practice however size distributions do not always fit a log-linear model (i.e. the observed rank-size plot might not be a straight line), and hence the estimated value of q might not necessarily be a robust proxy for distinguishing primate and convex distributions. Disciplines other than archaeology have overcome this issue by developing alternative models such as multi-fractal distributions (Haag 1994) or Double-Pareto lognormal distributions (Reed and Jorgensen 2004). These models are often very complex, and not necessarily useful for fitting a wider range of patterns. Furthermore, since the primary goal here is to describe the set of settlement sizes D, a much simpler method is desirable.

Drennan and Peterson (2004) provide a useful solution in this regard. Their A-coefficient quantifies the shape of the rank-size curve by calculating the area above and below a standardised log-log plot. This can be achieved with the following steps (see also figure 19):

1. Based on the observed number of units (n), and the size of the largest settlement S_1 compute equation 3.1, and obtain the expected size for the other settlements $\hat{S}_2, \hat{S}_3 ... \hat{S}_n$.

2. Standardise the log-log plot so that the difference $log(S_1) - log(\hat{S}_n)$ and $log(n) - log(1)$ are both equal to $\sqrt{2}$. Thus the area above the Zipf's law curve (which will be the diagonal cutting a square with edge size $\sqrt{2}$.) will be 1, as well as the area below it.

3. Plot the observed transformed sizes $S_2, S_3 ... S_n$. Notice that that smallest set-

tlement might have a value smaller than $\hat{S}_n$, and thus plotted "outside" the square defined by the Zipf's law diagonal.

4. Compute the area above the Zipf's law diagonal and below the observed rank-size curve (A_1), and then the area below the diagonal and above the empirical data (A_2). Notice that the maximum value for A_1 is by definition 1, while A_2 could exceed 1 for strongly primate systems where one or more observed settlement sizes are smaller than $\hat{S}_n$.

5. Finally, compute A as the difference $A_1 - A_2$.

Generally speaking, the resulting A coefficient will indicate a convex pattern (thus a dispersed pattern) with positive values of A, a primate (clumped) pattern for negative values, and a Zipf's law pattern when $A \approx 0$ (see figure 20). Thus, Drennan and Peterson's method offers a tool for directly assessing the continuous spectrum of variation between clumped and dispersed pattern using a single value, whose time-series could offer a way to test Uchiyama's hypothesis of cyclical change in the Jōmon settlement pattern.

There are however some limitations to this method. First, recall that A is the difference between A_1 and A_2. This means that in case of primo-convex, double convex or any other mixed pattern (as the ones shown in figure 19), the two values might be similar (and hence A will approach to 0), giving a false impression of a Zipfian distribution. A simple solution will consist of visualising the rank-size plot, or to produce as an output both A_1 and A_2.

Second, as Drennan and Peterson note, A-coefficient (along with other rank-size analyses) is strongly affected by sampling bias and hence the robustness of the observed value should be properly assessed. Since parametric tests are not feasible they suggest that a confidence interval of the observed A should be calculated using bootstrap techniques. This procedure will consist of resampling with replacement the observed settlement sizes for n times, compute for each the A coefficient, and then "shift" the observed distribution of A so that the mean will match the result (i.e. the empirical A) obtained from the raw dataset. Drennan

and Peterson note that the resulting distribution is not always normally shaped, and hence a quantile-based definition of the confidence interval should be used instead of standard Z-scores. This is not surprising as an observed primate distribution might easily be resampled as a Zipf's law or convex distributions if the largest settlement is not picked during the bootstrapping, leading to a bimodal distribution of possible values of A.

Third, in case the A-coefficient analysis is applied for count assessment of sizes there is a potential bias towards positive values, caused by the fact that the system is "bounded" for smaller values (i.e. there is limit threshold for the smallest size). A practical example can show why this could occur. Consider a distribution with 20 observations, with the highest settlement size S_1 equal to 15 units (e.g. 15 pithouses). According to equation 3.1, the smallest settlement ($\hat{S}_{20}$) should have 0.75 units with $q = 1$, which is clearly impossible. All settlements with $r > S_1 = 15$, will in fact have observed sizes above the expected size for a Zipf's law distribution, leading to a bias towards higher values of A_1. In practice this will not determine big differences in the results, as observations with lower ranks have smaller impact to the overall computation of A due to the logarithmic scale of the rank-size plot. However, in case the number of observations is high, or when the size of the largest settlement is comparatively small, the effect could be more prominent. A modified version of the A-coefficient where only settlements with ranks between $r = 1$ and $r = S_1$ (thus for the above case: $D = \{S_1, S_2...S_{15}\}$) are considered can remove this bias. This provides a partial description of the phenomena (the upper-tail), but will still offer a valid proxy for identifying clumped and dispersed patterns.

3.3.2 Spatial Analysis

As mentioned earlier, the second approach for tackling the problem of spatial uncertainty consists of adopting as the basic unit of analysis the most atomic available observation. This has the main advantage of overcoming the problem of how to define aggregate units, but leads to question how to relate the observed spatial pattern of residential units to the theoretical distinction between clumped and dis-

persed patterns. It is thus important to note that the objective here is not to provide an alternative to the A-coefficient analysis, but rather to seek a complementary tool where the primary aim is to describe the spatial distribution of Jōmon pithouses (rather than the size distribution of settlements). Ideally this will offer insights that are perhaps not directly comparable to Uchiyama's distinction, but nonetheless can highlight properties that might be relevant for understanding the observed phenomena.

From the perspective of a single residential unit, the distinction between clumped and dispersed pattern can be described as follows (see fig. 21). We first define e as one of the residential units, and $\lambda(d)$ as the density of other units at a distance d from e. When the size distribution is strongly primate (i.e. clumped), most residential units will be clustered in one location, while the remnant units will be sparsely distributed in the landscape. This means that if e is part of the largest cluster, the curve $\lambda(d)$ will be initially high, and then will decrease over distance. In contrast if e is part of one of the smaller settlements, the curve will be still initially decreasing, but will reach a sudden peak when d is equivalent to the distance to the largest settlement. On the contrary if the size distribution is strongly convex (i.e. dispersed), all events are likely to have similar values for $\lambda(d)$ and then depending on the inter-distance between settlements, a second peak (with similar value of λ) will be present. If we define $\bar{\lambda}(d)$ as the average of all $\lambda(d)$ from all events, we can predict that its shape will be a function of both the settlement size distribution *and* the spatial structure.

Table 4 shows some expected shapes of $\bar{\lambda}(d)$ based on different combination of spatial pattern and size distribution. The list shows how exclusively assessing $\bar{\lambda}(d)$ is not sufficient to determine whether an observed settlement pattern is clumped or dispersed, but when combined to rank-size analysis can offer a detailed insight on the spatial structure of the settlement pattern.

Recent advances in point-pattern analysis have fully integrated similar multi-scalar perspectives, effectively providing tools to explore how the spatial rela-

tionship vary at different spatial scales. Traditional methods such as Clark and Evan's nearest neighbour index (1954) or quadrat analysis (Thomas 1977), which have been, and are still widely used in archaeology (Pinder *et al.* 1979, Ebert 1992, Thompson and Turk 2009), are not suitable for such purposes, while such analyses as Ripley's K function (Ripley 1981) can offer the necessary multi-scalar perspective. Archaeological applications of the latter have been relatively successful in a wide range of contexts, including artefact level intra-site analysis (Orton 2004, Matinón-Torres *et al.* 2012), regional settlement patterns (Bevan and Connolly 2006, Mayer 2006), and meso-scale analysis of residential units (Crema *et al.* 2010).

The key concept of Ripley's K function consists of calculating the average number of observed points within a defined distance d from each focal point, and then dividing this by the global intensity of the process, obtained as the ratio between the total number of observed points and the spatial extent of the window of analysis. The result —technically referred as the sample estimate $\hat{K}$— is then compared to the theoretical value K expected from the same analysis applied to a complete spatially random process (CSR). If, at a given distance d, $\hat{K}$ is larger than K, the pattern is considered to be *clustered* at such a scale , and conversely if it is smaller it will be regarded as *dispersed*. In practice, deviations from the expected value of K will be always present, and hence spatially random points are generated through Monte-Carlo simulation in order to provide an envelope of theoretical K values to which $\hat{K}$ can be compared to.

This statistic is however an unsuitable proxy for $\bar{\lambda}(d)$, especially when high levels of clustering is known to be present at smaller scales. In fact, since K function has a cumulative nature, a strong aggregation at smaller scale will bias the results (Wiegand and Moloney 2004), leaving potentially a false impression of clustering for large values of d. Approaching the Jōmon settlement pattern by shifting the perspective to the spatial distribution of single residential units will most likely determine such a bias, since a high level of clustering at the lowest spatial scale is implied by the presence of settlements (which are by definition cluster of dwellings). An alternative statistic which can be a more direct proxy of $\bar{\lambda}(d)$

is offered by the *O-ring* function (Wiegand and Moloney 2004), a method closely related to Ripley's K, but based on density estimates within annuli rather than circles. In practice the analysis will compute the average density of neighbour points located between distances d_1 and d_2 from any given focal point i, with $d_2 > d_1$ and the difference $d_2 - d_1$ hold constant. The obtained value, which can be formally named $O(d_1, d_2)$,will be then compared to the expected density for a CSR, λ_{CSR}. The latter will be a constant, as a complete random process will have homogenous density through space, and can act as a null hypothesis. If $O(d_1, d_2) > \lambda_{CSR}$, then the pattern will be clustered at the specific annulus defined by d_1 and d_2, and conversely when $O(d_1, d_2) < \lambda_{CSR}$ a repulsive force will determine a dispersion (hence a lower density) at such a scale. As for Ripley's K function, establishing the relationship between O and λ_{CSR} is not simple, since the stochastic fluctuations in the density might lead to values slightly above or below the theoretical λ_{CSR} even if the observed pattern is truly random. In order to compensate such an effect a Monte-Carlo simulation of a CSR process can provide an envelope of λ_{CSR} to which the $O(d_1, d_2)$ can be compared.

Figure 22, shows a typical output of O-ring functions applied to three different simulated datasets. For simplicity the location of residential units has been approximated to the centroid of each hypothetical settlement, with their location and size (number of dwellings) shown on the right column. All three datasets share the same spatial structure; points are uniformly distributed, with an average inter-distance of 0.6 units and a minimum inter-distance above 0.2. Size distribution are instead different, with instances of Zipf's law ($A = -0.02$, fig. 22:**a**), primate ($A = -1.49$, fig. 22:**b**), and convex ($A = 0.88$, fig. 22:**c**) distributions. The left column shows the plots of the O-ring statistic, with the x-axis showing the distance bands and the y-axis indicating the density. The solid line represents $O(d_1, d_2)$, the horizontal dashed line λ_{CSR}, and the grey shaded area the envelope created by 100 Monte-Carlo simulation runs. As predicted by table 4, all three cases show an initial decreasing density. Clumped and dispersed patterns can be distinguished with the former showing evidence of repulsion (significantly low density) above

0.1, while the latter exhibiting attraction (significantly low density) from 0.4.

These examples of O-ring statistics briefly show the pros and the cons anticipated by the discussion of table 4. On one hand this method enables the assessment of the spatial pattern and overcomes the issue of unit definition. This provides information that is not retrievable by rank-size analysis, and offers a multi-scalar description of the empirical data. On the other hand, outcomes of the O-ring statistic assess the variation of density *over space* and hence two datasets with the same group size distribution but with different spatial pattern could easily generate different outputs. This is shown in the meta-analysis depicted in figure 23 where each plot shows the total proportion of significant clustering and dispersion within one hundred artificially created datasets of clumped ($A = -1.49$, **a** and **c**) and dispersed distributions ($A = 0.88$, **b** and **d**) with random (**a** and **b**) and uniform spatial patterns (**c** and **d**, with minimum inter-distance of 0.2). The figure show how small differences in spatial distributions sharing the same structural property still generate different outputs despite the same size distributions. The meta-analysis further supports the idea that O-ring function is not sufficient to identify whether a given settlement pattern is clumped or dispersed, but can provide information on detailed aspects of the spatial structure.

3.4 Summary

This chapter has first offered an overview of the theoretical aspects underpinning the statistical analyses that will be provided in the next chapter. Although models on the generative processes of clumped and dispersed patterns will be presented in chapter 5, discussion on the theoretical distinction between induced and inherent spatial dependency has served as a general framework for linking pattern and process.

The main purpose of the chapter has been the detailed description of the statistical tools to be used for the pattern-recognition exercise. Two analyses have been identified as the most suitable candidates for answering the first research question:

the A-coefficient analysis, which is capable of providing a numerical index for distinguishing clumped and dispersed pattern; and the O-ring function, which can offer additional and alternative insights on the spatial distribution of residential features. The former will be particularly relevant in the description of the simulation output (chapter 6 and 7) and its comparative evaluation with the analysis of the empirical data (chapter 8). The adoption of these methods is however not straightforward due to the problems arising from the spatial and temporal uncertainty of the archaeological data. The sensitivity analysis of the unit-definition criterion and the rejection of aggregate units have been proposed as two alternative solutions for dealing with the problem of spatial uncertainty, while the combination of aoristic analysis and Monte-Carlo simulation have been introduced as a technique for tackling the problem of temporal uncertainty. The next chapter will start by providing details on how the archaeological data-set of the two case studies have been pre-processed in order to realise these solutions and will then illustrate the results of spatial and temporal analysis before proceeding to offer an answer to the first research question.

Chapter 4

Applied Spatial and Temporal Analysis

4.1 Data Collection and Pre-processing

The case studies described in sections 2.3.1 and 2.3.2 offer two exceptional windows for understanding the dynamics of change in Jōmon settlement pattern, providing suitable contexts for answering the first research question (*whether episodes of alternation between clumped and dispersed pattern occurred*) using the methods introduced in the previous chapter. Chiba and Gunma are characterised by a high density of rescue excavations, fostered by modern urban expansion and the construction of a network of infrastructures covering a large portion of the Kantō region. The total number of archaeological sites in the two 15×15 km study areas exceeds 2,000 units (1249 for Chiba, 930 for Gunma) with ca 20% of them extensively excavated and published (267 for Chiba and 170 for Gunma). The spatial distribution of these sites (figure 24) is relatively uniform in Chiba, where most excavations are concentrated on the Shimousa Tableland, whereas in Gunma they tend to concentrate along the edges of the Tone and Agatsuma River valleys.

Site locations in Chiba have been obtained from the excavation reports (see appendix A) and integrated into the raw data obtained from an offline version of a webGIS published by the board of education of Chiba prefecture (url: `http://`

wwwp.pref.chiba.lg.jp/pbbunkazai/kiyaku.html, last accessed on 13th February 2012). Similarly, spatial data from Gunma has been primarily based on published reports and from the geographically referenced data publicly accessibly as a webGIS (url: http://www2.wagamachi-guide.com/gunma/top.asp, last accessed on 13th February 2012) and published by the board of education of Gunma prefecture.

To compensate for the effects of the arbitrary definition of archaeological sites (Dunnell 1992; section 3.2.1) and to reduce the bias caused by the spatially unequal intensity of archaeological investigations, the following set of procedures have been adopted. First, only sites that were known to be excavated down to the Jōmon occupational level have been considered. This allowed the detection of "non-site" locations (i.e. areas which can guarantee the absence of Jōmon features), which will assume a critical role in the implementation of the O-ring function. While this selection process had no impact on the sample size at Chiba, about 10-20 sites in the western portion of Gunma have been excluded from the analysis for this reason.

Second (see fig.25), each site was subdivided into subunits in those cases where: **a**) it was composed of multiple excavation plots; or **b**) it was a single oversized excavation plot. The former case can be found in rescue excavations associated with extremely large constructions (e.g. a golf club), where multiple and separated excavation areas have been identified by archaeologists. Each of these separate excavation plots has therefore been identified as a separate subunit. In contrast, single, oversized excavation plots have been subdivided following the procedure adopted by local archaeologists, who often identify multiple sectors within each excavation area. Each of these sectors have been identified as a subunit. This procedure provided a repeatable way to subdivide unusually large sites that were originally defined as such purely on the basis of the emergency context determining the excavation (see section 3.2.1). The purpose of this step was to standardise as much as possible the spatial extent of each unit of analysis, although this was not possible for few sites where the plans of the excavation areas were not published, in which

cases the idiosyncrasies of the data imposed often arbitrary segmentations based on the polygonal site extent defined in the webGIS. The centroids of so-obtained subunits (see fig.25:**b**) constitute the *basic unit of analysis* (BUA) for the two areas (369 points for Chiba and 221 for Gunma) and is shown in the leftmost column of figure 26 (see also appendix A).

The BUA should be conceived as the spatial distribution of "windows of analysis": portions of the landscape where the knowledge of presence or absence of observations are verified by archaeological excavations. This should ideally be represented as a series of polygonal features within which the exact location of individual residential features are depicted as point data. In practice this is not always feasible, as publications occasionally omit the shape of these polygons and sometimes even the position of the pithouses within these[1]. Thus the available information has been collapsed into a point data (where possible using the centroid of the polygons), which has then been *marked* with the aerial extent of the polygon they represent, recovered either from the excavation reports or manually computed using digitised geo-referenced maps.

While the BUA is suitable for the O-ring statistic (since each observed point corresponds to a *location* and not to a settlement or a group), the application of rank-size analysis requires further data-processing to generate group size distributions with different aggregation criteria (see section 3.2.1). In section 3.3.1 I described the basic procedure of the DBSCAN algorithm, which provides a method for aggregating point locations based on a spatial threshold parameter (*eps*). This has been applied to the BUA (see figure 25: **c** and **d**), so that clusters of locations have been bound together, with their mean centre of gravity providing the point coordinates of *aggregate units of analysis* (AUA). Figure 26 shows the results of this for the two case studies, with *eps* arbitrary set to 100, 150, and 250 meters[2]. Since the locations of pithouses will be linked to the BUA as a one-to-one relationship,

[1]This is particularly notable for some preliminary reports published by local cultural agencies where only a list of recovered residential features and their rough chronology are provided.

[2]The increments have been derived by preliminary exploration of the data-set where tangible changes in the number of clusters has been identified.

this procedure will in practice provide the same outcome of clustering pithouses into groups based on their positions (approximated in this case to the centroid of their excavation area).

The three alternative AUA will thus provide a spatial dataset where excavated residential features (each associated with a single point in the BUA) are aggregated. This makes it possible to generate rank-size distributions where each observation corresponds to the number of pithouses associated with each AUA.

A total of almost 3,000 pithouses (1,418 for Chiba and 1,432 for Gunma) dated between Early and Late Jōmon periods have been recovered from the excavations of the two case studies areas. For each of these residential units the following set of information has been retrieved from the reports:

1. *time-span* of possible existence (recorded in terms of pottery based relative chronology).

2. topological relation to other residential units from the same excavation area (recorded as a *before/after* relationship).

3. spatial location (recorded as a one-to-one membership to the BUA).

4.1.1 Aoristic Analysis and Monte-Carlo Simulation

The information retrieved from the excavation reports has been converted into an *aoristic* table, where rows represent each residential unit, columns refer to the temporal blocks, and each cell stores the aoristic weights. For the purpose of this thesis, a temporal resolution of 100 years has been chosen, leading to the creation of 37 time-blocks (columns), starting from t_1=7000-6900 cal BP and ending with t_{37}=3400-3300 cal BP. The choice of the resolution was regarded as the best compromise between the nature of the research question, the quality of the available data, and the estimated length of occupation of Jōmon pithouses, corresponding to ca 10 $\sim$ 15 years. The latter value was derived from ethnographic comparisons (Watanabe 1986, Muto 1995) and archaeological evidence (Kobayashi 2007), all suggesting

such an interval. This is slightly large compared to the chosen resolution, but still likely to have only a minor impact on the analytical outcome, as the probability of a pithouse existing in two consecutive time-blocks is only between 0.08 and 0.13 (see section 3.2.3)[3]. Coarser resolutions have been also explored, but were rejected as they tend to obscure fine grained dynamics of change that are suggested by the existing literature.

The pottery phase based chronological definition was first converted to an absolute interval using the most recent chronological sequence described in section 2.2.1. This was then converted into probability distributions using the method outlined in section 3.2.3 (figures 14 and 15).

The final step of the data pre-processing was to convert the probabilistic data obtained from the aoristic analysis into a series of simulated data where the temporal uncertainty is "removed" (i.e. the chronological definition is restricted to one of the 37 time-blocks instead of being represented as probability weights). This was achieved using the Monte-Carlo simulation technique introduced in section 3.2.3. For the purpose of the two case studies, the generation of 1,000 simulated spatio-temporal distributions was regarded as sufficient. This was established by sequentially increasing the number of runs and comparing the output of the analysis. In most cases a few hundred runs were sufficient to obtain a convergence in the results (see Crema *et al.* 2010 for details of such a convergence test), thus 1,000 runs was regarded as adequate in this case.

4.2 Results

The output of the Monte-Carlo simulation allows the application of traditional methods of analysis to data-sets where the temporal dimension is expressed in probabilistic terms. Results will shift from a single output (i.e. count of pithouses

[3]Recall that the working assumption of aoristic analysis is that events (pithouses in this case) have no duration in time, and hence can exist only in one time-block. However, when their duration are short compared to the length of the time-blocks this is expected to have negligible impact to the analytical output.

in a given time-block), to a distribution of outputs (i.e. n possible count of pithouses in a given time-block, with n equal to the number of simulation runs), which will then allow a probabilistic assessment of the observed pattern.

Notice that in the following pages reference to temporal coordinates will be often based on the time-blocks intervals rather than absolute dates, and these will be denoted using an italic "t" with the start date of the block shown as a subscript (e.g. the time-block starting at 3800 cal BP and ending at 3700 cal BP will be referred to as t_{3800}). Notice also that the labels of the x-axis of the figures will refer to the starting date of the time-blocks.

4.2.1 Non-spatial Analysis

Number of Pithouses

Figure 27 shows the temporal variation in the total counts of pithouses. All the 1,000 possible time-series (the raw output of the Monte-Carlo simulation) are depicted as grey lines, with the sequence of average pithouse counts per time-block (among all simulation runs) superimposed as a solid black line. A look at both line graphs suggests that the grey lines are bounded by a limited range of possible pithouse counts, defining an *envelope* of possible values, with the black line approximately passing through the middle. Visual analysis of the distribution of possible counts for each time-block (not shown here) indicates how the simulated values are normally distributed, providing confidence that the time-series of the mean can provide a robust description of the overall trend in the pithouse counts.

Broadly speaking, both areas exhibit multiple peaks in the time-series, with the highest being the one occurring during the first half of the 5th millennium cal BP. Other notable peaks shared by both regions are the one around 6000 cal BP (although this is much less prominent in Chiba) and the one at ca 5500-5400 cal BP. The biggest difference between the two regions is a peak in pithouse counts during the second half of the 5th millennium cal BP in Chiba, a pattern not observed in Gunma. Most of these general trends are not surprising and conform to existing

studies from other parts of the Kantō region (see Crema 2012). A more detailed inspection of figure 27 shows how the two regions are characterised by dissimilarities other than the one noticed between 4500 and 4000 cal BP. These include a generally larger number of pithouse in Gunma during the Early Jōmon period (7000-5470 cal BP) and a slight mismatch in the timing of the largest peak in the two regions. Chiba in fact reaches its highest peak around t_{4700}-t_{4600}, and shows a strong decline at t_{4500}, while Gunma has its highest peak earlier (t_{4800}), which is immediately followed by a decline in the subsequent time-block.

A more precise assessment of the temporal variation in pithouse counts can be obtained by computing the rate of change[4] for consecutive pairs of time-blocks within each run of the simulation. The resulting distributions (with length n, equal to the total number of runs) will provide a more robust method for assessing the temporal variation in pithouse counts. This will in fact maintain the conditional dependency of each event across all time-blocks [5], offering a probabilistic assessment of the increase or decrease of counts.

Figure 28 shows the result of this analysis for the two study areas, with error-bars defining a 95% envelope of the rate of change, and the x-axis showing the initial date of pairs of time-blocks. In many instances the error bars extend from positive to negative rates of change, indicating how either the magnitude of change was minimal or the uncertainty associated with the data-set is too large to determine with confidence whether there was an increase or decrease in the pithouse counts. This implies also that the statistical significance in the change (i.e. error bars entirely located in positive or negative regions of the plot) does not imply a

[4]The rate of change computed here uses the following formula:

$$R(c_t, c_{t+1}) = \frac{c_{t+1} - c_t}{d}$$

where c_t and c_{t+1} are the counts of pithouses at time-step t and $t+1$, and d is the duration of each time-block

[5]The existence of a pithouse in a given time-block will clearly indicate its nonexistence in all the other time-blocks. To maintain this information in the diachronic assessment of the time-series, analysis should be undertaken on each simulated count series independently and combined only at the end. Failure to do this will produce biased impressions of rates of change (see also Crema 2012).

strong magnitude of change (i.e. one with practical archaeological significance). As an additional remark, this study did not use the size of individual residential units as a proxy for inferring more directly the population size. This choice was prompted partly by the lack of such data for several pithouses, and by a generally low level of variation in the areal extent of the residential units in the two regions, suggesting that size variation of the habitation floors is an unlikely source of bias in population estimates (although other factors, such as the frequency of residential moves, might potentially bias the relationship between counts of residential units and population size).

Despite several time-block transitions showing higher levels of uncertainty, the results confirm that the two regions exhibit differences in their temporal dynamics. In Chiba, the Early Jōmon "collapse" (Imamura 1992, Habu 2001) can be identified in the transition $t_{5900} - t_{5800}$, while in Gunma potential decline can be observed in the transitions $t_{6000} - t_{5900}$, $t_{5900} - t_{5800}$, and $t_{5800} - t_{5700}$, although only the last one exhibit low levels uncertainty with both error bars below zero. Similarly, the divergence in the timing of the Middle Jōmon peak is confirmed, with Gunma showing an earlier decline. Figure 28 also depicts some dynamics that were less evident when the simple time-series were assessed, namely fluctuations in the magnitude of change during the Middle Jōmon period (ca 5500-4400 cal BP). Both areas in fact show three stages of growth alternated with two episodes of slight decline or reduced rate of growth. This is particularly evident for Gunma, which saw increasing growth between t_{5700} and t_{5400}, t_{5300}-t_{5000}, and t_{4900}-t_{4800}, contrasted with episodes of decline at t_{5400}-t_{5300} and t_{5000}-t_{4900}. Similar fluctuations can be observed in Chiba, where there is no evidence of decline during this interval (although the error-bars sometimes reaches negative values), but a fluctuation in the rate of increase, with low values at t_{5300}-t_{5200} and at t_{4900}-t_{4800}. Although the overall dynamics are similar, the absolute timing differs between the two case studies, suggesting either the possibility of a real difference in the *tempo*, or a bias resulting from differences in the pottery-based chronology (see section 4.3 for a more detailed discussion).

Number of Groups

One simple indicator for inferring possible changes in the settlement pattern is to count the number of groups for each time-block. Such a time-series must however be recreated for each different value of *eps*, our parameter defining the settlements. As mentioned earlier, convergence or divergence in the overall pattern will indicate whether the way we defined our aggregate unit of analysis (AUA) affects the outcome of the analysis, in turn suggesting whether the specific measure (in this case the time-series of group counts) is robust or not.

Figure 29 shows the combined set of all 3,000 (1,000 for each *eps* value) simulated group counts in grey lines, along with the average values for different settings of *eps* superimposed as solid (*eps*=100m), dash (*eps*=150 m) and dotted (*eps*=250 m) lines. In both case studies, variations in *eps* do not appear to determine changes in the trajectory of the time-series, and differences are restricted to a slightly lower group counts for *eps* = 250m. This convergence in the output suggests that the rate of change analysis can be undertaken with confidence that differences in the settlement definition criteria can be ignored.

A visual comparison between the pithouse counts (fig. 27) and the group counts (fig. 29) indicates how the relation between the two sets of time-series differs across the two regions. In Chiba they show similar trends, with the primary peak at t_{4700}, and a secondary peak between 4500 and 4000 cal BP. In Gunma however, the highest number of groups is attributed to the Early Jōmon (7000-5470 cal BP), with the subsequent Middle Jōmon (5470-4420 cal BP) characterised by roughly half the counts of the previous period. This divergence between pithouse and group counts in Gunma suggests the possibility that Early Jōmon settlements were much smaller and dispersed in number, while during the Middle Jōmon period they were aggregated into fewer but larger groups.

As for the pithouse counts, the rate of change analysis can provide a more robust inference on how the number of groups varied through time. Figure 30 illustrates this for *eps*=150 m, again with the error-bar representing the 95% confidence interval. As in figure 28, the bars often extend to both positive and negative

rates, indicating that we can identify the robust presence of an increase or decrease only for very few transitions. Nonetheless some interesting patterns can be still observed, suggesting further differences between pithouse and group count dynamics.

The rate of change at Chiba shows repeated "sparks" of increase towards the early stages of the Middle Jōmon period (t_{5600}-t_{5500}, t_{5200}-t_{5100}, t_{5000}-t_{4900} and t_{4800}-t_{4700}), and a strong decrease from t_{4700} to t_{4500} cal BP. Interestingly the decline in the number of groups seems to occur slightly earlier than the decrease in the pithouse number (occurring at t_{4600}-t_{4500}, see fig 28), suggesting that notable changes in the settlement pattern might have occurred before the conjunct drop in pithouse counts and settlements. This divergence in the *tempo* is, however, not detected for the Late Jōmon decline, which occurred at t_{4200}-t_{4100} for both the total number of residential units and settlements.

The dataset from Gunma appears to be generally affected by higher levels of uncertainty, with larger error bars ranging from negative to positive rates of change. Exceptions to this can be found in the declines at the end of the Early Jōmon (at t_{5800}-t_{5700}) and Middle Jōmon periods (at t_{4600}-t_{4500}). Interestingly, the latter is synchronic with the decrease observed at Chiba, indicating how from the standpoint of group counts the dynamic of change is shared in the two regions during this stage.

Median Group Size

A more direct attempt to assess further properties of these settlements is to investigate their median size. This will be a biased statistical measure (see section 3.3.1) influenced by the length and the width of the lower tail of the distribution (i.e. smaller settlements), but nonetheless offers some clues on how settlement size might have changed over time.

Figure 31 shows the time-series and figure 32 the rate of change analysis of this statistical measure for the two case studies (again with the latter referring to AUA with *eps*=150 m). It is immediately apparent from looking at the two figures

that the degree of uncertainty is much higher in this case, with both the envelope defined by the simulated time-series and the error bars of the rate of change being much larger than the ones shown for the pithouse and group counts. Nevertheless, a peak of the median group size at t_{4500} is confirmed for Chiba. Gunma also shows an increase of the median group size during the Middle Jōmon period, peaking at t_{5000}, although the rate of change fails to identify this as a moment of significant transition, partly because the increase was probably more gradual.

4.2.2 A-Coefficient

The non-spatial analyses presented in the previous subsection already showed how the time-series of pithouse counts, group counts, and median group size differ from each other, sometimes showing opposite trajectories (e.g. slight increase in pithouses and a sharp decrease of group count in Chiba from t_{4700} to t_{4600}) which might suggest the presence of changes in the group size distribution.

As introduced in the previous chapter (section 3.3.1), Drennan and Peterson's (2004) *A*-coefficient analysis offers a quantitative method for describing such variations, with the additional benefit of providing an index value directly referable to the spectrum of variation between clumped and dispersed patterns. In this case, however, the application of *A*-coefficient analysis was not straightforward and additional intermediate steps were required for its correct implementation.

First, as for the group counts and median group size, the problem of unit definition has been approached by using multiple AUA, effectively determining three sets of outcomes (with *eps* set to 100, 150 and 250 meters) for each case study. Second, the analysis has been repeated for each of the 1,000 simulated spatio-temporal data, and combined via the same method used for the time-series of pithouse counts and group counts. Third, in order to avoid potential biases resulting from the right tail of the distribution, a truncated version (see section 3.3.1) of the A-coefficient has been computed. Fourth, the analysis was restricted to instances where at least 5 groups (settlements) have been identified. This has been based on the principle that some known types of group size distribution (e.g. double

convex, primo-convex, etc.; see figure 18) require at least five observations to be realised.

The result of this modified version of the *A*-coefficient analysis is shown in figure 33. As with the group counts and median group size, the grey lines depict the whole set of 3,000 simulated time-series (1,000 for each *eps*) while solid, dashed and dotted lines shows the average *A*-coefficient for each *eps* settings.

The truncation of the right tail and the restriction to a minimum of five observations has greatly reduced the number of outputs for some portions of the time continuum. This is particularly the case for the Early Jōmon in Chiba and Late Jōmon in Gunma, where the number of runs with more than five settlements is too small for any robust interpretation of the results. Nonetheless, figure 33 shows how a fluctuating pattern in the *A*-coefficient is evident for both areas. In Chiba, two peaks of dispersed/convex distribution can be identified at t_{5300} and t_{4700}, alternating with episodes of clumped/primate distribution at t_{5000} , t_{4300} , and t_{3900}-t_{3800}. In addition there are also two instances where the average *A*-coefficient is close to zero, indicating a Zipf's law distribution at t_{4000} and t_{3500} . In Gunma, peaks of dispersed/convex distribution can be found at t_{6000} and t_{5200} , while clumped/primate patterns are found at t_{5700} and t_{4800} , and a Zipf's law distribution at t_{4500} .

Some of the results depicted on figure 33 should however be treated cautiously. Firstly, effects derived from different way we defined our AUA should be taken into account. In this case, however, variation in *eps* appears to be insignificant in almost all instances, with the only exception observed at t_{3900} in Chiba, when the average *A*-coefficient suggests a quasi-Zipfian pattern for *eps*=100 and a dispersed pattern for *eps*=150 and *eps*=250.

Another source of uncertainty, and potential error in the analytical output, can emerge from sampling biases in the input data itself and by the restricted vision of a 15 $\times$ 15 km window of analysis. As mentioned in section 3.3.1, Drennan and Peterson (2004) suggest the adoption of bootstrap techniques to overcome these problems. This will allow us to generate a simulated distribution of A, from which

a confidence interval of the sample estimate can be retrieved. Here, this procedure has been implemented by computing 1,000 bootstraps for each of the observed (simulated) 1,000 A-coefficients. Subsequently, instead of extracting the confidence interval for each result, the complete distribution (i.e. both the sample estimate and the bootstrap output) has been plotted, thereby using one million possible values of A for each time-block. Figure 34 shows this for *eps*=150, depicted as a violin plot [6] , with the fill colour indicating the proportion of effectively computed A-coefficients, the mean value as a solid red line, and the 10% and 90% percentiles shown as red dashed lines. Despite the strongly conservative nature of the bootstrap simulation, the results still maintain the general pattern observed in figure 33, especially for instances of dispersed patterns. Clumped patterns tend instead to have a bimodal shape (although their mean value still suggest a clumped distribution), most likely caused by the bootstrap resampling procedure failing to pick the largest settlement, hence occasionally generating a set of results with a less pronounced dominance of larger groups.

Temporal uncertainty and potential presence of complex rank-size distributions (e.g. primo-convex, double-convex etc.; see figure 18) should also lead to a cautious interpretation of the results. The first is partly addressed by visually assessing the envelope generated by the simulated time-series. For example, figure 33 shows how the dispersed pattern at ca 5300 cal BP is characterised by large envelopes suggesting that there is a small chance that the settlement size distribution was clumped. The second problem is less straightforward and requires the actual plotting of all the simulated rank-size plots on a single graph. This will require some mathematical transformations that will lose the absolute values of the observed sizes, but will maintain the ”shape” of the rank-size curve and its relationship to the theoretic Zip’s law distribution.

Figures 35-38 show such a combined rank-size plots along with the histograms of the A-coefficients for key time-blocks where notable peaks have been identified

[6] A violin-plot is a combination of box-plot and kernel density, with ”fatter” regions indicating higher frequencies and thinner regions indicating lower frequencies of a given observation.

(compare with fig. 33). All rank-size plots associated with positive A-coefficients do indeed suggest a convex pattern, while negative values of A seem to be characterised by either a primate (e.g. t_{4800} in Gunma, figure 37), or a primo-convex pattern (e.g. t_{3800} in Chiba, figure 35; see also 18), although the latter is often inferred from a relatively small number of effectively computed A-coefficients.

Despite the presence of possible primo-convex patterns, the detailed examination of individual rank-size plots for these time-blocks supports the idea that both study areas saw cycles of changes in the settlement size distribution. In Chiba, this was characterised by an almost regular interval, with similar values of the A-coefficient reappearing approximately every 500-600 years. In Gunma, similar regularity can be also identified in the interval between ca 6000 and 4300 cal BP, after a period of constant positive values of the A-coefficients. The frequency of the cycle seems, however, to be slightly longer (ca 800 years), and more irregular than was the case in Chiba. Both studies thus appear to strongly support Uchiyama's hypothesis, with repeated episodes of shifts between positive and negative values of A suggesting transition between clumped and dispersed patterns. Exact timings are different between the two areas, and the lack of data does not allow comparison for the full interval between Early and Late Jōmon periods. Nonetheless, both Chiba and Gunma appear to show the same "dispersed-clumped-dispersed" sequence during the Middle Jōmon period, providing further insights (see section 4.3 for more detailed discussion) into the rapid increase and decline in the pithouse counts shared by the two regions during the same interval.

4.2.3 O-ring Function

The A-coefficient analysis successfully offered a direct measure for determining whether the rank-size distribution of the settlements in the two case studies were primate (clumped) or convex (dispersed), but did not provide any insights into how these settlements were spatially distributed. O-ring statistics can overcome this problem by assessing how the density of neighbouring residential units varies as a function of distance. Although this does not constitute a valid proxy for de-

termining whether a settlement pattern can be regarded as clumped or dispersed, its comparison with other analysis can offer new and complementary perspectives (see section 3.3.2 and table 4). As with the A-coefficient analysis, direct application of this analysis is not trivial and requires several additional steps that must be undertaken first.

The implementation of O-ring statistics for large-scale regional studies will ideally require evidence that most sites have been identified. Furthermore, since pithouses are acting as units of analysis, a good portion of these archaeological sites should be extensively excavated, uncovering most parts of settlements. Failure to meet these requirements will involve assessing an archaeological distribution that will be partly derived from the spatial pattern of the archaeological investigation itself. In chapter 2 (sections 2.2.4 and 2.3), I have argued that Japanese CRM archaeology provides suitable data on this regard, but nonetheless some data limitations are still likely to be present.

In order to overcome these, a modified version of the O-ring function has been implemented. The main difference to the standard version is to obtain the density of neighbouring residential units from the ratio between: 1) the number of residential features at distance above d_1 and below d_2; and 2) the total sum of excavation areas within the same distance band (figure 39:**b**). Thus, while in a standard implementation of O-ring statistics the denominator will be computed as the annulus $\pi(d_2^2 - d_1^2)$ (see figure 39:**a**), the modified version will have a smaller value, which will vary depending on the location of the focal point and the intensity of the archaeological investigation. In practice this is the same result that would be obtained if we assume that the window of analysis is characterised by n sub-windows, each corresponding to an excavation area (or to the BUA in the specific case). Similarly, the complete spatial random process will be generated only within these excavation areas, effectively ignoring remnant portions of the landscape. The ideal implementation of this procedure would require the exact location of each individual residential unit and the computation of partial portions of excavation areas intersecting the annuli (figure 39:**b**). However, these data

are not always available and hence for the present study a further modified point data with two *marks* (i.e. attributes) —one indicating the count of residential units and the other representing the areal extent of the polygon referenced by the point location (figure 39:**c**)— was used. This method will be less accurate, but if the difference $d_2 - d_1$ is sufficiently large the bias will be minimal. Monte-Carlo simulation of the random spatial process will not be based on the creation of artificial points (residential units), but on the creation of alternative *marks* of each point location, based on a random draw from a Poisson distribution. This marked-version of O-ring statistic will be perfectly suited for the present case study, with the BUA becoming the basic input data.

The output of the O-ring statistic will be the same for all three versions described above: the observed density $O(d_1, d_2)$ is compared to the expected density for a complete spatial random process (λ_{CSR}), with the significance obtained from an envelope created by Monte-Carlo simulation. However, visualising each of the 1,000 (number of simulation runs) $\times$ 36 (number of time-blocks) outputs of the O-ring statistic is clearly not feasible, and hence the following method has been devised. For each distance bin (d_1, d_2), at each time-block (t), the proportion of $O(d_1, d_2)$ with significant (with *p-value* < 0.05) clustering among the 1,000 simulation runs has been defined as $C(d_1, d_2, t)$. Similarly the proportion of significant dispersion has been named $D(d_1, d_2, t)$. Both values will be bounded between 0 (no runs with significant clustering or dispersion) and 1 (all runs with significant clustering/dispersion).

Figure 40 and 41 is a matrix plot showing the difference $\Delta_{CD}(d_1, d_2, t) = C(d_1, d_2, t) - D(d_1, d_2, t)$ for each combination of t (x-axis) and distance band (y-axis), so that values close to 1 (coloured in red) will indicate higher probability of clustering and values close to -1 (coloured in green) will indicate higher probability of dispersion, with intermediate values (≈ 0, coloured in yellow) suggesting either a random pattern ($C(d_1, d_2, t) \approx D(d_1, d_2, t) \approx 0$) or a high level of uncertainty (both $C(d_1, d_2, t)$and $D(d_1, d_2, t)$ greater than zero). For the purpose of this study, the distance band interval has been fixed to 500 meters, with the highest value of d_2 equal

to 5km (i.e. the largest distance band is $d_1 = 4500$ m and $d_2 = 5000$ m), while the number of spatial Monte-Carlo simulations defining the envelope of CSR has been fixed to 99.

As expected (see section 3.3.2) the lowest distance band (0-500 m) exhibits significant clustering for all periods in both regions, while time-blocks with higher temporal uncertainties usually have $\Delta_{CD}(d_1, d_2, t)$ close to zero. The most interesting aspect of the two matrix plots is the presence of sudden changes of $\Delta_{CD}(d_1, d_2, t)$ from highly positive (or negative) values to negative (or positive) ones in a short interval of time, often within the transition from one time-block to another. For instance in Chiba (fig. 40) the distance band 3500-4000 m exhibit high probability of clustering between t_{5400} and t_{5100}, then at t_{5000} there is a sudden switch to a strong probability of dispersion in the same distance range. This rapid change in $O(d_1, d_2)$ suggests instances of a radical spatial re-organisation, and in this specific case it coincides with a strong negative peak in the *A*-coefficient, before a reversal in the group size distribution towards a dispersed/convex pattern. More generally, instances of change in the direction of the *A*-coefficient time-series often seem to be correlated with shifts in $\Delta_{CD}(d_1, d_2, t)$. For example, from t_{4800} to t_{4700}, when a strong decreasing trend in the *A*-coefficient is recorded (fig. 33), there is a sudden increase in the probability of clustering at 3500-5000 meters and a transition to a high probability of dispersion at 2000-2500 meters.

Close relationships between rank-size distribution and O-ring statistics seem, however, to be restricted to instances of rapid shifts and episodes of reversals in the *A*-coefficient. When a diachronic perspective is not adopted, the correlation between a given spatial inter-distancing depicted by the O-ring statistics and the size distribution described by the *A*-coefficient shows a variety of associations. For instance, when Gunma exhibits its lowest *A*-coefficient at t_{4800}, $\Delta_{CD}(d_1, d_2, t)$ shows mostly negative values, with a positive peak only at 4000-4500 m. Conversely the lowest *A*-coefficient at Chiba (occurring at t_{5100}-t_{5000}) is characterised by variation between spatial scales of high probability of clustering (1500-2500 and 3500-4000 m) and dispersion (500-1500, 2500-3500, and 4000-5000 m). These inconsistencies

indicate how a variety of different spatial configurations can lead to the generation of similar rank-size distributions, even within the same context of Jōmon hunter-gatherers.

4.3 Discussion

The analyses conducted in the previous sections enable us to assess how Jōmon settlement patterns varied in the two regions between 7000 and 3220 cal BP. Comparisons of each analysis have already shown key differences between the two regions, but a more detailed review focusing on how the five measures *co-varied* is crucial for providing a comprehensive description of the changes in settlement pattern.

Figures 42 and 43 depict the mean time-series for four of these statistics, using an AUA with *eps* equal to 150 m for group based measures (number of groups, median group size, and A-Coefficient). It is important to recall that choosing to show simultaneously the four time-series sacrifices the representation of the uncertainty associated to each measure, and hence continuous reference to the figures in the previous pages will be necessary.

4.3.1 Early Jōmon (t_{7000}-t_{5500})

The Early Jōmon period is characterised by a strong dissimilarity in the settlement density of the two regions, with Gunma showing its highest values (an average of 20 groups before 5800 cal BP), and Chiba its lowest (ca 5 groups before 5800 cal BP). Despite this difference in the absolute values, the two regions shared similar dynamics of change, with an increase in both residential and group counts towards the end of the 7th millennium cal BP, followed by a decline during the early 6th millennium. In Chiba the onset of this decline was slightly earlier, during the transition from t_{5900} and t_{5800} (see also fig 28), while in Gunma the trend became pronounced at the transition t_{5800}-t_{5700}, although a decrease was already noticeable earlier (fig. 28 and 30). This pattern of increase and decline provides

rigorous quantitative support for existing archaeological studies (Imamura 1992, Habu 2001) suggesting a "collapse" towards the end of the Early Jōmon period.

From the perspective of the rank-size distribution, the lack of data and high levels of uncertainty do not allow a robust assessment for Chiba, and hence the analysis is restricted to Gunma. Here, there was a dominance of a dispersed/convex pattern, which suddenly shifted to a clumped/primate pattern in synchrony with the decrease in the pithouse and settlement counts. A detailed examination of the latter trend (see fig. 37) shows how the rank-size distribution can be characterised as primo-convex, but that the *A*-coefficient was not computed for all simulation runs due to a lower number of settlements. This correlation between the nature of the group size distribution and residential density was also present at the very end of the Early Jōmon period, when the reprise in both pithouse counts and number of settlements was associated with a reversing of the *A*-coefficient, which increased and reached values proximal to zero. A similar reprise in settlement counts, pithouse number and also median group size occured from ca 5600 cal BP at Chiba, indicating how at the end of the Early Jōmon both regions still shared similar trends.

4.3.2 Middle Jōmon (t_{5500}-t_{4500})

The peak in the residential density, the finest chronological resolution (see table 3 in chapter 2), and the lowest levels of temporal uncertainty offer a wider range of robustly identifiable patterns (see for instance fig. 34) for this period, allowing a direct comparison of all statistical measures between the two regions of interest.

As noted in the previous sections, the dominant feature of this period was the steady increase of pithouse and settlement counts in the first few centuries, followed by a sharp decline towards its end. This general trend confirms existing studies on pithouse counts from other parts of Kantō (Imamura 1997, Kobayashi 2004, Crema 2012), and northern Japan (Habu 2008) where a similar rise and decline of pithouse counts has been observed. Despite this general parallelism, the two case studies exhibited differences in the timing of the events, and the positive

correlation between the four statistical measures observed during the Early Jōmon period (see figure 42 and 43) is no longer present.

The group size distribution and the spatial patterning of the residential units showed notable changes over time. Both regions started with a rank-size distribution moving towards a dispersed pattern, followed by a rapid shift towards negative values of A (suggesting a clumped/primate pattern), and a renewed increase towards positive values towards the end of the period. Similarities are however limited to this broad trend; both the timing of this fluctuation and its relationship to the other three statistical measures are in fact different between the two regions.

In Chiba, the first few centuries of the Middle Jōmon period were characterised by a steady growth in the pithouse counts coupled to a relative stability in the number of groups. Subsequently, in synchrony with the sudden shift from dispersed to clumped pattern (fig. 33), both pithouse and settlement counts saw a sharp increase (see also fig. 28 and 30) at t_{5200}-t_{5100}. This rapid change in the settlement pattern was also paralleled by shifts in the O-ring statistic (see fig. 40), suggesting a radical spatial reorganisation. The clumped pattern stage lasted for ca two centuries, before a sudden reversal of the A-coefficient from 5000 cal BP, coupled this time to an increase in the number of pithouses and settlements (which showed a small break in its increasing trend during the peak stage of the clumped pattern). From t_{4900} to t_{4800} the rate of increase in the pithouse counts slowed down slightly, while the median group size and the total number of groups exhibited a small decline. This pattern is however not supported by the rate of change analyses (fig. 28, 30, and 32) which indicate high levels of uncertainty. The transition to the subsequent time-block (t_{4700}) showed, however, a sharp increase in pithouse counts, groups counts, and median group size, paralleled with a transition toward a dispersed/convex settlement pattern.

The last three centuries of the Middle Jōmon period were characterised by a strong asynchrony of all statistical measures (fig. 42), associated with higher frequency shifts in the spatial distribution of the settlements themselves (see fig. 40). From t_{4700} to t_{4600}, the pithouse counts showed a slight increase (although the pat-

tern is not robust enough; see fig. 28) while the number of groups decreased dramatically (see also fig. 30). This divergence in the trajectory of the two measures vanished in the interval between t_{4600} and t_{4500}, with both pithouse counts and group number decreasing. However the same interval was characterised by the steepest increase of the median group size, which reached its highest peak for the whole interval between Early and Late Jōmon periods. The last transition between t_{4500} and t_{4400} was associated with a decrease in the median group size and pithouse counts, associated however with a renewed increase in the number of groups. From the perspective of group size distribution, the same interval between t_{4700} and t_{4400} was characterised by a decline of the *A*-coefficient suggesting a shift from convex to Zipf's law distribution.

One possible explanation for the combination of patterns observed in these few centuries could be the following.The rank-size distribution was initially convex with a large number of settlements and pithouses at t_{4700}. In the subsequent timeblock (t_{4600}) the number of groups decreased, while the total number of pithouses remained stable (with a small chance of increase). This could be explained by a nucleation (fusion) to larger groups (associated with the abandonment of smaller groups), which led to the formation of a stronger diversity in the group size distribution, and hence a decrease in the *A*-coefficient. An alternative explanation is that some settlements increased in size by internal growth, while others were characterised by the opposite trend. Regardless of the specific generative process, a peak in the median group size can be identified at t_{4500}, suggesting a potential combination between a decrease in the number of small settlements (shorter tail in the distribution) and a possible increase in size of the largest ones. This lasted only briefly with the following century characterised by a dramatic decrease in both pithouse counts and median group size. This is possibly associated with a fission to new offspring settlements, as suggested by an increase in the number of groups and a "break" in the decreasing trend of the *A*-coefficient. A more detailed examination of these possible dynamics in relation to human decision-making will be presented in chapter 8, where these observed patterns will be re-assessed in re-

lation to the outcome of the computer simulation model. Here it is sufficient to state that the late Middle Jōmon period was undoubtedly a phase of rapid and tumultuous reorganisation of the settlement system.

In Gunma, the increase of all statistical measures observed at the end of the Early Jōmon showed a short reversal of trend from t_{5400} to t_{5300}, although this can be stated with confidence only for the decrease in the pithouse counts (see fig. 28, 30, and 32). The parallel increase reoccured immediately after this break, although after t_{5200} the *A*-coefficient initiated a strong decrease after reaching its peak positive value (dispersed/convex pattern). At t_{5000}, when the median group size reached its highest peak, the rank-size distribution had a primate shape, while the number of groups showed a small decline (although this does not appear to be significant; see fig. 30). This phase was also associated with some transformation in the spatial pattern (see fig. 41), with the emergence of a strong repulsion between settlements, as shown by the dominance of negative values of $\Delta_{CD}(d_1, d_2, t)$ up to 4000-4500 meters. The number of groups showed a renewed increase around t_{4800}, when the pithouse count reached its maximum and the group size distribution showed the strongest degree of clumping (smallest *A*-coefficient). As for Chiba, the last few centuries of the Middle Jōmon were characterised by rapid changes in the settlement pattern. The O-ring statistic showed a reduction in the typical inter-distance between settlements from this stage (fig. 41), while the *A*-coefficient exhibited a rapid increase towards values typical of a Zipf's law distribution. From t_{4800} to t_{4700}, when the shift in the shape of the rank-size distribution was pronounced, the pithouse counts showed a strong decline, contra-posed to a slight increase (or at least stability; see fig. 30) in the number of groups. The parallel decrease of the median group size during the same interval might suggest a fission of larger groups and the consequent formation of new smaller groups. From t_{4700} however, most statistics show a decrease in their values (except for the *A*-coefficient, and a brief episode of increase in the median group size) until the end of the Middle Jōmon period, with group and pithouse counts both reaching low densities typical of the subsequent Late Jōmon period.

As mentioned previously, the two regions exhibited some common trends (a similar alternating sequence of group size distribution and a peak and decline in the number of pithouses and settlements), characterised however by different timings. This is particularly notable for the emergence of the clumped settlement pattern (at t_{5000} in Chiba and at t_{4800} in Gunma) and the onset of the decline in pithouse counts (from t_{4600} to t_{4500} in Chiba and from t_{4800} to t_{4700} cal BP in Gunma). Divergence in the timing of the latter can be explained in two different ways:

1. The events are synchronous, and the observed difference in the onset of the decline is a bias derived by an erroneous matching of the pottery sequences in the two regions (see table 3 in chapter 2).

2. The events are asynchronous, suggesting how the possible decrease in population that might be inferred from the pithouse counts was strongly related to difference (e.g. in the subsistence strategy or the environmental setting) between the two regions.

While the first hypothesis cannot be fully dismissed, a careful review of the pottery sequence suggests how the second is a stronger candidate. Figure 44 is a graphical illustration of the pottery *Kasori E* sub-phases in relation to the 100-year time-blocks used in this thesis. The strongest rate of decline in the pithouse counts in Gunma occurred sometime between t_{4800} and t_{4700} (see also fig. 28), which corresponds to the transition from *Kasori E2* pottery phase to *Kasori E3*. In Chiba the peak in the negative rate of change occurs in the transition from t_{4600} to t_{4500}, corresponding instead to the transition between *Kasori EIII* and *Kasori EIV* phases. As illustrated in figure 44 the largest difference in the roman number sequence at Chiba and the arabic number sequence in Gunma is in the relative duration of the pottery sub-phases *E2/EII* and *E3/EIII*. Possible controversy and revisions on the relation between the two parallel pottery sequences could arise on the timing of the transition between these two sub-phases, but the observed archaeological events appear to parallel the subsequent transition. This suggests that some level

of asynchronicity might be indeed present, and cannot be simply dismissed as a bias derived by an erroneous attribution of the duration of *Kasori E2/EII*.

4.3.3 Late Jōmon(t_{4400}-t_{3400})

The Late Jōmon period was the interval with the strongest divergence between the two regions. In Gunma this phase was characterised by low values in the number of pithouses and groups, and the lowest median group size. The data-set is unfortunately too small for a robust inference on the rank-size distribution as well.

On the contrary Chiba seems showed an initial increase in the total number of pithouse counts, with a peak at ca t_{4300}. This trend was paralleled by an increase in the median group size and group counts, with the latter already occurring at the very end of the Middle Jōmon period (t_{4500}-t_{4400}), when the pithouse count was still declining. The peak in these three statistical measures at t_{4300}-t_{4200} was also associated with a second onset of a strong clumped/primate pattern, thus showing opposite properties to the residential peak of the Middle Jōmon period, which was instead characterised by a dispersed pattern. At t_{4100} however there was a renewed decrease in the pithouse counts, group counts, and median group size, while the rank-size distribution of the groups showed a transition to a pattern close to a Zipfian distribution. The last few centuries of the Late Jōmon period saw the continuation of such a trend, with a slow decline in the pithouse and group counts and a further decrease of the *A*-coefficient, this time however characterised by a primo-convex pattern rather than a clumped one (see fig. 35). At t_{3500}, however there was a small peak in the pithouse and group counts, along with a slight growth in the median group size and a renewed increase in the *A*-coefficient. However this trend can be robustly inferred only for the pithouse and group counts, as other measures are associated with high levels of uncertainty.

4.4 Summary

As mentioned in the introductory remarks of this chapter, the spatial and temporal analysis introduced in sections 3.3.1 and 3.3.2 and applied in this chapter were chosen and designed to assess the first research question of the thesis: whether the Jōmon settlement pattern in Chiba and Gunma exhibited cyclical alternation between clumped and dispersed pattern.

The most direct method for tackling this — the *A*-coefficient analysis — has shown (fig. 33) that the two regions did indeed experience rapid and repeated shifts between clumped and dispersed pattern, with almost regular intervals of change. A more detailed overview involving parallel assessment with other measures of the metapopulation structure (number of groups, total number of recovered residential units, median settlement size, and O-ring statistic), along with a comparative perspective between the two regions, suggested however the presence of a much more complex picture, which is summarised in the following points:

- The two regions share some broad similarities in their spatio-temporal patterning, notably the presence of two peaks in the pithouse and settlement counts towards the end of the 7th millennium cal BP and the first half of the 5th millennium cal BP, and the same sequences of change in the rank-size distribution (dispersed, clumped, and dispersed again) during the Middle Jōmon period.

- During the Late Jōmon period, the two regions were characterised by strongly dissimilar trends, with Chiba exhibiting an renewed increase in the pithouse and group counts, associated with a clumped/primate distribution, and Gunma by an overall decline in residential density.

- While the onset of the Early Jōmon peak and decline in pithouse counts can be regarded as roughly synchronic between the two regions, the one observed during the Middle Jōmon period shows a mismatch of ca 200 years.

- Similarly, although both regions were characterised by fluctuations in the

settlement size distribution, they appear to be slightly out of phase for some time-blocks (see fig. 45).

- Each episode of strongly dispersed or clumped pattern was not necessarily associated with the same trends in the other statistical measures (see fig. 42 and 43). This suggests that while similar group size distributions reoccured during the 3,500 years interval, each episode might have been characterised by different underlying processes.

The identification of these cycles of change offers, for the first time, a direct and quantitative assessment of the claims made previously by several scholars in qualitative and descriptive terms (see section 2.4). The adoption of aoristic analysis has also allowed the shift from a relative to absolute chronological framework, providing the necessary foundation for establishing possible causal links to key environmental changes occurring during this interval (see fig. 3 in chapter 2; see also chapter 8 for detailed discussion). The majority of existing settlement studies still rely on relative pottery- based sequence but the analyses in this chapter show how new and more precise insights on Jōmon settlement dynamics are both possible and mandatory for pursuing any research on their causes. However, before proceeding to evaluate the possible role played by environmental change (chapter 8) we need to determine how clumped and dispersed patterns emerge in the first place. In order to tackle this issue we need to reverse the perspective, starting this time with plausible processes inferred from the ecological literature that might generate the observed patterns, rather than the other way around. This will be the main theme of the computational model building, developed as the core element of the third part of the thesis.

Part III

Model Building

Chapter 5

Theory and Method: Computational Model Building

A comparative review of two recent papers sharing the same magisterial title — *why model* —, provides grounds to support the choice of a computer simulation approach to understand the spatial and temporal changes in Jōmon settlements. The first paper (van der Leeuw 2004) was written by an archaeologist with a long-lasting interest in complex systems (van der Leeuw 1981, McGlade and van der Leeuw 1995) and simulation models (Kohler and Leeuw 2007), while the author of the second paper is a sociologist (Epstein 2008), who is a well known expert of computer simulations (Epstein 1996; 2007) with an active engagement in archaeological applications (Dean *et al.* 2000, Axtell *et al.* 2002).

The introductory line of the second paper offers a direct insight to the shared vision of the two authors:

> ”The first question that arises frequently—sometimes innocently and sometimes not— is simply, ”Why model?”. Imagining a rhetorical (non-innocent) inquisitor, my favorite retort is, ”You *are* a modeler.” Anyone who ventures a projection, or imagines how a social dynamic —an epidemic, war, or migration—would unfold is running *some* model” (emphasis original, Epstein 2008:1).

The key message here is that we already model all the time, and computational simulation simply offers *another* platform for pursuing this goal. The question which then follows is the choice of platform: why use algorithms, mathematical equations, and lines of computer program code instead of plain English (or for that matter any other language)? The answer, shared and explicitly acknowledged in the two papers, is that such models provide the advantage to be *explicit*, in that all assumptions and details need to be (in theory) formally expressed, giving other scholars the opportunity to recreate the same model (see Janssen 2009) in order to fully grasp its properties and confirm its results. In other words, computer simulations, along with mathematical and statistical models, provide the best way to communicate what we think about reality, without being lost in the misinterpretations and the limits of natural language (van der Leeuw 2004).

Simulations provide also an additional benefit for understand the dynamics observed in the real world. Once we have combined our ideas, assumptions, and details of a phenomenon into a model, we need to understand how this behaves. This can be achieved by reasoning on its structure, either through an informal rational or more desirably by means of analytical solutions provided by the formal language of mathematics and logic. The former will be biased by the limits imposed by natural language and human mind, the latter, whilst ideal in many contexts, is often impractical and too complex. Computer simulations offer a third alternative, where we can directly *observe* how our models unfold into dynamic processes, comparable to the real world phenomena that we ultimately want to understand (Doran and Gilbert 1994).

The wide variety of simulation models can be broadly classified into the following three distinct categories based on their function within the archaeological endeavour (Mithen 1994, Lake 2010): (1) *hypothesis-testing* models; (2) *methodological development* models; and (3) *theory-building* models.

The first group seeks to generate patterns that are directly compared to empirically observed data. This includes a relatively large number of examples (e.g. Chadwick 1978, Mithen 1990, Dean *et al.* 2000, Kohler *et al.* 2000, Lake 2000, Lans-

ing 2000, Conolly *et al.* 2008) where the core aim is usually the validation of a model through hypothesis testing procedures not dissimilar to the epistemic foundations of widely common statistical methods.

A typical problem of these computer-simulations is the tendency to unnecessarily increase the level of complexity. This is present in all types of models, but it is particularly noticeable in *hypothesis-testing* types. The deep cause of this trend lies in the reluctance to abandon specific aspects of reality, leading ultimately to the design of a hyper-realistic model where most conceivable details are explicitly integrated. The phenomenon is often referred to as Bonini's paradox (Bonini 1963, Zimmerman 1978), a problem that emerges when models are too complex to be understood, sometimes leading the modeller to, consciously or unconsciously, "drive" the outcome of the simulations to desired directions and outputs. The latter scenario will be hardly detectable, as complex models will require an additional effort by the reader in order to formally evaluate its assumptions and recreate its outputs.

Several studies illustrate how *hypothesis-testing* models can be generated without such a strong reliance on realism and without integrating an excessive number of assumptions and details. Lansing's simulation of the subak irrigation system in Bali (2000) is a good example of this: a simple game-theoretic model was in fact sufficient to describe the phenomena and generate datasets which were then tested against the observed empirical data.

At the opposite end of the spectrum between extreme realism and pure abstraction, we can find a range of abstract statistical models which rely heavily on computer simulations. Their implications are rarely discussed in the archaeological literature of simulation models, but nevertheless offer an alternative and important perspective on modelling. One example of this is offered in the assessment of point pattern data, which often relies on the quantitative comparison of an observed empirical measure to those generated via computer simulation (see Orton 1982; 2004, Bevan *et al.* under review). Usually this involves the creation of a random point pattern that acts as a null hypothesis, and significant deviations from this model

(i.e. aggregation or segregation) are often regarded as the most interesting results. This approach —where the model output provides a comparative *template*— is an important aspect that is sometimes missing in the application of hyper-realistic simulations, where models are often simplistically judged on the basis of their goodness of fit to the empirical data, and accordingly models which fit poorly are hastily dismissed. Additionally, statisticians long ago adopted more robust inferential frameworks, including maximum likelihood methods where alternative models are directly compared to each other. Such analytical sophistication is however missing in the great majority of archaeological hypothesis-testing simulation models. Most in fact focus on the model-building processes, and model validation, via quantitative comparisons between the simulated and empirical data, is left undeveloped and often based on informal visual comparisons. Perhaps, this limitation is partly derived from the nature of the empirical data itself, which in archaeological contexts is characterised by a much higher level of uncertainty compared to other disciplines. Additionally many of these simulations are not designed to model the archaeological formation process, and hence a direct comparison between their outputs and the empirical record might be potentially biassed. A possible solution might be the creation of simpler models designed to generate exclusively archaeological patterns rather than assessing their possible underlying processes (which might be suggested from ethnographic analogies or from the outcome of other models). These might be combined with *theory-building* models (see below) to form a modular research design, where process modelling (aimed to understand the structural properties of the observed system) and pattern modelling (i.e. the generation of artificial patterns that can be directly tested against the archaeological record) are approached sequentially rather than jointly.

The second type of archaeological simulation aims to refine and evaluate the pros and the cons of available tools for empirical pattern recognition. Most works of this category (e.g. Aldenderfer 1981, Gregg *et al.* 1991, Eerkens *et al.* 2005, Brantingham *et al.* 2007, Surovell and Brantingham 2007, Rubio *et al.* 2011) seek to recreate an artificial archaeological record in order to assess the limits of the

available methodological tools. Thus for example, the effects of post-depositional artefact movements can be modelled to test the robustness of certain spatial analysis (Gregg *et al.* 1991), or different types of cultural transmission can be simulated to explore their effects in phylogenetic analysis (Eerkens *et al.* 2005). The practical advantage of these models relies on the relative ease of the model building process, which primarily focuses on the generation of patterns, rather the exploration of the underlying processes and its driving forces.

The purpose of the last category —*theory-building* models— is to directly evaluate the relationship between range of possible causes and their effects (Lake 2010). The model could be derived from or inspired by enquiries related to specific archaeological contexts (e.g. Wobst 1974, Doran *et al.* 1995, Bentley *et al.* 2005, Powell *et al.* 2009), but more often seeks to formalise, investigate, and/or extend a defined body of theories (e.g. Costopoulos 2001, Shennan 2001, Smith and Choi 2007, Whitehead and Richerson 2009, Griffin 2011, Lake and Crema 2012). The distinction between these two subcategories are however fuzzy, as the abstract nature of these models allow their application to specific archaeological problems and at the same time generalisation to broader sets of phenomena. In opposition to *hypothesis-testing* models, the primary *modus operandi* of this category is to produce simulations with relatively few and often abstract parameters. This ensures better control and understanding of the model behaviour, which could sometimes even lead to *analytical* solutions, where the relationship between causative agents are expressed with mathematical rigour, which in turn eschews the need for computer simulation. The simple and abstract nature of these models could however lead to three types of problems (both applicable also for *hypothesis-testing* models): (1) the definition and quantification of the parameters could become highly abstract and unrelated to any "real" content (see Agar 2003 for discussion); (2) the temporal and spatial representation of the model might be too detached from reality (e.g. space being represented as a grid of environmental "patches"); and (3) the model could generate patterns which are not directly measurable in the archaeological record (e.g. the *fitness* of a forager). These potential limits often lead to critical dismissal

of such models as ”too abstract” or ”impossible to validate”. Such claims could be countered by stating that the aim of these models is not the emulation of reality but the development of a heuristic environment where the implications of our theories are *formally* explored (Zubrow 1981). Abstraction could undoubtedly lead to a mere intellectual exercise of anthropological theory, but *structural* similarities between artificial and real worlds can still be sought as a proxy for validating some of these models or as a basis for generating novel research questions.

This third type of model appears to be the best candidate for the research agenda of this thesis. One of the primary objectives required for answering the second research question (*can observed shifts in settlement pattern be explained without reference to environmental change?*) is to explore the wide range of possible generative processes behind observed shifts between clumped and dispersed patterns. Existing theories on human behaviour might however not be sufficient for this, and ideally they will need to be extended, revised, and combined to fit such an objective. This is a theory-building exercise, and an abstract computer simulation can provide the most flexible environment for this. Reviewing briefly how existing computer simulations have approached the problem of modelling settlement pattern can provide additional support to such a choice.

Most computer simulations of prehistoric settlement patterns appear to be closer to *hypothesis-testing* models. Recent examples include case studies of the Anasazi Indians of the long-house valley in Arizona (Dean *et al.* 2000, Axtell *et al.* 2002, Janssen 2009), the Pueblo of the Mesa Verde in Colorado (Kohler *et al.* 2000; 2005; 2007), early polities at Lake Titicaca between Peru and Bolivia (Griffin and Stanish 2007), and the Mesolithic hunter-gatherers of the southern Hebrides in Scotland (Lake 2000). Exceptions to this trend do however exist, such as Premo’s model of Plio-Pleistocene hominids (Premo 2006, although strictly speaking the model does not produce settlement patterns), or Griffin’s model of early complex polities (Griffin 2011). In both cases the primary focus is theory-building, although the underlying research questions originated from clearly defined archaeological contexts and problems.

The great majority of these simulations are *agent-based models* (ABM), that is, computer simulations based primarily on the interactions of *agents*, entities usually characterised by a goal-directed behaviour with certain levels of autonomy (capacity to make individual choices), social ability (capacity to interact with each other), and reactivity (capacity to perceive, interact and respond to the surrounding environment; Wooldridge and Jennings 1995). One of the main advantages of ABM rests in its spatial architecture, where different forms of representation can be easily adopted. This might include continuous spaces (e.g. Power 2009), grid-based subdivisions (e.g. Griffin 2011), and even relational networks (e.g. Bentley *et al.* 2005). Such a flexibility is clearly well suited for modelling settlement processes. Depending on the specific case, agents designed for these simulations can be single individuals (e.g. Lake 2000), households (e.g. Dean *et al.* 2000) or even entire settlements or cities (e.g. Bura *et al.* 1995). These agents are characterised by a series of quantitatively definable properties known as *state variables*, which play a fundamental role in determining their actions. When simulations are executed, agents interact with each other as well as with the local environment according to specific goals set by the modeller (e.g. maximise fitness or yields). These actions will often lead to a change in their *state variables*, which will in turn condition their future behaviour.

The parallel development of Geographic Information Systems (GIS) has increasingly allowed the possibility of integrating ABMs within a spatial database (see Lake 2000, Gimblett 2002), enabling the capacity to *situate* the agents within realistic landscapes. This technological achievement has probably encouraged an optimistic view on the generation of realistic models, pushing scholars to attempt building *hypothesis-testing* simulations. A possible side effect of this strong interest in GIS-integration is the prominence of models where the primary driver of the settlement process is an *induced* form of *spatial dependency* (see section 3.1), where external forces play an exclusive role in shaping the behaviour of the agents. In most cases the GIS dataset has in fact been transformed in to some form of *resource-scape*, where the value of each raster cell is representative of the degree of its at-

tractiveness or suitability for specific sets of behaviour. Agent mobility —which can be regarded as the primary cause of settlement pattern— is typically based on some sub-model where agent moves by trying to reach cells with the highest values. In most cases this is implemented using simple algorithms where agents have complete knowledge within a pre-defined search radius (as in Kohler *et al.* 2007), while in other instances the knowledge of the environment is assumed to be a state variable of each agent, which could be learned either individually (through an exploration of the landscape) or socially via cultural transmission (as in Lake 2000).

The emphasis placed on these external forces has, however, led to a relative underdevelopment of how the interaction between agents determines the spatial patterning (i.e. *inherent spatial dependency*; see section 3.1). The presence of other agents has in most cases been integrated through indirect effects on the decision-making of a focal individual. For example an agent could experience limited mobility because another agent is already occupying a possible destination, or its yield could be decreased by the consumption of the same resource pool by other individuals. However, the integration of direct forces (e.g. agents being attracted or repulsed by the density of other agents in the landscape) have been rarely applied, especially in modelling decision-making processes.

Integrating the role of "the others", and hence explicitly acknowledging "concurrent economic interdependence among different individuals' payoffs and penalties" (Giraldeau and Caraco 2000:3) has long been accepted by evolutionary ecologists as a critical aspect of foraging theory (see e.g. Waite and Field 2007) and its importance is extensively discussed in the context of group formation dynamics (see section 5.2 and Clark and Mangel 1986, Giraldeau and Caraco 1993, Gueron and Levin 1995, Hamilton 2000, Aureli *et al.* 2008). The existence of such a large body of literature suggests that in order to evaluate the long-term settlement dynamics we need to explicitly model variations that could arise internally, and not confine ourselves to the role played by variations in the external environment (see also discussion in section 3.1). At this stage, we do not have an explicit expec-

tation of what a settlement pattern should look like in an hypothetical ”flat” and ”homogenous” world (i.e. where resources are evenly distributed and topographical variation is negligible), and whether it will be stable or unstable over time. In order to provide a template for interpreting the patterns observed in chapter 4, we need to prioritise the development of theories derived from the existing literature on group formation, extend their features to model long-term dynamics, and translate and integrate this into a computer simulation.

5.1 Settlement Patterns as a Complex Adaptive System

Models of hunter-gatherer settlement pattern have often been based on a relatively static and synchronic vision, where the primary focus is explaining why the observed spatial distribution is well adapted to the specific properties of a given environment. The temporal dimension is integrated into these models, but in most cases this is narrowed to the seasonal variation of the resources and how the settlement system copes with such a spatio-temporal diversity. The fundamental question of how the observed pattern emerged in the first place, and how it changed over the evolutionary history of a region is often left aside. The most commonly found epistemic framework departs from the (often tacit) assumption that for a given type of environment, there will be an *expected* optimal settlement pattern, one that will maximise the average fitness of a given population. Consequently, a change in the environment will lead to the emergence of novel settlement patterns that will be better fit to the new properties of the environment. The exact process of how this occurs is rarely approached directly.

If we follow this reasoning, and consider Uchiyama’s distinction between *clumped* and *dispersed* patterns (2006), we would expect the former in environments where a centralised economic system is more suited, and latter when an extensive and dispersed one provides a higher benefit. Similarly, Binford’s *Collector-Forager* model

(Binford 1980) is deeply linked to the concepts of spatial and temporal "incongruence" of the resources (*ibid.*: 15), so that when these are high a collector system is more suitable and when low a forager system is expected.

We can formalise the basic logic of these models, such that given a specific environment, which we can label $\mathbf{E}_a$, there will be an *expected* pattern $\mathbf{P}_a$. This indirectly assumes that whatever is the initial condition of a system (i.e. its settlement pattern), given a new environment setting, this will ultimately converge on an expected state. The relationship between any instance of **E** and its associated spatial pattern **S** will be derived and supported from empirical observations (as in the case of Binford's model), or deduced from some form of economic model of optimality. In either case, the correlation between economic, cultural, or natural settings on the one hand and the spatial patterning on the other does not directly consider the diachronic changes that led a specific system to reach the observed pattern, often implying that the latter is at an equilibrium condition. If we adopt a simplistic vision, this would lead to the claim that as long as environment is in a given state $\mathbf{E}_a$, the observed pattern will ultimately always be $\mathbf{P}_a$, and consequently a change of the observed pattern will also necessitate and presume a change in environment.

It is clear how the primary aim of this epistemic framework is to describe *why* a specific pattern is being observed, rather than trying to understand *how* this emerged. While this is suitable for developing models aimed to explain the relationship between a given environmental setting and an observed settlement pattern, it does not provide sufficient explanatory power for describing *changes* between different patterns. Given an observed transition $\mathbf{P}_a \rightarrow \mathbf{P}_b$ we would seek explanation only by looking for evidence supporting a parallel transition $\mathbf{E}_a \rightarrow \mathbf{E}_b$. This resembles more a *prediction* rather than a proper *explanation*, since the mechanism of change itself is not modelled or explored and is more or less derived by an interpolation between known states ($\mathbf{P}_a$ and $\mathbf{P}_b$ in this case).

The problem of this approach becomes more evident if we consider the following example. Consider two distinct scenarios, one in which the observed pattern is $\mathbf{P}_a$ with the environment being $\mathbf{E}_a$, and another one where we have $\mathbf{P}_b$ associ-

ated with $\mathbf{E}_b$. At a given moment in time the background environment in both scenarios becomes $\mathbf{E}_c$, which has an expected optimal pattern $\mathbf{P}_c$. According to the explanatory framework presented above, we will expect the transition $\mathbf{P}_a \rightarrow \mathbf{P}_c$ for the first scenario and $\mathbf{P}_b \rightarrow \mathbf{P}_c$ for the latter. While, with other things being equal, the ultimate configuration of the system is expected to converge on $\mathbf{P}_c$, this form of reasoning does not help with explaining when this will occur, nor how. Both transitions will in fact require the expenditure of some energy (e.g. the cost involved in relocating each residential unit), a certain amount of time, and a given set of pre-adaptive knowledge. These are most likely different between $\mathbf{P}_a$ and $\mathbf{P}_b$, and hence their path leading to $\mathbf{P}_c$ will also be different, which also implies that for a certain amount of time the two scenarios will be characterised by different transitional settlement patterns. Consequently, if the environment $\mathbf{E}_c$ transforms (e.g. into $\mathbf{E}_d$) *before* one of the two (or both) transitions $\mathbf{P}_a \rightarrow \mathbf{P}_c$ and $\mathbf{P}_b \rightarrow \mathbf{P}_c$ is complete, then we would never see the convergent pattern $\mathbf{P}_c$, despite the existence of the same environmental change. Such a divergence in historical trajectories as a consequence of different initial conditions is known as *path-dependence* and indicates how historical contingency plays an active role in the evolution of a system.

A natural question that follows the example illustrated above is to establish how different must two initial conditions ($\mathbf{P}_a$ and $\mathbf{P}_b$ in this case) be in order to expect a divergence in their evolutionary paths. Of course the answer to this question depends on the idiosyncrasies of the system of interest and the temporal scale of observation, but a critical aspect is whether difference derived from some random fluctuation of the system is sufficient to obtain such a divergence. In other words, are differences in the spatial configuration of residential units arising from stochasticities in the individual decision-making sufficient to guarantee a long-term divergence in two settlement patterns? Or are external forces necessary for a divergence in historical trajectories?

Brain Arthur (1988) explored the relationship between two alternative systems, which he labels *convex* and *non-convex* [1] (fig. 46). The former describes systems

[1]Notice that Arthur derived this nomenclature from the shape of a probability function (not

that are resilient to small random fluctuations, while *non-convex* systems have weaker equilibria where smaller variations could have larger long-term consequences. Arthur concludes his paper suggesting that the choice between these two perspectives lies on the properties of the system itself, namely "whether small events in history matter in determining the pattern of spatial regional settlement in the economy reduces, strangely enough, to a question of topology. It reduces to whether the underlying structure of locational forces guiding the locational pattern as it form is convex or non-convex" (Arthur 1988:95).

Arthur's conclusion suggests that in order to determine the role played by path-dependence, we need to understand the structural properties of the system and then evaluate how this is susceptible to random events originating from inside and outside the system. But to do this, we first need to define exactly what we intend as a settlement pattern. If we ignore instances where some form of centralised institution or power imposes a given spatial structure (e.g. modern regional planning), any observed pattern could be regarded as the aggregate effect of individual decision-making. In other words, any spatial pattern can be considered as an *emergent* phenomena derived from the interaction of its components: each household, or perhaps each individual, will contribute to the generation of the macro-scale pattern by individually deciding where to move, live, and build their residential units (see also section 3.1). The concept of *emergence* (see Dessalles *et al.* 2007, Bedau and Humphreys 2008) is perhaps the most prominent justification of why agent-based simulation provides the most suitable model building environment. As briefly mentioned in the previous section, the core feature of ABM is that each agent will act based on its personal goals, and hence the macro-scale outcome is not designed by the modeller but a phenomenon that will emerge from the aggregate actions of the agents.

But how does defining settlement systems as *emergent* phenomena help understanding the transition between different patterns and how does this link to the concept of *path dependence*? In order to answer this question we need to: (1) es-

illustrated here), and not from the conceptual model depicted in figure 46

tablish the set of properties that are part of a given system at time $t-1$; (2) how these affect the individual decision-making at time t; and (3) how ultimately this will lead to the emergence of a novel pattern at $t+1$.

We can identify several broad properties of a system and its constituent parts that are likely to play a crucial role in the dynamics of change in settlement patterns. Firstly *biological* properties derived from specific life-styles are likely to be inherited over time, possibly driving the decision-making process in certain circumstances. These properties could be present as phenotypic expressions (e.g. individuals who are entirely dedicated to plant-gathering tasks will not develop certain muscular features which might be required for hunting activities) or deeply rooted at the gene level (e.g. a population without the lactase persistence gene will be less likely to switch to a diet based on dairy products). In a similar fashion the knowledge of the surrounding environment, the set of techniques required for certain subsistence tasks, the know-how for making specific tools, as well as any other form of information acquired either individually or via social learning will play a crucial role in the decision-making process. In other words *culture* will actively modify the decision-making, hindering certain choices and favouring others.

The combination and inter-dependence of these two inheritance systems has long been discussed and explicitly integrated in gene-culture co-evolution models (Cavalli-Sforza and Feldman 1981) and dual inheritance theory (Boyd and Richerson 1985). Both are supported by an extensive literature of theoretical studies, coupled by an increasing volume of empirical data illustrating how specific biological and cultural properties of the system will respond differently to external forces, ultimately determining alternative historical trajectories and exhibiting path-dependency (Boyd and Richerson 1992).

Advocates of niche construction theory (Odling-Smee *et al.* 2003) have recently pointed out that modified environments should also be regarded as an inheritance system and hence be regarded as a major driver of evolutionary trajectories. Landscape degradation and the creation of secondary forest environments (see section 2.2.2) are just few examples of how human groups can modify selec-

tive forces by generating artificial environments. A given subsistence strategy will, for instance, be interlinked to a network of *ecological* relationships (e.g. symbiosis, prey-predator interdependence, etc.), which will be actively modified by the behavioural choices of each individual and its consequences inherited through time. This will create a feedback process that will in turn drive subsequent decision-making. The net result can be regarded as a "triple inheritance system" (Laland *et al.* 2000; 2001, but see Olding-Smee 2007), where *ecological* inheritance is intermingled with *cultural* and *biological* ones.

The triple inheritance framework provides a useful set of theories and models which illustrates how even subtle differences in key properties of the system can determine divergent historical trajectories. We can further integrate this model with two additional heritable properties that are also likely to play a crucial role in settlement pattern change: population density and spatial structure.

The former might influence the process of change if adaptive forces have some form of frequency-dependence. For instance, figure 47 shows two different initial densities of a highly clustered settlement pattern (fig 47:**a**,**b**), which over time becomes unsuitable and hence fissions to a dispersed pattern. If the initial density is too high (fig 47:**a**), the lack of space after fission might force the settlements to have a smaller territory size than the one expected with lower initial density (fig 47:**b**). The resulting difference might lead to difference in the adaptive fitness, and even determine the formation of a completely different spatial patterning.

From an individual perspective, a change in settlement pattern will involve the physical relocation of each residential unit, which will be subject to certain costs. Since subsequent generations of offspring will inherit the spatial location of their parents, a spatio-temporal dependence will most likely affect the decision-making process. Such a *spatial* inheritance (see also Schauber *et al.* 2007) would have positive or negative effects depending on the degree of spatio-temporal autocorrelation in the suitability of the landscape. If the environment changes slowly, the optimal locations will be the same and hence the spatial inheritance will provide benefits, but if the suitability of landscape changes radically, an adaptive location could sud-

denly be maladaptive. This is the case illustrated in 47:**c**,**d**. The spatial area with higher suitability (the shaded grey area in the figure) is subject to some change over time. In both scenario **c** and **d** the settlement location becomes unsuitable and hence requires a shift in its location. However this will involve a longer distance (and hence a higher cost) for scenario **c** compared to **d**. The aggregate effects of similar constraints might ultimately determine a different *tempo* in the transition between settlement patterns, if not an entirely divergent trajectory.

Path-dependence illustrates how historical contingency matters and could determine divergence in evolutionary trajectories. The related concepts of equifinality and multifinality offer further warnings about how we establish the relationship between an observed pattern and its possible causes (see Premo 2010 for an extensive review). The former indicates instances where an observed state of a system can be reached from different initial conditions, possible through different trajectories. The latter refers to cases where we can observe the opposite: given the same initial condition we might in fact have different final states. Both strongly undermine the simplistic assumption that for a given environmental setting we should expect a specific optimal outcome [2]. In the present case, equifinality cautions that observing $\mathbf{P}_b$ at a given moment in time does not imply that environment was necessarily $\mathbf{E}_b$ (as alternative environmental condition could have generated the same pattern), while multifinality cautions that if the environment is $\mathbf{E}_a$, there are different possible responses and hence different patterns, where $\mathbf{P}_a$ is only one of the conceivable outcomes.

Luke Premo (2007) has recently borrowed a well-known metaphor offered by Stephen J. Gould, in which the evolutionary biologist asks what we would see if we could continuously rewind and observe what is being played on the "tape of life". Given the idiosyncrasies derived from path-dependence, equifinality, and multifinality we would expect to see different outcomes for each iteration. Each time the tape is played, small differences will determine different paths, which

[2]Notice that equifinality and multifinality problems refers also to the relationship between a process and the resulting pattern (see Fortin and Dale 2005:4) which in a similar fashion could exhibit convergence and divergence

will converge and diverge through time. This simple thought-experiment warns us to base our conclusions on the empirical evidence alone, since the "tape of life" has been played only once in the real world: watching it will tell us only *what* happened. In other words history is a single trajectory in time, but in order to understand *why* and *how* a specific path was followed we should evaluate its relationship to the alternative paths and bifurcations that were present at each point along its line.

The field of computational modelling is well suited for tackling this issue. Simulations provide us the opportunity to rewind and play the "tape of life" *in silico* as many times as our computational limits allow us. We can verify whether certain patterns occur more frequently than others, and establish this in probabilistic terms. This will help distinguish and classify different dynamics on the basis of the likelihood of their occurrence, and at the same identify instances of possible evolutionary convergence and divergence, thus directly addressing the issues of multifinality and equifinality. The process involved is strikingly similar to how physical experiments are conducted (see Parker 2009 and Winsberg 2010 for epistemological discussion in this regard): given a set of initial conditions, the modeller will run the computer simulation multiple times and then will record the distribution of its outcomes. This will be repeated for different *parameter* settings, which will define both the properties of the model and its initial condition. The ultimate product is often depicted as a *parameter space* where the variation of the simulation outcome is "mapped-out" on an n-dimensional space, where n is the number of the input parameters in the model. Exploration of such a space provides a multidimensional vision of the system of interest, showing how the sensibility of its behaviour varies between different variables and parameter settings.

5.1.1 Phase Space and Attractors

Given the potential complexity of the dynamics of change in human settlement pattern, a fundamental step that needs to be undertaken before assessing the role played by external perturbation is to evaluate the internal properties of the sys-

tem of interest. In the specific case, we need to establish whether transitions between *clumped* and *dispersed* pattern could occur without the onset of environmental changes, or on the contrary that these are essential to cause such changes. Undeniably, both could be possible, in which case we need to establish the boundaries within the parameter space where we would expect one or the other.

The literature of complex systems provides us with two key concepts that can help in formalising this endeavour: *phase space* and *attractors*. The former can be regarded as the "geometric representation of the universe of possibilities possessed by a system" (McGlade 1995:120). Thus in our case the phase space will represent all possible forms of spatial configurations that are theoretically possible for a given system. Notice that phase spaces represent variations (usually across time) within a single combination of parameters, and hence it should be distinguished from parameter spaces, which depict the variation of the system as a function of *different* parameter values. The second key concept —attractors— can be defined as specific points of the phase space where the system will ultimately converge. Thus if we have a one-dimensional phase space measured in A-coefficients (see section 3.3.1), and we know that ultimately the system will converge on an even distribution of settlement sizes, then we will define $A = 1$ as an attractor. An attractor is surrounded by its *basin of attraction*, so that if a system is "located" within that portion of the phase space, it will ultimate converge on the attractor itself.

The example provided above described the simplest form of attractor, known as a *point attractor*. McGlade (1995) provides a summary description of three other types of attractors: *limit-cycle attractors*, *toroidal attractors*, and *strange attractors*. The first type is characterised by a periodic fluctuation between two or more different regions of the phase space. The second is distinguished by a quasi-periodic pattern in which dynamics occurring at different scales determine an apparently chaotic behaviour of the system, which however is characterised by some form of periodicity. Finally *strange attractors* can be recognised by the presence of complex and chaotic dynamics in which there is no periodicity and no trajectory within the phase space is ever repeated.

We can apply the concept of attractors to our research question, assuming for a moment that the phase space can be described by a single dimension ranging from negative (primate/*clumped* pattern) to positive (convex/*dispersed* pattern) values of the *A*-coefficient (see section 3.3.1). Using this framework we can envisage the following set of possible outcomes for each unique combination of parameter settings:

1. Clumped and dispersed patterns are distinct point attractors (figure 48:**a**). In this case the system converges to one state or the other depending in which basin of attraction it was initially located and on the intrinsic properties of the system (thus its parameter combination) . Transitions from one settlement form to the other could possibly occur if a perturbation is strong enough to "move" the system from one basin of attraction to the other.

2. The two settlement forms are extremes of a limit-cycle or toroidal attractor (figure 48:**b** and **c**). In this scenario, changes between clumped (primate) and dispersed (convex) patterns occur endogenically. Perturbations in the system could either temporarily or permanently fixate the system in one state or another, or modify the frequency/magnitude of the fluctuations.

3. The system is chaotic and fluctuations between the two settlement patterns occurs aperiodically.

Other implications of perturbations on the system will be discussed in chapter 7, but it can be anticipated that these could actually trigger transitions between different types of attractors. A system that is in an equilibrium state around a point attractor could shift to a limit-cycle attractor, in which the original state becomes one of its poles. This is an example of a *bifurcation*, which refers to the transition of one system to another and could occur as a result of radical change in the system, caused for instance by the adoption of a novel form of subsistence strategy or technological innovation.

Previous models of complex sedentary groups have suggested that a point-attractor equilibrium of settlement system should not be taken for granted, and

that endogenic transition between different settlement forms could potentially emerge (see e.g. Renfrew and Poston 1979, Griffin 2011). For instance, Renfrew and Poston (1979:458) argued that transitions between nucleated and dispersed patterns can be generated by "smooth variations of the local factors", that "suddenly" determine a change in the system which resembles the effects caused by exogenous forces. Similarly Griffin (2011) has recently modelled the dynamics of the consolidation and collapse of early complex polities, showing that cycles of group fission and fusion observed at the macro-scale could emerge as a consequence of micro-level interaction. These theoretical studies are usually based on sedentary agricultural societies, and hence not directly applicable to mobile hunter-gatherer groups. Nonetheless, the relatively high degree of sedentism exhibited by complex hunter-gatherers (see chapter 2) indicates that some of the implications offered by these model should be considered, in particular that an unquestioned assumption that Jōmon settlement pattern constitutes a static point attractor —subject to change only when external forces are applied— should be carefully tested. In order to achieve this objective, we need to first review the basics principles of group formation, and then implement these in the dynamic environment of an ABM.

5.2 Models of Group Formation

The formation of groups is undeniably one of the fundamental processes generating variation in settlement size and hence it provides important insights for understanding the wide spectrum of variation between clumped and dispersed patterns.

The topic has been extensively explored in different disciplines, and often models proposed in one have been used and extended by others. Broadly speaking, we can recognise two distinct lines, each placing their emphasis on two different catalysts for aggregation. The first group of models have looked the effect of the environment, and more precisely the spatial distribution of the resources, as the determinant of the aggregation. This closely resembles the induced spatial dependence introduced in section 3.1, and portrays the emergence of groups as a consequence

of variation in the attractiveness of the physical landscape. To put it simply, individuals aggregate because space is heterogeneous, and they are attracted to specific locations according to their suitability. The second line of models place their emphasis on how the presence (or absence) of other individuals provides a selective advantage (or disadvantage). This is similar to the concept of inherent spatial dependency (see section 3.1), and views the emergence of groups as a function of cost-benefit ratio derived from the spatial proximity of other individuals and possible interactions derived from it. For example, individuals can be attracted to join a group because of the advantage derived by mutual defence against a common threat.

Before proceeding, it is important to stress that the two arguments are not mutually exclusive but complementary aspects of group formation. The distinction of the two perspectives should be viewed more as means to isolate the effects caused by each form of spatial dependency, rather than an explicit statement of a preferred perspective. This is born out by the fact that many of these model of group formation often incorporate both types of arguments.

One of the earliest models which explicitly linked the spatio-temporal distribution of the resources and the spatial structure of individual foragers was offered by Horn (1968) who developed a quantitative model seeking to explore the adaptive significance of blackbird colonial nests. The key argument in Horn's model was that the optimal location for a settlement (a nest in this case) is the one that minimise the foraging time travel. In order to compute this he proposed the following equation:

$$D(x_o, y_o) = 2kT \sum_i \sum_j t(x_i, y_j) \sqrt{(x_i - x_o)^2 + (y_j - y_o)^2} \tag{5.1}$$

where $D(x_o, y_o)$ is the average distance travelled from an origin located at x_o, y_o, T is a given unit of time, $2k$ is the number of round trips and $t(x_i, y_j)$ is a function of time which indicates the proportion of time where the specific location (x_i, y_j) provides the highest return. Equation 5.1 is ideally computed for each location

in a landscape, and coordinates with the lowest value of D can be regarded as the most suitable location to settle. Horn then proceeds to compare two extreme scenarios, one in which resources are stable and equally distributed in the landscape, and another in which the same amount of resource is concentrated in a single location which spatial coordinates vary as a function of time (defined by the variable $t(x_i, y_j)$). He then compares dispersed (multiple small settlements) and aggregated (a single large settlement) spatial patterns for each type of resource distribution, and using equation 5.1 concludes that dispersion is optimal for a homogeneous and static resource distribution, while aggregation is better in cases where resources are concentrated but their location is time varying.

In an extensive review of spatial organisation and habitat use of human foragers, Cashdan (1992) lists several successful applications of Horn's model (e.g. Wilmsen 1973, Dwyler and Minnegal 1985), pointing out also how its ultimate implication is similar to the power-spectrum model proposed by Harpending and Davis (1977). The key concept of the latter model was to describe the availability of one or more resources in terms of their spatial and temporal frequencies, and its main predictions can be summarised as follows: (**a**) when multiple resources have no coherence in space, and thus are homogeneously distributed in space, we should expect a dispersed settlement pattern; (**b**) when resources are correlated to each other (i.e. when the finding of one type of resource is likely to determine the finding of another type as well), and hence we expect a patchy resource distribution we should expect an aggregated settlement pattern; and (**c**) when the cross-correlation between the two resources is negative (i.e. when the finding of one precludes the finding of the other) we should again expect a dispersed pattern (Harpending and Davis 1977, Cashdan 1992).

The weakness of both models is that the main unit of analysis is the whole population, and as such does not take into account the effects of economic interdependence, competition, and interference caused by variation in local density. The ideal free distribution (IFD; Fretwell and Lucas 1970) and its derivative models (see e.g. Tregenza 1995, Greene and Stamps 2001) provide a useful framework which

combines the population density of the predator population *and* the resource abundance and spatial distribution of the prey population.

The simplest form of IFD can be described with the following equation:

$$\bar{\xi_p} = \frac{K_p}{n_p} \tag{5.2}$$

where $\bar{\xi_p}$ is the average individual gain at a given patch p, K_p is the resource input (amount of available resource) at p, and n_p is the number of individuals at p. The basic prediction of the model is that the yield of a specific patch is maximised when population is equal to 1, and that increasing population size causes a reduction of the amount of resources available for each individual. Given the assumptions that: (**a**) all individuals have full knowledge of the resource availability and (**b**) are free to relocate to any patch, equation 5.2 predicts that the evolutionary stable equilibrium will be achieved when ξ is identical for all individuals. In order to achieve such a state, the number of individuals in each patch must be proportional to the amount of resources available there.

The graphical representation of equation 5.2 (figure 49:**a**) provides an example of the dynamic by which this could occur. In this case K_A is larger than K_B, and hence if both patches are unoccupied, a new immigrant will choose to settle on patch A first. This trend will persist until the number of individuals on patch A will be equal to x. At this point, the productivity of patch A will decline to the level of patch B , and hence both locations will have the same probability of occupation, ultimately leading to a number of individuals per patch proportional to the amount of available resource (K).

This pattern is known as the *input matching rule* (Parker 1978), and is often ambiguously referred as the *habitat matching rule* (e.g. in Fagen 1987, Cashdan 1992). Tregenza (1994) notes that the latter term is unfortunate, as the key assumption of a constant and continuous resource input is not implied in its name. However, in many environments resources can be sparse, so that the negative effect of increased population density might be caused by reciprocal interference, rather than

the equal sharing of the available resources. Sutherland (1983) modelled this by introducing the interference constant m as follows:

$$\bar{\xi_p} = \frac{K_p}{n_p}^m \text{, Where } 0 \leq m \leq \infty \tag{5.3}$$

when $m = 0$, the patch will remain unexploited, while when $m = 1$ we have the same situation portrayed in equation 5.2. When $m > 1$, $\bar{\xi_p}$ will be lower than the equal share predicted by the standard IFD model. This results from the resource wastage caused by mutual interference, modelled by m.

Figure 49:**b** shows two patches where $K_A > K_B$ but also $m_A > m_B$, thus patch A has a higher amount of resource but its intrinsic properties determine a higher rate of interference among the predator population. As in figure 49:**a**, when the two patches are unoccupied, patch A will be invaded first, followed by an occupation of patch B when the number of individuals at A is equal or larger than x_1. However the long-term equilibrium is different compared to the one predicted by equation 5.2, as at higher population ($n > x_2$), patch B will have higher suitability (higher ξ) at equal population densities.

Equation 5.3 is a good example of how mutual economic independence can produce significantly different dynamics. The model however takes into account only the negative aspects of aggregation, and does not consider its possible benefits. Greene and Stamps (2001) propose an alternative model, which overcomes this issue by introducing what ecologists refer to as the "Allee effect" (i.e. instances of positive correlation between population density and individual fitness; Allee 1951):

$$\bar{\xi_p} = Q_p - B_p(n_p - M_p)^2 \tag{5.4}$$

where Q_p and B_p are scaling parameters, and M_p defines how the suitability of a specific patch p can be maximised. When $M_p = 0$, the model approximates a standard IFD model with a decreasing trend, however when $M_p > 0$, the model has a unimodal shape, with a peak value $\xi_p = Q_p$, reached when n_p is equal to M_p.

Figure 49:**c** shows two patches characterised by the Allee effect for small population densities (i.e. when $n_p < M_p$). As in the previous example, patch A is initially favoured, but this time the suitability of patch B will increase as the number of individuals located there increases. If B is unoccupied, individuals at patch A will consider relocating to the other patch when their number exceeds x_1. This will determine a positive feedback mechanism since the consequent increase of population at B will also increase its "attractiveness". The peak of this trend will be reached when the population density at B is M_B. In such a case individuals at B will have the highest fitness value, and individuals at A will be expected to migrate when their population density is over x_2.

Winterhalder and colleagues (2010) provide a series of examples where they explore how variations in the parameter values of equation 5.4 can determine different settlement histories, where the reciprocal economic interdependence between individuals can result in the occupation of different patches according to dynamics of population growth and dispersal. The complexity of the Allee effect is ultimately related to its unimodal shape, where the co-occurrence of *both* negative and positive frequency dependence is the key element.

The integration of interference (equation 5.3) and Allee effect (equation 5.4) in the IFD models shows how population density and the interaction caused by this could modify the attractiveness of specific locations. At the same time this introduces the core principle of other models, where such forces are the primary drivers of variation in the group size distribution.

Advantages derived from increased group size have been widely acknowledged in the anthropological and archaeological literature. Collective action and sharing (Hawkes 1992) are perhaps the two most commonly presented examples of positive frequency dependence among hunter-gather groups. The former refers to the execution of specific tasks (e.g. communal hunting, intensive plant gathering etc.) where the joint effort of multiple individuals determines a payoff that is higher than the one expected by the sum of individual foraging activities. The emergence of the latter has been debated among several behavioural ecologists

(see Hawkes 1992 for an extensive review) and broadly suggests that sharing is an effective strategy for decreasing the variance experienced in foraging tasks (Winterhalder 1986, Halstead and O'Shea 1989, Hawkes 1992) as well as a key element shaping the group demographic composition (Lee 2008).

The benefits of sharing have been extensively explored by Bruce Winterhalder (1986), who provides a simple mathematical model that highlights its key properties. The core component of the model is the assumption that foraging yields are subject to random forces which will lead to positive or negative deviations from an ideal mean. If resources are shared, the effects of such random forces will be reduced, as a function of: (**a**) the average correlation in the return rates of group members; and (**b**) the group size. When the former is positive, the random forces act in the same manner across the entire group, and hence sharing provides only a minor advantage with increasing group size, while when it is negative (and hence high yields of one individual tend to be associated with lower yields of another) a small increase of group size provides a relatively higher benefit to its members. The most important conclusion of Winterhalder's model is the diminishing rate of return of the benefit derived by variance-reduction: the larger is the group the smaller will be the rate of increase of the benefit derived from sharing.

Other advantages of a larger group size are mutual protection and defensibility (Gould and Yellen 1987), higher complexity in organisational tasks and division of labour (Hawkes 1992, Bonner 2004, Jeanson *et al.* 2007), increase in information acquisition (Clark and Mangel 1984), and higher rates of cultural evolution (Shennan 2001, Powell *et al.* 2009).

All these factors are associated with an increase in the per capita fitness. Determining whether this effect is unbounded or characterised by an asymptotic increase is not necessarily straightforward, although the latter scenario is expected to be common among instances where the presence of an upper threshold in the benefit can be assumed. For instance, Dunbar (1993) suggests that humans are characterised by a cognitive limit in the number of direct and stable social interactions they can maintain (equal to ca 150 individuals), and how groups exceeding

this threshold will tend to be less stable and more likely to be characterised by a high degree of social differentiation and hierarchy.

Clearly some factors can also determine negative frequency dependence, so that increase in group size is detrimental. For instance larger groups will be characterised by the psychological stress of increased interaction and crowding (Hill and Hawkes 1987), increased interference (Sutherland 1983), and a reduced availability of local resources (Hamilton *et al.* 2007), which will also lead to a higher costs in procurement and in the maintenance of larger territories (Cashdan 1992).

The combined effect of positive and negative frequency dependence, which has been anticipated by the concept of the Allee effect above, has been thoroughly explored by Roland Fletcher (1995) who examined the residential density and population size of human settlements ranging from simple mobile hunter-gatherers to agricultural societies and industrialised urban centres (see also section 3.1). The core explanatory framework adopted by Fletcher is based on the theoretical definition of a "stress matrix" structured by the following three types of constraints: (1) an *interaction limit*, which defines the upper level tolerable residential density; (2) a *communication limit*, which defines the spatial extent beyond which communication becomes inefficient; and (3) a *threshold limit*, the lower level residential density, below which settlements are unstructured. Not surprisingly, the three types of constraints are not equally relevant in all human societies, and different types of economic system or technological level determine different limit values. For example, sedentism seems to shift the *interaction limit*, as mobile groups tend to tolerate a much higher residential density.

The most relevant aspect of Fletcher's study is the cross-cultural presence of upper limits in settlement sizes, a pattern which has been observed in other studies (see e.g. Hamilton *et al.* 2007) and which supports the argument that above a certain threshold negative frequency dependence starts to predominate and lead to detrimental effects derived from grouping.

The combination of positive and negative frequency dependence described so far will determine variations in the individual fitness as a function of group size.

The exact shape of such a *fitness curve* could vary considerably depending on the complex interactions between the factors listed above and as such its precise form cannot be ascertained in archaeological studies. However a broad structural description is still possible if we choose to describe the fitness function by defining the relationships between the critical group sizes (see table 5) that are likely to be present in most conceivable models.

We first define individual fitness as an unknown function $\phi(g)$, where g is the size of the group. We can then define the smallest possible group size as m, and thus its fitness value $\phi(m)$. In the simplest case, m is referred to the single individual and hence is equal to 1, while in other instances this could be a fixed value representing a household, a small kin-group, or any other minimum aggregate unit. It is important to stress that the condition $g < m$ is never satisfied, either because of a physical impossibility (m cannot be less than 1) or by an underlying assumption that there is a smallest indivisible unit. The latter might not necessarily hold in the real world, where m could also be variable (e.g. differently sized households), but the effect of such a variability is presumed to be negligible in this context. It is worth mentioning here that m will be often referred to as an *individual*, despite potentially representing an aggregate of multiple individuals, and that g will be always a multiple of m.

It is assumed that in all cases the function $\phi(g)$ has a group size $g*$ where fitness is maximised: groups smaller or larger (but see below for an exception) than $g*$ will thus have a smaller fitness. The direct consequence of this is that the function $\phi(g)$ is assumed not to be flat or monotonic. The former would imply a complete absence of benefits (or drawbacks) derived from grouping, which contradicts the evidence listed above. Multimodality is, however, a possible condition, although its description would be a much more complex exercise. In theory, $\phi(g)$ can be regarded as a function which aggregates multiple sub-functions (i.e. $\phi(g) = \phi_1(g) + \phi_2(g) +, ... + \phi_n(g)$) representing each factor (e.g. benefit of cooperation, detrimental effect of interference, etc.). Thus if two or more sub-functions are characterised by a strong unimodal shape and their peaks are out of phase, then the resulting

aggregate fitness curve might exhibit multimodality. For the purpose of this thesis I will assume a unimodal shape, which is directly referable to existing studies (e.g. Sibly 1983, Clark and Mangel 1986, Giraldeau and Caraco 2000), generalisable to a broader number of cases, and simpler to model.

The two conditions discussed above allow us to predict and define a hypothetical group size $\bar{g}$ where the fitness is equal to the one obtained by the minimum possible group size, but $g > m$ (i.e. $\phi(m) = \phi(\bar{g})$). The existence of such a *saturation* size is not necessarily true for all types of fitness curves. For example a function characterised by unbounded growth would have $g* = \infty$ and $\bar{g}$ will consequently never exist.

Clark and Mangel (1986) describe four types of *fitness curve* based on the topological relationships between these specific values of g. When $g* = m$, we have a simple negative frequency dependence similar to the one portrayed for the basic ideal free distribution model depicted on figure 49:**a**: aggregation is always deleterious, and the optimal "group size" is m (figure 50:**a**). When $g* = \infty$, we have the opposite condition (figure 50:**b**), a larger group size provides additional benefit and we have a constant positive frequency dependence. A variant of this model can be characterised by a threshold size, above which group members are not affected by additional benefits or by detrimental effects (e.g. $\phi(g*) = \phi(g * +m)$). When $m < g* < \infty$ and $\bar{g} = \infty$, we have a pattern close to the Allee effect discussed above (figure 50:**c**). At small group size ($g < g*$) positive frequency dependence predominates, while at larger size ($g > g*$) negative frequency dependence is stronger. However positive effects due to aggregation will always exist in this case, and hence the decrease in fitness can be described as asymptotic. The last model portrayed by Clark and Mangel is described by the following relations: $m < g* < \infty$ and $\bar{g} < \infty$ (figure 50:**d**). The shape again shows an Allee effect with positive frequency dependence at $g < g*$ and negative frequency dependence above the critical size $g*$. This time however there is a specific size $\bar{g}$, above which being in a group becomes deleterious (i.e. $\phi(g > \bar{g}) < \phi(m)$).

5.2.1 Group Formation Dynamics

In order to explore how group formation dynamics could arise we need to establish which working model of a fitness curve is most appropriate. Given the evidence listed in the previous section, we can dismiss the first two types of model proposed by Clark and Mangel (figure 50:**a,b**). The latter two are more plausible candidates, where the contrast of negative and positive effects of aggregation are nicely portrayed in a single-humped curve (figure 50:**c,d**) not dissimilar to the one already explored in the context of IFD when the Allee effect has been explicitly explored (see figure 49:**c**). In the present thesis I will mainly focus on the second type of unimodal curve, which integrates the notion that negative forces of grouping can exceeds positive ones above certain group sizes. This is not an new concept in anthropology (see e.g. Smith 1983), and implies that increased group size can lead to a decline in the return rate, reaching levels below the ones expected by foraging alone and triggering different types of potential responses including group fission-fusion dynamics (Aureli *et al.* 2008).

The unimodal curve has extremely interesting properties in terms of its implications for group formation dynamics. One of these is the intrinsic instability of the optimal group size, which led several authors (Sibly 1983, Clark and Mangel 1984) to suggest that, counterintuitively, the expected group size is likely to be closer to $\bar{g}$ than $g*$. This expectation, which has been proven both empirically and theoretically, can easily be substantiated by the following thought experiment. Consider a small group with $m > g < g*$ with a fitness curve similar to the one portrayed in figure 50:**d**. Such a group will provide a higher fitness than the one expected by an individual in the smallest possible unit (i.e. $\phi(g) > \phi(m)$), and hence individuals will tend to migrate there. This will provide a benefit to both the members of the group and the newcomers, so long as $g < g*$. At a certain point the group will reach its optimal size $g*$, beyond which any additional unit will decrease the fitness of its members. However at this point the difference $\phi(g) - \phi(m)$ will have reached its highest value, meaning that the group "attractiveness" will also have reached its peak, leading to an increased rate of immigration. This will further in-

crease the group size until it reaches its saturation size $\bar{g}$. At this point, joining the group will no longer provide advantage, and hence immigration will cease, leading to an equilibrium state. We can denote this group size as the *equilibrium group size* and refer to it with the symbol $\dot{g}$ [3].

The dynamic portrayed above is biased as it considers only the perspective of the joiner and ignores the implications of his/her choice for existing group members. In fact, from the latter perspective, the presence of joiners is beneficial only for groups with sizes up to $g*$, after which any additional m will decrease the ϕ of group members. This determines a conflict of interest between incumbent members of a group (who will expect a decrease in fitness) and joiners (who will expect an increase in fitness). Several scholars (e.g. Smith 1983, Giraldeau and Caraco 1993; 2000) have explored different models of this, in most cases trying to establish whether incumbent members are willing to reject the newcomers for an hypothetical cost (expressed in terms of energy consumption or a decrease in fitness) or not. For example, Smith (1983; see also Boone 1992) developed a game theoretic model of group formation, which predictions successfully matched the ethnographically observed pattern of Inuit hunting groups.

When facing a declining fitness, incumbent members of a group might also consider leaving the group itself. In the case of the minimum possible group m, two different options are available: (**a**) join another group through *migration*; (**b**) become a solitary group ($g = m$) through *fission*. If we assume that individuals are free to join or leave a group and have complete knowledge of both the fitness of the origin group $\phi(g_o)$ and the destination group $\phi(g_d)$, we can easily predict conditions where one option is better than the other. Migration would be favoured if the destination provides a higher fitness than the origin ($\phi(g_d) > \phi(g_o)$), and the

[3] It is worth mentioning that the shape of the unimodal curve could determine a different outcome, leading $g*$ to be occasionally stable. Giraldeau and Gillis (1984) showed this exploring different shapes of unimodal fitness curves via computer simulation. They found that in certain situations, when "the fitness of joining a group of optimal size is less than that of remaining alone" (Giraldeau and Gillis 1984:667), the optimal size will be $g*$. The result of their analysis is partly due to that fact that their simulation was based on discrete values rather than continuous ones. In fact, in order to have the condition described by Giraldeau and Gillis, the condition $\phi(g*+m) < \phi(m)$ must be satisfied. In other words, the size $\bar{g}$ can never been reached because $(\bar{g} - g*) < m$. In a continuous mathematical model this is however possible.

expected fitness when foraging with the minimum possible size ($\phi(g_d) > \phi(m)$). When the second condition is not satisfied and $\phi(g_o) < \phi(m)$, fission will provide the highest increase in fitness.

If we assume that the fitness function is the same for all groups (e.g. by assuming for instance that all groups have the same subsistence strategy on a landscape with a homogenous distribution of resources), the viability of migration is entirely a function of the group size distribution, and could occur for any instance where the inequality $g \neq g*$ is satisfied. All other things being equal, fission will instead occur only when the economic return of members of a group is lower than $\phi(m)$. The threshold size above which fission provides an increase in the benefit will be referred to as the *fission size*, and will be labelled with the symbol $\hat{g}$. In normal conditions, clearly $\hat{g} = \bar{g}$, since as we recall from the description of the fitness curve, $\bar{g}$ is the group size when the fitness becomes equal to the one expected by foraging as a single unit. However, if we incorporate any costs involved in fissioning or we assume that the difference between $\phi(g)$ and $\phi(m)$ should be larger than a specific threshold value in order to fission, $\hat{g}$ (fission size) could theoretically be larger than $\bar{g}$ (saturation size).

So far we have considered only the independent decision-making of m, the minimum aggregate unit. An alternative scenario can be explored for instances where multiple subunits jointly decide to fission or migrate. We first define this group as a subset q of the parent group, where $q > m$. In theory the optimal value of q can be predicted as the one satisfying the inequality $\phi(q) > \phi(g)$, but in practical terms this is entirely dependent on the shape of the fitness curve. Figure 51 shows three groups of equal size and evaluates the diverse implications for $q = g/2$, given three alternative fitness curves sharing the same structure as the one portrayed in figure 50:**d** (thus with an unimodal shape and the $\bar{g} < \infty$).

Group fission does not necessarily involve the creation of equally sized subsets, in fact in the optimal choice is unlikely to be so. For instance, if we observe carefully the scenario portrayed in figure 51:**b**, we will notice how a group fission with $q \approx \frac{3}{4}g$ will provide a fitness close to the highest possible value. This, however, will

require the remnant members to form a group of size $\frac{1}{4}g$, which will reduce their fitness below that expected with the current group size g. This situation is known as a *zero-sum* game, where the gain of one player (one sub-group in this case) will unavoidably lead to a loss for the other(s). The perfect solution could occur only when the group size is $2g*$ [4], when a fission into two equally sized groups ($q = \frac{1}{2}g$) would provide the highest benefit both offspring groups. When this perfect solution is not tenable, an optimally sized group (the one sized $\frac{3}{4}g$ in the example above), and one or more sub-optimally sized groups will emerge after fission. This will in turn push the individuals located in groups with lower fitness to migrate towards the optimally sized group. As a consequence of these invasions, such a group will experience a decrease in fitness, since its size will be larger than $g*$. The long-term equilibrium will be the creation of two equally sized group.

Group decision-making has rarely been used in models of human settlement creation (but see Lake 2000 for an exception), and in most cases this involves a simple shift of the agency from the single individual to a larger composite unit, or to different variants of voting models (e.g. Lake 2000, Sellers *et al.* 2007). More sophisticated models are being developed (e.g. Sayama *et al.* 2011), but their extreme complexity appears to be inapt in this context.

One problem that affects both individual and group decision-making is the assumption that group members are aware of the shape of the fitness curve. In most scenarios, however, it is very likely that this and other parameters are unknown to the members of the group, and they can only approximate them based on direct observation and information exchange with individuals of other groups. Ethnographic data supports the existence of inter-group information sharing for several hunter-gatherer traditions (see examples in Whallon *et al.* 2011), either during occasional encounters or visits (e.g. Watanabe 1973, Meehan 1982), or as part of a regular trade network (e.g. Silberbauer 1981). These episodes will enable each individual to evaluate their conditions in a comparative fashion (for instance by

[4] In theory any multiple of $g*$ would lead to perfect solution, but in practice there would be no reason to not fission when the group reaches $2g*$

assessing their perceived payoff difference) and ultimately guide their decision-making.

5.3 Building the Model

The review presented in the previous section allow us to highlight the following points:

- Given the assumptions of the basic form of IFD model (see equation 5.2) and with the other things being equal, we should expect a long-term equilibrium where the population density matches the underlying resource distribution of the environmental patches.
- Once the IFD model integrates both positive and negative frequency dependence, the dynamics become more complex (see equation 5.4 and discussion on figure 49:**c**).
- The relationship between group size and the fitness of its member can be portrayed as an unimodal fitness curve, with an optimal size $g*$ (where fitness is maximised) and a saturation size $\bar{g}$ (above which being in the group no longer provides benefit).
- Individuals are expected to improve their condition (i.e. their fitness) by reallocating themselves. This might involve leaving or joining a group by means of migration and fission-fusion processes.
- Individuals are assumed to have only a comparative knowledge, that is, they are able to evaluate whether other individuals are performing better or worse than themselves but incapable to portray the exact shape of the fitness curves.

These points will form the basis of a computer simulation model[5], which allow us to explore the expected macro-level consequences (i.e. group size distribution)

[5]Technical details of the model are described in the Overview, Design and Details protocol in appendix B, while the computer code are provided in appendix C

of some of these assumptions. The adoption of ABM provides us the opportunity to combine some of the aspects introduced in the IFD models (e.g. a spatial structure formed by patches) to the assumption of an unimodal fitness curve. At the same time, key elements such as demographic processes (reproduction, death, and migration) and decision-making rules can be integrated, providing a simulation environment that can be later enriched by the integration of models apt to explore the effects of exogenic forces (see chapter 7).

The core of the model is the definition of a fitness function, which can be assumed (see section 5.2.1 for justifications) to have an unimodal shape similar to the one portrayed in figure 50:**d**. We start by defining ξ_i as the gain of the minimum aggregate subunit of foragers (of size m) with the index i, so that the gain of each forager of a group will be distinguished and coded $\xi_1, \xi_2, ...\xi_g$, with g being the group size expressed as the number of its constituent subunits (i.e. a group with three subunits m will have $g = 3$). We can further assume that individual gains are : (**a**) subject to randomness; and (**b**) dependent on the group size g.

The first aspect can be modelled as a random yield from a Gaussian probability function with mean μ, and a standard deviation ϵ. The choice is dictated by the assumption that foraging efficiency is affected by multiple random and independent factors (e.g. fluctuations in the availability of the resources, chance events during foraging activities, etc.) that can occasionally produce yields that are higher or lower than a certain average. The symmetric nature of the Gaussian curve implies also that there are no biases towards higher than or lower than average yields (i.e. stochastic deviations from the means have the same chance of being beneficial or detrimental), that the likelihood and magnitude of these events will be tuned by ϵ, and that in the long run the average yield of an individual will be μ. The choice of a Gaussian curve for modelling foraging yields is not new and has been widely adopted in the anthropological literature (e.g. Winterhalder 1986, Henrich 2001, Lake and Crema 2012).

The second aspect, that is the benefit derived by the presence of other members in the group, can be integrated as a positive surplus to the individual yield that

increases as a function of the group size. For the sake of simplicity this can be depicted as a linear model that increases μ as a function of the group size g.

The combination of these two assumptions is formalised in the following equation:

$$\xi_i = \mathcal{N}(\mu_i + (g-1)^b, \epsilon) \tag{5.5}$$

where $\mathcal{N}$ indicates a Gaussian probability distribution with mean $\mu_i + (g-1)^b$ and standard deviation ϵ. The exponent b is a scaling parameter which determines a concave curve for $b > 1$, a convex curve for $b < 1$ and a linear growth for $b = 1$ (see figure 52). Following the assumptions illustrated in section 5.2.1, the most sensible values of b appear to be below 1, since several types of benefit seem to follow a convex curve with a decreasing benefit caused by the presence of other individuals in the group.

At this stage the model resembles the one depicted on figure 50:**b**, with no negative frequency dependence due to large values of g. Furthermore, no effects of variance reduction are incorporated in the model, so a larger group will still experience the same stochasticity as the single subunits.

These two elements can be incorporated as follows. First we define Ξ as the total contribution of a given group, which is obtained by summing all ξ. More formally we have:

$$\Xi = \sum_{i}^{g} \xi_i \tag{5.6}$$

The resulting value will then be equally shared among the group members as follows:

$$\phi_i = \frac{\Xi}{g} \tag{5.7}$$

Thus, the stochastic effect derived by ϵ will be reduced with increasing group size, mimicking the outcome of sharing among foragers (see figure 53).

The negative frequency dependence at high values of g can be obtained by introducing a parameter defining the size of the resource pool (K) as shown previously for the IFD models (see equation 5.2). This leads to the following equation:

$$\phi_i \begin{cases} \Xi/g & \text{if } \Xi \leq K \\ K/g & \text{if } \Xi > K \end{cases} \tag{5.8}$$

where K is the resource input of the patch where the focal group is located. Equation 5.8 basically models the negative effects of overexploitation; when $\Xi > K$, the individual fitness ϕ will decrease due to the lack of available resources. As a result the fitness curve will have a unimodal shape, and given $\epsilon = 0$, we can predicted the critical size $g*$ as the one satisfying the condition $K = g(\mu + (g-1)^b)$, and $\bar{g}$ as equal to K/μ (see figure 54).

The combination of the parameters b, μ, and K and their effects on the fitness curve are described in figure 55: the increase the cooperation benefit (b) and the basic fitness (μ) combine to determine a decrease in the value of $g*$ but an increases in $\phi(g*)$. The former also considerably modifies the shape of the curve, with higher values determining a much higher initial rate of increase in ϕ. Variation of K is instead positively correlated to the variation of $g*$, $\phi(g*)$, and $\bar{g}$.

One of the critical aspects missing in the models presented in the previous section is the explicit integration of population dynamics. Fitness curve models such as the one portrayed by Clark and Mangel (1986) do not take account of the possibility of reproduction and death that can also determine variation in g. These can increase or decrease group size as a function of the fitness of its members, and hence we should expect that a group with $g = g*$ will most likely become larger over time, even if it does not accept any external members. Since most models look at short-term dynamics where the reproduction and death of individuals are not considered, I will refer to the equilibrium exhibited by these as *short-term*. We have already seen before that, with other things being equal, group sizes are expected to be roughly equal to $\bar{g}$ when the group members' fitness $\phi(g)$ is equal to the one expected when foraging as the minimum unit ($\phi(m)$, here on average equal

to μ). The group size that remains in equilibrium (i.e. is not subject to invasion or fission) can be defined as the short-term equilibrium group size, and be labelled with $\dot{g}$. However if we incorporate reproduction and death, the expected group size might be different from $\dot{g}$. In fact if $\phi(\dot{g})$ is sufficiently high, the group might continue to increase in size by internal growth and ultimately fission. We can thus define the *long-term equilibrium* size as the expected size when all demographic processes (migration, reproduction, and death) are incorporated and label this with $\breve{g}$. This will allow us to infer that the short ($\dot{g}$) and the long-term equilibrium size ($\breve{g}$) can coincide only when the group net growth rate (γ) is equal to zero at that size.

In order to integrate these concepts in the model, we need to convert fitness to probabilities of reproduction and death. The former could be represented as a linear function of the fitness so that:

$$r = \rho \frac{\phi}{\mu} \tag{5.9}$$

where r is the probability of reproduction and ρ is the basic reproduction rate that we will expect if the group size is m (since $\phi(m) \approx \mu$).

The probability of death could be formally described by the following equation:

$$d = \frac{1}{1 + e^{(\omega_1 \phi) - \omega_2}} \tag{5.10}$$

where d is the probability of death, and ω_1 and ω_2 are shape parameters, which ensure a sigmoidal shape with $d = 0.5$ when $\phi = \omega_2/\omega_1$. The choice of this shape is dictated by the following assumptions: 1) d will be low with high values of ϕ, but never equal to zero (ensuring the possibility that an agent has a small chance to die even when its fitness is high); 2) decrease in fitness will determine an exponential increase in d (i.e. a small initial decrease in ϕ will have a marginal effect, but with further decrease, d will become extremely large; see for example Pelletier *et al.* 1993).

Equations 5.9 and 5.10 allow us to define the net growth rate as follows:

$$\gamma = r - d \tag{5.11}$$

This will have positive values for expected growth and negative values for expected decline in the group size. Furthermore we can introduce the last critical group size $\tilde{g}$, which will be the value of g, for a given fitness curve, where $\gamma = 0$. Thus we can say that if only one group is present (and hence there is no possibility of immigration), the long-term equilibrium group size $\breve{g}$ would be equal to the zero net growth rate group size $\tilde{g}$. Table 5 provides a summary of all the critical group sizes and their annotations used in the thesis.

5.4 Implementing the Model in an Agent-Based Framework

The mathematical definition of the fitness curve (equations 5.5, 5.6, 5.7, and 5.8) and related demographic processes (equations 5.9, 5.10, and 5.11) provides the basic set of submodels which can be linked within an agent based simulation environment and at the same time establishes a theoretical bridge and extension to the previous studies introduced in section 5.2.

In order to achieve this objective a computer simulation has been created using R (R Development Core Team 2011), a programming language and software environment specifically designed to deal with statistical computing and graphics. Implementation of ABMs in R is not common (but see Lake and Crema 2012) but its flexible structure allows the creation of a hierarchical organisation of submodels, and its wide library of statistical tools enable the analysis of the simulation output in the same software environment. Although the simulation can be conducted on any desktop computer, a wider exploration of the *parameter space* requires its implementation on a high performance computer cluster. All simulation has thus been conducted on the UCL Legion high performance computing facility.

One of the major advantages of the model described in section 5.3 is that by

choosing to incorporate the resource input parameter K, we have established a structural framework which enables the integration of some key properties offered by IFD models. We can in fact create the *spatial environment* where the agents will act as a two-dimensional torus[6], subdivided into P patches, each with its own value of K.

The simulation will proceeds in discrete time steps $t = 0, 1, 2, 3, ..., T$, such that it terminates when $t = T$. At its initialisation, $N(t = 0)$ agents are created and randomly distributed among all patches. Each agent represents the minimum aggregate unit m, and if two or more agents are located in the same patch they will automatically form a group of size $g > m$. At this point the set of equations introduced in section 5.3 can be applied to each group, and hence the fitness of each individual can be computed on the basis of the predefined constant parameters (see table 7) and the group size g. The fitness will then be used to simulate the reproduction and death of individuals, thus mimicking basic population dynamics.

5.4.1 Decision-making

The model developed so far recreates the unimodal fitness curve introduced in section 5.2, and integrates biological forces of reproduction and death, but does not incorporate the decision-making process which guides the relocation of individual agents (via fission-fusion, migration, etc.) as an adaptive strategy. Such processes have been modelled in the literature of IFD (see Tregenza 1995) and fitness curves (e.g. Sibly 1983, Clark and Mangel 1986) with the core assumption that all individuals have full knowledge of the surrounding environment (including the fitness of other individuals) and that any decision will not involve costs or constraints (e.g. the "free" assumption on IFD).

These two assumptions do not always hold, as: (**a**) individuals' payoff will not be a function of the group size alone but also of other external forces; (**b**) fitness

[6] A torus is a geometrical shape resembling a doughnut which is widely used in ABM to avoid instances of edge effect. To put it simply given a square shaped area, any movement of an agent "outside" the edge will lead it back on the other side of the square. See also figure 56

of other individuals will be inferred by incomplete observations and indirect evidence, and hence knowledge of it is susceptible to error (see for example Ohmagari and Berkes 1997, Henrich 2001, Eerkens and Lipo 2005); and (**c**) spatial relocation (e.g. migration, fission etc.) will be affected by costs and constraints that will drive the decision-making.

The first point has been already addressed with the definition of the fitness curve. The presence of ϵ in equation 5.5 guarantees that stochasticity is present in the model, so that members of two equally sized groups can have different fitness due to random effects (although this will vanish as soon as the group demand Ξ exceeds the resource pool size K). The parameter K in equation 5.8 also provides the possibility of exploring the effects of both spatial and temporal variability, an aspect which will be extensively pursued in chapter 7. This section will tackle the second and the third point by modelling the cost and constraints of individual decision-making process and how these are shaped by the knowledge of other individuals.

In the present model, the trigger for decision-making is assumed to be some form of comparative evaluation occurring during social interaction between agents. The outcome of this process might eventually lead the agent to improve its current situation (fitness level) by relocating itself to a different patch. Kennedy (1998, see also Kennedy and Eberhart 2001) proposes a generic model of learning that can be applied in this context. Its basic structure is a three-step process starting from an *evaluation* of other individuals' behaviour, a *comparison* to its own and an eventual *imitation* of the other individuals' behaviour.

An individual will first need to evaluate the behavioural traits adopted by others. This could be a simple acknowledgement of difference to the focal individual' own behaviour, or a more sophisticated form of evaluation where the fitness of the other individual is calculated. For instance, one could determine how commonly a specific trait is adopted, or measure the success of an agent having such a trait. The literature of dual-inheritance theory provides many examples in this regard (see Boyd and Richerson 1985) and offers a series of mathematical models

which explore how the chosen measure can strongly affect the process of imitation and hence the ultimate distribution of behavioural traits. To put it simply *evaluation* involves the adoption of some heuristics that would decrease the costs of learning. In most cases this will involve some form of sampling (e.g. observe a randomly chosen individual), summary measures (e.g. what is the most common or uncommon trait), and/or selection process (e.g. who is the individual with the best performance), which will bias the process of cultural transmission (Boyd and Richerson 1985, Henrich and McElreath 2003). Several studies in ethnography (e.g. Hewlett and Cavalli-Sforza 1986, Henrich and Gil-White 2001 and psychology (e.g. Eriksson *et al.* 2007, Efferson *et al.* 2008) have further explored these models, seeking validation on empirical data. Archaeologists have instead tried to infer about different forms of cultural transmission bias by assessing, for example, the distribution of artefact traits (e.g. Shennan and Wilkinson 2001, Bettinger and Eerkens 1999). A common feature of all these forms of biased evaluation is that, in certain circumstances, a maladaptive trait can spread among the population. For example if a trait is characterised by a negative frequency dependence, then an evaluation based on the commonness of the trait will be deleterious, similarly if one copies a trait based on the fitness of the carrier, it might not consider the specific context in which the trait is successful (e.g. the trait might be beneficial only in certain environments) or the observed trait might have nothing to do with the success of the carrier at all.

Comparison occurs when the focal individual estimates its own strategy in relation to the observed trait. This might also be biased especially when the traits exhibits variability in their phenotypic expression. For example, Lake and Crema (2012) have recently shown that when the payoff derived from a trait is stochastic, model-biased transmission (i.e. a form of cultural transmission where traits are evaluated and selected on the basis of the properties of the individual who exhibit the trait itself) can occasionally lead to the abandonment of a trait for the adoption of less beneficial ones. This occurs since in their model-biased evaluation the focal individual observes the most successful individual, and hence it is not able to dis-

tinguish between success derived by chance and success derived by the intrinsic properties of the trait itself. If the number of individuals adopting a maladaptive trait is large enough, a successful individual is likely to emerge by pure chance, and hence the trait can spread among the population.

In most cases, the stochasticity of a trait can be acknowledged and hence incorporated in the process of evaluation. For example, in his mathematical model of environmental learning, Henrich (2001) introduced a parameter named *threshold of evidence*, which essentially measures the propensity of an individual to abandon the current trait and adopt a newly observed one. The key feature in this model is that individuals compare the outcome of their own trait and the outcome of a novel trait and then evaluate the difference between the two. If this difference is above the *threshold of evidence* the new trait will be adopted, conversely when it is below the threshold, the old trait will be maintained. We can easily infer from this simple model that, other things being equal, small *thresholds of evidence* will lead to a higher propensity to adopt novel traits, at the expense of erroneously copying a trait which is less adaptive than the one currently adopted. On the other hand, high values of the threshold will lead to conservatism, and thus obsolete traits could persist longer in the population.

This brief review of the literature provides the basis on which a model of the foragers' decision-making can be designed. First we assume that decision-making will occur at frequency z, a parameter mimicking the response time of individuals. High values of z will potentially determine higher rates of relocation and at the same time increase the likelihood of synchronic decision-making, low values on the other hand will determine a higher diversity in the response time.

The evaluation process will be based on a structure similar to a variant of model biased transmission used by Shennan (2001) and more recently by Lake and Crema (2012). This involves the selection of a model agent w, defined as the best agent among a subset of the population. In Shennan's work, and also in Lake and Crema's, this subset was defined as a purely random selection of x agents from the entire population, with x being controlled as a model parameter. In the

present model, two constraints will shape the size and nature of the subset population. Firstly, I assume that the evaluation process will be constrained by physical distance; this could be portrayed either as some form of distance-decay function (i.e. the further away an individual is, the less we know about him/her) or more simply by a threshold value. For the sake of simplicity this model will adopt the latter option by using the parameter s, representing a spatial neighbourhood expressed in grid-cell (known as Chebyshev) distance (see figure 56) from the patch where the focal agent i is located; any agent outside this neighbourhood will be ignored by the focal agent. We define the set of all agents within distance s from the focal agent i as $U(i, s)$, and use the operator $||$ to define its size. The agent will be further constrained by the parameter k, which represent the proportion of individuals from $U(i, s)$ from which the subset $u(k, i, s)$ is randomly drawn. The size of u will be defined as $\lceil k|U(i, s)|\rceil$, where the ceiling operator $\lceil\rceil$ ensures that even with extremely small values of k, the subset $u(k, i, s)$ will have at least one agent.

The agent will then choose its model w, which will be the one with the highest fitness among the subset $u(k, i, s)$. Notice that since members of the same group will have the same fitness (see equation 5.7), the focal individual will choose the group with highest fitness, with the model agent w being simply its representative. In practical terms, the combination of the parameter k and the size of each group will determine an unequal "visibility", with larger groups having a higher chance to be observed and selected as models. This is a satisfactory side effect of the model, since a higher visibility of larger groups is a plausible assumption in this case.

The next step involves the direct comparison of the focal agents' fitness ϕ_i to: (**a**) the model agent's fitness ϕ_w; and (**b**) the expected fitness of an individual forager (μ). The latter is assumed to be known by the focal agents, as individual units are expected to be capable of determining their own contribution to the group benefit. Each of these comparisons will be calibrated by different thresholds of evidence c, and will also depend on g_i — the size of the focal agents' group — and g_w — the size of the model agents' group — . As a result the focal agent will choose among

the following options:

Stay in the current group/patch. This will occur if the focal agent considers its own strategy to be the best possible or when some constraint(s) prevents the realisation of one of the other possible options. More specifically, the former will occur when the agent's fitness is better than the one expected for $g = m$ minus the threshold of evidence (i.e. $\phi_i > \mu - c_1$), and when it is better than the model's fitness, again minus the threshold of evidence ($\phi_i > \phi_w - c_2$ in case $g_i > m$, and $\phi_i > \phi_w - c_3$ in case $g_i = m$). The latter could occur when fission is not a viable option as all the patches within a distance of h are occupied by other groups (see below).

Migrate to another group. If the model agent's fitness is sufficiently larger than the focal agent's (i.e. when their difference is larger than the threshold of evidence), the latter will join the group through migration (when $g_i > m$) or through fusion (when $g_i = m$), provided that $g_w > m$. The threshold of evidence will be equal to c_2 when $g_i > m$ and to c_3 when $g_i = m$. Following the assumptions of the IFD models, migration is assumed to be unconstrained, that is members of the destination group cannot limit the access of the agent i. Notice also that the focal agent should determine at the same time that migration will be more productive than fission, and hence the condition $\phi_w > \mu - c_1$ will also need to be satisfied.

Fission and create a new group. If the agent is in a group ($g_i > m$), migration is not a viable option (either because $\lceil k|U(i,s)| \rceil = 0$ or because $\phi_i > \phi_w - c_2$), and empty patches are available within a distance of h, then the agent fissions and forms a new group of size $g_i = m$, as long as this is regarded as beneficial (i.e. $\phi_i > \mu - c_1$). Alternatively, if the model agent has a group size $g_w = m$, and $\phi_i < \phi_w - c_3$, then the focal agent will imitate its strategy (i.e. switch to individual mode), and hence fission. The underlying assumption in this case is that that the focal agent presumes that $g = m$ is the best option, and hence does not consider joining w to form a group.

Create a new group through fusion. If both focal and model agents have $g = m$, and the conditions $\phi_i < \mu$ and $\phi_w < \mu$ are both met, then the two will join and form a new group with size $g = 2m$. In practical terms, this assumes that fusion occurs as a cooperation between foraging units experiencing less than average payoff.

The four choices (see table 6 for a summary) allow each agent to adapt to the contingencies of group formation dynamics, which itself emerges as an aggregate effect of all agents' decision-making. There are three assumptions that justify how the behavioural rules of the agents have been designed:

Firstly, instances where multiple agents jointly fission to form a group larger than m have been omitted, leaving in the individual agent the *locus* of decision-making. The consequences of this assumption become apparent in certain situations where agents make temporarily suboptimal choices. For example, if a given group has $g = 2g*$, a fission to two half sized groups is the best theoretical option, and forming multiple groups of size m will only provide a partial improvement, which sooner or later will lead to the creation of larger groups through fusion. Removing the complexity of group decision-making (see 5.2.1) is however a necessary sacrifice in order to maintain the flexible and abstract nature of the simulation and to avoid an increase in the number of dimensions of the parameter space. Furthermore, these group processes cannot be solved by simply placing the agency at higher aggregate levels, since subgroup formation prior to fission should be modelled as a phenomena emerging from the interaction of the smallest units. These dynamics will however be strongly related to the underlying social network within and between groups which has not been modelled in this context. Thus, while acknowledging the existence of these dynamics, the model has been based purely on the perspective of a single agent, with all instances of group formation resulting from interactions between agents seeking to improve their own fitness.

The second key assumption of the model is the motivating force behind the decision-making. Steven Mithen (1990:31-32) distinguishes three distinct principles on the basis of different backgrounds — including psychology (Simon 1979)

and evolutionary biology (Dawkins 1982)— which have been applied, although to different degrees, in this context:

Optimising principle Agents try to achieve the highest possible fitness. In this case agents would always try to achieve a fitness equal to $\phi(g*)$. This driving force has not been integrated in to the model, as one of its assumptions is the full knowledge of such a hypothetical value. This principle is however the underlying assumption in many of the models described in section 5.2.1.

Meliorising principle. Agents try to improve their performance in a comparative and competitive fashion. This is integrated in the model for instances of migration ("move to the group which is doing better") and episodes of fission triggered as an imitation of another individual forager ("choose the behaviour which is doing better").

Satisficing principle. Agents change their behaviour only when this is regarded as unsatisfactory, and do not change their behaviour otherwise. This is partially integrated in the model when fission is triggered because no other options are available and the focal agents fitness is lower than $\mu - c_1$.

The third assumption is that agents do not have memory of past actions. This means that agents do not have the facility to learn, and hence to determine the shape of the fitness curve and to predict the consequence of their own decision-making. The most relevant implication can be observed in the process of fusion, in this case in the formation of a group of size $g = 2m$ as an union of two individual units. The assumption is that since agents have no knowledge of the benefit of group foraging (since they ignore the shape of the fitness function) fusion will not emerge immediately but only as an outcome of the cooperation of two individual units both experiencing a lower than average payoff (see above). For this model, such an event have a fixed probability of occurrence[7] of 0.25, although fusion itself

[7]The payoff of individual foragers are modelled as random draws from a normal distribution, and fusion occurs when both the focal and model agents have an yield minor to its mean μ. In order to determine the probability of fusion, we first need to establish the probability that an agent will

will occur only if all the other agents within the neighbourhood defined by s are individual units (since otherwise a migration/fusion to a group will be more likely to occur). Modelling agents as memory-less individuals implies that the duration of a single time-step is sufficiently long that the knowledge acquired during each decision-making episode is lost. Clearly defining how long is a single time-step in real-world terms is not possible given the abstract nature of the model. The implications of this will be discussed later; here it is sufficient to remind that the priority is to identify the broad behaviour of the system by mapping its parameter space for theory building purposes, rather than seeking a more realistic spatio-temporal reference system apt for hypothesis-testing models.

5.5 Summary of the Model

Before exploring the parameter space of the model and how its phase space will vary accordingly, I will briefly summarise the key features of the agent-based simulation (see also table 7 for a summary list of parameters and state variables) :

- Agents are minimum aggregate unit of foragers (e.g. a household or a close kin group) who seek to survive and pursue an increase in their fitness through spatial reallocation.
- Each spatial location (patch) will determine the fitness of the households located there. This will depend on the inherent properties of the environment (i.e. the amount of available resource, K) and the local population density (number of agents).
- The relationship between the number of agents in a group and the fitness its

have an yield smaller than its mean, which in the case of normal distribution is always 0.5. Hence the probability that *both* agents have such a lower than average yield will be the simple product between the two probabilities: $0.5 \times 0.5 = 0.25$. An alternative model could integrate a threshold of evidence as follows. If both agents have an yield of an amount c smaller than the average, then the two agents cooperates and create a new group. In such a scenario the value of c and ϵ play a crucial role. The higher is the former, the lower would be the chance of fusion but at the same time the higher is ϵ (the uncertainty derived by foraging) the higher would be the likelihood of such a event.

members have positive frequency dependence for small sizes, and negative frequency dependence for large sizes. This will determine a unimodal fitness curve with a single optimal size peak.

- The fitness of the agent will determine its probability of death and reproduction. The latter can be regarded as the splitting of the parent household into two offspring households, and does not involve a relocation process (i.e. the two offspring agents stay in the same patch/group).

- The fitness of an agent will change if the group size changes. To cope with this, agents have the possibility to relocate themselves. This could involve a movement to another occupied (migration and fusion) or unoccupied (fission) patch.

The ABM thus incorporates the major assumptions of existing IFD models and fitness curve models, adding to those demographic features such as reproduction, death and migration. The next chapter will illustrate how the metapopulation dynamics emerging from the model can be measured using some of the same tools used in chapter 3 to describe the empirical data of Jōmon settlements, and will then provide a guide through its parameter space.

Chapter 6

Applied Models of Endogenous Change

The previous chapter illustrated details of the agent-based model, which have been translated into a series of scripts written in R programming language (R Development Core Team 2011 ; see Appendix B). This chapter will illustrate the basic behaviour of such a model in order to understand what is the range of possible dynamics and their relationships to given sets of assumptions, with the latter expressed in terms of coordinates within the multidimensional parameter space. Ultimately, for each parameter combination, I will establish whether clumping and dispersion emerge and whether they reflect:

- equilibrium states (point attractors) that once reached are fixed and unchanging;
- polar states that are periodically or quasi-periodically reached (limit-cycle and toroidal attractors);
- or transitory states that are occasionally reached chaotically by the system (strange attractors);

Clearly there is no reason to presume a single, convergent response of the system for a given combination of parameters. As mentioned in the previous chapter,

small variation in the initial conditions and the effects of stochasticity in the model might determine divergence in the trajectories. In order to cope with this problem, multiple runs of the simulation have been computed for each parameter combination. This will provide a probabilistic assessment of the model, rather than unique results.

For the purpose of this thesis, the primary aim of the simulation is to establish what is the typical shape of the rank-size distribution for each parameter combination (which in turn will indicate whether we have a clumped or a dispersed pattern) and whether this varies as a function of time. The A-coefficient analysis introduced in section 3.3.1 is well-suited for this objective, as it provides a directly comparable measure to the archaeologically observed empirical data presented in chapter 4 and offers a proxy for distinguishing between clumped and dispersed settlement patterns.

Having established the shape of the rank-size distribution, the aim of the simulation is to determine whether this becomes asymptotically stable after a given number of time-steps (point attractor), or it varies through time without reaching any fixed equilibrium. In the latter case, the time-series of the A-coefficient should be assessed to establish whether the specific instance is a limit-cycle, toroidal, or strange attractor.

In order to better understand the dynamics of the model, the total number of agents N and groups G, and the median group size $\tilde{\lambda}$ have also been recorded. These statistics cannot be directly compared to the archaeological record, but their rate of change and reciprocal covariation can serve as broad templates to evaluate specifics of the empirical record.

6.1 Experiment Design and Parameter Sweeps

In order to explore the parameter space, we need to define its coordinate system by expressing quantitatively each parameter and how to "sweep" (i.e. sequentially vary) within ranges of meaningful values. Since many of the parameters

are virtually unbounded and/or expressed as continuous numbers, the range of possible values (and hence the size of the parameter space) is theoretically infinite. Even if we identify portions of the parameter space that are relevant to our interests, its exploration will be still constrained by computational limits. Thus, the choice of the parameters values and their "sweep" should be able to detect the highest variation of system behaviour (maximise the output information), using the smallest number of parameter combinations (minimise the input information). An alternative to this will require the development of metamodels that are specifically designed to seek portions of the phase space meeting user-defined criteria. For example, Stonedahl and Wilensky (2010) have recently developed a tool that combines genetic algorithms[1] and agent based simulation to quickly search the parameter space to seek where specific outcomes of the system are likely observed. While such a method provides a more sophisticated and faster solution, its goals are different from this context, since it provides a *searching* algorithm, while our aim in this case is pure exploration.

The core of the model — the unimodal fitness curve — provides several advantages for choosing meaningful values to sweep, as the essence of its structural properties can be described using the typologies of different relationships between critical values of g (see table 5) rather than absolute numbers. In other words, the design of the model and the theoretical framework provided by the existing literature suggests that the parameter space is likely characterised by repeated similarities (parameter combinations yielding the same relationship between critical values of g), and hence the choice of the sweep should try to exploit such a structural property.

I have already shown in section 5.3 (fig. 55) the effects derived from the variation of the basic fitness (μ), the scaling parameter defining the benefit derived from cooperation (b), and the size of the resource input (K). We can derive from this that

[1] A computational tool that mimics the process of natural evolution to solve mathematical and computational problems. In essence, it is defined by a population of possible solutions to the problems which will be naturally selected based on their fitness, measured as distance to the desired answer to the problem.

the variables mostly influencing the quantitative relationship between critical values of g appears to be b, since it is capable to modify the shape of the fitness curve itself. In fact, the cooperation parameter is likely to play a role in the initial stages of group formation (with lower values determining higher difference between $\phi(m)$ and $\phi(2m)$) and lead to different degree of inter-group diversity in fitness (higher values determining higher diversity). Starting from these assumptions we can then define three values for b : 0.3 (high initial advantage of aggregation economy and low inter-group diversity for larger sizes), 0.5 (intermediate initial advantage of aggregation economy and medium inter-group diversity for larger sizes), and 0.8 (small initial advantage of aggregation economy and high inter-group diversity at larger sizes).

One of the most critical aspects of the ABM is the explicit integration of key demographic processes such as reproduction and death. This is one of the two determinants of group size variation and directly relates ϕ to population dynamics. The three parameters related to reproduction (ρ) and death (ω_1 and ω_2) are, however, represented as continuous numerical values, and hence the range of different combinations is extremely large. One way to establish significant combination of these values is to formalise precise relationships with the fitness curve and critical group sizes. In the previous chapter, we defined $\tilde{g}$, as the group size where the net growth rate of the group (γ) is equal to zero. Since $\tilde{g}$ is partly derived from the three parameters listed above, we can identify four types of relationship between reproduction, death and critical values of g:

i. *The net growth rate is zero at the saturation group size ($\bar{g}$)* In this scenario (figure 57:**a**), the short-term (the evolutionarily stable size when reproduction and death is omitted; $\dot{g}$, see table 5) and long term (the evolutionarily stable size when reproduction and death is integrated in the model; $\breve{g}$, see table 5) equilibrium sizes are expected to be identical. When the fitness of group members declines to the level of individual subunit foragers (i.e. $g = \bar{g}$), the internal forces of population growth (γ) will also reach 0. As long as the threshold of evidence is larger than 0, changes in group size will be relatively rare and

will be driven by stochastic events modelled by ϵ.

ii. *The net growth rate is zero between the saturation group size ($\bar{g}$) and the optimal fission size ($\breve{g}$).* We already defined $\breve{g}$ as the group size where fission to individual units is the optimal solution. This will be reached when the individual fitness becomes equal to $\mu - c_1$ (see table 6). In this scenario (figure 57:**b**), the outcome will be similar to **i**, but the effect of ϵ will have a larger impact and hence, with other things being equal, instances of group reaching $\breve{g}$ by internal growth or immigration would be higher, especially if the threshold of evidence (c_1) is comparatively smaller. Notice that the size of c_1 is the width of the grey shaded area in figure 57:**b**.

iii. *The net growth rate is zero at the optimal fission size ($\breve{g}$)* If $\gamma(\breve{g}) = 0$, then the demographic pressure will vanish when the group reaches it optimal fission size. The probability of fission will thus be much higher than the previous scenarios (figure 57:**c**).

iv. *The net growth rate is zero above the optimal fission size ($\breve{g}$)* The dynamics of this scenario (figure 57:**d**) is likely to be close to the one predicted for **iii**, but group size will carry on increasing even after $g \geq \breve{g}$, and hence highly oversized group might emerge for a brief moment of time if z (the frequency of decision-making) is considerably low.

There are several ways to obtain the four type of relationships portrayed on figure 57. Here,[2] ρ (rate of reproduction) and ω_2 (second death parameter) have been fixed, while ω_1 has been swept from 0.8 to 1.4, with an interval of 0.2. The so-obtained four values ensure the following relationships: 1) $\omega_1 = 0.8 \Rightarrow \tilde{g} = \bar{g}$; 2) $\omega_1 = 1.0 \Rightarrow \bar{g} < \tilde{g} < \breve{g}$; 3) $\omega_1 = 1.2 \Rightarrow \tilde{g} = \breve{g}$; 4) $\omega_1 = 1.4 \Rightarrow \tilde{g} > \breve{g}$.

The second determinant of group size variation is derived from the agents' decision-making processes and its outcomes (fission, fusion, and migration). This will be tuned by their frequency of occurrence (z), and the degree of knowledge

[2]Notice that this solution applies for the specific combination of parameters shown in table 9.

obtained by the agents. The latter is characterised by two parameters: the spatial scale of knowledge (h, expressed as a cell neighbourhood size, see figure 56) and the sample proportion of the observed neighbour agents (k). We can use extreme values of each of the three parameters in order to explore their broad implications to the model. Hence we can use three values for z (0.1,0.5, and 1.0) and for k (10^{-7}, 0.5, 1)[3] while h will have two extremes resembling spatially local ($h = 1$) and global ($h = \infty$) versions of the model.

Other parameters of the model include the threshold values (c_1, c_2 and c_3), and the fission range (s). For simplicity, we can assume a constant value for the former ($c_1 = c_2 = c_3 = c$) and a fission range equal to the spatial scale of knowledge h. While the latter choice can be easily justified (we can safely assume that h and s are both derived by the same source of spatial knowledge), the arbitrary choice of c is more problematic. However, we can translate its effect in terms of probability of migration, which can be defined as the odds that the difference in the fitness between the model and the focal agent is smaller than the chosen threshold of evidence. From a mathematical standpoint, this will be the likelihood that the condition $(\phi_w - \phi_i) > c$ is satisfied. Figure 58 shows a level plot depicting such a probability for three different values of b (0.3, 0.5 and 0.8) and two values of c (1 and 3). Generally speaking, the plot shows higher probabilities for g_w (the model group) between 10 and 15 and for low ($g_i < 5$) and high value ($g_i > 15$) of the focal group (g_i). This is not surprising, since the unimodal shape of the fitness curve will determine higher attractiveness for a group with g close to the optimal size $g*$, and, at the same time, members of smaller and oversized groups (who over-exploit their resources and have declining fitness when $\Xi > K$) will be expected to migrate to there. Thus, both the variation of the shape in the fitness curve and the threshold of evidence will determine variation in the likelihood of migration. Figure 58 provides also some clues for deciding which value of c to choose. Since the primary focus of the experiment design is to determine possible variation in the system behaviour across the parameter space, the choice of c should be the

[3]The extremely small value of k ensures that only one random agent is being observed.

one allowing the highest diversity in terms of expected dynamics. In the specific case, the right column of figure 58 shows a higher variation in the probability of migration, and hence the threshold of evidence has been fixed to $c = 3$.

Table 9 shows both constant and sweep values for the parameters used in the model. This consists of 216 unique parameter combinations (3 sweeps for z, 3 for b, 3 for k, 2 for $s = h$ and 4 for ω_1; $3 \times 3 \times 3 \times 2 \times 4 = 216$). As mentioned earlier, each of these will require multiple runs in order to explore the effects derived by the stochastic components of the model (e.g. ϵ, reproduction, death, sampling of the observed neighbour agents, etc.). Preliminary runs of the simulation have shown that 100 runs are sufficient to capture the main properties of the model for each parameter combination, and hence a total of 21,600 simulation runs has been computed.

For each of these, the following four statistics have been measured:

- Total number of agents at each time step ($N(t)$).
- Total number of groups at each time step ($G(t)$).
- The median group size per time step ($\tilde{\lambda}(t)$)
- The A-Coefficient for each time step ($A(t)$)

The time-series of the A-coefficient are undeniably of primary interest here, as it is comparable to the observed archaeological data and offers a direct measure of the settlement size distribution. However, the other three measures provide further details that could indirectly be compared to the empirical data and could in theory distinguish apparent similarities observed in settlement pattern. For example positive $A(t)$ indicating a dispersed pattern could be characterised by many small groups, or alternatively by few large groups.

As noted at the beginning of the chapter, the main objective is to use $A(t)$ and the other three measures of group size distribution to determine whether a given parameter combination of the model will generate a point, limit-cycle, toroidal, or strange type of attractor. Ultimately, by sweeping the parameters we should be

able to establish how the variation of a specific parameter can drive the system of interest from one type of attractor to another, and by doing this, we would be able to highlight the structural properties of the model.

6.1.1 Visualising Simulation Outputs

Figure 59:**a** shows an example of a time-series of the A-coefficient for a single run of the simulation (see figure caption for details on the specific parameter combination). The plot shows how, in this specific case, the group size distribution can be mostly characterised as being dispersed/convex, although there are several moments when the settlement pattern rapidly shifts to lower values of A, indicating temporary transitions to Zipfian or even to weak clumped/primate patterns. We need to assess whether such a time-series represents a typical run for the specific parameter combination or not. Eyeballing each of the 100 runs is clearly impractical, and hence we need to devise a method capable to summarise the simulation output, minimising at the same time possible loss of information. Figure 59:**b** depicts a *combined plot* of all runs, with each time-series shown as a semi-transparent grey line. The graph shows how these occasional transitions to clumped/primate patterns are not rare. An alternative way to visualise the same information is to plot some key summary statistics as in figure 59:**c**, where the average value of $A(t)$ among all runs is depicted as a solid line, while the 10^{th} and 90^{th} percentiles, shown as a dashed lines, allow us to define the most typical group size distribution at each time-step. The plot suggests how the settlement pattern can be mostly characterised as dispersed/convex, although during the first hundred time-steps there is a strong decrease of $A(t)$ for all runs, showing a convergent short-term existence of a Zipfian rank-size distribution.

Plotting the raw data cumulatively (fig. 59:**b**) or using summary statistics (fig. 59:**c**) can both provide a visual insight of the model behaviour for each parameter settings. However, both forms of representation have some limits. For example, figure 59:**c** does not show how the system is characterised by occasional rapid transition to clumped/primate patterns, while combined plots are often hard to read.

Two derivative data representation techniques can offer alternative insights to the time series: *probability density* and *correlograms*.

Probability density plots are obtained from the frequency distribution of given measures (A, G, N, and $\tilde{\lambda}$ in our case) and essentially shows the length of time the system has spent in a given portion of the phase space. Figure 60 shows an example of this with the same parameter combination as the one illustrated for figure 59. The grey shaded bars are the probability histogram[4] of A with a bin size of 0.1, while the solid black line shows the probability density of the same data. The left graph shows the results for run number 12 (the same data depicted in figure 59:**a**), while the right panel depicts the probability density for all 100 runs (compare with figure 59:**b,c**). Probability density plots offer a way to visualise the long-term dynamics of the system, and can provide clues for determining which type of attractor can better describe the model behaviour. In the specific case, figure 60 shows a unimodal shape with a strong peak to higher values of A, indicating how the group size distribution is in most cases found to be dispersed/convex. This suggests that dynamics of the system can be categorised as a point attractor, although the left tail with low A values indicates that brief "escapes" from the basin of attraction (stages of clumped/primate pattern) do occur. Figure 60 shows also the limits of such a data representation technique. It is in fact not possible to distinguish whether tails with negative values of A represent short episode of clumping within each run, or whether they show how few distinct runs of the model were characterised as point attractors with negative values of A. We already know the answer in the specific case, since the combined plot on figure 59:**b** is characterised by a "rain-line" pattern, depicting rapid transition between positive and negative values of A.

The plot of the autocorrelation function —known as correlogram— could offer an alternative perspective for describing the time-series generated from the simulation. This is a widely used method in time-series analysis (Box and Jenkins 1976,

[4]Probability histogram depicts the likelihood that a specific value (the A coefficient here) can be found in a population. This is obtained by standardising the total area of a frequency histogram to 1.

Cowpertwait and Metcalfe 2009) and helps distinguishing whether at a given temporal interval (known as *lag*) from any moment in time t, there is a *positive autocorrelation* ("similarity" in the values) or negative autocorrelation ("difference" in the values). The most straightforward example can be observed when the time-series exhibit a regular limit-cycle. Figure 61:**b** shows an example of such a dynamic, along with its correlogram and probability density plots. The limit cycle has a negative autocorrelation at lag 6; meaning that if we observe the value of the time-series at any moment in time t, its value at $t + 6$ and $t - 6$ will be *regularly* and *significantly* dissimilar. At a larger temporal scale, the system exhibits positive autocorrelation (at ca lag 11-14), meaning that if we look at the value at any moment t and compare it to $t + 12$ or $t - 13$ they will be significantly similar.

Generally speaking, most systems exhibit some degree of positive autocorrelation that will decay at higher lags (meaning that, at such a scale, the knowledge of a value at t will no longer provide any information to predict its future and past values). The correlogram can help determining instances of limit-cycle and toroidal attractors, but since its underpinning mathematics determines similarities and dissimilarities based on the overall variability of the system, it might not help distinguish instances of point and strange attractors, especially if the former is characterised by small stochastic fluctuations within its basin of attraction. For example if we are measuring the correlogram of $A(t)$, and this is characterised by chaotic oscillations between 0.85 and 0.9, we can categorise the system as a point attractor, with a convex (dispersed) pattern being its long term equilibrium. However, the correlogram might indicate a complete absence of autocorrelation, since if the overall system is bounded between 0.85 and 0.9, random fluctuations within the two extremes will be regarded as an instance of strange attractor. In other words, such a system will be both a point attractor (at large scales) and a strange attractor (at smaller scales).

Figure 61 shows four examples of possible raw time-series of A for different types of attractors (**a**: point attractor; **b**: limit attractor; **c**: toroidal attractor; **d**: strange attractor), along with their correlograms and probability density plots.

This can be used as a rough guide to distinguish different types of attractors as follows:

- *Point attractors*. The raw time series will show asymptotic trends towards a fixed value with no or minor fluctuations. The correlogram will suggest high positive autocorrelation for short lags, with a declining trend likely to be a function of the time required by the system to reach its equilibrium state. The probability density plot will have a unimodal shape, with the mode being the centre of the basin of attraction (fig. 61 :**a**).

- *Limit-cycle attractors*. The time-series will be depicted as regular fluctuations between two polar values of A. The correlogram will show the frequency of such a cycle (i.e. the temporal interval between two moments where the settlement pattern is very similar), while the density plot will be bimodal, with the two modes corresponding to the poles of attraction and their inter-distance the magnitude of the fluctuations (fig. 61 :**b**).

- *Toroidal attractors*. This is similar to the previous type of attractor, although $A(t)$ will be characterised by multiple periodicities. The correlogram will show alternating peaks of positive and negative autocorrelations, while the probability density will be characterised by multi-modality (see fig. 61 :**d**). Toroidal attractors cannot be always identified easily, especially when multiple periodicities are "out of phase" or hidden under dominant patterns which mask smaller ones.

- *Strange attractors*. This can be recognised by a chaotic behaviour of the time-series, which will exhibit no significant instances of positive or negative autocorrelation for almost all temporal scales. The density plot will be irregular and possibly characterised by smaller peaks that might resemble the ones depicted for toroidal attractors (fig. 61 :**d**).

As for the density plots it is possible to depict the information of multiple runs of the same parameter settings in a single graph as follows:

1. Compute the autocorrelation function for each run of the simulation for a given parameter combination.

2. For each lag, count the number of cases where positive or negative autocorrelation are evident with a given statistical significance level (for instance, the horizontal dash lines in the correlogram of figure 61 indicates the threshold for $p < 0.05$).

3. Compute the proportion of significant runs.

4. Plot the results as a double-sided bar plot

Figure 62 shows how a combined correlogram would look like, using the same parameter combination of the examples used above. The left column shows the results for a single run and the right one shows its combined version. It is important to highlight the fact that, although visually similar, the two plots are showing different information. The standard correlogram (left column) shows the magnitude of the autocorrelation, while the plot on the right shows the frequency of runs where statistically significant positive (bars on the top) and negative (bars on the bottom) autocorrelation has been observed.

6.2 Results

Given the large number of parameter combinations (216), four distinct measures ($G(t)$, $\tilde{\lambda}(t)$, $N(t)$, and $A(t)$) and three representations (time-series, probability density and correlogram), a detailed account of each scenario will not be described (see however appendix D), and instead a broader discussion on the effects of each parameter will be provided after a general summary of the model.

6.2.1 General Properties of the Model

The experimental design described in the previous pages will require the exploration of a 5-dimensional parameter space, where each of the five parameters (b,

ω_1, k, z, and h) will represent its coordinates. Visualising such a multidimensional space is not trivial, especially when for each parameter combination we need to observe a plot (e.g. the combined raw time-series or the probability density plot) rather than a single value. One possible solution is to arrange the plots so that its location in the figure will suggest its parameter combination. This method allows the visualisation of a 4-dimensional parameter space (with coordinates b, ω_1, k, z), and thus a pair (one for $h = 1$ and one for $h = \infty$) would be sufficient to cover the entire range of parameter combination. Figure 63 shows the representation frame that will be used in the following pages. The parameter space is first divided in a 3×3 major set of quadrants, each referring to a combination of the parameters k (columns) and z (rows). Each of these quadrants will have a 3×4 matrix of plots, with the rows indicating variation in b and the columns indicating variation in ω_1. Thus, for example, the black filled square in figure 63, will have the following coordinates in the parameter space: $z = 0.1$, $k = 1.0$, $b = 0.5$ and $\omega_1 = 1.0$.

A-coefficient ($A(t)$)

Figure 64 and 65 are the summary statistic of the time-series for $h = 1$ and $h = \infty$ respectively. Each of the 216 (108+108) plots show the most typical time-series of $A(t)$ (the median A coefficient among all the 100 runs for each value of t) in solid line, juxtaposed on a shaded grey area representing the envelope between the 10$^{\text{th}}$ and 90$^{\text{th}}$ percentile and a red horizontal line showing the level for $A = 0$ (notice that the range of the y-axis is between -1 and +1).

The spatially local model ($h = 1$, fig.64) shows how, in large portions of the parameter space, point attractors with high positive values of A are present. In all instances such an equilibrium is reached after an initial fluctuation of $A(t)$, usually leading the system to reach temporarily a Zipf's-law group size distribution, before permanently resting to a dispersed/convex pattern. The only exception to this trend is visible with high values of k (proportion of observed agents) and z (frequency of decision-making), coupled to $\omega_1 \geq 1.0$ (positve net growth rate at the saturation group size), where the system can still be described as a point-attractor,

but with lower levels of A approaching median values close to those expected for a Zipf's-law distribution. Interestingly, variation in b does not show any sensitive variation in the time-series of $A(t)$.

The spatially global version of the model ($h = \infty$, fig.65) shows a strikingly dissimilar pattern to the one depicted in figure 64, with the exception of all models with the smallest values of z and k (the top-left quadrant in figure 64) where point attractors similar to the ones portrayed in figure 64 can be found. Similar patterns can also be observed in regions of the parameter space where the frequency of decision-making is extremely small ($z = 0.1$; first row of quadrants in fig. 65) or when the proportion of observed neighbour agents is small ($k = 10^{-7}$; first column in fig. 65). However, in the former case when $k \geq 0.5$ increasing values of ω_1 shows both a widening of the inter-percentile envelope and a slight decrease of the equilibrium value of $A(t)$. In the latter case (when $k = 10^{-7}$), instances where $\omega_1 = 0.8$ and $z = 1$ show also an increase in the envelope, while the median value appears to be chaotically oscillating. In some plots (e.g. at coordinates $k = 0.5$, $z = 0.5$, $b = 0.8$, $\omega_1 = 0.8$), both the median and the envelope vanish after few time-steps. This is caused by the fact that the number of groups is extremely small (less than three) and hence the A-coefficient cannot be computed for any of the runs (see section 4.2.2).

The most interesting pattern observed in figure 65 is the presence of extremely wide inter-percentile envelopes for high values of z and k. In some cases, these envelopes cover the full spectrum between dispersed and clumped patterns, indicating that these are unlikely to be instances of point-attractors. The median $A(t)$ is instead always fluctuating around 0, or to some slightly higher (i.e. towards a dispersed pattern) or lower (i.e. towards a clumped pattern) values.

Figure 67 and 68 show the probability density distribution of $A(t)$ for time-steps between 200 and 500, with the colour beneath the density curve indicating the proportion of computed A-coefficients. When no measures of A-coefficient were available between the temporal interval no plot has been depicted (e.g. in $k = 0.5$, $z = 0.5$, $b = 0.8$, $\omega_1 = 0.8$). When $h = 1$ (fig. 67), the patterns suggested by

figure 64 is confirmed: all curves have unimodal shapes, with no or small negative skews and with the mode being always positive, confirming the idea that these are indeed instances of point-attractors with an equilibrium as a dispersed/convex pattern (although with the tendency of smaller medians with higher k and z). With $h = \infty$ (fig. 68), the variation in the parameter space depicted already in figure 65 becomes even clearer. Generally speaking four types of pattern can be recognised:

- *Unimodal distribution with single small tail.* These are very likely instances of point attractors, and can be generally found where k and z are low. In all cases, the median is located at positive values of $A(t)$, and in some occasion a small tail of negative values can be observed, indicating possible short-term transition to clumped/primate patterns.

- *Unimodal distribution with single fat tail.* These instances are generally characterised by a unimodal shape with a pronounced negative skew, and a median located at high values of A. This could either indicate that the system is characterised by a dominance of convex rank-size distributions with occasional shifts to primate ones, or that two different point attractors —one dispersed and the other clumped— coexist, with the former having a larger basin of attraction. Detailed examination of the time-series plot (see appendix D) suggests that the tails of the probability density curves depict stochastic escapes from the main basin of attraction. Typical examples of this pattern can be found in regions of the parameter space with the following coordinates: $z = 0.5$, $k \geq 0.5$ and $b \leq 0.5$.

- *Unimodal distribution with double fat tail.* This is observed when $k \geq 0.5$,$z = 1.0$ and $b = 0.3$, and is characterised by a unimodal shape with mode $A \approx 0$, with tail reaching both extremes of the spectrum between dispersed and clumped pattern. Detailed discussion on this pattern will be presented later, here it can be anticipated that this is most likely the result of a toroidal attractor, or a limit cycle attractor with three polar states (clumped, dispersed and Zipf's-law distributions).

- *Bimodal distributions.* This is likely to be the result of a limit-cycle attractor, or a bifurcation of the system in to two distinct point-attractors. Visual assessment of fig. 65 seems to support the former hypothesis. This type of distribution can generally be observed when $z = 1.0$, with $b \geq 0.5$ and $k \geq 0.5$, and are characterised by two modes, one with highly positive A (dispersed group size distribution) and with a highly negative A (clumped group size distribution). In some cases, the pattern have some weak multimodality, although these modes tend to cluster together (see for instance $k = 0.5$,$z = 1.0$,$b = 0.5$,$\omega \geq 1.0$). These instances resemble the expected frequency distribution for toroidal attractors illustrated in figure 61. Instances of bimodality can also be observed for $z = 0.1$, $k \geq 0.5$, $\omega_1 = 1.4$, with the two modes of $A(t)$ being both positive.

- *Multimodal distributions.* A small region of the parameter space (i.e. when $k \geq 0.5$, $z = 0.5$, $b = 0.8$, $\omega_1 \geq 1.2$) exhibits a weak form of multimodality, with a central mode at $A \approx 0$ and two other modes with negative and positive values of A.

Exploring how the temporal autocorrelation of A varies across the parameter space can provide further insights on the four broad patterns identified above. Figure 69 and 70 show respectively the correlogram of $A(t)$ for the local ($h = 1$) and the global ($h = \infty$) versions of the model, both with 25 lags and using the whole set of time-steps. As in all other cases illustrated above, when $h = 1$ (fig. 69) there is a substantial homogeneity across the parameter space, with most plots showing a strong positive autocorrelation for all lags. Exception to this can be observed in regions of the parameter space with high frequency of decision making ($z = 1.0$) and a comparatively large proportion of observed agents ($k \geq 0.5$), where at larger lags the system starts to show both significant positive and negative autocorrelations (although the former is always dominant), indicating possibly a more chaotic behaviour of the system. With $h = \infty$, instances of fluctuating pattern can be observed in the correlogram (e.g. when $z = 1.0$, $k = 0.5$, $b = 0.5$, $\omega_1 \geq 1.0$), confirming

that the system is indeed characterised by limit-cycle attractors for some regions of the parameter space. In most cases a significant negative autocorrelation is observed around lag 5-10, followed either by a predominance of significant positive autocorrelation at lag 15-20 (e.g. when $z = 1.0$, $k = 0.5$, $b = 0.5$, $\omega_1 \geq 1.0$) or by equal proportions of positive and negative autocorrelation (e.g. when $z = 1.0$, $k = 0.8$, $b = 0.5$, $\omega_1 \geq 1.0$), indicating possibly a more irregular fluctuation in the shape of the rank-size distribution. A comparison with the frequency plot depicted in figure 68 indicates how instances with clear fluctuating pattern in the correlogram are associated with bimodal (with the two poles of attractions being strong convex/dispersed and primate/clumped patterns) and unimodal distributions with both positive and negative long tails.

As anticipated before, the behaviour of the latter is slightly more complex. Visual inspections of single runs (see fig. 66) show that the time-series is characterised by the combination of major shifts between clumped and dispersed patterns, and minor fluctuations around $A \approx 0$. This can be regarded as an instance of tri-polar limit attractor (with the three poles corresponding to convex, primate and Zipfian distributions) or a toroidal attractor with the coexistence of different periodicities.

Number of groups ($G(t)$), Population size ($N(t)$), and Median group size ($\lambda(t)$)

Figures 74 and 75 shows the time-series of the group counts. Notice that since each patch can contain only one group, we can define the upper limit of the phase space of G as equal to 100, the total number of patches. As for A-coefficient, the plots shows the median values and the envelop bounded by the 10^{th} and 90^{th} percentiles.

When the spatial range of interaction is local (i.e. $h = 1$, fig.74) the time-series show some level of diversity across the parameter space. The most notable trend is the positive correlation between ω_1, which defines the relationship between the net growth rate and critical group sizes, and the median value of G. This is not surprising, since high value of ω_1 will determine a positive growth rate for larger group sizes, leading to an increase likelihood of fission events and eventually to

an increase in the total number of groups. With $z = 0.5$ and $k \geq 0.5$, the total number of groups is also negatively correlated to b, the cooperation benefit. The inter-percentile range is relatively large in this case, and with high b, the median value of G is on the lower edge of the envelope. This could possibly indicate how the high attractiveness of larger groups determines a fusion process, which limits the expansion and the persistence of novel groups generated by fission. When the frequency of decision-making is high ($z = 1$) episodes of fission-fusion can be still inferred from the relatively wide inter-percentile envelope, but the median G is much larger, and despite occasional drops it is maintained at high levels.

Figure 75 shows the same statistics for $h = \infty$. As in figure 74 the positive correlation between ω_1 and G is still present in some portions of the parameter space. However, exceptions can be found where G remains considerably small. This can be found when $z = 0.5$, $k \geq 0.5$ with all values of b and ω_1. Several parameter combinations appear to determine a large inter-percentile envelope, with the median value of $G(t)$ often located on one or another of its extremes. For example, when $k = 10^{-7}$, $z = 0.5$, $b = 0.8$ and $\omega_1 \geq 1.2$, the median value is at its highest possible value (i.e. equal to P), although the lowest extreme of the inter-percentile envelope is located at low values. In contrast when $z = 0.1$,$k = 1.0$,$b \leq 0.5$ and $\omega_1 = 1.2$, the median value is at its lowest, while the envelope reaches extremely high values. As for some scenario illustrated when exploring the parameter space of $A(t)$, this pattern could either reflect occasional escapes from a point attractor, a limit-cycle attractor, or the presence of two distinct point attractors to which the system diverge depending on the initial conditions of the model. A uniform subregion of the parameter space can also be found at $k \geq 05$ and $z = 1.0$. In both quadrants, the inter-percentile envelope has an intermediate size, with relatively small median value of G located in its middle ($b \leq 0.5$) or higher edge ($b = 0.8$).

Probability density plots of G (figure 76 and 77) illustrates essentially the same information. With $h = 1$, most parameter combinations show an unimodal distribution although often characterised by either a tail (e.g. $z = 1.0$, $k = 1.0$, $\omega_1 \geq 1.0$) or a positive tail (e.g. $z = 0.5$, $k = 1.0$, $b \geq 0.5$, $\omega_1 \geq 1.0$). Exception to this

trend can be observed for $z = 0.1$, $k \geq 0.5$, $\omega_1 = 1.0$, where a bimodal distribution can be observed. In all cases, this is characterised by smaller peaks at lower values of G and greater peaks at larger values. Figure 71:**a** illustrates the combined time-series plot with the same parameter settings, showing how such a bimodal probability distribution reflect different timing in the transition of G from low values (ca10 groups) to the maximum allowed (100), rather than an effect derived by a limit-cycle attractor. This pattern essentially indicated that, at initialisation, the system is outside the basin of attraction of a point attractor located at $G = 100$; minor stochastic fluctuations of the system determine a rapid transition to such a point attractor at different timings. Similarly, most of the bimodal distribution observed in figure 77, where $h = \infty$, are characterised by such a pattern. For example figure 71:**b**, which depicts the combined time-series for $z = 0.1$, $k = 1.0$, $b = 0.5$, $\omega_1 = 1.4$, shows how the system is first characterised by low values of G, and suddenly —but with different timings— a global level fission process leads to the highest possible values of G, followed by a slight decrease in the number of settlements triggered by fusion. The only instances of bimodal distributions that are representative of a limit-cycle attractor can be observed when $z = 1.0$, $k \geq 0.5$ and $\omega \geq 1.0$. Figure 71:**c** for example shows the combined time-series plot for $z = 1.0$, $k = 1.0$, $b = 0.5$, $\omega_1 = 1.4$, with a typical pattern of dense vertical stripes indicating continuous fluctuations. The identification of such limit-cycle attractors are even more direct when the correlograms are examined (see fig. 78), and indicates how such a pattern is restricted in a relatively small region of the parameter space with $h = \infty$ (notice, however, how some of the bimodal distributions depicted in figure 77 do not show the typical undulating pattern in the correlogram, indicating how these cannot be described as instances of limit-cycle attractors, but are more likely instances of strange attractors).

The dynamics of the total number of agents (N) are a reflection of the total number of groups G, and detailed discussion will be omitted here. A more useful statistic is the median group size ($\tilde{\lambda}(t)$), which can provide additional insights on possible fission-fusion events. In the local version of the model ($h = 1$), three broad

patterns of point attractors can be recognised at high (>20-25), medium (≈10-20) and low (<10) values of $\tilde{\lambda}(t)$ (see figures 79 and 80). Interestingly the most relevant element causing this is not the net growth rate (defined by ω_1), but the frequency of decision-making (z). In fact, when $\omega_1 \geq 1.0$, at increasing value of z, $\tilde{\lambda}(t)$ becomes smaller (although this is less evident for $k = 10^{-7}$).

When spatial range of interaction is infinite ($h = \infty$; fig. 81), the negative correlation between the median $\tilde{\lambda}(t)$ and z is still visible, although this is restricted primarily for values of ω_1 equal or larger than 1.2. The most notable property of this parameter space is the much wider extent of the inter-percentile envelope in comparison to the local model. This can be further distinguished between instances where: (**a**) the envelope extends slightly above and below the median value of $\tilde{\lambda}(t)$ as a buffer (e.g. $z = 0.5$, $k \geq 0.5$); (**b**) the median value is high, and the envelope covers all the lower values of $\tilde{\lambda}(t)$ (e.g. $z = 1.0$, $k = 0.5$, $\omega_1 = 1.0$); (**c**) the median value is constantly low, and the envelope is characterised by spikes of high values (e.g. $z = 1.0$, $k \geq 0.5$, $\omega_1 \geq 1.2$).

Probability density plots (fig. 82) of these three different patterns of the inter-percentile envelopes show how pattern **a** is associated with an unimodal curve with two fat tails, pattern **b** is associated with a strong bimodality with higher $\tilde{\lambda}(t)$ being the dominant mode and pattern **c** to an unimodal curve with a long positive tail. The correlogram of the same portion of parameter space (fig. 84) shows how for **a** and **b** there is a positive autocorrelation for all lags, indicating that the bimodality observed for the latter is not the result of a limit cycle attractor. The bimodal probability density can be instead explained by examining the combined plot of the median group size. Figure 72:**a** shows one instance of this, with a dominance of vertical lines (indicating rapid transitions) and a highly dense "cloud" (suggesting smaller oscillations) at high values of $\tilde{\lambda}(t)$. Observing single runs of the simulation (fig. 72:**b,c**) shows better what is behind this pattern. In some cases, the median group size have occasional sparks to high median group size; these usually do not last long (see fig. 72:**b**), but sometimes the system remains stable at high values of $\tilde{\lambda}$ for a while (see fig. 72:**c**). The underlying process generating such

a pattern is most likely related to stochastic events triggering fission events. This is clearly a function of ω_1 (see figure 57); when the net growth rate is zero at the saturation group size ($\omega_1 = 0.8$) the system show stability at large median group sizes, when $\omega_1 \geq 1.2$ the system is characterised by sudden temporary peaks of high values. When ω_1 is equal to 1 (i.e. when the net growth rate is zero between the saturation and the optimal fission size), the system exhibits a mixed pattern where both dynamics co-exist.

The correlogram for the third type (**c**) of inter-percentile envelope confirms this idea, showing a fluctuating pattern (fig.78; e.g. $z = 1.0$, $k \geq 0.5$, $\omega_1 \geq 1.2$). This, however, varies in its structure as a function of the cooperation benefit b; smaller values of this parameter show a much more marked pattern with the peak of the first negative autocorrelation at higher lags (ca 14-16), while larger values of b depicts a much more irregular pattern, with peaks at lags 3-4. Figure 73 depicts the singles runs of the simulation, which illustrates the actual dynamics of $\tilde{\lambda}(t)$. In all cases, the median group size is usually low (≈ 1) and is occasionally interrupted by sudden peaks, which are more frequent and reaches higher values for larger values of b. This pattern can be explained by higher attractiveness of groups with larger b (see figure 58), which would determine a large-scale synchronic invasion to optimal groups when the frequency of decision-making (z) is high, followed by the formation of exceptionally large groups, which are unavoidably destined to collapse by means of fission and death of its members.

6.2.2 Parameter Sensitivity and Group Formation Dynamics

The previous section aimed to explore how A, G and $\tilde{\lambda}$ varied as a function of time, and how such dynamics were related to specific combinations of the five variables (i.e. spatial range of interaction h, frequency of decision-making z, sample proportion of observed agents k, cooperation benefit b, and death rate parameter ω_1) defining the parameter space. This section will review these results focusing on the sensitivity of each parameter —i.e. how strongly they affect the variation in the patterning— which in turn will shed some light on the underlying processes.

Undoubtedly the most sensitive parameter of the model is h (and hence also s, since the we assumed that $h = s$): the spatial scale of interaction. Generally speaking, the spatially local versions of the model (i.e. when $h = 1$) are characterised by point attractors, with all statistical measures of the group distribution consistently showing some form of equilibrium with only minor irregular variations. Groups are always characterised by a convex rank-size distribution, and often with a large numbers that occasionally reach the ceiling value of 100 units.

Spatial isolation, which constrain fission-fusion dynamics, is perhaps the primary cause of this pattern. Immigration will, in fact, be spatially restricted, since direct movement towards a given focal group will be limited to the 8 neighbouring patches (see fig 56), and similarly when a group exceeds it optimal fission size, only the first 8 agents will be able to fission, with other members most likely forced to stay in the group for a while and then to migrate to one of the newly formed offspring groups.

This reconstruction of the underlying dynamics of the model is further supported by the fact that with increasing frequency of decision-making (z) and sample proportion of observed neighbour agents (k), the equilibrium value of A becomes smaller, approaching values expected from a Zipf's-law rank-size distribution rather than a convex/dispersed one. Such a pattern can be explained as follows. With low ranges of spatial interaction (h and s), groups will be easily segregated through local fusion towards optimal groups. This will determine further isolation between groups and hence variation of group size will be primarily based on internal dynamics. When the frequency of decision-making (z) is low, spatial relocation will occur only occasionally but will be synchronous, because there will be sufficient "time" to allow all groups to reach similar situations (e.g. exceeding the optimal fission size) before the actual decision is made. In contrast when z is high, decisions (spatial relocation) are made immediately, and hence small diversity between distant groups will determine different onset of events such as fission. This effect will be cumulative, leading ultimately to different local histories of group formation dynamics. Thus, if one portion of the landscape is characterised by a

fission event, another could see a fusion process. Ultimately such a divergence in the evolutionary trajectories determines a mixed distribution of sizes at a global level that closely resemble a Zipf's-law pattern.

In the spatially global version of the model ($h = s = \infty$), such an isolation between groups does not exist, as any individual will have the opportunity to reach any patch in the landscape. This essentially means that if both the frequency of decision-making and the observed proportion of neighbour agents are set to 1, all agents will virtually take the same decision at the same time, with differences arising only from the state variables of the focal group (i.e. its size). As a consequence, if a given group is seen as the best destination, members of such a group will stay while all other agents will try to join it. The net result of this process is that we will expect a smaller number of often oversized groups and rapid fission-fusion dynamics where moments of dispersion with many small groups are alternated by sudden episodes of aggregation. Figure 85 shows a single run of the model where we can infer such dynamics by comparing the variation of $A(t)$, $\tilde{\lambda}$,$N(t)$, and $G(t)$. The figure shows how sudden peaks in the median group size are associated with drops in the total number of groups and agents, indicating a strong aggregation of individuals. The number of groups is so small that A cannot be measured during this stage. Shortly after such a strong aggregation, a sudden rise in the number of groups can be observed, as well as an increase in N and the emergence of a convex/dispersed distribution of group sizes. This is then followed by a gradual aggregation (decrease in A), a reduction in the number of groups, and an increase in population, until a sudden increase in the median group size resets the cycle.

The global version of the model shows how the degree of interconnectedness between groups plays a crucial role in the model. Small spatial interaction ($h = 1$) will determine patterns similar to the one expected with low rates of decision-making (low z) and proportion of observed agents (k). When, on the other hand, agents have full knowledge of their surrounding environment (high h, s and k) and are responsive (high z), their choice will likely determine higher reciprocal interdependence, ultimately leading to a *tragedy of commons*-like scenario, where the

joint demand for an optimal choice determines negative consequences (decrease in fitness) to the whole population. If we consider the total number of groups and agents as a proxy of adaptive success, then high interconnectedness, knowledge, and responsiveness all appears to determine only short-term benefits.

The remaining two parameters —the shape parameter of the fitness curve (b) and the relationship between internal growth rate and fission size (defined by ω_1)— also contribute to the dynamics of the model, but their impacts seem to be more predictable. This is especially the case of ω_1, which in essence controls the effect of internal growth. In all instances where $\omega_1 = 0.8$ (i.e. when the net growth rate becomes zero at the saturation group size) groups will not fission and hence changes in group size will be driven entirely by migration events; fission, and hence increase in G, will occur only for larger values of ω_1. This is nicely portrayed by the transitional state shown on figure 72. The role of b is less prominent than the other parameters. As shown in figure 58 the key effect that we can predict from its variation is the attractiveness of optimally sized groups, and hence we should expect more migration and invasion with higher values of b. This idea can be supported by the fact that b seems to affect the *tempo* of the fission-fusion dynamics. All correlograms with high values of z, k and h —when we expect cycles of fission-fusion dynamics as observed in figure 85— depict smaller lags for the first episode of negative autocorrelation for larger values of b. This suggest that higher cooperation benefit determines a faster rate of change in group size distribution. This is not surprising, as when b is high, migration from groups larger or smaller than the optimal size will occur more frequently, despite the effects derived by the stochasticity in foraging tasks (derived from ϵ).

6.2.3 Summary

The description of the parameter space offered in the previous two sections portrays the essential dynamics of the ABM and is sufficient to develop some conclusions concerning the expected variation of settlement patterns in a closed system.

First, the most evident outcome of the model is that *transitions between clum-*

ped/primate and dispersed/convex pattern could occur endogenically, without the presence of any exogenic catalyst. This can be observed in some regions of the parameter space where the model behaves as a limit-cycle or toroidal attractor. Detailed examinations of these cases have shown how such dynamics are more likely to emerge when the system has high levels of inter-connectivity, which in the present case is embodied by larger parameter values for the spatial neighbourhood of interaction (h and s), knowledge (k) , and degree of agent responsiveness (z). The underlying process that generates such a transition between the two extreme forms of group size distribution is an alternation of group fission and fusion, a phenomenon which influences also the number of groups, their median sizes, and the total counts of agents.

Second, the model has shown that most regions of the parameter space are occupied by point-attractors, where *dispersed/convex distributions of groups are permanently maintained in equilibrium*. The typical evolutionary trajectory sees an increasing tendency toward such a shape in the rank-size distribution, which —once reached— is permanently maintained. In some occasions this also determines a complete occupation of all patches, and consequently leads to the highest possible population size, with all groups reaching a relatively large size around $\tilde{g}$, the zero-growth group size. In other cases when the internal growth is low, groups remain in equilibrium without fissioning and maintain a relatively small size.

Third, occasionally the model exhibits equilibrium at lower values of A, close to the one expected for a Zipf's-law distribution, but it never exhibits a point attractor with negative A coefficient. In other words, *clumped/primate distributions are unstable for all examined regions of the parameter space*, and most likely such a statement is valid for unexamined regions as well. This is because, as long as we assume a free entry-rule where movement between groups are unconstrained, optimally-sized groups will be sooner or later invaded through migration unless it is not spatially isolated. However, in the latter case other groups will share the same destiny and hence ultimately we will observe a dispersed pattern with a relatively large group size. The only exception to this is when each group has independent evolution-

ary trajectories caused by spatial isolation. In such cases, divergence in the local histories might create an overall appearance of a Zipf's-law to weakly clumped distributions.

It is important at this point to highlight again one of the key assumptions of the model: a spatially homogenous distribution of the resource input K. In a real world context, spatial diversity of the resources could in theory determine variations in the group size and hence offer the opportunity for the emergence of a stable clumped/primate distribution, despite the maintenance of a free-entry rule assumption. This scenario will occur only if the groups are isolated from each other. In such a case the group size distribution will be unaffected by migration dynamics, which are central to the model developed so far. If a sufficient level of inter-connectedness is present, large groups located at optimal locations will still be invaded, ultimately triggering fission-fusion events. In other words, the only way to maintain a clumped/primate pattern is to impede the movement of individuals between groups. This could be obtained either by spatial segregation or the emergence of social mechanism that alters the free-entry rule assumption. In the case of human societies the latter will require the emergence of some form of "organised" violence, which will allow the maintenance of groups at its optimal size. Nonetheless, internal growth could —under certain conditions— still undermine such an equilibrium, leading in the long-term to a fission process. It is worth stressing that resource input (K) is constant here, so that a group with a net-growth rate equal to zero at its saturation size (see fig. 57:**a**) can be potentially located on the same patch forever. This unrealistic assumption will be relaxed in the next chapter, but here it is sufficient to anticipate that major differences in the simulation output can be observed when groups are isolated and have lower values of ω_1. In these scenarios, a decline in K might lead a group fission even when in normal conditions (i.e. when K is constant) this happens very rarely. For the remnant portions of the parameter space the unimodal shape of the fitness curve guarantees that some form of overexploitation is already integrated in the model (i.e. oversized groups having a decline in fitness) and this is sufficient to generate

the fission-fusion dynamics observed here.

The results provided by the ABM offer a cautionary tale about the dangers of assuming a static model of settlement pattern where variation is simply a function of external forces could be potentially misleading, since changes can easily occur through well-known endogenic processes such as migration flows, and fission-fusion events. This is not a novel statement, since other models of settlement pattern suggest similar conclusion (see Renfrew and Poston 1979, Griffin 2011) although starting from a different set of assumptions and theories. The critical aspect here is that the same conclusion has been achieved starting from entirely different perspective on group formation dynamics. This convergence in outcome is undoubtedly a strong support for being cautious of any assumption of a static settlement system.

The discussion above prompts two distinct avenues of further enquiry. On the one hand, once we have established that changes between clumped/primate and dispersed/convex pattern could occur endogenically, we need to determine what is then the expected effect of exogenic forces. This aspect will be explored on the next chapter. The second direction seeks to address whether the patterns observed in the model match to the one observed in the archaeological data. In other words, we need to validate the model through a direct comparison of the simulation output and the empirical data. The abstract and theory-building nature of the model makes this process less formal than the ones that can be offered by hypothesis-testing models, but nonetheless the simulation provides explicit expectations in the form of different directional trends in multiple statistical measures. These aspects will be discussed in chapter 8, in combination with the results offered in the next chapter.

Chapter 7

Applied Models with Disturbance Processes

7.1 Theoretical Introduction

The exploration of the ABM's parameter space has shown how the internal properties of the system are in some cases sufficient to stimulate dynamics of changes between clumped and dispersed patterns. This conclusion is already sufficient to undermine the assumption that these changes were episodes of cultural response to modified climatic conditions, since similar outcomes could possibly occur without any external perturbation to the system.

The purpose of this chapter is to further explore the model developed in chapter 5 by simulating external forces to the system. This will establish the expected response of the system for different forms of perturbations and ultimately help understanding whether a given change observed in the archaeological record is endogenous —i.e. originating from the internal forces of the system —, exogenous —i.e. emerging as a response of the system to an external perturbation —, or a combination of the two. More specifically my goal is to address the following questions for each parameter combination explored in chapter 6:

- Can external forcing produce shifts between clumped and dispersed pattern?

- Are these changes temporary (i.e. a variation which will eventually lead the system to return to its original equilibrium) or permanent (i.e. a variation leading the system to a new equilibrium) ?

- Are there any differences between externally and internally induced changes in the group size distribution?

Before proceeding to the details of how to model these perturbations to the system, it is important to briefly review how the effects of these forces have been formalised in the literature of ecology and complex systems and how the framework offered in those disciplines can be applied in this specific context.

The central notion, shared by many ecological models, is the concept of *disturbance*. White and Pickett (1985) offer a seminal definition stating that "any relatively discrete event in time that disrupts the ecosystem, community or population structure and changes the resources, substrate availability or physical environment" can be considered as *disturbance* (*ibid.*:7). This definition has been further extended and formalised by Petraitis and colleagues (1989), who defined *disturbances* as processes that are capable of modifying the birth and death rate of individuals. If we extend this definition to include any active response at the individual level (e.g. migration) that might determine changes at the macro-level (e.g. modification of the meta-population structure), we can generalise our definition of *disturbance* to any force capable of modifying the behaviour of a system of interest. White and Jentsch (2001) have noticed how this notion is often approached in relativist or absolutist terms. In the former case disturbance is defined as a force "causing deviation from the normal dynamics of an ecosystem" (*ibid.*: 405). In the latter, disturbance is measured by assessing the quantitative changes of some key variables, rather than relying on a comparative framework.

While acknowledging the benefits of relative definitions, White and Jentsch focus on the second view, and suggest how *disturbances* are relatively short and discrete *events* which can be characterised by three measurable properties: duration, abruptness, and magnitude (see figure 86).

They further seek generalities by distinguishing *stressors* from *disturbances*, defining the former as smaller and less abrupt perturbations to the system that affect its function but do not lead to an abrupt change in the system. *Disturbances* can be further divided into *exogenous disturbance* — " those in which the force originates outside the ecosystem (White and Jentsch 2001: 412)" and *endogenous disturbance* —"those in which the force [...] originates within [the system] or as a product of successional development (*ibid.*: 412)". Clearly, this dichotomy represents the two theoretical extremes of a continuous spectrum, but nonetheless it offers a valuable conceptual framework in the present context.

The key element in White and Jentsch's paper is the emphasis placed on the *tempo* of the disturbance, which switches the perspective from a trend-like slow variation to an event-like, sudden change to the system. The importance attributed to these events characterised by short duration and high magnitude (and consequently higher abruptness, see fig. 86) is increasing in the ecological and paleoclimatological literature (e.g. Adams *et al.* 1999, Jentsch *et al.* 2007, Lloret *et al.* 2012), where they are often regarded as a critical component shaping the evolutionary history of an ecosystem.

Jentsch and colleagues (2007) highlight this concept by indicating how, when assessing environmental changes, it is more important to track down the frequency of extreme events rather than changes in the mean state. This can be shown with a simple mathematical model (figure 87, *after* Jentsch *et al.* 2007: fig.3) where the variation in climate can be represented as random draws from a Gaussian curve (figure 87). For example, consider an agricultural community residing in a region with a mean annual precipitation rate equal to x_1 and a variance equal to v_1. We can further assume that when the precipitation rate is below a fixed threshold c, the crop productivity is too low to sustain the population. In the case of figure 87 such an episode of extreme draught would occur once every 200 years (the area shaded in black). Suppose that some climatic change shifts the mean from x_1 to x_2, and also increases the variance from v_1 to v_2. In the new environmental context, the decline in mean precipitation rate does not affect the system (i.e. $x_2 > c$), but the

probability of occurrence of extreme events below the threshold c becomes much higher, in this example once every 4 years (area shaded in grey). For present purposes the most relevant aspect of this theoretical model is the way it highlights the importance of the tail of distributions, an aspect that is often neglected and considered as a simple background noise. Very often we look at the mean climatic values and how this changes over time, but what matters more is how the frequency of rare events changes along with a shift in the mean. A decrease in the average temperature of 1-2 °C (see section 2.1) is not critical on its own, what matters is the increase in episodes of extreme frost.

One crucial property of these extremely severe events is the statistical shape of their distribution in relation to their frequency and magnitude. Generally speaking the greater the environmental change, the smaller the probability of their occurrence (Turner *et al.* 1998, White and Jentsch 2001). From a conceptual viewpoint this statement is supported by the analysis of ecological time-series recently formalised by Halley (1996), who noticed how a large number of ecological and environmental processes are characterised by variances that continuously increase over time, instead of stabilising within a defined boundary. This is caused by a long-term correlation of events, which can be described as an instance of a *1/f red (or pink) noise*. For our purposes, the most important aspect of red noise and related 1/f models is that these distributions are characterised by the dominance of small changes at shorter timescales interrupted by the occurrence of unusually larger changes over the long-term.

This temporal structure has profound implications for biological adaptation, since a slow sequence of small environmental changes will lead the system to be adaptive in the short-term, but brittle when facing high amplitude changes. Whitehead and Richerson (2009) have further explored the implications of this when combined with different mechanisms of cultural transmission. Their simulation-based analysis has shown how a red noise structure can determine the predominance of social learning at the expense of individual learning. This is because most environmental changes will be small, and thus an individual will do better

in copying rather than trying to individually track the changes. However, such an increase in conformism will also increase the weakness of the system, as very few individuals will be capable of tracking rare radical environmental changes through individual learning. Since red noises are characterised by such rare events, Whitehead and Richerson point out how such a structure in environmental change could determine the "collapse" of a system.

Although an explicit reference to red noise structure is not present, Prentiss and Chatters (Prentiss and Chatters 2003, Chatters and Prentiss 2005) offered a macro-evolutionary model of settlement system change which would be undoubtedly favoured by similar dynamics of environmental change. The key concept of their model relies on the assumption that during episodes of relative stability in climatic conditions parallel and alternative settlement patterns emerge. This *diversification* stage is followed by a *decimation* stage, when sudden changes in environmental conditions alter the selective forces, leading to the survival of only the most adaptive settlement strategies. A red noise structure in environmental time-series will create suitable conditions for the occurrence of these patterns of change, since prolonged periods of climatic stability will ensure the diversification of settlement strategies before their sudden decimations.

Environmental data supporting the presence of such a rare but radical changes has already been introduced in chapter 2. Bond cycles are often characterised by rapid change in the climate at a decadal timescale, often determining an average shift in the temperature of ca. 2 °C (Adams *et al.* 1999). Similarly Mayewski and colleagues' (2004) analysis of RCC (Rapid Climate Change) indicates how "many of these changes are sufficiently fast from the point of view of human civilization (i.e., a few hundred years and shorter) that they may be considered rapid" (*ibid.*: 245). This abruptness of climatic events has also been pointed out by other authors (e.g. deMenocal 2001, Anderson *et al.* 2007) and substantially indicates how exogenous *disturbances* have been and still are quite common.

We can relate the concept of *disturbance* described above with the notion of attractors introduced in chapter 5. A *disturbance* can in fact be formally defined as

a force sufficiently strong to shift the system out of its original basin of attraction and hence determining either a permanent or temporary transition to another basin. This allows us to introduce the notion of *resilience* as "the capacity of a system to absorb disturbance and reorganise while undergoing change so as to still retain essentially the same function, structure, identity, and feedbacks", which along with the concepts of *adaptability* —"the capacity of actors in a system to influence resilience"; – and *transformability* —"capacity to create a fundamentally new system when ecological, economic, or social (including political) conditions make the existing system untenable"; — determines the evolutionary trajectories of a system (Walker *et al.* 2004). A related concept —and in one sense a "measure" of resilience— is what has been defined as *engineering resilience*, defined as the time required for a system to return to its equilibrium state (Holling 1996).

The purpose of our modelling endeavour is to establish what condition determines the resilience of the system to a specific type of disturbance. In practical terms, given the equilibrium conditions identified in the previous chapter we need to determine whether the system-level response to given disturbances are distinguishable from variations which can be generated from its intrinsic stochasticity. For example, if a given parameter combination determines a point attractor to a stable dispersed pattern, a disturbance could manifest itself as a temporary transition to a clumped pattern or as a permanent transition to a given number of groups. The ultimate aim is to establish whether there are variations in the response of the system — which will help us identifying which parameter combinations are more resilient and which are more susceptible to exogenic forces —, or whether the impact of certain disturbances is so strong that the system converges to the same outcome (e.g. extinction). For example different frequencies in the decision-making (z) might determine different levels of resilience, with some values leading to a profound change in the settlement pattern, and others maintaining the system in the conditions observed before the disturbance event. Or on the contrary, such a parameter might be irrelevant, and the system might be driven to similar patterns regardless of the initial condition or show no sign of change after the disturbance

process.

7.2 Modelling Disturbance

In order to integrate disturbance processes with the basic model introduced in chapter 5, we need to design additional submodels mimicking their effects, maintaining at the same time the integrity of the model itself. The most straightforward solution to this is to create a function that induces variation in a model parameter or variable. If such a variation is dependent on the behaviour of the system, we will obtain an *endogenous disturbance*, while if this occurs independently we will simulate an *exogenous disturbance* (see section 7.1 and White and Jentsch 2001:412).

The ideal parameter/variable for modelling disturbance regimes is K, the amount of resource available at any given patch. So far this has been modelled as constant and fixed over time and space. The system was in fact assumed to be isolated from any external perturbation that might alter resource availability, and the rate of consumption by a group of agents had no long-term implications for the amount of resource located at a given patch, with K being "regenerated" at the end of each time-step, even in case of overexploitation (i.e. when $\Xi > K$, see equation 5.8 in section 5.3). This assumption facilitated the exploration of the intrinsic properties of the model, but at the same time led the system to reach some equilibrium states that are unlikely to occur in real world contexts. For example, when the range of spatial interaction leading to a fission-fusion dynamic is limited ($h = 1$), the simulation generated, in several regions of the parameter space, an equilibrium state where all patches were occupied by equally sized groups. This equilibrium state is reached by a predator-prey relationship in a constant static equilibrium, as if consumed resources were fully regenerated at the end of each time-step. In reality a continuous overexploitation (in the specific case a continuous satisfaction of the condition $\Xi > K$) might reduce the productivity of the prey population, if not lead it to extinction.

For the purpose of this thesis, two distinct sub-models of disturbance will be

integrated into the ABM. The first one will explore the effects of endogenic perturbation and will seek to determine whether a predator-prey relationship between foragers and resources could alter the dynamics observed in chapter 6. The second sub-model will instead focus on exogenic influences on the system, and will establish whether changes in K with different levels of abruptness, duration, and magnitude can lead to a temporary or permanent alteration of the evolutionary trajectories in the metapopulation structure.

7.2.1 Endogenic Disturbance: Predator-Prey Interaction Model

The most straightforward approach for modelling resource variation as a function of the predator population is to use the well-known and widely adopted Verhulst equation (Verhulst 1838) as follows:

$$K_t = K_{t-1} + \zeta K_{t-1}\left(1 - \frac{K_{t-1}}{\kappa}\right) \tag{7.1}$$

where K_t is the resource input at time t, κ is the theoretical maximum carrying capacity of the resource pool, and ζ is its intrinsic growth rate. This model produces a wide variety of dynamics from point attractors with $K \approx \kappa$ to limit cycles and chaotic oscillations (May 1976). We can then modify equation 7.1 by adding the term Ξ, the cumulative "demand" of a group of foragers in a given patch:

$$K_t = (K_{t-1} - \Xi) + \zeta(K_{t-1} - \Xi)\left(1 - \frac{K_{t-1} - \Xi}{\kappa}\right) \tag{7.2}$$

This will determine a predator-prey relationship where the intrinsic dynamics of the predator population will be modelled following the equations introduced in chapter 5 (equations 5.5,5.6,5.7, and 5.8) and the intrinsic dynamics of the prey population by the standard Verhulst equation (equation 7.1). The two will be related by the terms Ξ and K in a way similar to the so-called Lotka-Volterra models (see Hastings 1997 for a review), where predator and prey populations are both modelled as modified and interconnected versions of Verhulst equations.

The model introduced in chapter 5 assumes, however, that the predator pop-

ulation possess full knowledge and can cause the complete extinction of the prey (i.e. $\Xi \geq K$ is possible). This is an unrealistic assumption, as it is very likely that a portion β of the resource input is likely to remain unexploited by the predator population. While this is a marginal problem when we do not consider the possible effect of resource depletion, if we adopt equation 7.2 the predator population could easily deplete the resources and lead itself to extinction. In order to avoid this scenario, an upper threshold of Ξ will be defined as $K(1-\beta)$; the perceived availability of resources can thus be smaller than K if $\beta > 0$, or in other words an amount βK always survives predation by the agents. This allow us to slightly modify [1] equation 5.8 as follows:

$$\phi_{i \in j} \begin{cases} \Xi_j / g & \text{if } \Xi_j \leq K(1-\beta) \\ K(1-\beta)/g & \text{if } \Xi_j > K(1-\beta) \end{cases} \tag{7.3}$$

We investigate the implications of these changes by exploring our model in a simplified version of the ABM. Our aim in this case is to obtain a generic expectation derived exclusively from the predator-prey relationship, ignoring for a moment the effects of fission and fusion. This will be achieved by generating a single group in a world with one patch and allowing only the local processes to drive the population dynamics. Figure 88 shows the temporal variation in the group size and the variation in K for three different scenarios defined by different values of β. In the first scenario ($\beta = 0.3$, figure 88:**a**), the group size rapidly increases and overexploits K, which consequently drives the populations of predators to extinction. In the meantime the amount of resources starts to increase thanks to the proportion βK surviving the intense exploitation by the predator population, and subsequently fluctuates as a function of its own intrinsic growth rate ζ. In the sec-

[1] Notice that this implies also that in equation 7.2, the term Ξ should no longer represent the cumulative "demand". The term should be substituted with $\hat{\Xi}$, obtained as follows:

$$\hat{\Xi} \begin{cases} \Xi & \text{if } \Xi \leq (K_{t-1} - \beta K_{t-1}) \\ K_{t-1} - \beta K_{t-1} & \text{if } \Xi > (K_{t-1} - \beta K_{t-1}) \end{cases}$$

ond scenario ($\beta = 0.35$, figure 88:**b**), the predator population survives the episode of declined resource availability and exhibit a renewed growth followed by another crash. This time, the reduced number of individuals determines a smaller exploitation rate between time-steps 75 and 120, allowing an initially slow recovery of the prey population. The subsequent increase of the prey population leads to a second increase of the predator group size, followed again by another crash. In the last scenario (fig. 88:**c**), β is sufficiently high ($= 0.4$) to support an equilibrium population size of ca. 10 predators, affected only by minor stochastic fluctuations.

One of the most obvious consequences of this model is the emergence of spatial inhomogeneity in K as function of local historical processes. The persistence of such a diversity will be dependent upon the density of predators in a given patch and the values of β and ζ. If both resource resilience (β) and prey population intrinsic growth rate (ζ) are small, the recovery rate of K will also be small and thus spatial diversity will last longer. If on the other hand both values are high, such a diversity will last very briefly and its effect can be ignored if the frequency of decision-making (z) is sufficiently high.

The integration of resource depletion highlights possible inconsistencies with two of the assumptions used to model the predators' behaviour, namely the absence of joint migration and the incapacity of the predator to perceive the amount of available resources in a given patch when this is unoccupied. In a real world context, the minimum aggregate unit (m) will have the option to leave the group via fission, or alternatively the entire group could move *together* to an undepleted patch. All other things being equal, the second option is clearly optimal, at least in the short-term. Modelling such a behaviour, however, adds additional layers of complexity, since we would need to formalise our assumptions regarding group decision-making and any conflict with individual choices (see chapter 5 for further discussion), and how to model group-level knowledge of the spatial environment, which will determine "where" to move. For simplicity, here we assume that individuals will fission to a random patch (or migrate to another group) as a response to declining resources. This will ultimately determine the relocation of most mem-

bers of the group to new patches, thus offering a mid-term output which resembles a group-based decision-making.

The second assumption (agents being incapable of directly evaluating the productivity of an unknown patch) can be regarded as an acceptable compromise, and definitely preferable to alternative models where the agents have full-knowledge of patch productivity. Ideally the evaluation of a new environment should be a mixture between direct observation of the predator and the prey population, coupled with a direct assessment by means of a trial stage of exploitation. Here we reduce this to an observation of the predator population (the fitness of the model group), while the trial stage will be achieved in multiple time-steps (i.e. if an agent locates to a highly depleted patch, it will obtain a lower fitness value and hence will migrate in the subsequent time-step).

7.2.2 Exogenic Disturbance: Temporal Variation of K

The second type of disturbance is a force external to the system that decreases the amount of available resources as a function of time. This is a commonly used model of environmental change that varies from the simple linear decrease/increase, to more complex time-series adopting empirical data (e.g. Dean *et al.* 2000) or theoretical models (e.g. Whitehead and Richerson 2009).

For the purpose of this thesis, the following will be adopted:

$$K_t = K_{t-1} - \delta(t_s, t_e) \tag{7.4}$$

where the function $\delta(t_s, t_e)$ is:

$$\delta(t_s, t_e) \begin{cases} 0 & \text{if } t < t_s \\ 0 & \text{if } t > t_e \\ \eta & \text{if } t_s \leq t \leq t_e \end{cases} \tag{7.5}$$

with the condition $t_s < t_e$. In other words, K is initially constant, and then will

decrease by an amount η per time-step within the temporal interval bounded by t_s to t_e. This will conform the triadic description proposed by White and Jentsch (2001) and described in figure 86; $t_e - t_s + 1$ will indicate the duration, $\eta(t_e - t_s + 1)$ the magnitude, and η the abruptness of the disturbance process.

The major advantage of equations 7.4 and 7.5 is that the parameters t_s and t_e allow us to precisely define *when* the disturbance process occurs. This is not possible for more sophisticated models such as 1/f noise, where the stochastic components prevent a precise control of the onset of a disturbance event. Although equations 7.4 and 7.5 are abstract, they can describe the basic properties of a disturbance process inducing a decline in the availability of subsistence resources.

It is important to stress at this point that the purpose of the simulation is to establish the nature of the short-term response of the system, rather than its long-term adaptation. In other words, we need to explore the expected behavioural response within the range of decision-making rules defined in chapter 5 and establish their effects at the macro-scale. In a real world context we might expect a mid- or long-term cultural response that is not integrated in the model (e.g. technological innovation, exploitation of alternative resources, etc.), but capable to generate profound changes in the behaviour of individuals and ultimately lead to changes in the settlement pattern. This is outside the scope of the present study, where the primary focus is to establish the role played by the exogenic forces alone and its relationship to the equilibrium properties of the system explored in chapter 6.

7.3 Experimental Design

The additional parameters introduced above will considerably increase the dimensions and hence the overall size of the parameter space. Recall that the basic experimental design was based on the sweep of 5 parameters (h, b, k, ω_1, and z) resulting in 216 unique combinations. As discussed previously in chapter 6, it is important to minimise the number of parameter combinations, but at the same time explore the widest range of possible behaviour of the system.

A preliminary exploration of the endogenic disturbance model indicates how the predator-prey relationship exhibits three distinct types of behaviour within the constraint of a single patch world (see figure 88). This can be obtained by fixing the intrinsic growth parameter (ζ) to 2 (which generates a point attractor in the prey population dynamics in absence of predation), the prey carrying capacity (κ) to 200 (which conforms to the value chosen for K in the disturbance-free model explored in chapter 6), and sweeping the resilience parameter (β) with the values 0.3, 0.35, and 0.4. The range of variation of β covers a transitional portion of the parameter space for an individual group model, between domains where the system exhibits complete predator extinction and domains where an equilibrium predator population size is reached. Experimental runs have shown that between these two extremes, when $\beta \approx 0.35$, the system shows a limit cycle. Although these dynamics may not emerge when more than one group are present in simulation, this range of the parameter values provides a useful template for exploring the general behaviour of the system and the implications of fission-fusion dynamics.

The exogenic disturbance model is slightly more complicated to explore, as its core parameters and their relation to disturbance events are contingent upon the observed context. For example a shift in climate occurring in an interval of 20 years can be regarded as fast-paced in the real world, but 20 time-steps within the ABM do not itself allow us to determine whether the disturbance has a short or long duration. This limitation originates from the abstract structure of the model, where the spatial and temporal dimensions are detached from real world references (see chapter 5). In order to overcome this issue the parameter sweep must be selected in relation to known behaviour of the system. One possible candidate for this is to use the knowledge about the *tempo* of fission-fusion dynamics obtained from the analysis of the experiment results (i.e. the correlogram) presented in chapter 6. Recall that the correlogram of the simulation output exhibited often a strong evidence of negative autocorrelation in the A coefficient, the median group size, and the number of groups. This has been observed with lags between 3 and 15 time-steps depending on the parameter combination, and in cases where the sys-

tem exhibited a limit-cycle attractor, they represented the half-time of a full cycle (second peak in positive autocorrelation) of transition between clumped and dispersed patterns. This supports adoption of the premise that, for example and with other things being equal, a disturbance process with a duration over 30 time-steps will be slow compared to the basic dynamics of the system. In order to explore the system response to different types of disturbance regimes, the following three scenario have been conceived in relation to the output examined in the previous chapter:

Fast disturbance ($t_s = 301$, $t_e = 304$, $\eta = 25$). The duration of the disturbance is short (4 time-steps) and the abruptness is high (a decrease of 12.5% of the original value of K per time-step). This will represent a disturbance event where the available resources dramatically decrease in a relatively short period of time, reaching half of its original value $K_{t_e+1} = 100$ at a timing equal or faster than a single transition of settlement pattern induced by internal dynamics.

Intermediate disturbance ($t_s = 301$, $t_e = 318$, $\eta \approx 5.56$). The duration of the disturbance is sufficiently large to be longer than all observed cases of a single transition from one settlement system to another. The magnitude has been maintained so that the final amount of resource input is half the initial value; this is achieved by reducing the abruptness to ca. one-fifth of the fast disturbance scenario.

Slow disturbance ($t_s = 301$, $t_e = 348$, $\eta \approx 2.08$). The duration of the disturbance is large (between 2 to 8 cycles of transition between different settlement configurations) with a slow rate of decrease in K (a reduction of only 1% of the initial value of K). Again the final value of K is equal to 100, the same magnitude as the other two scenarios.

7.4 Results

Before outlining the results of the simulation experiments it is important to reemphasise the research design and the purpose of the disturbance model. Some parameter settings, such as the frequency of decision-making or core components of the model such as the fitness curve, are assumed to be fixed throughout each run of the simulation. There are pragmatic and inferential reasons for this. First, designing a model that allows the modification of these parameters — in effect mimicking deep structural changes in the society such as the adoption of new subsistence strategy — will add complexity to the model that will soon become intractable. Exploring the parameter space of the current model already requires a large number of simulation runs, and it is already a difficult task to provide a simple representation of the model behaviour. Second, before tackling the effects of these structural changes, we need to explore the long-term consequences with fixed structural conditions (i.e. fixed model parameters). This strategy has already demonstrated how some patterns observed in the archaeological data could emerge without any disturbance process at all (e.g. fluctuations between clumped and dispersed patterns).

In order to understand the implications of event-based exogenic disturbance we need to look at the short-term response of the system. When environmental changes abruptly, individual responses are expected to be fast-paced and the range of behavioural choices constrained by the available options that are known by the agents at the time. Although cultural responses capable of modifying the behaviour of the agents can ultimately lead to potentially more successful adaptations (e.g. by adopting a novel subsistence resource that might modify the shape of the fitness curve), understanding how the agents reacted within its range of behavioural choices (i.e. fission-fusion dynamics), and what are the their cumulative consequences can offer us important clues for assessing the role of exogenic forces.

7.4.1 Endogenic Disturbance Model

The endogenic disturbance model has been designed to explore the equilibrium properties of the system once a predator-prey relationship between agents and resources is introduced. The primary aim is to establish whether introducing such a relationship will lead to patterns that differ from those observed in the disturbance-free model (discussed in chapter 6). We can explore the model using the same statistics used in chapter 6: the A-coefficient for assessing whether the group size distribution is clumped or dispersed; the median group size as an additional statistic for describing the size distribution; and the number of groups and agents for determining the population and the metapopulation dynamics.

As for the experimental results provided in the previous chapter, the parameter space will be portrayed in a four dimensional space (with coordinates k, z, ω_1, and b). Hence the effects of the remaining two parameters (the range of interaction h and the prey resilience parameter β) will be recorded in different figures (effectively resulting in six four-dimensional parameter space plots), which can be found in appendix D. This section will illustrate only a subset of these plots that are sufficient for describing the system behaviour under endogenic disturbance processes.

A-coefficient ($A(t)$)

The spatially local version of the model ($h = 1$, fig. 89) exhibits a broad dominance of a convex distribution (positive A-coefficient) as a point attractor, a pattern similar to the one observed for the basic model described in chapter 6 (see fig. 64). However the equilibrium values of A appear to be generally lower, suggesting a metapopulation structure closer to those expected for a Zipfian distribution. This trend is more relevant when the prey population resilience (β) is smaller and especially when the net growth rate is zero at the saturation group size (i.e. when $\omega_1 = 0.8$). In the latter case the system exhibits also occasional shifts to a clumped (primate) distributional pattern.

Figure 90 shows a single run of the simulation (**a**) and a combined time-series with semi-transparent lines (**b**), with the prey resilience parameter (β) set to 0.35. The two plots confirm the idea that if both resource resilience and population growth rate are small, the rank-size distribution becomes less stable, leading the system to occasionally (although briefly) leave its basin of attraction and enter in the domain of primate distributions. With higher values of ω_1 this pattern is no longer visible; the system maintains its chaotic fluctuations but within a much narrower range of A, inside the domain of what can be classified as a convex distribution. This is most likely because the number of groups (G) is generally lower for these parameter combinations, often leading the system to extinction (see below).

In contrast to the disturbance-free model, variations of the parameters k (sample proportion of observed neighbour agents) and z (frequency of decision-making) seem to have only marginal effects to the system. While the former showed a consistent decrease of the average A with high values of both parameters when $\omega_1 \geq 1.0$, the endogenic disturbance model shows almost no effects derived from k and just a small impact of z, which becomes more visible for higher values of β. The decrease of the equilibrium value of A for increasing value of z becomes apparent only with higher resilience of the prey population. This is of course not surprising as high values of resilience (β) will lead to smaller effect of the disturbance process, bringing the system close to the disturbance-free basic model described in the previous chapter.

The endogenic disturbance process seems to have a much stronger impact on the group size distribution when the spatial range of interaction is infinite ($h = \infty$, fig.91). Recall that in the basic version of the model, two main attractor states were recognised: a convex point attractor dominating when the frequency of decision-making (z) and the proportion of observed agents (k) are low, and a limit cycle attractor present at the opposite end of the parameter space (see figure 65). When the local density of individuals affects the resource input size, the extent of the point attractor becomes smaller for small values of resource resilience (β). When $\beta = 0.3$, the equilibrium state is a convex distribution only when $\omega_1 = 1.4$, $k =$

10^{-8}, $z \geq 0.5$, with the remnant portions of the parameter space showing chaotic oscillations or limit cycles between dispersed and clumped pattern. When the prey resilience is increased by 0.05, convex equilibria become also visible with slightly lower values of ω_1 (≥ 1.2) and all values of z. Finally when $\beta = 0.4$, the convex point attractor region of the parameter space broadly matches the one observed in the basic model, although when net growth rate is zero at the saturation group size (i.e. when $\omega_1 = 0.8$) episodes of transition to clumped pattern are consistently present.

The reduced number of instances with point attractors does not mean that regular cycles of fluctuations (a limit cycle attractor) are dominant through the parameter space. A detailed examination of the correlogram and the probability density distribution (fig. 92 and 93) suggests a more irregular fluctuation between the two types of settlement pattern, with the latter (fig. 93) showing both unimodal and multimodal curves. Figure 94 shows an example of this, with the single run (**a**) showing irregular oscillations between the two states and the combined time-series (**b**) showing a typical "rain" pattern. In contrast to the pattern observed in figure 90, both dispersed and clumped patterns are now highly unstable, indicating a strange attractor. Again the appearance of unstable fluctuations between different types of group size distribution seems to be partly related to the presence of a comparatively low number of groups (see below), which continuously change their sizes as a function of migratory processes and internal dynamics derived from prey-predator interaction.

Number of groups ($G(t)$), Population size ($N(t)$), and Median group size ($\lambda(t)$)

The total number of agents ($N(t)$) and groups ($G(t)$) are expected to be strongly affected by a decline in resource availability. This reasoning relates to models that explain the decline of pithouse and settlement counts as a consequence of resource overexploitation (see section 2.4). Here, the primary aim of the model is to establish whether possible episodes of resource depletion can generate different meta-population dynamics leading perhaps to smaller equilibrium size for $N(t)$, $G(t)$

and median group size $\lambda(t)$. The population size is particularly interesting as the one-patch model portrayed in figure 88 can serve as a guideline for the expected behaviour of the system without meta-population structure (i.e. multiple groups) and fission-fusion dynamics. Difference in the output can tell us whether these two properties determine a selective advantage or not, and whether modelling these aspects matter if we seek to explore Jōmon population dynamics.

As anticipated above, in the local ($h = 1$, compare fig. 95 and 96) version of the model, the group count is dramatically reduced when the prey resilience is low, and when the net growth rate is zero at saturation group size ($\omega_1 = 0.8$), the system often exhibits extinction. The latter phenomenon is most likely related to a lower net growth rate and a comparatively lower propensity of the agents to fission in new groups and conforms to the expectation portrayed in figure 88:**a**. When ω_1 is increased, fission is enabled (as the groups can exceed the saturation size through internal growth) and this allows the survival of the population despite low prey resilience (β). Increasing β causes a marked increase of the average group counts, but this seems to be valid only for regions of the parameter space where the frequency of decision-making (z) and the sample proportion of observed agents (k) are low. With higher values of these parameters the positive effect derived from higher resilience of the prey population becomes almost undetectable, and the group count remains almost unaffected. Figure 97 depicts two extreme examples of this trend, with 97:**a** showing the effect of β for instances with lower interconnectivity (low z and k) between agents, and 97:**b** for instances of higher interconnectivity (high z and k).

A similar trend can be observed when the range of spatial interaction is ∞, however in this case a tangible correlation between group counts and β can be observed only for $z = 0.1$ and $k = 10^{-8}$, with other parameter combinations showing consistently low values of G.

Increase in the number of agents (N) and the median group size ($\tilde{\lambda}$) are also positively correlated with prey resilience when k and z are low, although the effect is less difficult to assess for the median group size. This linkage between number

of agents and groups is not surprising, and clearly the pattern is more visible when G is stable (i.e. when z and k are low).

In terms of dynamics, N, G, and $\tilde{\lambda}$ maintain their structural properties (i.e. the type of attractor) although with lower equilibrium values in the case of point attractors. This is noteworthy especially in relation to the expansion of limit-cycle and strange attractors for the parameter space of the A-coefficient, observed primarily in the global model (fig. 91). As mentioned above, these regions of the parameter space are characterised by extremely low number of groups, suggesting how the fluctuation between clumped and dispersed pattern is possibly explained by the stronger role of stochastic components in the model. Similarly the regularity in the variation of A observed for large values of k and z when coupled with high prey resilience is most likely related to a higher number of groups and agents, leading to a more stable and consistent response to the random effects derived from the predator-prey interactions.

7.4.2 Exogenic Disturbance Model

Since the aim of the exogenic disturbance model is to evaluate the short-term response of the system, the simulation output will be assessed primarily through the analysis of the time-series, rather than using tools designed to explore the equilibrium properties of the system (i.e. probability density plots and correlograms). The visualisation of the parameter space in this section (and in the appendix D) will thus be restricted to the combined time-series plots of the various statistical measures ($A(t)$, $G(t)$, etc.) between time-steps $t = 200$ and $t = 400$, with t_s and t_e (the interval within which the disturbance process is introduced to the system) shown as vertical dashed lines.

Since agents respond to declining fitness by means of spatial relocation, the expected cumulative and macro-scale effect of the disturbance process is either a temporary change of the system within its basin of attraction (followed by a return to its original equilibrium values) or a shift to a new basin, effectively leading to a permanent change in the size and the shape of the group distribution. How-

ever, in practice these patterns will not always be simple to detect, as we have already noticed how the internal dynamics of the model (see chapter 6) can generate sharp transitions between different metapopulation structures, resembling what we might classify as a system-level response to disturbance. A corollary of this is the role played by historical contingency (i.e. the state of the system during the externally induced resource decline), which might determine a divergence of responses between different runs of the simulation.

Given these expectations, the objective of this section is to identify patterns that are beyond the range of the "normal" behaviours (either in their timing, directionality, or magnitude) expected from the basic model during the interval following the onset of the disturbance regime. This conforms to the relativist definition of disturbance (White and Jentsch 2001, see section 7.1) and can set the basis for assessing the archaeological data (chapter 8) during intervals where we might expect changes in environment.

A-coefficient ($A(t)$)

Rank-size distribution is generally unaffected by slow disturbance processes, but some notable variations can be identified when resource decline is more abrupt. In the latter scenario the most relevant responses of the system depends on the behaviour exhibited by this prior to the disturbance process. For example, regions of the parameter space where a point attractor is observed during normal conditions are characterised by short-term changes in A outside the original basin of attraction, while regions where fluctuations between clumped and dispersed pattern are originally observed exhibit a temporary interruption of such a dynamic, with A converging to similar values despite different initial conditions of the system (i.e. time-series that are out-of-phase become in-phase).

When the range of spatial interaction is restricted ($h = 1$, fig. 98), two types of system response can be identified: 1) a sharp, short-term transition from a strongly convex to a Zipfian pattern (i.e a decrease of A); and 2) a permanent shift from a Zipfian distribution to a slightly more dispersed pattern. Both instances are de-

tectable when the disturbance process is fast, but the former becomes weaker in the medium and almost completely absent in the slow disturbance scenarios.

The strongest decrease of the A-coefficient can be observed in all instances when the net population growth rate is zero at the saturation group size (i.e. when $\omega_1 = 0.8$). As for the endogenic disturbance model, the generally smaller number of groups typical for these regions of the parameter space can perhaps explain this pattern. When the disturbance process occurs, the few large communities will fission, but this process will be constrained by low values of h and s, leaving the parent group to maintain a comparatively large size. This will generate a higher variation in the group size distribution, effectively lowering the A-coefficient. When $\omega_1 \geq 1.0$, the number of groups is larger, and hence the fission process will be more constrained (i.e. the number available empty patches within the neighbourhood defined by h will be smaller), leading to a comparatively smaller decrease of A.

When the rate of decision-making is high (i.e. $z = 1$) and the net growth rate is still positive at the saturation group size (i.e. when $\omega_1 \geq 1.0$), the opposite trend — a slight increase of the A-coefficient— can be noticed. This time the change is permanent, although the increase itself is minimal, and can be found for all three scenarios of disturbance integrated into the simulation. The underlying reason of for this divergent response can be found in the basic property of the system, characterised by a less dispersed pattern coupled to a higher frequency of spatial relocation (due to high values of z). The decline of K will determine a change in the fitness curve (see figure 55) and the consequent reduction of the average group size. As a consequence of this, the number of offspring groups generated by fission events will be smaller, and this will affect the tale of the rank-size distribution. The ultimate consequence of this is a slight decrease in the variability of group sizes and hence to a permanent (although minimal) increase of the average value of A. The ultimate convergence to similar equilibrium values of A for all three scenarios suggests how the observed variation in the group size distribution is probably unrelated to how the system behaved during the onset of the disturbance process. The decline of A is instead the consequence of the shift of the point-attractor equi-

librium imposed by the change in the resource input (K), and a slow variation of the system towards this new point.

When the spatial range of interaction is extended to the entire grid ($h = \infty$, fig. 99), the simulation output appears to maintain some of the properties of the local model (i.e. the decline of A in convex point attractors) coupled with some novel type of responses. Once again, the parameter space is characterised by a general bifurcation defined by z (although this time also k seems to play a relevant role) and variation in A can be observed mainly for fast to medium disturbance processes.

Figure 100 shows some of the most typical outputs of the simulation as box and whisker plots. This will aid in detecting variations in the group size distribution that are hard to assess by a visual inspection of the combined time-series plots. By examining figures 99 and 100, we can identify five types of system responses:

1. A sharp but temporary decline of A indicating a short-term transition from a strongly convex pattern to a group size distribution closer to what we would expect from Zipf's law (fig. 100:**a**; e.g. when $z = 0.1$. $k = 10^{-8}$, $\omega_1 = 1.0$);

2. A similarly sharp decline of A from a highly convex distribution followed however by a partial recovery to a weakly dispersed pattern (e.g. when $z = 0.1$, $k \geq 0.5$, $\omega_1 \geq 1.2$);

3. A weak decline of A within a highly convex point attractor, followed by a rapid recovery to the original equilibrium values (fig. 100:**b**, e.g. when $z = 0.5$, $k \geq 0.5$, $b = 0.3$);

4. A temporary increase of A within a system characterised by repeated fluctuations between dispersed and clumped pattern (fig. 100:**c**. e.g. when $z = 1.0$, $k = 0.5$, $\omega_1 = 1$)

5. No detectable response (fig. 100:**d**; e.g. when $k = 10^{-8}$ and $\omega_1 \geq 1.2$ or when $z = 0.5$, $k \geq 0.5$ and $b = 0.8$)

The first three scenarios (decrease of A-coefficient) are basically distinguished by the initial magnitude of change and the equilibrium level reached after the disturbance process. They are typically observed when both the frequency of decision-making (z) and the sample proportion of the observed agents (k) are small. As for the local model, this corresponds to portions of the parameter space where the rank-size distribution of group sizes is convex, either as a narrow point attractor, or as an instance of strange attractor confined within positive values of A. The sharp decline of K will in this case trigger a fission process, leading to higher diversity of the system. Instances where this decrease is not detected but still within low values of k and z (i.e. when $k = 10^{-8}$ and $\omega_1 \geq 1.2$) are most probably related to parameter combinations determining an extremely high value of G, which consequently impedes the fission process itself (no empty patches within a distance of 1). This "packing" effect will maintain the group size distribution in a highly convex pattern. The absence of variation in the rank-size distribution for extremely low values of ω_1 is instead explained by the fact that fission process itself does not occur in such a scenario, as the net growth rate at the group saturation size is equal to zero.

As for the local model, the transition towards lower values of A could occasionally be permanent, leading the system to enter into a new basin of attraction, although this time we see the emergence of a slightly more primate (instead of convex) pattern. Recall from the analysis of the time-series of $G(t)$ in chapter 6 that with this combination of parameters the dynamics of the disturbance-free model is characterised by different timings in the onset of a large-scale fission process, which leads to the occupation of all the available patches. While this was stochastically triggered in the basic model (see figure 71), here the disturbance process act as a catalyst leading to the generation of multiple offspring groups (see also below) at the same time. This causes a higher variability in group size distribution, and consequently a decline in $A(t)$.

The fourth scenario (a temporary increase of A) can be found in regions of the parameter space where we have previously recognised a dominance of limit-cycle

attractors. When both the frequency of decision-making (z) and the sample proportion of the model agent (k) are high, the exogenic disturbance appears to push the system towards a dispersed pattern, sustain that group size distribution for few time-steps, and then return to oscillate between positive and negative values of A (see fig. 100:**c**). However such a dynamic does not always appear, suggesting that the state of the system during the onset of the disturbance process could play a crucial role.

One way to examine this is to produce a scatterplot of $A(t)$ against $A(t-1)$, so that each point will represent the "movement" of the system within the phase space. If the disturbance process has no influence to the system, or more precisely if we are unable to identify significant divergences from the "normal" behaviour of the system, we should see no difference between the scatter plots with $t_s > t$ and $t_e < t$, and $t_s \geq t \leq t_e$. Of course, this plotting technique considers only instances when A is actually computed for both t and $t-1$, and excludes cases where a low number of groups do not allow the actual computation of the coefficient. An example of this phase scatterplot is provided in figure 101, where the "normal" behaviour of the system (a point attractor with a convex distribution equilibria, here obtained by plotting with values of t from 280 to 300) is plotted as black dots, and the behaviour of the system during the exogenic disturbance process ($t = t_s = 301$) is depicted in red. The black dots show the high stability of the system ($A(t)$ and $A(t-1)$ are perfectly correlated along a diagonal line) prior to disturbance, and they are clearly distinct from the red dots, which instead indicate a transition to a less dispersed pattern ($A(t-1)$ have higher values than $A(t)$).

Figure 102 shows the scatter plots for a subregion of the parameter space where a limit-cycle or a strange attractor has been identified in normal conditions (i.e. $z \geq 0.5$ and $k \geq= 0.5$). The results show how before the onset of disturbance z seems to determine the primary variation through the parameter space. When the frequency of decision-making (z) is equal to 0.5, the basic scatterplot (in black) shows a wedge shaped pattern, with a high cluster of points in the top right corner indicating relative stability of a highly dispersed pattern (both $A(t-1)$ and $A(t)$ are

large), coupled with occasional episodes of shifts towards and away from such a state (points on the top-left and bottom-right quadrants) . When $z = 1.0$, the points cluster along a diagonal line, suggesting the presence of multiple instances where both clumped and dispersed patterns are maintained between $t - 1$ and t. This is coupled with a cloud of more dispersed points extending to the left of the diagonal, which indicates the presence of episodes where A exhibits a slight decline. When the cooperation benefit is high ($b \geq= 0.5$), we can also identify a high concentration of dots in the top-left and bottom right quadrants, suggesting the presence of radical shifts between extreme values of A. Transitions from clumped to dispersed patterns are however depicted with a comparatively smaller number of dots (in the bottom right panel, for instance when $z = 1.0$. $k = 1.0$, $b = 0.5$,$\omega_1 \geq 1.2$); this is probably due to the fact that primate distributions in this region of the parameter space are often characterised by an insufficient number of groups to permit the computation of A.

Generally speaking, the introduction of a disturbance process does not seem to generate a substantial variation in the system behaviour (red dots in fig. 102). However a more careful examination of the scatterplots shows how, when $z = 0.5$, the high concentration of dots in the top right corner disappears when $\omega_1 \geq= 1.0$, demonstrating how the maintenance of a strongly dispersed pattern is no longer possible when the net growth rate is zero above the saturation group size. This is not always the case, and in some instances there are even transitions from clumped to dispersed patterns (dots in the bottom right panel), but nonetheless the pattern confirms the general decline of the A coefficient observed above. When $z = 1$, the distribution of the red dots does not seem to differ from the black ones, indicating how, according to this visualisation technique, there is no clear evidence of system response to the disturbance process. This is true even for parameter combinations where we previously observed a convergent increase of A (for instance when $z = 1.0$, $k = 1.0$,$b = 0.3$, and $\omega_1 = 1.0$, see also fig. 100:**c**), suggesting that the observed transition to a more dispersed system occurs only when the number of groups is extremely small and the A-coefficient cannot be computed (< 3 groups). In

such a scenario fission process generates a larger number of equally sized offspring groups across the landscape (since there are no spatial limitations dictated by the presence of other groups) thereby resulting in a high value for A.

Number of groups ($G(t)$), Population size ($N(t)$), and Median group size ($\lambda(t)$)

While the effects of the exogenic disturbance have mostly a short-term impact on the rank-size distribution, its repercussions for other properties of the system appears to be much larger and more frequently permanent. This is not surprising, as an overall decline in the availability of resources (K) will offer less energy for reproduction, leading to a population decline. Surprisingly this is not always the case, and the dynamics of $N(t)$ appear not to be only a function of the potential availability of the resources, but also of the colonisation rate of groups (i.e. the frequency of fission events). In some cases the latter appears to be triggered by a disturbance process without a subsequent fusion process, ultimately leading to an overall increase in the number of groups, and hence of agents.

Variation in the total number of groups (G) is generally characterised by an increase — confirming the idea of a fission process suggested by the analysis of the A coefficient — unless the number of groups is already at its maximum (100 units in the present case). Despite this broad similarity across the parameter space, the magnitude and more importantly the persistence of such a change varies in function to specific combinations of parameters.

When the range of spatial interaction is localised ($h = 1$, fig. 103) two types of system responses can be observed. Group count may exhibit an increase followed by stable values of G (e.g. when $z = 0.1$, $k = 10^{-8}$, and $\omega_1 = 1.0$), or by a decrease to values close to those observed prior to the disturbance process (e.g. when $z = 0.5$, $k \geq 0.5$, $b = 0.8$, and $\omega_1 \geq 1.0$). In the latter case, such a decline in G might occasionally reach values that are slightly lower than those observed before the decline of K (e.g. when $z = 1.0$, $k = 0.5$, $\omega_1 = 1.0$, and $b \geq 0.5$). Unsurprisingly, the magnitude of the increase is partly a function of the median group size and the number of empty patches in the lattice space. When a few large groups are

isolated from each other and the groups are on the cusp of a fission size (i.e. when $\omega_1 = 1.0$, see figure 57), disturbance provides the right incentive for a global fission, which will lead to the creation of a large number of new groups. If the frequency of decision-making is sufficiently small, these groups will remain in the landscape, permanently increasing the overall value of G. However if z is higher, and if b is large enough to determine a strong attraction towards optimally sized groups (see figure 58), this process is followed by fusion, which in turn determines a decrease of G to its original value. In some case this process is fast enough ($z = 1.0$) to reduce the overall number of groups to levels lower than those observed prior to the disturbance event.

When $h = \infty$ (fig. 104), the disturbance process appears to determine one of the following scenarios: 1) permanent increase (e.g. when $z = 0.1$, $k = 10^{-8}$, $\omega_1 = 1.0$); 2) temporary increase followed by a slight decline (e.g. when $z = 1.0$, $k = 0.5$, $\omega_1 = 1.0$); 3) decrease ($z = 1.0$, $k \geq 0.5$, $\omega_1 \geq 1.0$); and 4) absence of change (e.g. when $z = 0.5$, $k \geq 0.5$).

The underlying processes of the first two scenarios are most probably similar to the one inferred for the local version of the model. The decline in the resource input triggers a fission process, leading to an increase of G. This state of the system is either maintained or followed by a strong fusion process (and decline of G) when the attraction towards optimal groups is higher (high values of b). In regions of the parameter space characterised by repeated and continuous transitions between clumped and dispersed patterns, the decline of K causes a contraction in the occupied regions of the phase space, as the number of offspring groups will be reduced by the smaller size of the parent groups. This leads to a lower average value of G after the disturbance process, a trend that can be observed even when the disturbance process is slow. The last scenario seems to be confined to regions of the parameter space where the system shows a chaotic behaviour with extremely low values of G. Here, the disturbance process does not seem to generate any consistent change in the total number of groups, a pattern coupled with rapid shifts of the group size distribution. This suggests that an intermediate fre-

quency of decision-making allows, via an intense series of inter-group migration process, the resistance of the system to external disturbance.

Population size (N, fig. 105 and 106) is clearly a function of both the group size and the total number of groups, and hence the question is whether an increase in G leads also to an increase of N (i.e. whether the increase in the number of groups compensates the predicted decline of group size). As anticipated at the beginning of this section, for certain parameter combinations, the increase of G is sufficiently large to provoke an increase of the total population after an initial decline recorded during the disturbance process. We thus need to distinguish scenarios where the disturbance process interrupted the increase of G, from those where the system was at equilibrium before the disturbance. If we exclude instances of the former, we can still identify cases where N ultimately increased in a permanent fashion owing to the decline of K. This can for example be observed with the parameter combinations $z = 0.1$, $k = 10^{-8}$, $\omega_1 = 1.0$ in the local model ($h = 1$), and for $z = 0.1$, $k = 10^{-8}$, $\omega_1 = 1.0$ and for $z = 0.1$, $k \geq 0.5$, $b \leq 0.5$, $\omega_1 = 1.2$ in the global model ($h = \infty$). For all other parameter combinations the population level remains low, either because the increase of G is too small or because its increase is immediately followed by a decrease.

Finally a brief overview of the dynamics of the median group size ($\tilde{\lambda}$) confirms a rapid decline of the median group size which is noticeable in all parameter combinations, expect for instances where the basic value is very low (i.e. when $z = 1.0$ and $\omega_1 \geq 1.0$). In most cases the decline is permanent, but in some instances there is a slight recovery caused by a stronger initial fission process during the disturbance stage, and the formation of short-term large groups during the subsequent fusion stage.

7.5 Summary

7.5.1 Endogenic Disturbance Model

The main objective of the endogenic disturbance model was to establish whether introducing a dynamic relation between the prey (K) and the predator (the agents) population would lead to a noticeable change in the behaviour of the system initially modelled in chapter 6. A secondary objective, derived from the preliminary exploration of the prey-predator model, was to explore whether population dynamics observed in a stripped-down version of the ABM with a single patch (i.e. without providing the agents the opportunity to spatially reallocate) were also visible in the full version of the model.

The results of the simulation runs can be summarised in the following points:

- *The relationship between parameter combination and type of attractor for the A-coefficient does not seem to change much between the basic disturbance-free model and the endogenic disturbance model, especially when the prey resilience is high (i.e. when $\beta \geq 0.35$).* When the spatial range of interaction is limited ($h = 1$), the parameter space is dominated by convex distribution point attractors, while when the range is infinite ($h = \infty$) we can observe a trend from point attractors (again with a dispersed pattern) to strange/limit cycle attractors with increasing values of z and k. This implies that, broadly speaking, the relationship between the equilibrium properties of the rank-size distribution and the model parameters does not change with the introduction of endogenic disturbance: the main driver of settlement dynamics are still variables such as the spatial range of interaction (h), the frequency of decision-making (z) and the sample proportion of the observed agents (k).

- *The equilibrium properties of population size are different from the expectations derived from the single group predator-prey model explored in fig. 88.* The presence of a spatial structure and the consequent possibility of fission-fusion dynamics ensures the survival of the agents even when prey resilience is low

($\beta = 0.3$). Extinction occurs only when the net growth rate is zero at the saturation group size (i.e. when $\omega_1 = 0.8$), most probably because agents die before fissioning. This divergence between the non spatial and the spatial model (effectively a meta-population model) reminds us again how the models seeking to understand population dynamics requires the integration of fission-fusion processes. Additionally it shows how fission-fusion dynamics are an adaptive strategy which is fundamental for the survival of a population once resource can be potentially depleted by human exploitation.

- *When prey resilience is low ($\beta = 0.3$) and the system can be described as a point-attractor, the average A-coefficient is lower than the disturbance-free model, although the rank-size distribution is still convex.* This phenomenon is explained by a generally lower number of groups (hence a higher chance to have more diversified group size distribution) and by the spatial diversity in the availability of resources (K) caused by the predator-prey dynamics. The latter point is not surprising, and warns against the uncritical adoption of the habitat matching rule (see section 5.2) for environments with an uniform resource distribution: local episodes of overexploitation can generate spatial diversity, leading to a less dispersed settlement pattern.

- *When prey resilience is low ($\beta = 0.3$) and the range of spatial interaction is global, fluctuations between clumped and dispersed pattern seems to be occurring for a wider range of parameter combinations.* As for the previous point, the lower number of groups and the spatial diversity in resource availability play are critical for the generation of the observed patterns. Additionally, local depletion of the prey population —and the consequent fitness reduction—, generates an intense and continuous migration process. This plays a fundamental role when the spatial range interaction is high, as clumped pattern will continuously appear as an outcome of fusion processes. However, endogenic disturbance is not sufficient to generate stable primate distributions, as their appearance remains extremely short-termed. This is caused by the overexploitation of

local resources by large groups, which ultimately leads to fission. This generates a repeated sequence of fission and fusion similar to the ones observed in the disturbance-free model, when the range of spatial interaction (h), the frequency of decision-making (z), and the sample proportion of observed agents (k) are all high. The introduction of a prey-predator relationship between the agents and the resources result into a widening of such dynamics in the parameter space. This implies that, with a higher chance of endogenic disturbance processes (i.e. when β is low) we should expect to observe fluctuations between clumped and dispersed patterns for a wider range of assumptions, and that the main driver for the emergence of these dynamics is still the spatial range of interaction.

7.5.2 Exogenic Disturbance Model

In contrast to the endogenic disturbance model, the exogenic one was intended to explore the immediate response of the system when facing a global decline in the resource availability. Here it is important to distinguish changes that are simply due to a lower availability of the resources, and changes that are related to the disturbance process itself. The former refers to patterns that we would expect if the model were initiated by values of K equal to K_{t_e+1} (the amount of resources available at each patch after the disturbance process). Lower resource input will clearly modify the shape of the fitness curve (see fig. 55) and generate different equilibrium values (although it will not change the type of attractor), and hence variation in the simulation output is not surprising in the long-term. The latter instead refers to short-term responses of the system that are due to change (decline) in resource input. Possible responses include a temporary deviation of the system from its basin of attraction or a permanent change that leads the metapopulation to reach structures and configurations that are otherwise unreachable from a simple initialisation with lower values of K.

The most relevant outputs of the simulation include the following points:

- *Slow exogenic disturbance events lead only to a gradual change of the system towards equilibrium levels expected for lower resource input*. This implies that any observed changes in the system (e.g. lower median group size, lower population size, etc.) can be recreated by initialising the simulation setting K equal to K_{t_e+1}. The gradual decline of resource input ($\eta \approx 2.08$) does not affect much the fitness of the agents, and hence fission-fusion dynamics are only occasionally triggered, often with different timings in each group. From an archaeological viewpoint, this implies that variations in the settlement pattern will be indistinguishable from those expected from the disturbance free model, especially if we look at narrow temporal windows. Measurable changes will become identifiable only when a larger temporal scale of observation is adopted, but these will be confined mostly on aspects pertaining the average group size or the total population size rather than a change in the shape of the rank-size distribution.

- *Medium and Fast disturbance events induce fission events and spatial relocation.* This is clearly a function of the group size at the moment of the disturbance process: if the group is sufficiently small, the reduction of the available resources will not affect the fitness of its individuals (eg. group G_A in fig. 107), while if the group is large (eg. group G_B in fig. 107) the decrease of fitness could potentially be dramatic, leading agents to fission or to migrate to groups that in other conditions would be regarded as being too small and suboptimal. Both processes will clearly affect the metapopulation structure, leading to a sudden variation of the A-coefficient. In the majority of cases this will consist of a decrease of A, indicative of a trend towards a more clumped pattern (due to an increase in the tale of group size distribution). The only exception (an increase of A, and a transition towards a more dispersed distribution) is observed in a small region of the parameter space characterised by the occasional presence of few largely sized groups collapsing into numerous small offspring groups.

- *Regions of the parameter space characterised by a point attractor in the disturbance-free model are affected by an abrupt temporary decline of A, an increase in the number of groups, and a reduction in the median group size.* These changes (see an example in figure 108) are often characterised by a recovery of the system to either its original configuration or to those expected by a system with smaller values of K (i.e. to equilibrium states expected with lower resource input). However, in some instances the *total number of groups could permanently be modified, reaching values that are outside the original basin of attraction*. This will occur for systems that are highly conservative and requires a strong perturbation to modify their properties: once this happens we can observe metapopulation properties (in this case the number of groups) that cannot be expected as the long-term equilibrium for lower values of K. This novel structure effectively emerges from the disturbance process, and could in certain cases yield unexpected consequences such as an increase in the total number of individuals.

Conclusion

The brief overview of the exogenic disturbance model offered above seems to suggest similar conclusions to the ones observed for the endogenic model, indicating how, generally speaking, *disturbance processes lead to group fission, which in most cases drives the system to a more clumped pattern*. Once again, the disturbance process determines a decrease of A, but this does not allow the system to reach a stable clumped distribution. It is also important to highlight here that the basic properties of the system observed via a disturbance-free model in chapter 5 remain the same. Endogenously induced decline in the resource input size (K) does trigger or anticipate the onset of fission events, and this might enlarge the number of parameter combinations where fluctuations in the rank-size distributions are observed. Large groups will be less resilient, as their members will experience a decline in fitness even when there are no instances of immigration or internal growth. This does not change the dynamics of a highly integrated system with higher growth

rates, but with less integrated systems characterised by slow growth rate the introduction of endogenous disturbance might lead to the emergence of dynamics unobserved in the basic (disturbance free) model. The model also highlights two critical aspects that are important for interpreting the archaeologically observed data.

First, the state of the system during the onset of the disturbance could lead to a strongly divergent outcome, especially if the system is characterised by multiple equilibria. The scatter-plot analysis in figure 102 shows this effectively, pointing out how the system could stay stable or show transitions from clumped to dispersed pattern and vice-versa. The key to understand this divergence is shown in figure 107. In a hypothetical scenario where the system is affected by a disturbance process after a strong fission process, groups will most likely be small enough to sustain the decline of resources. Conversely, if the system is affected by a disturbance after a fusion process, groups will be less resilient, leading to their collapse and fission.

Second, and partly as a consequence of the first point, distinguishing patterns induced by exogenic forces and patterns emerging from purely internal dynamics is extremely complex. If the system has a single equilibrium state, disturbance can be measured as a deviation from its basin of attraction, but if the system has multiple equilibria or can be classified as chaotic, responses to disturbance will be often virtually identical to the normal behaviour of the system. This does not mean that a sudden decline of resources is not having any effects, on the contrary disturbance processes do have consequences, but often as catalysts capable of accelerating or retarding the onset of events that will occur in any case.

The formalisation of the behavioural processes generating changes in the rank-size distribution (chapter 5), its implementation as an agent-based model (chapter 6), and the exploration of possible responses to disturbance processes (this chapter), enable us to finally review the output of the analysis conducted on the archaeological data (chapter 4) and put this in relation to the broader background of the natural and socio-ecological processes presented in chapter 2. The fourth and last

part of the thesis will seek to achieve this goal.

Part IV

Discussion and Conclusions

Chapter 8

Discussion: the Pattern and Process of Jōmon Settlement Change

Part II and part III of the thesis have been dedicated to the analysis of Jomon settlement pattern from two different epistemological directions. Chapter 4 offered a data-driven and pattern-oriented perspective, and sought to assess Uchiyama's claim of alternation between clumped and dispersed settlement distributions by analysing the archaeological record from two case studies. Chapters 5,6, and 7 were instead theory-driven and process-oriented, and aimed to build expectations from a combination of different ecological models within the structural framework of agent-based simulation.

The two directions of enquiry helped to answer the first two research questions formulated in chapter 1. The former offered empirical and statistical support for Uchiyama's hypothesis, showing that indeed the two case studies were characterised by repeated shifts between different shapes of rank-size distributions; the latter suggested how these changes could potentially occur in the absence of any external forces, warning against the unquestioned assumption (see for example Uchiyama 2006) that these transformations were caused by environmental change. The third research question seeks to reexamine this assumption by combining the analysis of the empirical data (chapter 4), the available proxies of environmental change (chapter 2), and the expectations offered by the simulation model (chap-

ter 6-7). The process will involve establishing whether variations in the settlement pattern correlate to recorded environmental changes, and whether these are qualitatively similar to those observed in *silico*.

8.1 Empirical Data, Environmental Change, and Model Expectations

If we lay aside the detailed variations observed across the parameter space, the simulation output provides a broad set of expectations that are consistent in both the disturbance-free and endogenic disturbance models. Although the exact coordinates in the parameter space are different for the two models, the key axis of variation is still defined by three variables: the spatial range of interaction (h); the frequency of decision-making (z); and the sample proportion of observed neighbour agents (k). These three parameters determine how much the groups are interconnected. High values of h, z, and k will lead to a higher conformism in the decision-making (i.e. a higher proportion of agents will make similar choices at the same time) and higher rates of migration with a shared destination; low values of h, z, and k will instead cause group isolation and higher diversity in the choices made by the agents. Using this triadic axis as a guideline we can identify three major expectations:

1. Dispersed settlement patterns (i.e. an uniform distribution of settlement sizes) are widely found as point attractors at the lower range of the axis (low values of h, k and z).

2. Clumped settlement patterns (i.e. a hierarchical distribution of settlement sizes) never exist in an equilibrium state and their occurrence is always short-termed and unstable.

3. Shifts between dispersed and clumped settlement patterns can occur without any external force if the system is located at the higher end of the axis (high

values of h, k, and z)

Before proceeding to compare the archaeological data and the simulation output, it is useful to reassess the results of the A-coefficient analysis for Chiba and Gunma using probability density distributions and auto-correlation functions (fig. 109). These techniques were used to examine the long-term equilibrium properties of the simulation output in chapter 6 and 7, and can offer additional and comparative insights when applied to the empirical data. The probability density shows a bimodal curve for Chiba (fig. 109:**a**), with modes at ca -0.6 and -0.1, and a multimodal shape for Gunma (fig. 109:**b**), with a wide central peak between -0.1 and 0.5 and two minor peaks at -0.5 and -1.5. The results capture the "typical" (i.e. the most commonly found) shapes of the rank-size distribution in the two regions regardless of their order of occurrence. A visual comparison with the theoretical expectations illustrated in figure 61 would suggest that Chiba was possibly characterised by a limit-cycle attractor between primate (clumped) and Zipfian distributions, while Gunma can be classified as a toroidal or a strange attractor, with equilibrium points around Zipfian-convex (weakly dispersed) distributions and different intensities of primate distributions. The combined correlogram[1] provides further insights into the temporal structure of the settlement change, helping to distinguish instances of chaotic oscillations as opposed to a more regular and cyclical transitions between different values of A. The results show fairly strong signals of positive and negative autocorrelation for both regions, suggesting the presence of a relatively regular cycle of change in the shape of the rank-size distribution. This pattern is particularly robust for Chiba (fig. 109:**c**), where two negative peaks at lags of 400 years and 1,000 years, and two positive peaks at 100 and 600 years can be identified. This implies that, on average, similar shapes of rank-size distribution can be found every 600 years, and that these generally lasted for a short interval

[1]The combined correlogram has been created following the same procedure used for the simulation outputs (see section 6.1.1). The bars depict the proportion of significant (at $p \leq 0.05$) positive and negative autocorrelation within the each of the 1,000 time-series of A generated from the Monte-Carlo simulation.

of ca 200 years[2]. Comparison with the time-series depicted on figure 33 confirms these ideas, and suggest that the correlogram of Gunma shows a weaker pattern of positive/negative autocorrelation due to the longer initial stage of dispersed pattern (which is captured by the wide central mode in the probability density plot of figure 109:**b**).

If we incorrectly assume that the system was isolated from external forces, we would classify Chiba as an instance of a limit-cycle attractor (i.e. characterised by a regular alternation between two settlement patterns) and Gunma as a strange attractor (i.e. characterised by chaotic and irregular fluctuations between different patterns) with a weak basin of attraction around positive values of A. Both patterns are similar to those observed in regions of the parameter space at the high end of the triadic axis defined by h, k and z. While it is difficult to infer directly whether the frequency of decision-making was high or low, the range of spatial interaction (h) and the sample proportion of observed neighbours (k) could be partly inferred from the topographic properties of the landscape and potential inter-accessibility between settlements. Rugged landscapes might for example favour isolation between settlements, impeding the interaction (and hence the potential movement) between households located in different groups. Physical constraints in the movement between settlements can be inferred using GIS-led analysis (e.g. cost-weighted distance; see Conolly and Lake 2006), or more sophisticated techniques based on circuit-scape theory (McRae 2006). Lines of evidence indicating the potential presence (or absence) of interaction can also be obtained by examining the spatial distribution of stylistic traits in artefacts (see e.g. Lipo *et al.* 1997). Given the same spatial setting, and with all other things being equal, we should expect to see that periods of higher interaction exhibit higher spatial homogeneity in the stylistic traits.

The relatively small spatial extent of the study areas (15 $\times$ 15 km) lead some to infer that the range of spatial interaction and the sample proportion of ob-

[2]Notice that the duration of the time-blocks is 100 years, thus a positive autocorrelation at lag 0 indicates a positive autocorrelation within the time-block. Consequently a positive peak up to lag 1 (100 years) will suggest continuity for 200 years

served neighbours were relatively high, especially in the case of Chiba, where the Shimousa Tableland offers a landscape which might have facilitated the contact between settlements. The same assumption can be made for Gunma, although the presence of the Tone River and the slopes of the three volcanoes might have encouraged some level of isolation between clusters of settlements. These topographic properties could explain the maintenance of a dispersed settlement system in Gunma during the Early Jōmon period, when pottery styles also exhibit local features (*Ario* and *Kurohama* styles; see Ishizaka and Daikuhara 2001) suggesting potentially smaller interactions between the easter and western settlements in the study area.

The almost regular cycle of alternation between different shapes of rank-size distribution observed in Chiba and Gunma, the possibility that these settlements were highly interconnected (especially in the case of Chiba), and the assumption of a negligible role played by environmental change would suggest that transitions between clumped and dispersed patterns were generated by dynamics of fission-fusion not dissimilar from those described in the disturbance-free (chapter 6) and endogenic disturbance models (chapter 7). Clearly assuming that Jōmon settlements were isolated from environmental changes described in section 2.1 is most likely wrong. A regularity in the cycle of alternation between clumped and dispersed patterns is not sufficient to support the hypothesis of an endogenous change, as regular reappearance of similar exogenic forces might have driven the system to converge to similar patterns multiple times. We cannot dismiss the idea that both hypothesis can be true, as one shift in the settlement pattern might have been triggered by external forces, while another one might have emerged from internal dynamics.

In order to determine whether these changes were indeed product of internal forces or were instead driven by exogenic disturbance, we need to re-evaluate the co-variation of different statistical measures pertaining the settlement size distribution (i.e. total number of residential units, number of settlements, median settlement size and A-coefficient) and at the same time assess these in relation to the

onset of climatic changes that could constitute disturbance events.

The simulation output provides a set of expectations for each of the two hypotheses and offers a rough guide for reinterpreting the analysis of the empirical data. Notice that the following expectations do not refer to the long-term equilibria of different models, but to the combinations of parameter co-variations at a given transition between clumped and dispersed patterns:

I. *If the alternation between clumped and dispersed settlement pattern is purely endogenic and independent of disturbance processes, we should expect the following set of observations*:

   a) the emergence of a clumped pattern should occur independently from the disturbance processes;

   b) a clumped pattern could occur either regularly or irregularly, but in both cases it should be unstable and last for a shorter interval of time compared to dispersed patterns;

   c) a clumped pattern should be followed by a peak in the median group size, before a rapid transition to a dispersed pattern coupled with a sudden decrease of the median group size;

   d) transition to a clumped pattern should be associated with a decline in the number of settlements;

   e) transition to dispersed pattern should be associated with a sudden increase in the number of settlements and smaller group size.

   f) population size should show peaks during intermediate stages (Zipfian distribution), increasing after the transition to a dispersed pattern, and decreasing when the system approaches a clumped pattern.

II. *If the alternation between clumped and dispersed patterns is induced by an external disturbance process, we should expect*:

   a) variations in the system to be correlated with the disturbance process;

b) if during periods of no-disturbance the system is characterised by a stable dispersed pattern, a brief transition to a more clumped pattern with:

   i. a slight increase in the number of settlements;

   ii. a decrease in the median group size;

   iii. and a decrease in the number of pithouses.

c) if during periods of no-disturbance the settlement pattern is clumped, with a low number of settlements and a peak in the median group size, a transition to a dispersed pattern with:

   i. an increase in the number of settlements;

   ii. a decrease in the median group size;

   iii. and a decrease in the number of pithouses.

Before proceeding with a reassessment of the empirical data, it is important to emphasise that this overview of the hypothesis and its associated expectations is predicated on several model assumptions that do not necessarily hold within the observed contexts. One of these stems from the fact that the model was designed to explore the equilibrium properties of the system, and hence does not allow deep structural changes over time. This means that the parameters of the model remained fixed through the simulation runs, and as a result, transitions between different regions of the parameter space did not occur. This assumption does not always hold especially if we consider a large timeframe. Technological innovation and shifts in subsistence strategies are two typical processes that might cause a structural change, inducing the system to transit into different regions of the parameter space. Nevertheless, there are several reasons that justifies the choice of not modelling variations of the parameters triggered by the dynamics of the system. Firstly, such an endeavour will increase the complexity of the model and the number of variables. This will necessitate the exploration of a larger parameter space, and more crucially the interpretation of the simulation outputs will be strongly limited, and obscure the role played by each variable. Secondly, the

primary aim of the simulation was to establish the reaction of the system in response to disturbance processes, which have been indicated as the best candidate in explaining changes in the settlement pattern (see section 2.4). Thirdly, effects of variations in the main parameters defining the triadic axis described above (i.e. frequency of decision-making, spatial range of interaction, and the sample proportion of observed agents) can still be predicted by observing the parameter space without explicitly modelling the process that generates such a change. For example, if the archaeological evidence suggests an increase in the mobility and the range of interaction (perhaps triggered by a stronger reliance on game resources), we can predict that its long-term consequences is a transition from a stable dispersed pattern (fig. 64) to the potential occurrence of cyclical change between clumped and dispersed pattern (fig. 65).

Figures 110 and 111 show a summary of the analysis presented in Chapter 4, along with the absolute dates of key environmental changes that might have triggered some form of disturbance. The archaeological data include the time-series of the A-coefficient analysis and the rate of change of settlement counts, pithouse counts, and median group size. The choices of the environmental proxies has been confined to those that might have decreased the productivity of key resources, and are thus comparable to the type of exogenic disturbance modelled in chapter 7. These include instances of cooling and weakening in the monsoon events, which might have decreased the productivity of masts species (see Imamura 1999a, Kitagawa and Yasuda 2004), and episodes of rapid marine regression and cooling of sea temperature, which caused changes in the coastal environment and its biota, potentially leading to a decline of key maritime resources. It is mandatory to note that these proxies simply suggests interval of times where a decline in resource availability *might* have occurred. A cooling event will increase the likelihood of extreme frost, but, as mentioned in chapter 2, its effect is not always tangible (Kitagawa and Yasuda 2008) and could be lagged (see Davis and Botkin 1985). Similarly, regression events might create suitable environments where the reproductive fitness of certain molluscs might be favoured. Nevertheless, a comparison between

archaeological events and these intervals (colour shaded in figures 110 and 111) can set the basis for building novel and more specific hypothesis of settlement change, laying the foundation of future directions of studies.

Before proceeding, it is important to note how the temporal dimension of figures 110 and 111 are represented. In chapter 4 the labels in the x-axis represented the beginning of each time-block (i.e. 4500 referred to the time-block t_{4500}, starting at 4500 cal BP and ending at 4400 cal BP), here they represent the actual time-continuum. Consequently, the measurement points of the A-coefficient was positioned at the half of each time-block (i.e. an A-coefficient referring to t_{4500} will have a point at 4450 cal BP) while for the rate of change analysis they were positioned at the midpoint of each transition (i.e. a rate of change between blocks t_{5300} and t_{5200} will be centred at 5200 cal BP).

The climatic data in the two figures clearly show how it is difficult to define a precise temporal window when the likelihood of disturbance processes is higher. Different proxies point to different temporal intervals and defining *when* major climatic changes occurred within these intervals is not possible. Consequently, the available dataset cannot indicate whether the temporal relationship between two distinct environmental changes is real or a product of the uncertainties in the measurement of their proxies. Despite these limitations, we can still identify two periods of relative stability in the environmental conditions (between 7000 and 6000 cal BP, and between 5000 and 4600 cal BP), alternating with periods where multiple proxies suggest higher chances of exogenic disturbance (between 6100 and 5000 cal BP, and between 4600 and 3300 cal BP). Both figures 110 and 111 tries to visualise the fuzzy nature of these arbitrarily defined stages by depicting them with a semitransparent colour, so that periods with a high level of overlap will be shown darker. This rather simplistic visualisation technique is sufficient to highlight how the first cluster of disturbance proxies (7000-6100 cal BP) is characterised by "soft" boundaries with minor overlapping towards the beginning and the end of the interval, while the second cluster (4600-3300 cal BP) is characterised by a higher number of events occurring during the second half of the 5th millennium

cal BP.

A general overview of both case studies shows how shifts between clumped and dispersed patterns (as well as instances of notable changes in other measures such as total number of settlements and residential units) do not always appear to be related to environmental changes. For example, on the one hand we can identify at Chiba a slow trend from clumped to dispersed pattern (possibly reversed by a disturbance process at $t_{4700} - t_{4600}$), while on the other hand, we can also detect a similar reversion in Gunma (a trend towards clumped pattern reversed after t_{4800}) during an interval of environmental stasis.

The divergence of the two case studies illustrates the complexity of the situation, but nonetheless suggests that some shifts in the settlement pattern are likely to be independent of environmental changes. At the same time, these two examples also illustrate the limit imposed by temporal uncertainty. For example, the already-mentioned reversion observed at Chiba at the end of the Middle Jōmon (from t_{4700} onwards) appears to be related to the cooling of Tokyo bay described by Miyaji and colleagues (2010), but it is difficult to determine the temporal order between the two events, and hence infer their possible causal relationship. Furthermore, both cultural response and the appearance of perceivable effects to the biota could occur much after the actual onset of climatic change, which will be manifest as a lag between measured environmental change and the empirically observed shift in settlement pattern.

A further aspect, which will also be addressed later, is that each transition in settlement pattern is associated with different directions in the rate of change in pithouse counts, number of settlements, and median group size (see figures 110 and 111 and tables 10 and 11). This strongly suggests that the generative processes behind these changes were probably different and that the observed cyclical pattern is either induced by exogenic forces, or by the convergent outcome of different dynamics. The next two sections will provide a closer inspection to the most notable events of settlement change in both Chiba and Gunma, aiming to detect instances that are similar or dissimilar to the expectations derived from the simu-

lation output.

Chiba

The first transition in settlement pattern —a shift towards a primate (clumped) rank-size distribution — is observed towards the end of the 6th millennium cal BP in conjunction to episodes of rapid climatic changes (Mayewski *et al.* 2004). This shift is associated with a fairly robust chance of increase in settlement counts and a definite increase in the number of residential units. This combination of patterns partially conforms to the expectation offered by the ABM, where group fission is expected to occur when resource availability declines, leading often to the emergence of a clumped settlement pattern (decrease of A and increase in the number of groups). However, the strong and continuous increase in the number of pithouses (a trend also maintained in the subsequent time-block transition) does not conform to the prediction generated by the simulation output: according to this, a disturbance-induced fission process should lead to an overall decline in the total population size (see page 287).

One possible explanation for this divergence is that the steady growth in the number of pithouses, which characterised the first part of the Middle Jōmon period as a whole, and the coarse temporal resolution chosen for the aoristic analysis might combine to obscure a short-term population decrease. The first few centuries of the 5th millennium cal BP are, in fact, a period of relatively stable climatic conditions that might have created suitable environments for population growth. This is the hypothesis proposed by Toizumi (1999b) who suggests that the periods of stasis in the marine regression were associated with the formation of large shell deposits, signalling a possible increase in the availability of maritime resources. Furthermore, multiple studies (see section 2.2.3), including the results presented in chapter 4, have demonstrated that this period was characterised by an unusual increase in the number of pithouses. Thus, the improved climatic conditions might have occurred just after a declining phase at the end of the 6th millennium cal BP, possibly also stimulated by new offspring settlements generated from fission

events.

The clumped system observed at $t_{5200} - t_{5100}$ was unstable and soon followed by a transition towards a more convex (dispersed) distribution. Large settlements might have reached unsustainable sizes due to immigration flows and internal growth, perhaps leading to local resource depletion and fission. The increase of the A-coefficient and settlement counts supports this idea, and the formation of offspring groups might even have been an incentive for subsequent population growth. This combination of patterns conforms to the expectations suggested by the disturbance-free model (compare with fig. 85), although the simulation outputs suggest rapid shifts rather than gradual changes to convex rank-size distributions (dispersed pattern). A more detailed examination of the empirical time-series shows, however, that the increase of A was characterised by a "pulse and pause" pattern, with a rapid increase at $t_{5000} - t_{4900}$ and $t_{4800} - t_{4700}$ and a relative stasis at $t_{4900} - t_{4800}$. The increase of settlement counts shows exactly the same dynamics, suggesting that the transition to convex distributions was possibly characterised by a two-stage fission process.

The onset of the subsequent reversion from a dispersed to a clumped pattern can be summarised as follows:

1. Decline in A, associated with a strong decline in the number of settlements but a relatively stable number of pithouses ($t_{4700} - t_{4600}$).

2. Further decline in A, associated with both decline in the number of pithouses and settlements, but contrasted by a sudden increase in the median group size ($t_{4600} - t_{4500}$).

3. No significant variation in A, coupled to an increase in the number of groups and a decline of pithouse counts and median group size ($t_{4500} - t_{4400}$).

4. Renewed decline in A, associated with an increase in group counts and pithouse counts ($t_{4400} - t_{4300}$).

According to the expectations listed at page 287, transitions to clumped pattern induced by exogenic disturbance should be associated with an increase in the number of settlements and a decline in the number of pithouses. Neither pattern is observed during the first stage, with opposite trends being more likely for the former and high level of uncertainty associated with the other. The observed dynamics seems to be much closer to those expected from the disturbance-free model (see fig. 85). The only notable difference from the expectations of such a model can be found in the rate of change in the number of residential units, which despite being positive, is characterised by wide error bars. However, the fact that the median group size also exhibits a potential increase (although similarly associated with high levels of uncertainty) further supports this argument, which would suggest that the variation in the settlement pattern was triggered by internal processes and not by an externally induced decline of resource availability.

The second stage appears to show similar dynamics, providing additional support to this hypothesis. The A-coefficient reached negative values at t_{4500}, and the number of settlements showed further decline, this time coupled with a marked decrease in the pithouse counts and a sudden increase in the median group size. Again, this combination of patterns matches perfectly the dynamics observed on figure 85, where small groups disappear (decrease in the number of groups) by joining larger groups through fusion (increase of the median group size). The interval between t_{4700} and t_{4500}, which corresponds to the very end of the Middle Jōmon period, is usually regarded as a period characterised by major changes in the settlement pattern in conjunction with a sharp decline in the number of pithouses. Several authors (see for instance Imamura 1999a) have indicated that the cooling events occurring during this stage caused a "collapse" of the Middle Jōmon economy, leading to an overall decline in population. The pattern observed here suggests that changes towards a primate (clumped) rank-size distribution might have occurred before such cooling events. If we hypothesise that the effects of the disturbance process can be translated to a simple decline in resources, smaller groups will be more resilient as the chance of local overexploitation will be min-

imised for them (compare with Fagan 1999). The formation of large groups during this stage is counterintuitive, unless a technological innovation allowed a more efficient harvesting strategy or alternative staple resources (unaffected by the disturbance process) have been selected for a brief period of time. However no evidence of these changes have been detected in the archaeological record, and thus an alternative hypothesis should be sought. On the one hand, the highest coincidence of environmental change recorded at t_{4500} might have not caused a decline in resource availability or at least not a homogenous decline. If this is the case, then we should expect to observe — as we do — a combination of patterns similar to those expected from the disturbance-free model. Alternatively one should consider the fact that environmental change might have modified other parameters (e.g. the average individual yield μ) that might have favoured a fusion process. In other words, smaller settlements might have had a stronger decline in fitness compared to larger ones. This goes beyond the scenarios described by the model, but clearly available lines of evidence suggest that the pattern observed at the end of the Middle Jōmon period is much more complex than previously thought and cannot simply be dismissed by its apparent correlation with the climatic changes of the mid-5$^{\text{th}}$ millennium cal BP.

The subsequent stage is characterised by higher levels of uncertainty associated with the temporal variation of the A coefficient, and hence it is difficult to establish whether the shape of the rank-size distribution changed. A closer inspection of the Monte-Carlo simulation outputs show, however, that the distribution of the rate of change of A between t_{4500} and t_{4400} is normally shaped, with a mean of -6.18×10^{-5} and a standard deviation of 0.0018. This suggests that possible variations in A were extremely small, and hence we can assume relative stability in the shape of the rank-size distribution. Despite the likelihood of stability, this interval is characterised by renewed growth in the number of groups and a sharp decline in both median group size and number of residential units. If we assume that this third stage was also unaffected by the disturbance processes, and hence followed the fission-fusion cycle depicted in figure 85, we can regard this combination of

patterns as those expected when a clumped pattern shifts to a dispersed one. The sharp decline in the median group size and the emergence of new offspring settlements do indeed match the pattern expected by the simulation output when large group fissions to smaller groups. However, the decrease in the number of residential units and the stability of A (which, during the next stage, will decrease rather than increase) do not fully support such a hypothesis. The increase in the number of settlements can potentially be linked to the fission of large groups, which would also explain the decline in the median group size. This should however lead also to an increase in A as the decline in size of large groups and the appearance of small group should lead to a more homogenous settlement size distribution. One possible explanation can be sought in a decline in resource availability, which might have induced a decrease in the population size, but maintained at the same time a comparatively high mixture of differently sized groups. Furthermore, it should be remembered that in the simulation model, the generative process behind the rapid transition to a convex distribution is determined by the synchronic fission of large groups into *equally sized* subunits. In a real world context, subunits might not have the same size, and a disturbance process might have had different effects on differently sized groups. The combination of these factors can easily impede the transition to a pure dispersed pattern, with the substantial diversity in settlement sizes maintaining a relatively lower value of A.

The last stage ($t_{4400} - t_{4300}$) is characterised by a renewed decline of A, coupled this time by an increase in the number of settlements and pithouses. This combination does not appear in any of the simulation outputs, where transition towards a clumped pattern is usually the consequence of a fusion process, which is expected to lead to a decrease in the number of groups. There are multiple hypotheses that can explain why the observed pattern does not match this expectation. For example, some fission process might have occurred (which would explain the emergence of new settlements) but did not lead to the disappearance of the parent group, which is instead maintained to a comparatively large size (a pattern observed in the spatially local version of the ABM). Alternatively, fission-

fusion and growth dynamics might have been strongly heterogeneous, with some groups fissioning while other increased their sizes through internal growth. Both generative processes can equally well cause a decline in the observed values of A. The nature of a disturbance process is also difficult to define in this context. On the one hand, this stage is characterised by the overlap of multiple proxies suggesting a potential decline of resource availability, on the other hand, the archaeological record suggests a renewed increase in the marine exploitation (despite a stronger rate of marine regression recorded between 4500 and 3600 cal BP; Fukusawa *et al.* 1999), attested to by the formation of large scale shell-middens (Toizumi 1999b). This contrasting evidence warns against a simplistic correlation between environmental change and potential disturbance processes, suggesting that the same type of event (marine regression in this case) might have generated completely different responses in different circumstances.

After an interval of relative stability in the A coefficient, which suggests the maintenance of a clumped distribution, a renewed shift towards a Zipfian pattern can be observed from t_{4200} to t_{4100}. The transition is characterised by a decrease in all the settlement parameters and is associated with the disappearance of the large shell-middens that characterised the previous centuries. Again, the relationship with the potential onset of exogenic disturbance processes is difficult to define, as the available data suggests they were already present in the previous time-blocks. Perhaps their effects on resource availability were delayed in this case, but the absence of a regrowth in the number of settlements and pithouses seems to suggest that a profound and permanent change occurred during this stage.

Gunma

As mentioned earlier in chapter 4, the dynamics observed in Gunma (see fig. 111) share some similarities with those examined in Chiba (e.g. the broad fluctuating pattern of the settlement size distribution, the peak in the pithouse counts during the Middle Jōmon period, etc.) but are also characterised by minor (e.g. the timing of the decline in the number of residential units toward the mid-5th millennium

cal BP) and major (e.g. the lack of a second increase in the residential density during the Late Jōmon period and the stability of a dispersed system during the 7th cal BP) differences. The dataset is also characterised by slightly higher levels of uncertainty, especially concerning the rate of change in the group counts and temporal variation in the median group size.

There are several reasons why the presence of these differences in the settlement history of the two regions is not unexpected. Gunma is located in the mountainous regions of Northern Kantō, far from the flat intertidal zones of Chiba. The absence of maritime resources might determine a different shape for the fitness curve, which would in turn lead to different equilibrium sizes and hence divergent group formation dynamics. In addition, I have already mentioned at the beginning of this chapter how the geographical settings might have determined slightly different types of inter-group relationships. These are aspects that need to be taken in consideration during the interpretative process.

The interval between 7000 and 6000 cal BP is characterised by a long-term persistence of a convex rank-size distribution (dispersed pattern) associated with comparatively stable climatic conditions (fig. 111). Despite the high levels of temporal uncertainty, which characterise the archaeological record of this stage, we can safely state that the empirically observed rank-size distribution shares similarities with point-attractor equilibria that are typically observed in regions of the parameter space with small values in the range of spatial interaction (h and s), the sample proportion of observed agents (k), and the frequency of decision-making (z).

This period of relative stasis is followed by an increase of A associated with a gradual growth in the number of groups and residential units (at ca $t_{6100} - t_{6000}$). This can be associated with the cooling recorded at Lake Aoki (Adhikari *et al.* 2002), but it is difficult to establish whether such a climatic event caused a decline in resource availability and the consequent fission of large-sized settlements. The observed patterns (which is maintained in the subsequent centuries) seem rather to suggest an increase in the availability of resources. Nonetheless, simulation outputs have certainly warned that disturbance processes can trigger an increase

in the population size, so the role of resource decline should not be summarily dismissed.

Towards the beginning of the 6th millennium cal BP, a sudden decline in the number of settlements and pithouses, coupled with a sharp transition to a clumped pattern is observed. This occurred during a period in which the proxies of environmental change are the same as those observed during the increase in A, suggesting again how a more precise knowledge of the timing of climatic change is necessary. The combination of patterns matches the shift to a primate distribution identified in the disturbance-free model when the range of spatial interaction, the frequency of decision-making, and the proportion of observed agents are high. The underlying dynamic in this case would be a strong fusion process, but this should also cause a significant increase of the median group size, which is not observed in this case. It is difficult to explain this mismatch with the onset of a potential disturbance process, as this should lead to the fission of largely sized settlements, in turn causing an increase in the number of groups and a less convex rank-size distribution. Perhaps environmental change had a higher impact on smaller settlements, which might explain the decrease in the number of groups and residential units, as well as a transition to a more primate distribution. If, for example, the climatic change determined a decline in μ (the expected average yield from subsistence tasks), rather than K (the total amount of available resources), largely sized settlement would become more attractive and favour the onset of migration flows towards them.

After a ca 200 years when a slight reprise in the residential density can be inferred (although the rate of change does not show a robust pattern), the group size distribution at Gunma saw a relatively fast return to a dispersed pattern coupled again with an increase in the number of pithouses and a possible (the error-bars are quite wide) increase in the median group size and settlement counts ($t_{5600} - t_{5500}$; fig. 111). This corresponds to a stage where numerous proxies suggest climatic changes, including a strong weakening of the Asian monsoons (Wang *et al.* 2005). Whether or not this correlation indicates a possible role of climatic change as a

catalyst for triggering this transition, the combination of patterns suggests fission events of large-scale settlements (increase in group counts and A-coefficient) possibly followed by a population expansion (increase in the number of pithouses).

The subsequent few centuries (from ca 5400 to 5100 cal BP) appear to be characterised by a renewed dominance and maintenance of a dispersed system. The levels of uncertainty become high again and thus it is difficult to establish whether there were significant changes in the shape of the rank-size distribution. Generally speaking, the same interval has been characterised by an overall increase in the number of residential units and settlements, although a brief interval of decline can be recognised during the transition from t_{5400} to t_{5300}. The maintenance of a convex rank-size distribution share some similarities to the patterns observed during the 7$^{\text{th}}$ millennium cal BP, although the dynamics observed in other measures (pithouse counts, number of settlements, and median group size) suggest that this was not a period of stasis. The smaller rate of increase in settlement counts, contrasted by higher rates for pithouse counts and median group size, suggests that this period was characterised by a homogenous growth of each settlement with few episodes of fission-fusion. This would explain the maintenance of a dispersed pattern, but at the same time would suggest that this period was not characterised by disturbance events affecting the population growth of Jōmon communities, despite the presence of cooling events and rapid climate changes (see fig. 111).

From t_{5200} to t_{4800} we can observe a marked decrease of the A-coefficient, similar to the one observed in Chiba during the second half of the 5$^{\text{th}}$ millennium cal BP. We can again identify four distinct stages for this interval:

1. Decline of the A-coefficient suggesting a transition from a convex to Zipfian distribution, coupled with an increase in the pithouse counts and an increase in the median group size ($t_{5200} - t_{5100}$).

2. Further decline of the A-coefficient indicating the emergence of a primate distribution, coupled again with an increase in the pithouse counts and the median group size, but also to a possible decline in the total number of set-

tlements ($t_{5100} - t_{5000}$).

3. Stability of the A-coefficient, coupled with a decrease in the number of residential units and median group size, but also with a possible increase in the total number of settlements ($t_{5000} - t_{4900}$).

4. A renewed decline of A leading to a very strong clumped pattern, associated with a sharp increase in the number of residential units ($t_{4900} - t_{4800}$).

The patterns of the first two stages conforms to those observed in the simulation model when this exhibits a limit-cycle attractor of A. If the empirical data and the simulated data share the same generative process, the interval between $t_{5200} - t_{5000}$ would be characterised by group fusion, with an increasing flow towards large groups contra-posed to the presence of many small scale satellite settlements. This transition to a clumped pattern is, however, followed by a period of possible stasis of A (the average rate of change is 0.0006 with a standard deviation of 0.0019), during which both the total number of residential units and the median group size appear to decline. If we look at the dynamics observed in the simulation, this combination of patterns would suggest a fission process, although this would require a significant increase in the number of new settlements. The rate of change analysis does suggest such an increase, but the level of uncertainty is too high and the error bars extend to negative values, indicating a small possibility of decrease. Despite the lack of a robust pattern in the increase of settlement counts (which can perhaps be influenced by recovery biases; see below), temporary fission appears to be a plausible explanation, and the absence of disturbance proxies seems to suggest that this short-term reversal of trend was induced by internal dynamics of the system. Subsequently the A coefficient showed a renewed decline, reaching at t_{4800} its lowest value. This transition is coupled with a sharp increase in the number of pithouses and a relative stasis in the total number of settlements and the median group size. This could be potentially the result of a fusion process similar to those observed in the simulation output, but would require also a decrease in the number of settlements and an increase in the median group size. Neither patterns

are observed in this case, suggesting that alternative generative processes (such as an increased rate of growth of large settlements) should be sought.

The overall trend towards an increasingly primate distribution observed during the transition from the 6th and the 5th millennium cal BP, saw a reversal at $t_{4800} - t_{4700}$ (fig. 111). This paralleled by a strong decline in the number of residential units and a possible decrease in the median group size, although the latter is associated with high levels of uncertainty. I have already discussed the possibility that this sharp decline in the number of pithouse counts is comparable to those observed at Chiba few centuries later, and chances of a bias derived from the pottery-based chronology has already been discussed at the end of chapter 4 (section 4.3.2). If we assume that these absolute dates are correct, the observed pattern would have occurred before the onset of climatic events that might have triggered disturbance processes, and hence the increase of A and the decline of the pithouse counts should be explained by internal dynamics of the system. Predictions derived from the simulation output (see fig. 85), suggest a decline of the population size at the peak of clumped distribution, and hence one possible explanation might be provided by the coarse resolution of the temporal blocks which could have "blended" the observed patterns. This would show a "fake" signal of pithouse count decrease during the transition to a less primate pattern, when it actually occurred earlier. The comparatively high level of uncertainty does not allow a more robust inspection of the empirical data or the choice of a finer chronological resolution, but the pithouse counts appears to further decline in the subsequent time-blocks, in correspondence to an A coefficient value fluctuating around 0. This last stage (from t_{4700} onwards) is also contemporary with the high number of climatic events that might have triggered some disturbance processes, possibly explaining why a low residential density is observed.

8.2 Discussion

The review presented in the previous few pages has offered insights that can help establish: 1) whether observed changes in the settlement pattern were induced by exogenic forces or derived from internal dynamics of the system; and 2) whether they followed patterns expected from the agent-based model.

Given a time-span of over 3,000 years and the choice of two distinct geographical settings, a unique answer to these questions cannot be given, as each episode of transition might have been the convergent outcome of different generative processes. Tables 10 and 11 offer support to this hypothesis, similar transitions in the rank-size distribution (e.g. the primate to Zipfian distribution at t_{5000}-t_{4900} and at t_{4200}-t_{4100} in Chiba; table 10) are associated with different combinations of other measures of metapopulation dynamics (e.g. increase in the pithouse counts for the former transition in contrast to a decline in the latter). I have already mentioned in chapter 2 that underlying the apparent homogeneity of the Jōmon culture there is in fact a substantial spatial and temporal diversity, and hence each transition event between one settlement pattern to another was most likely characterised by different initial conditions and different structural properties, which led to a different system level responses. If we use the model's parameter space as a heuristic metaphor, the Jōmon system might have continuously moved within this space, perhaps exhibiting a dispersed point attractor at one stage and then a limit-cycle attractor in another. Hence when we assess the whole settlement history between Early and Late Jōmon periods, we need to take into consideration that each transition we are observing might be "internal" to a single type of attractor or the result of a deeper transition which involved the movement of the system across the parameter space. If we observe a shift from a clumped to dispersed settlement pattern, what we ultimately seek to know is whether this was: a) just part of a cyclical change fostered by episodes of local resource depletion and fission-fusion dynamics; b) a response to a decline in resource availability caused by cooling events, leading to the collapse of large groups; c) the outcome of a deeper struc-

tural transformation (e.g. a change in the shape of the fitness curve derived by some technological innovation); d) or some combination of the three. Examining the details of each settlement transition will require a much more detailed and focused analysis, where the integration of proxies beyond the settlement data is mandatory. This goes beyond the scope of this thesis, which aimed to explore the long-term dynamics of the Jōmon settlement evolution, setting the framework and the condition for generating more specific hypothesis for each episode of transition between clumping and dispersion.

Despite the wide diversity of patterns observed in the empirical data, two clues strongly suggests that transitions between clumping and dispersal were at least occasionally generated by forces internal to the system similar to those predicted by the ABM. The first line of evidence comes from the comparison between proxies of environmental change and the analysis of settlement data. The refined chronology based on the adoption of aoristic analysis and Monte-Carlo simulation have improved the assessment of the temporal relationship between these two and allowed us to identify episodes of *transitions between clumped and dispersed pattern during periods of environmental stasis* (see table 10 and 11). The correlation between these radical changes in the settlement pattern and possible episodes of environmental degradation has been the central assumption of several models proposed in the literature (see section 2.4), but the available evidence suggest that this is not the case.

The natural question arising from this is whether these changes are induced by some unknown external forces (or derived by an erroneous assessment of the temporal relationship between archaeological and environmental events), or are, in fact, emerging from internal dynamics of the system. The comparison between the simulation outputs of the disturbance-free model and the empirical evidence can offer insights on this regard. The transition from a convex (dispersed) to weakly primate (clumped) distributions at t_{4700}-t_{4500} in Chiba and at t_{5200}-t_{5000} in Gunma, and the shift towards a convex distribution at t_{4700} in Chiba all *resemble the pattern observed in the disturbance-free model*. The comparison is qualitative, and some lev-

els of uncertainty are present, but the rates of change in the median group size, pithouse counts, and number of settlements all appear to match the dynamics expected by the ABM in regions of the parameter space where a limit-cycle attractor has been observed. This further supports the idea that observed changes in rank-size distribution might have been generated from the internal dynamics of the system: migration flows, fission-fusion dynamics, and local resource depletion all played a role causing the emergence of novel settlement patterns. These endogenous changes in the settlement pattern have been predicted in other simulation studies, which showed how these can be often characterised by sudden transitions rather than gradual changes (e.g. Renfrew and Poston 1979, Griffin 2011, see chapter 5 for discussions), and stress how we should not assume *a priori* that Jōmon settlement systems are static point attractors.

Establishing the causes of settlement transitions during other periods, where environmental proxies suggest higher chances of disturbance processes, is more complex and limited by two broad sets of problems. The first one is related to the nature of these environmental changes. Figures 110 and 111 shows how the same type of environmental changes (e.g. regression events) occurred multiple times, but this does not imply that their properties were identical, and more importantly that their effect to the biota were similar. The assumption shared by the existing literature (see sections 2.1 and 2.4) indicates that most of these events determined a decline in resource availability. Reduced precipitation and cooling could decrease the productivity of mast species, while regression events can alter coastal ecosystems, in turn determining a change in its composition and a possible decline in the availability of certain species of molluscs. Some of these assumptions are supported by archaeological evidences (e.g. Toizumi 1999b, Kitagawa and Yasuda 2004), but establishing a precise link between environmental proxies (e.g. possible cooling) and the onset of a disturbance process (e.g. decline of chestnut productivity) is a complex task, and the available data can only suggest higher or lower likelihood of their occurrence.

The second set of problems is caused by the temporal uncertainty associated

with the archaeological and palaeoenvironmental data. The adoption of aoristic analysis and Monte-Carlo simulation can fully exploit the available information but does not allow us to support fine-grained sub-century temporal resolutions. This would be a problem if variations in the settlement distribution occurred at a comparatively higher frequency. Figure 112 shows three hypothetical time-series with different frequencies of change and how the adoption of a coarse chronological resolution could modify the archaeologically detectable pattern. If the underlying change is gradual, loss of information is minimal, but rapid changes in the system might give false signals of staticity. The results of the agent-based simulation have shown that a fast paced response of the system can be followed by a rapid recovery (e.g. a dispersed point attractor can exhibit a brief transition to a more clumped pattern); if such a process is comparatively fast, the pattern might be hidden under an apparent impression of staticity (fig. 112 :**c**).

A corollary of this problem is the reliability of the pottery-based chronology. Although Kobayashi's chronology is the only one providing a reference to absolute calibrated dates, the uncertainties of the radiocarbon dates from which such a sequence has been created have been lost in the creation of his pottery phases. As a consequence of this, the absolute temporal definition of time-blocks might be slightly shifted, potentially altering its "before/after" relationship to episodes of environmental changes. As mentioned in section 2.2.1, the adoption Bayesian techniques (Buck *et al.* 1992) could potentially improve the situation, suggesting that a large-scale reassessment of the radiocarbon dates aimed to enhance Kobayashi's sequence is a priority in the future.

The problem of temporal uncertainty affects also the environmental dataset. The chronological definition of most palaeoenvironmental datasets relies on age-depth models, where the observation of a proxy of change (e.g. the increase in frequency of a certain pollen type) is linked to the time-continuum by the interpolation of few known dates. For example, the chronological definition of Adhikari and colleagues' (2002) study at Lake Aoki is inferred from an age-depth model based on the linear interpolation of three known dates. Variation in the rate of de-

position between these points might determine a different age-depth relationship, altering the absolute chronology of the environmental record. This is a known issue, and can occasionally lead to high levels of imprecision masked by an apparent high resolution temporal framework. Recent studies based on Bayesian methods (e.g. Buck *et al.* 2003, Parnell *et al.* 2008) have demonstrated how the uncertainty in these records can be formally measured and expressed, providing a more robust framework for comparing archaeological and palaeoenvironmental data.

Given these limitations, it is difficult to determine whether each episode of transition in settlement pattern was actually associated with a decline in resource availability. Nonetheless, we can still compare the observed variations in the statistical measures of the metapopulation structure (i.e. median group size, number of pithouses, etc.; tables 10 and 11) and establish whether these conform to the expectations of the agent-based simulation (see page II). The results do not show any matching of patterns, suggesting that *there is no clear evidence pointing to shifts between clumped and dispersed pattern induced by a decline in resource availability*, if we assume that the predictions offered by the ABM are correct. Correlation between environmental change and other properties of Jōmon settlement are however observed, especially once we adopt a broader perspective. The most notable example is the population dynamics inferred from the number of pithouses and settlements which both appear to decline around the mid-5th millennium cal BP in Chiba (see figure 111). This and other potential correlations do not, however, imply causation, but suggest that the broad dynamics identified by this study require further investigation narrowed to each episode of settlement transition.

One general point that needs to be taken into consideration is the potential bias derived by limitations in the empirical data. The extent of the window of analysis and the potential presence of unrecovered settlements —despite the unparalleled intensity of archaeological investigation —, can both limit the match between the observed patterns and the simulation outputs, even when they share the same dynamics. For example, a lack of increase in the number of settlements might still be generated by a fission process where the offspring settlements are simply located

outside the study area or buried in the soil. Similarly, the appearance of a clumped pattern might be caused by the presence of new offspring settlements that were generated by the fission of settlements located outside the window of analysis or perhaps in less intensively examined areas. These examples illustrate how a mismatch between the simulation output and the empirical data does not necessarily imply that the underlying generative process were different, a phenomena which can be classified by an instance of multifinality driven by the limits imposed by archaeological data.

Alternative hypotheses

The problem of equifinality and multifinality (see section 5.1) highlights the importance of alternative hypotheses that could possibly explain the observed archaeological pattern. Some of these parallel models, and the reasons why the one proposed here was preferred, have already been discussed in chapter 2 and 5. Nonetheless it is useful to review them here, discussing whether they can still be regarded as potential alternative hypotheses or not and showing potential new directions of research. The following list presents the most relevant ones in order of increasing plausibility:

- *The observed variation in the rank-size distribution is due to a combination of recovery bias and the limited size of the window of analysis.*

  This hypothesis follows the argument presented above. Small settlements are in many cases less visible in the landscape and hence less likely to be identified and investigated, and as such the tail of the rank-size distribution might "shorten". Similarly, primate distributions (clumped settlement patterns) are heavily dependent on the identification of highly ranked sites, if these are not identified or are located outside the window of analysis, the resulting A coefficient will be biased towards higher values. The adoption of truncated rank-size analysis and bootstrap techniques (see chapter 4) has shown how, at least from a statistical viewpoint, the observed fluctuating pattern is ro-

bust. Nonetheless, a more direct formal analysis of the archaeological bias can perhaps improve the analytical output.

- *Difference in settlement size reflects different length of site occupation*.

  This argument is mainly derived from Kobayashi's settlement system model (Kobayashi 1973; 1992; see section 2.2.4), which states that large-scale settlements are simply the result of a longer and repeated occupation (inferred from the presence of multiple pottery phases). Although this hypothesis cannot be entirely dismissed, the adoption of Monte-Carlo simulations with temporal blocks of 100 years has considerably reduced the possibility that the observed variation in the settlement size was due to the length of occupational history.

- *Clumped and dispersed pattern emerge from direct inter-group competition and territoriality*

  Territorial expansion and conflict are potential solutions that might have been undertaken by Jōmon communities, and could have limited the growth of neighbouring communities, ultimately leading to the emergence of a hierarchy in the rank-size distribution. Empirical evidence of territorial organisation is conflicting. Taniguchi's (1993) suggested their existence in his study of Middle Jōmon settlements in Tokyo, but the analysis has been limited exclusively to the distribution of large-settlements and the adoption of a coarse chronological resolution. More detailed analysis at intermediate spatial scales (e.g. Crema *et al.* 2010) has shown how cluster of differently sized settlements can be located in close-proximity suggesting a lack of territorial competition between neighbouring communities. Although some evidence of conflict does exist (see Suzuki 1999) it is too weak to support this hypothesis.

- *Changes in the group size distribution reflect underlying variation in the resource availability*.

The basic prediction of the ideal free distribution model is that individuals distribute themselves among different patches in proportion to the availability of local resources (Tregenza 1995; see section 5.2). The dominance of a dispersed settlement pattern for large portions of the parameter space partly conforms to this prediction, as the non-disturbance model was designed with a homogenous value of K. Variations between clumped and dispersed patterns observed in the simulation outputs were, in other words, entirely caused by inherent spatial dependency, as induced spatial dependency was held constant.

An obvious critique and extension to this model is that resource distribution can be inhomogeneous, and more importantly its spatial structure could change over time. In such circumstances, the model expectation is that transitions between clumping and dispersal could arise simply because of a changed spatial distribution of the prey population. Instances when a dispersed pattern is observed could be indicative of a homogenous distribution, and conversely a clumped pattern could simply be the outcome of a high proportion of resources located in very few patches (where dominant settlements will reside).

In both case studies, the spatial variation of resource availability could potentially be determined by exogenic (e.g. marine regression will modify the productivity of intertidal zones) or endogenic (e.g. local resource depletion) forces. The former is difficult to support due to the relatively small size of the window of analysis: any disturbance process will most likely affect the region homogeneously. The implications of the latter hypothesis were explored by the endogenic disturbance model (chapter 7), which showed how the expected dynamics are not dissimilar to the non-disturbance model, although in some portions of the parameter space there is a slightly higher likelihood of transitions between clumping and dispersal.

Establishing whether the observed variation in settlement pattern is due to

changes in the induced spatial dependency will require further analysis. This would need to focus on specific transitions that have been identified in the present study, and adopt suitable techniques such as multivariate regression (which can establish the statistical relationship between temporal changes in the residential density and the background environment) or point-process modelling (which offers the possibility of testing different hypotheses concerning both inherent and induced spatial dependencies; Illian *et al.* 2008, Bevan *et al.* under review).

- *Clumped and dispersed patterns are results of different types of intra-annual fission-fusion process*.

  If fission-fusion dynamics occurred at high frequencies (e.g. seasonally), a clumped settlement pattern could be expected in the archaeological record as the result of overlap between different spatial configurations (compare with the notion of "remnant settlement patterns" in Dewar and McBride 1992). Large settlements could be the remnants of seasonal aggregation sites, while smaller settlements might be the result of a short-term fission process (compare with ethnographic examples in Watanabe 1986). Variations in such seasonal mobility patterns will thus produce an archaeologically visible variation between clumped and dispersed pattern. For example, if households cease to aggregate seasonally (e.g. due to change in the subsistence strategy), the size distribution of settlements will become less diverse, leading to an increase in the A-coefficient.

  A similar argument was made by Habu (2001) in her study of the late Early Jōmon collapse in southwest Kantō, where she suggested that observed changes in the archaeological record could be explained by temporary transitions between collector and forager systems. The former would be characterised by larger home-base settlements coupled with smaller task-specific sites (e.g. stations, caches, etc.), while a forager system would be characterised by lower levels of inter-site diversity. All other things being equal, the rank-size dis-

tribution of the settlements would have a primate shape for the former, and a convex shape for the latter.

In order to test this alternative hypothesis, a detailed analysis of the seasonality on these settlements would be mandatory. If indeed clumping is a result of seasonal fission-fusion dynamics, the analysis of faunal remains should exhibit a higher inter-site diversity (mainly between large and small settlements) in the season of occupation, and conversely a dispersed pattern should show a lower diversity. Such an analysis would, however, be biased towards the few settlements where such faunal remains are available (and hence would virtually exclude the whole dataset from Gunma). The few available datasets do not seem to support this alternative hypothesis. For example, Koike's analysis of the seashells recovered at Kidosaku site (1986), in Chiba (which is part of the current dataset), provides evidence of a year-long occupation during the early stages of the *Horinouchi* phase (4250-3820 cal BP). This phase is characterised by a clumped pattern first ($t_{4300} - t_{4200}$) followed by a stage with a comparatively high level of uncertainty (although on average A approaches 0 between $t_{4100} - t_{4000}$). If Kidosaku site —which is one of the settlements with the highest rank during this stage— were the result of a seasonal aggregation, we would not observe the evidence suggested by its malacofauna. Thus, this mismatch weakens the seasonal fission-fusion hypothesis, at least for the *Horinouchi* phase in Chiba.

An additional argument against the possibility of intra-annual fission-fusion dynamics points to the relatively small geographic variability in the study areas (especially in the case of Chiba), which does not seem to offer an adaptive advantage in terms of resource variability, although the limited window of analysis adopted here does not allow us to fully dismiss this hypothesis.[3]

[3]It should be noted that aggregation can be induced also by short-term collaborations (e.g. collective hunting) that are not based on external properties of the environment but instead on the presence of other individuals (i.e. on the basis of a short-term attractive inherent spatial dependency)

This brief review of possible alternative hypothesis allows us to place the model introduced in this thesis in a wider perspective, showing its potential and implications on the one hand, and its limits on the other. The key assumption that resides in the core of the model is that human groups are not fixed but modifiable entities characterised by multiple episodes of fission and fusion. Empirical evidence of fission can be found in every site; whether these are the remnants of seasonally formed task-specific subgroups or long-termed occupied settlements, their founders previously inhabited other places, settling at the new site after leaving their parent group. Evidence of group fusion is harder to find, since the simple decrease in the number of small settlements, paralleled to the growth of the large ones can be equally explained by the collapse of the former and increase, by internal growth, of the latter. Evidence of inter-group migration could, however, be inferred from the analysis of human remains. For example, Kusaka and colleagues (2011) showed, using strontium isotope analysis, that some individuals from two Final Jōmon sites in Aichi prefecture (Chūbu) were most likely immigrants.

The most relevant outcome emerging from the analysis of the empirical data and the simulation outputs is that shifts between different settlement patterns can arise from internal dynamics alone, without the need of external forces. As mentioned earlier, this is not itself a new conclusion in the literature of settlement dynamics, but the empirical evidence offered in the two cases studies, and the fact that the details of the simulation model differs from previous studies, further support this idea. The striking regularity of the transitions between clumped and dispersed pattern in Chiba (see fig. 109) would almost suggest that these changes were instances of a limit-cycle attractor, with environmental changes being only a weak external force incapable to trigger the observed patterns alone. The population dynamics inferred from the number of pithouse counts does not support this claim: the Middle Jōmon peak coincides with a period of stasis, and the decline observed at the end of the Early and Middle Jōmon periods appear to be broadly correlated with environmental change. However, these correlations cannot be robustly supported (see the decline in the residential units at Gunma at the end of

the Middle Jōmon period before the occurrence of any environmental change) due to the high levels of uncertainty associated with both archaeological and palaeoenvironmental data.

The exploration of the model's parameter space has shown that the key catalyst inducing change in the metapopulation structure is the level of intergroup connectivity and conformism in the decision-making. The lower is the number of restrictions impeding individuals to make the choice they regard as optimal the higher is the chance that the system reaches a static equilibrium. Isolated groups with few flows of migration can then become stable, and fission-fusion dynamics will be rare. The shape of the rank-size distribution will most likely match the underlying distribution of the resources, conforming to the predictions provided by the ideal free distribution models. When the opposite situation occurs, and individuals are free to make their choices with a greater knowledge of the surrounding environment, the effects derived by the relocation of the agents are not immediately absorbed by the system. Groups regarded as optimal will be quickly invaded, and the migration flow will inevitably lead the group itself to collapse and fission, enabling a continuous cycle of fluctuation between primate and convex distributions.

The instability of highly clumped distribution can be found in both empirical and simulated data. The archaeological record shows how these systems did not last for a long interval of time (contra-posed to a dispersed pattern; see the Early Jōmon in Gunma) and the exploration of the parameter space did not yield any instance of point-attractor with a negative equilibrium value of A. Nonetheless, these unstable metapopulation structure emerged multiple times during the Jōmon period, either as a response to an external stimuli or emerging from the cumulative effect of individual decision-makings. The underlying reason for this instability is that such a metapopulation structure is essentially derived by an initially adaptive choice (joining a group with higher expected fitness) that becomes maladaptive in the long-term. This closely resembles evolutionary trajectories observed in the well-known "tragedy of commons" (Hardin 1968), where the optimal (and self-

ish) choice of multiple individuals leads to a loss to the whole community. Similar models are widely present in the literature of game theory, were the interdependence of multiple decision-makings (e.g. migration to a shared destination) often leads to a system-level emergence (e.g. the formation of over-sized group) that has negative implications to the single individual (e.g. subsequent decline in fitness). Why do such dynamics arise? The ABM suggests that these cycles of change will emerge when agents make similar decisions at the same time. A high proportion of observed neighbour individuals (k) and larger spatial range of interaction (s) will lead the agents to look at the same pool of potential model individuals, while high frequency of decision-making (z) will induce them to reallocate spatially at the same time to the same place. If we take a step back from the specifics of this model, we can generalise that a decline in the diversity of choices leads the system to grow the seed of its own "collapse". Although their model was designed for completely different aims, the loss of resilience derived by excessive conformism plays a central role in Whitehead and Richerson's simulation model of collapse as well (2009; see discussion in section 2.4). The ABM presented in this thesis suggests also that this process is prone to be repeated multiple times, as the short-term benefit of specific behaviours will always prevail and have a selective advantage. If no constraints are imposed on the system, convergence in the choices will *always* lead the system to become more and more brittle until a break point (fission), which resets the cycle. Note also that clumped patterns are defined as such by the tail of the rank-size distribution, and not by the size of the largest settlement. Hence the instability of the system is also due to the behaviour of these settlements, which will likely merge (fusion) into larger settlements. This alternation of fission and fusion generate dynamics that are not dissimilar to the *adaptive cycles* advocated by some scholars (see Rosen and Rivera-Collazo 2012 for a recent archaeological application of this heuristic model) where a system repeatedly proceeds through phases of *growth* (increase in settlement size), *conservation* (stasis), *release* (fission), and *reorganisation* (fusion).

If we adopt the descriptive framework provided by the ABM, clumped systems can persist only through a modification of the fitness curve, but from the long-term perspective, their collapse and the consequent emergence of a cyclical behaviour appears to be unavoidable. Forced isolation by means of selective entry-rules can impede migration flows and perhaps sustain large-scale settlements, but will lead ultimately to a homogenous size distribution. A technological innovation might temporarily increase the positive effects derived by aggregation, and hence allow the persistence of the largest settlements. This situation will, however, not last long, and large groups will soon lose their supremacy in the rank-size distribution, leading to a turnover of the system (Bentley *et al.* 2008). Batty's analysis (2006) of US urban systems between 1790 and 2000 shows this pattern, warning at the same time that the maintenance of the same shape in the rank-size distribution could hide a continuous change in the ranks of its settlement. In a recent review paper on resilience theory where many of these ideas on adaptive change are explored, Janssen and colleagues (2007) state that the key component of these adaptive systems is *change* itself. Whether induced by some disturbance process or emerging from inherent properties of the system, the alternation between clumped and dispersed pattern is an example of adaptive process which underpinned the sustainment of the Jōmon culture for several thousand years.

Chapter 9

Conclusions

This thesis took its point of departure from the convergence of two lines of enquiry. The first one arose from the specifics of the archaeological record of Jōmon settlements while the second took shape from the broader question of how human groups form and change over space and time. This interest in both the particular and the general has deeply shaped the structure of the thesis, leading to the development of two distinct epistemological frameworks. On the one hand, statistical analysis of patterns in the empirical record aimed to test whether existing claims about Jōmon settlement change could be confirmed (part II of the thesis). On the other hand, a process-oriented approach, seeking to determine the possible generative dynamics behind the observed patterns, has been adopted through the creation a computer simulation model and a series of experiments derived from this (part III of the thesis). Despite the existence of these apparently separate tracks of enquiry, the two lines of research were conducted simultaneously with continuous feedback between each other. This endeavour culminated in the previous chapter, where the outcome from the two approaches were brought together.

In chapters 1 and 2, I illustrated how a number of studies have identified repeated episodes of transformations in the Jōmon settlement pattern. This fragmented body of work, often focused on narrow temporal windows, has been unified by Uchiyama's distinction between clumped and dispersed forms (Uchiyama 2006). The distinction between these two types was based on the size distribution

of the settlements; clumped patterns are characterised by the presence of few large clusters of residential units and many smaller settlements; while dispersed pattern by a more homogenous distribution of sizes. Uchiyama made two crucial points: 1) that these two forms appeared in cyclical fashion during the Jōmon period; and 2) that shifts between one form to another were ultimately due to changes in the environment. Although other authors stated similar claims (see for instance contributions in Suzuki and Suzuki 2010), no attempts to assess the long-term dynamics of Jōmon settlement pattern in a formal and unified fashion have been offered so far. The few exceptions are in fact in most cases semi-quantitative descriptions, and crucially with a temporal definition exclusively based on the relative chronological framework of pottery phases. Furthermore, Uchiyama did not made clear how these forms emerged in the first place and how they changed from one to another over time, with only few words pointing to possible differences in land-use.

This thesis aimed to fill this gap by combining the specific research problem of the Jōmon culture with the broader question of how human groups emerge and vary over time. This led to the formulation of three research questions: 1) whether transitions between clumped and dispersed pattern can be quantitatively observed; 2) whether these alternation can, at least in theory, occur without the presence of external forces; 3) determine the possible role played by these forces in shaping the evolution of Jōmon settlement pattern.

The first research question has been tackled by analysing the settlement data from two case studies in Central Japan. The qualitative distinction between clumped and dispersed pattern made necessary a formal redefinition. It was argued that rank-size analysis offers the best framework, with clumped patterns being comparable to primate distributions, and dispersed patterns to convex distributions. This formalisation also offered the opportunity to use a continuous measure (the A-coefficient, Drennan and Peterson 2004) for describing different settlement forms, enabling a switch from an arbitrary dichotomy to a full spectrum of variation, with the Zipfian distribution acting as a middle-point.

The application of this and other statistical measures of the settlement pattern

required some methodological developments for overcoming the limits imposed by the intrinsic spatial and temporal uncertainty of the archaeological record. Shifting the perspective to the distribution of single residential features, rather than relying on arbitrary and ambiguously defined archaeological sites tackled the former issue. The use of aoristic analysis (Ratcliffe and McCullagh 1998) and Monte-Carlo simulation tackled the second problem of temporal uncertainty. Aoristic analysis allowed the conversion of the relative chronological data associated with individual pithouses to a series of probability distributions within the framework of an absolute chronology. Monte-Carlo simulation employed such a transformed data and generated possible temporal sequences of settlement pattern that *might* have occurred on the basis of the current state of archaeological knowledge. This allowed the transition from a discrete assessment of the observed patterns to a probabilistic one, effectively maximising the information retrieved from the available data and distinguishing instances of lower or higher uncertainty.

The results (chapter 4) offered a formal and statistical account of the temporal changes in Jōmon settlement pattern and successfully supported Uchiyama's hypothesis by showing how *shifts between clumping and dispersion did occur multiple times in both case studies* with a surprisingly regular and cyclical fashion. However, it also made clear how the two case studies differed in their patterns, and that each cycle of change was characterised by a different combination of other measures of the metapopulation structure, including the total number of residential units, settlement counts, median group size, and the spatial inter-distance between clusters of pithouses. The most relevant difference between the two regions can be identified in the time-series of the residential units between the Middle and Late Jōmon periods. The number of residential units in Gunma declined abruptly between 4800 and 4600 cal BP and never recovered, while in Chiba the decline occurred later (between 4600 and 4400 cal BP) and was followed by an increase during the early phases of the Late Jōmon period (between 4400 and 4200 cal BP).

The second research question, concerning the necessity of external forces, has been tackled by looking at the existing anthropological and ecological literature

on group formation dynamics and extending these theories by means of an agent-based model. This was a necessary epistemological leap, aimed at building new theories and expectations rather than testing specific hypothesis of settlement change. The computer simulation sought to merge two leading ecological theories: the ideal free distribution (Fretwell and Lucas 1970, Tregenza 1995) and group foraging models (Sibly 1983, Clark and Mangel 1986). The former is centred on the role of the background distribution of resources, and how this drives the locational choice of each individual; the latter looks at the beneficial and detrimental effects of the presence (or absence) of others individuals and how this can exercise attractive and repulsive forces in group formation dynamics. The two models have been combined within a computational model, where multiple *agents* could form *groups* by locating themselves on the same *patch*, and, more importantly, enhance their condition by migration and fission-fusion dynamics. The spatial relocation of each agent, a consequence of individual decision-making, undoubtedly has effects on the other agents, triggering in turn their responses.

The simulation output showed how this cascade of actions and reactions leads the system to diverge in two different types of dynamics. On the one hand, when groups were spatially isolated from each other or when the frequency of decision-making and the level of knowledge of the surrounding environment were comparatively low, the system reached an equilibrium state characterised by a dispersed pattern. On the other hand, when the opposite preconditions were true (interconnected groups with high frequency of decision-making and knowledge), the system showed continuous alternation between clumped and dispersed pattern. The simulation output has thus suggested three broad expectations: 1) that dispersed patterns can be stable; 2) that clumped patterns are instead highly unstable; and crucially 3) that *shifts between the two can occur without external forces applied to the system*.

The results of the second research question have warned against the adoption of unquestioned assumptions with respect to shifts in settlement pattern. Transitions between clumping and dispersal do not appear to necessarily require the

presence of an environmental change, and concordantly the correlation between the two phenomena does not imply the presence of a causal relationship. These conclusions suggested that the third question, that is to determine the possible role played by external forces, should be addressed in two steps.

First, existing hypotheses about the effects of environmental changes have been translated in two simple models integrated into the agent-based simulation. One explored the effect derived from a predator-prey relationship between agents and resources, while the other focused on the consequences of a decline in resource availability independent of the agent behaviour, mimicking scenarios of environmental degradation derived for instance by cooling or decrease in rainfall. The simulation output showed in most cases the same characteristics as the basic model, but in some instances (especially when the decline of resource availability was abrupt) a temporary variation in the settlement pattern was observed, in most cases emerging from the synchronic fission of multiple groups.

Second, expectations derived from the simulation model have been compared to the archaeological data in conjunction with the available records on environmental change. The long temporal scale of analysis and the broad expectations offered by the model did not allow a detailed evaluation of each transition but has instead offered a general overview of the relationship between shifts in the settlement pattern and environmental change. The most notable results were: the identification of robust markers of *transitions between clumped and dispersed pattern during intervals of relatively stable environmental conditions*; and the *failure to identify precise correspondence between the archaeologically observed pattern and the model expectations when a possible decline in resource availability might have occurred*.

Problems arising while tackling the last research question have highlighted the limits and the potential new directions of enquiries suggested by this work. The comparison between the archaeological and environmental data has first showed the limits imposed by temporal uncertainty. Although the adoption of aoristic analysis and Monte-Carlo simulation offered the opportunity to overcome many of these problems, some critical problems were still apparent. A key point of the

method applied in this thesis has been the translation of a relative chronological framework to absolute sequences, based primarily on the works of Kobayashi (2004, 2008). While the latter offered an exceptional starting point, there are a number of problems that emerge from this, namely the absence of uncertainty in the absolute chronological definition of the pottery phases. The adoption of Bayesian modelling has already showed how the definition of archaeological phases can be formally and quantitatively modelled (see Buck *et al.* 1992, Ziedler *et al.* 1998), and the marriage of these techniques with the methods presented in chapter 4 could undoubtedly offer a more robust method for integrating temporal uncertainty in the analysis of the Jōmon settlement pattern. Similarly, the recalibration of the absolute dates of older palaeoenvironmental studies, and the quantitative treatment of the uncertainty associated with these and more recent data (see for instance Hegerl *et al.* 2007, Parnell *et al.* 2008) can dramatically enhance the quantitative assessment of the correlation between archaeologically observed pattern and climate data. Again the ideal framework for conducting this kind of research is Bayesian modelling, which would allow a probabilistic assessment of the temporal relationships between archaeological and climatic events.

A second crucial aspect, which needs to be addressed in order to make a more explicit assessment of the role played by environmental change, is to build a series of formal expectations of their impact to human communities. Existing studies (section 2.4) offer broad qualitative expectations, which can be translated to abstract models but are heavily limited if more realistic models are sought. An increasing number of studies, where the modelling aspects focused on the high-quality reconstruction of palaeoenvironment, have achieved some interesting results in this regard showing the great potential of these multidisciplinary works (see for instance Axtell *et al.* 2002, Kohler *et al.* 2007).

As discussed in chapter 5, simulation models can be broadly classified in three types depending on its primary purpose (Mithen 1994, Lake 2010). The agent-based model presented in this thesis was explicitly designed as a *theory-building* tool, apt for formally examining the consequences of our models when our param-

eterised assumptions are changed. The necessary processes of simplification and abstraction made, however, made the model inappropriate for formal hypothesis-testing. This is the main reason why the third research question was tackled by suggesting broad suggestions of possible scenarios, rather than conclusive and definitive answers on how specific transitions occurred. While the exploration of the parameter space and the integration of alternative assumptions and models must be carried on, the next stage of this research should be the creation of models capable of generating explicit and, more importantly, *testable* hypotheses. This will require more realistic spatio-temporal references (e.g. the simulation should proceed by time-steps comparable to the real world, such as single seasons or years), a precise definition of the initial conditions of the simulation runs, and the integration of a higher number of variables (e.g. different types of resources), including those related more directly to the formation of the archaeological record (e.g. taphonomic processes). Such a model will clearly become more complex, and will need to sacrifice its heuristic power (e.g. the exploration range of the parameter space will most likely be reduced) for enabling a sufficient level of realism in its output. The fine-tuning between realism and explanatory power is undoubtedly the biggest challenge in this endeavour as in any other application of formal and quantitative models in archaeology. One solution might be the creation of "middle-range" models, where specific behavioural responses (inferred from existing abstract models or ethnographic analogies) are imposed —rather than being generated through some form of emergence—, purely in order to establish their expectation in the archaeological record. This will leave to the abstract models the burden to answer *why something happened* (e.g. why a synchronic fission of large groups could occur in the system?) and leave space for a different model designed to answer *what happened* (e.g. is the observed pattern the result of the synchronic fission of large groups?).

Adopting such a solution will be best pursued if we go back to the detailed analysis of single transitions in settlement pattern, perhaps one of those identified in this thesis. The ideal candidate for such an endeavour could be the interval be-

tween the second half of the Middle Jōmon and the first half of the Late Jōmon. The analysis of the archaeological record from Chiba and Gunma had shown that the first few centuries of this time span (from ca. 5000 to 4500 cal BP) were characterised by profound transformations in the settlement pattern, despite a palaeoenvironmental record suggesting relatively stable conditions. This offers an ideal laboratory for determining how endogenous processes can induce changes between a clumped and dispersed pattern, perhaps by building a *hypothesis-testing* model from the foundations outlined by the computer simulation proposed in this thesis. The second half of this interval offers instead an excellent opportunity to investigate the effects derived from the environmental changes of the mid-5th millennium cal BP. This stage is characterised by a sharp decline in the number of residential units, observed also in other regions of central Japan (Imamura 2010, Crema 2012), and several authors (Koyama and Sugito 1984, Imamura 1999a) have suggested how this could have been caused by changed environmental conditions. It is unquestionable that this period offers an invaluable context for exploring the cultural responses of Jōmon hunter-gatherers to climate change.

The analysis of the empirical data presented in this thesis showed how the adoption of quantitative and statistical methods can set the ground for these and other venues of future research on Jōmon culture. At the same, the relevance of the patterns identified in the archaeological record goes beyond the field of Japanese prehistory and can contribute to worldwide debates on hunter-gatherer adaptation. By combining these results with the theoretical framework offered by the agent-based simulation, I believe this thesis has build new building blocks for enquiries on human settlement.

Bibliography

Adams, J., Maslin, M. and Thomas, E., 1999. Sudden climate transitions during the Quaternary. *Progress in Physical Geography*, 23, 1–36.

Adhikari, D. P., Kumon, F. and Kawajiri, K., 2002. Holocene climate variability as deduced from the organic carbon and diatom records in the sediments of Lake Aoki, central Japan. *Journal of the Geological Society of Japan*, 108, 249–265.

Agar, M., 2003. My Kingdom for a Function: Modeling Misadventures of the Innumerate. *Journal of Artificial Societies and Social Simulations*, 6, URL: `http://jasss.soc.surrey.ac.uk/6/3/8.html` (last retrieved on 27th July 2012).

Agarwal, H., Renaud, J. E., Preston, E. L. and Padmanabhan, D., 2004. Uncertainty quantication using evidence theory in multidisciplinary design optimization. *Reliability Engineering and System Safety*, 85, 281–294.

Aikens, C. M., 1981. The Last 10,000 years in Japan an Eastern North America: Parallels in Environment, Economic Adaptation, Growth of Social Complexity and the Adoption of Agriculture. In: S. Koyama and D. H. Thomas (eds.), *Affluent Foragers: Pacific Coasts East and West*, Osaka: Senri National Museum of Ethnology, 261–273.

Aikens, C. M., Ames, K. M. and Sanger, D., 1986. Affluent collectors at the edges of Eurasia and North America: Some comparisons and observations on the evolution of society among north-temperate coastal hunter-gatherers. In: T. Akazawa and C. M. Aikens (eds.), *Prehistoric Hunter-Gatherers in Japan: New Research Methods*, Tokyo: University of Tokyo, volume 27, 3–26.

Aikens, C. M. and Dumond, D. E., 1986. Convergence and Common Heritage: Some Parallels in the Archaeology of Japan and Western North America. In: R. J. Pearson; G. L. Barnes and K. L. Hutterer (eds.), *Windows on the Japanese Past: Studies in Archaeology and Prehistory*, Ann Arbor: Centre for Japanese Studies University of Michigan, 163–178.

Aizawa, S., 1990. Kazanbai no fudo. In: Gunmakenshi Hensan Shuiinkai (ed.), *Gunmakenshi Tsushihen 1 Genshikodai 1*, Maebashi: Gunmaken, 42–59.

Akayama, Y., 1990. Jomonjidai no shurakukouzou. In: Gunmakenshi Hensan Shuiinkai (ed.), *Gunmakenshi Tsushihen 1 Genshikodai 1*, Maebashi: Gunmaken.

Akazawa, T., 1986. Hunter-gatherer adaptations and the transition to food production in Japan. In: M. Zvelebil (ed.), *Hunters in transition: Mesolithic societies of temperate Eurasia ad their transition to farming*, Cambridge: Cambridge University Press, 151–165.

Aldenderfer, M. S., 1981. Computer Simulation for Archaeology: An Introductory Essay. In: J. A. Sabloff (ed.), *Simulations in archaeology*, Albuquerque: University of New Mexico Press, 11–49.

Allee, W., 1951. *The social life of animals*. Boston: Beacon Press.

Anderson, D. G., Maasch, K. A., Sandweiss, D. H. and Mayewki, P. A., 2007. Climate and cultural change: exploring Holocene transitions. In: D. G. Anderson; K. A. Maasch and D. H. Sandweiss (eds.), *Climate Change and Cultural Dynamics: a Global perspective on Mid-Holocene Transitions*, London: Academic Press, 1–24.

Anzai, M. (ed.), 2002a. *Jomonshakairon (ge)*. Tokyo: Douseisha.

Anzai, M. (ed.), 2002b. *Jomonshakairon (jo)*. Tokyo: Douseisha.

Aonuma, M., 1990. Chibashiiki no jomonjidaichukikohaniseki no bunpu to ricchi. Tokyowan engan ni okeru jomonchukishyumatsuki shurakukenkyu no shishin. *Kaizukahakubutsukankiyo*, 17, 42–71.

Aonuma, M., Tateishi, T., Furutani, W. and Morimoto, T., 2001. Chibashijomonjidaiichuki isekishitsudo kokuyouseki no gensanchisuitei. *Kaizukahakubutsukankiyo*, 28, 42–71.

Arnold, J., 1996. Archaeology of Complex Hunter-Gatherers. *Journal of Archaeological Method and Theory*, 3, 77–126.

Arthur, W. B., 1988. Urban Systems and Historical Path-Dependence. In: J. Ausubel and R. Herman (eds.), *Urban systems and Infrastructure*, Washington: National Academy of Sciences, 85–97.

Aureli, F., Schaffner, C. M., Boesch, C., K.Bearder, S., Call, J., Chapman, C. A., Connor, R., Fiore, A. D., Dunbar, R. I. M., Henzi, S. P., Holekamp, K., Korstjens, A. H., Layton, R., Lee, P., Lehmann, J., H.Manson, J., Ramos-Fernandez, G., Strier, K. B. and van Schaik, C. P., 2008. Fission-Fusion Dynamics: New Research Frameworks. *Current Anthropology*, 49, 627–654.

Axtell, R. L., Epstein, J. M., Dean, J. S., Gumerman, G. J., Swedlund, A. C., Harburger, J., Chakravarty, S., Hammond, R., Parker, J. and Parker, M., 2002. Population growth and collapse in a multiagent model of the Kayenta Anasazi in Long House Valley. *Proceedings of the National Academy of Sciences*, 99, 7275–7279.

Baddeley, A. and Lieshout, M. v., 1995. Area-Interaction Point Processes. *Annals of the Institute of Statistical Mathematics*, 47, 601–619.

Bailey, G., 1983. Concepts of Time in Quaternary Prehistory. *Annual Review of Anthropology*, 12, 165–192.

Bailey, T. and Gatrell, T., 1995. *Interactive Spatial Data Analysis*. Harlow: Longman.

Banks, W. E., d'Errico, F., Peterson, A. T., Vanhaeren, M., Kageyama, M., Sepulchre, P., Ramstein, G., Jost, A. and Lunt, D., 2008. Human ecological niches and ranges during the LGM in Europe derived from an application of eco-cultural niche modeling. *Journal of Archaeological Science*, 35, 481–491.

Batty, M., 2006. Rank clocks. *Nature*, 592–596.

Bedau, M. A. and Humphreys, P. (eds.), 2008. *Emergence: Contemporary Readings in Philosophy and Science*. London: MIT Press.

Bentley, A., Ormerod, P. and Batty, M., 2008. Evolution and turnover in scaling systems. *CASA Working Paper Series*, 135, 1–6.

Bentley, R. A., Lake, M. W. and Shennan, S. J., 2005. Specialisation and wealth inequality in a model of a clustered economic network. *Journal of Archaeological Science*, 32, 1346–1356.

Bentley, R. A., Ormerod, P. and Batty, M., 2009. An evolutionary model of long tailed distributions in the social sciences. *arXiv: [physics:soc-ph]*, 0903.2533v1, URL: `http://arxiv.org/abs/0903.2533` (last retrieved on 27th July 2012).

Bettinger, R. L. and Baumhoff, M. A., 1982. The Numic Spread: Great Basin Cultures in Competition. *American Antiquity*, 47, 485–503.

Bettinger, R. L. and Eerkens, J., 1999. Point Typologies, Cultural Transmission, and the Spread of Bow-and-Arrow Technology in the Prehistoric Great Basin. *American Antiquity*, 64, 231–242.

Bevan, A. and Connolly, J., 2006. Multiscalar Approaches to Settlement Pattern Analysis. In: G. Lock and B. Molyneaux (eds.), *Confronting Scale in Archaeology: Issues of Theory and Practice*, New York: Springer, 217–234.

Bevan, A. and Conolly, J., 2009. Modelling spatial heterogeneity and nonstationarity in artifact-rich landscapes. *Journal of Archaeological Science*, 36, 956–964.

Bevan, A., Conolly, J., Hennig, C., Johnston, A., Quercia, A., Spencer, L. and Vroom, J., in press. Measuring Chronological Uncertainty in Intensive Survey Finds. *Archaeometry*.

Bevan, A., Crema, E., Li, X. and Palmisano, A., under review. Intensities, Interactions and Uncertainties: Some New Approaches to Archaeological Distributions. In: A. Bevan and M. Lake (eds.), *Computational Approaches to Archaeological Space*.

Binford, L., 1977. General Introduction. In: L. Binford (ed.), *For Theory Building in Archaeology*, New York: Academic Press, 1–13.

Binford, L. R., 1964. A Consideration of Archaeological Research Design. *American Antiquity*, 29, 425–441.

Binford, L. R., 1980. Willow Smoke and Dogs' Tails: Hunter-Gatherer Settlement Systems and Archaeological Site Formation. *American Antiquity*, 45, 4–20.

Binford, L. R., 2001. *Constructing Frames of Reference: An Analytical Method for Archaeological Theory Building Using Ethnographic and Environmental Data Sets*. Berkeley and Los Angeles: University of California Press.

Bleed, P. and Matsui, A., 2010. Why Didn't Agriculture Develop in Japan? A Consideration of Jomon Ecological Style, Niche Construction, and the Origins of Domestication. *Journal of Archaeological Method and Theory*, 17, 356–370.

Bond, G., Showers, W., Cheseby, M., Lotti, R., Almasi, P., deMenocal, P., Priore, P., Cullen, H., Hajdas, I. and Bonani, G., 1997. A Pervasive Millennial-Scale Cycle in North Atlantic Holocene and Glacial Climates. *Science*, 287, 1257–1266.

Bonini, C. P., 1963. *Simulation of Information and Decision Systems in the Firm*. Englewood Cliffs, N.J.: Prentice-Hall.

Bonner, J., 2004. Perspective: The Size-Complexity Rule. *Evolution*, 58, 1883–1890.

Boone, J. L., 1992. Competition, Conflict, and The Development of Social Hierarchies. In: E. Smith and B. Winterhalder (eds.), *Evolutionary Ecology and Human Behaviour*, New York: Aldine de Gruyter, 301–337.

Box, G. E. P. and Jenkins, G., 1976. *Time Series Analysis: Forecasting and Control (Rev.Ed.)*. London: McGraw-Hill.

Boyd, R. and Richerson, P. J., 1985. *Culture and the Evolutionary Process*. Chicago: University of Chicago Press.

Boyd, R. and Richerson, P. J., 1992. How Microevolutionary Processes Give Rise to History. In: M. Niteki and D. Niteki (eds.), *Evolution and History*, Albany: State University of New York Press, 149–178.

Brantingham, P. J., Surovell, T. A. and Waguespack, N. M., 2007. Modeling post-depositional mixing of archaeological deposits. *Journal of Anthropological Archaeology*, 26, 517–540.

Broughton, J. M., Cannon, M. D. and Bartelink, E. J., 2010. Evolutionary Ecology, Resource Depression, and Niche Construction Theory: Applications to Central California Hunter-Gatherers and Mimbres-Mogollon Agriculturalists. *Journal of Archaeological Method and Theory*, 17, 371421.

Buck, C., Litton, C. and Smith, A., 1992. Calibration of Radiocarbon Results Pertaining to Related Archaeological Events. *Journal of Archaeological Science*, 19, 497–512.

Buck, C. and Millard, A. (eds.), 2003. *Tools for Constructing Chronologies: Crossing Disciplinary Boundaries.* London: Springer Verlag.

Buck, C. E., Cavanagh, W. G. and Litton, C. D., 1996. *Bayesian approach to interpreting archaeological data*. Chirchester: Wiley.

Buck, C. E., Higham, T. F. and Lowe, D. J., 2003. Bayesian tools for tephrochronology. *The Holocene*, 13, 639–647.

Bura, S., Guerin-Pace, F., Mathian, H., Pumain, D. and Sander, L., 1995. Cities can be agents too: a model for the evolution of settlement systems. In: N. Gilbert and R. Conte (eds.), *Artificial Societies: The Computer Simulation of Social Life*, London: UCL Press, 72–85.

Butzer, K., 1982. *Archaeology as human ecology : method and theory for a contextual approach*. Cambridge: Cambridge University Press.

Carneiro, R. L., 1970. A Theory of the Origin of the State. *Science*, 169, 733738.

Cashdan, E., 1992. Spatial organization and habitat use. In: E. Smith and B. Winterhalder (eds.), *Evolutionary Ecology and Human Behaviour*, New York: Aldine de Gruyter, 237–266.

Cavalli-Sforza, L. L. and Feldman, M. W., 1981. *Cultural Transmission and Evolution: A Quantitative Approach*. Princeton University Press.

Chadwick, A. J., 1978. A computer simulation of Mycenean settlement. In: I. Hodder (ed.), *Simulation studies in archaeology*, Cambridge: Cambridge Univerisity Press, 47–57.

Chatters, J. C. and Prentiss, W. C., 2005. A Darwinian macro-evolutionary perspective on the development of hunter-gatherer systems in Northwestern North America. *World Archaeology*, 37, 46–65.

Chino, Y., 1991. Jomonjidai ni nijirin ha attaka: isekishutsudo no shokubutsuseiibutsu kara no kento. *Tokyotobunkazaisentaa Kenkyuronshu*, 10, 215–249.

Clark, C. W. and Mangel, M., 1984. Foraging and Flocking Strategies: Information in an Uncertain Environment. *The American Naturalist*, 123, 626–641.

Clark, C. W. and Mangel, M., 1986. The Evolutionary Advantages of Group Foraging. *Theoretical Population Biology*, 30, 45–75.

Clark, P. J. and Evans, F. C., 1954. Distance to nearest neighbour as a measure of spatial relationships in populations. *Ecology*, 35, 445–453.

Clarke, D., 1973. Archaeology: the loss of innocence. *Antiquity*, 47, 6–18.

Cohen, M. N., 1981. Pacific Coast Foragers: Affluent or Overcrowded? In: S. Koyama and D. H. Thomas (eds.), *Affluent Foragers: Pacific Coasts East and West*, Osaka: Senri National Museum of Ethnology, 275–295.

Collins, S. L., Suding, K. N., Cleland, E. E., Batty, M., Pennings, S. C., Gross, K. L., Grace, J. B., Gough, L., Fargione, J. E. and Clark, C. M., 2008. Rank Clocks and Plant Community Dynamics. *Ecology*, 89, 3534–3541.

Conolly, J., College, S. and Shennan, S., 2008. Founder effect, drift, and adaptive change in domestic crop use in early Neolithic Europe. *Journal of Archaeological Science*, 35, 2797–2804.

Conolly, J. and Lake, M., 2006. *Geographical information systems in archaeology*. Cambridge: Cambridge University Press.

Costopoulos, A., 2001. Evaluating the impact of increasing memory on agent behaviour: Adaptive patterns in an agent based simulation of subsistence. *Journal of Artificial Societies and Social Simulations*, 4, URL: `http://jasss.soc.surrey.ac.uk/4/4/7.html` (last retrieved on 27th July 2012).

Cowpertwait, P. S. and Metcalfe, A. V., 2009. *Introductory Time Series with R*. Use R! London: Springer.

Crawford, G. W., 1983. *Paleoethnobotany of the Kameda peninsula Jomon*. Ann Arbor, Michigan: Museum of Anthropology, University of Michigan.

Crawford, G. W., 2008. The Jomon in early agriculture discourse: issues arising from Matsui, Kanehara and Pearson. *World Archaeology*, 40, 445–465.

Crawford, G. W., 2011. Advances in Understanding Early Agriculture in Japan. *Current Anthropology*, 52, S331–S345.

Crema, E. R., 2012. Modelling Temporal Uncertainty in Archaeological Analysis. *Journal of Archaeological Method and Theory*, 19, 440–461.

Crema, E. R., Bevan, A. and Lake, M., 2010. A probabilistic framework for assessing spatio-temporal point patterns in the archaeological record. *Journal of Archaeological Science*, 37, 1118–1130.

Crema, E. R. and Nishino, M., 2012. Spatio-Temporal Distributions of Middle to Late Jomon Pithouses in Oyumino, Chiba (Japan). *Journal of Open Archaeology Data*, 1, URL `http://dx.doi.org/10.5334/4f8eb4078284b` (last retrieved on 27th July 2012).

Currie, T. and Mace, R., 2011. Mode and tempo in the evolution of socio-political organization: reconciling 'Darwinian' and 'Spencerian' evolutionary approaches in anthropology. *Philosophical Transactions of the Royal Society B*, 366, 1108–1117.

Daikuhara, Y., 2002. Kokuyouseki no ryutsuu wo meguru shakai. In: M. Anzai (ed.), *Jomonshakairon (jo)*, Tokyo: Douseisha, 67–131.

Davis, M. B. and Botkin, D. B., 1985. Sensitivity of Cool-Temperate Forests and Their Fossil Pollen Record to Rapid Temperature Change. *Quaternary Research*, 23, 327–340.

Dawkins, R., 1982. *The Extended Phenotype*. Oxford: Oxford University Press.

De Wit, A., Bruin, S. D. and Torfs, P., 2008. Representing Uncertainty in Continental-Scale Gridded Precipitation Fields for Agrometeorological Modeling. *Journal of Hydrometerology*, 9, 1172–1190.

Dean, J. S., 1978. Independent Dating in Archaeological Analysis. *Advances in Archaeological Method and Theory*, 1, 223–255.

Dean, J. S., Gumerman, G. J., Epstein, J. M., Axtell, R. L., Swedlund, A. C., Parker, M. T. and McCaroll, S., 2000. Understanding Anasazi Culture Change Through Agent Base Modeling. In: T. A. Kohler and G. J. Gumerman (eds.), *Dynamics in Human and Primate Societies: Agent Based Modeling of Social and Spatial Processes*, Oxford: Oxford University Press, 179–205.

deMenocal, P. B., 2001. Cultural Responses to Climate Change During the Late Holocene. *Science*, 292, 667–673.

Deravignone, L. and Janica, G. M., 2006. Artificial Neural Networks in archaeology. *Archeologia e Calcolatori*, 17, 121–136.

Dessalles, J. L., Müller, J. P. and Phan, D., 2007. Emergence in Multi-agent Systems: Conceptual and Methodological Issues. In: D. Phan and F. Amblard (eds.), *Agent-Based Modelling and Simulation in Social and Human Sciences*, Oxford: The Bardwell Press, 327–355.

Dewar, R. E., 1991. Incorporating Variation in Occupation Span into Settlement-Pattern Analysis. *American Antiquity*, 56, 604–620.

Dewar, R. E. and McBride, K. A., 1992. Remnant Settlement Patterns. In: J. Rossignol and L. Wandsnider (eds.), *Space, time, and archaeological landscapes*, New York: Plenum Press, 257–282.

Dobney, K., Ervynck, A. and Albarella, U., 2007. The transition from wild boar to domestic pig in Eurasia, illustrated by a tooth developmental defect and biometrical data. In: U. Albarella; K. Dobney; A. Ervynck and P. Rowley-Conwy (eds.), *Pigs and Humans 10,000 years of Interaction*, Oxford: Oxford University Press, 57–82.

Doi, Y., 1991. 1990nen noJomonjidai gakki doko: Shuraku Ryoikiron. *Jomonjidai*, 2, 216–218.

Doran, J. and Gilbert, N., 1994. Simulating societies: an introduction. In: N. Gilbert and J. Doran (eds.), *Simulating societies: The computer simulation of social phenomena*, London: UCL press, 1–18.

Doran, J., Palmer, M., Gilbert, N. and Mellars, P., 1995. The EOS project: modelling Upper Palaeolithic social change. In: N. Gilbert and J. Doran (eds.), *Simulating societies: The computer simulation of social phenomena*, London: UCL Press, 195–221.

Drennan, R. D. and Peterson, C. E., 2004. Comparing archaeological settlement systems with rank-size graphs: a measure of shape and statistical confidence. *Journal of Archaeological Science*, 31, 533–549.

Drucker, P., 1951. *The Northern and Central Northern Tribes*. Washington: Bureau of American Ethnology Bulletin 144, Smithsonian Institute.

Dunbar, R. I. M., 1993. Coevolution of neocortical size, group size and language in humans. *Behavioral and Brain Sciences*, 16, 681–735.

Dunnell, R., 1971. *Systematics in prehistory*. New York: Free Press.

Dunnell, R., 1992. The Notion Site. In: J. Rossignol and L. Wandsnider (eds.), *Space, time, and archaeological landscape*, New York: Plenum Press, 21–41.

Dwyler, P. D. and Minnegal, M., 1985. Andaman Islanders, Pygmies, and an Extension of Horn's Model. *Human Ecology*, 13, 111–119.

Ebert, J. E., 1992. *Distributional Archaeology*. Albuquerque: University of New Mexico Press.

Eerkens, J. and Lipo, C., 2005. Cultural transmission, copying errors, and the generation of variation in material culture and the archaeological record. *Journal of Anthropological Archaeology*, 24, 316–334.

Eerkens, J. W., Bettinger, R. L. and McElreath, R., 2005. Cultural transmission, phylogenetics, and the archaeological record. In: C. P. Lipo; M. O'Brien; M. Collard and S. J. Shennan (eds.), *Mapping Our Ancestors: Phylogenic Methods in Anthropology and Prehistory*, Somerset: Transaction Publishers, 169–183.

Efferson, C., Lalive, R., Richerson, P. J. and McElreath, R., 2008. Conformists and mavericks: the empirics of frequency-dependent cultural transmission. *Evolution and Human Behavior*, 29, 56–64.

Epstein, J., 1996. *Growing Artificial Societies: Social Science From the Bottom Up*. London: MIT Press.

Epstein, J. (ed.), 2007. *Generative Social Science: Studies in Agent-Based Computational Modeling*. Princeton: Princeton University Press.

Epstein, J. M., 2008. Why Model? *Journal of Artificial Societies and Social Simulations*, 11, URL: `http://jasss.soc.surrey.ac.uk/11/4/12.html` (last retrieved on 27th July 2012).

Eriksson, K., Enquist, M. and Ghirlanda, S., 2007. Critical points in current theory of conformist social learning. *Journal of Evolutionary Psychology*, 5, 67–87.

Ester, M., Kriegel, H.-P., Sander, J. and Xu, X., 2009. A Density-Based Algorithm for Discovering Clusters in Large Spatial Databases with Noise. In: E. Simoudis; J. Han and U. M. Fayyad (eds.), *Proceedings of 2nd International Conference on Knowledge Discovery and Data Mining (KDD-96)*, Portland: AAAI Press, 226–231.

Evans, T., Knappett, C. and Rivers, R., 2009. Using Statistical Physics to Understand Relational Space: A Case Study from Mediterranean Prehistory. In: D. Lane; D. Pumain; S. E. van der Leeuw and G. West (eds.), *Complexity Perspectives in Innovation and Social Change*, Berlin: Springer, 451–479.

Fagan, B., 1999. *Floods, Famines, and Emperors: El Nino and the Fate of Civilizations*. New York: Basic Books.

Fagen, R., 1987. A generalized habitat matching rule. *Evolutionary Ecology*, 1, 5–10.

Falconer, S. E. and Savage, S. H., 1995. Heartlands and Hinterlands: Alternative Trajectories of Early Urbanization in Mesopotamia and the Southern Levant. *American Antiquity*, 60, 37–58.

Farina, A. and Belgrano, A., 2004. The eco-field: A new paradigm for landscape ecology. *Ecological Research*, 19, 107–110.

Fitzhugh, B., 2003. *The Evolution of Complex Hunter-Gatherers: Archaeological Evidence from the North Pacific*. New York: Kluwer.

Fletcher, R., 1981. People and space: a case study on material behaviour. In: I. Hodder; G. Isaac and N. Hammond (eds.), *Pattern of the past: Studies in honour of avid Clarke*, Cambridge: Cambridge University Press, 97–128.

Fletcher, R., 1995. *The Limits of Settlement Growth: a theoretical outline*. Cambridge: Cambridge University Press.

Foley, R., 1981. A model of regional archaeological structure. *Proceedings of the Prehistoric Society*, 47, 1–17.

Fortin, M.-J. and Dale, M., 2005. *Spatial Analysis: A Guide for Ecologists*. Cambridge: Cambridge University Press.

Fretwell, S. and Lucas, H., 1970. On territorial behaviour and other factors influencing habitat distribution in birds. *Acta Biotheoretica*, 19, 16–36.

Fukusawa, H., Yamada, K. and Kato, M., 1999. High-Resolution Reconstruction of Paleoenvironmental Changes by Using Varved Lake Sediments and Loess-Paleosik Sequences in East Asia Japan. *Kokuritsu RekishiMinzokuHakbutsukan KenkyuHoukoku*, 81, 463–481.

Gibson, J. G., 1977. The Theory of Affordances. In: R. Shaw and J. Bransford (eds.), *Perceiving, Acting, and Knowing*, Hillsdale: Erlbaum, 67–82.

Gimblett, H. R. (ed.), 2002. *Integrating Geographic Information Systems and Agent-based Modeling Techniques for Simulating Social and Ecological Processes*. Oxford: Oxford University Press.

Giraldeau, L.-A. and Caraco, T., 1993. Genetic relatedness and group size in an aggregation economy. *Evolutionary Ecology*, 7, 429–438.

Giraldeau, L.-A. and Caraco, T., 2000. *Social Foraging Theory*. Princeton: Princeton University Press.

Giraldeau, L.-A. and Gillis, D., 1984. Optimal Group Size Can Be Stable: A Reply to Sibly. *Animal Behaviour*, 33, 666–667.

Gould, P., 1970. Is statistix inferens the geographical name for a wild goose? *Economic Geography*, 46, 439–448.

Gould, R. A. and Yellen, J. E., 1987. Man the Hunterd: Determinants of Household Spacing in Desert and Tropical Foraging Societies. *Journal of Anthropological Archaeology*, 6, 77–103.

Green, C., 2011. *Winding Dali's clock : the construction of a fuzzy temporal-GIS for archaeology*. Oxford: Archaeopress.

Greene, C. M. and Stamps, J. A., 2001. Habitat Selection at low population densities. *Ecology*, 82, 2091–2100.

Gregg, S. A., Kintigh, K. W. and Whallon, R., 1991. Linking Ethnoarchaeological Interpretation and Archaeological Data: The Sensitivity of Spatial Analytical Methods to Postdepositional Disturbance. In: E. M. Kroll and T. D. Price (eds.), *The Interpretation of Archaeological Spatial Patterning*, New York: Plenum Press, 149–196.

Griffin, A. F., 2011. Emergence of fusion/fission cycling and self-organized criticality from a simulation model of early complex polities. *Journal of Archaeological Science*, 38, 873–883.

Griffin, A. F. and Stanish, C., 2007. An Agent-based Model of Prehistoric Settlement Patterns and Political Consolidation in the Lake Titicaca Basin of Peru and Bolivia. *Structure and Dynamics: eJournal of Anthropological and Related Sciences*, 2, URL: `http://escholarship.org/uc/item/2zd1t887` (last retrieved on 27th July 2012).

Grimm, V., Berger, U., Bastiansen, F., Eliassen, S., Ginot, V., Giske, J., Goss-Custard, J., Grand, T., Heinz, S. K., Huse, G., Huth, A., Jepsen, J. U., Jrgensen, C., Mooij, W. M., ller, B. M., Peer, G., Piou, C., Railsback, S. F., Robbins, A. M., Robbins, M. M., Rossmanith, E., ger, N. R., Strand, E., Souissi, S., Stillman, R. A., Vab, R., Visser, U. and DeAngelis, D. L., 2006. A standard protocol for describing individual-based and agent-based models. *Ecological Modelling*, 198, 115–126.

Grimm, V., Berger, U., DeAngelis, D. L., Polhill, J. G., Giske, J. and Railsback, S. F., 2010. The ODD protocol: A review and first update. *Ecological Modelling*, 221, 2760–2768.

Grove, M., 2011. A Spatio-Temporal Kernel Method for Mapping Change in Prehistoric Land-Use Patterns. *Archaeometry*, 53, 1012–1030.

Gueron, S. and Levin, S. A., 1995. The Dynamics of Group Formation. *Mathematical Biosciences*, 128, 243–264.

Haag, G., 1994. The Rank-Size Distribution of Settlements as a Dynamic Multifractal Phenomenon. *Chaos, Solitons and Fractals*, 4, 519–534.

Habu, J., 1988. Number of Pit Dwellings in Early Jomon Moroiso Stage Sites. *The Journal of the Anthropological Society of Nippon*, 96, 147–165.

Habu, J., 2001. *Subsistence-Settlment Systems and Intersite Variability in the Moroiso Phase of the Early Jomon Period of Japan*. International Monographs in Prehistory. Ann Arbor: International Monographs in Prehistory.

Habu, J., 2002. Jomon Collectors and Foragers: Regional Interactions and Long-term Changes in Settlement Systems among Prehistoric Hunter-Gatherers in Japan. In: B. Fitzhugh and J. Habu (eds.), *Beyond Foraging and Collecting: Evolutionary Change in Hunter-Gatherer Settlement Systems*, New York: Kluwer Academic/Plenum Publishers, 53–72.

Habu, J., 2004. *Ancient Jomon of Japan*. Cambridge: University of Cambridge Press.

Habu, J., 2008. Growth and decline in complex hunter-gatherer societies: a case study from the Jomon period Sannai Maruyama site, Japan. *Antiquity*, 82, 571–584.

Habu, J., Matsui, A., Yamamoto, N. and Kanno, T., 2011. Shell midden archaeology in Japan: Aquatic food acquisition and long-term change in the Jomon culture. *Quaternary International*, 239, 19–27.

Halley, J. M., 1996. Ecology, evolution and 1/f-noise. *TREE*, 11, 33–37.

Halstead, P. and O'Shea, J., 1989. Introduction: cultural responses to risk and uncertainty. In: P. Halstead and J. O'Shea (eds.), *Bad year economics: Cultural responses to risk and uncertainty*, Cambridge: Cambridge University Press, 1–7.

Hamilton, I. M., 2000. Recruiters and Joiners: Using Optimal Skew Theory to Predict Group Size and the Division of Resources within Groups of Social Foragers. *The American Naturalist*, 155, 684–695.

Hamilton, M. J., Milne, B. T., Walker, R. S. and Brown, J. H., 2007. Nonlinear scaling of space use in human hunter gatherers. *Proceedings of the National Academy of Sciences*, 104, 4765–4769.

Han, X., Hui, C. and Zhang, Y., 2009. Effects of time-lagged niche construction on metapopulation dynamics and environmental heterogeneity. *Applied Mathematics and Computation*, 215, 449–458.

Hardin, G., 1968. The Tragedy of Commons. *Science*, 162, 1243–1248.

Harpending, H. and Davis, H., 1977. Some Implications for Hunter-Gatherer Ecology Derived from the Spatial Structure of Resources. *World Archaeology*, 8, 275–286.

Harunari, H., 1986. Rules of residence in the Jomon period, based on the analysis of tooth extraction. In: R. J. Pearson; G. L. Barnes and K. L. Hutterer (eds.), *Windows on the Japanese Past: Studies in Archaeology and Prehistory*, Ann Arbor: Centre for Japanese Studies University of Michigan, 293–310.

Harunari, H., Fujio, S., Imamura, M. and Sakamoto, M., 2003. Yayoi jidai no kaishi nendai: C14 nendai no sokutei kekka ni tsuite. In: Nihon KoukogakuKyokai (ed.), *Nihon Koukogaku Kyokai dai 68 kai Sokai Kenkyu Happyo Yoshi*, Tokyo: NihonKokogakuKyokai, 65–68.

Hastings, A., 1997. *Population biology : concepts and models*. London: Springer.

Hawkes, K., 1992. Sharing and Collective Action. In: E. Smith and B. Winterhalder (eds.), *Evolutionary Ecology and Human Behaviour*, New York: Aldine de Gruyter, 269–300.

Hayashi, K., 2001. *Jomonshakai no Kokogaku*. Tokyo: Douseisha.

Hegerl, G. C., Crowley, T. J., Allen, M., Hyde, W. T., Pollack, H. N., Smerdon, J. and Zorita, E., 2007. Detection of Human Influence on a New, Validated 1500-Year Temperature Reconstruction. *Journal of Climate*, 20, 650–666.

Hennig, C., 2010. *fpc: Flexible procedures for clustering*. URL `http://CRAN.R-project.org/package=fpc`. R package version 2.0-3.

Henrich, J., 2001. Cultural Transmission and the Diffusion of Innovations: Adoption Dynamics Indicate That Biased Cultural Transmission Is the Predominate Force in Behavioral Change. *American Anthropologist*, 103, 992–1013.

Henrich, J. and Gil-White, F. J., 2001. The evolution of prestige Freely conferred deference as a mechanism for enhaning the benefits of cultural transmission. *Evolution and Human Behavior*, 22, 165–196.

Henrich, J. and McElreath, R., 2003. The evolution of cultural evolution. *Evolutionary Anthropology*, 12, 123–135.

Hewlett, B. S. and Cavalli-Sforza, L., 1986. Cultural Transmission among Aka Pygmies. *American Anthropologist*, 88, 922–934.

Hijmans, R. J., Cameron, S. E., Parra, J. L., Jones, P. G. and Jarvis, A., 2005. Very high resolution interpolated climate surfaces for global land areas. *International Journal of Climatology*, 25, 1965–1978.

Hill, K. and Hawkes, K., 1987. Neotropical Hunting among the Ach of Eastern Paraguay. In: R. B. Hames and W. T. Vickers (eds.), *Adaptive Responses of Native Amazonians*, New York: Academic Press, 139–188.

Hodder, I. and Okell, E., 1978. An Index for assessing the association between distributions of points in archaeology. In: I. Hodder (ed.), *Simulation studies in Archaeology*, London: Cambdrige University Press, 97–107.

Holdaway, S. and Wandsnider, L. (eds.), 2008. *Time in archaeology : time perspectivism revisited*. Salt Lake City: University of Utah Press.

Holling, C., 2001. Understanding the Complexity of Economic, Ecological, and Social Systems. *Ecosystems*, 4, 390–405.

Holling, C. S., 1996. Engineering resilience versus ecological resilience. In: P. C. Schulze (ed.), *Engineering within ecological constraints*, Washington, D.C.: National Academy Press, 31–44.

Hongo, H., Anezaki, T., Yamazaki, K., Takahashi, O. and Sugawara, H., 2007. Hunting or management? The status of Sus in the Jomon period in Japan. In: U. Albarella; K. Dobney; A. Ervynck and P. Rowley-Conwy (eds.), *Pigs and Humans 10,000 years of Interaction*, Oxford: Oxford University Press, 109–130.

Horikoshi, M., 1992. Zenkoku no Kaizukabunpu to chiiki no kaizukagun. *Kikan Kokogaku*, 41, 35–40.

Horn, H. S., 1968. The Adaptive Signficance of Colonial Nesting in the Brewer's Blackbird (Euphagus Cyanocephalus). *Ecology*, 49, 682–694.

Hui, C., Li, Z. and Yue, D.-x., 2004. Metapopulation dynamics and distribution, and environmental heterogeneity induced by niche construction. *Ecological Modelling*, 177, 107–118.

Ikawa-Smith, F., 1992. Kanjodori: Communal cemeteries of the Late Jomon Hokkaido. In: C. M. Aikens and S. N. Rhee (eds.), *Pacific Northeast Asia in Prehistory: Hunter-Fisher-Gatherers, Farmers, and Sociopolitical Elites*, Pullman: Washington State University Press, 83–90.

Illian, J., Penttinen, A., Stoyan, H. and Stoyan, D., 2008. *Statistical Analysis and Modelling of Spatial Point Patterns*. Statistics in Practice. Chirchester: Wiley.

Imamura, K., 1983. Otoshiana. In: S. Kato; T. Kobayashi and T. Fujimoto (eds.), *Jomonbunka no Kenkyu 2: Seigyo*, Tokyo: Yuzankaku, 148–160.

Imamura, K., 1992. Jomonzenkimatsu no Kanto ni okeru Jinkogenshyo to soreni kanrensuru shyogenshyo. In: Yoshida-Itaru-Sensei-Koki-Kinenen-Ronbunshu-Kanko-Kai (ed.), *Musashino no Koukogaku:Yoshida Itaru Sensei Koki Kinenen Ronbunshu*, Tokyo: Yoshida-Itaru-Sensei-Koki-Kinenen-Ronbunshu-Kanko-Kai, 85–115.

Imamura, K., 1996. *Prehistoric Japan: New perspectives on insular East Asia*. London: UCL Press.

Imamura, K., 1997. Jomon jidai no jyukyoatosu to jinko no hendo. In: I. Fujimoto (ed.), *Hashira no Kokogaku*, Tokyo: Douseisha, 45–60.

Imamura, K., 1999a. *Jomon no jitsuzo wo motomete*. Tokyo: Yoshikawakoubunkan.

Imamura, K., 2002. *Jomon no yutakasa to genkai*. Tokyo: Yamakawa.

Imamura, K., 2005. Doki: nendaigaku-keishikigaku. In: Narabunkazaikekyujo; M. Sahara and W. Steinhaus (eds.), *Nihon no Koukogaku*, Tokyo: Gakuseisha, 180–186.

Imamura, K., 2010. Jomonjidai no jinkodoutai. In: Y. Kosugi; Y. Taniguchi; Y. Nishida; K. Mizunoe and K. Yano (eds.), *Jomonjidai no koukogaku 1: Jomonbunka no rinkaku -hikakubunkaron ni yoru soutaika-*, Tokyo: Douseisha, 63–73.

Imamura, M., 1999b. Koseido 14C nendai sokutei to kokogaku. *Gekkan Chikyu Special Issue*, 26, 23–31.

Inada, A., Saito, T., Nirei, T., Nishimura, S., Ohama, K., Kaneko, S., Kaneko, Y., Shimamura, K. and Shimizu, S., 2008. Chibaken yachiyoshishinkawateichi ni okeru kanshinsei no shokuseihennsen to insasaku kaishijiki. *Dai Yonki kenkyu*, 47, 313–327.

Inoue, J., Nishimura, R. and Takahara, H., 2012. A 7500-year history of intentional fires and changing vegetation on the Soni Plateau, Central Japan, reconstructed from macroscopic charcoal and pollen records within mire sediment. *Quaternary International*, 254, 12–17.

Ishikawa, S., Suzuki, T., Nakayama, T. and Kashima, K., 2009. Tokyotochiodakuhibiyakouen to Kotokuarasuna ni okeru keisoukaseki ni yoru kanshinsei no kokankyofukugen. *Chirigakuzasshi*, 118, 245–260.

Ishizaka, S., 2002. Jomonjidaichuukimatsuba no kanjoshuraku no hokai to kanjoresseki no shutsugen. *GunmakenMaizobunkazai Chosa Gigyoudan Kenkyukiyo*, 20, 72–102.

Ishizaka, S. and Daikuhara, Y., 2001. Gunmaken ni okeru jomojidai shuraku no shoyouso. In: Jomonjidaikenkyukai (ed.), *Rettou ni okeru jomonjidaishuraku no shoyouso*, Tokorosawa: Jomonjidaikenkyukai, 183–248.

Ito, Y., 1999. Bousou ni okeru jomonjidai no kogatajyuusyuryou. *DoubutsuKokogaku*, 13, 17–32.

Janssen, M. A., 2009. Understanding Artificial Anasazi. *Journal of Artificial Societies and Social Simulations*, 12, URL: `http://jasss.soc.surrey.ac.uk/12/4/13.html` (last retrieved on 27th July 2012).

Janssen, M. A., Anderies, J. M. and Ostrom, E., 2007. Robustness of Social-Ecological Systems to Spatial and Temporal Variability. *Society and Natural Resources*, 20, 307–322.

Jeanson, R., Fewell, J. H., Gorelick, R. and Bertram, S. M., 2007. Emergence of increased division of labor as a function of group size. *Behavioral Ecology and Sociobiology*, 62, 289–298.

Jentsch, A., Kreyling, J. and Beierkuhnlein, C., 2007. A new generation of climate change experiments: events, not trends. *Frontiers in Ecology and the Environment*, 5, 365–374.

Jochim, M. A., 1976. *Hunter-gatherer subsistence and settlement : a predictive model*. London: Academic Press.

Johnson, G. A., 1980. Rank-Size Convexity and System Integration: A View from Archaeology. *Economic Geography*, 56, 234–247.

Johnson, I., 2004. Aoristic Analysis: seeds of a new approach to mapping archaeological distributions through time. In: K. Ausserer; W. B. rner; M. Goriany and L. K.-V. . ckl (eds.), *[Enter the Past] the E-way into the Four Dimensions of Cultural Heritage: CAA2003. BAR International Series 1227.*, Oxford: Archaeopress, 448–452.

Kaneda, A., Tsumura, H. and Niiro, I., 2001. *Koukogaku no tameno GIS nyumon*. Tokyo: Kokonshoin.

Kaneko, H., Nishimoto, T. and Nagahama, M., 1982. Shuryo/Gyorou taishodoubutsu no chiikisei. *Kikan Kokogaku*, 1, 18–24.

Kani, M., 1993. Jomonjidai no setorumento shisutemu. *Kikan Kokogaku*, 44, 77–81.

Kano, M., 2001. Chibaken ni okeru Jomonjidaishuraku no shoyouso. In: Jomonjidaikenkyukai (ed.), *Rettou ni okeru jomonjidaishuraku no shoyouso*, Tokorosawa: Jomonjidaikenkyukai, 265–286.

Kano, M., 2002. Hikyojyuuikihe no Bunsannkyojyuu ga shimesu shyakai. In: M. Anzai (ed.), *Jomonshakairon 1*, Tokyo: Douseisha, volume 235-258.

Kariya, Y., Sasaki, A. and Arai, F., 1998. Sankokuchitairyapposan ni bunpu suru daiyonkimakki no tefuraso. *Chigakuzasshi*, 107, 92–103.

Karlsson, H. (ed.), 2001. *It's about time : the concept of time in archaeology*. Goteborg: Bricoleur.

Kawahata, H., Yamamoto, H., Ohkushi, K., Yokoyama, Y., Kimoto, K., Ohshima, H. and Matsuzaki, H., 2009. Changes of environments and human activity at

the Sannai-Maruyama ruins in Japan during the mid-Holocene Hypsithermal climatic interval. *Quaternary Science Reviews*, 28, 964–974.

Keally, C. T., 2004. Bad Science and the Distortion of History: Radiocarbon Dating in Japanese Archaeology. *Sophia International Review*, 26, 1–16.

Keeley, L. H., 1988. Hunter-gatherer Economic Complexity and "Population Pressure": A Cross-Cultural Analysis. *Journal of Anthropological Archaeology*, 7, 373–411.

Kelly, R. L., 1995. *The Foraging Spectrum: Diversity In Hunter-Gatherer Lifeways*. Washington, DC: Smithsonian Institution Press.

Kennedy, J., 1998. Methods of Agreement: Inference Among the EleMentals. In: *Intelligent Control (ISIC), 1998. Held jointly with IEEE International Symposium on Computational Intelligence in Robotics and Automation (CIRA), Intelligent Systems and Semiotics (ISAS), Proceedings*. Piscataway, NJ: IEEE Service Center, 883–887.

Kennedy, J. and Eberhart, R. C., 2001. *Swarm Intelligence*. London: Morgan Kaufmann Publishers/Academic Press.

Kikuchi, M., 1997. Shimousadaichi tokyowanganchiiki ni okeru jomonjidai no isekiricchi. *Busshitsubunka*, 62, 34–47.

Kikuchi, M., 2001. Bosohanto ni okeru jomonjidaishuraku no ricchi: shimousawanganchiiki kujyukurihamachiiki no jirei. *Dai Yonki kenkyu*, 40, 171–183.

Kitagawa, H., Fukusawa, H., Okamura, T., Takemura, M., Hayashida, K. and Yasuda, Y., 1995. AMS14C dating of varved sediments from Lake Suigetsu, central Japan and atmospheric change during the late Pleisticene. *Radiocarbon*, 37, 371–378.

Kitagawa, J. and Yasuda, Y., 2004. The influence of climatic change on chestnut and horse chestnut preservation aroundJomon sites in Northeastern Japan with special reference to the Sannai-Maruyama and Kamegaoka sites. *Quaternary International*, 123-125, 89–103.

Kitagawa, J. and Yasuda, Y., 2008. Development and distribution of Castanea and Aesculus culture during the Jomon Period in Japan. *Quaternary International*, 184, 42–55.

Kobashi, T., Severinghaus, J. P., Brook, E. J., Barnola, J.-M. and Grachev, A. M., 2007. Precise timing and characterization of abrupt climate change 8200 years ago from air trapped in polar ice. *Quaternary Science Reviews*, 26, 1212–1222.

Kobayashi, K., 2004. *Jomonkenkyu no shinsiten: tanso14nenndaiokutei no riyo*. Tokyo: Rokuichishobo.

Kobayashi, K., 2007. AMS 14C Nendaisokuteishiryo no kento to Jomonjykyoky-ojukikan no kento. *Kokogaku Kenkyu*, 54, 50–69. Duration of Jomon pithouse is between 10 to 20 years.

Kobayashi, K., 2008. Jomonjidai no rekinendai. In: Y. Kosugi; Y. Taniguchi; Y. Nishida; W. Mizunoe and K. Yano (eds.), *Rekishi no monosashi: : Jomon jidai kenkyu no hennen taikei*, Tokyo: Douseisha, 257–269.

Kobayashi, T., 1973. Tama New Town no senjyusha: omo toshite jomonjidai no setorumento shisutemy ni tsuite. *Gekkan Bunkazai*, 112, 20–26.

Kobayashi, T., 1992. Patterns and Levels of Social Complexity in Jomon Japan. In: C. M. Aikens and S. N. Rhee (eds.), *Pacific Northeast Asia in Prehistory: Hunter-Fisher-Gatherers, Farmers. and Sociopolitical Elites*, Pullman: Washigton State University Press, 91–98.

Kobayashi, T., 2002. *Jomon doki no kenkyu*. Tokyo: Gakuseisha.

Kohler, T. A., Gummerman, G. J. and Reynolds, R. G., 2005. Simulating Ancient Societies. *Scientific American*, 293, 76–84.

Kohler, T. A., Johnson, C. D., Varien, M., Ottman, S., Reynolds, R., Kobti, Z., Cowan, J., Kolm, K., Smith, S. and Yap, L., 2007. Settlement Ecodynamics in the Prehispanic Central Mesa Verde Region. In: T. A. Kohler and S. E. v. d.

Leeuw (eds.), *The model-based archaeology of socionatural systems*, Sante Fe: SAR Press, 61–104.

Kohler, T. A., Kresl, J., West, C. V., Carr, E. and Wilshusen, R. H., 2000. Be There Then: A Modeling Approach to Settlement Determinants and Spatial Efficiency Among Late Ancestral Pueblo Populations of the Mesa Verde Region, U.S. Southwest. In: T. A. Kohler and G. J. Gumerman (eds.), *Dynamics in Human and Primate Societies: Agent Based Modeling of Social and Spatial Processes*, Oxford: Oxford University Press, 145–178.

Kohler, T. A. and Leeuw, S. E. v. d. (eds.), 2007. *The Model-Based Archaeology of Socionatural Systems*. Santa Fe: SAR Press.

Kohler, T. A. and Parker, S. C., 1986. Predictive Models for Archaeological Resource Location. *Advances in Archaeological Method and Theory*, 9, 397–452.

Koike, H., 1980. *Seasonal dating by growth-line counting of the clam, Meretrix lusoria*. Tokyo: University Musuem, University of Tokyo.

Koike, H., 1986. Prehistoric Hunting Pressure and Paleobiomass: An Environmental Reconstruction and Archaeozoological Analysis of a Jomon Shellmound Area. In: T. Akazawa and C. M. Aikens (eds.), *Prehistoric Hunter-Gatherers in Japan: New Research Methods*, Tokyo: University of Tokyo Press, 27–53.

Koike, H., 1992a. Exploitation Dynamics During the Jomon Period. In: C. M. Aikens and S. N. Rhee (eds.), *Pacific Northeast Asia in Prehistory: Hunter-Fisher-Gatherers, Farmers, and Sociopolitical Elites*, Pullman: Washington State University Press, 53–57.

Koike, H., 1992b. Umi no seitaikei kara mita Jomon-jidai no kairui saishu: kaigara no ookisa, nenrei kousei, soshite hoshokuatsu. *Bulletin of the Chiba Municipal Museum of Kasori Shell-Mideen*, 18–38.

Kokawa, S., 1983. Jomonjin no omona shokubutsushokuryou. In: S. Kato;

T. Kobayashi and T. Fujimoto (eds.), *Jomonbunka no kenkyu1*, Tokyo: Yuzankaku, 42–49.

Komiya, H., 1989. Bousou ni okeru jomonjidai wo chusin to suru kokankyou no hensen: chikei no hensen. *Chibakenbunkazaisentaa KenkyuKiyo*, 9, 1–39.

Kosugi, Y., 1991. Jomonjidai ni kaikyushakai wa sonzaishitanoka. *Koukogakukenkyu*, 37, 97–121.

Kosugi, Y., 2002. Shinzo ga kaiku suru shakai. In: M. Anzai (ed.), *Jomonshakairon (jo)*, Tokyo: Douseisha, 133–180.

Koyama, S., 1978. Jomon Subsistence and Population. *Senri Ethnological Studies*, 2, 1–65.

Koyama, S., 1996. *Jomongaku heno michi*. Tokyo: Nihonhousoushuppankyoukai.

Koyama, S. and Sugito, S., 1984. Jomon jinko simulation. *Bulletin of the National Museum of Ethnology*, 9, 1–39.

Koyama, S. and Thomas, D. H. (eds.), 1981. *Affluent Foragers: Pacific Coasts East and West*. Senri Ethnological Series No.9. Osaka: National Museum of Ethnology.

Kudo, Y., 2007. The Temporal Correspondences between the Archaeological Chronology and Environmental Changes from 11,500 to 2,800 cal BP on the Kanto Plain, Eastern Japan. *The Quaternary Research*, 46, 187–194.

Kudo, Y., Sasaki, Y., Sakamoto, M., Kobayashi, K. and Matsuzaki, H., 2007. Tokyo-to Shimoyakebeiseki kara shutsudo shita Jomonjidai kouhanki no shokubutsuriyou ni kanrensuru ikou/ibutsu no nendaitekikenkyu. *Shokuseishikenkyu*, 15, 5–17.

Kuroo, K., 2009. Jomoniseki keiseikatei: kanjoshuraku no keisei prosesu. In: Y. Kosugi; Y. Taniguchi; Y. Nishida; K. Mizunoe and K. Yano (eds.), *Jomonjidai no koukogaku 8: seikatsukukan*, Tokyo: Douseisha, 85–98.

Kusaka, S., Nakano, T., Yumoto, T. and Nakatsukasa, M., 2011. Strontium isotope evidence of migration and diet in relation to ritual tooth ablation: a case study from the Inariyama Jomon site, Japan. *Journal of Archaeological Science*, 38, 166–174.

Kuwahata, M., 2002. Koukogakushiryo karamita kikaiakahoyafunka no jiki to eikyo. *Daiyonkikenkyu*, 41, 317–339.

Kuzmin, Y. V., 2006. Chronology of the earliest pottery in East Asia: progress and pitfalls. *Antiquity*, 80, 362–371.

Lake, M., 2010. The Uncertain Future of Simulating the Past. In: A. Costopoulos and M. Lake (eds.), *Simulating Change: Archaeology Into the Twenty-First Century*, Salt Lake City: University of Utah Press, 12–20.

Lake, M. W., 2000. MAGICAL Computer Simulation of Mesolithic Foraging. In: T. A. Kohler and G. J. Gumerman (eds.), *Dynamics in Human and Primate Societies: Agent-Based Modeling of Social and Spatial Processes*, Oxford: Oxford University Press, 107–143.

Lake, M. W. and Crema, E. R., 2012. The Cultural Evolution of Adaptive-Trait Diversity when Resources are Uncertain and Finite. *Advances in Complex Systems*, 15, 1150013–1 – 1150013–19.

Lake, M. W. and Woodman, P. E., 2000. Viewshed analysis of site location on Islay. In: S. J. Mithen (ed.), *Hunter-Gatherer Landscape Archaeology: The Southern Hebrides Mesolithic Project, 1988-98, Volume 2: Archaeological Fieldwork on Colonsay, Computer Modelling, Experimental Archaeology, and Final Interpretations*, Cambridge: The Mcdonald Institute for Archaeological Research, 497–503.

Laland, K., Olding-Smee, F. and Feldman, M., 1999. Evolutionary consequences of niche construction and their implications for ecology. *Proceedings of the National Academy of Sciences of the United States of America*, 96, 10242–10247.

Laland, K. N., Olding-Smee, J. and Feldman, M., 2001. Cultural niche construction and human evolution. *Journal of Evolutionary Biology*, 14, 22–33.

Laland, K. N., Olding-Smee, J. and Feldman, M. W., 2000. Niche construction, biological evolution, and cultural change. *Behavioral and Brain Sciences*, 23, 131–175.

Lansing, J. S., 2000. Anti-Chaos, Common Proprety, and the Emergence of Cooperation. In: T. a. Kohler and G. J. Gumerman (eds.), *Dynamics in Human and Primate Societies: Agent-Based Modeling of Social and Spatial Processes*, Oxford: Oxford University Press, 207–223.

Layton, R., Foley, R. and Williams, E., 1991. The Transition Between Hunting and Gathering and the Specialized Husbandry of Resources: A Socio-ecological Approach. *Current Anthropology*, 32, 255–274.

Lee, R., 2008. Sociality, selection, and survival: Simulated evolution of mortality with intergenerational transfers and food sharing. *Proceedings of the National Academy of Sciences*, 105, 7124–7128.

Lee, R. B., 1979. *The !Kung San: Men, women, and wotk in a foraging society*. Cambridge: Cambridge University Press.

Lipo, C. P., Madsen, M. E., Dunnell, R. C. and Hunt, T., 1997. Population Structure, Cultural Transmission, and Frequency Seriation. *Journal of Anthropological Archaeology*, 16, 301–333.

Lloret, F., Escudero, A., Iriondo, J. M., Martinez-Vilalta, J. and Valladares, F., 2012. Extreme climatic events and vegetation: the role of stabilizing processes. *Global Change Biology*, 18, 797–805.

Lock, G. and Harris, D., 2002. Analysing change through time within a cultural landscape: conceptual and functional limitations of a GIS approach. In: P. Sinclair (ed.), *The Development of Urbanism from a Global Perspective*, Uppsala Univer-

sitet: Uppsaka, URL: http://www.arkeologi.uu.se/digitalAssets/9/9453_LockAll.pdf (last retrieved on 27th July 2012).

Lyman, R. L. and O'Brein, M., 2006. *Measuring Time with Artifacts: A History of Methods in American Archaeology*. Lincoln: University of Nebraska Press.

Martin, M. K., 1974. *The foraging adaptation: Uniformity or diversity?* Reading, Massachusetts: Addison-wesley.

Maschner, H. D. and Stein, J. W., 1995. Multivariate approaches to site location on the Northwest Coast of North America. *Antiquity*, 69, 61–73.

Matinón-Torres, M., Li, X. J., Bevan, A., Xia, Y., Kun, Z. and Rehren, T., 2012. Making Weapons for the Terracotta Army. *Archaeology International*, 13/14, 65–75.

Matsugi, T., 2007. *Rettosouseiki*. Tokyo: Shogakukan.

Matsui, A., 1996. Archaeological Investigations of Anadromous Salmonid Fishing in Japan. *World Archaeology*, 27, 444–460.

Matsushima, Y., 1982. Gyoryotaishodobutsu (kairuo) no chiikisei. *Kikan Kokogaku*, 1, 25–27.

Mauss, M. and Beuchat, H., 1904. Essai sur les variations saisonnìres des sociétés Eskimos. *L'Année Sociologique*, 1904-1905, 39–132.

May, R., 1976. Simple mathematical models with very complicated dynamics. *Nature*, 261, 459–467.

Mayer, C., 2006. Making Use of Distances: Estimating Parameters of Spatial Processes. In: M. W. Mehrer and K. L. Wescott (eds.), *GIS and Archaeological Site Location Modeling*, Boca Raton: Taylor and Francis, 148–166.

Mayewski, P. A., Rohling, E. E., Stager, J. C., Karlen, W., Maasch, K. A., Meeker, L. D., Meyerson, E. A., Gasse, F., Kreveld, S. v., Holmgren, K., Lee-Thorp, J., Rosqvist, G., Rack, F., Staubwasser, M., Schneider, R. R. and Steig, E. J., 2004. Holocene climate variability. *Quaternary Research*, 62, 242–255.

McGlade, J., 1995. Archaeology and the ecodynamics of human-modified landscapes. *Antiquity*, 69, 113–132.

McGlade, J. and van der Leeuw, S., 1995. Introduction: Archaeology and non-linear dynamics -new approaches to long-term change. In: S. v. d. Leeuw and J. McGlade (eds.), *Time, Process and Structured Transformation in Archaeology*, London: Routledge, 1–31.

Mcgrayne, S. B., 2011. *The theory that would not die*. London: Yale University Press.

McRae, B. H., 2006. Isolation by resistance. *Evolution*, 60, 1551–1561.

Meehan, B., 1982. *Shell Ned to Shell Midden*. Canberra: Australian Institute of Aboriginal Studies.

Mikami, T., 1996. Arioyoshikidoki. In: M. Tozawa (ed.), *Jomonjidai kenkyu jiten*, Tokyo: Tokyodo, 207.

Millard, A., 2005. What can Bayesian statistics do for archaeological predictive modelling? In: P. M. v. Leusen and H. Kamermans (eds.), *Predictive modelling for archaeological heritage management: a research agenda*, Amersfoort: Rijkdienst voor het Oudheidkundig Bodemonderzoek, 169–182.

Minagawa, M. and Akazawa, T., 1992. Dietry Patterns of Japanese Jomon Hunter-Gatherers: Stable Nitrogen and Carbon Isotope Analyses of Human Bones. In: C. M. Aikens and S. N. Rhee (eds.), *Pacific Northeast Asia in Prehistory: Hunter-Fisher-Gatherers, Farmers, and Sociopolitical Elites*, Pullman: Washington State University Press, 59–68.

Minaki, M., 1994. Jomonjidai iko no kur (Castanea crenata Sieb. et. Zucc.) kajutsu no oogataka. *Shokuseishikenkyu*, 2, 3–10.

Mitchell, D. and Donald, L., 2001. Sharing Resources on the North Pacific Coast of North America: The Case of the Eulachon Fishery. *Anthropologica*, 43, 19–35.

Mithen, S., 1990. *Thoughtful foragers : a study of prehistoric decision making*. New York: Cambridge University Press.

Mithen, S., 1994. Simulating Prehistoric Hunter-Gatherers. In: N. Gilbert and J. Doran (eds.), *Simulating Societies: The Computer Simulation of Social Phenomena*, London: UCL Press, 165–193.

Miyaji, T., Tanabe, K., Matsushima, Y., Sato, S., Yokoyama, Y. and Matsuzaki, H., 2010. Response of daily and annual shell growth patterns of the intertidal bivalve Phacosoma japonicum to Holocene coastal climate change in Japan. *Palaeogeography, Palaeoclimatology, Palaeoecology*, 286, 107–120.

Möller, J. and Waagepetersen, R. P., 2004. *Statistical Inference and Simulation for Spatial Point Processes*. London: Chapman and Hall/Crc.

Morse, E. S., 1879. *Shell Mounds of Omori*. Tokyo: University of Tokyo.

Murdock, G., 1949. *Social Structure*. New York: The Macmillan Company.

Murray, T. (ed.), 1999. *Time and Archaeology*. London: Routledge.

Muto, Y., 1995. Minzokushi kara mita jomonjidai no tateanajukyo. *Teikyou Daigaku Yamanashi bunkazaikenkyujyo kenkyuhoukoku*, 6, 267–301.

Nakamura, O., 2002. Kaisoushakai. *Kikan Kokogaku*, 80, 38–41.

Nakamura, T., 1996. Seugyokatusdo to isekigun. *Kikan Kokogaku*, 55, 56–61.

Naylor, J. C. and Smith, F. M., 1988. An Archaeological Inference Problem. *Journal of the American Statistical Association*, 83, 588–595.

Nicolucci, F. and Hermon, S., 2002. Estimating subjectivity of typologists and typological classification with fuzzy logic. *Archeologia e Calcolatori*, 12, 217–232.

Nishida, M., 1983. The Emergence of Food Production in Neolithic Japan. *Journal of Anthropological Archaeology*, 2, 305–322.

Nishida, M., 1989. *Jomonjidai no seitaishikan*. Tokyo: Tokyodaigaku shuppankai.

Nishida, M., 2002. Another Neolithic in Holocene Japan. *Documenta Praehistorica*, XXIX, 21–28.

Nishimoto, T., 1983. Inu. In: S. Kato; T. Koabayshi and T. Fujimoto (eds.), *Jomon Bunka no Kenkyu 2: Seigyo*, Tokyo: Yuzankaku.

Nishimoto, T., 1991. Jomonjidai no sika/inoshishi shuryou. *Kodai*, 91, 114–132.

Nishimoto, T., 1995. Sakana to tori no nikushoku seikatsu: Sannai Maruyama iseki no doubutsu-shitsu shokuryo no mondai. In: T. Umehara and Y. Yasuda (eds.), *Jomon Bunmei no Hakken: Kyoi no Sannai Maruyama Iseki*, Tokyo: PHP Kenkyujo, 207–213.

Nishimoto, T., 2003. Jomonjidai no butakachiku ni tsuite. *Kokuritsu RekishiMinzokuHakbutsukan KenkyuHoukoku*, 108, 1–15.

Nishimoto, T., Tsumura, H., Kobayashi, K., Sakaguchi, T. and Tatieshi, T., 2001. Jomonshuraku no seitairon 1. *Doubutsukoukogaku*, 17, 73–82.

Nishino, M., 1999. Jomon chuuki no daikaizuka to seikatsukatusdo: ariyoshikita kaizuka bunsekikekka. *Chibakenbunkazaisentaa KenkyuKiyo*, 19, 135–150.

Nishino, M., 2005. Tokyowanhigashigan No Oogatakaizuka Wo Sasaeta Seisankyoujyuyoshiki. In: *Chiiki to Bunka No Koukogaku I*, Tokyo: Department of Archaeology, Meiji University, 695–711.

Nishino, M., 2008. Chuki no kanjokaizuka to shuraku. *Kikan Kokogaku*, 105, 29–33.

Odling-Smee, F. J., Laland, K. N. and Feldman, M. W., 2003. *Niche Construction: The Neglected Process in Evolution*. New Jersey: Princeton University Press.

Ogawa, N., 1996a. Futatsushikidoki. In: M. Tozawa (ed.), *Jomonjidai kenkyu jiten (3rd edition)*, Tokyo: Tokyodo, 371.

Ogawa, N., 1996b. Okitsushikidoki. In: M. Tozawa (ed.), *Jomonjidai kenkyu jiten (3rd edition)*, Tokyo: Tokyodo, 241–242.

Ogawa, N., 1996c. Ukishimashikidoki. In: M. Tozawa (ed.), *Jomonjidai kenkyu jiten (3rd edition)*, Tokyo: Tokyodo, 219–220.

Ohmagari, K. and Berkes, F., 1997. Transmission of Indigenous Knowledge and Bush Skills Among the Western James Bay Cree Women of Subarctic Canada. *Human Ecology*, 25, 197–222.

Okamura, M., 2005a. Gendai nihon no maizobunkazaiseigyo. In: Narabunkazaikekyujo; M. Sahara and W. Steinhaus (eds.), *Nihon no Koukogaku*, Tokyo: Gakuseisha, 736–742.

Okamura, M., 2005b. Naze Jomonbunka wa owaranakkatanoka. In: Narabunkazaikekyujo; M. Sahara and W. Steinhaus (eds.), *Nihon no Koukogaku*, Tokyo: Douseisha, 244–249.

Olding-Smee, J., 2007. Niche Inheritance: A Possible Basis for Classifying Multiple Inheritance Systems in Evolution. *Biological Theory*, 2, 276–289.

Olson, D. M., Dinerstein, E., Wikramanayake, E. D., Burgess, N. D., Powell, G. V., Underwood, E. C., D'Amico, H., Itoua, I., Strand, H. E., Morrison, J. C., Loucks, C. J., Allnutt, T. F., Ricketts, T. H., Kura, Y., Lamoreux, J. F., Wettengel, W. W., Hedao, P. and Kenneth R, . K., 2001. Terrestrial Ecoregions of the World: A new Map of Life on Earth. *BioScience*, 51, 933–938.

Oota, H., Pakendorf, B., Weiss, G., Haeseler, A. v., Pookajorn, S., Settheetham-Ishida, W., Tiwawech, D., Ishida, T. and Stoneking, M., 2005. Recent Origin and Cultural Reversion of a HunterGatherer Group. *Plos Biology*, 3.

Openshaw, S., 1984. *The Modifiable Areal Unit Problem*. Norwich: Geobooks.

Orton, C., 1982. Stochastic Process and Archaeological Mechanism in Spatial Analysis. *Journal of Archaeological Science*, 9, 1–23.

Orton, C., 2000. *Sampling in Archaeology*. Cambridge: Cambridge University Press.

Orton, C., 2004. Point Pattern Analysis Revisited. *Archeologia e Calcolatori*, 15, 299–315.

O'Sullivan, D. and Unwin, D., 2003. *Geographic information analysis*. Hoboken: Wiley.

Ouchi, C., 2008. Chibken niu okeru shokiboshuraku no buseki. In: K. Kobayashi and Settlement-KenkyuKai (eds.), *Jomon Kenkyu no shinchiheu (zoku): Tateana-jukyo shyurakuchousa no research*, Tokyo: Rokuichihobo, 99–106.

Parker, G., 1978. Searching for mates. In: J. R. Krebs and N. B. Davies (eds.), *Behavioural Ecology (1st Edition)*, Oxford: Blackwell, 214–244.

Parker, W. S., 2009. Does matter really matter? Computer simulations, experiments, and materiality. *Synthese*, 169, 483–496.

Parnell, A., Haslett, J., Allen, J., Buck, C. and Huntley, B., 2008. A flexible approach to assessing synchroneity of past events using Bayesian reconstructions of sedimentation history. *Quaternary Science Reviews*, 27, 1872–1885.

Pearson, R., 2006. Jomon hot spot: increasing sedentism in south-western Japan in the Incipient Jomon (14,0009250 cal. BC) and Earliest Jomon (9250-5300 cal. BC) periods. *World Archaeology*, 38, 239–258.

Pearson, R., 2007. Debating Jomon Social Complexity. *Asian Perspectives*, 46, 361–388.

Pelletier, D. L., Frongillo, E. A. and Habicht, J.-P., 1993. Epidemiologic Evidence for a Potentiating Effect of Malnutrition on Child Mortality. *American Journal of Public Health*, 83, 1130–1133.

Petraitis, P. S., Latham, R. E. and Niesenbaum, R. A., 1989. The maintenance of species diversity by disturbance. *The Quarterly Review of Biology*, 64, 393–418.

Pinder, D., Shimada, I. and Gregory, D., 1979. The Nearest-Neighbor Statistic: Archaeological Application and New Developments. *American Antiquity*, 44, 430–445.

Plog, F. T., 1973. Diachronic Anthropology. In: C. L. Redman (ed.), *Research and Theory in Current Archeology*, New York: Wiley, 181–198.

Powell, A., Shennan, S. and Thomas, M. G., 2009. Late Pleistocene Demography and the Appearance of Modern Human Behavior. *Science*, 324, 1298–1301.

Power, C., 2009. A Spatial Agent-Based Model of N-Person Prisoner's Dilemma Cooperation in a Socio-Geographic Community. *Journal of Artificial Societies and Social Simulations*, 12, URL `http://jasss.soc.surrey.ac.uk/12/1/8.html` (last retrieved on 27th July 2012).

Premo, L., 2010. Equifinality and Explanation:The Role of Agent-Based Modeling in Postpositivist Archaeology. In: A. Costopoulos and M. Lake (eds.), *Simulating Change: Archaeology into the Twenty-First century*, Salt Lake City: University of Utah Press, 28–37.

Premo, L. S., 2006. *Patchiness an Prosociality: Modeling the Evolution and Archaeology of Plio-Pleistocene Homin Food Sharing*. Ph.D. thesis, University of Arizona.

Premo, L. S., 2007. Exploratory Agent-based Models: Towards an Experimental Ethnoarchaeology. In: J. T. Clark and E. M. Hagemeister (eds.), *Digital Discovery: Exploring New Frontiers in Human Heritage, CAA 2006. Computer Applications and Quantitative Methods in Archaeology*, Budapest: Archeolingua Press, 29–36.

Prentiss, W. C. and Chatters, J. C., 2003. Cultural Diversification and Decimation in the Prehistoric Record. *Current Anthropology*, 44, 33–58.

Price, T. D., 1981. Complexity in "Non-complex" Societies. In: S. van der Leeuw (ed.), *Archaeological Approaches to the Study of Complexity*, Amstredam: Universiteit van Amstredam, 54–97.

Price, T. D. and Brown, J. A. (eds.), 1985. *Prehistoric Hunter-Gatherers: The Emergence of Cultural Complexity*. Studies in Archaeology. San Diego: Academic Press.

R Development Core Team, 2011. *R: A Language and Environment for Statistical Computing*. R Foundation for Statistical Computing, Vienna, Austria. URL `http://www.R-project.org`. ISBN 3-900051-07-0.

Ramenofsky, A. F., 1998. The Illusion of Time. In: A. F. Ramenofsky and A. Steffen (eds.), *Unit Isues in Archaeology: Measuring Time, Space, and Material*, Utah: University of Utah Press, 74–84.

Ratcliffe, J. H., 2000. Aoristic analysis: the spatial interpretation of unspecifed temporal events. *International Journal of Geographical Information Science*, 14, 669–679.

Ratcliffe, J. H. and McCullagh, M. J., 1998. Aoristic crime anaylsis. *International Journal of Geographical Information Science*, 12, 751–764.

Reed, W. J. and Jorgensen, M., 2004. The Double Pareto-Lognormal DistributionA New Parametric Model for Size Distributions. *Communications in Statistics - Theory and Methods*, 33, 1733–1753.

Renfrew, C. and Poston, T., 1979. Discontinuities in the Endogenous Change of Settlement Pattern. In: C. Renfrew and K. L. Cooke (eds.), *Transformations: Mathematical Approaches to Culture Change*, New York: Academic Press, 437–461.

Renssen, H., Seppaä, H., Heiri, O., Roche, D. M., Goosse, H. and Fichefet, T., 2009. The spatial and temporal complexity of the Holocene thermal maximum. *Nature Geoscience*, 2, 411–414.

Rhode, M. P. and Arriaza, B. T., 2006. Influence of Cranial Deformation on Facial Morphology Among Prehistoric South Central Andean Populations. *American Journal of Physical Anthropology*, 130, 462–470.

Rick, J. W., 1976. Downslope Movement and Archaeological Intrasite Spatial Analysis. *American Antiquity*, 41, 133–144.

Rihill, T. and Wilson, A., 1987. Spatial Interaction and Structural Models in Historical Analysis: Some Possibilities and an Example. *Histoire & Mesure*, 2, 5–32.

Ripley, B., 1981. *Spatial Statistics*. Hoboken, New Jersey: Wiley and Sons.

Robert, C. and Casella, G., 2004. *Monte Carlo Statistical Methods (2nd Ed.)*. New York: Springer.

Roberts, B. K., 1996. *Landscapes of Settlement: prehistory to the present*. London: Routeledge.

Rochette, S., Lobry, J., Lepage, M. and Boet, P., 2009. Dealing with uncertainty in qualitative models with a semi-quantitative approach based on simulations. Application to the Gironde estuarine food web (France). *Ecological Modelling*, 220, 122–132.

Rosen, A. M. and Rivera-Collazo, I., 2012. Climate change, adaptive cycles, and the persistence of foraging economies during the late Pleistocene/Holocene transition in the Levant. *Proceedings of the National Academy of Sciences*, 109, 3640–3645.

Rouse, I., 1972. Settlement Patterns in Archaeology. In: P. Ucko; R. Tringham and G. Dimblelby (eds.), *Man, Settlement and Urbanism*, London: Duckworth, 95–107.

Rowley-Conwy, P., 2001. Time, change, and the archaeology of hunter-gatherers: how original is the'Original Affluent Society'. In: C. Panter-Brick; R. H. Layton and P. Rowley-Conwy (eds.), *Hunter-Gatherer: An Interdisciplinary Perspective*, Cambridge: Cambridge University Press, 39–72.

Rowley-Conwy, P. and Zvelebil, M., 1989. Saving it for later: storage by prehistoric hunter-gatherers in Europe. In: P. Halstead and J. O'Shea (eds.), *Bad year economics: Cultural responses to risk and uncertainty*, Cambrdige: Cambrdige University Press, 40–56.

Rubio, X. C., Cela, J. M. and Cardona, F. X. H., 2011. Simulating archaeologists? Using agent-based modelling to improve battlefield excavations. *Journal of Archaeological Science*, 39, 347–356.

Sakaguchi, T., 2009. Storage adaptations among hunter-gatherers: A quantitative approach to the Jomon period. *Journal of Anthropological Archaeology*, 26, 290–303.

Sasaki, F., 2000. Jomontekishakaizo no saikousei: futatsu no -atarashii jomonkan- no hazamade. *Ibou*, 18, 82–107.

Sasaki, F., 2002. Kanjoresseki to Jomonshikikaisoshakai. In: M. Anzai (ed.), *Jomonshakairon (ge)*, Tokyo: Douseisha, 3–50.

Sasaki, F., 2010. Jomonjidai no dankaikubun. In: Y. Kosugi; Y. Taniguchi; Y. Nishida; K. Mizunoe and K. Yano (eds.), *Jomonjidai no koukogaku 1: Jomonbunka no rinkaku -hikakubunkaron ni yoru soutaika-*, Tokyo: Douseisha, 107–126.

Sato, H., 2005. Socio-ecological Research of the Trap-pit Hunting in Jomon Period, Japan. *Bulletin of the Department of Archaeology, The University of Tokyo*, 19, 105–124.

Sato, Y., Yamanaka, S. and Takahashi, M., 2003. Evidence for Jomon Plant Cultivation Based on DNA Analysis of Chestnut Remains. In: J. Habu; J. M. Savelle; S. Koyama and H. Hongo (eds.), *Hunter-Gatherers of the North Pacific Rim (Senri Ethnological Studies 63)*, Osaka: Senri National Museum of Ethnology, 187–197.

Savage, S. H., 1997. Assessing Departures from Log-Normality in the Rank-Size Rule. *Journal of Archaeological Science*, 24, 233–244.

Sayama, H., Farrell, D. L. and Dionne, S. D., 2011. The Effects of Mental Model Formation on Group Decision Making: An Agent-Based Simulation. *Complexity*, 16, 49–57.

Schafer, J. L., 1999. Multiple imputation: a primer. *Statistical Methods in Medical Research*, 8, 3–15.

Schauber, E. M., Goodwin, B. J., Jones, C. G. and Ostfeld, R. S., 2007. Spatial Selection and Inheritance: Applying Evolutionary Concepts to Population Dynamics in Heterogenous Space. *Ecology*, 88, 1112–1118.

Schiffer, M. B., 1972. Archaeological context and systemic context. *American Antiquity*, 37, 156–165.

Schiffer, M. B., 1987. *Formation Processes of the Archaeological Record*. Albuquerque, N.M.: University of New Mexico Press.

Schlaepfer, M. A., Runge, M. C. and Sherman, P. W., 2002. Ecological and evolutionary traps. *TRENDS in Ecology and Evolution*, 17, 474–480.

Schone, B. R., Oschmann, W., Tanabe, K., Dettman, D., Fiebig, J., Houk, S. D. and Kanie, Y., 2004. Holocene seasonal environmental trends at Tokyo Bay, Japan, reconstructed from bivalve mollusk shellsimplications for changes in the East Asian monsoon and latitudinal shifts of the Polar Front. *Quaternary Science Reviews*, 23, 1137–1150.

Schrire, C., 1980. An Inquiry into the Evolutionary Status and Apparent Identity of San Hunter-Gatherers. *Human Ecology*, 8, 9–32.

Seguchi, S., 2009. *Jomonshuraku no koukogaku: nishinihon mi okeru teijyushuraku no seiritsu to tenkai*. Kyoto: Showado.

Seguchi, S., 2010. Kansaichiho no Jomonshuraku to Jomonshakai. In: K. Suzuki and Y. Suzuki (eds.), *Shuraku no Hensen to Chiikisei*, Tokyo: Yuzankaku, 185–218.

Sekiguchi, T., 1989. Bousou ni okeru jomonjidai wo chusin to suru kokankyou no hensen: shokusei no hensen. *Chibakenbunkazaisentaa KenkyuKiyo*, 9, 40–74.

Sellers, W., Hill, R. H. and Logan, B., 2007. An agent-based model of group decision making in baboons. *Philosophical Transactions of the Royal Society B*, 362, 1699–1710.

Serizawa, C., 1960. *Sekki Jidai no Nihon*. Tokyo: Tsukiji Shokan.

Shennan, S., 2001. Demography and Cultural Innovations: a Model and its Implications for the Emergence of Modern Human Culture. *Cambridge Archaeological Journal*, 11, 5–16.

Shennan, S. and Wilkinson, J., 2001. Ceramic Style Change and Neutral Evolution: A Case Study from Neolithic Europe. *American Antiquity*, 66, 577–593.

Shibutani, F., 1998. Tateanajyukyo no shouchyuketsuichinitsuite. *Matsudoshiritusuhakubutsukankiyou*, 27–48.

Shnirelman, V. A., 1992. Complex hunter-gatherers: Exception or common phenomenon? *Dialectical Anthropology*, 17, 183–196.

Sibly, R., 1983. Optimal Group Size is Unstable. *Animal Behaviour*, 31, 947–948.

Silberbauer, G., 1981. *Hunter and Habitat in the Central Kalahari Desert*. New York: Cambridge University Press.

Simon, H. A., 1979. *Models of Thought*. New Haven: Yale University Press.

Sinn, H.-W., 1980. A Rehabilitation of the Principle of Insufficient Reason. *The Quarterly Journal of Economics*, 94, 493–506.

Smith, B. D., 2001. Low-Level Food Production. *Journal of Archaeological Research*, 9, 1–43.

Smith, B. D., 2007. The Ultimate Ecosystem Engineers. *Science*, 315, 1797–1798.

Smith, B. D., 2011. General patterns of niche construction and the management of wild plant and animal resources by small-scale pre-industrial societies. *Philosophical Transactions of the Royal Society B*, 366, 836–848.

Smith, E. A., 1983. Anthropological Applications of Optimal Foraging Theory: A Critical Review. *Current Anthropology*, 24, 625–651.

Smith, E. A. and Choi, J.-K., 2007. The emergence of inequality in small-scale societies: simple scenarios and agent-based simulations. In: T. Kohler and S. v. d. Leeuw (eds.), *The Model-based Archaeology of Socionatural Systems*, Santa Fe: SAR Press, 105–119.

Soda, T., Noto, T. and Arai, F., 1988. Kusatsushiranekazankigen, kumakurakaruishiso no funnkanendai. *Touhokuchiri*, 40, 272–275.

Stewart, H., 1982. Kaishin, kaitai. In: S. Kato; T. Koabayshi and T. Fujimoto (eds.), *Jomon Bunka no Kenkyu I: Jomonjin to sono Kankyo*, Tokyo: Yuzankaku, 130–142.

Stonedahl, F. and Wilensky, U., 2010. Evolutionary Robustness Checking in the Artificial Anasazi Model. *AAAI Fall Symposium Series*, URL: `http://www.aaai.org/ocs/index.php/FSS/FSS10/paper/view/2181/2622` (last retrieved on 27th July 2012).

Sugiyama, S., 2002. Kikaiakahoyafunka ga minamikyusgu no shokusei ni aterta eikyo. *Dai Yonki kenkyu*, 41, 311–316.

Surovell, T. A. and Brantingham, P. J., 2007. A note on the use of temporal frequency distributions in studies of prehistoric demography. *Journal of Archaeological Science*, 34, 1868–1877.

Surovell, T. A., Finley, J. B., Smith, G. M., Brantingham, P. J. and Kelly, R., 2009. Correcting temporal frequency distributions for taphonomic bias. *Journal of Archaeological Science*, 36, 1715–1724.

Sutherland, W., 1983. Aggregation and the "ideal free" distribution. *Journal of Animal Ecology*, 52, 821–828.

Suzuki, K., 1986. Volumetry and Nutritional Analysis of a Jomon Shell-Midden. In: T. Akazawa and C. M. Aikens (eds.), *Prehistoric Hunter-Gatherers in Japan (The University Musuern Bulletin No. 27)*, Tokyo: University of Tokyo Press, 55–72.

Suzuki, K., 1989. *Kaizuka no Kokogaku*. Tokyo: Tokyodaigakushuppankai.

Suzuki, K., 2010a. Tohokuchiho no Jomonshuraku no shakaisoshiki to sonraku. In: K. Suzuki and Y. Suzuki (eds.), *Shuraku no Hensen to Chiikisei*, Tokyo: Yuzankaku, 51–94.

Suzuki, K. and Suzuki, Y. (eds.), 2010. *Shuraku no Hensen to Chiikisei*. Tokyo: Yuzankaku.

Suzuki, M., 1982. Yumiya to Yari. *Kikan Kokogaku*, 1, 32–35.

Suzuki, M., 1991. *Sekkinyumonjiten Jomon*. Tokyo: Hakushobo.

Suzuki, M., 1996. Jomonjidai no shuraku to kaizuka no keisei: kidosakuiseki ni okeru kanjoshuraku to kanjokaizuka no kaitai. *Kikan Kokogaku*, 55, 44–49.

Suzuki, T., 1999. Hontouni ni nakattanoka Jomonjin no shudanteki tatakai. In: T. Kobayashi (ed.), *Jomongaku no sekai*, Tokyo: Asahishinbunsha, 36–47.

Suzuki, Y., 2006. *Jomonjidai shuraku no kenkyu*. Tokyo: Yuzankaku.

Suzuki, Y., 2010b. Kanto/Tokaichiho no Jomonshuraku to Jomonshakai. In: K. Suzuki and Y. Suzuki (eds.), *Shuraku no Hensen to Chiikisei*, Tokyo: Yuzankaku, 96–143.

Takahashi, R., 2004. *Jomonbunka kenkyu no saizensen*. Tokyo: Waseda Daigaku.

Takahashi, R. and Hosoya, L. A., 2002. Nut exploitation in Jomon society. In: J. G. Hather and S. L. R. Mason (eds.), *Hunter-Gatherer Archaeobotany: Perspectives from the northern temperate zone*, London: The Institute of Archaeology, UCL, 146–155.

Taniguchi, Y., 1993. Jomonshuraku no ryouiki. *Kikan Kokogaku*, 44, 67–71.

Taniguchi, Y., 2002. Kanjosguraku to Buzokushakai: Zen, Chuki no retto chuoobu. In: M. Anzai (ed.), *Jomonshkairon (jo)*, Tokyo: Douseisha, 19–65.

Taniguchi, Y., 2005. *Kanjoshuraku to Jomonshakaikouzo*. Tokyo: Gakuseisha.

Tateishi, T., Tsumura, H. and Ninomiya, S., 2004. Kasoriminamikaizukashutsudokokuyouseki no gensanchi suitei. *KaizukaHakubutsukankiyou*, 31, 1–15.

Temple, D. H., 2007. Dietary Variation and Stress Among Prehistoric Jomon Foragers From Japan. *American Journal of Physical Anthropology*, 133, 1035–1046.

Terrell, J. E., Hart, J. P., Barut, S., Cellinese, N., Curet, A., Denham, T., Kusimba, C. M., Latinis, K., Oka, R., Palka, J., Pohl, M. E. D., Pope, K. O., Williams, P. R., Haines, H. and Staller, J. E., 2003. Domesticated Landscapes: The Subsistence Ecology of Plant and Animal Domestication. *Journal of Archaeological Method and Theory*, 10, 323–368.

Testart, A., 1982. The Significance of Food Storage among Hunter-Gatherers: Residence Patterns, Population Densities, and Social Inequalities. *Current Anthropology*, 23, 523–537.

Thomas, R., 1977. *An Introduction to Quadrat Analysis*. Norwich: Geo Abstracts Ltd.

Thompson, V. D. and Turk, J. A., 2009. Adaptive Cycles of Coastal Hunter-Gatherers. *American Antiquity*, 74, 255–278.

Toizumi, T., 1999a. *Kaisou no Kenkyu I*. Chiba: Chibashi Kasorikaizukahakubutsukan.

Toizumi, T., 1999b. Tokyowanchiiki ni okeru kanshinsei no kaiyokankyohensen to jomonkaizukakeiseishi. *Kokuritsuminzokuhakubutsukankenkyuhoukoku*, 81, 289–310. In Japanese.

Toizumi, T., 2005. Kaizuka: shuryo to gyoryo. In: Narabunkazaikekyujo; M. Sahara and W. Steinhaus (eds.), *Nihon no Koukogaku*, Tokyo: Gakuseisha, 167–172.

Toizumi, T., 2007. Kaigaraseichosen karamita Jomonshuraku no keisei. *Koukogaku Jyaanaru*, 563, 9–13.

Toizumi, T. and Nishino, M., 1999. Jomonkouki no miyakogawa muratagawaryouiki-kaizukagun. *Chibakenbunkazaisentaa KenkyuKiyo*, 19, 151–171.

Tozawa, M., 1996. Yakemachishikidoki. In: M. Tozawa (ed.), *Jomonjidai kenkyu jiten (3rd edition)*, Tokyo: Tokyodo, 395–396.

Tregenza, T., 1994. Common misconceptions in applying ideal free distribution. *Animal Behaviour*, 47, 485–487.

Tregenza, T., 1995. Building on the Ideal Free Distribution. *Advances in Ecological Research*, 26, 253–302.

Trigger, B. G., 1968. The Determinants of Spatial Pattern. In: K. Chang (ed.), *Settlement Archaeology*, Palo ALto, California: National Press Books, 53–78.

Tsude, H., 1995. Archaeological Theory in Japan. In: P. J. Ucko (ed.), *Theory in Archaeology: A world perspective*, London: Routledge, 298–311.

Tsuji, S., 1999. Kouseido 14Cnendai ni okeru sannaimaruyama iseki no hennen. *Gekkanchikyu*, 26, 32–38.

Tsukada, M., 1986. Vegetation in Prehistoric Japan: The Last 20,000 Years. In: R. J. Pearson; G. L. Barnes and K. L. Hutterer (eds.), *Windows on the Japanese Past: Studies in Archaeology and Prehistory*, Ann Arbor: Centre for Japanese Studies University of Michigan, 11–56.

Tsumura, H., 2002. Kukan compulekkusu no chuushutsu to isekikankankeihyoka no houhou: kokukogaku ni okeri kuukanbunseki 2. *Doubutsukoukogaku*, 18, 39–54.

Tsumura, H., 2006. Isekiricchi no teiryotekikaiseki to isekizonzaiyosoku moderu. In: T. Uno (ed.), *Jissen Koukogaku GIS: sentangijutsu de rekishi wo yomu*, Tokyo: NTT shuppan, 248–268.

Tsumura, H., Kobayashi, K., Sakaguchi, T., Tateishi, T. and Nishimoto, T., 2002a. Jomonshuraku no seitairon 2. *Doubutsukoukogaku*, 18, 1–38.

Tsumura, H., Kobayashi, K., Sakaguchi, T., Tateishi, T. and Nishimoto, T., 2002b. Jomonshuraku no seitairon 3-1. *Doubutsukoukogaku*, 19, 39–72.

Tsumura, H., Kobayashi, K., Sakaguchi, T., Tateishi, T. and Nishimoto, T., 2003. Jomonshuraku no seitairon 3-2. *Doubutsukoukogaku*, 20, 41–64.

Turner, M. G., Baker, W. L., Peterson, C. J. and Peet, R. K., 1998. Factors influencing succession: lessons from large, infrequent natural disturbances. *Ecosystems*, 1, 511–523.

Uchiyama, J., 2006. The Environmental troublemaker's Burden?: Jomon Perspectives on Foraging Land Use Change. In: C. Grier; J. Kim and J. Uchiyama (eds.), *Beyond Affluent Foragers: rethinking Hunter-Gatherer Complexity*, Oxford: Oxbow Books, 136–168.

Uchiyama, J., 2008. Vertical landscape or horizontal landscape? The prehistoric long-term perspectives on the history of the East Asian Inland Seas. In: A. Schottenhammer (ed.), *The East Asian "Mediterranean": Maritime Crossroads of Culture, Commerce and Human Migration*, Wiesbaden: Harrassowitz Verlag, 25–53.

van der Leeuw, S. (ed.), 1981. *Archaeological Approaches to the Study of Complexity*. Amsterdam: Universiteit van Amsterdam.

van der Leeuw, S., 2004. Why Model? *Cybernetics and Systems*, 35, 117–128.

Verhagen, P. and Whitley, T. G., 2011. Integrating Archaeological Theory and Predictive Modeling: a Live Report from the Scene. *Journal of Archaeological Method and Theory*, 18, 1–52.

Verhulst, P.-F., 1838. Notice sur la loi que la population poursuit dans son accroissement. *Correspondance mathématique et physique*, 10, 112–121.

Waite, T. A. and Field, K. L., 2007. Foraging with Others: Games Social Foragers Play. In: D. W. Stephens; J. S. Brown and R. C. Ydenberg (eds.), *Foraging: Behavior and Ecology*, Chicago: The University of Chicago Press, 331–362.

Wajima, S., 1948. Genshi Shuraku no Kosei. In: T.-D. R. Kenkyukai (ed.), *Nihon Rekishi-gaku Koza*, Tokyo: Tokyo Daigaku Shuppan-kai, 1–32.

Wajima, S. and Okamoto, I., 1958. Nanbori kaizuka to genshi shuraku. In: *Yokohama Shi-shi I*, Yokohama: Yokohama-shi, 29–46.

Walker, B., Holling, C., Carpenter, S. R. and Kinzig, A., 2004. Resilience, Adaptability and Transformability in Social ecological Systems. *Ecology and Society*, 9, URL: `http://www.ecologyandsociety.org/vol9/iss2/art5/` (last retrieved on 27th July 2012).

Wandsnider, L., 1998. Regional Scale Processes and Archaeological Landscape Units. In: A. F. Ramenofsky and A. Steffen (eds.), *Unit Isues in Archaeology: Measuring Time, Space, and Material*, Utah: University of Utah Press, 87–102.

Wang, Y., Cheng, H., Lawrence R, E., He, Y., Kong, X., An, Z., Wu, J., Kelly, M. J., Dykoski, C. A. and Li, X., 2005. The Holocene Asian Monsoon: Links to Solar Changes and North Atlantic Climate. *Science*, 308, 854–856.

Wanner, H., Beer, J., Butikofer, J., Crowley, T. J., Cubasch, U., Fluckiger, J., Goosse, H., Grosjean, M., Joos, F., Kaplan, J. O., Kuttel, M., Muller, S. A., Prentice, C., Solomina, O., Stocker, T. F., Tarasov, P., Wagner, M. and Widmann, M., 2008. Mid- to Late Holocene climate change: an overview. *Quaternary Science Reviews*, 27, 1791–1828.

Watanabe, H., 1968. Subsistence and Ecology of Northern Food Gatherers with Special Reference to the Ainu. In: R. B. Lee and I. DeVore (eds.), *Man the Hunter*, Chicago: Aldine de Gruyter, 69–77.

Watanabe, H., 1973. *The Ainu Ecosystem: Environment and Group Structure*. Seattle: Wahington University Press.

Watanabe, H., 1986. Community Habitation and Food Gathering in Prehistoric Japan: An Ethnographic Interpretation of the Archaeological Evidence. In: R. J. Pearson; G. L. Barnes and K. L. Hutterer (eds.), *Windows on the Japanese Past: Studies in Archaeology and Prehistory*, Ann Arbor: Centre for Japanese Studies University of Michigan, 229–254.

Watanabe, H., 1990. *Jomonshikikaisokashakai*. Rokkoichishobo.

Watanabe, H., 1992. The Northern Pacific Maritime Culture Zone: A Viewpoint on Hunter-Gatherer Mobility and Sedentism. In: C. M. Aikens and S. N. Rhee (eds.), *Pacific Northeast Asia in Prehistory: Hunter-Fisher-Gatherers, Farmers, and Sociopolitical Elites*, Pullman: Washington State University Press, 105–109.

Watanabe, M., 1975. *Jomonjidai no Shokubutsusyoku*. Tokyo: Yuzankaku.

Wescott, K. L. and Brandon, R. J. (eds.), 2000. *Practical Applications of GIS for Archaeologists: A Predictive Modelling Kit.* London: Taylor and Francis.

Whallon, R., Lovis, W. A. and Hitchcock, R. K. (eds.), 2011. *Information and its role in hunter-gatherer bands*. Los Angeles: Cotsen Institute of Archaeology Press.

Wheatley, D., 2004. Making space for an archaeology of place. *Internet Archaeology*, 15.

White, P. and Pickett, S., 1985. Natural disturbance and patch dynamics, an introduction. In: P. White and S. Pickett (eds.), *The ecology of natural disturbance and patch dynamics*, New York: Academic Press, 3–13.

White, P. S. and Jentsch, A., 2001. The Search for Generality in Studies of Disturbance and Ecosystem Dynamics. *Progress in Botany*, 62, 399–449.

Whitehead, H. and Richerson, P. J., 2009. The evolution of conformist social learning can cause population collapse in realistically variable environments. *Evolution and Human Behavior*, 30, 261–273.

Whitehead, P., Smith, S., Wade, A., Mithen, S., Finlayson, B., Sellwood, B. and Valdes, P., 2008. Modelling of hydrology and potential population levels at Bronze Age Jawa, Northern Jordan: a Monte Carlo approach to cope with uncertainty. *Journal of Archaeological Science*, 35, 517–529.

Whitelaw, T., 1991. Some dimensions of variability in the social organization of community space among foragers. In: C. Gamble and W. Boismer (eds.), *Ethnoarchaeological Approaches to Mobile Campsites: Hunter-Gatherer and Pastoralist Case Studies*, Ann Arbor, Michigan: International Monographs in Prehistory, 139–188.

Wiegand, T. and Moloney, K. A., 2004. Rings, circles, and null-models for point pattern analysis in ecology. *Oikos*, 104, 209–229.

Wilmsen, E. N., 1973. Interaction, Spacing Behavior, and the Organization of Hunting Bands. *Journal of Anthropological Research*, 29, 1–31.

Winsberg, E. B., 2010. *Science in the Age of Computer Simulation*. London: The University of Chicago Press.

Winterhalder, B., 1986. Diet Choice, Risk, and Food Sharing in a Stochastic Environment. *Journal of Anthropological Archaeology*, 5, 369–392.

Winterhalder, B., Baillargeon, W., Cappelletto, F., Jr., I. R. D. and Prescott, C., 1988. The Population Ecology of Hunter-Gatherers and Their Prey. *Journal of Anthropological Archaeology*, 7, 289–328.

Winterhalder, B., Kennett, D. J., Grote, M. N. and Bartruff, J., 2010. Ideal free settlement of California's Northern Channel Islands. *Journal of Anthropological Archaeology*, 29, 469–490.

Wobst, H. M., 1974. Boundary Conditions for Palaeolithic Social Systems. *American Antiquity*, 39, 147–178.

Wobst, H. M., 1978. The Archaeo-Ethnology of Hunter-Gatherers or the Tyranny of the Ethnographic Record in Archaeology. *American Antiquity*, 43, 303–309.

Woodburn, J., 1968. Stability and Flexibility in Hadza Residential Groupings. In: R. B. Lee and I. DeVore (eds.), *Man the Hunter*, Chicago: Aldine de Gruyter, 103–110.

Woodburn, J., 1982. Egalitarian Societies. *Man*, 17, 431–451.

Wooldridge, M. and Jennings, J. R., 1995. Intelligent agents: theory and practice. *Knowledge Engineering Review*, 10, 115–152.

Wright, Z. S., 1932. The roles of mutation, inbreeding, crossbreeding, and selection in evolution. *Proceedings of the Sixth International Congress on Genetics*, 1, 355–366.

Wylie, A., 2008. Mapping Ignorance in Archaeology: The Advantages of Historical Hindsight. In: R. Proctor and L. Schiebinger (eds.), *Agnotology: The Making and Unmaking of Ignorance*, Stanford: Stanford University Press, 183–208.

Yamamoto, T., Nagaoka, F., Onda, I. and Matsuda, K., 2001. Kanagawaken ni okeru Jomonjidaishuraku no shoyouso. In: Jomonjidaikenkyukai (ed.), *Rettou ni okeru jomonjidaishuraku no shoyouso*, Tokorosawa: Jomonjidaikenkyukai, 339–364.

Yamanouchi, S., 1964. Nihon senshi jidai gaisetsu. In: *Nihon Genshi Bijutsu IL Jomon-shiki Doki*, Tokyo: Kodansha, 135–158.

Yamanouchi, S. and Sato, T., 1962. Jomondoki no furusa. *Kagaku Yomiuri*, 14.

Yoneda, M., 2010. Douitaishokuseibunseki karamita Jomonbunka no tekiousenryaku. In: Y. Kosugi; Y. Taniguchi; Y. Nishida; K. Mizunoe and K. Yano (eds.), *Jomonjidai no koukogaku 4: Hito to doubutsu no kakawariai*, Tokyo: Douseisha, 207–221.

Ziedler, J. A., Buck, C. E. and Litton, C. D., 1998. Integration of Archaeological Phase Information and Radiocarbon Results from the Jama River Valley, Ecuador: A Bayesian Approach. *Latin American Antiquity*, 9, 160–179.

Zimmerman, L. J., 1978. Simulating prehistoric locational behaviour. In: I. Hodder (ed.), *Simulation studies in archaeology*, Cambridge: Cambdrige University Press, 27–38.

Zipf, G., 1949. *Human Behavior and the Principle of Least Effort*. Cambridge: Harvard University Press.

Zubrow, E. B., 1981. Simulation as a Heuristic Device in Archaeology. In: J. Sabloff (ed.), *Simulations in Archaeology*, Albuquerque: University of New Mexico Press, 143–188.

Zuck, T., Carpendale, S. and Glanzman, W., 2005. Visualizing Temporal Uncertainty in 3D Virtual Reconstructions. In: M. Mudge; N. Ryan and R. Scopigno

(eds.), *Proceedings of the 6th International Symposium on Virtual Reality, Archaeology and Cultural Heritage (VAST 2005)*, Pisa: Eurographics Association, 99–106.

Spatial and Temporal Models of Jōmon Settlement

VOLUME 2

PLATES

Figures

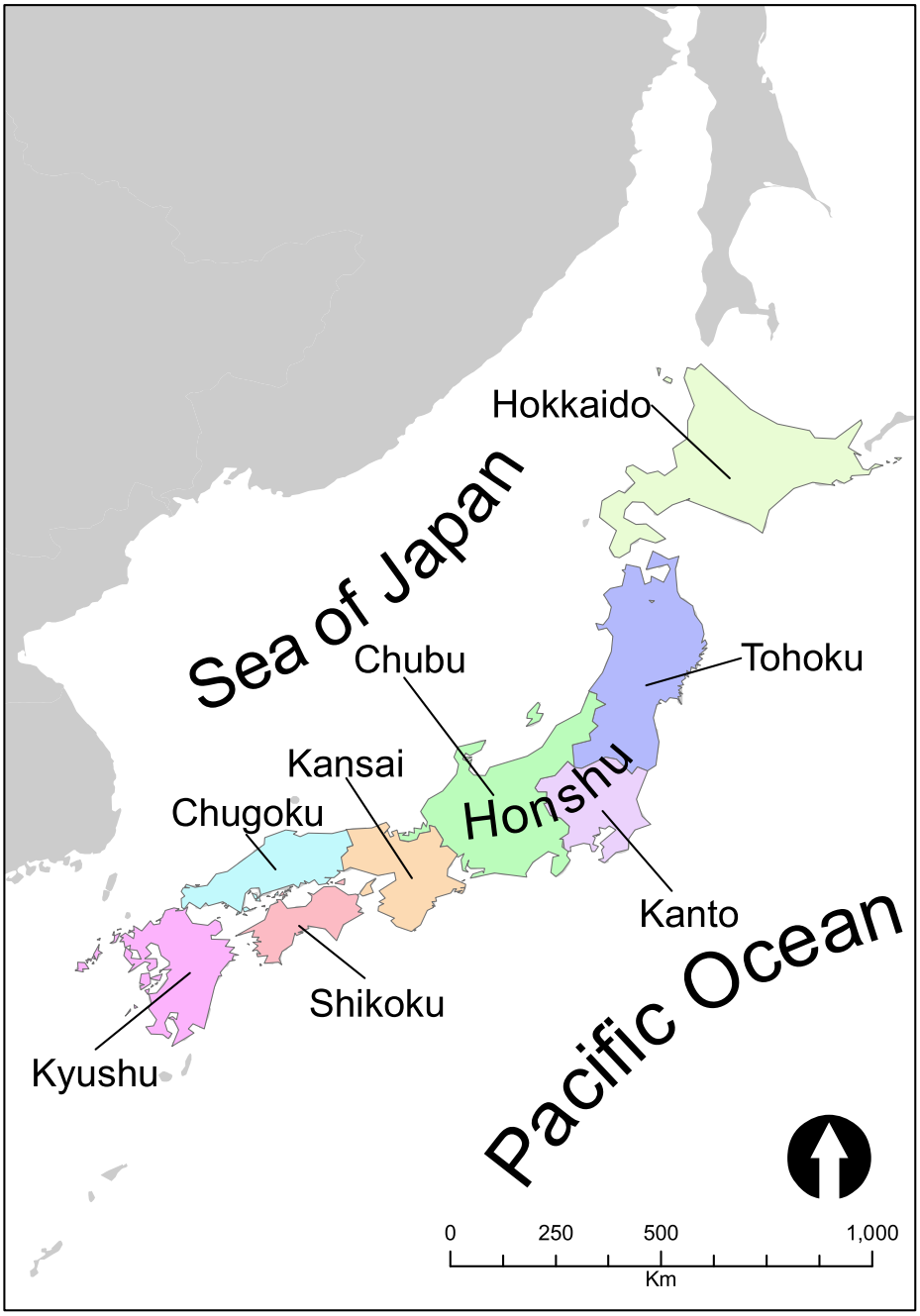

Figure 1: Main political and administrative subdivision of Japan

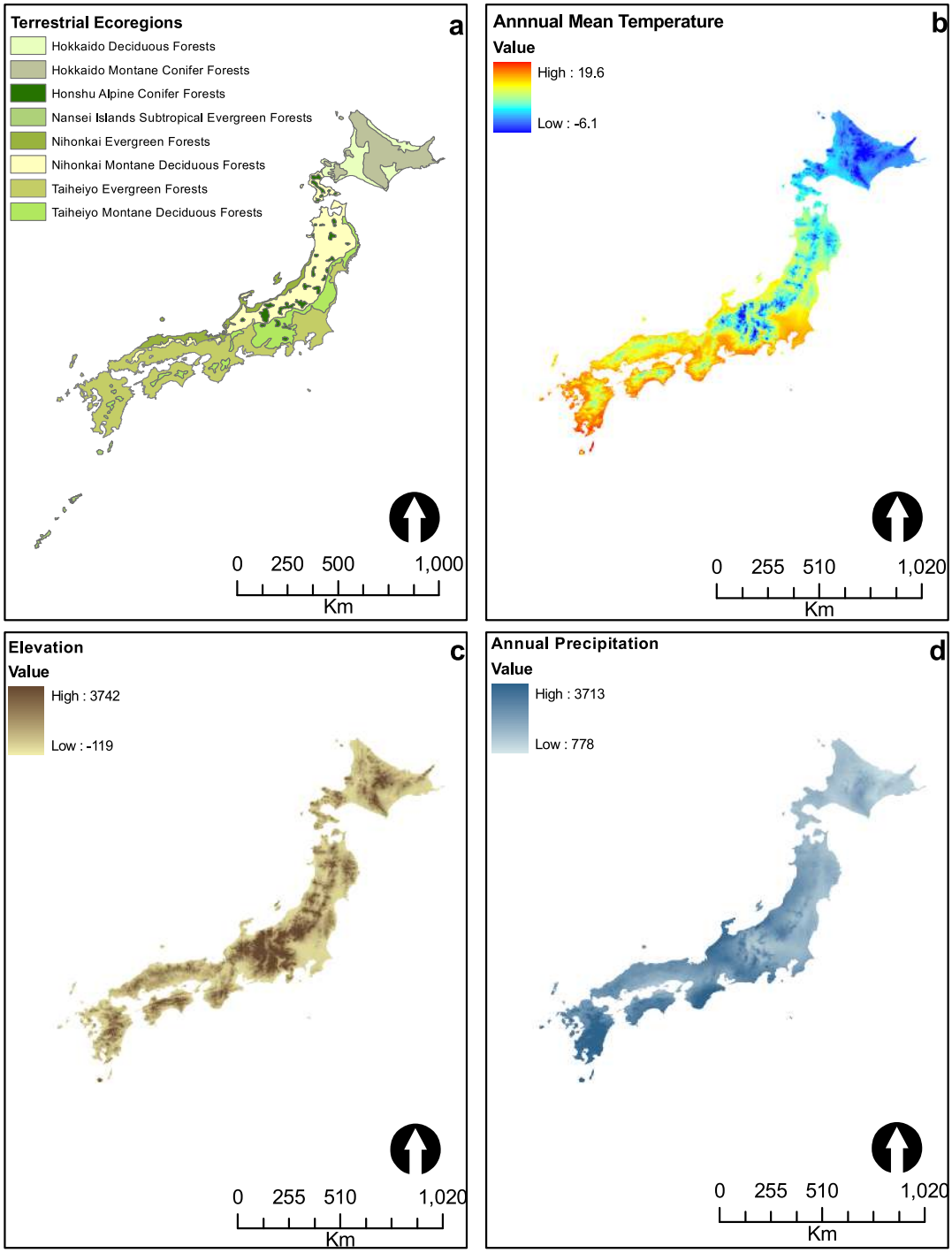

Figure 2: **a** terrestrial ecoregions (after Olsen *et al.* 2001, retrieved from: `http://www.worldwildlife.org/science/ecoregions/item1267.html`; **b**: annual mean temperature (1950-2000, after Hijmans et al. 2005, retrieved from: `http://www.worldclim.org/`); **c**: elevation (CGIAR-CSI SRTM 90m Database, retrieved from: `http://srtm.csi.cgiar.org`); **d**: annual precipitation (1950-2000, after Hijmans et al. 2005, retrieved from: `http://www.worldclim.org/`) of Japan.

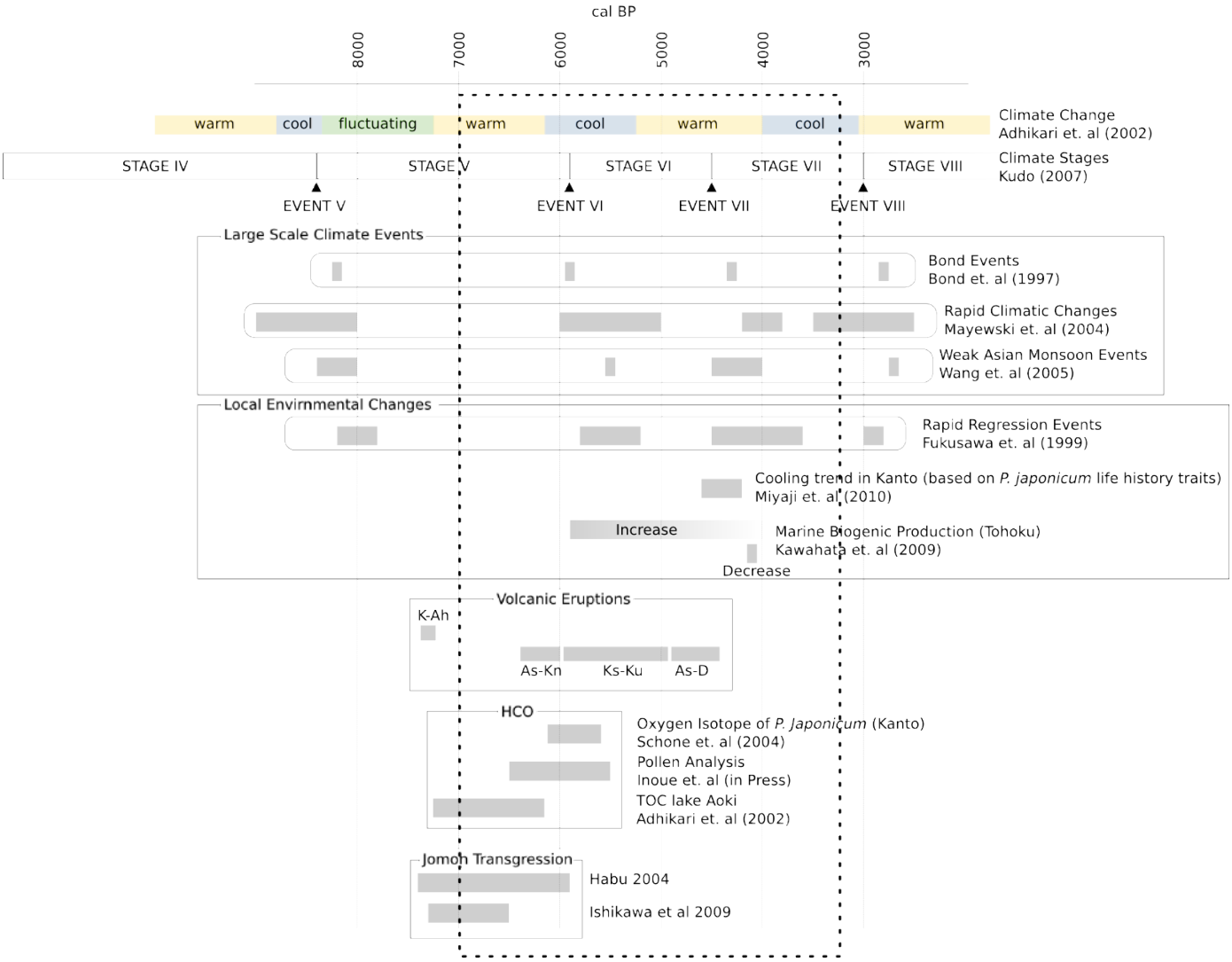

Figure 3: Major environmental changes in the Japanese archipelago (notice that studies based on uncalibrated dates and mentioned in the text has been omitted). The dotted-square defines the temporal scope of the present study.

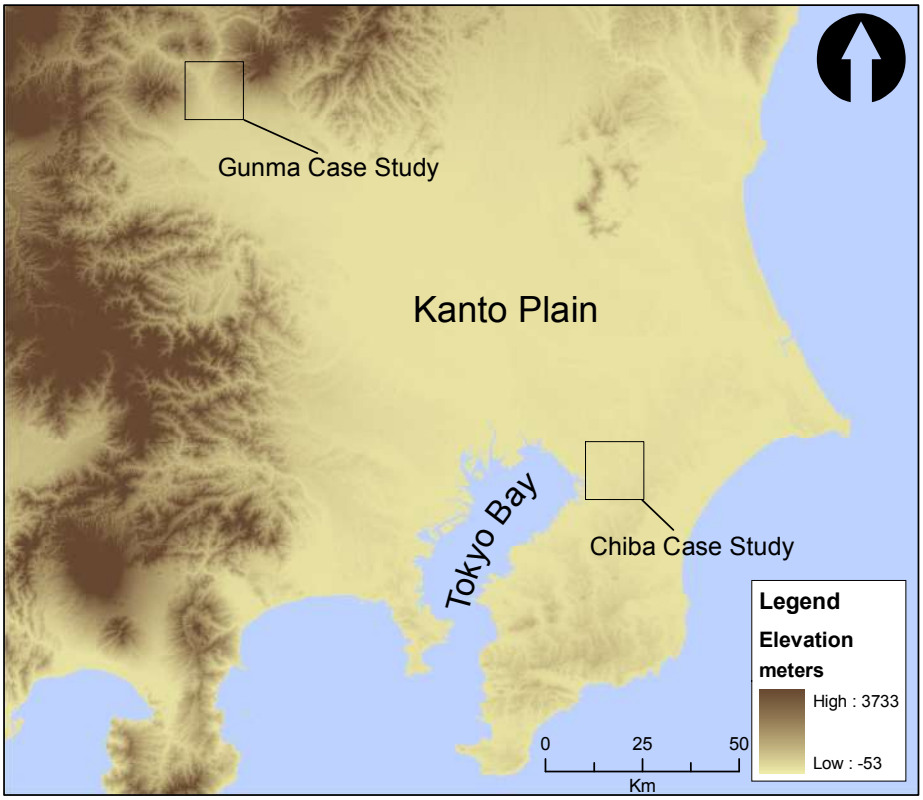

Figure 4: Location of the two case studies in Kantō

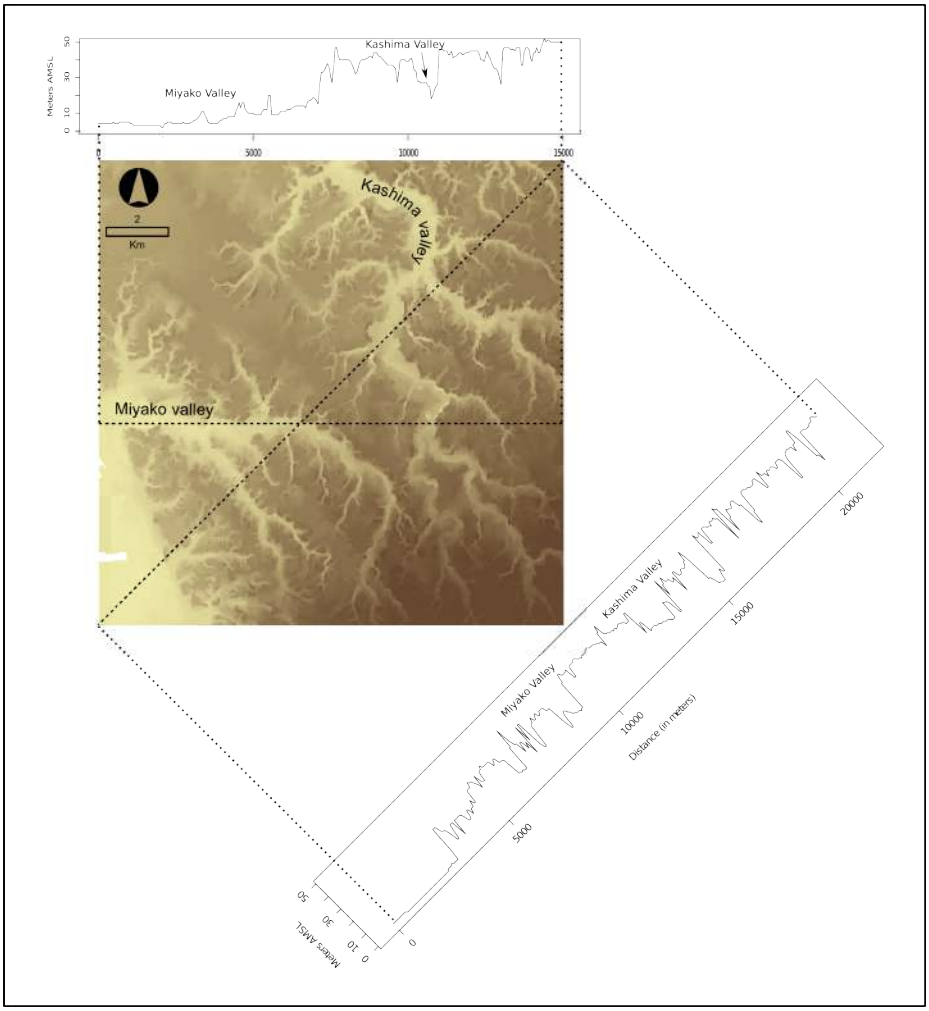

Figure 5: Case study at Chiba with elevation profile

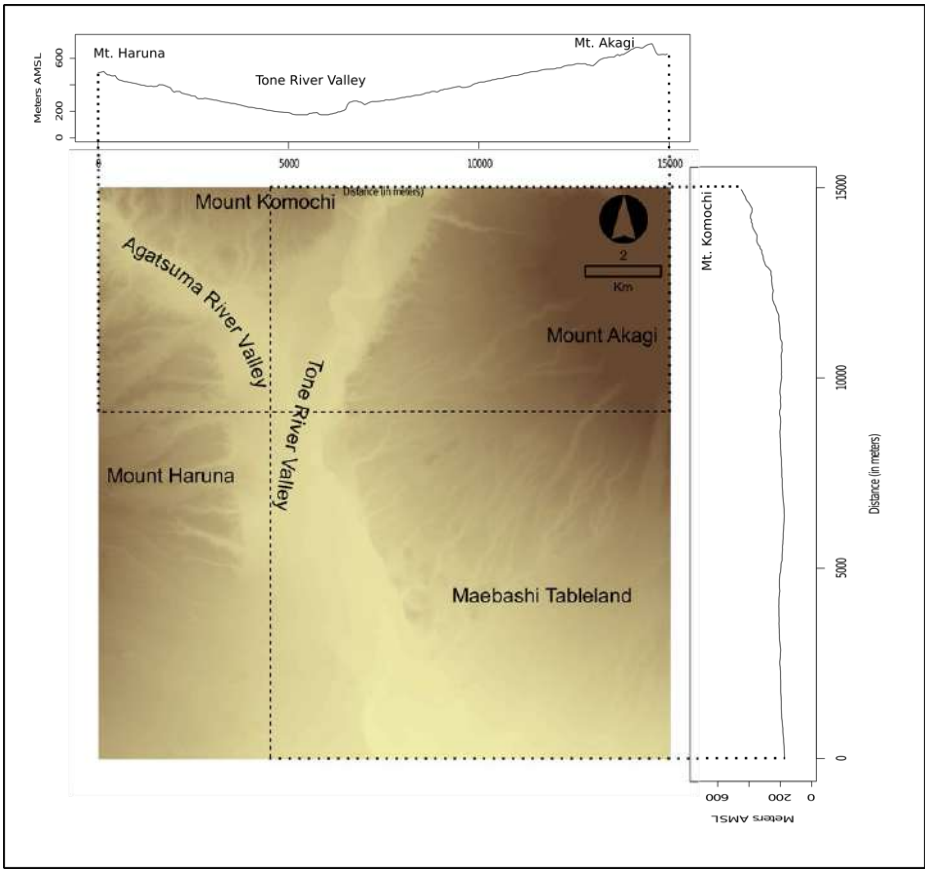

Figure 6: Case study at Gunma with elevation profile

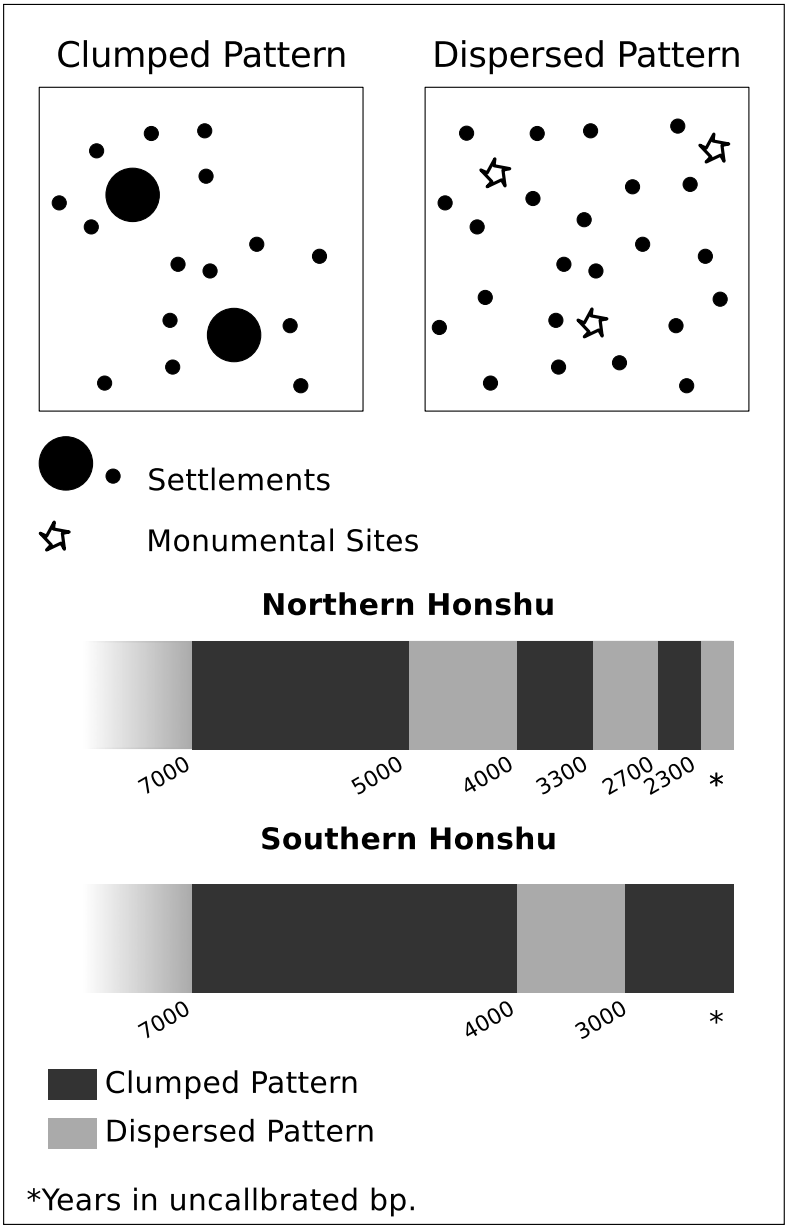

Figure 7: Uchiyama's model of clumped and dispersed settlement pattern (above) and the suggested sequence in Northern and Southern Honshū, (*after* Uchiyama 2006: 140-141)

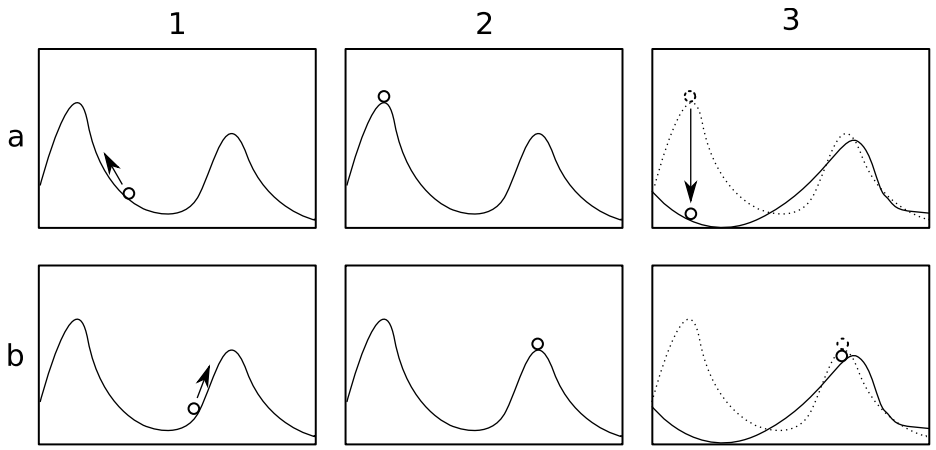

Figure 8: The concept of evolutionary trap. Individual *a* climbs the fitness landscape (1) and eventually reaches the global optimum (2, the highest peak), while individual *b* reaches a less adaptive local peak. This divergence is determined by small differences in the initial conditions (1). When environmental changes (3), individual *b* sees only a marginal decrease in its fitness, while individual *a* is strongly affected.

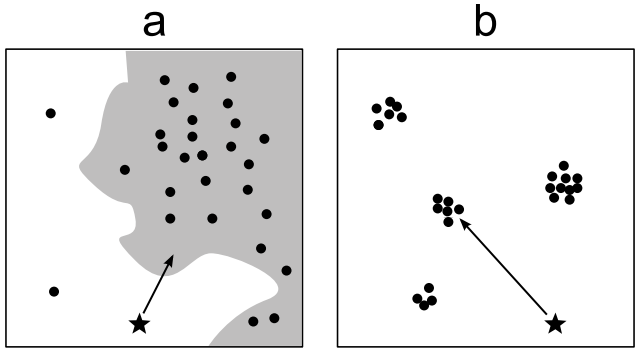

Figure 9: Abstract examples of induced (**a**) and inherent (**b**) spatial dependencies. In the former case, the focal individual (depicted as a star) is attracted to absolute locations with higher suitability (shown as a grey-shaded area). In the latter, he/she is attracted to locations where clusters of other individuals are already present. Notice that if we remove all the points from the first example, the expected behaviour of the focal individual will remain unchanged (i.e. spatial dependency is absolute), while in the latter case the removal of the cluster of individuals in the middle will lead to a different outcome (i.e. spatial dependency is relative).

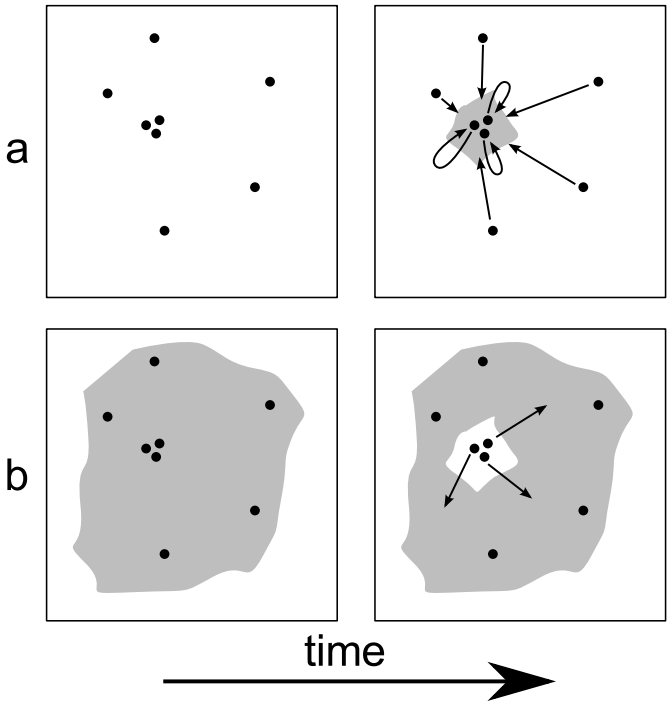

Figure 10: Examples of positive (**a**) and negative (**b**) niche construction and their spatio-temporal effects. In the former case (first row), the presence of individuals enhances the suitability of a local patch (coloured in grey) which in turn determines positive attraction to all individuals (including those already residing there). In the latter case (second row), the presence of individuals generates an unsuitable environment (coloured in white), which leads to the formation of a repulsive force over time.

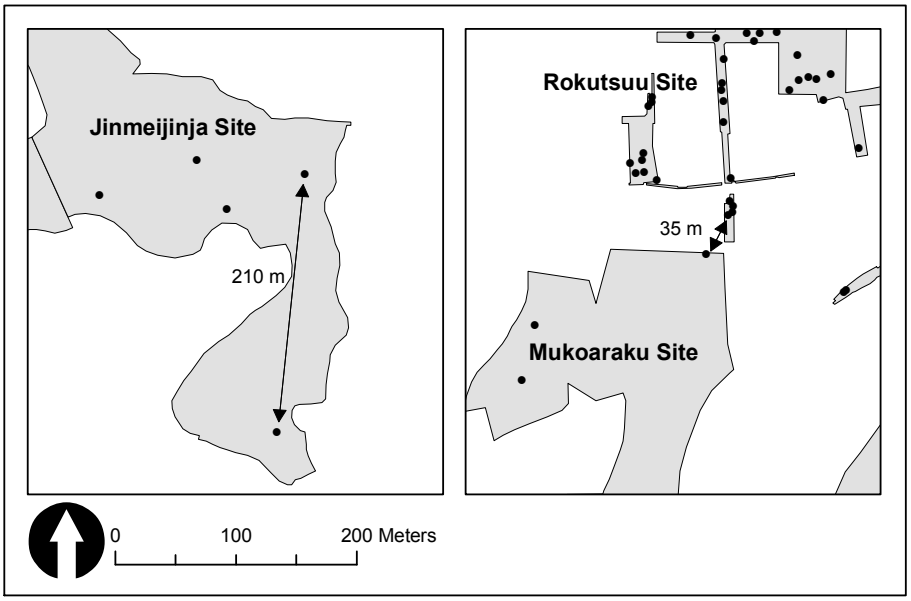

Figure 11: Examples of pithouse inter-distance at Jimenjinja, Mukoaraku, and Rokutsuu sites at Chiba

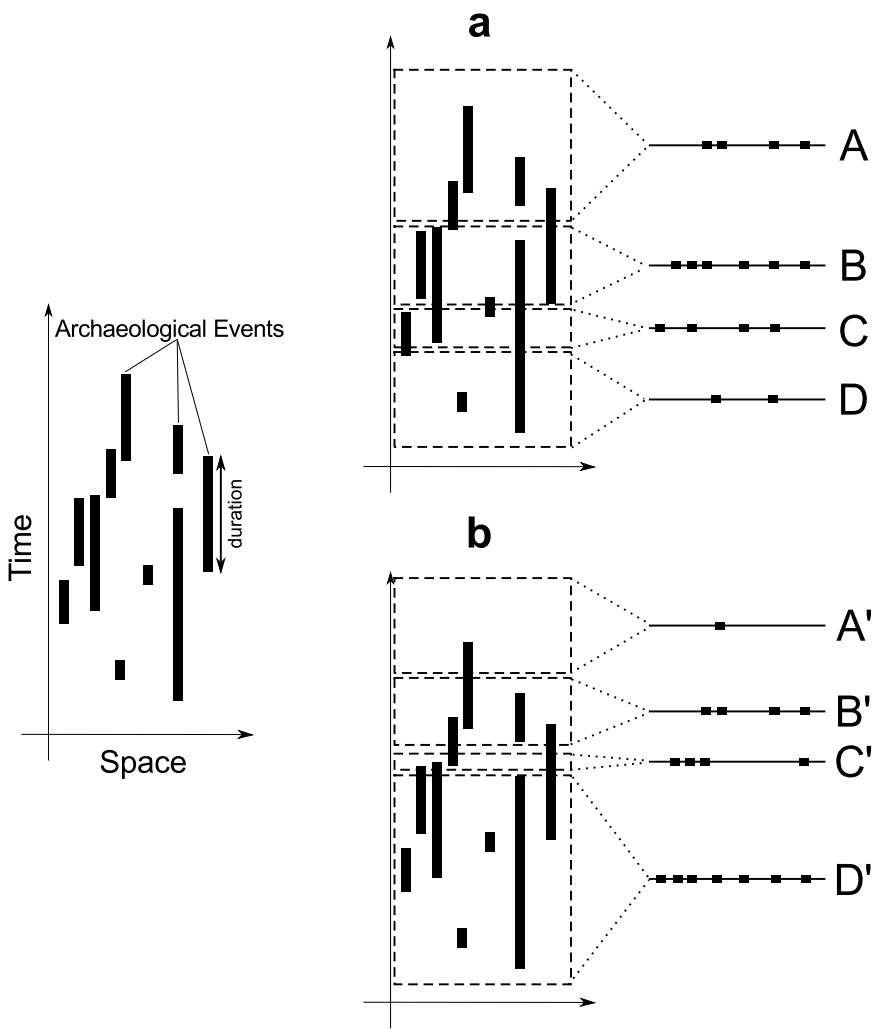

Figure 12: Abstract representation of a spatio-temporal process (left) and the effects derived from different temporal slicing (right top and bottom; **a** and **b**). Archaeological events are portrayed as black bar with specific spatial location (horizontal axis) and a temporal duration (vertical axis). The definition of temporal units are shown as differently sized dashed rectangles, from which snapshots of the spatio-temporal pattern (horizontal line with black squares) are derived. Notice that despite being the same process, different criteria of temporal slicing (**a** and **b**) generates different sequence of spatial patterns (A-B-C-D and A'-B'-C'-D').

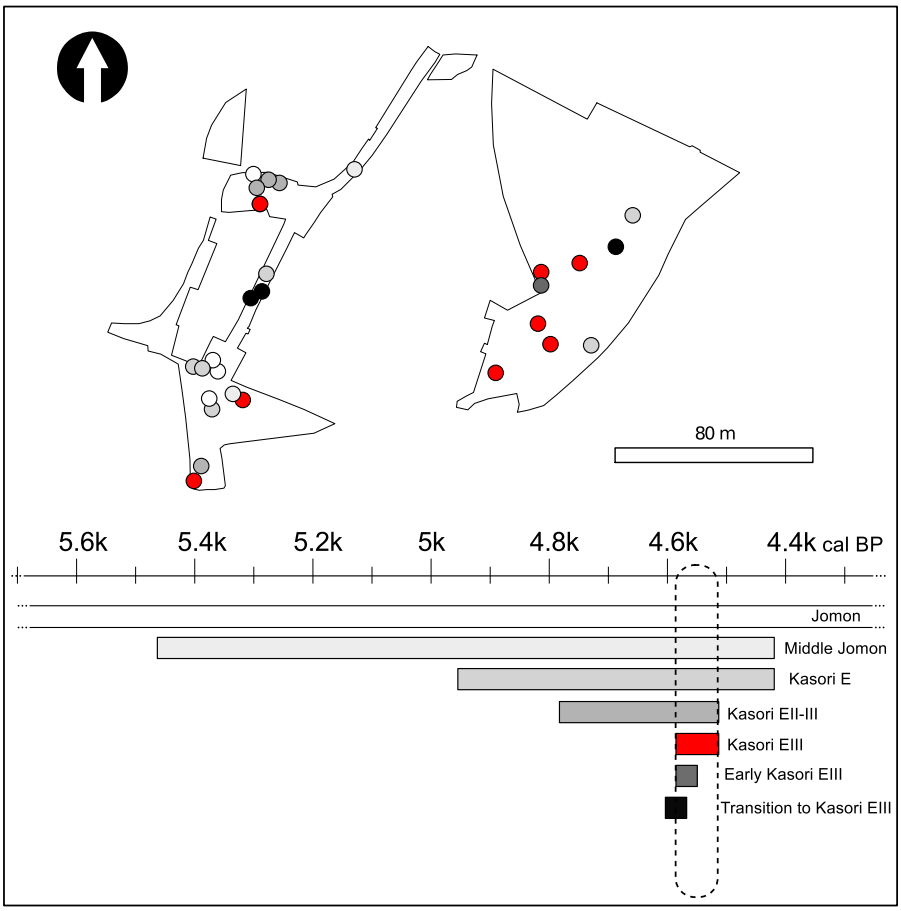

Figure 13: Pithouse locations at *Ariyoshi-minami* site in Chiba with chronological attribution overlapping with *Kasori EIII* phase. Colours of the dots indicate their relative chronology shown in absolute range on the bottom.

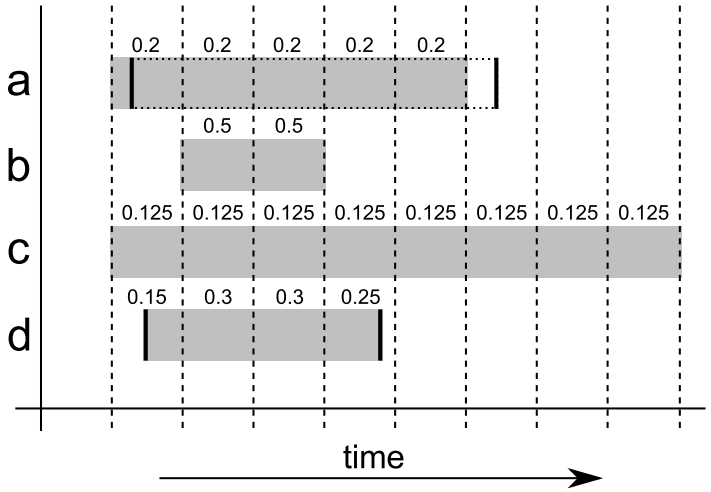

Figure 14: Aoristic analysis of four events (labelled **a**,**b**,**c** and **d**) with their relative *time-spans* shown as grey shaded rectangle, vertical dashed lines depicting the time-blocks, and aoristic weights written above each portion of the time-span. In **a**, the *terminus ante quem* and the *terminus post quem* (vertical solid lines) are rounded to the time-block boundaries, so that the aoristic weight is uniformly distributed within the *time-span* (i.e. 0.2). In **d**, aoristic weights are derived from a continuous uniform distribution, and hence the values will differ and be proportional to the amount of time-span within each time block.

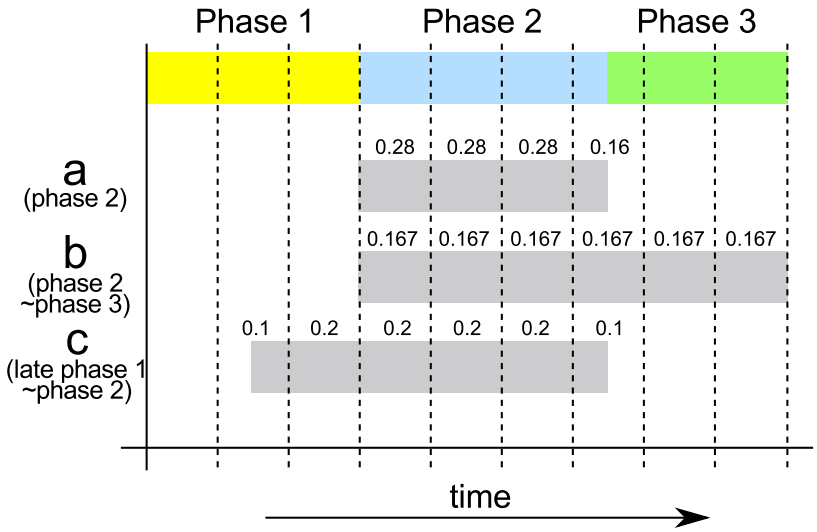

Figure 15: Examples of conversion from relative chronology to aoristic weights (compare with figures 13 and 14). The coloured sequence on the top show the duration of three abutting archaeological phases (phase 1, 2, and 3), while the grey bar shows the time-span of each event. Event **a** is attributed to phase 2, event **b** to both phase 2 and 3, and event **c** to the interval from the second half of phase 1 to the end of phase 2. Numbers above the time-blocks within the time-spans indicate the distribution of aoristic weights for each event.

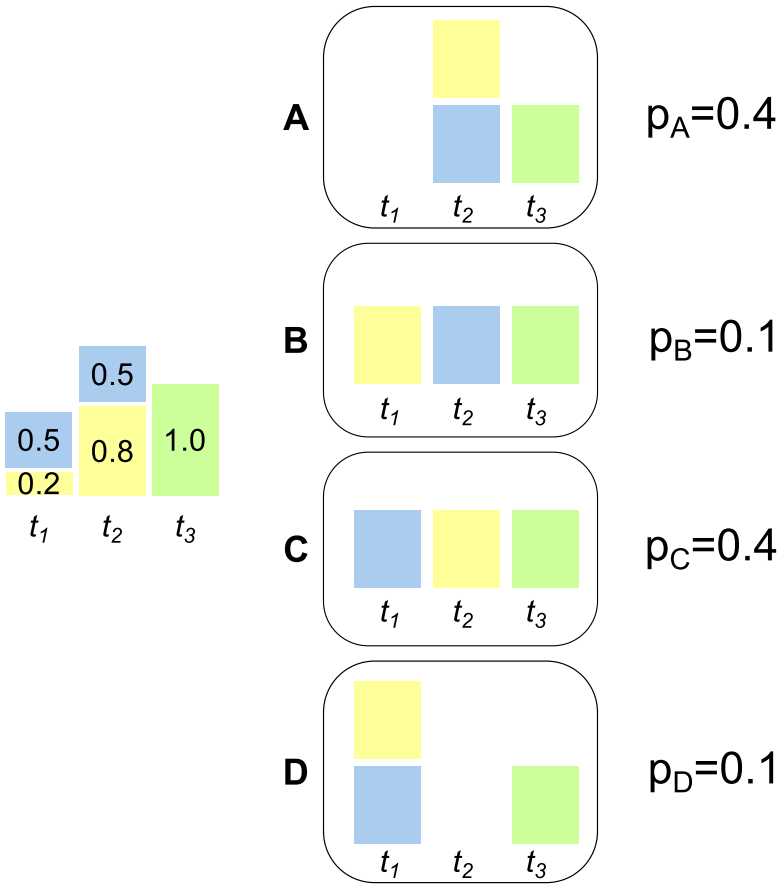

Figure 16: Aoristic sum and diachronic analysis. The left time-series shows the aoristic sum of three events (shown as yellow, green and blue rectangles), while the right four time-series shows four possible scenarios (A,B,C, and D) with their probability of occurrence (p_A, p_B, p_C, and p_D) obtained using the multiplication rule.

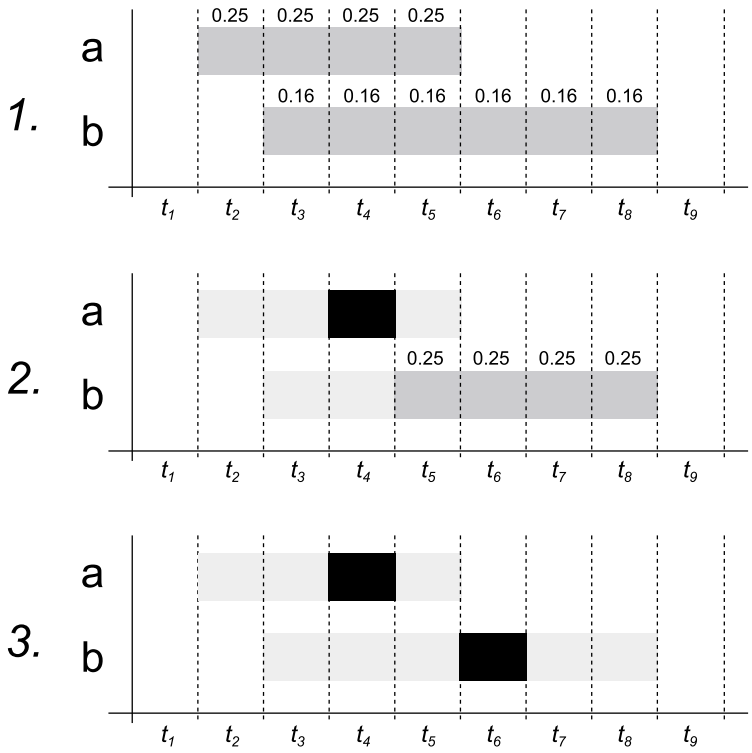

Figure 17: Integrating topological relationships in the Monte Carlo simulation. Event b is known to have occurred *after* a, thus $t_b > t_a$. The time-spans of the two events are shown in the first row. The second row shows a possible simulated value for the event a (t_4), and the consequent updating of the time-span of event b. The last row then shows the simulated time for event b (t_6), which satisfies the required condition $t_b > t_a$.

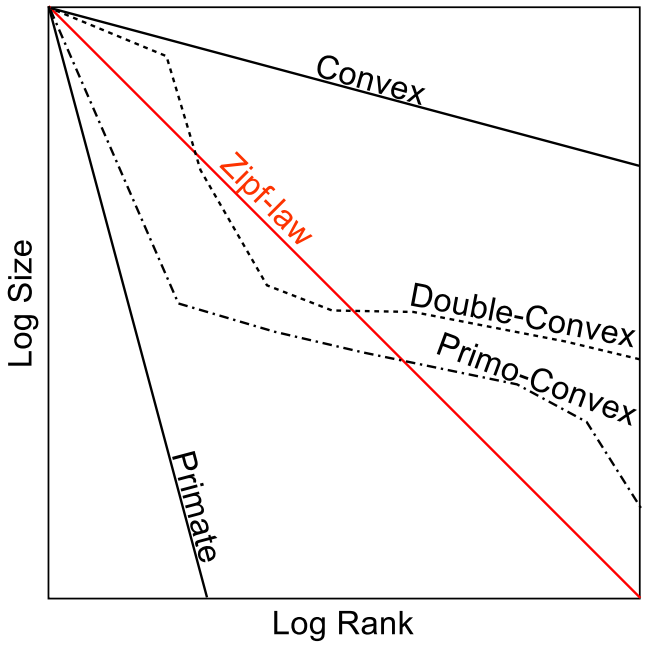

Figure 18: Different type of deviations from the theoretical Zipf's law distribution (modified from Savage 1997)

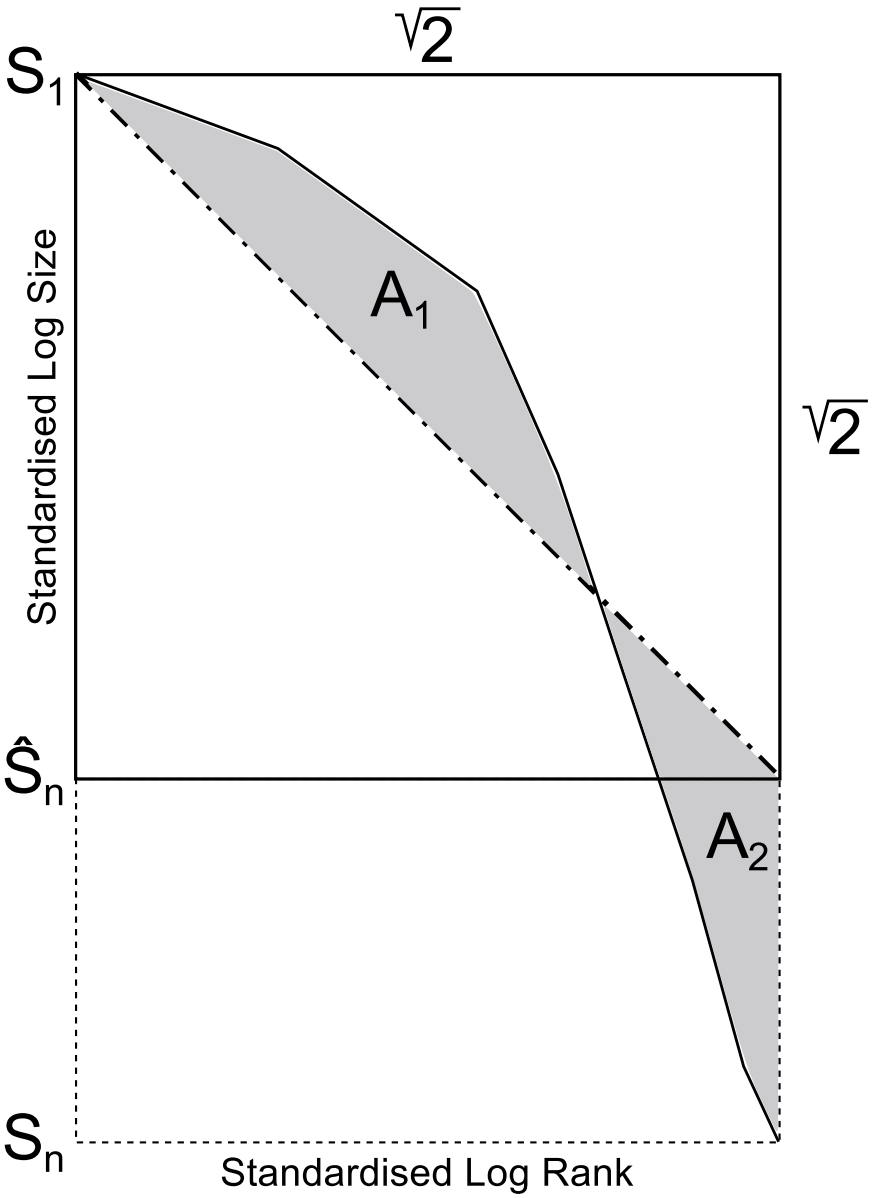

Figure 19: *A* coefficient calculation (see description in the text)

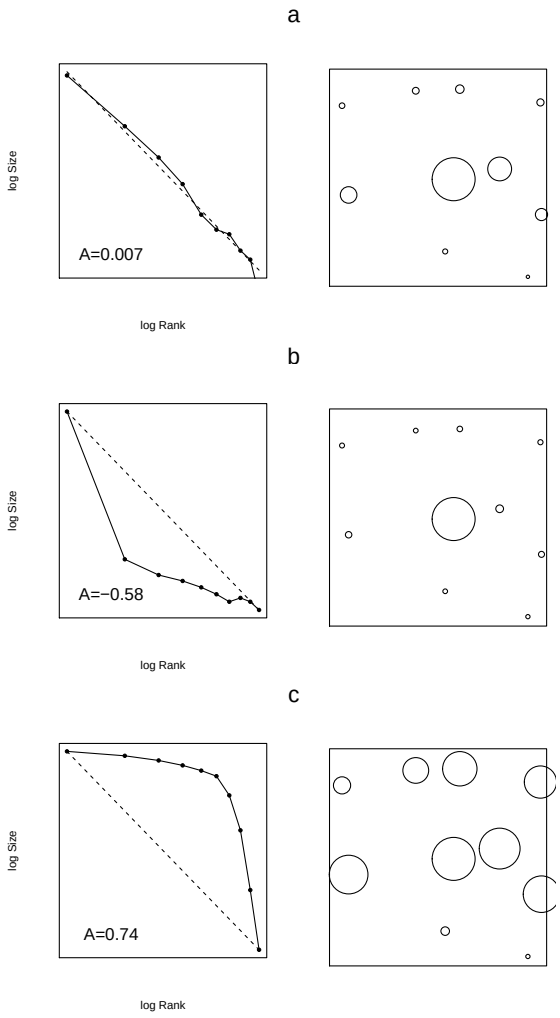

Figure 20: A-coefficient for Zipf's law (**a**), primate/clumped (**b**), and convex/dispersed (**c**) distributions. The left column shows the standardised rank-size plot, the right column shows the location of possible settlements with symbols proportional to their sizes.

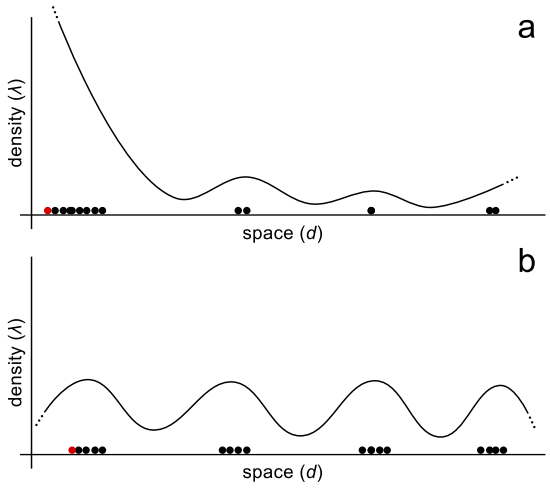

Figure 21: Variation of density over a one-dimensional space portrayed as distance from a focal point (shown as a red point): (**a**) clumped/primate distribution; (**b**) dispersed/convex distribution.

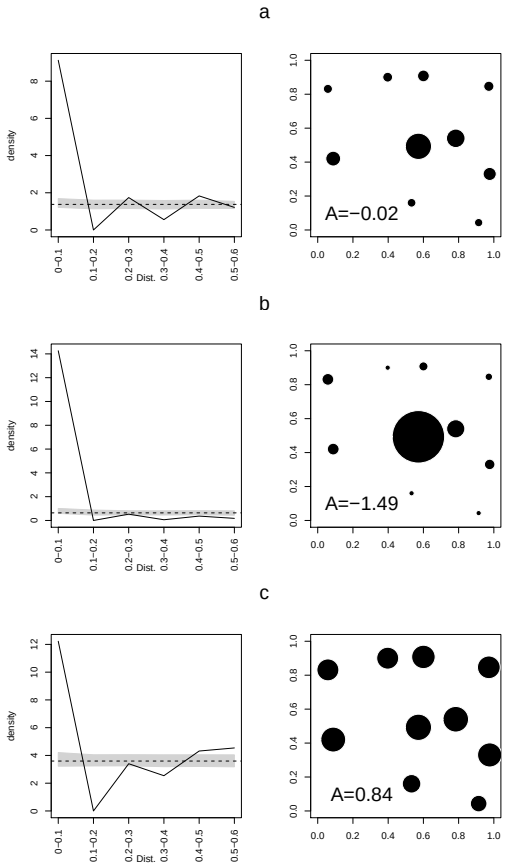

Figure 22: *A* coefficient and O-ring statistics for Zipf's law (**a**), primate/clumped (**b**), and convex/dispersed (**c**) distributions.

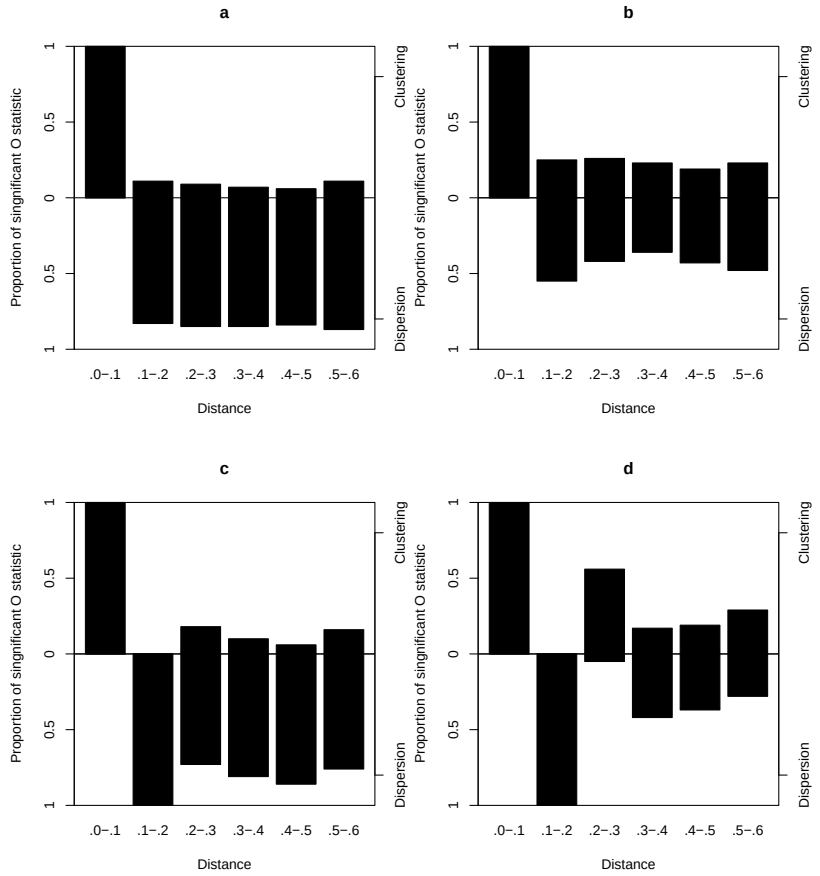

Figure 23: Meta-analysis of O-ring function in relation to different spatial structures and size distributions. Each plot depicts the proportion, among 100 artificial datasets, of significant ($p < 0.05$) clustering (bars above the horizontal line) and dispersion (bars below the line) for different distance intervals: (**a**) primate distribution ($A = -1.49$) with random point pattern; (**b**) convex distribution ($A = 0.88$) with random point pattern; (**c**) primate distribution ($A = -1.49$) with a uniform pattern and an average inter-distance of 0.2; **d** convex distribution ($A = -0.88$) with a uniform pattern and an average inter-distance of 0.2.

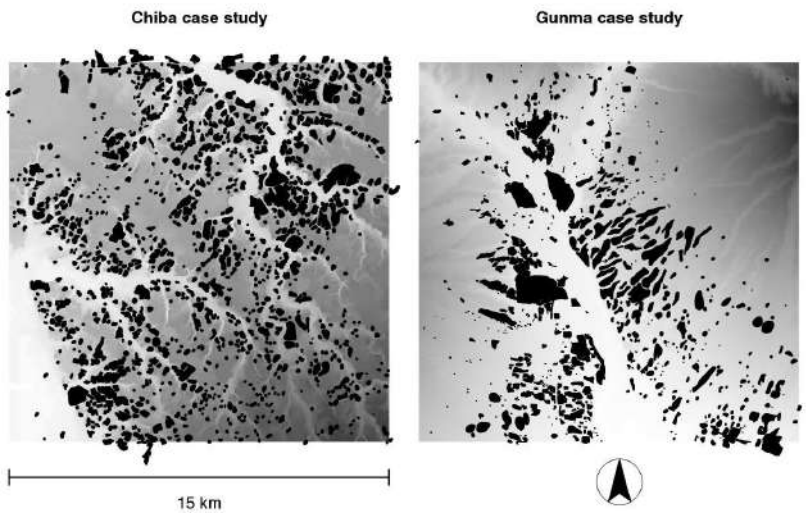

Figure 24: Archaeological site locations (all periods) at the study areas in Chiba and Gunma.

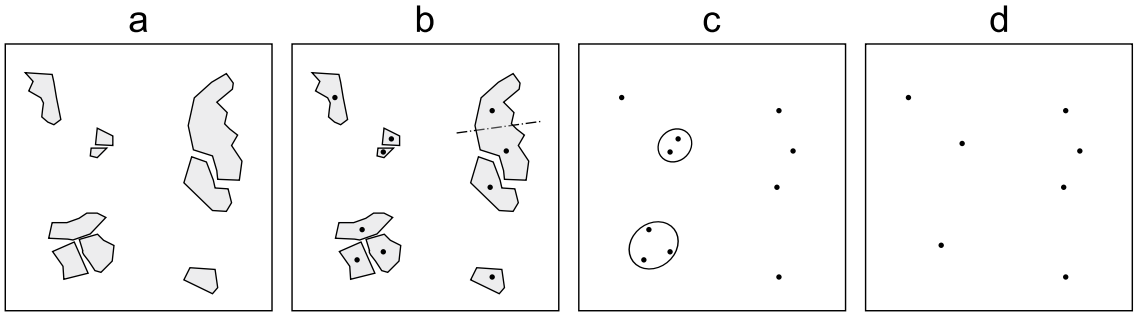

Figure 25: Generation of the basic unit of analysis (BUA) and aggregate unit of analysis (AUA): (**a**) locations of excavation areas; (**b**) definition of the BUA; (**c**) DBSCAN clustering; and (**d**) definition of the AUA.

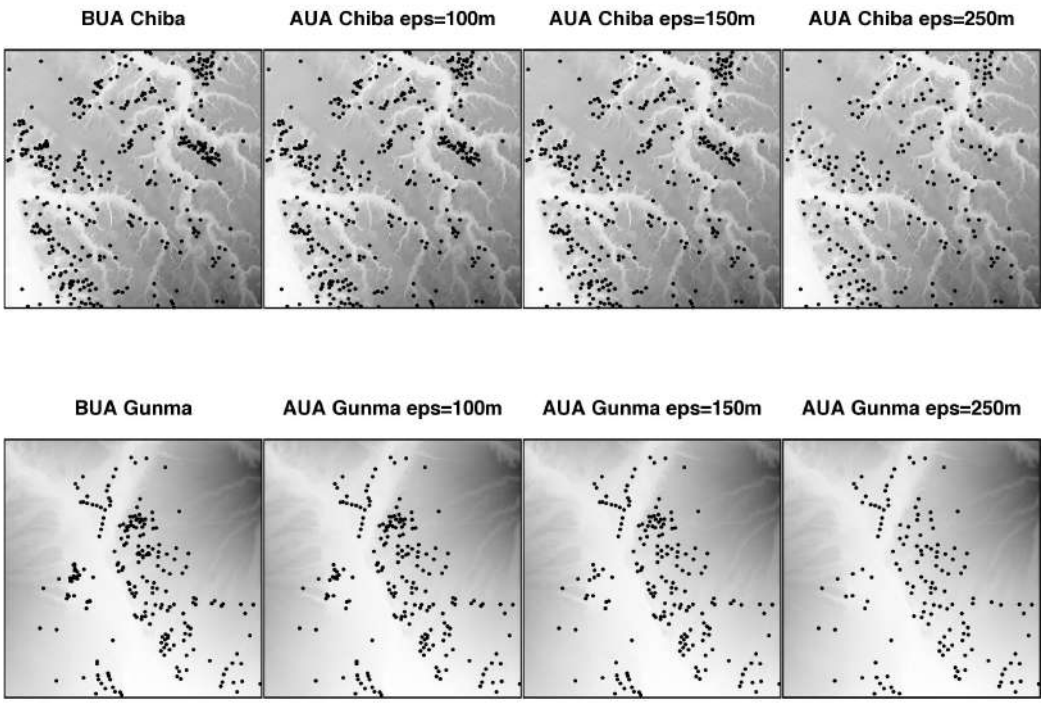

Figure 26: BUA and AUA of Chiba and Gunma with different values of *eps*.

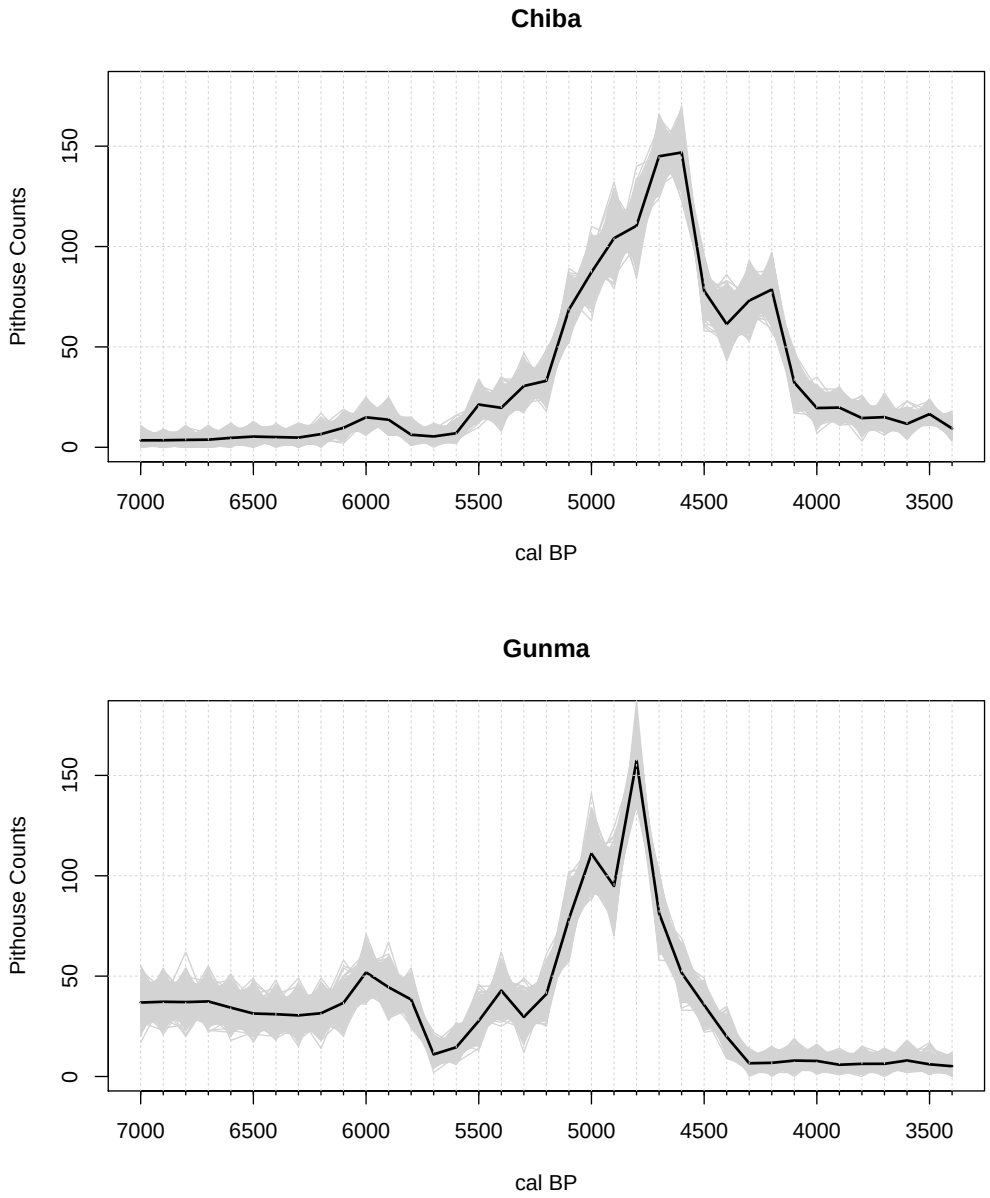

Figure 27: Time-series of pithouse counts for Chiba (n=1418) and Gunma (n=1432). Grey lines indicate each run of the Monte-Carlo simulation, while the black solid line shows the most typical (average) time-series.

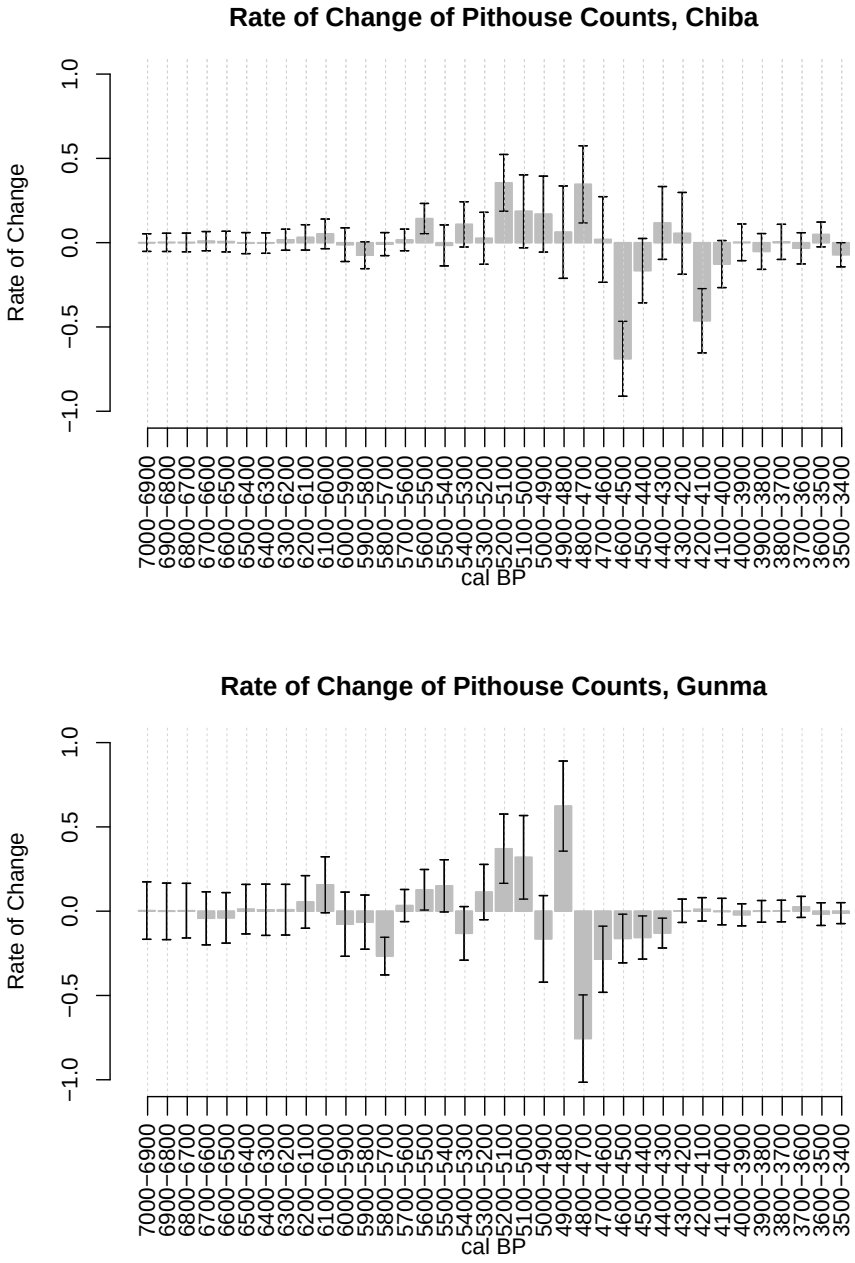

Figure 28: Rate of change analysis for the pithouse counts in Chiba and Gunma. The error-bars indicate the confidence envelope at 95%. Dates in the x-axis refer to the initial dates of each pair of time-blocks.

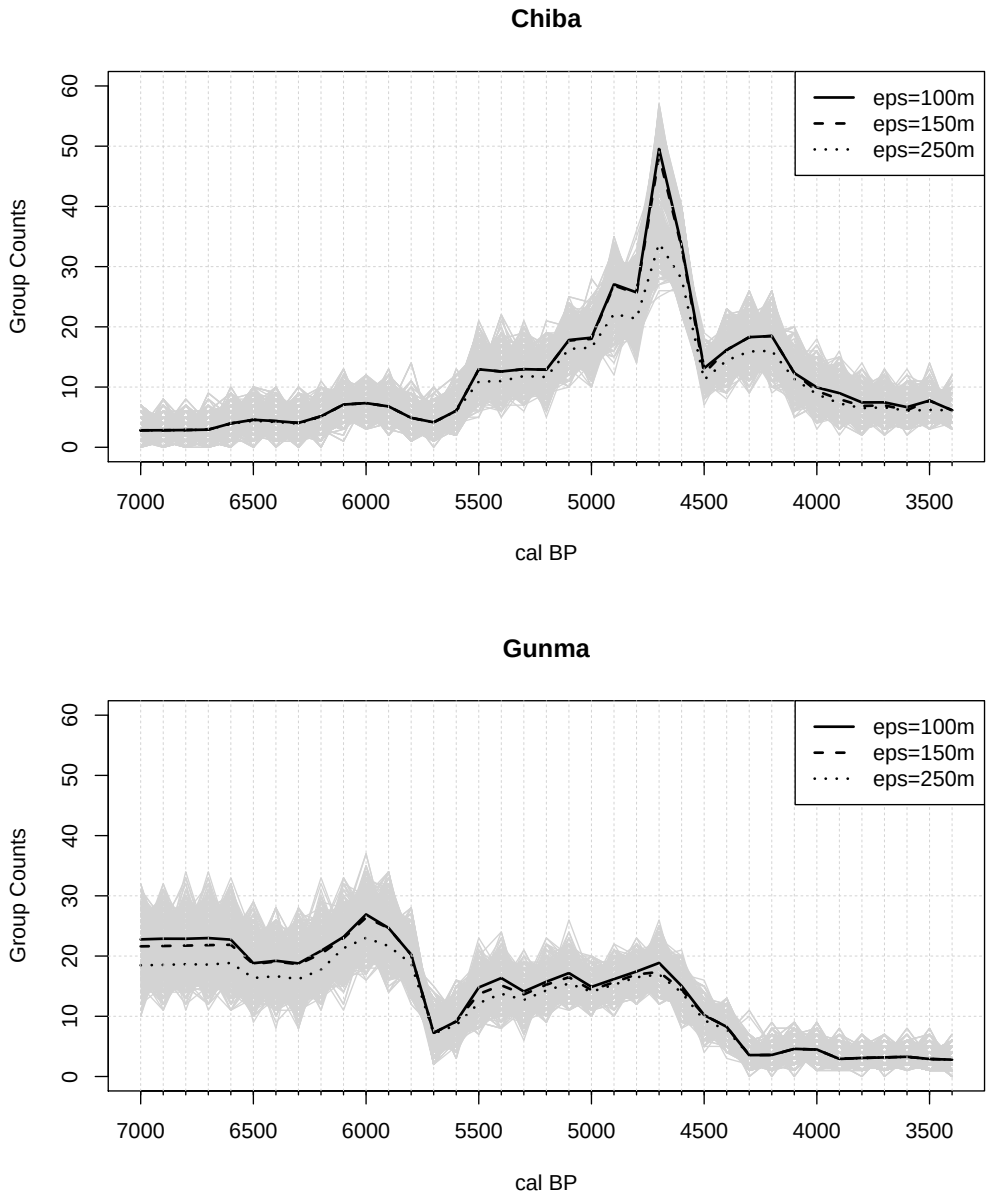

Figure 29: Time-series of group counts for Chiba and Gunma, with three different *eps* settings (100, 150, and 250 meters). Grey lines indicate each run of the Monte-Carlo simulation for all three settings, while solid, dashed, and dotted lines show the most typical (average) time-series for each *eps* value.

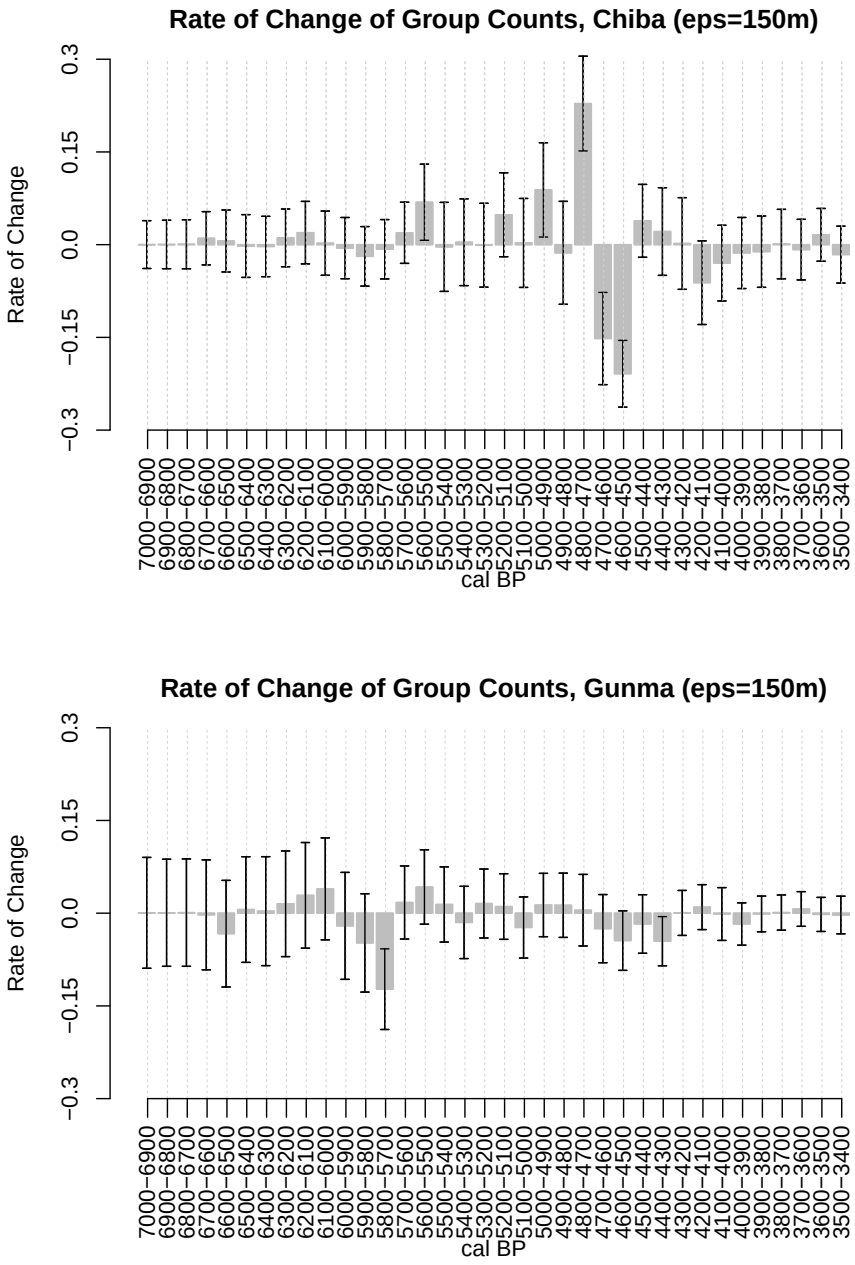

Figure 30: Rate of change analysis for the groups counts in Chiba and Gunma with *eps*=150 meters. The error-bars indicate the confidence envelope at 95%. Dates in the x-axis refers to the initial dates of each pair of time-blocks.

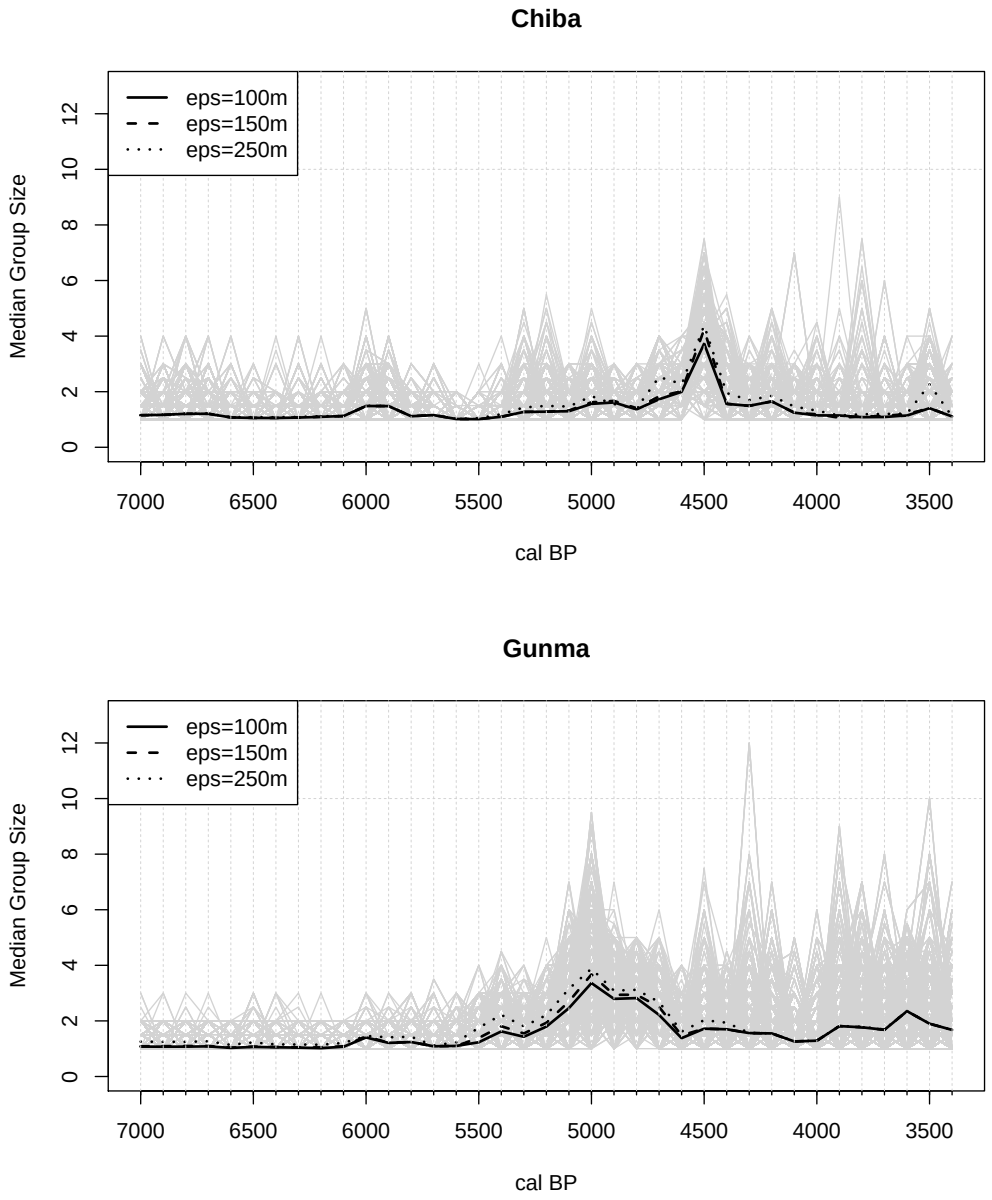

Figure 31: Time-series of the median group size for Chiba and Gunma, with three different *eps* settings (100, 150, and 250 meters). Grey lines indicate each run of the Monte-Carlo simulation for all three settings, while the solid, dashed, and dotted lines show the most typical (average) time-series for each *eps* value.

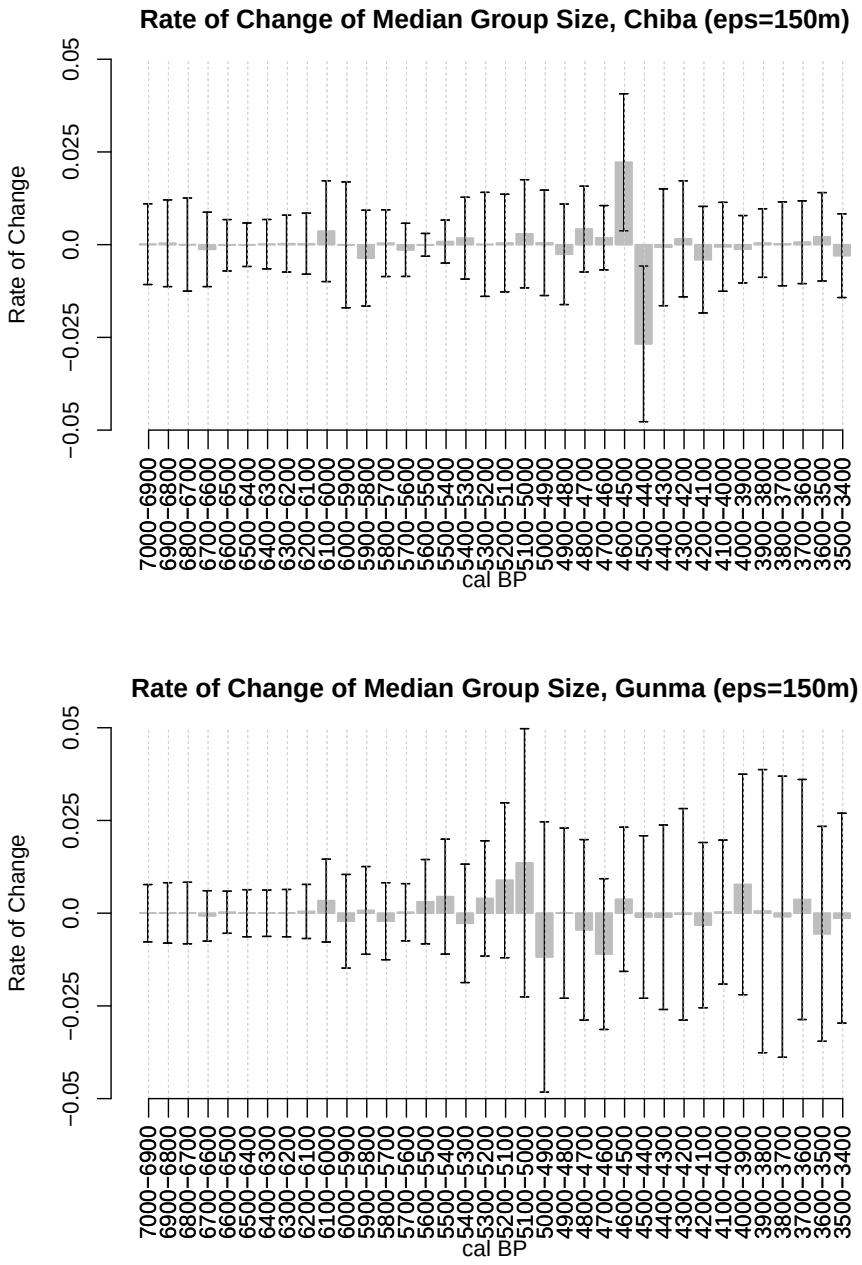

Figure 32: Rate of change analysis for the median group size in Chiba and Gunma with *eps*=150 meters. The error-bars indicate the confidence envelope at 95%. Dates in the x-axis refer to the initial dates of each pair of time-blocks.

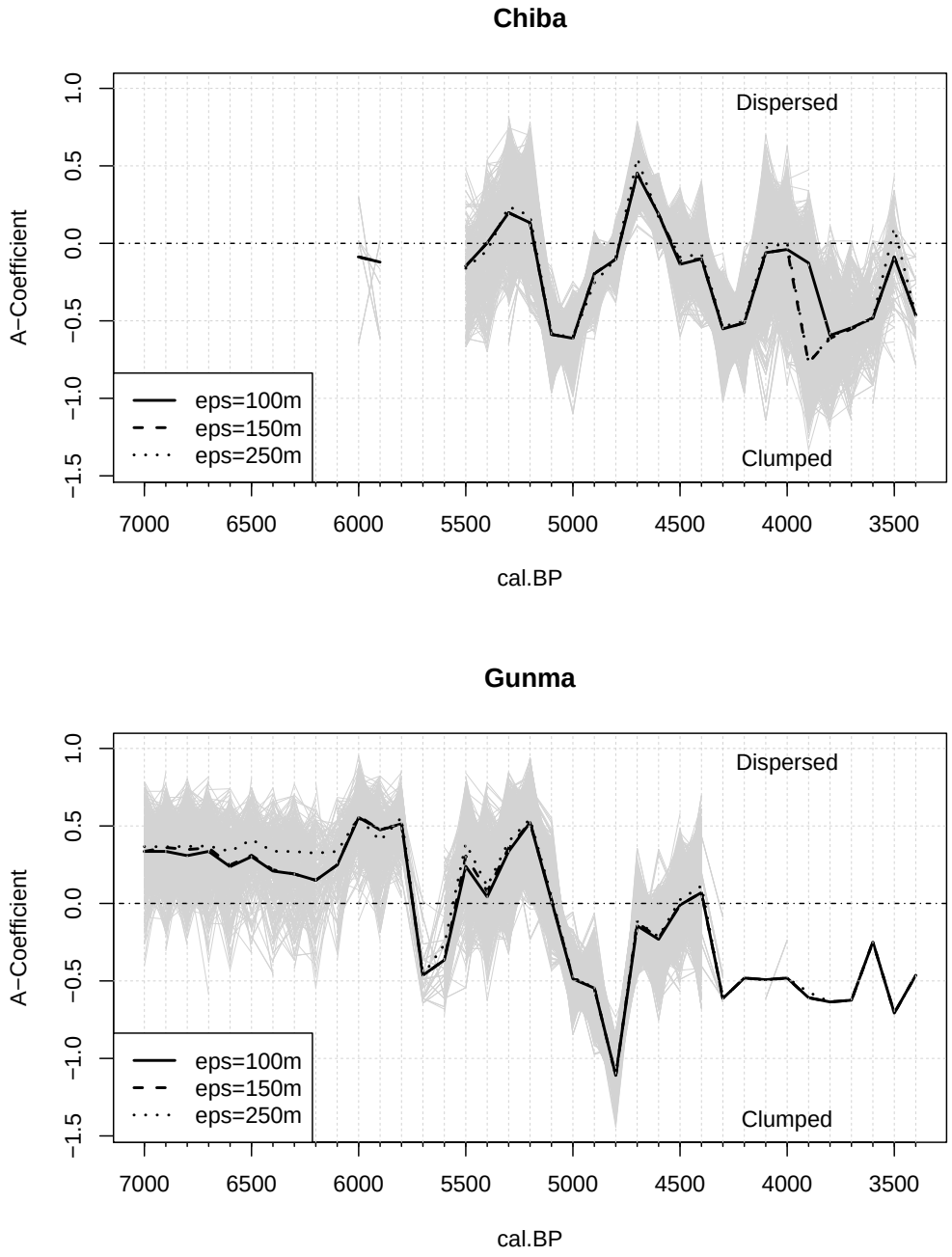

Figure 33: Time-series of the *A*-coefficient for Chiba and Gunma, with three different *eps* settings (100, 150, and 250 meters). Grey lines indicate each run of the Monte-Carlo simulation for all three settings, while the solid, dashed, and dotted lines shows the most typical (average) time-series for each *eps* value.

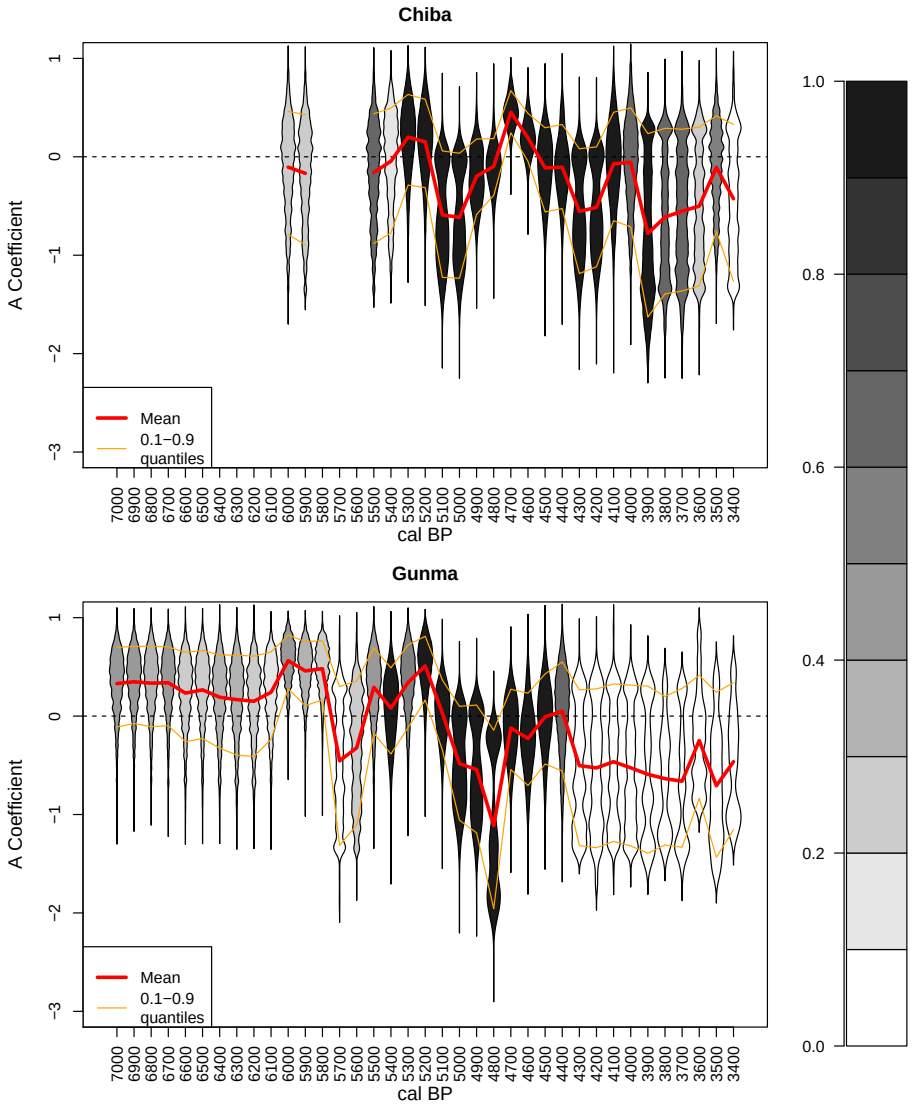

Figure 34: Violin plot of the bootstrapped version of the *A*-coefficient analysis. The fill colour indicates the proportion of successfully computed *A*-coefficients, the solid red line the mean and the dotted line the 0.1 and 0.9 quantiles.

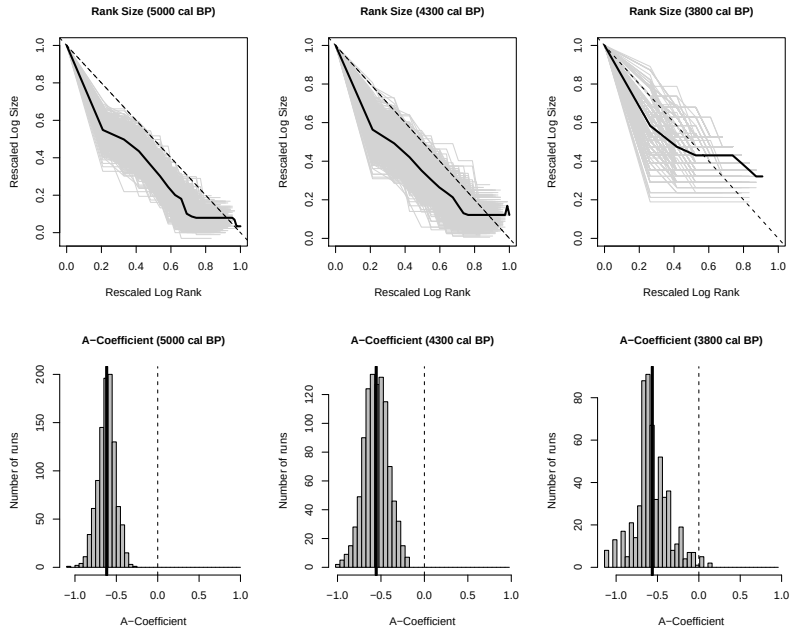

Figure 35: Cumulative rank-size plot and frequency distribution of A-coefficients for at Chiba for t_{5000} , t_{4300}, and t_{3800}

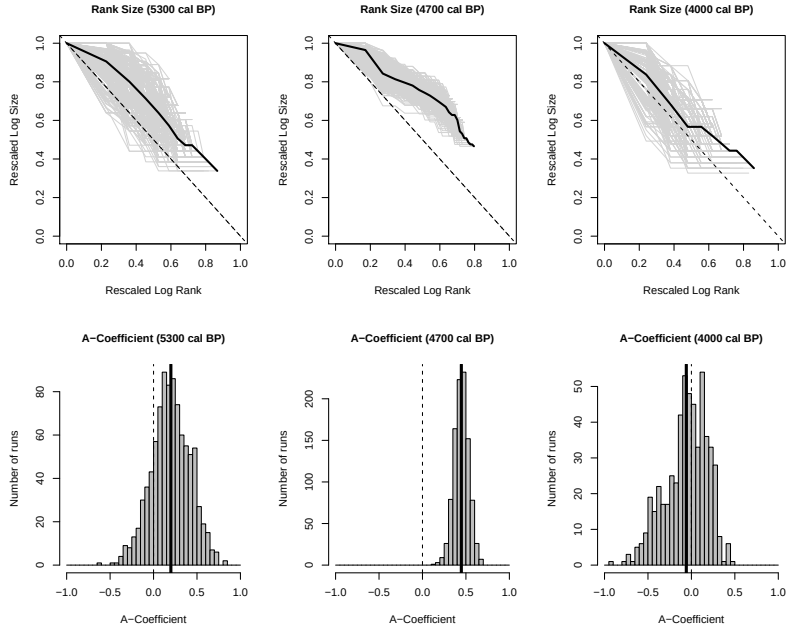

Figure 36: Cumulative rank-size plot and frequency distribution of A-coefficients for at Chiba for t_{5300} , t_{4700}, and t_{4000}

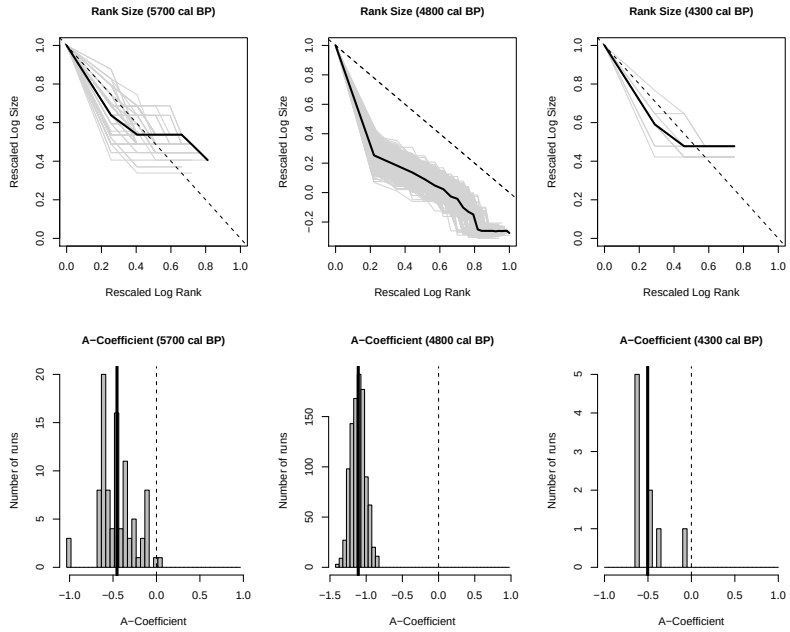

Figure 37: Cumulative rank-size plot and frequency distribution of A-coefficients for at Gunma for t_{5700}, t_{4800}, and t_{4300}

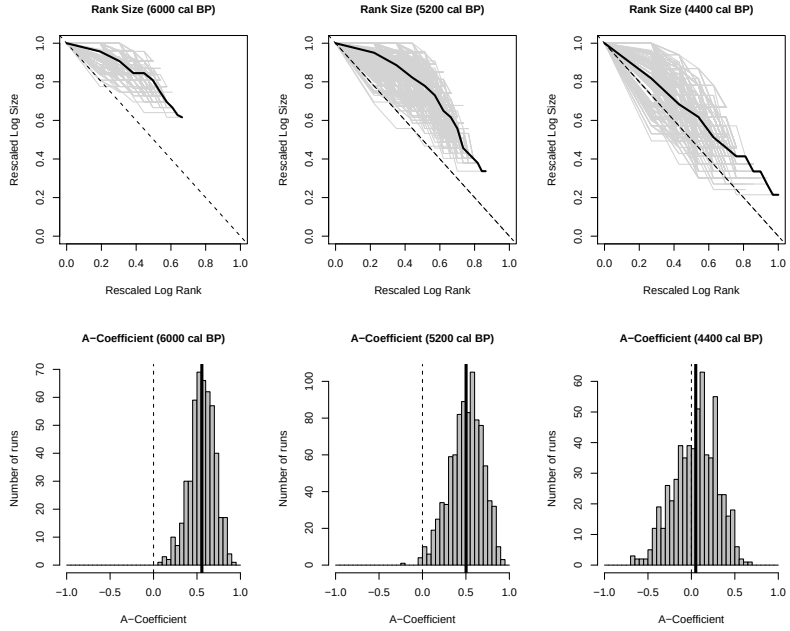

Figure 38: Cumulative rank-size plot and frequency distribution of A-coefficients for at Gunma for t_{6000}, t_{5200}, and t_{4400}

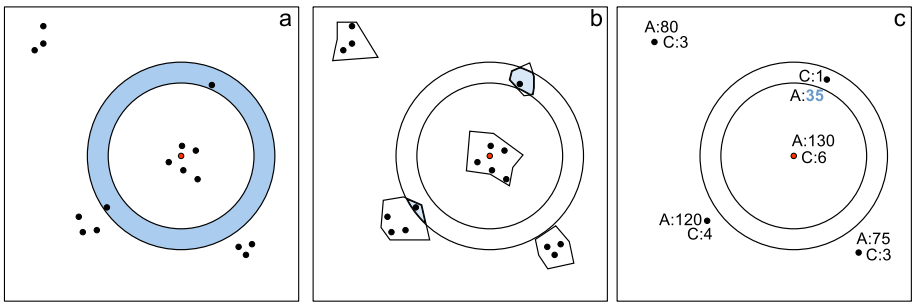

Figure 39: Standard, modified, and marked versions of the O-ring statistic. The density of the neighbour point is calculated using: (**a**) the area of the annulus defined by d_1 and d_2; (**b**) the intersection area between the annulus defined by d_1 and d_2, and the polygonal windows of analysis; and (**c**) marked values of the area (**A**) associated with point locations within the annulus defined by d_1 and d_2 (with **C** indicating the number of points there).

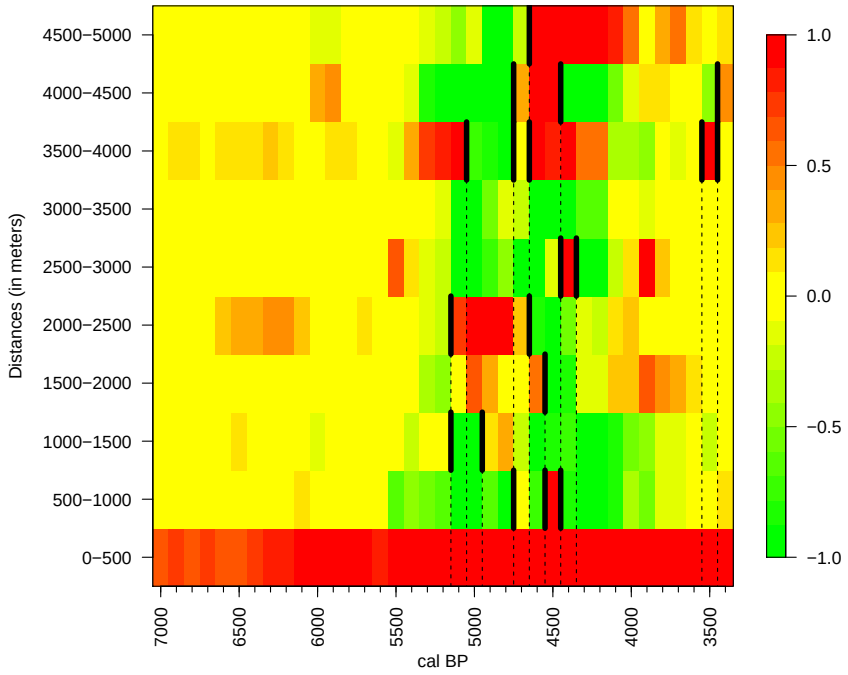

Figure 40: Matrix of $\Delta_{CD}(d_1, d_2, t)$ for Chiba. The black vertical bars indicates transitions where $|\Delta_{CD}(d_1, d_2, t) - \Delta_{CD}(d_1, d_2, t+1)| \geq 0.95$.

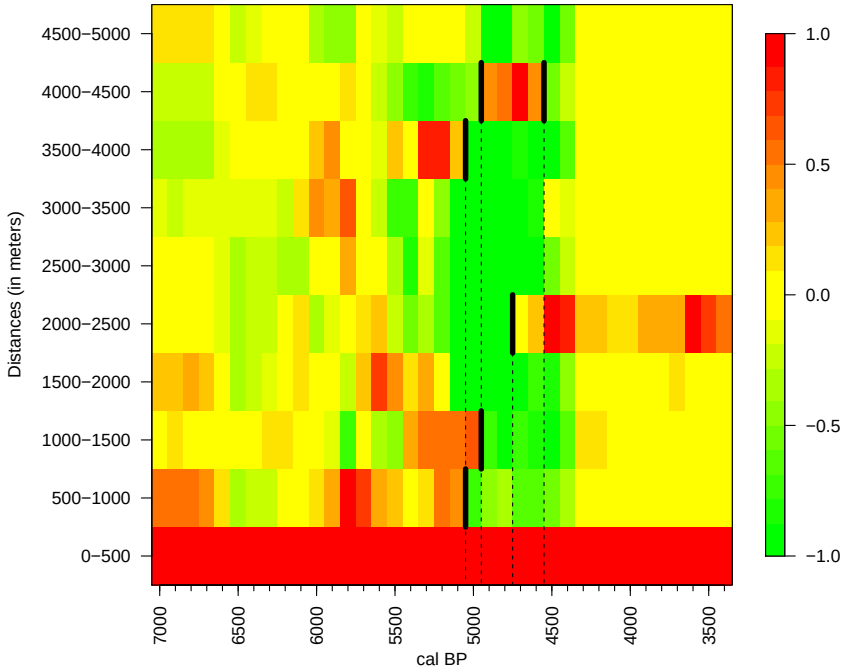

Figure 41: Matrix of $\Delta_{CD}(d_1, d_2, t)$ for Gunma. The black vertical bars indicates transitions where $|\Delta_{CD}(d_1, d_2, t) - \Delta_{CD}(d_1, d_2, t+1)| \geq 0.95$.

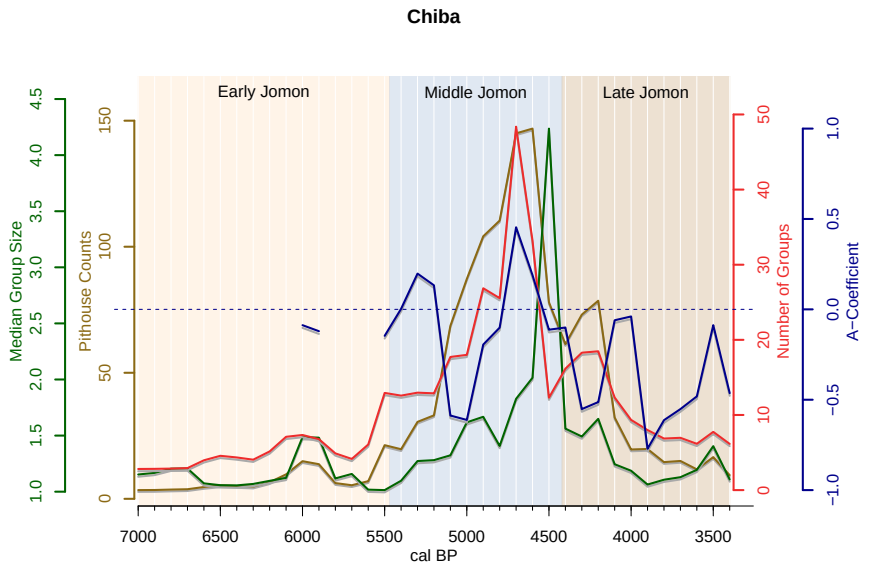

Figure 42: Comparative time-series of mean pithouse counts (brown), number of groups (red), median group size (green) and *A*-coefficient (blue) in Chiba.

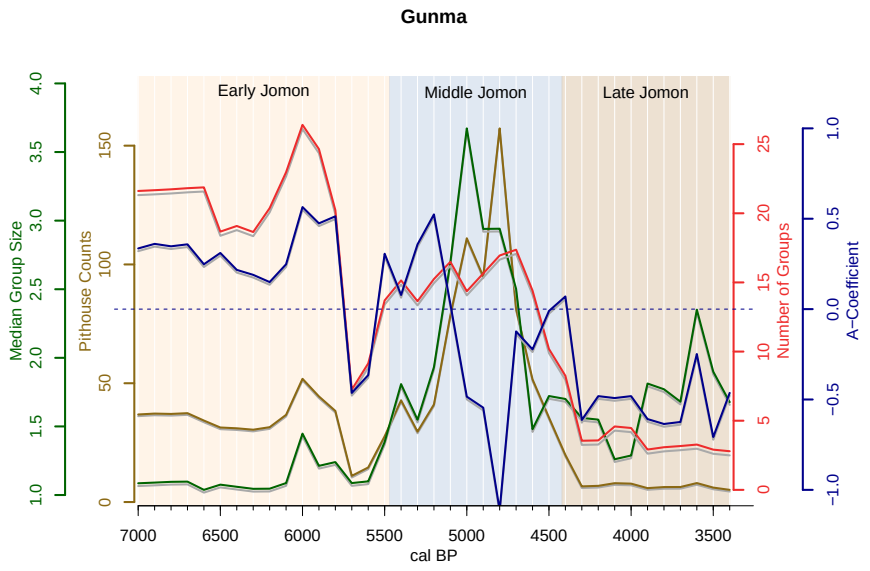

Figure 43: Comparative time-series of mean pithouse counts (brown), number of groups (red), median group size (green) and *A*-coefficient (blue) in Gunma.

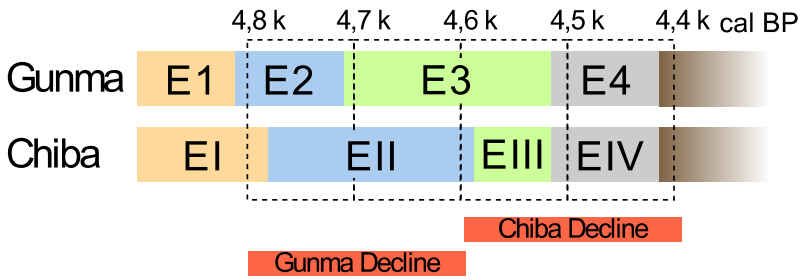

Figure 44: Timing of the pithouse count decline and the relative pottery sequence in Chiba and Gunma.

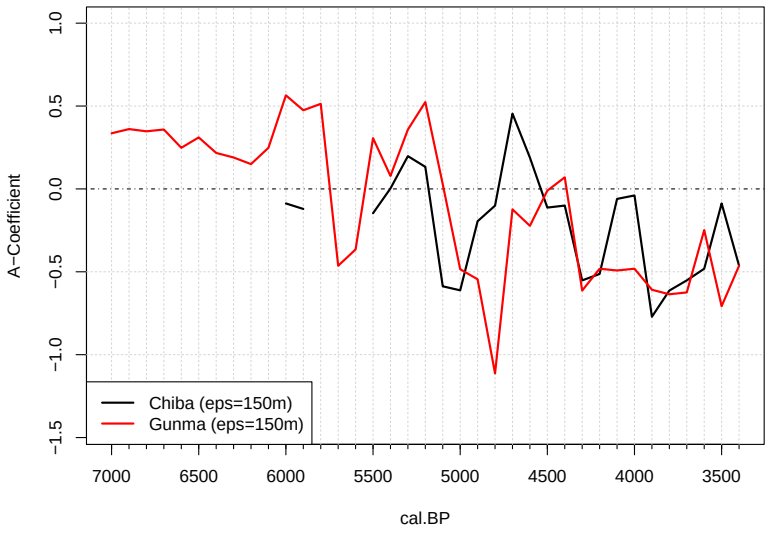

Figure 45: Comparison of the average A-coefficients between the two case studies (with *eps*=150m)

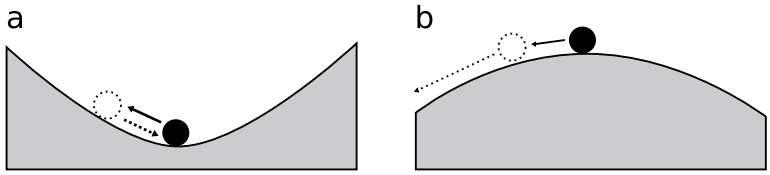

Figure 46: Convex (**a**) and non-convex (**b**) systems. In the former case, small perturbations (solid arrow) during the initial stages of a system (solid circle) determine a shift of the system state (hollow circle) which however recovers immediately returning to its original state (dashed arrow). In the latter case, similar small fluctuations are sufficient to determine a transition of the system into a new state (*after* Arthur 1988, fig.6).

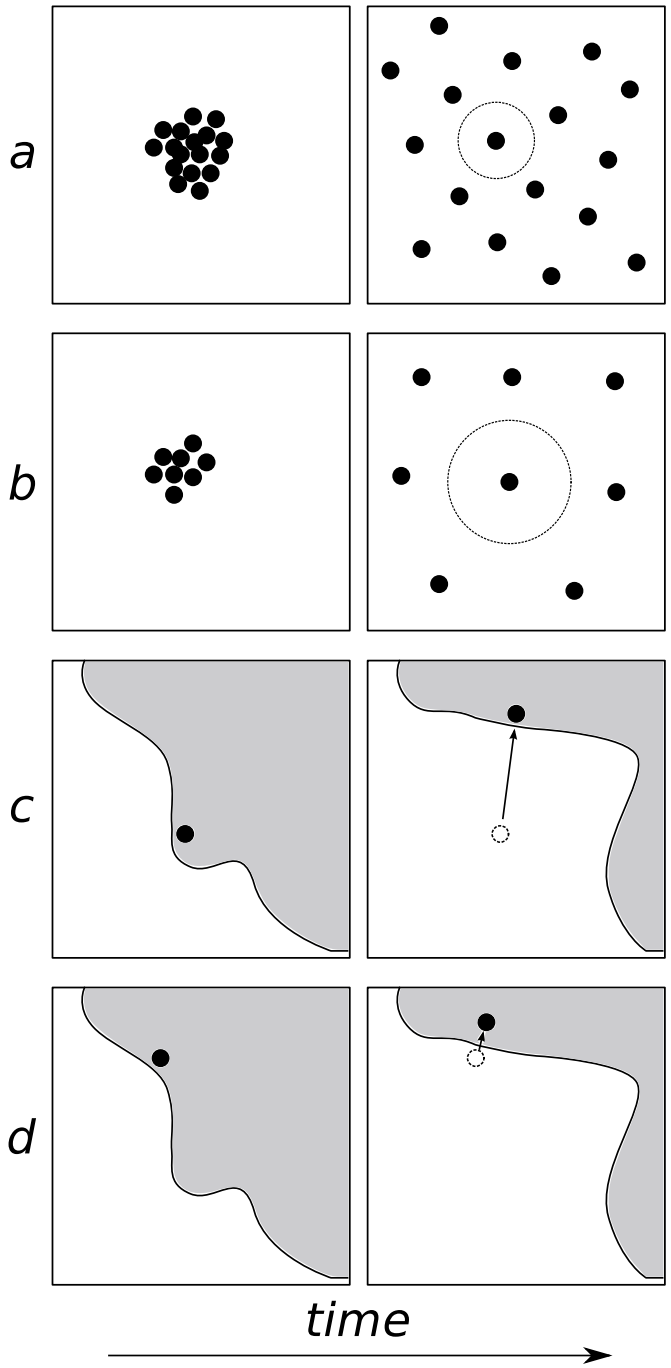

Figure 47: Effects of density (**a**,**b**) and spatial inheritance (**c**,**d**). See text for description.

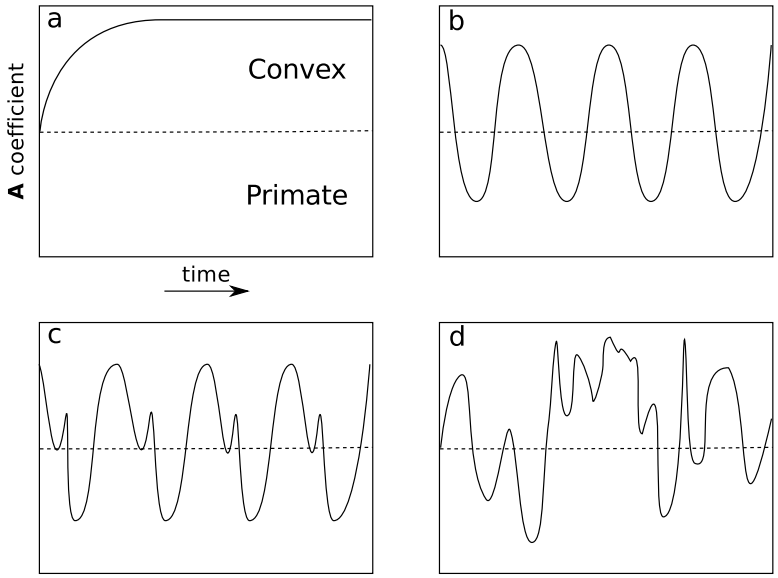

Figure 48: Four different types of dynamics for the change in the settlement size distribution: (**a**) Asymptotically reach a convex distribution (point attractor); (**b**) Periodically fluctuate between convex and primate distributions (limit-cycle attractor); (**c**) Quasi-periodically fluctuate between convex and primate patterns (toroidal attractor); (**d**) Chaotically change between primate and convex patterns (strange attractor).

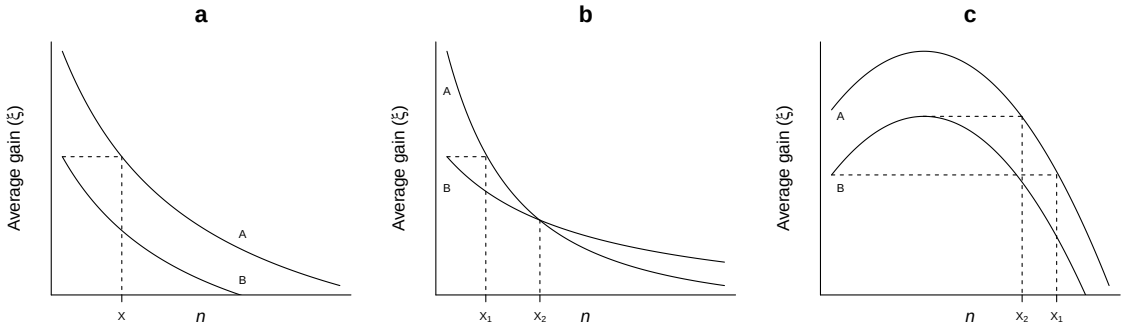

Figure 49: Graphical depiction of the ideal free distribution with: (**a**) negative frequency dependence (Eq. 5.2); (**b**) negative frequency dependence with interference (Eq. 5.3); and (**c**) Allee effect (Eq. 5.4). Further details can be found in the text.

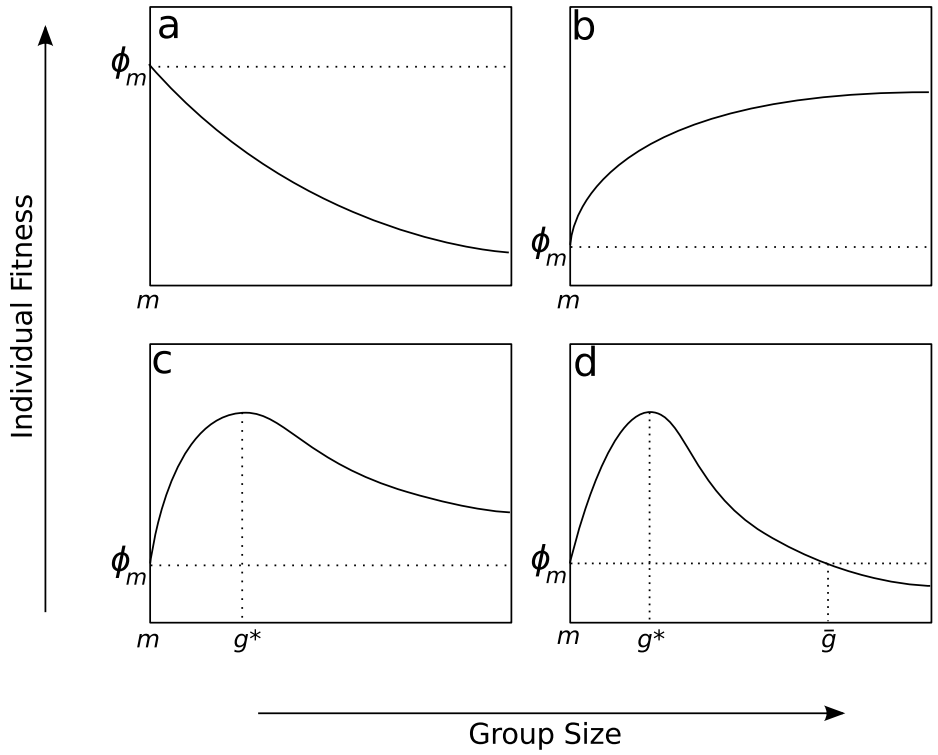

Figure 50: Four different shapes of the fitness function $\phi(g)$: (**a**) Decreasing fitness function; (**b**) Increasing fitness function; (**c**) Unimodal function with $\phi(\infty) \geq \phi(m)$ (**d**) Unimodal function with $\phi(\infty) < \phi(m)$; (modified from Clark and Mangel 1986)

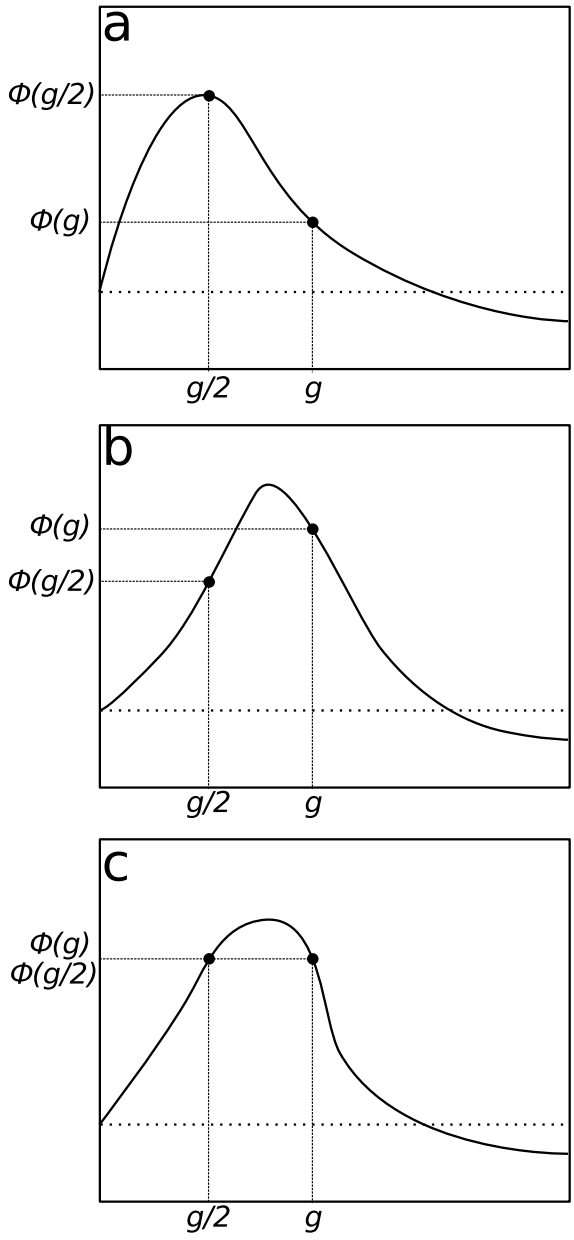

Figure 51: Variations in fitness after a group fission with $q = g/2$ under the assumption of different fitness curves: (**a**) fission provides an increase in fitness ($\phi(g/2) > \phi(g)$); (**b**) fission determines a decrease in fitness ($\phi(g/2) < \phi(g)$); fission does not determine any change in the fitness ($\phi(g/2) = \phi(g)$)

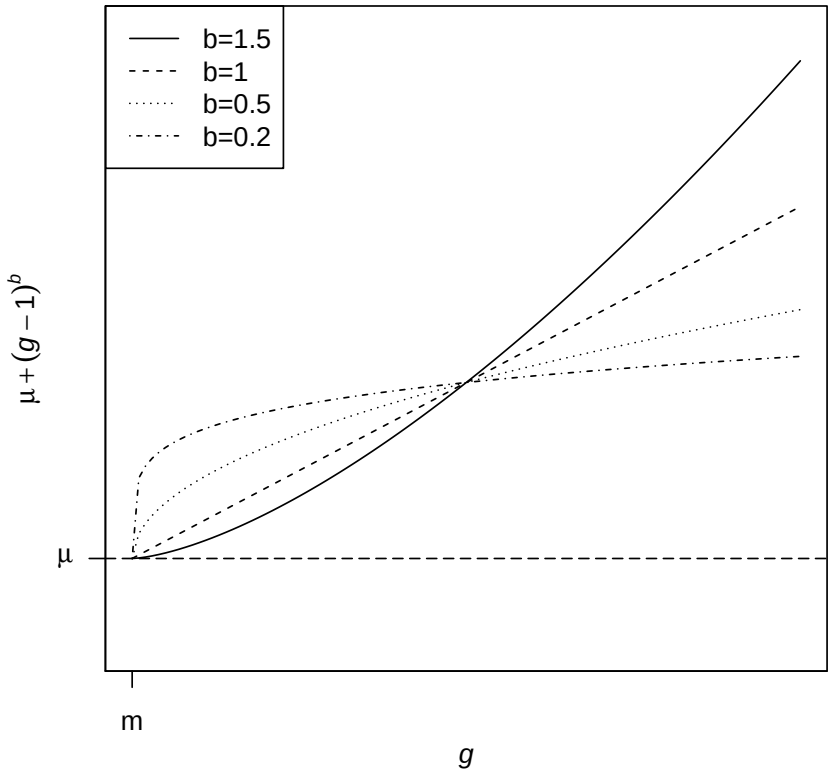

Figure 52: Variation of $\mu + (g-1)^b$ as function of the group size g and the cooperation parameter b. When $b = 1$, the growth is linear, when $b < 1$, the rate of change of $\mu + (g-1)^b$ decreases as a function of g, while when $b > 1$ the rate of change increases as the group size becomes bigger.

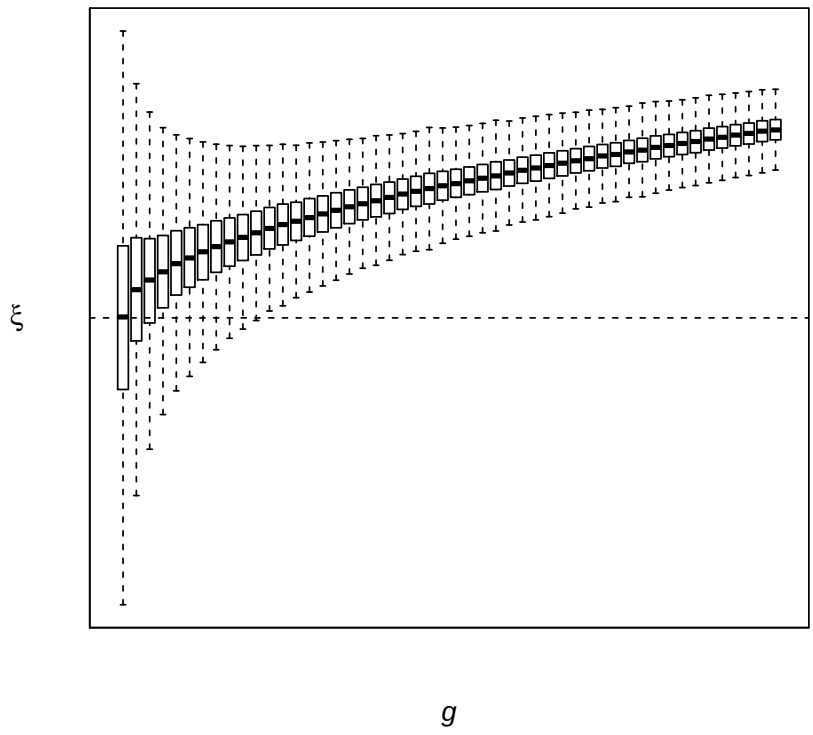

Figure 53: Box-plot showing the distribution of ξ and how this is affected by increased group size (data obtained from 10,000 simulation runs, with g between 1 and 50, $\epsilon = 4$, $\mu = 10$ and $b = 0.5$).

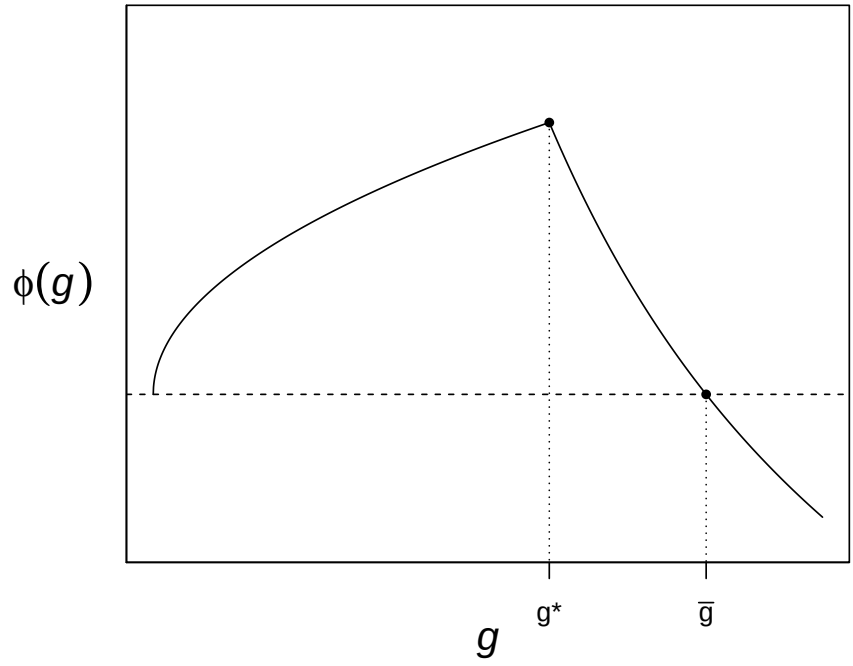

Figure 54: Fitness curve of equation 5.8. For simplicity ϵ is set to 0.

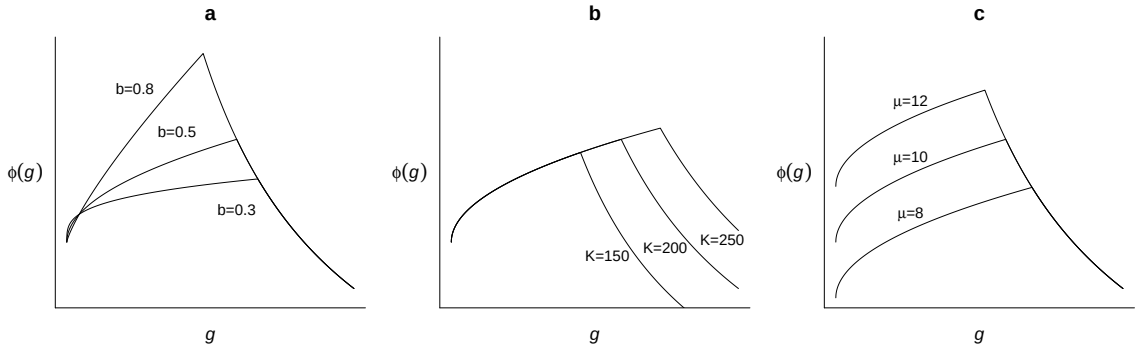

Figure 55: Variation of the fitness curve as function of its main parameters: (**a**) effect of the cooperation parameter b; (**b**) effect of the resource input size K; and (**c**) effect of the basic fitness μ.

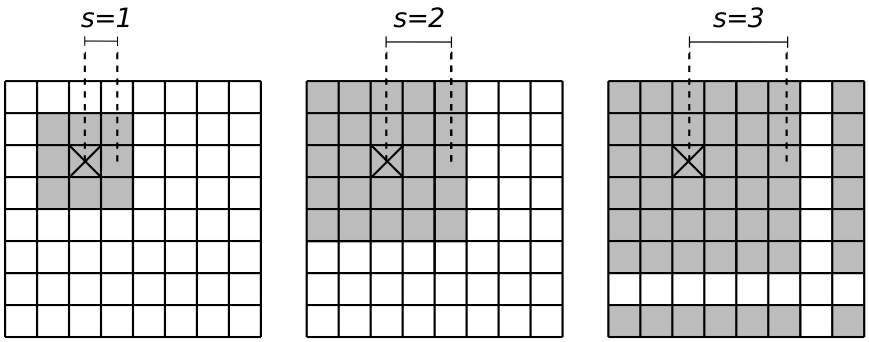

Figure 56: Three different values of s expressed in grid-cell size (Chebyshev distance) from the location of the focal agent (marked with an X). The grey shaded area is within distance s. Notice that in case of $s = 3$, the toroidal nature of the landscape can be observed, with the grey shaded area appearing on the other ”side” of the grid.

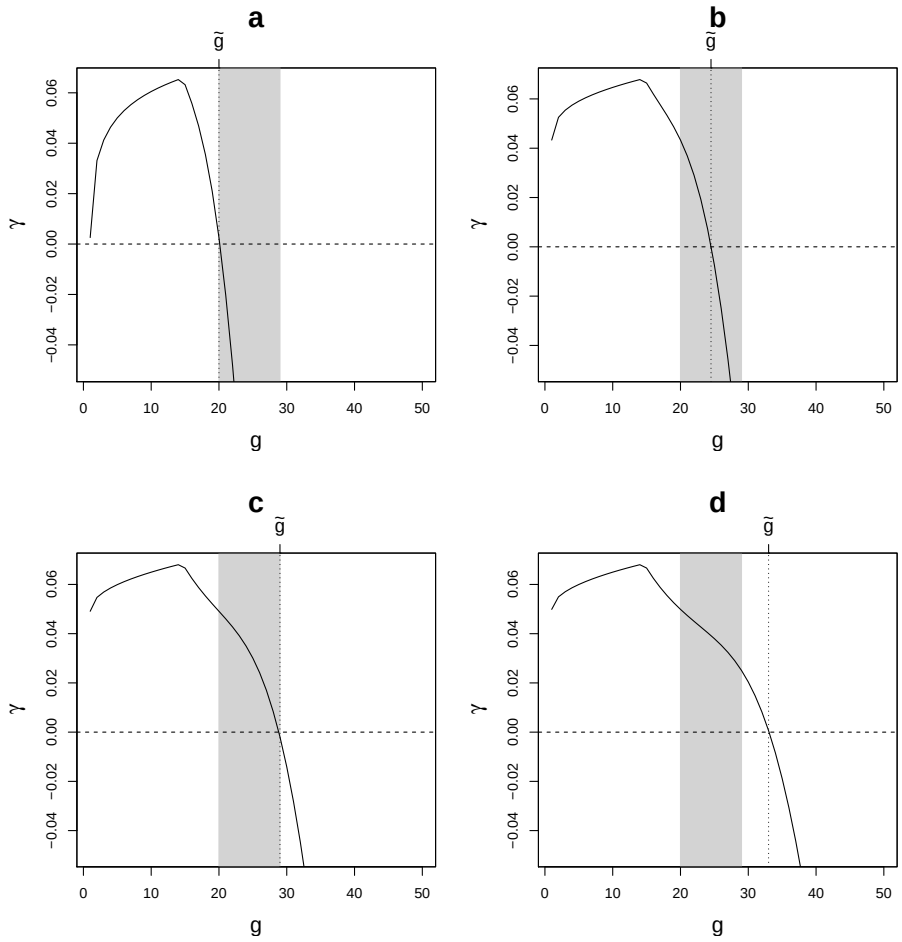

Figure 57: Four types of relation between critical values of g. The grey shaded areas represent the interval between $\bar{g}$ and $\breve{g}$, while the vertical line is located at the value of g when $\gamma = 0$ ($\tilde{g}$). In (**a**), $\tilde{g} = \bar{g}$, in (**b**) $\breve{g} > \tilde{g} > \bar{g}$, in (**c**) $\tilde{g} = \breve{g}$ and in (**d**) $\tilde{g} > \breve{g}$. The net growth rate curve has been derived from a fitness curve with the following parameters: $m = 1$, $\mu = 10$, $b = 0.5$, $K = 200$ and $c_1 = 3$. Variation of the net growth rate curve has been conducted by fixing $\rho = 0.05$ and $\omega_2 = 5$ and by sweeping ω_1 through 0.8 (**a**), 1.0 (**b**) ,1.2 (**c**) and 1.4 (**d**).

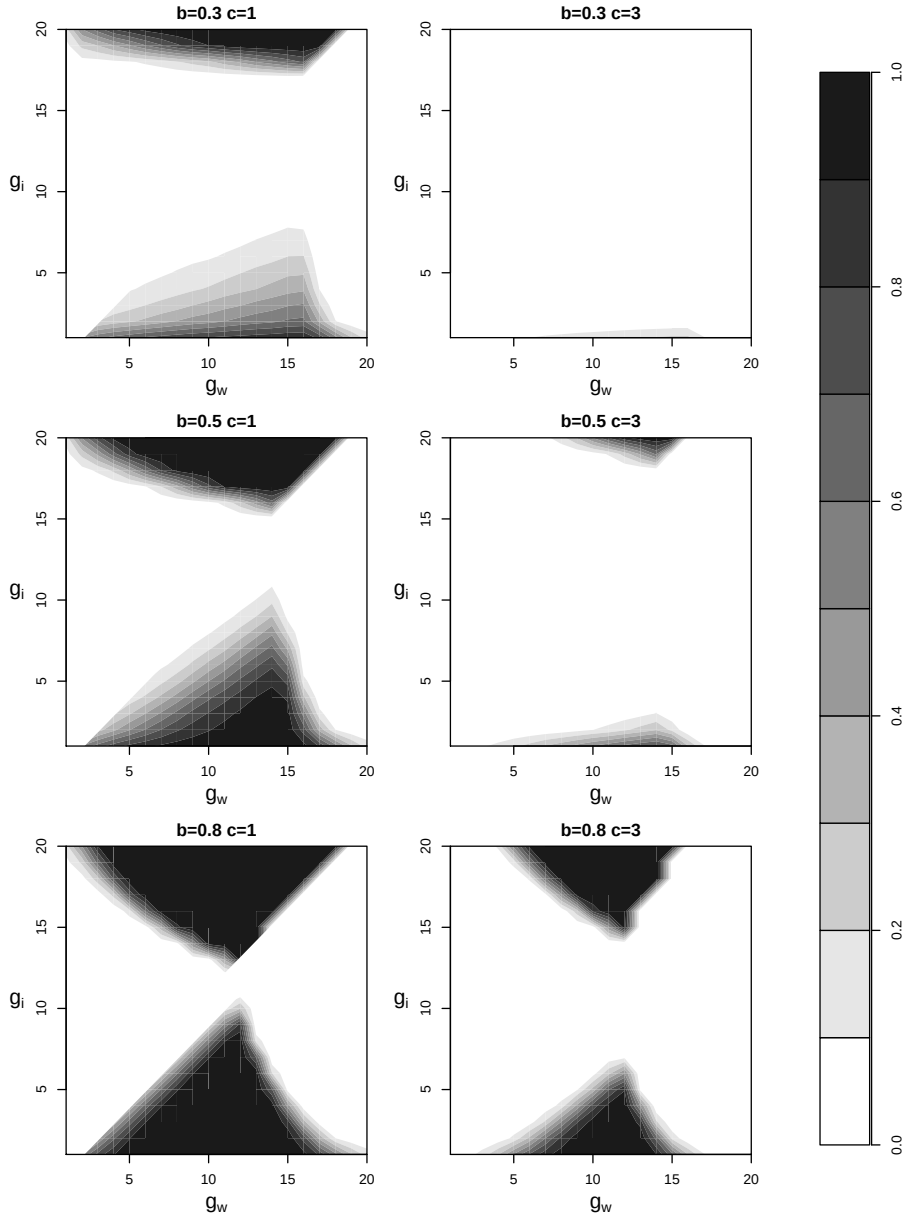

Figure 58: Probability of migration for different values of b and c, for each possible combination of group sizes for the focal (y-axis) and model (x-axis) agent. Probabilities obtained from 10,000 simulation runs for each parameter combination with $\mu = 10$, $K = 200$ and $\epsilon = 1$.

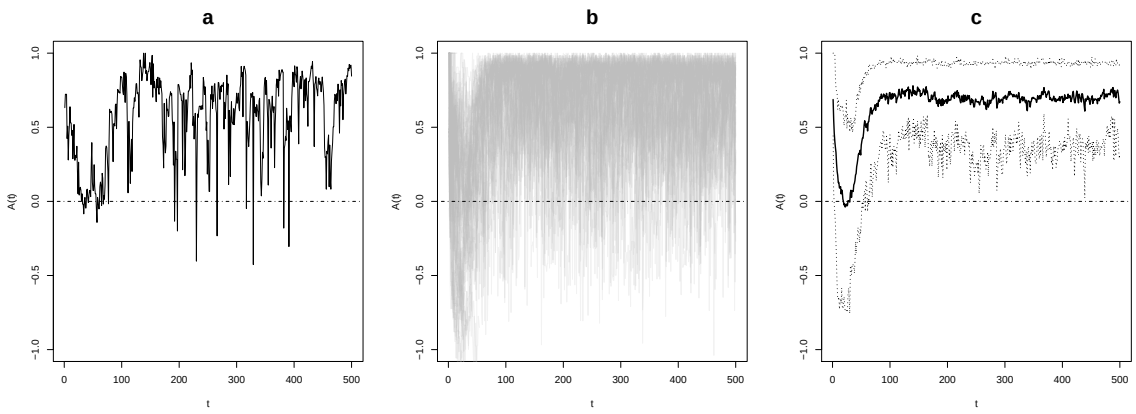

Figure 59: Time-series of $A(t)$: **a** single run (run number=10); **b** combined plot of all runs; **c** summary statistics (solid line=mean, dotted line=0.1 and 0.9 quantiles). Sweep parameters values: $z = 0.5$, $k = 0.5$, $b = 0.3$, $s = 1$, $\omega_1 = 0.8$. Basic parameters are the ones listed in table 9.

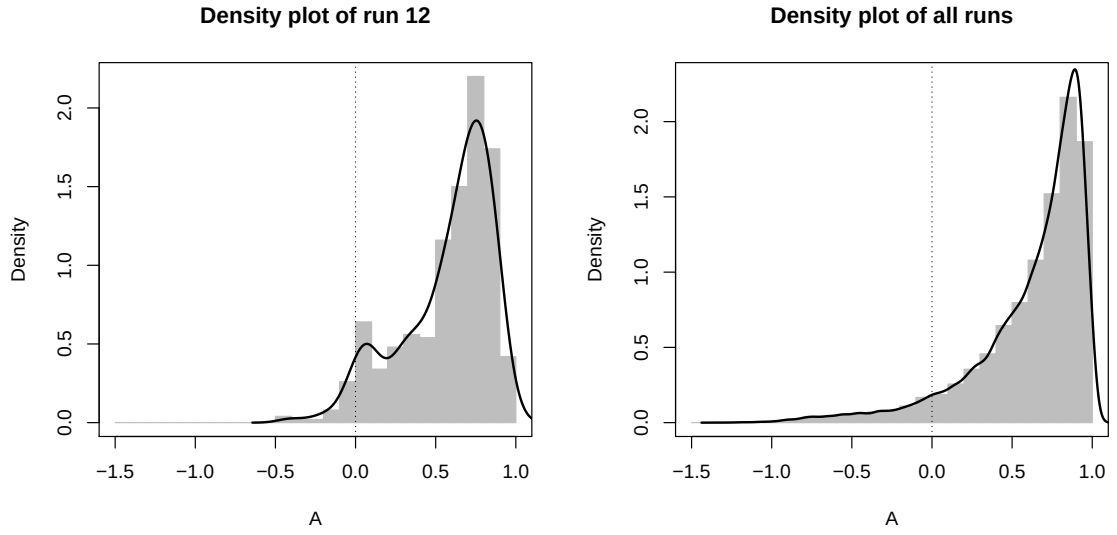

Figure 60: Frequency plot and density curves of A for a single run (left) and all runs (right). Sweep parameters values: $z = 0.5$, $k = 0.5$, $b = 0.3$,$s = 1$,$\omega_1 = 0.8$. Basic parameters are the ones listed in table 9, the bin-size of the histogram is 0.1

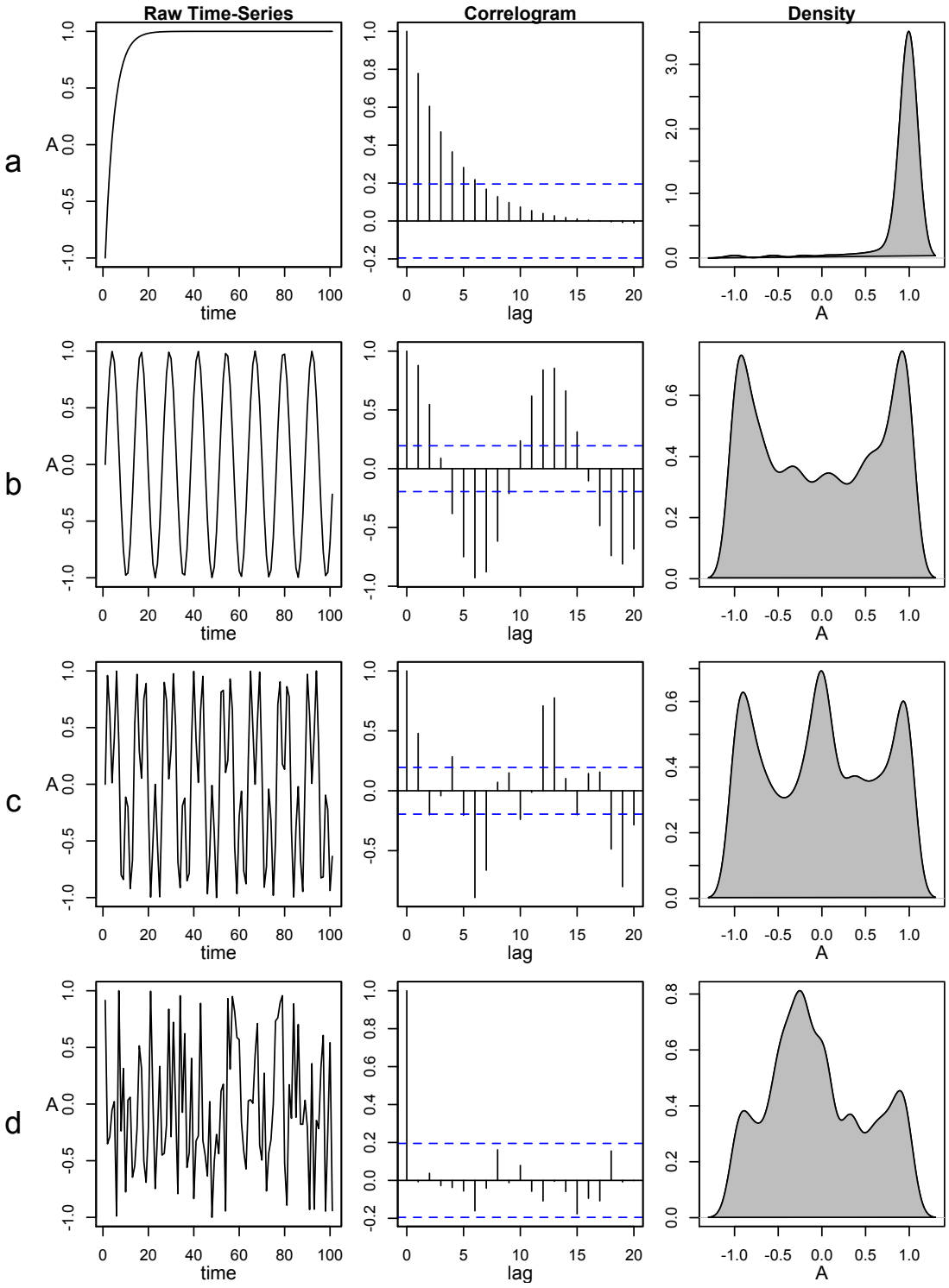

Figure 61: Raw time series, correlograms, and frequency plots for four different types of attractors: **a** point attractor; **b** limit-cycle attractor; **c** toroidal attractor; and **d** strange attractor.

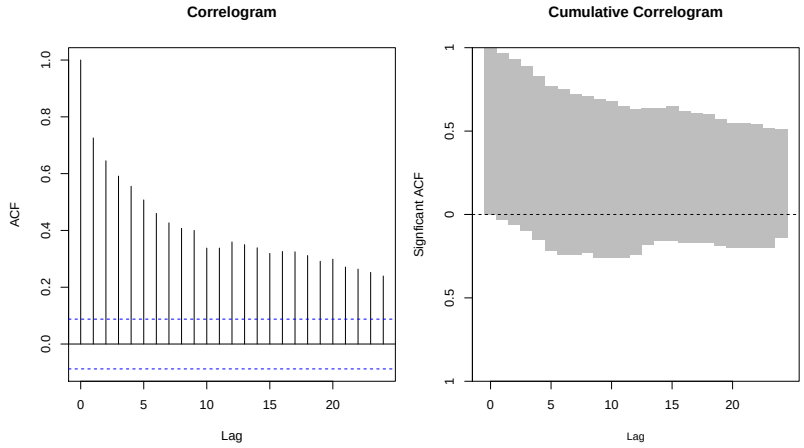

Figure 62: Correlogram of a single run (from the raw data depicted in fig.59**a**) and the combined correlogram of all runs (using the same parameter settings adopted in fig.59).

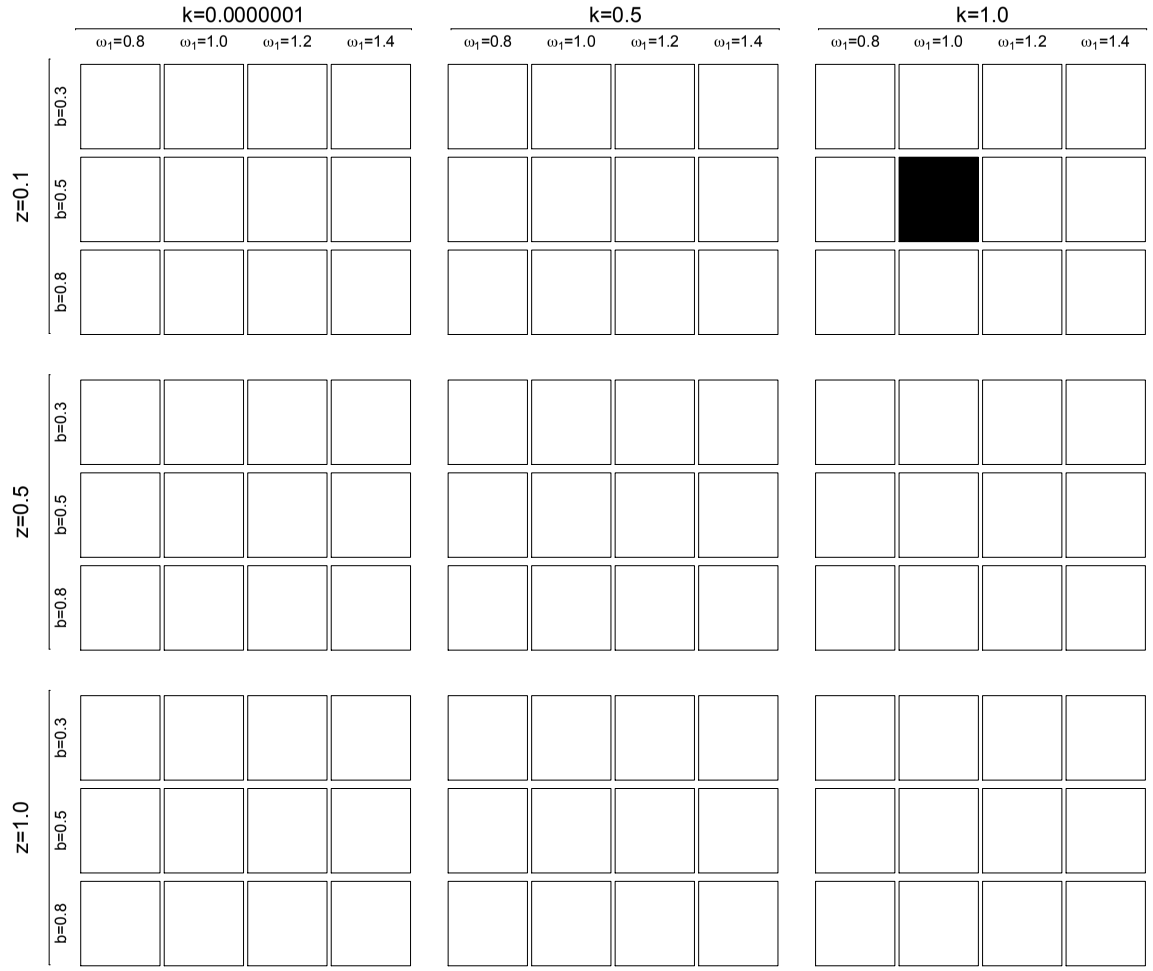

Figure 63: Frame for the 4-dimensional parameter space.

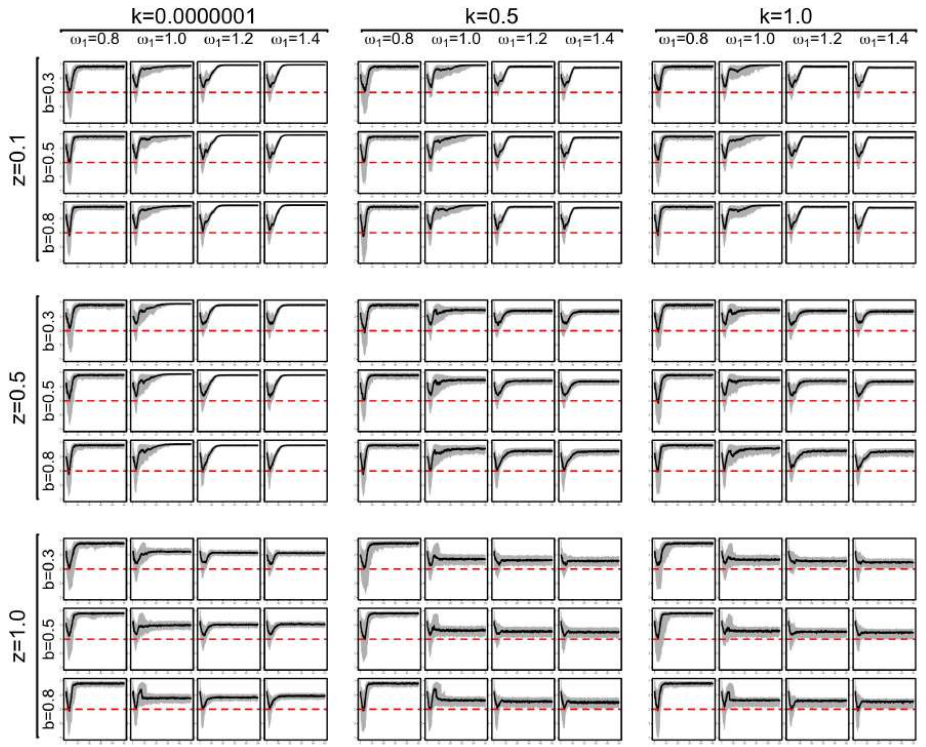

Figure 64: Summary statistics of $A(t)$ with $h = 1$. The solid line is the median A for each t, while the grey shaded area is the envelope bounded by the 10^{th} and 90^{th} percentile. The y-axis of each plot represents A and ranges between -1 and +1, while the x-axis represents t and ranges between 0 and 500.

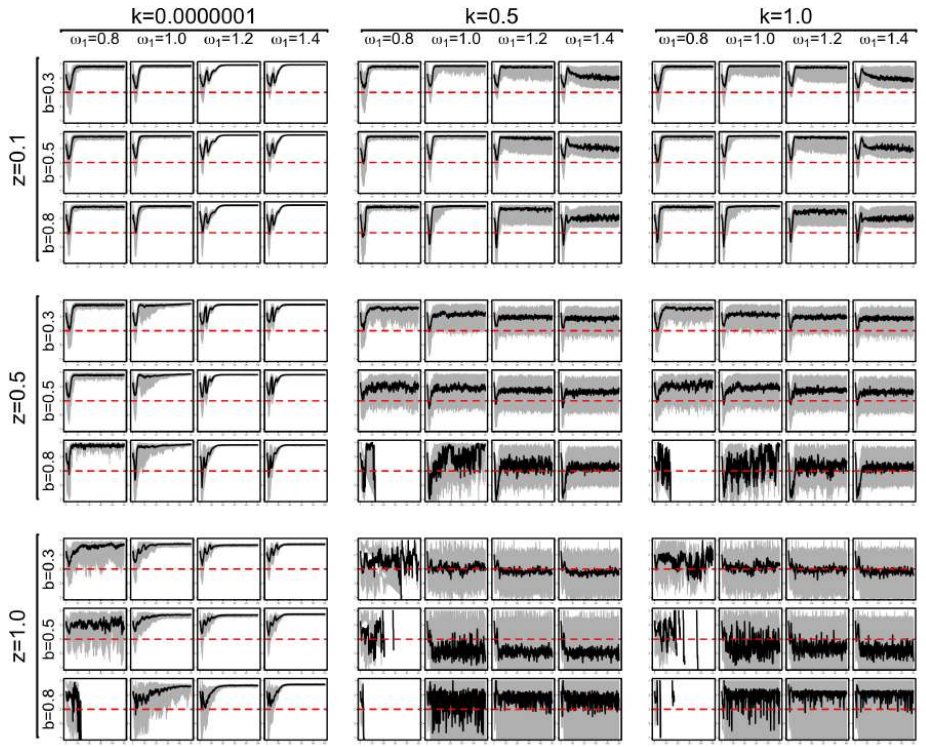

Figure 65: Summary statistics of $A(t)$ with $h = \infty$. The solid line is the median A for each t, while the grey shaded area is the envelope bounded by the 10^{th} and 90^{th} percentile. The y-axis of each plot represents A and ranges between -1 and +1, while the x-axis represents t and ranges between 0 and 500.

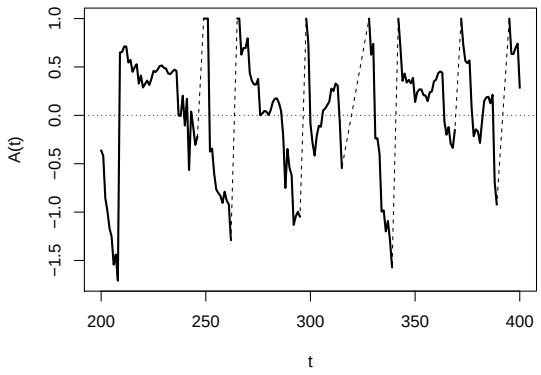

Figure 66: A coefficient time-series with $z = 1.0$,$k = 1.0$,$b = 0.3$ and $\omega_1 = 1.2$. Single run (run number 30), with missing values of $A(t)$ linearly interpolated and shown as dashed line.

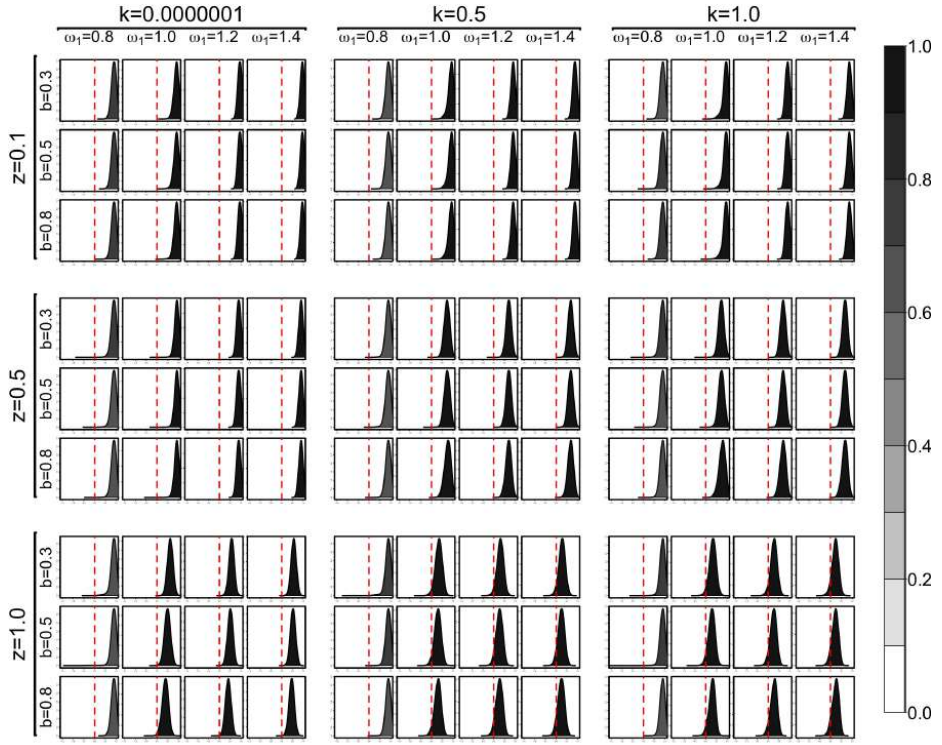

Figure 67: Probability density of the distribution of A with $h = 1$ and a kernel bandwidth of 0.1. The fill colour depicts the proportion of calculated values of A within each complete set of 30,000 values (300 t $\times$ 100 simulation runs). The x-axis represents the A coefficient with a range from -1.5 to +1. The y-axis represents the probability density. Notice that the range of the latter axis is different for each plot for comparative purposes.

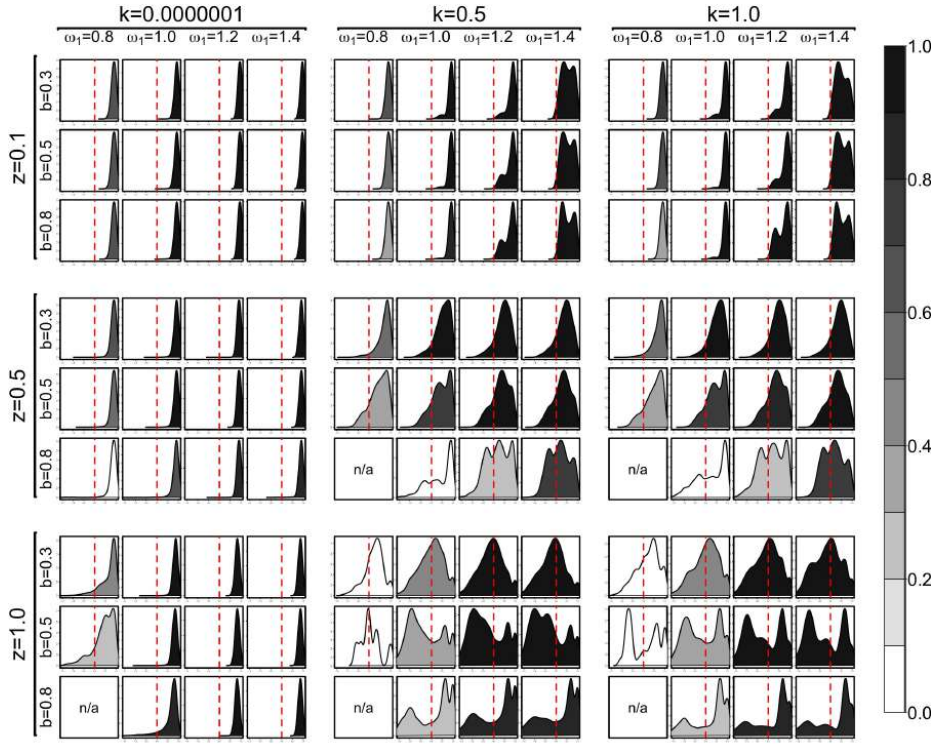

Figure 68: Probability density of the distribution of A with $h = \infty$ and a kernel bandwidth of 0.1. The fill colour depicts the proportion of calculated values of A within each complete set of 30,000 values (300 t $\times$ 100 simulation runs). The x-axis represents the A coefficient with a range from -1.5 to +1. The y-axis represents the probability density. Notice that the range of the latter axis is different for each plot for comparative purposes.

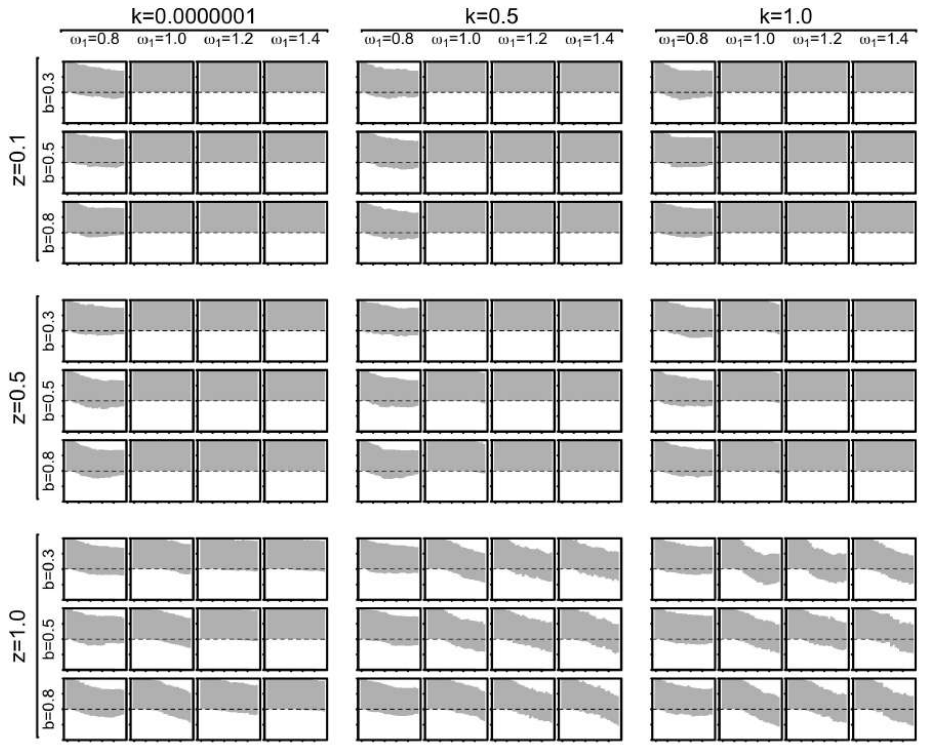

Figure 69: Correlogram of A with $h = 1$. The y-axis shows the proportion of significant positive (above the dashed line) and negative (below the dashed line) autocorrelation, while the x-axis depicts the time lags, with a range from 1 to 25.

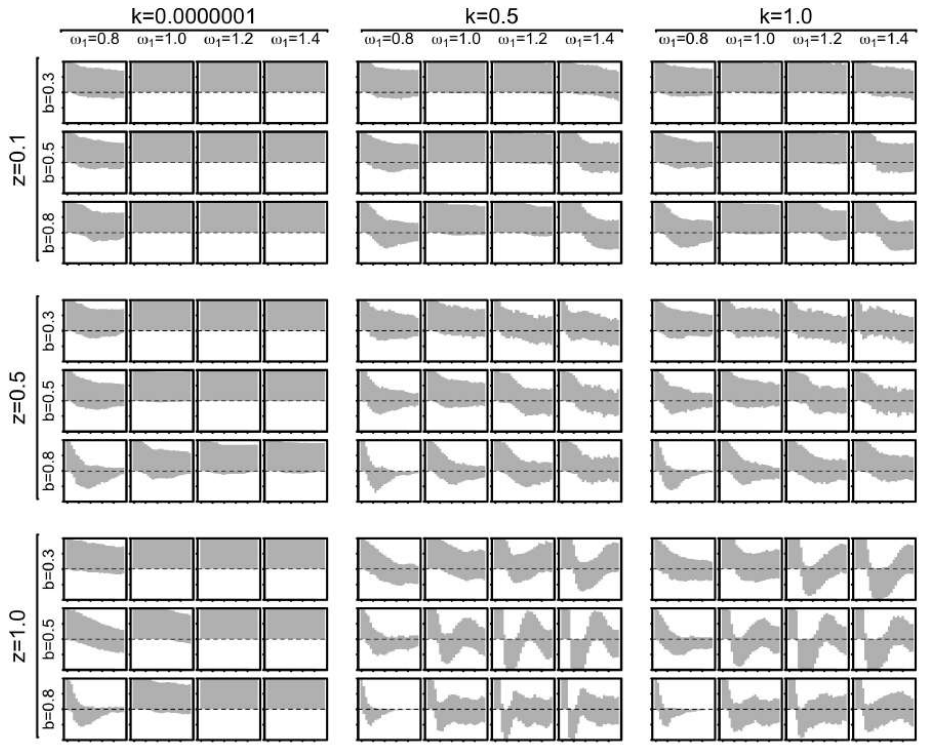

Figure 70: Correlogram of A with $h = \infty$.The y-axis shows the proportion of significant positive (above the dashed line) and negative (below the dashed line) autocorrelation, while the x-axis depicts the time lags, with a range from 1 to 25.

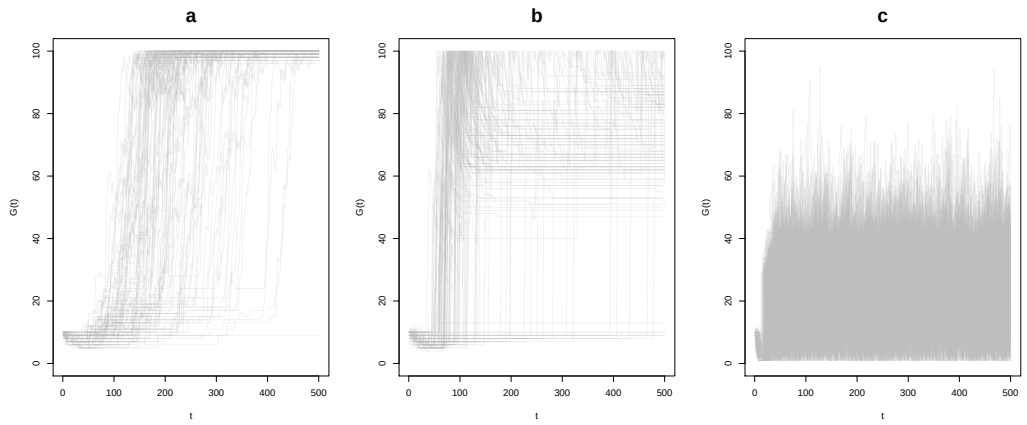

Figure 71: Cumulative time-series plot for: (**a**) $h = 1$, $z = 0.1$, $k = 1.0$, $b = 0.5$,$\omega_1 = 1.0$; (**b**) $h = \infty$, $z = 0.1$, $k = 1.0$, $b = 0.5$, $\omega_1 = 1.4$; (**c**) $h = \infty$, $z = 1.0$, $k = 1.0$, $b = 0.5$, $\omega_1 = 1.4$;

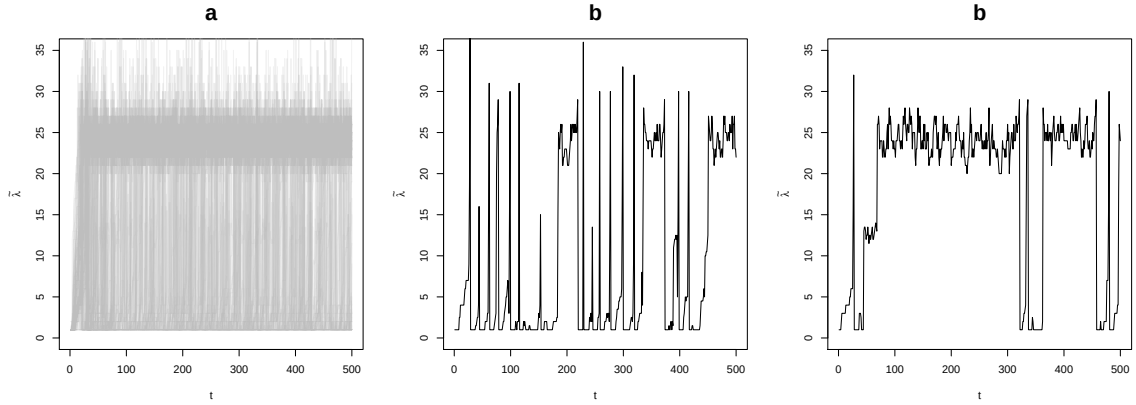

Figure 72: Cumulative plot (**a**), and single run time-series (**b**:run 11; **c**: run 31) of the median group size with $h = \infty$, $z = 1.0$, $k = 0.5$, $\omega_1 = 1.0$ and $b = 0.5$.

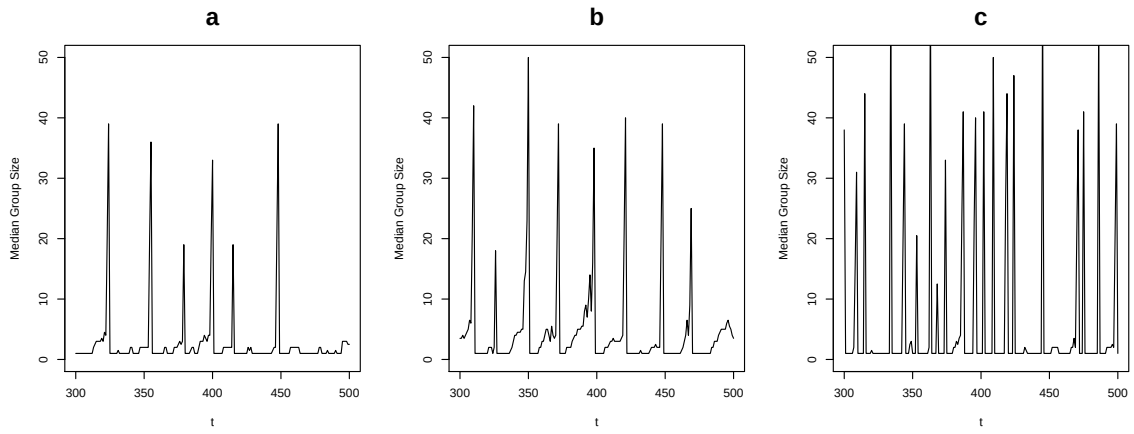

Figure 73: Time-series of median group size ($\tilde{\lambda}(t)$) between $t = 300$ and $t = 500$ for a single run (run n. 22). Parameters: $h = \infty$,$z = 1.0$,$k = 1.0$,$= \omega_1 = 1.4$, and $b = 0.3$ (**a**), $b = 0.5$ (**b**), and $b = 0.8$ (**c**).

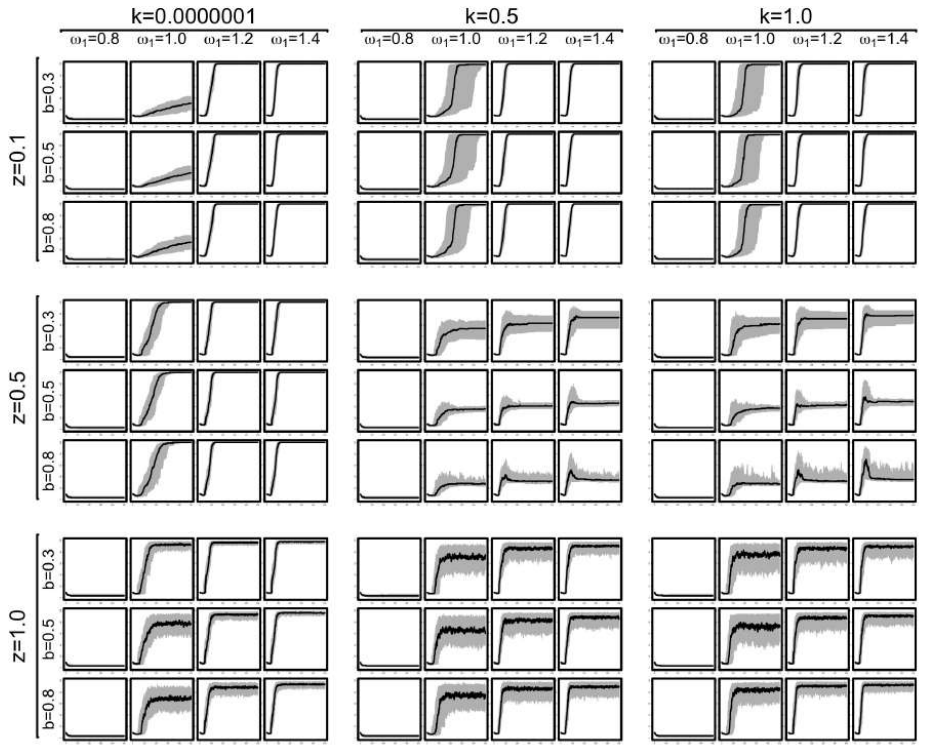

Figure 74: Summary statistics of $G(t)$ with $h = 1$. The solid line is the median G for each t, while the grey shaded area is the envelope bounded by the 10^{th} and 90^{th} percentile. The y-axis of each plot represents G and ranges between 0 and 100, while the x-axis represents t and ranges between 0 and 500.

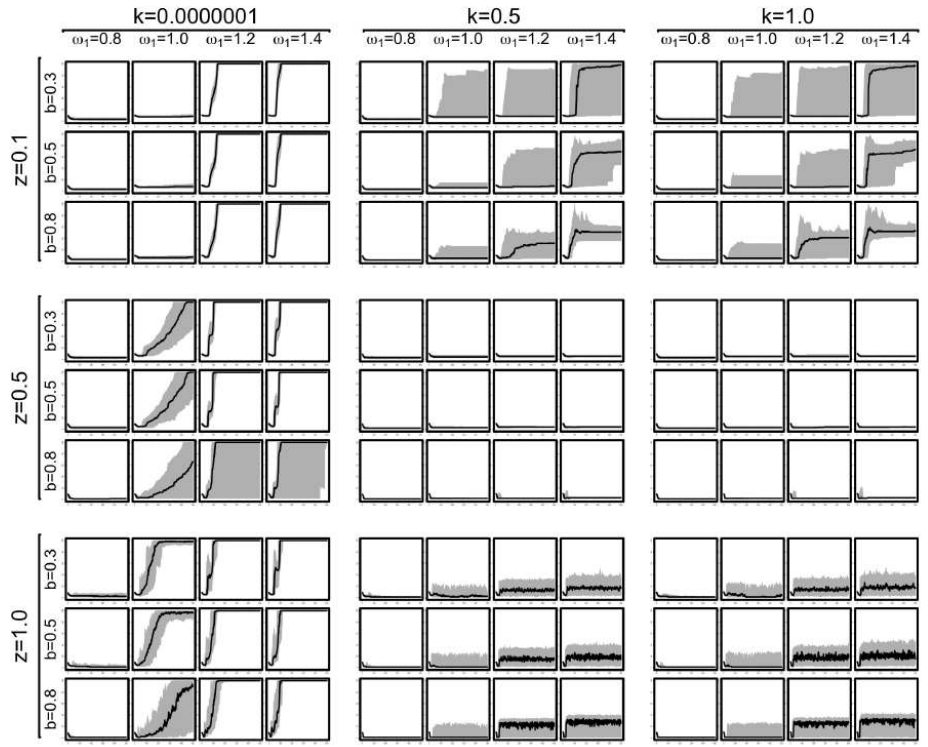

Figure 75: Summary statistics of $G(t)$ with $h = \infty$. The solid line is the median G for each t, while the grey shaded area is the envelope bounded by the 10^{th} and 90^{th} percentile. The y-axis of each plot represents G and ranges between 0 and 100, while the x-axis represents t and ranges between 0 and 500.

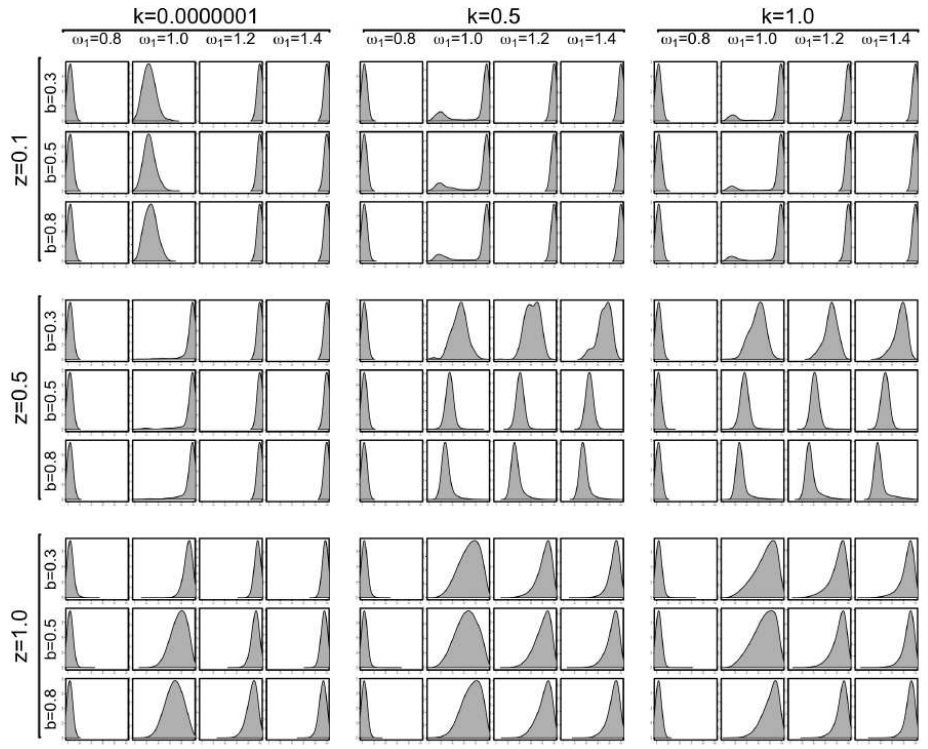

Figure 76: Probability density of the distribution of G with $h = 1$ and a kernel bandwidth of 5. The x-axis represents G with a range from 0 to 100. The y-axis represents the probability density. Notice that the range of the latter axis is different for each plot for comparative purposes.

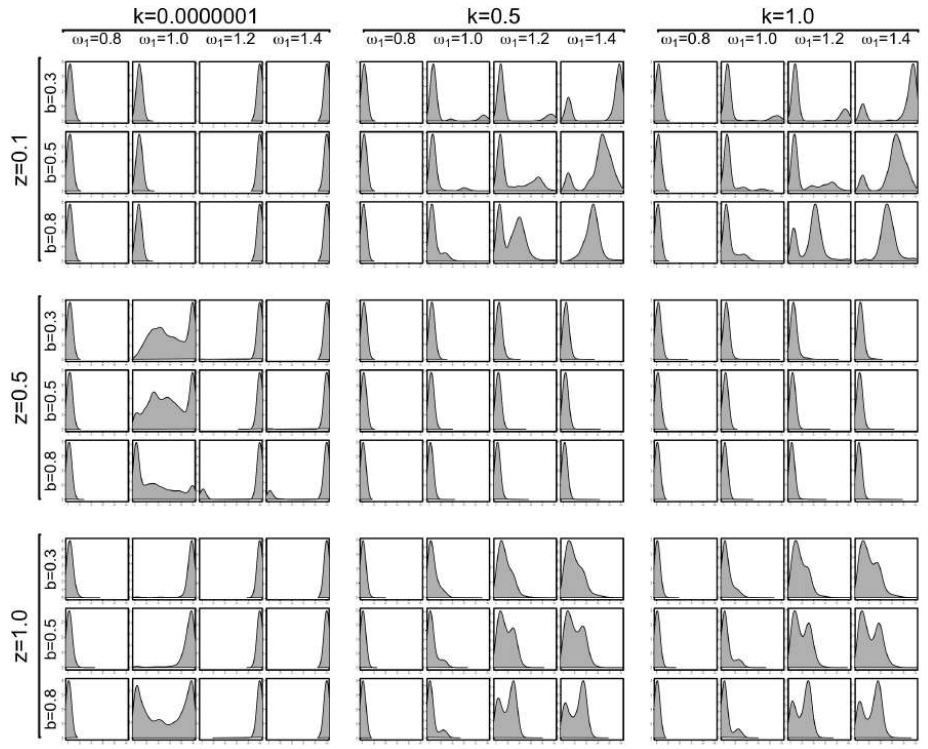

Figure 77: Probability density of the distribution of G with $h = \infty$ and a kernel bandwidth of 5. The x-axis represents G with a range from 0 to 100. The y-axis represents the probability density. Notice that the range of the latter axis is different for each plot for comparative purposes.

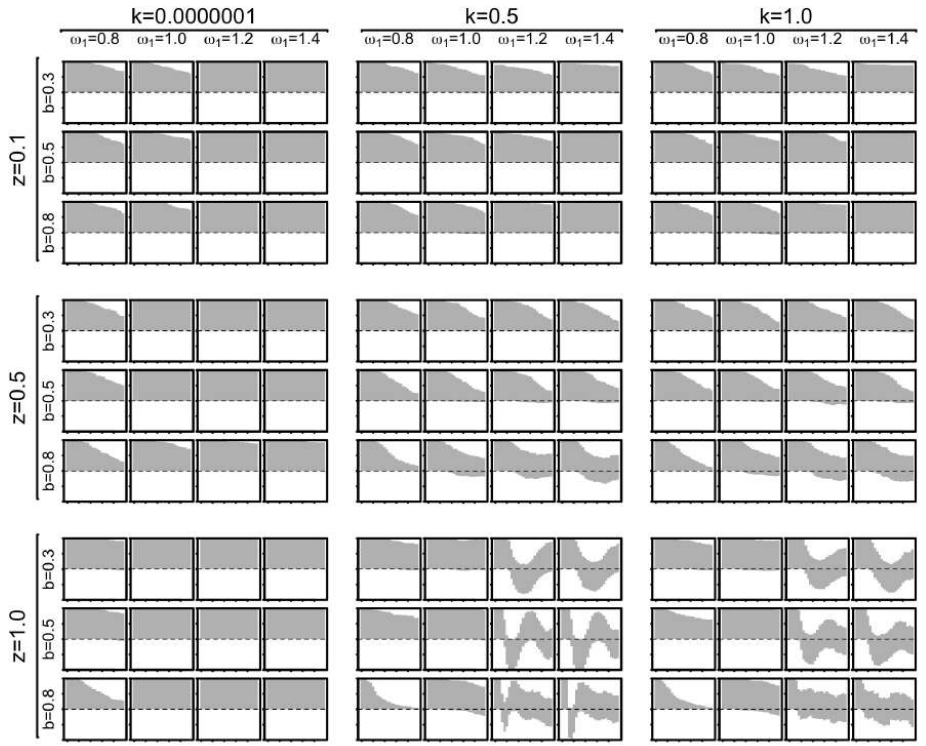

Figure 78: Correlogram of G with $h = \infty$. The y-axis shows the proportion of significant positive (above the dashed line) and negative (below the dashed line) autocorrelation, while the x-axis depicts the time lags, with a range from 1 to 25.

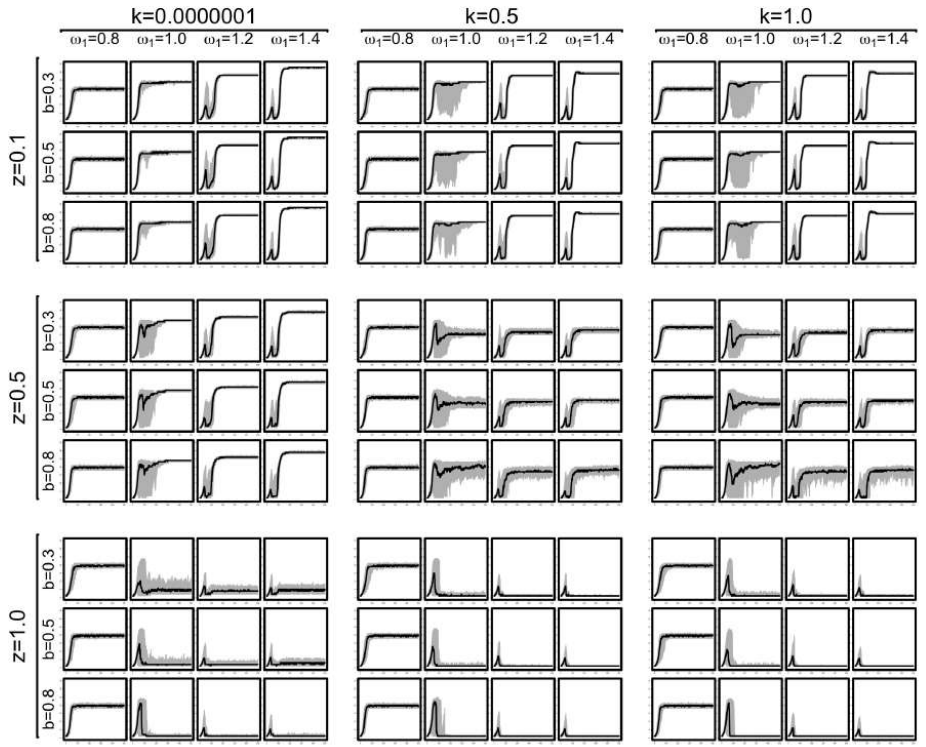

Figure 79: Summary statistics of $\tilde{\lambda}(t)$ with $h = 1$. The solid line is the median $\tilde{\lambda}(t)$ for each t, while the grey shaded area is the envelope bounded by the 10^{th} and 90^{th} percentile. The y-axis has a range between 0 and 35, while the x-axis ranges from 0 to 500.

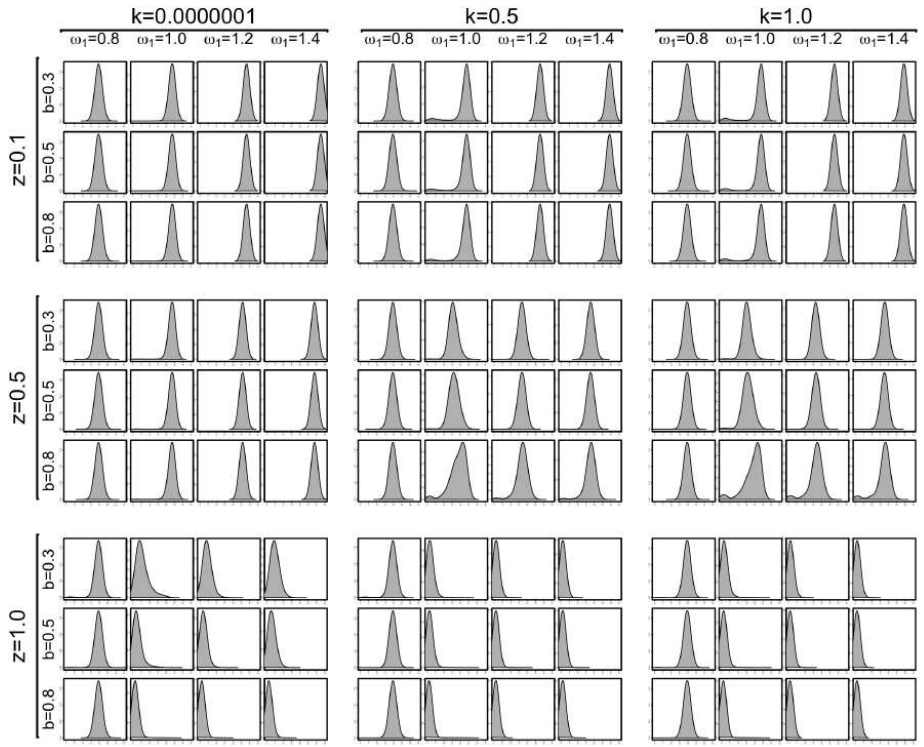

Figure 80: Probability density of the distribution of $\tilde{\lambda}(t)$ with $h = 1$ and a kernel bandwidth of 2. The x-axis represents the $\tilde{\lambda}(t)$ with a range from 0 to 100. The y-axis represents the probability density. Notice that the range of the latter axis is different for each plot for comparative purposes.

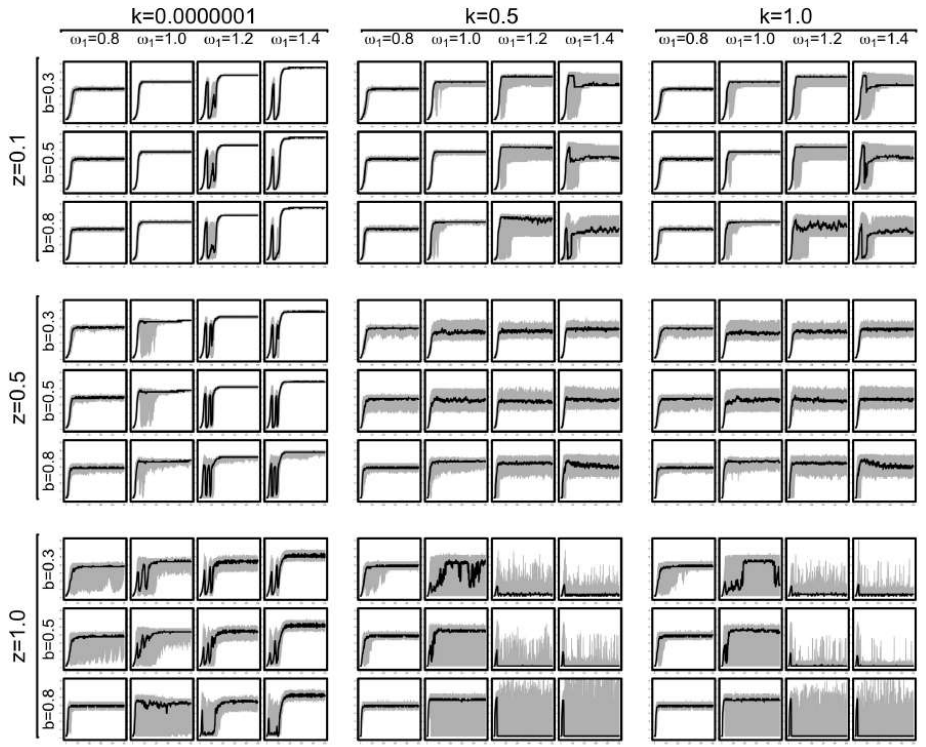

Figure 81: Summary statistics of $\tilde{\lambda}(t)$ with $h = \infty$. The solid line is the median $\tilde{\lambda}(t)$ for each t, while the grey shaded area is the envelope bounded by the 10^{th} and 90^{th} percentile. The y-axis has a range between 0 and 35, while the x-axis ranges from 0 to 500.

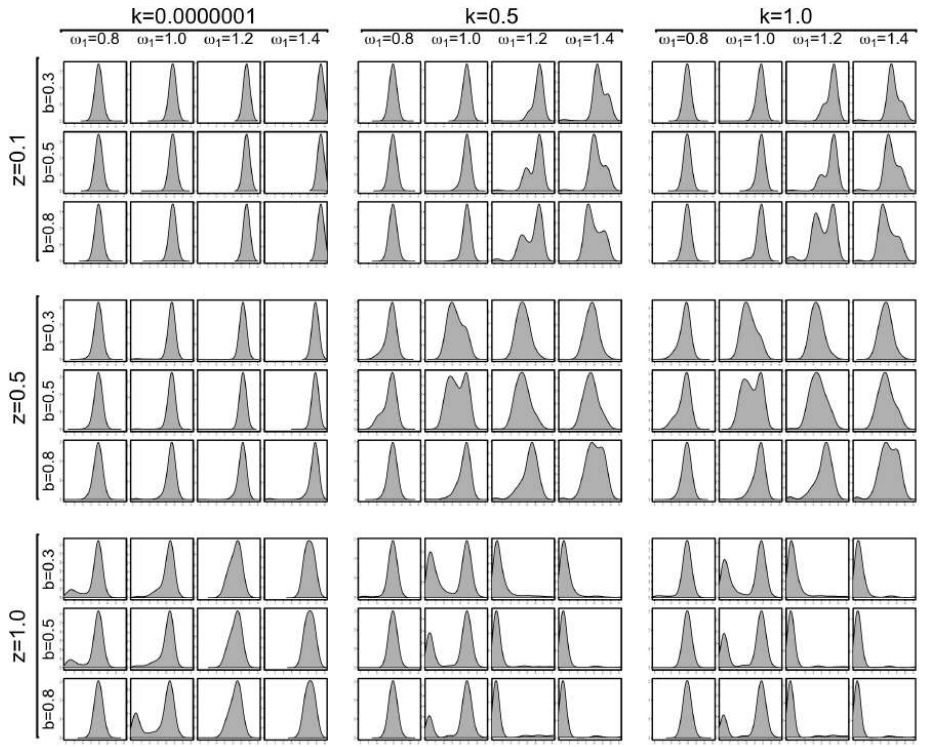

Figure 82: Probability density of the distribution of $\tilde{\lambda}(t)$ with $h = \infty$ and a kernel bandwidth of 2. The x-axis represents the $\tilde{\lambda}(t)$ with a range from 0 to 100. The y-axis represents the probability density. Notice that the range of the latter axis is different for each plot for comparative purposes.

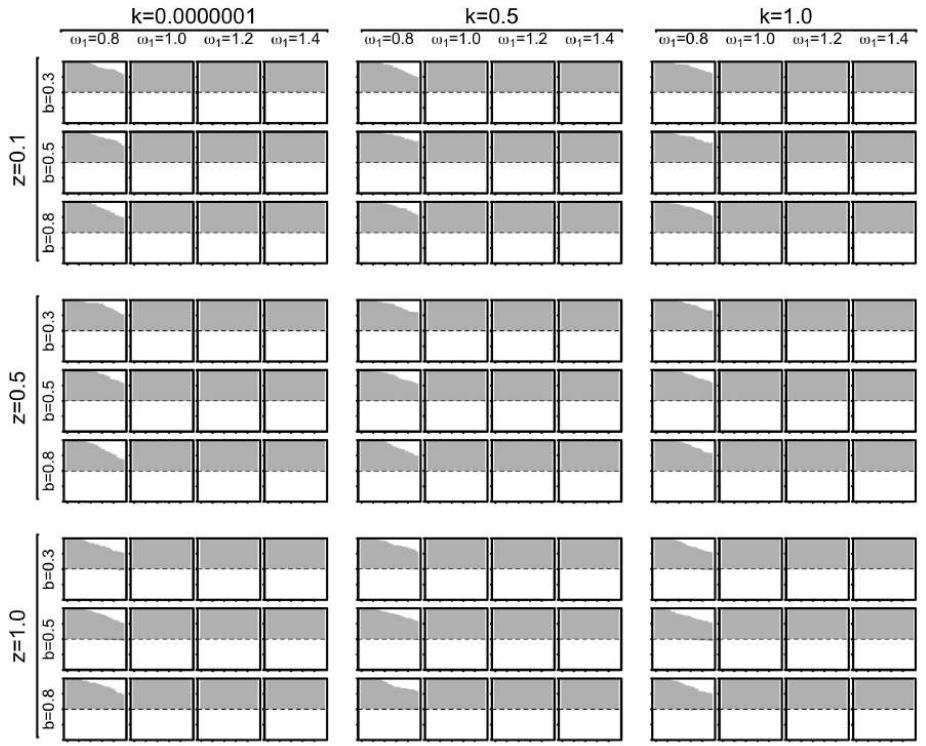

Figure 83: Correlogram of $\tilde{\lambda}(t)$ with $h = 1$. The y-axis shows the proportion of significant positive (above the dashed line) and negative (below the dashed line) autocorrelation, while the x-axis depicts the time lags, with a range from 1 to 25.

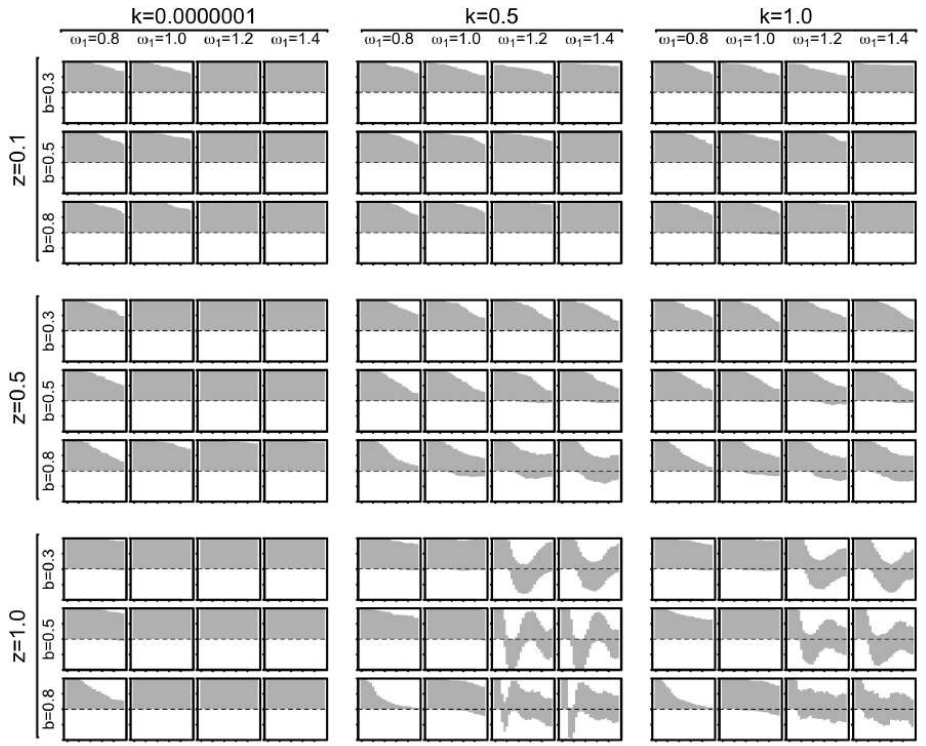

Figure 84: Correlogram of $\tilde{\lambda}(t)$ with $h = \infty$. The y-axis shows the proportion of significant positive (above the dashed line) and negative (below the dashed line) autocorrelation, while the x-axis depicts the time lags, with a range from 1 to 25.

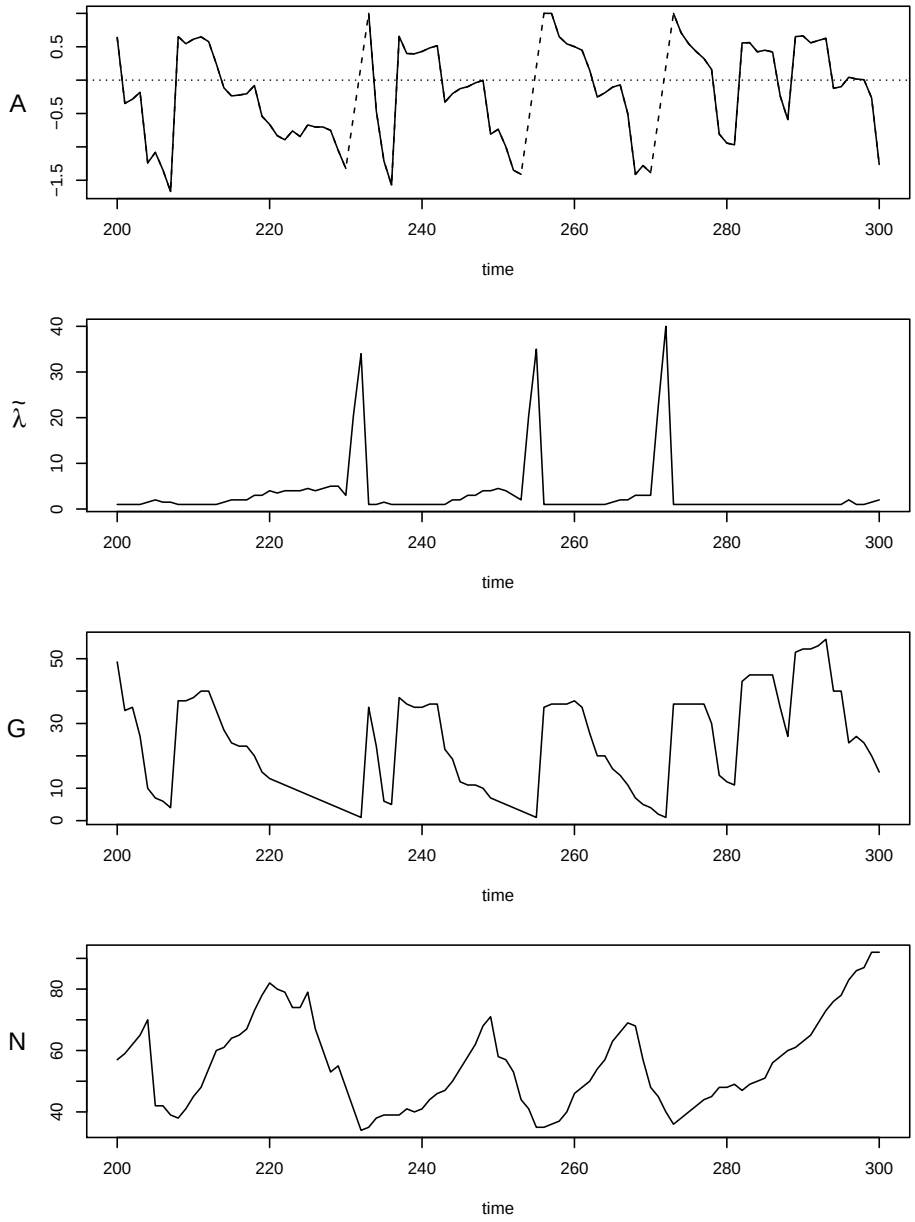

Figure 85: Dynamics of $A(t)$, $\tilde{\lambda}(t)$, $G(t)$, and $N(t)$ for a single run of the simulation (run n.10). Parameters: $h = \infty$, $k = 1.0$, $z = 1.0$, $b = 0.5$, and $\omega_1 = 1.4$. Unknown values of $A(t)$ have been obtained through linear interpolation and are shown as dashed line.

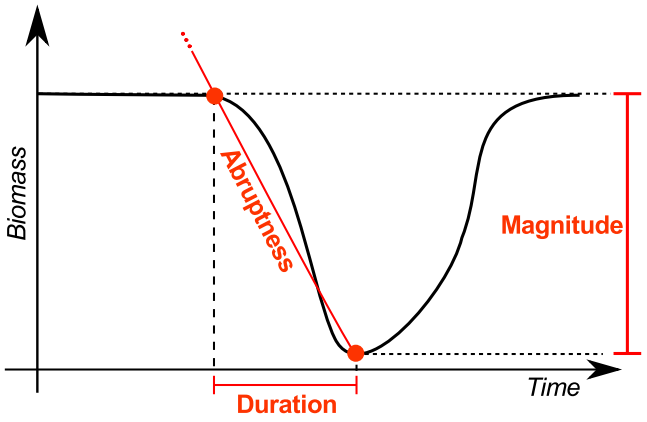

Figure 86: The three properties of disturbance (modified from White and Jentsch 2001:fig.2)

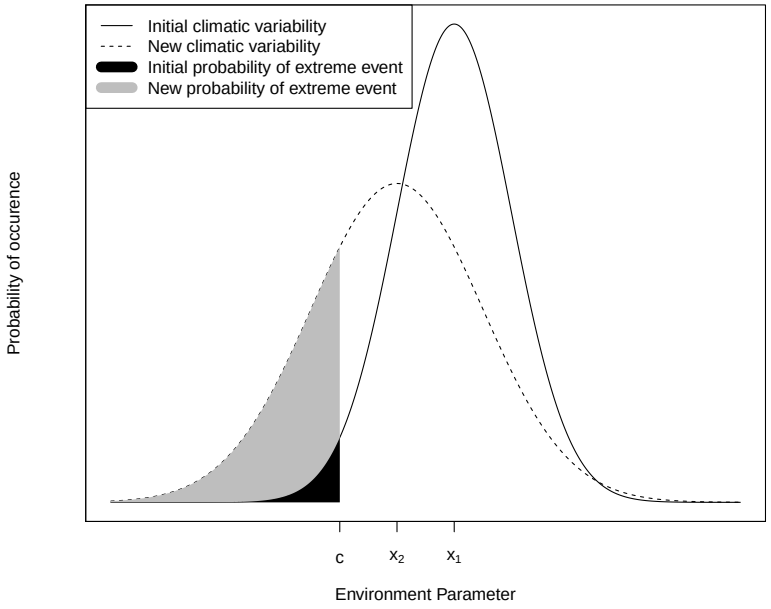

Figure 87: A simple model of change in the occurrence of extreme environmental changes (modified from Jentsch *et al.* 2007: fig. 3). See details in the text.

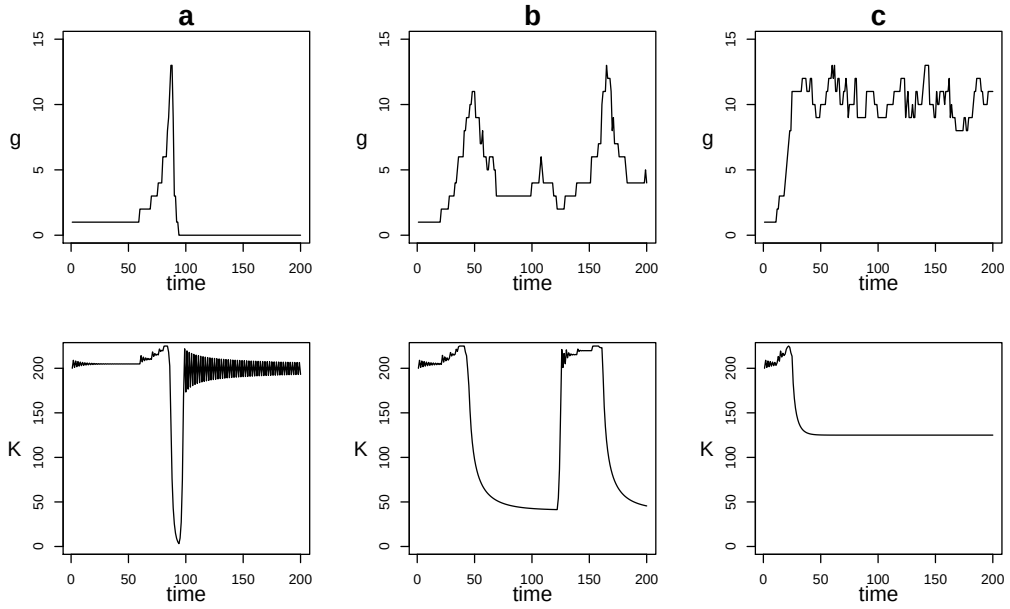

Figure 88: Effects derived by the variation of the resource resilience parameter β. The upper row depicts the group size variation over time, while the bottom row shows the corresponding variation of K: **a**) $\beta = 0.3$, **b**) $\beta = 0.35$; **c**) $\beta = 0.4$. Generated from a single run of the simulation with a starting value of K equal to 200, $\mu = 10$, $\kappa = 200$, $\zeta = 2$, $b = 0.5$, $\rho = 0.05$, $\omega_1 = 1.2$, $\omega_2 = 5$. The simulation has been initialised with a single agent (i.e. with an initial value of g equal to 1).

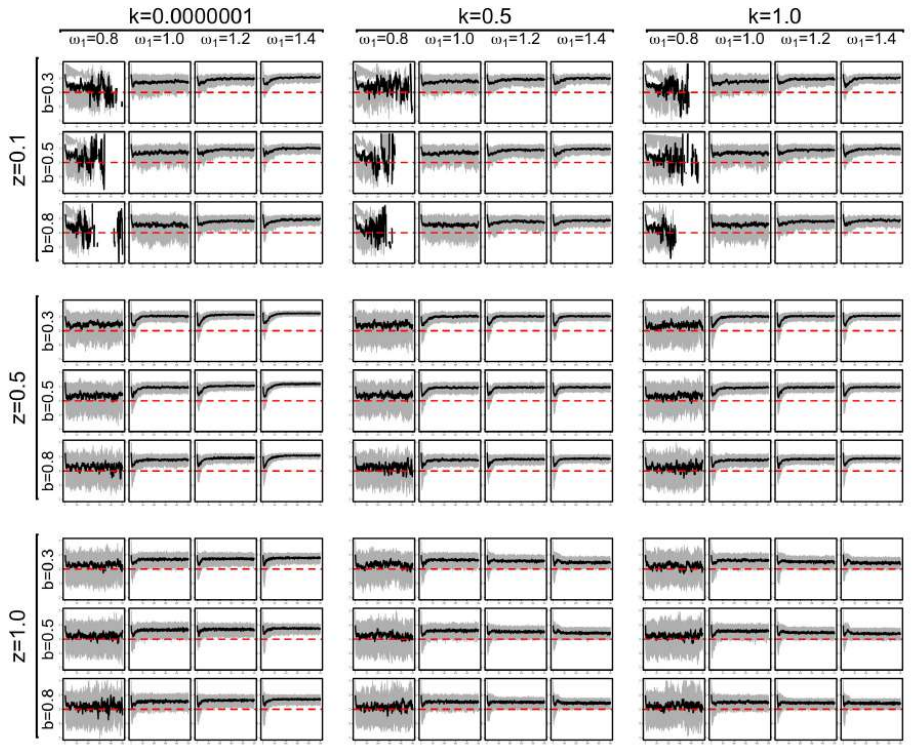

Figure 89: Summary statistics of $A(t)$ with $h = 1$ and $\beta = 0.30$. The solid line is the median A for each t, while the grey shaded area is the envelope bounded by the 10th and 90th percentile. The y-axis of each plot represents A and ranges between -1 and +1, while the x-axis represents t and ranges between 0 and 500.

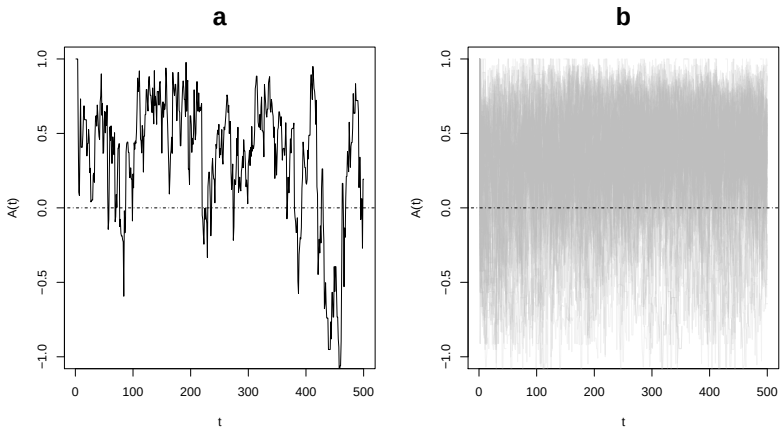

Figure 90: Emergence of chaotic shifts between clumped and dispersed pattern within a local version of the model: **a** single run; **b** combined plot. Model parameters: $h = 1$,$\beta = 0.35$, $b = 0.5$,$k = 10^{-7}$,$z = 1$, and $\omega_1 = 0.8$

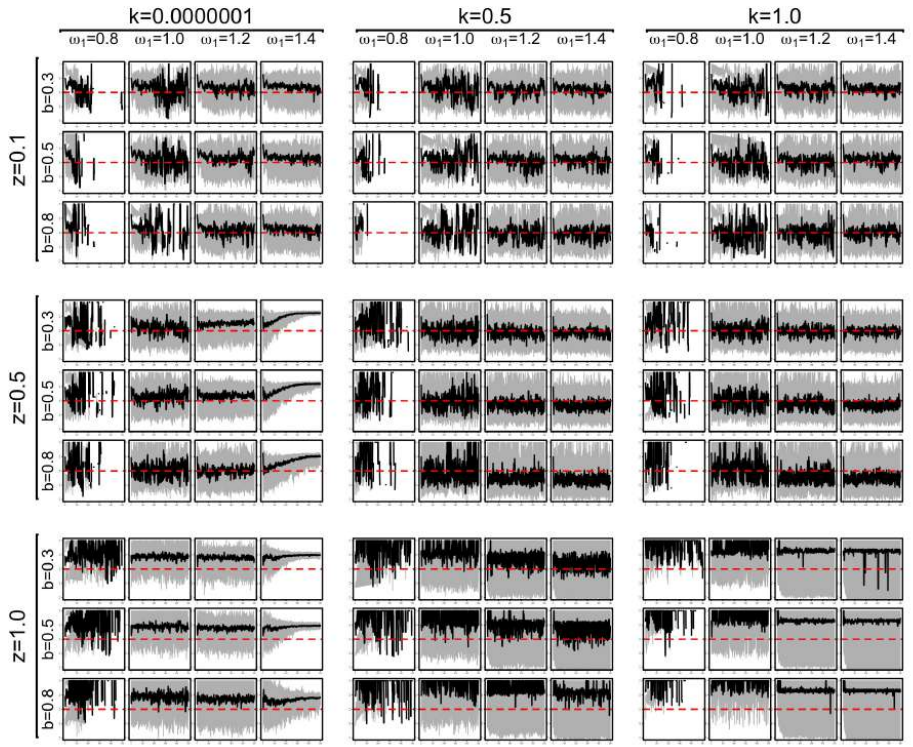

Figure 91: Summary statistics of $A(t)$ with $h = \infty$ and $\beta = 0.30$. The solid line is the median A for each t, while the grey shaded area is the envelope bounded by the 10^{th} and 90^{th} percentile. The y-axis of each plot represents A and ranges between -1 and +1, while the x-axis represents t and ranges between 0 and 500.

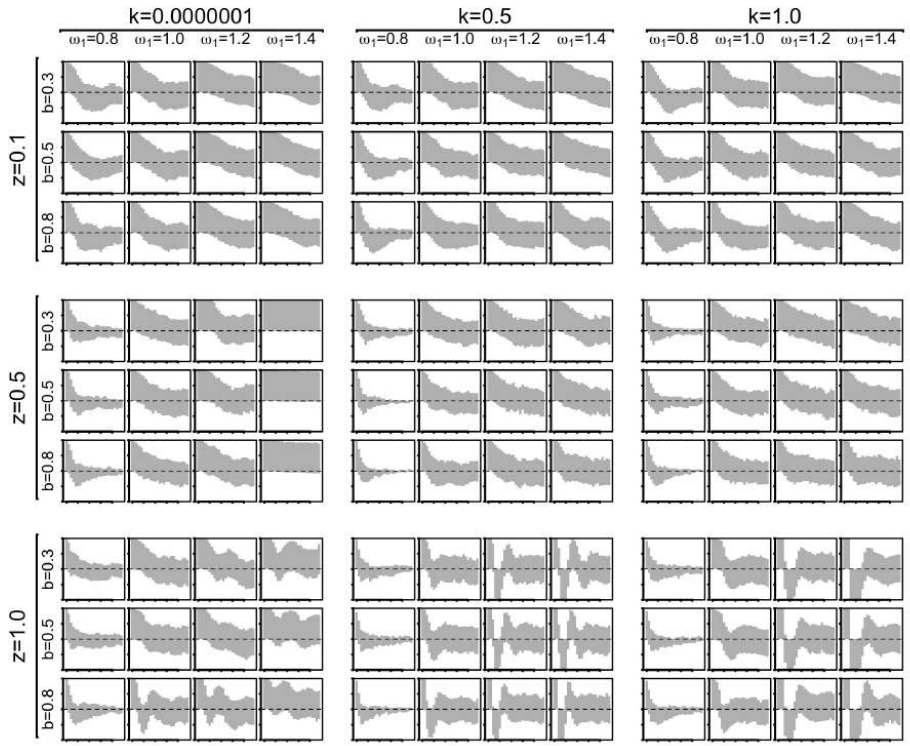

Figure 92: Correlogram of A with $h = \infty$ and $\beta = 0.3$. The y-axis shows the proportion of significant positive (above the dashed line) and negative (below the dashed line) autocorrelation, while the x-axis depicts the time lags, with a range from 1 to 25.

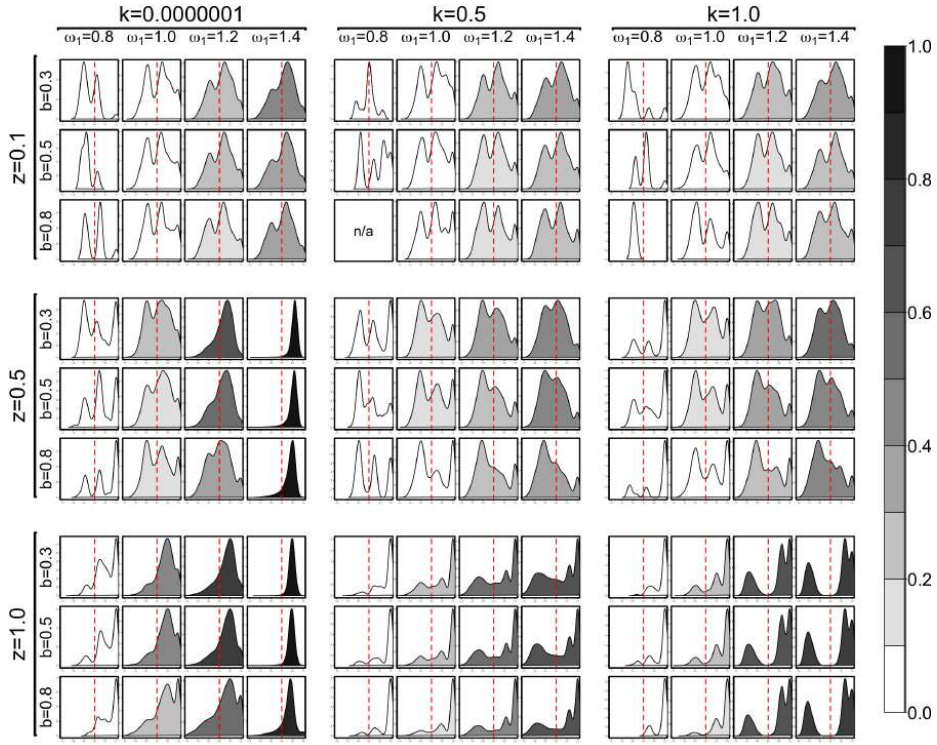

Figure 93: Probability density of the distribution of A with $h = \infty$, $\beta = 0.3$, and a kernel bandwidth of 5. The x-axis represents the A coefficient with a range from -1.5 to +1. The y-axis represents the probability density. Notice that the range of the latter axis is different for each plot for comparative purposes

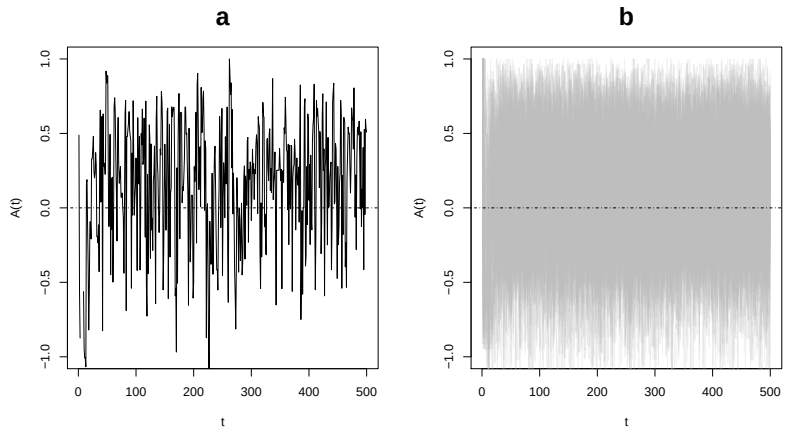

Figure 94: Emergence of chaotic shifts between clumped and dispersed pattern within the global version of the model: **a** single run; **b** combined plot. Model parameters: $h = \infty$,$\beta = 0.35$, $b = 0.5$,$k = 0.5$,$z = 0.5$, and $\omega_1 = 1.2$

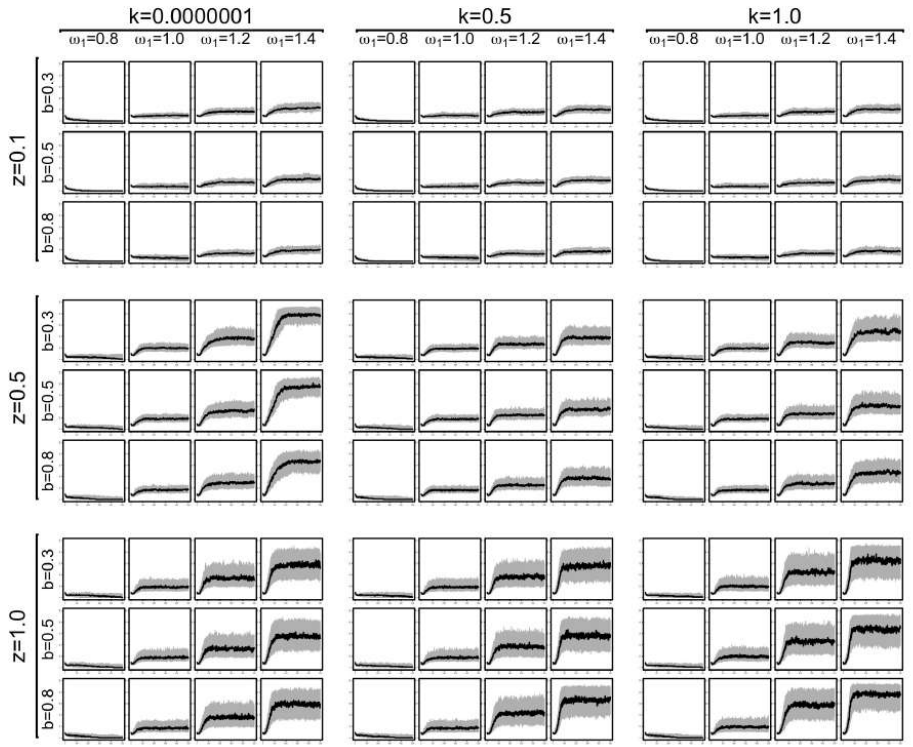

Figure 95: Summary statistics of $G(t)$ with $h = 1$ and $\beta = 0.30$. The solid line is the median G for each t, while the grey shaded area is the envelope bounded by the 10^{th} and 90^{th} percentile. The y-axis of each plot represents G and ranges between 0 and 100, while the x-axis represents t and ranges between 0 and 500.

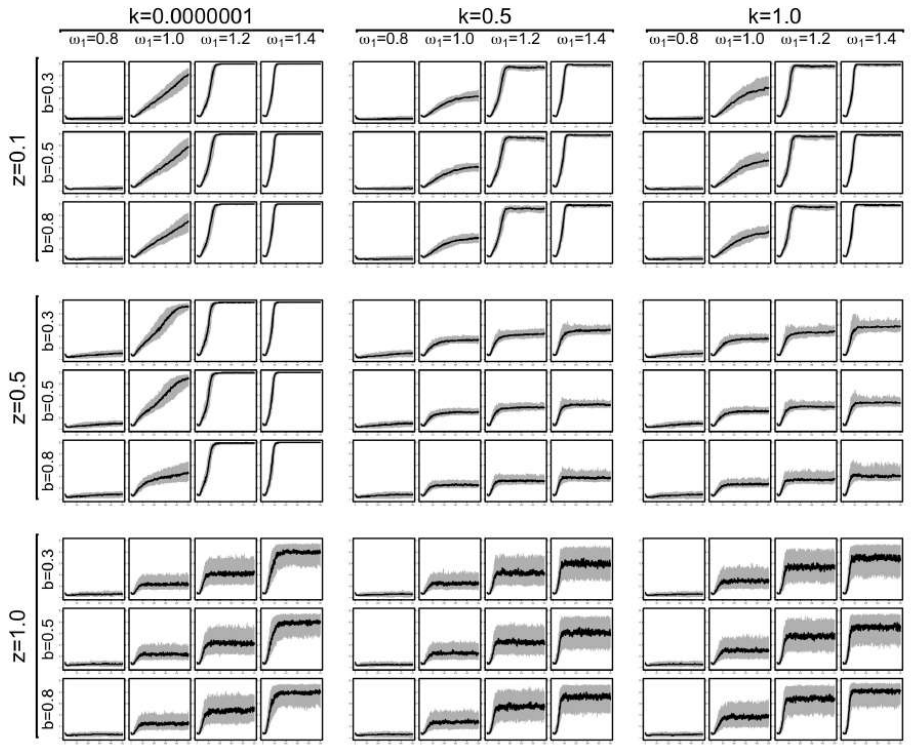

Figure 96: Summary statistics of $G(t)$ with $h = 1$ and $\beta = 0.4$. The solid line is the median G for each t, while the grey shaded area is the envelope bounded by the 10^{th} and 90^{th} percentile. The y-axis of each plot represents G and ranges between 0 and 100, while the x-axis represents t and ranges between 0 and 500.

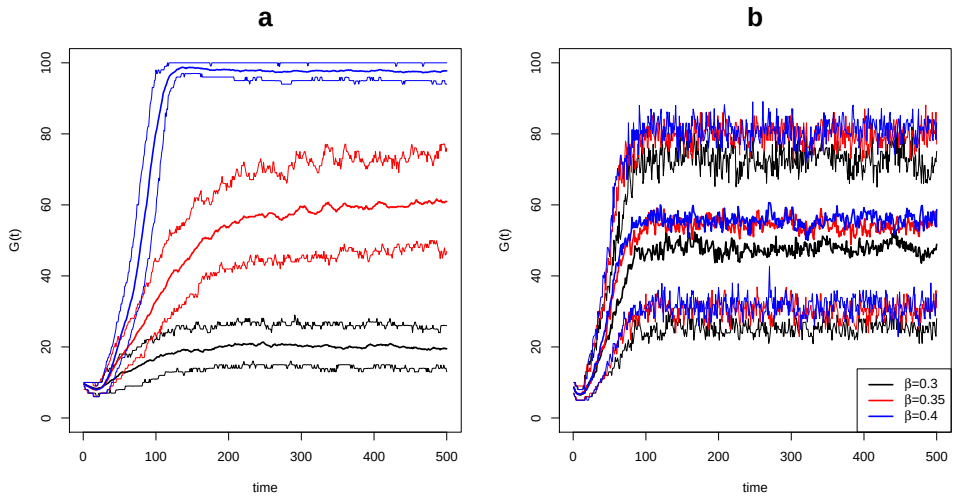

Figure 97: Effect of variation of β in the local version of the model. The thick line shows the mean, while the thin lines define the 10^{th} and 90^{th} percentiles. Parameters: **a**) $h = 1$, $z = 0.1$, $k = 0.5$,$b = 0.3$, and $\omega_1 = 1.4$; and **b**) $h = 1$, $z = 1$, $k = 1$,$b = 0.5$, and $\omega_1 = 1.2$

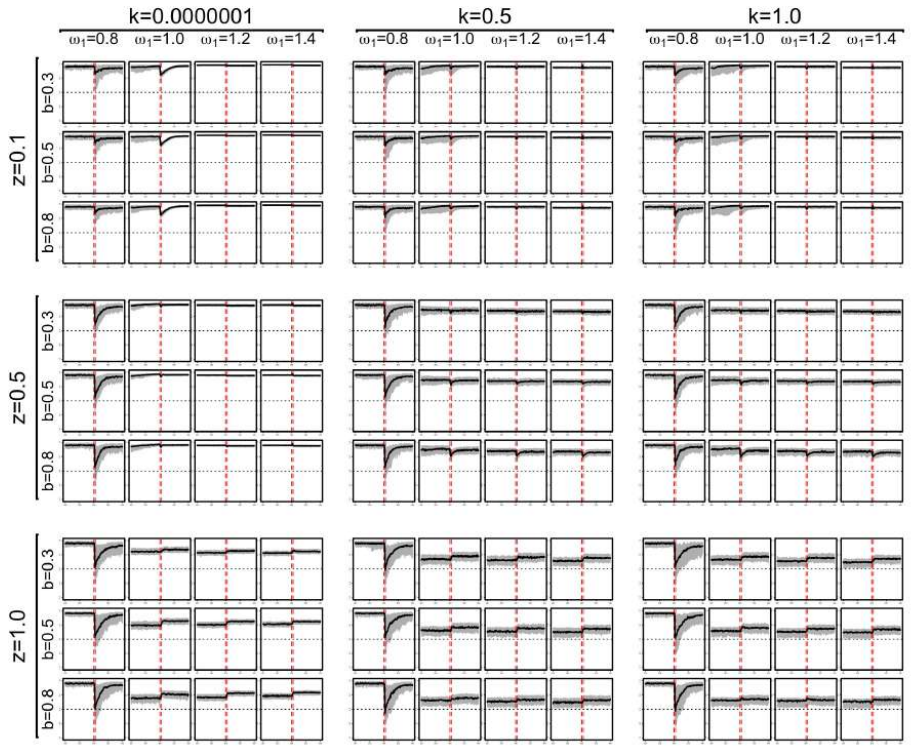

Figure 98: Summary statistics of $A(t)$ with $h = 1$, and a fast disturbance process ($t_s = 301$, $t_e = 304$, $\eta = 25$). The solid line is the median A for each t, while the grey shaded area is the envelope bounded by the 10$^{\text{th}}$ and 90$^{\text{th}}$ percentile. The t_s and t_e are shown as dashed vertical lines. The y-axis of each plot represents A and ranges between -1 and +1, while the x-axis represents t and ranges between 200 and 400.

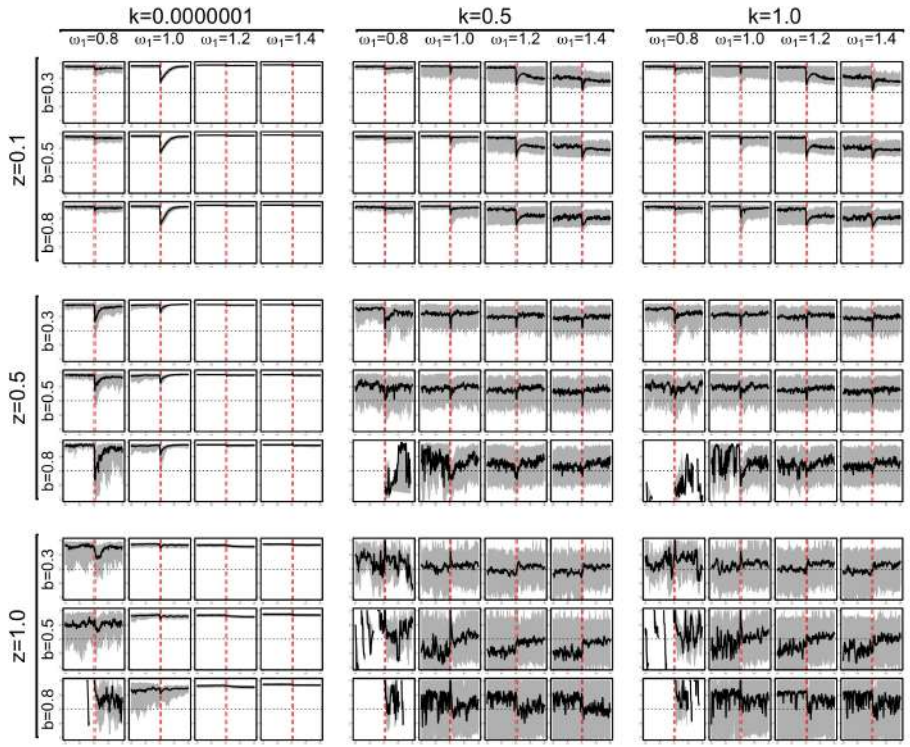

Figure 99: Summary statistics of $A(t)$ with $h = \infty$, and a fast disturbance process ($t_s = 301$, $t_e = 304$, $\eta = 25$). The solid line is the median A for each t, while the grey shaded area is the envelope bounded by the 10$^{\text{th}}$ and 90$^{\text{th}}$ percentile. The t_s and t_e are shown as dashed vertical lines. The y-axis of each plot represents A and ranges between -1 and +1, while the x-axis represents t and ranges between 200 and 400.

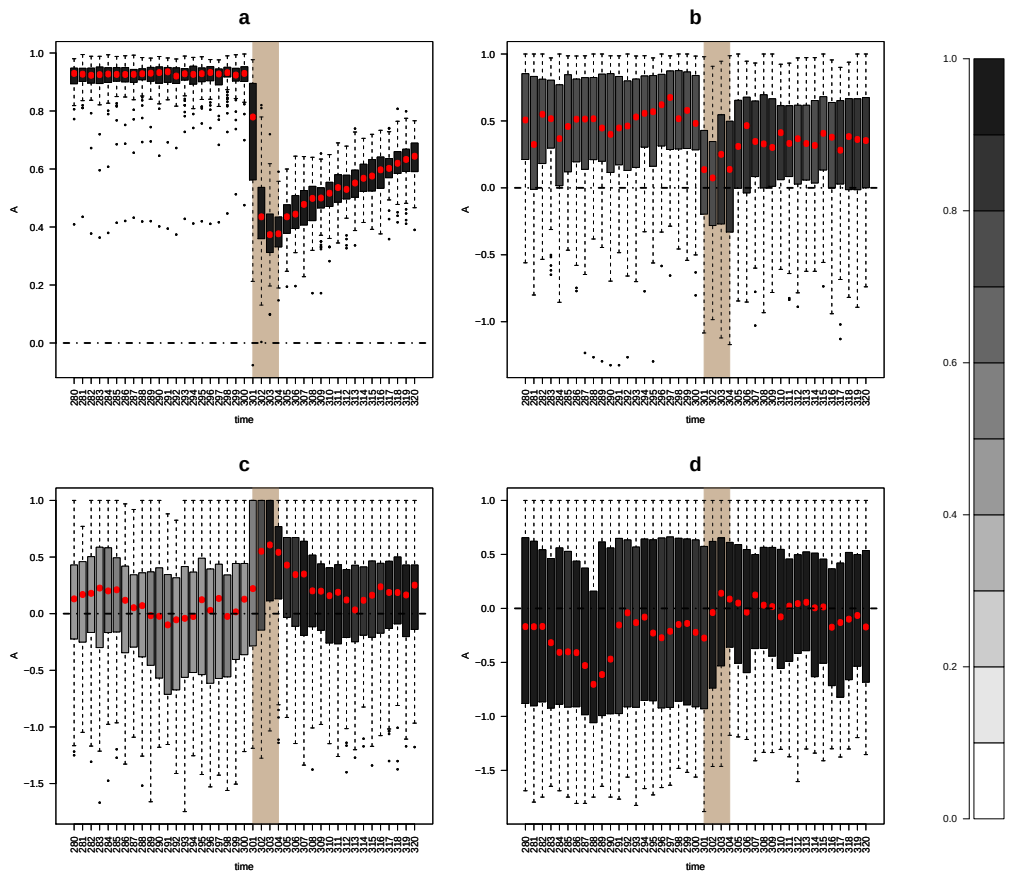

Figure 100: Boxplots of different types of group distribution change (A-coefficient) in response to a fast exogenic disturbance ($t_s = 301$, $t_e = 304$, $\eta = 25$): **a**) $h = 100$, $z = 0.1$, $k = 10^{-8}$,$b = 0.3$, and $\omega_1 = 1.0$; **b**) $h = 100$, $z = 0.5$, $k = 1.0$,$b = 0.5$, and $\omega_1 = 1.0$; **c**) $h = 100$, $z = 1.0$, $k = 1.0$,$b = 0.3$, and $\omega_1 = 1.0$; and **d**) $h = 100$, $z = 1.0$, $k = 1.0$,$b = 0.5$, and $\omega_1 = 1.2$. The fill colour of the boxes indicates the proportion of computed A-coefficients, the red dots depict the median value for each time-step, and the brown strip indicates the timing of the disturbance process.

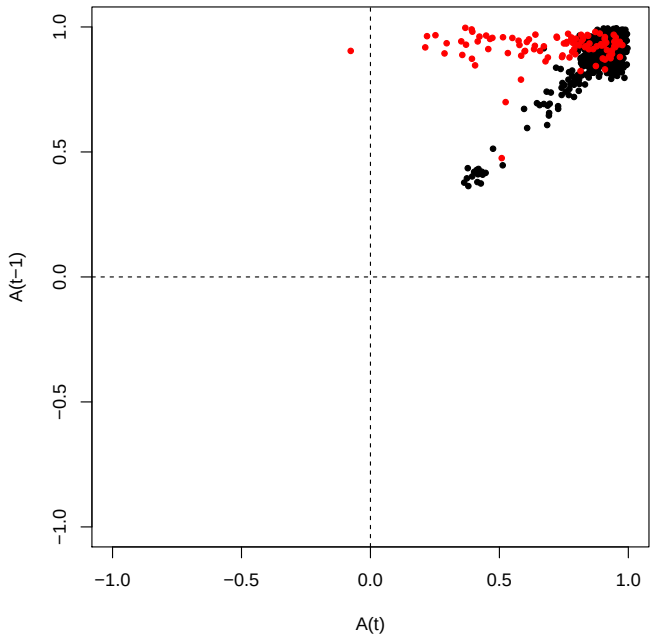

Figure 101: Phase scatterplot of $A(t)$ against $A(t-1)$ for $h = 1$, $z = 0.1$, $k = 10^{-8}$, $b = 0.3$, $\omega_1 = 1.0$. Black dots refer to t ranging from 280 to 300, while the red dots to $t = 301$.

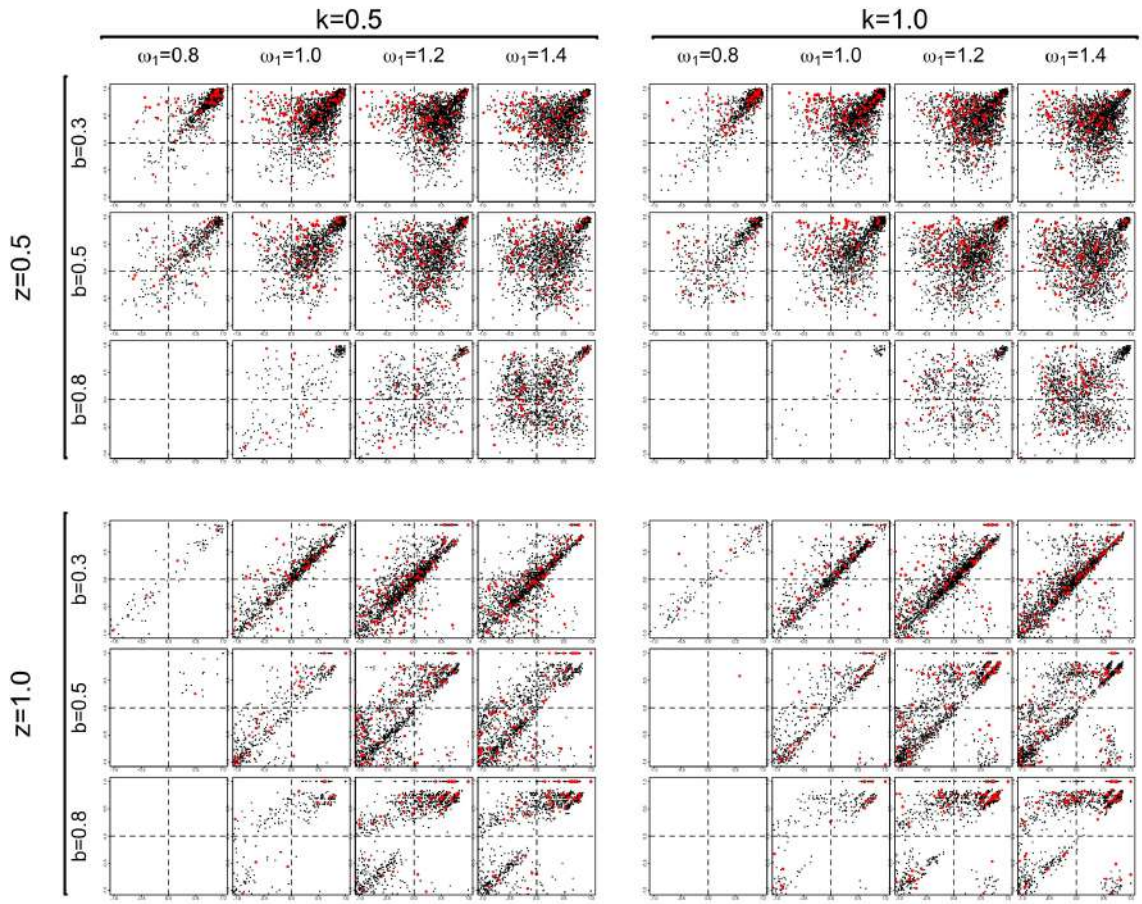

Figure 102: Phase scatterplots of $A(t)$ against $A(t-1)$ for a subregion of the parameter space ($h = \infty$, $z \geq= 0.5$, $k \geq= 0.5$). Black dots refer to t ranging from 280 to 300, while the red dots to $t = 301$. Both x and y axis range from -1 to +1.

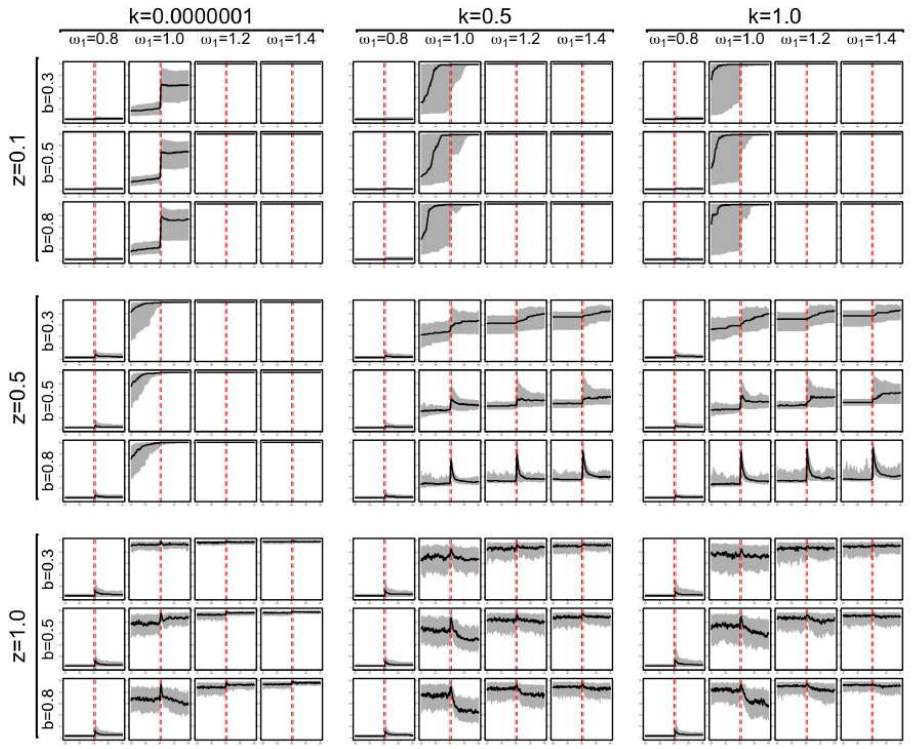

Figure 103: Summary statistics of $G(t)$ with $h = 1$, and a fast disturbance process ($t_s = 301$, $t_e = 304$, $\eta = 25$). The solid line is the median G for each t, while the grey shaded area is the envelope bounded by the 10$^{\text{th}}$ and 90$^{\text{th}}$ percentile. The dashed vertical lines represent t_s and t_e. The y-axis of each plot represents G and ranges between 0 and 100, while the x-axis represents t and ranges between 200 and 400.

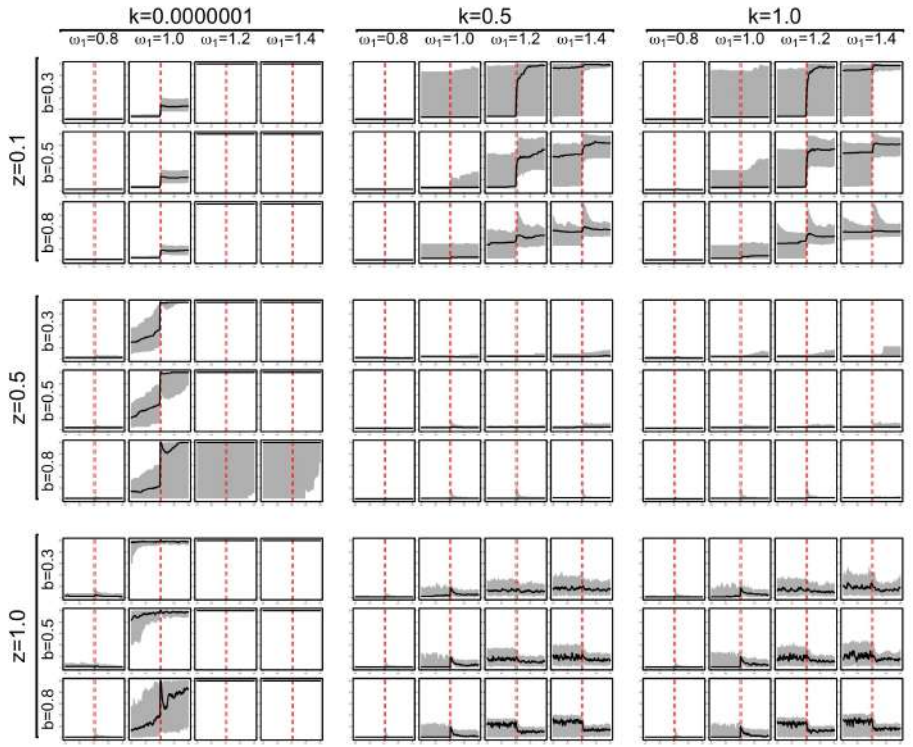

Figure 104: Summary statistics of $G(t)$ with $h = \infty$, and a fast disturbance process ($t_s = 301$, $t_e = 304$, $\eta = 25$). The solid line is the median G for each t, while the grey shaded area is the envelope bounded by the 10$^{\text{th}}$ and 90$^{\text{th}}$ percentile. The dashed vertical lines represent t_s and t_e. The y-axis of each plot represents G and ranges between 0 and 100, while the x-axis represents t and ranges between 200 and 400.

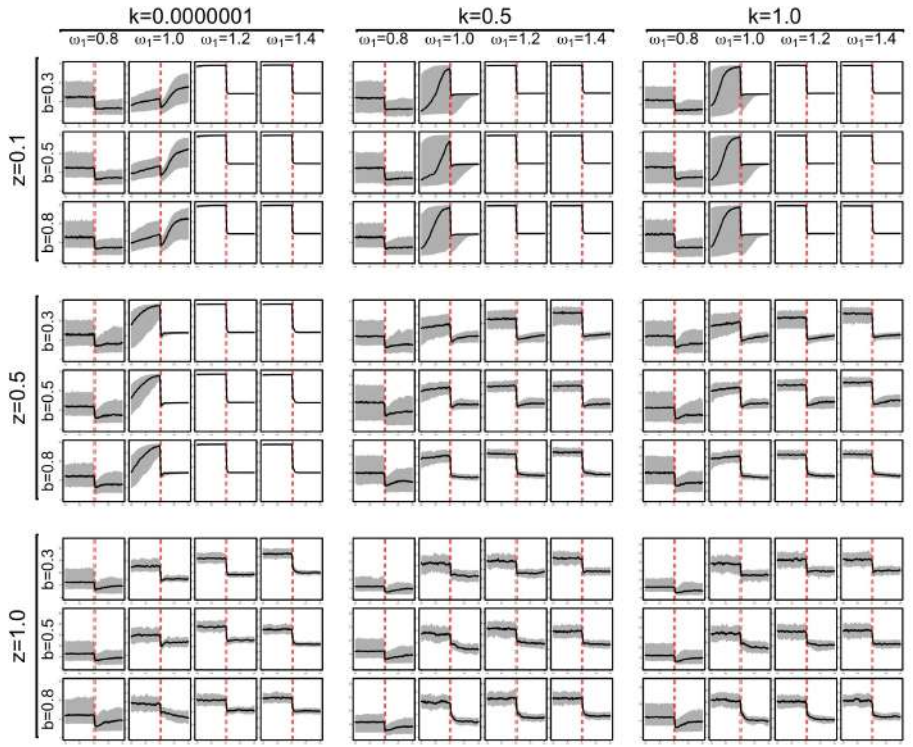

Figure 105: Summary statistics of $N(t)$ with $h = 1$, and a fast disturbance process ($t_s = 301$, $t_e = 304$, $\eta = 25$). The solid line is the median N for each t, while the grey shaded area is the envelope bounded by the 10$^{\text{th}}$ and 90$^{\text{th}}$ percentile. The dashed vertical lines represent t_s and t_e. Notice that the y-axis is scaled to each parameter combination, while the x-axis ranges between 200 and 400.

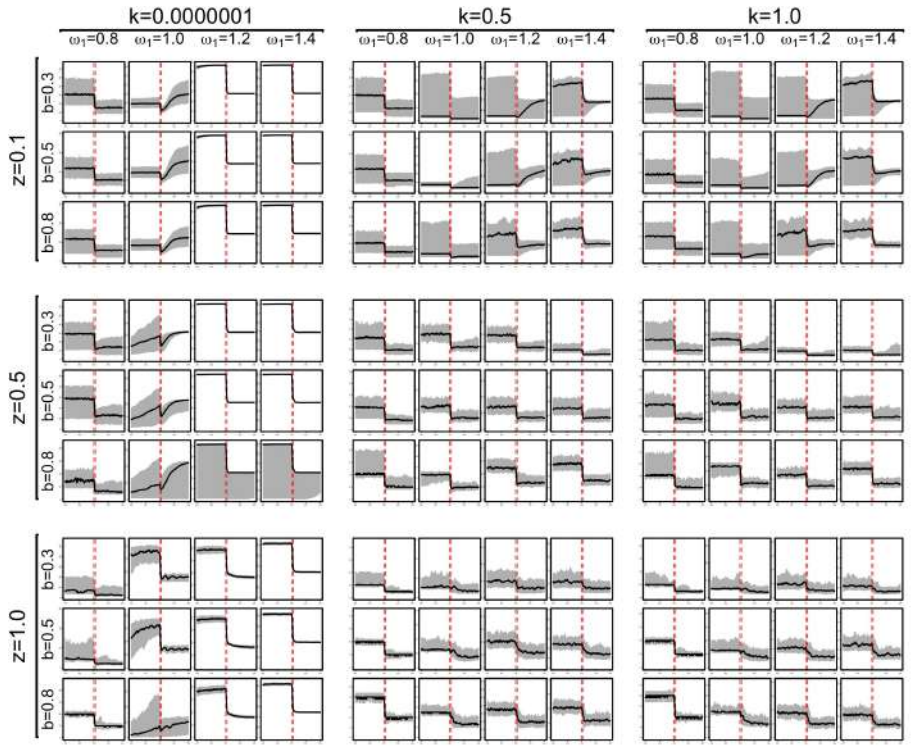

Figure 106: Summary statistics of $N(t)$ with $h = \infty$, and a fast disturbance process ($t_s = 301$, $t_e = 304$, $\eta = 25$). The solid line is the median N for each t, while the grey shaded area is the envelope bounded by the 10$^{\text{th}}$ and 90$^{\text{th}}$ percentile. The dashed vertical lines represent t_s and t_e. Notice that the y-axis is scaled to each parameter combination, while the x-axis ranges between 200 and 400.

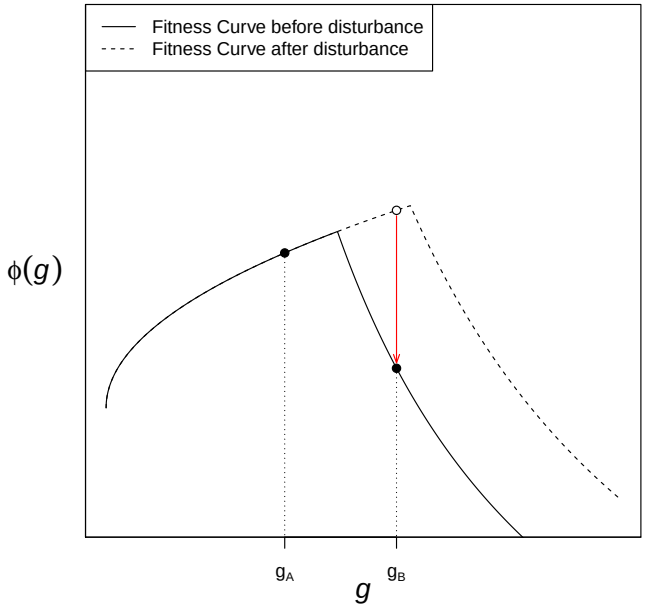

Figure 107: Changes in the fitness of two differently sized groups (G_A and G_B) facing a reduction in K. G_A does not incur any fitness reduction, while the fitness of the members of G_B are subject to decline.

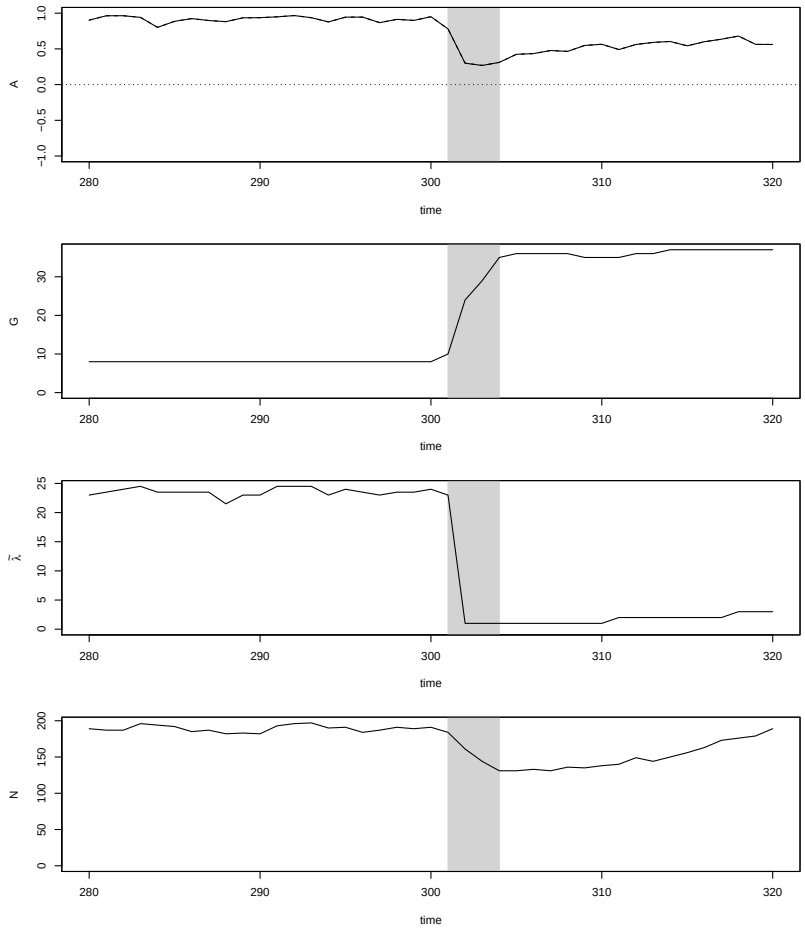

Figure 108: Dynamics of $A(t)$, $\tilde{\lambda}(t)$, $G(t)$, and $N(t)$ for a single run of the simulation (run n.10). Parameters: $h = \infty$, $k = 10^{-8}$, $z = 0.1$, $b = 0.3$, and $\omega_1 = 1.0$. The interval from t_s to t_e is shaded in grey.

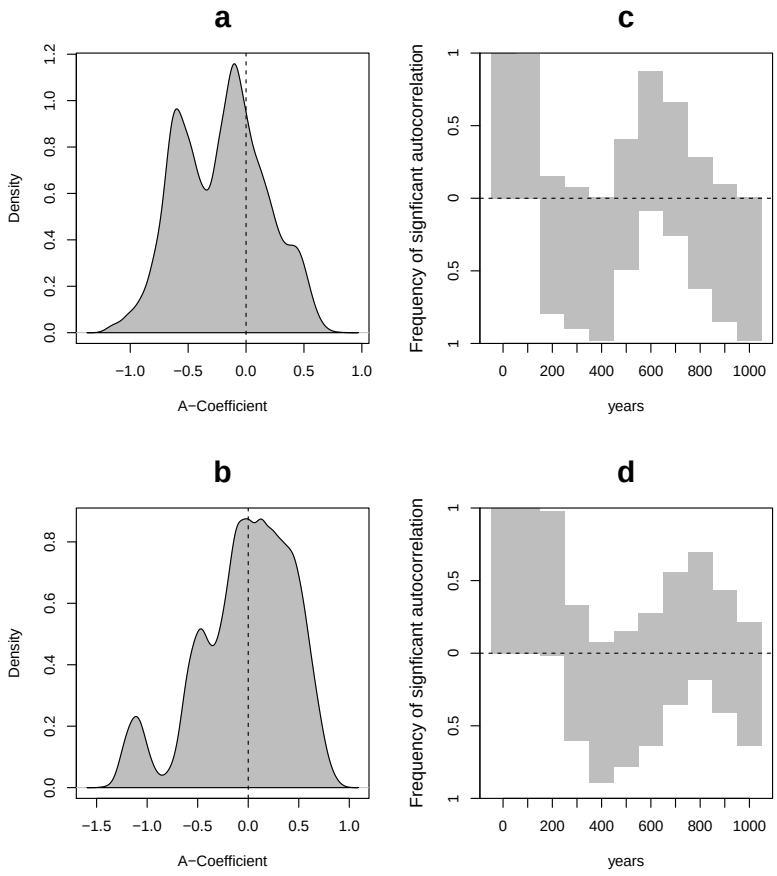

Figure 109: Equilibrium analysis of the empirical A-coefficient distributions: **a**) Probability density (Chiba); **b**) Probability density (Gunma); **c**) Correlogram (Chiba); and **d**) Correlogram (Gunma). Probability densities were obtained with a kernel bandwidth of 0.05; the correlogram plots indicates the proportion of significant positive and negative autocorrelation for 1,000 Monte Carlo simulation runs, for 10 lags of 100 years using the same method described in page 228

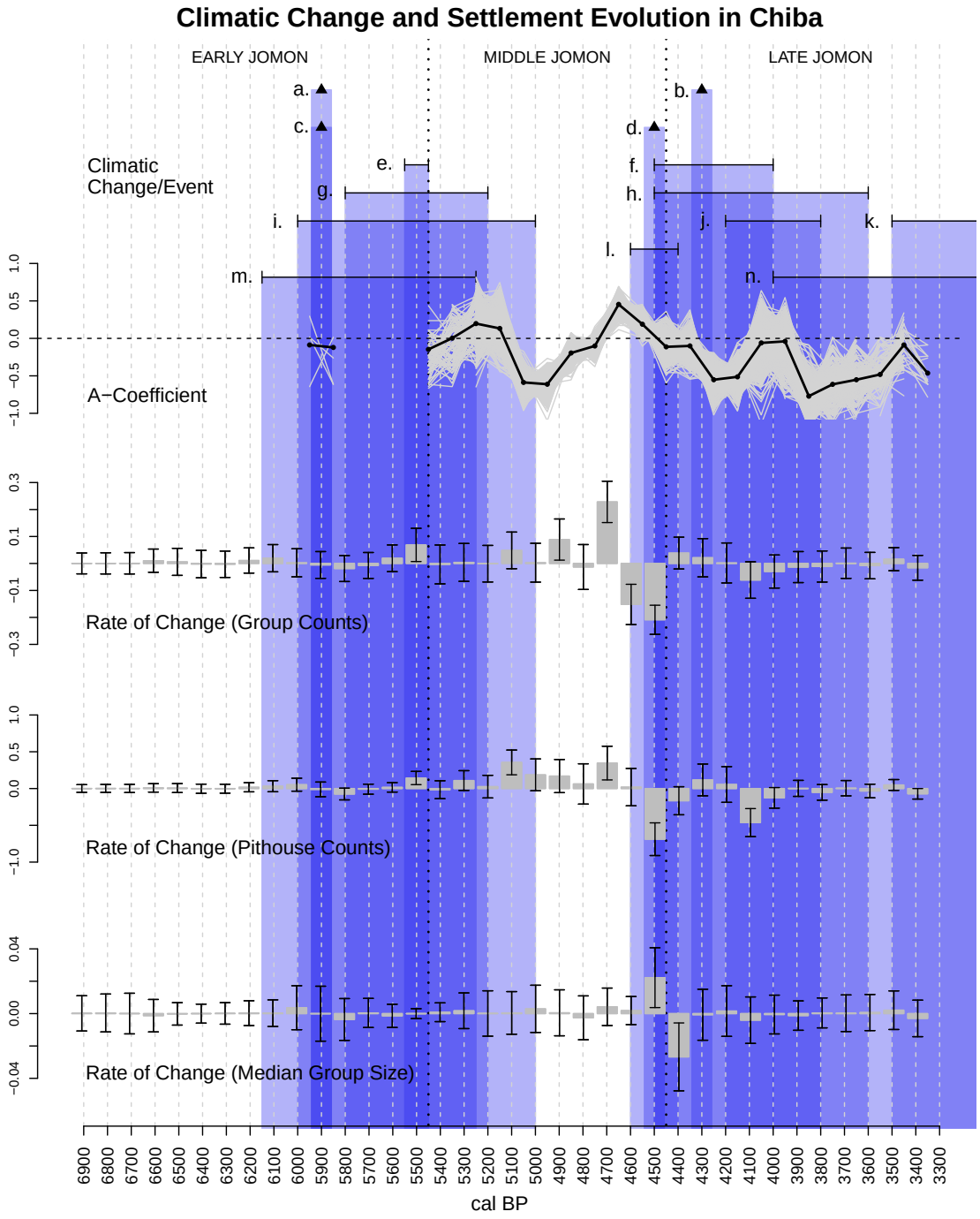

Figure 110: Summary plot of settlement change in Chiba. Climatic events: **a** & **b** : Bond Events (Bond *et al.* 1997); **c** & **d**: Kudo Events (Kudo 2007); **e** & **f**: weak Asian monsoon events (Wang *et al.* 2005); **g** & **h**: strong marine regression events (Fukusawa *et al.* 1999); **i**, **j** & **k**: rapid climate change (Mayewski *et al.* 2004); **l** cooling in Tokyo bay (Miyaji *et al.* 2010); **m** & **n** cooling in Aoki Lake (Adhikari *et al.* 2002) (see detailed discussion in section 2.1). Settlement change data are *A* coefficient time-series and rate of change of settlement counts, pithouse counts and median group size (see figures 28, 30, 32 and 33 and chapter 4 for details). Notice that point-data for the time-series have been shifted to the mid-century (i.e. a value observed at the time-block 4500 cal BP, will have a point at 4450 cal BP), while the rate of change is depicted at mid-point (i.e. a rate of change between blocks 5300-5200 cal BP and 5200-5100 cal BP will be depicted at 5200 cal BP).

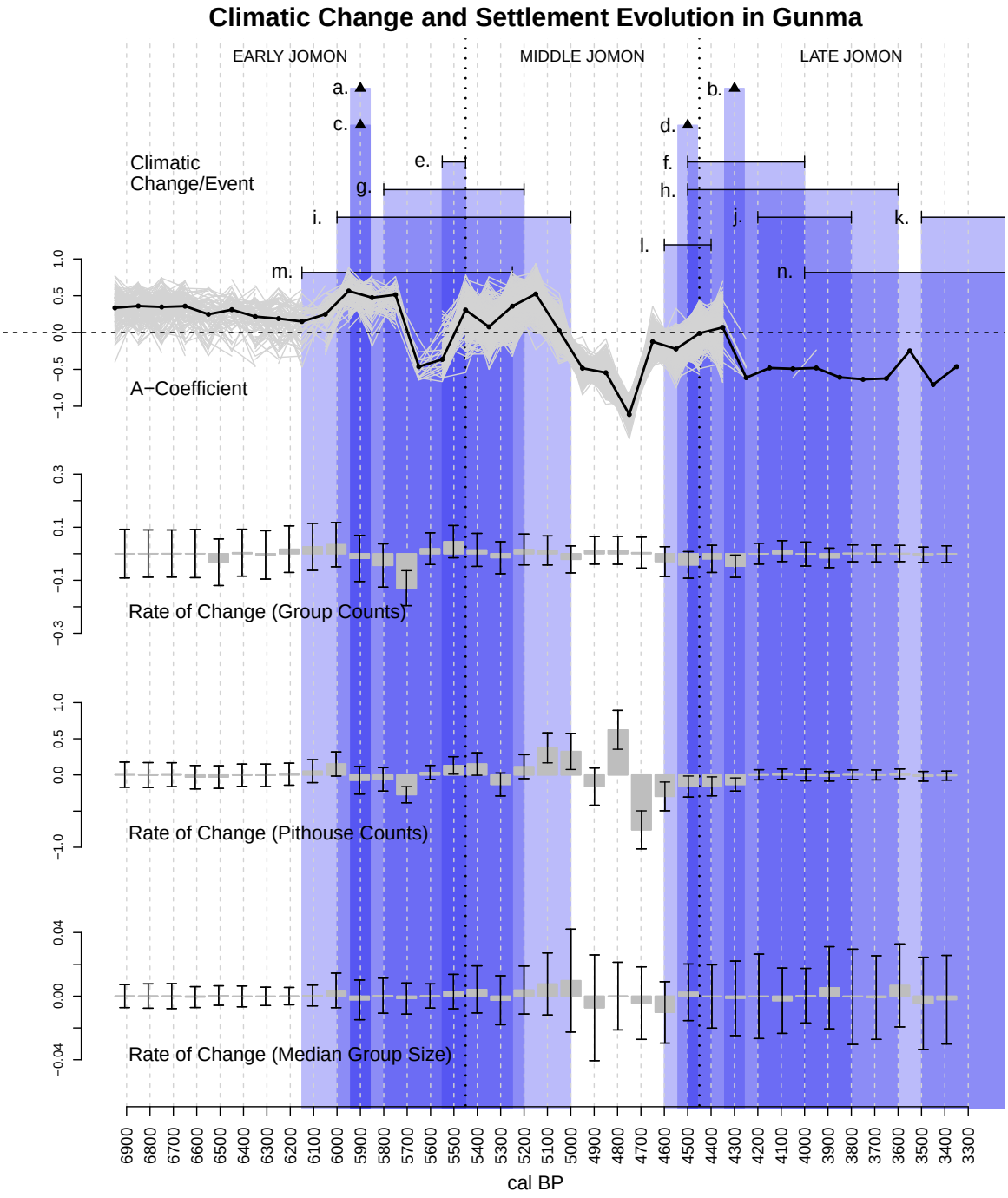

Figure 111: Summary plot of settlement change in Gunma. Climatic events: **a** & **b** : Bond Events (Bond *et al.* 1997); **c** & **d**: Kudo Events (Kudo 2007); **e** & **f**: weak Asian monsoon events (Wang *et al.* 2005); **g**, **h** & **i**: rapid climate change (Mayewski *et al.* 2004); **j** & **k** cooling in Aoki Lake (Adhikari *et al.* 2002) (see detailed discussion in section 2.1). Settlement change data are *A* coefficient time-series and rate of change of settlement counts, pithouse counts and median group size (see figures 28, 30, 32 and 33 and chapter 4 for details). Notice that point-data for the time-series have been shifted to the mid-century (i.e. a value observed at the time-block 4500 cal BP, will have a point at 4450 cal BP), while the rate of change is depicted at mid-point (i.e. a rate of change between blocks 5300-5200 cal BP and 5200-5100 cal BP will be depicted at 5200 cal BP).

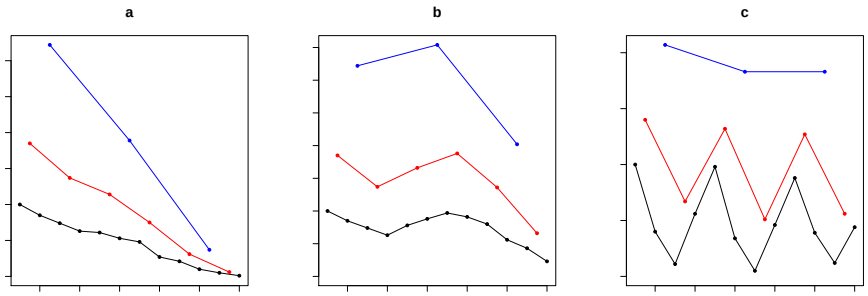

Figure 112: Effects of variation in the temporal resolution for different types of time-series. The resolution ratio is 1:2:4 with the red time-series being twice the resolution of the black one, and the blue time-series being four times coarser.

Tables

Period	Pottery Phase	cal BP
Early Jōmon	Hanazumi Kasō/Sekiyama	ca7000-?
	Sekiyama	?(6450)
	Kurohama	6450-6050
	Moroiso a	6050-5950
	Moroiso b	5950-5750
	Moroiso c	5750-5600
	Jūsanbodai	5600-5470
Middle Jōmon	Goryōgadai 1	5470-5440
	Goryōgadai 2	5440-5380
	Katsuzaka 1	5380-5280
	Katsuzaka 2	5280-5080
	Katsuzaka 3	5080-4900
	Kasori E1	4900-4810
	Kasori E2	4810-4710
	Kasori E3	4710-4520
	Kasori E4	4520-4420
Late Jōmon	Shōmyōji 1	4420-4300
	Shōmyōji 2	4300-4250
	Horinouchi 1	4250-3980
	Horinouchi 2	3980-3820
	Kasori B1	3820-3680
	Kasori B2	3680-3530
	Kasori B3	3530-3470
	Soya	3470-3400
	Angyō 1	3400-3300
	Angyō 2	3300-3220

Table 1: Absolute dates of pottery phases in Kantō

a	b	c
ca7000-	Hanazumi Kasō	-
?	Sekiyama I	Futatsuki
?	Sekiyama II	-
6450-6050	Kurohama	Ario
6050-5950	Moroiso a	Ukishima Ia
5950-	Moroiso b	Ukishima Ib
-	|	Ukishima II
-5750	|	Ukishima IIII
5750-5600	Moroiso c	Okitsu
5600-5470	Jūsanbodai	|

a: cal BP

b: Southwest Kantō Sequence

c: Chiba Sequence

Table 2: Comparison of Early Jōmon pottery sequences. The ″|″ sign indicates continuity of a pottery tradition.

a	b	c	d	e	f
5470-5440	1	Goryōgadai 1			
5440-5420	2	Goryōgadai 2			
5420-5400	3	|			
5400-5380	4	|			
5380-5360	5a	Katsuzaka 1	Kakusawa	Otamadai Ia	
5360-5340	5b	|	|	|	
5340-5320	5c	|	|	Otamadai Ib	
5320-5300	6a	|	Aramichi	|	
5300-5280	6b	|	|	Otamadai II	
5280-5250	7a	Katsuzaka 2	Fujiuchi 1	|	
5250-5220	7b	|	|	|	
5220-5150	8a	|	Fujiuchi 2	|	
5150-5080	8b	|	|	Otamadai III	
5080-5000	9a	Katsuzaka 3	Idojiri 1	|	Miharada-Yakemachi
5000-4920	9b	|	Idojiri 3	Otamadai IV	|
4920-4900	9c	|	Nashikubo B	Nakabyō	Miharada
4900-4870	10a	Kasori E1	Sori 1	Kasori EI	|
4870-4849	10b	|	|	|	|
4840-4810	10c	|	Sori 2	|	|
4810-4780	11a	Kasori E2	Sori 3 old	|	|
4780-4750	11b	|	|	Kasori EII	
4750-4730	11c1	|	|	|	
4730-4710	11c2	|	|	|	
4710-4670	12a	Kasori E3	Sori 3 new	|	
4670-4590	12b	|	|	|	
4590-4520	12c	|	Sori 4	Kasori EIII	
4520-4470	13a	Kasori E4	Sori 5	Kasori EIV	
4470-4420	13b	|	|	|	

a: cal BP
b: Shinchihei Sequence
c: Southwest Kantō Sequence
d: Chūbu Sequence
e: Chiba Sequence
f: Gunma Sequence

Table 3: Comparison of Middle Jōmon pottery sequences. The "|" sign indicates continuity of a pottery tradition. Notice that where the pottery phase is not specified, the local chronological sequence is inferred from those of other regions.

Size Distribution	**Spatial Pattern**	**Expected shape of $\bar{\lambda}(d)$**
Clumped/Primate	Random	Monotonic decrease.
Clumped/Primate	Uniform	Monotonic decrease.
Clumped/Primate	Clustered	Monotonic decrease.
Clumped/Primate	Equal distance of small settlements to S_1	Initial decrease with peak at $\bar{\lambda}(x)$, with x being the typical distance to S_1.
Clumped/Primate (with S_2 being close in size to S_1)	Random	Initial decrease with peak at $\bar{\lambda}(x)$, with x being the distance between S_1 and S_2.
Dispersed/Convex	Random	Monotonic decrease.
Dispersed/Convex	Uniform	Initial decrease with peak at $\bar{\lambda}(x)$, with x being the typical inter-distance between settlements.
Dispersed/Convex	Clustered	Monotonic decrease from $\bar{\lambda}(x)$, where x is the size of settlements cluster.

Table 4: Expected shape of $\bar{\lambda}(d)$ for different combinations of spatial structure and size distributions.

Symbol	Name	Notes
m	Minimum subunit.	-
g	Current group size.	-
$g*$	Optimal group size.	$\phi(g < g*) < \phi(g*) > \phi(g > g*)$
$\bar{g}$	Saturation group size.	$\phi(\bar{g}) = \phi(m)$
$\dot{g}$	short-term equilibrium group size.	Expected group size with no reproduction/death.
$\breve{g}$	long-term equilibrium group size.	Expected group size with reproduction/death.
$\tilde{g}$	Zero growth group size.	Group size where $\gamma = 0$.
$\hat{g}$	Fission size.	Expected size above which fission is likely to occur

Table 5: List of critical values of g.

Scenario	Condition	Decision
$g_i > m \; AND \; g_w > m$	$\mu - c_1 < \phi_i \geq \phi_w$	No Change
	$\phi_i \leq (\mu - c_1) \; AND \; [\phi_w \leq (\mu - c_1) \; OR \; \phi_i \geq \phi_w]$	Fission
	$[\phi_i \leq (\phi_w - c_2) \; OR \; \phi_i \leq (\mu - c_1)] \; AND \; \phi_w > (\mu - c_1)$	Migration
$g_i > m \; AND \; g_w = m$	$\phi_i \geq \phi_w \; AND \; \phi \geq (\mu - c_1)$	No Change
	$\phi_i < (\phi_w - c_1) \; OR \; \phi_i < (\mu - c_1)$	Fission
$g_i = m \; AND \; g_w > m$	$\phi_i > (\phi_w - c_3)$	No Change
	$\phi_i \leq (\phi_w - c_3)$	Fusion
$g_i = m \; AND \; g_w = m$	$\phi_i \geq \phi_w$	No Change
	$\phi_i < \mu \; AND \; \phi_w < \mu$	Fusion
$g_i > m \; AND \; g_w = NULL$	$\phi_i \leq (\mu - c_1)$	Fission
$g_i = m \; AND \; g_w = NULL$	-	No Change

Table 6: Summary of decision-making criteria. *NULL* indicates that not other groups are located within distance s (hence $\lceil k|U(i,s)| \rceil = 0$). Fission assumes the presence of at least one empty patch within distance h, otherwise the agent will make no changes.

General Settings	
$N(t)$	Number of agents at timestep t
t	Time-step
T	Total number of time-steps
g	Group size
$G(t)$	Total number of groups at time-step t
P	Total number of patches
i	Index referring to the focal agent
j	Index referring to the focal group
Fitness curve related	
μ	Basic individual payoff
ϵ	Payoff variance
b	Cooperation benefit
ξ	Individual contribution
Ξ	Group contribution
ϕ	Individual fitness
K	Resource input
Reproduction and death related	
r	Reproduction rate
d	Death rate
ρ	Basic reproduction rate
ω_1	Death parameter 1
ω_2	Death parameter 2
γ	Net Growth rate of a given group
Γ	Net Growth rate of the entire population
Fission/fusion/migration related	
z	Frequency of decision-making
k	Sample proportion of observed agents
s	Neighbour search distance
$U(s,i)$	Agents within distance s from i
$u(k,s,i)$	Randomly sampled agents from U
w	Index indicating the model agent
h	Fission distance
c_1	Treshold of evidence for fission
c_2	Treshold of evidence for migration
c_3	Treshold of evidence for fusion

Table 7: Symbols and definitions of the model parameters and variables

Constant Parameters		
$N(t=0)$	Number of agents at time-step t	10
T	Total number of time-steps	500
P	Total number of patches	100
μ	Basic individual payoff	10
ϵ	Payoff variance	1
K	Resource input	200
ρ	Basic reproduction rate	0.05
ω_2	Death parameter 2	5
h	Fission distance	s
c_1	Treshold of evidence for fission	3
c_2	Treshold of evidence for migration	3
c_3	Treshold of evidence for fusion	3
Sweep Parameters		
z	Frequency of decision-making	0.1, 0.5, and 1.0
b	Cooperation benefit	0.3, 0.5, and 0.8
k	Sample proportion of observed agents	10^{-7}, 0.5, and 1.0
s	Neighbour search distance	1 and ∞
ω_1	Death parameter 1	0.8, 1.0, 1.2, and 1.4

Table 8: Constant and sweep parameter values

Constant Parameters		
κ	Prey population carrying capacity	200
ζ	Prey population growth rate	2
t_s	Starting time-step of the disturbance event	301
Sweep Parameters		
β	Prey population growth resilience	0.3, 0.35, and 0.4
t_e	Ending time-step of the disturbance event	304, 308, and 348
η	Abruptness of the disturbance event	25, ca 5.56, and ca 2.08

Table 9: Constant and sweep parameter values for disturbance models

Temporal Interval	Rank-Size Distribution[a]	Settlement Counts [b]	Pithouse Counts [b]	Median Group Size [b]	Environmental Change [c]
$t_{5200}-t_{5100}$	Z(0.13)-C(-0.59)	Increase	Increase*	?	RCC
$t_{5000}-t_{4900}$	C(-0.61)-Z(-0.19)	Increase*	Increase	?	-
$t_{4900}-t_{4800}$	Z(-0.19)-Z(-0.10)	?	?	?	-
$t_{4800}-t_{4700}$	Z(-0.10)-D(0.45)	Increase*	Increase	?	-
$t_{4700}-t_{4600}$	D(0.45)-Z(0.18)	Decrease*	?	?	CTB
$t_{4600}-t_{4500}$	Z(0.18)-Z(-0.11)	Decrease*	Decrease*	Increase*	CTB; MR;WM
$t_{4500}-t_{4400}$	Z(-0.11)-Z(-0.10)	Increase	Decrease	Decrease*	CTB; MR; WM
$t_{4400}-t_{4300}$	Z(-0.10)-C(-0.55)	?	Increase	Increase?	MR; WM
$t_{4300}-t_{4200}$	C(-0.55)-C(-0.51)	?	?	?	RCC; MR; WM
$t_{4200}-t_{4100}$	C(-0.51)-Z(-0.06)	Decrease	Decrease*	?	RCC; MR; WM

a. Z: Zipf's law rank-size distribution; C: Clumped rank-size distribution; D: Dispersed rank-size distribution. The number in brackets refers to the mean A-coefficient.

b. The asterisk (*) indicates strongly significant case of increase/decrease; The question mark (?) refers to instance with high uncertainty. The distinction has been based on the position of the error-bars.

c. RCC: Rapid Climate Change (Mayewski *et al.* 2004); CTB: Cooling in Tokyo Bay (Miyaji *et al.* 2010); MR: Strong marine regression (Fukusawa *et al.* 1999); WM: Weak Asian monsoon events (Wang *et al.* 2005).

Table 10: Major settlement transitions in Chiba.

Temporal Interval	Rank-Size Distribution[a]	Settlement Counts [b]	Pithouse Counts [b]	Median Group Size [b]	Environmental Change [c]
$t_{6100}-t_{6000}$	D(0.25)-D(0.56)	Increase	Increase	?	CAL;RCC
$t_{5800}-t_{5700}$	D(0.51)-C(-0.46)	Decrease*	Decrease*	Decrease	CAL;RCC
$t_{5600}-t_{5500}$	C(-0.37)-D(0.30)	Increase	Increase	?	CAL;RCC;WM
$t_{5200}-t_{5100}$	D(0.52)-Z(0.03)	?	Increase*	Increase	RCC
$t_{5100}-t_{5000}$	Z(0.03)-Z(-0.48)	?	Increase*	Increase	RCC
$t_{5000}-t_{4900}$	C(-0.48)-C(-0.54)	?	?	Decrease	-
$t_{4900}-t_{4800}$	C(-0.54)-C(-1.11)	?	Increase*	Unknown	-
$t_{4800}-t_{4700}$	C(-1.11)-Z(-0.12)	?	Decrease*	Decrease	-
$t_{4700}-t_{4600}$	Z(-0.12)-Z(-0.22)	Decrease	Decrease*	Decrease	-

a. Z: Zipf's law rank-size distribution; C: Clumped rank-size distribution; D: Dispersed rank-size distribution. The number in brackets refers to the mean A-coefficient.

b. The asterisk (*) indicates strongly significant case of increase/decrease; The question mark (?) refers to instance with high uncertainty. The distinction has been based on the position of the error-bars.

c. CAL: Cooling at Aoki Lake (Adhikari *et al.* 2002); RCC: Rapid Climate Change (Mayewski *et al.* 2004); WM: Weak Asian monsoon events (Wang *et al.* 2005).

Table 11: Major settlement transitions in Gunma

APPENDICES

Appendix A

Supplementary Data

This appendix provides the raw data used for the spatial analysis discussed in chapter 4, comprising the following tables:

- Pithouse data (tables A.1 and A.2). For each pithouse, these two tables provide: an unique identifier (**Pithouse ID**); a linker to tables A.3 and A.4 (**BUA ID**); the associated pottery phase (**Period**; which links to table A.6), a linker to table A.5 (**REF**), and the original ID used in the published reports (when available).

- BUA (tables A.3 and A.4). The two tables provide the following set of information: an unique identifier which can be linked to tables A.1 and A.2 (**BUA ID**); the spatial coordinates of the BUA (**x** and **y**, in UTM Zone 54N, WGS84); and the total areal extent of the BUA in square meters (**Area**).

- List of excavation reports (table A.5). For each entry the table provides: an unique identifier (**REF Id**, which can be linked to tables A.1 and A.2); year of publication (**Year**); publishing institution (**Institution(s)**); title of the report (**Title**). In few cases the pithouse data has been obtained from books or articles, in such cases the bibliographic entry has been provided in the last column (**Other references**).

- Aoristic weights for the pottery phases (table A.6) . This table provides the

probability distribution for each pottery phase (**Pottery Phase**; which can serve as a linker to tables A.1 and A.2). Columns **t1,t2,t3**...**t37** refers to the temporal blocks starting from 7000-6900 and ending at 3400-3300, while the columns **B.** and **A.** provide the cumulative aoristic weights of all the time-intervals before 7000 cal BP (**B.**) and after 3300 cal BP (**A.**).

Table A.1: Pithouses at Gunma

BUA ID	Pithouse ID	Period	REF	original ID
348	348-001	Early Jomon	HGEASR2005	
348	348-002	Early Jomon	HGEASR2005	
348	348-003	Early Jomon	HGEASR2005	
348	348-004	Jomon	HGEASR2005	
348	348-005	Jomon	HGEASR2005	
348	348-006	Jomon	HGEASR2005	
348	348-007	Jomon	HGEASR2005	
348	348-008	Jomon	HGEASR2005	
348	348-009	Jomon	HGEASR2005	
348	348-010	Jomon	HGEASR2005	
348	348-011	Middle Jomon	HGEASR2005	
348	348-012	Middle Jomon	HGEASR2005	
348	348-013	Middle Jomon	HGEASR2005	
348	348-014	Middle Jomon	HGEASR2005	
348	348-015	Middle Jomon	HGEASR2005	
348	348-016	Middle Jomon	HGEASR2005	
348	348-017	Middle Jomon	HGEASR2005	
348	348-018	Middle Jomon	HGEASR2005	
348	348-019	Middle Jomon	HGEASR2005	
348	348-020	Middle Jomon	HGEASR2005	
348	348-021	Middle Jomon	HGEASR2005	
348	348-022	Middle Jomon	HGEASR2005	
348	348-023	Middle Jomon	HGEASR2005	
348	348-024	Middle Jomon	HGEASR2005	
348	348-025	Middle Jomon	HGEASR2005	
348	348-026	Middle Jomon	HGEASR2005	
348	348-027	Middle Jomon	HGEASR2005	
348	348-028	Middle Jomon	HGEASR2005	
348	348-029	Middle Jomon	HGEASR2005	
348	348-030	Middle Jomon	HGEASR2005	
348	348-031	Middle Jomon	HGEASR2005	
348	348-032	Middle Jomon	HGEASR2005	
348	348-033	Middle Jomon	HGEASR2005	
348	348-034	Middle Jomon	HGEASR2005	
370	370-001	Early Jomon (Final)	NGKB1981	
370	370-002	Kasori EIV	NGKB1981	
370	370-003	Kasori EII-EIII	NGKB1981	
370	370-004	Kasori EII-EIII	NGKB1981	
370	370-005	Kasori EII-EIII	NGKB1981	
370	370-006	Kasori EII-EIII	NGKB1981	
370	370-007	Kasori EII-EIII	NGKB1981	

Continued on next page

Table A.1: Pithouses at Gunma

BUA ID	Pithouse ID	Period	REF	original ID
370	370-008	Kasori EII-EIII	NGKB1981	
370	370-009	Kasori EII-EIII	NGKB1981	
370	370-010	Kasori EII-EIII	NGKB1981	
370	370-011	Kasori EII-EIII	NGKB1981	
370	370-012	Kasori EII-EIII	NGKB1981	
370	370-013	Kasori EII-EIII	NGKB1981	
489	489-001	Kasori EIV - Horinouchi1	HGKMY1990	Ek-1
489	489-002	Shomyoji - Horinouchi	HGKMY1990	Ek-2
489	489-003	Shomyoji - Horinouchi	HGKMY1990	Ek-3
489	489-004	Shomyoji - Horinouchi	HGKMY1990	Ek-4
489	489-005	Kurohama - Moroiso c	HGKMY1990	1
489	489-006	Kurohama - Moroiso c	HGKMY1990	2
489	489-007	Sekiyama - Kurohama	HGKMY1990	5
489	489-008	Early Jomon (Early)	HGKMY1990	6
489	489-009	Jomon	HGKMY1990	7
489	489-010	Moroiso c	HGKMY1990	8
489	489-011	Sekiyama - Kurohama	HGKMY1990	9
489	489-012	Sekiyama - Kurohama	HGKMY1990	10
489	489-013	Jomon	HGKMY1990	11
489	489-014	Moroiso c	HGKMY1990	12
489	489-015	Early Jomon	HGKMY1990	13
489	489-016	Kasori EIV - Horinouchi1	HGKMY1990	14
489	489-017	Early Jomon - Late Jomon	HGKMY1990	15
489	489-018	Early Jomon	HGKMY1990	16
489	489-019	Early Jomon	HGKMY1990	17
489	489-020	Moroiso b	HGKMY1990	18
489	489-021	Moroiso	HGKMY1990	19
489	489-022	Sekiyama - Moroiso c	HGKMY1990	20
489	489-023	Early Jomon	HGKMY1990	21
489	489-024	Kasori EIV - Shomyoji	HGKMY1990	22(JH-22)
546	546-001	Horinouchi 2	NSKB1993	J-1
581	581-001	Moroiso a	KWST1998	1
581	581-002	Kurohama / Ario	KWST1998	2
581	581-003	Kurohama / Ario	KWST1998	3
581	581-004	Kurohama / Ario	KWST1998	4
581	581-005	Kurohama / Ario	KWST1998	5
581	581-006	Kurohama / Ario	KWST1998	6
581	581-007	Kurohama / Ario	KWST1998	7
581	581-008	Moroiso b	KWST1998	8
581	581-009	Moroiso b	KWST1998	9
581	581-010	Kurohama / Ario	KWST1998	10

Continued on next page

Table A.1: Pithouses at Gunma

BUA ID	Pithouse ID	Period	REF	original ID
581	581-011	Kurohama / Ario	KWST1998	11
581	581-012	Kurohama / Ario	KWST1998	12
581	581-013	Kurohama / Ario	KWST1998	13
581	581-014	Moroiso b	KWST1998	14
581	581-015	Kurohama / Ario	KWST1998	15
581	581-016	Moroiso b	KWST1998	16
581	581-017	Kurohama / Ario	KWST1998	17
581	581-018	Kurohama / Ario	KWST1998	18
581	581-019	Jomon	KWST1998	19
581	581-020	Kurohama / Ario	KWST1998	20
581	581-021	Kurohama / Ario	KWST1998	21
581	581-022	Kurohama / Ario	KWST1998	22
6460	6460-001	Moroiso c	RKMAN1993	1
6494	6494-001	Shomyoji	MZRGO2003	J-1
6494	6494-002	Shomyoji	MZRGO2003	J-2
6494	6494-003	Shomyoji	MZRGO2003	J-3
6494	6494-004	Shomyoji	MZRGO2003	J-4
6494	6494-005	Shomyoji	MZRGO2003	J-5
6494	6494-006	Shomyoji	MZRGO2003	J-6
6494	6494-007	Shomyoji	MZRGO2003	J-7
6494	6494-008	Shomyoji	MZRGO2003	J-8
6494	6494-009	Shomyoji	MZRGO2003	J-9
6494	6494-010	Shomyoji	MZRGO2003	J-10
6494	6494-011	Shomyoji	MZRGO2003	J-11
6494	6494-012	Shomyoji	MZRGO2003	J-12
6494	6494-013	Shomyoji	MZRGO2003	J-13
6494	6494-014	Shomyoji	MZRGO2003	J-14
6494	6494-015	Shomyoji	MZRGO2003	J-15
6494	6494-016	Shomyoji	MZRGO2003	J-16
6494	6494-017	Shomyoji	MZRGO2003	J-17
6494	6494-018	Shomyoji	MZRGO2003	J-18
6494	6494-019	Shomyoji	MZRGO2003	J-19
6494	6494-020	Shomyoji	MZRGO2003	J-20
6510	6510-001	Sekiyama I (Middle - Early)	MTJS2005	J-1
6510	6510-002	Sekiyama I (Late) - II	MTJS2005	J-2
6510	6510-003	Sekiyama I (Ealry - Middle)	MTJS2005	J-3
6510	6510-004	Sekiyama I (Middle - Early)	MTJS2005	J-4
6510	6510-005	Sekiyama I (Late) - II	MTJS2005	J-5
6510	6510-006	Sekiyama II	MTJS2005	J-6
6510	6510-007	Sekiyama I (Ealry - Middle)	MTJS2005	J-7
6510	6510-008	Sekiyama I (Middle - Early)	MTJS2005	J-8

Continued on next page

Table A.1: Pithouses at Gunma

BUA ID	Pithouse ID	Period	REF	original ID
6510	6510-009	Sekiyama I (Ealry - Middle)	MTJS2005	J-9
6510	6510-010	Sekiyama I (Middle - Early)	MTJS2005	J-10
6510	6510-011	Sekiyama II	MTJS2005	J-11
6510	6510-012	Kasori E2	MTJS2005	J-12
6510	6510-013	Sekiyama I (Early)	MTJS2005	J-13
6511	6511-001	Sekiyama	TKZYNG2005	J-1
6519	6519-001	Moroiso	UMHTK2004	
6519	6519-002	Moroiso	UMHTK2004	
6519	6519-003	Moroiso	UMHTK2004	
6519	6519-004	Moroiso	UMHTK2004	
6519	6519-005	Moroiso	UMHTK2004	
6519	6519-006	Moroiso	UMHTK2004	
6519	6519-007	Moroiso	UMHTK2004	
6519	6519-008	Moroiso	UMHTK2004	
6522	6522-001	Miharada	MIHA1990	1-1
6522	6522-002	Kasori E2	MIHA1990	1-2
6522	6522-003	Kasori E3 (Early)	MIHA1990	1-3
6522	6522-004	Miharada	MIHA1990	1-4
6522	6522-005	Kasori E2 - E3 (Early)	MIHA1990	1-5
6522	6522-006	Kasori E2	MIHA1990	1-6
6522	6522-007	Miharada	MIHA1990	1-7
6522	6522-008	Miharada	MIHA1990	1-8
6522	6522-009	Kasori E2	MIHA1990	1-9
6522	6522-010	Kasori E2	MIHA1990	1-10
6522	6522-011	Kasori E2	MIHA1990	1-11
6522	6522-012	Kasori E2	MIHA1990	1-12
6522	6522-013	Kasori E3 (Late)	MIHA1990	1-13
6522	6522-014	Kasori E3 (Early)	MIHA1990	1-14
6522	6522-015	Kasori E2	MIHA1990	1-15
6522	6522-016	Kasori E2	MIHA1990	1-16
6522	6522-017	Kasori E3 (Late)	MIHA1990	1-17
6522	6522-018	Miharada	MIHA1990	1-18
6522	6522-019	Miharada	MIHA1990	1-19
6522	6522-020	Kasori E3 (Early)	MIHA1990	1-20
6522	6522-021	Kasori E3 (Early)	MIHA1990	1-21
6522	6522-022	Kasori E3 (Late)	MIHA1990	1-22
6522	6522-023	Jomon	MIHA1990	1-23
6522	6522-024	Kasori E3 (Middle)	MIHA1990	1-25
6522	6522-025	Kasori E3 (Middle)	MIHA1990	1-26
6522	6522-026	Kasori E2	MIHA1990	1-28
6522	6522-027	Kasori E2	MIHA1990	1-29

Continued on next page

Table A.1: Pithouses at Gunma

BUA ID	Pithouse ID	Period	REF	original ID
6522	6522-028	Kasori E3 (Late)	MIHA1990	1-30
6522	6522-029	Kasori E3 (Early)	MIHA1990	1-31
6522	6522-030	Jomon	MIHA1990	1-32
6522	6522-031	Kasori E3 (Middle)	MIHA1990	1-33
6522	6522-032	Kasori E3 (Late)	MIHA1990	1-34
6522	6522-033	Kasori E3 (Middle)	MIHA1990	1-35
6522	6522-034	Kasori E4	MIHA1990	1-36
6522	6522-035	Miharada	MIHA1990	1-37
6522	6522-036	Kasori E3 (Middle)	MIHA1990	1-38
6522	6522-037	Jomon	MIHA1990	1-39
6522	6522-038	Jomon	MIHA1990	1-40
6522	6522-039	Kasori E3 (Middle)	MIHA1990	1-42
6522	6522-040	Initial Jomon	MIHA1990	1-43
6522	6522-041	Shomyoji 2	MIHA1990	1-44
6522	6522-042	Kasori E4	MIHA1990	1-45
6522	6522-043	Yakemachi	MIHA1990	1-46
6522	6522-044	Kasori E3 (Early)	MIHA1990	1-47
6522	6522-045	Shomyoji 1	MIHA1990	1-48
6522	6522-046	Kasori E3 (Middle)	MIHA1990	1-49
6522	6522-047	Shindo	MIHA1990	1-50
6522	6522-048	Kasori E3 (Early)	MIHA1990	1-51
6522	6522-049	Kasori E3 (Middle)	MIHA1990	1-52
6522	6522-050	Kasori E3 (Middle)	MIHA1990	1-53
6522	6522-051	Kasori E4	MIHA1990	1-54
6522	6522-052	Jomon	MIHA1990	1-55
6522	6522-053	Kasori E4	MIHA1990	1-56
6522	6522-054	Kasori E4	MIHA1990	1-57
6522	6522-055	Kasori E3 (Late)	MIHA1990	1-58
6522	6522-056	Miharada	MIHA1990	1-59
6522	6522-057	Miharada	MIHA1990	1-60
6522	6522-058	Jomon	MIHA1990	1-63
6522	6522-059	Jomon	MIHA1990	1-64
6522	6522-060	Kasori E3 (Early)	MIHA1990	1-65
6522	6522-061	Shomyoji	MIHA1990	1-66
6522	6522-062	Jomon	MIHA1990	1-67
6522	6522-063	Kasori E3 (Middle)	MIHA1990	1-68
6522	6522-064	Jomon	MIHA1990	1-69
6522	6522-065	Miharada	MIHA1990	1-70
6522	6522-066	Kasori E3 (Middle)	MIHA1990	1-71
6522	6522-067	Kasori E3 (Late)	MIHA1990	1-73
6522	6522-068	Kasori E3 (Middle)	MIHA1990	1-74

Continued on next page

Table A.1: Pithouses at Gunma

BUA ID	Pithouse ID	Period	REF	original ID
6522	6522-069	Kasori E3 (Late)	MIHA1990	1-75
6522	6522-070	Kasori E3 (Late)	MIHA1990	1-76
6522	6522-071	Kasori E3 (Late)	MIHA1990	1-77
6522	6522-072	Miharada	MIHA1990	1-78
6522	6522-073	Kasori E3 (Middle)	MIHA1990	1-79
6522	6522-074	Jomon	MIHA1990	1-80
6522	6522-075	Jomon	MIHA1990	1-81
6522	6522-076	Kasori E3 (Late)	MIHA1990	1-82
6522	6522-077	Kasori E3 (Late)	MIHA1990	1-83
6522	6522-078	Kasori E3 (Late)	MIHA1990	1-84
6522	6522-079	Kasori E4	MIHA1990	1-85
6522	6522-080	Shomyoji 1	MIHA1990	2-1
6522	6522-081	Shomyoji 1	MIHA1990	2-2
6522	6522-082	Kasori E3 (Early)	MIHA1990	2-3
6522	6522-083	Kasori E3 (Middle)	MIHA1990	2-4
6522	6522-084	Kasori E3 (Middle)	MIHA1990	2-5
6522	6522-085	Kasori E3 (Late)	MIHA1990	2-6
6522	6522-086	Kasori E3 (Late)	MIHA1990	2-7
6522	6522-087	Kasori E3 (Late)	MIHA1990	2-8
6522	6522-088	Kasori E3 (Late)	MIHA1990	2-9
6522	6522-089	Kasori E4	MIHA1990	2-10
6522	6522-090	Shomyoji 1	MIHA1990	2-11
6522	6522-091	Kasori E4	MIHA1990	2-12
6522	6522-092	Kasori E3 (Middle)	MIHA1990	2-13
6522	6522-093	Shomyoji 1	MIHA1990	2-15
6522	6522-094	Kasori E3 (Late)	MIHA1990	2-16
6522	6522-095	Kasori E3 (Early)	MIHA1990	2-17
6522	6522-096	Kasori E4	MIHA1990	2-19
6522	6522-097	Kasori E3 (Late)	MIHA1990	2-20
6522	6522-098	Kasori E3 (Late)	MIHA1990	2-22
6522	6522-099	Jomon	MIHA1990	2-23
6522	6522-100	Kasori E3 (Late)	MIHA1990	2-24
6522	6522-101	Kasori E3 (Early)	MIHA1990	2-25
6522	6522-102	Jomon	MIHA1990	2-26
6522	6522-103	Kasori E3 (Late)	MIHA1990	2-27
6522	6522-104	Jomon	MIHA1990	2-28
6522	6522-105	Miharada	MIHA1990	2-30
6522	6522-106	Miharada	MIHA1990	2-33
6522	6522-107	Miharada	MIHA1990	2-33′
6522	6522-108	Kasori E4	MIHA1990	2-34
6522	6522-109	Kasori E4	MIHA1990	2-35

Continued on next page

Table A.1: Pithouses at Gunma

BUA ID	Pithouse ID	Period	REF	original ID
6522	6522-110	Kasori E2	MIHA1990	2-36
6522	6522-111	Kasori E3 (Early)	MIHA1990	2-37A
6522	6522-112	Kasori E3 (Middle)	MIHA1990	2-37B
6522	6522-113	Kasori E2	MIHA1990	2-38
6522	6522-114	Kasori E3 (Middle)	MIHA1990	2-39
6522	6522-115	Kasori E2	MIHA1990	2-40
6522	6522-116	Kasori E3 (Early)	MIHA1990	2-41
6522	6522-117	Miharada	MIHA1990	2-42
6522	6522-118	Kasori E3 (Late)	MIHA1990	2-43
6522	6522-119	Kasori E2	MIHA1990	2-44
6522	6522-120	Kasori E3 (Early)	MIHA1990	2-45
6522	6522-121	Kasori E2	MIHA1990	2-46
6522	6522-122	Miharada	MIHA1990	2-47
6522	6522-123	Kasori E3 (Middle)	MIHA1990	2-48
6522	6522-124	Kasori E3 (Early)	MIHA1990	2-49
6522	6522-125	Kasori E2	MIHA1990	2-50
6522	6522-126	Kasori E2	MIHA1990	2-51
6522	6522-127	Kasori E3 (Late)	MIHA1990	2-52
6522	6522-128	Kasori E2	MIHA1990	2-53
6522	6522-129	Kasori E3 (Early)	MIHA1990	2-54
6522	6522-130	Kasori E3 (Middle)	MIHA1990	2-55
6522	6522-131	Miharada	MIHA1990	2-56
6522	6522-132	Shomyoji 2 - Horinouchi 1	MIHA1990	2-57
6522	6522-133	Jomon	MIHA1990	2-58
6522	6522-134	Kasori E3 (Late)	MIHA1990	2-R1
6522	6522-135	Kasori E3 (Late) - E4	MIHA1990	3-1
6522	6522-136	Kasori E3 (Middle)	MIHA1990	3-2
6522	6522-137	Kasori E3 (Late)	MIHA1990	3-3
6522	6522-138	Kasori E3 (Middle)	MIHA1990	3-4
6522	6522-139	Kasori E3 (Middle)	MIHA1990	3-5
6522	6522-140	Kasori E3 (Middle)	MIHA1990	3-6
6522	6522-141	Kasori E3 (Middle)	MIHA1990	3-7
6522	6522-142	Kasori E3 (Middle)	MIHA1990	3-8
6522	6522-143	Jomon	MIHA1990	3-9
6522	6522-144	Jomon	MIHA1990	3-10
6522	6522-145	Kasori E3 (Middle)	MIHA1990	3-11
6522	6522-146	Kasori E3 (Middle)	MIHA1990	3-12
6522	6522-147	Jomon	MIHA1990	3-13A
6522	6522-148	Kasori E3 (Middle)	MIHA1990	3-13B
6522	6522-149	Kasori E3 (Early)	MIHA1990	3-14A
6522	6522-150	Jomon	MIHA1990	3-14B

Continued on next page

Table A.1: Pithouses at Gunma

BUA ID	Pithouse ID	Period	REF	original ID
6522	6522-151	Kasori E3 (Middle)	MIHA1990	3-15
6522	6522-152	Kasori E3 (Middle)	MIHA1990	3-16A
6522	6522-153	Kasori E3 (Middle)	MIHA1990	3-16B
6522	6522-154	Kasori E3 (Early)	MIHA1990	3-17
6522	6522-155	Yakemachi	MIHA1990	3-18
6522	6522-156	Kasori E3 (Early)	MIHA1990	3-19
6522	6522-157	Kasori E3 (Early)	MIHA1990	3-20
6522	6522-158	Kasori E3 (Early)	MIHA1990	3-21
6522	6522-159	Kasori E3 (Early)	MIHA1990	3-22
6522	6522-160	Kasori E2	MIHA1990	3-23
6522	6522-161	Miharada	MIHA1990	3-24
6522	6522-162	Kasori E3 (Early)	MIHA1990	3-25
6522	6522-163	Kasori E2	MIHA1990	3-26
6522	6522-164	Shomyoji 2	MIHA1990	3-27
6522	6522-165	Kasori E3 (Early)	MIHA1990	3-28
6522	6522-166	Horinouchi 2	MIHA1990	3-29
6522	6522-167	Kasori E3 (Early)	MIHA1990	3-30
6522	6522-168	Kasori E3 (Middle)	MIHA1990	3-31
6522	6522-169	Jomon	MIHA1990	3-32
6522	6522-170	Kasori E3 (Middle)	MIHA1990	3-33
6522	6522-171	Kasori E3 (Late) - E4	MIHA1990	3-34
6522	6522-172	Jomon	MIHA1990	3-35A
6522	6522-173	Kasori E3 (Early)	MIHA1990	3-35B
6522	6522-174	Kasori E3 (Early)	MIHA1990	3-36
6522	6522-175	Kasori E3 (Middle)	MIHA1990	3-37
6522	6522-176	Kasori E3 (Early)	MIHA1990	3-38
6522	6522-177	Kasori E2 - E3 (Early)	MIHA1990	3-39
6522	6522-178	Kasori E2	MIHA1990	3-40
6522	6522-179	Kasori E2	MIHA1990	3-41
6522	6522-180	Otamadai II	MIHA1990	3-42
6522	6522-181	Kasori E3 (Early)	MIHA1990	3-43
6522	6522-182	Kasori E2	MIHA1990	3-44
6522	6522-183	Kasori E4	MIHA1990	3-45
6522	6522-184	Kasori E2	MIHA1990	3-46
6522	6522-185	Kasori E3 (Late)	MIHA1990	3-47
6522	6522-186	Kasori E3 (Early)	MIHA1990	3-48
6522	6522-187	Kasori E3 (Middle)	MIHA1990	3-48′
6522	6522-188	Middle Jomon (Early)	MIHA1990	3-49
6522	6522-189	Kasori E2	MIHA1990	3-50
6522	6522-190	Jomon	MIHA1990	3-51
6522	6522-191	Kasori E3 (Early)	MIHA1990	3-52

Continued on next page

Table A.1: Pithouses at Gunma

BUA ID	Pithouse ID	Period	REF	original ID
6522	6522-192	Jomon	MIHA1990	3-53
6522	6522-193	Kasori E2	MIHA1990	3-54
6522	6522-194	Jomon	MIHA1990	3-55
6522	6522-195	Jomon	MIHA1990	3-56
6522	6522-196	Jomon	MIHA1990	3-R1
6522	6522-197	Yakemachi	MIHA1990	4-1
6522	6522-198	Jomon	MIHA1990	4-2
6522	6522-199	Miharada	MIHA1990	4-3
6522	6522-200	Miharada	MIHA1990	4-4
6522	6522-201	Miharada	MIHA1990	4-5
6522	6522-202	Kasori E4	MIHA1990	4-6
6522	6522-203	Jomon	MIHA1990	4-7
6522	6522-204	Kasori E2	MIHA1990	4-8
6522	6522-205	Kasori E3 (Middle)	MIHA1990	4-9
6522	6522-206	Miharada	MIHA1990	4-10
6522	6522-207	Kurohama / Ario	MIHA1990	4-12
6522	6522-208	Kasori E3 (Early)	MIHA1990	4-13
6522	6522-209	Kurohama / Ario	MIHA1990	4-14
6522	6522-210	Kasori E3 (Late)	MIHA1990	4-15
6522	6522-211	Jomon	MIHA1990	4-16
6522	6522-212	Kasori E1	MIHA1990	4-17
6522	6522-213	Miharada	MIHA1990	4-18
6522	6522-214	Kasori E4	MIHA1990	4-19
6522	6522-215	Miharada	MIHA1990	4-20
6522	6522-216	Kasori E2	MIHA1990	4-21
6522	6522-217	Miharada	MIHA1990	4-22
6522	6522-218	Kasori E2	MIHA1990	4-23
6522	6522-219	Yakemachi	MIHA1990	4-24
6522	6522-220	Otamadai II	MIHA1990	4-25
6522	6522-221	Jomon	MIHA1990	4-R1
6522	6522-222	Otamadai II	MIHA1990	5-1
6522	6522-223	Kasori E3 (Middle)	MIHA1990	5-2
6522	6522-224	Kasori E3 (Middle)	MIHA1990	5-3
6522	6522-225	Kasori E3 (Late)	MIHA1990	5-4
6522	6522-226	Kasori E3 (Middle)	MIHA1990	5-5
6522	6522-227	Kasori E3 (Early)	MIHA1990	5-6
6522	6522-228	Shomyoji 1	MIHA1990	5-7
6522	6522-229	Kasori E3 (Middle)	MIHA1990	5-8A
6522	6522-230	Jomon	MIHA1990	5-8B
6522	6522-231	Kasori E3 (Middle)	MIHA1990	5-9
6522	6522-232	Kasori E3 (Middle)	MIHA1990	5-10A

Continued on next page

Table A.1: Pithouses at Gunma

BUA ID	Pithouse ID	Period	REF	original ID
6522	6522-233	Jomon	MIHA1990	5-10B
6522	6522-234	Kasori E3 (Late)	MIHA1990	5-11
6522	6522-235	Kasori E3 (Late)	MIHA1990	5-12
6522	6522-236	Kasori E3 (Middle)	MIHA1990	5-13
6522	6522-237	Kasori E3 (Early)	MIHA1990	5-14
6522	6522-238	Kasori E2	MIHA1990	5-15
6522	6522-239	Kasori E3 (Early)	MIHA1990	5-16
6522	6522-240	Kasori E3 (Middle)	MIHA1990	5-17
6522	6522-241	Kasori E4	MIHA1990	5-19
6522	6522-242	Miharada	MIHA1990	5-20
6522	6522-243	Kasori E3 (Middle)	MIHA1990	5-21
6522	6522-244	Kasori E3 (Late) - E4	MIHA1990	6-1
6522	6522-245	Kasori E3 (Early)	MIHA1990	6-2
6522	6522-246	Kasori E2	MIHA1990	6-3
6522	6522-247	Kasori E3 (Early)	MIHA1990	6-4
6522	6522-248	Kasori E3 (Late)	MIHA1990	6-6
6522	6522-249	Shomyoji 1	MIHA1990	6-7
6522	6522-250	Kasori E3 (Late)	MIHA1990	6-8
6522	6522-251	Kasori E1	MIHA1990	6-9
6522	6522-252	Kasori E3 (Early)	MIHA1990	6-10
6522	6522-253	Kasori E3 (Early - Middle)	MIHA1990	6-11
6522	6522-254	Kasori E3 (Early)	MIHA1990	6-12
6522	6522-255	Miharada	MIHA1990	6-13
6522	6522-256	Miharada	MIHA1990	6-14
6522	6522-257	Kasori E3 (Middle)	MIHA1990	6-15
6522	6522-258	Jomon	MIHA1990	6-16
6522	6522-259	Kasori E3 (Middle)	MIHA1990	6-18
6522	6522-260	Jomon	MIHA1990	6-19
6522	6522-261	Kasori E3 (Early)	MIHA1990	6-20
6522	6522-262	Kasori E3 (Late) - E4	MIHA1990	6-26
6522	6522-263	Kasori E3 (Middle)	MIHA1990	6-27
6522	6522-264	Kasori E3 (Middle)	MIHA1990	6-28
6522	6522-265	Kasori E3 (Early)	MIHA1990	6-29
6522	6522-266	Kasori E3 (Middle)	MIHA1990	6-30
6522	6522-267	Kasori E3 (Middle)	MIHA1990	6-31A
6522	6522-268	Kasori E3 (Late) - E4	MIHA1990	6-31B
6522	6522-269	Kasori E3 (Middle)	MIHA1990	6-32
6522	6522-270	Jomon	MIHA1990	6-33
6522	6522-271	Kasori E3 (Late)	MIHA1990	6-35
6522	6522-272	Kasori E3 (Middle)	MIHA1990	6-36
6522	6522-273	Kasori E3 (Late)	MIHA1990	6-37

Continued on next page

Table A.1: Pithouses at Gunma

BUA ID	Pithouse ID	Period	REF	original ID
6522	6522-274	Kasori E3 (Middle)	MIHA1990	6-38A
6522	6522-275	Jomon	MIHA1990	6-38B
6522	6522-276	Kasori E2	MIHA1990	6-39
6522	6522-277	Kasori E3 (Middle)	MIHA1990	6-40
6522	6522-278	Kasori E3 (Middle)	MIHA1990	6-41
6522	6522-279	Kasori E3 (Middle)	MIHA1990	6-42
6522	6522-280	Kasori E2	MIHA1990	6-44
6522	6522-281	Kasori E4	MIHA1990	6-45
6522	6522-282	Kasori E4	MIHA1990	6-46
6522	6522-283	Jomon	MIHA1990	6-47
6522	6522-284	Jomon	MIHA1990	6-48
6522	6522-285	Kasori E2	MIHA1990	7-1A
6522	6522-286	Kasori E3 (Early)	MIHA1990	7-1B
6522	6522-287	Kasori E2	MIHA1990	7-3
6522	6522-288	Kasori E2	MIHA1990	7-4
6522	6522-289	Kasori E1	MIHA1990	7-5
6522	6522-290	Kasori E3 (Early)	MIHA1990	7-6
6522	6522-291	Kasori E3 (Early)	MIHA1990	7-7
6522	6522-292	Kasori E2 - E3 (Early)	MIHA1990	7-8
6522	6522-293	Kasori E2	MIHA1990	7-9
6522	6522-294	Kasori E1	MIHA1990	7-10
6522	6522-295	Kasori E3 (Late)	MIHA1990	7-11
6522	6522-296	Kasori E1	MIHA1990	7-12
6522	6522-297	Kasori E2	MIHA1990	7-13
6522	6522-298	Miharada	MIHA1990	7-14
6522	6522-299	Kasori E3 (Middle)	MIHA1990	7-15A
6522	6522-300	Kasori E3 (Middle)	MIHA1990	7-15B
6522	6522-301	Jomon	MIHA1990	7-15C
6522	6522-302	Otamadai II	MIHA1990	7-17
6522	6522-303	Miharada	MIHA1990	7-18
6522	6522-304	Shindo	MIHA1990	7-19
6522	6522-305	Miharada	MIHA1990	7-20
6522	6522-306	Otamadai II	MIHA1990	7-21
6522	6522-307	Jomon	MIHA1990	7-22
6522	6522-308	Initial Jomon	MIHA1990	7-23
6522	6522-309	Otamadai II	MIHA1990	7-24
6522	6522-310	Otamadai II	MIHA1990	7-25A
6522	6522-311	Otamadai II	MIHA1990	7-25B
6522	6522-312	Kasori E1	MIHA1990	7-27
6522	6522-313	Kasori E4	MIHA1990	7-29
6522	6522-314	Kasori E1	MIHA1990	7-30

Continued on next page

Table A.1: Pithouses at Gunma

BUA ID	Pithouse ID	Period	REF	original ID
6522	6522-315	Kasori E3 (Middle)	MIHA1990	7-31
6522	6522-316	Kasori E3 (Late)	MIHA1990	7-32
6522	6522-317	Kasori E2	MIHA1990	7-33
6522	6522-318	Kasori E2-E3	MIHA1990	7-35
6522	6522-319	Kasori E4	MIHA1990	7-36
6522	6522-320	Jomon	MIHA1990	7-37
6522	6522-321	Shindo	MIHA1990	7-38
6522	6522-322	Jomon	MIHA1990	7-R1
6522	6522-323	Shomyoji 1	MIHA1990	7-R2
6522	6522-324	Jomon	MIHA1990	7-R3
6522	6522-325	Kasori E4	MIHA1990	7-R4
6522	6522-326	Jomon	MIHA1990	7-R6
6522	6522-327	Kasori E3 (Late)	MIHA1990	7-R8
6522	6522-328	Jomon	MIHA1990	7-R9
6522	6522-329	Miharada	MIHA1990	8-1
6522	6522-330	Jomon	MIHA1990	8-2
6522	6522-331	Yakemachi	MIHA1990	8-4
6522	6522-332	Otamadai II	MIHA1990	8-5
6522	6522-333	Shomyoji 1	MIHA1990	8-7
6522	6522-334	Yakemachi	MIHA1990	8-8
6522	6522-335	Miharada	MIHA1990	8-9
6522	6522-336	Yakemachi	MIHA1990	8-10
6522	6522-337	Jomon	MIHA1990	8-11
6522	6522-338	Miharada	MIHA1990	8-13
6522	6522-339	Otamadai II	MIHA1990	8-14
6522	6522-340	Jomon	MIHA1990	8-15
6522	6522-341	Yakemachi	MIHA1990	8-16
6522	6522-342	Otamadai II	MIHA1990	8-20
6544	6544-001	Moroiso b (Middle)	NAKSW1986	3
6544	6544-002	Moroiso b (Late)	NAKSW1986	4
6544	6544-003	Kurohama / Ario	NAKSW1986	5
6544	6544-004	Moroiso a	NAKSW1986	6
6544	6544-005	Kurohama / Ario	NAKSW1986	7
6544	6544-006	Early Jomon	NAKSW1986	8
6523	6523-001	Shomyoji	NAKSW2000	1
6523	6523-002	Moroiso b	NAKSW2000	2
6513	6513-002	Jomon	TKZSK2008	H10-J1
6513	6513-003	Kasori B	TKZSK2008	H10-J2
6513	6513-004	Kasori E	TKZSK2008	H10-J3
6513	6513-005	Kurohama / Ario	TKZSK2008	H10-J4
6513	6513-006	Moroiso c	TKZSK2008	H10-J5

Continued on next page

Table A.1: Pithouses at Gunma

BUA ID	Pithouse ID	Period	REF	original ID
6513	6513-007	Kasori E	TKZSK2008	H10-J6
6513	6513-008	Kasori B2	TKZSK2008	H10-J7
6513	6513-009	Angyo 3	TKZSK2008	H10-J8
6513	6513-010	Late Jomon (Middle) - Final Jomon	TKZSK2008	H10-J9
6513	6513-011	Angyo 3	TKZSK2008	H10-J10
6513	6513-012	Katsuzaka	TKZSK2008	H10-J11
6513	6513-013	Angyo2-3	TKZSK2008	H10-J12
6513	6513-014	Angyo 3	TKZSK2008	H10-J13
6513	6513-015	Kasori B	TKZSK2008	H10-J14
6513	6513-016	Kasori E3	TKZSK2008	H11-J1
6513	6513-017	Kasori E3	TKZSK2008	H11-J2
6513	6513-018	Shomyoji	TKZSK2008	H12-J1
6513	6513-019	Middle Jomon - Late Jomon (Initial)	TKZSK2008	H12-J2
6513	6513-020	Middle Jomon	TKZSK2008	H12-J3
6513	6513-021	Kasori E2	TKZSK2008	H13-J1
6513	6513-022	Kasori EI (Early) / Miharada	TKZSK2008	H13-J2
6513	6513-023	Yakemachi / Katsuzaka / Otamadai	TKZSK2008	H13-J3
6513	6513-024	Kasori E3	TKZSK2008	H13-J4
6513	6513-025	Kasori E3	TKZSK2008	H16-J1
6543	6543-001	Sekiyama	NAKSW1986	1
6543	6543-002	Katsuzaka / Otamadai	NAKSW1986	2
6543	6543-003	Sekiyama	NAKSW1986	3
6543	6543-004	Sekiyama	NAKSW1986	4
6543	6543-005	Moroiso a	NAKSW1986	5
6543	6543-006	Sekiyama	NAKSW1986	7
6543	6543-007	Sekiyama	NAKSW1986	8
6543	6543-008	Katsuzaka / Otamadai	NAKSW1986	9
6543	6543-009	Sekiyama	NAKSW1986	10
6543	6543-010	Sekiyama	NAKSW1986	11
6543	6543-011	Sekiyama	NAKSW1986	12
6543	6543-012	Sekiyama	NAKSW1986	13
6524-I-II	6524-I-II-001	Sekiyama	MIHASW2004a	I-J-1
6524-I-II	6524-I-II-002	Kurohama / Ario	MIHASW2004a	I-J-3
6524-I-II	6524-I-II-003	Kurohama / Ario	MIHASW2004a	I-J-4
6524-I-II	6524-I-II-004	Kurohama / Ario	MIHASW2004a	I-J-5
6524-I-II	6524-I-II-005	Sekiyama	MIHASW2004a	I-J-7
6524-I-II	6524-I-II-006	Sekiyama	MIHASW2004a	I-J-9
6524-I-II	6524-I-II-007	Kurohama / Ario	MIHASW2004a	I-J-10
6524-I-II	6524-I-II-008	Kurohama / Ario	MIHASW2004a	I-J-11
6524-I-II	6524-I-II-009	Kurohama / Ario	MIHASW2004a	II-J-1
6524-I-II	6524-I-II-010	Sekiyama	MIHASW2004a	II-J-3

Continued on next page

Table A.1: Pithouses at Gunma

BUA ID	Pithouse ID	Period	REF	original ID
6524-I-II	6524-I-II-011	Sekiyama	MIHASW2004a	II-J-4
6524-I-II	6524-I-II-012	Sekiyama	MIHASW2004a	II-J-5
6524-I-II	6524-I-II-013	Kurohama / Ario	MIHASW2004a	II-J-6
6524-I-II	6524-I-II-014	Sekiyama	MIHASW2004a	II-J-7
6524-I-II	6524-I-II-015	Sekiyama	MIHASW2004a	II-J-8
6524-I-II	6524-I-II-016	Kurohama / Ario	MIHASW2004a	II-J-9
6524-I-II	6524-I-II-017	Sekiyama	MIHASW2004a	II-J-10
6524-I-II	6524-I-II-018	Jomon	MIHASW2004a	II-J-11
6524-I-II	6524-I-II-019	Kurohama / Ario	MIHASW2004a	II-J-12
6524-I-II	6524-I-II-020	Katsuzaka / Otamadai	MIHASW2005a	I-J-1
6524-I-II	6524-I-II-021	Katsuzaka / Otamadai	MIHASW2005a	II-J-2
6524-III	6524-III-001	Lower Hanazumi	MIHASW2004a	III-J-2
6524-III	6524-III-002	Katsuzaka / Otamadai	MIHASW2005a	III-J-1
6524-III	6524-III-003	Middle Jomon (Early)	MIHASWMK2009	1
6524-III	6524-III-004	Jomon	MIHASWMK2009	2
6525	6525-001	Moroiso b (Late)	MHHUAN1987	1
6525	6525-002	Lower Hanazumi	MHHUAN1987	2
6525	6525-003	Lower Hanazumi	MHHUAN1987	3
6525	6525-004	Lower Hanazumi	MHHUAN1987	4
6525	6525-005	Lower Hanazumi	MHHUAN1987	6
6525	6525-006	Lower Hanazumi	MHHUAN1987	7
6525	6525-007	Lower Hanazumi	MHHUAN1987	8
6525	6525-008	Lower Hanazumi	MHHUAN1987	9
6525	6525-009	Lower Hanazumi	MHHUAN1987	10
6540	6540-001	Kurohama / Ario	KAHNY1988	1
6540	6540-002	Sekiyama	KAHNY1988	2
6540	6540-003	Sekiyama-Kurohama-Moroiso	KAHNY1988	3
6540	6540-004	Moroiso a	KAHNY1988	4
6540	6540-005	Sekiyama I	KAHNY1988	5
6540	6540-006	Sekiyama	KAHNY1988	6
6540	6540-007	Sekiyama	KAHNY1988	7
6540	6540-008	Kurohama / Ario	KAHNY1988	8
6540	6540-009	Sekiyama I	KAHNY1988	9
6540	6540-010	Sekiyama II	KAHNY1988	10
6540	6540-011	Sekiyama II	KAHNY1988	11
6540	6540-012	Jomon	KAHNY1988	12
6540	6540-013	Jomon	KAHNY1988	13
6540	6540-014	Moroiso a	KAHNY1988	14
6541	6541-001	Early Jomon (Middle) - Middle Jomon (Middle)	MTCH1985	J1
6541	6541-002	Kurohama / Ario	MTCH1985	J2
6541	6541-003	Kurohama / Ario	MTCH1985	J3

Continued on next page

Table A.1: Pithouses at Gunma

BUA ID	Pithouse ID	Period	REF	original ID
6541	6541-004	Kurohama / Ario	MTCH1985	J5
6541	6541-005	Kuorhama / Ario - Moroiso	MTCH1985	J6
6541	6541-006	Kurohama / Ario	MTCH1985	J7
6541	6541-007	Otamadai - Kasori E	MTCH1985	J8
6541	6541-008	Sekiyama	MTCH1985	J9
6542	6542-001	Otamadai - Kasori E	MTCH1985	1
6542	6542-002	Kasori E	MTCH1985	2
6542	6542-003	Kuorhama / Ario - Otamadai	MTCH1985	3
6542	6542-004	Middle Jomon (Early-Middle)	MTCH1985	4
6558	6558-001	Moroiso b	MHDMTD2001	9
6558	6558-002	Early Jomon (Final)	MHDMTD2001	10
6558	6558-003	Early Jomon	MHDMTD2001	11
6558	6558-004	Goryogadai	MHDMTD2001	15
6558	6558-005	Early Jomon (Late)	MHDMTD2001	26
6558	6558-006	Moroiso a - b	MHDMTD2001	33
6558	6558-007	Moroiso a - b	MHDMTD2001	34
6558	6558-008	Moroiso a - b	MHDMTD2001	36
6558	6558-009	Moroiso a - b	MHDMTD2001	39
6558	6558-010	Moroiso a	MHDMTD2001	40
6559	6559-001	Moroiso b	UMHM2001	J1
6559	6559-002	Moroiso b	UMHM2001	J2
6559	6559-003	Moroiso b	UMHM2001	J3
6559	6559-004	Moroiso b	UMHM2001	J4
6563	6563-001	Kurohama / Ario	UMHHONM2002	31
6563	6563-002	Kurohama / Ario	UMHHONM2002	32
6563	6563-003	Sekiyama - Kurohama	UMHHONM2002	33
6563	6563-004	Sekiyama - Kurohama	UMHHONM2002	34
6563	6563-005	Kurohama / Ario	UMHHONM2002	35
6563	6563-006	Otamadai	UMHHONM2002	36
6563	6563-007	Lower Hanazumi / Futatsuki	UMHHONM2002	37
6563	6563-008	Moroiso b	UMHHONM2002	38
6563	6563-009	Sekiyama	UMHHONM2002	39
6563	6563-010	Moroiso a - b	UMHHONM2002	40
6563	6563-011	Kurohama / Ario	UMHHONM2002	41
6563	6563-012	Sekiyama	UMHHONM2002	42
6564	6564-001	Lower Hanazumi / Futatsuki	HTMTSH2003	J-1
6564	6564-002	Middle Jomon (Early)	HTMTSH2003	J-2
6564	6564-003	Futatsuki	HTMTSH2003	J-3
6564	6564-004	Futatsuki	HTMTSH2003	J-4
6564	6564-005	Moroiso c	HTMTSH2003	J-5
6564	6564-006	Futatsuki	HTMTSH2003	J-6

Continued on next page

Table A.1: Pithouses at Gunma

BUA ID	Pithouse ID	Period	REF	original ID
6564	6564-007	Futatsuki	HTMTSH2003	J-7
6564	6564-008	Futatsuki	HTMTSH2003	J-8
6564	6564-009	Futatsuki	HTMTSH2003	J-9
6564	6564-010	Futatsuki	HTMTSH2003	J-10
6564	6564-011	Futatsuki	HTMTSH2003	J-11
6564	6564-012	Futatsuki	HTMTSH2003	J-12
6564	6564-013	Middle Jomon (Early)	HTMTSH2003	J-13
6564	6564-014	Futatsuki	HTMTSH2003	J-14
6564	6564-015	Futatsuki	HTMTSH2003	J-15
6564	6564-016	Futatsuki	HTMTSH2003	J-16
6567	6567-001	Katsuzaka / Otamadai	HTMTSH2003	J-1
6567	6567-002	Sekiyama	HTMTSH2003	J-2
6567	6567-003	Katsuzaka / Otamadai	HTMTSH2003	J-3
6567	6567-004	Katsuzaka / Otamadai	HTMTSH2003	J-4
6567	6567-005	Katsuzaka / Otamadai	HTMTSH2003	J-5
6567	6567-006	Moroiso c	HTMTSH2003	J-6
6567	6567-007	Katsuzaka / Otamadai	HTMTSH2003	J-7
6567	6567-008	Moroiso c	HTMTSH2003	J-8
6567	6567-009	Kasori E - Shomyoji	HTMTSH2003	J-9
6567	6567-010	Jomon	HTMTSH2003	J-10
6567	6567-011	Moroiso c	HTMTSH2003	J-11
6569	6569-001	Moroiso b (Middle - Late)	MHRNKI2004	1
6569	6569-002	Moroiso b (Middle - Late)	MHRNKI2004	2
6569	6569-003	Lower Hanazumi	MHRNKI2004	3
6569	6569-004	Kurohama / Ario	MHRNKI2004	4
6569	6569-005	Sekiyama II	MHRNKI2004	5
6569	6569-006	Sekiyama II	MHRNKI2004	6
6569	6569-007	Moroiso b (Middle - Late)	MHRNKI2004	7
6569	6569-008	Lower Hanazumi	MHRNKI2004	8
6571	6571-001	Lower Hanazumi	UMHNKTT2004	J-1
6575	6575-001	Shomyoji	TZTATNH2005	1
6575	6575-002	Sekiyama	TZTB2005	12
6575	6575-003	Kasori E3 - Shomyoji	TZTB2005	13
6575	6575-004	Sekiyama	TZTB2005	18
6575	6575-005	Moroiso c	TZTCTZEDO2005	24
6576	6576-001	Early Jomon (Final) - Middle Jomon (Initial)	TZTCTZEDO2005	J-1
6577-I-II	6577-I-II-001	Kurohama - Moroiso	MTCAS2005	J-1
6577-III	6577-III-001	Lower Hanazumi	MTCA2005b	J-2
6577-III	6577-III-002	Lower Hanazumi	MTCA2005b	J-3
6582-I	6582-I-001	Shomyoji	MTCHHACH2008	I-J-1
6582-I	6582-I-002	Shomyoji	MTCHHACH2008	I-J-2

Continued on next page

Table A.1: Pithouses at Gunma

BUA ID	Pithouse ID	Period	REF	original ID
6582-I	6582-I-003	Shomyoji	MTCHHACH2008	I-J-3
6582-I	6582-I-004	Shomyoji	MTCHHACH2008	I-J-4
6582-I	6582-I-005	Shomyoji	MTCHHACH2008	I-J-5
6582-I	6582-I-006	Kasori E3 - Shomyoji	MTCHHACH2008	I-J-6
6582-I	6582-I-007	Shomyoji	MTCHHACH2008	I-J-7
6582-I	6582-I-008	Jomon	MTCHHACH2008	I-J-8
6582-I	6582-I-009	Sekiyama - Kurohama	MTCHHACH2008	I-J-9
6582-I	6582-I-010	Sekiyama - Kurohama	MTCHHACH2008	I-J-10
6582-I	6582-I-011	Sekiyama - Kurohama	MTCHHACH2008	I-J-11
6582-I	6582-I-012	Sekiyama - Kurohama	MTCHHACH2008	I-J-12
6582-I	6582-I-013	Jomon	MTCHHACH2008	I-J-13
6582-I	6582-I-014	Early Jomon	MTCHHACH2008	I-J-14
6582-II	6582-II-001	Sekiyama - Kurohama	MTCHHACH2008	II-J-1
6582-II	6582-II-002	Sekiyama - Kurohama	MTCHHACH2008	II-J-2
6582-II	6582-II-003	Sekiyama - Kurohama	MTCHHACH2008	II-J-3
6586	6586-001	Sekiyama I	BGHS1986	1
6586	6586-002	Sekiyama I	BGHS1986	2
6586	6586-003	Sekiyama I	BGHS1986	3
6586	6586-004	Sekiyama I	BGHS1986	4
6586	6586-005	Kurohama (Early)	BGHS1986	5
6586	6586-006	Kurohama (Early)	BGHS1986	7
6586	6586-007	Kurohama (Early)	BGHS1986	10
6586	6586-008	Kurohama (Early)	BGHS1986	6
6586	6586-009	Kurohama (Early)	BGHS1986	8
6586	6586-010	Kurohama (Early)	BGHS1986	9
6586	6586-011	Moroiso a	BGHS1986	11
6588-1	6588-001	Katsuzaka / Otamadai	BOUYT1989	1
6588-1	6588-002	Jusanboda-Gorogadai-Otamadai-Katsuzaka	BOUYT1989	20
6588-1	6588-003	Otamadai I - II / Katsuzaka	BOUYT1989	21
6588-1	6588-004	Otamadai I - II / Katsuzaka	BOUYT1989	22
6588-1	6588-005	Katsuzaka / Otamadai	BOUYT1989	23
6588-1	6588-006	Katsuzaka / Otamadai	BOUYT1989	24
6588-1	6588-007	Katsuzaka / Otamadai	BOUYT1989	25
6588-1	6588-008	Katsuzaka / Otamadai	BOUYT1989	26
6588-1	6588-009	Katsuzaka / Otamadai	BOUYT1989	27
6588-1	6588-010	Katsuzaka / Otamadai	BOUYT1989	28
6588-1	6588-011	Katsuzaka / Otamadai	BOUYT1989	29
6588-1	6588-012	Jomon	BOUYT1989	30
6588-1	6588-013	Yakemachi	BOUYT1989	31
6588-1	6588-014	Otamadai / Yakemachi	BOUYT1989	32
6588-1	6588-015	Katsuzaka / Otamadai	BOUYT1989	33

Continued on next page

Table A.1: Pithouses at Gunma

BUA ID	Pithouse ID	Period	REF	original ID
6588-1	6588-016	Katsuzaka / Otamadai	BOUYT1989	34
6588-1	6588-017	Katsuzaka / Otamadai	BOUYT1989	35
6588-1	6588-018	Katsuzaka / Otamadai	BOUYT1989	36
6588-IV	6588-019	Katsuzaka / Otamadai	HOKV1997	J-1
6588-IV	6588-020	Otamadai Ia - IIa / Katsuzaka 1	HOKVIII2000	J-2
6588-IV	6588-021	Otamadai Ia - IIa / Katsuzaka 1	BOUYT2001	J-3
6590	6590-001	Sekiyama II	HOKIV1996	J1
6595-kita	6595-001	Initial Jomon - Early Jomon	KITTANO1996	J-1(A)
6595-kita	6595-002	Initial Jomon - Early Jomon	KITTANO1996	J-2(B)
6595-kita	6595-003	Initial Jomon - Early Jomon	KITTANO1996	J-3(E)
6595-kita	6595-004	Initial Jomon - Early Jomon	KITTANO1996	J-4(E)
6595-kita	6595-005	Initial Jomon - Early Jomon	KITTANO1996	J-5(E)
6595-kita	6595-006	Initial Jomon - Early Jomon	KITTANO1996	J-6(E)
6595-kita	6595-007	Initial Jomon - Early Jomon	KITTANO1996	J-7(E)
6595-kita	6595-008	Initial Jomon - Early Jomon	KITTANO1996	J-1(D)
6600-lowerACDE	6600-001	Katsuzaka 3	TOTHRAC2008	J-1(A)
6600-lowerACDE	6600-002	Moroiso b	TOTHRAC2008	J-2(A)
6600-lowerACDE	6600-003	Moroiso b	TOTHRAC2008	J-3(A)
6600-lowerACDE	6600-004	Katsuzaka 3	TOTHRAC2008	J-4(A)
6600-lowerACDE	6600-005	Otamadai II	TOTHRAC2008	J-1(C)
6600-lowerACDE	6600-006	Moroiso b	TOTHRAC2008	J-2(C)
6600-lowerACDE	6600-007	Katsuzaka 2	TOTHRAC2008	J-3(C)
6600-lowerACDE	6600-008	Kasori E4	TOTHRAC2008	J-9(C)
6600-lowerACDE	6600-009	Sekiyama II	TOTHRAC2008	J-16(C)
6600-lowerACDE	6600-010	Moroiso b	TOTHRAC2008	J-6(C)
6600-lowerACDE	6600-011	Katsuzaka 2	TOTHRAC2008	J-7(C)
6600-lowerACDE	6600-012	Otamadai II	TOTHRAC2008	J-8(C)
6600-lowerACDE	6600-013	Sekiyama II	TOTHRAC2008	J-10(C)
6600-lowerACDE	6600-014	Moroiso b - Kasori E2	TOTHRAC2008	J-11(C)
6600-lowerACDE	6600-015	Jomon	TOTHRAC2008	J-12(C)
6600-lowerACDE	6600-016	Moroiso b	TOTHRAC2008	J-13(C)
6600-lowerACDE	6600-017	Moroiso b	TOTHRAC2008	J-14(C)
6601-3	6601-001	KasoriE-3	MISOIII1999	J-1
6601-3	6601-002	Moroiso b	MISOIII1999	J-2
6601-3	6601-003	Early Jomon (Final) - Middle Jomon (Middle)	MISOIII1999	J-3
6602-n	6602-001	Sekiyama II - Kurohama (Early)	MITCHK1990	1
6602-n	6602-002	Sekiyama II - Kurohama (Early)	MITCHK1990	4
6602-n	6602-003	Moroiso b	MITCHK1990	3
6602-n	6602-004	Middle Jomon	MITCHK1990	2
6603-12	6603-001	Early Jomon	HOKI1993	
6607-edited	6607-001	Early Jomon	HOK11993	

Continued on next page

Table A.1: Pithouses at Gunma

BUA ID	Pithouse ID	Period	REF	original ID
6608-edited	6608-001	Sekiyama II	SHMY1990	5
6608-edited	6608-002	Sekiyama II	SHMY1990	8
6608-edited	6608-003	Sekiyama II	SHMY1990	1
6608-edited	6608-004	Kurohama / Ario	SHMY1990	3
6608-edited	6608-005	Kurohama / Ario	SHMY1990	2
6608-edited	6608-006	Moroiso	SHMY1990	4
6608-edited	6608-007	Moroiso	SHMY1990	6
6608-edited	6608-008	Finale-Middle Jomon	SHMY1990	7
6610-edited	6610-001	Jomon	TNJN1997	
6611-edited1	6611-001	Kasori E3 - E4	HKD1999	J-1
6611-edited1	6611-002	Jomon	HKD1999	J-2
6611-edited1	6611-003	Kasori E3 - Horinouchi	HKD1999	J-3
6611-edited1	6611-004	Jomon	HKD1999	J-4
6611-edited1	6611-005	Kasori E4 - Shomyoji	HKD1999	J-5
6611-edited1	6611-006	Jomon	HKD1999	J-6
6611-edited1	6611-007	Jomon	HKD1999	J-8
6611-edited1	6611-008	Kasori E4 - Shomyoji	HKD1999	J-9
6611-edited1	6611-009	Kasori E	HKD1999	J-10
6611-edited1	6611-010	Kasori E3 - Shomyoji	HKD1999	J-11
6611-edited1	6611-011	Moroiso b	HKD1999	J-12
6611-edited1	6611-012	Jomon	HKD1999	J-13
6611-edited1	6611-013	Kasori E3 - Shomyoji	HKD1999	J-14
6611-edited1	6611-014	Middle Jomon	HKD1999	J-15
6611-edited1	6611-015	Jomon	HKD1999	J-16
6611-edited1	6611-016	Jomon	HKD1999	J-17
6611-edited1	6611-017	Jomon	HKD1999	J-18
6611-edited1	6611-018	Futatsuki	HKD1999	J-19
6611-edited1	6611-019	Moroiso b	HKD1999	J-20
6611-edited1	6611-020	Futatsuki	HKD1999	J-21
6611-edited1	6611-021	Jomon	HKD1999	J-22
6611-edited1	6611-022	Early Jomon - Middle Jomon	HKD1999	J-23
6611-edited1	6611-023	Early Jomon - Middle Jomon	HKD1999	J-25
6611-edited1	6611-024	Early Jomon - Middle Jomon	HKD1999	J-26
6611-edited1	6611-025	Early Jomon - Middle Jomon	HKD1999	J-27
6611-edited1	6611-026	Initial Jomon	HKD1999	J-28
6611-edited1	6611-027	Moroiso a	HKD1999	J-29
6611-edited1	6611-028	Moroiso a	HKD1999	J-30
6613-edited	6613-001	Jomon	SHBA1993	J-1
6613-edited	6613-002	Moroiso	SHBA1993	J-2
6613-edited	6613-003	Moroiso	SHBA1993	J-3
6613-edited	6613-004	Moroiso	SHBA1993	J-4

Continued on next page

Table A.1: Pithouses at Gunma

BUA ID	Pithouse ID	Period	REF	original ID
6613-edited	6613-005	Lower Hanazumi - Futatsuki	SHBA1993	J-5
6613-edited	6613-006	Moroiso	SHBA1993	J-6
6613-edited	6613-007	Moroiso	SHBA1993	J-7
6613-edited	6613-008	Moroiso	SHBA1993	J-8
6613-edited	6613-009	Kasori E3 - E4	SHBA1993	J-9
6613-edited	6613-010	Lower Hanazumi - Futatsuki	SHBA1993	J-10
6613-edited	6613-011	Lower Hanazumi - Futatsuki	SHBA1993	J-11
6613-edited	6613-012	Kurohama / Ario	SHBA1993	J-12
6613-edited	6613-013	Moroiso	SHBA1993	J-13
6613-edited	6613-014	Lower Hanazumi - Futatsuki	SHBA1993	J-14
6613-edited	6613-015	Kurohama / Ario	SHBA1993	J-15
6613-edited	6613-016	Kurohama / Ario	SHBA1993	J-16
6613-edited	6613-017	Kurohama / Ario	SHBA1993	J-17
6614-edited	6614-001		HOKVI1998	H-1
6616-west	6616-001	Inaridai	SHYA1989	1
6616-west	6616-002	Inaridai	SHYA1989	2
6616-west	6616-003	Inaridai	SHYA1989	3
6616-west	6616-004	Initial Jomon	SHYA1989	4
6616-west	6616-005	Inaridai	SHYA1989	5
6616-west	6616-006	Inaridai	SHYA1989	6
6619-edited	6619-001	Jomon	HSUY1990	2
6619-edited	6619-002	Katsuzaka / Otamadai	HSUY1990	1
6625-kom1	6625-001	Kasori EIII-Shomyoji	KOSH1968	1
6625-kom1	6625-002	Kasori EIII-Shomyoji	KOSH1968	2
6625-komtak1	6625-003	Kasori E2-E3	KOSH2005	J-9
6625-komtak1	6625-004	Katsuzaka 3	KOSH2005	J-23
6625-komtak1	6625-005	Katsuzaka 1 - 2	KOSH2005	J-24
6625-komtak1	6625-006	Kasori E1	KOSH2005	J-25
6625-komtak1	6625-007	Katsuzaka 1 / Miharada	KOSH2005	J-26
6625-komtak1	6625-008	Early Jomon - Middle Jomon	KOSH2005	J-28
6625-komtak1	6625-009	Kasori E1-E2	KOSH2005	J-27
6625-komtak1	6625-010	Kasori E2-E3	KOSH2005	J-29
6625-komtak1	6625-011	Kasori E2-E3	KOSH2005	J-31
6625-komtak1	6625-012	Kasori E2	KOSH2005	J-30
6625-komtak1	6625-013	Kasori E1	KOSH2006	J-1
6625-komtak1	6625-014	KasoriE-3	KOSH2006	J-2
6625-komtak1	6625-015	KasoriE-3	KOSH2006	J-3
6625-komtak1	6625-016	KasoriE-3	KOSH2006	J-21
6625-komtak1	6625-017	KasoriE-3	KOSH2006	J-4
6625-komtak1	6625-018	Kasori E	KOSH2006	J-5
6625-komtak1	6625-019	Kasori E1	KOSH2006	J-6

Continued on next page

Table A.1: Pithouses at Gunma

BUA ID	Pithouse ID	Period	REF	original ID
6625-komtak1	6625-020	Kasori E3	KOSH2006	J-7
6625-komtak1	6625-021	KasoriE-3	KOSH2006	J-8
6625-komtak1	6625-022	KasoriE-3	KOSH2006	J-10
6625-komtak1	6625-023	Kasori E2-E3	KOSH2006	J-11
6625-komtak1	6625-024	Kasori E1-E2	KOSH2006	J-12
6625-komtak1	6625-025	Kasori E1	KOSH2006	J-15
6625-komtak1	6625-026	Kasori E2	KOSH2006	J-13
6625-komtak1	6625-027	Katsuzaka 3	KOSH2006	J-14
6625-komtak1	6625-028	KasoriE-3	KOSH2006	J-16
6625-komtak1	6625-029	KasoriE-3	KOSH2006	J-17
6625-komtak1	6625-030	KasoriE-3	KOSH2006	J-18
6625-komtak1	6625-031	KasoriE-3	KOSH2006	J-19
6625-komtak1	6625-032	Kasori E3	KOSH2006	J-20
6625-komtak1	6625-033	Middle Jomon	KOSH2006	J-22
6625-komtak4	6625-034	Kasori EI-EII	HOKXII2005	J-1
6625-komtak4	6625-035	Kasori EI-EII	HOKXII2005	J-2
6629-mak	6629-001	Initial Jomon	HKD1999	J-1
6630-edited	6630-001	Sekiyama - Kurohama	KAIHT1995	J-1
6630-edited	6630-002	Sekiyama - Kurohama	KAIHT1995	J-2
6630-edited	6630-003	Sekiyama - Kurohama	KAIHT1995	J-3
6631-edited	6631-001	Early Jomon	GNMY1971	1
6631-edited	6631-002	Early Jomon	GNMY1971	2
6631-edited	6631-003	Early Jomon	GNMY1971	3
6633-edited	6633-001	Katsuzaka 3 - Kasori E1	HOKVII1999	J-1
6633-edited	6633-002	Middle Jomon (Middle)	HOKVII1999	J-6
6633-edited	6633-003	Kasori EI-EII	HOKVII1999	J-2
6633-edited	6633-004	Kasori EI-EII	HOKVII1999	J-3
6633-edited	6633-005	Kasori EI-EII	HOKVII1999	J-5
6633-edited	6633-006	Kasori EI-EII	HOKVII1999	J-4
6633-edited	6633-007	Kasori EI-EII	HOKVII1999	J-12
6633-edited	6633-008	Middle Jomon	HOKVII1999	J-10
6633-edited	6633-009	Middle Jomon	HOKVII1999	J-11
6633-edited	6633-010	Middle Jomon	HOKVII1999	J-7
6633-edited	6633-011	Otamadai - Kasori EII	HOKVII1999	J-8
6633-edited	6633-012	Middle Jomon	HOKVII1999	J-9
6633-edited	6633-013	Yakemachi / Otamadai	DOK2001	J-1
6633-edited	6633-014	Yakemachi - Kasori E2	DOK2001	J-17
6633-edited	6633-015	Kasori E1	DOK2001	J-2
6633-edited	6633-016	Katsuzaka 3	DOK2001	J-3
6633-edited	6633-017	Katsuzaka 3	DOK2001	J-4
6633-edited	6633-018	Kasori E1 / Miharada	DOK2001	J-5

Continued on next page

Table A.1: Pithouses at Gunma

BUA ID	Pithouse ID	Period	REF	original ID
6633-edited	6633-019	Katsuzaka 2 - 3	DOK2001	J-6
6633-edited	6633-020	Katsuzaka 2 - 3	DOK2001	J-7
6633-edited	6633-021	Otamadai III - Katsuzaka 3	DOK2001	J-8
6633-edited	6633-022	Otamadai III - Katsuzaka 3	DOK2001	J-12
6633-edited	6633-023	Kasori E1	DOK2001	J-9
6633-edited	6633-024	Miharada / Yakimachi	DOK2001	J-10
6633-edited	6633-025	Katsuzaka 3	DOK2001	J-11
6633-edited	6633-026	Katsuzaka 3 - Kasori E1 / Miharada	DOK2001	J-13
6633-edited	6633-027	Kasori E1 / Miharada	DOK2001	J-14
6633-edited	6633-028	Katsuzaka 2	DOK2001	J-15
6633-edited	6633-029	Kasori E2	DOK2001	J-16
6633-edited	6633-030	Katsuzaka 2 - 3	DOK2001	J-18
6633-edited	6633-031	Kasori E1(Early)	DOK2001	J-19
6633-edited	6633-032	Katsuzaka 2 - 3	DOK2001	J-20
6633-edited	6633-033	Kasori E2	DOK2001	J-21
6633-edited	6633-034	Kasori E1 / Miharada	DOK2001	J-22
6633-edited	6633-035	Before Miharada-KasoriE-1	DOK2001	J-28
6633-edited	6633-036	Katsuzaka 3 - Yakemachi	DOK2001	J-23
6633-edited	6633-037	Katsuzaka 2 - 3	DOK2001	J-25
6633-edited	6633-038	Jomon	DOK2001	J-26
6633-edited	6633-039	Kasori E1-E2	DOK2001	J-27
6635-got	6635-001	Kurohama / Ario	GOT2006	J-1
6639-nisw	6639-001	Kurohama / Ario	NISW1992	J-1
6639-nisw	6639-002	Kurohama / Ario	NISW1992	J-2
6639-nisw	6639-003	Moroiso b	NISW1992	J-3
6639-nisw	6639-004	Early Jomon	NISW1992	J-4
6639-shir	6639-005	Kurohama / Ario	HOKIX2001	
6640-edited	6640-001	Kurohama / Ario	MORY1986	1
6640-edited	6640-002	Kurohama / Ario	MORY1986	2
6749-edited	6749-001	Kurohama / Ario	OSHT1987	
6827-edited	6827-001	Jomon	SHNSH1993	J1
6827-edited	6827-002	Kasori EIII (Late) - EIV	SHNSH1993	J2
6827-edited	6827-003	Kasori EIII	SHNSH1993	J3
6847-edited	6847-001	Moroiso c	SHBSHI2008	1
6847-edited	6847-002	Kurohama / Ario - Moroiso b	SHBSHI2008	2
6847-edited	6847-003	Kurohama / Ario - Moroiso b	SHBSHI2008	3
6847-edited	6847-004	Katsuzaka / Otamadai	SHBSHI2008	4
6847-edited	6847-005	Katsuzaka / Otamadai	SHBSHI2008	5
6847-edited	6847-006	Kurohama / Ario - Moroiso b	SHBSHI2008	6
6847-edited	6847-007	Katsuzaka / Otamadai	SHBSHI2008	7
6847-edited	6847-008	Ealry Jomon (Middle) - Middle Jomon (Early)	SHBSHI2008	8

Continued on next page

Table A.1: Pithouses at Gunma

BUA ID	Pithouse ID	Period	REF	original ID
6847-edited	6847-009	Ealry Jomon (Middle) - Middle Jomon (Early)	SHBSHI2008	9
6847-edited	6847-010	Ealry Jomon (Middle) - Middle Jomon (Early)	SHBSHI2008	10
6847-edited	6847-011	Ealry Jomon (Middle) - Middle Jomon (Early)	SHBSHI2008	11
6847-edited	6847-012	Katsuzaka / Otamadai	SHBSHI2008	12
6847-edited	6847-013	Ealry Jomon (Middle) - Middle Jomon (Early)	SHBSHI2008	13
6849-ush	6849-001	Sekiyama	SHNSH1988	6
6849	6849-002	Sekiyama - Kurohama	SHNSH1993	9
6849	6849-003	Sekiyama - Kurohama	SHNSH1993	10
6849	6849-004	Sekiyama - Kurohama	SHNSH1993	11
6849-kam	6849-005	Sekiyama II	KAMMT1998	6
6849-kam	6849-006	Sekiyama II	KAMMT1998	10
6849-kam	6849-007	Sekiyama II	KAMMT1998	2
6909-IV	6909-001	Sekiyama - Kurohama	SWNKIV2001	8
6920-12567812	6920-001	Sekiyama	NAKSJ1987	JH-1
6920-12567812	6920-002	Sekiyama	NAKSJ1987	JH-2
13557-I-IV	13557-001	Sekiyama	FKYA2007	III-1
13557-I-IV	13557-002	Sekiyama	FKYA2007	IV-1
13557-I-IV	13557-003	Sekiyama	FKYA2007	IV-2
13557-I-IV	13557-004	Sekiyama	FKYA2007	IV-3
13557-I-IV	13557-005	Early Jomon	FKYA2007	IV-4
13557-I-IV	13557-006	Sekiyama - Moroiso b	FKYA2007	IV-5
13557-V-VII	13557-007	Moroiso	FKYA2007	V-1
13558-edited	13558-001	Middle Jomon	NAKG2008	
13558-edited	13558-002	Middle Jomon	NAKG2008	
13558-edited	13558-003	Middle Jomon	NAKG2008	
13558-edited	13558-004	Middle Jomon	NAKG2008	
13558-edited	13558-005	Middle Jomon	NAKG2008	
13558-edited	13558-006	Middle Jomon	NAKG2008	
13558-edited	13558-007	Middle Jomon	NAKG2008	
13558-edited	13558-008	Early Jomon - Late Jomon	NAKG2008	
13558-edited	13558-009	Early Jomon - Late Jomon	NAKG2008	
13558-edited	13558-010	Early Jomon - Late Jomon	NAKG2008	
13558-edited	13558-011	Early Jomon - Late Jomon	NAKG2008	
13558-edited	13558-012	Early Jomon - Late Jomon	NAKG2008	
13558-edited	13558-013	Early Jomon - Late Jomon	NAKG2008	
13558-edited	13558-014	Early Jomon - Late Jomon	NAKG2008	
13558-edited	13558-015	Early Jomon - Late Jomon	NAKG2008	
13558-edited	13558-016	Early Jomon - Late Jomon	NAKG2008	
13558-edited	13558-017	Early Jomon - Late Jomon	NAKG2008	
13558-edited	13558-018	Early Jomon - Late Jomon	NAKG2008	
13558-edited	13558-019	Early Jomon - Late Jomon	NAKG2008	

Continued on next page

Table A.1: Pithouses at Gunma

BUA ID	Pithouse ID	Period	REF	original ID
13558-edited	13558-020	Early Jomon - Late Jomon	NAKG2008	
13558-edited	13558-021	Early Jomon - Late Jomon	NAKG2008	
13558-edited	13558-022	Early Jomon - Late Jomon	NAKG2008	
13558-edited	13558-023	Early Jomon - Late Jomon	NAKG2008	
13558-edited	13558-024	Early Jomon - Late Jomon	NAKG2008	
13558-edited	13558-025	Early Jomon - Late Jomon	NAKG2008	
13558-edited	13558-026	Early Jomon - Late Jomon	NAKG2008	
13558-edited	13558-027	Early Jomon - Late Jomon	NAKG2008	
13558-edited	13558-028	Early Jomon - Late Jomon	NAKG2008	
13558-edited	13558-029	Early Jomon - Late Jomon	NAKG2008	
13558-edited	13558-030	Early Jomon - Late Jomon	NAKG2008	
13558-edited	13558-031	Early Jomon - Late Jomon	NAKG2008	
13558-edited	13558-032	Early Jomon - Late Jomon	NAKG2008	
13558-edited	13558-033	Early Jomon - Late Jomon	NAKG2008	
13558-edited	13558-034	Early Jomon - Late Jomon	NAKG2008	
13558-edited	13558-035	Early Jomon - Late Jomon	NAKG2008	
13558-edited	13558-036	Early Jomon - Late Jomon	NAKG2008	
13558-edited	13558-037	Early Jomon - Late Jomon	NAKG2008	
13558-edited	13558-038	Early Jomon - Late Jomon	NAKG2008	
13558-edited	13558-039	Early Jomon - Late Jomon	NAKG2008	
13558-edited	13558-040	Early Jomon - Late Jomon	NAKG2008	
13558-edited	13558-041	Early Jomon - Late Jomon	NAKG2008	
13558-edited	13558-042	Early Jomon - Late Jomon	NAKG2008	
13558-edited	13558-043	Early Jomon - Late Jomon	NAKG2008	
13558-edited	13558-044	Early Jomon - Late Jomon	NAKG2008	
13558-edited	13558-045	Early Jomon - Late Jomon	NAKG2008	
13558-edited	13558-046	Early Jomon - Late Jomon	NAKG2008	
13558-edited	13558-047	Early Jomon - Late Jomon	NAKG2008	
13558-edited	13558-048	Early Jomon - Late Jomon	NAKG2008	
13558-edited	13558-049	Early Jomon - Late Jomon	NAKG2008	
13558-edited	13558-050	Early Jomon - Late Jomon	NAKG2008	
13558-edited	13558-051	Early Jomon - Late Jomon	NAKG2008	
13558-edited	13558-052	Early Jomon - Late Jomon	NAKG2008	
13558-edited	13558-053	Early Jomon - Late Jomon	NAKG2008	
13558-edited	13558-054	Early Jomon - Late Jomon	NAKG2008	
13558-edited	13558-055	Early Jomon - Late Jomon	NAKG2008	
13558-edited	13558-056	Early Jomon - Late Jomon	NAKG2008	
13558-edited	13558-057	Early Jomon - Late Jomon	NAKG2008	
13558-edited	13558-058	Early Jomon - Late Jomon	NAKG2008	
13558-edited	13558-059	Early Jomon - Late Jomon	NAKG2008	
13558-edited	13558-060	Early Jomon - Late Jomon	NAKG2008	

Continued on next page

Table A.1: Pithouses at Gunma

BUA ID	Pithouse ID	Period	REF	original ID
13558-edited	13558-061	Early Jomon - Late Jomon	NAKG2008	
13558-edited	13558-062	Early Jomon - Late Jomon	NAKG2008	
13558-edited	13558-063	Early Jomon - Late Jomon	NAKG2008	
13558-edited	13558-064	Early Jomon - Late Jomon	NAKG2008	
13558-edited	13558-065	Early Jomon - Late Jomon	NAKG2008	
13558-edited	13558-066	Early Jomon - Late Jomon	NAKG2008	
13558-edited	13558-067	Early Jomon - Late Jomon	NAKG2008	
13558-edited	13558-068	Early Jomon - Late Jomon	NAKG2008	
13558-edited	13558-069	Early Jomon - Late Jomon	NAKG2008	
13558-edited	13558-070	Early Jomon - Late Jomon	NAKG2008	
13558-edited	13558-071	Early Jomon - Late Jomon	NAKG2008	
13558-edited	13558-072	Early Jomon - Late Jomon	NAKG2008	
13558-edited	13558-073	Early Jomon - Late Jomon	NAKG2008	
13558-edited	13558-074	Early Jomon - Late Jomon	NAKG2008	
13558-edited	13558-075	Early Jomon - Late Jomon	NAKG2008	
13558-edited	13558-076	Early Jomon - Late Jomon	NAKG2008	
13558-edited	13558-077	Early Jomon - Late Jomon	NAKG2008	
13558-edited	13558-078	Early Jomon - Late Jomon	NAKG2008	
13558-edited	13558-079	Early Jomon - Late Jomon	NAKG2008	
13558-edited	13558-080	Early Jomon - Late Jomon	NAKG2008	
13558-edited	13558-081	Early Jomon - Late Jomon	NAKG2008	
13558-edited	13558-082	Early Jomon - Late Jomon	NAKG2008	
13558-edited	13558-083	Early Jomon - Late Jomon	NAKG2008	
13558-edited	13558-084	Early Jomon - Late Jomon	NAKG2008	
13558-edited	13558-085	Early Jomon - Late Jomon	NAKG2008	
13558-edited	13558-086	Early Jomon - Late Jomon	NAKG2008	
13558-edited	13558-087	Early Jomon - Late Jomon	NAKG2008	
13558-edited	13558-088	Early Jomon - Late Jomon	NAKG2008	
13558-edited	13558-089	Early Jomon - Late Jomon	NAKG2008	
13558-edited	13558-090	Early Jomon - Late Jomon	NAKG2008	
13558-edited	13558-091	Early Jomon - Late Jomon	NAKG2008	
13558-edited	13558-092	Early Jomon - Late Jomon	NAKG2008	
13558-edited	13558-093	Early Jomon - Late Jomon	NAKG2008	
13558-edited	13558-094	Early Jomon - Late Jomon	NAKG2008	
13558-edited	13558-095	Early Jomon - Late Jomon	NAKG2008	
13558-edited	13558-096	Early Jomon - Late Jomon	NAKG2008	
13558-edited	13558-097	Early Jomon - Late Jomon	NAKG2008	
13558-edited	13558-098	Early Jomon - Late Jomon	NAKG2008	
13558-edited	13558-099	Early Jomon - Late Jomon	NAKG2008	
13558-edited	13558-100	Early Jomon - Late Jomon	NAKG2008	
13558-edited	13558-101	Early Jomon - Late Jomon	NAKG2008	

Continued on next page

Table A.1: Pithouses at Gunma

BUA ID	Pithouse ID	Period	REF	original ID
13558-edited	13558-102	Early Jomon - Late Jomon	NAKG2008	
13558-edited	13558-103	Early Jomon - Late Jomon	NAKG2008	
13558-edited	13558-104	Early Jomon - Late Jomon	NAKG2008	
13558-edited	13558-105	Early Jomon - Late Jomon	NAKG2008	
13558-edited	13558-106	Early Jomon - Late Jomon	NAKG2008	
13558-edited	13558-107	Early Jomon - Late Jomon	NAKG2008	
13558-edited	13558-108	Early Jomon - Late Jomon	NAKG2008	
13558-edited	13558-109	Early Jomon - Late Jomon	NAKG2008	
13558-edited	13558-110	Early Jomon - Late Jomon	NAKG2008	
13558-edited	13558-111	Early Jomon - Late Jomon	NAKG2008	
13558-edited	13558-112	Early Jomon - Late Jomon	NAKG2008	
13558-edited	13558-113	Early Jomon - Late Jomon	NAKG2008	
13558-edited	13558-114	Early Jomon - Late Jomon	NAKG2008	
13558-edited	13558-115	Early Jomon - Late Jomon	NAKG2008	
13558-edited	13558-116	Early Jomon - Late Jomon	NAKG2008	
13558-edited	13558-117	Early Jomon - Late Jomon	NAKG2008	
13558-edited	13558-118	Early Jomon - Late Jomon	NAKG2008	
13558-edited	13558-119	Early Jomon - Late Jomon	NAKG2008	
13558-edited	13558-120	Early Jomon - Late Jomon	NAKG2008	
13558-edited	13558-121	Early Jomon - Late Jomon	NAKG2008	
13558-edited	13558-122	Early Jomon - Late Jomon	NAKG2008	
13558-edited	13558-123	Early Jomon - Late Jomon	NAKG2008	
13558-edited	13558-124	Early Jomon - Late Jomon	NAKG2008	
13558-edited	13558-125	Early Jomon - Late Jomon	NAKG2008	
13558-edited	13558-126	Early Jomon - Late Jomon	NAKG2008	
13558-edited	13558-127	Early Jomon - Late Jomon	NAKG2008	
13558-edited	13558-128	Early Jomon - Late Jomon	NAKG2008	
13558-edited	13558-129	Early Jomon - Late Jomon	NAKG2008	
13558-edited	13558-130	Early Jomon - Late Jomon	NAKG2008	
13558-edited	13558-131	Early Jomon - Late Jomon	NAKG2008	
13558-edited	13558-132	Early Jomon - Late Jomon	NAKG2008	
13558-edited	13558-133	Early Jomon - Late Jomon	NAKG2008	
13558-edited	13558-134	Early Jomon - Late Jomon	NAKG2008	
13558-edited	13558-135	Early Jomon - Late Jomon	NAKG2008	
13558-edited	13558-136	Early Jomon - Late Jomon	NAKG2008	
13558-edited	13558-137	Early Jomon - Late Jomon	NAKG2008	
13558-edited	13558-138	Early Jomon - Late Jomon	NAKG2008	
13559-edited	13559-001	Early Jomon (Early)	GUNMA23	
13559-edited	13559-002	Early Jomon (Early)	GUNMA23	
13559-edited	13559-003	Early Jomon (Early)	GUNMA23	
13560-edited	13560-001	Moroiso c	SHRJN2008	1

Continued on next page

Table A.1: Pithouses at Gunma

BUA ID	Pithouse ID	Period	REF	original ID
13560-edited	13560-002	Moroiso b	SHRJN2008	2
13560-edited	13560-003	Moroiso b - c	SHRJN2008	3
13560-edited	13560-004	Moroiso b	SHRJN2008	7
13560-edited	13560-005	Moroiso b	SHRJN2008	4A
13560-edited	13560-006	Moroiso b	SHRJN2008	4B
13560-edited	13560-007	Moroiso b	SHRJN2008	6
13560-edited	13560-008	Moroiso b	SHRJN2008	5
13560-edited	13560-009	Moroiso b	SHRJN2008	8
13560-edited	13560-010	Moroiso b - c	SHRJN2008	10
13560-edited	13560-011	Moroiso c	SHRJN2008	12
13560-edited	13560-012	Moroiso c	SHRJN2008	11
13561-edited	13561-001	Early Jomon (Late)	GUNMA23	
13561-edited	13561-002	Early Jomon (Late)	GUNMA23	
13561-edited	13561-003	Early Jomon (Late)	GUNMA23	
13561-edited	13561-004	Early Jomon (Late)	GUNMA23	
13561-edited	13561-005	Early Jomon (Late)	GUNMA23	
13561-edited	13561-006	Early Jomon (Late)	GUNMA23	
13563-edited	13563-001	Kurohama / Ario	SHFKIFKNK1998	1
13564-edited	13564-001	Kurohama (Early)	SHFKIFKNK1998	1
13564-edited	13564-002	Kasori E3	SHFKIFKNK1998	2
13564-edited	13564-003	Moroiso a	SHFKIFKNK1998	3
10000	10000-001	Kasori E3 (late)	HKDTK2001	J-1
6964-jomon	6964-001	Goryogadai - Otamadai Ib (Early)	HNDMH1994	163
6964-jomon	6964-002	Moroiso a - Goryogadai	HNDMH1994	164
6964-jomon	6964-003	Sekiyama - Goryogadai	HNDMH1994	165
6964-jomon	6964-004	Moroiso a - Goryogadai	HNDMH1994	166
6964-jomon	6964-005	Moroiso b - Goryogadai 2	HNDMH1994	167
6964-jomon	6964-006	Sekiyama - Kurohama	HNDMH1994	168
6964-jomon	6964-007	Kurohama - Moroiso b	HNDMH1994	169
6964-jomon	6964-008	Jusanbodai-Goryogadai-Katsuzaka1	HNDMH1994	170
6964-jomon	6964-009	Jomon	HNDMH1994	171
6964-jomon	6964-010	Jomon	HNDMH1994	172
6964-jomon	6964-011	Moroiso b	HNDMH1994	173
6964-jomon	6964-012	Jomon	HNDMH1994	174
6964-jomon	6964-013	Jomon	HNDMH1994	175
6964-jomon	6964-014	Jomon	HNDMH1994	176
6964-jomon	6964-015	Jomon	HNDMH1994	177
6964-jomon	6964-016	Jomon	HNDMH1994	178
6964-jomon	6964-017	Daigi 7b	HNDMH1994	179
6964-jomon	6964-018	Jomon	HNDMH1994	180
6964-jomon	6964-019	Sekiyama - Kurohama	HNDMH1994	181

Continued on next page

Table A.1: Pithouses at Gunma

BUA ID	Pithouse ID	Period	REF	original ID
6964-jomon	6964-020	Kurohama - Moroiso a	HNDMH1994	182
6964-jomon	6964-021	Kurohama - Moroiso b	HNDMH1994	183
6964-jomon	6964-022	Early Jomon (Early)	HNDMH1994	184
6964-jomon	6964-023	Early Jomon (Early)	HNDMH1994	185
6964-jomon	6964-024	Jomon	HNDMH1994	186
6964-jomon	6964-025	Early Jomon (Early)	HNDMH1994	187
6964-jomon	6964-026	Early Jomon (Early)	HNDMH1994	188
6964-jomon	6964-027	Early Jomon (Early)	HNDMH1994	189
6964-jomon	6964-028	Jomon	HNDMH1994	190
6935-AB	6935-001	Kasori E1	MYKTYM1987	1
6935-AB	6935-002	Kasori E1	MYKTYM1987	2
6935-AB	6935-003	Kasori E3 (Early)	MYKTYM1987	3
6935-AB	6935-004	Katsuzaka 3	MYKTYM1987	4
6935-AB	6935-005	Kasori E1	MYKTYM1987	5
6935-AB	6935-006	Kasori E2	MYKTYM1987	6
6935-AB	6935-007	Kasori E3 (Early)	MYKTYM1987	7
6935-AB	6935-008	Kasori E2	MYKTYM1987	8
6935-AB	6935-009	Kasori E1	MYKTYM1987	9
6935-AB	6935-010	Kasori E2	MYKTYM1987	10
6935-AB	6935-011	Kasori E2	MYKTYM1987	11
6935-AB	6935-012	Kasori E3 (Early)	MYKTYM1987	12
6935-AB	6935-013	Kasori E1	MYKTYM1987	13
6935-AB	6935-014	Kasori E2	MYKTYM1987	14
6935-AB	6935-015	Kasori E3 (Early)	MYKTYM1987	15
6935-AB	6935-016	Kasori E3 (Early)	MYKTYM1987	16
6935-AB	6935-017	Katsuzaka 3	MYKTYM1987	17
6935-AB	6935-018	Kasori E3 (late)	MYKTYM1987	18
6935-AB	6935-019	Kasori E2	MYKTYM1987	19
6935-AB	6935-020	Kasori E2	MYKTYM1987	20
6935-AB	6935-021	Jomon	MYKTYM1987	21
6935-AB	6935-022	Katsuzaka 3	MYKTYM1987	22
6935-AB	6935-023	Kasori E1	MYKTYM1987	23
6935-AB	6935-024	Jomon	MYKTYM1987	24
6935-AB	6935-025	Kasori E2	MYKTYM1987	25
6935-AB	6935-026	Jomon	MYKTYM1987	26
6935-AB	6935-027	Kasori E2	MYKTYM1987	27
6935-AB	6935-028	Kasori E2	MYKTYM1987	28
6935-AB	6935-029	Kasori E2-E3	MYKTYM1987	29
6935-AB	6935-030	Katsuzaka 3	MYKTYM1987	30
6935-AB	6935-031	Kasori E2-E3	MYKTYM1987	31
6935-AB	6935-032	Kasori E3 (Early)	MYKTYM1987	32

Continued on next page

Table A.1: Pithouses at Gunma

BUA ID	Pithouse ID	Period	REF	original ID
6935-AB	6935-033	Kasori E1	MYKTYM1987	33
6935-AB	6935-034	Kasori E3 (Early)	MYKTYM1987	34
6935-AB	6935-035	Kasori E3 (Early)	MYKTYM1987	35
6935-AB	6935-036	Kasori E3 (Early)	MYKTYM1987	36
6935-AB	6935-037	Kasori E1	MYKTYM1987	37
6935-AB	6935-038	Kasori E2	MYKTYM1987	38
6935-AB	6935-039	Kasori E3 (Early)	MYKTYM1987	39
6935-AB	6935-040	Kasori E1	MYKTYM1987	40
6927	6927-001	Kasori EIV - Shomyoji	KRSW1978	JH-1
6927	6927-002	Kasori EIII-EIV	KRSW1978	JH-2
6927	6927-003	Kasori EIII-EIV	KRSW1978	JH-3
6927	6927-004	Kasori E	KRSW1980	
6927	6927-005	Kasori E	KRSW1980	
6927	6927-006	Kasori E	KRSW1980	
6927	6927-007	Kasori E	KRSW1980	
6927	6927-008	Kasori E	KRSW1980	
6927	6927-009	Kasori E	KRSW1980	
6927	6927-010	Kasori E	KRSW1980	
6927	6927-011	Kasori E	KRSW1980	
6927	6927-012	Kasori E	KRSW1980	
6927	6927-013	Kasori E	KRSW1980	
6927	6927-014	Kasori E	KRSW1980	
6927	6927-015	Kasori E	KRSW1980	
6927	6927-016	Kasori E	KRSW1980	
6927	6927-017	Kasori E	KRSW1980	
6927	6927-018	Kasori E	KRSW1980	
6927	6927-019	Kasori E	KRSW1980	
6927	6927-020	Kasori E	KRSW1980	
6927	6927-021	Kasori E	KRSW1980	
6927	6927-022	Kasori E	KRSW1980	
6927	6927-023	Kasori E	KRSW1980	
6927	6927-024	Sekiyama	KRSW1980	
6927	6927-025	Kasori EIII-EIV	KRSW1982	JH-24
6927	6927-026	Kasori E4	KRSW1985	JH-26
6927	6927-027	Kasori E	KRSW1985	JH-27
6927	6927-028	Kasori E	KRSW1985	JH-28
6927	6927-029	Kasori E	KRSW1985	JH-29
6927	6927-030	Kasori E	KRSW1985	JH-30
6927	6927-031	Kasori E	KRSW1985	JH-31
6927	6927-032	Kasori E	KRSW1985	JH-32
6927	6927-033	Kasori E	KRSW1985	JH-33

Continued on next page

Table A.1: Pithouses at Gunma

BUA ID	Pithouse ID	Period	REF	original ID
6927	6927-034	Kasori E	KRSW1985	JH-34
6927	6927-035	Katsuzaka / Otamadai	KRSW1985	
6927	6927-036	Kasori E	KRSW1985	
6927	6927-037	Kasori E	KRSW1985	
6927	6927-038	Kasori E	KRSW1985	
6927	6927-039	Kasori E	KRSW1985	
6927	6927-040	Kasori E	KRSW1985	
6927	6927-041	Kasori E	KRSW1986	JH-41
6927	6927-042	Middle Jomon	KRSW1988	
6927	6927-043	Middle Jomon	KRSW1988	
6927	6927-044	Middle Jomon	KRSW1988	
6927	6927-045	Middle Jomon	KRSW1988	
6927	6927-046	Middle Jomon	KRSW1988	
6927	6927-047	Middle Jomon	KRSW1988	
6927	6927-048	Middle Jomon	KRSW1988	
6927	6927-049	Middle Jomon	KRSW1988	
6927	6927-050	Middle Jomon	KRSW1988	
6927	6927-051	Middle Jomon	KRSW1988	
6927	6927-052	Middle Jomon	KRSW1988	
6927	6927-053	Middle Jomon (Late)	KRSW1991	JH-53
6927	6927-054	Middle Jomon (Late)	KRSW1991	JH-54
6927	6927-055	Middle Jomon (Late)	KRSW1991	JH-55
6927	6927-056	Middle Jomon (Late)	KRSW1991	JH-56
10011-nishishita	10011-001	Moroiso	JNBSHJ1991	
10011-nishishita	10011-002	Moroiso	JNBSHJ1991	
10011-nishishita	10011-003	Moroiso	JNBSHJ1991	
10011-nishishita	10011-004	Moroiso	JNBSHJ1991	
10011-higashishita	10011-005	Lower Hanazumi - Moroiso a	JNBSHJ1991	
10011-higashishita	10011-006	Lower Hanazumi - Moroiso a	JNBSHJ1991	
10011-higashishita	10011-007	Lower Hanazumi - Moroiso a	JNBSHJ1991	
10011-higashishita	10011-008	Lower Hanazumi - Moroiso a	JNBSHJ1991	
10011-higashishita	10011-009	Lower Hanazumi - Moroiso a	JNBSHJ1991	
10011-higashishita	10011-010	Kasori E	JNBSHJ1991	
10011-higashi	10011-011	Sekiyama - Moroiso b	JNBSHJ1991	
10011-higashi	10011-012	Sekiyama - Moroiso b	JNBSHJ1991	
10011-higashi	10011-013	Sekiyama - Moroiso b	JNBSHJ1991	
10011-higashi	10011-014	Sekiyama - Moroiso b	JNBSHJ1991	
10012-edited	10012-001	Sekiyama - Kurohama	JNBSHJ1991	
10012-edited	10012-002	Sekiyama - Kurohama	JNBSHJ1991	
10012-edited	10012-003	Sekiyama - Kurohama	JNBSHJ1991	
10012-edited	10012-004	Moroiso c (Early)	JNBSHJ1991	

Continued on next page

Table A.1: Pithouses at Gunma

BUA ID	Pithouse ID	Period	REF	original ID
10012-edited	10012-005	Moroiso c (Early)	JNBSHJ1991	
10012-edited	10012-006	Moroiso c (Early)	JNBSHJ1991	
10012-edited	10012-007	Moroiso c (Early)	JNBSHJ1991	
10012-edited	10012-008	Kasori E	JNBSHJ1991	
10012-edited	10012-009	Kasori E	JNBSHJ1991	
10012-edited	10012-010	Kasori E	JNBSHJ1991	
10012-edited	10012-011	Kasori E	JNBSHJ1991	
10012-edited	10012-012	Kasori E	JNBSHJ1991	
10012-edited	10012-013	Kasori E	JNBSHJ1991	
10012-edited	10012-014	Kasori E	JNBSHJ1991	
10012-edited	10012-015	Kasori E	JNBSHJ1991	
10012-edited	10012-016	Kasori E	JNBSHJ1991	
10012-edited	10012-017	Kasori E	JNBSHJ1991	
10012-edited	10012-018	Kasori E	JNBSHJ1991	
10012-edited	10012-019	Kasori E	JNBSHJ1991	
10012-edited	10012-020	Kasori E	JNBSHJ1991	
10012-edited	10012-021	Kasori E	JNBSHJ1991	
10012-edited	10012-022	Kasori E	JNBSHJ1991	
10012-edited	10012-023	Shomyoji	JNBSHJ1991	
10012-edited	10012-024	Shomyoji	JNBSHJ1991	
10012-edited	10012-025	Jomon	JNBSHJ1991	
10014	10014-001	Early Jomon (Early)	TNKTSM1986	J-1
10014	10014-002	Moroiso b (Early)	TNKTSM1986	J-2
10015	10015-001	Moroiso c	ATGYSAH1994	1
10015	10015-002	Moroiso b	ATGYSAH1994	2
10015	10015-003	Kurohama / Ario	ATGYSAH1994	3
10015	10015-004	Moroiso b	ATGYSAH1994	4
10015	10015-005	Moroiso b	ATGYSAH1994	5
10015	10015-006	Moroiso b	ATGYSAH1994	6
10015	10015-007	Moroiso b	ATGYSAH1994	7
10015	10015-008	Moroiso b	ATGYSAH1994	8
10015	10015-009	Moroiso b	ATGYSAH1994	9
10015	10015-010	Moroiso b	ATGYSAH1994	10
10015	10015-011	Moroiso b	ATGYSAH1994	11
10015	10015-012	Jomon	ATGYSAH1994	12
10016-edited	10016-001	Early Jomon	MKIWTNYI1987	1
10016-edited	10016-002	Moroiso c	MKIWTNYI1987	2
10029-ABC	10029-001	Early Jomon	MKIWTNYI1987	J-1
10029-DEF	10029-002	Moroiso b - c	MKIWTNYI1987	J-6
10029-DEF	10029-003	Early Jomon	MKIWTNYI1987	J-10
10029-DEF	10029-004	Katsuzaka / Otamadai	MKIWTNYI1987	J-7

Continued on next page

Table A.1: Pithouses at Gunma

BUA ID	Pithouse ID	Period	REF	original ID
10029-DEF	10029-005	Katsuzaka / Otamadai	MKIWTNYI1987	J-12
10029-DEF	10029-006	Katsuzaka / Otamadai	MKIWTNYI1987	J-9
10029-DEF	10029-007	Katsuzaka / Otamadai	MKIWTNYI1987	J-8B
10029-DEF	10029-008	Katsuzaka / Otamadai	MKIWTNYI1987	J-8A
10029-DEF	10029-009	Katsuzaka / Otamadai	MKIWTNYI1987	J-13
10029-DEF	10029-010	Katsuzaka / Otamadai	MKIWTNYI1987	J-11
10029-ABC	10029-011	Middle Jomon	MKIWTNYI1987	J-2
10029-ABC	10029-012	Middle Jomon	MKIWTNYI1987	J-3
10029-ABC	10029-013	Middle Jomon	MKIWTNYI1987	J-4
10030-A	10030-001	Katsuzaka / Otamadai	TNKTSM1986	J-1
10030-A	10030-002	Katsuzaka / Otamadai	TNKTSM1986	J-2
10031-edited	10031-001	Early Jomon (Early)	TNKTSM1986	J-1
10051	10051-001	Moroiso b - c	HRMN1992	J-2
10051	10051-002	Moroiso b (Final)	HRMN1992	J-3
10051	10051-003	Moroiso b - c	HRMN1992	J-4
10051	10051-004	Moroiso b (Final) - Moroiso c	HRMN1992	J-5
10051	10051-005	Moroiso b - c	HRMN1992	
10051	10051-006	Moroiso b - c	HRMN1992	
10051	10051-007	Moroiso b - c	HRMN1992	
10051	10051-008	Moroiso b - c	HRMN1992	
10051	10051-009	Moroiso b - c	HRMN1992	
10051	10051-010	Moroiso b - c	HRMN1992	
10068-J1	10068-001	Kurohama / Ario	OBRM1998	1
10068-J1	10068-002	Kurohama / Ario	OBRM1998	2
10068-J1	10068-003	Kurohama / Ario	OBRM1998	3
10068-J1	10068-004	Kurohama / Ario	OBRM1998	4
10068-J1	10068-005	Kurohama / Ario	OBRM1998	5
10068-J1	10068-006	Kurohama / Ario	OBRM1998	6
10068-J234	10068-007	Early Jomon	OBRM1998	7
10078	10078-001	Horinouchi 2	SHKWYMKBT1989	J-1
10078	10078-002	Moroiso a	SHKWYMKBT1989	J-2
10079	10079-001	Early Jomon (Initial)	SHKWYMKBT1989	J-1
10079	10079-002	Early Jomon (Initial)	SHKWYMKBT1989	J-2
10079	10079-003	Early Jomon (Initial)	SHKWYMKBT1989	J-3
10079	10079-004	Early Jomon (Initial)	SHKWYMKBT1989	J-4
10079	10079-005	Early Jomon (Initial)	SHKWYMKBT1989	J-5
10079	10079-006	Early Jomon (Initial)	SHKWYMKBT1989	J-6
10080	10080-001	Kurohama / Ario	SHKWYMKBT1989	J-1
10080	10080-002	Kurohama / Ario	SHKWYMKBT1989	J-2
10084-EF	10084-001	Early Jomon (Late)	SKGM1994	1
10084-EF	10084-002	Jomon	SKGM1994	2

Continued on next page

Table A.1: Pithouses at Gunma

BUA ID	Pithouse ID	Period	REF	original ID
10085-edited	10085-001	Middle Jomon (Early)	AKGCSJ1993	EJ-1
10085-edited	10085-002	Kasori EIII (Late)	AKGCSJ1993	CJ-1
10088-edited	10088-001	Moroiso b (Late) - c (Ealy)	KMHTERMAG1995	J-1
10088-edited	10088-002	Moroiso b (Late)	KMHTERMAG1995	J-2
10088-edited	10088-003	Moroiso b (Late) - c (Ealy)	KMHTERMAG1995	J-3
10088-edited	10088-004	Moroiso b (Late) - c (Ealy)	KMHTERMAG1995	J-4
10088-edited	10088-005	Moroiso c (Early)	KMHTERMAG1995	J-5
10088-edited	10088-006	Moroiso c (Early)	KMHTERMAG1995	J-6A
10088-edited	10088-007	Moroiso c (Early)	KMHTERMAG1995	J-6B
10089-edited	10089-001	Early Jomon (Middle)	KMHTERMAG1995	J-1
10089-edited	10089-002	Moroiso a	KMHTERMAG1995	J-2A
10089-edited	10089-003	Moroiso a	KMHTERMAG1995	J-2B
10105-edited	10105-001	Early Jomon	SHFJMM1997	
10149	10149-001	Kasori E3	JNM1999	B-1
10149	10149-002	Kasori E3	JNM1999	C-1
10149	10149-003	Kasori E3	JNM1999	C-2
10149	10149-004	Kasori E3	JNM1999	C-3a
10149	10149-005	Kasori E3	JNM1999	C-4
10149	10149-006	Kasori E3	JNM1999	C-5
10149	10149-007	Kasori E3	JNM1999	C-3b
10149	10149-008	Kasori E3	JNM1999	C-3c
10149	10149-009	Kasori E3	JNM1999	C-6
10149	10149-010	Kasori E3	JNM1999	C-7
10149	10149-011	Kasori E3	JNM1999	C-8
10149	10149-012	Kasori E3	JNM1999	C-9
10149	10149-013	Kasori E3	JNM1999	C-10
10149	10149-014	Kasori E3	JNM1999	C-11
10149	10149-015	Kasori E3	JNM1999	D-1
10149	10149-016	Kasori E3	JNM1999	D-2
10149	10149-017	Jomon	JNM1999	D-3
10149	10149-018	Kasori E3	JNM1999	E-1
10149	10149-019	Kasori E3	JNM1999	E-2
10149	10149-020	Kasori E2	JNM1999	E-3
10159	10159-001	Late Jomon - Final Jomon	KYN2005	A-J1
10159	10159-002	Late Jomon (Late) - Final Jomon (Early)	KYN2005	A-J2
10159	10159-003	Late Jomon (Late) - Final Jomon (Early)	KYN2005	A-J3
10159	10159-004	Late Jomon (Final) - Final Jomon (Early)	KYN2005	A-J4
10159	10159-005	Final Jomon (Early)	KYN2005	A-J5
10159	10159-006	Jomon	KYN2005	A-J6
10159	10159-007	Jomon	KYN2005	A-J7
10159	10159-008	Angyo3a-3b	KYN2005	A-J8A

Continued on next page

Table A.1: Pithouses at Gunma

BUA ID	Pithouse ID	Period	REF	original ID
10159	10159-009	Horinouchi, Kasori B, Takaihigashi	KYN2005	A-J8B
10159	10159-010	Jomon	KYN2005	A-J8C
10159	10159-011	Late Jomon - Final Jomon	KYN2005	A-J11
10159	10159-012	Jomon	KYN2005	A-J12
10159	10159-013	Takaihigashi	KYN2005	A-J13
10159	10159-014	Takaihigashi	KYN2005	A-J14
10159	10159-015	Jomon	KYN2005	A-J15A
10159	10159-016	Angyo 3a-3b	KYN2005	A-J15B
10159	10159-017	Jomon	KYN2005	A-J16A
10159	10159-018	Jomon	KYN2005	A-J16B
10159	10159-019	Jomon	KYN2005	A-J17
10159	10159-020	Jomon	KYN2005	A-J18
10159	10159-021	Jomon	KYN2005	B-J1
10159	10159-022	Jomon	KYN2005	B-J2
10159	10159-023	Angyo1, Shinchi,Takaihigashi	KYN2005	A-J9
10310-B	10310-001	Moroiso b	SHTKON1986	1
10322-edited	10322-001	Otamadai II - Kasori EI (Early)	NMMN1999	90
10322-edited	10322-002	Otamadai II - Kasori EI (Early)	NMMN1999	91
10322-edited	10322-003	Yakemachi	NMMN1999	92
10322-edited	10322-004	Otamadai II - Kasori EI (Early)	NMMN1999	93
10322-edited	10322-005	Late Jomon	NMMN1999	94
10322-edited	10322-006	Otamadai II - Kasori EI (Early)	NMMN1999	95
10322-edited	10322-007	Kasori E	NMMN1999	96
10322-edited	10322-008	Kasori E	NMMN1999	97
10322-edited	10322-009	Kasori E	NMMN1999	98
10322-edited	10322-010	Kasori E	NMMN1999	99
10322-edited	10322-011	Kasori E	NMMN1999	100
10322-edited	10322-012	Kasori E	NMMN1999	101
10322-edited	10322-013	Kasori E	NMMN1999	102
10322-edited	10322-014	Kasori E	NMMN1999	103
10322-edited	10322-015	Kasori EI (Early)	NMMN1999	104
10322-edited	10322-016	Kasori E	NMMN1999	105
10322-edited	10322-017	Otamadai II - Kasori EI (Early)	NMMN1999	106
10322-edited	10322-018	Otamadai II - Kasori EI (Early)	NMMN1999	107
10322-edited	10322-019	Moroiso a	NMMN1999	108
10322-edited	10322-020	Kasori E	NMMN1999	109
10322-edited	10322-021	Otamadai II - Kasori EI (Early)	NMMN1999	110
10322-edited	10322-022	Otamadai II - Kasori EI (Early)	NMMN1999	111
10322-edited	10322-023	Otamadai II - Kasori EI (Early)	NMMN1999	112
10322-edited	10322-024	Otamadai II - Kasori EI (Early)	NMMN1999	113
10322-edited	10322-025	Otamadai II - Kasori EI (Early)	NMMN1999	114

Continued on next page

Table A.1: Pithouses at Gunma

BUA ID	Pithouse ID	Period	REF	original ID
10322-edited	10322-026	Otamadai II - Kasori EI (Early)	NMMN1999	115
10322-edited	10322-027	Otamadai II - Kasori EI (Early)	NMMN1999	117
10322-edited	10322-028	Otamadai II - Kasori EI (Early)	NMMN1999	116
10322-edited	10322-029	Otamadai II - Kasori EI (Early)	NMMN1999	118
10322-edited	10322-030	Otamadai II - Kasori EI (Early)	NMMN1999	119
10322-edited	10322-031	Otamadai II - Kasori EI (Early)	NMMN1999	120
10322-edited	10322-032	Otamadai II - III	NMMN1999	122
10322-edited	10322-033	Otamadai II - Kasori EI (Early)	NMMN1999	121
10322-edited	10322-034	Otamadai II - Kasori EI (Early)	NMMN1999	123
10322-edited	10322-035	Moroiso b	NMMN1999	124
10322-edited	10322-036	Otamadai II - Kasori EI (Early)	NMMN1999	125
10322-edited	10322-037	Otamadai II - Kasori EI (Early)	NMMN1999	126
10322-edited	10322-038	Otamadai II - Kasori EI (Early)	NMMN1999	127
10322-edited	10322-039	Otamadai II - Kasori EI (Early)	NMMN1999	128
10322-edited	10322-040	Kasori EI (Early)	NMMN1999	129
10322-edited	10322-041	Otamadai II - III	NMMN1999	130
10322-edited	10322-042	Otamadai II - Kasori EI (Early)	NMMN1999	131
10322-edited	10322-043	Otamadai II - Kasori EI (Early)	NMMN1999	132
10324-edited	10324-001	Late Jomon (Early)	STMNGK1986	1-1
10324-edited	10324-002	Kasori EI (late)	STMNGK1986	13-1
10324-edited	10324-003	Kasori EII	STMNGK1986	13-2
10324-edited	10324-004	Kasori EIII	STMNGK1986	13-3
10324-edited	10324-005	Kasori EII (Middle) - EIII	STMNGK1986	13-4
10324-edited	10324-006	Kasori EII (Middle) - EIII	STMNGK1986	13-5
10324-edited	10324-007	Kasori EIII	STMNGK1986	13-6
10324-edited	10324-008	Kasori EII (Middle-Late)	STMNGK1986	13-8
10324-edited	10324-009	Kasori EIII	STMNGK1986	13-9
10324-edited	10324-010	Kasori EII (Middle-Late)	STMNGK1986	13-10
10324-edited	10324-011	Kasori EIV	STMNGK1986	13-11
13556-edited	13556-001	Moroiso b (Late)	ISMR2006	I-1
13556-edited	13556-002	Moroiso b (Late)	ISMR2006	I-2
13556-edited	13556-003	Moroiso b (Late)	ISMR2006	I-4
13556-edited	13556-004	Moroiso b (Late)	ISMR2006	I-5
13556-edited	13556-005	Moroiso b (Late)	ISMR2006	I-6
6718-edited	6718-001	Kurohama / Ario	GUNMAKENSHI	
6718-edited	6718-002	Sekiyama	GUNMAKENSHI	
6718-edited	6718-003	Sekiyama	GUNMAKENSHI	
6718-edited	6718-004	Sekiyama	GUNMAKENSHI	

Table A.2: Pithouses at Chiba

BUA ID	Pithouse ID	Period	REF	original ID
2010625_edited	10010-001	Middle Jomon	CHNEN1998	
2010625_edited	10010-002	Otamadai	BOUYS2000	1
2010625_edited	10010-003	Otamadai	BOUYS2000	2
2010625_edited	10010-004	Kasori EII - EIV	BOUYS2000	3
2010625_edited	10010-005	Kasori EIII - EIV	BOUYS2000	4
2010625_edited	10010-006	Kasori EIII - EIV	BOUYS2004	5
2010625_edited	10010-007	Kasori EIII - EIV	BOUYS2004	6
2010524_edited1	10018-001	Horinouchi	UNRSZ2001	3
2010524_edited1	10018-002	Kasori EIV - Shomyoji	UNRSZ2001	6
2010524_edited1	10018-003	Horinouchi 1	UNRSZ2001	9
2010524_edited1	10018-004	Horinouchi 1	UNRSZ2001	11
2010524_edited1	10018-005	Kasori EIV - Shomyoji	UNRSZ2001	10
2010524_edited1	10018-006	Kasori EIV	UNRSZ2001	12
2010524_edited1	10018-007	Kasori EIV - Shomyoji	UNRSZ2001	13
2010524_edited1	10018-008	Shomyoji 1a	UNRSZ2001	5
2010524_edited1	10018-009	Kasori EIV	UNRSZ2001	15
2010524_edited1	10018-010	Horinouchi	UNRSZ2001	16
2010524_edited1	10018-011	Kasori EIV	UNRSZ2001	17
2010524_edited1	10018-012	Shomyoji I	UNRSZ2001	18
2010524_edited1	10018-013	Middle Jomon - Late Jomon	UNRSZ2001	19
2010524_edited1	10018-014	Middle Jomon - Late Jomon	UNRSZ2001	14
2010524_edited2	10018-015	Kasori EIV	UNRSZ2004	A-002
2010524_edited2	10018-016	Kasori EIV	UNRSZ2004	A-007
2010524_edited2	10018-017	Kasori EIII	UNRSZ2004	A-010
2010524_edited2	10018-018	Kasori EIII	UNRSZ2004	A-014
2010524_edited2	10018-019	Kasori EIII	UNRSZ2004	A-015
2010524_edited2	10018-020	Kasori EIV	UNRSZ2004	A-016
2010524_edited2	10018-021	Shomyoji 1	UNRSZ2004	A-017
2010524_edited2	10018-022	Kasori EIII	UNRSZ2004	A-019
2010524_edited2	10018-023	Shomyoji 1	UNRSZ2004	A-020
2010524_edited2	10018-024	Kasori EIII	UNRSZ2004	A-021
2010524_edited2	10018-025	Kasori EIV - Shomyoji	UNRSZ2004	A-023
2010524_edited2	10018-026	Kasori EIV	UNRSZ2004	A-024
2010524_edited2	10018-027	Kasori EIV	UNRSZ2004	A-025
2010524_edited2	10018-028	Shomyoji 1	UNRSZ2004	A-026
2010524_edited2	10018-029	Kasori EIV	UNRSZ2004	A-027
2010524_edited2	10018-030	Kasori EIV	UNRSZ2004	A-028
2010524_edited2	10018-031	Kasori EIII	UNRSZ2004	A-029
2010524_edited2	10018-032	Kasori EIV	UNRSZ2004	A-030
2010524_edited2	10018-033	Shomyoji 1	UNRSZ2004	A-031
2010524_edited2	10018-034	Shomyoji 1	UNRSZ2004	A-033

Continued on next page

Table A.2: Pithouses at Chiba

BUA ID	Pithouse ID	Period	REF	original ID
2010524_edited2	10018-035	Kasori EIV - Shomyoji	UNRSZ2004	A-034
2010524_edited2	10018-036	Kasori EIV	UNRSZ2004	A-035
2010524_edited2	10018-037	Kasori EIII	UNRSZ2004	A-037
2010524_edited2	10018-038	Kasori EIII	UNRSZ2004	A-038
2010524_edited2	10018-039	Kasori EIV	UNRSZ2004	A-039
2010524_edited2	10018-040	Kasori EIV	UNRSZ2004	A-040
2010524_edited2	10018-041	Kasori E	UNRSZ2004	A-043
2010524_edited2	10018-042	Kasori EIV	UNRSZ2004	A-044
2010524_edited2	10018-043	Kasori EIII	UNRSZ2004	A-045
2010524_edited2	10018-044	Kasori EIV	UNRSZ2004	A-046
2010524_edited2	10018-045	Shomyoji 1	UNRSZ2004	A-049
2010524_edited2	10018-046	Kasori EIV	UNRSZ2004	A-054
2010524_edited2	10018-047	Shomyoji 1	UNRSZ2004	A-055
2010524_edited2	10018-048	Kasori EIII	UNRSZ2004	A-057
2010524_edited2	10018-049	Kasori EIV	UNRSZ2004	A-058
2010524_edited2	10018-050	Kasori EIII	UNRSZ2004	A-059
2010524_edited2	10018-051	Kasori EIV	UNRSZ2004	A-060
2010524_edited2	10018-052	Shomyoji 2 - Horinouchi	UNRSZ2004	A-062
2010524_edited2	10018-053	Kasori EIV	UNRSZ2004	A-063
2010524_edited2	10018-054	Horinouchi	UNRSZ2004	A-064
2010524_edited2	10018-055	Horinouchi	UNRSZ2004	A-065
2010524_edited2	10018-056	Horinouchi 1	UNRSZ2004	A-066
2010524_edited2	10018-057	Shomyoji 1	UNRSZ2004	A-067
2010524_edited2	10018-058	Shomyoji 1 - Horinouchi 1	UNRSZ2004	A-068
2010524_edited2	10018-059	Kasori EIV	UNRSZ2004	A-069
2010524_edited2	10018-060	Shomyoji 1	UNRSZ2004	A-070
2010524_edited2	10018-061	Kasori EIV	UNRSZ2004	A-071
2010524_edited2	10018-062	Middle Jomon - Late Jomon	UNRSZ2004	A-072
2010524_edited2	10018-063	Middle Jomon - Late Jomon	UNRSZ2004	A-073
2010524_edited2	10018-064	Kasori EIII	UNRSZ2004	A-074
2010524_edited2	10018-065	Shomyoji 1	UNRSZ2004	A-075
2010524_edited2	10018-066	Horinouchi 1	UNRSZ2004	A-076
2010524_edited2	10018-067	Kasori EIII - Horinouchi 1	UNRSZ2004	A-078a
2010524_edited2	10018-068	Kasori EIII - Horinouchi 1	UNRSZ2004	A-078b
2010524_edited2	10018-069	Kasori EIV	UNRSZ2004	A-079
2010524_edited2	10018-070	Shomyoji 1	UNRSZ2004	A-080a
2010524_edited2	10018-071	Shomyoji 1	UNRSZ2004	A-080b
2010524_edited2	10018-072	Horinouchi 1	UNRSZ2004	A-081a
2010524_edited2	10018-073	Horinouchi 1	UNRSZ2004	A-081b
2010524_edited2	10018-074	Horinouchi 1	UNRSZ2004	A-081c
2010524_edited2	10018-075	Horinouchi 1	UNRSZ2004	A-081d

Continued on next page

Table A.2: Pithouses at Chiba

BUA ID	Pithouse ID	Period	REF	original ID
2010524_edited2	10018-076	Shomyoji 1	UNRSZ2004	A-082
2010524_edited2	10018-077	Kasori EIV	UNRSZ2004	A-083
2010524_edited2	10018-078	Kasori EIV	UNRSZ2004	A-084
2010524_edited2	10018-079	Shomyoji 2	UNRSZ2004	A-085
2010632_edited	10029-001	Shomyoji	TBKTMG2003	A-001
2010632_edited	10029-002	Kasori EIII	TBKTMG2003	A-003
2010632_edited	10029-003	Kasori EIII - EIV	TBKTMG2003	A-004
2010632_edited	10029-004	Kasori B	TBKTMG2003	A-007
2010632_edited	10029-005	Kasori B	TBKTMG2003	A-008
2010632_edited	10029-006	Kasori B	TBKTMG2003	A-009
2010632_edited	10029-007	Kasori EIV	TBKTMG2003	A-010
2010632_edited	10029-008	Soya - Angyo 3a	TBKTMG2003	A-012
2010632_edited	10029-009	Soya - Angyo 1	TBKTMG2003	A-013
2010632_edited	10029-010	Soya - Angyo 1	TBKTMG2003	A-014
2010632_edited	10029-011	Horinouchi 1	TBKTMG2003	A-015
2010632_edited	10029-012	Kasori EIV	TBKTMG2003	A-021
2010633_edited	10030-001	Jomon	CHNEN1998	
2014008_edited	10038-001	Kasori EIII	TBKTMG2003	A-002
2014008_edited	10038-002	Horinouchi 1	TBKTMG2003	A-008
2010239	10086-001	Kasori EIV	HOMESI2003	1
2014013	10116-001	Horinouchi 1	SIM2007	1
2014013	10116-002	Kasori EIV	SIM2007	2
2014013	10116-003	Kasori B1	SIM2007	3
2014013	10116-004	Kasori EIV	SIM2007	4
2014014	10117-001	Kasori EIII	SIM2007	2
2014015_edited	10118-001	Late Jomon	SIM2007	2
2014015_edited	10118-002	Angyo 2	SIM2007	3
2014016	10119-001	Kasori EIV	SIM2007	14
2014017	10120-001	Kasori EIV	SIM2007	1
2014017	10120-003	Kurohama	SIM2007	3
2014017	10120-004	Early Jomon	SIM2007	4
2014017	10120-005	Early Jomon	SIM2007	5
2014017	10120-006	Shomyoji 1	SIM2007	6
2014017	10120-007	Shomyoji 1	SIM2007	7
2014017	10120-008	Shomyoji 1	SIM2007	8
2014017	10120-009	Kasori EII (up to)	SIM2007	9
2014017	10120-010	Shomyoji 1	SIM2007	10
2014017	10120-011	Shomyoji 1	SIM2007	11
2014019	10120-012	Shomyoji 1	SIM2007	12
2014019	10122-001	Kasori B3	SIM2007	1
2014019	10122-002	Kasori B1	SIM2007	2

Continued on next page

Table A.2: Pithouses at Chiba

BUA ID	Pithouse ID	Period	REF	original ID
2014019	10122-003	Kasori B1	SIM2007	3
2014019	10122-004	Kasori B1	SIM2007	4
2014019	10122-005	Kasori B1	SIM2007	5
2014019	10122-006	Kasori B1	SIM2007	6
2014019	10122-007	Kasori EIII	SIM2007	7
2014019	10122-008	Kasori B1	SIM2007	8
2010448_edited	10150-001	Jomon	KWKBMN2002	
2010422_edited	10159-001	Middle Jomon	MAICH1996	
2010422_edited	10159-002	Otamadai	EAUKA1999	1
2010422_edited	10159-003	Otamadai - Kasori E	EAUKA1999	2
2010427	10160-001	Kasori E	CHNEN1998	
2010427	10160-003	Kasori E	CHNEN1999	
2010427	10160-004	Kasori E	CHNEN1999	
2010427	10160-005	Kasori E	CHNEN1999	
2010427	10160-006	Horinouchi	CHNEN1999	
2010427	10160-007	Horinouchi	CHNEN1999	
2010439_edited	10177-002	Kasori EI (up to)	MUKY1987	3
2010439_edited	10177-003	Otamadai	MUKY1987	4
2010439_edited	10177-004	Nakabyo	MUKY1987	5
2010439_edited	10177-005	Kasori EI (up to)	MUKY1987	6
2010439_edited	10177-006	Kasori EII (up to)	MUKY1987	7
2010439_edited	10177-007	Kasori EII (up to)	MUKY1987	8
2010785_edited	10250-001	Horinouchi 1	HAG2007	1a
2010785_edited	10250-002	Horinouchi 1	HAG2007	1b
2010785_edited	10250-003	Horinouchi 1	HAG2007	4
2010785_edited	10250-004	Kasori B	HAG2007	2
2010782_edited	10272-001	Horinouchi 1	KOMGM1984	15
2010782_edited	10272-002	Horinouchi 1	KOMGM1984	23
2010782_edited	10272-003	Horinouchi 1	KOMGM1984	
2010782_edited	10272-004	Horinouchi 1	KOMGM1984	
2010673_n	10273-001	Kasori EII	HAG2007	14
2010673_sw	10273-002	Horinouchi 1	HAG2007	16a
2010673_sw	10273-003	Kasori EII -EIII	HAG2007	16b
2010673_sw	10273-004	Kasori EII -EIII	HAG2007	21
2010673_sw	10273-005	Kasori EII -EIII	HAG2007	22
2010673_sw	10273-006	Kasori EII -EIII	HAG2007	23
2010673_sw	10273-007	Kasori EII -EIII	HAG2007	25
2010673_sw	10273-008	Kasori EII -EIII	HAG2007	26
2010673_sw	10273-009	Kasori EIII	HAG2007	27
2010673_sw	10273-010	Horinouchi 1	HAG2007	28
2010673_n	10273-011	Kasori EIII	HAG2007	39

Continued on next page

Table A.2: Pithouses at Chiba

BUA ID	Pithouse ID	Period	REF	original ID
2010673_sw	10273-012	Kasori EIII	HAG2007	50
2010673_sw	10273-013	Horinouchi 1	HAG2007	57
2010673_sw	10273-014	Jomon	HAG2007	58
2010673_e	10273-015	Kasori EIII	HAG2007	59
2010673_e	10273-016	Kasori EIII	HAG2007	60
2010673_sw	10273-017	Jomon	HAG2007	61
2010673_sw	10273-018	Jomon	HAG2007	62
2010673_sw	10273-019	Jomon	HAG2007	63
2010673_sw	10273-020	Kasori B	HAG2007	79
2010673_c	10273-021	Kasori EII -EIII	HAG2007	85
2010673_c	10273-022	Kasori EII	HAG2007	91
2010673_c	10273-023	Kasori EII -EIII	HAG2007	99
2010673_c	10273-024	Kasori EII -EIII	HAG2007	106
2010673_c	10273-025	Jomon	HAG2007	108
2010673_c	10273-026	Jomon	HAG2007	113
2010673_c	10273-027	Jomon	HAG2007	114
2010673_n	10273-028	Nakabyo	HAG2007	115
2010673_n	10273-029	Kasori EIII	HAG2007	132
2010673_n	10273-030	Kasori EIII	HAG2007	133
2010673_n	10273-031	Kasori EIII	HAG2007	134
2010673_n	10273-032	Kasori EIV	HAG2007	135
2010673_n	10273-033	Kasori EIV	HAG2007	137
2010673_sw	10273-034	Kasori EII	HAG2007	147
2010673_sw	10273-035	Kasori EII	HAG2007	149
2010673_sw	10273-036	Kasori EII	HAG2007	152
2010673_sw	10273-037	Kasori EII	HAG2007	153
2010673_sw	10273-038	Kasori EII	HAG2007	154
2010673_sw	10273-039	Kasori EII	HAG2007	155
2010673_n	10273-040	Kasori E	HAG2007	171
2014021	10308-001	Kasori EIII	CHNEN1998	
2014021	10308-002	Kasori EIII	CHNEN1998	
2014021	10308-003	Kasori EIII	CHNEN1998	
2014021	10308-004	Kasori EIII	CHNEN1998	
2010810	10315-001	Middle Jomon	CHNEN1998	
2010802_edited	10344-001	Kasori EIV	NAKNS1976	1
2010802_edited	10344-002	Kasori EIV	NAKNS1976	2
2010802_edited	10344-003	Kasori EIV	NAKNS1976	3
2010802_edited	10344-004	Kasori EIV	NAKNS1976	4
2010802_edited	10344-005	Kasori EIV	NAKNS1976	5
2010802_edited	10344-006	Kasori EIV	NAKNS1976	6
2010802_edited	10344-007	Horinouchi	NAKNS1976	7

Continued on next page

Table A.2: Pithouses at Chiba

BUA ID	Pithouse ID	Period	REF	original ID
2010802_edited	10344-008	Kasori EIV	NAKNS1976	8
2010802_edited	10344-009	Kasori EIV	NAKNS1976	9
2010802_edited	10344-010	Kasori EIV	NAKNS1976	10
2010802_edited	10344-011	Kasori EIV - Shomyoji	NAKNS1976	11
2010802_edited	10344-012	Kasori EIV	NAKNS1976	12
2010475_edited	10395-001	Horinouchi 1	YHG1981	11
2010475_edited	10395-002	Horinouchi 1	YHG1981	12
2010475_edited	10395-003	Horinouchi 2	YHG1981	13
2010475_edited	10395-004	Jomon	YHG1981	14
2010475_edited	10395-005	Horinouchi 1	YHG1981	15
2010475_edited	10395-006	Horinouchi 1	YHG1981	16
2010610_edited	10435-002	Kurohama	YMNKM1989	59
2010596_edited	10460-001	Middle Jomon	HTND1990	1
2010596_edited	10460-002	Kasori E	HTND1990	2
2010596_edited	10460-003	Middle Jomon	MAICHI1991	
2010597_edited	10461-001	Kasori EII (up to)	CHIBAKEN, NIHON4	1
2010597_edited	10461-002	Kasori EII (up to)	CHIBAKEN, NIHON4	2
2010597_edited	10461-003	Kasori EII (up to)	CHIBAKEN, NIHON4	3
2010597_edited	10461-004	Kasori EII (up to)	CHIBAKEN, NIHON4	4
2010831_known	10488-001	Jomon	OOMC1981	1
2010861	10519-001	Kasori EII (Early)	CHBNEWT17	141
2010861	10519-002	Kasori EII (Early)	CHBNEWT17	294
2010857	10520-001	Horinouchi 1	CHBNEWT31	W001
2010857	10520-002	Horinouchi 1	CHBNEWT31	W002
2010857	10520-003	Horinouchi 1	CHBNEWT31	E101
2010867_edited	10523-001	Kasori EI (Early)	CHBNEWT22	12
2010867_edited	10523-002	Kasori EI (Early)	CHBNEWT22	13
2010867_edited	10523-003	Kasori EI (Early)	CHBNEWT22	16
2010867_edited	10523-004	Kasori EI (up to)	CHBNEWT22	17
2010867_edited	10523-005	Nakabyo - Kasori EI	CHBNEWT22	23
2010867_edited	10523-006	Transition between Kasori EI and Kasori EII	CHBNEWT22	24
2010867_edited	10523-007	Nakabyo - Kasori EI	CHBNEWT22	25
2010867_edited	10523-008	Kasori EII (up to)	CHBNEWT22	31
2010867_edited	10523-009	Kasori EII (up to)	CHBNEWT22	33
2010867_edited	10523-010	Kasori EI (Late) - EII (Early)	CHBNEWT22	35
2010867_edited	10523-011	Kasori EI (up to)	CHBNEWT22	36
2010867_edited	10523-012	Kasori EI (up to)	CHBNEWT22	37
2010867_edited	10523-013	Kasori EI (up to)	CHBNEWT22	51
2010867_edited	10523-014	Nakabyo	CHBNEWT22	52
2010867_edited	10523-015	Jomon	CHBNEWT22	41
2010867_edited	10523-016	Nakabyo	CHBNEWT22	60

Continued on next page

Table A.2: Pithouses at Chiba

BUA ID	Pithouse ID	Period	REF	original ID
2010867_edited	10523-017	Nakabyo - Kasori E1	KMTRB2007	10
2010867_edited	10523-018	Kasori EI	KMTRB2007	11
2010867_edited	10523-019	Kasori EII	KMTRB2007	12
2011222_edited	10526-001	Kasori EII (Early)	CHBNEWT18	2
2011222_edited	10526-002	Kasori EIII (old)	CHBNEWT18	4
2011222_edited	10526-003	Kasori EIII (old)	CHBNEWT18	5
2011222_edited	10526-004	Kasori EIII (old)	CHBNEWT18	6
2011222_edited	10526-005	Kasori EIII (old)	CHBNEWT18	7
2011222_edited	10526-006	Kasori EII (Early)	CHBNEWT18	9
2011222_edited	10526-007	Kasori EII (Early)	CHBNEWT18	013A
2011222_edited	10526-008	Kasori EIII (old)	CHBNEWT18	40
2011222_edited	10526-009	Kasori EIII (old)	CHBNEWT18	42
2011222_edited	10526-010	Kasori E	CHBNEWT18	12
2011222_edited	10526-011	Jomon	CHBNEWT18	13B
2011222_edited	10526-012	Kasori E (Late)	CHBNEWT18	8
2010874_edited	10528-001	Kasori EII (up to)	CHBNEWT12	11
2010874_edited	10528-002	Kasori EII (Middle)	CHBNEWT12	13
2010874_edited	10528-003	Kasori EII (up to)	CHBNEWT12	18
2010874_edited	10528-004	Otamadai III	CHBNEWT12	47
2010874_edited	10528-005	Kasori EI - EII	CHBNEWT12	70
2010874_edited	10528-006	Kasori EI - EII	CHBNEWT12	87
2010874_edited	10528-007	Kasori EII (up to)	CHBNEWT12	88
2010874_edited	10528-008	Kurohama (Early)	CHBNEWT12	48
2010865_edited	10529-001	Kasori E (Late)	Nishino Pers.	8
2010865_edited	10529-002	Kasori E	Nishino Pers.	12
2010865_edited	10529-003	Middle Jomon	Nishino Pers.	41
2010865_edited	10529-004	Kasori EI (up to)	CHBNEWT19	SB001
2010865_edited	10529-005	Otamadai III	CHBNEWT19	SB004
2010865_edited	10529-006	Kasori EI - EII	CHBNEWT19	SB009
2010865_edited	10529-007	Kasori EI - EII	CHBNEWT19	SB010
2010865_edited	10529-008	Kasori EII (up to)	CHBNEWT19	SB011
2010865_edited	10529-009	Kasori EII (up to)	CHBNEWT19	SB012
2010865_edited	10529-010	Kasori EII (up to)	CHBNEWT19	SB013A
2010865_edited	10529-011	Kasori EII (up to)	CHBNEWT19	SB013B
2010865_edited	10529-012	Kasori EII (up to)	CHBNEWT19	SB017
2010865_edited	10529-013	Otamadai II - Kasori EII	CHBNEWT19	SB018A
2010865_edited	10529-014	Otamadai II - Kasori EII	CHBNEWT19	SB018B
2010865_edited	10529-015	Kasori EII (up to)	CHBNEWT19	SB019
2010865_edited	10529-016	Nakabyo	CHBNEWT19	SB021A
2010865_edited	10529-017	Kasori EII (up to)	CHBNEWT19	SB047A
2010865_edited	10529-018	Kasori EII (up to)	CHBNEWT19	SB047B

Continued on next page

Table A.2: Pithouses at Chiba

BUA ID	Pithouse ID	Period	REF	original ID
2010865_edited	10529-019	Kasori EII (up to)	CHBNEWT19	SB048A
2010865_edited	10529-020	Kasori EII (up to)	CHBNEWT19	SB048B
2010865_edited	10529-021	Kasori EII	CHBNEWT19	SB048C
2010865_edited	10529-022	Kasori EII	CHBNEWT19	SB048D
2010865_edited	10529-023	Kasori EII	CHBNEWT19	SB048E
2010865_edited	10529-024	Kasori EII (up to)	CHBNEWT19	SB049A
2010865_edited	10529-025	Kasori EII (up to)	CHBNEWT19	SB049B
2010865_edited	10529-026	Kasori EII (up to)	CHBNEWT19	SB051A
2010865_edited	10529-027	Kasori EII (up to)	CHBNEWT19	SB051B
2010865_edited	10529-028	Kasori EII (up to)	CHBNEWT19	SB052A
2010865_edited	10529-029	Kasori EII (up to)	CHBNEWT19	SB052B
2010865_edited	10529-030	Kasori EII (up to)	CHBNEWT19	SB053
2010865_edited	10529-031	Kasori EI (up to)	CHBNEWT19	SB054
2010865_edited	10529-032	Kasori EII (up to)	CHBNEWT19	SB056
2010865_edited	10529-033	Kasori EII (up to)	CHBNEWT19	SB057
2010865_edited	10529-034	Nakabyo - Kasori EI	CHBNEWT19	SB058A
2010865_edited	10529-035	Kasori EI (up to)	CHBNEWT19	SB058B
2010865_edited	10529-036	Kasori EII (up to)	CHBNEWT19	SB059
2010865_edited	10529-037	Kasori EII (up to)	CHBNEWT19	SB060
2010865_edited	10529-038	Jomon	CHBNEWT19	SB061
2010865_edited	10529-039	Kasori EII (up to)	CHBNEWT19	SB062
2010865_edited	10529-040	Kasori EII (up to)	CHBNEWT19	SB063
2010865_edited	10529-041	Otamadai III - Nakabyo	CHBNEWT19	SB064A
2010865_edited	10529-042	Otamadai III - Nakabyo	CHBNEWT19	SB064B
2010865_edited	10529-043	Kasori EII (up to)	CHBNEWT19	SB065
2010865_edited	10529-044	Nakabyo - Kasori EI	CHBNEWT19	SB068
2010865_edited	10529-045	Nakabyo - Kasori EI	CHBNEWT19	SB070
2010865_edited	10529-046	Otamadai IV - Nakabyo	CHBNEWT19	SB071
2010865_edited	10529-047	Kasori EII (up to)	CHBNEWT19	SB073
2010865_edited	10529-048	Nakabyo - Kasori EI	CHBNEWT19	SB074A
2010865_edited	10529-049	Nakabyo - Kasori EI	CHBNEWT19	SB074B
2010865_edited	10529-050	Nakabyo - Kasori EI	CHBNEWT19	SB074C
2010865_edited	10529-051	Kasori EII (up to)	CHBNEWT19	SB077
2010865_edited	10529-052	Nakabyo - Kasori EI	CHBNEWT19	SB079
2010865_edited	10529-053	Kasori EII (up to)	CHBNEWT19	SB081A
2010865_edited	10529-054	Kasori EII (up to)	CHBNEWT19	SB081B
2010865_edited	10529-055	Kasori EII (up to)	CHBNEWT19	SB082
2010865_edited	10529-056	Kasori EI (up to)	CHBNEWT19	SB084A
2010865_edited	10529-057	Kasori EI (up to)	CHBNEWT19	SB084B
2010865_edited	10529-058	Kasori EI (up to)	CHBNEWT19	SB084C
2010865_edited	10529-059	Kasori EI (up to)	CHBNEWT19	SB085A

Continued on next page

Table A.2: Pithouses at Chiba

BUA ID	Pithouse ID	Period	REF	original ID
2010865_edited	10529-060	Kasori EI (up to)	CHBNEWT19	SB085B
2010865_edited	10529-061	Nakabyo - Kasori EI	CHBNEWT19	SB086A
2010865_edited	10529-062	Nakabyo - Kasori EI	CHBNEWT19	SB086B
2010865_edited	10529-063	Kasori EII (up to)	CHBNEWT19	SB086C
2010865_edited	10529-064	Nakabyo	CHBNEWT19	SB087
2010865_edited	10529-065	Kasori EI (up to)	CHBNEWT19	SB088
2010865_edited	10529-066	Kasori EI (up to)	CHBNEWT19	SB089A
2010865_edited	10529-067	Otamadai III - Nakabyo	CHBNEWT19	SB089B
2010865_edited	10529-068	Kasori EI	CHBNEWT19	SB090
2010865_edited	10529-069	Nakabyo - Kasori EI	CHBNEWT19	SB091
2010865_edited	10529-070	Nakabyo - Kasori EI	CHBNEWT19	SB093A
2010865_edited	10529-071	Nakabyo - Kasori EI	CHBNEWT19	SB093B
2010865_edited	10529-072	Kasori EI (up to)	CHBNEWT19	SB094
2010865_edited	10529-073	Otamadai IV - Nakabyo	CHBNEWT19	SB095
2010865_edited	10529-074	Nakabyo	CHBNEWT19	SB096A
2010865_edited	10529-075	Nakabyo	CHBNEWT19	SB096B
2010865_edited	10529-076	Nakabyo - Kasori EI	CHBNEWT19	SB096C
2010865_edited	10529-077	Kasori EII (up to)	CHBNEWT19	SB097
2010865_edited	10529-078	Kasori EII (up to)	CHBNEWT19	SB098A
2010865_edited	10529-079	Kasori EII (up to)	CHBNEWT19	SB098B
2010865_edited	10529-080	Kasori EII (up to)	CHBNEWT19	SB098C
2010865_edited	10529-081	Kasori EII (up to)	CHBNEWT19	SB099
2010865_edited	10529-082	Nakabyo - Kasori EI	CHBNEWT19	SB100
2010865_edited	10529-083	Kasori EII (up to)	CHBNEWT19	SB107
2010865_edited	10529-084	Jomon	CHBNEWT19	SB109
2010865_edited	10529-085	Kasori EI (up to)	CHBNEWT19	SB114
2010865_edited	10529-086	Jomon	CHBNEWT19	SB115
2010865_edited	10529-087	Nakabyo	CHBNEWT19	SB116
2010865_edited	10529-088	Kasori EII (up to)	CHBNEWT19	SB117
2010865_edited	10529-089	Jomon	CHBNEWT19	SB119
2010865_edited	10529-090	Nakabyo	CHBNEWT19	SB120
2010865_edited	10529-091	Kasori EII (up to)	CHBNEWT19	SB121A
2010865_edited	10529-092	Kasori EII (up to)	CHBNEWT19	SB121B
2010865_edited	10529-093	Kasori EII (up to)	CHBNEWT19	SB122
2010865_edited	10529-094	Kasori EII	CHBNEWT19	SB124
2010865_edited	10529-095	Kasori EII (up to)	CHBNEWT19	SB125
2010865_edited	10529-096	Jomon	CHBNEWT19	SB126
2010865_edited	10529-097	Kasori EI (up to)	CHBNEWT19	SB127
2010865_edited	10529-098	Kasori EII (up to)	CHBNEWT19	SB128
2010865_edited	10529-099	Kasori EI (up to)	CHBNEWT19	SB130
2010865_edited	10529-100	Jomon	CHBNEWT19	SB131

Continued on next page

Table A.2: Pithouses at Chiba

BUA ID	Pithouse ID	Period	REF	original ID
2010865_edited	10529-101	Kasori EI - EII	CHBNEWT19	SB132
2010865_edited	10529-102	Jomon	CHBNEWT19	SB133
2010865_edited	10529-103	Jomon	CHBNEWT19	SB135
2010865_edited	10529-104	Kasori EII (up to)	CHBNEWT19	SB136
2010865_edited	10529-105	Kasori EII (up to)	CHBNEWT19	SB137
2010865_edited	10529-106	Otamadai II - IV	CHBNEWT19	SB139
2010865_edited	10529-107	Nakabyo	CHBNEWT19	SB142A
2010865_edited	10529-108	Nakabyo - Kasori EI	CHBNEWT19	SB142B
2010865_edited	10529-109	Nakabyo	CHBNEWT19	SB167
2010865_edited	10529-110	Kasori EI (up to)	CHBNEWT19	SB172A
2010865_edited	10529-111	Kasori EI (up to)	CHBNEWT19	SB172B
2010865_edited	10529-112	Nakabyo	CHBNEWT19	SB173
2010865_edited	10529-113	Otamadai I - II	CHBNEWT19	SB174
2010865_edited	10529-114	Kasori EII (up to)	CHBNEWT19	SB175A
2010865_edited	10529-115	Kasori EII (up to)	CHBNEWT19	SB175B
2010865_edited	10529-116	Kasori EII (up to)	CHBNEWT19	SB176
2010865_edited	10529-117	Kasori EI - EII	CHBNEWT19	SB177A
2010865_edited	10529-118	Kasori EI - EII	CHBNEWT19	SB177B
2010865_edited	10529-119	Kasori EI (up to)	CHBNEWT19	SB178
2010865_edited	10529-120	Kasori EI - EII	CHBNEWT19	SB180A
2010865_edited	10529-121	Kasori EI - EII	CHBNEWT19	SB180B
2010865_edited	10529-122	Kasori EI (up to)	CHBNEWT19	SB182
2010865_edited	10529-123	Kasori EII (up to)	CHBNEWT19	SB184
2010865_edited	10529-124	Kasori EI (up to)	CHBNEWT19	SB185A
2010865_edited	10529-125	Kasori EI (up to)	CHBNEWT19	SB185B
2010865_edited	10529-126	Kasori EI (up to)	CHBNEWT19	SB186A
2010865_edited	10529-127	Kasori EI (up to)	CHBNEWT19	SB186B
2010865_edited	10529-128	Kasori EI (up to)	CHBNEWT19	SB186C
2010865_edited	10529-129	Kasori EI (up to)	CHBNEWT19	SB186D
2010865_edited	10529-130	Kasori EII (up to)	CHBNEWT19	SB187
2010865_edited	10529-131	Kasori EI (up to)	CHBNEWT19	SB190
2010865_edited	10529-132	Kasori EI?	CHBNEWT19	SB191A
2010865_edited	10529-133	Kasori EI (up to)	CHBNEWT19	SB191B
2010865_edited	10529-134	Nakabyo - Kasori EI	CHBNEWT19	SB192
2010865_edited	10529-135	Kasori EI - EII	CHBNEWT19	SB193
2010865_edited	10529-136	Kasori EI - EII	CHBNEWT19	SB194A
2010865_edited	10529-137	Kasori EII (up to)	CHBNEWT19	SB194B
2010865_edited	10529-138	Kasori EI (up to)	CHBNEWT19	SB195A
2010865_edited	10529-139	Kasori EI (up to)	CHBNEWT19	SB195B
2010865_edited	10529-140	Kasori EI (up to)	CHBNEWT19	SB195C
2010865_edited	10529-141	Jomon	CHBNEWT19	SB196

Continued on next page

Table A.2: Pithouses at Chiba

BUA ID	Pithouse ID	Period	REF	original ID
2010865_edited	10529-142	Kasori EI (up to)	CHBNEWT19	SB197
2010865_edited	10529-143	Kasori EI (up to)	CHBNEWT19	SB199
2010865_edited	10529-144	Kasori EI (up to)	CHBNEWT19	SB200
2010865_edited	10529-145	Kasori EI	CHBNEWT19	SB203
2010865_edited	10529-146	Jomon	CHBNEWT19	SB204A
2010865_edited	10529-147	Kasori EI (up to)	CHBNEWT19	SB204B
2010865_edited	10529-148	Jomon	CHBNEWT19	SB205
2010865_edited	10529-149	Kasori EI - EII	CHBNEWT19	SB207
2010865_edited	10529-150	Otamadai III-Nakabyo	CHBNEWT19	SB208
2010865_edited	10529-151	Jomon	CHBNEWT19	SB209
2010865_edited	10529-152	Jomon	CHBNEWT19	SB210
2010865_edited	10529-153	Kasori EI (up to)	CHBNEWT19	SB211
2010865_edited	10529-154	Nakabyo	CHBNEWT19	SB213
2010865_edited	10529-155	Jomon	CHBNEWT19	SB216
2010865_edited	10529-156	Kasori EIII - EIV	CHBNEWT19	SB225
2010865_edited	10529-157	Kasori EIII - EIV	CHBNEWT19	SB226
2010865_edited	10529-158	Kasori EI (up to)	CHBNEWT19	SB231
2010865_edited	10529-159	Kasori EIII - EIV	CHBNEWT19	SB236
2010865_edited	10529-160	Kasori EII (up to)	CHBNEWT19	SB238
2010865_edited	10529-161	Kasori EI (up to)	CHBNEWT19	SB239
2010865_edited	10529-162	Kasori EI - EII	CHBNEWT19	SB241
2010865_edited	10529-163	Kasori EI (up to)	CHBNEWT19	SB243A
2010865_edited	10529-164	Kasori EII (up to)	CHBNEWT19	SB243B
2010865_edited	10529-165	Otamadai (Late)	CHBNEWT19	SB244
2010865_edited	10529-166	Kasori EI (up to)	CHBNEWT19	SB245
2010865_edited	10529-167	Kasori EII (up to)	CHBNEWT19	SB246
2010865_edited	10529-168	Jomon	CHBNEWT19	SB247
2010865_edited	10529-169	Kasori EII (up to)	CHBNEWT19	SB248
2010865_edited	10529-170	Kasori EIII	CHBNEWT19	SB249A
2010865_edited	10529-171	Kasori EII (after)	CHBNEWT19	SB249B
2010865_edited	10529-172	Horinouchi 1	CHBNEWT19	SB113
2010871	10531-001	Kasori EII (Late)	CHBNEWT40	26
2010871	10531-002	Kasori EII (Late)	CHBNEWT40	28
2010871	10531-003	Kasori E	CHBNEWT40	33
2010871	10531-004	Kasori EIII	CHBNEWT40	40
2010871	10531-005	Kasori EII (Late)	CHBNEWT40	41
2010871	10531-006	Kasori EII (Late) - EIII	CHBNEWT40	44
2010871	10531-007	Kasori EII (Late)	CHBNEWT40	51
2010871	10531-008	Kasori EII - EIII	CHBNEWT40	52
2010871	10531-009	Kasori EII (Early)	CHBNEWT40	53
2010871	10531-010	Kasori EII (Late) - EIII	CHBNEWT40	77

Continued on next page

Table A.2: Pithouses at Chiba

BUA ID	Pithouse ID	Period	REF	original ID
2010871	10531-011	Kasori EII (Early)	CHBNEWT40	78
2010871	10531-012	Kasori EII (up to)	CHBNEWT40	79
2010871	10531-013	Kasori EIII	CHBNEWT40	80
2010871	10531-014	Kasori EII (Late)	CHBNEWT40	81
2010871	10531-015	Kasori E	CHBNEWT40	82
2010871	10531-016	Kasori EI (up to)	CHBNEWT40	83
2010871	10531-017	Kasori EIII	CHBNEWT40	108
2010871	10531-018	Kasori EIII	CHBNEWT40	110
2010871	10531-019	Kasori EII (Late)	CHBNEWT40	113
2010871	10531-020	Kasori EII (Late) - EIII	CHBNEWT40	116
2010871	10531-021	Kasori EII (Middle-Late)	CHBNEWT40	123
2010871	10531-022	Kasori E	CHBNEWT40	125
2010871	10531-023	Kasori EII (Middle-Late)	CHBNEWT40	126
2010871	10531-024	Kasori EII (Early)	CHBNEWT40	130
2010871	10531-025	Kasori EII (up to)	CHBNEWT40	131
2010871	10531-026	Kasori EII (Middle)	CHBNEWT40	133
2010871	10531-027	Kasori E	CHBNEWT40	136
2010871	10531-028	Kasori EI - EII (Early)	CHBNEWT40	143
2010871	10531-029	Kasori EII (Late)	CHBNEWT40	169
2010871	10531-030	Kasori EII (Middle-Late)	CHBNEWT40	206
2010871	10531-031	Kasori E	CHBNEWT40	208
2010871	10531-032	Kasori EIII	CHBNEWT40	234
2010871	10531-033	Kasori EII (Late) - EIII	CHBNEWT40	235
2010871	10531-034	Kasori EIII	CHBNEWT40	247
2010871	10531-035	Kasori E	CHBNEWT40	269
2010871	10531-036	Kasori E	CHBNEWT40	274
2010871	10531-037	Kasori EII (up to)	CHBNEWT40	275
2010871	10531-038	Kasori EII (up to)	CHBNEWT40	300
2010871	10531-039	Middle Jomon	CHBNEWT40	301
2010871	10531-040	Kasori EII (Early)	CHBNEWT40	302
2010871	10531-041	Kasori EII (Middle)	CHBNEWT40	305
2010871	10531-042	Middle Jomon	CHBNEWT40	318
2010871	10531-043	Kasori EI (up to)	CHBNEWT40	352
2010871	10531-044	Kasori EI (up to)	CHBNEWT40	354
2010871	10531-045	Kasori EI (up to)	CHBNEWT40	372
2010871	10531-046	Kasori EII (Middle)	CHBNEWT40	373
2010871	10531-047	Kasori EII (Late)	CHBNEWT40	375
2010871	10531-048	Kasori EI - EII (Early)	CHBNEWT40	378
2010871	10531-049	Kasori E	CHBNEWT40	402
2010871	10531-050	Kasori EII (Middle)	CHBNEWT40	407
2010871	10531-051	Kasori EII (Middle-Late)	CHBNEWT40	500

Continued on next page

Table A.2: Pithouses at Chiba

BUA ID	Pithouse ID	Period	REF	original ID
2010871	10531-052	Kasori EI (up to)	CHBNEWT40	518
2010871	10531-053	Kasori EII (Late) - EIII	CHBNEWT40	523
2010871	10531-054	Kasori EII (Late) - EIII	CHBNEWT40	525
2010871	10531-055	Middle Jomon	CHBNEWT40	578
2010871	10531-056	Middle Jomon	CHBNEWT40	580
2010871	10531-057	Middle Jomon	CHBNEWT40	581
2010871	10531-058	Middle Jomon	CHBNEWT40	583
2010871	10531-059	Kasori EII (Late) - EIII	CHBNEWT40	507B
2010875_edited	10534-001	Kasori EII (up to)	CHBNEWT25	SI-11
2010875_edited	10534-002	Lower Hanazumi	CHBNEWT25	SI-41
2010875_edited	10534-003	Kasori EIV	CHBNEWT25	SI-42
2010985	10535-001	Moroiso b / Ukishima I	CHBNEWT30	SB-049
2010995	10537-001	Horinouchi	CHBNEWT7	27(011A)
2010995	10537-002	Horinouchi	CHBNEWT7	28(042A)
2010995	10537-003	Horinouchi	CHBNEWT7	29(042B)
2010995	10537-004	Horinouchi 1	CHBNEWT7	30(042C)
2010995	10537-005	Horinouchi	CHBNEWT7	31(042E)
2010995	10537-006	Horinouchi	CHBNEWT7	32(046)
2010995	10537-007	Horinouchi 1	CHBNEWT7	33(047)
2010995	10537-008	Horinouchi 1	CHBNEWT7	34(048)
2010995	10537-009	Horinouchi 1	CHBNEWT7	35(049)
2010995	10537-010	Horinouchi	CHBNEWT7	36(050)
2010998	10539-001	Kasori B	CHBNEWT9	1(DW03)
2010998	10539-002	Kasori B	CHBNEWT9	2(DW04)
2011008_east	10544-001	Kasori EII (up to)	CHBNEWT35	23
2011011	10553-001	Kasori EIV	CHBNEWT10	1(136)
2011011	10553-002	Kasori EIV	CHBNEWT10	2(141)
2011011	10553-003	Horinouchi 1	CHBNEWT10	3(120)
2011011	10553-004	Horinouchi 1	CHBNEWT10	4(122)
2011011	10553-005	Horinouchi 1	CHBNEWT10	5(123)
2011011	10553-006	Horinouchi 1	CHBNEWT10	6(131)
2011011	10553-007	Horinouchi 1	CHBNEWT10	7(134)
2011011	10553-008	Horinouchi 1	CHBNEWT10	8(135)
2011011	10553-009	Horinouchi 1	CHBNEWT10	9(140)
2011011	10553-010	Horinouchi 1	CHBNEWT10	10(142)
2011011	10553-011	Horinouchi 1	CHBNEWT10	11(143)
2011011	10553-012	Horinouchi 1	CHBNEWT10	12(145)
2011011	10553-013	Horinouchi 1	CHBNEWT10	13(146)
2011011	10553-014	Horinouchi 1	CHBNEWT10	14(148)
2011011	10553-015	Horinouchi 1	CHBNEWT10	15(149)
2011011	10553-016	Horinouchi 1	CHBNEWT10	16(154)

Continued on next page

Table A.2: Pithouses at Chiba

BUA ID	Pithouse ID	Period	REF	original ID
2011011	10553-017	Horinouchi 1	CHBNEWT10	17(150)
2011011	10553-018	Horinouchi 1	CHBNEWT10	18(151)
2011011	10553-019	Horinouchi 1	CHBNEWT10	19(152)
2010992	10554-001	Shomyoji (Early)	CHBNEWT37	SI001
2010992	10554-002	Kasori EIV - Shomyoji (Early)	CHBNEWT37	SI002
2010992	10554-003	Middle Jomon - Late Jomon	CHBNEWT37	SI003
2010992	10554-004	Jomon	CHBNEWT37	SI004
2010992	10554-005	Shomyoji (Early)	CHBNEWT37	SI005
2010992	10554-006	Shomyoji (Early)	CHBNEWT37	SI006
2010992	10554-007	Shomyoji (Early)	CHBNEWT37	SI007
2010992	10554-008	Kasori EIII	CHBNEWT37	SI008
2010992	10554-014	Shomyoji (Early)	CHBNEWT37	SI015
2010992	10554-016	Angyo 1 - 3b	CHBNEWT37	SI017
2010992	10554-017	Angyo 1	CHBNEWT37	SI019
2010992	10554-018	Angyo 1	CHBNEWT37	SI020
2010992	10554-020	Soya	CHBNEWT37	SI023
2010992	10554-021	Jomon	CHBNEWT37	SI024
2010992	10554-022	Late Jomon - Final Jomon	CHBNEWT37	SI025
2010992	10554-023	Jomon	CHBNEWT37	SI026
2010992	10554-024	Jomon	CHBNEWT37	SI027
2010992	10554-027	Jomon	CHBNEWT37	SI030
2010992	10554-028	Late Jomon / Angyo	CHBNEWT37	SI032
2010992	10554-029	Jomon	CHBNEWT37	SI034
2010992	10554-030	Jomon	CHBNEWT37	SI038
2010992	10554-031	Jomon	CHBNEWT37	SI039
2010992	10554-032	Jomon	CHBNEWT37	SI040
2010992	10554-033	Jomon	CHBNEWT37	SI041
2010992	10554-034	Jomon	CHBNEWT37	SI043
2010992	10554-036	Middle Jomon - Late Jomon	CHBNEWT37	SI045
2010992	10554-037	Middle Jomon - Late Jomon	CHBNEWT37	SI046
2010992	10554-038	Jomon	CHBNEWT37	SI047
2010992	10554-039	Jomon	CHBNEWT37	SI048
2010992	10554-040	Jomon	CHBNEWT37	SI054
2010735_edited	10590-001	Kasori EI (up to)	HSNA1969	1
2010735_edited	10590-002	Kasori EI (up to)	HSNA1969	2
2010735_edited	10590-003	Kasori EI (up to)	HSNA1969	3
2010735_edited	10590-004	Kasori EI (up to)	HSNA1969	4
2010735_edited	10590-005	Kasori EI (up to)	HSNA1969	5
2010735_edited	10590-006	Otamadai - Kasori EII	HSNA1969	6
2010735_edited	10590-007	Otamadai - Kasori EII	HSNA1969	7
2010740_edited	10594-001	Jomon	HRKT2004	1

Continued on next page

Table A.2: Pithouses at Chiba

BUA ID	Pithouse ID	Period	REF	original ID
2010740_edited	10594-001	Jomon	HRKT2004	1
2010740_edited	10594-002	Otamadai	HRKT2004	1(33)
2010756_edited	10601-001	Kasori EIII - EIV	TKJHRK1978	1
2010756_edited	10601-002	Kasori E	TKJHRK1978	2
2010756_edited	10601-004	Angyo 2 - 3a	TSKJD2000	1a
2010756_edited	10601-005	Angyo 2 - 3a	TSKJD2000	1b
2010756_edited	10601-006	Angyo 2 - 3a	TSKJD2000	1c
2010756_edited	10601-007	Angyo 2 - 3a	TSKJD2000	2a
2010756_edited	10601-008	Angyo 2 - 3a	TSKJD2000	2b
2010756_edited	10601-009	Angyo 2 - 3a	TSKJD2000	3
2010756_edited	10601-010	Angyo 2 - 3a	TSKJD2000	4
2010756_edited	10601-011	Angyo 2 - 3a	TSKJD2000	5
2010756_edited	10601-012	Late Jomon - Final Jomon	TSKJD2000	6
2010756_edited	10601-013	Late Jomon - Final Jomon	TSKJD2000	7
2010756_edited	10601-014	Late Jomon - Final Jomon	TSKJD2000	8
2010756_edited	10601-015	Angyo 1 - 3a	TSKJD2000	9
2010756_edited	10601-016	Kasori B3	TSKJD2000	10
2010756_edited	10601-017	Angyo 2	TSKJD2000	11
2010756_edited	10601-018	Kasori B	TSKJD2000	12
2010756_edited	10601-019	Jomon	TSKJD2000	13
2011246_edited	10621-001	Kasori EI (up to)	HTSY1986	001(021)
2011246_edited	10621-002	Kasori EI (up to)	HTSY1986	002(032)
2011246_edited	10621-003	Kasori EI (up to)	HTSY1986	003(28)
2011246_edited	10621-004	Jomon	HTSY1986	004(029)
2010882	10682-001	Kasori EII	KMFKZW1993	3
2120385a	3931-001	Otamadai 3 - Kasori E3	GDBS1996	2
2120385a	3931-002	Kasori EII -EIII	GDBS1996	5
2120385a	3931-003	Jomon	GDBS1996	6
2120385a	3931-004	Kasori E	GDBS1996	7
2120385a	3931-005	Jomon	GDBS1996	8
2120385b	3931-006	Otamadai Ib	GDBS1996	1
2120469	4015-001	Otamadai	SKT1999	1
2120469	4015-002	Kasori E1 (Late)	SKT1999	2
2120469	4015-003	Kasori EI	SKT1999	3
2120469	4015-004	Kasori EI	SKT1999	4
2120469	4015-005	Kasori E1 (Late)	SKT1999	5
2120469	4015-006	Jomon	SKT1999	setwd
2120469	4015-007	Kasori EI - EII	SKT1999	7
2120469	4015-008	Kasori EI - EII	SKT1999	8
2120469	4015-009	Kasori EI - EII	SKT1999	9
2120531_i	4076-001	Kasori EIII	MIYU1998	I-1

Continued on next page

Table A.2: Pithouses at Chiba

BUA ID	Pithouse ID	Period	REF	original ID
2120531_rest	4076-002	Horinouchi 1	MIYU2009	II-2
2120531_rest	4076-003	Horinouchi 1	MIYU2009	II-3
2120531_rest	4076-004	Horinouchi	MIYU2009	II-4
2120531_rest	4076-005	Horinouchi	MIYU2009	II-6
2120531_rest	4076-006	Horinouchi 1	MIYU2009	II-8
2120531_rest	4076-007	Horinouchi 1	MIYU2009	II-9
2120531_rest	4076-008	Horinouchi 1	MIYU2009	II-10
2120531_rest	4076-009	Horinouchi 1	MIYU2009	II-11
2120531_rest	4076-010	Horinouchi 1	MIYU2009	II-12
2120531_rest	4076-011	Jomon	MIYU2009	II-14
2120531_rest	4076-012	Horinouchi 1	MIYU2009	II-15
2120531_rest	4076-013	Horinouchi 1	MIYU2009	II-16A
2120531_rest	4076-014	Horinouchi 1	MIYU2009	II-16B
2120531_rest	4076-015	Horinouchi 1	MIYU2009	II-17
2120531_rest	4076-016	Horinouchi 1	MIYU2009	II-19
2120531_rest	4076-017	Horinouchi 1	MIYU2009	II-20
2120531_rest	4076-018	Horinouchi 1	MIYU2009	II-21
2120531_rest	4076-019	Horinouchi 1	MIYU2009	II-22
2120531_rest	4076-020	Horinouchi 1	MIYU2009	II-23
2120531_rest	4076-021	Horinouchi 1	MIYU2009	II-24
2120531_rest	4076-022	Horinouchi 1	MIYU2009	II-25
2120531_rest	4076-023	Horinouchi 1	MIYU2009	II-26
2120531_rest	4076-024	Horinouchi 1	MIYU2009	II-27
2120531_rest	4076-025	Horinouchi 1	MIYU2009	II-28
2120531_rest	4076-026	Jomon	MIYU2009	II-29
2120531_rest	4076-027	Horinouchi 1	MIYU2009	II-31
2120531_rest	4076-028	Horinouchi 1	MIYU2009	II-32
2120531_rest	4076-029	Horinouchi 1	MIYU2009	II-33
2120531_rest	4076-030	Horinouchi 1	MIYU2009	II-34
2120531_rest	4076-031	Horinouchi 1	MIYU2009	II-35
2120531_rest	4076-032	Horinouchi 1	MIYU2009	II-36
2120531_rest	4076-033	Kasori B3	MIYU2009	II-37
2120531_rest	4076-034	Horinouchi 1	MIYU2009	II-38
2120531_rest	4076-035	Horinouchi 1	MIYU2009	II-39
2120531_rest	4076-036	Horinouchi 1	MIYU2009	II-40
2120531_rest	4076-037	Horinouchi - Kasori B	MIYU2009	II-45
2120531_rest	4076-038	Kasori EIV	MIYU2009	II-46
2120531_rest	4076-039	Horinouchi 1	MIYU2009	II-48
2120531_rest	4076-040	Horinouchi 1	MIYU2009	II-49
2120531_rest	4076-041	Horinouchi 1	MIYU2009	II-53
2120531_rest	4076-042	Shomyoji	MIYU2009	II-57

Continued on next page

Table A.2: Pithouses at Chiba

BUA ID	Pithouse ID	Period	REF	original ID
2120531_rest	4076-044	Kasori B	MIYU2009	II-59
2120531_rest	4076-045	Kasori EIV	MIYU2009	II-61
2120531_rest	4076-048	Jomon	MIYU2009	II-63B
2120531_rest	4076-049	Shomyoji	MIYU2009	II-66
2120531_rest	4076-050	Kasori EIV	MIYU2009	II-67
2120531_rest	4076-051	Horinouchi 1	MIYU2009	II-69
2120531_rest	4076-052	Horinouchi 1	MIYU2009	II-71
2120531_rest	4076-053	Jomon	MIYU2009	II-76
2120531_rest	4076-054	Jomon	MIYU2009	II-77
2120531_rest	4076-055	Kasori EIV	MIYU2009	II-78
2120531_rest	4076-057	Horinouchi 1	MIYU2009	II-81
2120531_rest	4076-058	Horinouchi 1	MIYU2009	II-82
2120531_rest	4076-059	Horinouchi 1	MIYU2009	II-83
2120531_rest	4076-060	Jomon	MIYU2009	II-84
2120531_rest	4076-061	Jomon	MIYU2009	II-85
2120531_rest	4076-062	Horinouchi 1	MIYU2009	II-87
2120531_rest	4076-063	Horinouchi 1	MIYU2009	II-88
2120531_rest	4076-064	Horinouchi 1	MIYU2009	II-91
2120531_rest	4076-065	Horinouchi 1	MIYU2009	II-95
2120531_rest	4076-066	Horinouchi 2	MIYU2009	II-96
2120531_rest	4076-067	Jomon	MIYU2009	II-97
2120531_rest	4076-068	Jomon	MIYU2009	II-98
2120531_rest	4076-069	Jomon	MIYU2009	II-99
2120531_rest	4076-070	Kasori EIV	MIYU2009	II-100
2120531_rest	4076-071	Kasori EIV	MIYU2009	II-101
2120531_rest	4076-072	Angyo 1	MIYU2009	II-102
2120531_rest	4076-073	Angyo 1	MIYU2009	II-103
2120531_rest	4076-074	Shomyoji	MIYU2009	II-106
2120531_rest	4076-075	Horinouchi 1	MIYU2009	II-108
2120531_rest	4076-076	Horinouchi - Kasori B	MIYU2009	II-109
2120531_rest	4076-077	Horinouchi - Kasori B	MIYU2009	II-110
2120531_rest	4076-078	Jomon	MIYU2009	II-111
2120531_rest	4076-079	Kasori B2	MIYU2009	II-112
2120531_rest	4076-080	Kasori B2 - Soya	MIYU2009	II-113
2120531_rest	4076-081	Kasori B2 - Soya	MIYU2009	II-114
2120531_rest	4076-082	Jomon	MIYU2009	II-115
2120531_rest	4076-083	Horinouchi 1	MIYU2009	II-117
2120531_rest	4076-085	Jomon	MIYU2009	II-119
2120531_rest	4076-086	Angyo 2	MIYU2009	II-120
2120531_rest	4076-087	Horinouchi	MIYU2009	II-121
2120531_rest	4076-088	Kasori EIV	MIYU2009	II-122

Continued on next page

Table A.2: Pithouses at Chiba

BUA ID	Pithouse ID	Period	REF	original ID
2120531_rest	4076-089	Jomon	MIYU2009	II-123
2120531_rest	4076-090	Jomon	MIYU2009	II-124A
2120531_rest	4076-091	Kasori B2	MIYU2009	II-124B
2120531_rest	4076-092	Horinouchi 1	MIYU2009	II-125
2120531_rest	4076-093	Shomyoji	MIYU2009	II-126
2120531_rest	4076-094	Horinouchi 1	MIYU2009	II-127
2120531_rest	4076-095	Horinouchi 1	MIYU2009	II-128
2120531_rest	4076-096	Kasori EIV	MIYU2009	II-129
2120531_rest	4076-097	Horinouchi 1	MIYU2009	II-130
2120531_rest	4076-098	Kasori B	MIYU2009	II-135A
2120531_rest	4076-099	Kasori B	MIYU2009	II-135B
2120531_rest	4076-100	Shomyoji	MIYU2009	II2-1
2120531_rest	4076-101	Horinouchi 1	MIYU2009	II2-2
2120531_rest	4076-102	Horinouchi 1	MIYU2009	II2-6
2120531_rest	4076-103	Horinouchi 1	MIYU2009	II2-8
2120531_rest	4076-104	Jomon	MIYU2009	II2-10
2120531_rest	4076-105	Kasori EIV	MIYU2009	II2-12
2120531_rest	4076-106	Horinouchi 1	MIYU2009	II2-13
2120531_rest	4076-107	Kasori B2	MIYU2009	II2-14
2120531_rest	4076-108	Horinouchi 1	MIYU2009	II2-15
2120531_rest	4076-109	Horinouchi 1	MIYU2009	II2-16
2120531_rest	4076-110	Horinouchi 1	MIYU2009	II2-17
2120531_rest	4076-111	Kasori EIV	MIYU2009	II2-18
2120531_rest	4076-112	Horinouchi 1	MIYU2009	II2-19
2120531_rest	4076-114	Jomon	MIYU2009	II2-22
2120531_rest	4076-115	Horinouchi 1	MIYU2009	II2-23
2120531_rest	4076-116	Horinouchi 1	MIYU2009	II2-25
2120531_rest	4076-117	Horinouchi 1	MIYU2009	II2-26
2120531_rest	4076-118	Soya	MIYU2009	II2-27
2120531_rest	4076-119	Horinouchi	MIYU2009	II2-28
2120531_rest	4076-120	Horinouchi 1	MIYU2009	II2-30
2120531_rest	4076-121	Angyo 1	MIYU2009	II2-31
2120531_rest	4076-122	Horinouchi 1	MIYU2009	II2-32
2120531_rest	4076-123	Horinouchi 1	MIYU2009	II2-33
2120531_rest	4076-124	Horinouchi 1	MIYU2009	III-1
2120531_rest	4076-125	Horinouchi 1	MIYU2009	III-2
2120531_rest	4076-126	Kasori B1	MIYU2009	III-3
2120531_rest	4076-127	Kasori B1	MIYU2009	III-4
2120531_rest	4076-128	Kasori B	MIYU2009	III-5
2120531_rest	4076-129	Horinouchi - Kasori B	MIYU2009	III-6
2120531_rest	4076-130	Kasori EIII	MIYU2009	III-7

Continued on next page

Table A.2: Pithouses at Chiba

BUA ID	Pithouse ID	Period	REF	original ID
2120531_rest	4076-131	Jomon	MIYU2009	III-8
2120531_rest	4076-132	Horinouchi - Kasori B	MIYU2009	III-9
2120531_rest	4076-133	Horinouchi - Kasori B	MIYU2009	III-10
2120531_rest	4076-134	Horinouchi - Kasori B	MIYU2009	III-11
2120531_rest	4076-135	Jomon	MIYU2009	III-12
2120531_rest	4076-136	Jomon	MIYU2009	III-13
2120531_rest	4076-137	Jomon	MIYU2009	III-14
2120531_rest	4076-138	Jomon	MIYU2009	III-15
2120531_rest	4076-139	Jomon	MIYU2009	III-16
2120531_rest	4076-140	Jomon	MIYU2009	III-17
2120531_rest	4076-141	Jomon	MIYU2009	III-18
2120531_rest	4076-142	Jomon	MIYU2009	III-19
2120531_rest	4076-143	Jomon	MIYU2009	III-20
2120531_rest	4076-144	Jomon	MIYU2009	III-21
2120531_rest	4076-145	Jomon	MIYU2009	III-22
2120531_rest	4076-146	Jomon	MIYU2009	III-23
2120531_rest	4076-147	Jomon	MIYU2009	III-24
2120531_rest	4076-148	Jomon	MIYU2009	III-25
2120531_rest	4076-149	Jomon	MIYU2009	III-26
2120531_rest	4076-150	Jomon	MIYU2009	III-27
2120531_rest	4076-151	Jomon	MIYU2009	III-28
2120531_rest	4076-152	Jomon	MIYU2009	III-29
2120531_rest	4076-153	Jomon	MIYU2009	III-30
2120531_rest	4076-154	Jomon	MIYU2009	III-31
2120531_rest	4076-155	Jomon	MIYU2009	III-32
2120531_rest	4076-156	Jomon	MIYU2009	III-33
2120531_rest	4076-157	Jomon	MIYU2009	III-34
2120531_rest	4076-158	Jomon	MIYU2009	III-35
2120531_rest	4076-159	Jomon	MIYU2009	III-36
2120531_rest	4076-160	Jomon	MIYU2009	III-37
2120531_rest	4076-161	Jomon	MIYU2009	III-38
2120531_rest	4076-162	Jomon	MIYU2009	III-40
2120531_rest	4076-163	Jomon	MIYU2009	III-41
2120531_rest	4076-164	Jomon	MIYU2009	III-42
2120531_rest	4076-165	Jomon	MIYU2009	III-43
2120531_rest	4076-166	Jomon	MIYU2009	III-44
2120531_rest	4076-167	Jomon	MIYU2009	III-45
2120531_rest	4076-168	Jomon	MIYU2009	III-46
2120531_rest	4076-169	Jomon	MIYU2009	III-47
2120531_rest	4076-170	Jomon	MIYU2009	III-48
2120531_rest	4076-171	Jomon	MIYU2009	III-49

Continued on next page

Table A.2: Pithouses at Chiba

BUA ID	Pithouse ID	Period	REF	original ID
2120531_rest	4076-172	Jomon	MIYU2009	III-50
2120531_rest	4076-173	Jomon	MIYU2009	III-51A
2120531_rest	4076-174	Jomon	MIYU2009	III-51B
2120531_rest	4076-175	Jomon	MIYU2009	III-52
2120531_rest	4076-176	Jomon	MIYU2009	III-53
2120531_rest	4076-177	Jomon	MIYU2009	III-54
2120531_rest	4076-178	Jomon	MIYU2009	III-55
2120531_rest	4076-179	Jomon	MIYU2009	III-56
2120531_rest	4076-180	Jomon	MIYU2009	III-57
2120531_rest	4076-181	Jomon	MIYU2009	III-58
2120531_rest	4076-182	Jomon	MIYU2009	III-59
2120531_rest	4076-183	Jomon	MIYU2009	III-60
2120531_rest	4076-184	Angyo 1	MIYU2009	III2-1
2120531_rest	4076-185	Horinouchi 1	MIYU2009	III2-2
2120531_rest	4076-186	Horinouchi 1	MIYU2009	III2-3
2120531_rest	4076-187	Horinouchi 1	MIYU2009	III2-4
2120531_rest	4076-188	Horinouchi 1	MIYU2009	III2-5
2120531_rest	4076-189	Kasori B1	MIYU2009	III2-6
2120531_rest	4076-190	Horinouchi - Kasori B	MIYU2009	III2-7
2120531_rest	4076-191	Kasori EIV	MIYU2009	III2-8
2120531_rest	4076-192	Jomon	MIYU2009	III2-9
2120531_rest	4076-193	Kasori B	MIYU2009	III2-10
2120531_rest	4076-194	Horinouchi 1	MIYU2009	III2-11
2120531_rest	4076-195	Horinouchi 1	MIYU2009	III2-12
2120531_rest	4076-196	Horinouchi 1	MIYU2009	III2-13
2120531_rest	4076-197	Horinouchi - Kasori B	MIYU2009	III2-14
2120531_rest	4076-198	Kasori B	MIYU2009	III2-15A
2120531_rest	4076-199	Kasori B	MIYU2009	III2-15B
2120531_rest	4076-200	Horinouchi - Kasori B	MIYU2009	III2-16
2120531_rest	4076-201	Horinouchi 1	MIYU2009	III3-1
2120531_rest	4076-202	Horinouchi 1	MIYU2009	III3-2
2120531_rest	4076-203	Horinouchi 1	MIYU2009	III3-4
2120531_rest	4076-204	Horinouchi 1	MIYU2009	III3-5
2120531_rest	4076-205	Horinouchi 1	MIYU2009	III3-6
2120531_rest	4076-207	Angyo 1	MIYU2009	III3-8
2120531_rest	4076-210	Horinouchi 1	MIYU2009	III3-11
2120531_rest	4076-211	Kasori B	MIYU2009	III3-12
2120531_rest	4076-212	Horinouchi 1	MIYU2009	III3-13
2120531_rest	4076-213	Jomon	MIYU2009	III3-14
2120531_rest	4076-215	Kasori B - Soya	MIYU2009	III3-16
2120531_rest	4076-216	Horinouchi	MIYU2009	IV-1

Continued on next page

Table A.2: Pithouses at Chiba

BUA ID	Pithouse ID	Period	REF	original ID
2120531_rest	4076-217	Jomon	MIYU2009	IV-2
2120531_rest	4076-218	Jomon	MIYU2009	IV-3
2120531_rest	4076-219	Jomon	MIYU2009	VI-1
2120531_rest	4076-220	Horinouchi 1	MIYU2009	VI-2
2120531_rest	4076-221	Jomon	MIYU2009	VI-3
2120531_rest	4076-222	Horinouchi 1	MIYU2009	VI-4
2120531_rest	4076-223	Jomon	MIYU2009	VI-5
2120531_rest	4076-224	Jomon	MIYU2009	VI-6
2120531_rest	4076-225	Jomon	MIYU2009	VI-7
2120531_rest	4076-226	Jomon	MIYU2009	VI-8
2120531_rest	4076-227	Horinouchi 1	MIYU2009	VI-9
2120531_rest	4076-228	Horinouchi 1	MIYU2009	VI-10
2120531_rest	4076-229	Horinouchi 1	MIYU2009	VI-11
2120531_rest	4076-230	Jomon	MIYU2009	VI-12
2120531_rest	4076-231	Jomon	MIYU2009	VI-13
2120531_rest	4076-232	Jomon	MIYU2009	VI-14
2120531_rest	4076-233	Jomon	MIYU2009	VI-15
2120531_rest	4076-234	Jomon	MIYU2009	VI-16
2120531_rest	4076-235	Jomon	MIYU2009	VI-17
2120531_rest	4076-236	Jomon	MIYU2009	VI-18
2120531_rest	4076-237	Jomon	MIYU2009	VI-19
2120531_rest	4076-238	Jomon	MIYU2009	VI-20
2120531_rest	4076-239	Jomon	MIYU2009	VI-21
2120531_rest	4076-240	Jomon	MIYU2009	VI-22
2120533_3	4078-002	Middle Jomon - Late Jomon (Late)	NISMIM2006	2
2120533_3	4078-003	Ukishima	NISMIM2006	3
2120533_3	4078-004	Horinouchi	NISMIM2006	4
2120533_3	4078-005	Horinouchi 2 - Kasori B1	NISMIM2006	5
2120533_3	4078-006	Kasori B	NISMIM2006	6
2120536c	4081-001	Horinouchi	NISMI2006	1
2120616_23	4161-001	Late Jomon	SKHH2005	?
2120616_23	4161-002	Late Jomon	SKHH2005	?
2120616_23	4161-003	Kasori B	SKHH2005	1
2120660	4205-001	Pre-Kasori E	SKHH2001	2
2120660	4205-002	Jomon	SKHH2001	3
2120660	4205-003	Kasori E	SKHH2001	4
2120660	4205-004	Jomon	SKHH2001	5
2120881_h	4404-001	Kasori EIII	UCHT2008	Area3-1
2120881_b	4404-002	Kasori EIII	UCHT2008	Area4-1
2120881_b	4404-003	Kasori E	UCHT2008	Area4-5
2120881_a	4404-004	Kasori EIII	UCHT2008	Area7HA-3

Continued on next page

Table A.2: Pithouses at Chiba

BUA ID	Pithouse ID	Period	REF	original ID
2120881_a	4404-005	Kasori EIII	UCHT2008	Area7HA-7
2120881_a	4404-006	Jomon	UCHT2008	Area7HA-10
2120881_h	4404-007	Kasori EIII	UCHT2008	Clubhouse-2
2120881_h	4404-008	Kasori EIII	UCHT2008	Clubhouse-3
2120881_h	4404-009	Kasori EIII	UCHT2008	Clubhouse-4
2120881_h	4404-010	Kasori EIII	UCHT2008	Clubhouse-37
2120881_h	4404-011	Kasori E	UCHT2008	Clubhouse-38
2120881_h	4404-012	Middle Jomon	UCHT2008	Clubhouse-66
2120813_edited	4414-001	Moroiso	MUKH1989	1
2120813_edited	4414-002	Kasori E	MUKH1989	2
2120813_edited	4414-003	Moroiso b	MUKH1989	3
2120813_edited	4414-004	Moroiso b	MUKH1989	4
2120813_edited	4414-005	Kasori EIII	MUKH1989	5
2120813_edited	4414-006	Moroiso	MUKH1989	6
2120813_edited	4414-007	Kasori EIII	MUKH1989	7
2120812	4415-001	Jomon	OOSK1990	1
2120813_edited	4420-001	Jomon	RKSB1994	33
2120813_edited	4421-001	Kasori EIII (Late) - EIV	IKMUK1995	15
2120813_edited	4421-002	Kasori EIII (Late) - EIV	IKMUK1995	16
2120813_edited	4421-003	Kasori EIV	IKMUK1995	17
2120813_edited	4421-004	Kasori EIV	IKMUK1995	18
2120813_edited	4421-005	Kasori EIV	IKMUK1995	19
2120813_edited	4421-006	Kasori EIII	IKMUK1995	20
2120813_edited	4421-007	Kasori EIII (Late) - EIV	IKMUK1995	21
2120813_edited	4421-008	Jomon	IKMUK1995	22
2120813_edited	4421-009	Kasori E	IKMUK1995	23
2120813_edited	4421-010	Jomon	IKMUK1995	24
2120813_edited	4421-011	Kasori EIV - Shomyoji	IKMUK1995	25
2120813_edited	4421-012	Kasori EIV	IKMUK1995	26
2120813_edited	4421-013	Jomon	IKMUK1995	27
2120813_edited	4421-014	Kasori EIII (Early)	IKMUK1995	28
2120813_edited2	4421-015	Kasori EIV	SKHH2003	1
2120813_edited2	4421-016	Kasori E	SKHH2003	2
2280067_edited	4917-001	Jomon	YAMAK2005	
2280069_edited2	4919-001	12b - 12c	YAMAK2005	1
2280070	4920-001	Jomon	SHIW2004	1
2280070	4920-002	Jomon	SHIW2004	2
2280116_II_III	4966-007	Ukishima II (Early)	WRBI1991	7
2280116_II_III	4966-008	Ukishima III	WRBI1991	8
2280116_II_III	4966-009	Ukishima II / Moroiso b (Late)	WRBI1991	9
2280116_II_III	4966-010	Moroiso b (Middle - Late)	WRBI1991	10

Continued on next page

Table A.2: Pithouses at Chiba

BUA ID	Pithouse ID	Period	REF	original ID
2280116_II_III	4966-011	Ukishima III / Moroiso b	WRBI1991	11
2280116_II_III	4966-012	Moroiso (Late)	WRBI1991	12
2280116_II_III	4966-013	Moroiso b (Late)	WRBI1991	13
2280116_II_III	4966-014	Moroiso b (Late)	WRBI1991	14
2280116_II_III	4966-015	Ukishima III / Moroiso b	WRBI1991	15
2280116_II_III	4966-016	Ukishima III	WRBI1991	16
2280117_edited	4967-001	Kasori E	WRBI1991	20
2280118_edited	4968-001	Kasori E	WRBI1991	17
2280118_edited	4968-002	Kasori E	WRBI1991	18
2280118_edited	4968-003	Middle Jomon - Late Jomon	WRBI1991	19
2280122_edited	4972-001	Lower Hanazumi	YYMS1987	1
2280122_edited	4972-002	Jomon	YYMS1987	2
2280122_edited	4972-003	Lower Hanazumi	YYMS1987	3
2280122_edited	4972-004	Jomon	YYMS1987	4
2280122_edited	4972-005	Natsushima - Lower Hanazumi	YYMS1987	5
2280122_edited	4972-006	Jomon	YYMS1987	6
2280122_edited	4972-007	Jomon	YYMS1987	7
2280122_edited	4972-008	Lower Hanazumi	YYMS1987	8
2280122_edited	4972-009	Natsushima - Lower Hanazumi	YYMS1987	9
2280122_edited	4972-010	Tado - Kasori EII	YYMS1987	10
2280122_edited	4972-011	Jomon	YYMS1987	11
2280122_edited	4972-012	Kasori EII (up to)	YYMS1987	12
2280122_edited	4972-013	12b - 12c	YYMS1987	13
2280122_edited	4972-014	Kasori EII (up to)	YYMS1987	14
2280122_edited	4972-015	Natsushima - Lower Hanazumi	YYMS1987	15
2280122_edited	4972-016	Natsushima - Lower Hanazumi	YYMS1987	16
2280122_edited	4972-018	Jomon	YYMS1987	18
2280122_edited	4972-019	12b - 12c	YYMS1987	19
2280122_edited	4972-020	12b - 12c	YYMS1987	20
2280122_edited	4972-021	12b - 12c	YYMS1987	21
2280122_edited	4972-022	12b - 12c	YYMS1987	22
2280122_edited	4972-023	Kasori EII (up to)	YYMS1987	23
2280122_edited	4972-024	Kasori EII (up to)	YYMS1987	24
2280122_edited	4972-025	12b - 12c	YYMS1987	25
2280122_edited	4972-026	Kasori EII (up to)	YYMS1987	26
2280122_edited	4972-027	Jomon	YYMS1987	27
2280122_edited	4972-028	12b - 12c	YYMS1987	28
2280124	4974-001	Otamadai III	YOTSHH2005	2
2280128	4978-001	Angyo 1 - 2	SHIMYOT1986	6
2280147_edited	4997-001	Jomon	WRYM1986	Area2-1
2280147_edited	4997-002	Jomon	WRYM1986	Area3-1

Continued on next page

Table A.2: Pithouses at Chiba

BUA ID	Pithouse ID	Period	REF	original ID
2280148_edited	4998-001	Otamadai	UNDC1993	1
2280148_edited	4998-002	Otamadai	UNDC1993	2
2280148_edited	4998-003	Otamadai	UNDC1993	3
2280148_edited	4998-004	Otamadai	UNDC1993	4
2280148_edited	4998-005	Shimoono	UNDC1993	5
2280148_edited	4998-006	Kasori EIII	UNDC1993	6
2280148_edited	4998-007	Kasori EIII	UNDC1993	7
2280148_edited	4998-008	Kasori EIII	UNDC1993	8
2280155_edited2	5005-001	Kasori EIII	UNDC1993	1
2280160_edited2	5010-001	Middle Jomon	YOTSHH2001	
2280160_edited2	5010-002	Middle Jomon	YOTSHH2001	
2280163_1	5013-001	Kasori EIII	UKY2004	16
2280164_edited	5014-001	Otamdai III - IV	MNSK2007	63
2280164_edited	5014-002	Otamdai III - IV	MNSK2007	64
2280164_edited	5014-003	Otamadai III (Late) - IV	MNSK2007	71
2280164_edited	5014-004	Otamdai III - IV	MNSK2007	72
2280164_edited	5014-005	Otamdai III - IV	MNSK2007	73
2280164_edited	5014-006	Otamadai III	MNSK2007	76
2280164_edited	5014-007	Otamadai III	MNSK2007	77
2280164_edited	5014-008	Otamadai III (Late) - IV	MNSK2007	80
2280164_edited	5014-009	Otamdai III - IV	MNSK2007	92
2280164_edited	5014-010	Otamdai III - IV	MNSK2007	94
2280164_edited	5014-011	Otamdai III - IV	MNSK2007	95
2280164_edited	5014-012	Otamdai III - IV	MNSK2007	96
2280164_edited	5014-013	Otamdai III - IV	MNSK2007	97
2280164_edited	5014-014	Otamdai III - IV	MNSK2007	126
2280164_edited	5014-015	Otamadai - Kasori EIII	MNSK2007	128
2280164_edited	5014-016	Otamadai III (Late) - IV	MNSK2007	132
2280164_edited	5014-017	Otamdai III-IV	MNSK2007	136
2280164_edited	5014-018	Otamdai III-IV	MNSK2007	137
2280164_edited	5014-019	Otamadai III (Late) - IV	MNSK2007	142
2280164_edited	5014-020	Otamdai III-IV	MNSK2007	143
2280164_edited	5014-021	Otamadai III (Late) - IV	MNSK2007	152
2280164_edited	5014-022	Kasori EIII	MNSK2007	160
2280193	5043-001	Kurohama	YOSIG1986	3
2280193	5043-002	Kurohama	YOSIG1986	5
2280193	5043-003	Ukishima I / Moroiso a	YOSIG1986	10
2280193	5043-004	Ukishima I / Moroiso a	YOSIG1986	20
2280193	5043-005	Ukishima I / Moroiso a	YOSIG1986	21
2280196	5046-001	Kurohama	YOSIG1986	1
2280196	5046-002	Jomon	YOSIG1986	2

Continued on next page

Table A.2: Pithouses at Chiba

BUA ID	Pithouse ID	Period	REF	original ID
2280196	5046-003	Kasori EIII	YOSIG1986	3
2280196	5046-004	Kasori EIII	YOSIG1986	4
2280199_edited	5049-001	Ukishima III	YOSIG1986	1
2280199_edited	5049-002	Ukishima III	YOSIG1986	2
2280199_edited	5049-003	Ukishima III (Early) / Moroiso b	YOSIG1986	3
2280199_edited	5049-004	Moroiso b	YOSIG1986	4
2280199_edited	5049-005	Ukishima III Kouritsu	YOSIG1986	5
2280199_edited	5049-006	Ukishima II	YOSIG1986	6
2280199_edited	5049-007	Okitsu	YOSIG1986	7
2280199_edited	5049-008	Ukishima I (Late) / Moroiso b	YOSIG1986	8
2280222_edited	5065-001	Early Jomon (Final)	KDSK1994	1
2280222_edited	5065-002	Ukishima II / Moroiso a	KDSK1994	2
2280222_edited	5065-003	Kurohama / Moroiso a - b / Ukishima I - II	KDSK1994	3
2280222_edited	5065-004	Kurohama / Moroiso a - b / Ukishima I - II	KDSK1994	4
2280222_edited	5065-005	Kurohama / Moroiso a - b / Ukishima I - II	KDSK1994	5
2280222_edited	5065-006	Kurohama / Moroiso a - b / Ukishima I - II	KDSK1994	6
2280222_edited	5065-007	Kurohama / Moroiso a - b / Ukishima I - II	KDSK1994	7
2280222_edited	5065-008	Kurohama / Moroiso a - b / Ukishima I - II	KDSK1994	8
2010105	9652-001	Kurohama - Moroiso b	KWBCIM1987	1
2010105	9652-002	Ukishima I	KWBCIM1987	2
2010105	9652-003	Early Jomon (Final)	KWBCIM1987	3
2010105	9652-004	Early Jomon (Final)	KWBCIM1987	4
2010105	9652-005	Kasori EII - EIII	KWBCIM1987	5
2010105	9652-006	Early Jomon (Final)	KWBCIM1987	6
2010105	9652-007	Early Jomon (Final)	KWBCIM1987	7
2010105	9652-008	Kasori EII (Late)	KWBCIM1987	8
2010105	9652-009	Kurohama - Ukishima	KWBCIM1987	9
2010105	9652-010	Shomyoji	KWBCIM1987	10
2011005_edited	9804-001	Middle Jomon - Late Jomon	MONCHI1986	D-002
2010251	9808-001	Middle Jomon (Late)	CHNEN1994	
2010251	9808-002	Middle Jomon (Late)	CHNEN1994	
2010251	9808-003	Middle Jomon (Late)	CHNEN1994	
2010188_1	9815-003	Kasori EI (up to)	CHIBAKEN	Area I
2010188_1	9815-004	Kasori EII (up to)	CHIBAKEN	Area I
2010188_1	9815-005	Kasori EII (up to)	CHIBAKEN	Area I
2010188_1	9815-006	Kasori EII (up to)	CHIBAKEN	Area I
2010188_1	9815-007	Kasori EII (up to)	CHIBAKEN	Area I
2010188_1	9815-008	Kasori EII (up to)	CHIBAKEN	Area I
2010188_1	9815-009	Shomyoji 2	CHIBAKEN	Area I
2010188_1	9815-010	Horinouchi 1	CHIBAKEN	Area I
2010188_1	9815-011	Horinouchi 1	CHIBAKEN	Area I

Continued on next page

Table A.2: Pithouses at Chiba

BUA ID	Pithouse ID	Period	REF	original ID
2010188_1	9815-012	Horinouchi 1	CHIBAKEN	Area I
2010188_1	9815-013	Kasori EIV - Shomyoji	CHIBAKEN	Area I
2010188_1	9815-014	Kasori EIV - Shomyoji	CHIBAKEN	Area I
2010188_1	9815-015	Kasori EIV - Shomyoji	CHIBAKEN	Area I
2010188_1	9815-016	Kasori EIV - Shomyoji	CHIBAKEN	Area I
2010188_1	9815-017	Kasori EIV - Shomyoji	CHIBAKEN	Area I
2010188_1	9815-018	Kasori EIV - Shomyoji	CHIBAKEN	Area I
2010188_1	9815-019	Kasori EIV - Shomyoji	CHIBAKEN	Area I
2010188_1	9815-020	Kasori EIV - Shomyoji	CHIBAKEN	Area I
2010188_1	9815-021	Kasori EIV - Shomyoji	CHIBAKEN	Area I
2010188_1	9815-022	Kasori EIV - Shomyoji	CHIBAKEN	Area I
2010188_1	9815-023	Kasori EIV - Shomyoji	CHIBAKEN	Area I
2010188_1	9815-024	Kasori EIV - Shomyoji	CHIBAKEN	Area I
2010188_1	9815-025	Kasori EIV - Shomyoji	CHIBAKEN	Area I
2010188_1	9815-026	Kasori EIV - Shomyoji	CHIBAKEN	Area I
2010188_1	9815-027	Kasori EIV - Shomyoji	CHIBAKEN	Area I
2010188_1	9815-028	Kasori EIV - Shomyoji	CHIBAKEN	Area I
2010188_1	9815-029	Kasori EIV - Shomyoji	CHIBAKEN	Area I
2010188_1	9815-030	Kasori EIV - Shomyoji	CHIBAKEN	Area I
2010188_1	9815-031	Kasori EIV - Shomyoji	CHIBAKEN	Area I
2010188_1	9815-032	Kasori EIV - Shomyoji	CHIBAKEN	Area I
2010188_1	9815-033	Kasori EIV - Shomyoji	CHIBAKEN	Area I
2010188_1	9815-034	Kasori EIV - Shomyoji	CHIBAKEN	Area I
2010188_1	9815-035	Kasori EIV - Shomyoji	CHIBAKEN	Area I
2010188_1	9815-036	Kasori EIV - Shomyoji	CHIBAKEN	Area I
2010188_1	9815-037	Kasori EIV - Shomyoji	CHIBAKEN	Area I
2010188_1	9815-038	Kasori EIV - Shomyoji	CHIBAKEN	Area I
2010188_1	9815-039	Kasori EIV - Shomyoji	CHIBAKEN	Area I
2010188_1	9815-040	Kasori EIV - Shomyoji	CHIBAKEN	Area I
2010188_1	9815-041	Kasori EIV - Shomyoji	CHIBAKEN	Area I
2010188_1	9815-042	Kasori EIV - Shomyoji	CHIBAKEN	Area I
2010188_1	9815-043	Kasori EIV - Shomyoji	CHIBAKEN	Area I
2010188_1	9815-044	Kasori EIV - Shomyoji	CHIBAKEN	Area I
2010188_1	9815-045	Kasori EIV - Shomyoji	CHIBAKEN	Area I
2010188_1	9815-046	Kasori EIV - Shomyoji	CHIBAKEN	Area I
2010188_1	9815-047	Kasori EIV - Shomyoji	CHIBAKEN	Area I
2010188_1	9815-048	Kasori EIV - Shomyoji	CHIBAKEN	Area I
2010188_1	9815-049	Kasori EIV - Shomyoji	CHIBAKEN	Area I
2010188_1	9815-050	Kasori EIV - Shomyoji	CHIBAKEN	Area I
2010188_1	9815-051	Kasori EIV - Shomyoji	CHIBAKEN	Area I
2010188_1	9815-052	Kasori EIV - Shomyoji	CHIBAKEN	Area I

Continued on next page

Table A.2: Pithouses at Chiba

BUA ID	Pithouse ID	Period	REF	original ID
2010188_1	9815-053	Kasori EIV - Shomyoji	CHIBAKEN	Area I
2010188_1	9815-054	Kasori EIV - Shomyoji	CHIBAKEN	Area I
2010188_1	9815-055	Kasori EIV - Shomyoji	CHIBAKEN	Area I
2010188_1	9815-056	Kasori EIV - Shomyoji	CHIBAKEN	Area I
2010188_1	9815-057	Kasori EIV - Shomyoji	CHIBAKEN	Area I
2010188_1	9815-058	Kasori EIV - Shomyoji	CHIBAKEN	Area I
2010188_1	9815-059	Kasori EIV - Shomyoji	CHIBAKEN	Area I
2010188_1	9815-060	Kasori EIV - Shomyoji	CHIBAKEN	Area I
2010188_1	9815-061	Kasori EIV - Shomyoji	CHIBAKEN	Area I
2010188_1	9815-062	Kasori EIV - Shomyoji	CHIBAKEN	Area I
2010188_1	9815-063	Kasori EIV - Shomyoji	CHIBAKEN	Area I
2010188_1	9815-064	Kasori EIV - Shomyoji	CHIBAKEN	Area I
2010188_1	9815-065	Kasori EIV - Shomyoji	CHIBAKEN	Area I
2010188_1	9815-066	Kasori EIV - Shomyoji	CHIBAKEN	Area I
2010188_1	9815-067	Kasori EIV - Shomyoji	CHIBAKEN	Area I
2010188_1	9815-068	Kasori EIV - Shomyoji	CHIBAKEN	Area I
2010188_1	9815-069	Kasori EIV - Shomyoji	CHIBAKEN	Area I
2010188_1	9815-070	Kasori EIV - Shomyoji	CHIBAKEN	Area I
2010188_1	9815-071	Kasori EIV - Shomyoji	CHIBAKEN	Area I
2010188_1	9815-072	Kasori EIV - Shomyoji	CHIBAKEN	Area I
2010188_1	9815-073	Kasori EIV - Shomyoji	CHIBAKEN	Area I
2010188_1	9815-074	Kasori EIV - Shomyoji	CHIBAKEN	Area I
2010188_1	9815-075	Kasori EIV - Shomyoji	CHIBAKEN	Area I
2010188_1	9815-076	Kasori EIV - Shomyoji	CHIBAKEN	Area I
2010188_1	9815-077	Kasori EIV - Shomyoji	CHIBAKEN	Area I
2010188_1	9815-078	Kasori EIV - Shomyoji	CHIBAKEN	Area I
2010188_1	9815-079	Kasori EIV - Shomyoji	CHIBAKEN	Area I
2010188_1	9815-080	Kasori EIV - Shomyoji	CHIBAKEN	Area I
2010188_1	9815-081	Kasori EIV - Shomyoji	CHIBAKEN	Area I
2010188_1	9815-082	Kasori EIV - Shomyoji	CHIBAKEN	Area I
2010188_1	9815-083	Kasori EIV - Shomyoji	CHIBAKEN	Area I
2010188_1	9815-084	Kasori EIV - Shomyoji	CHIBAKEN	Area I
2010188_1	9815-085	Kasori EIV - Shomyoji	CHIBAKEN	Area I
2010188_3	9816-001	Kasori EIII - IV	KAID1972	1
2010188_3	9816-002	Kasori EIII - IV	KAID1972	2
2010189	9816-003	Kasori EIII - IV	KAID1972	3
2010189	9816-004	Kasori EIII - IV	KAID1972	4
2010189	9816-005	Kasori EIII - IV	KAID1972	5
2010189	9816-006	Kasori EIII - IV	KAID1972	6
2010189	9816-007	Kasori EIII - IV	KAID1972	7
2010189	9816-008	Kasori EIII - IV	KAID1972	8

Continued on next page

Table A.2: Pithouses at Chiba

BUA ID	Pithouse ID	Period	REF	original ID
2010189	9816-009	Kasori EIII - IV	KAID1972	9
2010189	9816-010	Kasori EIII - IV	KAID1972	10
2010189	9816-011	Kasori EIII - IV	KAID1972	11
2010189	9816-012	Kasori EIII - IV	KAID1972	12
2010195_edited	9818-002	Jomon	MINM2001	4
2011263_edited	9823-001	Early Jomon	MINM2001	3
2011263_edited	9823-002	Jomon	MINM2001	4
2011263_edited	9823-003	Jomon	MINM2001	5
2011244	9825-001	Shomyoji 1	AIOI2000	1
2011244	9825-002	Shomyoji 1	AIOI2000	2
2011244	9825-003	Shomyoji 1	AIOI2000	3
2011244	9825-004	Shomyoji 1	AIOI2000	4
2011244	9825-005	Kasori EIV	AIOI2000	5
2011244	9825-006	Kasori EIV	AIOI2000	6
2011244	9825-007	Kasori EIV	AIOI2000	7
2011244	9825-008	Shomyoji I	AIOI2000	8
2011244	9825-009	Kasori EIV	AIOI2000	9
2011244	9825-010	Kasori EIV	AIOI2000	10
2011244	9825-011	Kasori EIV	AIOI2000	11
2011244	9825-012	Kasori EIV	AIOI2000	12
2011244	9825-013	Kasori EIV	AIOI2000	13
2011244	9825-014	Kasori EIV	AIOI2000	14
2011244	9825-015	Kasori EIV	AIOI2000	15
2011244	9825-016	Kasori EIV	AIOI2000	16
2011244	9825-017	Shomyoji 1	AIOI2000	17
2011244	9825-018	Shomyoji 1	AIOI2000	18
2011244	9825-019	Kasori EIV	AIOI2000	19
2010271_h4h8	9832-001	Ukishima	KAIR1996	8
2010271_h4h8	9832-002	Kasori EIV	KAIR1996	12
2010271_h4h8	9832-003	Kasori EIV	KAIR1996	23
2010271_h4h8	9832-004	Kasori EIV	KAIR1996	24
2010271_h4h8	9832-005	Shomyoji (Early)	KAIR1996	26
2010271_h4h8	9832-006	Shomyoji (Early)	KAIR1996	29
2010271_h4h8	9832-007	Shomyoji (Early)	KAIR1996	31
2010271_h4h8	9832-008	Shomyoji (Early)	KAIR1996	32
2010271_h4h8	9832-009	Kasori EIV - Shomyoji	KAIR1996	35
2010271_h4h8	9832-010	Shomyoji (Early)	KAIR1996	36
2010271_h4h8	9832-011	Kasori EIV - Shomyoji	KAIR1996	37
2010271_h4h8	9832-012	Kasori EIV	KAIR1996	38
2010271_h4h8	9832-013	Shomyoji (Early)	KAIR1996	39
2010271_h4h8	9832-014	Shomyoji (Early)	KAIR1996	40

Continued on next page

Table A.2: Pithouses at Chiba

BUA ID	Pithouse ID	Period	REF	original ID
2010271_h4h8	9832-015	Ukishima	KAIR1996	41
2010271_h4h8	9832-016	Shomyoji (Early)	KAIR1996	43
2010271_h4h8	9832-017	Shomyoji (Early)	KAIR1996	44
2010271_h4h8	9832-018	Kasori EIV - Shomyoji	KAIR1996	45
2010271_h4h8	9832-019	Shomyoji (Late)	KAIR1996	61
2010271_h4h8	9832-020	Shomyoji (Early)	KAIR1996	63
2010271_h4h8	9832-021	Kasori EIV - Shomyoji	KAIR1996	64
2010271_h4h8	9832-022	Jomon	KAIR1996	65
2010271_h4h8	9832-023	Shomyoji (Early)	KAIR1996	66
2010271_h4h8	9832-024	Jomon	KAIR1996	67
2010271_h4h8	9832-025	Kasori EIV - Shomyoji	KAIR2000	69
2010271_h4h8	9832-026	Kasori EIV - Shomyoji	KAIR2000	73
2010271_h4h8	9832-027	Kasori EIV - Shomyoji	KAIR2000	79
2010269_1	9840-001	Kasori EIII (Renkomon)	TOBS1998	183
2010289_ABDEF	9850-001	Otamadai Ib	NESK1997	4
2010289_ABDEF	9850-002	Otamadai	NESK1997	14
2010289_ABDEF	9850-003	Otamadai Ib	NESK1997	15
2010289_ABDEF	9850-004	Otamadai Ib	NESK1997	18
2010289_ABDEF	9850-005	Otamadai Ib	NESK1997	20
2010289_ABDEF	9850-006	Kasori B	NESK1997	26
2010289_ABDEF	9850-007	Jomon	NESK1997	29
2010289_ABDEF	9850-008	Otamadai Ib	NESK1997	38
2010289_ABDEF	9850-009	Otamadai Ib	NESK1997	40
2010289_ABDEF	9850-010	Otamadai Ib	NESK1997	42
2010289_C	9850-011	Jomon	CHIBAH2	
2010289_C	9850-012	Jomon	CHIBAH2	
2010289_C	9850-013	Jomon	CHIBAH2	
2010289_C	9850-014	Jomon	CHIBAH2	
2014001_1	9852-001	Middle Jomon	DAIHT1996	1
2014001_1	9852-002	Otamadai	DAIHT1996	2
2014001_1	9852-003	Middle Jomon	DAIHT1996	3
2014001_2	9852-004	Otamadai Ib	DAIHT2004	27
2014002	9853-001	Late Jomon	CHIBAS63	
2010272_B	9860-001	Middle Jomon - Late Jomon	KEIO1973	B-1
2010297_edited	9885-001	Horinouchi 1	ARYTSM1986	1(008)
2010297_edited	9885-002	Kasori EIII	ARYTSM1986	3 (014)
2010349	9890-001	Kasori EII (up to)	CHIBAKEN	
2010349	9890-002	Kasori EII (up to)	CHIBAKEN	
2010349	9890-003	Middle Jomon (Early)	CHIBAKEN	
2010355	9891-001	Jomon	CHIBAH14	
2010355	9891-002	Jomon	CHIBAH14	

Continued on next page

Table A.2: Pithouses at Chiba

BUA ID	Pithouse ID	Period	REF	original ID
2010355	9891-003	Jomon	CHIBAH14	
2010355	9891-004	Jomon	CHIBAH14	
2010355	9891-005	Jomon	CHIBAH14	
2010355	9891-006	Jomon	CHIBAH14	
2010355	9891-007	Jomon	CHIBAH14	
2010355	9891-008	Jomon	CHIBAH14	
2010355	9891-009	Jomon	CHIBAH14	
2010355	9891-010	Jomon	CHIBAH14	
2010355	9891-011	Jomon	CHIBAH14	
2010355	9891-012	Jomon	CHIBAH14	
2010346_edited	9892-001	Kasori EIV	CHNEN1998	
2010346_edited	9892-002	Kasori EIV	CHNEN1998	
2010346_edited	9892-003	Kasori EIV	CHNEN1998	
2010346_edited	9892-004	Kasori EIV	CHNEN1998	
2010346_edited	9892-005	Kasori EIV	CHNEN1998	
2010346_edited	9892-006	Kasori EIV	CHNEN1998	
2010346_edited	9892-007	Kasori EIV	CHNEN1998	
2010346_edited	9892-008	Kasori EIV	CHNEN1998	
2010346_edited	9892-009	Kasori EIV	ARYTSM1986	3(009)
2010299_east	9917-001	Otamadai	KAID1981a	JD No6
2010299_east	9917-002	Otamadai	KAID1981a	JD No15
2010299_east	9917-003	Kasori E	KAID1981a	JD No7
2010299_east	9917-004	Kasori E	KAID1981a	JD No8
2010299_east	9917-005	Kasori E	KAID1981a	JD No9
2010299_east	9917-006	Kasori EII (up to)	KAID1981a	JD No11
2010299_east	9917-007	Kasori EII (up to)	KAID1981a	JD No12
2010299_east	9917-008	Kasori EII (up to)	KAID1981a	JD No13
2010299_east	9917-009	Kasori EII (up to)	KAID1981a	JD No14
2010299_east	9917-010	Kasori EII (up to)	KAID1981a	JD No10
2010299_east	9917-011	Kasori B	KAID1981a	JD No3
2010299_east	9917-012	Angyo 1	KAID1981a	Jd No1
2010299_east	9917-013	Kasori EII (up to)	KAID1981b	JD No16
2010299_east	9917-014	Kasori EIII	KAID1981b	JD No17
2010299_east	9917-015	Horinouchi 1	KAID1981b	JD No18
2010299_east	9917-016	Kasori EII (up to)	KAID1981b	JD No19
2010299_east	9917-017	Kasori B	KAID1982a	JD No20
2010299_east	9917-018	Sekiyama	KAID1981a	JD No4
2010299_east	9917-019	Kurohama	KAID1981a	JD No5
2010299_south	9917-020	Otamadai	KASM1976	17
2010299_south	9917-021	Otamadai	KASM1976	22
2010299_south	9917-022	Otamadai	KASM1976	23

Continued on next page

Table A.2: Pithouses at Chiba

BUA ID	Pithouse ID	Period	REF	original ID
2010299_south	9917-023	Otamadai	KASM1976	25
2010299_south	9917-024	Kasori EIII - EIV	KASM1976	5
2010299_south	9917-025	Kasori EIII - Shomyoiji	KASM1976	19
2010299_south	9917-026	Kasori E	KASM1976	31
2010299_south	9917-027	Kasori EII - EIII	KASM1976	32
2010299_south	9917-028	Shomyoji	KASM1976	27
2010299_south	9917-029	Shomyoji	KASM1976	29
2010299_south	9917-030	Horinouchi 1	KASM1976	1
2010299_south	9917-031	Horinouchi 1	KASM1976	2
2010299_south	9917-032	Horinouchi 1	KASM1976	3
2010299_south	9917-033	Horinouchi 1	KASM1976	6
2010299_south	9917-034	Horinouchi 1	KASM1976	7
2010299_south	9917-035	Horinouchi 1	KASM1976	8
2010299_south	9917-036	Horinouchi 1	KASM1976	9
2010299_south	9917-037	Horinouchi 1	KASM1976	10
2010299_south	9917-038	Horinouchi 1	KASM1976	11
2010299_south	9917-039	Horinouchi 1	KASM1976	12
2010299_south	9917-040	Horinouchi 1	KASM1976	16
2010299_south	9917-041	Horinouchi 1	KASM1976	21
2010299_south	9917-042	Horinouchi	KASM1976	26
2010299_south	9917-043	Kasori B2	KASM1976	4
2010299_south	9917-044	Kasori B	KASM1976	13
2010299_south	9917-045	Kasori B	KASM1976	14
2010299_south	9917-046	Kasori B	KASM1976	15
2010299_south	9917-047	Kasori B	KASM1976	28
2010299_south	9917-048	Kasori B	KASM1976	30
2010299_south	9917-049	Angyo 1 - 2	KASM1976	20
2010299_south	9917-051	Jomon	KASM1976	18
2010299_north	9917-052	Kasori EI (up to)	KASK1977	1
2010299_north	9917-053	Kasori EI (up to)	KASK1977	2
2010299_north	9917-054	Kasori EII (up to)	KASK1977	3
2010299_north	9917-055	Kasori EII (up to)	KASK1977	4
2010299_north	9917-056	Kasori EII (up to)	KASK1977	5
2010299_north	9917-057	Horinouchi 1	KASK1977	6
2010299_north	9917-058	Horinouchi 1	KASK1977	7
2010299_north	9917-059	Horinouchi 1	KASK1977	8
2010299_north	9917-060	Kasori EII (up to)	KASK1977	9
2010299_north	9917-061	Horinouchi 1	KASK1977	10
2010299_north	9917-062	Kasori EII (up to)	KASK1977	11
2010299_north	9917-063	Otamadai	KASK1977	12
2010299_north	9917-064	Kasori EII (up to)	KASK1977	13

Continued on next page

Table A.2: Pithouses at Chiba

BUA ID	Pithouse ID	Period	REF	original ID
2010299_north	9917-065	Kasori EII (up to)	KASK1977	14
2010299_north	9917-066	Otamadai	KASK1977	15
2010299_north	9917-067	Otamadai	KASK1977	16
2010299_north	9917-068	Kasori EII (up to)	KASK1977	17
2010299_north	9917-069	Kasori EII (up to)	KASK1977	18
2010299_north	9917-070	Kasori EII (up to)	KASK1977	19
2010299_north	9917-071	Otamadai	KASK1977	20
2010299_north	9917-072	Horinouchi 1	KASK1977	21
2010299_north	9917-073	Kasori EI (up to)	KASK1977	22
2010299_north	9917-074	Kasori EII (up to)	KASK1977	23
2010299_north	9917-075	Pre-Kasori E	KASK1977	24
2010299_north	9917-076	Horinouchi 1	KASK1977	25
2010299_north	9917-077	Kasori EII (up to)	KASK1977	26
2010299_north	9917-078	Kasori EII (up to)	KASK1977	27
2010299_north	9917-079	Kasori EI (up to)	KASK1977	28
2010299_north	9917-080	Katsuzaka	KASK1977	29
2010299_north	9917-081	Kasori EII (up to)	KASK1977	30
2010299_north	9917-082	Otamadai	KASK1977	31
2010299_north	9917-083	Kasori EII	KASK1977	32
2010299_north	9917-084	Otamadai - Kasori EI	KASK1977	33
2010299_north	9917-085	Otamadai - Kasori EI	KASK1977	34
2010299_north	9917-086	Otamadai - Kasori EI	KASK1977	35
2010299_north	9917-087	Kasori EII	KASK1977	36
2010299_north	9917-088	Kasori EI (up to)	KASK1977	37
2010299_north	9917-089	Kasori EII (up to)	KASK1977	38
2010299_north	9917-090	Kasori EII (up to)	KASK1977	39
2010299_north	9917-091	Kasori EII (up to)	KASK1977	40
2010299_north	9917-092	Kasori EII (up to)	KASK1977	41
2010299_north	9917-093	Kasori EI - EII	KASK1977	42
2010299_north	9917-094	Kasori EII (up to)	KASK1977	43
2010299_north	9917-095	Pre-Kasori E	KASK1977	44
2010299_north	9917-096	Kasori EI (up to)	KASK1977	45
2010299_north	9917-097	Kasori EI (up to)	KASK1977	46
2010299_north	9917-098	Kasori EII (up to)	KASK1977	47
2010299_north	9917-099	Angyo 1	KASKIV1971	1
2010299_north	9917-100	Angyo 1	KASKIV1971	2
2010299_north	9917-101	Kasori EII (up to)	KASKIV1971	3
2010299_north	9917-102	Kasori EII (up to)	KASKIV1971	4
2010299_north	9917-103	Kasori EI (up to)	KASKIV1971	5
2010299_north	9917-104	Kasori EI (up to)	KASKIV1971	6
2010299_north	9917-105	Otamadai	KASKIV1971	7

Continued on next page

Table A.2: Pithouses at Chiba

BUA ID	Pithouse ID	Period	REF	original ID
2010299_north	9917-106	Otamadai	KASKIV1971	8
2010299_north	9917-107	Otamadai	KASKIV1971	9
2010299_north	9917-108	Otamadai	KASKIV1971	10
2010299_north	9917-109	Otamadai	KASKIV1971	11
2010299_north	9917-110	Otamadai	KASKIV1971	12
2010299_north	9917-111	Otamadai	KASKIV1971	13
2014004_edited	9918-001	Kasori EIV	CHNEN1989	
2014004_edited	9918-002	Kasori EIV	CHNEN1989	
2011242_edited	9922-001	Kasori EI - EII	MONCHI1986	
2011242_edited	9922-002	Kasori EI - EII	MONCHI1986	
2011242_edited	9922-003	Kasori EI - EII	MONCHI1986	
2011242_edited	9922-004	Kasori EI - EII	MONCHI1986	
2010300_edited	9925-001	Kasori EIII - EIV	CHIBAKEN	
2010300_edited	9925-002	Kasori EIII - EIV	CHIBAKEN	
2010300_edited	9925-003	Kasori EIII - EIV	CHIBAKEN	
2010300_edited	9925-004	Kasori EIII - EIV	CHIBAKEN	
2010300_edited	9925-005	Kasori EIII - EIV	CHIBAKEN	
2010300_edited	9925-006	Kasori EIII - EIV	CHIBAKEN	
2010300_edited	9925-007	Kasori EIII - EIV	CHIBAKEN	
2010300_edited	9925-008	Kasori EIII - EIV	CHIBAKEN	
2010300_edited	9925-009	Kasori EIII - EIV	CHIBAKEN	
2010301_edited	9926-001	Kasori EIII - EIV	NAKNG1986	1
2010301_edited	9926-002	Kasori EIII - EIV	NAKNG1986	3
2010301_edited	9926-003	Kasori EIII - EIV	NAKNG1986	5
2010301_edited	9926-004	Kasori EIII - EIV	NAKNG1986	6
2010309	9929-001	Kasori EIII - EIV	HRGS1984	1
2010309	9929-002	Kasori EIII - EIV	HRGS1984	2
2010309	9929-003	Kasori EIII - EIV	HRGS1984	3
2010309	9929-004	Kasori EIII - EIV	HRGS1984	4
2010309	9929-005	Kasori EIII - EIV	HRGS1984	5
2010309	9929-006	Kasori EIV	HRGS1984	6
2010309	9929-007	Kasori EIV	HRGS1984	7
2010302_edited	9939-001	Middle Jomon (Early)	MONCHI1986	1
2010302_edited	9939-002	Middle Jomon (Early)	MONCHI1986	2
2010302_edited	9939-003	Middle Jomon (Early)	MONCHI1986	3
2010359_edited	9943-001	Horinouchi	HNW2006	
2010359_edited	9943-002	Horinouchi	HNW2006	
2010359_edited	9943-003	Horinouchi	HNW2006	
2010359_edited	9943-004	Horinouchi	HNW2006	
2010359_edited	9943-005	Horinouchi	HNW2006	
2010359_edited	9943-006	Horinouchi	HNW2006	

Continued on next page

Table A.2: Pithouses at Chiba

BUA ID	Pithouse ID	Period	REF	original ID
2010359_edited	9943-007	Horinouchi	HNW2006	
2010359_edited	9943-008	Horinouchi	HNW2006	
2010359_edited	9943-009	Horinouchi	HNW2006	
2010359_edited	9943-010	Horinouchi	HNW2006	
2010359_edited	9943-011	Horinouchi	HNW2006	
2010359_edited	9943-012	Horinouchi	HNW2006	
2010359_edited	9943-013	Horinouchi	HNW2006	
2010359_edited	9943-014	Horinouchi	HNW2006	
2010359_edited	9943-015	Horinouchi	HNW2006	
2010359_edited	9943-016	Horinouchi	HNW2006	
2010359_edited	9943-017	Horinouchi	HNW2006	
2010359_edited	9943-018	Horinouchi	HNW2006	
2010359_edited	9943-019	Horinouchi	HNW2006	
2010359_edited	9943-020	Horinouchi	HNW2006	
2010359_edited	9943-021	Horinouchi	HNW2006	
2010359_edited	9943-022	Horinouchi	HNW2006	
2010359_edited	9943-023	Horinouchi	HNW2006	
2010359_edited	9943-024	Horinouchi	HNW2006	
2010359_edited	9943-025	Horinouchi	HNW2006	
2010359_edited	9943-026	Horinouchi	HNW2006	
2010359_edited	9943-027	Horinouchi	HNW2006	
2010359_edited	9943-028	Horinouchi	HNW2006	
2010377	9948-001	Ukishima III - Okitsu	FRYM1990	1
2010377	9948-002	Ukishima III - Okitsu	FRYM1990	2
2010377	9948-003	Early Jomon (Late) / Kaminoki	FRYM1990	3
2010377	9948-004	Otamadai Ia	FRYM1990	4
2010417_edited	9981-001	Otamadai III	WRBI1982	1
2010417_edited	9981-002	Otamadai I - III	WRBI1982	2
2010417_edited	9981-003	Otamadai	WRBI1982	9
2010417_edited	9981-004	Otamadai III	WRBI1982	12
2010417_edited	9981-005	Jomon	WRBI1982	14
2010417_edited	9981-006	Otamadai III	WRBI1982	15
2010417_edited	9981-007	Otamadai III - IV	WRBI1982	17
2010417_edited	9981-008	Otamadai III	WRBI1982	18
2010417_edited	9981-009	Otamadai III	WRBI1982	19
2010417_edited	9981-010	Otamadai III	WRBI1982	20
2010417_edited	9981-011	Otamadai III	WRBI1982	21
2010417_edited	9981-012	Otamadai III	WRBI1982	24
2010417_edited	9981-013	Otamadai III - IV	WRBI1982	25
2010417_edited	9981-014	Otamadai III	WRBI1982	26
2010417_edited	9981-015	Otamadai III	WRBI1982	29

Continued on next page

Table A.2: Pithouses at Chiba

BUA ID	Pithouse ID	Period	REF	original ID
2010417_edited	9981-016	Otamadai III - IV	WRBI1982	34
2010417_edited	9981-017	Otamadai III - IV	WRBI1982	44
2010417_edited	9981-018	Jomon	WRBI1982	45
2010417_edited	9981-019	Otamadai III - IV	WRBI1982	47
2010417_edited	9981-020	Otamadai III	WRBI1982	49
2010417_edited	9981-021	Jomon	WRBI1982	50
2010417_edited	9981-022	Jomon	WRBI1982	52
2010499_edited	9987-001	Otamadai III - Kasori EI	SHRNKS1979	1
2010499_edited	9987-002	Otamadai III - Kasori EI	SHRNKS1979	3
2010499_edited	9987-003	Otamadai III - Kasori EI	SHRNKS1979	146
2010499_edited	9987-004	Otamadai III - Kasori EI	SHRNKS1979	22
2010499_edited	9987-005	Otamadai III - Kasori EI	SHRNKS1979	102
2010499_edited	9987-006	Otamadai III - Kasori EI	SHRNKS1979	119
2010499_edited	9987-007	Otamadai III - Kasori EI	SHRNKS1979	159
2010499_edited	9987-008	Otamadai III - Kasori EI	SHRNKS1979	143
2010499_edited	9987-009	Otamadai III - Kasori EI	SHRNKS1979	171
2010504_B	9988-001	Horinouchi	CHNEN1990	
2010504_B	9988-002	Jomon	CHNEN1990	
2120879_n	4402-003	Horinouchi	NISMIS2007	6
2120879_n	4402-005	Horinouchi	NISMIS2007	8
2120879_n	4402-006	Horinouchi	NISMIS2007	9
2120879_n	4402-007	Horinouchi	NISMIS2007	17
2120879_n	4402-008	Kasori EIV	NISMIS2007	41
2120879_n	4402-009	Horinouchi	NISMIS2007	42

Table A.3: BUA at Gunma

BUA ID	x	y	Area
49	330159	4032636	320
63	330394	4034278	39
348	330456	4033256	60757
489	329940	4033187	8500
6460	324893	4046220	1500
6494	326790	4043125	11085
6516	324296	4042193	900
6522	323424	4041545	21000
6523	323662	4041994	3000
6544	323761	4042051	5797
6513-h14	324334	4042704	2295
6514-hx	324553	4042690	1959
6543	323748	4042247	8638
6524-I-II	323856	4042265	8521
6524-III	323981	4042339	1944
6525	323818	4041655	6400
6563	324645	4042224	6000
6564	324776	4042398	8371
6570	324288	4042627	2722
6575	324481	4042941	2143
6577-I-II	323342	4042298	8283
6577-III	323546	4042397	1049
6588-1	323709	4041294	16000
6588-III	323628	4041192	1400
6588-IV	323581	4041173	2988
6590-nishi	323030	4040806	130
6595-kita	323194	4040033	4290
6595-kita2	323248	4040135	360
6600-lowerB	323884	4038914	250
6600-lowerACDE	323835	4038998	1200
6601-12	324923	4039069	1100
6601-3	324666	4039316	1000
6602-n	324198	4038763	7144
6602-s	323918	4038582	10282
6603-12	324046	4038370	500
6603-5	324279	4038398	652
6603-h19	324185	4038187	419
6608-edited	324204	4037110	2800
6610-edited	324864	4037789	2212
6611-edited1	325235	4038392	74000
6612-edited	325405	4037694	1600

Continued on next page

Table A.3: BUA at Gunma

BUA ID	x	y	Area
6613-edited	325250	4037164	14989
6614-edited	324807	4037304	108
6616-west	324309	4036985	361
6616-east	324603	4036861	4975
6616-north	324628	4037021	235
6619-edited	325091	4036582	665
6622-edited	324421	4041119	1
6624-rok	324652	4040852	410
6624-nishi	324987	4041106	35
6624-maenaka1234	324470	4040634	7700
6624-maenaka567	324439	4040719	476
6624-maenaka8	324364	4040662	1
6625-kom1	325039	4040624	100
6625-komtak1	324894	4040610	2020
6625-komtak2	324672	4040533	4430
6625-komtak3	324688	4040441	480
6625-komtak4	325000	4040708	34
6625-ueasa	324428	4040184	50
6629-shimo2	325316	4038976	56
6629-mak	325237	4038703	1858
6630-edited	325497	4038655	2500
6631-edited	326030	4038492	24
6582-I	324221	4042869	2077
6582-II	324078	4042813	1666
6586-north	323536	4039881	12606
6586-south	323471	4039725	15416
6633-edited	326240	4039501	3415
6635-higashi	325883	4039702	22
6635-got	326514	4040342	100
6636-edited	325548	4039979	60
6637-edited	325567	4040483	10
6638-edited	325592	4040773	8
6639-nisw	325248	4040958	1686
6639-shir	325625	4041197	7
6640-edited	326072	4040651	1200
6641-edited	326615	4040997	64
6643-nak	327202	4039905	50
6643-zen	327327	4040687	5538
6645-t12	323265	4039641	6600
6717-edited	326983	4039539	266
6749-edited	320754	4044735	469

Continued on next page

Table A.3: BUA at Gunma

BUA ID	x	y	Area
6751-edited	321195	4045153	1618
6761-edited	321446	4044013	2688
6804-edited	321071	4043670	4638
6805-edited	321225	4043684	5063
6806-edited	321441	4043608	3569
6827-edited	320867	4039211	130
6838-edited	321399	4037502	463
6847-edited	319801	4039201	314
6849-kam	321448	4037865	150
6849-ush	321603	4037892	460
6849-ush2	321582	4037942	430
6852-edited	320675	4038228	400
6909-III	320720	4039814	500
6909-IV	320707	4040019	780
6909-V	320767	4039726	11977
6909-VI	320635	4040030	6360
6909-VII	320709	4039694	250
6909-VIII	320693	4040069	800
6913-edited	321259	4039765	2900
6917-edited	321783	4039298	1300
6920-12567812	320533	4039060	338
6920-349	320451	4039080	190
6920-1011	320452	4039167	70
6928-edited	320737	4039254	1135
13556-edited	322709	4043914	2700
6935-AB	320238	4038062	17385
6935-D	320360	4038205	588
6935-EC	320292	4038302	1766
13557-V-VII	322581	4044331	9467
13557-I-IV	322670	4044633	7921
13558-edited	322957	4045156	22286
13559-edited	323101	4045587	2614
13560-edited	322786	4043731	3688
13561-edited	322759	4043481	19025
13562-edited	322488	4043221	5600
13563-edited	322235	4043367	10200
13564-edited	321987	4043474	8200
13565-edited	322146	4041674	8200
13566-edited	322255	4042089	21825
13567-edited	322326	4042410	9145
13568-edited	322394	4042752	18535

Continued on next page

Table A.3: BUA at Gunma

BUA ID	x	y	Area
6964-jomon	322926	4035638	5300
10011-nishi	325813	4035834	1800
10011-kita	326003	4035995	300
10011-higashi	326141	4035914	5000
10011-higashishita	326119	4035779	6500
10011-nishishita	325966	4035674	5000
10012-edited	325754	4035502	6000
10016-edited	326474	4035348	280
10020-edited	326785	4033829	110
10029-ABC	325785	4037705	669
10029-DEF	325722	4037526	638
10030-A	326481	4037720	870
10030-B	326241	4037579	1564
10031-edited	326113	4037373	3808
10091-edited	330633	4037206	5000
10096-edited	326671	4033547	454
10100-II	329347	4037747	1537
10100-I	329249	4037645	3400
10105-edited	326660	4034054	310
10106-edited	330912	4035925	5560
10108-edited	330377	4037723	660
10111-edited	325918	4035209	110
10214-edited	319661	4036258	12
10268-edited	322014	4034275	6540
10273-edited	322018	4034415	11925
10310-A	322058	4033601	10111
10310-B	322096	4033372	16830
10312-edited	322652	4033719	2500
10313-edited	322704	4033563	1400
10317-edited	322771	4033362	8000
10322-edited	322928	4032907	4125
10324-edited	322502	4032832	8000
10333-edited	323056	4032648	1164
6718-edited	320879	4044500	983
6546-edited	325987	4045692	66
10000	327125	4036642	121
10013	326052	4035401	68
10014	325732	4035014	3971
10015	326332	4036257	7000
10023	327223	4033904	397
10044	329303	4033208	550

Continued on next page

Table A.3: BUA at Gunma

BUA ID	x	y	Area
10051	330153	4034849	2247
10076	326228	4035085	80
10077	325926	4034784	983
10078	327411	4035964	20293
10079	327057	4035632	10236
10080	327142	4036033	17162
10094	327027	4037200	500
10095	329212	4032965	2656
10101	328581	4034452	180
10102	327621	4035092	442
10104	327222	4034766	340
10110	331104	4037706	357
10149	319644	4033287	1750
10159	318699	4036341	8000
10332	323356	4032622	635
123	326881	4033401	3160
360	321234	4033464	4130
364	321948	4032529	1500
370	322266	4033130	8000
546	323448	4032458	420
581	331502	4033104	485
6510	325245	4042644	5747
6511	325217	4043076	3055
6515	324515	4041705	600
6519	325453	4042168	2800
6540	324513	4043860	6000
6541	323918	4042818	16000
6542	324338	4043375	1620
6550	323997	4046266	250
6558	324130	4042269	6000
6559	324713	4041794	4000
6567	324668	4042619	1500
6569	323976	4042547	3128
6571	324501	4042513	236
6572	324236	4045954	1230
6576	324823	4042674	261
6580	325274	4042139	371
6615	324836	4037037	2778
6807	321741	4043529	8874
6914	320862	4039623	1977
6919	320428	4039258	57

Continued on next page

Table A.3: BUA at Gunma

BUA ID	x	y	Area
6921	320623	4039278	120
6927	320846	4039347	4142
6931	320648	4039373	150
6937	318900	4038664	2692
9995	327306	4036445	213
10085-edited	327454	4036328	965
10088-edited	329382	4033655	5100
10089-edited	329884	4034313	3500
10090-edited	329536	4033962	1500
6975-edited	320985	4039430	4970
10068-J5	327745	4037716	2195
10068-J1	327589	4037828	15627
10068-J234	327627	4038108	7601
10068-J6	327757	4038038	5213
10084-AB	328685	4037775	15897
10084-EF	328847	4037937	6023

Table A.4: BUA at Chiba

BUA ID	x	y	Area
2010105	420283	3948082	16000
2010189	421570	3944727	14000
2010226	428222	3944818	1508
2010235	428666	3944091	2600
2010239	429106	3944941	627
2010244	422038	3943014	140
2010251	420360	3942873	1650
2010263	420962	3944010	307
2010278	422090	3942681	100
2010280	422132	3943511	48
2010298	423208	3943058	1806
2010309	424633	3943335	5000
2010342	421845	3942570	535
2010349	422651	3942325	2014
2010355	422426	3942439	229
2010357	422158	3942510	1800
2010367	422940	3941334	200
2010377	424572	3942039	4000
2010383	424524	3941160	128
2010399	425597	3941871	640
2010406	426084	3941713	6059
2010427	428420	3941516	6030
2010434	429705	3941947	150
2010441	428720	3942144	200
2010483	421196	3940376	10692
2010485	422090	3939680	33900
2010490	423202	3940112	7110
2010494	423468	3941028	10000
2010503	422483	3940327	200
2010547	429759	3940036	6200
2010568	430646	3939928	2375
2010581	421701	3938966	30401
2010598	422663	3938689	12560
2010652	429182	3938110	824
2010686	430315	3938110	300
2010688	431410	3939345	1220
2010716	433159	3938823	1340
2010728	422767	3937794	800
2010742	425556	3937021	110
2010783	429406	3937735	207
2010804	432847	3937615	1300

Continued on next page

Table A.4: BUA at Chiba

BUA ID	x	y	Area
2010806	432512	3937734	2100
2010810	432475	3937144	7110
2010857	423822	3935405	15000
2010861	424297	3935775	51000
2010870	425329	3935333	45000
2010871	424977	3935235	10265
2010873	424644	3935423	7000
2010882	427143	3935393	1550
2010887	426878	3935130	10000
2010906	428711	3935637	200
2010943	430021	3935212	210
2010985	423879	3934476	19700
2010988	423092	3934885	616
2010992	425639	3934335	10664
2010994	424061	3934769	18000
2010995	424930	3934775	10750
2010998	425430	3934482	4000
2011006	425011	3934495	1000
2011011	425201	3934372	30000
2011020	426670	3934282	1000
2011032	428722	3934937	4050
2011036	429798	3934483	4795
2011040	428928	3934375	600
2011041	429714	3934630	5428
2011054	429869	3934265	10725
2011143	432364	3934616	9950
2011223	423846	3935003	58000
2011227	421365	3934323	825
2011244	421593	3945902	4255
2011248	426466	3937155	1000
2011258	422033	3938632	600
2011266	423118	3941355	1900
2014000	422250	3943593	8700
2014002	422075	3943693	200
2014006	424925	3941377	1450
2014010	428236	3939134	500
2014011	427989	3942449	218
2014012	431871	3942762	240
2014013	431780	3943213	2150
2014014	431280	3943262	25003
2014016	432040	3942686	21270

Continued on next page

Table A.4: BUA at Chiba

BUA ID	x	y	Area
2014017	432214	3942565	17000
2014018	431763	3942916	150
2014019	431433	3943405	26557
2014021	432140	3937095	5311
2014023	432147	3936663	1170
2014024	432275	3936881	1125
2016001	425556	3937237	356
2120389	429788	3948462	50
2120410	428507	3949020	1600
2120413	428229	3949112	494
2120460	430143	3947288	4505
2120469	429343	3946290	360
2120483	429794	3945857	1640
2120484	429488	3945744	24100
2120577	431524	3945148	332
2120582	430938	3945395	12100
2120584	430780	3945724	315
2120592	431438	3946281	120
2120593	431446	3945961	650
2120610	431140	3946695	496
2120660	432152	3949087	1836
2120794	431230	3947636	530
2120807	431734	3947569	1800
2120809	431271	3948036	2000
2120811	431551	3948348	33000
2120812	431769	3948225	118900
2120814	431515	3947750	4500
2120815	432012	3948292	11450
2120816	432121	3947639	30938
2120817	431803	3948540	19494
2120818	432119	3948462	18700
2120821	431379	3947849	6850
2120880	431843	3942963	3500
2120900	431831	3948692	1500
2280026	426298	3949132	341
2280064	426188	3947538	16
2280066	425315	3947293	2596
2280070	425399	3946695	1322
2280124	427070	3948299	1032
2280128	427894	3948118	2400
2280136	426562	3947683	300

Continued on next page

Table A.4: BUA at Chiba

BUA ID	x	y	Area
2280169	427794	3946348	322
2280190	427861	3944776	300
2280191	427996	3944624	60
2280193	427570	3944453	44900
2280196	427386	3943711	4100
2280197	427257	3943840	620
2280198	426910	3943681	1018
2280208	425650	3947452	792
2120385a	430981	3948784	350
2120385b	430859	3948614	50
2120385c	430981	3948653	2600
2120414a	428463	3949120	1320
2120494_2005	430351	3944625	4671
2120528_10ha	431285	3943861	1135
2120528_11h	431402	3943825	340
2120528_13a	431315	3943779	1255
2120528_14hb	431407	3943718	745
2120529_12h	431694	3943805	1220
2120529_1	431651	3943630	3570
2120529_2	431514	3943492	1860
2120529_14ha15ha	431542	3943679	691
2120531_i	431677	3943538	22353
2120531_rest	431577	3943361	81217
2120533_12	432092	3943493	3946
2120533_3	432032	3943323	9268
2120536a	432307	3943198	6200
2120536b	432289	3942909	9000
2120536c	432494	3942813	6640
2120536d	432443	3943111	434
2120616_1	431591	3947241	475
2120616_23	431798	3947234	376
2120638_1998	432518	3948101	340
2120661_edited	432061	3948845	385
2120677_edited	431331	3948991	7810
2120678_1	430947	3948113	81
2120678_2	431070	3948000	504
2120847_edited	430726	3948564	72
2120873_edited	432898	3948727	223
2120876_edited	432180	3944656	1376
2120879_n	432069	3942946	10346
2120879_s	431973	3942862	9625

Continued on next page

Table A.4: BUA at Chiba

BUA ID	x	y	Area
2120808_edited	431324	3948522	10045
2120810_edited	431495	3948114	4800
2120819_edited	431619	3948621	17700
2120820_edited	431383	3948712	10700
2120813_edited	432014	3947888	57625
2120813_edited2	431756	3947847	660
2280029_edited	427039	3948853	17000
2280030_edited	425774	3948803	70
2280067_edited	425204	3946795	1826
2280068_edited	425446	3947149	420
2280068_edited2	425477	3947349	2020
2280069_edited	425493	3947126	1400
2280069_edited2	425617	3947050	484
2280072_new	424478	3946284	362
2280079_edited	423260	3947526	938
2280110_edited	422143	3948570	47
2280116_I	423900	3946166	75
2280116_II_III	424133	3946346	31525
2280116_IV	424336	3946407	20000
2280117_edited	424500	3946356	12850
2280117_edited2	424434	3946213	1350
2280118_edited	424343	3946097	6430
2280119_edited	424057	3945486	727
2280120_1	424391	3945306	2020
2280120_2	424615	3945519	632
2280122_edited	424957	3945962	11200
2280121_edited	424653	3945938	3902
2280123_edited	426701	3948417	600
2280126_edited	427396	3948676	450
2280141_edited	426258	3946155	210
2280143_edited	425591	3945879	375
2280147_edited	426796	3945856	4600
2280148_edited	426985	3945825	4815
2280155_edited	427091	3946026	7415
2280155_edited2	427179	3946218	2430
2280156_edited	428384	3947509	29830
2280160_edited	428074	3946725	364
2280160_edited2	428170	3946685	950
2280163_1	428597	3947007	13460
2280163_2	428507	3946774	686
2280164_edited	428759	3946830	27750

Continued on next page

Table A.4: BUA at Chiba

BUA ID	x	y	Area
2280167_edited	428180	3946373	790
2280168_edited	428006	3946576	410
2280170_edited	427664	3946247	326
2280180_edited	426873	3945051	6000
2280195_edited	427382	3943970	800
2280201_edited	426701	3943278	1200
2280222_edited	427248	3943559	1153
2300091_edited	433892	3943927	1922
2011259_edited	420208	3942802	1905
2011005_edited	420613	3944892	3100
2010249_edited	420501	3943332	20840
2010188_1	420899	3944871	24400
2010188_2	420872	3945098	5000
2010188_3	421066	3945109	6130
2010188_4	421127	3944967	5000
2010190_edited	421305	3944502	1000
2010195_edited	421123	3944445	5940
2011263_edited	421025	3944341	1090
2010271_h7h9	421352	3943419	6060
2010271_h4h8	421252	3943405	9500
2010271_s58	421070	3943455	1100
2010245_edited	421589	3943017	16800
2010269_1	421048	3943105	29889
2010269_2	421011	3943177	6743
2010269_0	421240	3943208	15184
2010289_s5859	422399	3943739	4300
2010289_IJ	422479	3943622	880
2010289_C	422331	3943727	3000
2010289_G	422492	3943747	168
2010289_ABDEF	422450	3943912	18400
2010289_K	422403	3943648	1397
2014001_1	421795	3943518	7800
2014001_2	421941	3943480	700
2010272_B	422254	3942791	690
2010272_A	422245	3942946	1573
2010277_edited	422685	3942999	2000
2010297_edited	423052	3942886	3724
2010347_edited	423090	3942417	186
2010346_edited	422729	3942614	5262
2010371_edited	422888	3941985	800
2010299_north	424343	3942631	846

Continued on next page

Table A.4: BUA at Chiba

BUA ID	x	y	Area
2010299_south	424285	3942437	7255
2010299_east	424507	3942400	25200
2014004_edited	424108	3942253	3134
2011242_edited	424350	3942997	1850
2010300_edited	424594	3943141	3300
2010301_edited	425715	3942698	5000
2010302_edited	424694	3942871	850
2010351_h3h5	423544	3941559	2245
2010417_edited	426134	3942111	8894
2010499_edited	423723	3939975	10187
2010504_B	425174	3940310	80
2010504_A	425403	3939958	25
2010510_edited	424169	3939726	4200
2010611_edited	425223	3939211	1073
2010625_edited	424793	3939070	3834
2010628_edited	424946	3939295	47
2010509_edited	424533	3939573	1000
2010524_edited1	427330	3939622	760
2010524_edited2	427490	3939518	32150
2010632_edited	427422	3938997	32925
2010633_edited	427899	3939413	3482
2014008_edited	427301	3939177	21000
2014009_edited	427231	3939243	1460
2010523_edited	427549	3940459	583
2010225_edited	429239	3944436	2500
2014015_edited	431550	3942938	8630
2010446_edited	431178	3941822	400
2010451_edited	430609	3941205	1065
2010448_edited	430158	3941658	405
2010422_edited	428496	3941642	3396
2010426_edited	428791	3941428	1387
2010425_edited	428332	3941450	1662
2010439_edited	429885	3941575	6000
2010647_edited	428849	3939162	556
2010785_edited	430236	3937449	250
2010782_edited	429485	3937991	7400
2010692_edited	430801	3939334	120
2010565_edited	431023	3941044	7156
2011245_edited	432545	3941480	1500
2010802_edited	433303	3936700	23000
2010951_edited	433266	3936013	23500

Continued on next page

Table A.4: BUA at Chiba

BUA ID	x	y	Area
2010358_edited	422819	3941484	4807
2011226_edited	423126	3934587	1150
2010475_edited	421927	3940655	2250
2010489_edited	422310	3940241	931
2010478_edited	421253	3939693	2840
2010591_edited	421884	3939105	9669
2011262_edited1	421610	3938688	475
2011262_edited2	421797	3938610	265
2010608_edited	422598	3938970	2330
2010580_edited	421934	3938968	4129
2010592_edited1	422548	3938554	7500
2010592_edited2	422378	3938554	298
2010594_edited	422119	3938786	20709
2010610_edited	422274	3938698	9300
2015000_edited	422592	3938197	130
2010595_edited	422832	3938234	13699
2010720_edited2	422830	3937561	257
2010720_edited1	422622	3937424	11145
2010723_edited	423417	3937681	5000
2010724_edited	423623	3937536	3250
2010731_edited	423688	3937458	2150
2010743_edited	424079	3937220	13055
2010596_edited	423765	3939167	1833
2010597_edited	423700	3939410	350
2010736_edited	424544	3937740	840
2010719_1992	423903	3936750	19909
2010719_200x	424439	3937019	6145
2010836_edited	423000	3936613	413
2010830_edited	421036	3935318	700
2010831_known	423307	3936234	6753
2010831_2	423256	3936122	12468
2010848_north	422866	3936206	5520
2010848_south	422633	3936020	20730
2010859_edited	423562	3936329	2876
2011286_edited	424163	3936394	8100
2010853_edited	423313	3935315	16
2010837_edited	423378	3935422	114
2010854_edited	423425	3935627	176
2010404_edited	423174	3937912	3400
2010867_edited	424780	3935885	7900
2011222_edited	425078	3935638	23000

Continued on next page

Table A.4: BUA at Chiba

BUA ID	x	y	Area
2010832_1	424014	3935772	10000
2010832_2	423944	3935559	20000
2010832_3	423796	3935639	5000
2010832_4	423877	3935781	9000
2010874_edited	424592	3935755	12000
2010865_edited	424890	3935551	29030
2010875_edited	424412	3935287	56380
2010997_edited	424366	3934252	22200
2011008_west	424507	3934540	10000
2011008_east	424722	3934463	33726
2016000_edited	424876	3937240	576
2010735_edited	424996	3937292	211
2010740_edited	425819	3937193	4900
2010756_edited	426152	3937851	3718
2011246_edited	426623	3935191	27000
2016005_edited	426446	3935093	50
2011056_edited	432700	3934587	1153
2010673_sw	431002	3938605	12564
2010673_n	431006	3938857	19794
2010673_c	431105	3938716	3756
2010673_e	431297	3938603	3370
2010673_se	431183	3938376	5784
2120881_a	430301	3944119	6264
2120881_b	430563	3944155	7767
2120881_l	430436	3944026	494
2120881_d	430177	3943751	15100
2120881_c	430248	3943817	13583
2120881_e	430380	3943823	11500
2120881_f	430555	3943837	3654
2120881_g	430742	3943898	2220
2120881_h	430758	3943630	43290
2120881_i	430910	3943678	3845
2120881_j	431120	3943614	1709
2120881_k	431045	3943462	1400
2010386	425097	3941141	200
2011284	422073	3934441	2770
2120468	429031	3946206	330
2010359_edited	424078	3941612	1300
2010381_edited	424914	3941846	2262
2010402_edited	425631	3941371	366
2280199_edited	427016	3943335	9750

Continued on next page

Table A.4: BUA at Chiba

BUA ID	x	y	Area

Table A.5: List of Excavation Reports

REF Id	Year	Institution(s)	Title	Other references
AIOI2000	2000	Chibashi; Chibashi bunkazaichousa kyoukai	Chibashi aioi iseki	
AKGCSJ1993	1993	Fujimimura kyouiku iinkai	Akagi iseki chousenji iseki: fujimichiku isekigun :heisei 3nendo kenei hojou seibi jigyou fujimichiku ni tomonau maizou bunkazai hakkutsu chousa houkokusho	
AKGN1996	1996	Akagimura kyouiku iinkai	Akagimuranai iseki II	
AKGN1997	1997	Akagimura kyouiku iinkai	Akagimuranai iseki III	
AOYG1983	1984	Maebashi shi maizou bunkazai hakkutsu chousadan	Aoyagi yorii isekigun	
ARK1998	1998	Chibashi kyouiku iinkai; Arakuiseki hakkutsu chousadan	Chibaken chibashi araku iseki : hakkutsu chousa houkokusho	
ARKU1989	1989	Chibaken bunkazai sentaa	Chiba kenritsu chuuou hakubutsukan yagai kansatsuchi kensetsu ni tomonau maizou bunkazai hakkutsu chousa houkokusho	
ARKU1989b	1989	Chibaken bunkazai sentaa	Chiba kenritsu chuuou hakubutsukan yagai kansatsuchi kensetsu ni tomonau maizou bunkazai hakkutsu chousa houkokusho	
ARKU1991	1991	Chibaken bunkazai sentaa	Chiba kenritsu chuuou hakubutsukan yagai kansatsuchi kensetsu ni tomonau maizou bunkazai hakkutsu chousa houkokusho	
ARMA1989	1989	Gunmaken kyouiku iinkai; Gunmaken maizoubunkazai chousa jigyoudan	Arima iseki 1; ookubo Biseki	
ARMA1990	1990	Gunmaken kyouiku iinkai; Gunmaken maizoubunkazai chousa jigyoudan	Arima iseki	

Continued on next page

Table A.5: List of Excavation Reports

REF Id	Year	Institution(s)	Title	Other references
ARMDYK1999	1999	Shibukawa shi kyouiku iinkai shyogaigakushuuka	Arima douyama kofungun :heisei 6nendo shidou1341gousen douro kairyou kouji oyobi heisei 9nendo arima kigyou danchi zousei kouji ni tomonau maizou bunkazai hakkutsu chousa heisei7nendo arima kigyou danchi zousei yoteichinai niokeru kakunin chousa houkokusho	
ARMJ1987	1987	Shibukawa shi kyouiku iinkai	Arima haiji ato hakkutsu chousa gaihou	
ARMJ1988	1988	Shibukawa shi kyouiku iinkai	Arima haiji ato: 1986nendo chousa ni tomonau houkokusho	
ARMJRR1983	1983	Shibukawa shi kyouiku iinkai	Arima jouri iseki : okita chiku	
ARMJRR1989	1989	Gunmaken kyouiku iinkai; Gunmaken maizoubunkazai chousa jigyoudan	Arima jyouri iseki	
ARMKBT1997	1997	Shibukawa shi kyouiku iinkai; Shibukawa shi kyouiku iinkai shyogaigakushuuka	Arima kuguumado iseki	
ARMKGT1997	1997	Shibukawa shi kyouiku iinkai; Shibukawa shi kyouiku iinkai shyogaigakushuuka	Arima kokaido iseki	
ARNHND2005	2005	Chibashi kyouiku iinkai; Chibaken kyouiku shinkou zaidan bunkazai sentaa	Arayashikinishi iseki hishinadai iseki : chibashi	
ARYHSN2005	2005	Chibashi kyouiku iinkai; Chibaken kyouiku shinkou zaidan maizou bunkazaichousa sentaa	Arayashikinishi iseki hishinadai iseki : chibashi	
ARYS1976	1976	Chibaken bunkazai sentaa	Chibashi arayashiki kaizuka : kaizuka gaienbu ikou kakunin chousa houkoku	
ARYS1976b	1978	Chibaken bunkazai sentaa	Chibashi arayashiki kaizuka : kaizuka chuuoubu hakkutsu chousa houkoku	

Continued on next page

Table A.5: List of Excavation Reports

REF Id	Year	Institution(s)	Title	Other references
ARYTSM1986	1986	Chibaken bunkazai sentaa	Chibashi arayashiki kita kaizuka yatsugami sumabori iseki : ippan kokudou 51gou kita chiba baipasu kaichiku kouji ni tomonau maizou bunkazai hakkutsu chousa houkokusho	
ASHKB1998	1998	Fujimimura kyouiku iinkai	Asahikubo Biseki :kyoudou juutaku kensetsu ni tomonau maizou bunkazai hakkutsu chousa houkokusho	
ASHTK1985	1985	Hokkitsumura kyouiku iinkai	Asahizuka kofun :hakkutsu chousa no gaiyou	
ATGYSAH1994	1994	Fujimimura kyouiku iinkai	Atagoyama iseki shomuro kofun atago iseki hinata iseki : fujimi chiku isekigun	
AZMTB1998	1998	Fujimimura kyouiku iinkai	Ozawa matoba iseki : jimusho kensetsu ni tomonau maizou bunkazai hakkutsu chousa houkokusho	
BGHS1986	1986	Hokkitsumura kyouiku iinkai	Bungouhassaki iseki	
BOUYS2000	2000	Chibashi bunkazaichousa kyoukai; Chibaken kyouiku shinkou zaidan bunkazai sentaa	Chibashi bouyashiki iseki	
BOUYS2004	2004	Chibaken kyouiku shinkou zaidan bunkazai sentaa	Chibashi bouyashiki iseki	
BOUYT1989	1989	Gunmaken kyouiku iinkai; Gunmaken maizoubunkazai chousa jigyoudan	Bougaito iseki	
BOUYT1992	1992	Gunmaken kyouiku iinkai;Gunmaken maizoubunkazai chousa jigyoudan	Bougaito iseki 1	
BOUYT2001	2001	Hokkitsumura kyouiku iinkai	Bougaito iseki	
CHBNEWT1	1975	Chibaken bunkazai sentaa	Chiba tounanbu nyuutaun 1	
CHBNEWT10	1982	Chibaken bunkazai sentaa	Chiba tounanbu nyuutaun 10	
CHBNEWT11	1981	Chibaken bunkazai sentaa	Chiba tounanbu nyuutaun 11	
CHBNEWT12	1983	Chibaken bunkazai sentaa	Chiba tounanbu nyuutaun 12	

Continued on next page

Table A.5: List of Excavation Reports

REF Id	Year	Institution(s)	Title	Other references
CHBNEWT14	1983	Chibaken bunkazai sentaa	Chiba tounanbu nyuutaun 14	
CHBNEWT15	1984	Chibaken bunkazai sentaa	Chiba tounanbu nyuutaun 15	
CHBNEWT17	1990	Chibaken bunkazai sentaa	Chiba tounanbu nyuutaun 17	
CHBNEWT18	1992	Chibaken bunkazai sentaa	Chiba tounanbu nyuutaun 18	
CHBNEWT19	1998	Chibaken bunkazai sentaa	Chiba tounanbu nyuutaun 19	
CHBNEWT2	1975	Chibaken bunkazai sentaa	Chiba tounanbu nyuutaun 2	
CHBNEWT21	1999	Chibaken bunkazai sentaa	Chiba tounanbu nyuutaun 21	
CHBNEWT21	1999	Chibaken bunkazai sentaa	Chiba tounanbu nyuutaun 21	
CHBNEWT22	1999	Chibaken bunkazai sentaa	Chiba tounanbu nyuutaun 22	
CHBNEWT25	2002	Chibaken bunkazai sentaa	Chiba tounanbu nyuutaun 25	
CHBNEWT26	2003	Chibaken bunkazai sentaa	Chiba tounanbu nyuutaun 26	
CHBNEWT28	2004	Chibaken bunkazai sentaa	Chiba tounanbu nyuutaun 28	
CHBNEWT3	1975	Chibaken bunkazai sentaa	Chiba tounanbu nyuutaun 3	
CHBNEWT30	2004	Chibaken bunkazai sentaa	Chiba tounanbu nyuutaun 30	
CHBNEWT31	2005	Chibaken bunkazai sentaa	Chiba tounanbu nyuutaun 31	
CHBNEWT32	2005	Chibaken bunkazai sentaa	Chiba tounanbu nyuutaun 32	
CHBNEWT33	2005	Chibaken bunkazai sentaa	Chiba tounanbu nyuutaun 33	
CHBNEWT34	2006	Chibaken bunkazai sentaa	Chiba tounanbu nyuutaun 34	
CHBNEWT35	2006	Chibaken bunkazai sentaa	Chiba tounanbu nyuutaun 35	
CHBNEWT37	2007	Chibaken bunkazai sentaa	Chiba tounanbu nyuutaun 37	
CHBNEWT38	2008	Chibaken bunkazai sentaa	Chiba tounanbu nyuutaun 38	
CHBNEWT40	2008	Chibaken bunkazai sentaa	Chiba tounanbu nyuutaun 40	
CHBNEWT5	1978	Chibaken bunkazai sentaa	Chiba tounanbu nyuutaun 5	
CHBNEWT6	1979	Chibaken bunkazai sentaa	Chiba tounanbu nyuutaun 6	
CHBNEWT7	1979	Chibaken bunkazai sentaa	Chiba tounanbu nyuutaun 7	
CHBNEWT8	1979	Chibaken bunkazai sentaa	Chiba tounanbu nyuutaun 8	

Continued on next page

Table A.5: List of Excavation Reports

REF Id	Year	Institution(s)	Title	Other references
CHBNEWT9	1980	Chibaken bunkazai sentaa	Chiba tounanbu nyuutaun 9	
CHGNS63	1988	Chibashi kyouiku iinkai	Chibashi isekigun hakkustiu chousa houkokusho showa63	
CHIB1976	1976	Chibashi kyouiku iinkai	Chibashi bunkazaichousa houkokusho dai 1 shu	
CHIB1984	1984	Chibashi kyouiku iinkai	Chibashi bunkazai chousa houkoku sho 8	
CHIBAKEN	2007	Chibakenshiryou kenkyuzaidan	Chibaken no rekisi (Genshi Kodai)	
CHIBAS56	1981	Chibaken kyouikuchou bunkaka	Chibaken maizou bunkazai hakkutsuchousa showa56nendo	
CHIBAS60	1985	Chibaken kyouikuchou bunkaka	Chibaken maizou bunkazai hakkutsuchousa showa60nendo	
CHKYUK1983	1984	Chibaken bunkazai sentaa	Washiyatsu iseki kannonzuka iseki yamanokami iseki oomori daiichi iseki aradachi iseki	
CHKYUK1986	1986	Chibaken bunkazai sentaa	Ookita iseki yatsu iseki urisaku iseki ikeda kofungun	
CHNEN1989	1989	Chibashi bunkazaichousa kyoukai	Zaidan houjin chibashi bunkazai chousa kyoukai nenpou 1	
CHNEN1992	1992	Chibashi bunkazaichousa kyoukai	Zaidan houjin chibashi bunkazai chousa kyoukai nenpou 4	
CHNEN1990	1990	Chibashi bunkazaichousa kyoukai	Zaidan houjin chibashi bunkazai chousa kyoukai nenpou 2	
CHNEN1992	1992	Chibashi bunkazaichousa kyoukai	Zaidan houjin chibashi bunkazai chousa kyoukai nenpou 4	
CHNEN1994	1994	Chibashi bunkazaichousa kyoukai	Zaidan houjin chibashi bunkazai chousa kyoukai nenpou 6	
CHNEN1995	1995	Chibashi bunkazaichousa kyoukai	Zaidan houjin chibashi bunkazai chousa kyoukai nenpou 7	

Continued on next page

Table A.5: List of Excavation Reports

REF Id	Year	Institution(s)	Title	Other references
CHNEN1997	1997	Chibashi bunkazaichousa kyoukai	Zaidan houjin chibashi bunkazai chousa kyoukai nenpou 9	
CHNEN1998	1998	Chibashi bunkazaichousa kyoukai	Zaidan houjin chibashi bunkazai chousa kyoukai nenpou 10	
COLON1976	1976	Chibaken bunkazai sentaa	Chibashi honda kenritsu koroniinai iseki	
DAIHT1996	1996	Chibashi bunkazaichousa kyoukai	Daihata iseki	
DAIHT2004	2004	Chibaken kyouiku shinkou zaidan bunkazai sentaa	Chibashi daihata iseki	
DGCH2004	2004	Inbagunshi bunkazai sentaa	Yotsukaidoushi yamanashi nabasamasen maizou bunkazai chousa houkokusho	
DNAT1995	1995	Chibaken bunkazai sentaa	Yotsukaidoushi dounoushiro iseki : shuyou chihoudou hamano yotsukaidou naganumasen juutaku takuchi kanren jigyou ni tomonau maizou bunkazai chousa houkokusho	
DOJO1998	1998	Yoshiokamura kyouiku iinkai	Doujyou iseki	
DOK2001	2001	Hokkitsumura kyouiku iinkai	Doukunmae iseki : kenou dai2 suidou jousuijou kensetsutou ni tomonau hakkutsu chousa houkokusho	
EAUKA1999	1999	Chibashi kyouiku iinkai; Chibashi bunkazaichousa kyoukai	Enokisaku iseki amita iseki utsushino isekigun kairou iseki arayashiki kaizuka : chibashi	
ENOK1992	1992	Chibaken bunkazai sentaa	Chibashi enokisaku iseki	
ETTTMU2001	2001	Chibashi kyouiku iinkai; Chibashi bunkazaichousa kyoukai	Enokisaku iseki tanegayatsu iseki tatebori jouseki takaari iseki miyanoushiro iseki yatou uenodai iseki : chibashi	
FKY2007	2007	Gunmaken maizoubunkazai chousa jigyoudan	Fukiya koujiya iseki	
FKYA2007	2007	Gunmaken maizoubunkazai chousa jigyoudan	Fukiya iseki	

Continued on next page

Table A.5: List of Excavation Reports

REF Id	Year	Institution(s)	Title	Other references
FKYSNK2007	2007	Gunmaken maizoubunkazai chousa jigyoudan	Fukiya mikado iseki	
FRYM1990	1990	Chibashi bunkazaichousa kyoukai	Chibashi furuyama iseki	
GDBS1996	1996	Inbagunshi bunkazai sentaa	Chibaken sakurashi goudoboushita iseki hakkutsu chousa houkokusho : nanbu chuugakkou maizou bunkazai chousa jigyou	
GDBS2004	2004	Inbagunshi bunkazai sentaa	Chibaken sakurashi goudoboushita iseki C chiten: nanbu chuugakkou maizou bunkazai chousa	
GDSM2006	2006	Inbagunshi bunkazai sentaa	Goudo shukumukai iseki : chibaken sakurashi :mawatashikyoku maizou bunkazai chousa	
GHTNK1995	1995	Shibukawa shi kyouiku iinkai; Shibukawa shi kyouiku iinkai shyogaigakushuuka	Miyukida hatakenaka Biseki	
GKN1982	1982	Maebashi shi kyouiku iinkai	Gokan iseki :tenjin shougakkou kensetsu nitomonau maizou bunkazai kakunin chousa gaihou	
GNMY1971	1971	Gunmaken suitochi kairyou chiiki maizou bunkazai chousa iinkai	Gunmaken suitochi kairyou chiiki maizou bunkazai chousa	
GOD1989	1989	Chibaken bunkazai sentaa	Chibashi hamanogawa goudo iseki tei shicchi kaizuka no hakkutsu chousa : toshi shou kasen kaishuu jigyou sokushin hamanogawa ni tomonau maizou bunkazai hakkutsu chousa houkokusho	
GOD1991	1991	Chibashi kyouiku iinkai; Chibashi bunkazai-chousa kyoukai	Chibashi goudo iseki : joumon jidai sou_zenki o shutoshita teishicchi iseki no chousa	
GONO2002	2002	Inbagunshi bunkazai sentaa	Chibaken yotsukaidoushi gouno iseki	
GOT2006	2006	Hokkitsumura kyouiku iinkai	Gotanda iseki	
GUNMA12	1993	Gunmaken maizoubunkazai chousa jigyoudan	Nenpou 12	

Continued on next page

Table A.5: List of Excavation Reports

REF Id	Year	Institution(s)	Title	Other references
GUNMA13	1994	Gunmaken maizoubunkazai chousa jigyoudan	Nenpou 13	
GUNMA14	1995	Gunmaken maizoubunkazai chousa jigyoudan	Nenpou 14	
GUNMA15	1996	Gunmaken maizoubunkazai chousa jigyoudan	Nenpou 15	
GUNMA18	1999	Gunmaken maizoubunkazai chousa jigyoudan	Nenpou 18	
GUNMA21	2002	Gunmaken maizoubunkazai chousa jigyoudan	Nenpou 21	
GUNMA24	2004	Gunmaken maizoubunkazai chousa jigyoudan	Nenpou 24	
GUNMA25	2005	Gunmaken maizoubunkazai chousa jigyoudan	Nenpou 25	
GUNMA26	2007	Gunmaken maizoubunkazai chousa jigyoudan	Nenpou 26	
GUNMA5	1986	Gunmaken maizoubunkazai chousa jigyoudan	Nenpou 5	
GUNMA8	1989	Gunmaken maizoubunkazai chousa jigyoudan	Nenpou 8	
HAG1988	1988	Chibashi bunkazaichousa kyoukai	Chibashi hagawa iseki : hakkutsu chousa houkokusho showa61nendo chousa	
HAG1992	1992	Chibashi kyouiku iinkai	Chibashi hagawa iseki : hakkutsu chousa houkokusho heisei2nendo chousa	
HAG1993	1993	Chibashi kyouiku iinkai	Chibashi hagawa iseki : hakkutsu chousa houkokusho heisei3nendo chousa	

Continued on next page

Table A.5: List of Excavation Reports

REF Id	Year	Institution(s)	Title	Other references
HAG1994	1994	Chibashi kyouiku iinkai	Chibashi hagawa iseki : hakkutsu chousa houkokusho heisei4nendo chousa	
HAG1996	1996	Chibashi kyouiku iinkai	Chibashi hagawa iseki : hakkutsu chousa houkokusho heisei6nendo chousa	
HAG1998	1998	Chibashi kyouiku iinkai	Chibashi hagawa iseki : hakkutsu chousa houkokusho heisei8nendo chousa	
HAG2007	2007	Chibashi kyouiku iinkai; Chibaken kyouiku shinkou zaidan maizou bunkazaichousa sentaa	Chibashi hagawa iseki	
HAGARK1987	1987	Chibashi bunkazaichousa kyoukai	Hagawa iseki ; oota araku iseki	
HCMN2002	2002	Maebashi shi kyouiku iinkai; Maebashi shi kyouiku iinkai bunkazai hogo ka	Shiseki hachimanyama kofun	
HGEASR1984	1984	Maebashi shi kyouiku iinkai	Haga toubu danchi iseki 1	
HGEASR1988	1988	Maebashi shi kyouiku iinkai	Haga toubu danchi iseki 2	
HGEASR1990	1990	Maebashi shi kyouiku iinkai	Haga toubu danchi iseki 3	
HGEASR1998	1998	Maebashi shi maizou bunkazai hakkutsu chousadan	haga toubu danchi iseki :haga toubu juutaku danchi kakuchou jigyou ni tomonau maizou bunkazai hakkutsu chousa houkokusho	
HGEASR2005	2005	Maebashi shi maizou bunkazai hakkutsu chousadan	Haga toubu danchi iseki III	
HGGR1977	1977	Chibashi kyouiku iinkai	Tougorou iseki hakkutsu chousa houkokusho	
HGKH1992	1991	Maebashi shi maizou bunkazai hakkutsu chousadan	Haga kitahara iseki minkan kaihatsu haidenyou hendensho shinsetsu ni tomonau maizou bunkazai hakkutsu chousa gaihou	

Continued on next page

Table A.5: List of Excavation Reports

REF Id	Year	Institution(s)	Title	Other references
HGKMY1990	1990	Maebashi shi maizou bunkazai hakkutsu chousadan	Haga kita kuruwa iseki :juutaku danchi zousei jigyou ni tomonau maizou bunkazai hakkutsu chousa houkokusho	
HGMSS1998	1998	Gunmaken maizoubunkazai chousa jigyoudan	Azumachou sekishita iseki	
HGNOR1994	1994	Maebashi shi kyouiku iinkai	Haga hokubu danchi iseki	
HGNSH1991	1991	Maebashi shi kyouiku iinkai	Haga seibu danchi iseki	
HGTJ1970	1971	Chibaken bunkazai hogo kyoukai	Higashikantou jidoushadou(chiba–naritasen)kankei maizou bunkazai hakkutsu chousa houkokusho	
HKD1999	1999	Hokkitsumura kyouiku iinkai	Hakoda iseki gun(uenohara;sankaku iseki);makabe suwa iseki	
HKDTK2001	2001	Fujimimura kyouiku iinkai	Hikida takazeki iseki :soudensen shinsetsu jigyou ni tomonau maizou bunkazai hakkutsu chousa houkokusho	
HKE1982	1982	Maebashi shi kyouiku iinkai	Hake iseki gun 1	
HKE1984	1984	Maebashi shi kyouiku iinkai	Hake iseki gun 2	
HKR1985	1988	Sunaga kankyou sokutei kabushikigaisha;Maebashi shi kyouiku iinkai	Hikikirizuka iseki :bunjou juutakuchi zousei jigyou ni tomonau maizou bunkazai hakkutsu chousa houkokusho	
HKR1993	1993	Maebashi shi kyouiku iinkai	Hikikirizuka 2iseki minkan kaihatsu takuchi zousei ni sakidatsu maizou bunkazai hakkutsu chousa	
HKSS1982	1982	Tokyo denryoku hokusousen iseki chousa kai	Hokusousen : toukyou denryoku hokusousen secchi kouji ni tomonau maizou bunkazai chousa houkokusho	
HMGU1995	1995	Chibashi bunkazaichousa kyoukai	Chibashi hamaguriyatsuue iseki	
HNDKDMT1991	1991	Shibukawa shi kyouiku iinkai shakai kyouiku ka	Handa kougyou danchi toritsuke douro iseki	

Continued on next page

Table A.5: List of Excavation Reports

REF Id	Year	Institution(s)	Title	Other references
HNDMH1994	1994	Shibukawa shi kyouiku iinkai; Shibukawa shi kyouiku iinkai shyogaigakushuuka	Handa minamihara iseki	
HNDNMH1994	1994	Shibukawa shi kyouiku iinkai shyogaigakushuuka; Gunmaken kigyoukyoku	Handa nakahara minamihara iseki	
HNDTSKJ1996	1996	Shibukawa shi kyouiku iinkai; Shibukawa shi kyouiku iinkai shyogaigakushuuka	Hatsuda tsukijimae iseki	
HNDYKSJ1995	1995	Shibukawa shi kyouiku iinkai; Shibukawa shi kyouiku iinkai shyogaigakushuuka	Handa yakushi iseki	
HNW2006	2006	Chibashi kyouiku iinkai; Chibaken kyouiku shinkou zaidan bunkazai sentaa	Chibashi hanawa kaizuka : kakunin chousa houkoku	
HOKI1993	1993	Hokkitsumura kyouiku iinkai	Sonnai Iseki II	
HOKII1994	1994	Hokkitsumura kyouiku iinkai	Hokkitsumura nai iseki 2	
HOKIII1995	1995	Hokkitsumura kyouiku iinkai	Hokkitsumura nai iseki 3	
HOKIV1996	1996	Hokkitsumura kyouiku iinkai	Hokkitsumura nai iseki 4	
HOKIX2001	2001	Hokkitsumura kyouiku iinkai	Hokkitsumura nai iseki 9	
HOKV1997	1997	Hokkitsumura kyouiku iinkai	Hokkitsumura nai iseki 5	
HOKVI1998	1998	Hokkitsumura kyouiku iinkai	Hokkitsumura nai iseki 6	
HOKVII1999	1999	Hokkitsumura kyouiku iinkai	Hokkitsumura nai iseki 7	
HOKVIII2000	2000	Hokkitsumura kyouiku iinkai	Hokkitsumura nai iseki 8	
HOKX2002	2002	Hokkitsumura kyouiku iinkai	Hokkitsumura nai iseki 10	
HOKXI2004	2004	Hokkitsumura kyouiku iinkai	Hokkitsumura nai iseki 11	
HOKXII2005	2005	Hokkitsumura kyouiku iinkai	Hokkitsumura nai iseki 12	
HOKXIII2006	2006	Hokkitsumura kyouiku iinkai	Hokkitsumura nai iseki 13	
HOMESI2003	2003	Chibashi kyouiku iinkai; Chibaken kyouiku shinkou zaidan bunkazai sentaa	Horinouchijou ato menyatsu iseki shihota iseki :chibashi	

Continued on next page

Table A.5: List of Excavation Reports

REF Id	Year	Institution(s)	Title	Other references
HONDTAK1990	1991	Chibaken bunkazai sentaa	Chibashi honda takada kaizuka kakunin chousa houkokusho	
HRGS1984	1984	Chibashi iseki chousa kai	Hirogasaku iseki : chousa houkoku	
HRIS1988	1988	Yoshiokamura kyouiku iinkai	Hiraishi isekigun hakkutsu chousa houkokusho	
HRKT2004	2004	Chibashi kyouiku iinkai; Chibaken kyouiku shinkou zaidan maizou bunkazaichousa sentaa	Chibashi koshikawato iseki	
HRKW1988	1988	Chibashi bunkazaichousa kyoukai	Hirakawa isekigun : hakkutsu chousa houkokusho	
HRMN1992	1992	Fujimimura kyouiku iinkai	Hiromen iseki :kogurechiku isekigun :heisei 2nendo kenei hojou seibi jigyou minechiku ni tomonau maizou bunkazai hakkutsu chousa gaiyou houkokusho	
HRNGSW1998	1998	Fujimimura kyouiku iinkai	Haranogou unagizawa iseki : jimusho koujou kensetsu ni tomonau maizou bunkazai hakkutsu chousa houkokusho	
HSNA1969	1969	-	-	Goto,K., and Atsushi, T. ”ChibashiHirayamamachi Hishinakaizuka Chousagaihou”, Kaizukahakubutsukankiyou 2, pp18-38
HSUY1990	1990	Hokkitsumura kyouiku iinkai	Higashishino iseki uriyama iseki : shouwa63nendo kenei fujimi kitatachibana chiku hojou seibi jigyou ni tomonau maizou bunkazai hakkutsu chousa houkokusho	
HSYT1978	1978	Chibaken bunkazai sentaa	Sakurashi hoshinoyatsu iseki	
HTKN2000	2000	Yoshiokamura kyouiku iinkai	Hatakenaka iseki	
HTMTSH2003	2003	Akagimura kyouiku iinkai	Mitachimine iseki 2takizawa hinatabori iseki : joumon jidai zenki chuuki kofun jidai nara heian jidai shuurakutou no chousa	

Continued on next page

Table A.5: List of Excavation Reports

REF Id	Year	Institution(s)	Title	Other references
HTND1990	1990	Chibashi kyouiku iinkai; Chibashi bunkazai-chousa kyoukai	Chibashi hetanodai kaizuka	
HTSY1986	1986	Chibaken bunkazai sentaa	Chibashi heta sanya iseki : chibaken shouni iryou sentaa kashou kensetsu yoteichinai maizou bunkazai chousa houkokusho	
HTYIG1977	1977	Chibaken bunkazai sentaa	Higashiterayama ishigami iseki	
IAI1983	1983	Chibashi iseki chousa kai	Iai iseki hakkutsu chousa houkokusho	
ICHHRAJ1999	1999	Chibaken bunkazai sentaa	Ichiharashi ichihara jourisei iseki :higashikantou jidoushadou chiba futtsusen ichihara shidou 80gousen maizou bunkazai chousahoukokusho	
IHSIH2003	2003	Chibashi kyouiku iinkai; Chibaken kyouiku shinkou zaidan maizou bunkazaichousa sentaa	Chibashi inohanajou ato saraike higashi iseki	
IIDAD2003	2005	Inbagunshi bunkazai sentaa	Iizuka arachidai iseki : chibaken sakurashi :chiba risaachipaaku kaihatsu jigyou yoteichinai maizou bunkazai chousa 3 : kashou chiba risaachipaaku jigyou kanren douro seibi jigyou yoteichinai maizou bunkazai chousa	
IKMUK1995	1995	Chibaken bunkazai sentaa	Sakurashi ikemukai iseki	
INHJ1999	1999	Chibashi kyouiku iinkai; Chibashi bunkazai-chousa kyoukai	Chibashi inohanajou ato	
INHJH19	2007	Chibadaigaku koukogaku kenkyushitsu	Chibashi chuuouku inohana jouseki	
INHJSI2003	2003	Chibashi kyouiku iinkai; Chibaken kyouiku shinkou zaidan maizou bunkazaichousa sentaa	Chibashi inohanajou ato saraike higashi iseki	

Continued on next page

Table A.5: List of Excavation Reports

REF Id	Year	Institution(s)	Title	Other references
INRD1990	1991	Chibashi kyouiku iinkai; Chibashi bunkazai-chousa kyoukai	Inaridai iseki	
ISHHE2001	2001	Shibukawa shi kyouiku iinkai	Ishihara higashi isekiEku	
ISHHF2001	2001	Shibukawa shi kyouiku iinkai	Ishihara higashi isekiFku	
ISHHG1997	1997	Shibukawa shi kyouiku iinkai	Ishihara higashi kofungun	
ISHHII1994	1994	Shibukawa shi kyouiku iinkai	Ishihara higashi iseki : kendou shibukawa agatsumasen douro kairyou kouji ni tomonau maizou bunkazai hakkutsu chousa houkokusho	
ISHHIII1995	1995	Shibukawa shi kyouiku iinkai	Ishihara higashi iseki 3	
ISHNKHNKK1993	1993	Shibukawa shi kyouiku iinkai shyo-gaigakushuuka	Ishihara higashi iseki ;nakamura hiyakida iseki ;nakamura kubota iseki :kendou shibukawa agatsumasen douro kairyou kouji ni tomonau maizou bunkazai hakkutsu chousa houkokusho	
ISHNU1986	1986	Shibukawa shi kyouiku iinkai shakai kyouiku ka	Nishiura iseki :ishihara tegawa tochi kairyou jigyou ni tomonau hakkutsu chousa gaihou	
ISHNU1995	1995	Shibukawa shi kyouiku iinkai;Shibukawa shi kyouiku iinkai shyogaigakushuuka	Ishihara nishiura iseki	
ISHSBYM1997	1997	Fujimimura kyouiku iinkai	Ishii shibayama iseki	
ISHSM1995	1995	Shibukawa shi kyouiku iinkai	Ishihara shimizuda iseki: heisei 6nendo toukyou denryoku kabushiki gaisha gunma shiten shibukawa koumusho kensetsu kouji ni tomonau maizou bunkazai hakkutsu chousa houkokusho	
ISHSWNKV2005	2005	Gunmaken maizoubunkazai chousa jigyoudan	Ishihara higashi iseki Dku suwanoki Viseki	
ISMR2006	2006	Gunmaken maizoubunkazai chousa jigyoudan	Fujiya isenomori iseki	

Continued on next page

Table A.5: List of Excavation Reports

REF Id	Year	Institution(s)	Title	Other references
ITYAOA2003	2003	Sanbugunshi bunkazai sentaa	Ikeda maruyama yamaaraku okiaraku iseki	
IWSHTM2001	2002	Maebashi shi maizou bunkazai hakkutsu chousadan	Ogikubo iwashizuka iseki ogikubo higashizume iseki : ogikubo chiku kaihatsu seibi jigyou ni tomonau maizou bunkazai hakkutsu chousa houkokusho	
IWTEN2000	2000	Inbagunshi bunkazai sentaa	Chibaken sakurashi iwatomi enokido iseki	
IWTHG1986	1986	Inbagunshi bunkazai sentaa	Miroku higurashidai iseki iwatomi hagiyama iseki hakkutsu chousa houkokusho	
IWTUYT1983	1983	Sakurashi kyouiku iinkai	Iwatomi urushiyatsu ootashuku	
JNBSHJ1991	1991	Fujimimura kyouiku iinkai	Jinba shoujihara kofungun :fujimi chiku isekigun :heisei gannendo kenei hoba seibi jigyou fujimi chiku ni tomonau maizou bunkazai hakkutsu chousa houkokusho	
JNM1999	1999	Shintoumura kyouiku iinaki	Jyunimae iseki	
JZYM1992	1992	Chibaken bunkazai sentaa	Juutaku toshi seibi koudan chibatera chiku maizou bunkazai hakkutsu chousa houkokusho	
JZYM1993	1993	Chibaken bunkazai sentaa	Juutaku toshi seibi koudan chibatera chiku maizou bunkazai hakkutsu chousa houkokusho	
KAHNY1988	1988	Gunmaken kyouiku iinkai;Gunmaken maizoubunkazai chousa jigyoudan	Katsuhozawa nakayama iseki 1	
KAHNY1989	1989	Gunmaken maizoubunkazai chousa jigyoudan	Katsuhozawa nakayama iseki 2	
KAID1972	1972	Chibashi kasori kaizuka hakubutsukan	Kaizukahakubutsukankiyou	Goto,K. and Atsushi, T. ”Susukiyamaiseki Hakkutsuchousagaihou ”, Kaizukahakubutsukankiyou 5, pp1-17
KAID1981a	1973	-	-	Goto,K., Atsushi, T., and Goto, M. ”Showa 45 46 nendo kasori kaizuka higashi shamen iseki genkai kakuninchousa gaihou ”, Kaizukahakubutsukankiyou 6, pp1-40

Continued on next page

Table A.5: List of Excavation Reports

REF Id	Year	Institution(s)	Title	Other references
KAID1981b	1974	-	-	Goto,K., and Atsushi, T. ”Showa 47 nendo kasoriminami gawa heitanbu dai yonji iseki genkai kakunin chousagai-hou”, Kaizukahakubutsukankiyou 7, pp1-20
KAID1982a	1975	-	-	Goto,K., Atsushi, T. and Iizuka, H. ”Showa 48 nendo ka-sori kaizuka higashi syamen dai5ji hakkutsuchousa gai-hou”, Kaizukahakubutsukankiyou 8, pp1-21
KAIHT1995	1995	Hokkitsumura kyouiku iinkai	Kaihatsu iseki :heisei 5nendo dantaiei hojou seibi jigyou shichihashichiku ni tomonau maizou bunkazai hakkutsu chousa houkokusho	
KAIR1986	1986	Chibashi iseki chousa kai	Kairou iseki hakkutsu chousa houkokusho	
KAIR1996	1996	Chibashi bunkazaichousa kyoukai	Chibashi kairou iseki	
KAIR1997	1997	Chibashi bunkazaichousa kyoukai	Kairou iseki	
KAIR2000	2000	Chibashi bunkazaichousa kyoukai	Chibashi kairou iseki	
KAMMT1998	1988	Shibukawa shi kyouiku iinkai	Jinguuji nishi iseki hakkutsu chousa houkokusho	
KANT21996	1996	Yotsukaidou bunkazai sentaa	Kanezuka No.2 iseki : yotsukaidou NTT idou tsuushin-mou kensetsu yoteichinai maizou bunkazai chousa	
KASK1977	1977	-	-	Sugihara, S. and Takiguchi, H. (Eds.)”Kasorikitakaizuka” Tokyo: Chuoukouronbijyutsushyuppan.
KASKIV1971	1971	-	-	Takeda, M, Takiguchi, H, and Chiba Kasori Kaizuka Hakubutsukan. ”Kasorikaizuka 4”, Chiba: Chibaky-ouiku iinkai.
KASM1976	1976	-	-	Sugihara, S. and Takiguchi, H. (Eds.)”Kasoriminamikaizuka” Tokyo: Chuoukouronbi-jyutsushyuppan.
KDSK1994	1994	Inbagunshi bunkazai sentaa	Kidosaki iseki : onaridai danchi takuchi zousei jigyouch-inai maizou bunkazai chousa	

Continued on next page

Table A.5: List of Excavation Reports

REF Id	Year	Institution(s)	Title	Other references
KECHIBS46	1973	Chibaken toshikousha	Keiyou : keiyou douro dai4ki ippan kokudou16gousen kensetsu kouji ni tomonau maizou bunkazai hakkutsu chousa houkoku 1973	
KEIO1973	1973	Chibashitoshi kousha; Nihon douro koudan tokyo shisha; Kantou chihou shisetsu kyoku	Keiyou : keiyou douro dai4ki ippan kokudou16gousen kensetsu kouji ni tomonau maizou bunkazai hakkutsu chousa houkoku 1973	
KGMA1997	1997	Shibukawa shi kyouiku iinkai	Arima kuguumado iseki	
KITTANO1996	1996	Hokkitsumura kyouiku iinkai	Kitamachi iseki tanoho iseki heisei5_6nendo shuyou chihoudou shibukawa_oogosen tokushu kairyou kouji ni tomonau maizou bunkazai hakkutsu chousa houkokusho	
KMANT2000	2000	Komochimura kyouiku iinkai	Kitamoku ainota iseki :shoukibo tochi kairyou jigyou ni tomonau maizou bunkazai hakkutsu chousa houkokusho	
KMFKZW1993	1993	Chibashi bunkazaichousa kyoukai	Chibashi kamifukamizawa iseki	
KMGT1996	1996	Inbagunshi bunkazai sentaa	Chibaken yachimatashi yonegatouge iseki :yachimata kantoriikurabu zousei ni tomonau maizou bunkazai chousa	
KMHTERMAG1995	1995	Fujimimura kyouiku iinkai	Kamihyakudayama iseki terama iseki magota iseki :kogure chiku isekigun :heisei5nendo kenei hoba seibi jikyou minechiku ni tomonau maizou bunkazai hakkutsu chousa houkokusho	
KMHY1996	1996	Fujimimura kyouiku iinkai	Kamihyakudayama iseki : kogure chiku isekigun	
KMJK1996	1996	Sanbu koukogaku kenkyujyo	Kenritsu monjokan iseki: gunmaken maebashishi	
KMN2000	2000	Chibashi bunkazaichousa kyoukai	Chibashi komasu iseki	
KMNDN1990	1990	Chibashi bunkazaichousa kyoukai	Chibashi kumanodai nishi iseki	

Continued on next page

Table A.5: List of Excavation Reports

REF Id	Year	Institution(s)	Title	Other references
KMNHT1995	1995	Yoshiokamura kyouiku iinkai	Kumano- Hedama iseki	
KMNKHR1996	1996	Sunaga kankyou sokutei kabushikigaisha	Kuminokihara iseki	
KMTRB2007	2007	Chibaken kyouiku shinkou zaidan maizou bunkazaichousa sentaa	Chibashi kamatoribadai iseki	
KMTRSM1998	1998	Maebashi shi maizou bunkazai hakkutsu chousadan; Sunaga kankyou sokutei kabushikigaisha	Kamiizumi tarou sanmae iseki :manshon kensetsu ni tomonau maizou bunkazai hakkutsu chousa houkokusho	
KNCHN1994	1994	Yoshiokamura kyouiku iinkai	Kinchikusai iseki	
KNIST1975	1975	Shibukawa shi kyouiku iinkai	Imaiseitetsu iseki	
KNMHII1997	1997	Shibukawa shi kyouiku iinkai	Kanei maehara2 iseki : heisei8nendo bunjou juu-taku ni tomonau maizou bunkazai hakkutsu chousa houkokusho	
KNZJZYM2004	2004	Chibaken bunkazai sentaa	Chibashi kannonzuka iseki jizouyama iseki 3	
KOMG1978	1978	Komagata iseki chousa dan; Chibaken bunkazai hogo kyoukai	Komagata iseki : dai1ji dai 2ji hakkutsu chousa houkokusho	
KOMGM1984	1984	Chibashi iseki chousa kai	Komagome iseki hakkutsu chousa gaiyou houkoku	
KOSH1968	1968	Hokkitsumura kyouiku iinkai	Komuro iseki	
KOSH2005	2005	Hokkitsumura kyouiku iinkai	Komuro takada iseki I ii :houfuna ibutsu o tomonau joumon jidai chuuki chuuyou chuuki kouhan no oogata kanjou shuuraku sono ichibu no chousa : heisei gannen 1989kojin juutaku kensetsu ni tomonau hakkutsu chousa houkokusho	

Continued on next page

Table A.5: List of Excavation Reports

REF Id	Year	Institution(s)	Title	Other references
KOSH2006	2006	Hokkitsumura kyouiku iinkai	Komuro takada iseki I i II :houfuna ibutsu o tomonau joumon jidai chuuki chuuyou chuuki kouhan no oogata kanjou shuuraku sono ichibu no chousa : heisei gannen 1989kitatachibanamura tochi kaihatsu kousha bunjou juutaku danchi zousei ni tomonau hakkutsu chousa Ii : heisei 2nen1990 minkan bunjou juutaku danchi zousei ni tomonau hakkutsu chousa IIhoukokusho	
KOSM1987	1987	Chibaken dochikaihatsu kousha; Chibaken bunkazai sentaa	Sakurashi koshimaki iseki	
KOYNU2008	2007	Chibaken kyouiku shinkou zaidan bunkazai sentaa	Yotsukaidou koyanouchi iseki 3	
KOYNU2007	2006	Chibaken kyouiku shinkou zaidan bunkazai sentaa	Yotsukaidou koyanouchi iseki 2	
KRKT1984	1984	Shintoumura kyouiku iinaki	Kurakaido iseki	
KROI1990	1991	Komochimura kyouiku iinkai	Kuroimine iseki hakkutsu chousa houkokusho	
KRSW1978	1978	Shibukawa shi kyouiku iinkai	Karasawa iseki	
KRSW1980	1980	Shibukawa shi kyouiku iinkai	Karasawa iseki dainiji suwanoki iseki hakkutsu chousa gaihou	
KRSW1982	1982	Shibukawa shi kyouiku iinkai	Karasawa iseki (dai 3 ji)	
KRSW1985	1985	Shibukawa shi kyouiku iinkai	Karasawa iseki (dai 5 ji) I;J;K;L; chiten hakkutsu chousa gaihou	
KRSW1986	1986	Shibukawa shi kyouiku iinkai shakai kyouiku ka	Karasawa iseki (dai 6 ji) M; N chiten hakkustu chousa houkokusho	
KRSW1987	1987	Shibukawa shi kyouiku iinkai	Karasawa iseki (O chiten)	
KRSW1988	1988	Shibukawa shi kyouiku iinkai	Karasawa iseki P chiten hakkutsu chousa gaihou houkokusho	

Continued on next page

Table A.5: List of Excavation Reports

REF Id	Year	Institution(s)	Title	Other references
KRSW1989	1989	Shibukawa shi kyouiku iinkai	Karasawa iseki Q;R;S chiten hakkustu chousa houokokusho	
KRSW1990	1990	Shibukawa shi kyouiku iinkai shakai kyouiku ka	Karasawa iseki T;U chiten hakkutsu chousa houkokusho	
KRSW1991	1991	Shibukawa shi kyouiku iinkai shakai kyouiku ka	Karasawa iseki V;W;X;Y; chiten hakkutsu chousa houkokusho	
KRSWN2003	2003	Shibukawa shi kyouiku iinkai	Karasawanishi iseki	
KSTINB1981	1982	Gunmaken maizoubunkazai chousa jigyoudan	Kiyosato jinba iseki	
KSTKSN1981	1981	Gunmaken maizoubunkazai chousa jigyoudan	Kiyosato koushinzuka iseki	
KTHMK1999	1999	Akagimura kyouiku iinkai	Katsuhosawa kamisorikubo iseki :karasuyama jidousha seibi koujou kensetsu jigyou ni tomonau maizou bunkazai hakkutsu chousa houkokusho :harunasan futatsudake karuishi ni maibotsushita kofun jidai shuuraku no chousa	
KTMOOG2004	2004	Gunmaken maizoubunkazai chousa jigyoudan	Kitamoku oosakai iseki	
KTNKM1996	1996	Yoshiokamura kyouiku iinkai	Kinchikusai A iseki; nakachou iseki	
KURN1991	1991	Chibaken bunkazai sentaa	Sakurashi kurino 1 2 iseki	
KWBCIM1987	1987	Chibashi kyouiku iinkai; Chibashi bunkazai-chousa kyoukai	Kowashimizu iseki bouchi iseki ichimaita iseki	
KWKBB1998	1998	Shibukawa shi kyouiku iinkai	Kawashima kubouchi baba iseki	
KWKBMN2002	2002	Chibashi kyouiku iinkai; Chibashi bunkazai-chousa kyoukai	Kawasaki iseki ; kusakariba kita iseki ; miso kusano iseki : chibashi	

Continued on next page

Table A.5: List of Excavation Reports

REF Id	Year	Institution(s)	Title	Other references
KWMHK1982	1982	Gunmaken kyouiku iinkai bunkazai hokan ka	Kawamagari iseki ;higashikuden kofun	
KWST1998	1998	Sanbu koukogaku kenkyujyo	Kawashirota iseki	
KYN2005	2006	Shintoumura kyouiku iinaki	Shiseki kayano iseki : hojou seibi jigyou ni tomonau hakkutsu chousa oyobi iseki hani kakunin chousa houkokusho	
MAICH1990	1989	Chibashi kyouiku iinkai	Maizoubunkazaichousa (shinaiisekihun) houkokusho Heisei gannenn	
MAICH1992	1992	Chibashi kyouiku iinkai	Maizoubunkazaichousa (shinaiisekihun) houkokusho Heisei 3nenn	
MAICH1994	1994	Chibashi kyouiku iinkai	Maizoubunkazaichousa (shinaiisekihun) houkokusho Heisei 5nenn	
MAICH1995	1992	Chibashi kyouiku iinkai	Maizoubunkazaichousa (shinaiisekihun) houkokusho Heisei 6nenn	
MAICH1995	1995	Chibashi kyouiku iinkai	Maizoubunkazaichousa (shinaiisekihun) houkokusho Heisei 6nenn	
MAICH1996	1996	Chibashi kyouiku iinkai	Maizoubunkazaichousa (shinaiisekihun) houkokusho Heisei 7nenn	
MAICH1997	1997	Chibashi kyouiku iinkai	Maizoubunkazaichousa (shinaiisekihun) houkokusho Heisei 8nenn	
MAICH1998	1998	Chibashi kyouiku iinkai	Maizoubunkazaichousa (shinaiisekihun) houkokusho Heisei 9nenn	
MAICH1999	1999	Chibashi kyouiku iinkai	Maizoubunkazaichousa (shinaiisekihun) houkokusho Heisei 10nenn	
MAICH2001	2001	Chibashi kyouiku iinkai	Maizoubunkazaichousa (shinaiisekihun) houkokusho Heisei 12nenn	

Continued on next page

Table A.5: List of Excavation Reports

REF Id	Year	Institution(s)	Title	Other references
MATSM1992	1992	Chibaken bunkazai sentaa	Sakurashi matsumukaisaku iseki	
MHDMTD2001	2001	Akagimura kyouiku iinkai	Miharada santanda iseki: joumon jidai zenki kofun jidai shotou heian jidai shuuraku no chousa	
MHHUAN1987	1987	Gunmaken kyouiku iinkai;Gunmaken maizoubunkazai chousa jigyoudan	Miharadajou iseki hatsusaki joushi hatsusakizuka kamiaonashi kofun	
MHRA2002	2002	Yoshiokamura kyouiku iinkai	Maehara iseki	
MHRNKI2004	2004	Akagimura kyouiku iinkai	Miharada nakai iseki :joumon jidai zenki shuurakuato no chousa	
MIHA1990	1990	Gunmaken kigyou kaihatsu ka	Miharada iseki 2	
MIHASW2004a	2004	Akagimura kyouiku iinkai	Miharada suwagami iseki 1	
MIHASW2004b	2004	Akagimura kyouiku iinkai	Miharada suwagami iseki 2	
MIHASW2005a	2005	Akagimura kyouiku iinkai	Miharada suwagami iseki 3	
MIHASW2005b	2005	Akagimura kyouiku iinkai	Miharada suwagami iseki 4	
MIHASWMK2009	2009	Shibukawa shi kyouiku iinkai	Miharada suwagami iseki 5 ;nagumo moromine iseki : joumon jidai chuuki heian jidai shuuraku no chousa	
MINM2001	2001	Chibashi bunkazaichousa kyoukai; Chibashi minamotochou dainijichikuka seirukumikai	Chibashi minamotochou isekigun	
MISOIII1999	1999	Hokkitsumura kyouiku iinkai	Misono iseki	
MITCHK1990	1990	Hokkitsumura kyouiku iinkai	Suisenji chiku isekigun :shouwa62nendo shouwa63nendo dantaiei suisenji chiku hojou seibi jigyou oyobi heisei gannendo kokko hojo jigyou ni tomonau maizou bunkazai chousa houkokusho	
MIYMIA1992	1992	Inbagunshi bunkazai sentaa	Miyamoto miyanoushiro iseki Bchiku hakkutsu chousa houkokusho	

Continued on next page

Table A.5: List of Excavation Reports

REF Id	Year	Institution(s)	Title	Other references
MIYMIA2001	2001	Inbagunshi bunkazai sentaa	Miyamoto miyanoushiro iseki Bchiku : odei saisei shori sentaa kensetsu jigyou ni tomonau maizou bunkazai chousa	
MIYU1998	1998	Inbagunshi bunkazai sentaa	Chibaken sakurashi miyauchi idosaku iseki Ichiku	
MIYU2003	2003	Inbagunshi bunkazai sentaa	Miyauchi idosaku iseki hakkutsu chousa gaihou: chiba risaachi paaku kaihatsu jigyou yoteichinai maizou bunkazai chousa	
MIYU2009	2009	Inbagunshi bunkazai sentaa	Miyauchi idosaku iseki: chibaken sakurashi	
MKAE1991	1991	Chibashi bunkazaichousa kyoukai	Hirakawachou mukee iseki dainiji chousa hakkutsu chousa houkokusho	
MKBMK1995	1995	Hokkitsumura kyouiku iinkai	Makabe mukouyama iseki : bunjou juutaku kyoudou ju-utaku kensetsu ni tomonau maizou bunkazai hakkutsu chousa houkokusho	
MKDS61	1986	Chibashi iseki chousa kai	Mukoudai iseki hakkutsu chousa houkoku	
MKIWTNYI1987	1987	Fujimimura kyouiku iinkai	Mukoufuppari iseki ;iwanoshita iseki ; tanaka iseki ; yorii iseki : fujimi isekigun :shouwa 6061nendo kenei hojou seibijigyou fujimi chiku ni kakawaru maizou bunkazai hakkutsu chousa houkokusho	
MKNDARKU2006	2006	Chibaken kyouiku shinkou zaidan	Chibashi nakanodai iseki araku iseki 4	
MMKF1987	1987	Chibaken dochikaihatsu kousha; Chibaken bunkazai sentaa	Sakurashi mukaiyamayatsu mishirodai kidoba furuuchi iseki	
MNHR1993	1993	Chibaken bunkazai sentaa	Sakurashi minamihiro iseki	
MNKM1985	1985	Chibashi iseki chousa kai	Minami kanmyou iseki hakkutsu chousa houkokusho	
MNM1987	1987	Inbagunshi bunkazai sentaa	Mochikusa miyanomae iseki hakkutsu chousa houkokusho	

Continued on next page

Table A.5: List of Excavation Reports

REF Id	Year	Institution(s)	Title	Other references
MNMNK1985	1985	Maebashi shi maizou bunkazai hakkutsu chousadan	Minamitanokuchi iseki :suidoukyoku haisuijou shisetsu kensetsu ni tomonau maizou bunkazai hakkutsu chousa houkoku	
MNSK2007	2007	Inbagunshi bunkazai sentaa	Minamisaku iseki : chibaken yotsukaidoushi	
MONCHI1986	1986	Chibaken bunkazai sentaa	Chiba toshi monoreeru kankei maizou bunkazai hakkutsu chousa houkokusho : gominoki iseki tonoyama horikome iseki tsuiheijijou ato nesaki iseki kyougandai iseki yanagisawa iseki	
MORY1986	1987	Hokkitsumura kyouiku iinkai	Moriyama iseki	
MRTHTT1985	1985	Chibaken bunkazai sentaa	Chibashi murata hattori iseki : ippan kokudou16gou murata chiku maizou bunkazai hakkutsu chousa houkokusho	
MTAS1998	1998	Akagimura kyouiku iinkai	Miyata atago iseki : ippan kendou shimokuya shibukawasen tandoku tokubetsu douro kairyou jigyou ni tomonau maizou bunkazai hakkutsu chousa houkokusho :harunasan futatsudake karuishi ni maibotsushita kofun jidai saishiato	
MTCA2005b	2005	Akagimura kyouiku iinkai	Mitachi aiyoshi iseki 3	
MTCAS2005	2005	Akagimura kyouiku iinkai	Mitachi aiyoshi iseki 1 2	
MTCH1985	1985	Akagimura kyouiku iinkai	Mitachi tamei iseki mitachi ookubo iseki	
MTCHHACH2008	2008	Shibukawa shi kyouiku iinkai	Mitachi hachiman iseki: joumon jidai zenki kouki shuuraku shuumatsuki kofun no chousa	
MTJK1991	1991	Yoshiokamura kyouiku iinkai	Motojuku iseki hakkutsu chousa houkokusho	
MTJS2005	2005	Akagimura kyouiku iinkai	Mitachi juusanzuka iseki 1_2 :joumon jidai zenki shuuraku no chousa	

Continued on next page

Table A.5: List of Excavation Reports

REF Id	Year	Institution(s)	Title	Other references
MTN1985	1985	Maebashi shi maizou bunkazai hakkutsu chousadan	Minamitanokuchi iseki :suidoukyoku haisuijou shisetsu kensetsu ni tomonau maizou bunkazai hakkutsu chousa houkoku	
MTSGKA1995	1995	Chibashi bunkazaichousa kyoukai	Chibashi matsugaoka iseki	
MTSHMZ2007	2007	Shibukawa shi kyouiku iinkai	Mitachi shimizu iseki :kofun jidai zenki juukyoato tou no chousa	
MTSNKM2004	2004	Akagimura kyouiku iinkai	Miyata suwahara iseki3 neko mochikubo iseki :harunasan funka ni yotte umoreta kofun jidai saishi iseki no chousa	
MTTSB2005	2005	Akagimura kyouiku iinkai	Mitachi tamei2 iseki : kofun jidai houkei shuukoubo no chousa	
MTY1996	1996	Yoshiokamura kyouiku iinkai	Mitsuya kofun:hakkakukeifun no chousa	
MUKH1989	1989	Chibaken bunkazai sentaa	Sakurashi mukaihara iseki	
MUKY1987	1987	Chibashi bunkazaichousa kyoukai	Mukaeyama	
MURAUI1993	1993	Hokkitsumura kyouiku iinkai	Sonnai Iseki I	
MYKDMNM1994	1994	Shibukawa shi kyouiku iinkai	Miyukida nabara iseki	
MYKTYM1987	1987	Shibukawa shi kyouiku iinkai	Miyukidayama iseki	
MYTKBK1995	1995	Akagimura kyouiku iinkai	Miyata kobunoki iseki: ippan kendou shimokuya shibukawasen kinkyuu chihou douro seibi A(kairyou)jigyou ni tomonau maizou bunkazai hakkutsu chousa houkokusho	
MYTSW2005	2005	Akagimura kyouiku iinkai	Miyada suwabara isekiI II : heisei 1314nendo kinkyuu chihou douro seibi Ashimokuya shibukawasen douro kairyou jigyou ni kakaru maizou bunkazai hakkutsu chousa houkokusho :harunasan funka karuishi kazanbai ni maibotsushita kofun jidai saishi iseki	

Continued on next page

Table A.5: List of Excavation Reports

REF Id	Year	Institution(s)	Title	Other references
MYTSW2005b	2005	Akagimura kyouiku iinkai	Miyada suwabara isekiIV : heisei 1617nendo kendou shimokuya shibukawasen douro kairyou jigyou ni kakaru maizou bunkazai kakunin chousa houkokusho :harunasan funka karuishi ni maibotsu shita kofun jidai saishi iseki	
MZRGO2003	2003	Akagimura kyouiku iinkai	Mizorogi oomidou iseki: heisei 1314nendo kenei hatake chitai sougou seibi jigyou ninaite ikuseigata akagi dai2mozorogi chiku ni kakaru maizou bunkazai hakkutsu chousa houkokusho :joumon jidai kouki shotou shuuraku shikiishi juukyoato no chousa	
NAKG2008	2008	Gunmaken maizoubunkazai chousa jigyoudan	Nakagou iseki	
NAKNG1986	1986	Chibaken bunkazai sentaa	Chibashi nakanagi iseki : chiba higashisho kensetsu ni tomonau maizou bunkazai hakkutsu chousa houkokusho	
NAKNS1976	1977	Chibaken bunkazai sentaa	Chibashi nakano soumidou iseki	
NAKSJ1987	1987	Shibukawa shi kyouiku iinkai shakai kyouiku ka; Shibukawa shi kyouiku iinkai	Nakasuji iseki: hakkutsu chousa gaiyou houkokusho	
NAKSJ1988	1988	Shibukawa shi kyouiku iinkai shakai kyouiku ka; Shibukawa shi kyouiku iinkai	Nakasuji iseki: hakkutsu chousa gaiyou houkokusho	
NAKSJ1991	1991	Shibukawa shi kyouiku iinkai shakai kyouiku ka; Shibukawa shi kyouiku iinkai	Nakasuji iseki: hakkutsu chousa gaiyou houkokusho	
NAKSJ1993	1993	Shibukawa shi kyouiku iinkai shakai kyouiku ka; Shibukawa shi kyouiku iinkai	Nakasuji iseki: hakkutsu chousa gaiyou houkokusho	
NAKSJ1995	1995	Shibukawa shi kyouiku iinkai shakai kyouiku ka; Shibukawa shi kyouiku iinkai	Nakasuji iseki: hakkutsu chousa gaiyou houkokusho	

Continued on next page

Table A.5: List of Excavation Reports

REF Id	Year	Institution(s)	Title	Other references
NAKSJ1998	1998	Shibukawa shi kyouiku iinkai shakai kyouiku ka; Shibukawa shi kyouiku iinkai	Nakasuji iseki: hakkutsu chousa gaiyou houkokusho	
NAKSW1986	1986	Gunmaken kyouiku iinkai;Gunmaken maizoubunkazai chousa jigyoudan	Nakaune iseki; suwanishi iseki	
NAKSW2000	2000	Akagimura kyouiku iinkai	Nakaune iseki suwanishi iseki :joumon jidai kouki no shikiishi juukyoato kouki kofun no chousa	
NESK1995	1995	Chibashi bunkazaichousa kyoukai	Chibashi nesaki iseki (I chiku) : heisei 6nendo hakkutsu chousa houkokusho	
NESK1997	1997	Chibashi bunkazaichousa kyoukai	Nezaki iseki	
NESK1999	1999	Chibashi bunkazaichousa kyoukai	Chibashi nezaki iseki : kchiten	
NGKB1981	1986	Gunmaken maizoubunkazai chousa jigyoudan	Kiyosato nagakubo iseki	
NGSK1992	1993	Chibashi bunkazaichousa kyoukai	Chibashi nagasaku kita iseki	
NGSK2009	2009	Yoshiokamura kyouiku iinkai	Nagasawa kofun	
NIHON4	1951	Nihon koukogaku kyoukai	Nihonkoukogaku nenpo 4	
NISMI2006	2006	Inbagunshi bunkazai sentaa	Nishimikado araoi iseki C D chiku ; miyauchi minamidai iseki ; miyauchi imodo iseki :chibaken sakurashi : chiba risaachipaaku kaihatsu jigyou yoteichinai maizou Bunkazai chousa 4	
NISMIM2006	2007	Inbagunshi bunkazai sentaa	Nishimikado myoujindai iseki : chibaken sakurashi : chiba risaachipaaku kaihatsu jigyou yoteichinai maizou bunkazai chousa 5 : kashou chiba risaachipaaku genchi jimusho kensetsu ni tomonau maizou bunkazai chousa	
NISMIS2007	2007	Inbagunshi bunkazai sentaa	Nishimikado shinzutsumi iseki : chibaken sakurashi : chiba risaachipaaku kaihatsu jigyou yoteichinai maizou bunkazai chousa 6	

Continued on next page

Table A.5: List of Excavation Reports

REF Id	Year	Institution(s)	Title	Other references
NISW1992	1992	Hokkitsumura kyouiku iinkai	nishisakawaki iseki : sonei komuro tochi kairyou sougou seibi jigyou ni tomonau maizou bunkazai hakkutsu chousa houkokusho	
NKGD2001	2001	Yoshiokamura kyouiku iinkai	Nakagoshyo iseki	
NKGIKB2006	2006	Gunmaken maizoubunkazai chousa jigyoudan	Nakagou ikubo iseki	
NKGTJ2007	2007	Gunmaken maizoubunkazai chousa jigyoudan	Nakagou tajiri iseki	
NKMR1986	1986	Shibukawa shi kyouiku iinkai	Nakamura iseki	
NKNNH2	1990	Chibaken bunkazai sentaa	Chibashi nakahara kamaato kakunin chousa houkokusho	
NKOKM2001	2001	Shibukawa shi kyouiku iinkai	Nakamura okamae iseki	
NKRSW1996	1996	Chibaken bunkazai sentaa	Chibashi nishikarasawa iseki : kazusa akademia paaku daitai youchi maizou bunkazai chousa houkokusho	
NMMN1999	1999	Gunmaken maizoubunkazai chousa jigyoudan	Numaminami iseki	
NRFNSI1979	1979	Chibaken bunkazai sentaa	Chibashi nagidai fujisawa nakashiba shimizusaku iseki : chiba ooami shirasato yuuryou douro kensetsu kouji ni tomonau chousa	
NSHKM1985	1985	Komochimura kyouiku iinkai	Nishigumi iseki hakkutsu chousa houkokusho	
NSKB1993	1993	Maebashi shi maizou bunkazai hakkutsu chousadan;Sunaga kankyou sokutei kabushikigaisha	Nishikubo iseki: takuchi zousei jigyou ni tomonau maizou bunkazai hakkutsu chousa houkokusho	
NSYSK1979	1979	Chibaken bunkazai sentaa	Chibashi nishiyashiki iseki	
NTN1995	1995	Chibashi bunkazaichousa kyoukai	Chibashi nitona iseki : heisei 4 5nendo chousa houkoku	

Continued on next page

Table A.5: List of Excavation Reports

REF Id	Year	Institution(s)	Title	Other references
OBRM1998	1998	Fujimimura kyouiku iinkai; Shin gijyutsu konsaru	Obarame iseki: fujimi kenshuu danchi zousei kouji ni tomonau maizou bunkazai hakkutsu chousa houkokusho	
OCH1991	1991	Chibashi kyouiku iinkai	Chiba ochaya goten ato : chousa gaihou dai3ji	
OCH1993	1993	Chibashi kyouiku iinkai	Chiba ochaya goten ato : chousa gaihou dai5ji	
OGHSCH1996	1996	Sanbu koukogaku kenkyujyo	Kogure higashi shinchi iseki	
OGRKUC1998	1998	Sunaga kankyou sokutei kabushikigaisha; Fujimimura kyouiku iinkai	Kogure kita ukechi iseki :jiin konryuu ni tomonau maizou bunkazai hakkutsu chousa houkokusho	
OGSN1984	1984	Chibashi iseki chousa kai	Chibaken chibashi oguramachi sannou iseki hakkutsu chousa houkokusho	
OHR1985	1980	Shintoumura kyouiku iinaki	Ohori iseki hakkutsu chousa houkokusho	
OKTKS1982	1982	Yoshiokamura kyouiku iinkai	Ookubo A iseki; takizawa kofun	
OOKBA1986a	1986	Yoshiokamura kyouiku iinkai	Ookubi A iseki 1ku	
OOKBA1986b	1986	Yoshiokamura kyouiku iinkai	Ookubi A iseki 2ku	
OOMC1981	1981	Chibashi kyouiku iinkai	Oomichi iseki	
OOMOY1983	1983	Chibaken bunkazai sentaa	Chibashi oomichi iseki oyumijouseki hakkutsu chousa houkokusho	
OONGSK1998	1998	Inbagunshi bunkazai sentaa	Chibaken sakurashi oota nagasaku iseki :tokubetsu yougo roujin hoomu kensetsu ni tomonau maizou bunkazai chousa dai1ji	
OONGSK2005	2005	Inbagunshi bunkazai sentaa	Chibaken sakurashi oota nagasaku iseki :tokubetsu yougo roujin hoomu kensetsu ni tomonau maizou bunkazai chousa dai2ji	
OOSHT1993	1993	Yoshiokamura kyouiku iinkai	Ooshita iseki hakkutsu chousa houkokusho	
OOSK1990	1990	Chibaken bunkazai sentaa	Sakurashi oosaku iseki	

Continued on next page

Table A.5: List of Excavation Reports

REF Id	Year	Institution(s)	Title	Other references
OOTOOS1978	1978	Nihon bunkazai kenkyujo	Oota ooshinozuka : chibaken sakurashi oota ooshinozuka iseki hakkutsu chousa gaihou	
OSHD22003	2003	Sakurashi kyouiku iinkai	Ooshinozuka nishidai 2goufun : futokutei iseki hakkutsu chousa josei jigyou	
OSHT1987	1987	Komochimura kyouiku iinkai	Oshide iseki hakkutsu chousa gaihou	
OYUMI2000	2000	Chibashi bunkazaichousa kyoukai	Chibashi oyumi jouseki	
OYUMI2001	2001	Chibashi bunkazaichousa kyoukai	Chibashi oyumi jouseki	
OYUMI2002	2002	Chibashi bunkazaichousa kyoukai	Chibashi oyumi jouseki	
RKMAN1993	1993	Sanbu koukogaku kenkyujyo	Rokuman iseki: hakkutsu chousa houkokusho	
RKSB1994	1994	Chibaken bunkazai sentaa	Sakurashi rokujyuubu iseki	
RKTD1997	1997	Hokkitsumura kyouiku iinkai	Rokutanda iseki	
RPNG1997	1997	Akagimura kyouiku iinkai	Roppongi juusanzuka iseki	
SHBA1993	1993	Hokkitsumura kyouiku iinkai	Shibayama iseki : heisei 23nendo kenei fujimi kitatachibana chiku hojou seibi jigyou ni tomonau maizou bunkazai hakkutsu chousa houkokusho	
SHBSHI2008	2008	Shibukawa shi kyouiku iinkai	Shinai iseki I	
SHCM2002	2002	Yoshiokamura kyouiku iinkai	Shimohachiman minami iseki	
SHFJMM1997	1997	Fujimimura kyouiku iinkai	Shinai iseki heisei 8 nendo	
SHFJMM1998	1998	Fujimimura kyouiku iinkai	Shinai iseki heisei 9 nendo	
SHFJMM1999	1999	Fujimimura kyouiku iinkai	Shinai iseki heisei 10 nendo	
SHFJMM2001	2001	Fujimimura kyouiku iinkai	Shinai iseki heisei 12 nendo	
SHFJMM2002	2002	Fujimimura kyouiku iinkai	Shinai iseki heisei 13 nendo	
SHFJMM2003	2003	Fujimimura kyouiku iinkai	Shinai iseki heisei 14 nendo	
SHFKIFKNK1998	1996	Gunmaken maizoubunkazai chousa jigyoudan	Shiroi kitanakamichiII iseki fukiya inukozuka iseki fukiya nakahara iseki	

Continued on next page

Table A.5: List of Excavation Reports

REF Id	Year	Institution(s)	Title	Other references
SHIMYOT1986	1986	Nakanoiseki chousadan	Shimofusanokuni yotsukaidou chiiki no iseki chousa houkokusho : ikenojiri yakataato tozaki yakataato maehiro iseki	
SHINAI2000	1999	Maebashi shi kyouiku iinkai	Shinai iseki hakkutsu chousa houkokusho heisei 11 nendo	
SHIW2004	2004	Inbagunshi bunkazai sentaa	Shikawatashi iseki	
SHKWYMKBT1989	1989	Fujimimura kyouiku iinkai	Shirakawa iseki ;yoshimori iseki; kubota iseki: fujimi chiku isekigun :shouwa62nendo kenei hojou seibijigyou fujimi chiku ni kakaru maizou bunkazai hakkutsu chousa houkokusho	
SHMAI1999	1999	Shintoumura kyouiku iinaki	Shimoarai iseki	
SHMKT2000	2000	Shintoumura kyouiku iinaki	Kiyomizu kaito iseki	
SHMY1990	1990	Gunmaken maizoubunkazai chousa jigyoudan	Shimohakoda mukouyama iseki : ippan kokudou 17gou makabe kousaten kairyou kouji ni tomonau maizou bunkazai hakkutsu chousa houkokusho	
SHNAI1994	1994	Maebashi shi kyouiku iinkai	Shinai iseki hakkutsu chousa houkokusho heisei 6 nendo	
SHNAI1996	1995	Maebashi shi kyouiku iinkai	Shinai iseki hakkutsu chousa houkoku sho heisei 7 nendo	
SHNDN1993	1993	Chibashi kyouiku iinkai	Chibashi shinden iseki	
SHNSH1988	1988	Shibukawa shi kyouiku iinkai	Shinai iseki 1	
SHNSH1989	1989	Shibukawa shi kyouiku iinkai	Shinai iseki 2	
SHNSH1992	1992	Shibukawa shi kyouiku iinkai	Shinai iseki 5	
SHNSH1993	1993	Shibukawa shi kyouiku iinkai	Shinai iseki 6	
SHNSH1994	1994	Shibukawa shi kyouiku iinkai	Shinai iseki 7	
SHNSH1996	1996	Shibukawa shi kyouiku iinkai	Shinai iseki 9	
SHNSH1997	1997	Shibukawa shi kyouiku iinkai	Shinai iseki 10	
SHNSH1998	1998	Shibukawa shi kyouiku iinkai	Shinai iseki 11	

Continued on next page

Table A.5: List of Excavation Reports

REF Id	Year	Institution(s)	Title	Other references
SHNSH1999	1999	Shibukawa shi kyouiku iinkai	Shinai iseki 12	
SHNSH1999	1999	Shibukawa shi kyouiku iinkai	Shinai iseki 12	
SHNSH2000	2000	Shibukawa shi kyouiku iinkai	Shinai iseki 13	
SHNSH2003	2003	Shibukawa shi kyouiku iinkai	Shinai iseki 16	
SHNSH2005	2005	Shibukawa shi kyouiku iinkai	Shinai iseki 18	
SHRAI1998	1998	Gunmaken maizoubunkazai chousa jigyoudan	Shiroi maruiwa iseki shiroi kitanakamichi iseki	
SHRJN2008	2008	Gunmaken maizoubunkazai chousa jigyoudan	Shiroi jyuni iseki	
SHRNKS1979	1979	Chibaken bunkazai sentaa	Chibashi shironokoshi iseki	
SHTKON1986	1986	Yoshiokamura kyouiku iinkai	Nanokaichi iseki ;takizawa kofun; onnazuka iseki	
SHYA1989	1989	Hokkitsumura kyouiku iinkai	Jouyama iseki: shouwa62nendo kenei fujimi kitatachibana chiku hojou seibi jigyou ni tomonau maizou bunkazai hakkutsu chousa houkokusho	
SHYH10	1998	Chibaken bunkazai sentaa	Sasamezawa iseki tanegayatsu iseki oomichi iseki	
SHYM1978	1978	Shinyama iseki hakkutsu chousa dan	Chibashi hirayamachou shinyama iseki hakkutsu chousa gaihou : dosha saishu nitomonau kinkyuu hakkutsu chousa	
SIM2007	2007	Chibaken kyouiku shinkou zaidan maizou bunkazaichousa sentaa	Shiraikedai iseki shintsutsumi iseki myoujindai iseki hayamakoshi iseki ookusadai kofungun kamiyatsu dai1 iseki kamiyatsu dai2 iseki idosaku minami iseki	
SJSG1985	1985	Sanbu koukogaku kenkyujyo	Souja sakuragaoka iseki	
SKGM1994	1994	Fujimimura kyouiku iinkai	Sakagami iseki: fujimi kougyou danchi zousei ni kakaru maizou bunkazai hakkutsu chousa houkokusho	
SKHH1996	1994	Sakurashi kyouiku iinkai	Sakurashi maizou bunkazai hakkutsu chousa houkokusho heisei 6 nendo	

Continued on next page

Table A.5: List of Excavation Reports

REF Id	Year	Institution(s)	Title	Other references
SKHH1991	1990	Sakurashi kyouiku iinkai	Sakurashi maizou bunkazai hakkutsu chousa houkokusho heisei 2 nendo	
SKHH1988	1987	Sakurashi kyouiku iinkai	Sakurashi maizou bunkazai hakkutsu chousa houkokusho showa 62 nendo	
SKHH1989	1988	Sakurashi kyouiku iinkai	Sakurashi maizou bunkazai hakkutsu chousa houkokusho showa 63 nendo	
SKHH1998	1996	Sakurashi kyouiku iinkai	Sakurashi maizou bunkazai hakkutsu chousa houkokusho heisei 8 nendo	
SKHH2000	1998	Sakurashi kyouiku iinkai	Sakurashi maizou bunkazai hakkutsu chousa houkokusho heisei 10 nendo	
SKHH2001	1999	Sakurashi kyouiku iinkai	Sakurashi maizou bunkazai hakkutsu chousa houkokusho heisei 11 nendo	
SKHH2003	2001	Sakurashi kyouiku iinkai	Sakurashi maizou bunkazai hakkutsu chousa houkokusho heisei 13 nendo	
SKHH2004	2002	Sakurashi kyouiku iinkai	Sakurashi maizou bunkazai hakkutsu chousa houkokusho heisei 14 nendo	
SKHH2005	2003	Sakurashi kyouiku iinkai	Sakurashi maizou bunkazai hakkutsu chousa houkokusho heisei 15 nendo	
SKHH2008	2008	Sakurashi kyouiku iinkai	Sakurashi maizou bunkazai hakkutsu chousa houkokusho heisei 18 nendo	
SKHH2009	1997	Sakurashi kyouiku iinkai	Sakurashi maizou bunkazai hakkutsu chousa houkokusho heisei 9 nendo	
SKNSH1988	1988	Shibukawa shi kyouiku iinkai	Sakanoshita iseki hakkutsu chousa houkokusho	
SKT1999	1999	Inbagunshi bunkazai sentaa	Sakado nenbutsuzuka nishi iseki : chibaken sakurashi	
SMYOOM1996	1996	Chibashi bunkazaichousa kyoukai	Chibashi someyatsu iseki oomori dai1 iseki	
SNG1988	1988	Chibashi bunkazaichousa kyoukai	Chibashi sunago iseki	

Continued on next page

Table A.5: List of Excavation Reports

REF Id	Year	Institution(s)	Title	Other references
SNGC1990	1990	Chibashi bunkazaichousa kyoukai	Sunago iseki C-ku	
SNGD1991	1991	Chibashi bunkazaichousa kyoukai	Sunago iseki D-ku	
SNISM2003	2003	Chibashi kyouiku iinkai; Chibaken kyouiku shinkou zaidan bunkazai sentaa	Chibashi miyakochou sannou iseki isamudai iseki	
SNNAB1995	1995	Inbagunshi bunkazai sentaa	Shiraikedai iseki nishimikado araoi iseki A chiku nishimikado araoi iseki B chiku : chiba risaachipaaku kaihatsu jigyou yoteichinai maizou bunkazai chousa 1	
SNNK1990	1990	Tokyo denryoku kanushiki gaisha;Hokkitsumura kyouiku iinkai	Shimonamuro nakoune iseki :tettou kensetsu ni tomonau maizou bunkazai hakkutsu chousa houkokusho	
SNNO2000	2000	Sannou iseki hakkutsu chousadan	Chibaken chibashi sannou iseki : hakkutsu chousa houkokusho	
SNNO1995a	1995	Chibashi bunkazaichousa kyoukai	Sannou iseki	
SNNO1995b	1995	Chibashi bunkazaichousa kyoukai	Sannou iseki	
SNNO2002	2002	Chibashi bunkazaichousa kyoukai	Chibashi miyakochou sannou iseki : heisei13nendo chousa	
STMNGK1986	1986	Gunmaken maizoubunkazai chousa jigyoudan	Kiyosato nagakubo iseki	
SWN1995	1995	Gunmaken kyouiku iinkai	Suwa nishi iseki: shu takasaki shibukawasen baipasu douro kairyou kouji ni kakawaru maizou bunkazai hakkutsu chousa	
SWNK1981	1981	Shibukawa shi kyouiku iinkai shakai kyouiku ka	Suwanoki iseki: hakkutsu chousa houkoku	
SWNKII2000	2000	Shibukawa shi kyouiku iinkai	Suwanoki 2 iseki	
SWNKIII2001	2001	Shibukawa shi kyouiku iinkai	Suwanoki 3iseki: kendou nakamura kamigousen kensetsu kouji ni tomonau maizou bunkazai hakkutsu chousa houkokusho	

Continued on next page

Table A.5: List of Excavation Reports

REF Id	Year	Institution(s)	Title	Other references
SWNKIV2001	2001	Shibukawa shi kyouiku iinkai	Suwanoki6iseki : shidou2544gousen kensetsu kouji ni tomonau maizou bunkazai hakkutsu chousa houkokusho	
SWNKVI2006	2006	Gunmaken maizoubunkazai chousa jigyoudan	Suwanoki 6 iseki	
SWNKVII2003	2003	Shibukawa shi kyouiku iinkai	Suwanoki7iseki : shidou2221gousen kensetsu kouji ni tomonau maizou bunkazai hakkutsu chousa houkokusho	
SWNKVIII-IX2004	2004	Shibukawa shi kyouiku iinkai	Suwanoki 8-9iseki : heisei14nendo to3.3.1nakamura kamigousen kinkyuu chihou douro seibi jigyou A oyobi shidou2139gousen kensetsu kouji ni tomonau maizou bunkazai hakkutsu chousa houkokusho	
SWSONI2004	2004	Chibashi kyouiku iinkai; Chibaken kyouiku shinkou zaidan maizou bunkazaichousa sentaa	Sawa iseki shimonokiri iseki opparaikomi iseki haseshita iseki isamudai iseki : chibashi	
TAKSH2001	2001	Takasaki shi kyouiku iinkai	Takasaki shinai iseki maizou bunkazai	
TANH9	1997	Shibukawa shi kyouiku iinkai	Tanaka iseki	
TAR1985	1985	Chibaken dochikaihatsu kousha; Chibaken bunkazai sentaa	Sakurashi tarukasaku iseki	
TBKTMG2003	2003	Chibashi kyouiku iinkai; Chibaken kyouiku shinkou zaidan bunkazai sentaa	Tabeta kaizuka kaigarazuka iseki muguri iseki	
TBTK2001	2001	Chibashi kyouiku iinkai; Chibashi bunkazaichousa kyoukai	Chibashi tabeta kaizuka	
TCHM1996	1996	Chibadaigaku koukogaku kenkyushitsu	Tachiki minami iseki	
TCYM1983	1983	Chibaken dochikaihatsu kousha	Sakurashi tateyama iseki	
TJMA1987	1987	Hokkitsumura kyouiku iinkai	Gunmaken setagun kitatachibana mura keijimae iseki	

Continued on next page

Table A.5: List of Excavation Reports

REF Id	Year	Institution(s)	Title	Other references
TJRI2005	2005	Komochimura kyouiku iinkai	Tajiri iseki :dai11 chiten :shoukibo tochi kairyou jigyou ni tomonau maizou bunkazai hakkutsu chousa gaiyou houkokusho	
TKJHRK1978	1978	Chibaken bunkazai sentaa	Chibashi tsukijidai kaizuka hirayama kofun	
TKMINHJ2007	2007	Chibashi kyouiku iinkai; Chibaken kyouiku shinkou zaidan maizou bunkazaichousa sentaa	Takadaimukai iseki inohanajou ato : chibashi	
TKSSHIN1987	1987	Inbagunshi bunkazai sentaa	Takasaki shinyama iseki hakkutsu chousa houkokusho	
TKSW1997	1997	Yoshiokamura kyouiku iinkai	Takizawa iseki	
TKZSK2008	2008	Shibukawa shi kyouiku iinkai	Shiseki takizawa sekki jidai iseki	
TKZWNT1998	1998	Fujimimura kyouiku iinkai	Tokizawa nakaya iseki :kyoudou juutaku kensetsu ni tomonau maizou bunkazai hakkutsu chousa houkokusho	
TKZYNG2005	2005	Akagimura kyouiku iinkai	Takizawa yanagihara iseki : joumon jidai zenki shuuraku tou no chousa :heisei 15nendo sonei sougou gurando kensetsu jigyou ni kakaru maizou bunkazai hakkutsu chousa houkokusho :fu _yokonomura kasouba ato	
TMHSTMMS2006	2006	Kokudo kotsuu shou; Gunmaken maizoubunkazai chousa jigyoudan	Tomida hosoda iseki tomida miyashita iseki	
TNGYT1985	1985	Chibaken bunkazai sentaa	Chibashi tanegayatsu iseki : kendou oyumi honnousen douro kensetsu kouji ni tomonau maizou bunkazai hakkutsu chousa houkokusho	
TNGYT1989	1989	Chibaken bunkazai sentaa	Chibashi tanegayatsu iseki	
TNH2001	2001	Hokkitsumura kyouiku iinkai	Tanoho iseki :gunma no suiden nougyou suishin jigyou ni tomonau maizou bunkazai hakkutsu chousa houkokusho	

Continued on next page

Table A.5: List of Excavation Reports

REF Id	Year	Institution(s)	Title	Other references
TNJN1997	1997	Hokkitsumura kyouiku iinkai	Tenjinyama iseki	
TNKTSM1986	1986	Fujimimura kyouiku iinkai	Fujimi isekigun tanakada iseki kubogaido iseki mirume iseki : kenei hojou seibi jigyou fujimichiku ni kakaru maizou bunkazai hakkutsu chousa houkokusho	
TOBS1977	1977	Chibaken bunkazai sentaa	Chibashi higashi terayama tobarisaku iseki : keiyou	
TOBS1998	1998	Chibashi bunkazaichousa kyoukai	Chibashi tobarisaku iseki 1	
TOBS1999	1999	Chibashi bunkazaichousa kyoukai	Chibashi tobarisaku iseki 2	
TOTB2000	2000	Chibashi kyouiku iinkai; Chibashi bunkazai-chousa kyoukai	Chibashi tootsubo iseki	
TOTBS2007	2007	Sunaga kankyou sokutei kabushiki-gaisha;Maebashi shi maizou bunkazai hakkutsu chousadan	Tottori banjo iseki hakkutsu chousa houkokusho	
TOTHRAC2008	2008	Shibukawa shi kyouiku iinkai	Shimotouhara iseki A Cku :heisei 3nen1991nousanbutsu chokubaijo kensetsu ni tomonau hakkutsu chousa Aku :heisei 3nen1991 rekishi minzoku shiryoukan kensetsu ni tomonau hakkutsu chousa Cku houkokusho :joumon jidai zenki shuuraku joumon jidai chuuki shuuraku yayoi jidai kofun jidai zenki shuuraku	
TRFNT1999	1999	Akagimura kyouiku iinkai	Tarufunato iseki : ippan kendou shimokuya shibukawa sen kinkyuu chihou douro seibi Bfumikiri jigyou ni tomonau maizou bunkazai hakkutsu chousa houkokusho :akagisan seiroku ni okeru kofun jidai zenki shuurakuato no chousa	
TRUC1975	1975	Tadao Inoue	Terauchi iseki : futatsugadake fusekisouka no kofun jidai shuuraku	

Continued on next page

Table A.5: List of Excavation Reports

REF Id	Year	Institution(s)	Title	Other references
TRUC1996	1996	Akagimura kyouiku iinkai	Terauchi katsuhosawajou iseki hakkutsu chousa gaihou :sougenji sanmon zousei jigyou ni tomonau terauchi iseki hakkutsu chousa gaihou	
TSKJD2000	2000	Chibashi bunkazaichousa kyoukai	Chibashi tsukijidai kaizuka	
TSKUEA2009	2009	Shibukawa shi kyouiku iinkai	Tsukuda kamiajiro iseki: heian jidai seitetsuro o tomonau shuuraku no chousa	
TSKZ2005	2005	Akagimura kyouiku iinkai	Tsukuda kanezuka kofun: harunasan funka karuishi ni maibotsu shita shoki yokoanashiki sekishitsu kofun	
TSSKMK1997	1997	Akagimura kyouiku iinkai	Nagumo terago iseki tsukuda sakuranoki iseki	
TSTKZ2004	2004	Akagimura kyouiku iinkai	Tsukuda kezouji iseki :chuuseibo tou no chousa	
TZTATNH2005	2005	Akagimura kyouiku iinkai	Takizawa tenjin iseki - A chiten tanashita hibarizuka	
TZTB2005	2005	Akagimura kyouiku iinkai	Takizawa tenjin iseki : B chiten	
TZTCTZEDO2005	2005	Akagimura kyouiku iinkai	Takizawa tenjin iseki - C chiten takizawa edo kubo iseki	
UCHKRD1991	1991	Chibaken bunkazai sentaa	Yotsukaidoushi uchikuroda isekigun : uchikuroda tokutei tochi kukaku seiri jigyouchinai maizou bunkazai hakkutsu chousa houkokusho	
UCHT2008	2008	Inbagunshi bunkazai sentaa	Uchida hayamakoshi iseki : chibaken sakurashi :chiba risaachi paaku kaihatsu jigyou yoteichinai maizou bunkazai chousa 7	
UEMOBTK2005	2005	Akagimura kyouiku iinkai	Kamimiharada oobatake iseki	
UHKUN2006	2006	Hokkitsumura kyouiku iinkai	Kamihakoda uenohara iseki: kokudou353gou yamaguchi baipasu douro kairyou jigyou ni tomonau hakkutsu chousa houkokusho	
UKY2004	2004	Inbagunshi bunkazai sentaa	Ukiya iseki 1 2	

Continued on next page

Table A.5: List of Excavation Reports

REF Id	Year	Institution(s)	Title	Other references
UMHHONM2002	2002	Akagimura kyouiku iinkai	Kamimiharada hinata iseki kamimiharada oomiya iseki kamimiharada nakatsubomae iseki mitachimine iseki 1 : kofun jidai suiden joumon zenki nara heian jidai shuuraku tou no chousa	
UMHHPTMT2002	2002	Akagimura kyouiku iinkai	Kamimiharada hinata iseki kamimiharada oomiya iseki kamimiharada nakatsubomae iseki mitachimine iseki 1 : kofun jidai suiden joumon zenki nara heian jidai shuuraku tou no chousa	
UMHM2001	2001	Akagimura kyouiku iinkai	Kamimiharada higashimine iseki 1	
UMHM2002	2002	Akagimura kyouiku iinkai	Kamimiharada higashimine iseki 2	
UMHNKTT2004	2004	Akagimura kyouiku iinkai	Kamimiharada nakatsubo iseki nakatsubo kobo : joumon jidai zenki shuuraku chuuseibo no chousa	
UMHTK2004	2004	-	-	Kobayashi, O. ”Uwamiharadakaratsuka to Baikakyo”, Gunmakoukogaku techou 14, p43-48
UNDC1993	1993	Inbagunshi bunkazai sentaa	Chibaken yotsukaidoushi ueno iseki deguchi iseki hakkutsu chousa houkokusho :yotsukaidou sougou kouen jigyouchinai maizou bunkazai chousa	
UNRSZ2004	2004	Chibashi kyouiku iinkai; Chibaken kyouiku shinkou zaidan bunkazai sentaa	Unarasuzu iseki	
UNRSZ2001	2001	Chibashi bunkazaichousa kyoukai	Chibashi unarasuzu iseki	
UOMG1985	1985	Chibashi iseki chousa kai	Uchiomago iseki hakkutsu chousa houkokusho	
USRTN2003	2003	Chibaken kyouiku shinkou zaidan maizou bunkazaichousa sentaa	Chibashi ushirodani iseki	
UTNARI2005	2005	Komochimura kyouiku iinkai	Utsuno arise iseki : hani kakunin chousa jigyou ni tomonau maizou bunkazai gaiyou houkokusho	

Continued on next page

Table A.5: List of Excavation Reports

REF Id	Year	Institution(s)	Title	Other references
UTSAH3	1992	Chibaken bunkazai sentaa	Chibashi utsushino kamaato kakunin chousa houkokusho	
WASHYTS2002	2002	Chibaken bunkazai sentaa	Chibashi washiyatsu iseki	
WBOYS1990	1991	Inbagunshi bunkazai sentaa	Warabi oyashiki iseki hakkutsu chousa houkokusho	
WKGO1993	1993	Chibashi bunkazaichousa kyoukai	Chibashi wakagou iseki : heisei 3nendo hakkutsu chousa houkokusho	
WKM1998	1998	Shibukawa shi kyouiku iinkai	Wakamiya iseki : soseki hanchiku o motsu tateana juukyo	
WKSR1987	1987	Shintoumura kyouiku iinaki	Wakebu hachimanshita iseki sarufu shinden iseki	
WRBI1977	1977	Warabidachi iseki hakkutsu chousadan	Warabitachi iseki : chibashi ni okeru hokusousenNo.65 tettou tatekae kouji ni tomonau maizou bunkazai chousa houkokusho	
WRBI1982	1982	-	-	Okazaki, F. and Ishii, S. "Iseki kenkyu ronshu II Warabidachiiseki wo chuushin toshita jomonchuukishotou shuurakuato no kenkyu" Chiba: Isekikenkyukai.
WRBI1991	1991	Inbagunshi bunkazai sentaa	Warabi iseki hakkutsu chousa houkokusho :chibaken yotsukaidoushi : yotsukaidoushi warabichiku maizou bunkazai chousa	
WRYM1986	1986	Inbagunshi bunkazai sentaa	Wariyama iseki : yotsukaidou sougou undou kouen yoteichinai maizou bunkazai chousa houkokusho	
YAMAK2005	2005	Inbagunshi bunkazai sentaa	Yatsuda iseki Aku honchousa dai1 chiten maehara no.2 iseki honchousa dai1 dai2 chiten kidoba iseki honchousa dai1 chiten : chibaken yotsukaidoushi	
YGHKB1997	1997	Shibukawa shi kyouiku iinkai	Yagihara kubo iseki	
YGHOKT1993	1993	Shibukawa shi kyouiku iinkai	Yagihara okita 3 iseki	
YGHOKT1993b	1993	Shibukawa shi kyouiku iinkai	Yagihara okita 4 5 iseki	

Continued on next page

Table A.5: List of Excavation Reports

REF Id	Year	Institution(s)	Title	Other references
YGHOKT1995	1995	Shibukawa shi kyouiku iinkai	Yagihara okita6 iseki : kofun jidai no shuuraku to suiden chousa	
YGHOKT1996	1996	Shibukawa shi kyouiku iinkai	Yagihara okita 7 iseki	
YGHOKT1996b	1996	Shibukawa shi kyouiku iinkai	Yagihara okita 8 9 iseki	
YGHOKT1998	1998	Shibukawa shi kyouiku iinkai	Yagihara okita 10 iseki	
YHG1981	1981	Chibaken bunkazai sentaa	Chibashi yahagi kaizuka	
YHG1994	1994	Chibaken bunkazai sentaa	Chiba jousuijou jounai renrakukan fusetsu kouji ni tomonau maizou bunkazai chousa houkokusho	
YMNKM1989	1989	Chibashi bunkazaichousa kyoukai	Chibashi yamanokami iseki	
YNDD21991	1990	Yotsukaidou kyouiku iinkai	Irinodai dai2 iseki hakkutsu chousa houkokusho	
YOSIG1986	1986	Yotsukaidousjo yoshiokaisekigun chousakai	Yoshioka isekigun : yotsukaidoushi : hakkutsu chousa houkokusho	
YOTSHH1990	1990	Yotsukaidou kyouiku iinkai	Yotsukaidoushinai iseki hakkutsu chousa houkokusho 1990	
YOTSHH1991	1991	Yotsukaidou kyouiku iinkai	Yotsukaidoushinai iseki hakkutsu chousa houkokusho 1991	
YOTSHH1992	1992	Yotsukaidou kyouiku iinkai	Yotsukaidoushinai iseki hakkutsu chousa houkokusho 1992	
YOTSHH1994	1994	Yotsukaidou kyouiku iinkai	Yotsukaidoushinai iseki hakkutsu chousa houkokusho 1994	
YOTSHH1995	1995	Yotsukaidou kyouiku iinkai	Yotsukaidoushinai iseki hakkutsu chousa houkokusho 1995	
YOTSHH1996	1996	Yotsukaidou kyouiku iinkai	Yotsukaidoushinai iseki hakkutsu chousa houkokusho 1996	
YOTSHH1997	1997	Yotsukaidou kyouiku iinkai	Yotsukaidoushinai iseki hakkutsu chousa houkokusho 1997	

Continued on next page

Table A.5: List of Excavation Reports

REF Id	Year	Institution(s)	Title	Other references
YOTSHH1998	1998	Yotsukaidou kyouiku iinkai	Yotsukaidoushinai iseki hakkutsu chousa houkokusho 1998	
YOTSHH1999	1999	Yotsukaidou kyouiku iinkai	Yotsukaidoushinai iseki hakkutsu chousa houkokusho 1999	
YOTSHH2008	2008	Yotsukaidou kyouiku iinkai	Yotsukaidoushinai iseki hakkutsu chousa houkokusho heisei 20 nendo	
YOTSHH2003	2003	Yotsukaidou kyouiku iinkai	Yotsukaidoushinai iseki hakkutsu chousa houkokusho heisei15 nendo	
YOTSHH2000	1999	Yotsukaidou kyouiku iinkai	Yotsukaidoushinai iseki hakkutsu chousa houkokusho heisei 11 nendo	
YOTSHH2001	2003	Yotsukaidou kyouiku iinkai	Yotsukaidoushinai iseki hakkutsu chousa houkokusho 2001	
YOTSHH2003	2002	Yotsukaidou kyouiku iinkai	Yotsukaidoushinai iseki hakkutsu chousa houkokusho heisei 14 nendo	
YOTSHH2003	2003	Yotsukaidou kyouiku iinkai	Yotsukaidoushinai iseki hakkutsu chousa houkokusho 2003	
YOTSHH2003	2003	Yotsukaidoushi kyouiku iinkai	Yotsukaidou shinai iseki chousa hakkutsu houkokusho 2003	
YOTSHH2004	2004	Yotsukaidou kyouiku iinkai	Yotsukaidoushinai iseki hakkutsu chousa houkokusho 2004	
YOTSHH2005	2005	Yotsukaidou kyouiku iinkai	Yotsukaidoushinai iseki hakkutsu chousa houkokusho 2005	
YOTSHH2007	2007	Yotsukaidou kyouiku iinkai	Yotsukaidoushinai iseki hakkutsu chousa houkokusho heisei 18 nendo	
YOTSHH2009	2009	Yotsukaidoushi kyouiku iinkai	Yotsukaidou shinai iseki chousa hakkutsu houkokusho 2009	

Continued on next page

Table A.5: List of Excavation Reports

REF Id	Year	Institution(s)	Title	Other references
YTS1994	1994	Hokkitsumura kyouiku iinkai	Yatsu iseki :bunjou juutaku kensetsu ni tomonau maizou bunkazai hakkutsu chousa houkokusho	
YYMS1987	1987	Inbagunshi bunkazai sentaa	Yotsukaidoushi yotsukaidou minami tochi kukaku seiri jigyouchinai hakkutsu chousa houkokusho :nakayama iseki mizunagare iseki higashihara iseki	
ZNGM2001	2001	Hokkitsumura kyouiku iinkai	Zenigami iseki hakoda isekigun hoi :kenou dai2suidou jousuijou kensetsu tou ni tomonau hakkutsu chousa houkokusho	
ZTK2004	2004	Yoshiokamura kyouiku iinkai	Zentoku iseki :daikibo tenpo kensetsu nitomonau maizou bunkazai hakkutsu chousa	

Table A.6: Aoristic Weights and Pottery Phases

Pottery Phase	B.	t1	t2	t3	t4	t5	t6	t7	t8	t9	t10	t11	t12	t13	t14	t15	t16	t17	t18	t19	t20	t21	t22	t23	t24	t25	t26	t27	t28	t29	t30	t31	t32	t33	t34	t35	t36	t37	A.
12b - 12c	0.00	0.00	0.00	0.00	0.00	0.00	0.00	0.00	0.00	0.00	0.00	0.00	0.00	0.00	0.00	0.00	0.00	0.00	0.00	0.00	0.00	0.00	0.00	0.47	0.53	0.00	0.00	0.00	0.00	0.00	0.00	0.00	0.00	0.00	0.00	0.00	0.00	0.00	0.00
Angyo 1	0.00	0.00	0.00	0.00	0.00	0.00	0.00	0.00	0.00	0.00	0.00	0.00	0.00	0.00	0.00	0.00	0.00	0.00	0.00	0.00	0.00	0.00	0.00	0.00	0.00	0.00	0.00	0.00	0.00	0.00	0.00	0.00	0.00	0.00	0.00	0.00	1.00	0.00	0.00
Angyo 1 - 2	0.00	0.00	0.00	0.00	0.00	0.00	0.00	0.00	0.00	0.00	0.00	0.00	0.00	0.00	0.00	0.00	0.00	0.00	0.00	0.00	0.00	0.00	0.00	0.00	0.00	0.00	0.00	0.00	0.00	0.00	0.00	0.00	0.00	0.00	0.00	0.56	0.44	0.00
Angyo 1 - 3a	0.00	0.00	0.00	0.00	0.00	0.00	0.00	0.00	0.00	0.00	0.00	0.00	0.00	0.00	0.00	0.00	0.00	0.00	0.00	0.00	0.00	0.00	0.00	0.00	0.00	0.00	0.00	0.00	0.00	0.00	0.00	0.00	0.00	0.00	0.00	0.29	0.29	0.43
Angyo 1 - 3b	0.00	0.00	0.00	0.00	0.00	0.00	0.00	0.00	0.00	0.00	0.00	0.00	0.00	0.00	0.00	0.00	0.00	0.00	0.00	0.00	0.00	0.00	0.00	0.00	0.00	0.00	0.00	0.00	0.00	0.00	0.00	0.00	0.00	0.00	0.00	0.22	0.22	0.56
Angyo 2	0.00	0.00	0.00	0.00	0.00	0.00	0.00	0.00	0.00	0.00	0.00	0.00	0.00	0.00	0.00	0.00	0.00	0.00	0.00	0.00	0.00	0.00	0.00	0.00	0.00	0.00	0.00	0.00	0.00	0.00	0.00	0.00	0.00	0.00	0.00	0.00	1.00	0.00
Angyo 2	0.00	0.00	0.00	0.00	0.00	0.00	0.00	0.00	0.00	0.00	0.00	0.00	0.00	0.00	0.00	0.00	0.00	0.00	0.00	0.00	0.00	0.00	0.00	0.00	0.00	0.00	0.00	0.00	0.00	0.00	0.00	0.00	0.00	0.00	0.00	0.00	1.00	0.00
Angyo 2 - 3a	0.00	0.00	0.00	0.00	0.00	0.00	0.00	0.00	0.00	0.00	0.00	0.00	0.00	0.00	0.00	0.00	0.00	0.00	0.00	0.00	0.00	0.00	0.00	0.00	0.00	0.00	0.00	0.00	0.00	0.00	0.00	0.00	0.00	0.00	0.00	0.00	0.35	0.65
Angyo 3	0.00	0.00	0.00	0.00	0.00	0.00	0.00	0.00	0.00	0.00	0.00	0.00	0.00	0.00	0.00	0.00	0.00	0.00	0.00	0.00	0.00	0.00	0.00	0.00	0.00	0.00	0.00	0.00	0.00	0.00	0.00	0.00	0.00	0.00	0.00	0.00	0.04	0.96
Angyo 3a-3b	0.00	0.00	0.00	0.00	0.00	0.00	0.00	0.00	0.00	0.00	0.00	0.00	0.00	0.00	0.00	0.00	0.00	0.00	0.00	0.00	0.00	0.00	0.00	0.00	0.00	0.00	0.00	0.00	0.00	0.00	0.00	0.00	0.00	0.00	0.00	0.00	0.07	0.93
Angyo1, Shinchi,Takaihigashi	0.00	0.00	0.00	0.00	0.00	0.00	0.00	0.00	0.00	0.00	0.00	0.00	0.00	0.00	0.00	0.00	0.00	0.00	0.00	0.00	0.00	0.00	0.00	0.00	0.00	0.00	0.00	0.00	0.00	0.00	0.00	0.00	0.00	0.00	0.00	0.41	0.59	0.00	0.00
Angyo2-3	0.00	0.00	0.00	0.00	0.00	0.00	0.00	0.00	0.00	0.00	0.00	0.00	0.00	0.00	0.00	0.00	0.00	0.00	0.00	0.00	0.00	0.00	0.00	0.00	0.00	0.00	0.00	0.00	0.00	0.00	0.00	0.00	0.00	0.00	0.00	0.00	0.05	0.95
Before Miharada-KasoriE1	0.68	0.02	0.02	0.02	0.02	0.02	0.02	0.02	0.02	0.02	0.02	0.02	0.02	0.02	0.02	0.02	0.02	0.02	0.02	0.02	0.02	0.02	0.00	0.00	0.00	0.00	0.00	0.00	0.00	0.00	0.00	0.00	0.00	0.00	0.00	0.00	0.00	0.00	0.00
Daigi 7b	0.00	0.00	0.00	0.00	0.00	0.00	0.00	0.00	0.00	0.00	0.00	0.00	0.00	0.00	0.00	0.00	0.27	0.33	0.33	0.07	0.00	0.00	0.00	0.00	0.00	0.00	0.00	0.00	0.00	0.00	0.00	0.00	0.00	0.00	0.00	0.00	0.00	0.00	0.00
Early Jomon	0.00	0.07	0.07	0.07	0.07	0.07	0.07	0.07	0.07	0.07	0.07	0.07	0.07	0.07	0.07	0.02	0.00	0.00	0.00	0.00	0.00	0.00	0.00	0.00	0.00	0.00	0.00	0.00	0.00	0.00	0.00	0.00	0.00	0.00	0.00	0.00	0.00	0.00	0.00
Early Jomon - Late Jomon	0.00	0.03	0.03	0.03	0.03	0.03	0.03	0.03	0.03	0.03	0.03	0.03	0.03	0.03	0.03	0.03	0.03	0.03	0.03	0.03	0.03	0.03	0.03	0.03	0.03	0.03	0.03	0.03	0.03	0.03	0.03	0.03	0.03	0.03	0.03	0.03	0.02	0.00
Early Jomon - Middle Jomon	0.00	0.04	0.04	0.04	0.04	0.04	0.04	0.04	0.04	0.04	0.04	0.04	0.04	0.04	0.04	0.04	0.04	0.04	0.04	0.04	0.04	0.04	0.04	0.04	0.01	0.00	0.00	0.00	0.00	0.00	0.00	0.00	0.00	0.00	0.00	0.00	0.00	0.00
Early Jomon (Early)	0.00	0.22	0.22	0.22	0.22	0.11	0.00	0.00	0.00	0.00	0.00	0.00	0.00	0.00	0.00	0.00	0.00	0.00	0.00	0.00	0.00	0.00	0.00	0.00	0.00	0.00	0.00	0.00	0.00	0.00	0.00	0.00	0.00	0.00	0.00	0.00	0.00	0.00
Early Jomon (Final)	0.00	0.00	0.00	0.00	0.00	0.00	0.00	0.00	0.00	0.00	0.00	0.18	0.36	0.36	0.11	0.00	0.00	0.00	0.00	0.00	0.00	0.00	0.00	0.00	0.00	0.00	0.00	0.00	0.00	0.00	0.00	0.00	0.00	0.00	0.00	0.00	0.00	0.00
Early Jomon (Final) - Middle Jomon (Initial)	0.00	0.00	0.00	0.00	0.00	0.00	0.00	0.00	0.00	0.00	0.00	0.14	0.27	0.27	0.27	0.05	0.00	0.00	0.00	0.00	0.00	0.00	0.00	0.00	0.00	0.00	0.00	0.00	0.00	0.00	0.00	0.00	0.00	0.00	0.00	0.00	0.00	0.00
Early Jomon (Final) - Middle Jomon (Middle)	0.00	0.00	0.00	0.00	0.00	0.00	0.00	0.00	0.00	0.00	0.00	0.06	0.12	0.12	0.12	0.12	0.12	0.12	0.12	0.09	0.00	0.00	0.00	0.00	0.00	0.00	0.00	0.00	0.00	0.00	0.00	0.00	0.00	0.00	0.00	0.00	0.00	0.00
Early Jomon (Initial)	0.00	0.22	0.22	0.22	0.22	0.11	0.00	0.00	0.00	0.00	0.00	0.00	0.00	0.00	0.00	0.00	0.00	0.00	0.00	0.00	0.00	0.00	0.00	0.00	0.00	0.00	0.00	0.00	0.00	0.00	0.00	0.00	0.00	0.00	0.00	0.00	0.00	0.00
Early Jomon (Late)	0.00	0.00	0.00	0.00	0.00	0.00	0.00	0.00	0.00	0.00	0.10	0.21	0.21	0.21	0.21	0.06	0.00	0.00	0.00	0.00	0.00	0.00	0.00	0.00	0.00	0.00	0.00	0.00	0.00	0.00	0.00	0.00	0.00	0.00	0.00	0.00	0.00	0.00
Early Jomon (Late) / Kaminoki	0.00	0.00	0.00	0.00	0.00	0.00	0.00	0.00	0.00	0.09	0.17	0.17	0.17	0.17	0.17	0.05	0.00	0.00	0.00	0.00	0.00	0.00	0.00	0.00	0.00	0.00	0.00	0.00	0.00	0.00	0.00	0.00	0.00	0.00	0.00	0.00	0.00	0.00
Early Jomon (Middle)	0.00	0.00	0.00	0.00	0.00	0.00	0.00	0.00	0.00	0.17	0.33	0.33	0.17	0.00	0.00	0.00	0.00	0.00	0.00	0.00	0.00	0.00	0.00	0.00	0.00	0.00	0.00	0.00	0.00	0.00	0.00	0.00	0.00	0.00	0.00	0.00	0.00	0.00
Early Jomon (Middle) - Middle Jomon (Early)	0.00	0.00	0.00	0.00	0.00	0.00	0.00	0.00	0.00	0.06	0.12	0.12	0.12	0.12	0.12	0.12	0.12	0.10	0.00	0.00	0.00	0.00	0.00	0.00	0.00	0.00	0.00	0.00	0.00	0.00	0.00	0.00	0.00	0.00	0.00	0.00	0.00	0.00

Continued on next page

Table A.6: Aoristic Weights and Pottery Phases

Pottery Phase	B.	t1	t2	t3	t4	t5	t6	t7	t8	t9	t10	t11	t12	t13	t14	t15	t16	t17	t18	t19	t20	t21	t22	t23	t24	t25	t26	t27	t28	t29	t30	t31	t32	t33	t34	t35	t36	t37	A.
Early Jomon (Middle) - Middle Jomon (Middle)	0.00	0.00	0.00	0.00	0.00	0.03	0.07	0.07	0.07	0.07	0.07	0.07	0.07	0.07	0.07	0.07	0.07	0.07	0.07	0.07	0.05	0.00	0.00	0.00	0.00	0.00	0.00	0.00	0.00	0.00	0.00	0.00	0.00	0.00	0.00	0.00	0.00	0.00
Final Jomon (Early)	0.00	0.00	0.00	0.00	0.00	0.00	0.00	0.00	0.00	0.00	0.00	0.00	0.00	0.00	0.00	0.00	0.00	0.00	0.00	0.00	0.00	0.00	0.00	0.00	0.00	0.00	0.00	0.00	0.00	0.00	0.00	0.00	0.00	0.00	0.00	0.00	0.04	0.96
Futatsuki	0.00	0.22	0.22	0.22	0.22	0.11	0.00	0.00	0.00	0.00	0.00	0.00	0.00	0.00	0.00	0.00	0.00	0.00	0.00	0.00	0.00	0.00	0.00	0.00	0.00	0.00	0.00	0.00	0.00	0.00	0.00	0.00	0.00	0.00	0.00	0.00	0.00	0.00
Goryogadai	0.00	0.00	0.00	0.00	0.00	0.00	0.00	0.00	0.00	0.00	0.00	0.00	0.00	0.00	0.00	0.78	0.22	0.00	0.00	0.00	0.00	0.00	0.00	0.00	0.00	0.00	0.00	0.00	0.00	0.00	0.00	0.00	0.00	0.00	0.00	0.00	0.00	0.00
Goryogadai - Otamadai Ib (Early)	0.00	0.00	0.00	0.00	0.00	0.00	0.00	0.00	0.00	0.00	0.00	0.00	0.00	0.00	0.00	0.50	0.50	0.00	0.00	0.00	0.00	0.00	0.00	0.00	0.00	0.00	0.00	0.00	0.00	0.00	0.00	0.00	0.00	0.00	0.00	0.00	0.00	0.00
Horinouchi	0.00	0.00	0.00	0.00	0.00	0.00	0.00	0.00	0.00	0.00	0.00	0.00	0.00	0.00	0.00	0.00	0.00	0.00	0.00	0.00	0.00	0.00	0.00	0.00	0.00	0.00	0.00	0.12	0.23	0.23	0.23	0.19	0.00	0.00	0.00	0.00	0.00	0.00
Horinouchi - Kasori B	0.00	0.00	0.00	0.00	0.00	0.00	0.00	0.00	0.00	0.00	0.00	0.00	0.00	0.00	0.00	0.00	0.00	0.00	0.00	0.00	0.00	0.00	0.00	0.00	0.00	0.00	0.00	0.06	0.13	0.13	0.13	0.13	0.13	0.13	0.04	0.00	0.00	0.00
Horinouchi 1	0.00	0.00	0.00	0.00	0.00	0.00	0.00	0.00	0.00	0.00	0.00	0.00	0.00	0.00	0.00	0.00	0.00	0.00	0.00	0.00	0.00	0.00	0.00	0.00	0.00	0.00	0.00	0.19	0.37	0.37	0.07	0.00	0.00	0.00	0.00	0.00	0.00	0.00
Horinouchi 2	0.00	0.00	0.00	0.00	0.00	0.00	0.00	0.00	0.00	0.00	0.00	0.00	0.00	0.00	0.00	0.00	0.00	0.00	0.00	0.00	0.00	0.00	0.00	0.00	0.00	0.00	0.00	0.00	0.00	0.00	0.50	0.50	0.00	0.00	0.00	0.00	0.00	0.00
Horinouchi 2 - Kasori B1	0.00	0.00	0.00	0.00	0.00	0.00	0.00	0.00	0.00	0.00	0.00	0.00	0.00	0.00	0.00	0.00	0.00	0.00	0.00	0.00	0.00	0.00	0.00	0.00	0.00	0.00	0.00	0.00	0.00	0.00	0.27	0.33	0.33	0.07	0.00	0.00	0.00	0.00
Horinouchi, Kasori B, Takaihigashi	0.00	0.00	0.00	0.00	0.00	0.00	0.00	0.00	0.00	0.00	0.00	0.00	0.00	0.00	0.00	0.00	0.00	0.00	0.00	0.00	0.00	0.00	0.00	0.00	0.00	0.00	0.00	0.06	0.12	0.12	0.12	0.12	0.12	0.12	0.12	0.00	0.00	0.00
Initial Jomon	1.00	0.00	0.00	0.00	0.00	0.00	0.00	0.00	0.00	0.00	0.00	0.00	0.00	0.00	0.00	0.00	0.00	0.00	0.00	0.00	0.00	0.00	0.00	0.00	0.00	0.00	0.00	0.00	0.00	0.00	0.00	0.00	0.00	0.00	0.00	0.00	0.00	0.00
Initial Jomon	1.00	0.00	0.00	0.00	0.00	0.00	0.00	0.00	0.00	0.00	0.00	0.00	0.00	0.00	0.00	0.00	0.00	0.00	0.00	0.00	0.00	0.00	0.00	0.00	0.00	0.00	0.00	0.00	0.00	0.00	0.00	0.00	0.00	0.00	0.00	0.00	0.00	0.00
Initial Jomon	1.00	0.00	0.00	0.00	0.00	0.00	0.00	0.00	0.00	0.00	0.00	0.00	0.00	0.00	0.00	0.00	0.00	0.00	0.00	0.00	0.00	0.00	0.00	0.00	0.00	0.00	0.00	0.00	0.00	0.00	0.00	0.00	0.00	0.00	0.00	0.00	0.00	0.00
Initial Jomon - Early Jomon	0.76	0.02	0.02	0.02	0.02	0.02	0.02	0.02	0.02	0.02	0.02	0.02	0.02	0.02	0.02	0.01	0.00	0.00	0.00	0.00	0.00	0.00	0.00	0.00	0.00	0.00	0.00	0.00	0.00	0.00	0.00	0.00	0.00	0.00	0.00	0.00	0.00	0.00
Jomon	0.49	0.01	0.01	0.01	0.01	0.01	0.01	0.01	0.01	0.01	0.01	0.01	0.01	0.01	0.01	0.01	0.01	0.01	0.01	0.01	0.01	0.01	0.01	0.01	0.01	0.01	0.01	0.01	0.01	0.01	0.01	0.01	0.01	0.01	0.01	0.01	0.01	0.11
Jusanboda-Gorogadai-Otamadai-Katsuzaka	0.00	0.00	0.00	0.00	0.00	0.00	0.00	0.00	0.00	0.00	0.00	0.00	0.00	0.00	0.00	0.00	0.17	0.21	0.21	0.21	0.21	0.00	0.00	0.00	0.00	0.00	0.00	0.00	0.00	0.00	0.00	0.00	0.00	0.00	0.00	0.00	0.00	0.00
Jusanbodai-Goryogadai-Katsuzaka1	0.00	0.00	0.00	0.00	0.00	0.00	0.00	0.00	0.00	0.00	0.00	0.00	0.00	0.00	0.14	0.14	0.14	0.14	0.14	0.14	0.14	0.00	0.00	0.00	0.00	0.00	0.00	0.00	0.00	0.00	0.00	0.00	0.00	0.00	0.00	0.00	0.00	0.00
Kasori B	0.00	0.00	0.00	0.00	0.00	0.00	0.00	0.00	0.00	0.00	0.00	0.00	0.00	0.00	0.00	0.00	0.00	0.00	0.00	0.00	0.00	0.00	0.00	0.00	0.00	0.00	0.00	0.00	0.00	0.00	0.00	0.06	0.29	0.29	0.29	0.09	0.00	0.00
Kasori B - Soya	0.00	0.00	0.00	0.00	0.00	0.00	0.00	0.00	0.00	0.00	0.00	0.00	0.00	0.00	0.00	0.00	0.00	0.00	0.00	0.00	0.00	0.00	0.00	0.00	0.00	0.00	0.00	0.00	0.00	0.00	0.00	0.05	0.24	0.24	0.24	0.24	0.00	0.00
Kasori B1	0.00	0.00	0.00	0.00	0.00	0.00	0.00	0.00	0.00	0.00	0.00	0.00	0.00	0.00	0.00	0.00	0.00	0.00	0.00	0.00	0.00	0.00	0.00	0.00	0.00	0.00	0.00	0.00	0.00	0.00	0.00	0.14	0.71	0.14	0.00	0.00	0.00	0.00
Kasori B2	0.00	0.00	0.00	0.00	0.00	0.00	0.00	0.00	0.00	0.00	0.00	0.00	0.00	0.00	0.00	0.00	0.00	0.00	0.00	0.00	0.00	0.00	0.00	0.00	0.00	0.00	0.00	0.00	0.00	0.00	0.00	0.00	0.00	0.53	0.47	0.00	0.00	0.00
Kasori B2 - Soya	0.00	0.00	0.00	0.00	0.00	0.00	0.00	0.00	0.00	0.00	0.00	0.00	0.00	0.00	0.00	0.00	0.00	0.00	0.00	0.00	0.00	0.00	0.00	0.00	0.00	0.00	0.00	0.00	0.00	0.00	0.00	0.00	0.00	0.29	0.36	0.36	0.00	0.00
Kasori B3	0.00	0.00	0.00	0.00	0.00	0.00	0.00	0.00	0.00	0.00	0.00	0.00	0.00	0.00	0.00	0.00	0.00	0.00	0.00	0.00	0.00	0.00	0.00	0.00	0.00	0.00	0.00	0.00	0.00	0.00	0.00	0.00	0.00	0.00	0.50	0.50	0.00	0.00
Kasori E	0.00	0.00	0.00	0.00	0.00	0.00	0.00	0.00	0.00	0.00	0.00	0.00	0.00	0.00	0.00	0.07	0.10	0.10	0.10	0.10	0.10	0.10	0.10	0.10	0.10	0.08	0.00	0.00	0.00	0.00	0.00	0.00	0.00	0.00	0.00	0.00	0.00	0.00
Kasori E	0.00	0.00	0.00	0.00	0.00	0.00	0.00	0.00	0.00	0.00	0.00	0.00	0.00	0.00	0.00	0.07	0.10	0.10	0.10	0.10	0.10	0.10	0.10	0.10	0.10	0.08	0.00	0.00	0.00	0.00	0.00	0.00	0.00	0.00	0.00	0.00	0.00	0.00

Continued on next page

Table A.6: Aoristic Weights and Pottery Phases

Pottery Phase	B.	t1	t2	t3	t4	t5	t6	t7	t8	t9	t10	t11	t12	t13	t14	t15	t16	t17	t18	t19	t20	t21	t22	t23	t24	t25	t26	t27	t28	t29	t30	t31	t32	t33	t34	t35	t36	t37	A.
Kasori E - Shomyoji	0.00	0.00	0.00	0.00	0.00	0.00	0.00	0.00	0.00	0.00	0.00	0.00	0.00	0.00	0.00	0.00	0.00	0.00	0.00	0.00	0.04	0.15	0.15	0.15	0.15	0.15	0.15	0.07	0.00	0.00	0.00	0.00	0.00	0.00	0.00	0.00	0.00	0.00	0.00
Kasori E (Early) / Miharada	0.00	0.00	0.00	0.00	0.00	0.00	0.00	0.00	0.00	0.00	0.00	0.00	0.00	0.00	0.00	0.00	0.00	0.00	0.00	0.00	0.45	0.45	0.09	0.00	0.00	0.00	0.00	0.00	0.00	0.00	0.00	0.00	0.00	0.00	0.00	0.00	0.00	0.00	0.00
Kasori E (Late)	0.00	0.00	0.00	0.00	0.00	0.00	0.00	0.00	0.00	0.00	0.00	0.00	0.00	0.00	0.00	0.00	0.00	0.00	0.00	0.00	0.00	0.00	0.00	0.00	0.53	0.47	0.00	0.00	0.00	0.00	0.00	0.00	0.00	0.00	0.00	0.00	0.00	0.00	0.00
Kasori E1	0.00	0.00	0.00	0.00	0.00	0.00	0.00	0.00	0.00	0.00	0.00	0.00	0.00	0.00	0.00	0.00	0.00	0.00	0.00	0.00	0.50	0.50	0.00	0.00	0.00	0.00	0.00	0.00	0.00	0.00	0.00	0.00	0.00	0.00	0.00	0.00	0.00	0.00	0.00
Kasori E1	0.00	0.00	0.00	0.00	0.00	0.00	0.00	0.00	0.00	0.00	0.00	0.00	0.00	0.00	0.00	0.00	0.00	0.00	0.00	0.00	0.50	0.50	0.00	0.00	0.00	0.00	0.00	0.00	0.00	0.00	0.00	0.00	0.00	0.00	0.00	0.00	0.00	0.00	0.00
Kasori E1 - E2	0.00	0.00	0.00	0.00	0.00	0.00	0.00	0.00	0.00	0.00	0.00	0.00	0.00	0.00	0.00	0.00	0.00	0.00	0.00	0.00	0.20	0.67	0.13	0.00	0.00	0.00	0.00	0.00	0.00	0.00	0.00	0.00	0.00	0.00	0.00	0.00	0.00	0.00	0.00
Kasori E1 (Early)	0.00	0.00	0.00	0.00	0.00	0.00	0.00	0.00	0.00	0.00	0.00	0.00	0.00	0.00	0.00	0.00	0.00	0.00	0.00	0.00	1.00	0.00	0.00	0.00	0.00	0.00	0.00	0.00	0.00	0.00	0.00	0.00	0.00	0.00	0.00	0.00	0.00	0.00	0.00
Kasori E1 / Miharada	0.00	0.00	0.00	0.00	0.00	0.00	0.00	0.00	0.00	0.00	0.00	0.00	0.00	0.00	0.00	0.00	0.00	0.00	0.00	0.00	0.45	0.45	0.09	0.00	0.00	0.00	0.00	0.00	0.00	0.00	0.00	0.00	0.00	0.00	0.00	0.00	0.00	0.00	0.00
Kasori E2	0.00	0.00	0.00	0.00	0.00	0.00	0.00	0.00	0.00	0.00	0.00	0.00	0.00	0.00	0.00	0.00	0.00	0.00	0.00	0.00	0.00	0.78	0.22	0.00	0.00	0.00	0.00	0.00	0.00	0.00	0.00	0.00	0.00	0.00	0.00	0.00	0.00	0.00	0.00
Kasori E2	0.00	0.00	0.00	0.00	0.00	0.00	0.00	0.00	0.00	0.00	0.00	0.00	0.00	0.00	0.00	0.00	0.00	0.00	0.00	0.00	0.00	0.78	0.22	0.00	0.00	0.00	0.00	0.00	0.00	0.00	0.00	0.00	0.00	0.00	0.00	0.00	0.00	0.00	0.00
Kasori E2 - E3 (Early)	0.00	0.00	0.00	0.00	0.00	0.00	0.00	0.00	0.00	0.00	0.00	0.00	0.00	0.00	0.00	0.00	0.00	0.00	0.00	0.00	0.00	0.30	0.43	0.26	0.00	0.00	0.00	0.00	0.00	0.00	0.00	0.00	0.00	0.00	0.00	0.00	0.00	0.00	0.00
Kasori E2-E3	0.00	0.00	0.00	0.00	0.00	0.00	0.00	0.00	0.00	0.00	0.00	0.00	0.00	0.00	0.00	0.00	0.00	0.00	0.00	0.00	0.00	0.20	0.29	0.29	0.23	0.00	0.00	0.00	0.00	0.00	0.00	0.00	0.00	0.00	0.00	0.00	0.00	0.00	0.00
Kasori E3	0.00	0.00	0.00	0.00	0.00	0.00	0.00	0.00	0.00	0.00	0.00	0.00	0.00	0.00	0.00	0.00	0.00	0.00	0.00	0.00	0.00	0.00	0.31	0.38	0.31	0.00	0.00	0.00	0.00	0.00	0.00	0.00	0.00	0.00	0.00	0.00	0.00	0.00	0.00
Kasori E3	0.00	0.00	0.00	0.00	0.00	0.00	0.00	0.00	0.00	0.00	0.00	0.00	0.00	0.00	0.00	0.00	0.00	0.00	0.00	0.00	0.00	0.00	0.31	0.38	0.31	0.00	0.00	0.00	0.00	0.00	0.00	0.00	0.00	0.00	0.00	0.00	0.00	0.00	0.00
Kasori E3 - E4	0.00	0.00	0.00	0.00	0.00	0.00	0.00	0.00	0.00	0.00	0.00	0.00	0.00	0.00	0.00	0.00	0.00	0.00	0.00	0.00	0.00	0.00	0.00	0.33	0.37	0.30	0.00	0.00	0.00	0.00	0.00	0.00	0.00	0.00	0.00	0.00	0.00	0.00	0.00
Kasori E3 - Horinouchi	0.00	0.00	0.00	0.00	0.00	0.00	0.00	0.00	0.00	0.00	0.00	0.00	0.00	0.00	0.00	0.00	0.00	0.00	0.00	0.00	0.00	0.00	0.08	0.10	0.10	0.10	0.10	0.10	0.10	0.10	0.10	0.08	0.00	0.00	0.00	0.00	0.00	0.00	0.00
Kasori E3 - Shomyoji	0.00	0.00	0.00	0.00	0.00	0.00	0.00	0.00	0.00	0.00	0.00	0.00	0.00	0.00	0.00	0.00	0.00	0.00	0.00	0.00	0.00	0.00	0.15	0.19	0.19	0.19	0.19	0.09	0.00	0.00	0.00	0.00	0.00	0.00	0.00	0.00	0.00	0.00	0.00
Kasori E3 - Shomyoji	0.00	0.00	0.00	0.00	0.00	0.00	0.00	0.00	0.00	0.00	0.00	0.00	0.00	0.00	0.00	0.00	0.00	0.00	0.00	0.00	0.00	0.00	0.15	0.19	0.19	0.19	0.19	0.09	0.00	0.00	0.00	0.00	0.00	0.00	0.00	0.00	0.00	0.00	0.00
Kasori E3 (Early - Middle)	0.00	0.00	0.00	0.00	0.00	0.00	0.00	0.00	0.00	0.00	0.00	0.00	0.00	0.00	0.00	0.00	0.00	0.00	0.00	0.00	0.00	0.00	0.44	0.56	0.00	0.00	0.00	0.00	0.00	0.00	0.00	0.00	0.00	0.00	0.00	0.00	0.00	0.00	0.00
Kasori E3 (Early)	0.00	0.00	0.00	0.00	0.00	0.00	0.00	0.00	0.00	0.00	0.00	0.00	0.00	0.00	0.00	0.00	0.00	0.00	0.00	0.00	0.00	0.00	0.62	0.38	0.00	0.00	0.00	0.00	0.00	0.00	0.00	0.00	0.00	0.00	0.00	0.00	0.00	0.00	0.00
Kasori E3 (Early)	0.00	0.00	0.00	0.00	0.00	0.00	0.00	0.00	0.00	0.00	0.00	0.00	0.00	0.00	0.00	0.00	0.00	0.00	0.00	0.00	0.00	0.00	0.62	0.38	0.00	0.00	0.00	0.00	0.00	0.00	0.00	0.00	0.00	0.00	0.00	0.00	0.00	0.00	0.00
Kasori E3 (late)	0.00	0.00	0.00	0.00	0.00	0.00	0.00	0.00	0.00	0.00	0.00	0.00	0.00	0.00	0.00	0.00	0.00	0.00	0.00	0.00	0.00	0.00	0.00	0.56	0.44	0.00	0.00	0.00	0.00	0.00	0.00	0.00	0.00	0.00	0.00	0.00	0.00	0.00	0.00
Kasori E3 (Late)	0.00	0.00	0.00	0.00	0.00	0.00	0.00	0.00	0.00	0.00	0.00	0.00	0.00	0.00	0.00	0.00	0.00	0.00	0.00	0.00	0.00	0.00	0.00	0.56	0.44	0.00	0.00	0.00	0.00	0.00	0.00	0.00	0.00	0.00	0.00	0.00	0.00	0.00	0.00
Kasori E3 (Late) - E4	0.00	0.00	0.00	0.00	0.00	0.00	0.00	0.00	0.00	0.00	0.00	0.00	0.00	0.00	0.00	0.00	0.00	0.00	0.00	0.00	0.00	0.00	0.20	0.40	0.40	0.00	0.00	0.00	0.00	0.00	0.00	0.00	0.00	0.00	0.00	0.00	0.00	0.00	0.00
Kasori E3 (Middle)	0.00	0.00	0.00	0.00	0.00	0.00	0.00	0.00	0.00	0.00	0.00	0.00	0.00	0.00	0.00	0.00	0.00	0.00	0.00	0.00	0.00	0.00	0.44	0.56	0.00	0.00	0.00	0.00	0.00	0.00	0.00	0.00	0.00	0.00	0.00	0.00	0.00	0.00	0.00
Kasori E4	0.00	0.00	0.00	0.00	0.00	0.00	0.00	0.00	0.00	0.00	0.00	0.00	0.00	0.00	0.00	0.00	0.00	0.00	0.00	0.00	0.00	0.00	0.00	0.20	0.80	0.00	0.00	0.00	0.00	0.00	0.00	0.00	0.00	0.00	0.00	0.00	0.00	0.00	0.00

Continued on next page

Table A.6: Aoristic Weights and Pottery Phases

Pottery Phase	B.	t1	t2	t3	t4	t5	t6	t7	t8	t9	t10	t11	t12	t13	t14	t15	t16	t17	t18	t19	t20	t21	t22	t23	t24	t25	t26	t27	t28	t29	t30	t31	t32	t33	t34	t35	t36	t37	A.
Kasori E4	0.00	0.00	0.00	0.00	0.00	0.00	0.00	0.00	0.00	0.00	0.00	0.00	0.00	0.00	0.00	0.00	0.00	0.00	0.00	0.00	0.00	0.00	0.00	0.00	0.20	0.80	0.00	0.00	0.00	0.00	0.00	0.00	0.00	0.00	0.00	0.00	0.00	0.00	0.00
Kasori E4 - Shomyoji	0.00	0.00	0.00	0.00	0.00	0.00	0.00	0.00	0.00	0.00	0.00	0.00	0.00	0.00	0.00	0.00	0.00	0.00	0.00	0.00	0.00	0.00	0.00	0.00	0.07	0.37	0.37	0.19	0.00	0.00	0.00	0.00	0.00	0.00	0.00	0.00	0.00	0.00	0.00
Kasori EI	0.00	0.00	0.00	0.00	0.00	0.00	0.00	0.00	0.00	0.00	0.00	0.00	0.00	0.00	0.00	0.00	0.00	0.00	0.00	0.00	0.20	0.67	0.13	0.00	0.00	0.00	0.00	0.00	0.00	0.00	0.00	0.00	0.00	0.00	0.00	0.00	0.00	0.00	0.00
Kasori EI - EII (Early)	0.00	0.00	0.00	0.00	0.00	0.00	0.00	0.00	0.00	0.00	0.00	0.00	0.00	0.00	0.00	0.00	0.00	0.00	0.00	0.00	0.12	0.41	0.41	0.06	0.00	0.00	0.00	0.00	0.00	0.00	0.00	0.00	0.00	0.00	0.00	0.00	0.00	0.00	0.00
Kasori EI (Early)	0.00	0.00	0.00	0.00	0.00	0.00	0.00	0.00	0.00	0.00	0.00	0.00	0.00	0.00	0.00	0.00	0.00	0.00	0.00	0.00	0.40	0.60	0.00	0.00	0.00	0.00	0.00	0.00	0.00	0.00	0.00	0.00	0.00	0.00	0.00	0.00	0.00	0.00	0.00
Kasori EI (late)	0.00	0.00	0.00	0.00	0.00	0.00	0.00	0.00	0.00	0.00	0.00	0.00	0.00	0.00	0.00	0.00	0.00	0.00	0.00	0.00	0.00	0.73	0.27	0.00	0.00	0.00	0.00	0.00	0.00	0.00	0.00	0.00	0.00	0.00	0.00	0.00	0.00	0.00	0.00
Kasori EI (Late) - EII (Early)	0.00	0.00	0.00	0.00	0.00	0.00	0.00	0.00	0.00	0.00	0.00	0.00	0.00	0.00	0.00	0.00	0.00	0.00	0.00	0.00	0.00	0.32	0.59	0.09	0.00	0.00	0.00	0.00	0.00	0.00	0.00	0.00	0.00	0.00	0.00	0.00	0.00	0.00	0.00
Kasori EI (up to)	0.00	0.00	0.00	0.00	0.00	0.00	0.00	0.00	0.00	0.00	0.00	0.00	0.00	0.00	0.00	0.00	0.00	0.00	0.00	0.00	0.20	0.67	0.13	0.00	0.00	0.00	0.00	0.00	0.00	0.00	0.00	0.00	0.00	0.00	0.00	0.00	0.00	0.00	0.00
Kasori EI-EII	0.00	0.00	0.00	0.00	0.00	0.00	0.00	0.00	0.00	0.00	0.00	0.00	0.00	0.00	0.00	0.00	0.00	0.00	0.00	0.00	0.09	0.29	0.29	0.29	0.03	0.00	0.00	0.00	0.00	0.00	0.00	0.00	0.00	0.00	0.00	0.00	0.00	0.00	0.00
Kasori EII	0.00	0.00	0.00	0.00	0.00	0.00	0.00	0.00	0.00	0.00	0.00	0.00	0.00	0.00	0.00	0.00	0.00	0.00	0.00	0.00	0.00	0.00	0.42	0.53	0.05	0.00	0.00	0.00	0.00	0.00	0.00	0.00	0.00	0.00	0.00	0.00	0.00	0.00	0.00
Kasori EII - EIII	0.00	0.00	0.00	0.00	0.00	0.00	0.00	0.00	0.00	0.00	0.00	0.00	0.00	0.00	0.00	0.00	0.00	0.00	0.00	0.00	0.00	0.00	0.31	0.38	0.31	0.00	0.00	0.00	0.00	0.00	0.00	0.00	0.00	0.00	0.00	0.00	0.00	0.00	0.00
Kasori EII -EIV	0.00	0.00	0.00	0.00	0.00	0.00	0.00	0.00	0.00	0.00	0.00	0.00	0.00	0.00	0.00	0.00	0.00	0.00	0.00	0.00	0.00	0.00	0.22	0.28	0.28	0.22	0.00	0.00	0.00	0.00	0.00	0.00	0.00	0.00	0.00	0.00	0.00	0.00	0.00
Kasori EII (after)	0.00	0.00	0.00	0.00	0.00	0.00	0.00	0.00	0.00	0.00	0.00	0.00	0.00	0.00	0.00	0.00	0.00	0.00	0.00	0.00	0.00	0.00	0.42	0.53	0.05	0.00	0.00	0.00	0.00	0.00	0.00	0.00	0.00	0.00	0.00	0.00	0.00	0.00	0.00
Kasori EII (Early)	0.00	0.00	0.00	0.00	0.00	0.00	0.00	0.00	0.00	0.00	0.00	0.00	0.00	0.00	0.00	0.00	0.00	0.00	0.00	0.00	0.00	0.00	1.00	0.00	0.00	0.00	0.00	0.00	0.00	0.00	0.00	0.00	0.00	0.00	0.00	0.00	0.00	0.00	0.00
Kasori EII (Late)	0.00	0.00	0.00	0.00	0.00	0.00	0.00	0.00	0.00	0.00	0.00	0.00	0.00	0.00	0.00	0.00	0.00	0.00	0.00	0.00	0.00	0.00	0.00	0.85	0.15	0.00	0.00	0.00	0.00	0.00	0.00	0.00	0.00	0.00	0.00	0.00	0.00	0.00	0.00
Kasori EII (Late) - EIII	0.00	0.00	0.00	0.00	0.00	0.00	0.00	0.00	0.00	0.00	0.00	0.00	0.00	0.00	0.00	0.00	0.00	0.00	0.00	0.00	0.00	0.00	0.00	0.41	0.59	0.00	0.00	0.00	0.00	0.00	0.00	0.00	0.00	0.00	0.00	0.00	0.00	0.00	0.00
Kasori EII (Middle-Late)	0.00	0.00	0.00	0.00	0.00	0.00	0.00	0.00	0.00	0.00	0.00	0.00	0.00	0.00	0.00	0.00	0.00	0.00	0.00	0.00	0.00	0.00	0.15	0.77	0.08	0.00	0.00	0.00	0.00	0.00	0.00	0.00	0.00	0.00	0.00	0.00	0.00	0.00	0.00
Kasori EII (Middle)	0.00	0.00	0.00	0.00	0.00	0.00	0.00	0.00	0.00	0.00	0.00	0.00	0.00	0.00	0.00	0.00	0.00	0.00	0.00	0.00	0.00	0.00	0.31	0.69	0.00	0.00	0.00	0.00	0.00	0.00	0.00	0.00	0.00	0.00	0.00	0.00	0.00	0.00	0.00
Kasori EII (Middle) - EIII	0.00	0.00	0.00	0.00	0.00	0.00	0.00	0.00	0.00	0.00	0.00	0.00	0.00	0.00	0.00	0.00	0.00	0.00	0.00	0.00	0.00	0.00	0.00	0.53	0.47	0.00	0.00	0.00	0.00	0.00	0.00	0.00	0.00	0.00	0.00	0.00	0.00	0.00	0.00
Kasori EII (up to)	0.00	0.00	0.00	0.00	0.00	0.00	0.00	0.00	0.00	0.00	0.00	0.00	0.00	0.00	0.00	0.00	0.00	0.00	0.00	0.00	0.00	0.00	0.42	0.53	0.05	0.00	0.00	0.00	0.00	0.00	0.00	0.00	0.00	0.00	0.00	0.00	0.00	0.00	0.00
Kasori EIII	0.00	0.00	0.00	0.00	0.00	0.00	0.00	0.00	0.00	0.00	0.00	0.00	0.00	0.00	0.00	0.00	0.00	0.00	0.00	0.00	0.00	0.00	0.00	0.00	1.00	0.00	0.00	0.00	0.00	0.00	0.00	0.00	0.00	0.00	0.00	0.00	0.00	0.00	0.00
Kasori EIII - EIV	0.00	0.00	0.00	0.00	0.00	0.00	0.00	0.00	0.00	0.00	0.00	0.00	0.00	0.00	0.00	0.00	0.00	0.00	0.00	0.00	0.00	0.00	0.00	0.00	0.53	0.47	0.00	0.00	0.00	0.00	0.00	0.00	0.00	0.00	0.00	0.00	0.00	0.00	0.00
Kasori EIII - Horinouchi 1	0.00	0.00	0.00	0.00	0.00	0.00	0.00	0.00	0.00	0.00	0.00	0.00	0.00	0.00	0.00	0.00	0.00	0.00	0.00	0.00	0.00	0.00	0.00	0.00	0.15	0.16	0.16	0.16	0.16	0.16	0.03	0.00	0.00	0.00	0.00	0.00	0.00	0.00	0.00
Kasori EIII - Shomyoji	0.00	0.00	0.00	0.00	0.00	0.00	0.00	0.00	0.00	0.00	0.00	0.00	0.00	0.00	0.00	0.00	0.00	0.00	0.00	0.00	0.00	0.00	0.00	0.00	0.26	0.29	0.29	0.15	0.00	0.00	0.00	0.00	0.00	0.00	0.00	0.00	0.00	0.00	0.00
Kasori EIII (Early)	0.00	0.00	0.00	0.00	0.00	0.00	0.00	0.00	0.00	0.00	0.00	0.00	0.00	0.00	0.00	0.00	0.00	0.00	0.00	0.00	0.00	0.00	0.00	0.00	1.00	0.00	0.00	0.00	0.00	0.00	0.00	0.00	0.00	0.00	0.00	0.00	0.00	0.00	0.00
Kasori EIII (Late)	0.00	0.00	0.00	0.00	0.00	0.00	0.00	0.00	0.00	0.00	0.00	0.00	0.00	0.00	0.00	0.00	0.00	0.00	0.00	0.00	0.00	0.00	0.00	0.00	1.00	0.00	0.00	0.00	0.00	0.00	0.00	0.00	0.00	0.00	0.00	0.00	0.00	0.00	0.00

Continued on next page

Table A.6: Aoristic Weights and Pottery Phases

Pottery Phase	B.	t1	t2	t3	t4	t5	t6	t7	t8	t9	t10	t11	t12	t13	t14	t15	t16	t17	t18	t19	t20	t21	t22	t23	t24	t25	t26	t27	t28	t29	t30	t31	t32	t33	t34	t35	t36	t37	A.
Kasori EIII (Late) - EIV	0.00	0.00	0.00	0.00	0.00	0.00	0.00	0.00	0.00	0.00	0.00	0.00	0.00	0.00	0.00	0.00	0.00	0.00	0.00	0.00	0.00	0.00	0.00	0.00	0.43	0.57	0.00	0.00	0.00	0.00	0.00	0.00	0.00	0.00	0.00	0.00	0.00	0.00	0.00
Kasori EIII (Renkomon)	0.00	0.00	0.00	0.00	0.00	0.00	0.00	0.00	0.00	0.00	0.00	0.00	0.00	0.00	0.00	0.00	0.00	0.00	0.00	0.00	0.00	0.00	0.00	0.00	1.00	0.00	0.00	0.00	0.00	0.00	0.00	0.00	0.00	0.00	0.00	0.00	0.00	0.00	0.00
Kasori EIV	0.00	0.00	0.00	0.00	0.00	0.00	0.00	0.00	0.00	0.00	0.00	0.00	0.00	0.00	0.00	0.00	0.00	0.00	0.00	0.00	0.00	0.00	0.00	0.00	0.20	0.80	0.00	0.00	0.00	0.00	0.00	0.00	0.00	0.00	0.00	0.00	0.00	0.00	0.00
Kasori EIV - Horinouchi 1	0.00	0.00	0.00	0.00	0.00	0.00	0.00	0.00	0.00	0.00	0.00	0.00	0.00	0.00	0.00	0.00	0.00	0.00	0.00	0.00	0.00	0.00	0.00	0.00	0.07	0.37	0.37	0.19	0.00	0.00	0.00	0.00	0.00	0.00	0.00	0.00	0.00	0.00	0.00
Kasori EIV - Shomyoji	0.00	0.00	0.00	0.00	0.00	0.00	0.00	0.00	0.00	0.00	0.00	0.00	0.00	0.00	0.00	0.00	0.00	0.00	0.00	0.00	0.00	0.00	0.00	0.00	0.07	0.37	0.37	0.19	0.00	0.00	0.00	0.00	0.00	0.00	0.00	0.00	0.00	0.00	0.00
Kasori EIV - Shomyoji (Early)	0.00	0.00	0.00	0.00	0.00	0.00	0.00	0.00	0.00	0.00	0.00	0.00	0.00	0.00	0.00	0.00	0.00	0.00	0.00	0.00	0.00	0.00	0.00	0.00	0.09	0.45	0.45	0.00	0.00	0.00	0.00	0.00	0.00	0.00	0.00	0.00	0.00	0.00	0.00
Katsuzaka	0.00	0.00	0.00	0.00	0.00	0.00	0.00	0.00	0.00	0.00	0.00	0.00	0.00	0.00	0.00	0.00	0.17	0.21	0.21	0.21	0.21	0.00	0.00	0.00	0.00	0.00	0.00	0.00	0.00	0.00	0.00	0.00	0.00	0.00	0.00	0.00	0.00	0.00	0.00
Katsuzaka / Otamadai	0.00	0.00	0.00	0.00	0.00	0.00	0.00	0.00	0.00	0.00	0.00	0.00	0.00	0.00	0.00	0.00	0.17	0.21	0.21	0.21	0.21	0.00	0.00	0.00	0.00	0.00	0.00	0.00	0.00	0.00	0.00	0.00	0.00	0.00	0.00	0.00	0.00	0.00	0.00
Katsuzaka 1 - 2	0.00	0.00	0.00	0.00	0.00	0.00	0.00	0.00	0.00	0.00	0.00	0.00	0.00	0.00	0.00	0.00	0.27	0.33	0.33	0.07	0.00	0.00	0.00	0.00	0.00	0.00	0.00	0.00	0.00	0.00	0.00	0.00	0.00	0.00	0.00	0.00	0.00	0.00	0.00
Katsuzaka 1 / Mirahada	0.00	0.00	0.00	0.00	0.00	0.00	0.00	0.00	0.00	0.00	0.00	0.00	0.00	0.00	0.00	0.00	0.13	0.17	0.17	0.17	0.17	0.17	0.03	0.00	0.00	0.00	0.00	0.00	0.00	0.00	0.00	0.00	0.00	0.00	0.00	0.00	0.00	0.00	0.00
Katsuzaka 2	0.00	0.00	0.00	0.00	0.00	0.00	0.00	0.00	0.00	0.00	0.00	0.00	0.00	0.00	0.00	0.00	0.00	0.40	0.50	0.10	0.00	0.00	0.00	0.00	0.00	0.00	0.00	0.00	0.00	0.00	0.00	0.00	0.00	0.00	0.00	0.00	0.00	0.00	0.00
Katsuzaka 2 - 3	0.00	0.00	0.00	0.00	0.00	0.00	0.00	0.00	0.00	0.00	0.00	0.00	0.00	0.00	0.00	0.00	0.00	0.21	0.26	0.26	0.26	0.00	0.00	0.00	0.00	0.00	0.00	0.00	0.00	0.00	0.00	0.00	0.00	0.00	0.00	0.00	0.00	0.00	0.00
Katsuzaka 3	0.00	0.00	0.00	0.00	0.00	0.00	0.00	0.00	0.00	0.00	0.00	0.00	0.00	0.00	0.00	0.00	0.00	0.00	0.00	0.44	0.56	0.00	0.00	0.00	0.00	0.00	0.00	0.00	0.00	0.00	0.00	0.00	0.00	0.00	0.00	0.00	0.00	0.00	0.00
Katsuzaka 3	0.00	0.00	0.00	0.00	0.00	0.00	0.00	0.00	0.00	0.00	0.00	0.00	0.00	0.00	0.00	0.00	0.00	0.00	0.00	0.44	0.56	0.00	0.00	0.00	0.00	0.00	0.00	0.00	0.00	0.00	0.00	0.00	0.00	0.00	0.00	0.00	0.00	0.00	0.00
Katsuzaka 3 - Kasori E1	0.00	0.00	0.00	0.00	0.00	0.00	0.00	0.00	0.00	0.00	0.00	0.00	0.00	0.00	0.00	0.00	0.00	0.00	0.00	0.38	0.48	0.14	0.00	0.00	0.00	0.00	0.00	0.00	0.00	0.00	0.00	0.00	0.00	0.00	0.00	0.00	0.00	0.00	0.00
Katsuzaka 3 - Kasori E1 / Miharada	0.00	0.00	0.00	0.00	0.00	0.00	0.00	0.00	0.00	0.00	0.00	0.00	0.00	0.00	0.00	0.00	0.00	0.00	0.00	0.27	0.33	0.33	0.07	0.00	0.00	0.00	0.00	0.00	0.00	0.00	0.00	0.00	0.00	0.00	0.00	0.00	0.00	0.00	0.00
Katsuzaka 3 - Yakemachi	0.00	0.00	0.00	0.00	0.00	0.00	0.00	0.00	0.00	0.00	0.00	0.00	0.00	0.00	0.00	0.00	0.00	0.00	0.00	0.27	0.33	0.33	0.07	0.00	0.00	0.00	0.00	0.00	0.00	0.00	0.00	0.00	0.00	0.00	0.00	0.00	0.00	0.00	0.00
Kuohama / Ario - Otamadai	0.00	0.00	0.00	0.00	0.00	0.03	0.07	0.07	0.07	0.07	0.07	0.07	0.07	0.07	0.07	0.07	0.07	0.07	0.07	0.07	0.05	0.00	0.00	0.00	0.00	0.00	0.00	0.00	0.00	0.00	0.00	0.00	0.00	0.00	0.00	0.00	0.00	0.00	0.00
Kuorhama / Ario - Moroiso	0.00	0.00	0.00	0.00	0.00	0.06	0.12	0.12	0.12	0.12	0.12	0.12	0.12	0.12	0.00	0.00	0.00	0.00	0.00	0.00	0.00	0.00	0.00	0.00	0.00	0.00	0.00	0.00	0.00	0.00	0.00	0.00	0.00	0.00	0.00	0.00	0.00	0.00	0.00
Kuorhama / Ario - Moroiso b	0.00	0.00	0.00	0.00	0.00	0.07	0.14	0.14	0.14	0.14	0.14	0.14	0.07	0.00	0.00	0.00	0.00	0.00	0.00	0.00	0.00	0.00	0.00	0.00	0.00	0.00	0.00	0.00	0.00	0.00	0.00	0.00	0.00	0.00	0.00	0.00	0.00	0.00	0.00
Kurohama - Moroiso	0.00	0.00	0.00	0.00	0.00	0.06	0.12	0.12	0.12	0.12	0.12	0.12	0.12	0.12	0.00	0.00	0.00	0.00	0.00	0.00	0.00	0.00	0.00	0.00	0.00	0.00	0.00	0.00	0.00	0.00	0.00	0.00	0.00	0.00	0.00	0.00	0.00	0.00	0.00
Kurohama - Moroiso a	0.00	0.00	0.00	0.00	0.00	0.10	0.20	0.20	0.20	0.20	0.10	0.00	0.00	0.00	0.00	0.00	0.00	0.00	0.00	0.00	0.00	0.00	0.00	0.00	0.00	0.00	0.00	0.00	0.00	0.00	0.00	0.00	0.00	0.00	0.00	0.00	0.00	0.00	0.00
Kurohama - Moroiso b	0.00	0.00	0.00	0.00	0.00	0.07	0.14	0.14	0.14	0.14	0.14	0.14	0.07	0.00	0.00	0.00	0.00	0.00	0.00	0.00	0.00	0.00	0.00	0.00	0.00	0.00	0.00	0.00	0.00	0.00	0.00	0.00	0.00	0.00	0.00	0.00	0.00	0.00	0.00
Kurohama - Moroiso b	0.00	0.00	0.00	0.00	0.00	0.07	0.14	0.14	0.14	0.14	0.14	0.14	0.07	0.00	0.00	0.00	0.00	0.00	0.00	0.00	0.00	0.00	0.00	0.00	0.00	0.00	0.00	0.00	0.00	0.00	0.00	0.00	0.00	0.00	0.00	0.00	0.00	0.00	0.00
Kurohama - Moroiso c	0.00	0.00	0.00	0.00	0.00	0.13	0.25	0.25	0.25	0.13	0.00	0.00	0.00	0.00	0.00	0.00	0.00	0.00	0.00	0.00	0.00	0.00	0.00	0.00	0.00	0.00	0.00	0.00	0.00	0.00	0.00	0.00	0.00	0.00	0.00	0.00	0.00	0.00	0.00
Kurohama - Ukishima	0.00	0.00	0.00	0.00	0.00	0.07	0.14	0.14	0.14	0.14	0.14	0.14	0.07	0.00	0.00	0.00	0.00	0.00	0.00	0.00	0.00	0.00	0.00	0.00	0.00	0.00	0.00	0.00	0.00	0.00	0.00	0.00	0.00	0.00	0.00	0.00	0.00	0.00	0.00

Continued on next page

Table A.6: Aoristic Weights and Pottery Phases

Pottery Phase	B.	t1	t2	t3	t4	t5	t6	t7	t8	t9	t10	t11	t12	t13	t14	t15	t16	t17	t18	t19	t20	t21	t22	t23	t24	t25	t26	t27	t28	t29	t30	t31	t32	t33	t34	t35	t36	t37	A.
Kurohama (Early)	0.00	0.00	0.00	0.00	0.00	0.25	0.50	0.25	0.00	0.00	0.00	0.00	0.00	0.00	0.00	0.00	0.00	0.00	0.00	0.00	0.00	0.00	0.00	0.00	0.00	0.00	0.00	0.00	0.00	0.00	0.00	0.00	0.00	0.00	0.00	0.00	0.00	0.00
Kurohama (Late)	0.00	0.00	0.00	0.00	0.00	0.00	0.00	0.25	0.50	0.25	0.00	0.00	0.00	0.00	0.00	0.00	0.00	0.00	0.00	0.00	0.00	0.00	0.00	0.00	0.00	0.00	0.00	0.00	0.00	0.00	0.00	0.00	0.00	0.00	0.00	0.00	0.00	0.00
Kurohama / Ario	0.00	0.00	0.00	0.00	0.00	0.13	0.25	0.25	0.25	0.13	0.00	0.00	0.00	0.00	0.00	0.00	0.00	0.00	0.00	0.00	0.00	0.00	0.00	0.00	0.00	0.00	0.00	0.00	0.00	0.00	0.00	0.00	0.00	0.00	0.00	0.00	0.00	0.00
Kurohama / Ario	0.00	0.00	0.00	0.00	0.00	0.13	0.25	0.25	0.25	0.13	0.00	0.00	0.00	0.00	0.00	0.00	0.00	0.00	0.00	0.00	0.00	0.00	0.00	0.00	0.00	0.00	0.00	0.00	0.00	0.00	0.00	0.00	0.00	0.00	0.00	0.00	0.00	0.00
Kurohama / Moroiso a - b / Ukishima I - II	0.00	0.00	0.00	0.00	0.00	0.07	0.14	0.14	0.14	0.14	0.14	0.14	0.07	0.00	0.00	0.00	0.00	0.00	0.00	0.00	0.00	0.00	0.00	0.00	0.00	0.00	0.00	0.00	0.00	0.00	0.00	0.00	0.00	0.00	0.00	0.00	0.00	0.00
Late Jomon	0.00	0.00	0.00	0.00	0.00	0.00	0.00	0.00	0.00	0.00	0.00	0.00	0.00	0.00	0.00	0.00	0.00	0.00	0.00	0.00	0.00	0.00	0.00	0.00	0.00	0.02	0.08	0.08	0.08	0.08	0.08	0.08	0.08	0.08	0.08	0.08	0.07	0.00
Late Jomon - Final Jomon	0.00	0.00	0.00	0.00	0.00	0.00	0.00	0.00	0.00	0.00	0.00	0.00	0.00	0.00	0.00	0.00	0.00	0.00	0.00	0.00	0.00	0.00	0.00	0.00	0.00	0.01	0.05	0.05	0.05	0.05	0.05	0.05	0.05	0.05	0.05	0.05	0.05	0.45
Late Jomon (Early)	0.00	0.00	0.00	0.00	0.00	0.00	0.00	0.00	0.00	0.00	0.00	0.00	0.00	0.00	0.00	0.00	0.00	0.00	0.00	0.00	0.00	0.00	0.00	0.00	0.00	0.05	0.23	0.23	0.23	0.23	0.05	0.00	0.00	0.00	0.00	0.00	0.00	0.00
Late Jomon (Final) - Final Jomon (Early)	0.00	0.00	0.00	0.00	0.00	0.00	0.00	0.00	0.00	0.00	0.00	0.00	0.00	0.00	0.00	0.00	0.00	0.00	0.00	0.00	0.00	0.00	0.00	0.00	0.00	0.00	0.00	0.00	0.00	0.00	0.00	0.00	0.00	0.00	0.00	0.15	0.15	0.70
Late Jomon (Late) - Final Jomon (Early)	0.00	0.00	0.00	0.00	0.00	0.00	0.00	0.00	0.00	0.00	0.00	0.00	0.00	0.00	0.00	0.00	0.00	0.00	0.00	0.00	0.00	0.00	0.00	0.00	0.00	0.00	0.00	0.00	0.00	0.00	0.00	0.00	0.00	0.00	0.09	0.14	0.14	0.64
Late Jomon (Middle) - Final Jomon	0.00	0.00	0.00	0.00	0.00	0.00	0.00	0.00	0.00	0.00	0.00	0.00	0.00	0.00	0.00	0.00	0.00	0.00	0.00	0.00	0.00	0.00	0.00	0.00	0.00	0.00	0.12	0.23	0.23	0.23	0.19	0.00	0.00	0.00	0.00	0.00	0.00	0.00
Late Jomon / Angyo	0.00	0.00	0.00	0.00	0.00	0.00	0.00	0.00	0.00	0.00	0.00	0.00	0.00	0.00	0.00	0.00	0.00	0.00	0.00	0.00	0.00	0.00	0.00	0.00	0.00	0.00	0.00	0.00	0.00	0.00	0.00	0.00	0.00	0.00	0.00	0.56	0.44	0.00
Lower Hanazumi	0.00	0.22	0.22	0.22	0.22	0.11	0.00	0.00	0.00	0.00	0.00	0.00	0.00	0.00	0.00	0.00	0.00	0.00	0.00	0.00	0.00	0.00	0.00	0.00	0.00	0.00	0.00	0.00	0.00	0.00	0.00	0.00	0.00	0.00	0.00	0.00	0.00	0.00
Lower Hanazumi - Futatsuki	0.00	0.22	0.22	0.22	0.22	0.11	0.00	0.00	0.00	0.00	0.00	0.00	0.00	0.00	0.00	0.00	0.00	0.00	0.00	0.00	0.00	0.00	0.00	0.00	0.00	0.00	0.00	0.00	0.00	0.00	0.00	0.00	0.00	0.00	0.00	0.00	0.00	0.00
Lower Hanazumi - Moroiso a	0.00	0.11	0.11	0.11	0.11	0.11	0.11	0.11	0.11	0.05	0.00	0.00	0.00	0.00	0.00	0.00	0.00	0.00	0.00	0.00	0.00	0.00	0.00	0.00	0.00	0.00	0.00	0.00	0.00	0.00	0.00	0.00	0.00	0.00	0.00	0.00	0.00	0.00
Lower Hanazumi / Futatsuki	0.00	0.22	0.22	0.22	0.22	0.11	0.00	0.00	0.00	0.00	0.00	0.00	0.00	0.00	0.00	0.00	0.00	0.00	0.00	0.00	0.00	0.00	0.00	0.00	0.00	0.00	0.00	0.00	0.00	0.00	0.00	0.00	0.00	0.00	0.00	0.00	0.00	0.00
Middle Jomon	0.00	0.00	0.00	0.00	0.00	0.00	0.00	0.00	0.00	0.00	0.00	0.00	0.00	0.00	0.00	0.07	0.10	0.10	0.10	0.10	0.10	0.10	0.10	0.10	0.10	0.08	0.00	0.00	0.00	0.00	0.00	0.00	0.00	0.00	0.00	0.00	0.00	0.00
Middle Jomon - Late Jomon	0.00	0.00	0.00	0.00	0.00	0.00	0.00	0.00	0.00	0.00	0.00	0.00	0.00	0.00	0.00	0.03	0.04	0.04	0.04	0.04	0.04	0.04	0.04	0.04	0.04	0.04	0.04	0.04	0.04	0.04	0.04	0.04	0.04	0.04	0.04	0.04	0.04	0.00
Middle Jomon - Late Jomon (Initial)	0.00	0.00	0.00	0.00	0.00	0.00	0.00	0.00	0.00	0.00	0.00	0.00	0.00	0.00	0.00	0.06	0.08	0.08	0.08	0.08	0.08	0.08	0.08	0.08	0.08	0.08	0.08	0.04	0.00	0.00	0.00	0.00	0.00	0.00	0.00	0.00	0.00	0.00
Middle Jomon (Early-Middle)	0.00	0.00	0.00	0.00	0.00	0.00	0.00	0.00	0.00	0.00	0.00	0.00	0.00	0.00	0.00	0.13	0.19	0.19	0.19	0.19	0.13	0.00	0.00	0.00	0.00	0.00	0.00	0.00	0.00	0.00	0.00	0.00	0.00	0.00	0.00	0.00	0.00	0.00
Middle Jomon (Early)	0.00	0.00	0.00	0.00	0.00	0.00	0.00	0.00	0.00	0.00	0.00	0.00	0.00	0.00	0.00	0.28	0.40	0.32	0.00	0.00	0.00	0.00	0.00	0.00	0.00	0.00	0.00	0.00	0.00	0.00	0.00	0.00	0.00	0.00	0.00	0.00	0.00	0.00
Middle Jomon (Final)	0.00	0.00	0.00	0.00	0.00	0.00	0.00	0.00	0.00	0.04	0.09	0.09	0.09	0.09	0.09	0.09	0.09	0.09	0.09	0.09	0.06	0.00	0.00	0.00	0.00	0.00	0.00	0.00	0.00	0.00	0.00	0.00	0.00	0.00	0.00	0.00	0.00	0.00
Middle Jomon (Late)	0.00	0.00	0.00	0.00	0.00	0.00	0.00	0.00	0.00	0.00	0.00	0.00	0.00	0.00	0.00	0.07	0.10	0.10	0.10	0.10	0.10	0.10	0.10	0.10	0.10	0.08	0.00	0.00	0.00	0.00	0.00	0.00	0.00	0.00	0.00	0.00	0.00	0.00
Middle Jomon (Middle)	0.00	0.00	0.00	0.00	0.00	0.00	0.00	0.00	0.00	0.00	0.00	0.00	0.00	0.00	0.00	0.00	0.17	0.21	0.21	0.21	0.21	0.00	0.00	0.00	0.00	0.00	0.00	0.00	0.00	0.00	0.00	0.00	0.00	0.00	0.00	0.00	0.00	0.00
Miharada	0.00	0.00	0.00	0.00	0.00	0.00	0.00	0.00	0.00	0.00	0.00	0.00	0.00	0.00	0.00	0.00	0.00	0.00	0.00	0.00	0.45	0.45	0.09	0.00	0.00	0.00	0.00	0.00	0.00	0.00	0.00	0.00	0.00	0.00	0.00	0.00	0.00	0.00
Miharada / Yakemachi	0.00	0.00	0.00	0.00	0.00	0.00	0.00	0.00	0.00	0.00	0.00	0.00	0.00	0.00	0.00	0.00	0.00	0.00	0.00	0.27	0.33	0.33	0.07	0.00	0.00	0.00	0.00	0.00	0.00	0.00	0.00	0.00	0.00	0.00	0.00	0.00	0.00	0.00

Continued on next page

Table A.6: Aoristic Weights and Pottery Phases

Pottery Phase	B.	t1	t2	t3	t4	t5	t6	t7	t8	t9	t10	t11	t12	t13	t14	t15	t16	t17	t18	t19	t20	t21	t22	t23	t24	t25	t26	t27	t28	t29	t30	t31	t32	t33	t34	t35	t36	t37	A.
Moroiso	0.00	0.00	0.00	0.00	0.00	0.00	0.00	0.00	0.00	0.11	0.22	0.22	0.22	0.22	0.00	0.00	0.00	0.00	0.00	0.00	0.00	0.00	0.00	0.00	0.00	0.00	0.00	0.00	0.00	0.00	0.00	0.00	0.00	0.00	0.00	0.00	0.00	0.00
Moroiso	0.00	0.00	0.00	0.00	0.00	0.00	0.00	0.00	0.00	0.11	0.22	0.22	0.22	0.22	0.00	0.00	0.00	0.00	0.00	0.00	0.00	0.00	0.00	0.00	0.00	0.00	0.00	0.00	0.00	0.00	0.00	0.00	0.00	0.00	0.00	0.00	0.00	0.00
Moroiso (Late)	0.00	0.00	0.00	0.00	0.00	0.00	0.00	0.00	0.00	0.00	0.00	0.29	0.36	0.36	0.00	0.00	0.00	0.00	0.00	0.00	0.00	0.00	0.00	0.00	0.00	0.00	0.00	0.00	0.00	0.00	0.00	0.00	0.00	0.00	0.00	0.00	0.00	0.00
Moroiso a	0.00	0.00	0.00	0.00	0.00	0.00	0.00	0.00	0.00	0.50	0.50	0.00	0.00	0.00	0.00	0.00	0.00	0.00	0.00	0.00	0.00	0.00	0.00	0.00	0.00	0.00	0.00	0.00	0.00	0.00	0.00	0.00	0.00	0.00	0.00	0.00	0.00	0.00
Moroiso a - b	0.00	0.00	0.00	0.00	0.00	0.00	0.00	0.00	0.00	0.17	0.33	0.33	0.17	0.00	0.00	0.00	0.00	0.00	0.00	0.00	0.00	0.00	0.00	0.00	0.00	0.00	0.00	0.00	0.00	0.00	0.00	0.00	0.00	0.00	0.00	0.00	0.00	0.00
Moroiso a - Goryogadai	0.00	0.00	0.00	0.00	0.00	0.00	0.00	0.00	0.00	0.07	0.15	0.15	0.15	0.15	0.15	0.15	0.03	0.00	0.00	0.00	0.00	0.00	0.00	0.00	0.00	0.00	0.00	0.00	0.00	0.00	0.00	0.00	0.00	0.00	0.00	0.00	0.00	0.00
Moroiso b	0.00	0.00	0.00	0.00	0.00	0.00	0.00	0.00	0.00	0.00	0.25	0.50	0.25	0.00	0.00	0.00	0.00	0.00	0.00	0.00	0.00	0.00	0.00	0.00	0.00	0.00	0.00	0.00	0.00	0.00	0.00	0.00	0.00	0.00	0.00	0.00	0.00	0.00
Moroiso b - c	0.00	0.00	0.00	0.00	0.00	0.00	0.00	0.00	0.00	0.00	0.14	0.29	0.29	0.29	0.00	0.00	0.00	0.00	0.00	0.00	0.00	0.00	0.00	0.00	0.00	0.00	0.00	0.00	0.00	0.00	0.00	0.00	0.00	0.00	0.00	0.00	0.00	0.00
Moroiso b - Goryogadai 2	0.00	0.00	0.00	0.00	0.00	0.00	0.00	0.00	0.00	0.00	0.09	0.18	0.18	0.18	0.18	0.18	0.04	0.00	0.00	0.00	0.00	0.00	0.00	0.00	0.00	0.00	0.00	0.00	0.00	0.00	0.00	0.00	0.00	0.00	0.00	0.00	0.00	0.00
Moroiso b - Kasori E2	0.00	0.00	0.00	0.00	0.00	0.00	0.00	0.00	0.00	0.00	0.04	0.09	0.09	0.09	0.09	0.09	0.09	0.09	0.09	0.09	0.09	0.09	0.02	0.00	0.00	0.00	0.00	0.00	0.00	0.00	0.00	0.00	0.00	0.00	0.00	0.00	0.00	0.00
Moroiso b (Early)	0.00	0.00	0.00	0.00	0.00	0.00	0.00	0.00	0.00	0.00	0.50	0.50	0.00	0.00	0.00	0.00	0.00	0.00	0.00	0.00	0.00	0.00	0.00	0.00	0.00	0.00	0.00	0.00	0.00	0.00	0.00	0.00	0.00	0.00	0.00	0.00	0.00	0.00
Moroiso b (Final)	0.00	0.00	0.00	0.00	0.00	0.00	0.00	0.00	0.00	0.00	0.00	0.50	0.50	0.00	0.00	0.00	0.00	0.00	0.00	0.00	0.00	0.00	0.00	0.00	0.00	0.00	0.00	0.00	0.00	0.00	0.00	0.00	0.00	0.00	0.00	0.00	0.00	0.00
Moroiso b (Final) - Moroiso c	0.00	0.00	0.00	0.00	0.00	0.00	0.00	0.00	0.00	0.00	0.00	0.20	0.40	0.40	0.00	0.00	0.00	0.00	0.00	0.00	0.00	0.00	0.00	0.00	0.00	0.00	0.00	0.00	0.00	0.00	0.00	0.00	0.00	0.00	0.00	0.00	0.00	0.00
Moroiso b (Late)	0.00	0.00	0.00	0.00	0.00	0.00	0.00	0.00	0.00	0.00	0.00	1.00	0.00	0.00	0.00	0.00	0.00	0.00	0.00	0.00	0.00	0.00	0.00	0.00	0.00	0.00	0.00	0.00	0.00	0.00	0.00	0.00	0.00	0.00	0.00	0.00	0.00	0.00
Moroiso b (Late) - c (Early)	0.00	0.00	0.00	0.00	0.00	0.00	0.00	0.00	0.00	0.00	0.00	0.28	0.56	0.17	0.00	0.00	0.00	0.00	0.00	0.00	0.00	0.00	0.00	0.00	0.00	0.00	0.00	0.00	0.00	0.00	0.00	0.00	0.00	0.00	0.00	0.00	0.00	0.00
Moroiso b (Middle -Late)	0.00	0.00	0.00	0.00	0.00	0.00	0.00	0.00	0.00	0.00	0.00	0.62	0.38	0.00	0.00	0.00	0.00	0.00	0.00	0.00	0.00	0.00	0.00	0.00	0.00	0.00	0.00	0.00	0.00	0.00	0.00	0.00	0.00	0.00	0.00	0.00	0.00	0.00
Moroiso b (Middle)	0.00	0.00	0.00	0.00	0.00	0.00	0.00	0.00	0.00	0.00	0.00	1.00	0.00	0.00	0.00	0.00	0.00	0.00	0.00	0.00	0.00	0.00	0.00	0.00	0.00	0.00	0.00	0.00	0.00	0.00	0.00	0.00	0.00	0.00	0.00	0.00	0.00	0.00
Moroiso b / Ukishima I	0.00	0.00	0.00	0.00	0.00	0.00	0.00	0.00	0.00	0.17	0.33	0.33	0.17	0.00	0.00	0.00	0.00	0.00	0.00	0.00	0.00	0.00	0.00	0.00	0.00	0.00	0.00	0.00	0.00	0.00	0.00	0.00	0.00	0.00	0.00	0.00	0.00	0.00
Moroiso c	0.00	0.00	0.00	0.00	0.00	0.00	0.00	0.00	0.00	0.00	0.00	0.00	0.33	0.67	0.00	0.00	0.00	0.00	0.00	0.00	0.00	0.00	0.00	0.00	0.00	0.00	0.00	0.00	0.00	0.00	0.00	0.00	0.00	0.00	0.00	0.00	0.00	0.00
Moroiso c (Early)	0.00	0.00	0.00	0.00	0.00	0.00	0.00	0.00	0.00	0.00	0.00	0.00	0.00	1.00	0.00	0.00	0.00	0.00	0.00	0.00	0.00	0.00	0.00	0.00	0.00	0.00	0.00	0.00	0.00	0.00	0.00	0.00	0.00	0.00	0.00	0.00	0.00	0.00
Morosio b (Middle - Late)	0.00	0.00	0.00	0.00	0.00	0.00	0.00	0.00	0.00	0.00	0.00	0.62	0.38	0.00	0.00	0.00	0.00	0.00	0.00	0.00	0.00	0.00	0.00	0.00	0.00	0.00	0.00	0.00	0.00	0.00	0.00	0.00	0.00	0.00	0.00	0.00	0.00	0.00
Nakabyo	0.00	0.00	0.00	0.00	0.00	0.00	0.00	0.00	0.00	0.00	0.00	0.00	0.00	0.00	0.00	0.00	0.00	0.00	0.00	0.00	1.00	0.00	0.00	0.00	0.00	0.00	0.00	0.00	0.00	0.00	0.00	0.00	0.00	0.00	0.00	0.00	0.00	0.00
Nakabyo - Kasori EI	0.00	0.00	0.00	0.00	0.00	0.00	0.00	0.00	0.00	0.00	0.00	0.00	0.00	0.00	0.00	0.00	0.00	0.00	0.00	0.00	0.45	0.45	0.09	0.00	0.00	0.00	0.00	0.00	0.00	0.00	0.00	0.00	0.00	0.00	0.00	0.00	0.00	0.00
Natsushima - Lower Hanazumi	0.91	0.02	0.02	0.02	0.02	0.01	0.00	0.00	0.00	0.00	0.00	0.00	0.00	0.00	0.00	0.00	0.00	0.00	0.00	0.00	0.00	0.00	0.00	0.00	0.00	0.00	0.00	0.00	0.00	0.00	0.00	0.00	0.00	0.00	0.00	0.00	0.00	0.00
Oatamadai II - III	0.00	0.00	0.00	0.00	0.00	0.00	0.00	0.00	0.00	0.00	0.00	0.00	0.00	0.00	0.00	0.00	0.04	0.22	0.22	0.22	0.22	0.09	0.00	0.00	0.00	0.00	0.00	0.00	0.00	0.00	0.00	0.00	0.00	0.00	0.00	0.00	0.00	0.00
Oatamadai II - Kasori EI (Early)	0.00	0.00	0.00	0.00	0.00	0.00	0.00	0.00	0.00	0.00	0.00	0.00	0.00	0.00	0.00	0.00	0.04	0.22	0.22	0.22	0.22	0.09	0.00	0.00	0.00	0.00	0.00	0.00	0.00	0.00	0.00	0.00	0.00	0.00	0.00	0.00	0.00	0.00

Continued on next page

Table A.6: Aoristic Weights and Pottery Phases

Pottery Phase	B.	t1	t2	t3	t4	t5	t6	t7	t8	t9	t10	t11	t12	t13	t14	t15	t16	t17	t18	t19	t20	t21	t22	t23	t24	t25	t26	t27	t28	t29	t30	t31	t32	t33	t34	t35	t36	t37	A.
Okitsu	0.00	0.00	0.00	0.00	0.00	0.00	0.00	0.00	0.00	0.00	0.00	0.00	0.18	0.36	0.36	0.11	0.00	0.00	0.00	0.00	0.00	0.00	0.00	0.00	0.00	0.00	0.00	0.00	0.00	0.00	0.00	0.00	0.00	0.00	0.00	0.00	0.00	0.00
Otamadai	0.00	0.00	0.00	0.00	0.00	0.00	0.00	0.00	0.00	0.00	0.00	0.00	0.00	0.00	0.00	0.00	0.18	0.22	0.22	0.22	0.16	0.00	0.00	0.00	0.00	0.00	0.00	0.00	0.00	0.00	0.00	0.00	0.00	0.00	0.00	0.00	0.00	0.00
Otamadai - Kasori E	0.00	0.00	0.00	0.00	0.00	0.00	0.00	0.00	0.00	0.00	0.00	0.00	0.00	0.00	0.00	0.00	0.08	0.10	0.10	0.10	0.10	0.10	0.10	0.10	0.10	0.08	0.00	0.00	0.00	0.00	0.00	0.00	0.00	0.00	0.00	0.00	0.00	0.00
Otamadai - Kasori EI	0.00	0.00	0.00	0.00	0.00	0.00	0.00	0.00	0.00	0.00	0.00	0.00	0.00	0.00	0.00	0.00	0.13	0.17	0.17	0.17	0.17	0.17	0.03	0.00	0.00	0.00	0.00	0.00	0.00	0.00	0.00	0.00	0.00	0.00	0.00	0.00	0.00	0.00
Otamadai - Kasori EII	0.00	0.00	0.00	0.00	0.00	0.00	0.00	0.00	0.00	0.00	0.00	0.00	0.00	0.00	0.00	0.00	0.10	0.13	0.13	0.13	0.13	0.13	0.13	0.13	0.01	0.00	0.00	0.00	0.00	0.00	0.00	0.00	0.00	0.00	0.00	0.00	0.00	0.00
Otamadai - Kasori EII	0.00	0.00	0.00	0.00	0.00	0.00	0.00	0.00	0.00	0.00	0.00	0.00	0.00	0.00	0.00	0.00	0.10	0.13	0.13	0.13	0.13	0.13	0.13	0.13	0.01	0.00	0.00	0.00	0.00	0.00	0.00	0.00	0.00	0.00	0.00	0.00	0.00	0.00
Otamadai - Kasori EIII	0.00	0.00	0.00	0.00	0.00	0.00	0.00	0.00	0.00	0.00	0.00	0.00	0.00	0.00	0.00	0.00	0.09	0.12	0.12	0.12	0.12	0.12	0.12	0.12	0.09	0.00	0.00	0.00	0.00	0.00	0.00	0.00	0.00	0.00	0.00	0.00	0.00	0.00
Otamadai (Late)	0.00	0.00	0.00	0.00	0.00	0.00	0.00	0.00	0.00	0.00	0.00	0.00	0.00	0.00	0.00	0.00	0.00	0.07	0.34	0.34	0.24	0.00	0.00	0.00	0.00	0.00	0.00	0.00	0.00	0.00	0.00	0.00	0.00	0.00	0.00	0.00	0.00	0.00
Otamadai / Yakemachi	0.00	0.00	0.00	0.00	0.00	0.00	0.00	0.00	0.00	0.00	0.00	0.00	0.00	0.00	0.00	0.00	0.18	0.22	0.22	0.22	0.16	0.00	0.00	0.00	0.00	0.00	0.00	0.00	0.00	0.00	0.00	0.00	0.00	0.00	0.00	0.00	0.00	0.00
Otamadai I - II	0.00	0.00	0.00	0.00	0.00	0.00	0.00	0.00	0.00	0.00	0.00	0.00	0.00	0.00	0.00	0.00	0.50	0.50	0.00	0.00	0.00	0.00	0.00	0.00	0.00	0.00	0.00	0.00	0.00	0.00	0.00	0.00	0.00	0.00	0.00	0.00	0.00	0.00
Otamadai I - II / Katsuzaka	0.00	0.00	0.00	0.00	0.00	0.00	0.00	0.00	0.00	0.00	0.00	0.00	0.00	0.00	0.00	0.00	0.17	0.21	0.21	0.21	0.21	0.00	0.00	0.00	0.00	0.00	0.00	0.00	0.00	0.00	0.00	0.00	0.00	0.00	0.00	0.00	0.00	0.00
Otamadai I - III	0.00	0.00	0.00	0.00	0.00	0.00	0.00	0.00	0.00	0.00	0.00	0.00	0.00	0.00	0.00	0.00	0.21	0.26	0.26	0.26	0.00	0.00	0.00	0.00	0.00	0.00	0.00	0.00	0.00	0.00	0.00	0.00	0.00	0.00	0.00	0.00	0.00	0.00
Otamadai Ia	0.00	0.00	0.00	0.00	0.00	0.00	0.00	0.00	0.00	0.00	0.00	0.00	0.00	0.00	0.00	0.00	1.00	0.00	0.00	0.00	0.00	0.00	0.00	0.00	0.00	0.00	0.00	0.00	0.00	0.00	0.00	0.00	0.00	0.00	0.00	0.00	0.00	0.00
Otamadai Ia - IIa / Katsuzaka 1	0.00	0.00	0.00	0.00	0.00	0.00	0.00	0.00	0.00	0.00	0.00	0.00	0.00	0.00	0.00	0.00	0.50	0.50	0.00	0.00	0.00	0.00	0.00	0.00	0.00	0.00	0.00	0.00	0.00	0.00	0.00	0.00	0.00	0.00	0.00	0.00	0.00	0.00
Otamadai Ib	0.00	0.00	0.00	0.00	0.00	0.00	0.00	0.00	0.00	0.00	0.00	0.00	0.00	0.00	0.00	0.00	0.80	0.20	0.00	0.00	0.00	0.00	0.00	0.00	0.00	0.00	0.00	0.00	0.00	0.00	0.00	0.00	0.00	0.00	0.00	0.00	0.00	0.00
Otamadai II	0.00	0.00	0.00	0.00	0.00	0.00	0.00	0.00	0.00	0.00	0.00	0.00	0.00	0.00	0.00	0.00	0.20	0.80	0.00	0.00	0.00	0.00	0.00	0.00	0.00	0.00	0.00	0.00	0.00	0.00	0.00	0.00	0.00	0.00	0.00	0.00	0.00	0.00
Otamadai II - IV	0.00	0.00	0.00	0.00	0.00	0.00	0.00	0.00	0.00	0.00	0.00	0.00	0.00	0.00	0.00	0.00	0.05	0.26	0.26	0.26	0.18	0.00	0.00	0.00	0.00	0.00	0.00	0.00	0.00	0.00	0.00	0.00	0.00	0.00	0.00	0.00	0.00	0.00
Otamadai II - Kasori EII	0.00	0.00	0.00	0.00	0.00	0.00	0.00	0.00	0.00	0.00	0.00	0.00	0.00	0.00	0.00	0.00	0.03	0.14	0.14	0.14	0.14	0.14	0.14	0.14	0.01	0.00	0.00	0.00	0.00	0.00	0.00	0.00	0.00	0.00	0.00	0.00	0.00	0.00
Otamadai III	0.00	0.00	0.00	0.00	0.00	0.00	0.00	0.00	0.00	0.00	0.00	0.00	0.00	0.00	0.00	0.00	0.00	0.09	0.45	0.45	0.00	0.00	0.00	0.00	0.00	0.00	0.00	0.00	0.00	0.00	0.00	0.00	0.00	0.00	0.00	0.00	0.00	0.00
Otamadai III - IV	0.00	0.00	0.00	0.00	0.00	0.00	0.00	0.00	0.00	0.00	0.00	0.00	0.00	0.00	0.00	0.00	0.00	0.07	0.34	0.34	0.24	0.00	0.00	0.00	0.00	0.00	0.00	0.00	0.00	0.00	0.00	0.00	0.00	0.00	0.00	0.00	0.00	0.00
Otamadai III - Kasori EI	0.00	0.00	0.00	0.00	0.00	0.00	0.00	0.00	0.00	0.00	0.00	0.00	0.00	0.00	0.00	0.00	0.00	0.05	0.23	0.23	0.23	0.23	0.05	0.00	0.00	0.00	0.00	0.00	0.00	0.00	0.00	0.00	0.00	0.00	0.00	0.00	0.00	0.00
Otamadai III - Nakabyo	0.00	0.00	0.00	0.00	0.00	0.00	0.00	0.00	0.00	0.00	0.00	0.00	0.00	0.00	0.00	0.00	0.00	0.07	0.34	0.34	0.24	0.00	0.00	0.00	0.00	0.00	0.00	0.00	0.00	0.00	0.00	0.00	0.00	0.00	0.00	0.00	0.00	0.00
Otamadai III (Late) - IV	0.00	0.00	0.00	0.00	0.00	0.00	0.00	0.00	0.00	0.00	0.00	0.00	0.00	0.00	0.00	0.00	0.00	0.00	0.06	0.56	0.39	0.00	0.00	0.00	0.00	0.00	0.00	0.00	0.00	0.00	0.00	0.00	0.00	0.00	0.00	0.00	0.00	0.00
Otamadai III / Katsuzaka 3	0.00	0.00	0.00	0.00	0.00	0.00	0.00	0.00	0.00	0.00	0.00	0.00	0.00	0.00	0.00	0.00	0.00	0.00	0.33	0.33	0.33	0.00	0.00	0.00	0.00	0.00	0.00	0.00	0.00	0.00	0.00	0.00	0.00	0.00	0.00	0.00	0.00	0.00
Otamadai IV - Nakabyo	0.00	0.00	0.00	0.00	0.00	0.00	0.00	0.00	0.00	0.00	0.00	0.00	0.00	0.00	0.00	0.00	0.00	0.00	0.00	0.00	1.00	0.00	0.00	0.00	0.00	0.00	0.00	0.00	0.00	0.00	0.00	0.00	0.00	0.00	0.00	0.00	0.00	0.00
Pre-Kasori E	0.00	0.00	0.00	0.00	0.00	0.00	0.00	0.00	0.00	0.00	0.00	0.00	0.00	0.00	0.00	0.00	0.00	0.00	0.00	0.45	0.45	0.09	0.00	0.00	0.00	0.00	0.00	0.00	0.00	0.00	0.00	0.00	0.00	0.00	0.00	0.00	0.00	0.00

Continued on next page

Table A.6: Aoristic Weights and Pottery Phases

Pottery Phase	B.	t1	t2	t3	t4	t5	t6	t7	t8	t9	t10	t11	t12	t13	t14	t15	t16	t17	t18	t19	t20	t21	t22	t23	t24	t25	t26	t27	t28	t29	t30	t31	t32	t33	t34	t35	t36	t37	A.
Sekiyama	0.00	0.22	0.22	0.22	0.22	0.11	0.00	0.00	0.00	0.00	0.00	0.00	0.00	0.00	0.00	0.00	0.00	0.00	0.00	0.00	0.00	0.00	0.00	0.00	0.00	0.00	0.00	0.00	0.00	0.00	0.00	0.00	0.00	0.00	0.00	0.00	0.00	0.00	0.00
Sekiyama - Goryogadai	0.00	0.07	0.07	0.07	0.07	0.07	0.07	0.07	0.07	0.07	0.07	0.07	0.07	0.07	0.07	0.07	0.01	0.00	0.00	0.00	0.00	0.00	0.00	0.00	0.00	0.00	0.00	0.00	0.00	0.00	0.00	0.00	0.00	0.00	0.00	0.00	0.00	0.00	0.00
Sekiyama - Kurohama	0.00	0.12	0.12	0.12	0.12	0.12	0.12	0.12	0.12	0.06	0.00	0.00	0.00	0.00	0.00	0.00	0.00	0.00	0.00	0.00	0.00	0.00	0.00	0.00	0.00	0.00	0.00	0.00	0.00	0.00	0.00	0.00	0.00	0.00	0.00	0.00	0.00	0.00	0.00
Sekiyama - Moroiso b	0.00	0.09	0.09	0.09	0.09	0.09	0.09	0.09	0.09	0.09	0.09	0.09	0.04	0.00	0.00	0.00	0.00	0.00	0.00	0.00	0.00	0.00	0.00	0.00	0.00	0.00	0.00	0.00	0.00	0.00	0.00	0.00	0.00	0.00	0.00	0.00	0.00	0.00	0.00
Sekiyama - Moroiso b	0.00	0.09	0.09	0.09	0.09	0.09	0.09	0.09	0.09	0.09	0.09	0.09	0.04	0.00	0.00	0.00	0.00	0.00	0.00	0.00	0.00	0.00	0.00	0.00	0.00	0.00	0.00	0.00	0.00	0.00	0.00	0.00	0.00	0.00	0.00	0.00	0.00	0.00	0.00
Sekiyama - Moroiso c	0.00	0.08	0.08	0.08	0.08	0.08	0.08	0.08	0.08	0.08	0.08	0.08	0.08	0.08	0.00	0.00	0.00	0.00	0.00	0.00	0.00	0.00	0.00	0.00	0.00	0.00	0.00	0.00	0.00	0.00	0.00	0.00	0.00	0.00	0.00	0.00	0.00	0.00	0.00
Sekiyama I	0.00	0.22	0.22	0.22	0.22	0.11	0.00	0.00	0.00	0.00	0.00	0.00	0.00	0.00	0.00	0.00	0.00	0.00	0.00	0.00	0.00	0.00	0.00	0.00	0.00	0.00	0.00	0.00	0.00	0.00	0.00	0.00	0.00	0.00	0.00	0.00	0.00	0.00	0.00
Sekiyama I (Early - Middle)	0.00	0.22	0.22	0.22	0.22	0.11	0.00	0.00	0.00	0.00	0.00	0.00	0.00	0.00	0.00	0.00	0.00	0.00	0.00	0.00	0.00	0.00	0.00	0.00	0.00	0.00	0.00	0.00	0.00	0.00	0.00	0.00	0.00	0.00	0.00	0.00	0.00	0.00	0.00
Sekiyama I (Early)	0.00	0.22	0.22	0.22	0.22	0.11	0.00	0.00	0.00	0.00	0.00	0.00	0.00	0.00	0.00	0.00	0.00	0.00	0.00	0.00	0.00	0.00	0.00	0.00	0.00	0.00	0.00	0.00	0.00	0.00	0.00	0.00	0.00	0.00	0.00	0.00	0.00	0.00	0.00
Sekiyama I (Late) - II	0.00	0.22	0.22	0.22	0.22	0.11	0.00	0.00	0.00	0.00	0.00	0.00	0.00	0.00	0.00	0.00	0.00	0.00	0.00	0.00	0.00	0.00	0.00	0.00	0.00	0.00	0.00	0.00	0.00	0.00	0.00	0.00	0.00	0.00	0.00	0.00	0.00	0.00	0.00
Sekiyama I (Middle - Late)	0.00	0.22	0.22	0.22	0.22	0.11	0.00	0.00	0.00	0.00	0.00	0.00	0.00	0.00	0.00	0.00	0.00	0.00	0.00	0.00	0.00	0.00	0.00	0.00	0.00	0.00	0.00	0.00	0.00	0.00	0.00	0.00	0.00	0.00	0.00	0.00	0.00	0.00	0.00
Sekiyama II	0.00	0.22	0.22	0.22	0.22	0.11	0.00	0.00	0.00	0.00	0.00	0.00	0.00	0.00	0.00	0.00	0.00	0.00	0.00	0.00	0.00	0.00	0.00	0.00	0.00	0.00	0.00	0.00	0.00	0.00	0.00	0.00	0.00	0.00	0.00	0.00	0.00	0.00	0.00
Sekiyama II - Kurohama (Early)	0.00	0.12	0.12	0.12	0.12	0.12	0.12	0.12	0.12	0.06	0.00	0.00	0.00	0.00	0.00	0.00	0.00	0.00	0.00	0.00	0.00	0.00	0.00	0.00	0.00	0.00	0.00	0.00	0.00	0.00	0.00	0.00	0.00	0.00	0.00	0.00	0.00	0.00	0.00
Shimoono	0.00	0.00	0.00	0.00	0.00	0.00	0.00	0.00	0.00	0.00	0.00	0.00	0.00	0.00	0.00	0.78	0.22	0.00	0.00	0.00	0.00	0.00	0.00	0.00	0.00	0.00	0.00	0.00	0.00	0.00	0.00	0.00	0.00	0.00	0.00	0.00	0.00	0.00	0.00
Shindo	0.00	0.00	0.00	0.00	0.00	0.00	0.00	0.00	0.00	0.00	0.00	0.00	0.00	0.00	0.00	0.50	0.50	0.00	0.00	0.00	0.00	0.00	0.00	0.00	0.00	0.00	0.00	0.00	0.00	0.00	0.00	0.00	0.00	0.00	0.00	0.00	0.00	0.00	0.00
Shomyoji	0.00	0.00	0.00	0.00	0.00	0.00	0.00	0.00	0.00	0.00	0.00	0.00	0.00	0.00	0.00	0.00	0.00	0.00	0.00	0.00	0.00	0.00	0.00	0.00	0.00	0.12	0.59	0.29	0.00	0.00	0.00	0.00	0.00	0.00	0.00	0.00	0.00	0.00	0.00
Shomyoji - Horinouchi	0.00	0.00	0.00	0.00	0.00	0.00	0.00	0.00	0.00	0.00	0.00	0.00	0.00	0.00	0.00	0.00	0.00	0.00	0.00	0.00	0.00	0.00	0.00	0.00	0.00	0.03	0.17	0.17	0.17	0.17	0.17	0.13	0.00	0.00	0.00	0.00	0.00	0.00	0.00
Shomyoji (Early)	0.00	0.00	0.00	0.00	0.00	0.00	0.00	0.00	0.00	0.00	0.00	0.00	0.00	0.00	0.00	0.00	0.00	0.00	0.00	0.00	0.00	0.00	0.00	0.00	0.00	0.17	0.83	0.00	0.00	0.00	0.00	0.00	0.00	0.00	0.00	0.00	0.00	0.00	0.00
Shomyoji (Early)	0.00	0.00	0.00	0.00	0.00	0.00	0.00	0.00	0.00	0.00	0.00	0.00	0.00	0.00	0.00	0.00	0.00	0.00	0.00	0.00	0.00	0.00	0.00	0.00	0.00	0.17	0.83	0.00	0.00	0.00	0.00	0.00	0.00	0.00	0.00	0.00	0.00	0.00	0.00
Shomyoji (Late)	0.00	0.00	0.00	0.00	0.00	0.00	0.00	0.00	0.00	0.00	0.00	0.00	0.00	0.00	0.00	0.00	0.00	0.00	0.00	0.00	0.00	0.00	0.00	0.00	0.00	0.00	1.00	0.00	0.00	0.00	0.00	0.00	0.00	0.00	0.00	0.00	0.00	0.00	0.00
Shomyoji 1	0.00	0.00	0.00	0.00	0.00	0.00	0.00	0.00	0.00	0.00	0.00	0.00	0.00	0.00	0.00	0.00	0.00	0.00	0.00	0.00	0.00	0.00	0.00	0.00	0.00	0.17	0.83	0.00	0.00	0.00	0.00	0.00	0.00	0.00	0.00	0.00	0.00	0.00	0.00
Shomyoji 1	0.00	0.00	0.00	0.00	0.00	0.00	0.00	0.00	0.00	0.00	0.00	0.00	0.00	0.00	0.00	0.00	0.00	0.00	0.00	0.00	0.00	0.00	0.00	0.00	0.00	0.17	0.83	0.00	0.00	0.00	0.00	0.00	0.00	0.00	0.00	0.00	0.00	0.00	0.00
Shomyoji 1 - Horinouchi 1	0.00	0.00	0.00	0.00	0.00	0.00	0.00	0.00	0.00	0.00	0.00	0.00	0.00	0.00	0.00	0.00	0.00	0.00	0.00	0.00	0.00	0.00	0.00	0.00	0.00	0.05	0.23	0.23	0.23	0.23	0.05	0.00	0.00	0.00	0.00	0.00	0.00	0.00	0.00
Shomyoji 2	0.00	0.00	0.00	0.00	0.00	0.00	0.00	0.00	0.00	0.00	0.00	0.00	0.00	0.00	0.00	0.00	0.00	0.00	0.00	0.00	0.00	0.00	0.00	0.00	0.00	0.00	1.00	0.00	0.00	0.00	0.00	0.00	0.00	0.00	0.00	0.00	0.00	0.00	0.00
Shomyoji 2 - Horinouchi	0.00	0.00	0.00	0.00	0.00	0.00	0.00	0.00	0.00	0.00	0.00	0.00	0.00	0.00	0.00	0.00	0.00	0.00	0.00	0.00	0.00	0.00	0.00	0.00	0.00	0.00	0.00	0.21	0.21	0.21	0.21	0.17	0.00	0.00	0.00	0.00	0.00	0.00	0.00
Shomyoji 2 - Horinouchi 1	0.00	0.00	0.00	0.00	0.00	0.00	0.00	0.00	0.00	0.00	0.00	0.00	0.00	0.00	0.00	0.00	0.00	0.00	0.00	0.00	0.00	0.00	0.00	0.00	0.00	0.00	0.00	0.21	0.21	0.21	0.21	0.17	0.00	0.00	0.00	0.00	0.00	0.00	0.00

Continued on next page

Table A.6: Aoristic Weights and Pottery Phases

Pottery Phase	B.	t1	t2	t3	t4	t5	t6	t7	t8	t9	t10	t11	t12	t13	t14	t15	t16	t17	t18	t19	t20	t21	t22	t23	t24	t25	t26	t27	t28	t29	t30	t31	t32	t33	t34	t35	t36	t37	A.
Soya	0.00	0.00	0.00	0.00	0.00	0.00	0.00	0.00	0.00	0.00	0.00	0.00	0.00	0.00	0.00	0.00	0.00	0.00	0.00	0.00	0.00	0.00	0.00	0.00	0.00	0.00	0.00	0.00	0.00	0.00	0.00	0.00	0.00	0.00	1.00	0.00	0.00	0.00
Soya - Angyo 1	0.00	0.00	0.00	0.00	0.00	0.00	0.00	0.00	0.00	0.00	0.00	0.00	0.00	0.00	0.00	0.00	0.00	0.00	0.00	0.00	0.00	0.00	0.00	0.00	0.00	0.00	0.00	0.00	0.00	0.00	0.00	0.00	0.00	0.00	0.41	0.59	0.00	0.00
Soya - Angyo 3a	0.00	0.00	0.00	0.00	0.00	0.00	0.00	0.00	0.00	0.00	0.00	0.00	0.00	0.00	0.00	0.00	0.00	0.00	0.00	0.00	0.00	0.00	0.00	0.00	0.00	0.00	0.00	0.00	0.00	0.00	0.00	0.00	0.00	0.00	0.17	0.24	0.24	0.36
Tado - Kasori EII	0.00	0.00	0.00	0.00	0.00	0.00	0.00	0.00	0.00	0.00	0.00	0.00	0.00	0.00	0.00	0.00	0.00	0.00	0.00	0.00	0.00	0.00	0.42	0.53	0.05	0.00	0.00	0.00	0.00	0.00	0.00	0.00	0.00	0.00	0.00	0.00	0.00	0.00
Takaihigashi	0.00	0.00	0.00	0.00	0.00	0.00	0.00	0.00	0.00	0.00	0.00	0.00	0.00	0.00	0.00	0.00	0.00	0.00	0.00	0.00	0.00	0.00	0.00	0.00	0.00	0.00	0.00	0.00	0.00	0.00	0.00	0.00	0.00	0.00	1.00	0.00	0.00	0.00
Transition between Kasori EI and Kasori EII	0.00	0.00	0.00	0.00	0.00	0.00	0.00	0.00	0.00	0.00	0.00	0.00	0.00	0.00	0.00	0.00	0.00	0.00	0.00	0.00	0.00	0.32	0.59	0.09	0.00	0.00	0.00	0.00	0.00	0.00	0.00	0.00	0.00	0.00	0.00	0.00	0.00	0.00
Ukishima	0.00	0.00	0.00	0.00	0.00	0.00	0.00	0.00	0.00	0.17	0.33	0.33	0.17	0.00	0.00	0.00	0.00	0.00	0.00	0.00	0.00	0.00	0.00	0.00	0.00	0.00	0.00	0.00	0.00	0.00	0.00	0.00	0.00	0.00	0.00	0.00	0.00	0.00
Ukishima I	0.00	0.00	0.00	0.00	0.00	0.00	0.00	0.00	0.00	0.30	0.60	0.10	0.00	0.00	0.00	0.00	0.00	0.00	0.00	0.00	0.00	0.00	0.00	0.00	0.00	0.00	0.00	0.00	0.00	0.00	0.00	0.00	0.00	0.00	0.00	0.00	0.00	0.00
Ukishima I (Late) / Moroiso b	0.00	0.00	0.00	0.00	0.00	0.00	0.00	0.00	0.00	0.00	0.25	0.50	0.25	0.00	0.00	0.00	0.00	0.00	0.00	0.00	0.00	0.00	0.00	0.00	0.00	0.00	0.00	0.00	0.00	0.00	0.00	0.00	0.00	0.00	0.00	0.00	0.00	0.00
Ukishima I / Moroiso a	0.00	0.00	0.00	0.00	0.00	0.00	0.00	0.00	0.00	0.30	0.60	0.10	0.00	0.00	0.00	0.00	0.00	0.00	0.00	0.00	0.00	0.00	0.00	0.00	0.00	0.00	0.00	0.00	0.00	0.00	0.00	0.00	0.00	0.00	0.00	0.00	0.00	0.00
Ukishima II	0.00	0.00	0.00	0.00	0.00	0.00	0.00	0.00	0.00	0.00	0.00	1.00	0.00	0.00	0.00	0.00	0.00	0.00	0.00	0.00	0.00	0.00	0.00	0.00	0.00	0.00	0.00	0.00	0.00	0.00	0.00	0.00	0.00	0.00	0.00	0.00	0.00	0.00
Ukishima II (Early)	0.00	0.00	0.00	0.00	0.00	0.00	0.00	0.00	0.00	0.00	0.00	1.00	0.00	0.00	0.00	0.00	0.00	0.00	0.00	0.00	0.00	0.00	0.00	0.00	0.00	0.00	0.00	0.00	0.00	0.00	0.00	0.00	0.00	0.00	0.00	0.00	0.00	0.00
Ukishima II / Moroiso a	0.00	0.00	0.00	0.00	0.00	0.00	0.00	0.00	0.00	0.21	0.43	0.36	0.00	0.00	0.00	0.00	0.00	0.00	0.00	0.00	0.00	0.00	0.00	0.00	0.00	0.00	0.00	0.00	0.00	0.00	0.00	0.00	0.00	0.00	0.00	0.00	0.00	0.00
Ukishima II / Moroiso b (Late)	0.00	0.00	0.00	0.00	0.00	0.00	0.00	0.00	0.00	0.00	0.00	0.50	0.50	0.00	0.00	0.00	0.00	0.00	0.00	0.00	0.00	0.00	0.00	0.00	0.00	0.00	0.00	0.00	0.00	0.00	0.00	0.00	0.00	0.00	0.00	0.00	0.00	0.00
Ukishima III	0.00	0.00	0.00	0.00	0.00	0.00	0.00	0.00	0.00	0.00	0.00	0.25	0.75	0.00	0.00	0.00	0.00	0.00	0.00	0.00	0.00	0.00	0.00	0.00	0.00	0.00	0.00	0.00	0.00	0.00	0.00	0.00	0.00	0.00	0.00	0.00	0.00	0.00
Ukishima III - Okitsu	0.00	0.00	0.00	0.00	0.00	0.00	0.00	0.00	0.00	0.00	0.00	0.05	0.29	0.29	0.29	0.09	0.00	0.00	0.00	0.00	0.00	0.00	0.00	0.00	0.00	0.00	0.00	0.00	0.00	0.00	0.00	0.00	0.00	0.00	0.00	0.00	0.00	0.00
Ukishima III (Early) / Moroiso b	0.00	0.00	0.00	0.00	0.00	0.00	0.00	0.00	0.00	0.00	0.25	0.50	0.25	0.00	0.00	0.00	0.00	0.00	0.00	0.00	0.00	0.00	0.00	0.00	0.00	0.00	0.00	0.00	0.00	0.00	0.00	0.00	0.00	0.00	0.00	0.00	0.00	0.00
Ukishima III / Moroiso b	0.00	0.00	0.00	0.00	0.00	0.00	0.00	0.00	0.00	0.00	0.25	0.50	0.25	0.00	0.00	0.00	0.00	0.00	0.00	0.00	0.00	0.00	0.00	0.00	0.00	0.00	0.00	0.00	0.00	0.00	0.00	0.00	0.00	0.00	0.00	0.00	0.00	0.00
Yakemachi	0.00	0.00	0.00	0.00	0.00	0.00	0.00	0.00	0.00	0.00	0.00	0.00	0.00	0.00	0.00	0.00	0.04	0.22	0.22	0.22	0.22	0.09	0.00	0.00	0.00	0.00	0.00	0.00	0.00	0.00	0.00	0.00	0.00	0.00	0.00	0.00	0.00	0.00
Yakemachi - Kasori E2	0.00	0.00	0.00	0.00	0.00	0.00	0.00	0.00	0.00	0.00	0.00	0.00	0.00	0.00	0.00	0.00	0.00	0.00	0.27	0.33	0.33	0.07	0.00	0.00	0.00	0.00	0.00	0.00	0.00	0.00	0.00	0.00	0.00	0.00	0.00	0.00	0.00	0.00
Yakemachi / Katsuzaka / Otamadai	0.00	0.00	0.00	0.00	0.00	0.00	0.00	0.00	0.00	0.00	0.00	0.00	0.00	0.00	0.00	0.00	0.18	0.22	0.22	0.22	0.16	0.00	0.00	0.00	0.00	0.00	0.00	0.00	0.00	0.00	0.00	0.00	0.00	0.00	0.00	0.00	0.00	0.00
Yakemachi / Otamadai	0.00	0.00	0.00	0.00	0.00	0.00	0.00	0.00	0.00	0.00	0.00	0.00	0.00	0.00	0.00	0.00	0.00	0.00	0.27	0.33	0.33	0.07	0.00	0.00	0.00	0.00	0.00	0.00	0.00	0.00	0.00	0.00	0.00	0.00	0.00	0.00	0.00	0.00

Appendix B

ODD Protocol of the Agent Based Simulation

The following description of the Agent Based model is based on the ODD protocol proposed by Grimm and colleagues (2006, 2010).

B.1 PURPOSE

The purpose of the model is to:

1. combine the basic concepts of ideal free distribution (Fretwell and Lucas 1970) and several ecological models of group formation based on the notion of fitness curves (e.g. Clark and Mangel 1986);

2. explore group fission-fusion dynamics by modelling the knowledge of individual agents;

3. assess the rank-size distribution of the groups, and determine whether this is characterised by a fixed equilibrium or not.

The basic model is further extended to explore the effect o two different forms of disturbance, one generated by the behaviour of the agent themselves (*endogenic*

disturbance model) and the other originating from outside the system (*exogenic disturbance model*).

B.2 ENTITIES, STATE VARIABLES, AND SCALES

The model is structured by two scales of human aggregation: *minimum aggregate units* and *groups*. The former are represented by the basic units of the simulation model (the agents) and refer to inseparable groups of human individuals who share the same decision-making process. This could be a household or any other form of close-tied aggregation of individuals (e.g. kinship groups). These units are generally inseparable unless a fission process occurs via reproduction (see below). The second and highest scale of the model are represented by *groups*. They can be defined as *minimum aggregate units* who reside on the same *patch*, a discrete portion of a toroidal lattice representing the spatial environment of the agents. Each *patch* is characterised by a single state variable, K, representing the local resource input. Agents of the same group are characterised also by the same fitness ϕ, which in turn will determine their death and reproduction rate.

Fitness is computed as a function of K, the group size g (the number of *minimum aggregate units*, i.e. agents, located on the same patch), and the fixed parameters μ (the basic fitness for $g = 1$), b (shape of the fitness function) and ϵ (stochastic component of the fitness function). Although agents of the same group have the same fitness, the actual *locus* of the decision-making is in the individual agent, and is a function of five fixed parameters: h (spatial range of movement), s (spatial range of observation), z (frequency of decision-making), k (sample proportion of observed agents), c (threshold for fitness comparison). The outcome of the decision-making will be the potential spatial relocation of the agent to another *patch*, which mimics instances of migration and group fission-fusion.

Three variants of the model are proposed. In the basic *disturbance-free model* K is fixed, in the *endogenic disturbance model* K is modelled as prey population, and in the *exogenic disturbance model* K is decreased following a set of parameters.

Table B.1 shows the list of parameters used in the simulation.

B.3 PROCESS OVERVIEW AND SCHEDULING

The model proceeds by discrete steps $t = 1, 2, 3, ...T$ that are not directly referable to real-world temporal scales (i.e. they do not represent years, months, or days). Each time-step can be defined as the amount of time sufficient for all agents to make a decision, reproduce, and die. Within each step the following sequence of events occur:

1. Externally induced modification of K (only for the *exogenic disturbance model*).
2. Fitness evaluation.
3. Reproduction and death.
4. Resource regeneration (only for the *endogenic disturbance model*).
5. Migration and fission-fusion processes.
6. Data collection.

The update of the agents' state variable is synchronic for all points expect for 5., where this is sequential and initialised with a different ordering at each time-step.

B.4 DESIGN CONCEPTS

B.4.1 Basic Principles

The core principle of the model is a combination between group formation models —designed to explore the implication of positive and negative frequency dependence in fitness curves (e.g. Sibly 1983, Clark and Mangel 1986), and ideal free distribution models (e.g. Fretwell and Lucas 1970, Tregenza 1995), —designed for

building expectation on how individual allocates in relation to resource distribution—. By combining these two theoretical frameworks, the agent-based model seeks to integrate induced and inherent spatial dependencies (Fortin and Dale 2005) in metapopulation dynamics.

B.4.2 Emergence

Population and meta-population dynamics emerge from the behaviour of agents in response to either the decision-making of other agents or to an external force to the system, and are not imposed by the model architecture.

B.4.3 Adaptation

Agents adapt to changing condition (usually a decline in their fitness) by moving to another group (migration) or by creating a new group (fission and fusion).

B.4.4 Objectives

The objective of each agent is to improve their fitness in a comparative (i.e. do better than another agent) or absolute fashion (i.e. do better than a given value).

B.4.5 Learning

Agents are capable to copy the behaviour of other agents (e.g. the choice to be in a specific group), by means of a variant of model-biased transmission (see Henrich and McElreath 2003) coupled with a comparative threshold-based assessment of their own condition (see Kennedy 1998, Henrich 2001).

B.4.6 Sensing

Agents are spatially constrained in their knowledge by the parameters h and s, temporally by z, and qualitatively by k. The first two variables indicate the Chebyshev distance within a focal agent can observe the behaviour of the other agents

and the spatial range where the fission process is allowed (see below), the third refers to the frequency by which the agent gains knowledge about groups located in the neighbourhood defined by s, and the fourth indicate the sample proportion of other agents from which the best individual (the model) is chosen.

B.4.7 Interaction

Interactions between agents are primarily modelled by the fitness function, which assumes that the co-presence of multiple individuals in the same patch leads to either an increase or a decrease of an agent's fitness. Other indirect forms of interactions include the "packing" effect, when agents are unable to fission to a new group due to the occupation (by other agents) of all available patches.

B.4.8 Stochasticity

The following procedures includes stochastic components:

- Fitness evaluation (partly based on a random draw from a continuous normal distribution).
- Death and reproduction (bernoulli draws with function-based probability of success).
- Scheduling order (random permutation of the order of execution).
- Choice of the model agent during the learning stage (random draw from a discrete uniform distribution).
- Choice of the fission destination (random draw from a discrete uniform distribution).

B.4.9 Collectives

The only collectives in the model are *groups*, agents located on the same environment patch sharing the same fitness.

B.4.10 Observations

Temporal variation in the metapopulation structure (group size distribution) are calculated by computing the distribution of group sizes. This can be then used to compute measures including the total population size and the total number of groups, or more complex statistics such as the A-coefficient (Drennan and Peterson 2004).

B.5 INITIALISATION

The simulation is initialised by the creation of n agents randomly scattered in space. Agents located on the same patch will automatically form groups.

B.6 INPUT DATA

The simulation does not involve the input of any external data.

B.7 SUB-MODELS

B.7.1 Fitness Evaluation

The payoff ϕ_i of a focal agent i, is computed as a function of the resource input K and the group size g. The core assumption of the sub-model is that, with other things being equal, increasing group size will have positive effects to the group, until the group reaches an optimal size $g*$, where ϕ is maximised. When $g > g*$, fitness will decrease so the frequency dependence will be reversed, with larger group size determining smaller ϕ. Positive frequency dependence is modelled by formalising two additional assumptions: (1) larger group will be less prone to random fluctuations in the payoff; and (2) larger group will enhance the quality of their subsistence activities by means of cooperation and specialisation. Negative frequency dependence will be simply a function of limited resource pool size.

The basic component of the model is the yield of the individual subsistence task. This will be modelled with the following equation

$$\xi_i = \mathcal{N}(\mu_i + (g-1)^b, \epsilon) \tag{B.1}$$

where $\mathcal{N}()$ indicates a random draw from a normal distribution, with the first parameter indicating the mean ($\mu_i + (g-1)^b$) and the second indicating the standard deviation (ϵ). Equation (B.1) predicts that, on average, individual yield will linearly increase with increased group size, while the variance will remain constant.

Once the contribution ξ_i of each individual i of a group j is computed, the total yield of the group will be computed as follows:

$$\Xi_j = \sum_{i=1, i \in j}^{g} \xi_i \tag{B.2}$$

The total contribution of the group will then be shared among individuals of the group. Thus, when g is large, the effect derived by ϵ will become smaller. This essentially mimics the outcome of sharing as a risk-reducing strategy. However Ξ_j is constrained by K, so that when $\Xi_j > K$, Ξ_j is reduced to the amount of available resources in the patch. These two concepts are combined in the following equation:

$$\phi_{i \in j} \begin{cases} \Xi_j / g & \text{if } \Xi_j \leq K \\ K/g & \text{if } \Xi_j > K \end{cases} \tag{B.3}$$

The sequence of equations B.1, B.2 and B.3 will determine a function where the relation between the group size g and individual payoff ϕ can be depicted as a single humped curve, on the condition that $K < \infty$.

B.7.2 Reproduction and Death

Reproduction

Reproduction occurs with frequency r derived from the following equation:

$$r = \rho \frac{\phi}{\mu} \tag{B.4}$$

where ρ is the basic reproduction rate, so that when $\phi = \mu$, $r = \rho$. In other words, fitness will be linearly and positively correlated to the chance of reproduction.

Death

Death is also triggered as a bernoulli draw with a probability of success (death) equal to d, derived from the following logistic equation:

$$d = \frac{1}{1 + e^{(\omega_1 \phi) - \omega_2}} \tag{B.5}$$

where, ω_1 and ω_2 are shape parameters, and e is the base of the natural logarithm.

B.7.3 Fission-Fusion and Migration

Agents have the possibility improve their payoff through spatial relocation. This will involve a two-step process. Firstly each focal agent i will evaluate the surrounding environment and determine if other agents do better, subsequently the agent will have the opportunity to leave its own group to either forage alone or to join another group.

First we define $q_i(s)$ as the set composed by agents within a Chebyshev distance of s from the focal agent i. Each agent, with frequency z will have the opportunity to observe a subset of $q_i(s)$ of size $\lceil k|q_i(s)| \rceil$, where k is a proportion between 0 and 1. We then define the agent with the highest fitness among such a subset w.

The focal agent's fitness (ϕ_i) is then compared to both the model agent's fitness (ϕ_w) and the basic fitness (μ). Each comparison will be calibrated by a predefined *threshold of evidence* (c_1,c_2, and c_3). These value will essentially represent the propensity of the agent to change its behaviour. When c is small, the agent will

change its behaviour to minimal disadvantage of its behaviour compared to the model or the individual foraging mode. When, on the other hand c is high, the agent will be conservative and more likely persists with its own strategy.

Depending on the outcome of the comparison, the state variables of both agents, and the presence/absence of agents in a defined neighbourhood, the following set of decisions can be undertaken by the focal agent (see also table B.2):

No Change This occurs either because the agent is satisfied with the current situation (usually when $\phi_i > \phi_w$ AND $\phi_i > \mu - c_1$) or because the agent is unable to make its choice. The latter condition occurs when the agent decides to fission (see next bullet point) but no empty patches are available within a Chebyshev distance of h.

Fission Fission allows the agent to leave and form a group composed by itself, with the expectation to achieve an average payoff equal to μ. This occurs when one of the following three conditions are met:

1. Both focal agent and the model agents are in a group of size > 1, the focal agents' payoff is smaller than $\mu - c_1$ and either the agents' payoff is larger than the model's ($\phi_i > \phi_w$) or the model agent's payoff is also smaller than $\mu - c_1$. The agent choose to go and forage alone as: 1) being in its own group is no longer profitable; and 2) joining the other group will produce lower yields than being alone. Notice that in both cases the assumption is that the agents know the amount of the basic payoff μ.
2. The focal agent is in a group and the model agent is alone, with the agents' payoff being smaller than $\phi_w - c_1$ or $\mu - c_1$. In this case the agent decides to forage alone by imitating the model agent's strategy.
3. The focal agent's group is isolated (i.e. no other agents are located within distance s) and its payoff is lower than $\mu - c_1$.

In all three cases fission is triggered only if an unoccupied patch is present within a Chebyshev distance of h from the focal agent.

Fusion and Migration Migration occurs when the focal agent is located in a group and decides to move to another. This occurs when the focal agent's fitness is smaller than $\phi_w - c_2$ and the model agent's fitness is greater than $\mu - c_1$. An agent can also migrate to another group when its fitness is below $\phi_i - c_1$, but the model agent's fitness should be still greater than $\mu - c_1$.

Fusion occurs when the focal agent is alone (i.e. $g_i = m$) and the model agent is in a group. This is triggered when the fitness of the model agent minus the threshold of evidence c_3 is larger than ϕ_i.

Fusion and Group Formation If both the focal and the model agent have a group size of 1 (i.e. when $g_i = g_w = m$), then the two agents can form a group if both their fitness are below μ. Notice that the model agent will not be able to make any further choice during the time-step (i.e. the decision is assumed to be made by both agents).

B.7.4 Variation of the Resource Pool Size K

The basic setting of the model assumes a fixed value for K. By relaxing this assumption, and allowing a dynamic value for K, it is possible to mimic two different types of disturbance processes. The first models K as a function of the agents behaviour, and thus can be regarded as an endogenic disturbance process; the second imposes a variation of the resource input from outside, and thus can be referred to as exogenic disturbance process.

Verhulst model of resource growth (*endogenic disturbance model*)

This version of the disturbance process models K as a prey population defined by a modified version of the Verhulst equation (Verhulst 1838):

$$K_t = (K_{t-1} - \hat{\Xi}) + \zeta(K_{t-1} - \hat{\Xi}) \left(1 - \frac{K_{t-1} - \hat{\Xi}}{\kappa}\right) \tag{B.6}$$

where κ is the theoretical maximum carrying capacity of the resource pool and ζ is its intrinsic growth rate. Equation (B.6) models the resource pool as a population located at each patch, with its own internal dynamics perturbed by the amount consumed by the predator agents ($\hat{\Xi}$). This will be formally defined as follows:

$$\hat{\Xi} \begin{cases} \Xi & \text{if } \Xi \leq (K_{t-1} - \beta K_{t-1}) \\ K_{t-1} - \beta K_{t-1} & \text{if } \Xi > (K_{t-1} - \beta K_{t-1}) \end{cases} \tag{B.7}$$

Equation (B.7) assumes that the predator population (the agents in this case) is constrained in their exploitation of the prey population. This is modelled as function of the resource resilience parameter β, which varies between 0 and 1. When $\beta = 0$, $\hat{\Xi}$ can be equal to K_{t-1}, and hence the predator population can drive the prey population to extinction. However, if $\beta > 0$, $\hat{\Xi}$ will always be smaller than K_{t-1}, ensuring the survival of the prey population (i.e. K_t can never be smaller than βK_{t-1}). Notice that in this scenario, equation B.3 will be updated as follows:

$$\phi_{i \in j} = \hat{\Xi}_j / g \tag{B.8}$$

Linear decrease over time (*exogenic disturbance model*)

The exogenic disturbance will be modelled as a linear decrease of the resource input K of all patches with the following function:

$$K_t = K_{t-1} - \delta(t_s, t_e) \tag{B.9}$$

where $\delta(t_s, t_e)$ is defined as follows:

$$\delta(t_s, t_e) \begin{cases} 0 & \text{if } t < t_s \\ 0 & \text{if } t > t_e \\ \eta & \text{if } t_s \leq t \leq t_e \end{cases} \tag{B.10}$$

K will thus have a constant value K_s until time-step t_s, then it will decrease its

value linearly and reach its final value K_e at t_e.

	General Settings
T	Total number of time-steps
P	Total number of patches
	Fitness curve related
μ	Basic individual payoff
ϵ	Payoff variance
b	Cooperation benefit
K	Resource input
	Reproduction and Death related
r	Reproduction rate
d	Death rate
ρ	Basic reproduction rate
ω_1	Death parameter 1
ω_2	Death parameter 2
	Fission/fusion/migration related
z	Frequency of decision-making
k	Sample proportion of observed agents
s	Neighbour search distance
h	Fission distance
c_1	Treshold of evidence for fission
c_2	Treshold of evidence for migration
c_3	Treshold of evidence for fusion
	Disturbance related
κ	Prey population carrying capacity
ζ	Prey population growth rate
β	Prey population resilience
$\hat{\Xi}$	Predator consumption
t_s	Start time-step of disturbance process
t_e	End time-step of disturbance process
η	Resource decline rate

Table B.1: Model parameters

Condition 1	Condition 2	Decision
$g_i > 1\ AND\ g_w > 1$	$\mu - c_1 < \phi_i \geq \phi_w$	No Change
	$\phi_i \leq (\mu - c_1)\ AND\ [\phi_w \leq (\mu - c_1)\ OR\ \phi_i \geq \phi_w]$	Fission
	$[\phi_i \leq (\phi_w - c_2)\ OR\ \phi_i \leq (\mu - c_1)]\ AND\ \phi_w > (\mu - c_1)$	Migration
$g_i > 1\ AND\ g_w = 1$	$\phi_i \geq \phi_w$	No Change
	$\phi_i < (\phi_w - c_1)\ OR\ \phi_i < (\mu - c_1)$	Fission
$g_i = 1\ AND\ g_w > 1$	$\phi_i \geq \phi_w$	No Change
	$\phi_i \leq (\phi_w - c_3)$	Migration
$g_i = 1\ AND\ g_w = 1$	$\phi_i \geq \phi_w$	No Change
	$\phi_i < \mu\ AND\ \phi_w < \mu$	Fusion
$g_w = NULL$	$\phi_i \leq (\mu - c_1)$	Fission

Table B.2: Summary of Fission Fusion decision-making criteria. *NULL* indicates that the information is unavailable.

Appendix C

ABM Code

C.1 Disturbance-free Model

All versions of the agent-based models are written in R statistical computing language and can be executed once all scripts are sourced. The main function `FF()` will require a series of sub-functions (`initialise()`, `evaluateFitness()`, `repDeath()`, `fissionfusion()`) for its execution.

FF()

```
#
# *disturbance free model*
#
#
# MODEL PARAMETERS:
# ini       ... Initial Number of Agents
# P         ... Square root of the number of patches
# K         ... Resource Input Size
# mu        ... Basic Payoff
# b         ... group benefit
# sigma     ... payoff uncertainty
# c1        ... cost 1 for FissionFusion
# c2        ... cost 2 for FissionFusion
# c3        ... cost 3 for FissionFusion
# c4        ... cost 4 for FissionFusion ///New Parameter///
# timesteps ... number of timesteps
# k         ... Number of sampled neighbour agents for the model Biased Transmission
# z         ... Frequency of Decision Making (transmission rate)
```

```
# h          ... Fission Distance (in Chebyshev distance)
# s          ... Observation Distance (in Chebyshev distance)
# omega1      ... Mortality Parameter 1
# omega2       ... Mortality Parameter 2
# r          ... Reproduction Rate
# run        ... run number (to be used only for HPC)
#
#

FF <- function(ini = 10, P = 10, K = 200, mu = 10, c1 = 3, c2 = 3, c3 = 0, c4 = 0,
               k = 1, b = 0.5, sigma = 1, timesteps = 300, r = 0.05,
               omega1 = 1.0, omega2 = 5, size = P, h = 1 , s = 1,
               z = 1, run = 1)
{
# The following line prints the run number for HPC
print(paste("RunNumber=",run,sep=""));


#Initialise model
tmp <- initialise(ini = ini, P = P, K = K); #initialise model
groupSpace <- tmp$groupSpace; #extract groupSpace

Raw <- cbind(groupSpace$R, groupSpace$C);
RawMat <- matrix(0, nrow=length(groupSpace$R), ncol=timesteps);
Raw <- cbind(Raw, RawMat);


for (t in seq(timesteps)){

# STEP1 Fitness Evaluation (computed by group):
groupSpace <- evaluateFitness(groupSpace, mu = mu, b = b, sigma = sigma);

# STEP2 Reproduction & Death:
groupSpace <- repDeath(groupSpace = groupSpace, mu = mu, r = r, omega1 = omega1,
                       omega2 = omega2);


#Loophole in case of extinction:
if(sum(groupSpace$groupSize) == 0)
  {
    print("extinction!");
    return(Raw);
    break();
  }
```

```
#STEP 3 FissionFusion
groupSpacePre<-groupSpace
groupSpace <- fissionfusion(groupSpace, k=k, c1=c1,
                                                c2=c2, c3=c3, c4=c4, P=P, h=h, s=s, z=z, mu=mu);
groupSpaceAfter<-groupSpace
if (any(groupSpace$groupSize<0)){break()}


#STEP 4 Record group size distribution
Raw[,t+2] <- groupSpace$groupSize


#RETURN ARGUMENTS
return(Raw)

}
```

initialise()

```
# Initialise function
# Reads P (...square root of the Patch number), ini (... the initial number of agents),
# and K (...the resource input size)
# Ouputs:
#
# agentSet ... a data.frame with the number of rows corresponding to "ini"
#              containing the following columns:
#              R ... row coordinate
#              C ... column coordinate
#              fitness ... initial fitness (set to 0)
#              contribution ... initial contribution (set to 0)
#              groupID ... linker to specific groups

# groupSpace...a data.frame with row number equal to P^2  with the following columns:
#              R             ... row coordinate
#              C             ... column coordinate
#              occupied      ... 1=occupied; 0=not occupied
#              preoccupied   ... 1=previously occupied; 0=previously not occupied
#              groupSize     ... current groupSize
#              pregroupSize  ... previous groupSIze
#              T             ... Total Group Contribution
#              K             ... Resource Input Size
#              fit           ... Individual Fitness

# world    ...matrix of P by P representing the world
```

```
initialise <- function(P, ini, K)
{
#Create World
world <- matrix(0, P, P);
#Create Agent Space

agentSet <- data.frame(R=sample(1:P, ini, TRUE), C = sample(1:P, ini, TRUE),
                    fitness = numeric(length=ini), contribution = numeric(length=ini),
                    groupID = numeric(length=ini));

groupSpace <- expand.grid(R=1:P,C=1:P);

groupSpace <- cbind(groupSpace, occupied = rep(0, length = P^2),
               preoccupied = rep(0, length=P^2), groupSize = numeric(length=P^2),
               pregroupSize = numeric(length=P^2), T = numeric(length = P^2),
               K = rep(K, length=P^2),fit = numeric(length = P^2));


#Define Agent's group and update groupSpace and agentSet
for (i in seq(ini))
{
agentSet$groupID[i] = which(groupSpace$R == agentSet$R[i]&groupSpace$C == agentSet$C[i]);
groupSpace[agentSet$groupID[i], ]$groupSize = groupSpace[agentSet$groupID[i], ]$groupSize + 1;
groupSpace[agentSet$groupID[i], ]$occupied = 1;
}

#Define Group rank
groupSpace$preoccupied = groupSpace$occupied;
groupSpace$pregroupSize = groupSpace$groupSize;
return(list(agentSet = agentSet, groupSpace = groupSpace, world = world))
}
```

evaluateFitness()

```
# evaluateFitness function
# input: groupSpace, mu, b, sigma
# outputs:groupSpace (updated)

evaluateFitness <- function(groupSpace, mu, b, sigma)
{
index<-which(groupSpace$occupied==1);
```

```
for (i in index)
{
g <- groupSpace[i, ]$groupSize; #collect group size
groupSpace[i, ]$T =  sum(rnorm(n = g, mean = mu+(g^b)-1, sd = sigma));
                     #compute group contribution

if (groupSpace[i, ]$T>groupSpace[i, ]$K){
   groupSpace[i,]$T=groupSpace[i,]$K}
   #In case of overexploitation use K instead of T

groupSpace[i, ]$fit = groupSpace[i,]$T/g;
                      #compute individual fitness
}

return(groupSpace)
}
```

repDeath()

```
# repDeath function
# Inputs: groupSpace, mu, r, omega1 and omega2
# Exports:  groupSpace (updated)
#
#
repDeath <- function(groupSpace, mu, r, omega1, omega2)
{
index <- which(groupSpace$occupied == 1); #retrieve index of occupied patches

for (i in index)
{
Fit <- groupSpace[i, ]$fit; #collect fitness
G <- groupSpace[i, ]$groupSize; #collect groupSize
births <- 0
#births
births <- sum(runif(G)<((Fit/mu)*r))
#death:
deathProb <- 1/(1+exp(1)^((omega1*Fit)-omega2)); #probability of death
deaths <- sum(runif(G)<deathProb); #actual number of death

#update group size
G <- G+births-deaths

# IN case of extinction set everything to 0:
if (G<=0){
    groupSpace[i,]$groupSize <- 0;
    groupSpace[i,]$occupied <- 0;
```

```
    groupSpace[i,]$T <- 0;
    groupSpace[i,]$fit <- 0;
  }
if (G>0){
    groupSpace[i,]$groupSize <- G;
  }
}

return(groupSpace)

}
```

fissionfusion()

```
# inputs ...groupSpace, k,c1,c2,c3,s,h,P,z
# outputs.... updated groupSpace
# reverse dependencies ...FF()

fissionfusion <- function(groupSpace, k, c1, c2, c3, c4, s, h, P, z, mu)
{

#utility function for finding neighbours:
matNeighbour <- function(D, myLoc, size)
{
if (size < Inf){
  sizeSeq <- (-size:size)}

if (size == Inf){
  sizeSeq = 1:D}

if (length(sizeSeq) < D){

 L <- length(sizeSeq);
 coordinates <- expand.grid(r=sizeSeq, c=sizeSeq);
 rev <- D:1;
for (x in 1:L^2)
{
tmpR <- coordinates[x, 1] + myLoc[1];
tmpC <- coordinates[x, 2] + myLoc[2];
if (tmpR <= 0){
tmpR <- rev[abs(tmpR)+1];
}

if (tmpC <= 0)
{
```

```
tmpC <- rev[abs(tmpC)+1];
}
if (tmpR > D){
tmpR <- tmpR-D;
}
if (tmpC > D){
tmpC <- tmpC-D
}
coordinates[x, 1] <- tmpR;
coordinates[x, 2] <- tmpC;
}
}
if (length(sizeSeq) >= D){
    coordinates <- expand.grid(r=1:D, c=1:D);
  }
return(coordinates)
}



#Create AgentSet with the following columns:
  #id       ...agents' id
  #R        ...row coordinate
  #C        ...column coordinate
  #fitness  ...fitness
  #groupSize...group Size
  #groupID  ...group ID
  #moved    ...boolean (1=decision taken; 0=decision to be taken)

########################
####CREATE AGENTSET#####
########################

N = sum(groupSpace$groupSize);
agentSet = data.frame(id = 1:N, R = numeric(length=N), C = numeric(length=N),
                      fitness = numeric(length=N), groupSize = numeric(length=N),
                      groupID = numeric(length=N), moved = rep(1,N));

index <- which(groupSpace$occupied == 1);
counter = 1;
for (i in index)
{
G <- groupSpace[i,]$groupSize;
inputR <- counter:(counter+G-1);
counter <- counter+G;
```

```
agentSet[inputR, ]$R <- groupSpace[i, ]$R;
agentSet[inputR, ]$C <- groupSpace[i, ]$C;
agentSet[inputR, ]$fitness <- groupSpace[i, ]$fit;
agentSet[inputR, ]$groupSize <-G;
agentSet[inputR, ]$groupID <-as.numeric(rownames(groupSpace[i, ]));
}


################################
#####SELECT DECISIONMAKERS######
################################

#Randomize Order of Execution
order <- sample(1:N)
#Set frequency of execution
decisionmakers <- order[runif(N)<z]
if (length(decisionmakers)>0)
{
  #decisionmakers still need to make their decision (moved=0) w
  #while all the other agents are treated as if they've already
  #made their choices
  agentSet[decisionmakers,]$moved=0



for (x in decisionmakers)
  {

####################################
##########LOOK AROUND################
####################################


  #Look only at other groups

    #Spatially within the neighbourhood:
    myLoc <- c(agentSet[x, ]$R, agentSet[x, ]$C);
    destinations <- matNeighbour(D=P, myLoc=myLoc, size=s)
    # the following selects agents from the agentset with the coordinates of destinations
    # but without the groupID of the focal agent
    others <- which(agentSet$R %in% destinations$r & agentSet$C %in% destinations$c &
                    agentSet$groupID != agentSet[x,]$groupID)

    #if other is not empty (this could happen if the group is isolated spatially)
    if (length(others) > 0){
```

```
    #evaluate empty patches
    #Problem of synchronisation, as any refers to the current group space
    #however if this is referred to the <spaces> object, then it will lead to
    #the problem of co-occurence of agents in the same location.
    #for now the emptyPatches will refer to groupSpace no to spaces

    #evaluate emptypatches
    tmp <- matNeighbour(D=P, myLoc=myLoc, size=h);
    tmp2 <- which(groupSpace$R%in%tmp$r & groupSpace$C%in%tmp$c);
    emptyPatches <- any(groupSpace[tmp2, ]$occupied == 0);


####################################
##########CHOOSE MODEL STAGE#########
####################################
#reset the value of K (K UPPERCASE is the actual "k" used for sampling agents)

    K=k;
    K<-length(others)*K;
    K<-ceiling(K);

    if (K > length(others)){
      K <- length(others);
      }

    modelIDs=sample(x=others,size=K)

  #Choose the best fit agent among k individuals
  modelID <- modelIDs[which(agentSet[modelIDs, ]$fitness ==
                     max(agentSet[modelIDs, ]$fitness))[1]];
  modelF <- agentSet[modelID, ]$fitness
  modelG <- agentSet[modelID, ]$groupSize
  modelGID <- agentSet[modelID, ]$groupID
  myF <- agentSet[x, ]$fitness
  myG <- agentSet[x, ]$groupSize
  myGID <- agentSet[x, ]$groupID

####################################
##########COMPARISON STAGE########
####################################
if (agentSet[x, ]$moved != 1)
  {
#CASE 1: G vs G#
```

```
if (myG>1 & modelG>1)
  {
    if((myF>=modelF) & (myF>(mu-c1)))
      {
        #STAY, DO NOTHING
        agentSet[x, ]$moved <- 1
      }

    if (myF <= (mu-c1) & emptyPatches & ((myF>=modelF) | (modelF<=(mu-c1))))
      {
        #EMERGENCY FISSION
        #Reduce former group Size
        groupSpace[myGID, ]$groupSize <- groupSpace[myGID, ]$groupSize-1;
        #set occupied to 0 if there were no more agents
        if (groupSpace[myGID, ]$groupSize == 0) {
          groupSpace[myGID,  ]$occupied <- 0;
          }

        #Create a new group

        if(length(which(groupSpace$occupied==0))>1)
        {newPlace <- sample(x=which(groupSpace$occupied == 0),size=1);}
        if(length(which(groupSpace$occupied==0))==1)
        {newPlace <- which(groupSpace$occupied == 0)}
        if (groupSpace[newPlace, ]$groupSize > 0) {print("ERROR line 159")}
        groupSpace[newPlace, ]$groupSize <- 1
        groupSpace[newPlace, ]$occupied <- 1
        agentSet[x, ]$moved <- 1
      }

    if ((myF <= (modelF-c2) | (myF <= (mu-c1))) & modelF > (mu-c1)){
        #GUIDED MIGRATION
        #Change Group Sizes
        groupSpace[modelGID, ]$groupSize <- groupSpace[modelGID, ]$groupSize+1;
        agentSet[x, ]$moved <- 1
        #ensure the new group now is occupied
        groupSpace[modelGID, ]$occupied <- 1
        groupSpace[myGID, ]$groupSize <- groupSpace[myGID, ]$groupSize-1;
        if (groupSpace[myGID, ]$groupSize==0) {
          groupSpace[myGID, ]$occupied <- 0;
          }

      }

  }
```

```
#CASE 2: G vs L

if (myG>1 & modelG == 1){
    if(myF >= modelF){
        #STAY, DO NOTHING
      agentSet[x, ]$moved <- 1
      #  print("option4")
      }
     if ((myF < (modelF-c1) | (myF<=(mu-c1))) & emptyPatches)
      {
        #FISSION & EMERGENCY FISSION
        #Reduce former group Size
        groupSpace[myGID, ]$groupSize <- groupSpace[myGID, ]$groupSize-1;
        #handle local extinction
        if (groupSpace[myGID, ]$groupSize == 0) {
          groupSpace[myGID, ]$occupied <- 0}
        #Create a new group
        if(length(which(groupSpace$occupied==0))>1)
        {newPlace <- sample(x=which(groupSpace$occupied == 0),size=1);}
        if(length(which(groupSpace$occupied==0))==1)
        {newPlace <-which(groupSpace$occupied == 0)}
        groupSpace[newPlace, ]$groupSize <- 1;
        groupSpace[newPlace, ]$occupied <- 1;
        agentSet[x, ]$moved <- 1
      #  print("option5")
      }
    if ((myF > (modelF-c1) | (myF>(mu-c1))))
      {
        agentSet[x, ]$moved <- 1
      }

  }

#CASE 3: L vs G

if (myG == 1 & modelG > 1){
    if(myF >= modelF){
        #STAY, DO NOTHING
      agentSet[x, ]$moved <- 1
      }
    if (myF <= (modelF-c3)){
        #FUSION from SINGLE
        groupSpace[modelGID, ]$groupSize <- groupSpace[modelGID, ]$groupSize+1;
        groupSpace[modelGID, ]$occupied <- 1;
```

```
        groupSpace[myGID, ]$groupSize <- groupSpace[myGID, ]$groupSize-1;
        groupSpace[myGID, ]$occupied <- 0;
        agentSet[x, ]$moved <- 1
      }

  }

#CASE 4: L vs L

if (myG==1&modelG==1)
  {
    if(myF>=mu)
      {
        #STAY, DO NOTHING
        agentSet[x, ]$moved <- 1
      }

  #the third condition is to ensure that
  #the other agent did not make any decision, since this step
  # involves both agent making a decision.
    if (myF<(mu-c4) & modelF<(mu-c4) & agentSet[modelID, ]$moved == 0){
        #FUSION between SINGLES
        groupSpace[myGID, ]$groupSize <- groupSpace[myGID, ]$groupSize-1;
        groupSpace[myGID, ]$occupied <- 0;
        groupSpace[modelGID, ]$groupSize <- groupSpace[modelGID, ]$groupSize+1;
        groupSpace[modelGID, ]$occupied <- 1;
        agentSet[modelID, ]$moved <- 1;
        agentSet[x, ]$moved <- 1
      }

  }
}
  }


# CASE 5 : no other groups, emergency fission is still possible:
  if(length(others) == 0&agentSet[x, ]$moved != 1){
    myF <- agentSet[x, ]$fitness;
    emptyPatches <- any(groupSpace$occupied == 0);
    myGID <- agentSet[x, ]$groupID;

if (myF<(mu-c1) & emptyPatches){
        #EMERGENCY FISSION
        #Reduce former group Size
        groupSpace[myGID, ]$groupSize <- groupSpace[myGID, ]$groupSize-1;
```

```
        if (groupSpace[myGID, ]$groupSize == 0){
          groupSpace[myGID, ]$occupied <- 0;}

        #Create a new group
        if(length(which(groupSpace$occupied==0))>1)
        {newPlace <- sample(x=which(groupSpace$occupied == 0),size=1);}
        if(length(which(groupSpace$occupied==0))==1)
        {newPlace <-which(groupSpace$occupied== 0)}
        groupSpace[newPlace, ]$groupSize <- 1;
        groupSpace[newPlace, ]$occupied <- 1;
        agentSet[x, ]$moved <- 1
        #print("option10")
      }

    }

#After the decision is taken the agent is "moved"
agentSet[x, ]$moved <- 1;

  }
}
return(groupSpace)
}
```

C.2 Predator-prey model

The predator-prey version of the model is based on a slightly modified version of the main function `FF()`, along with a modified version of `evaluateFitness()` and the addition of the new sub-function `regenerateResources()`.

FF2()

```
#
# *Predator-prey model model*
#
#
# Additional MODEL PARAMETERS:
#  Kini ... Initial prey population size
#  KMax ... Prey carrying capacity (kappa)
#  gR ... Prey population growth rate (zeta)
#  beta ... Prey population reslience
```

```
FF2 <- function(ini = 10, P = 10, K = 200, mu = 10, c1 = 3, c2 = 3, c3 = 0, c4 = 0,
               k = 1, b = 0.5, sigma = 1, timesteps = 300, r = 0.05,
               omega1 = 1.0, omega2 = 5, size = P, h = 1 , s = 1,
               z = 1, run = 1, Kini=200, KMax=200, gR=2, beta=0.3)
{
# The following line prints the run number for HPC
print(paste("RunNumber=",run,sep=""));


#Initialise model
tmp <- initialise(ini = ini, P = P, K = K); #initialise model
groupSpace <- tmp$groupSpace; #extract groupSpace

Raw <- cbind(groupSpace$R, groupSpace$C);
RawMat <- matrix(0, nrow=length(groupSpace$R), ncol=timesteps);
Raw <- cbind(Raw, RawMat);


for (t in seq(timesteps)){

# STEP1 Fitness Evaluation (computed by group):
groupSpace <- evaluateFitness2(groupSpace, mu = mu, b = b, sigma = sigma, beta=beta);

# STEP2 Reproduction & Death:
groupSpace <- repDeath(groupSpace = groupSpace, mu = mu, r = r, omega1 = omega1,
                     omega2 = omega2);

# STEP3 Resource regeneration:
groupSpace <- regenerateResources(groupSpace=groupSpace, KMax=KMax, gR=gR);


#Loophole in case of extinction:
if(sum(groupSpace$groupSize) == 0)
  {
    print("extinction!");
    return(Raw);
    break();
  }



#STEP 4 FissionFusion
groupSpacePre<-groupSpace
groupSpace <- fissionfusion(groupSpace, k=k, c1=c1,
```

```
                                                    c2=c2, c3=c3, c4=c4, P=P, h=h, s=s, z=z, mu=mu);
groupSpaceAfter<-groupSpace
if (any(groupSpace$groupSize<0)){break()}


#STEP 5 Record group size distribution
Raw[,t+2] <- groupSpace$groupSize


#RETURN ARGUMENTS
return(Raw)

}
```

evaluateFitness2()

```
# evaluateFitness function
# input: groupSpace, mu, b, sigma, baseline
# output: groupSpace (updated)
#
#

evaluateFitness <- function(groupSpace, mu, b, sigma, beta)
{
index<-which(groupSpace$occupied == 1);


for (i in index)
{
startK <- groupSpace[i, ]$K;
g <- groupSpace[i, ]$groupSize; #collect group size
groupSpace[i, ]$T =  sum(rnorm(g, mean = mu+(g-1)^b, sd = sigma));
                     #compute group contribution

if (groupSpace[i, ]$T > (startK-startK*beta)){
   groupSpace[i,]$T <- startK-startK*beta}
   #In case of overexploitation use (K-K* beta) instead of T

groupSpace[i, ]$fit = groupSpace[i,]$T/g
                      #compute individual fitness

}

return(groupSpace)
}
```

regenerateResources()

```
# regenerateResources function
# input: groupSpace, KMax, gR
# output: groupSpace (updated)

regenerateResources <- function (groupSpace, KMax, gR)
{
  diff <- (groupSpace$K - groupSpace$T);
  groupSpace$K <- diff + (diff * gR * (1- diff/KMax));
  groupSpace$K[which(groupSpace$K<0)]=1 ;
  #exit strategy in case there is complete depletion
  #this should never happen, provided that beta>0
  groupSpace$T <- 0 ;
 return(groupSpace)
}
```

C.3 Exogenic Disturbance Model

The exogenic disturbance model is also based on a slightly modified version of the main function `FF()`.

FF3()

```
#
# *disturbance free model*
#
#
# Additional MODEL PARAMETERS:
# Kseq ...Vector (with length timesteps) representing the change of K over time.
#
#

FF <- function(ini = 10, P = 10, K = 200, mu = 10, c1 = 3, c2 = 3, c3 = 0, c4 = 0,
               k = 1, b = 0.5, sigma = 1, timesteps = 300, r = 0.05,
               omega1 = 1.0, omega2 = 5, size = P, h = 1 , s = 1,
               z = 1, run = 1,  Kseq=c(rep(200,299),
               seq(from=200,t=100,length=5),rep(100,196)))
{
# The following line prints the run number for HPC
print(paste("RunNumber=",run,sep=""));


#Initialise model
```

```
tmp <- initialise(ini = ini, P = P, K = K); #initialise model
groupSpace <- tmp$groupSpace; #extract groupSpace

Raw <- cbind(groupSpace$R, groupSpace$C);
RawMat <- matrix(0, nrow=length(groupSpace$R), ncol=timesteps);
Raw <- cbind(Raw, RawMat);


for (t in seq(timesteps)){

# STEP1 Environment Change
groupSpace$K<-Kseq[t]

# STEP2 Fitness Evaluation (computed by group):
groupSpace <- evaluateFitness(groupSpace, mu = mu, b = b, sigma = sigma);

# STEP3 Reproduction & Death:
groupSpace <- repDeath(groupSpace = groupSpace, mu = mu, r = r, omega1 = omega1,
                       omega2 = omega2);


#Loophole in case of extinction:
if(sum(groupSpace$groupSize) == 0)
  {
    print("extinction!");
    return(Raw);
    break();
  }

#STEP 4 FissionFusion
groupSpacePre<-groupSpace
groupSpace <- fissionfusion(groupSpace, k=k, c1=c1,
                                              c2=c2, c3=c3, c4=c4, P=P, h=h, s=s, z=z, mu=mu);
groupSpaceAfter<-groupSpace
if (any(groupSpace$groupSize<0)){break()}


#STEP 5 Record group size distribution
Raw[,t+2] <- groupSpace$groupSize


#RETURN ARGUMENTS
return(Raw)

}
```

Appendix D

Parameter Space Visualisation

The following pages show the simulation outputs using the parameter space visualisation techniques discussed in chapter 6 (sections 6.1.1 and 6.2.1). The combined time-series show the median value in solid line, and the envelope bounded by the 10% and 90% percentile in shaded grey. The y axes range from -1 to +1 for the A-coefficient, 0 to 100 for the group counts (G), and 0 to 35 for the median group size ($\tilde{\lambda}$). The y axes range of the agent counts (N) are specified in the caption of each figure. The x-axes of all combined time-series plots represent the time-steps and range from 0 to 500, with the exception of exogenic disturbance models where the interval is between 200 and 400, with the beginning and end of the disturbance stage shown as dashed lines. The x-axes do not represent time in the probability density plots where they instead represent the A-coefficient (from -1 to +1), the total number of groups (from 0 to 100), the median group size (from 0 to 35), and the number of agents (with range specified for each plot). Notice that the y-axes differ for each plot. The probability density plots of A-coefficients are coloured in shaded grey, with darker colours indicating higher proportion of computed A-coefficients. Finally, the correlograms are based on 25 lags (x-axis) with the y-axis showing the proportion of significant (with $p \leq 0.05$) positive and negative autocorrelation respectively above and below the horizontal line.

D.1 Disturbance-free model

D.1.1 A-Coefficient (A)

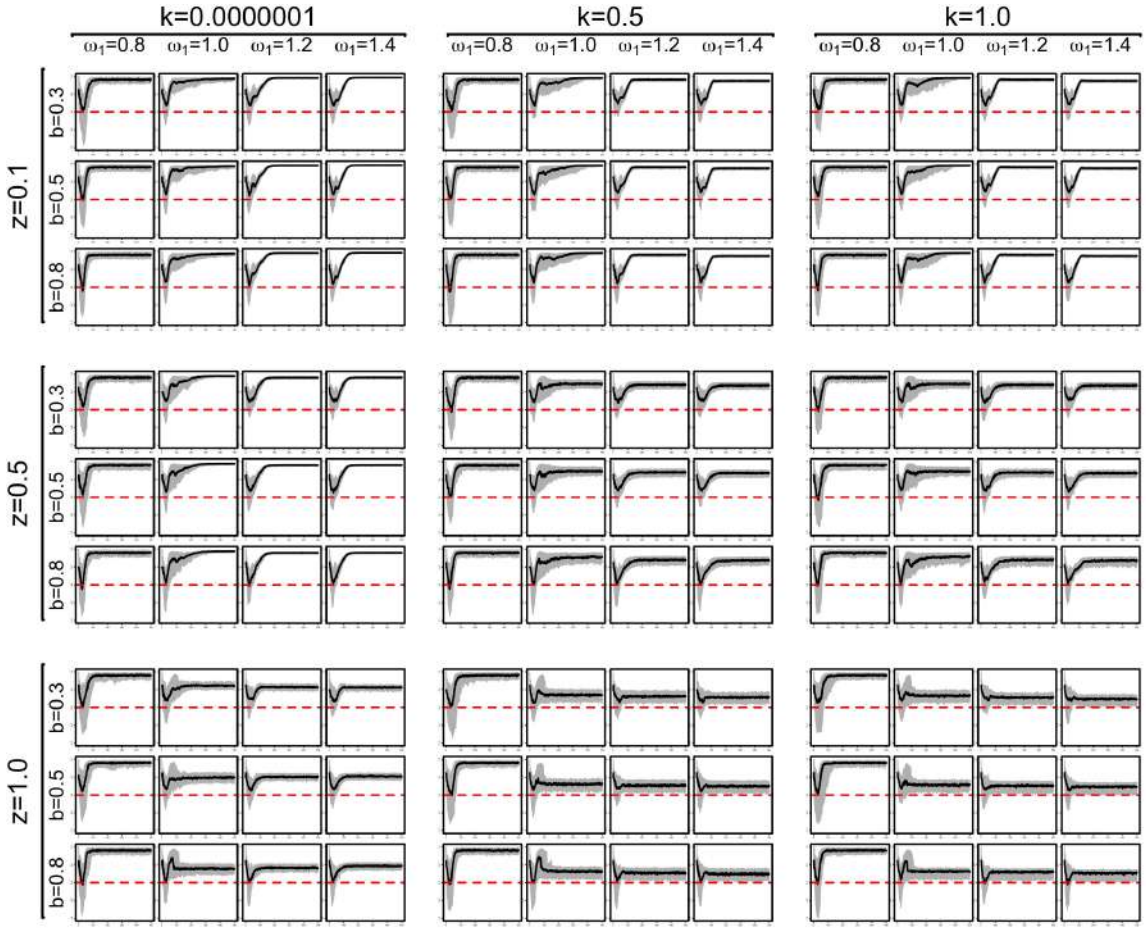

Combined time-series of A [disturbance-free model, $h = 1$]

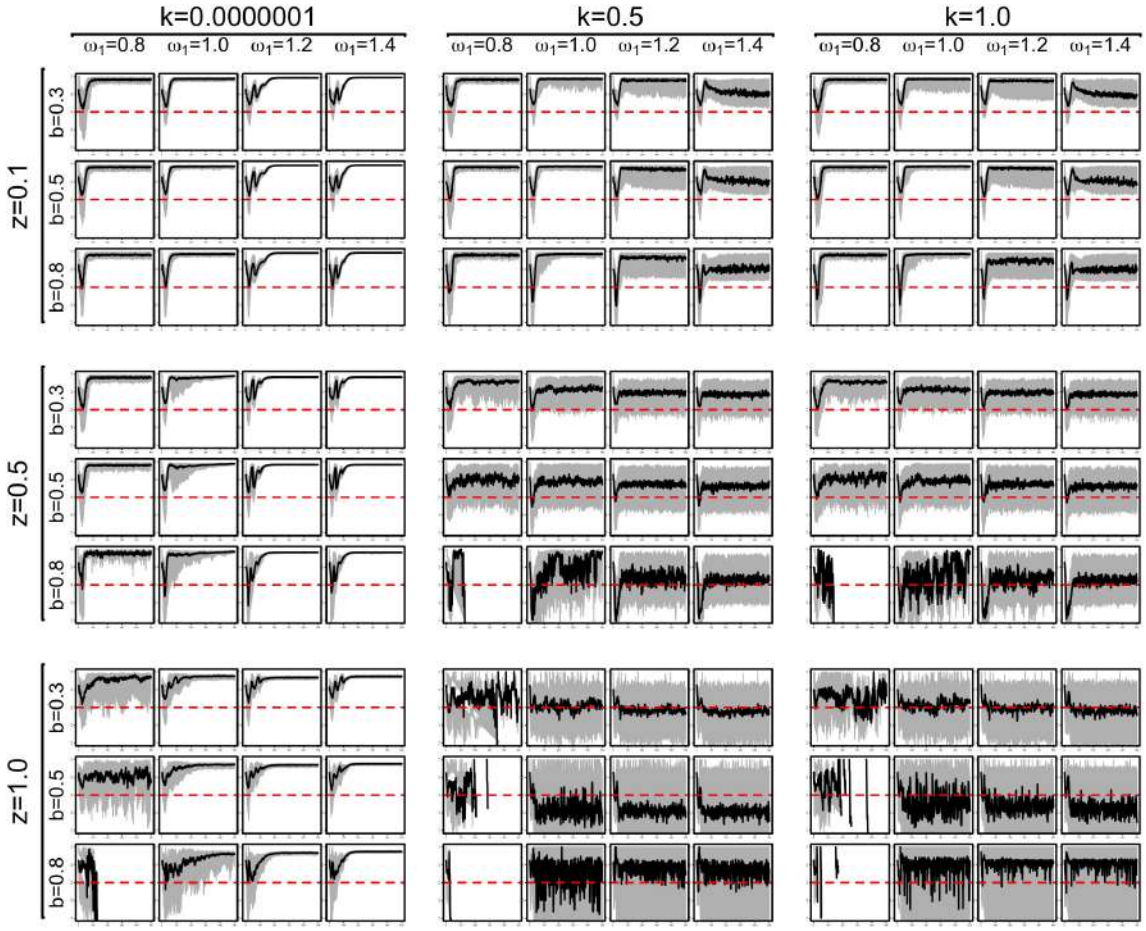

Combined time-series of A [disturbance-free model, $h = \infty$]

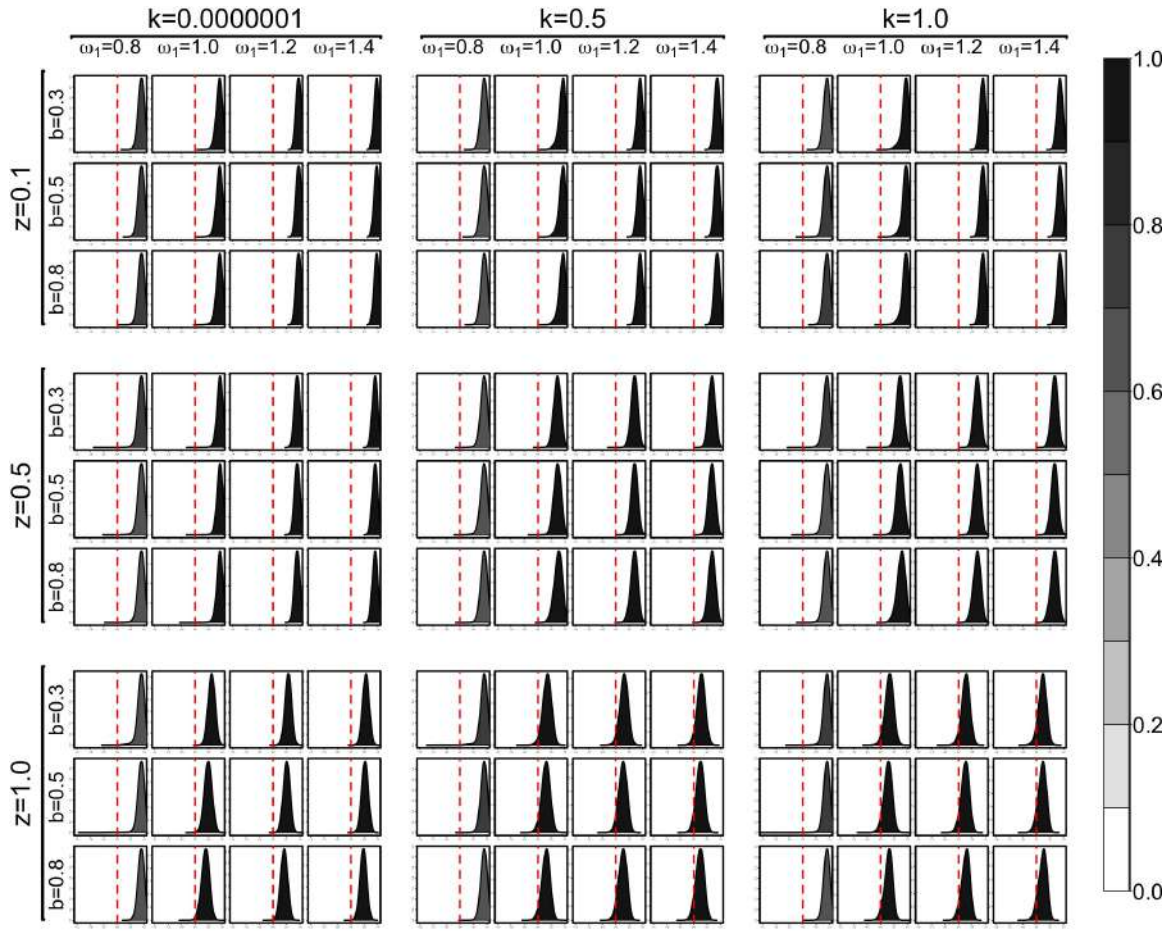

Probability density of A [disturbance-free model, $h = 1$]

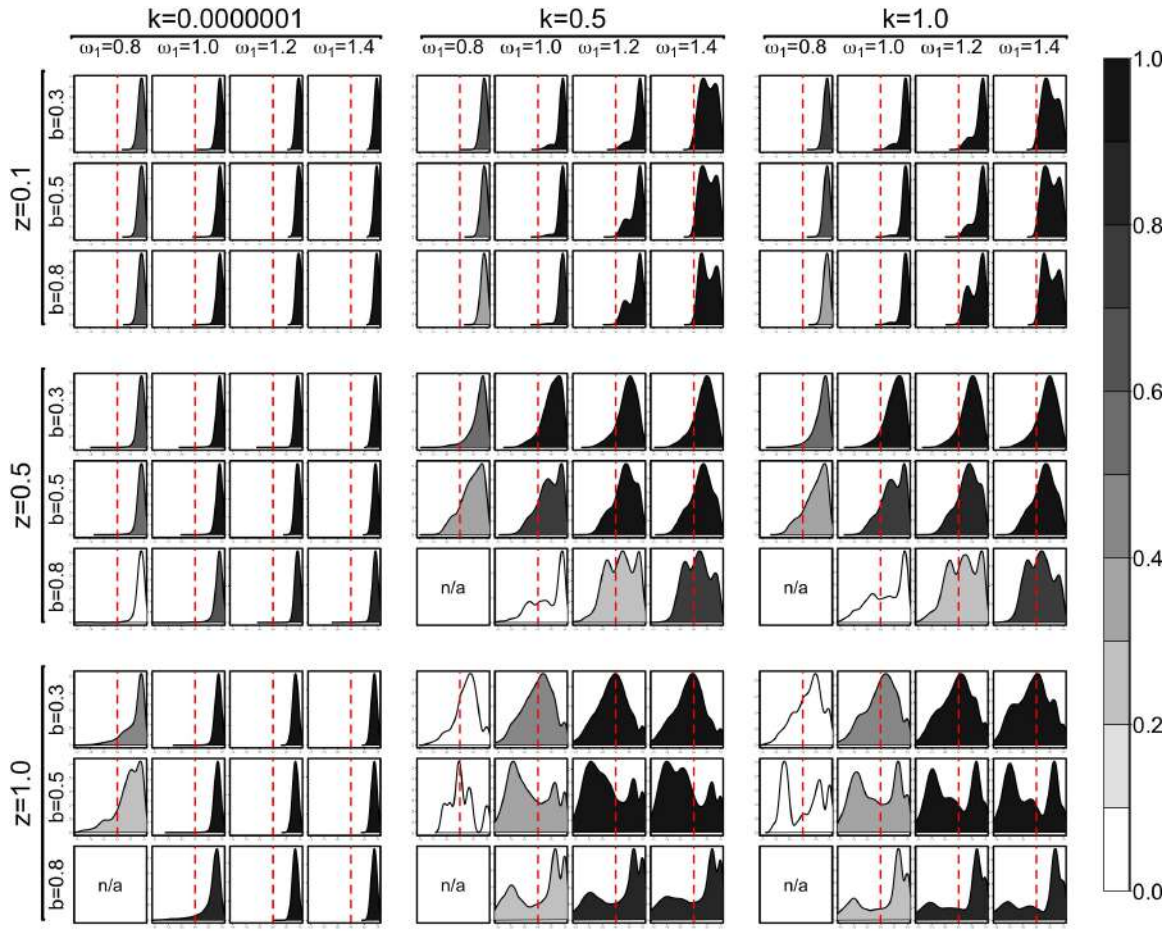

Probability density of A [disturbance-free model, $h = \infty$]

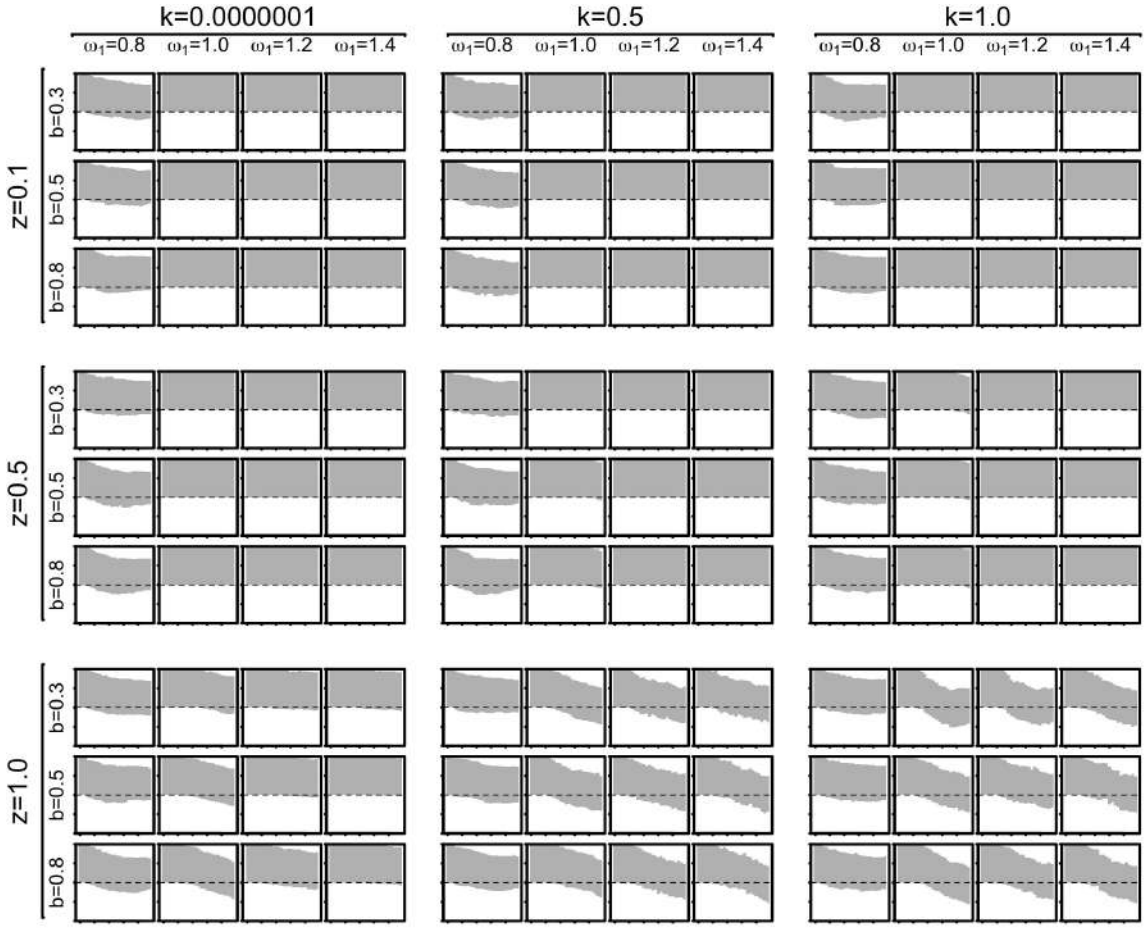

Correlogram of A [disturbance-free model, $h = 1$]

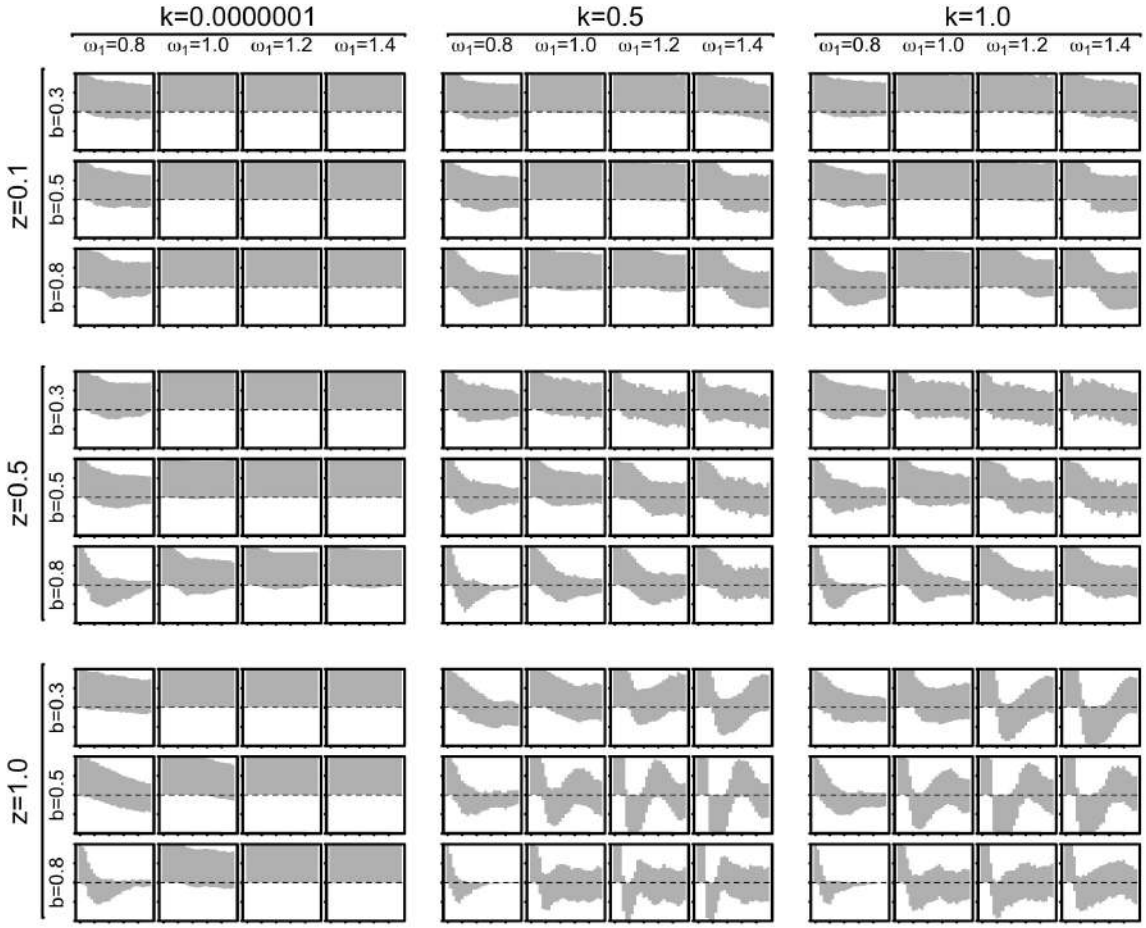

Correlogram of A [disturbance-free model, $h = \infty$]

D.1.2 Number of Groups (G)

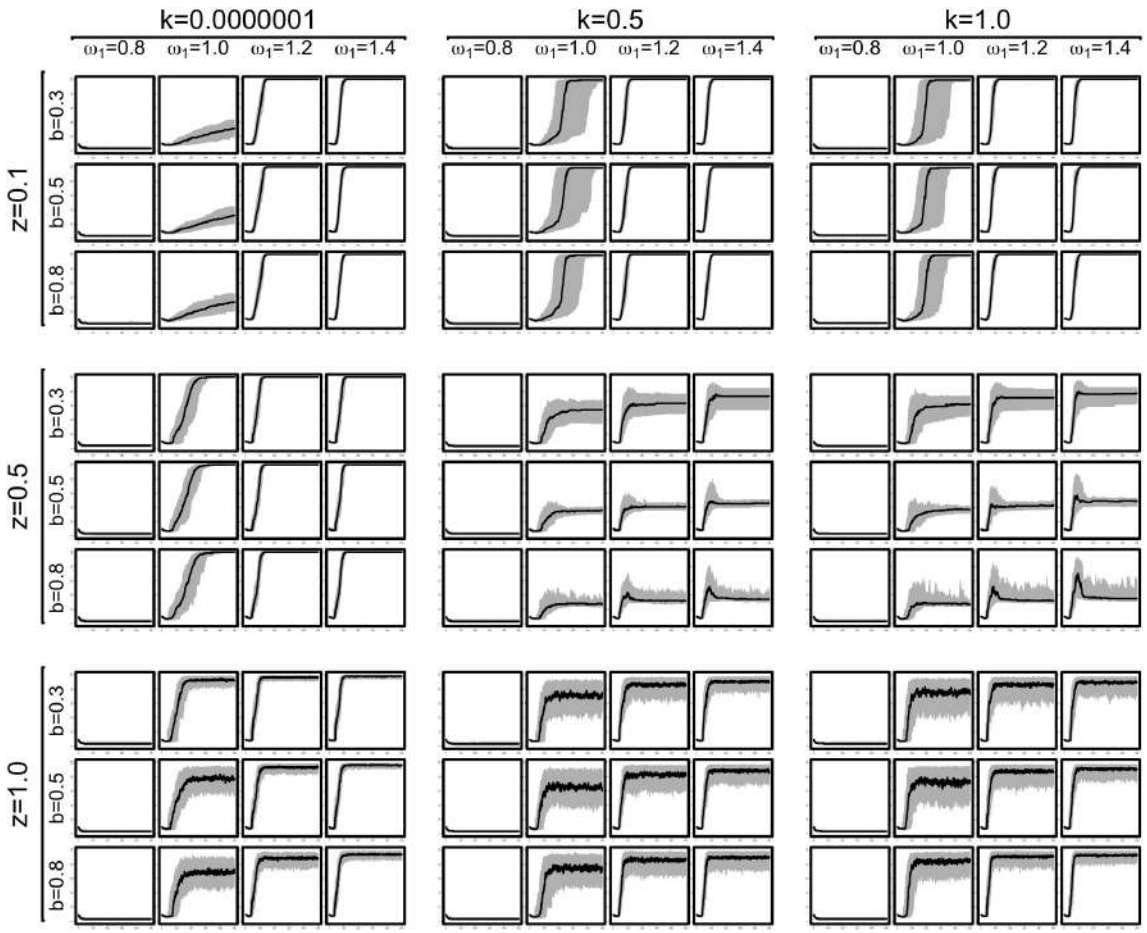

Combined time-series of G [disturbance-free model, $h = 1$]

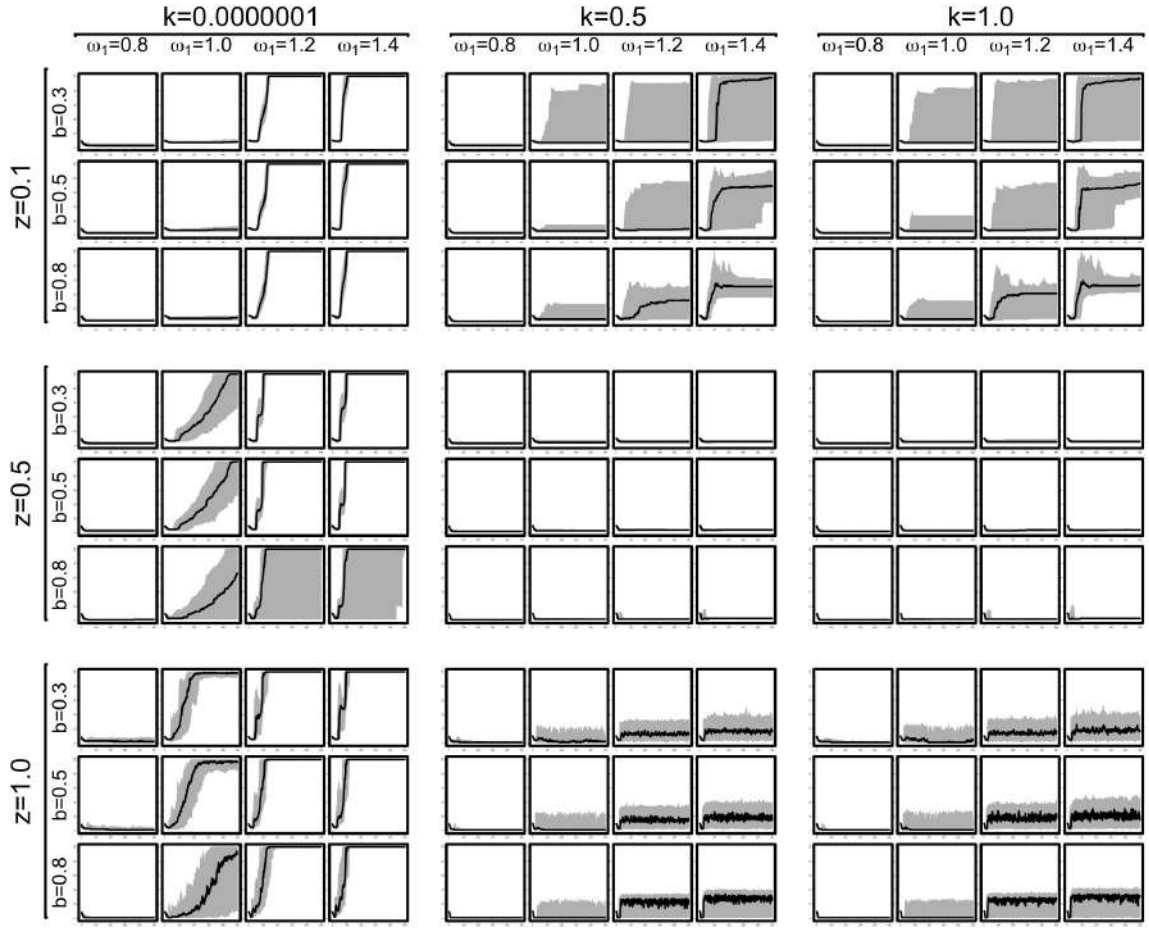

Combined time-series of G [disturbance-free model, $h = \infty$]

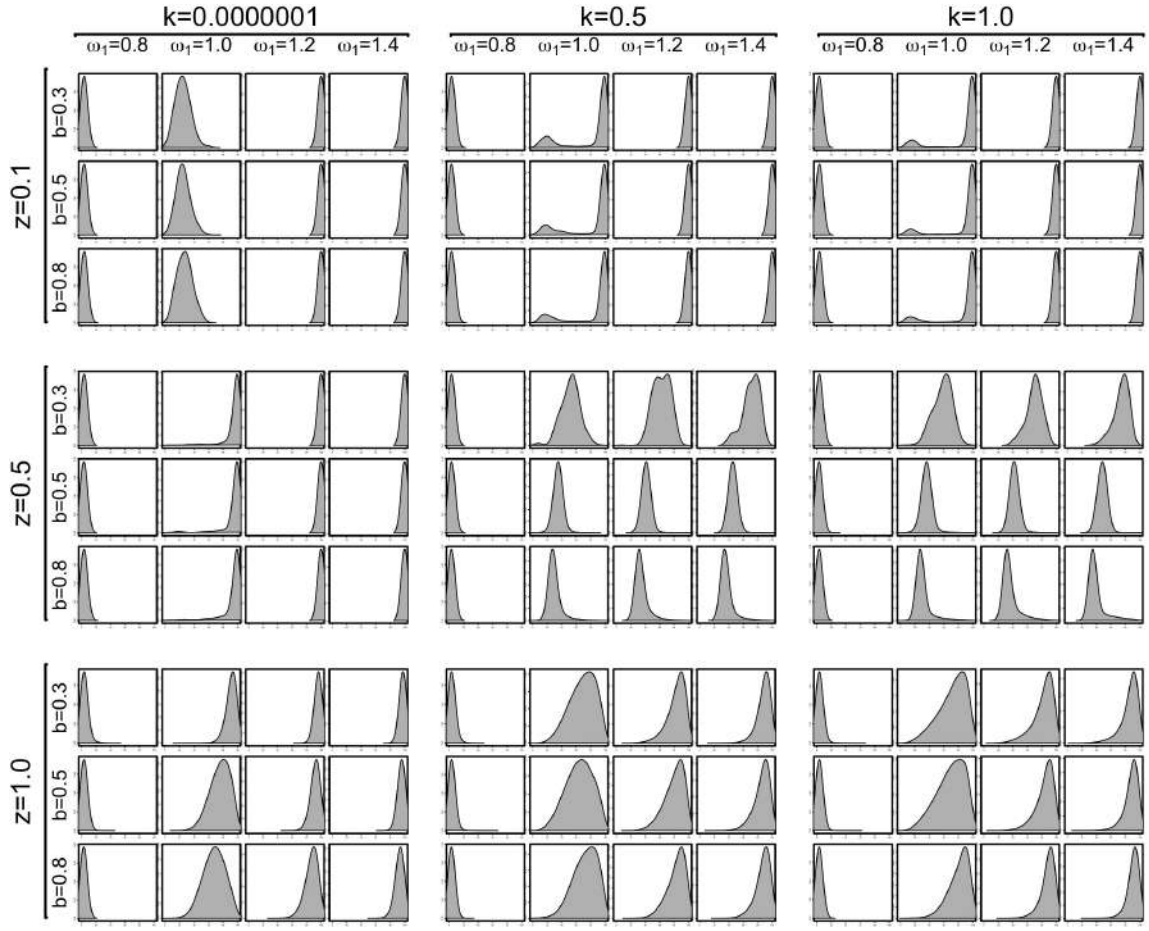

Probability density of G [disturbance-free model, $h = 1$]

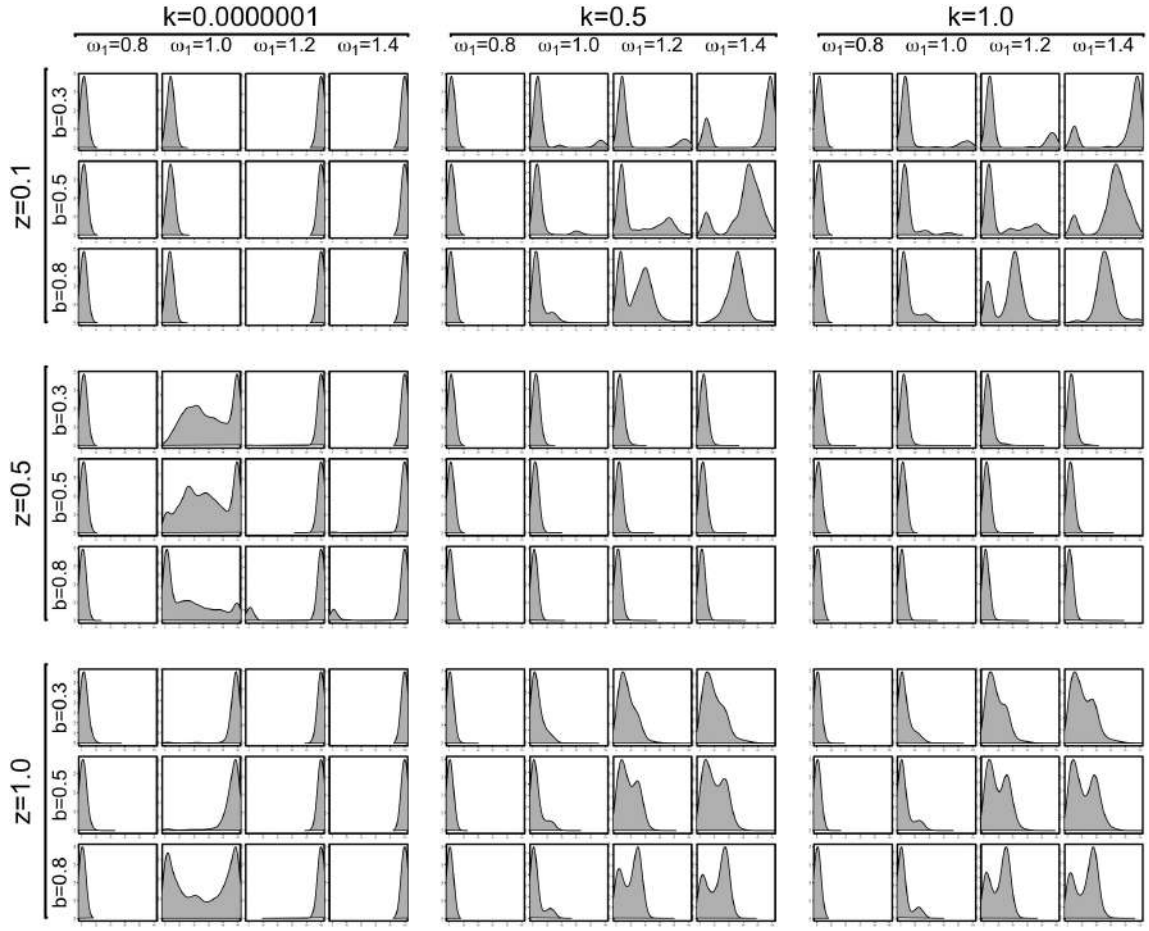

Probability density of G [disturbance-free model, $h = \infty$]

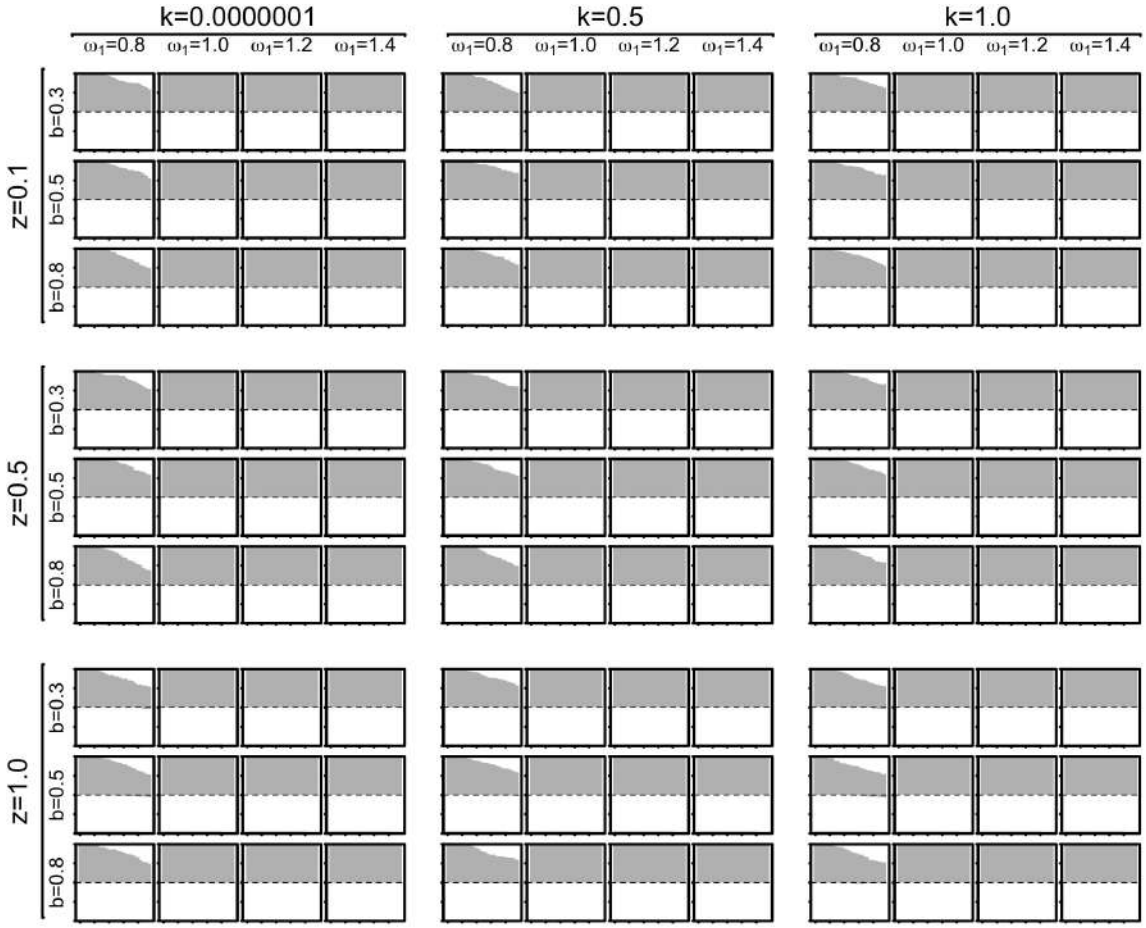

Correlogram of G [disturbance-free model, $h = 1$]

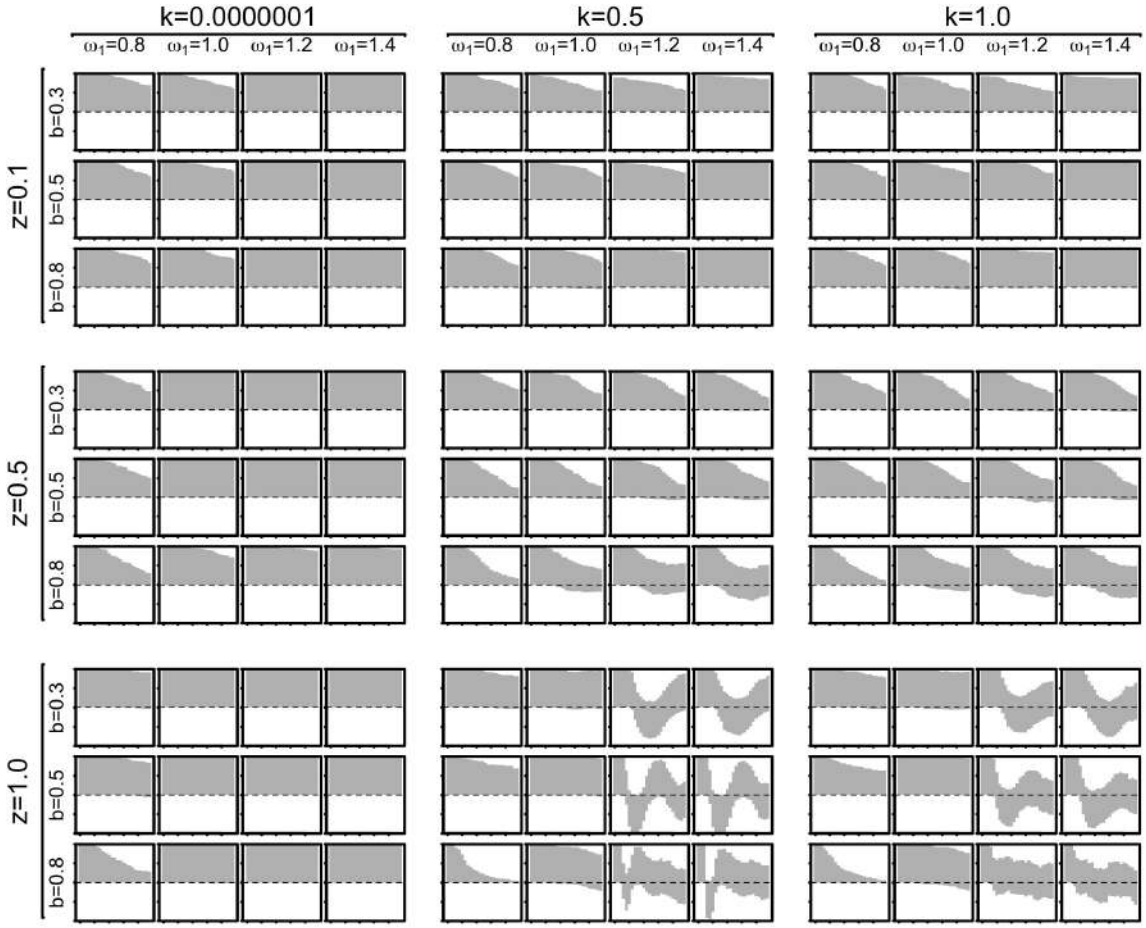

Correlogram of G [disturbance-free model, $h = \infty$]

D.1.3 Number of Agents (N)

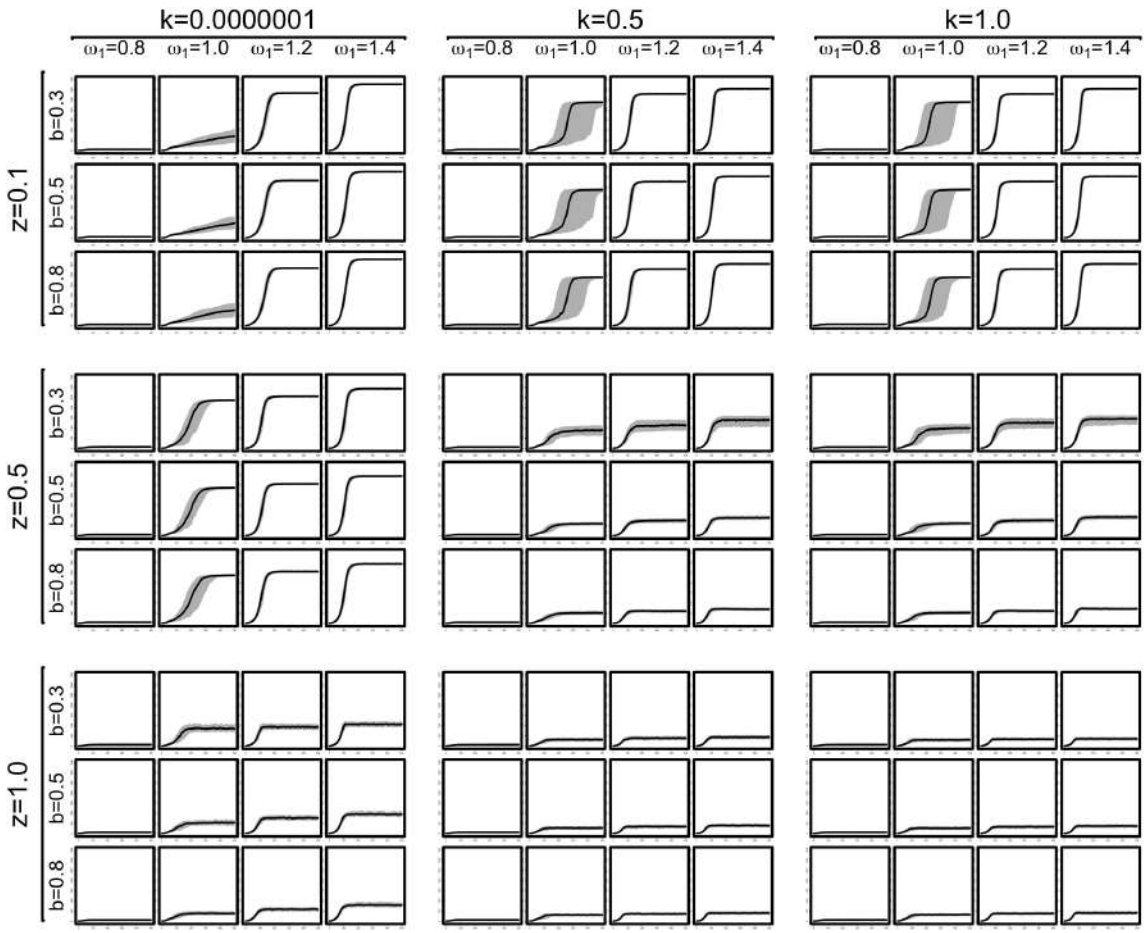

Combined time-series of N [disturbance-free model, $h = 1$, y-axis range from 0 to 3500]

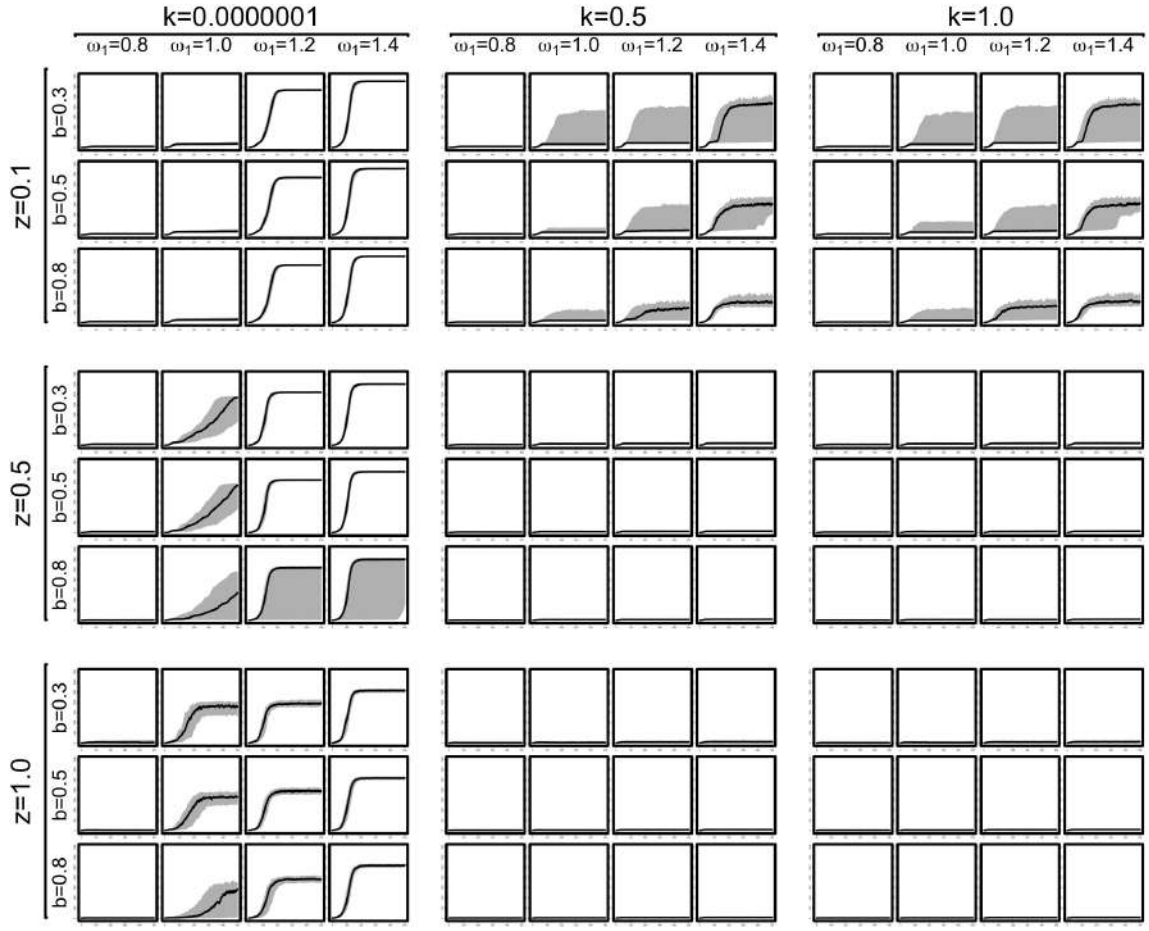

Combined time-series of N [disturbance-free model, $h = \infty$, y-axis range from 0 to 3500]

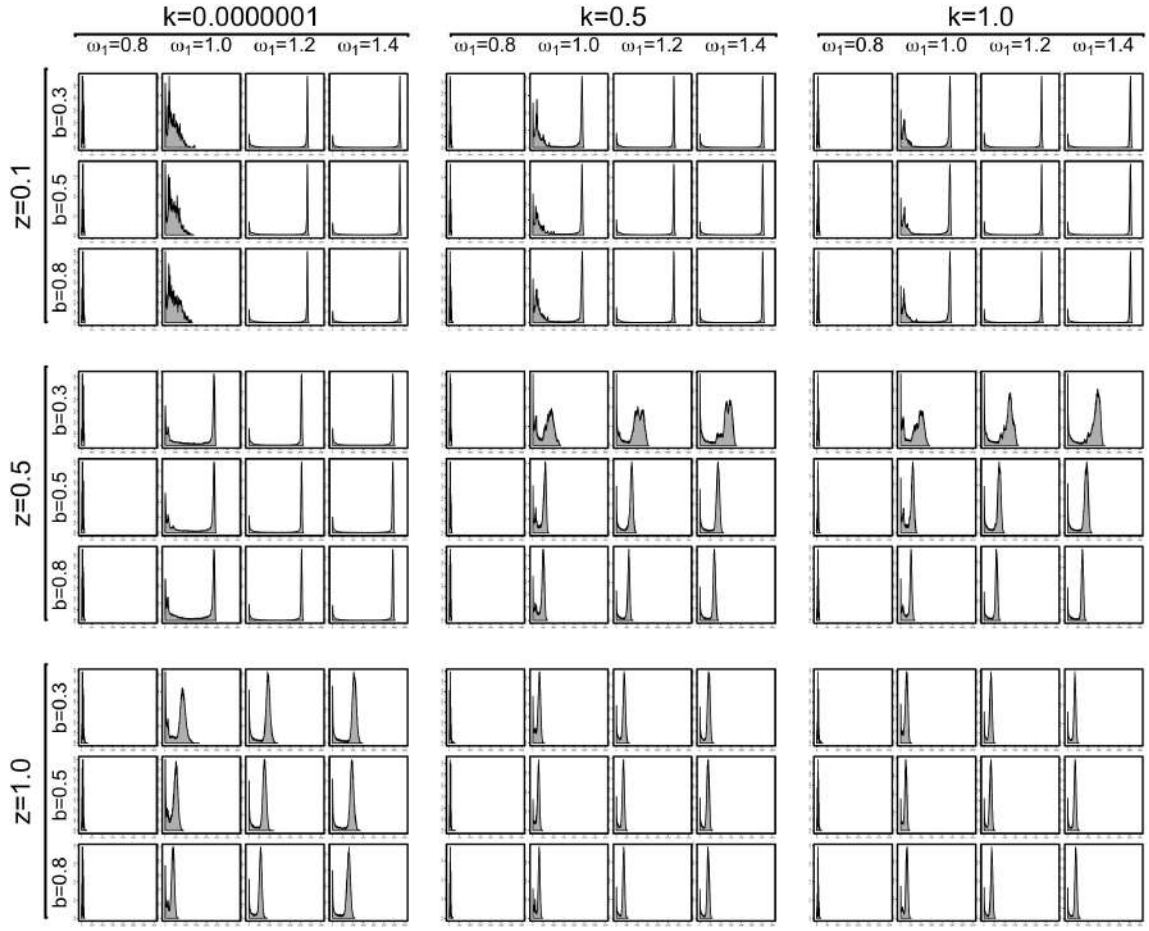

Probability density of N [disturbance-free model, $h = 1$, x-axis range from 0 to 3500]

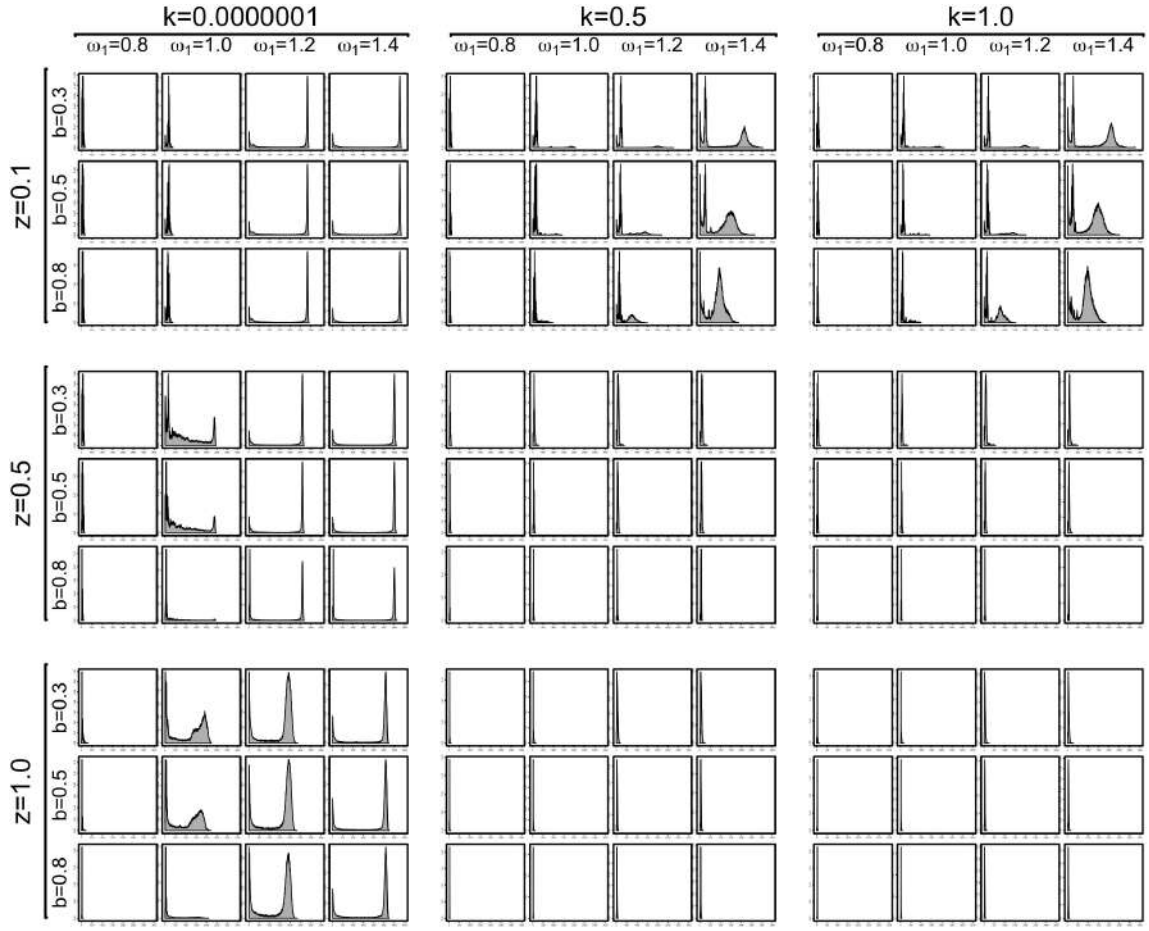

Probability density of N [disturbance-free model, $h = \infty$, x-axis range from 0 to 3500]

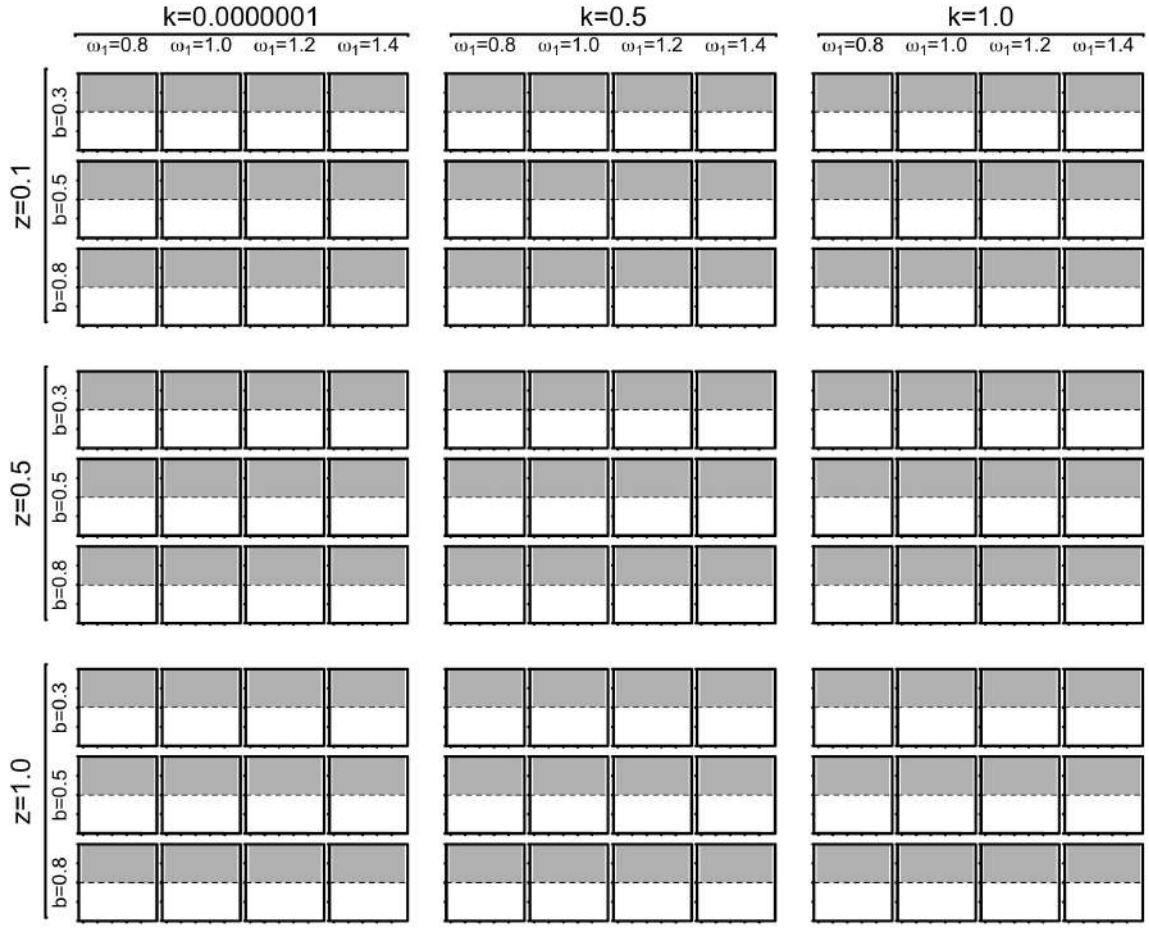

Correlogram of N [disturbance-free model, $h = 1$]

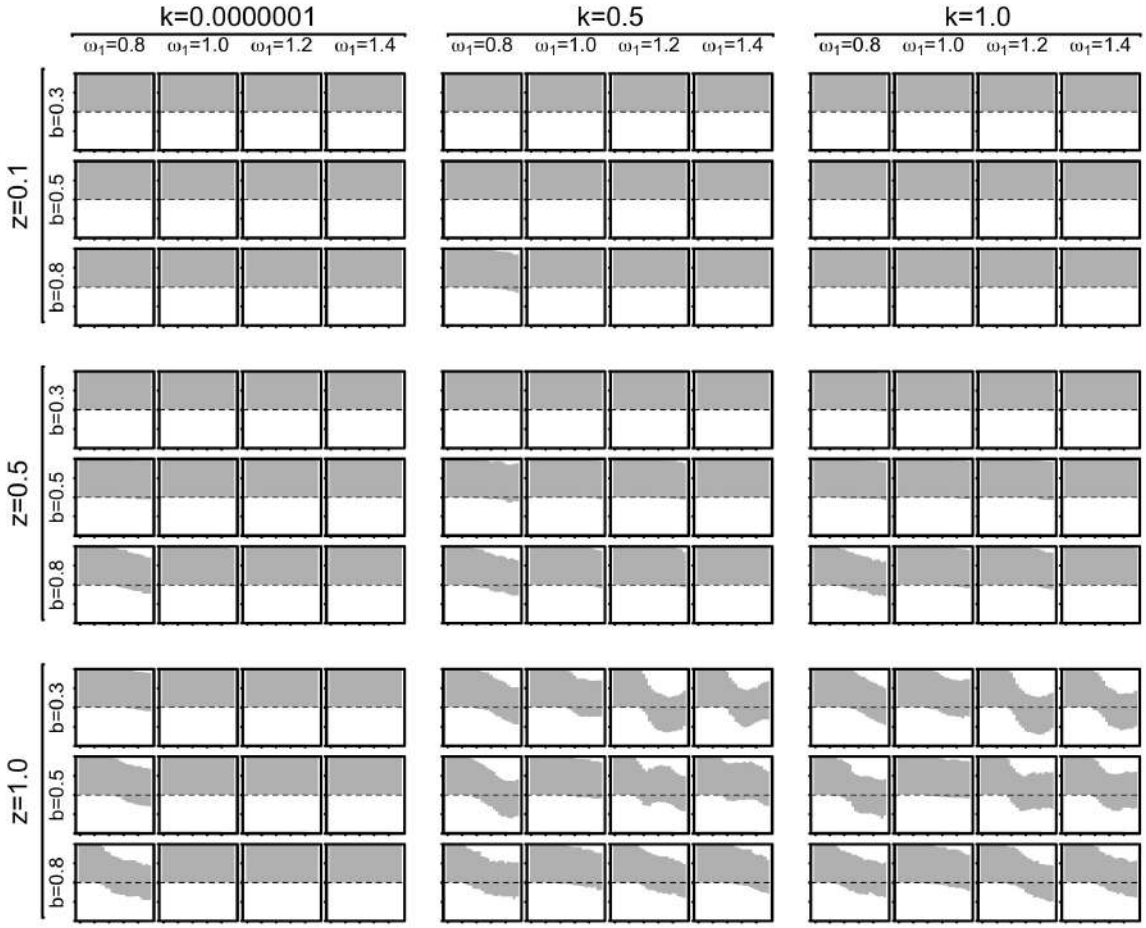

Correlogram of N [disturbance-free model, $h = \infty$]

D.1.4 Median Group Size ($\tilde{\lambda}$)

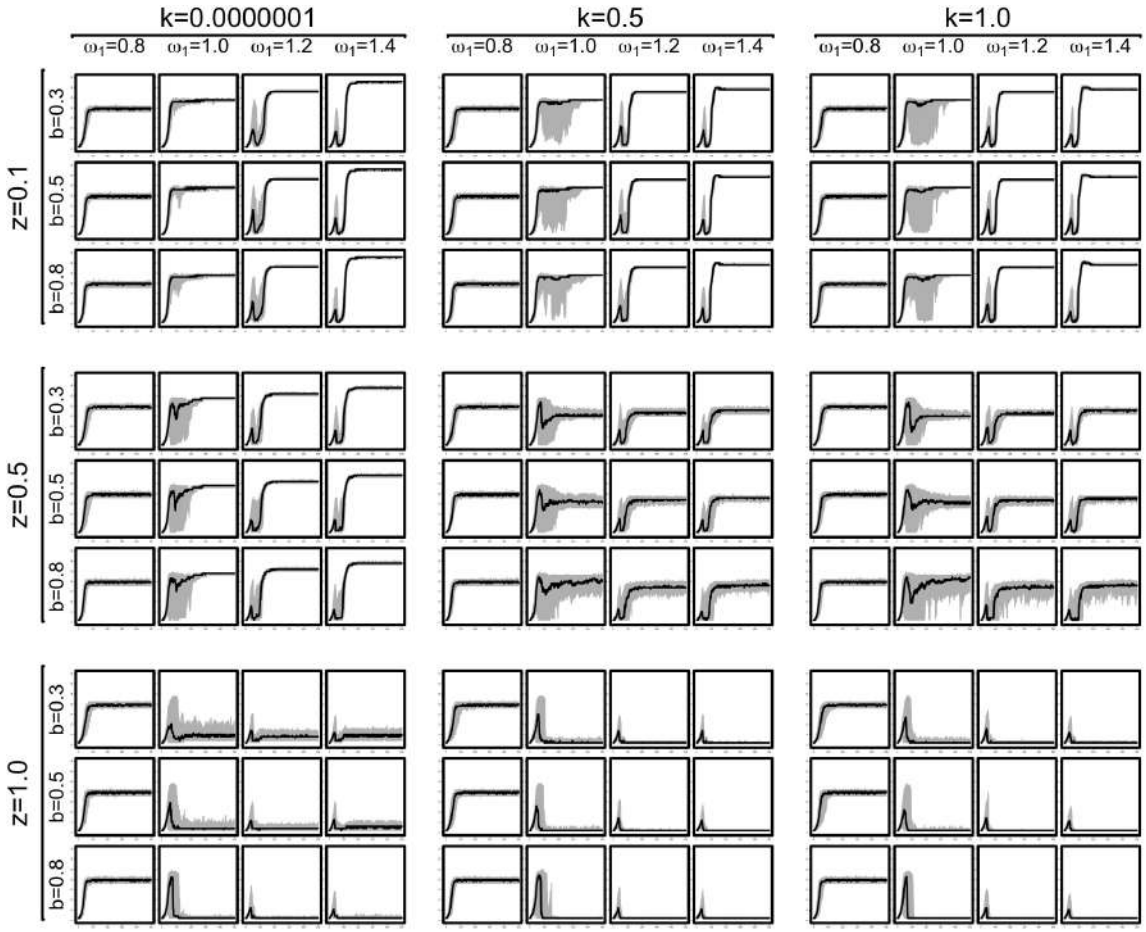

Combined time-series of $\tilde{\lambda}$ [disturbance-free model, $h = 1$]

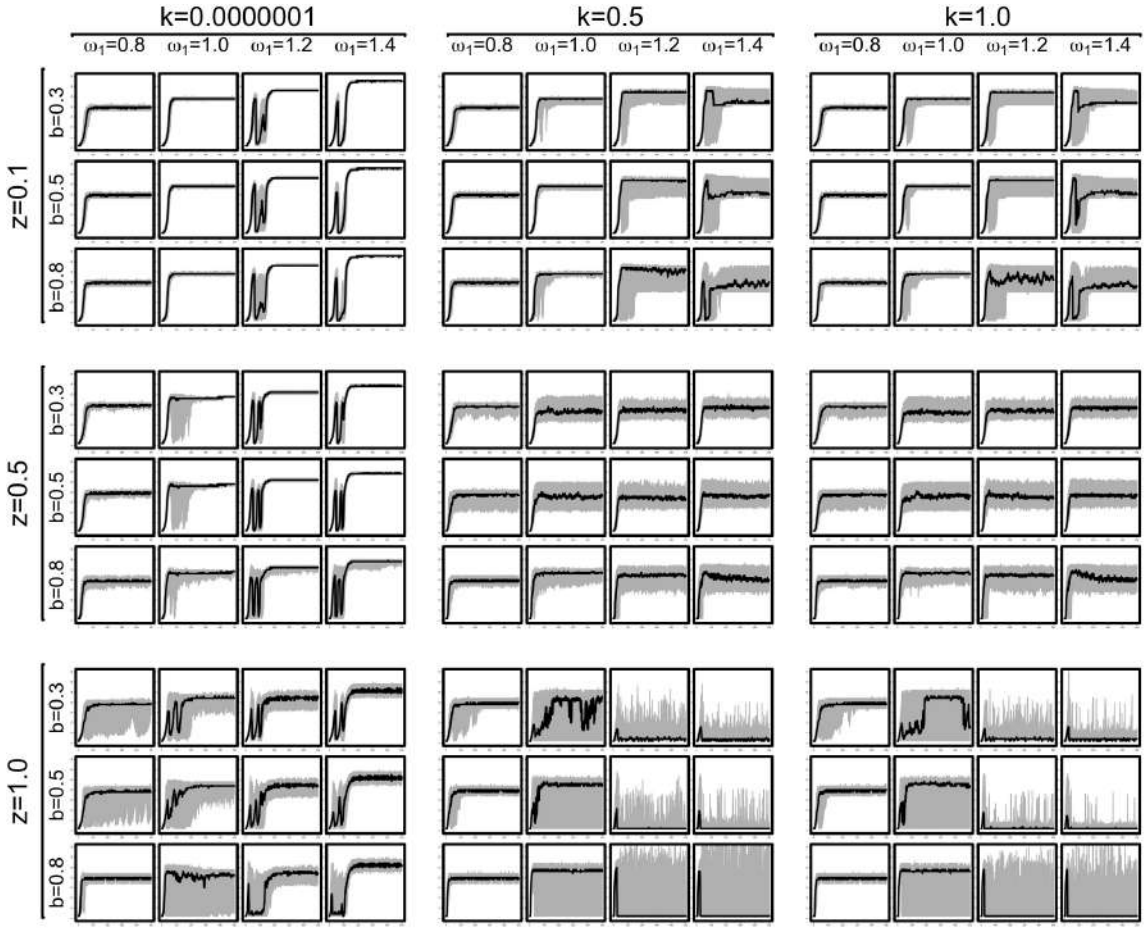

Combined time-series of $\tilde{\lambda}$ [disturbance-free model, $h = \infty$]

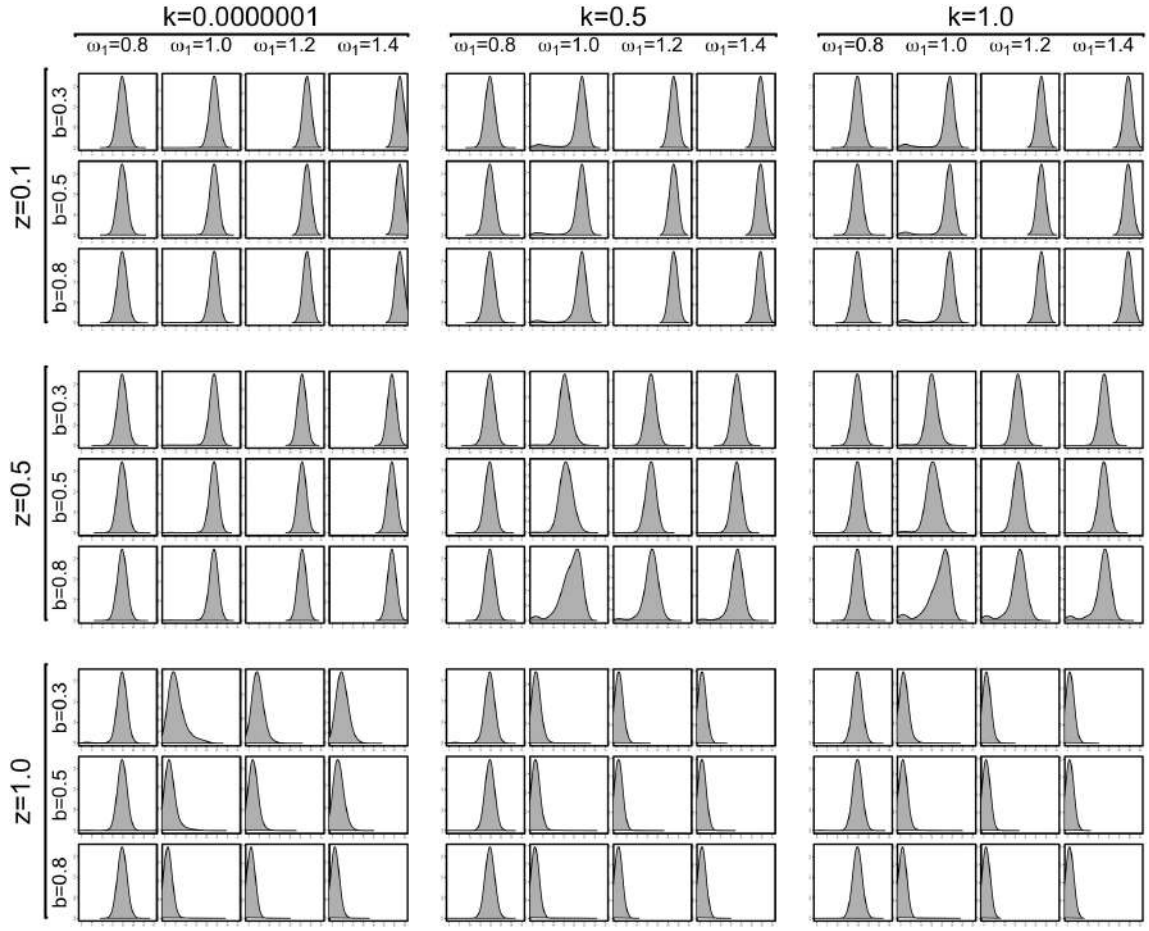

Probability density of $\tilde{\lambda}$ [disturbance-free model, $h = 1$]

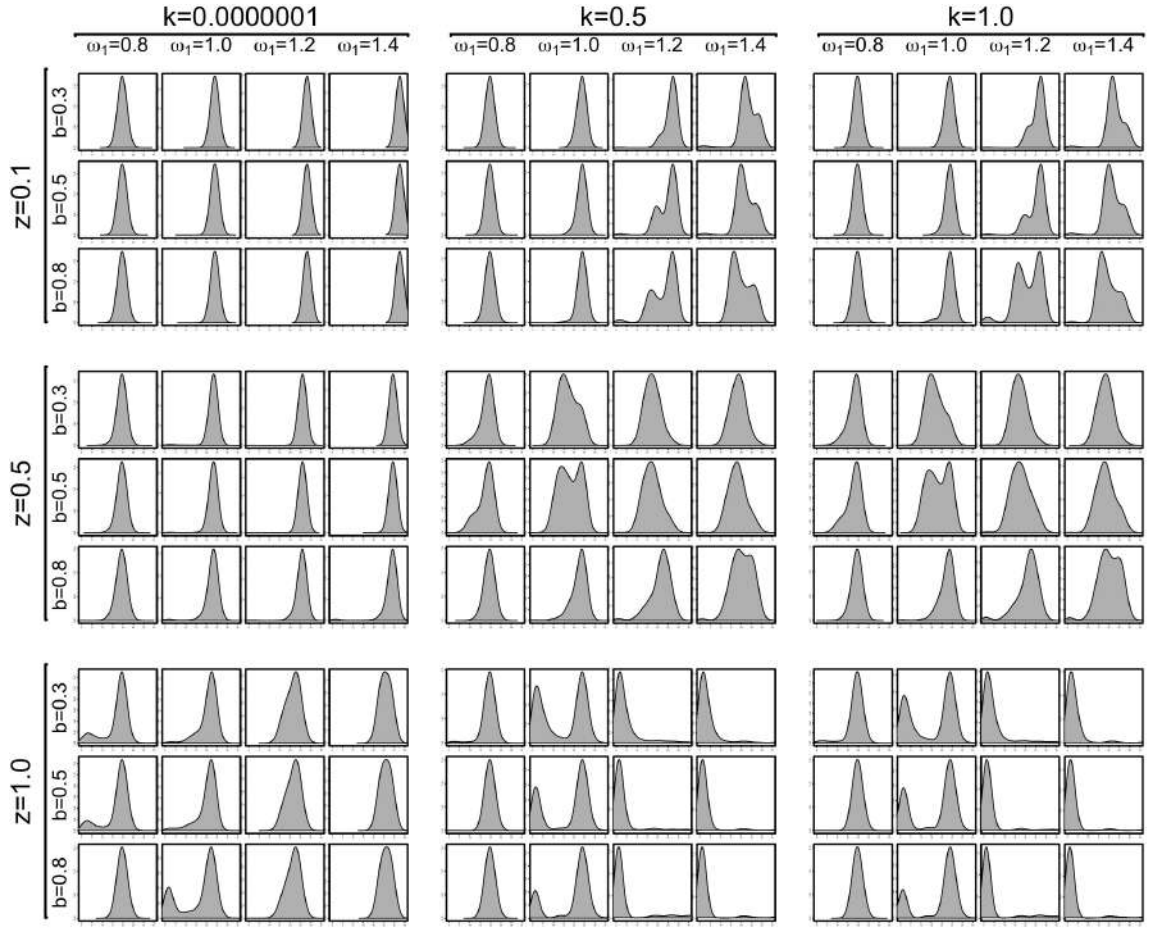

Probability density of $\tilde{\lambda}$ [disturbance-free model, $h = \infty$]

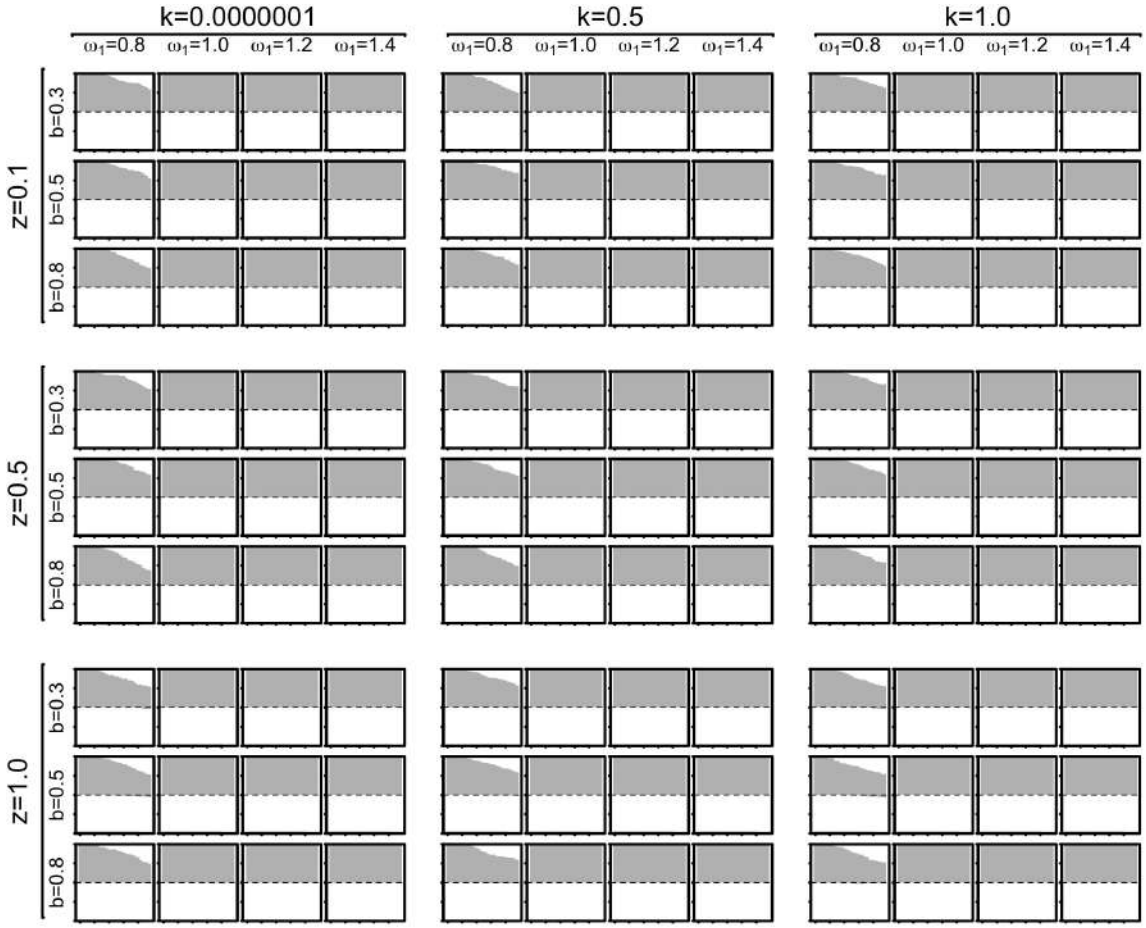

Correlogram of $\tilde{\lambda}$ [disturbance-free model, $h = 1$]

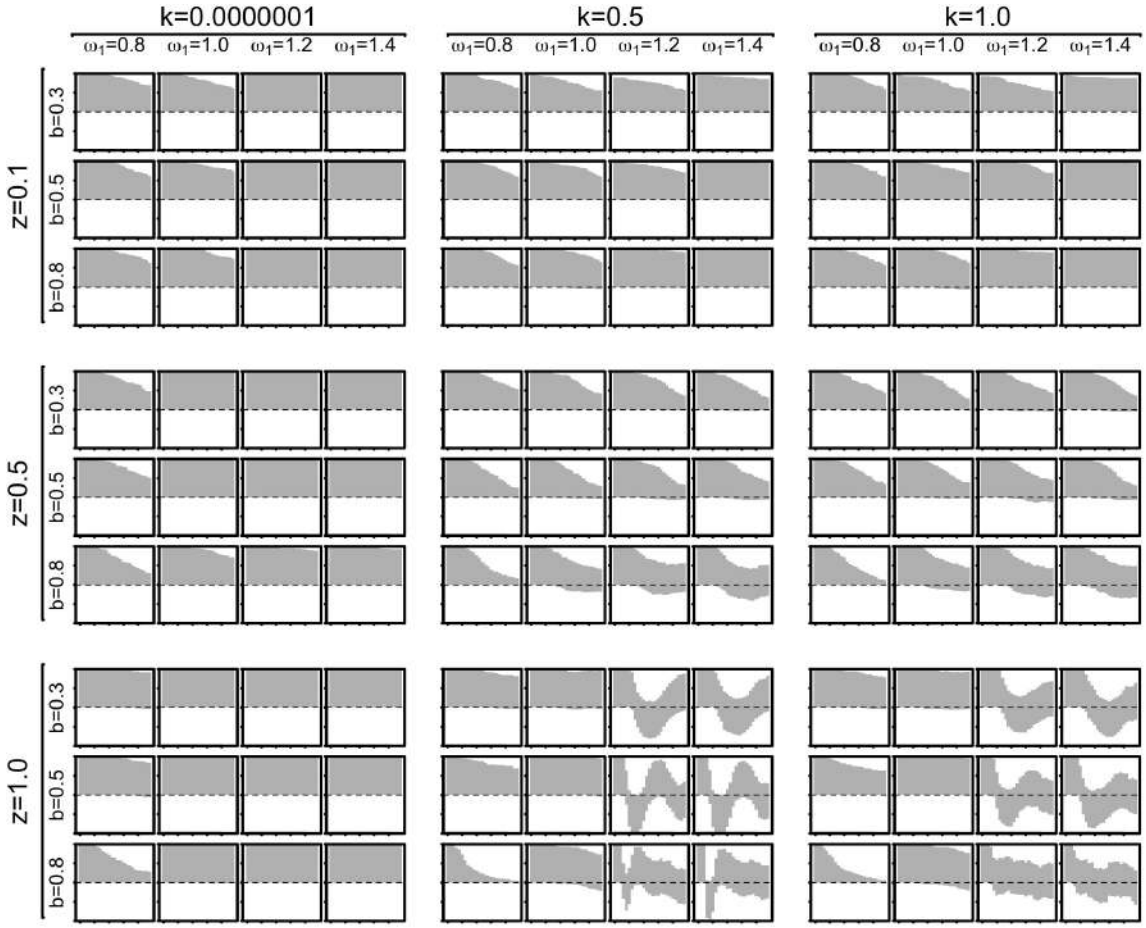

Correlogram of $\tilde{\lambda}$ [disturbance-free model, $h = \infty$]

D.2 Predator-prey model

D.2.1 A-Coefficient (A)

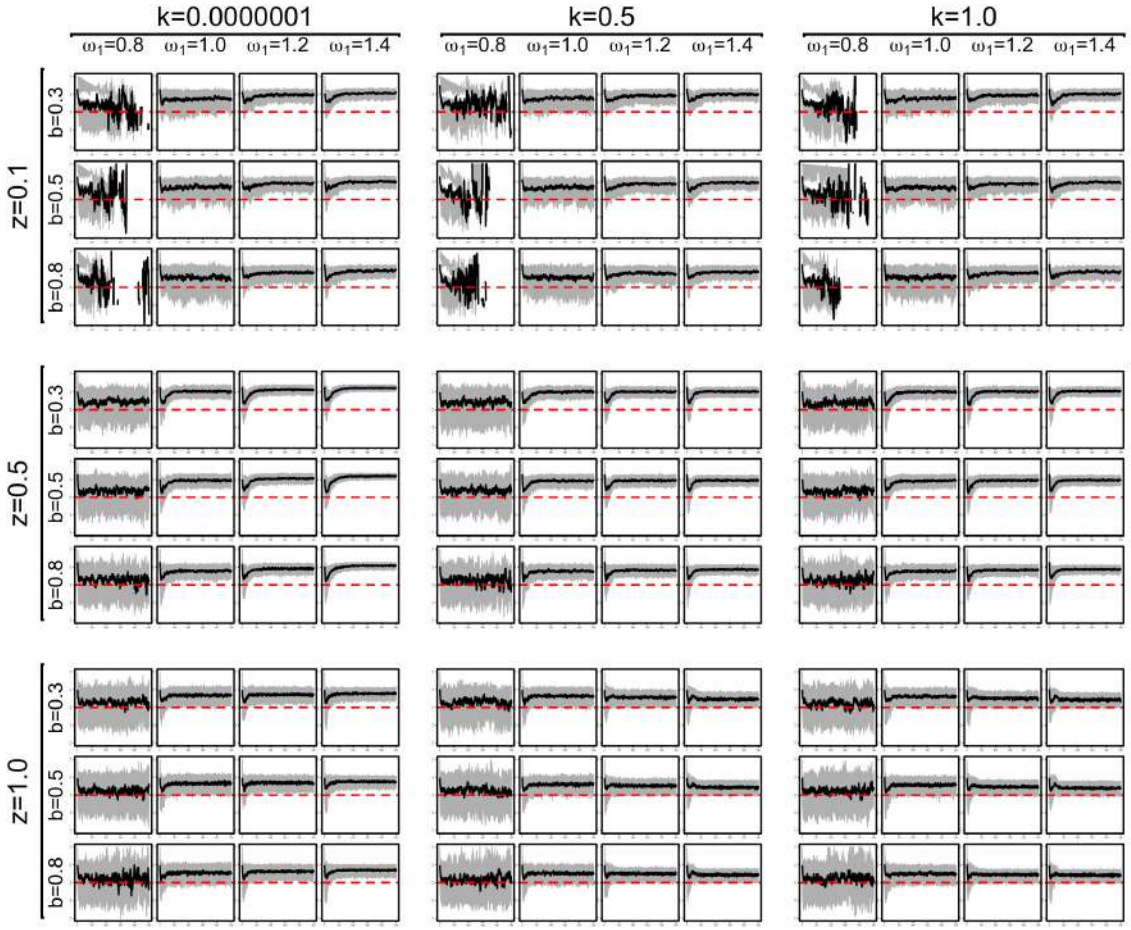

Combined time-series of A [predator-prey model, $\beta = 0.3$, $h = 1$]

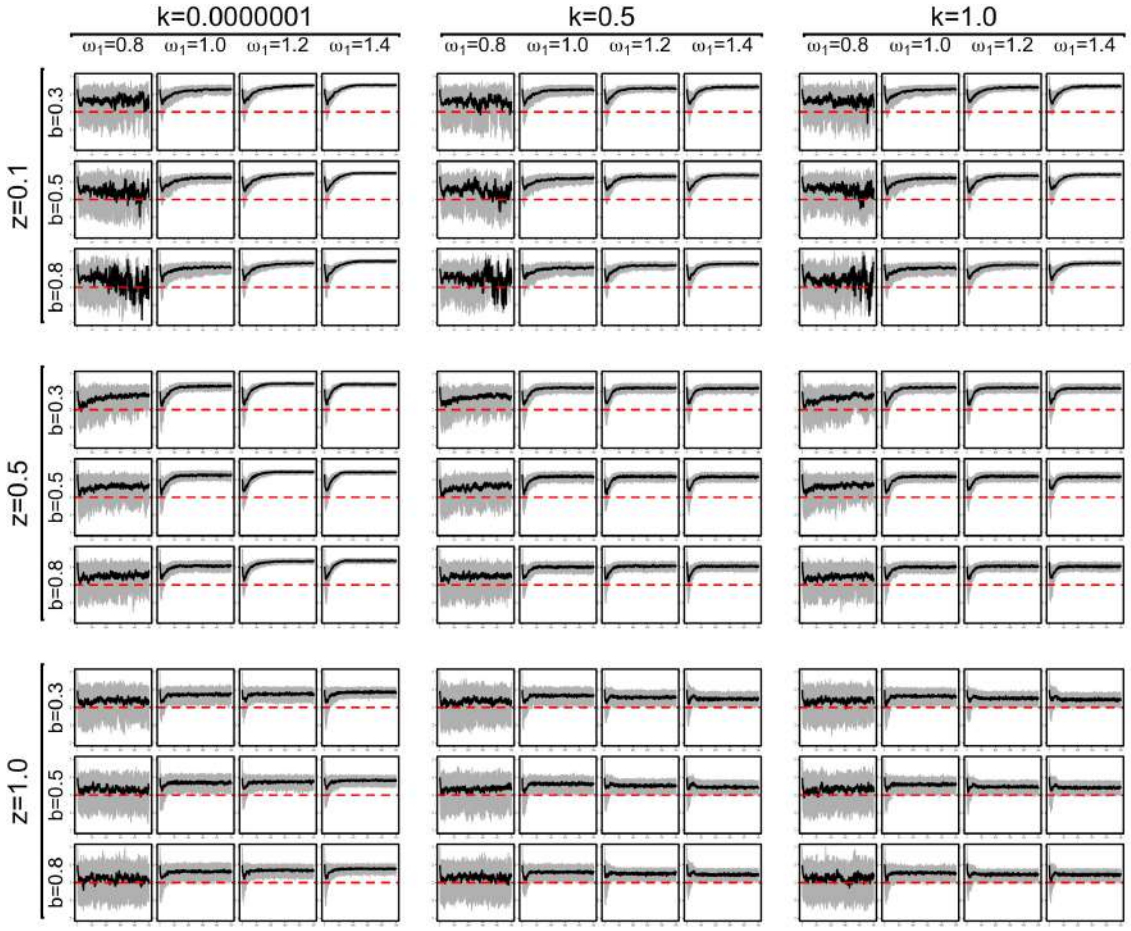

Combined time-series of A [predator-prey model, $\beta = 0.35$, $h = 1$]

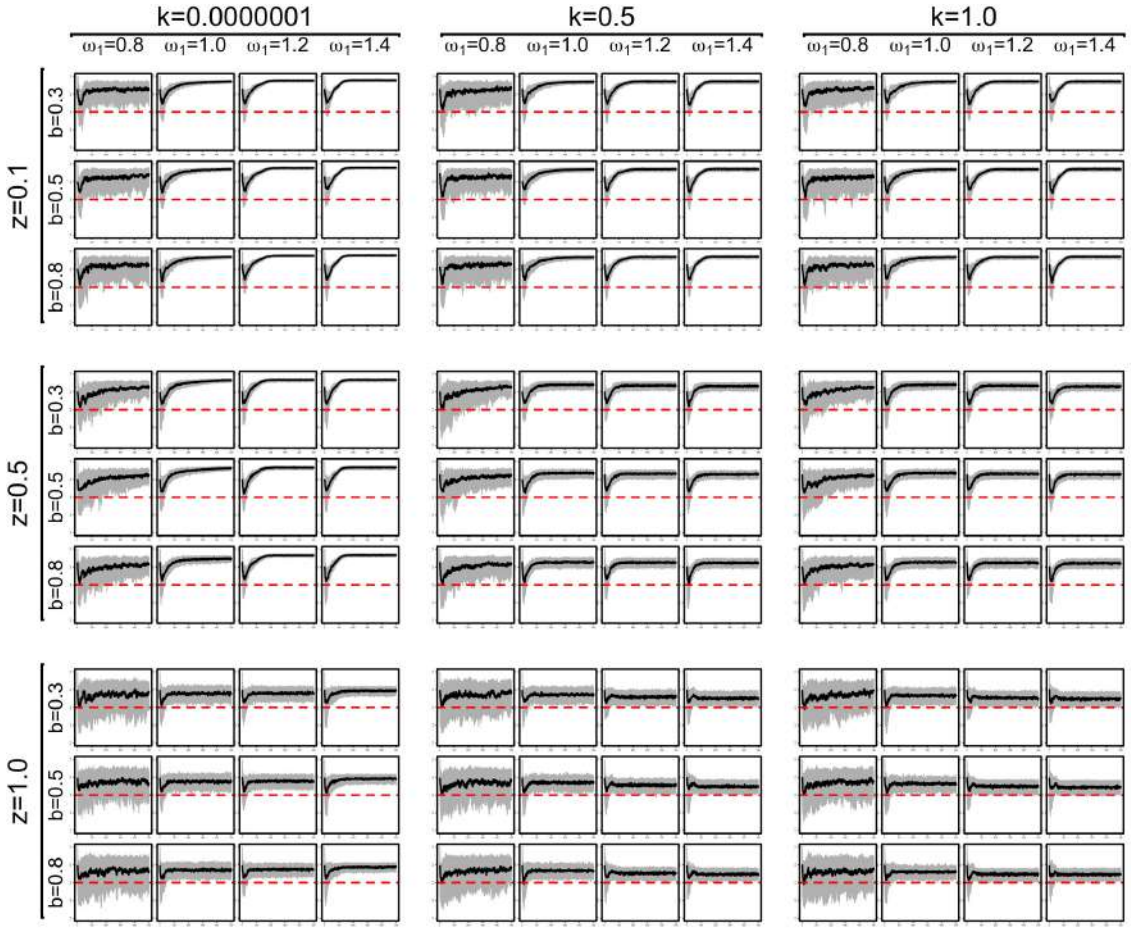

Combined time-series of A [predator-prey model, $\beta = 0.4$, $h = 1$]

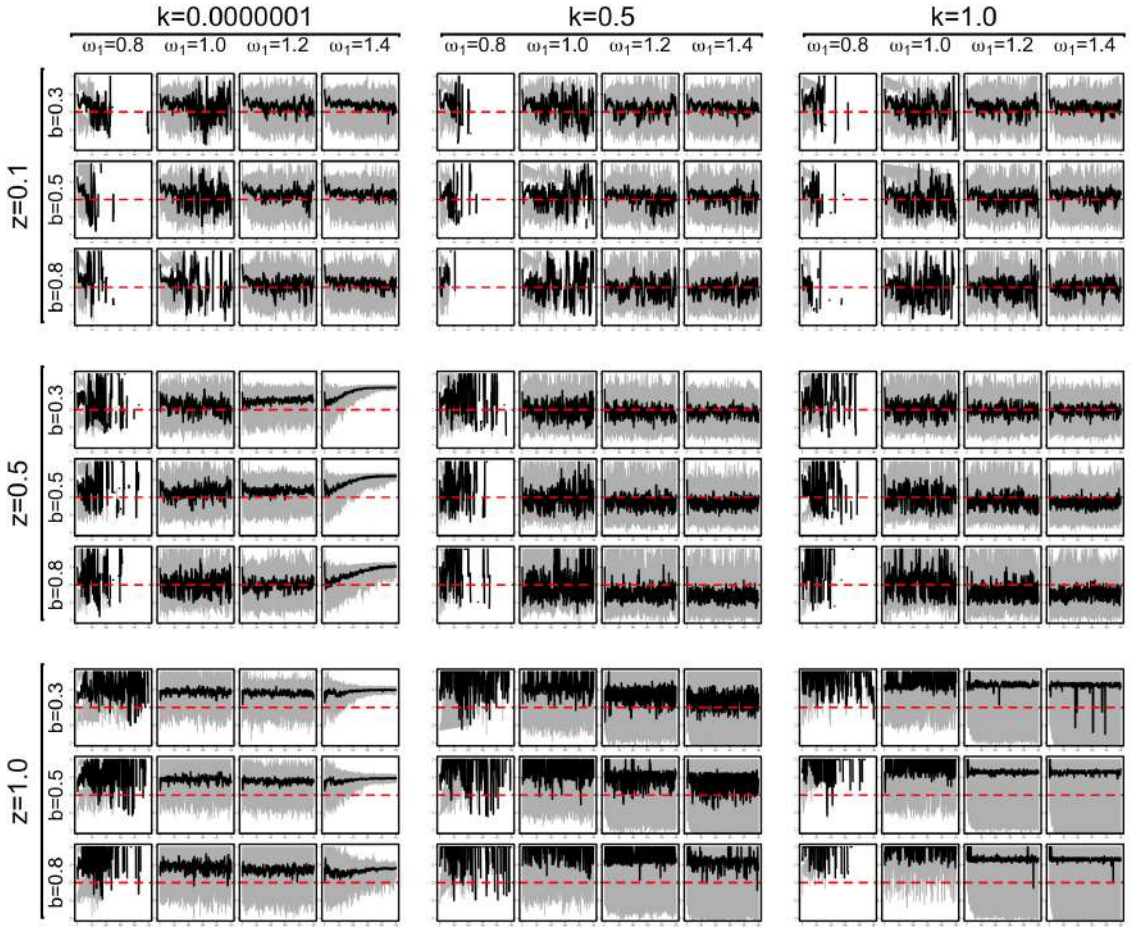

Combined time-series of A [predator-prey model, $\beta = 0.3$, $h = \infty$]

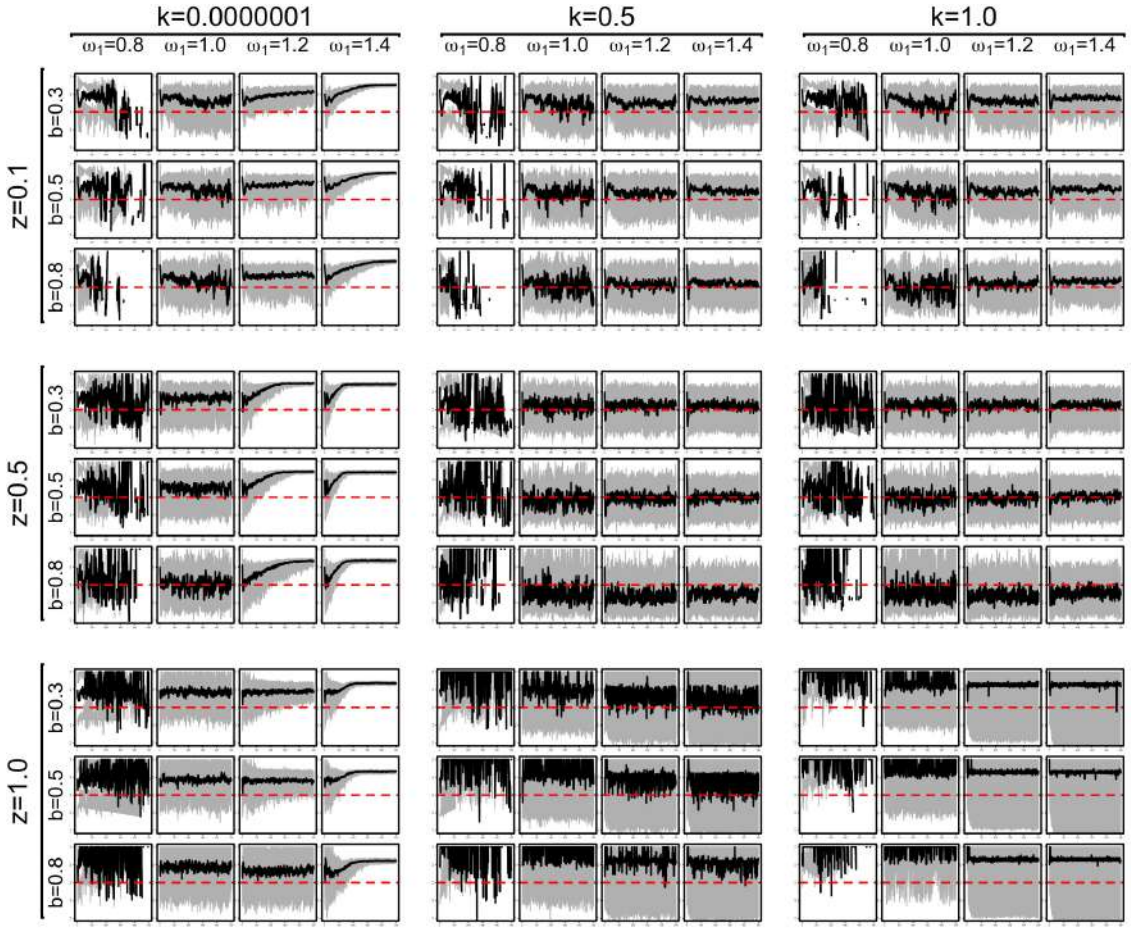

Combined time-series of A [predator-prey model, $\beta = 0.35$, $h = \infty$]

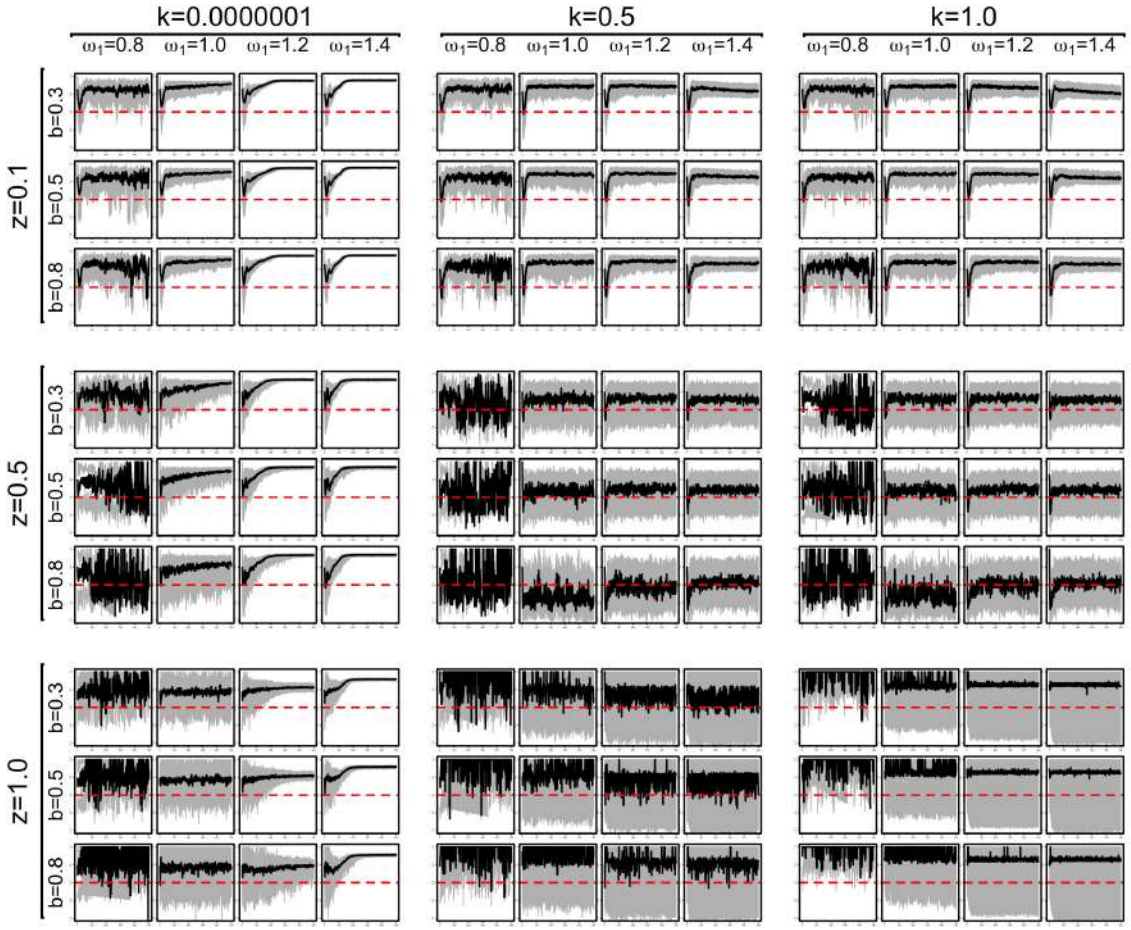

Combined time-series of A [predator-prey model, $\beta = 0.4$, $h = \infty$]

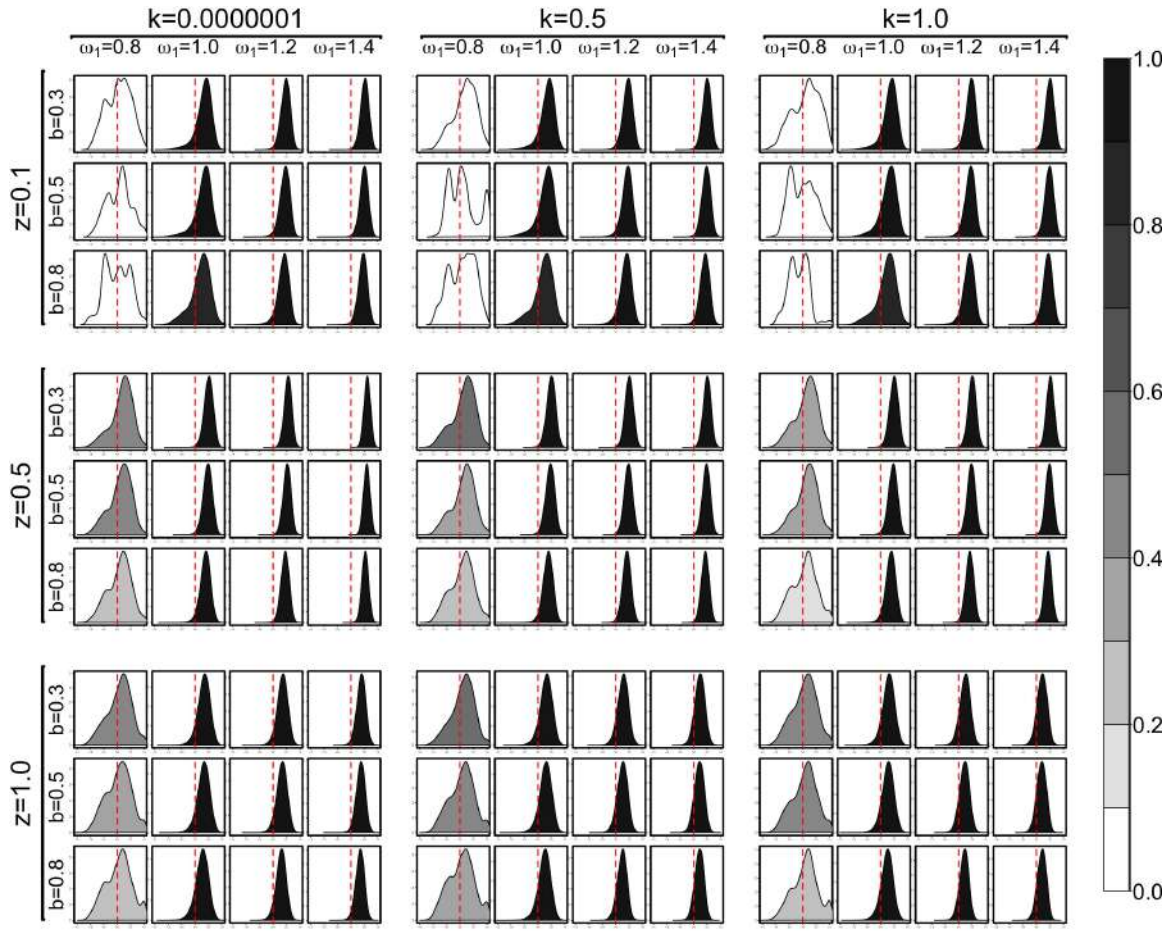

Probability density of A [predator-prey model, $\beta = 0.3$, $h = 1$]

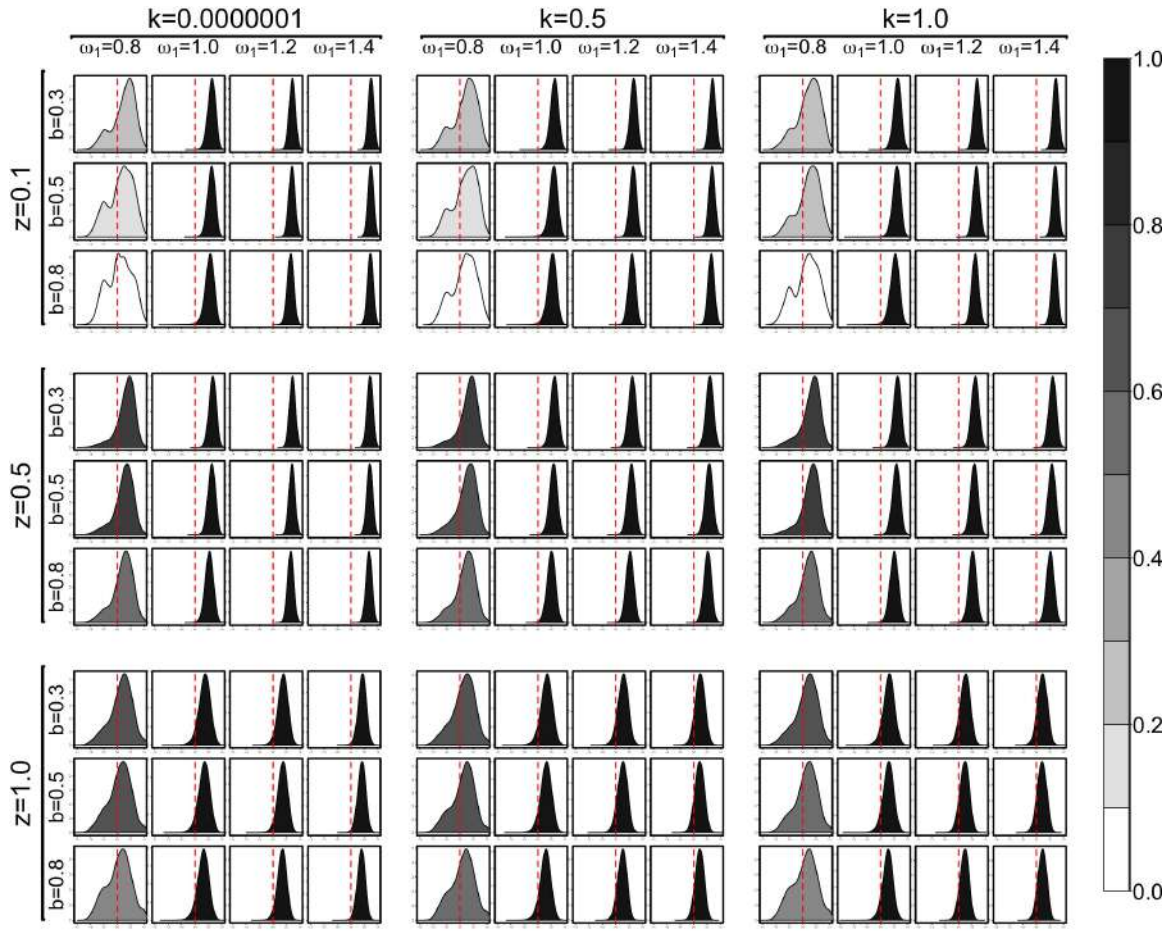

Probability density of A [predator-prey model, $\beta = 0.35$, $h = 1$]

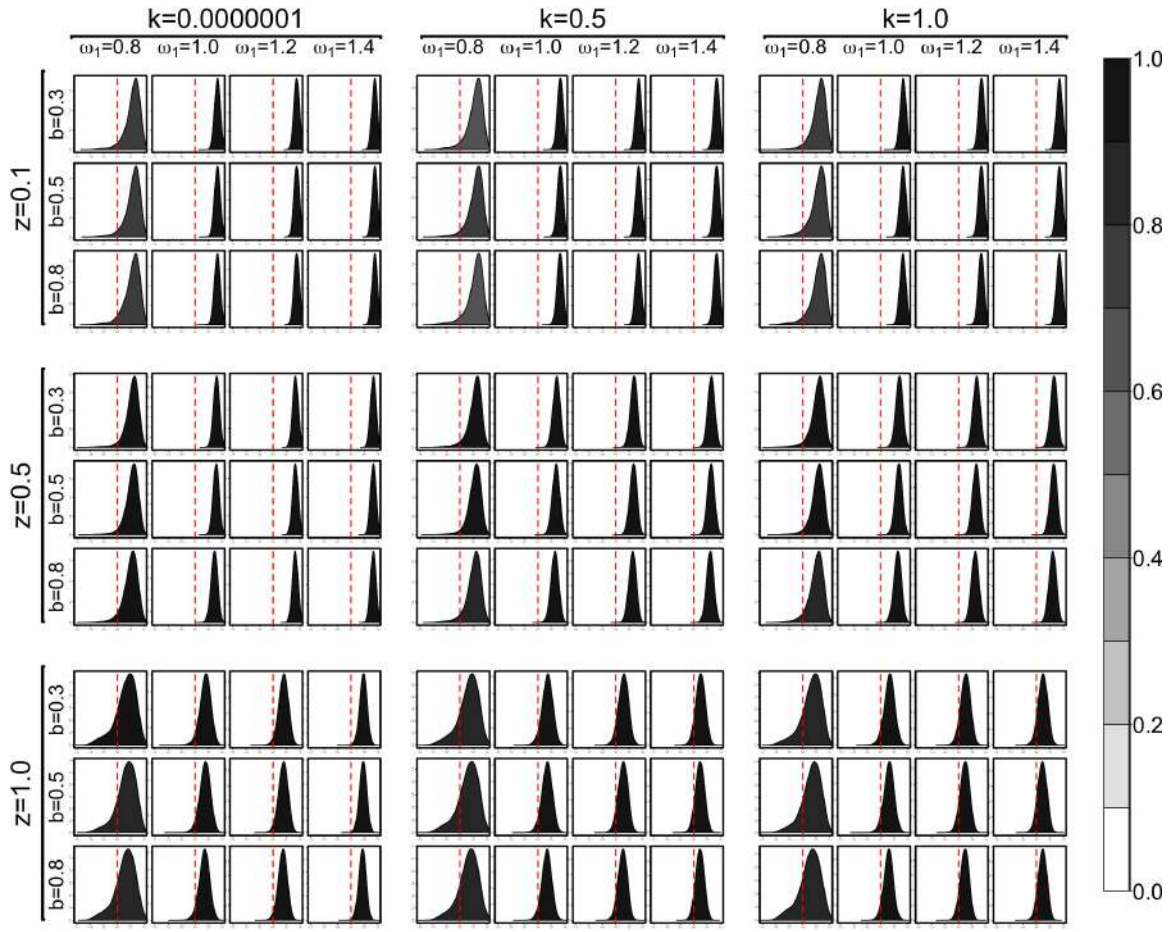

Probability density of A [predator-prey model, $\beta = 0.4$, $h = 1$]

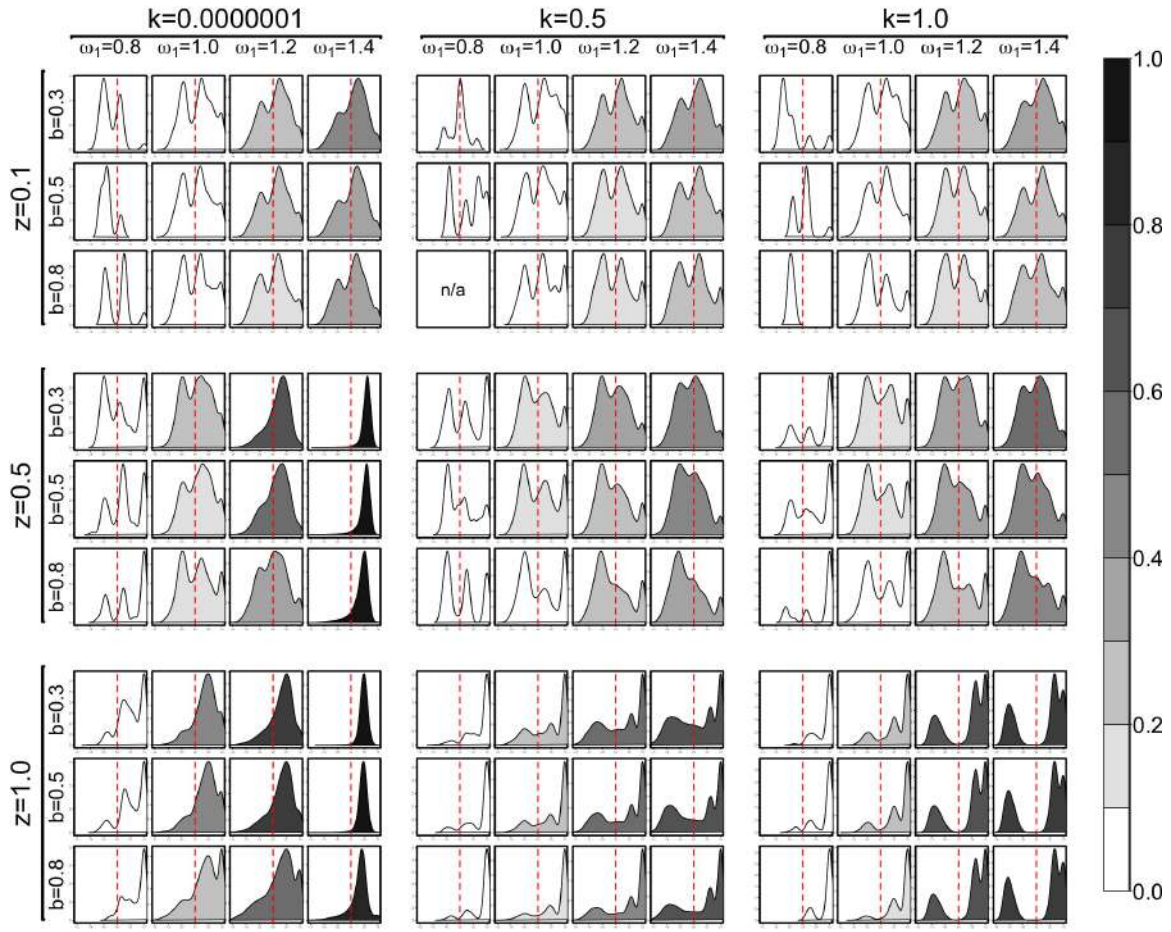

Probability density of A [predator-prey model, $\beta = 0.3$, $h = \infty$]

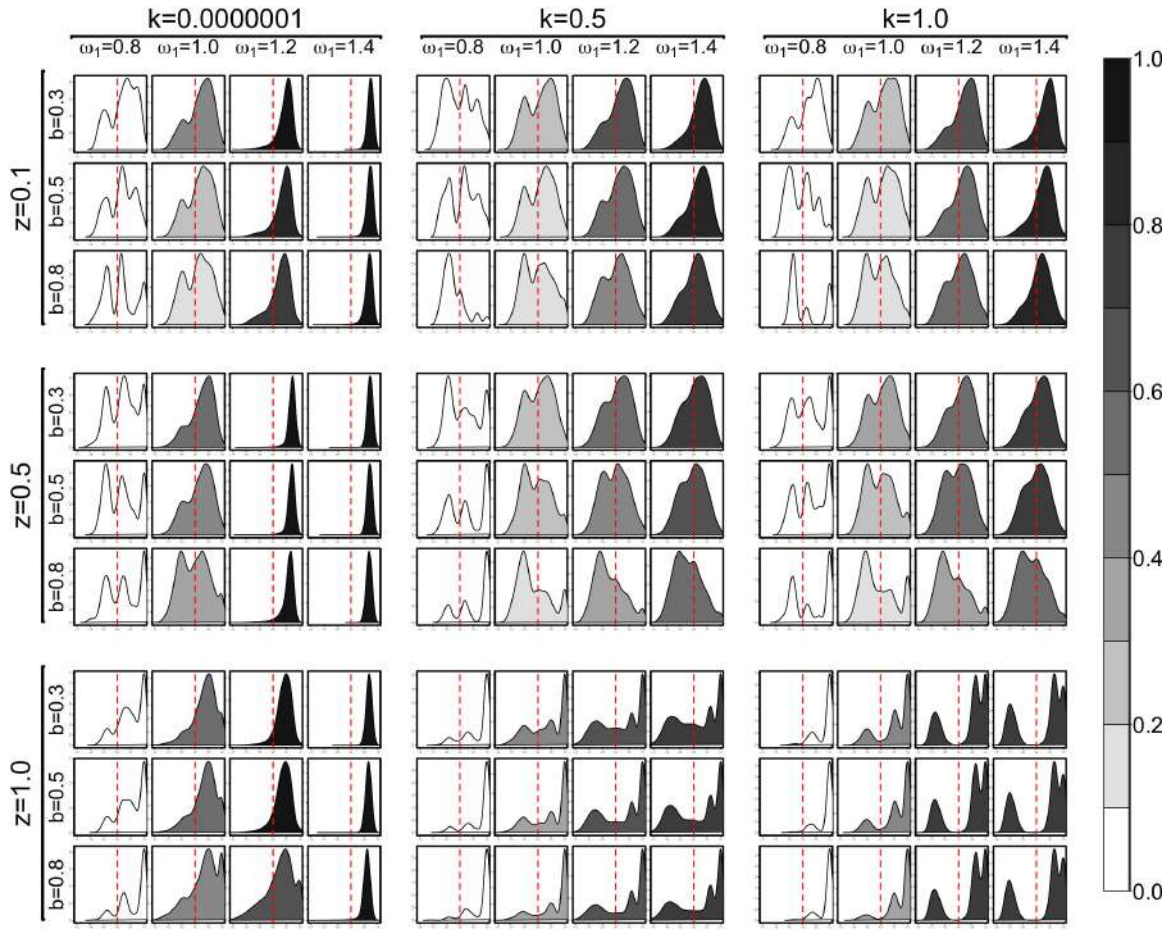

Probability density of A [predator-prey model, $\beta = 0.35$, $h = \infty$]

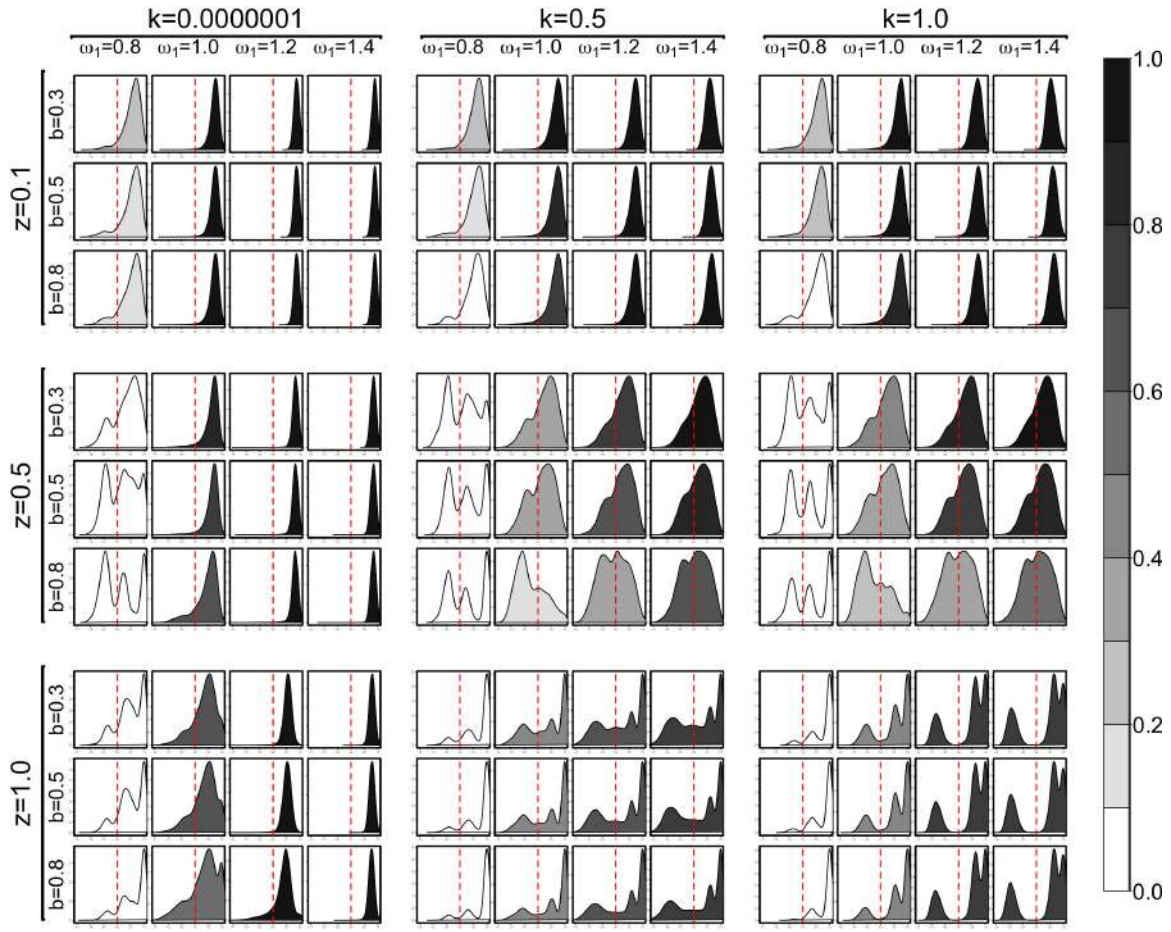

Probability density of A [predator-prey model, $\beta = 0.4$, $h = \infty$]

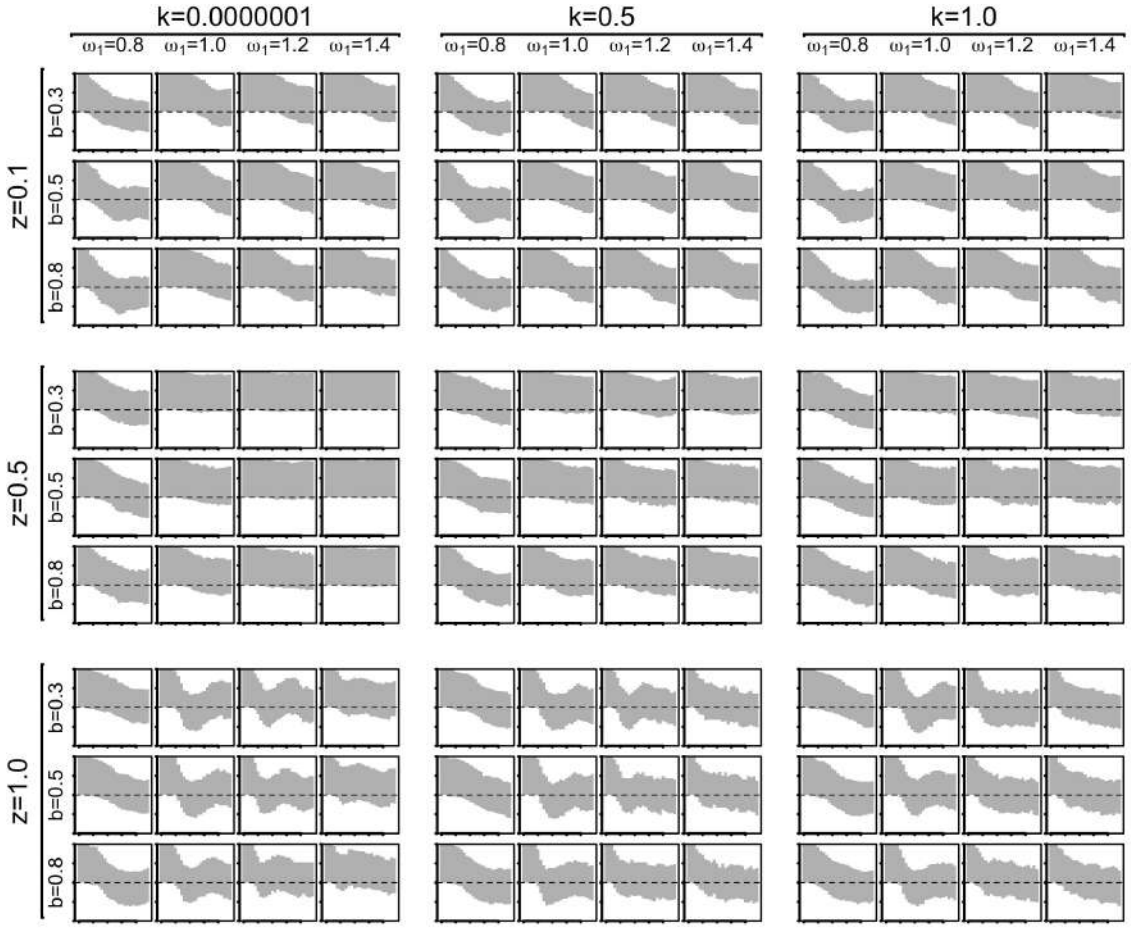

Correlogram of A [predator-prey model, $\beta = 0.3$, $h = 1$]

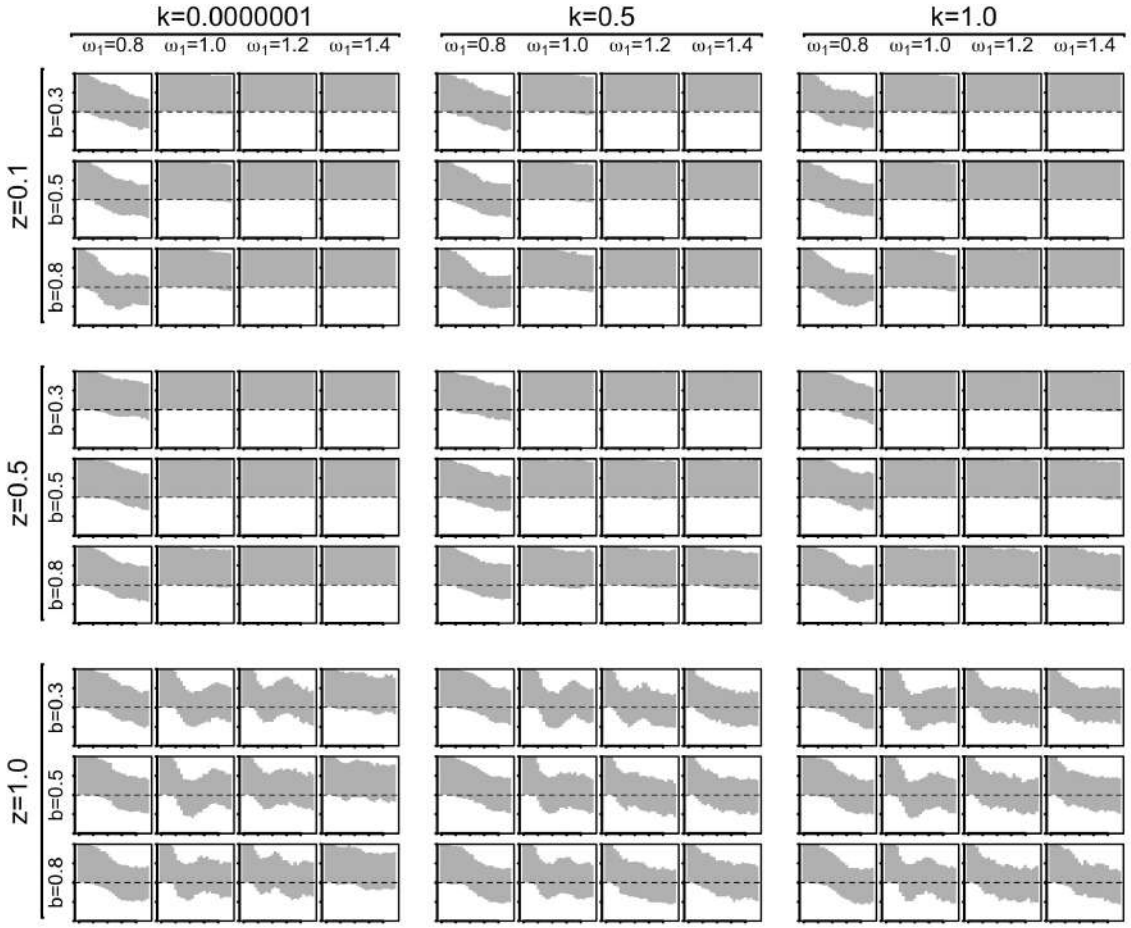

Correlogram of A [predator-prey model, $\beta = 0.35$, $h = 1$]

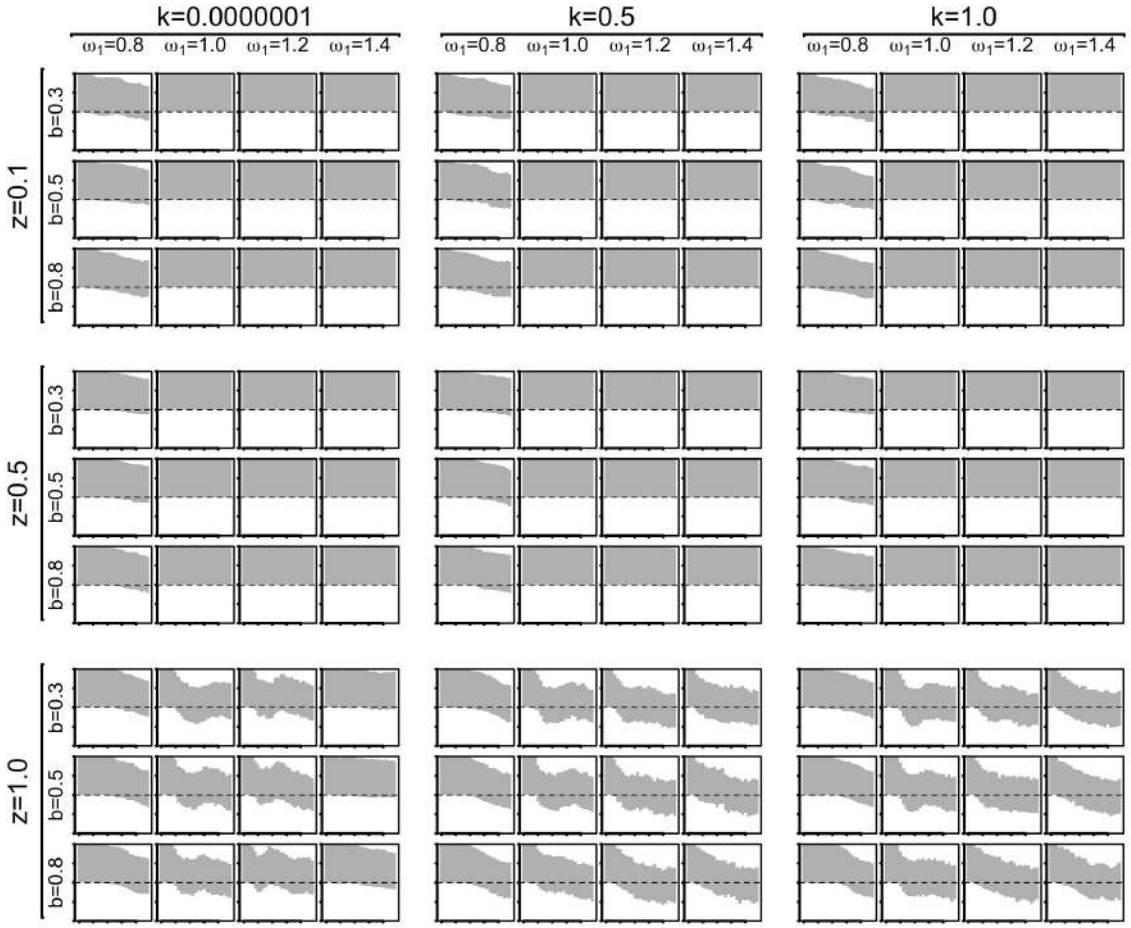

Correlogram of A [predator-prey model, $\beta = 0.4$, $h = 1$]

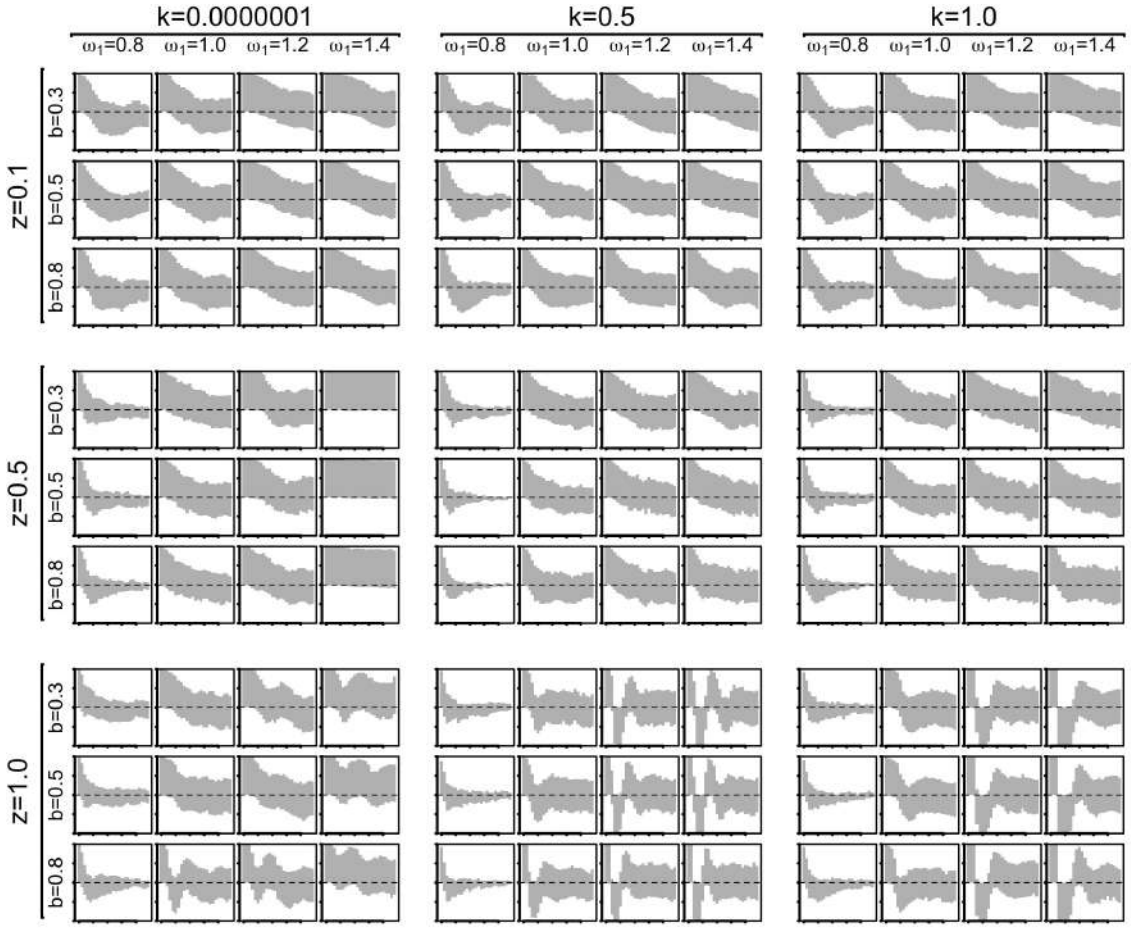

Correlogram of A [predator-prey model, $\beta = 0.3$, $h = \infty$]

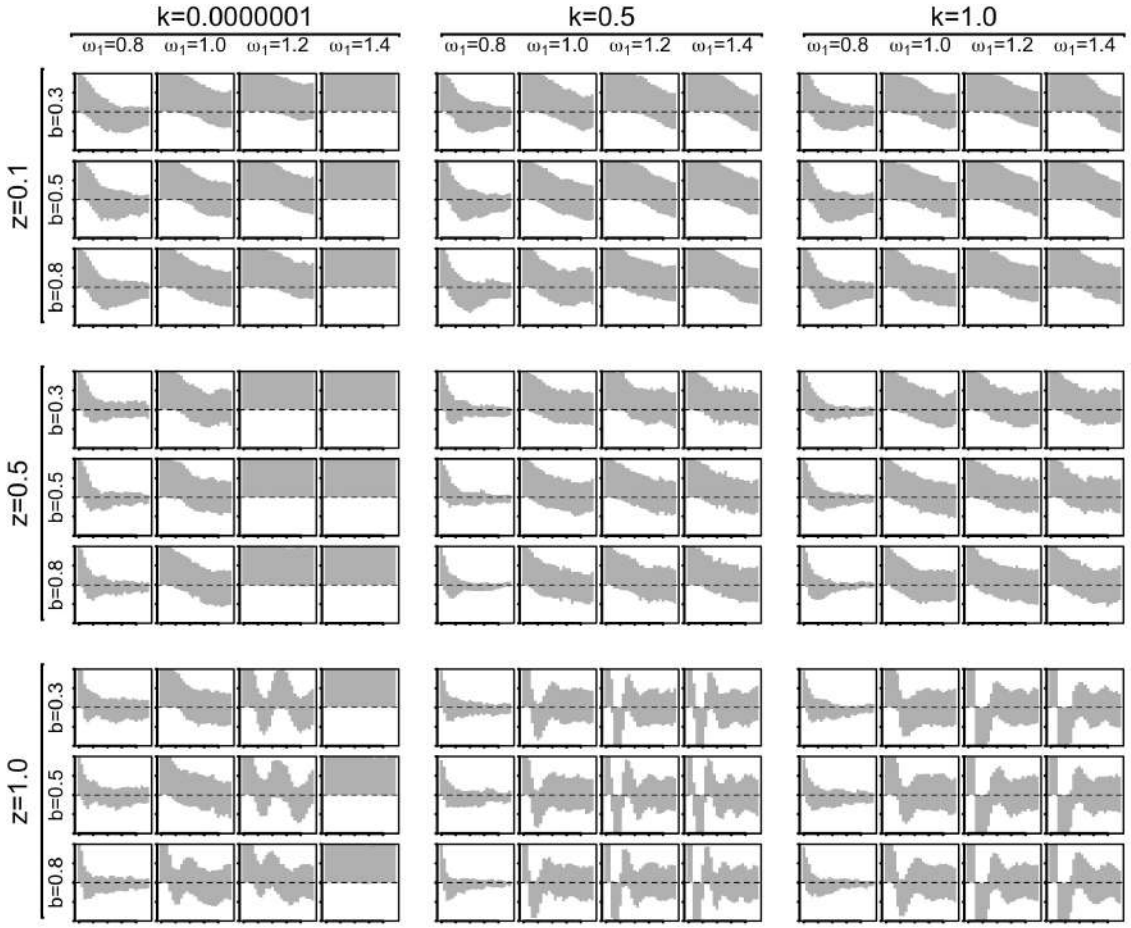

Correlogram of A [predator-prey model, $\beta = 0.35$, $h = \infty$]

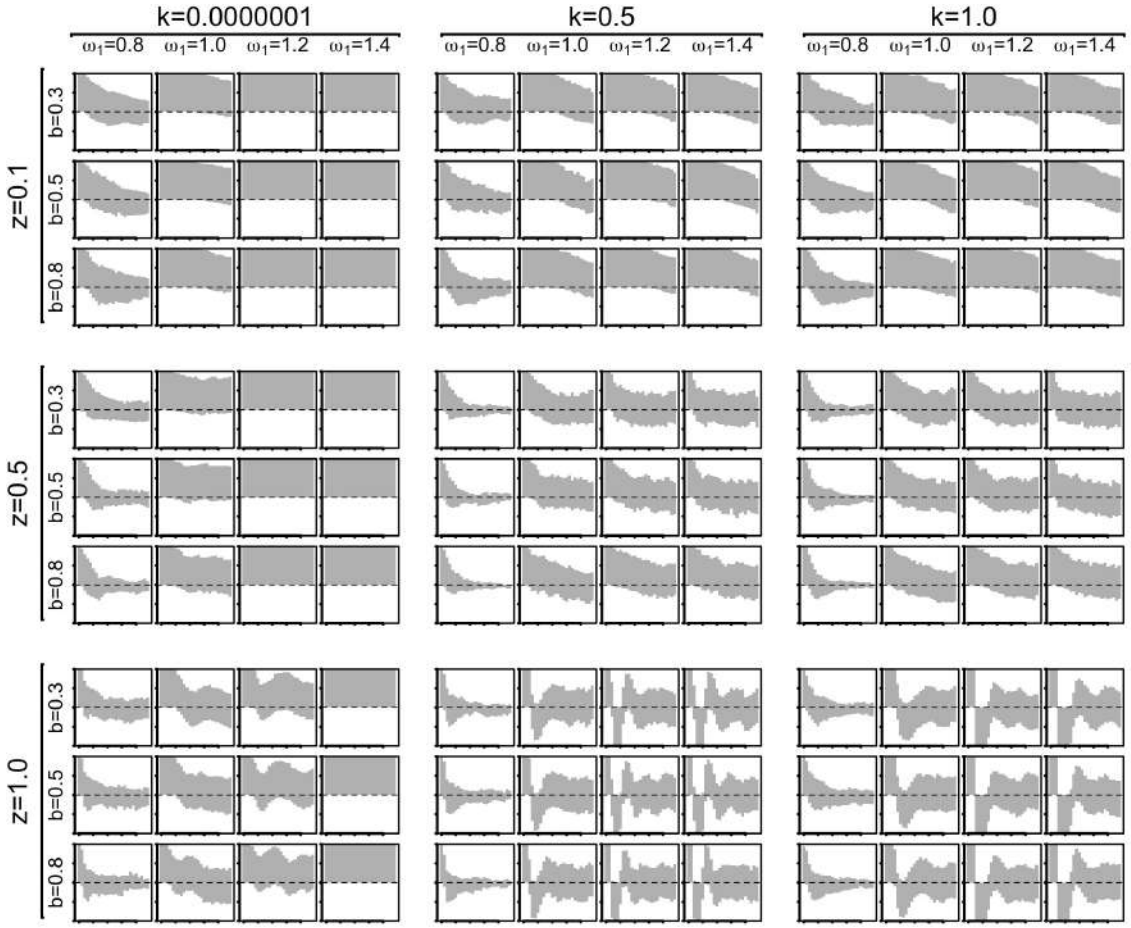

Correlogram of A [predator-prey model, $\beta = 0.4$, $h = \infty$]

D.2.2 Number of Groups (G)

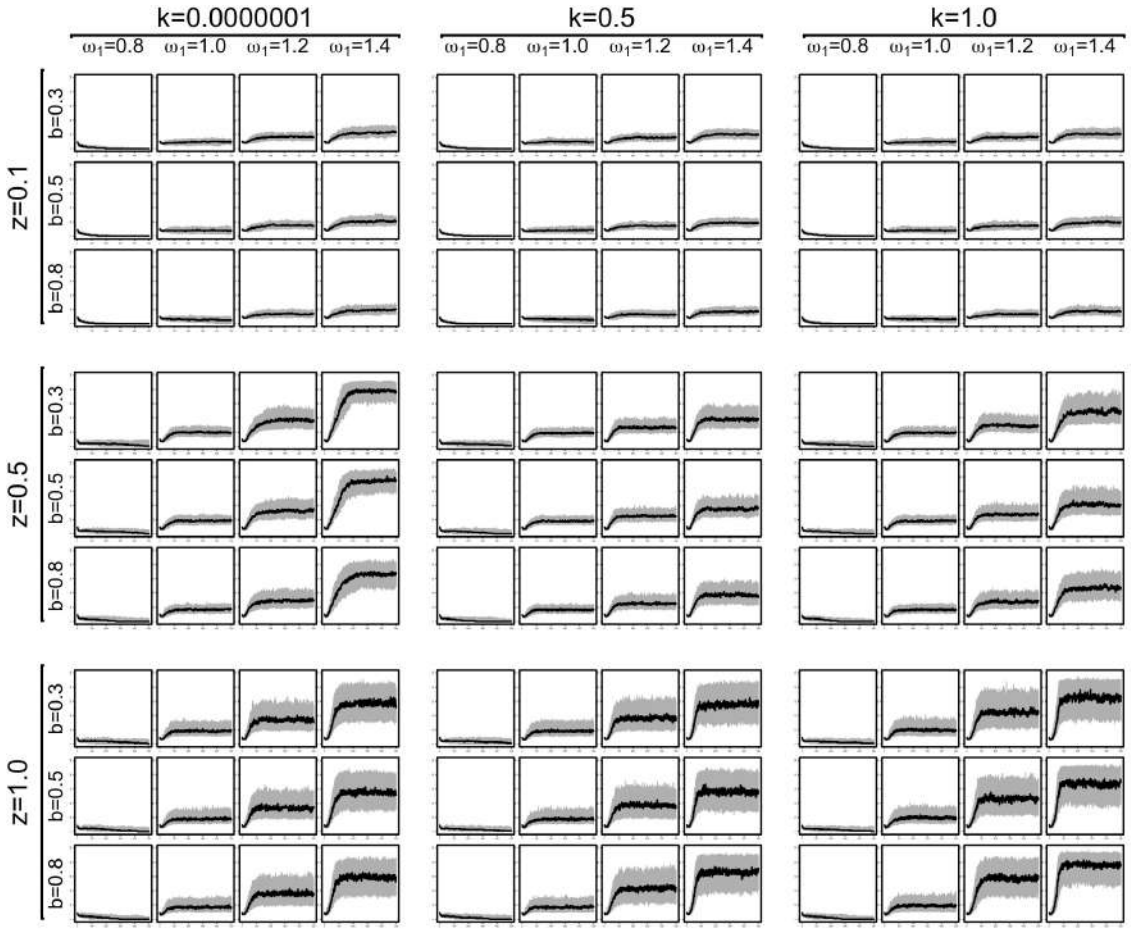

Combined time-series of G [predator-prey model, $\beta = 0.3$, $h = 1$]

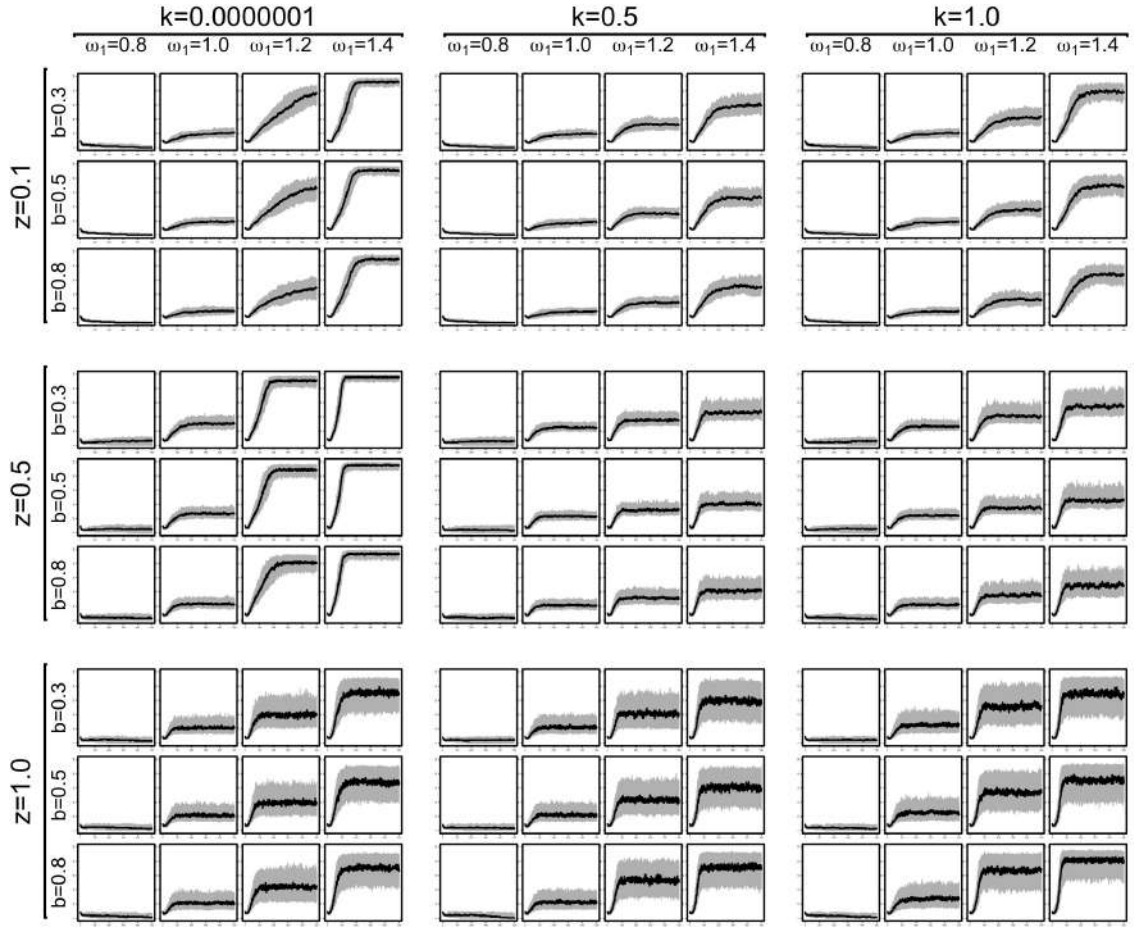

Combined time-series of G [predator-prey model, $\beta = 0.35$, $h = 1$]

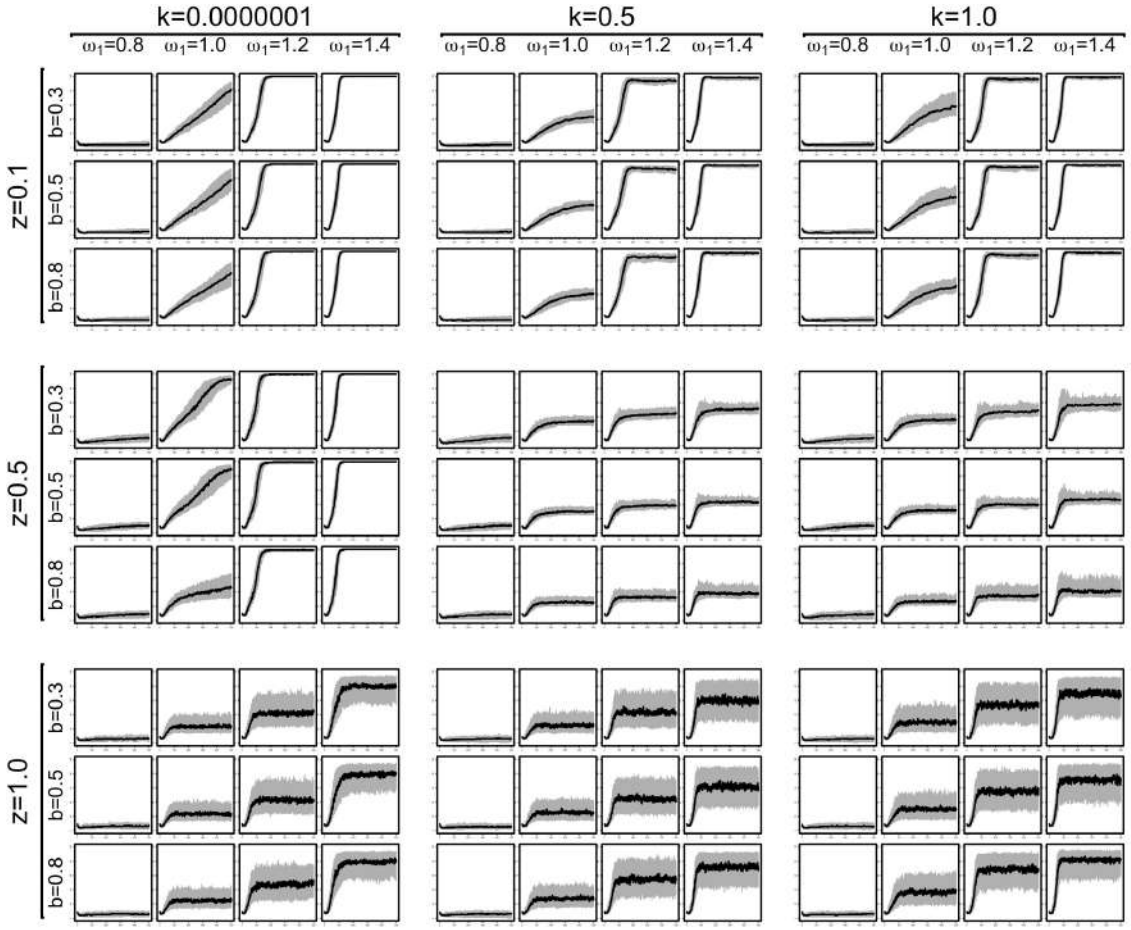

Combined time-series of G [predator-prey model, $\beta = 0.4$, $h = 1$]

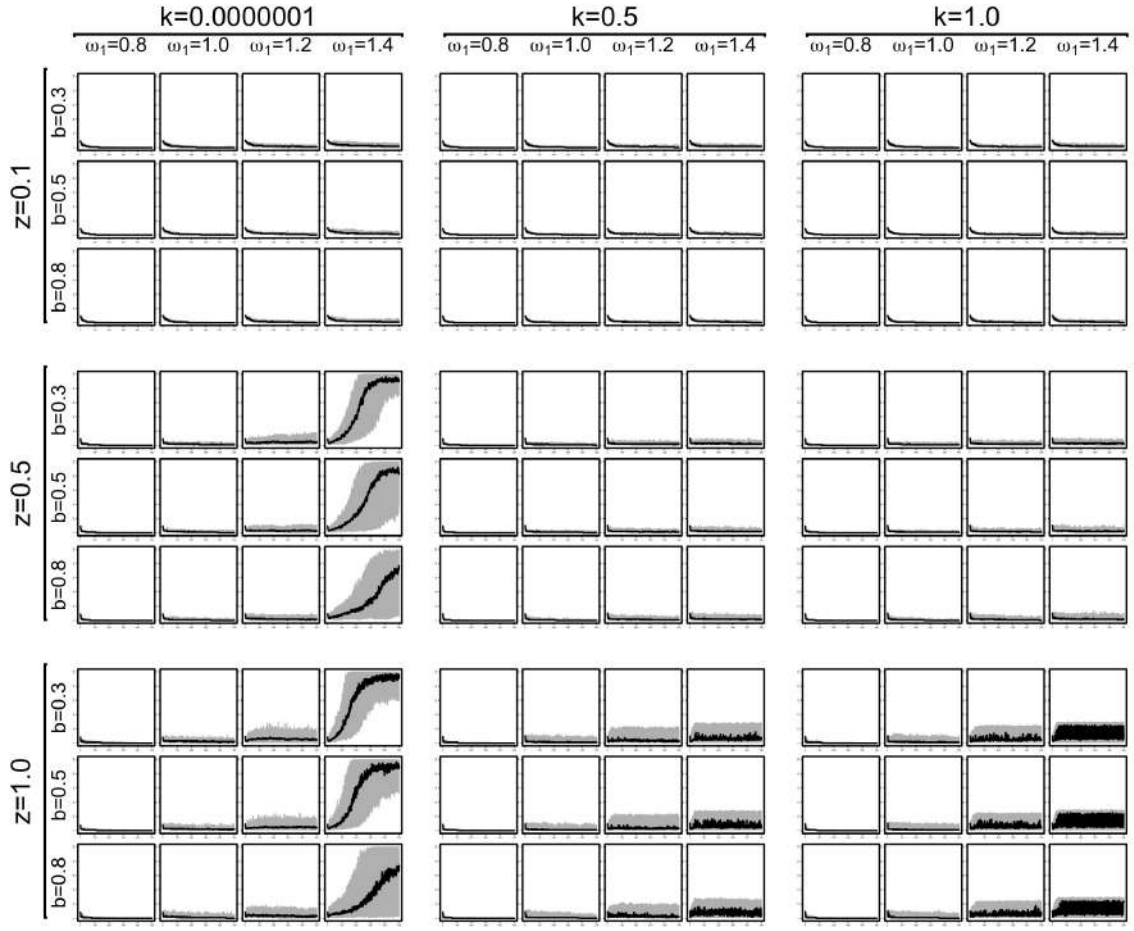

Combined time-series of G [predator-prey model, $\beta = 0.3$, $h = \infty$]

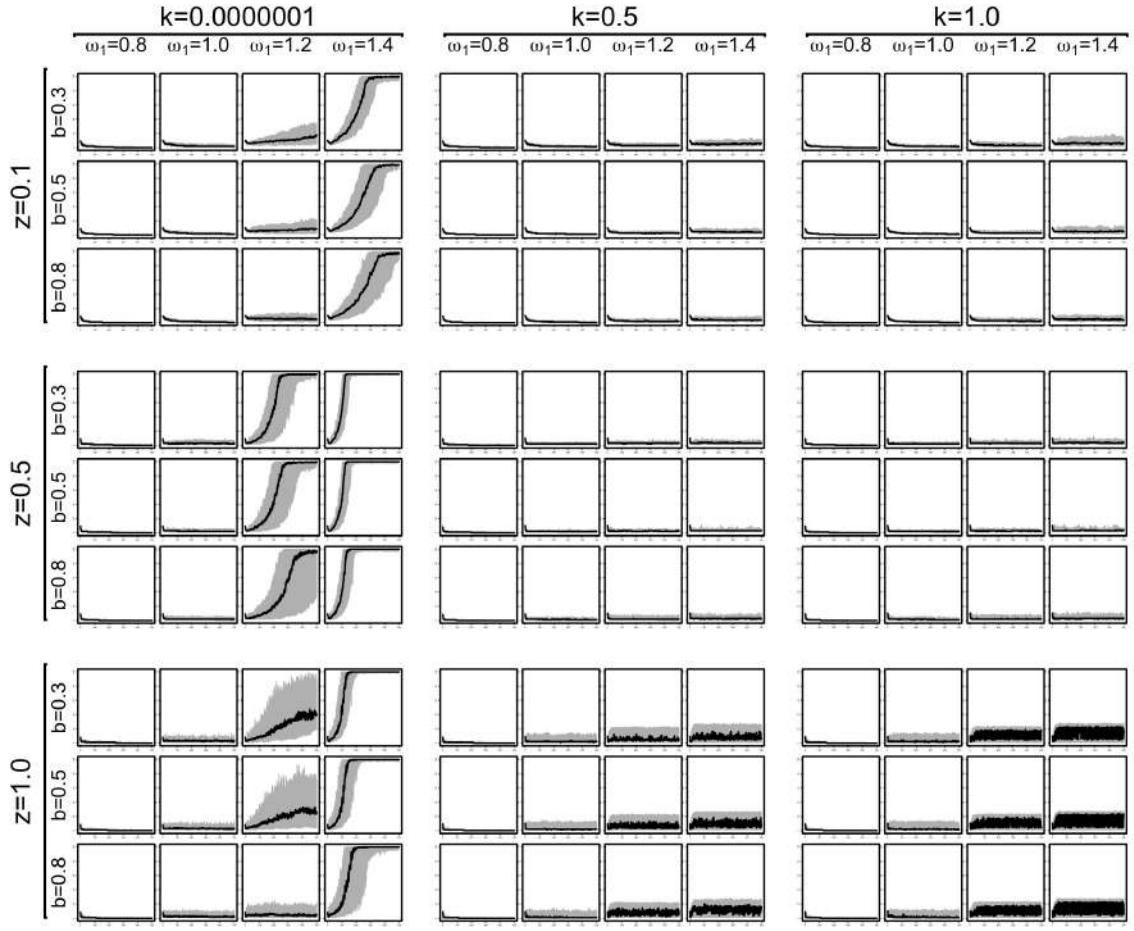

Combined time-series of G [predator-prey model, $\beta = 0.35$, $h = \infty$]

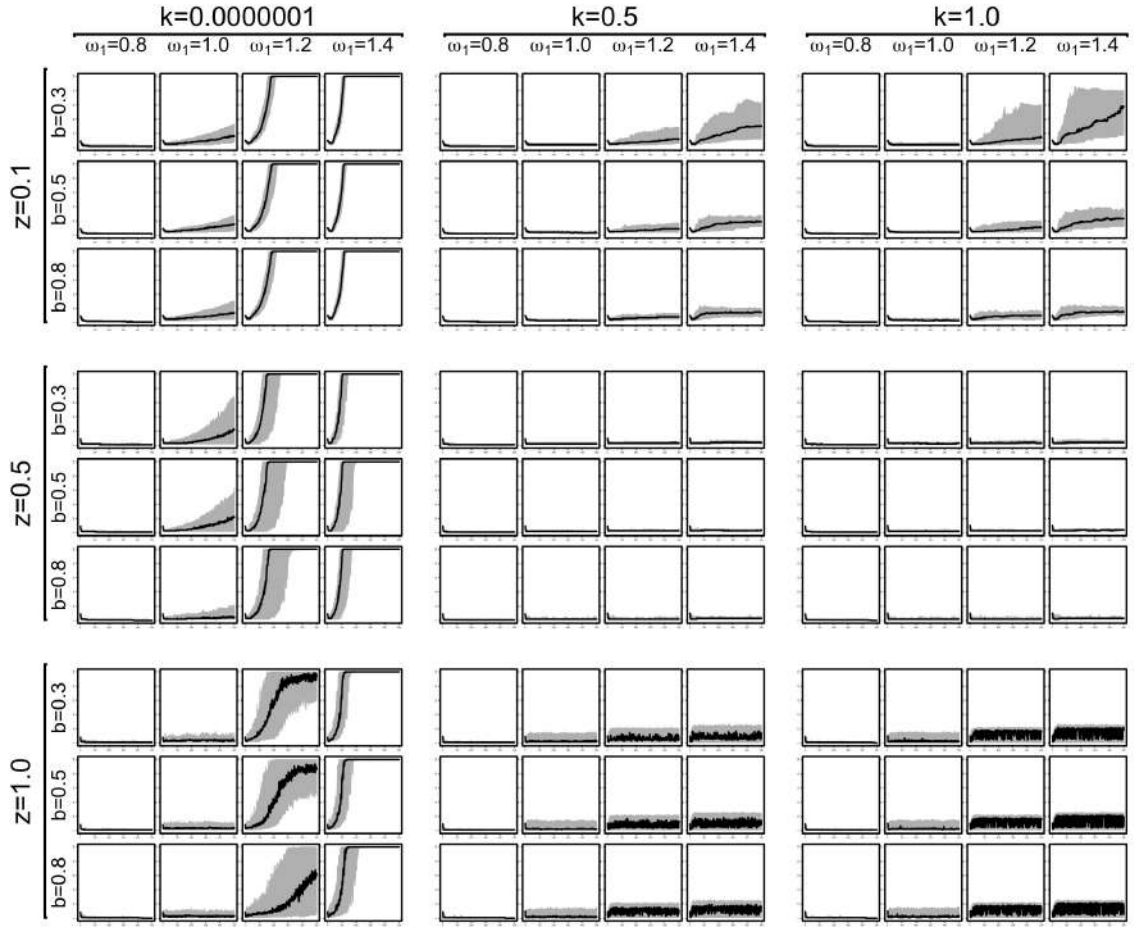

Combined time-series of G [predator-prey model, $\beta = 0.4$, $h = \infty$]

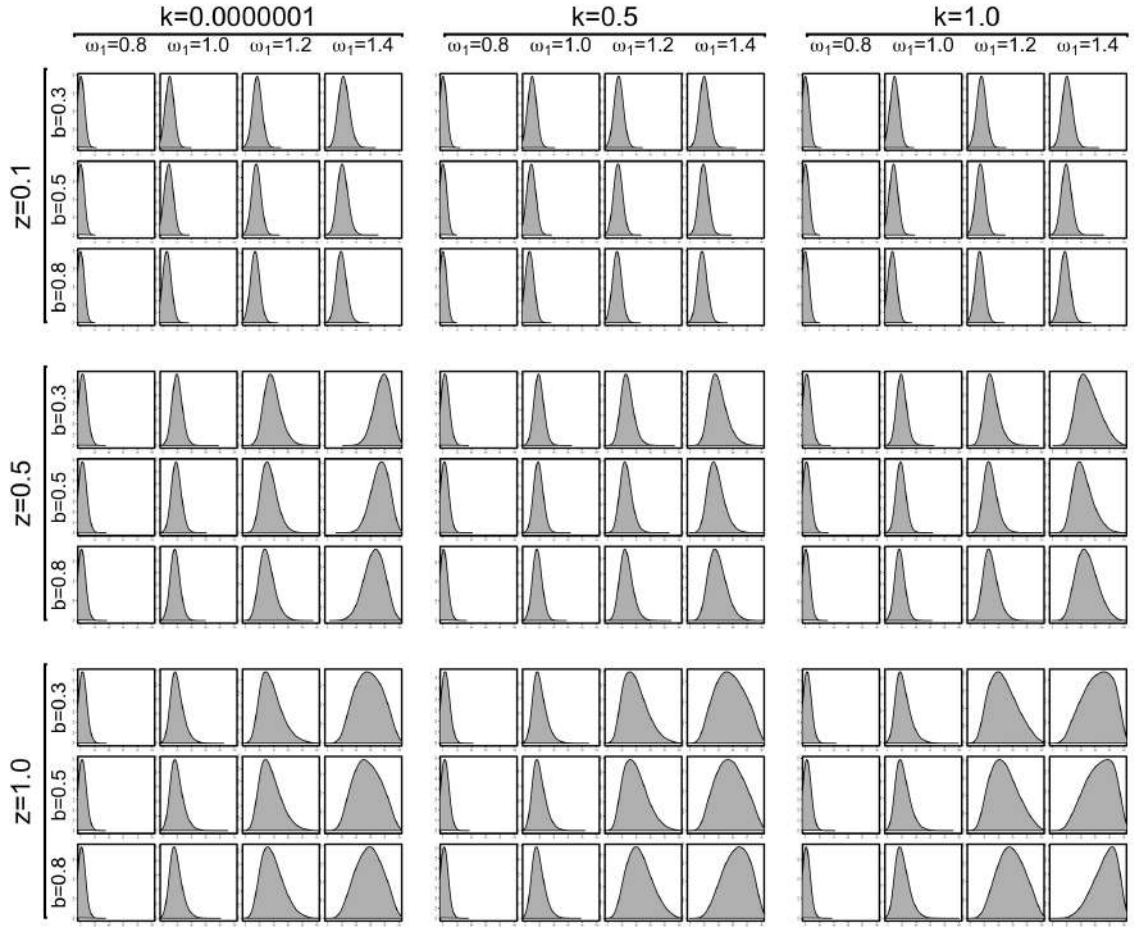

Probability density of G [predator-prey model, $\beta = 0.3$, $h = 1$]

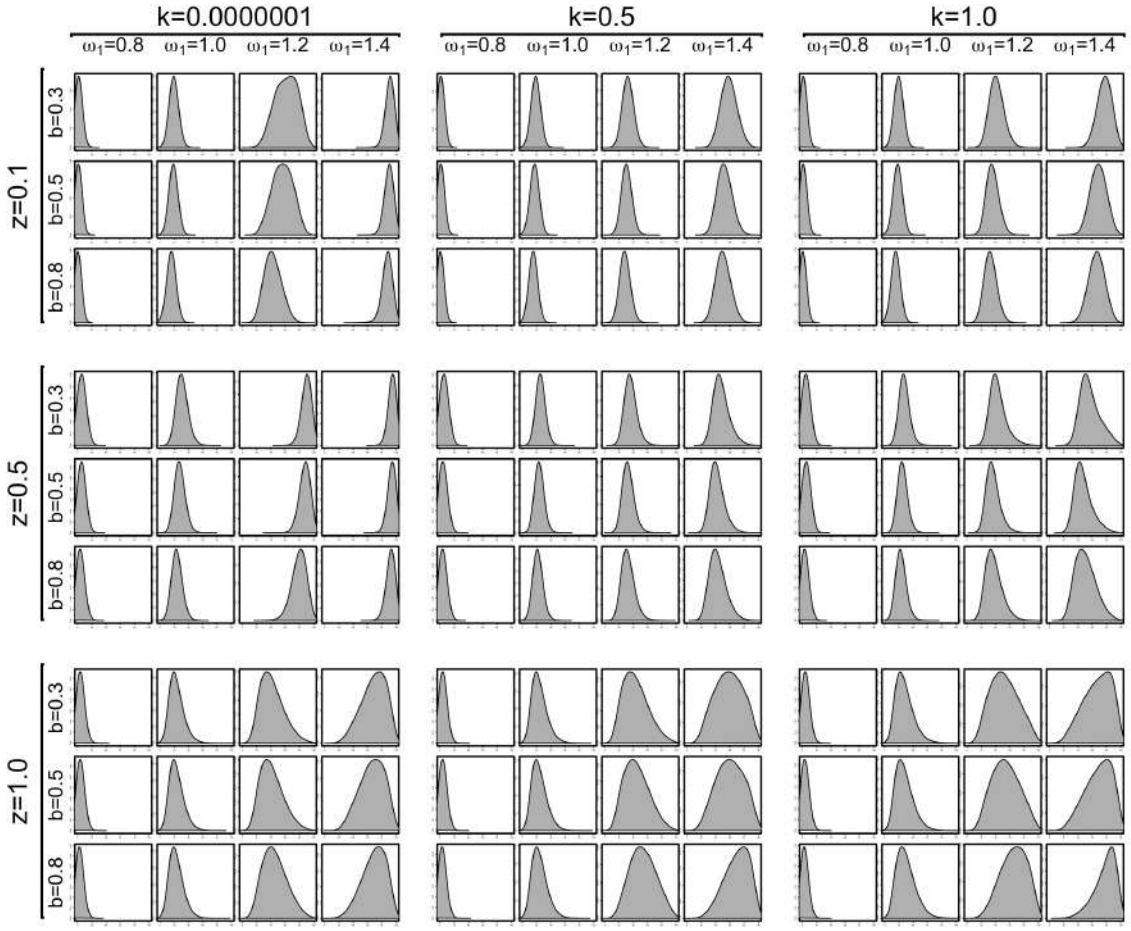

Probability density of G [predator-prey model, $\beta = 0.35$, $h = 1$]

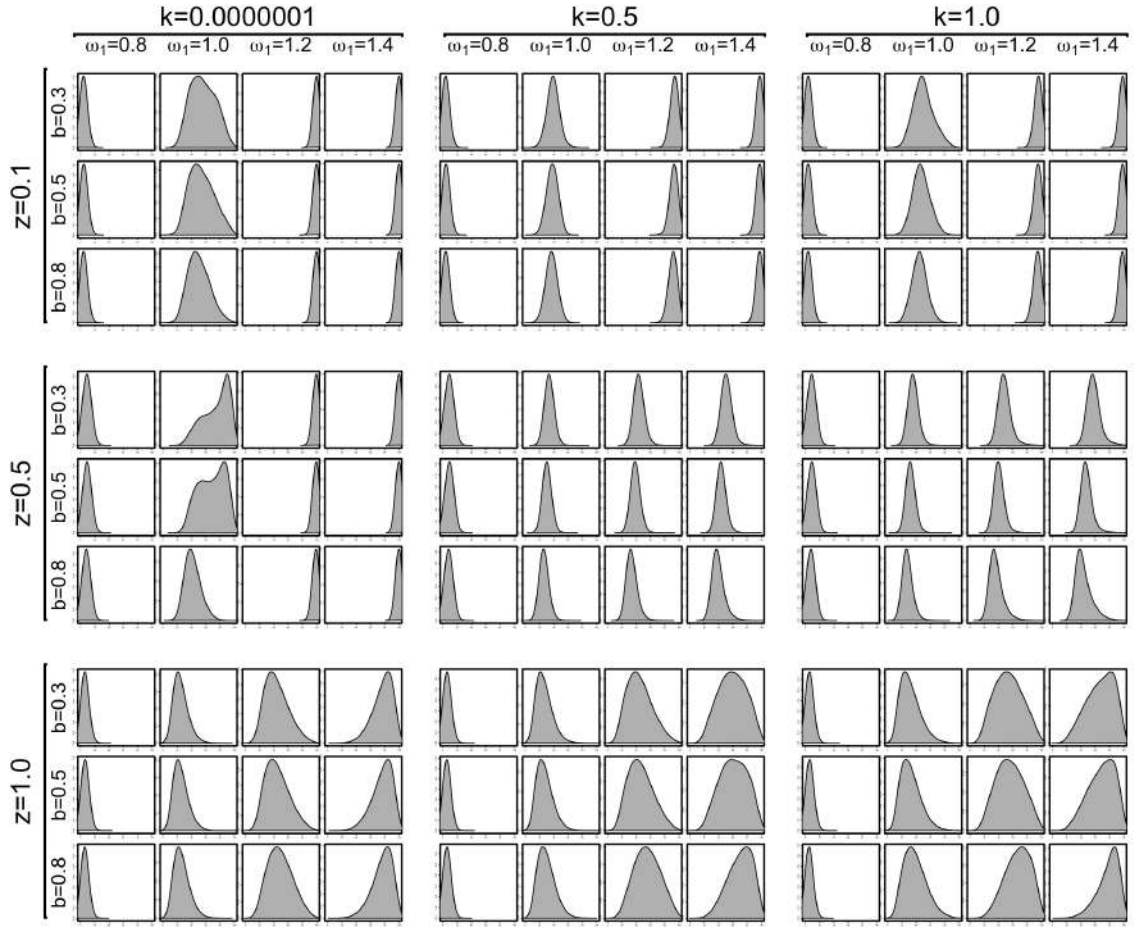

Probability density of G [predator-prey model, $\beta = 0.4$, $h = 1$]

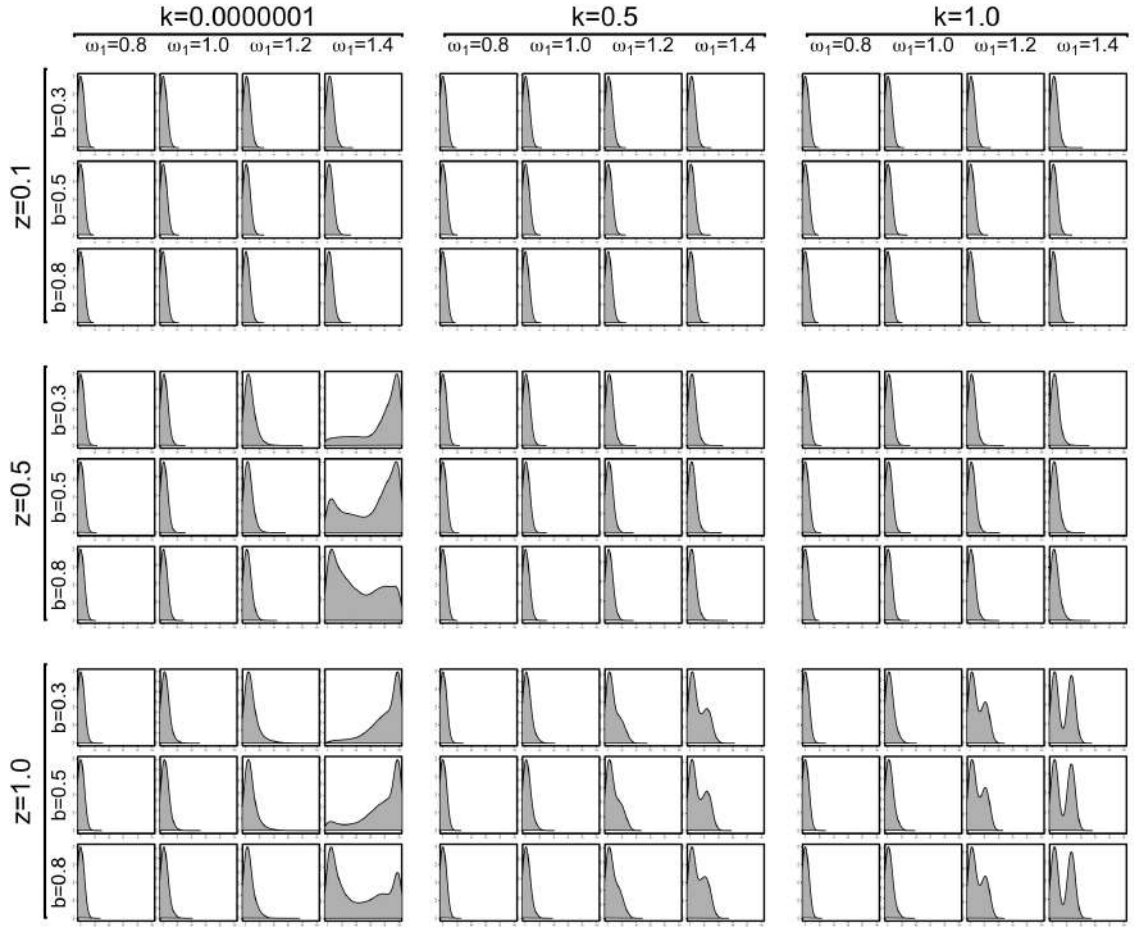

Probability density of G [predator-prey model, $\beta = 0.3$, $h = \infty$]

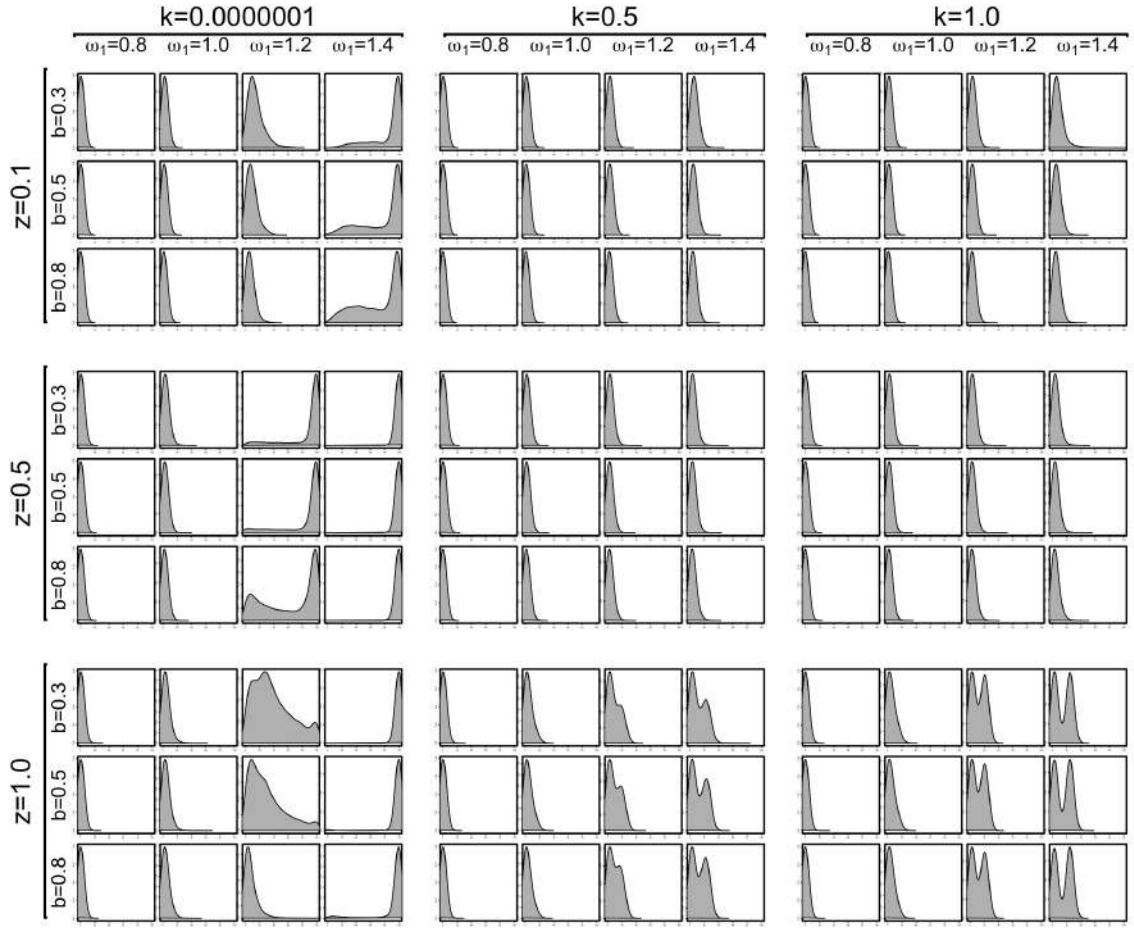

Probability density of G [predator-prey model, $\beta = 0.35$, $h = \infty$]

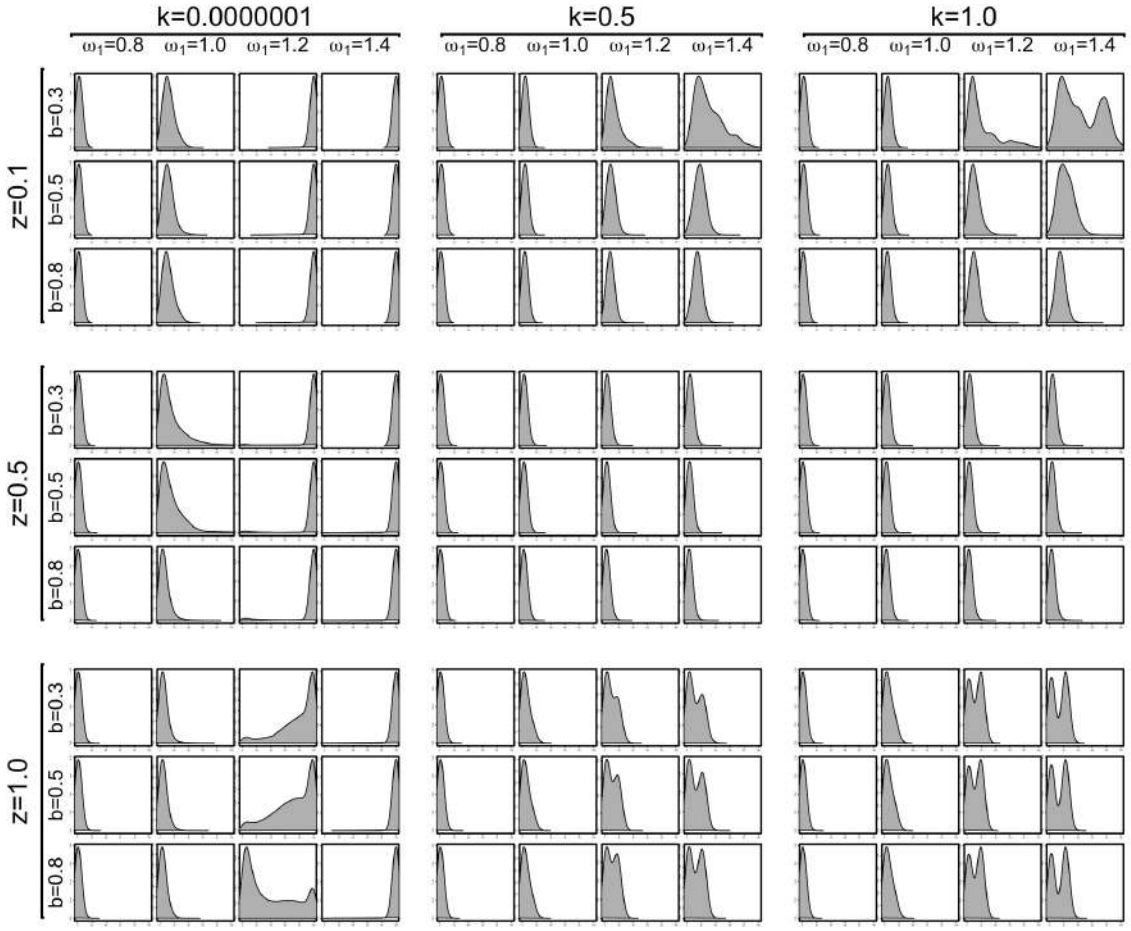

Probability density of G [predator-prey model, $\beta = 0.4$, $h = \infty$]

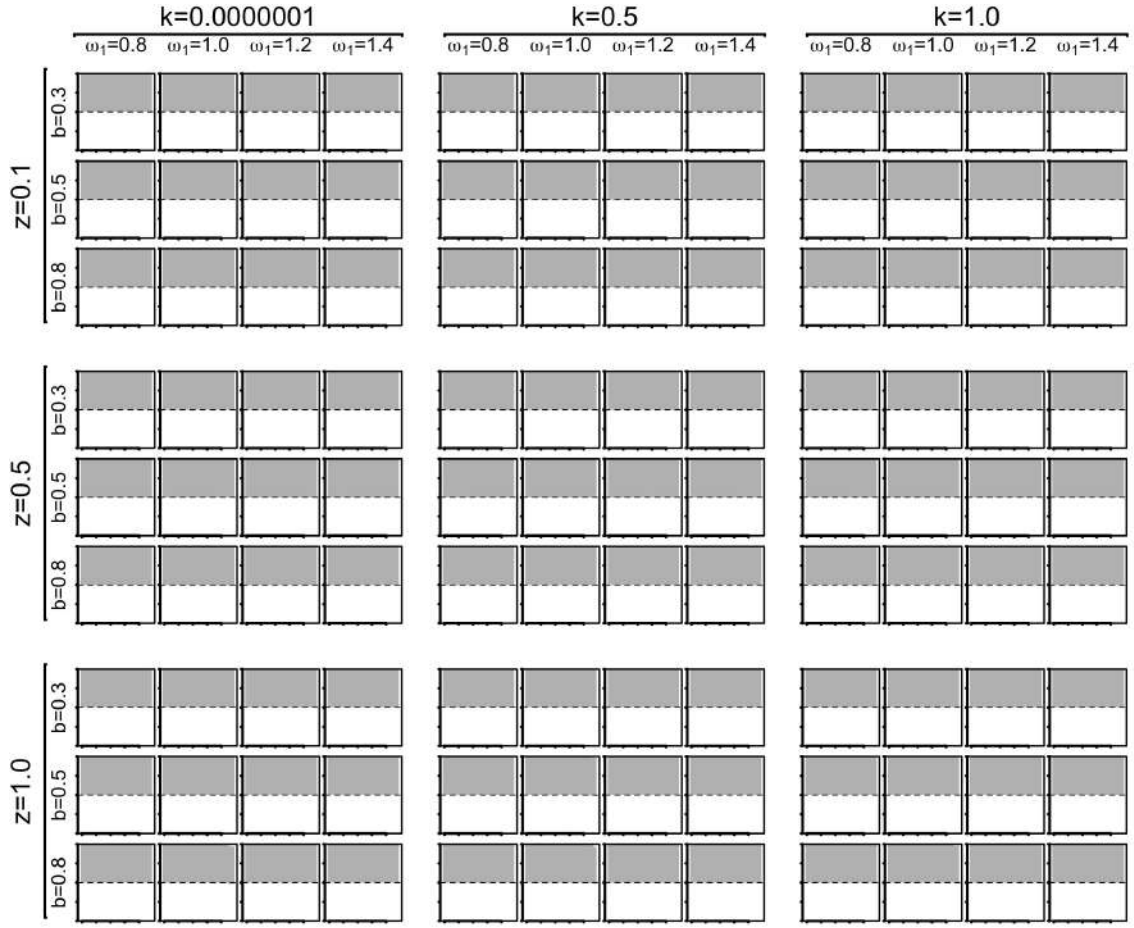

Correlogram of G [predator-prey model, $\beta = 0.3$, $h = 1$]

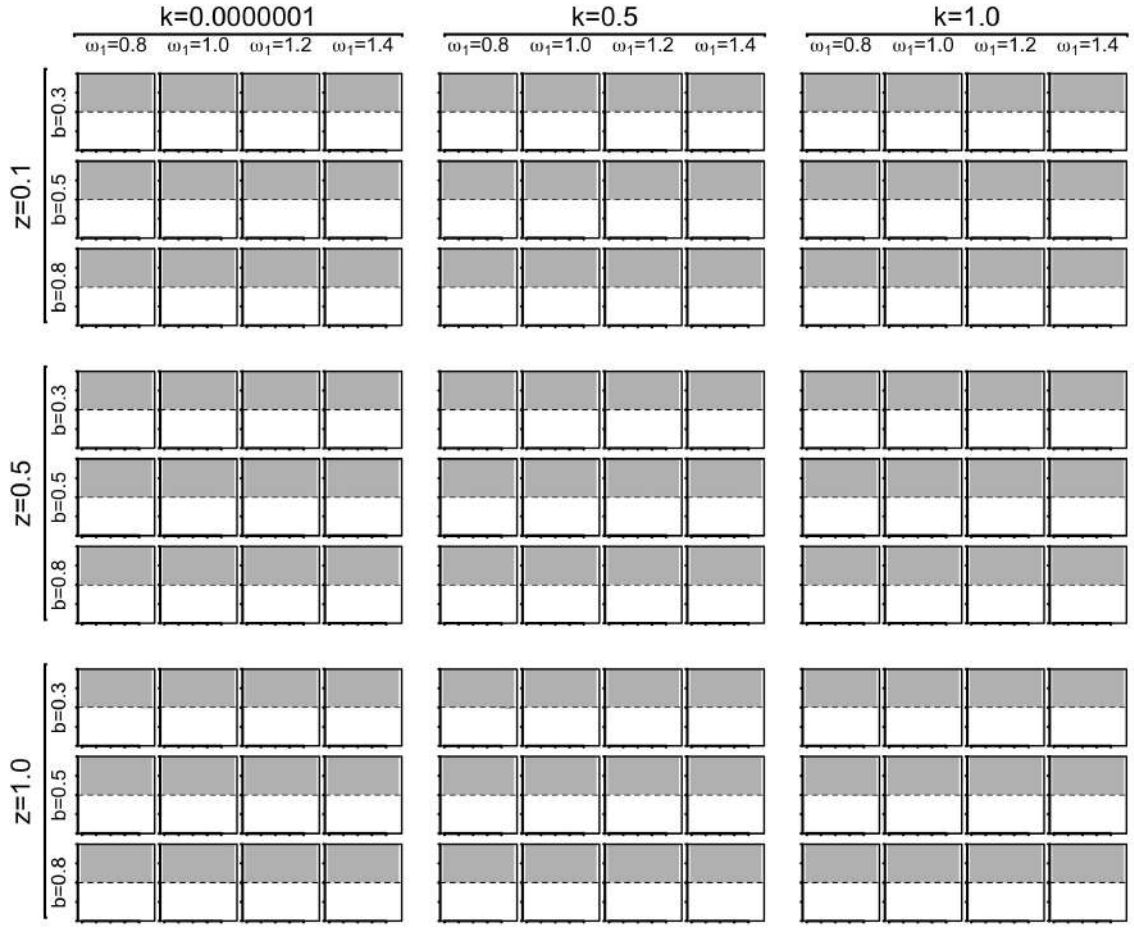

Correlogram of G [predator-prey model, $\beta = 0.35$, $h = 1$]

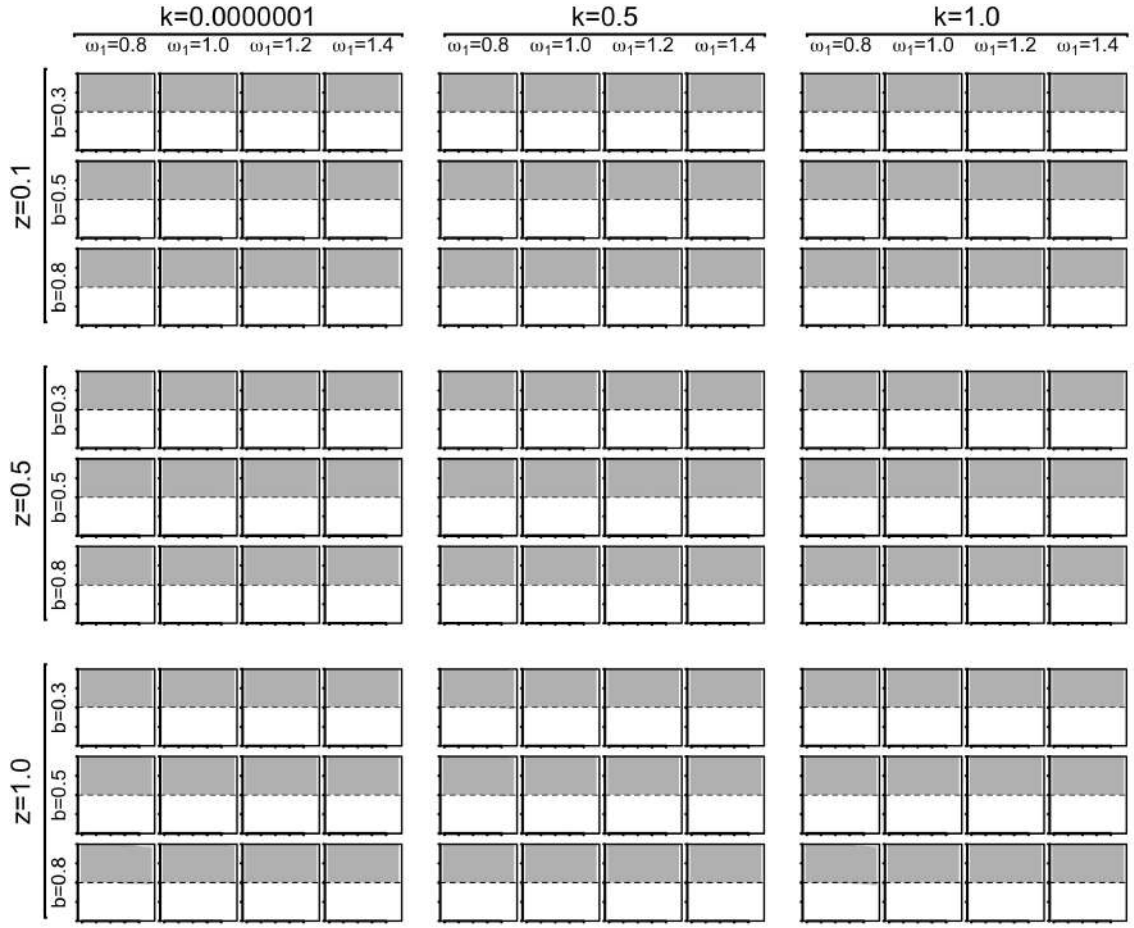

Correlogram of G [predator-prey model, $\beta = 0.4$, $h = 1$]

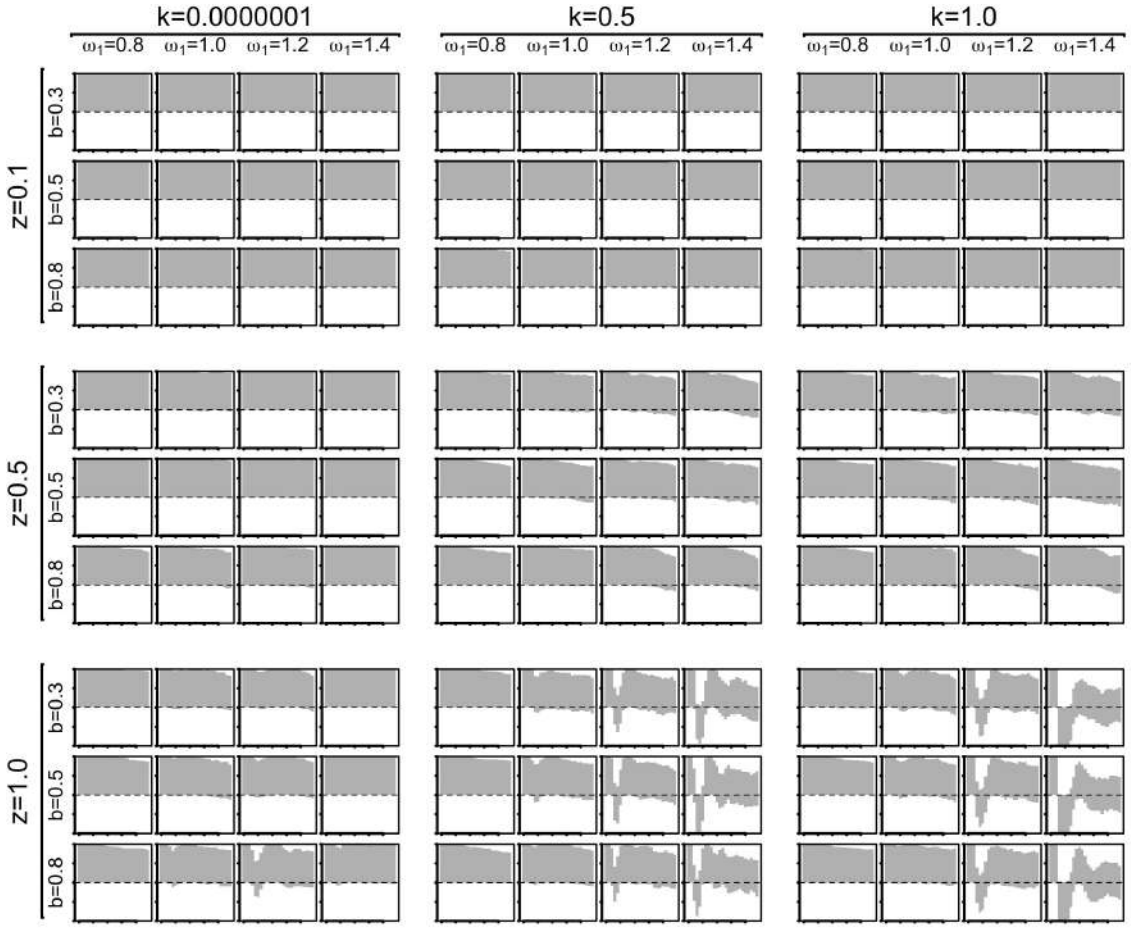

Correlogram of G [predator-prey model, $\beta = 0.3$, $h = \infty$]

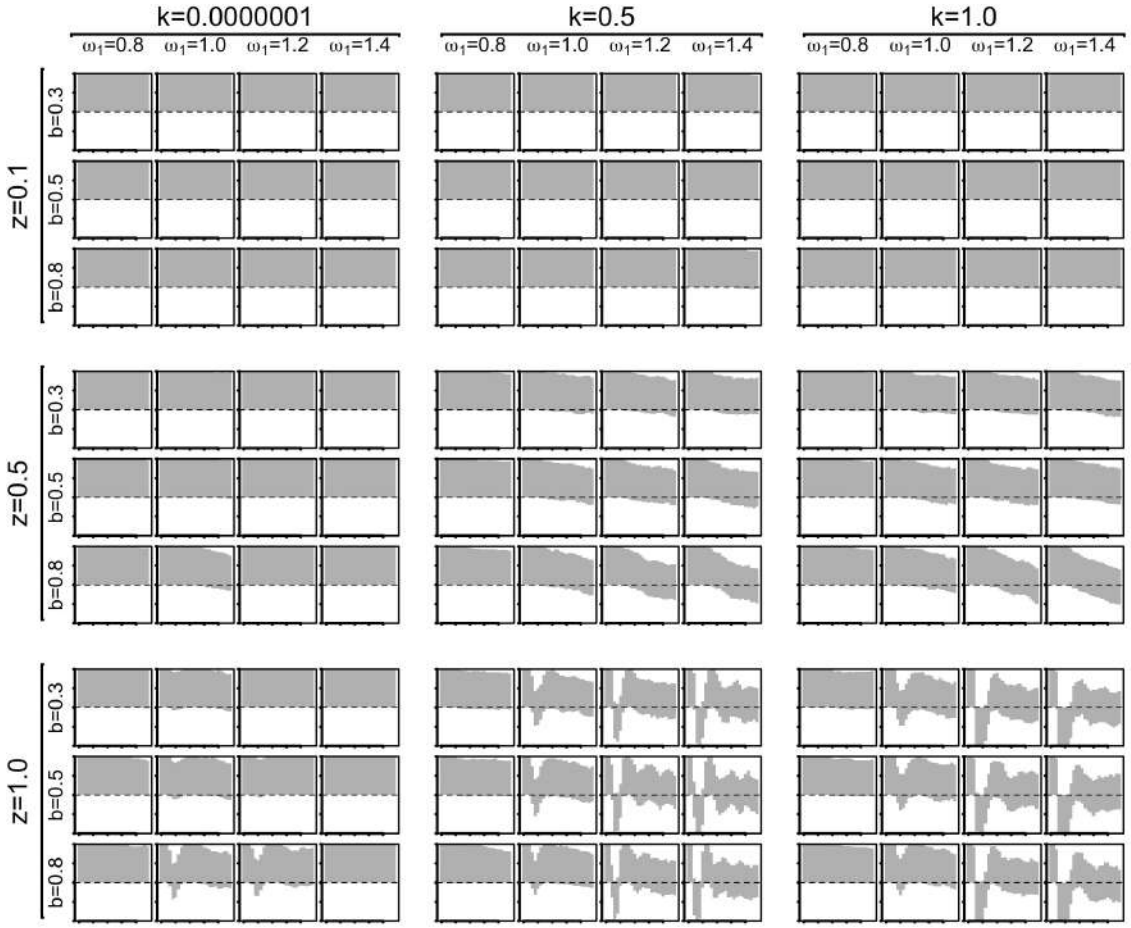

Correlogram of G [predator-prey model, $\beta = 0.35$, $h = \infty$]

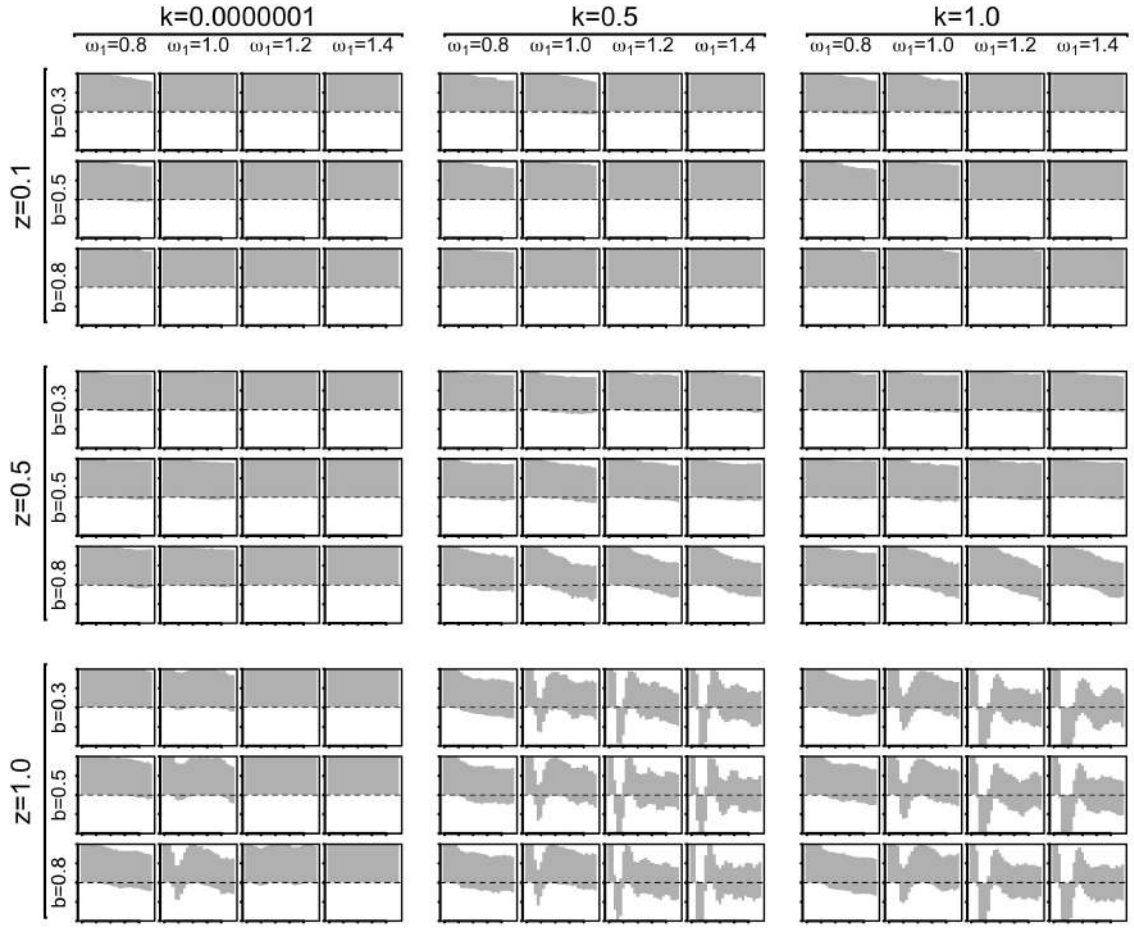

Correlogram of G [predator-prey model, $\beta = 0.4$, $h = \infty$]

D.2.3 Number of Agents (N)

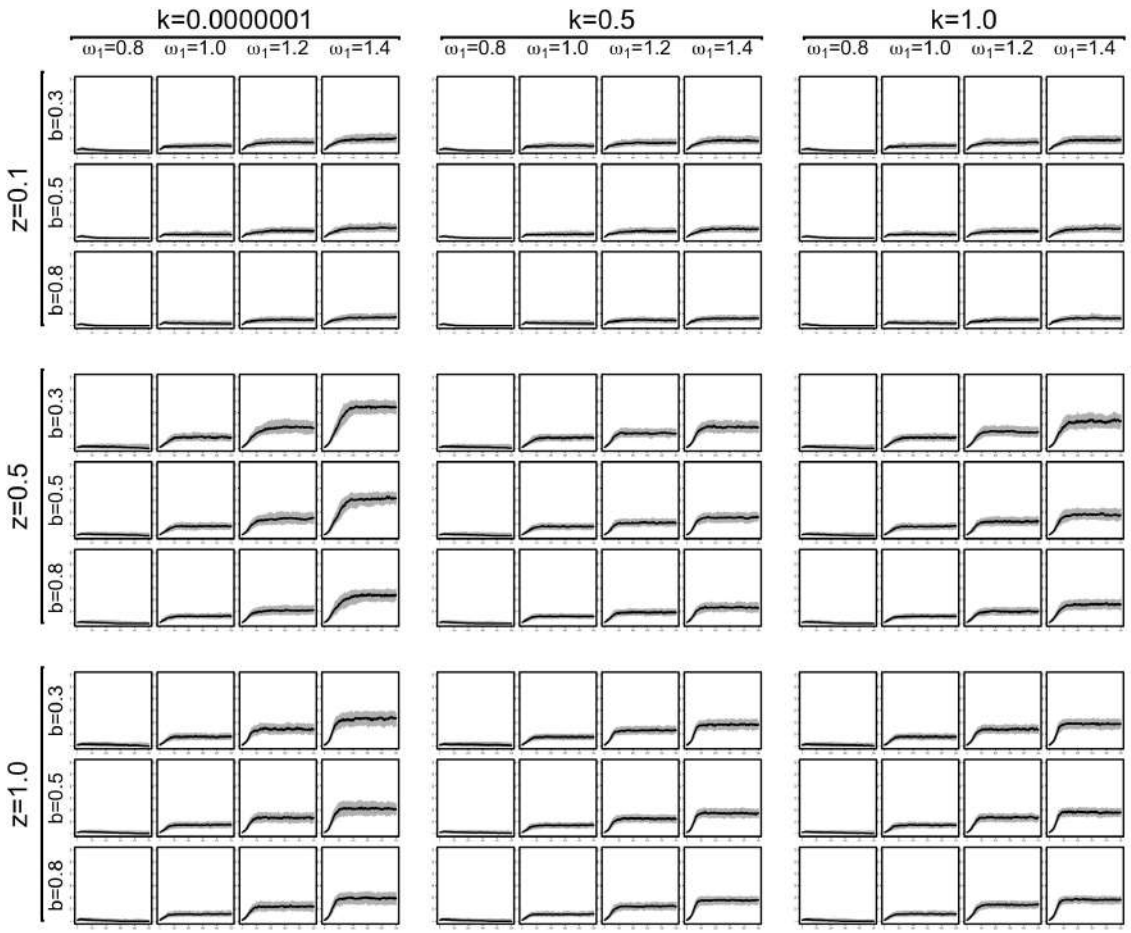

Combined time-series of N [predator-prey model, $\beta = 0.3$, $h = 1$, y-axis range from 0 to 600]

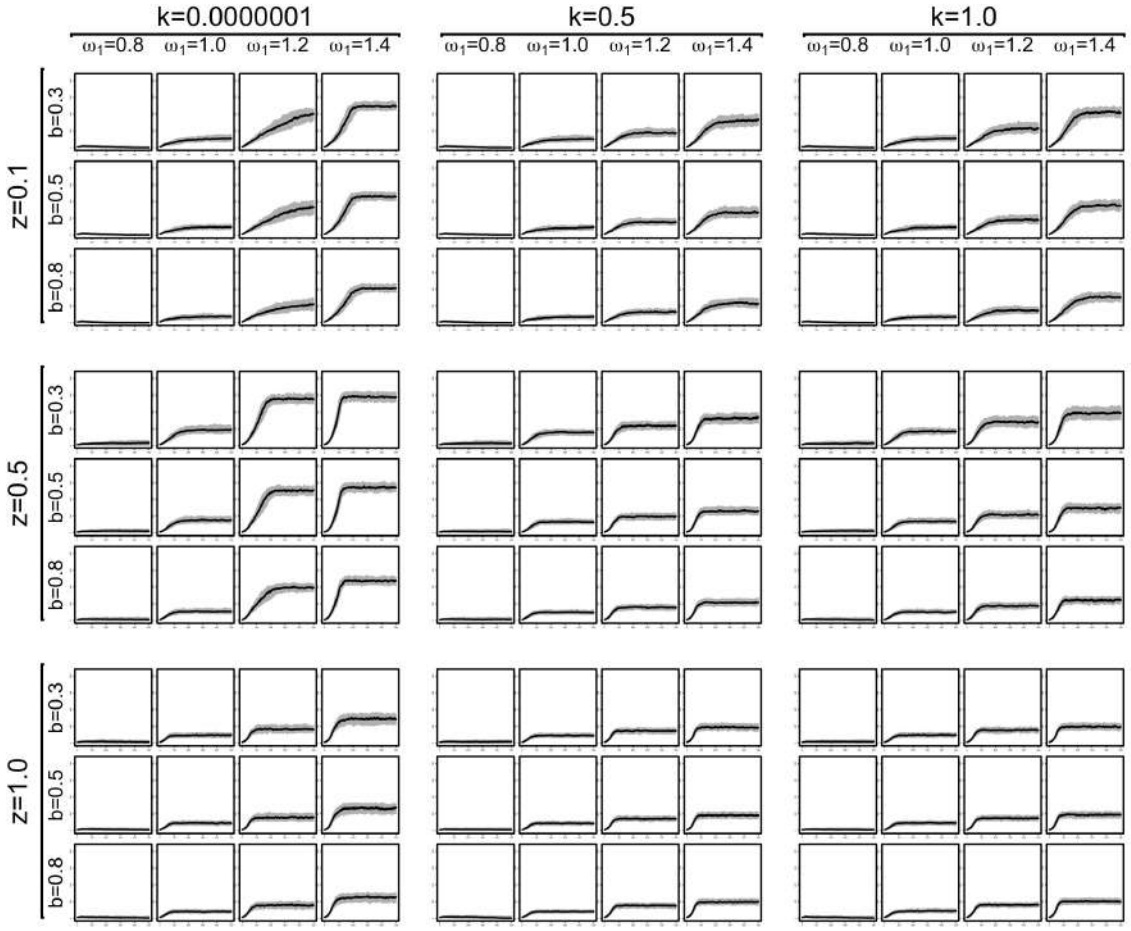

Combined time-series of N [predator-prey model, $\beta = 0.35$, $h = 1$, y-axis range from 0 to 850]

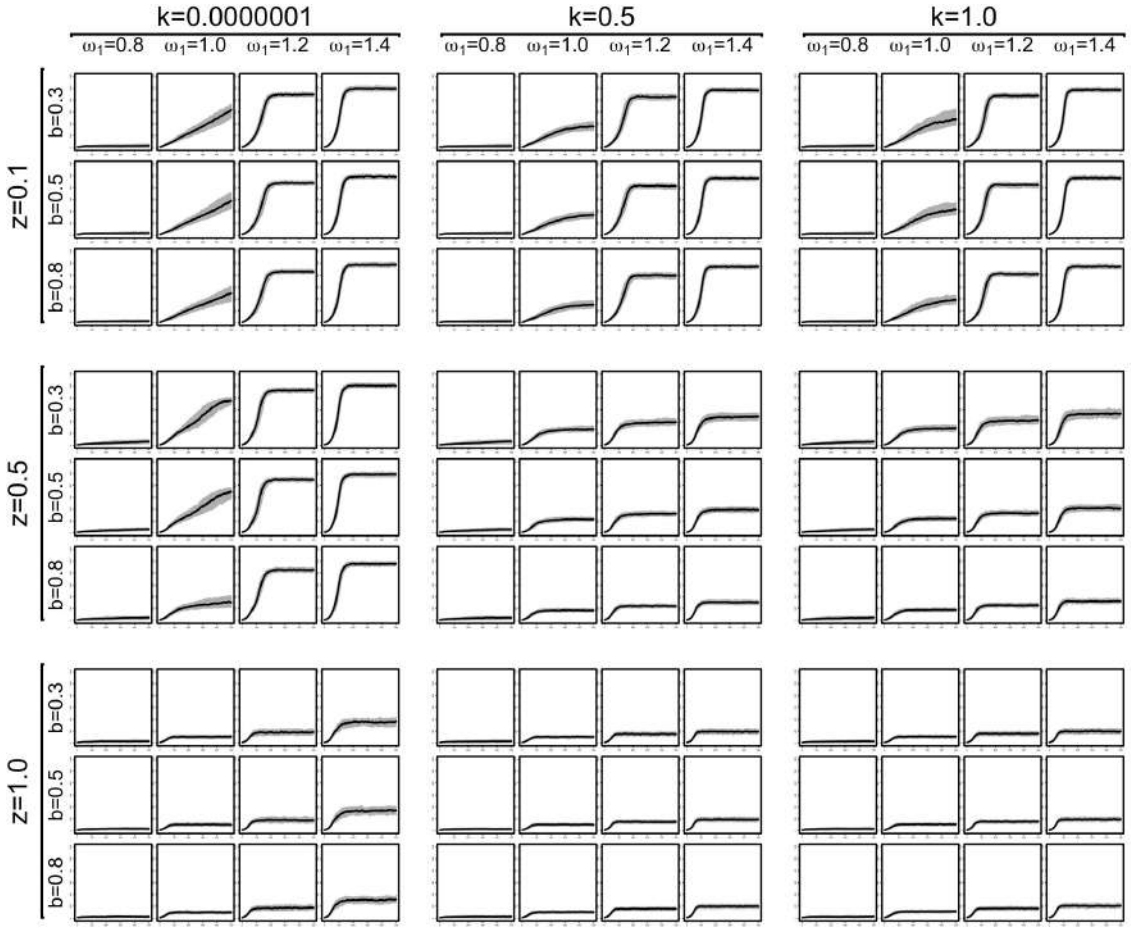

Combined time-series of N [predator-prey model, $\beta = 0.4$, $h = 1$, y-axis range from 0 to 1200]

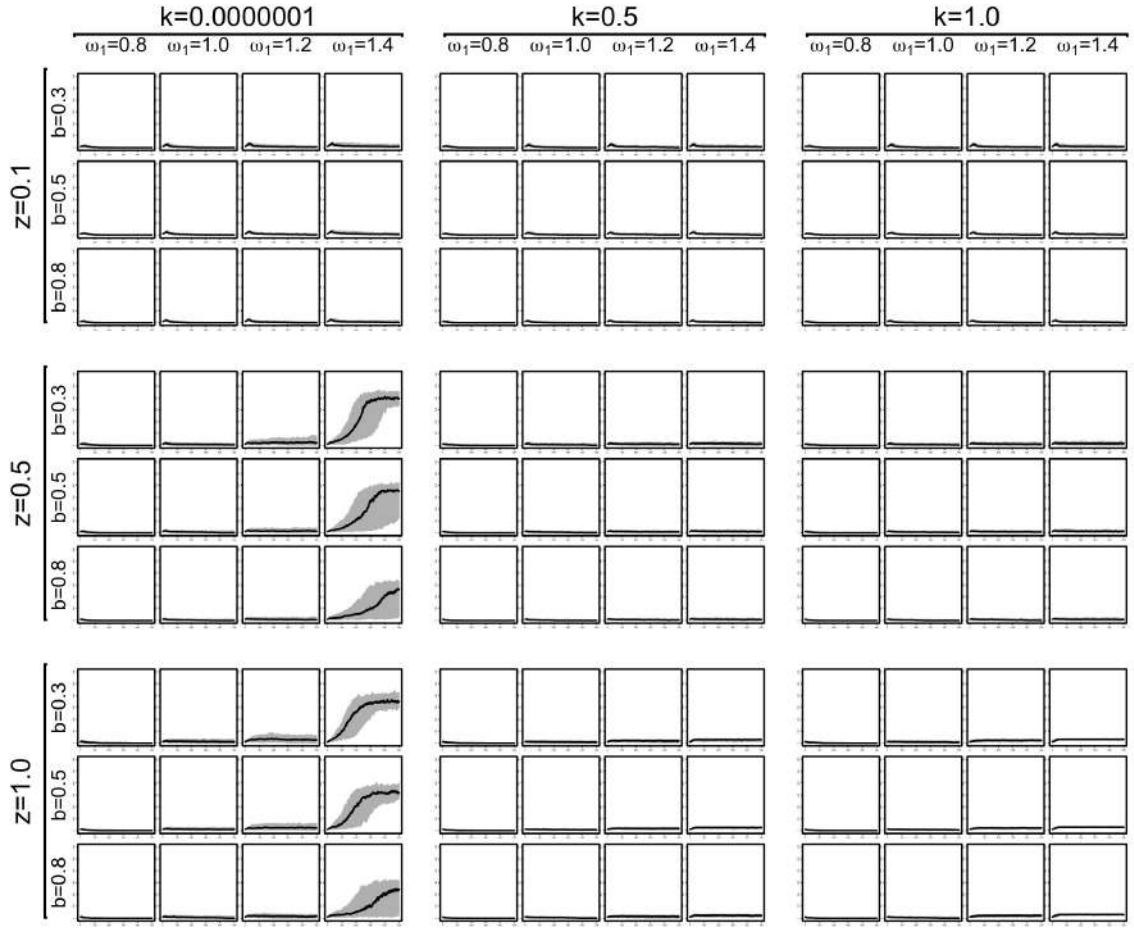

Combined time-series of N [predator-prey model, $\beta = 0.3$, $h = \infty$, y-axis range from 0 to 600]

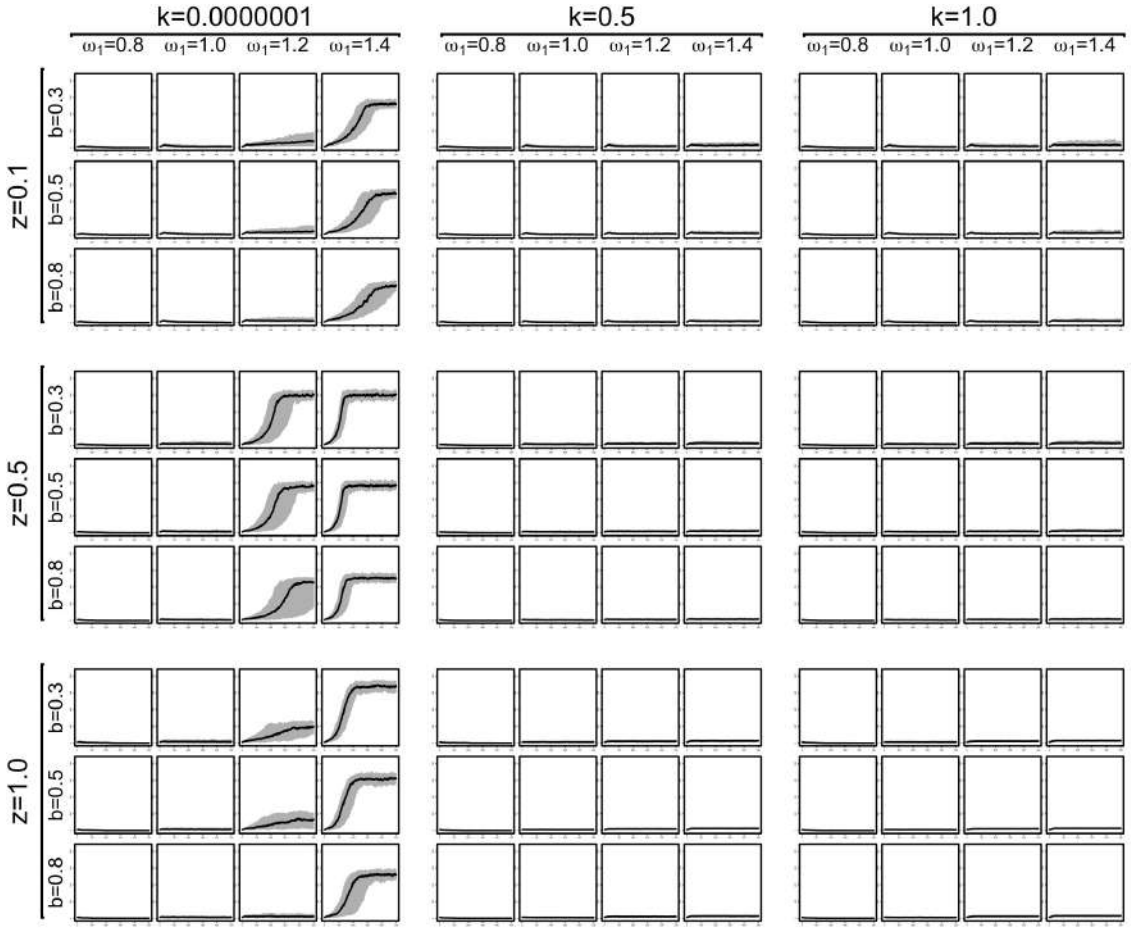

Combined time-series of N [predator-prey model, $\beta = 0.35$, $h = \infty$, y-axis range from 0 to 850]

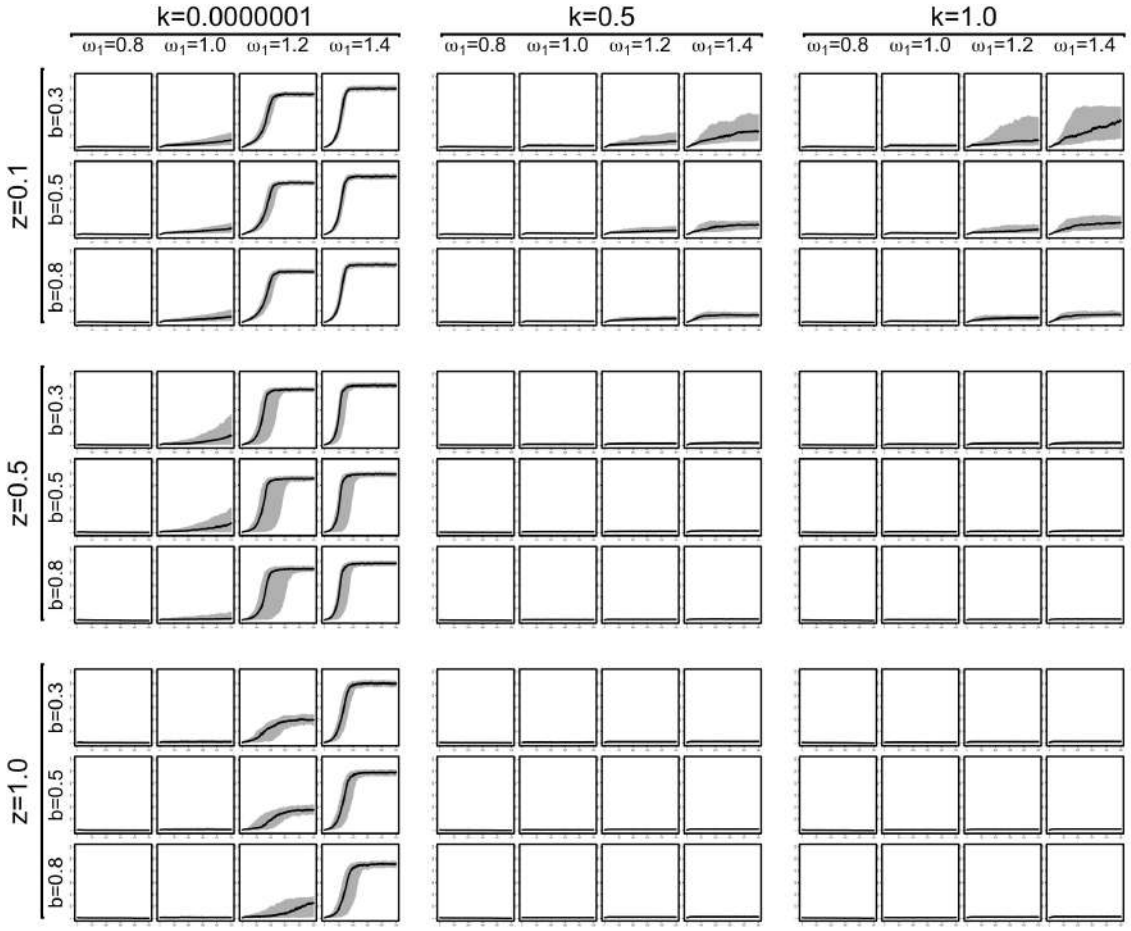

Combined time-series of N [predator-prey model, $\beta = 0.4$, $h = \infty$, y-axis range from 0 to 1200]

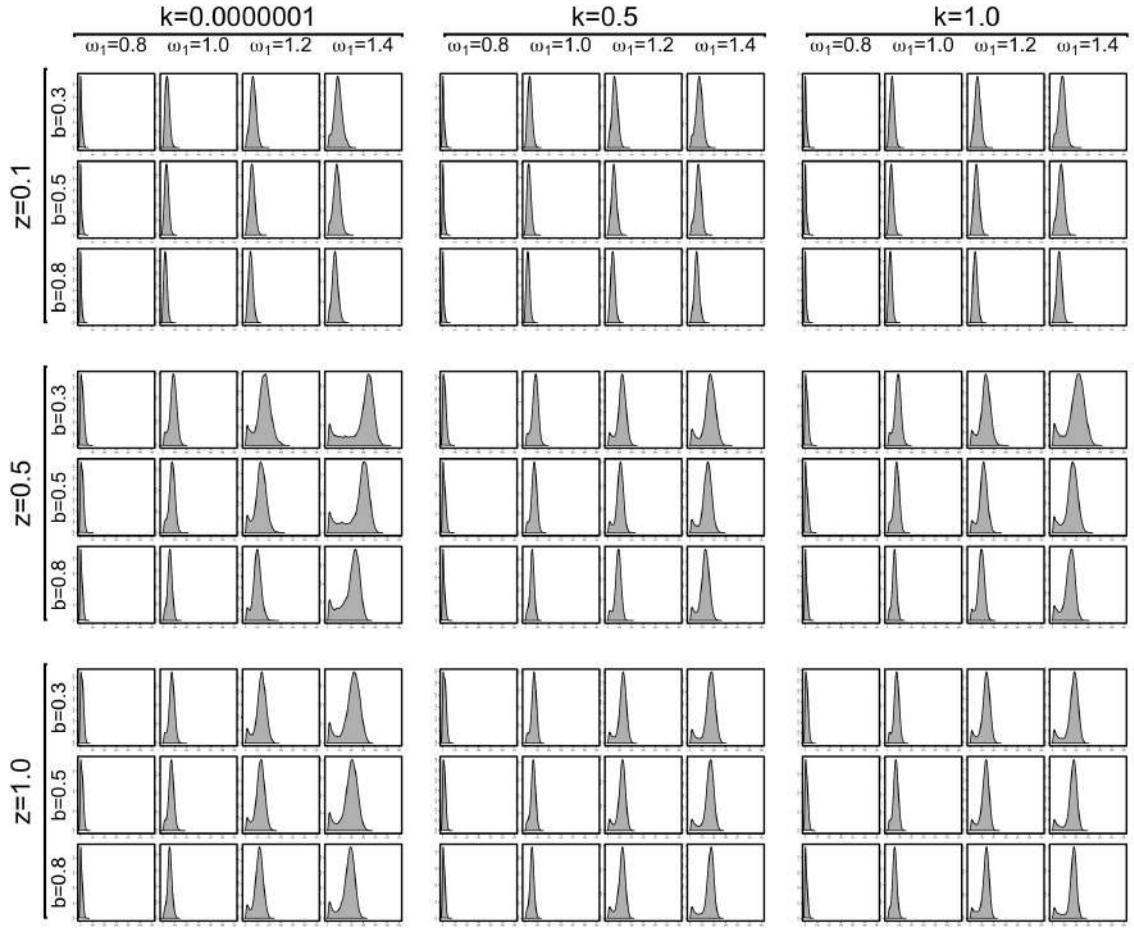

Probability density of N [predator-prey model, $\beta = 0.3$, $h = 1$; x-axis range from 0 to 600]

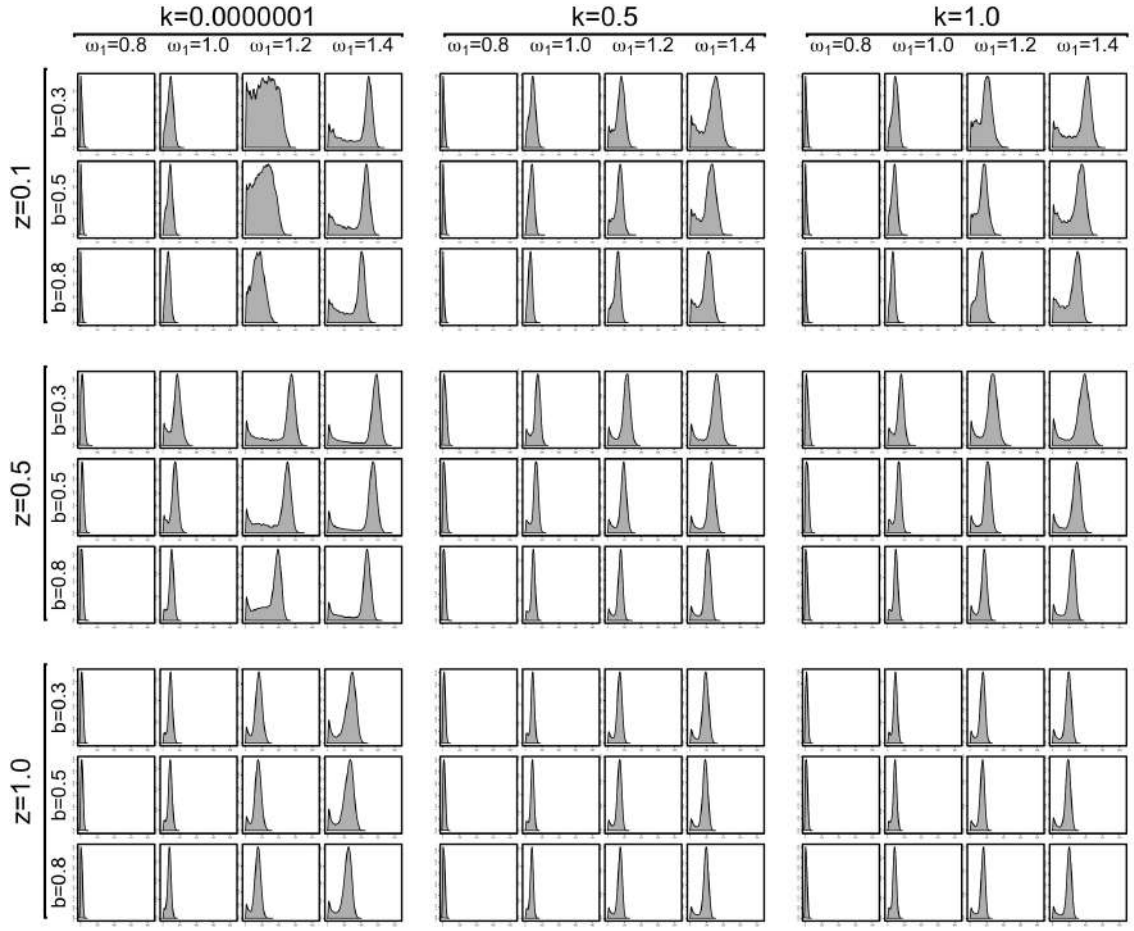

Probability density of N [predator-prey model, $\beta = 0.35$, $h = 1$; x-axis range from 0 to 850]]

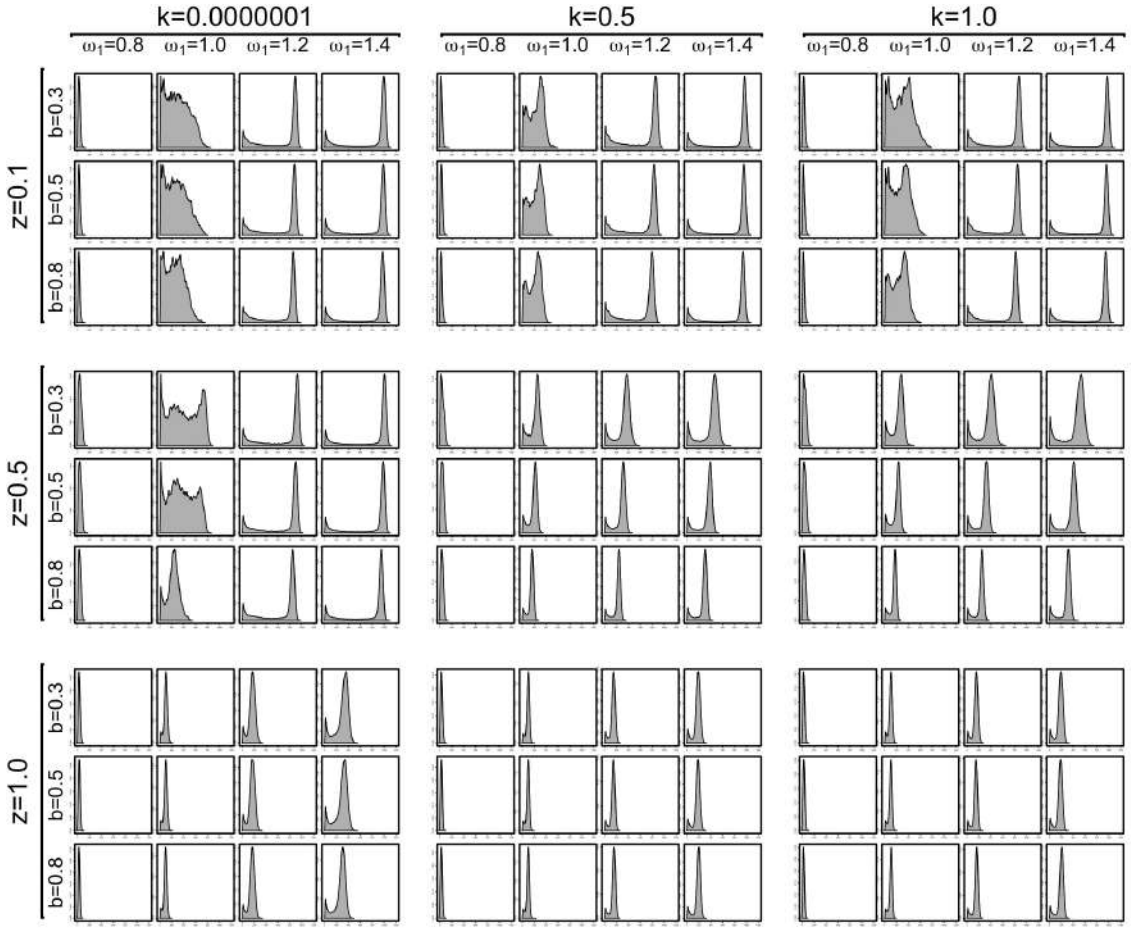

Probability density of N [predator-prey model, $\beta = 0.4$, $h = 1$; x-axis range from 0 to 1200]]

Probability density of N [predator-prey model, $\beta = 0.3$, $h = 1$; x-axis range from 0 to 600]

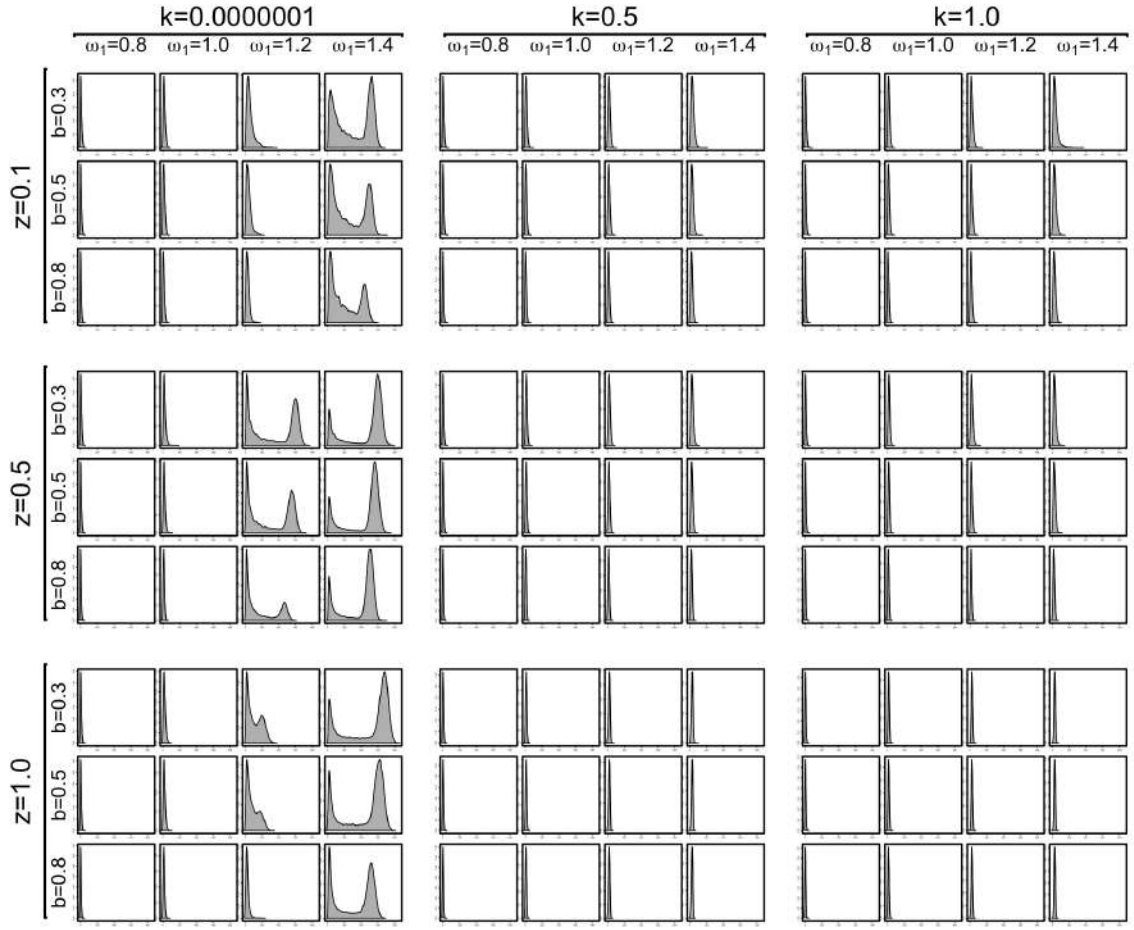

Probability density of N [predator-prey model, $\beta = 0.35$, $h = 1$; x-axis range from 0 to 850]

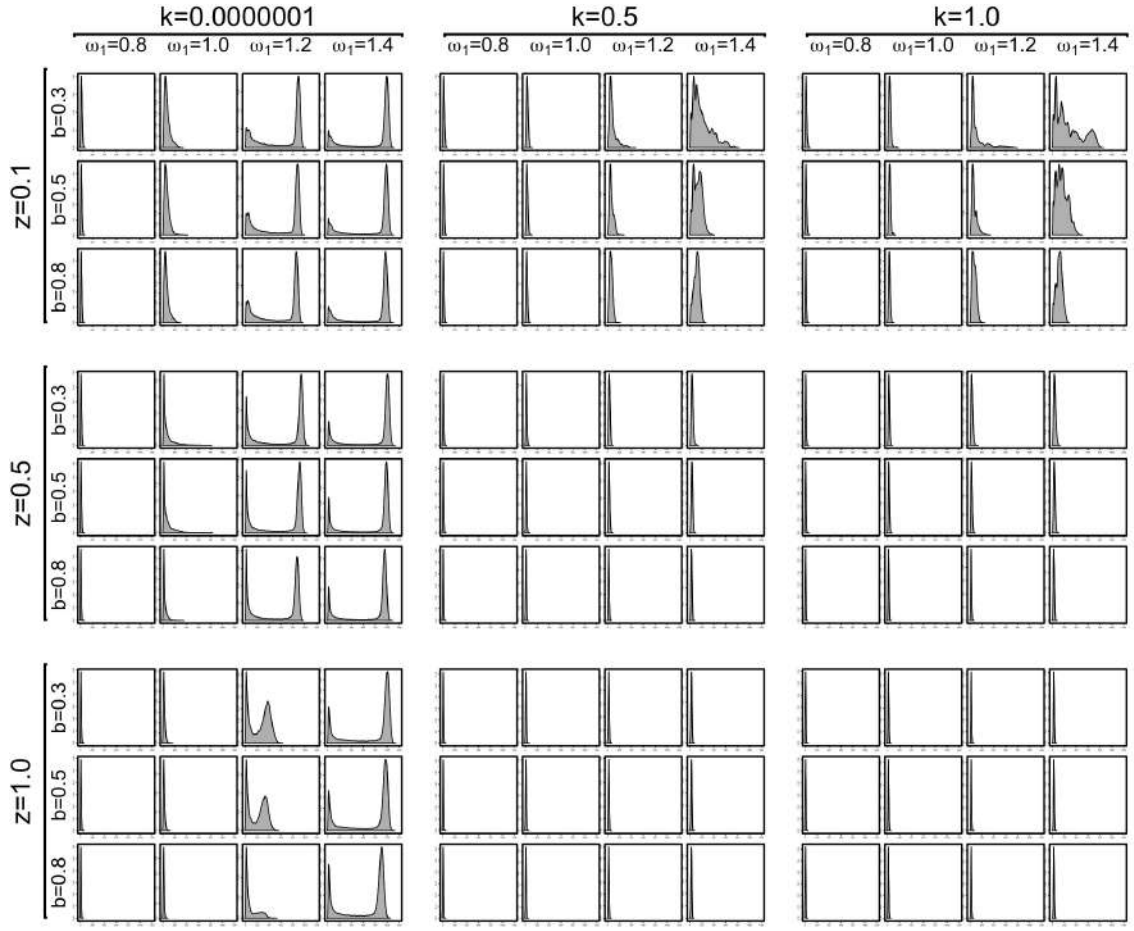

Probability density of N [predator-prey model, $\beta = 0.4$, $h = 1$; x-axis range from 0 to 1200]

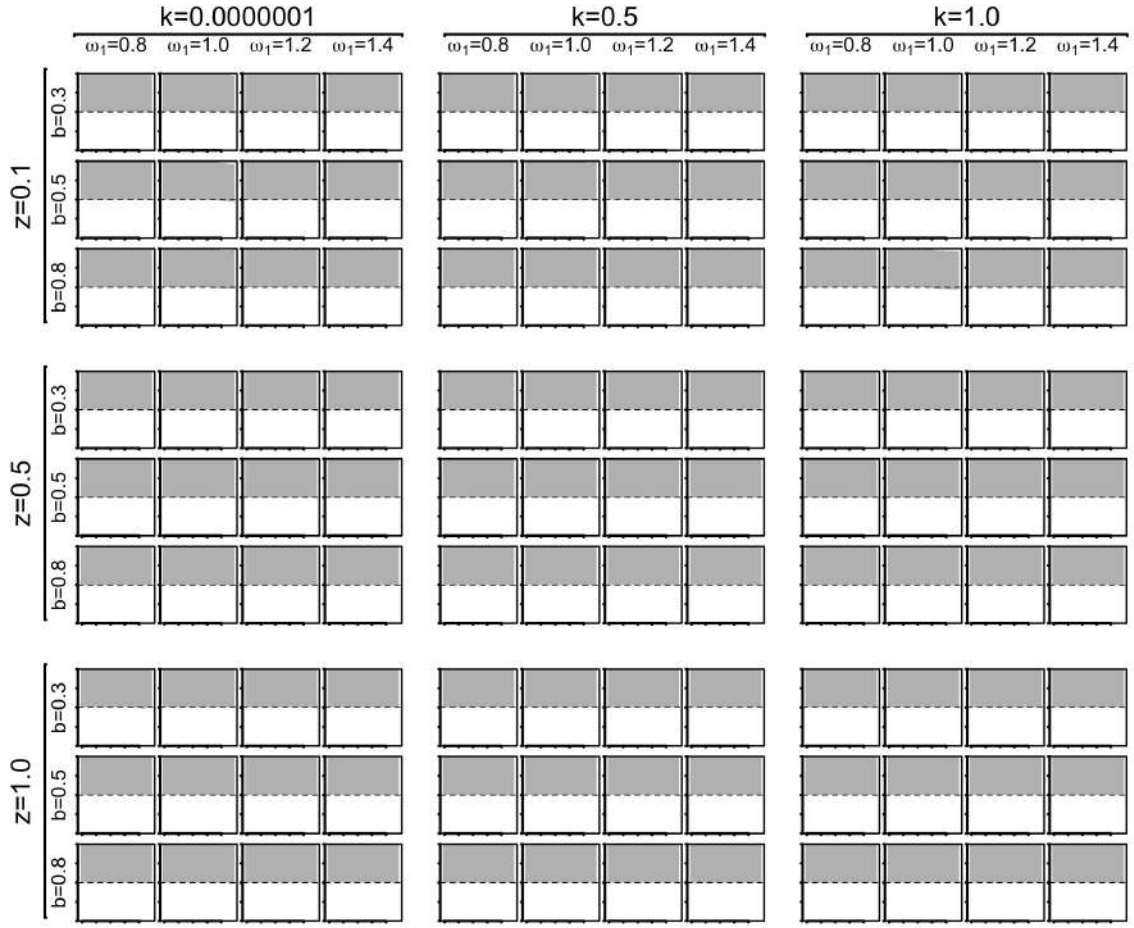

Correlogram of N [predator-prey model, $\beta = 0.3$, $h = 1$]

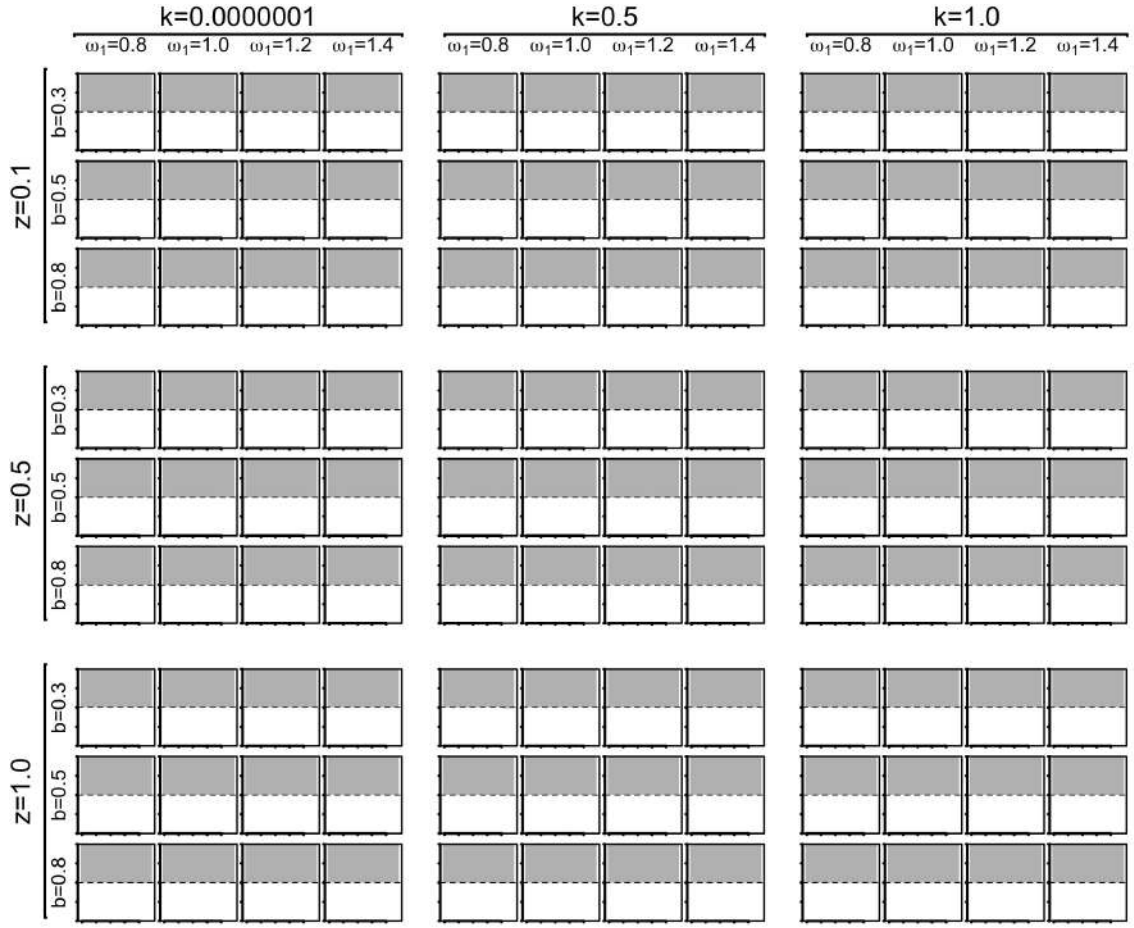

Correlogram of N [predator-prey model, $\beta = 0.35$, $h = 1$]

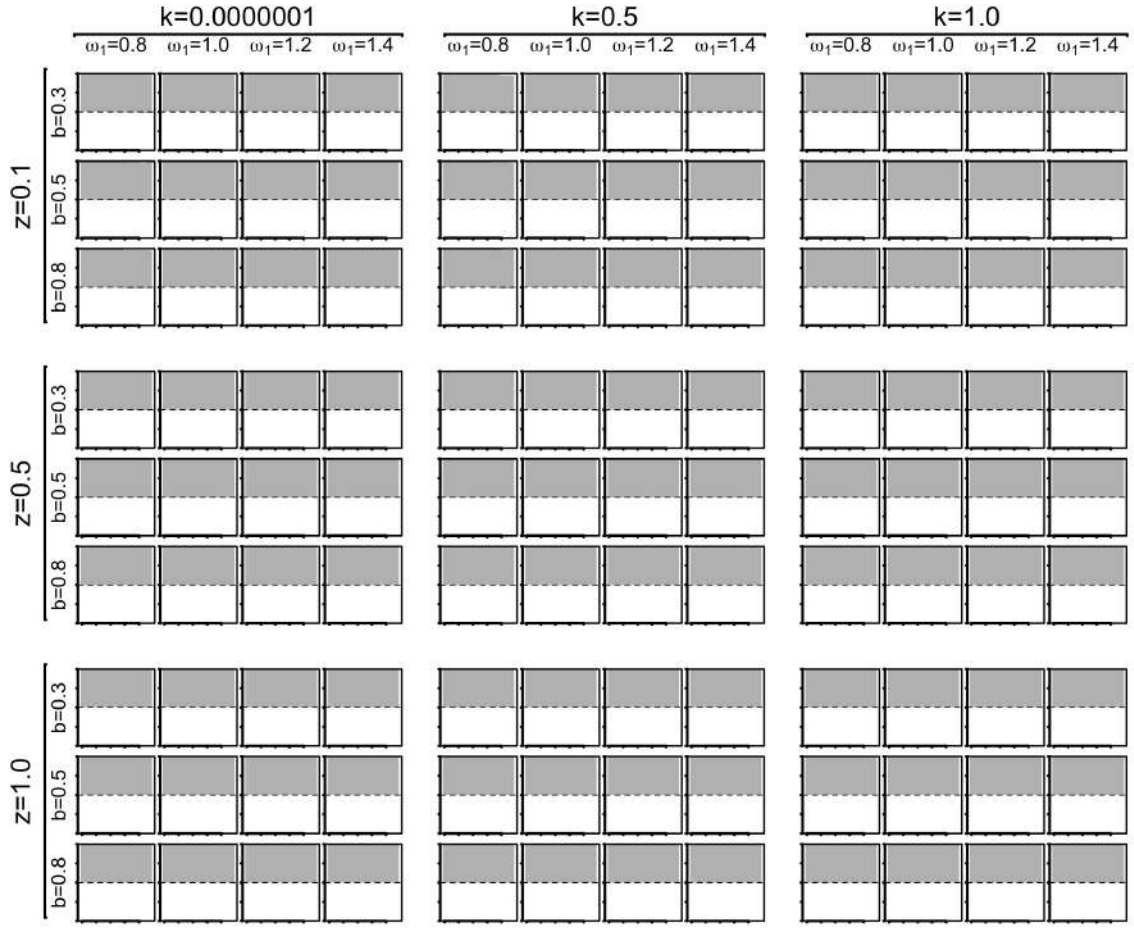

Correlogram of N [predator-prey model, $\beta = 0.4$, $h = 1$]

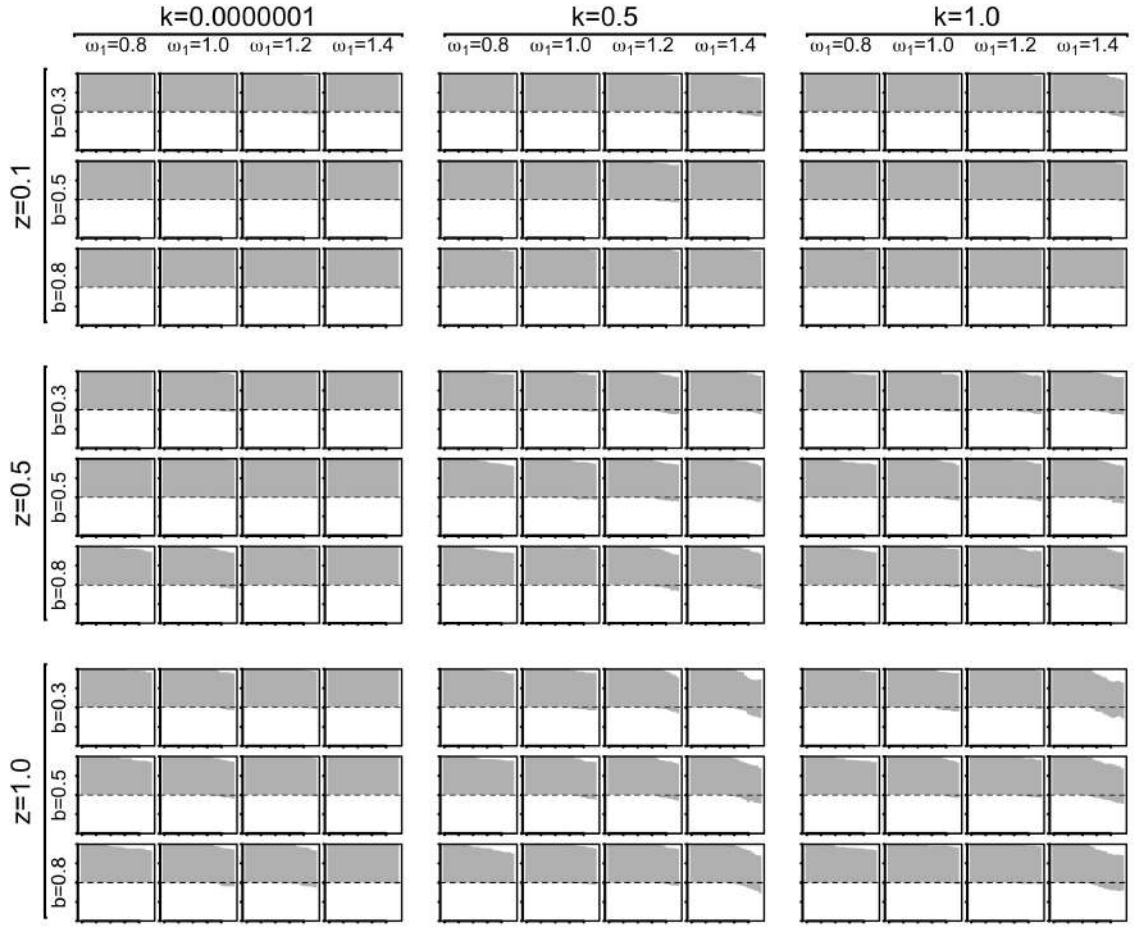

Correlogram of N [predator-prey model, $\beta = 0.3$, $h = \infty$]

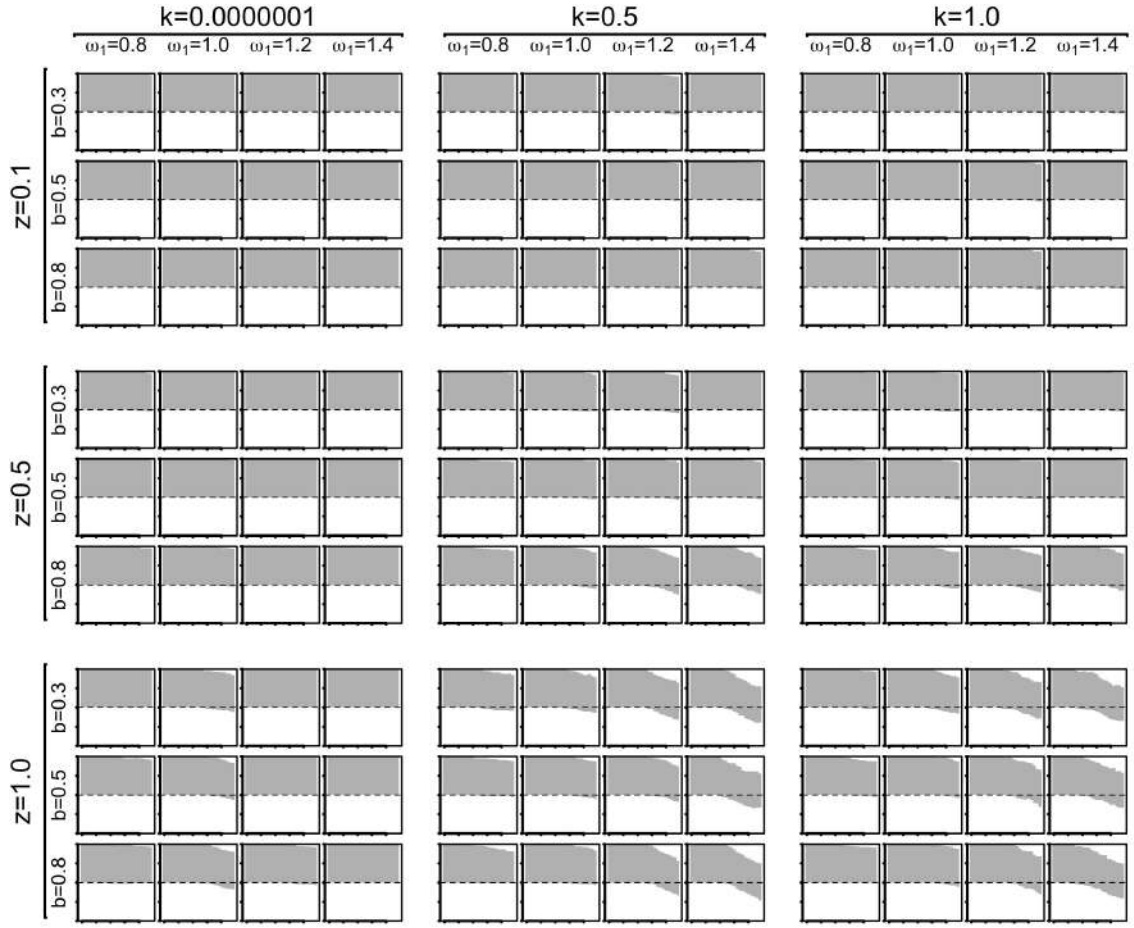

Correlogram of N [predator-prey model, $\beta = 0.35$, $h = \infty$]

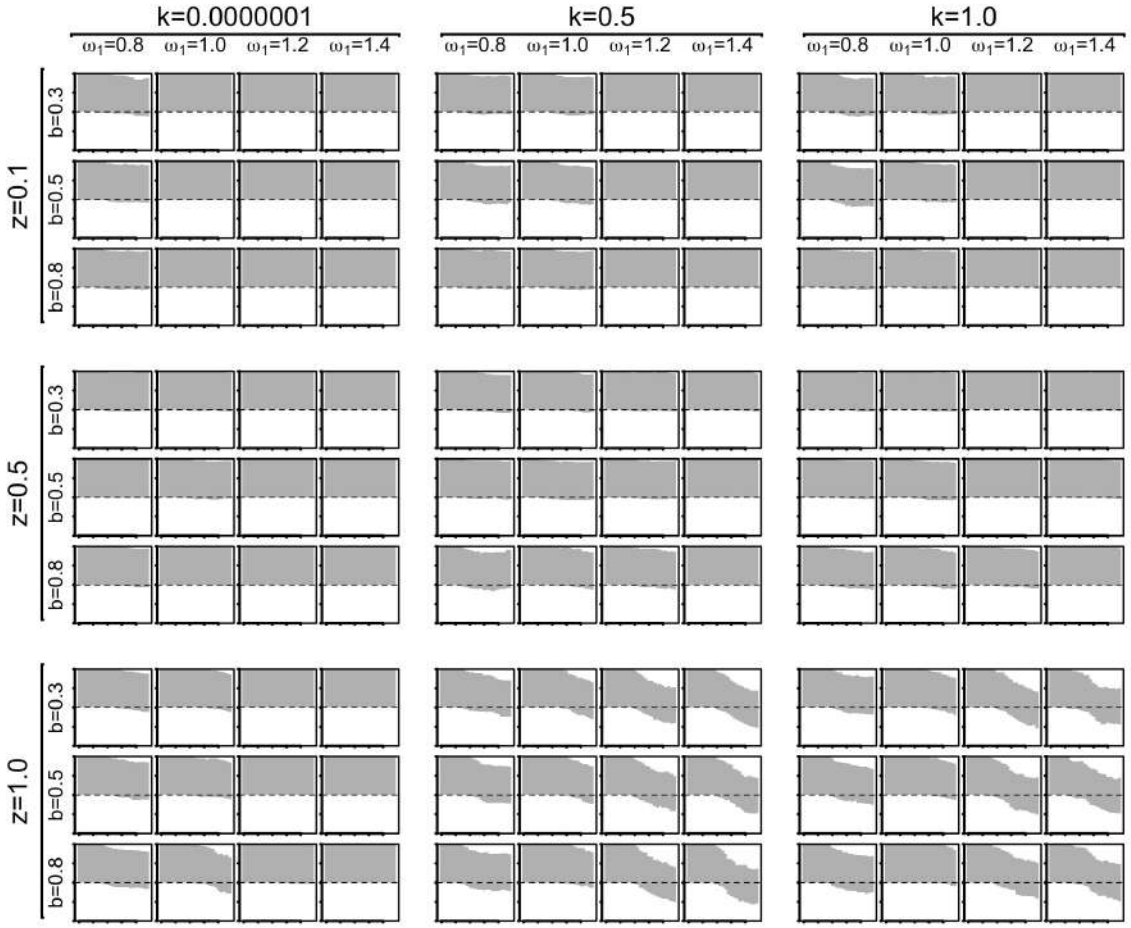

Correlogram of N [predator-prey model, $\beta = 0.4$, $h = \infty$]

D.2.4 Median Group Size ($\tilde{\lambda}$)

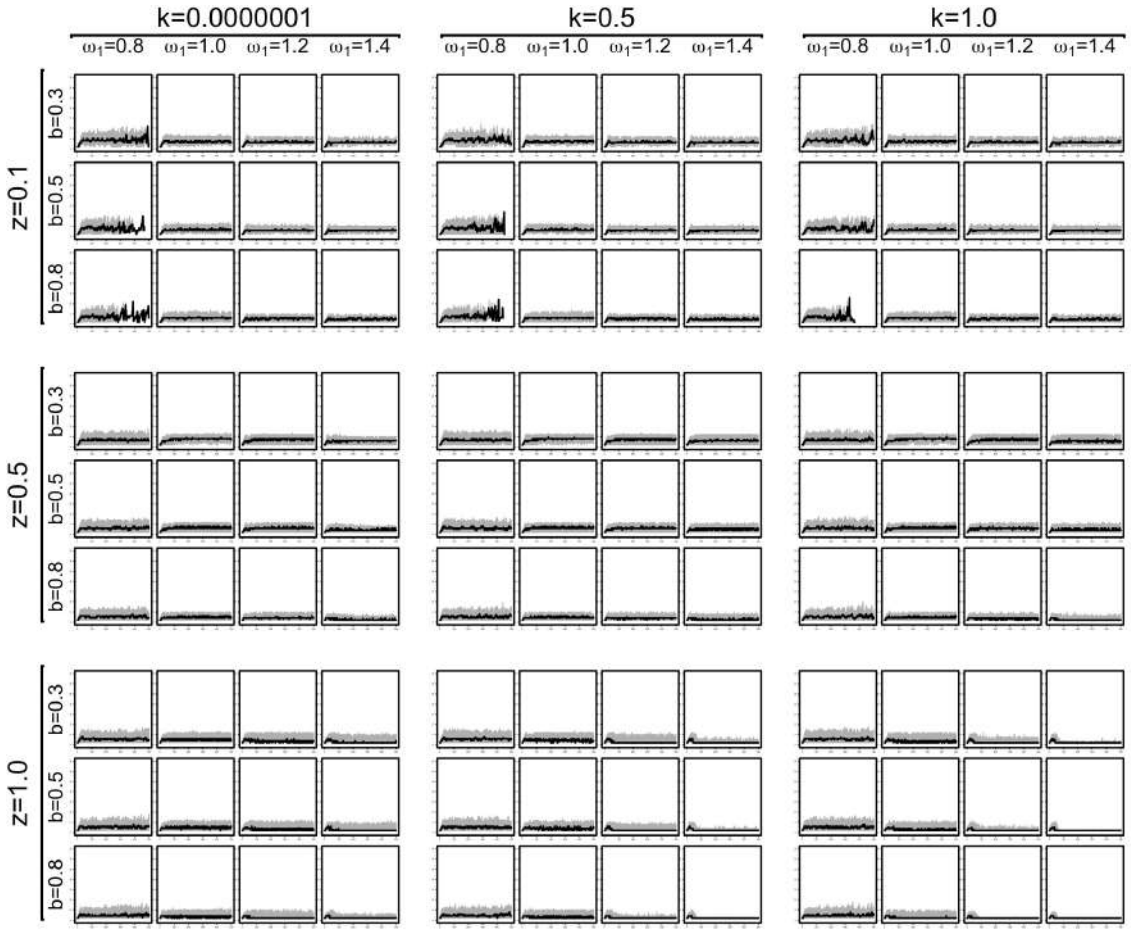

Combined time-series of $\tilde{\lambda}$ [predator-prey model, $\beta = 0.3$, $h = 1$]

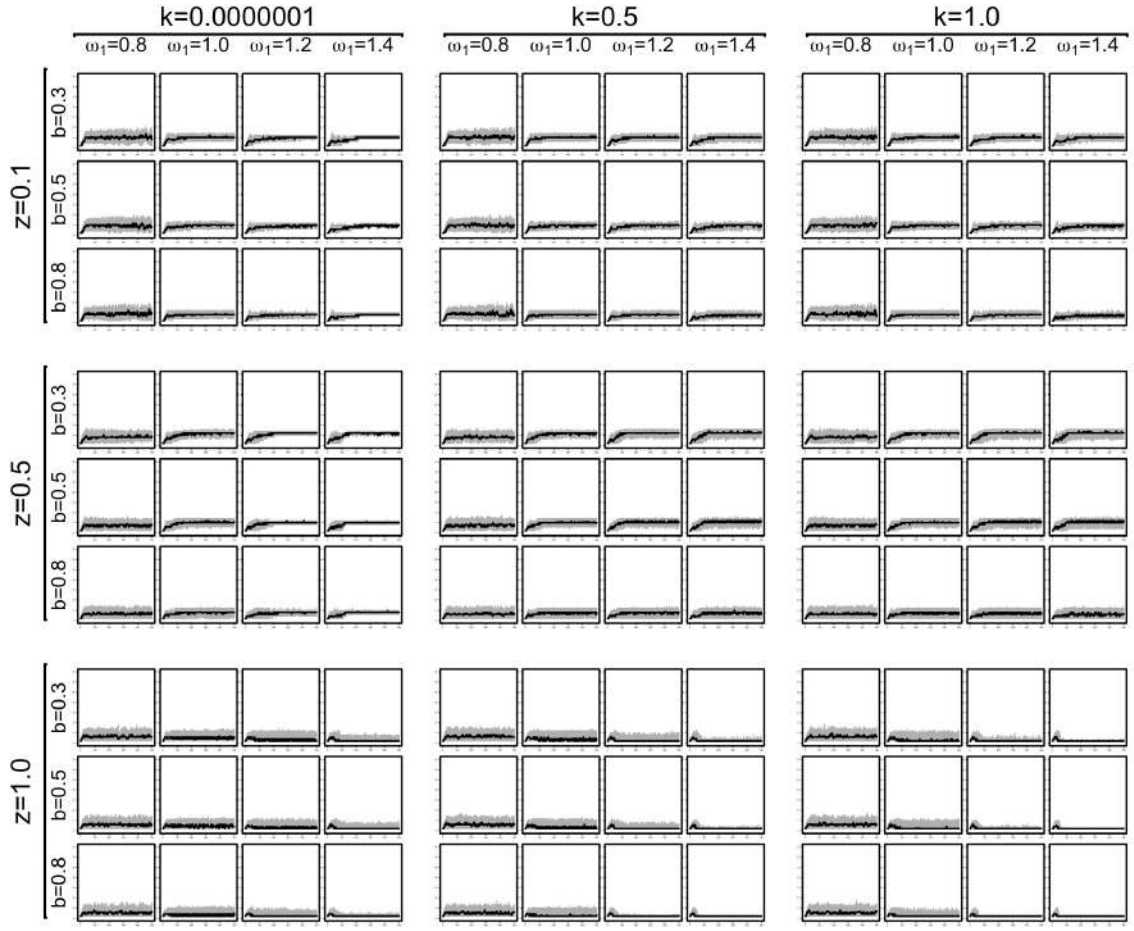

Combined time-series of $\tilde{\lambda}$ [predator-prey model, $\beta = 0.35$, $h = 1$]

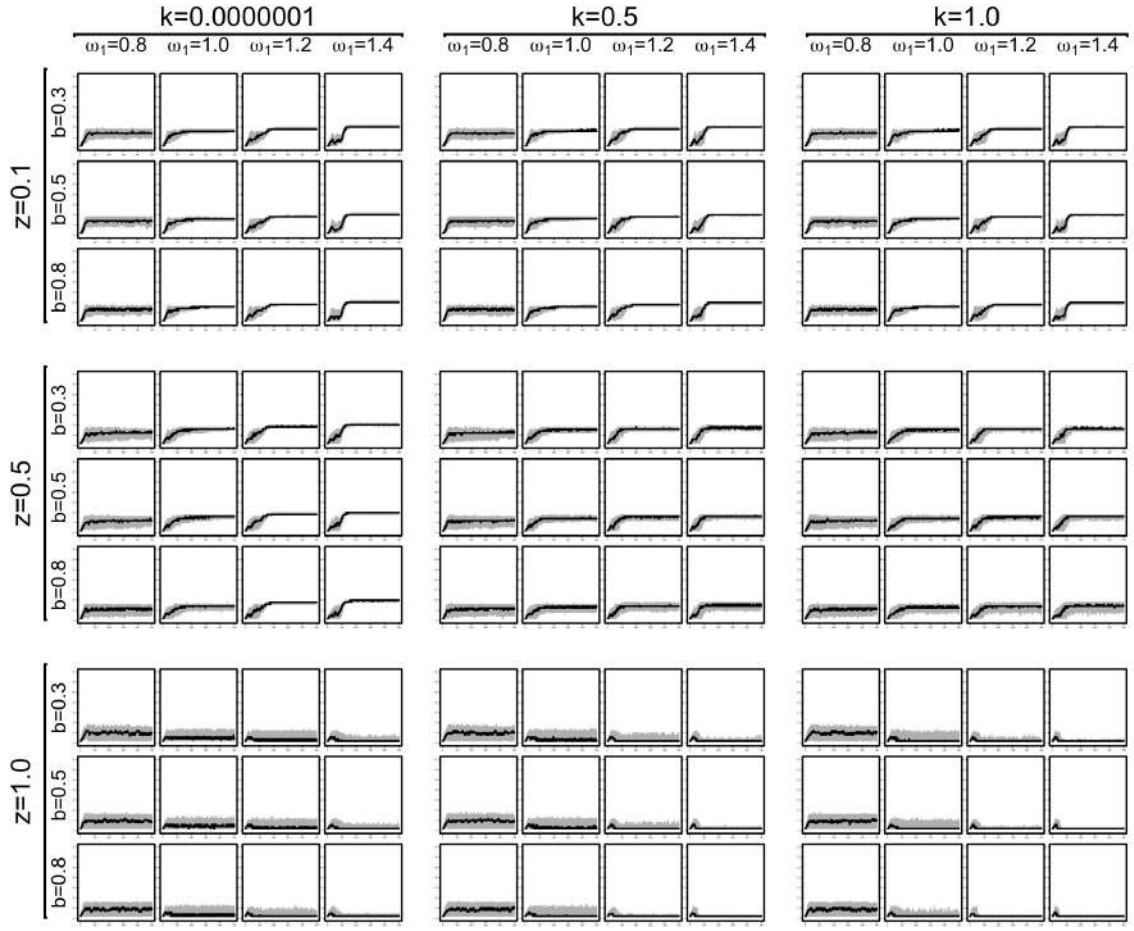

Combined time-series of $\tilde{\lambda}$ [predator-prey model, $\beta = 0.4$, $h = 1$]

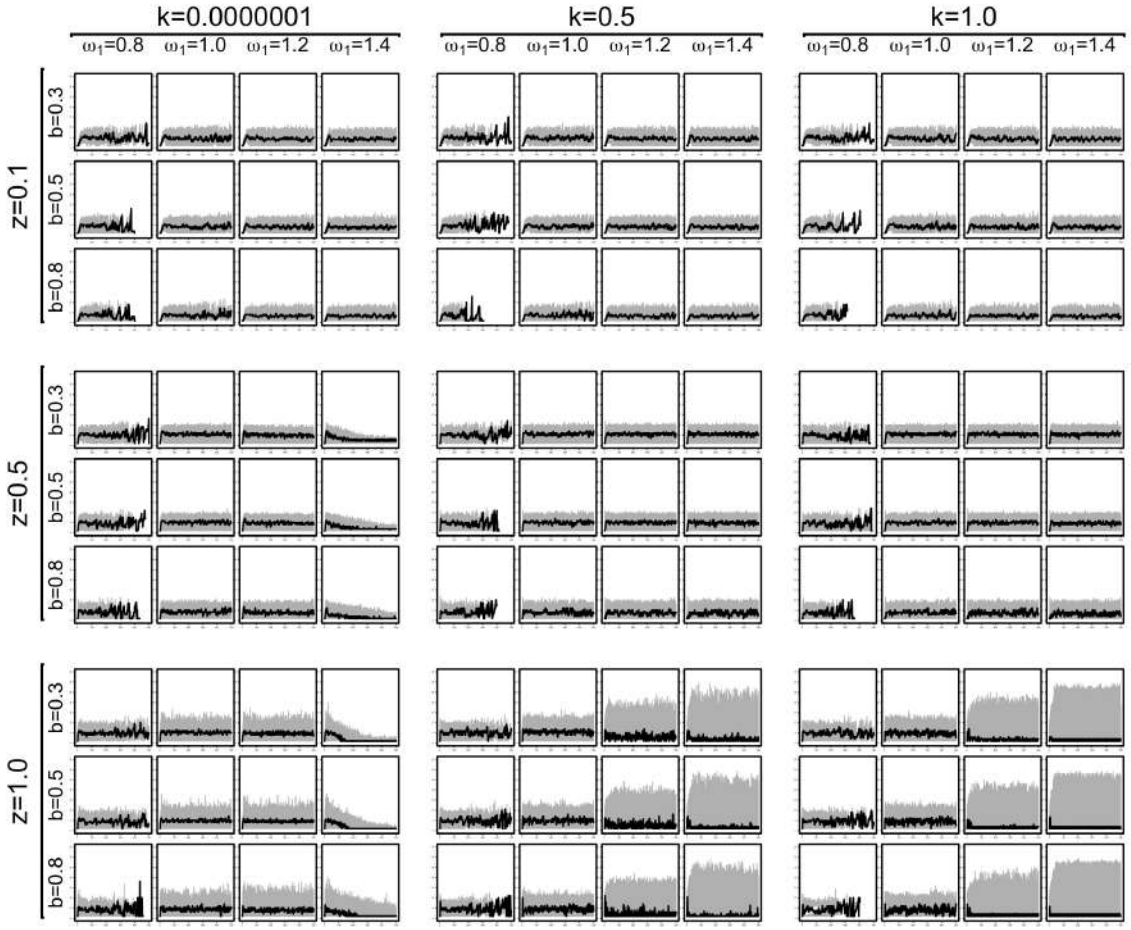

Combined time-series of $\tilde{\lambda}$ [predator-prey model, $\beta = 0.3$, $h = \infty$]

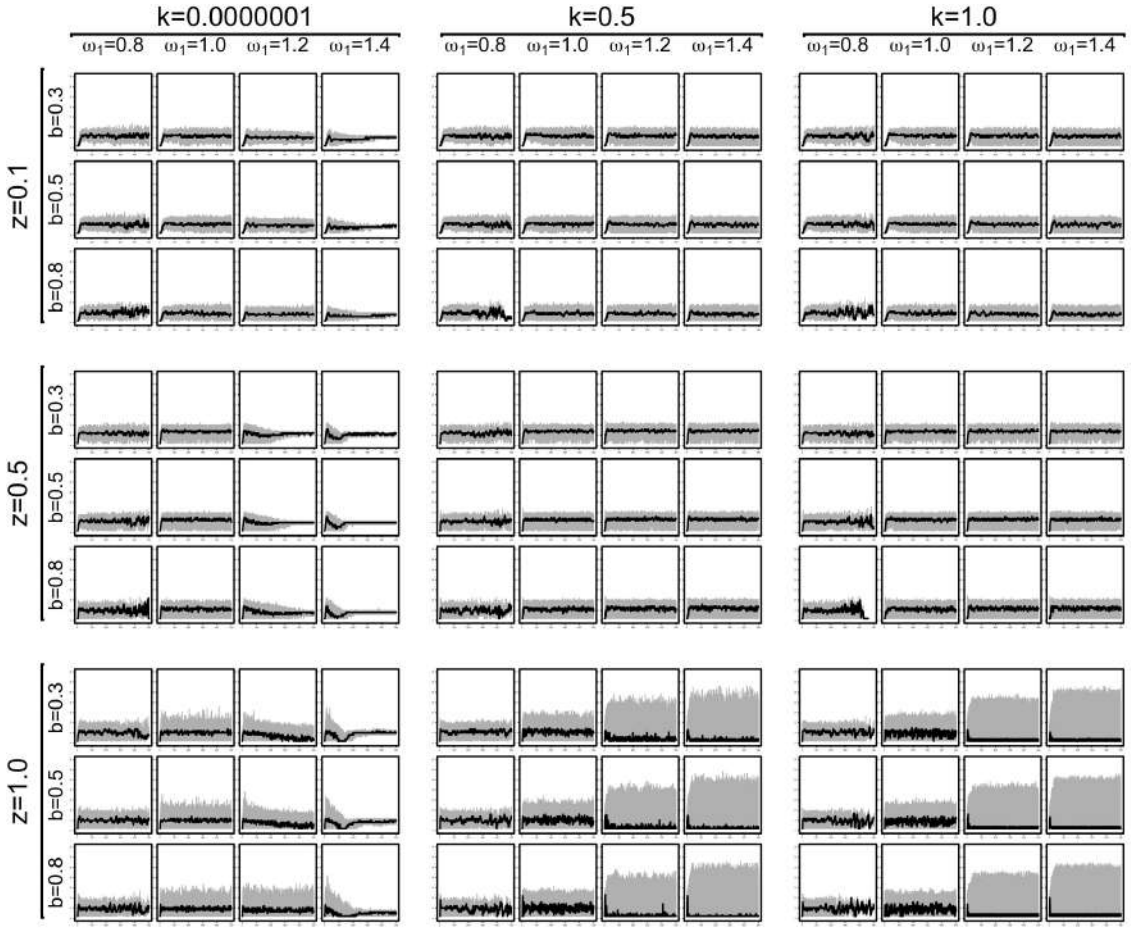

Combined time-series of $\tilde{\lambda}$ [predator-prey model, $\beta = 0.35$, $h = \infty$]

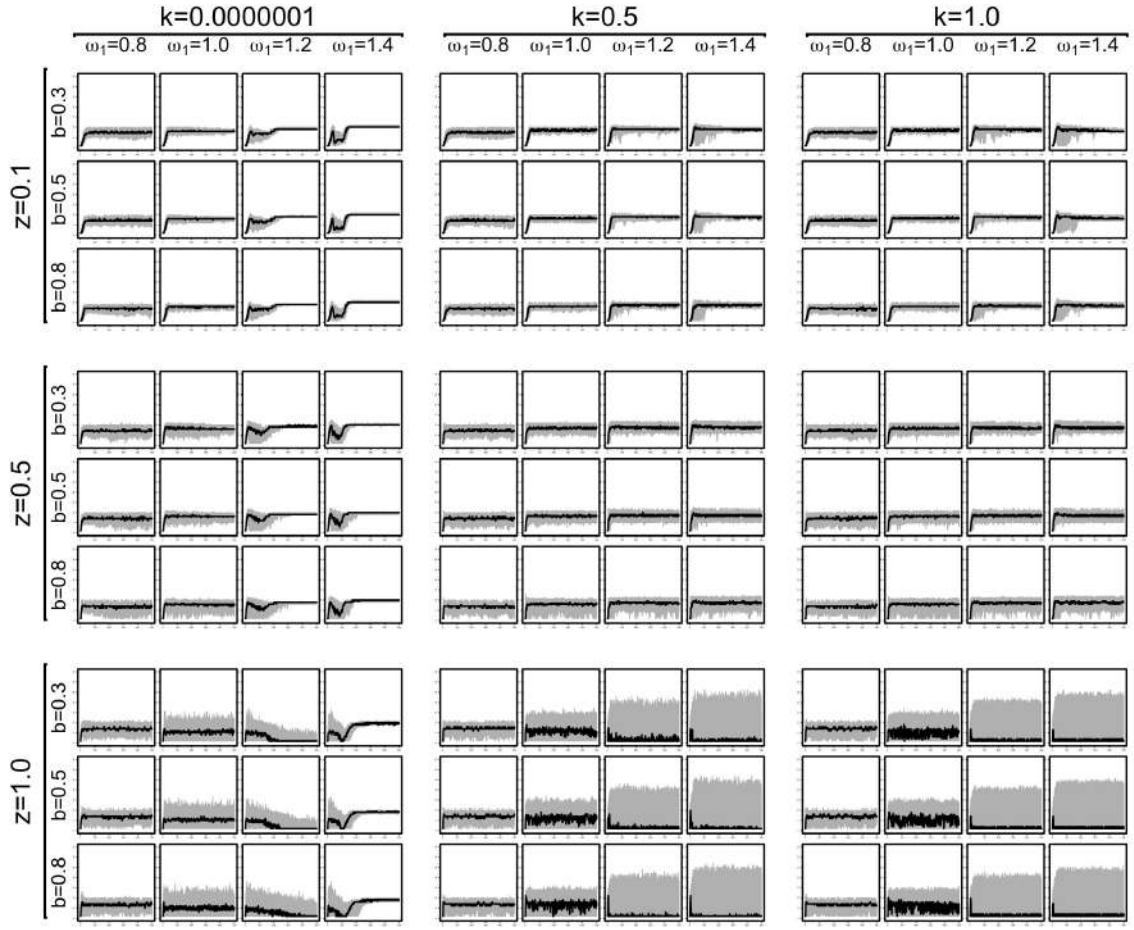

Combined time-series of $\tilde{\lambda}$ [predator-prey model, $\beta = 0.4$, $h = \infty$]

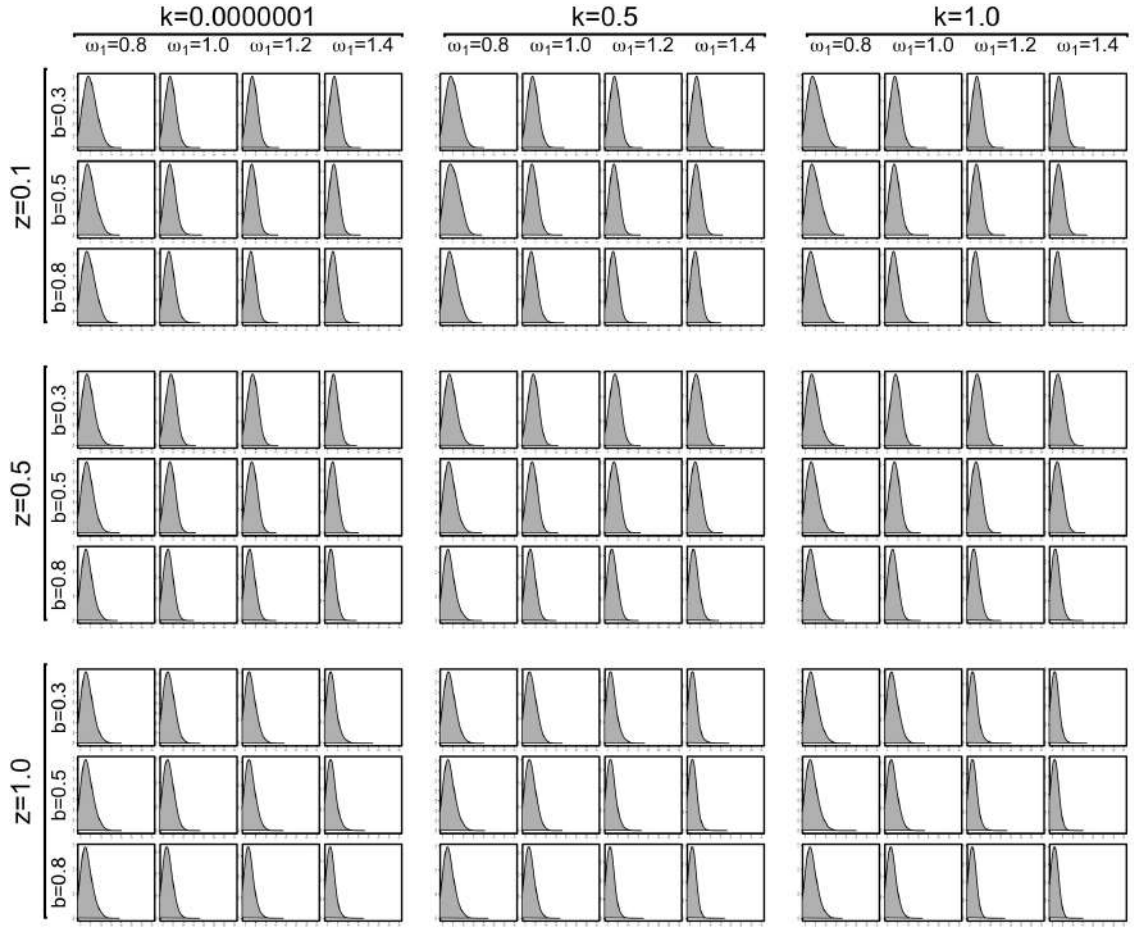

Probability density of $\tilde{\lambda}$ [predator-prey model, $\beta = 0.3$, $h = 1$]

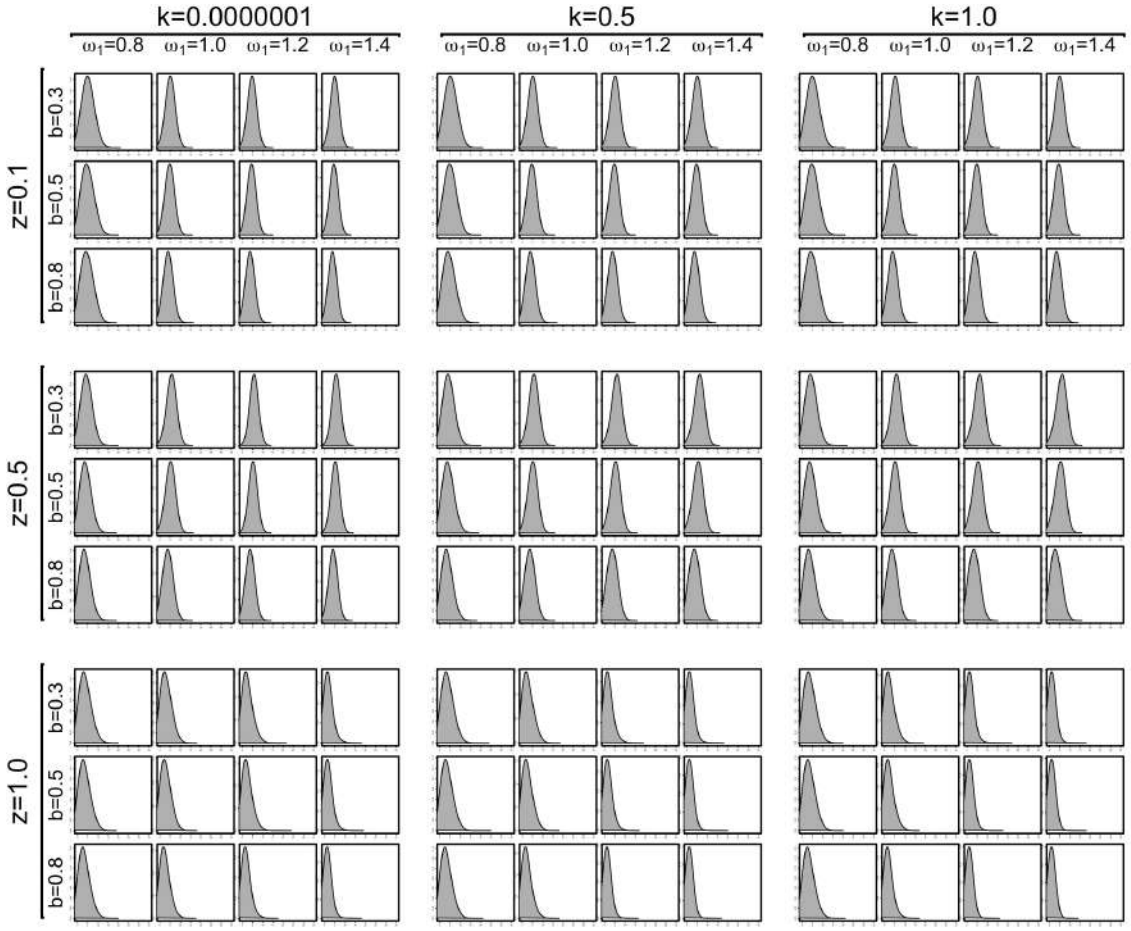

Probability density of $\tilde{\lambda}$ [predator-prey model, $\beta = 0.35$, $h = 1$]

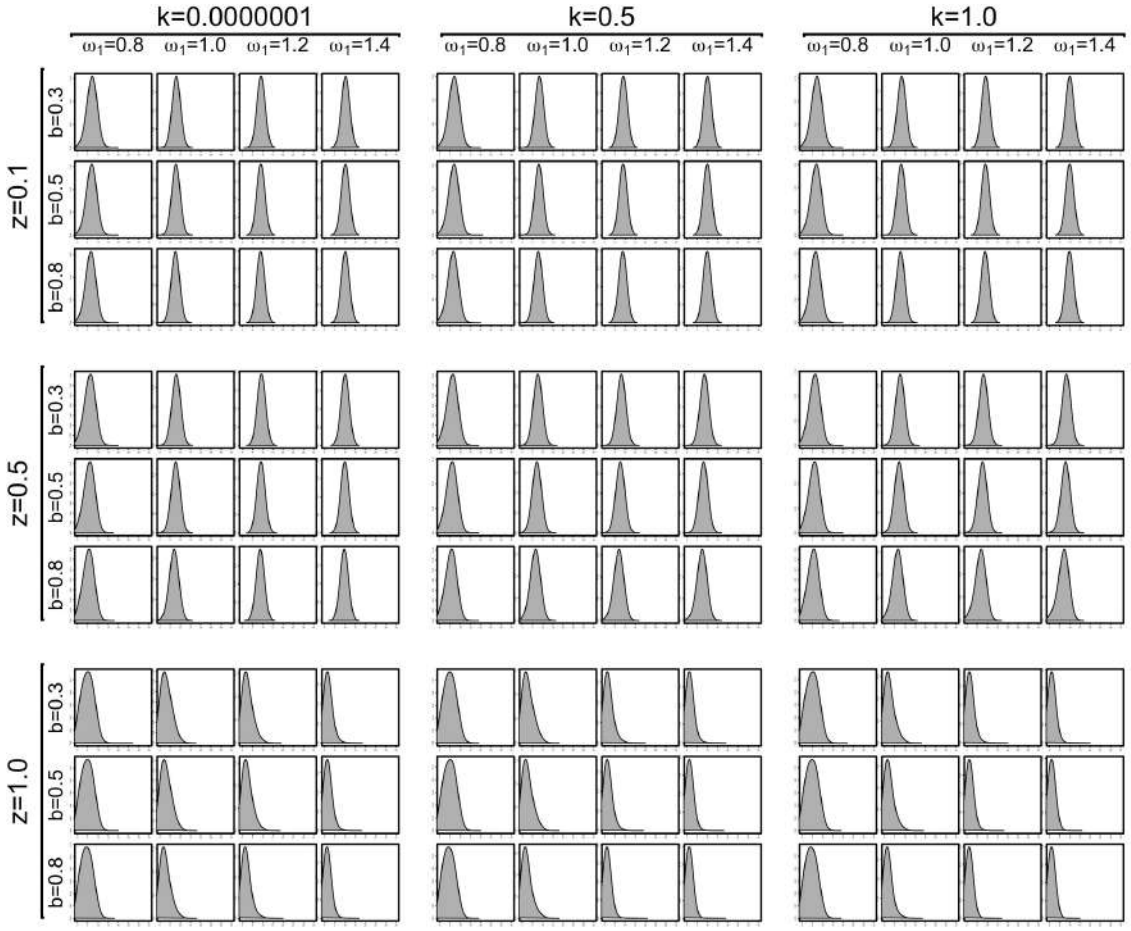

Probability density of $\tilde{\lambda}$ [predator-prey model, $\beta = 0.4$, $h = 1$]

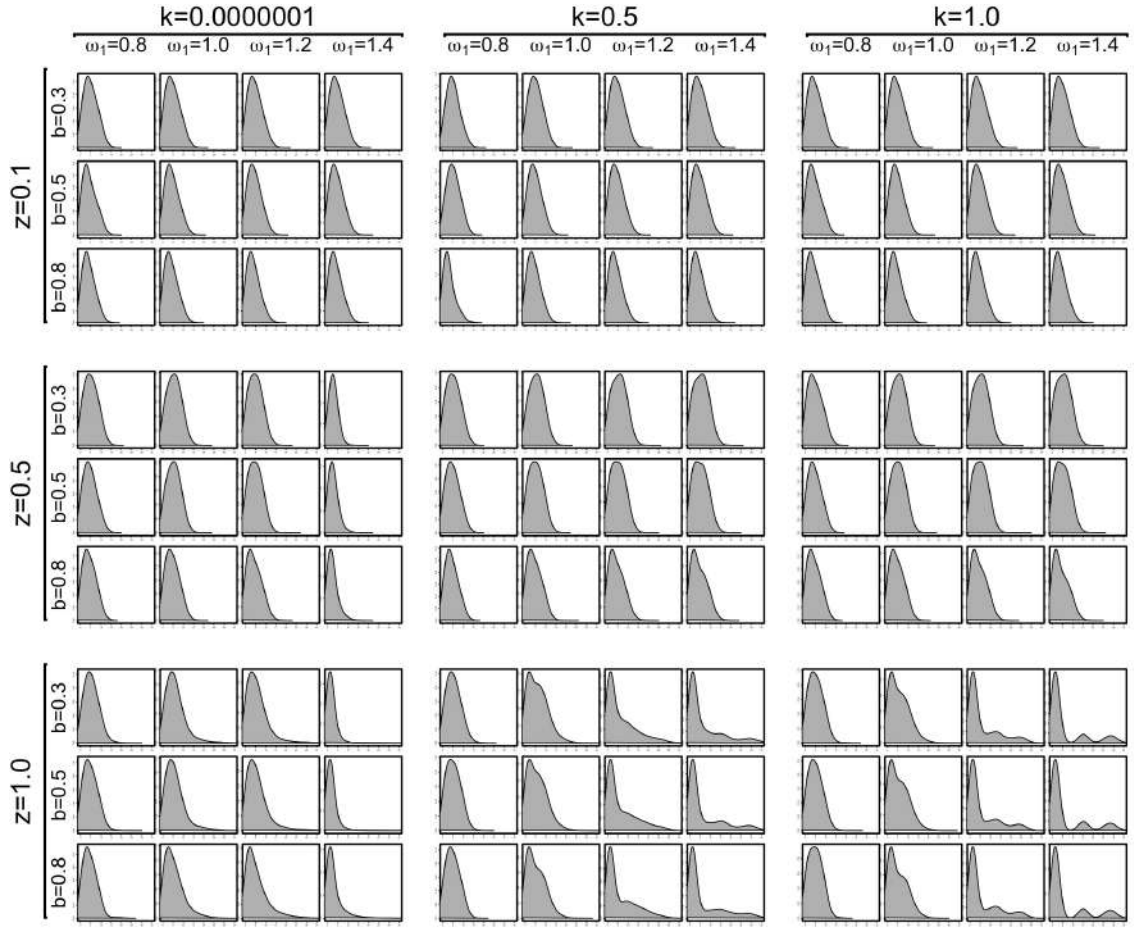

Probability density of $\tilde{\lambda}$ [predator-prey model, $\beta = 0.3$, $h = \infty$]

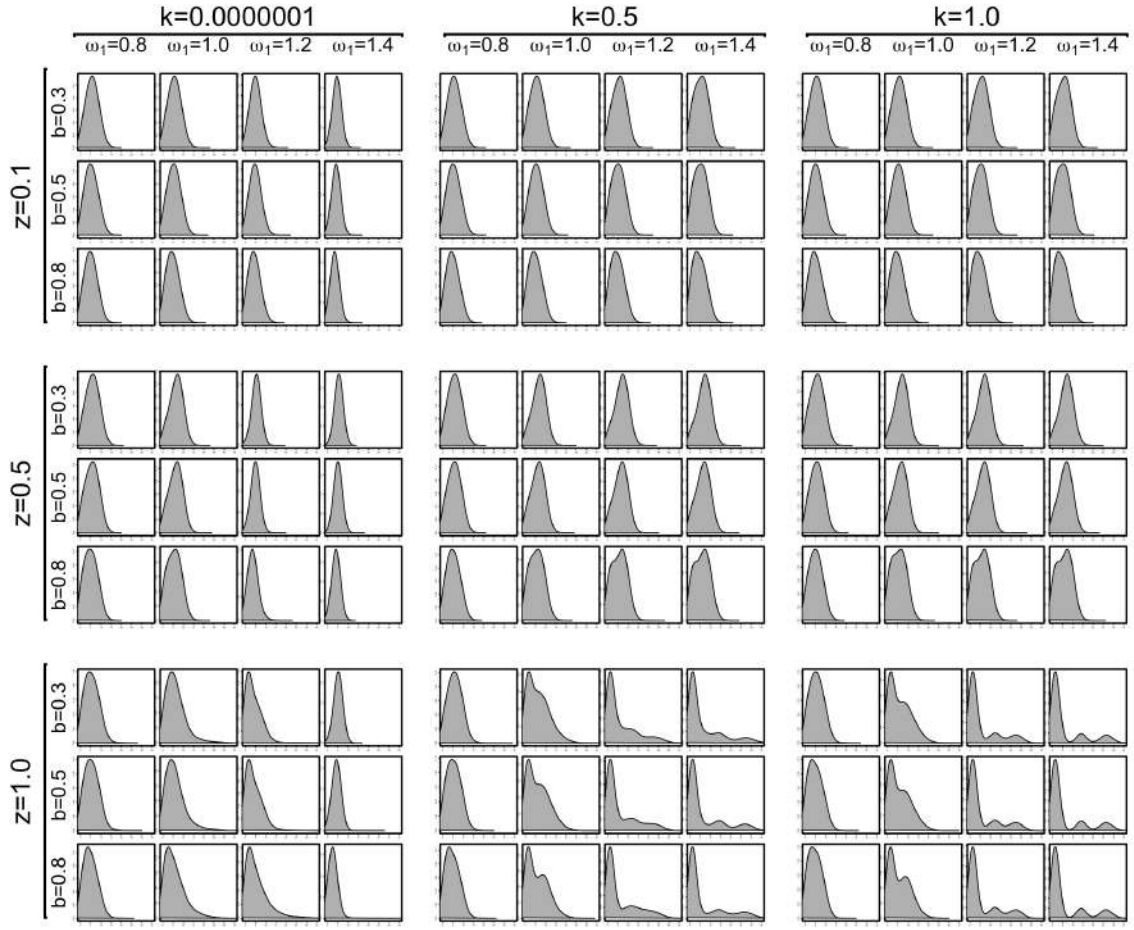

Probability density of $\tilde{\lambda}$ [predator-prey model, $\beta = 0.35$, $h = \infty$]

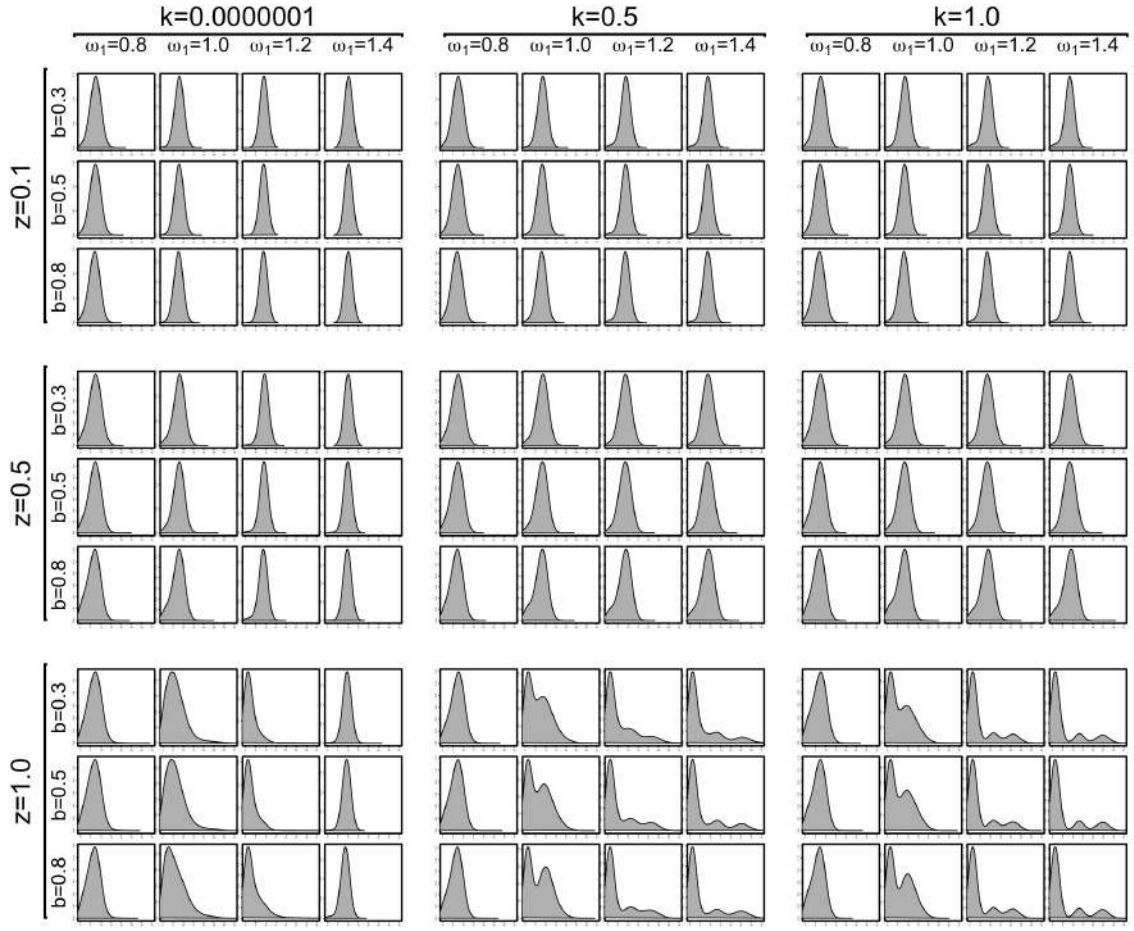

Probability density of $\tilde{\lambda}$ [predator-prey model, $\beta = 0.4$, $h = \infty$]

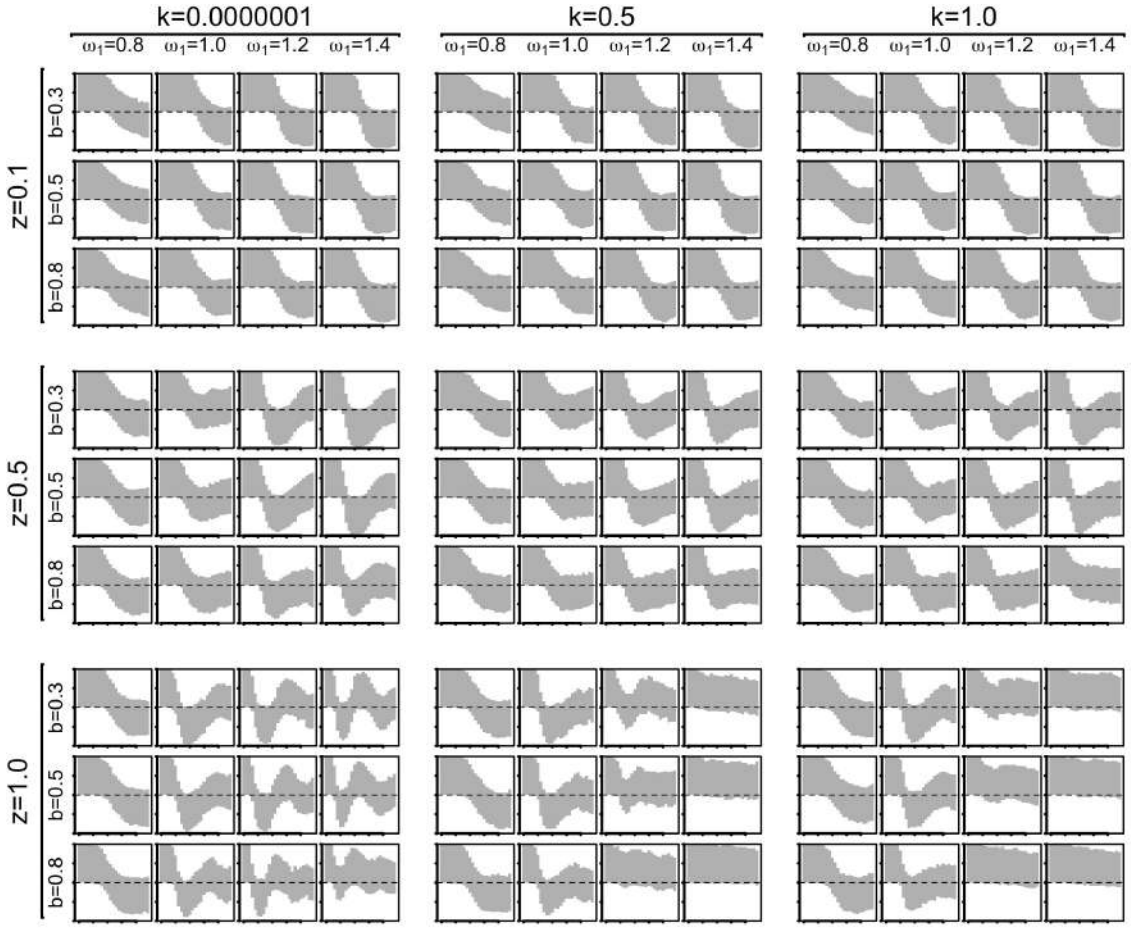

Correlogram of $\tilde{\lambda}$ [predator-prey model, $\beta = 0.3$, $h = 1$]

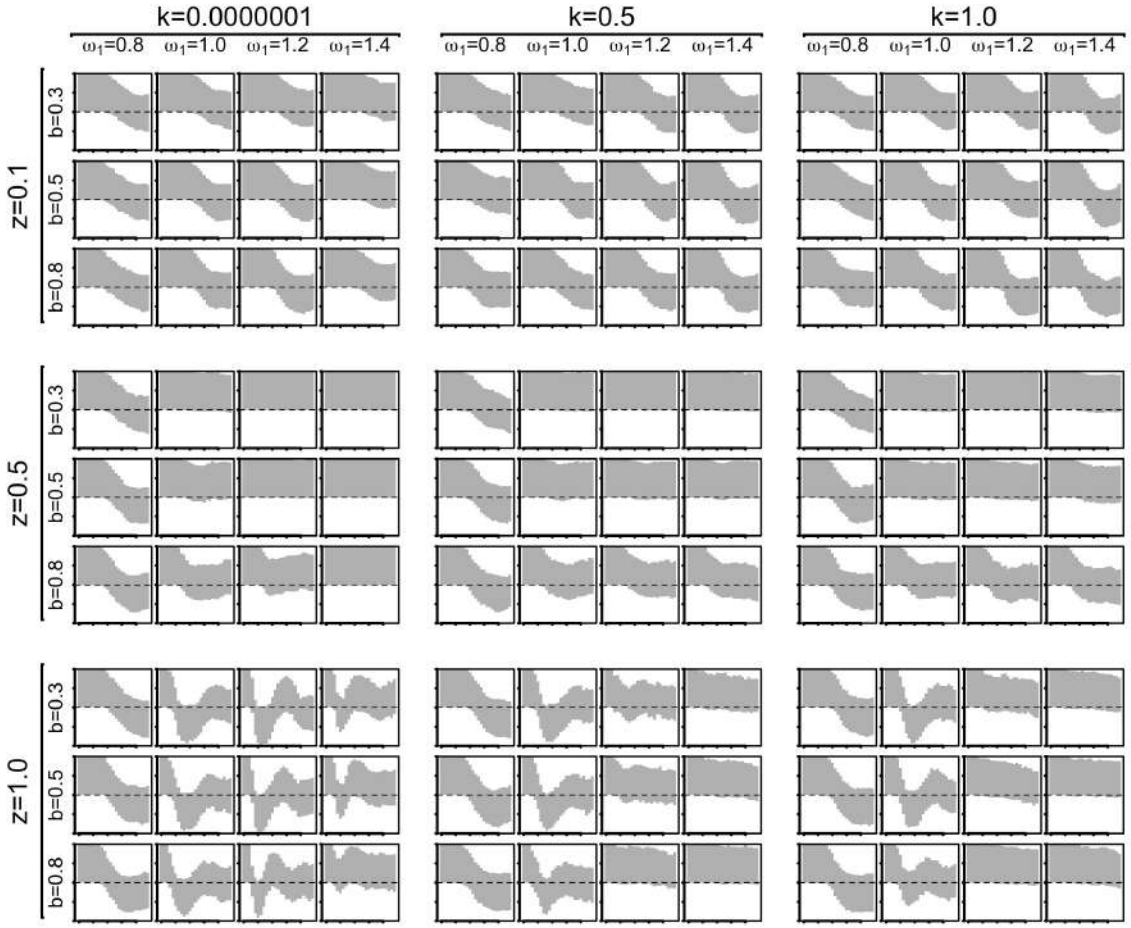

Correlogram of $\tilde{\lambda}$ [predator-prey model, $\beta = 0.35$, $h = 1$]

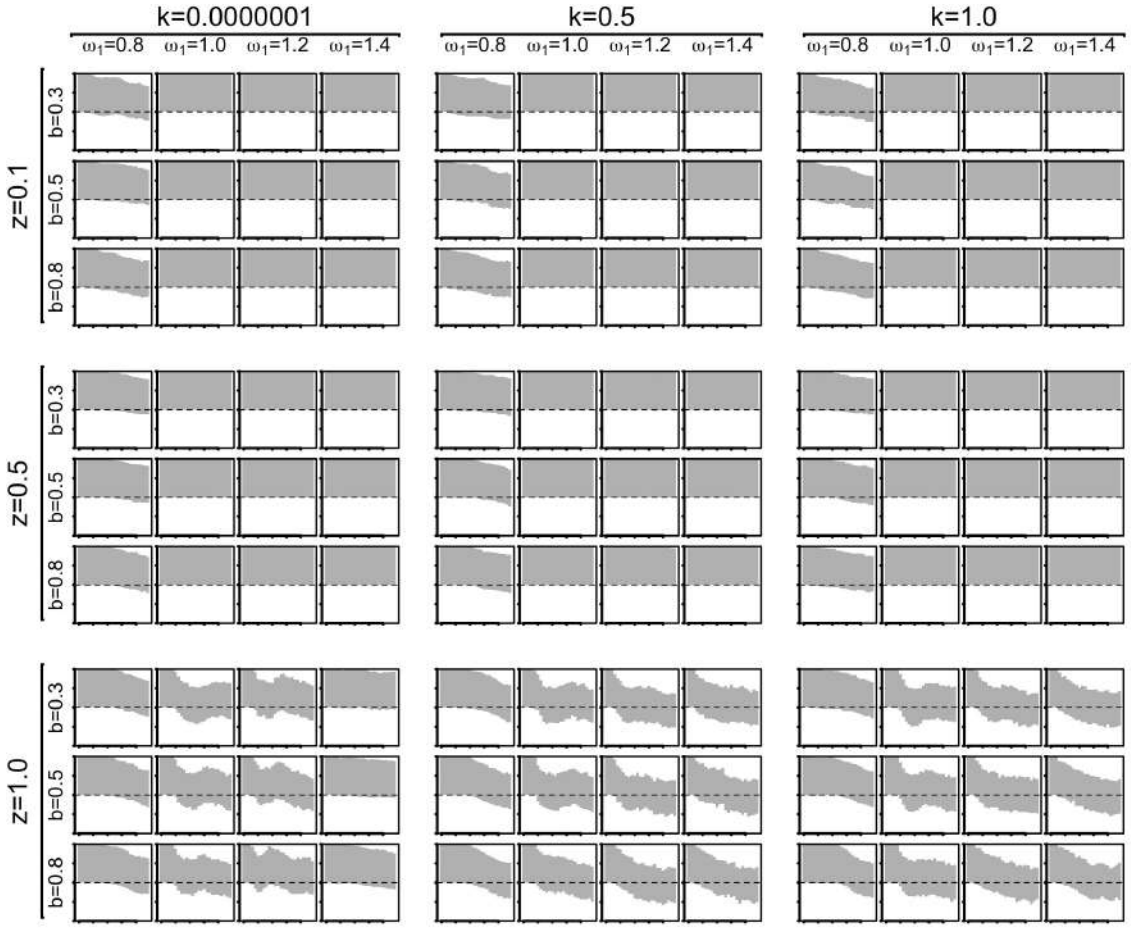

Correlogram of $\tilde{\lambda}$ [predator-prey model, $\beta = 0.4$, $h = 1$]

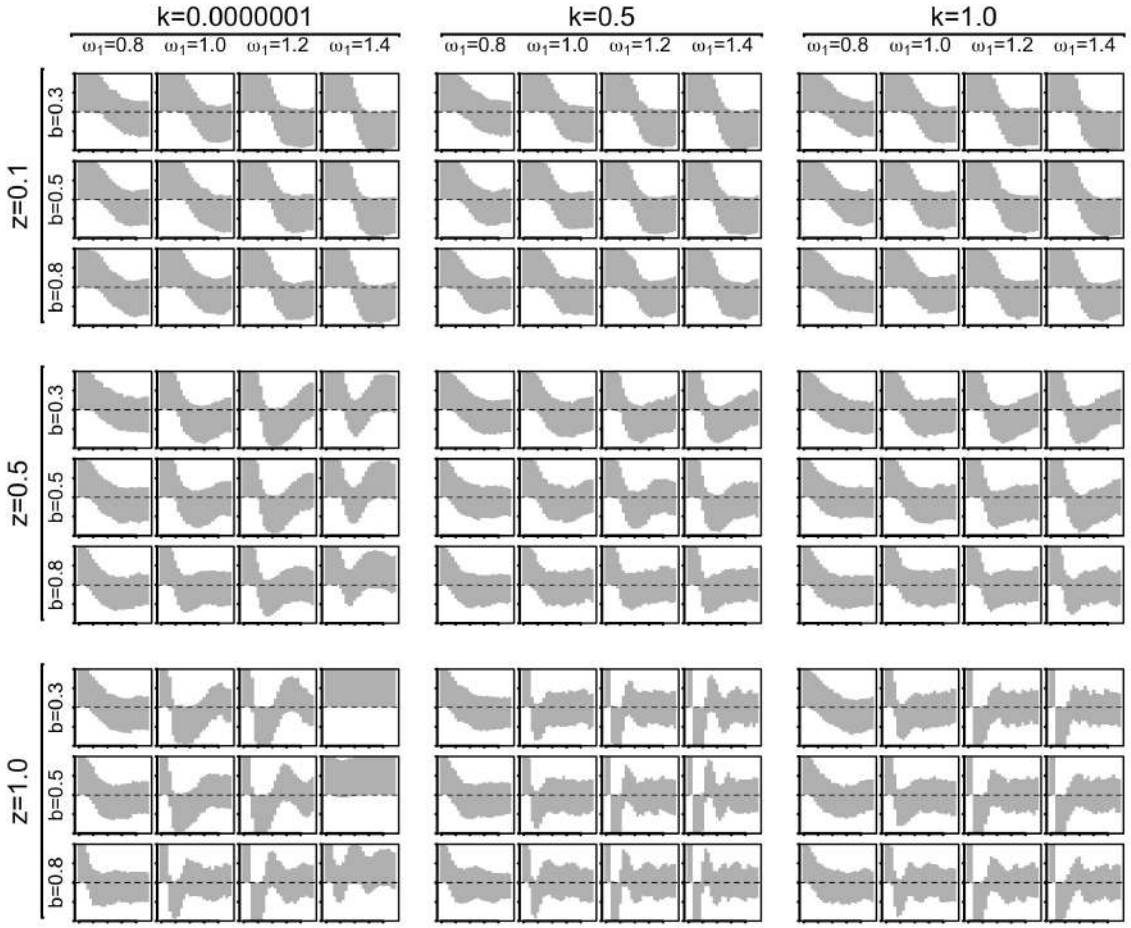

Correlogram of $\tilde{\lambda}$ [predator-prey model, $\beta = 0.3$, $h = \infty$]

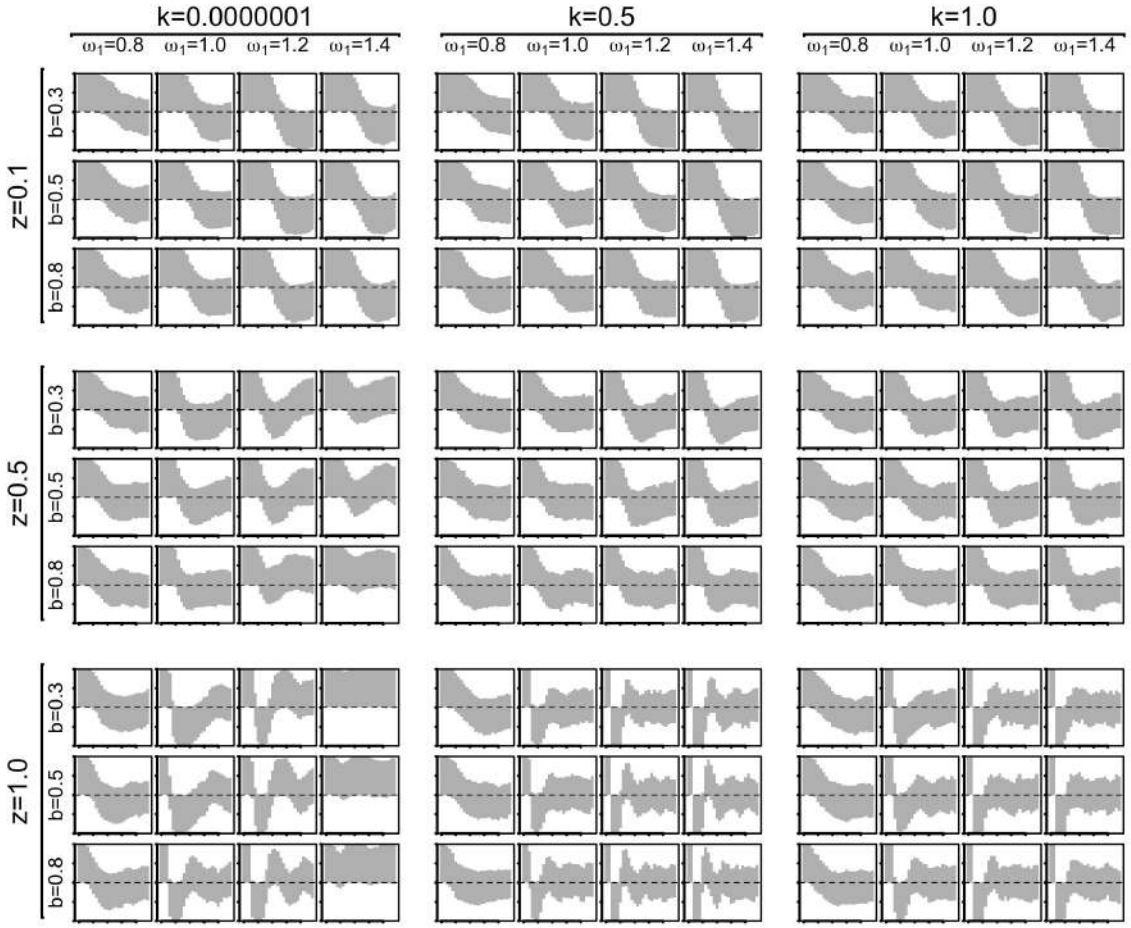

Correlogram of $\tilde{\lambda}$ [predator-prey model, $\beta = 0.35$, $h = \infty$]

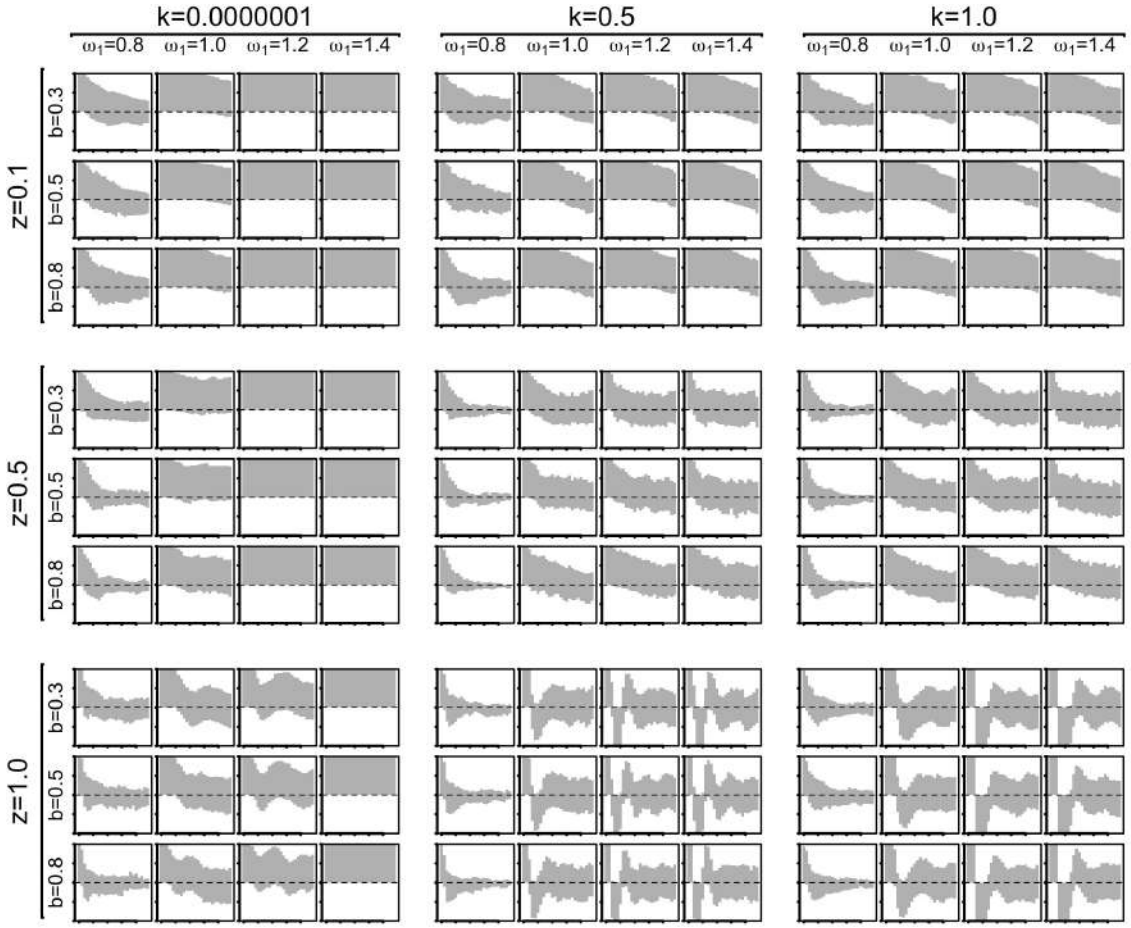

Correlogram of $\tilde{\lambda}$ [predator-prey model, $\beta = 0.4$, $h = \infty$]

D.3 Exogenic Disturbance Model

D.3.1 A-Coefficient (A)

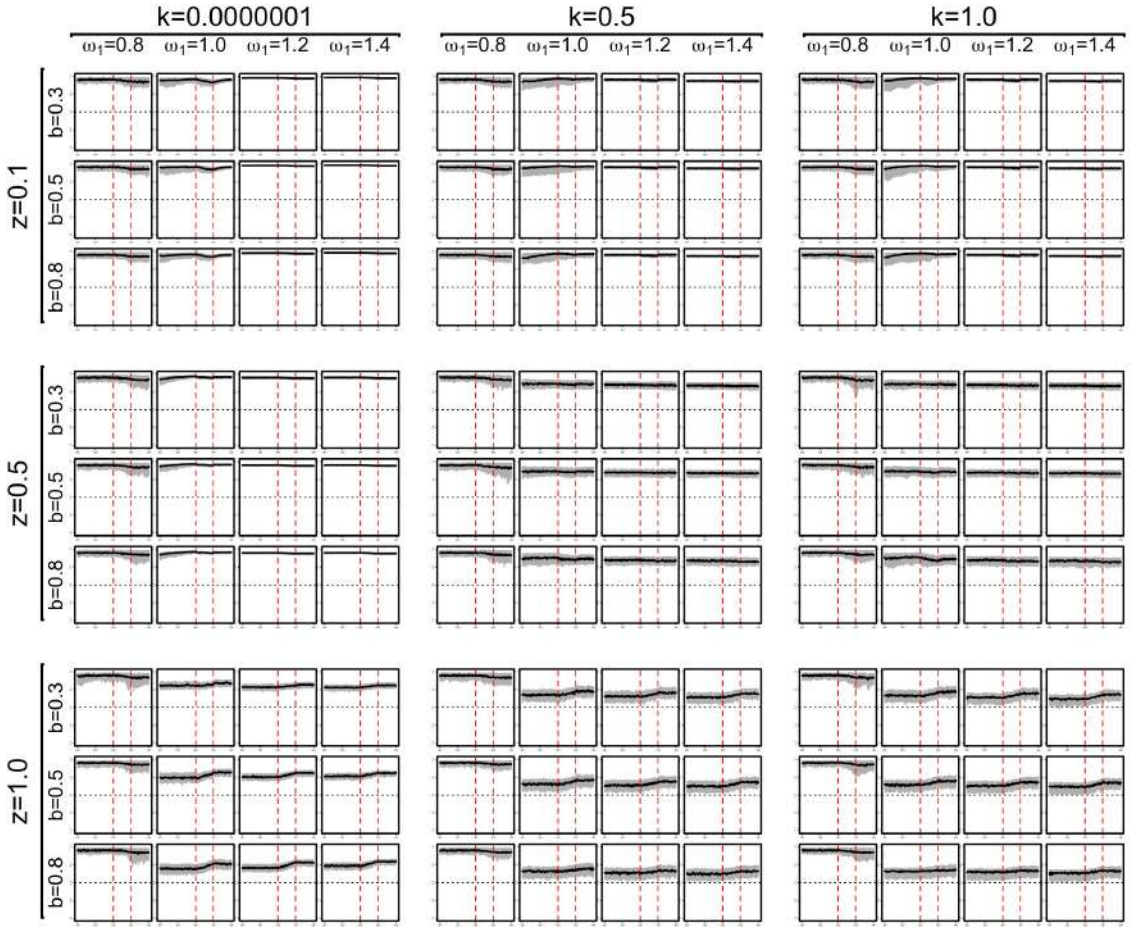

Combined time-series of A [disturbance model, $t_s = 301$, $t_e = 348$, $\eta = 2.08$, $h = 1$]

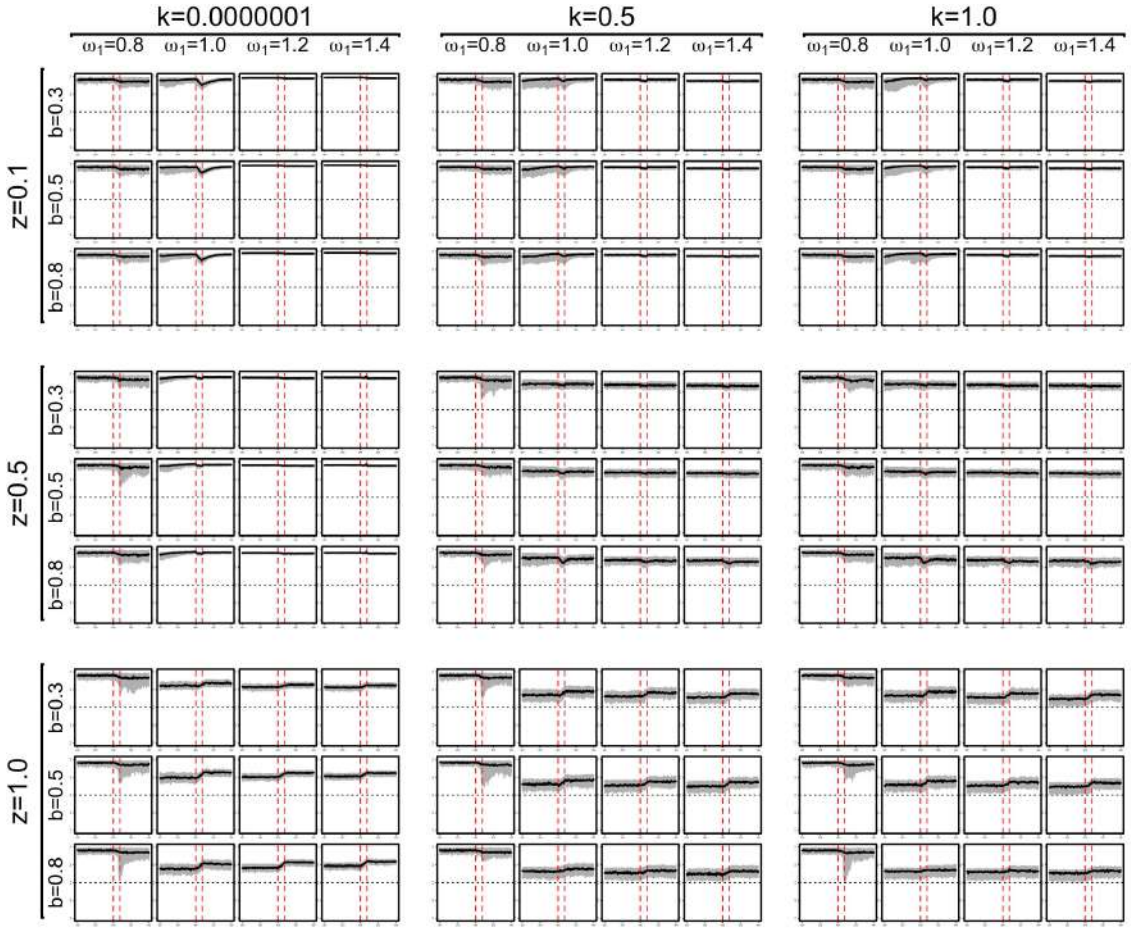

Combined time-series of A [disturbance model, $t_s = 301$, $t_e = 308$, $\eta = 5.56$, $h = 1$]

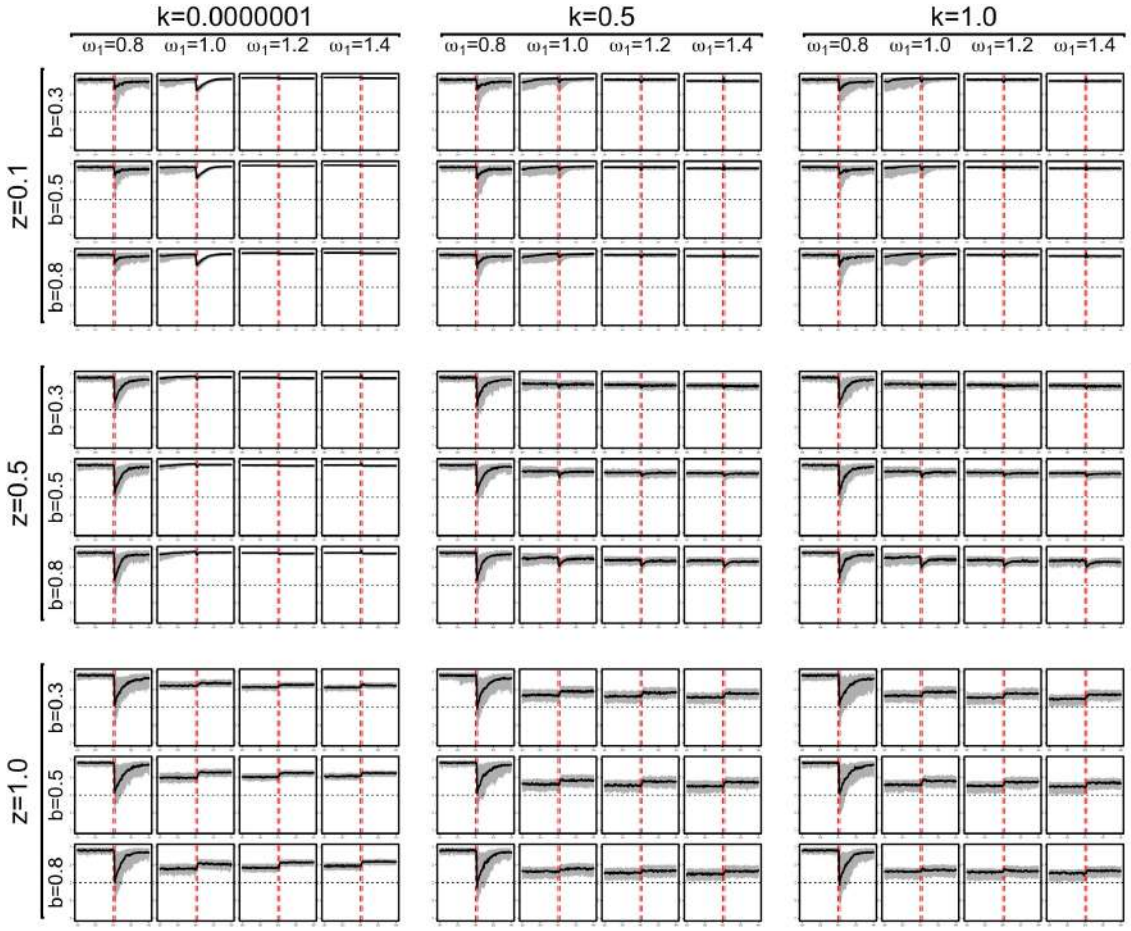

Combined time-series of A [disturbance model, $t_s = 301$, $t_e = 304$, $\eta = 25$, $h = 1$]

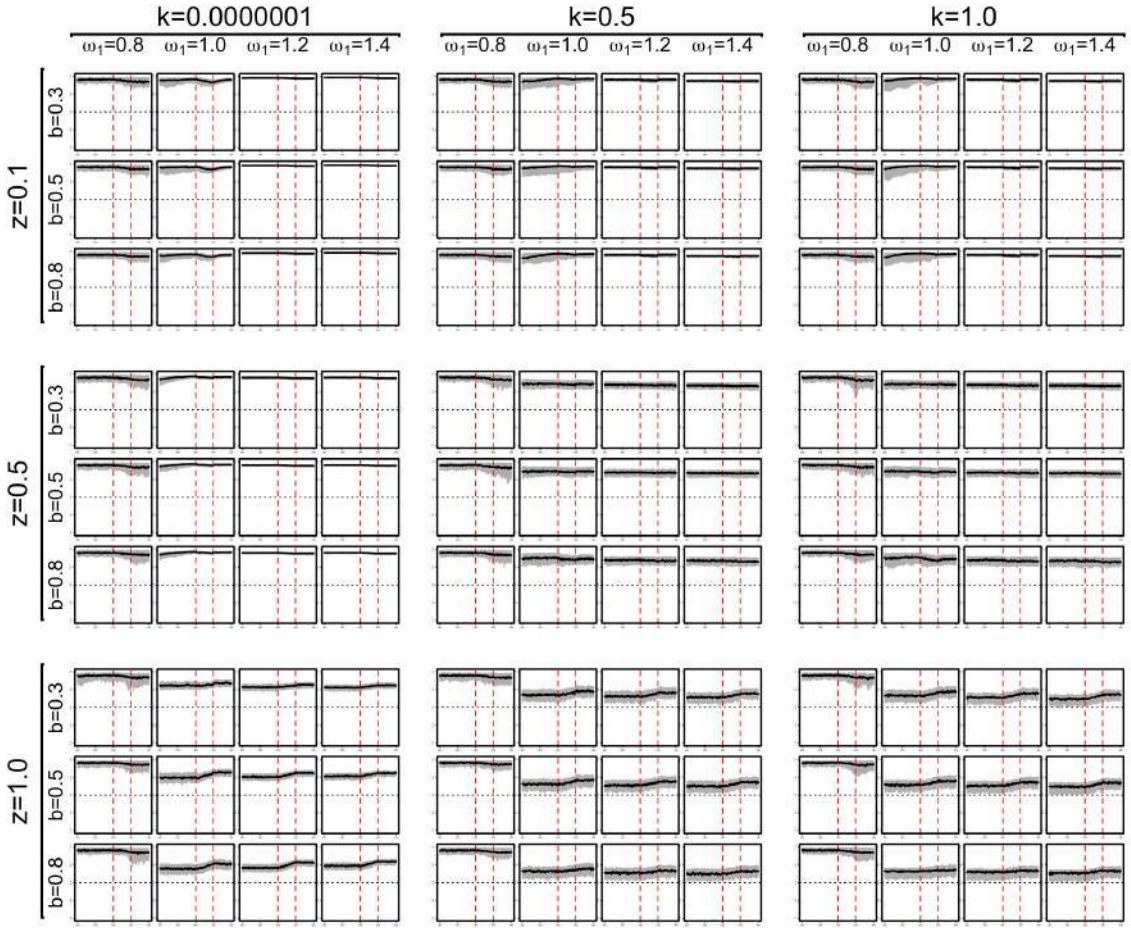

Combined time-series of A [disturbance model, $t_s = 301$, $t_e = 348$, $\eta = 2.08$, $h = \infty$]

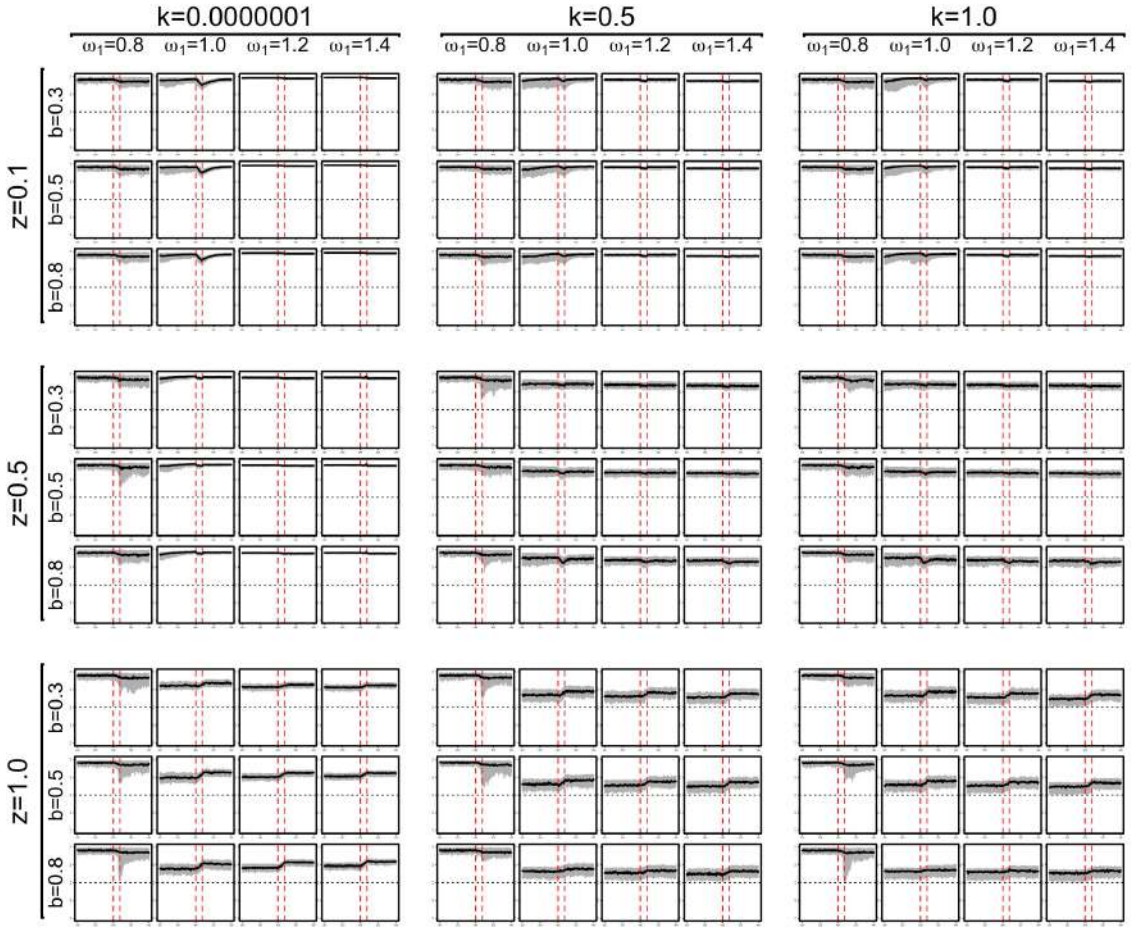

Combined time-series of A [disturbance model, $t_s = 301$, $t_e = 308$, $\eta = 5.56$, $h = \infty$]

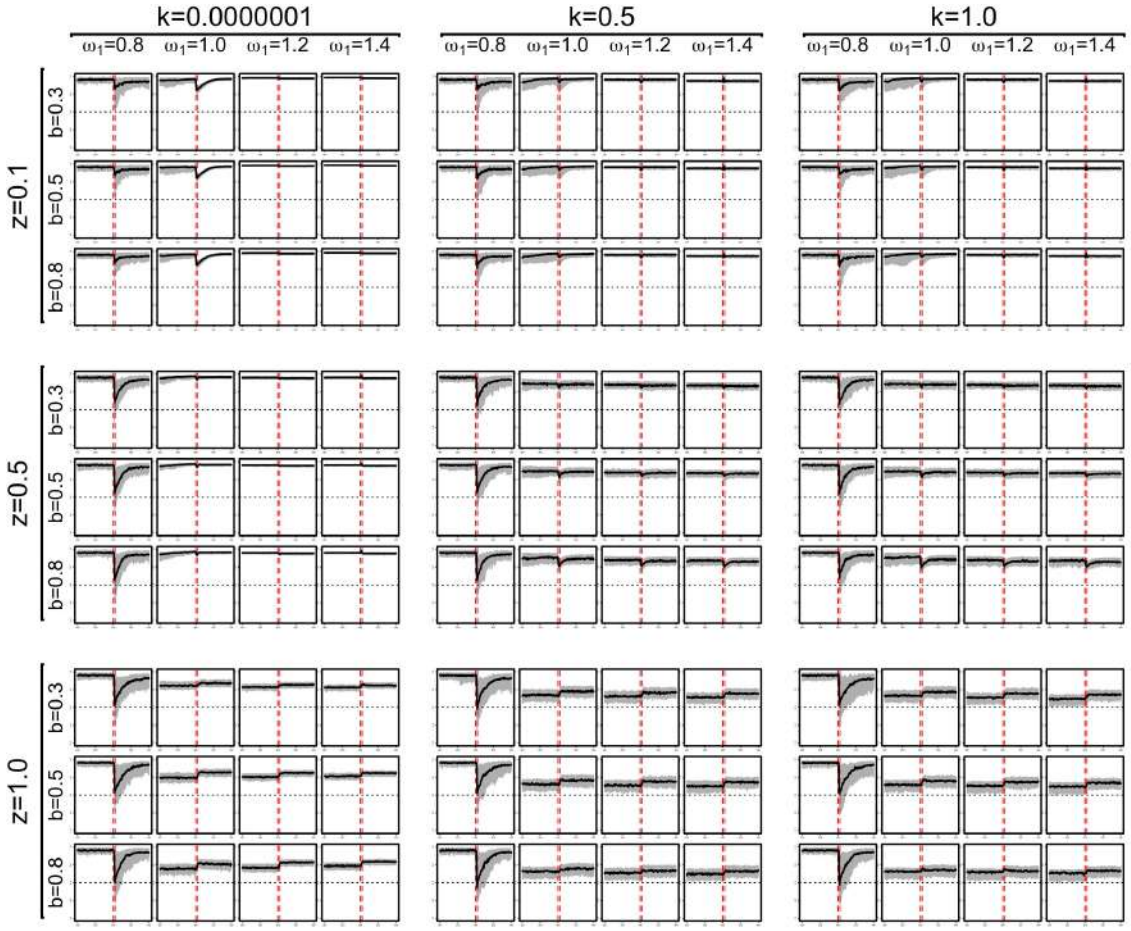

Combined time-series of A [disturbance model, $t_s = 301$, $t_e = 304$, $\eta = 25$, $h = \infty$]

D.3.2 Number of Groups (G)

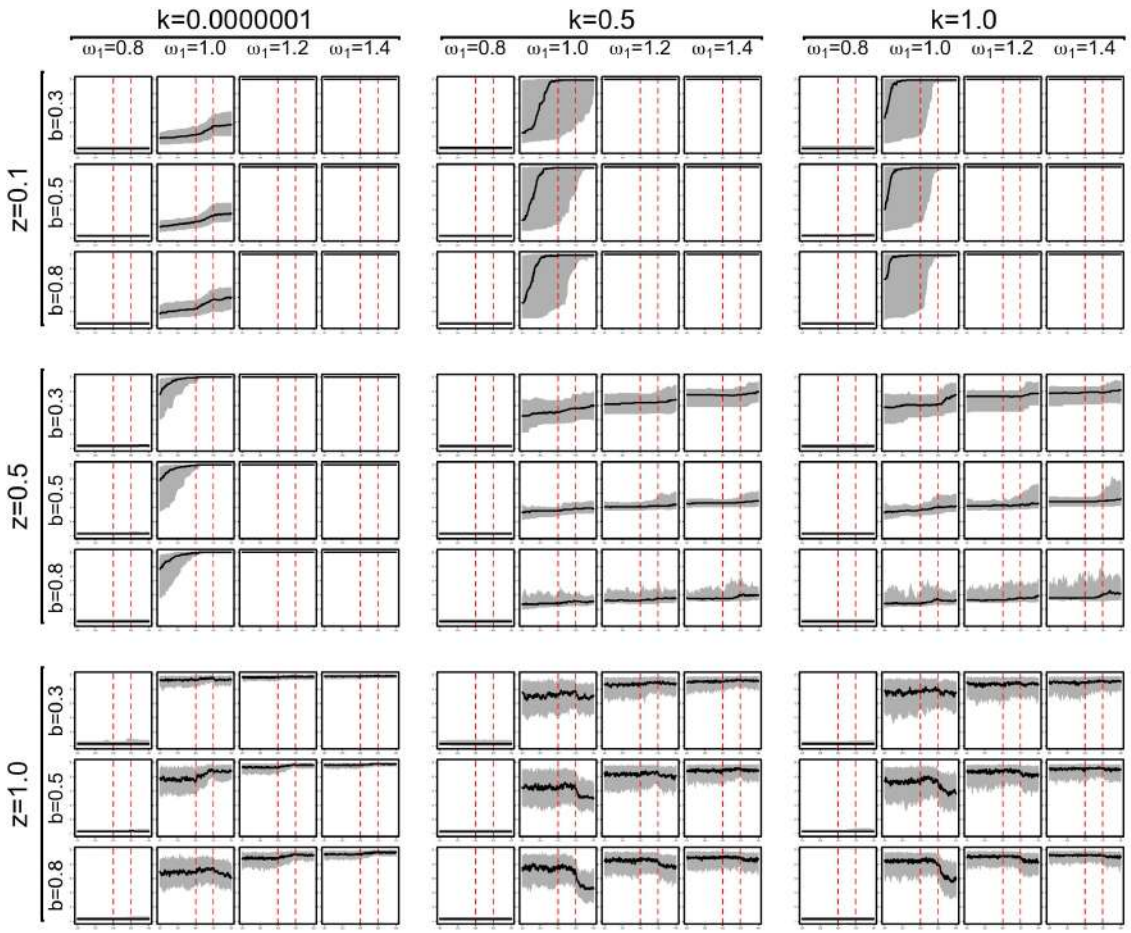

Combined time-series of G [disturbance model, $t_s = 301$, $t_e = 348$, $\eta = 2.08$, $h = 1$]

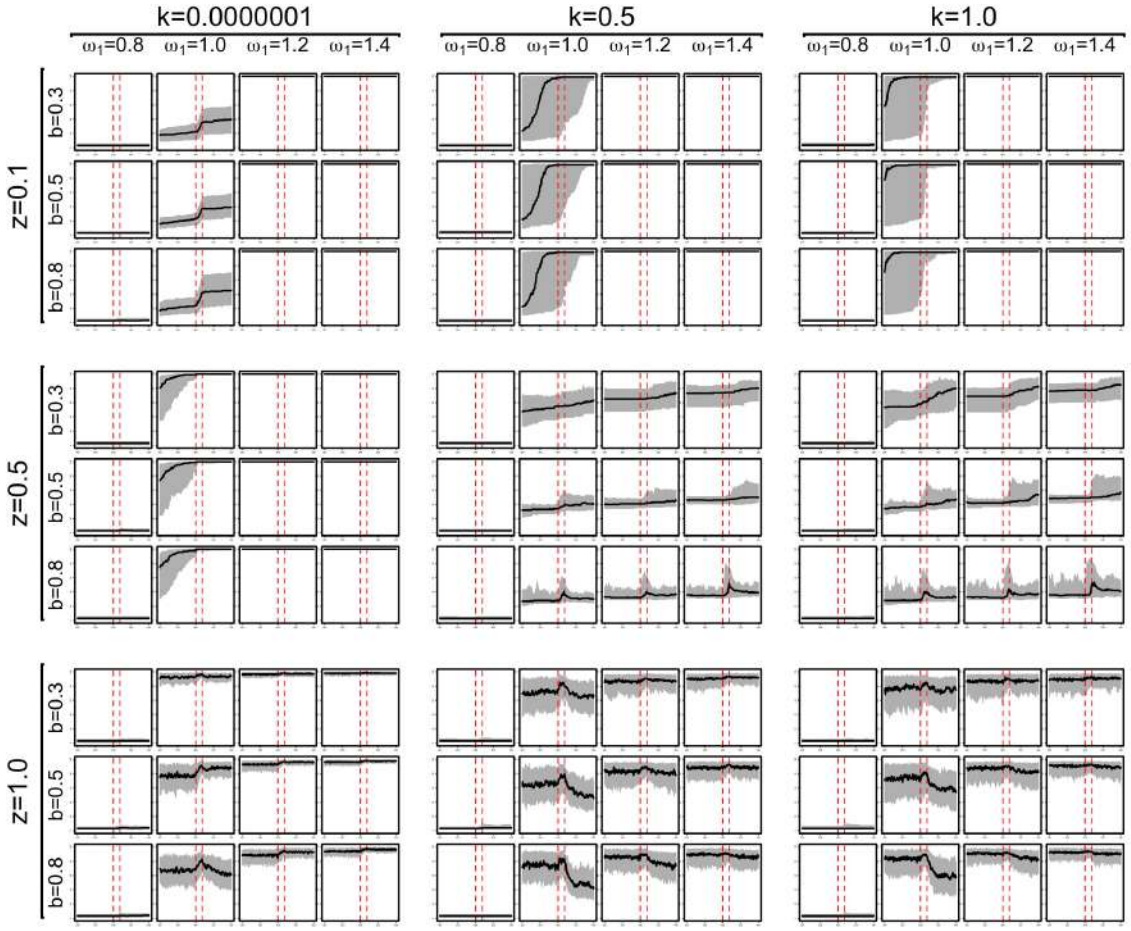

Combined time-series of G [disturbance model, $t_s = 301$, $t_e = 308$, $\eta = 5.56$, $h = 1$]

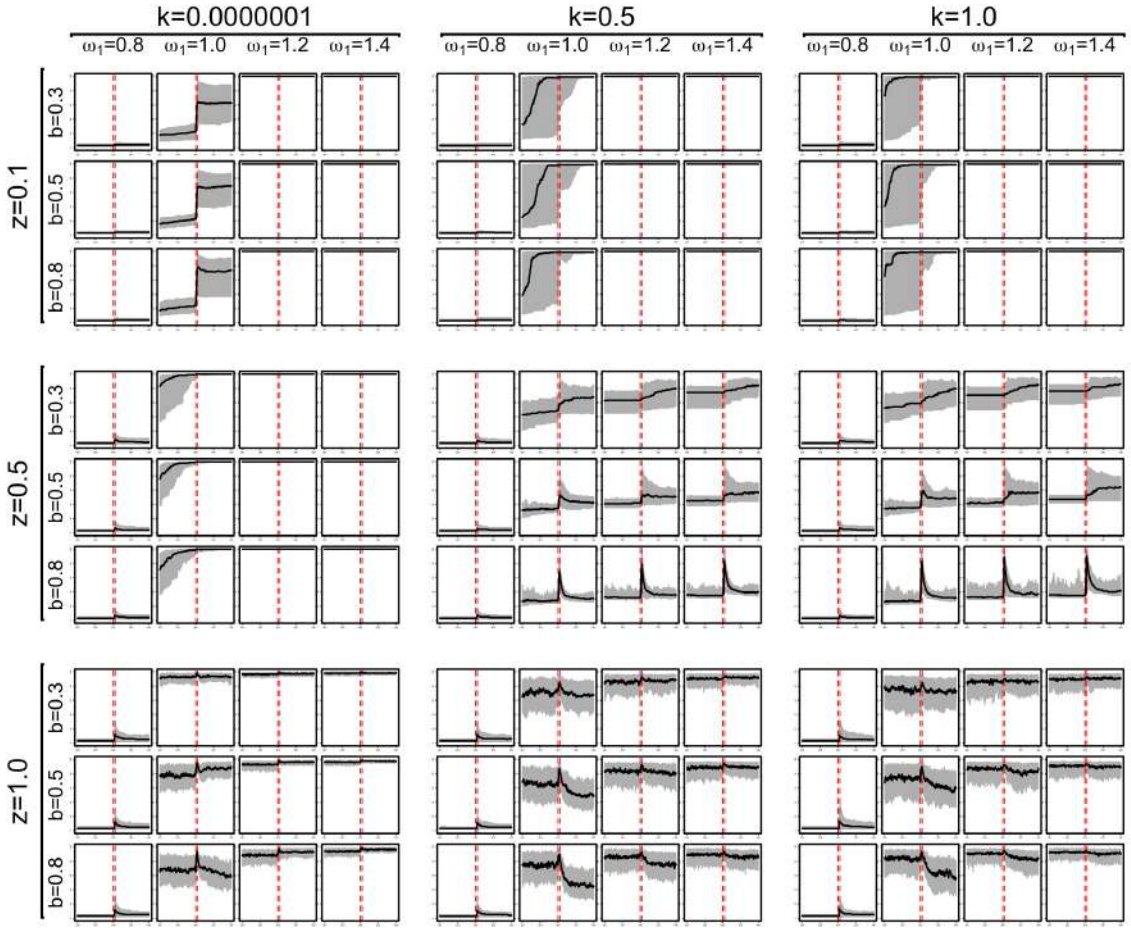

Combined time-series of G [disturbance model, $t_s = 301$, $t_e = 304$, $\eta = 25$, $h = 1$]

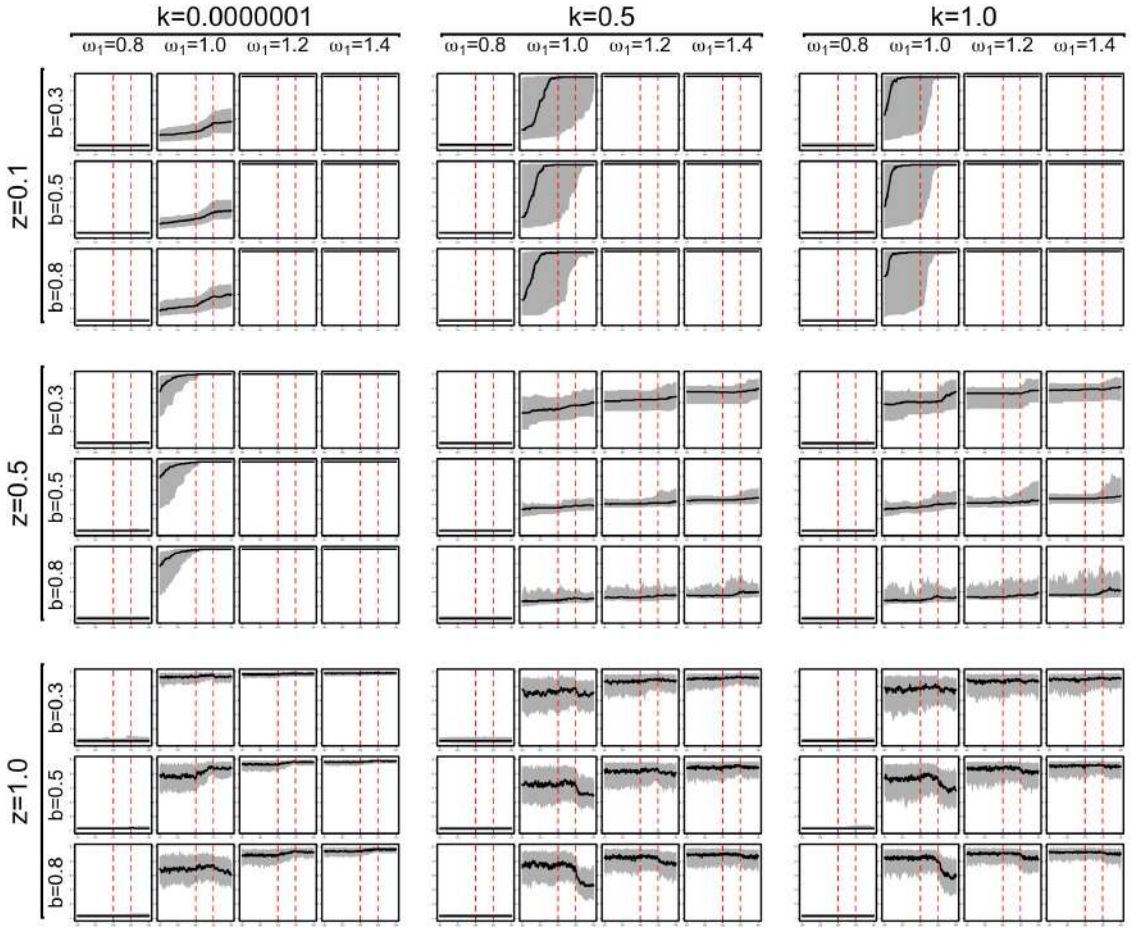

Combined time-series of G [disturbance model, $t_s = 301$, $t_e = 348$, $\eta = 2.08$, $h = \infty$]

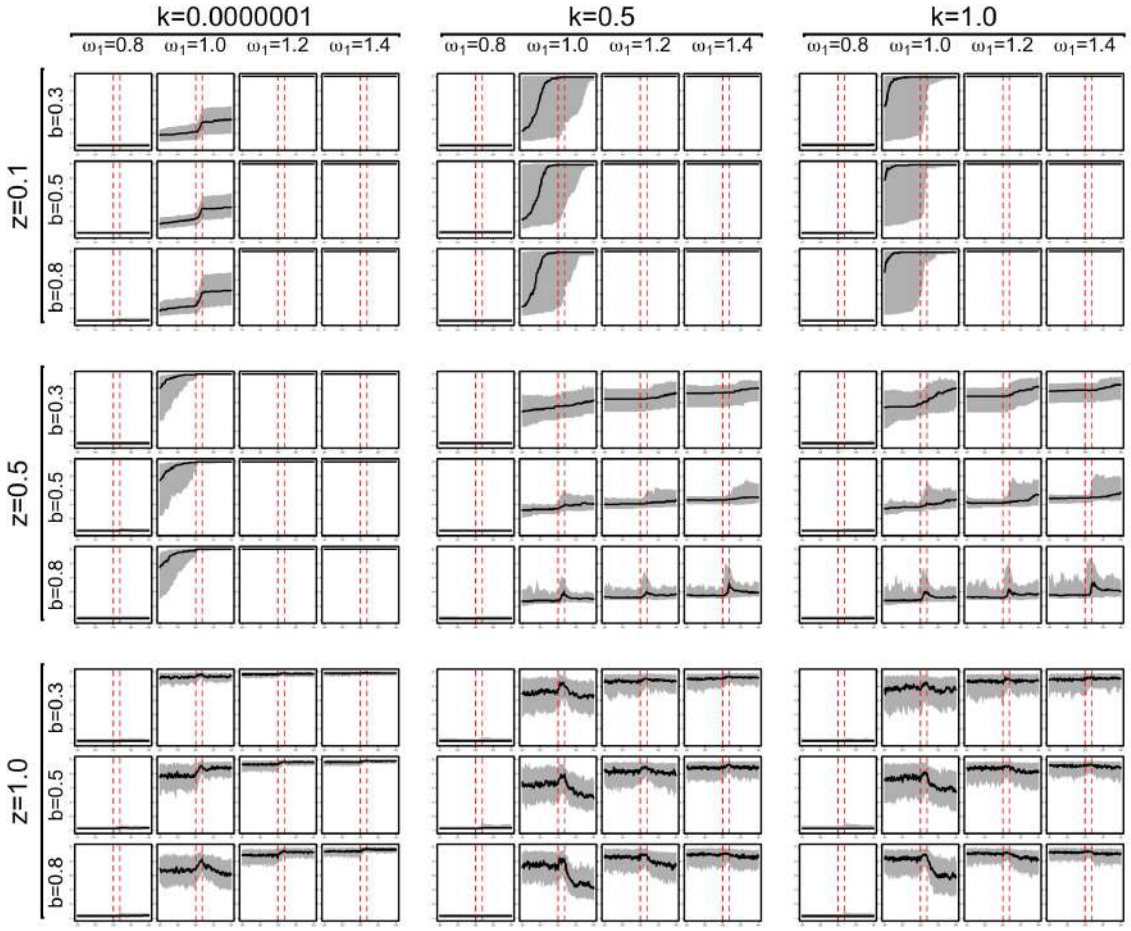

Combined time-series of G [disturbance model, $t_s = 301$, $t_e = 308$, $\eta = 5.56$, $h = \infty$]

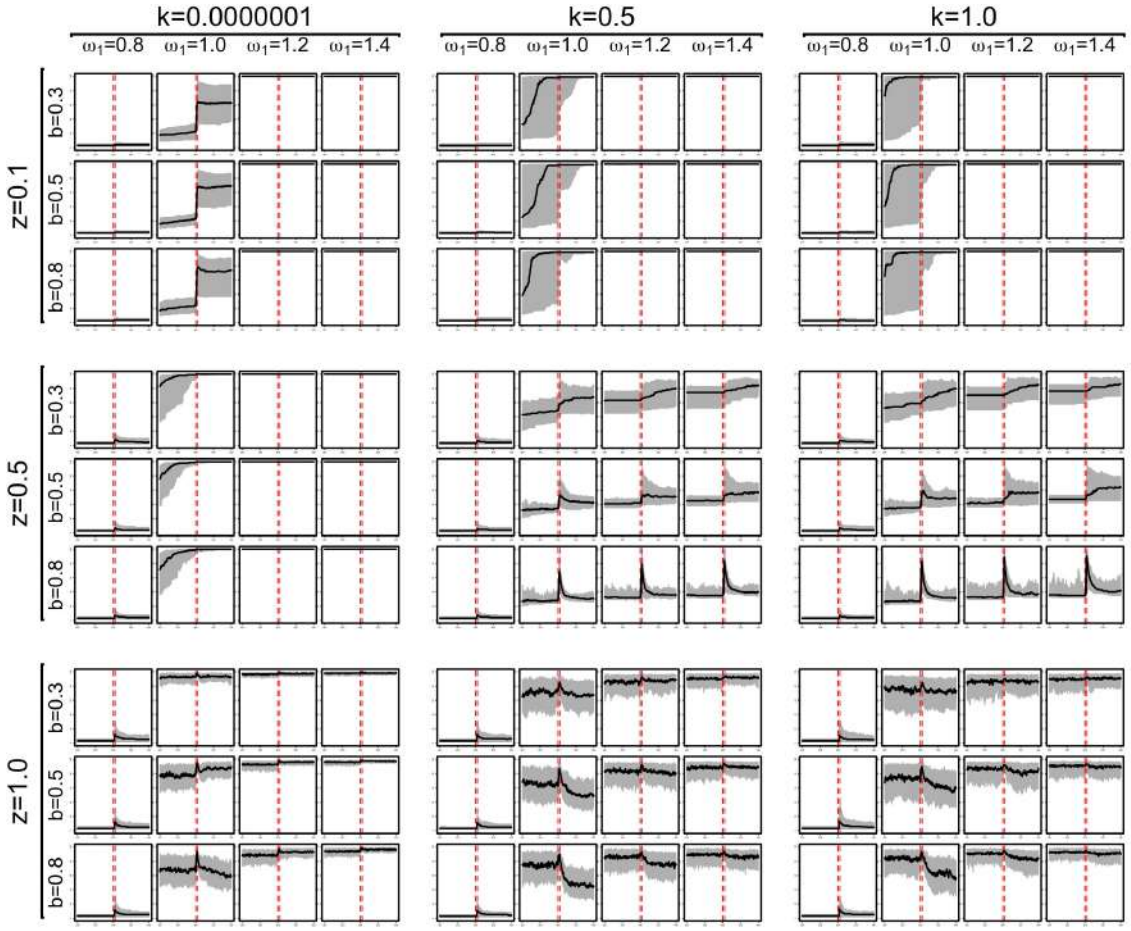

Combined time-series of G [disturbance model, $t_s = 301$, $t_e = 304$, $\eta = 25$, $h = \infty$]

D.3.3 Number of Agents (N)

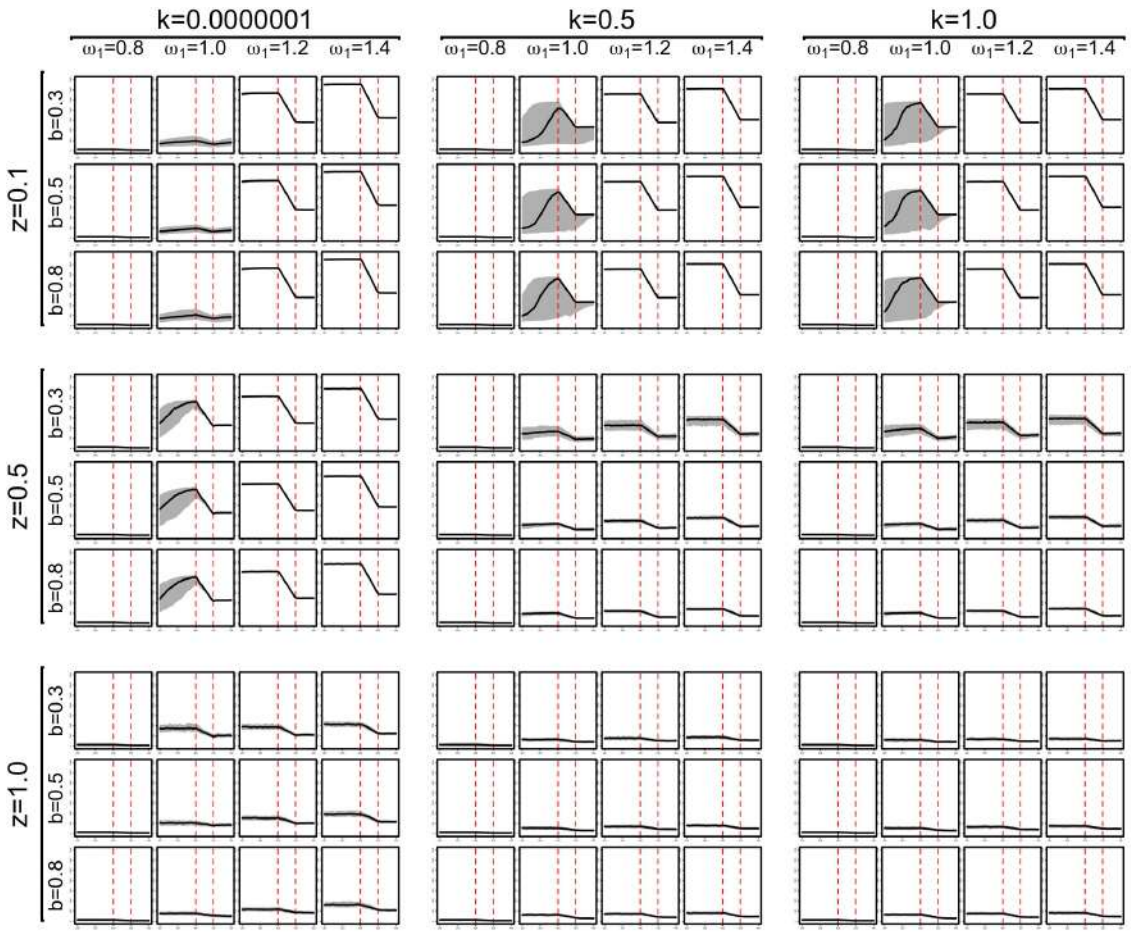

Combined time-series of N [disturbance model, $t_s = 301$, $t_e = 348$, $\eta = 2.08$, $h = 1$, y-axis range from 0 to 3500]

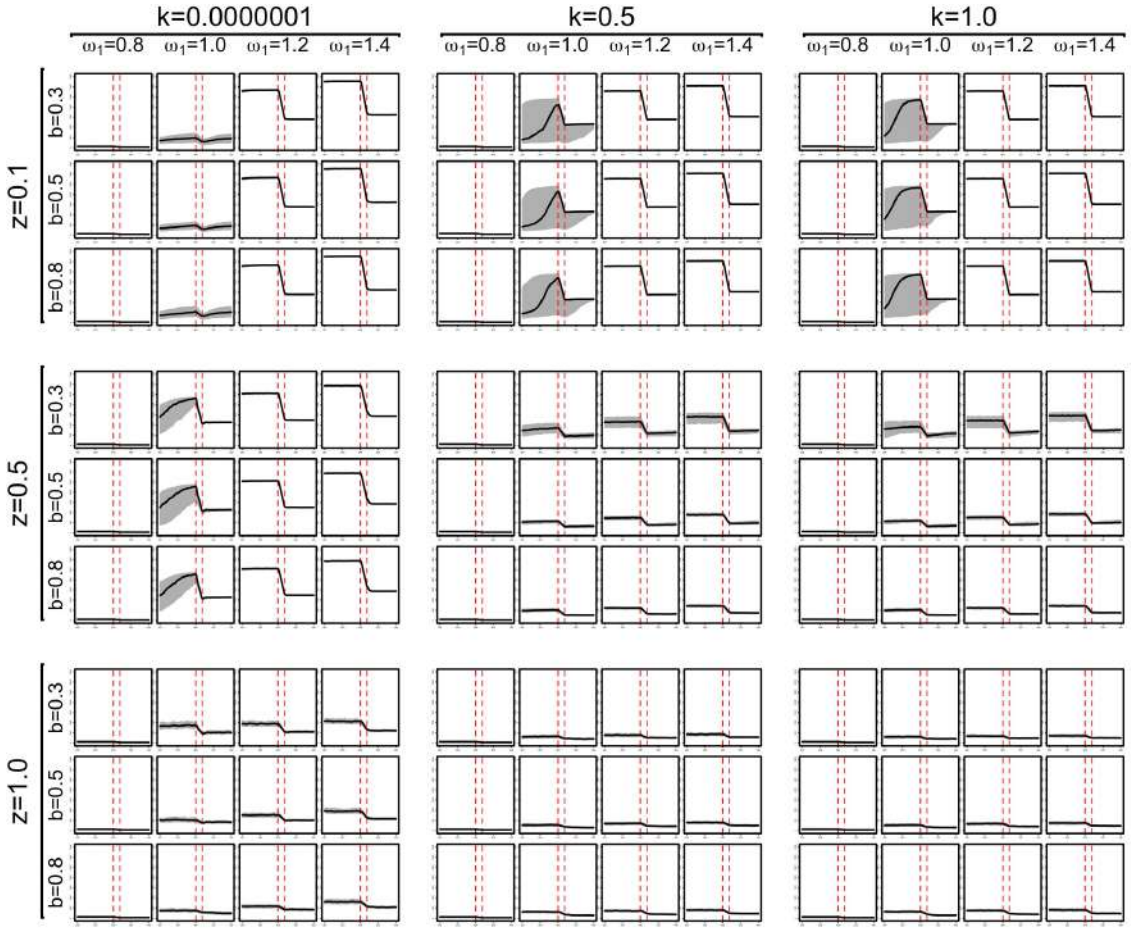

Combined time-series of N [disturbance model, $t_s = 301$, $t_e = 308$, $\eta = 5.56$, $h = 1$, y-axis range from 0 to 3500]

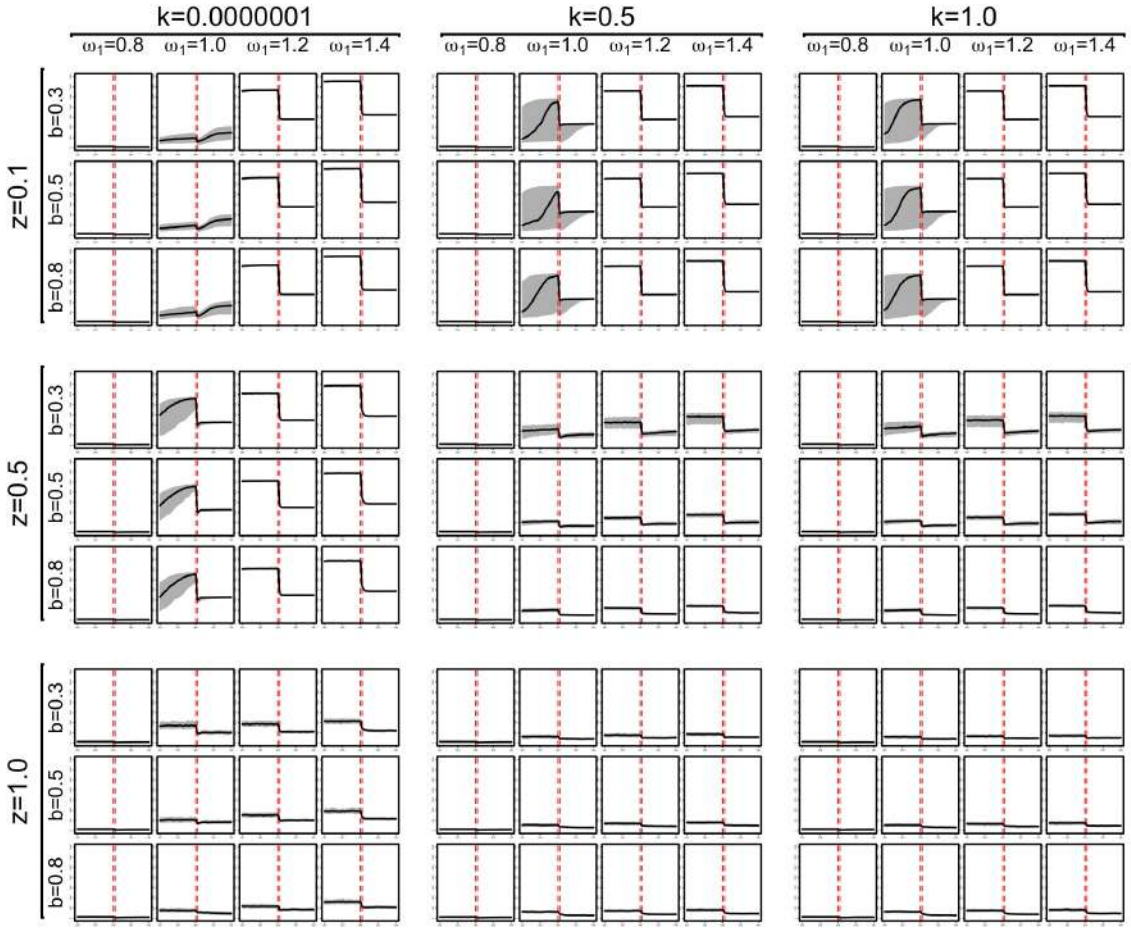

Combined time-series of N [disturbance model, $t_s = 301$, $t_e = 304$, $\eta = 25$, $h = 1$, y-axis range from 0 to 3500]

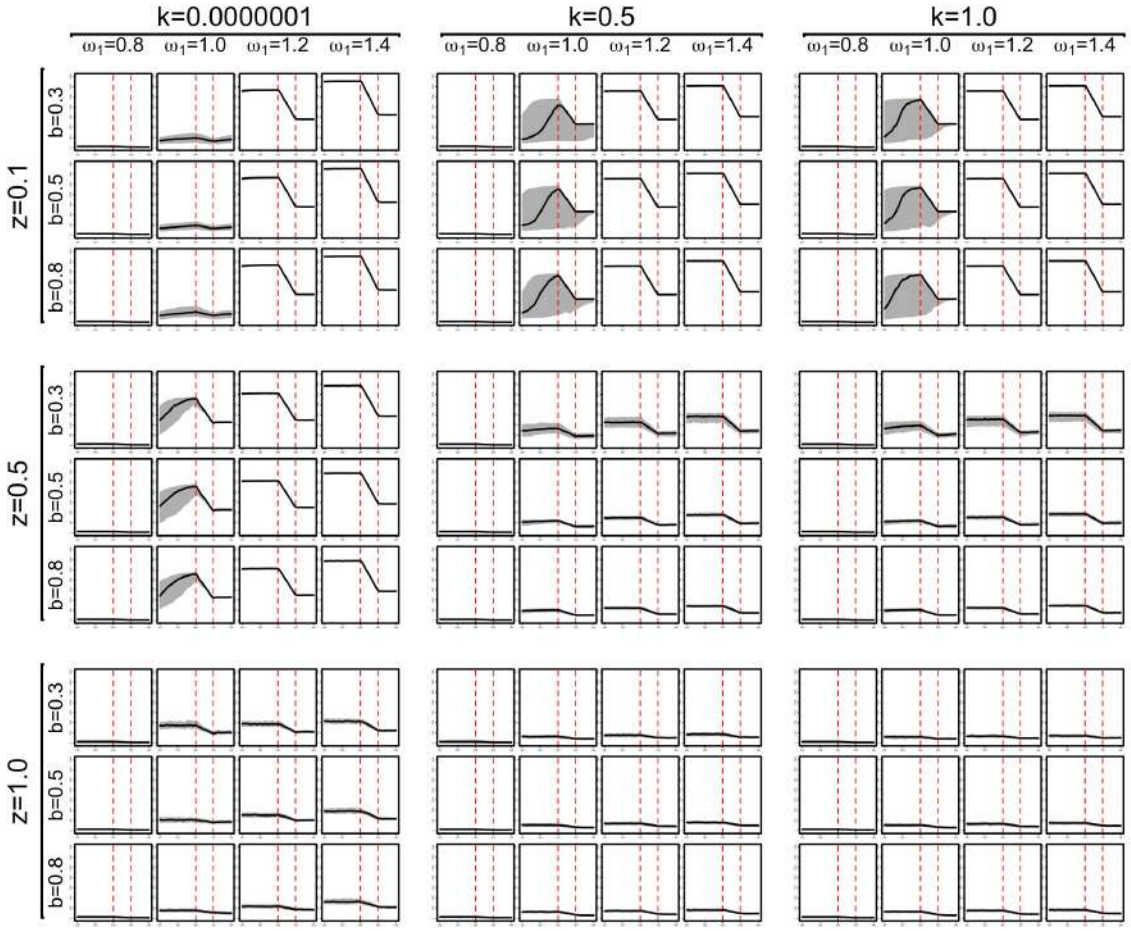

Combined time-series of N [disturbance model, $t_s = 301$, $t_e = 348$, $\eta = 2.08$, $h = \infty$, y-axis range from 0 to 3500]

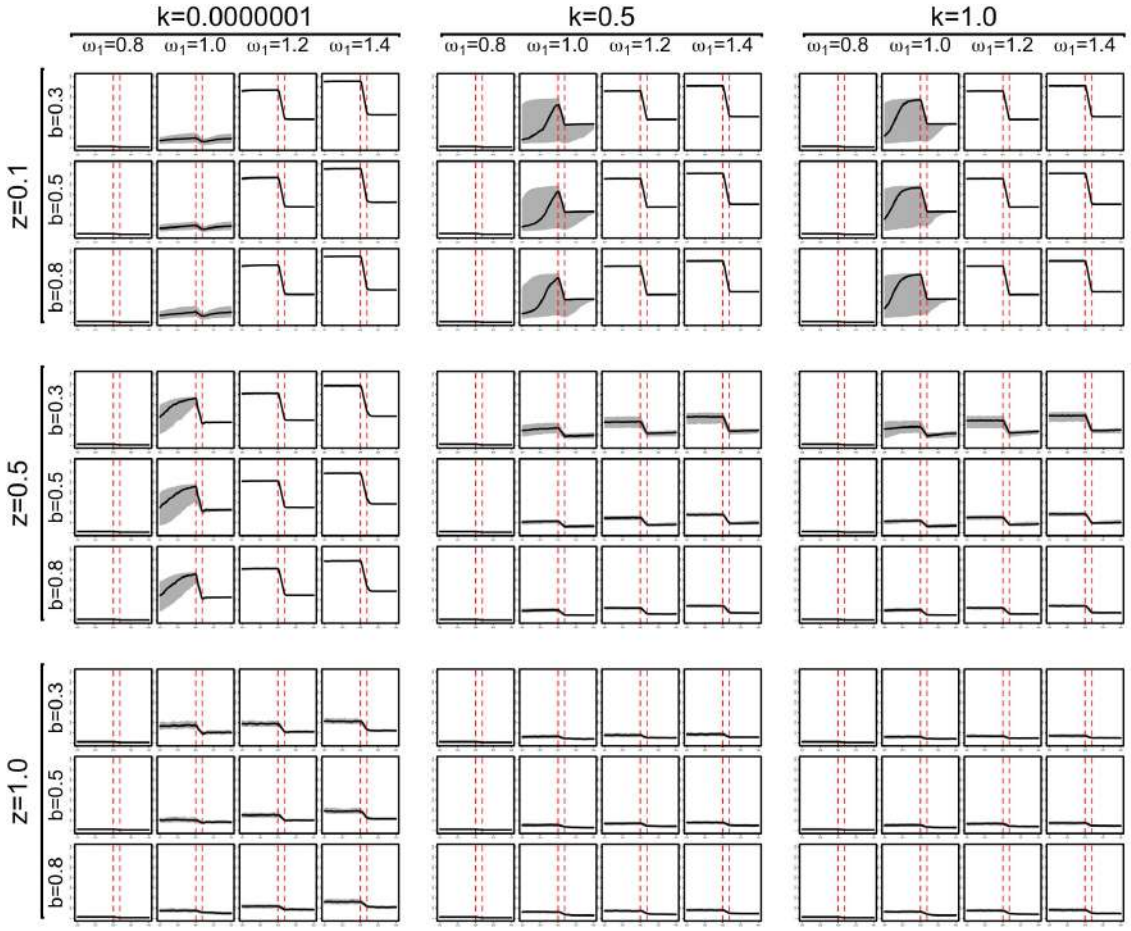

Combined time-series of N [disturbance model, $t_s = 301$, $t_e = 308$, $\eta = 5.56$, $h = \infty$, y-axis range from 0 to 3500]

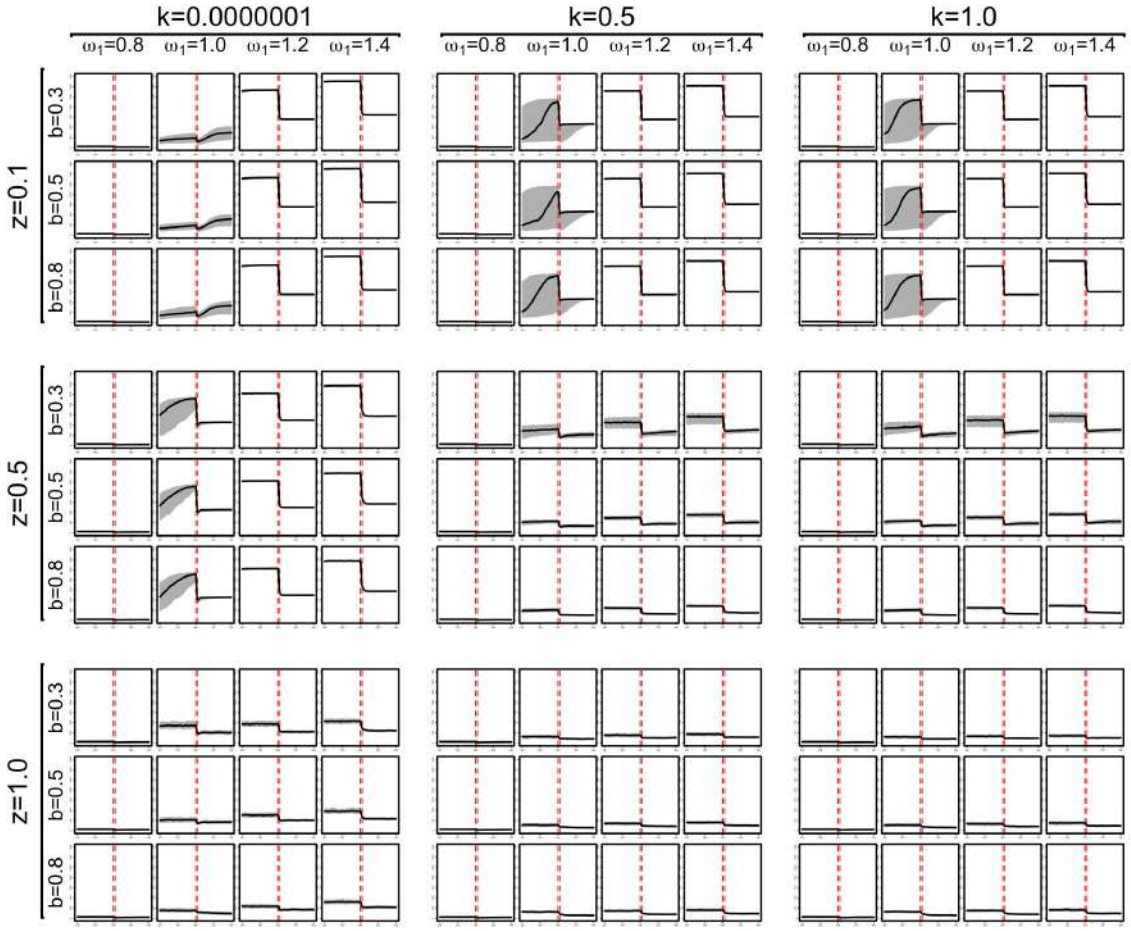

Combined time-series of N [disturbance model, $t_s = 301$, $t_e = 304$, $\eta = 25$, $h = \infty$, y-axis range from 0 to 3500]

D.3.4 Median Group Size ($\tilde{\lambda}$)

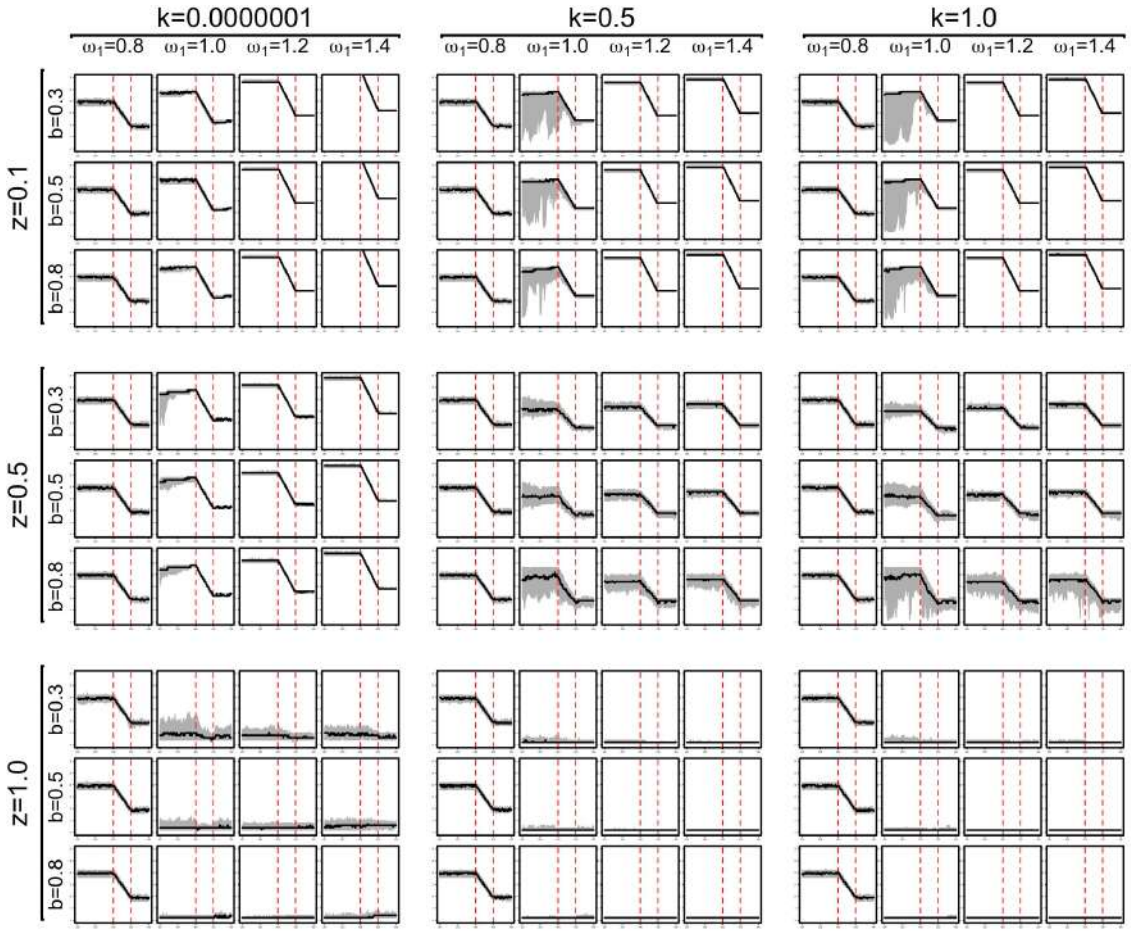

Combined time-series of $\tilde{\lambda}$ [disturbance model, $t_s = 301$, $t_e = 348$, $\eta = 2.08$, $h = 1$]

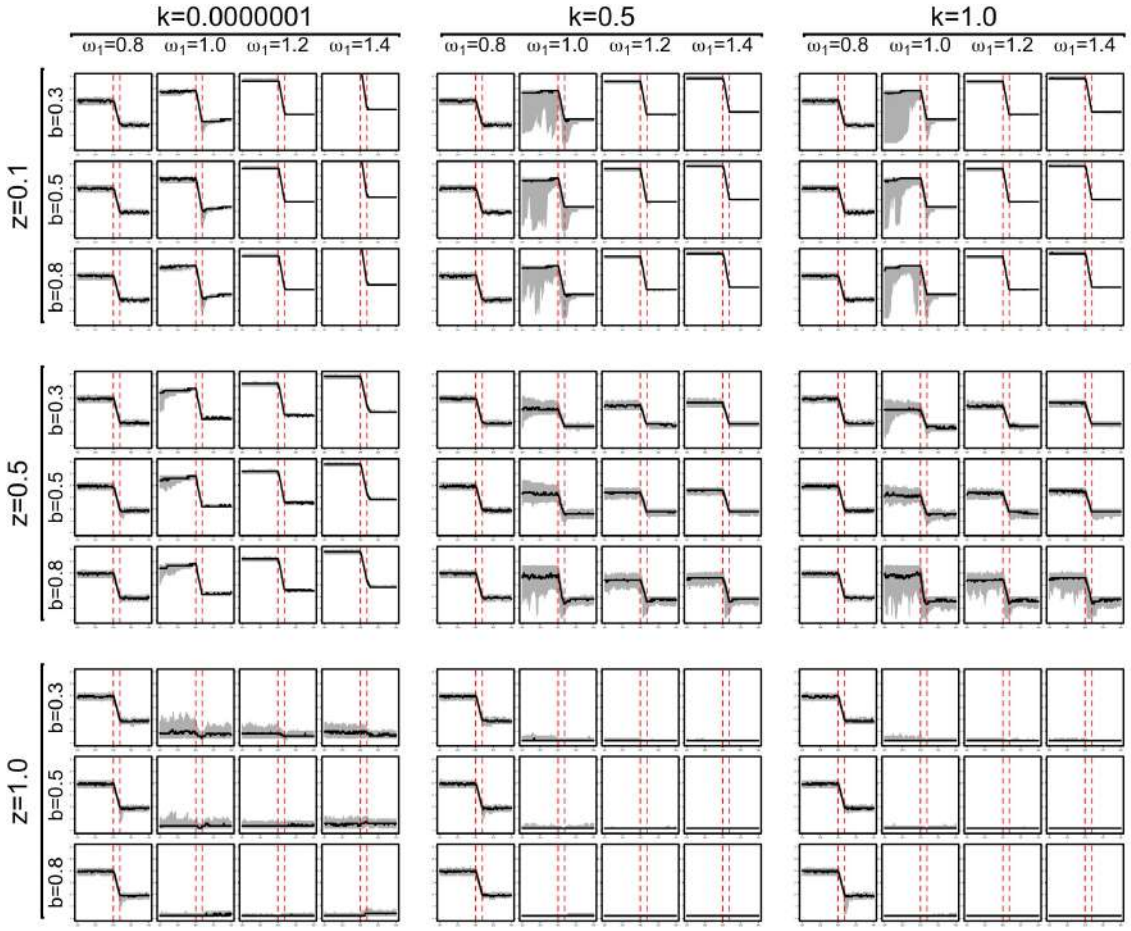

Combined time-series of $\tilde{\lambda}$ [disturbance model, $t_s = 301$, $t_e = 308$, $\eta = 5.56$, $h = 1$]

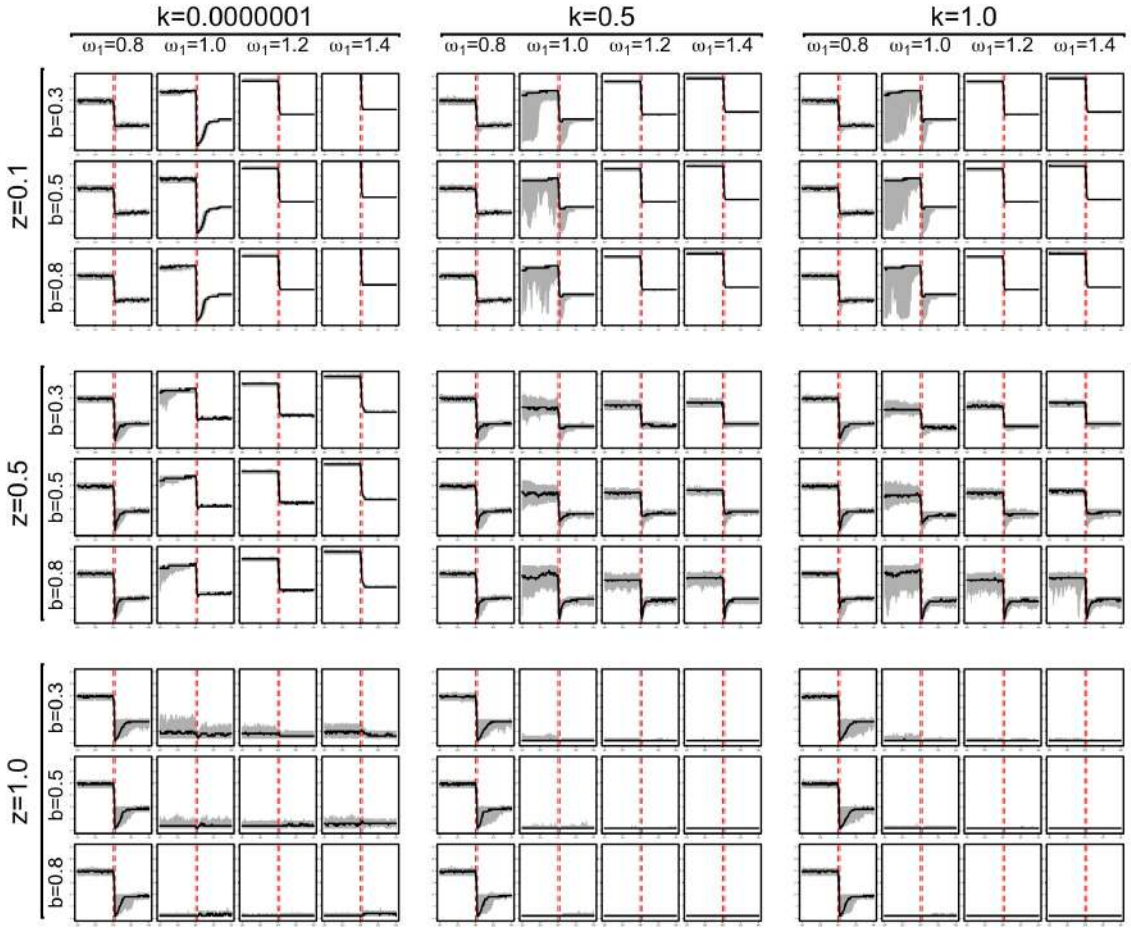

Combined time-series of $\tilde{\lambda}$ [disturbance model, $t_s = 301$, $t_e = 304$, $\eta = 25$, $h = 1$]

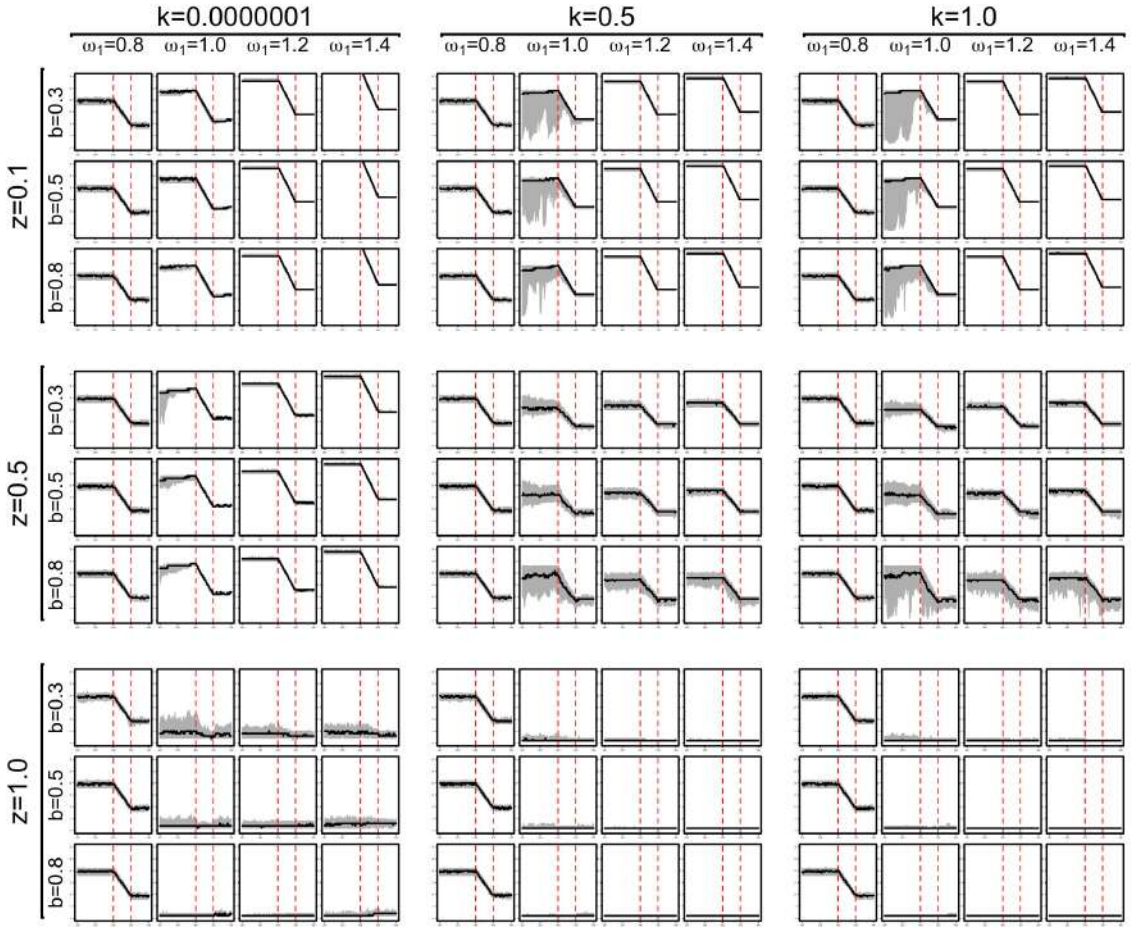

Combined time-series of $\tilde{\lambda}$ [disturbance model, $t_s = 301$, $t_e = 348$, $\eta = 2.08$, $h = \infty$]

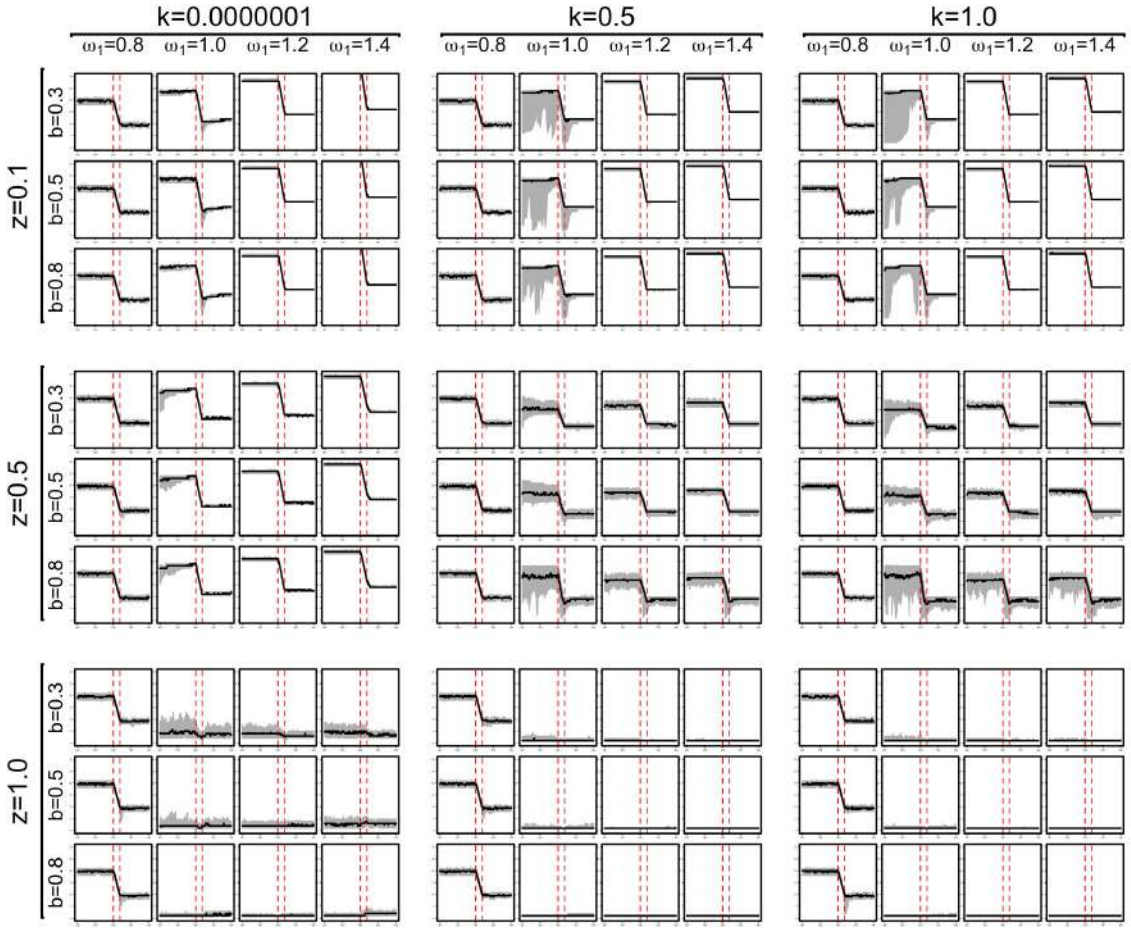

Combined time-series of $\tilde{\lambda}$ [disturbance model, $t_s = 301$, $t_e = 308$, $\eta = 5.56$, $h = \infty$]

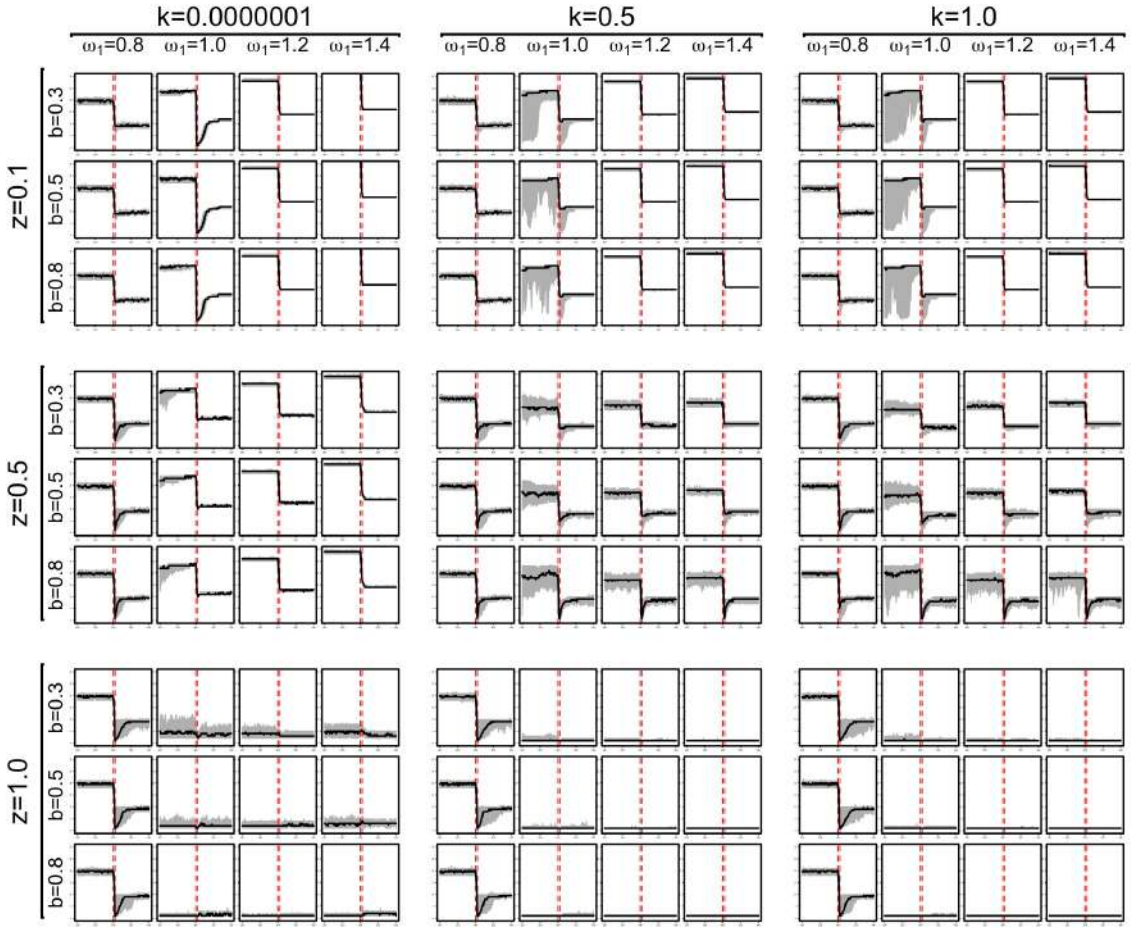

Combined time-series of $\tilde{\lambda}$ [disturbance model, $t_s = 301$, $t_e = 304$, $\eta = 25$, $h = \infty$]